



Phytochemical profiling and anti-microbial studies of Australian marine and terrestrial organisms: The search for new natural product derived anti-biotic and anti-fungal agents

A thesis submitted in fulfilment of the requirements for the degree of Doctor of Philosophy

Robert Brkljača

B. Sc. (Appl. Chem), Hons. (Appl. Chem.)

School of Applied Sciences

College of Science Engineering and Health

RMIT University

March 2015

Declaration

I certify that except where due acknowledgement has been made, the work is that of the author alone; the work has not been submitted previously, in whole or in part, to qualify for any other academic award; the content of the thesis/project is the result of work which has been carried out since the official commencement date of the approved research program; any editorial work, paid or unpaid, carried out by a third party is acknowledged; and, ethics procedures and guidelines have been followed.

Robert Brkljača

13 March 2015

Listed below are the bibliographic details of the publications that appear in this thesis along with my contribution to each publication.

Chapter 2: NMR Spectroscopy for the Identification of Natural Products

Brkljača, Robert, & Urban, Sylvia. (2014). Selected Applications of NMR Spectroscopy – Natural Products. In J. Fisher (Ed.), *Modern NMR Techniques for Synthetic Chemistry*. Florida, USA: CRC Press.

Author	Contribution
Robert Brkljača	Experimental, First Draft, Revision
Sylvia Urban	Revision

Chapter 3: HPLC-NMR for Chemical Profiling

Brkljača, Robert, & Urban, Sylvia. (2011). Recent Advancements in HPLC-NMR and Applications for Natural Product Profiling and Identification. *Journal of Liquid Chromatography & Related Technologies*, 34(12), 1063-1076.

Author	Contribution
Robert Brkljača	First Draft, Revision
Sylvia Urban	Revision

Chapter 4: Limit of Detection of HPLC-NMR

Brkljača, Robert, & Urban, Sylvia. (2015). Limit of Detection Studies for Application to Natural Product Identification using High Performance Liquid Chromatography Coupled to nuclear Magnetic Resonance Spectroscopy. *Journal of Chromatography A*, 1375, 69-75.

Author	Contribution
Robert Brkljača	Experimental, First Draft, Revision
Sylvia Urban	Revision

Chapter 5: Constituents from the Australian Plant *Macropidia fuliginosa*

Brkljača, Robert, White, Jonathan M., & Urban, Sylvia. (2015). Phytochemical investigation of the constituents derived from the Australian plant *Macropidia fuliginosa*. *Journal of Natural Products*, 78(7), 1600-1608.

Author	Contribution
Robert Brkljača	Experimental, First Draft, Revision
Sylvia Urban	Revision
Jonathan M. White	X-ray Structures

Chapter 6: Chemical Profiling and Isolation of Secondary Metabolites from

Haemodorum spicatum

Brkljača, Robert, & Urban, Sylvia. (2015). Chemical Profiling/HPLC-NMR and HPLC-MS profiling and bioassay-guided identification of secondary metabolites from the Australian plant *Haemodorum spicatum*. *Journal of Natural Products*, 78(7), 1486-1494.

Author	Contribution
Robert Brkljača	Experimental, First Draft, Revision
Sylvia Urban	Revision

Chapter 7: Secondary Metabolites of the Fungus *Leucocoprinus birnbaumii*

Brkljača, Robert, & Urban, Sylvia. (2015). Rapid Dereplication and Identification of the Bioactive Constituents from the Fungus, *Leucocoprinus birnbaumii*. *Natural Product Communications*, 10(1), 95-98.

Author	Contribution
Robert Brkljača	Experimental, First Draft, Revision
Sylvia Urban	Revision

Chapter 8: Dereplication and Chemotaxonomical Profiling of Seven Marine Algae by HPLC-NMR & HPLC-MS

Brkljača, Robert, Göker, Emrehan S., & Urban, Sylvia. (2015). Dereplication and Chemotaxonomical Studies of Marine Algae of the Ochrophyta and Rhodophyta Phyla. *Marine Drugs*, 13(5), 2714-2731.

Author	Contribution
Robert Brkljača	Experimental (6 algae), First Draft, Revision
Sylvia Urban	Revision
Emrehan S. Göker	Experimental (1 alga)

Chapter 9: Chemical Profiling and Isolation Studies of the Marine Brown Alga

Sargassum paradoxum

Brkljača, Robert, & Urban, Sylvia. (2015). Chemical Profiling (HPLC-NM & HPLC-MS), Isolation and Identification of Bioactive Meroditerpenoids from the Southern Austrian Marine Brown Alga *Sargassum paradoxum*. *Marine Drugs*, 13(1), 102-127.

Author	Contribution
Robert Brkljača	Experimental, First Draft, Revision
Sylvia Urban	Revision

Chapter 10: Dereplication and Structural Identification Studies of Marine Algae of the Genus *Cystophora*

Brkljača, Robert, & Urban, Sylvia. (2015). HPLC-NMR and HPLC-MS investigation of antimicrobial constituents in *Cystophora monilifera* and *Cystophora subfarcinata*. *Phytochemistry*, 117, 200-208.

Author	Contribution
Robert Brkljača	Experimental, First Draft, Revision
Sylvia Urban	Revision

Chapter 11: Relative Configuration Studies of the Marine Natural Product

Elatenyne

Brkljača, Robert, & Urban, Sylvia. (2013). Relative Configuration of the Marine Natural Product Elatenyne using NMR Spectroscopic and Chemical Derivatization Methodologies. *Natural product Communications*, 8(6), 729-732.

Author	Contribution
Robert Brkljača	Experimental, First Draft, Revision
Sylvia Urban	Revision

Acknowledgments

Dr Sylvia Urban, thank you for the opportunity to be part of the MATNAP research group. You were a fantastic supervisor and I have learned a great deal from you. Your encouragement and dedication to my PhD did not go unnoticed and without your assistance, I would not have completed such a high quality PhD. To my second supervisor, Dr Julie Niere, your constant advice and discussions in terms of NMR acquisition and interpretation were much appreciated.

To the various people responsible (Dr Daniel Dias; Ms Priyanka Reddy; Mr Roderick Watson, Victorian Marine Science Consortium; Mr Allan Tinker; Dr Rick Tinker; Dr Sylvia Urban) for the collection of my specimens, the various people (Dr Gerald Kraft, The University of Melbourne; Prof. Anne Lawrie, RMIT University; Mr Allan Tinker) responsible for the taxonomic identifications, and to the members of the MATNAP research group that conducted preliminary work on my specimens, thank you for your contributions.

Lastly, I am grateful to all the technical staff I was in contact with throughout my PhD studies. In particular, thanks to Ms Gill Ellis, University of Canterbury, Christchurch, New Zealand (for conducting some of the biological activity of the crude extracts); Ms Nerida Thurbon, RMIT University (for assistance and providing access to micro-organisms for anti-microbial assays); Dr John Ryan, Agilent Australia (NMR specialist, for his useful advice); Dr Mark Rizzacasa, The University of Melbourne and Bio21 Institute (for providing access to ozone generator); Dr Jonathan White, The University of Melbourne and Bio21 Institute (for

conducting single crystal X-ray crystallographic studies); and Ms Sally Duck, Monash University (for acquisition of high resolution mass spectrometry and providing access to HPLC-MS facility).

Publications Resulting from PhD Thesis

Journal Publications

1. **Brkljača, Robert**, White, Jonathan M., & Urban, Sylvia. (2015). Phytochemical Investigation of the Constituents Derived from the Australian Plant *Macropidia fuliginosa*. *Journal of Natural Products*, 78(7), 1600-1608.
2. **Brkljača, Robert**, & Urban, Sylvia. (2014). HPLC-NMR & HPLC-MS profiling and bioassay-guided identification of secondary metabolites from the Australian plant *Haemodorum spicatum*. *Journal of Natural Products*, 78(7), 1486-1494.
3. **Brkljača, Robert**, & Urban, Sylvia. (2015). HPLC-NMR and HPLC-MS investigation of antimicrobial constituents in *Cystophora monilifera* and *Cystophora subfarcinata*. *Phytochemistry*, 117, 200-208.
4. **Brkljača, Robert**, Göker, Emrehan S., & Urban, Sylvia. (2015). Dereplication and Chemotaxonomical Studies of Marine Algae of the Ochrophyta and Rhodophyta Phyla. *Marine Drugs*, 13(5), 2714-2731.
5. **Brkljača, Robert**, & Urban, Sylvia. (2015). Limit of Detection Studies for Application to Natural Product Identification using High Performance Liquid Chromatography Coupled to Nuclear Magnetic Resonance Spectroscopy. *Journal of Chromatography A*, 1375, 69-75.

6. **Brkljača, Robert**, & Urban, Sylvia. (2015). Rapid Dereplication and Identification of the Bioactive Constituents from the Fungus, *Leucocoprinus birnbaumii*. *Natural Product Communications*, 10(1), 95-98.
7. **Brkljača, Robert**, & Urban, Sylvia. (2015). Chemical Profiling (HPLC-NMR & HPLC-MS), Isolation and Identification of Bioactive Meroditerpenoids from the Southern Australian Marine Brown Alga *Sargassum paradoxum*. *Marine Drugs*, 13(1), 102-127.
8. **Brkljača, Robert**, & Urban, Sylvia. (2013). Relative Configuration of the Marine Natural Product Elatenyne using NMR Spectroscopic and Chemical Derivatization Methodologies. *Natural Product Communications*, 8(6), 729-732.
9. Urban, Sylvia, Timmers, Michael A., **Brkljača, Robert**, & White, Jonathan M. (2013). Phenylphenalenones and Oxabenzochrysenones from the Australian Plant *Haemodorum simulans*. *Phytochemistry*, 95, 351-359.
10. **Brkljača, Robert**, & Urban, Sylvia. (2011). Recent Advancements in HPLC-NMR and Applications for Natural Product Profiling and Identification. *Journal of Liquid Chromatography & Related Technologies*, 34(12), 1063-1076.

Book section/Book chapter

1. **Brkljača, Robert, & Urban, Sylvia.** (2014). Selected Applications of NMR Spectroscopy - Natural Products. In J. Fisher (Ed.), *Modern NMR Techniques for Synthetic Chemistry*. Florida, USA: CRC Press.

Conference Proceedings

Oral Presentations

1. Chemical Profiling (HPLC-NMR & HPLC-MS), Isolation and Identification of Bioactive Meroditerpenoids from the Southern Australian Marine Brown Alga *Sargassum paradoxum*, 39th Annual Synthesis Symposium, Bio21 Institute, Melbourne University, 5th December 2014.
2. Phytochemical Profiling and Biological Activity Studies of the Southern Australian Marine Alga, *Sargassum paradoxum*, 14th International Symposium on Marine Natural Products (MANAPRO XIV), La Toja Island, Spain 15-20th September 2013.
3. Natures Medicine Chest: Treatments from the Ground and Cures from the Deep, School of Applied Sciences Annual Research Day, 3 Minute Thesis Competition, 15th June 2012.
4. Chemical Profiling of Australian Marine and Terrestrial Organisms, Applications of NMR Spectroscopy, Bio21 Institute, 17th April 2012.

Poster Presentations

1. Relative Configuration Study of the Marine Natural Product Elatenyne using NMR Spectroscopic and Chemical Derivatisation Methodologies, 14th International Symposium on Marine Natural Products (MANAPRO XIV), La Toja Island, Spain 15-20th September 2013.

2. Chemical Investigation of the Australian Plant *Conospermum patens*, poster presentation, 27th International Symposium on the Chemistry of Natural Products (ISCNP27), Brisbane 10-15th July 2011.

3. Recent Advancements in HPLC-NMR and its Applications to Rapidly Profile Marine Natural Products, poster presentation, 27th International Symposium on the Chemistry of Natural Products (ISCNP27), Brisbane 10-15th July 2011.

Abstract

This thesis describes the identification of sixty five secondary metabolites from thirteen separate organisms (three terrestrial and ten marine specimens). A total of twenty two new and forty two known secondary metabolites, as well as one new natural product derivative were identified by chemical profiling utilising HPLC-NMR and HPLC-MS together with traditional off-line isolation strategies. Of the new compounds identified, fourteen displayed antibiotic activity. For nine of the compounds identified the 2D NMR characterisation is now reported for the first time in addition to five carbon and one proton NMR chemical shift reassignments. The single X-ray crystallographic structures for three of the compounds identified were also reported. Five previously reported compounds are now reported as natural products for the first time. HPLC-NMR was vital in the identification of an unstable meroditerpenoid that could not be isolated by off-line approaches. This PhD study also resulted in the first report of the acquisition of a gHMBCAD NMR spectrum obtained in the stop-flow HPLC-NMR mode, without pre-concentration, microcoils or cryogenically cooled probes.

Chapters 1-3 provide an introduction to natural products, isolation techniques as applied to natural products, an explanation and examples of dereplication strategies, an outline of the common NMR experiments used for natural product identification and a review of the recent advancements made in HPLC-NMR as well as its application to natural product identification.

Chapter 4 details the limit of detection determined for five key NMR experiments in HPLC-NMR, which were found to be within the 700 ng to 1 mg range, typical of that observed in natural product crude extracts. HPLC-NMR was subsequently successfully applied to a natural product crude extract for which complete 2D NMR data could be obtained for the major component.

Chapter 5 outlines the constituents identified from the flowers and bulbs of the Australian plant, *Macropidia fuliginosa*. The flowers and bulbs produced very different chemistry, and a total of sixteen compounds were identified, including six new and ten previously reported compounds. The single X-ray crystal structure for three compounds is also presented.

Chapter 6 describes the identification of eleven compounds including two new phenylphenalenones and two new chromenes from the bulbs of the Australian plant *Haemodorum spicatum*.

Chapter 7 summarises the identification of three fatty acids from the yellow fungus *Leucocoprinus birnbaumii*. The positions of the double bonds were secured by ozonolysis methods.

Chapter 8 outlines the dereplication of compounds from seven marine algae. Compounds were dereplicated using HPLC-NMR and HPLC-MS data in conjunction with the MarinLit database. Sixteen compounds were dereplicated including four new compounds.

Chapter 9 highlights the identification of four new and nine known meroditerpenoids from the brown alga *Sargassum paradoxum*. HPLC-NMR was vital for the identification of an unstable meroditerpenoid that oxidised during off-line isolation.

Chapter 10 describes the dereplication and identification of phloroglucinols from two *Cystophora* species, including four new and eight known phloroglucinols. HPLC-NMR and HPLC-NMR was able to rapidly establish that both marine algae contained the same structure class of compounds.

Chapter 11 summaries the relative configuration of elatenyne which was proposed on the basis of 1D nOe NMR and chemical derivatisation methods.

List of Abbreviations

$[\alpha]_D$specific optical rotation
$^{\circ}\text{C}$degrees Celsius
1Done dimensional
$^1\text{H NMR}$proton NMR spectroscopy
2Dtwo dimensional
$^{13}\text{C NMR}$carbon NMR spectroscopy
\AAangstrom (unit of length = 10^{-10} m used for bond length)
δchemical shift in parts per million
ϵmolar absorptivity
λ_{max}wavelength of maximum absorbance
μmicro
ν_{max}maximum wavenumber
bsbroad singlet
C_{18}octadecyl stationary phase (chromatography)
CALCcalculated
CHmethine
CH_2methylene
CH_3methyl

CH₃CN.....acetonitrile

CD.....Circular Dichroism

CDCl₃.....deuterated chloroform

CD₃OD.....deuterated methanol

CHCl₃.....chloroform

CIGAR.....Constant time Inverse-Detection Gradient Accordion Rescaled

cm⁻¹.....reciprocal centimeters (FT-IR spectroscopy)

d.....doublet

D₂O.....deuterated water

*d*₆-acetone.....deuterated acetone

*d*₆-DMSO.....deuterated dimethyl sulfoxide

DCM.....dichloromethane

DEPT.....Distortionless Enhanced by Polarisation Transfer

DMSO.....dimethyl sulfoxide

EI.....electron impact

EtOH.....ethanol

EtOAc.....ethyl acetate

ESI.....Electrospray Ionisation

ESI-MS.....Electrospray Ionisation-Mass Spectrometry

FDA.....U.S. Food and Drug Administration

FT-IR.....Fourier Transform-Infrared Spectroscopy

g.....grams

GCMS.....Gas Chromatography-Mass Spectrometry

gCOSY.....gradient Correlation Spectroscopy

gHMBC.....gradient Heteronuclear Multiple Bond Correlation

gHMBCAD.....gradient Heteronuclear Multiple Bond Correlation with ADiabatic pulses

gHSQCAD.....gradient Heteronuclear Single Bond Coherence with ADiabatic pulses

H₂O.....water

HCl.....hydrochloric acid

HDO.....residual water in D₂O

HPLC.....High Pressure Liquid Chromatography

HPLC-MS.....High Pressure Liquid Chromatography-Mass Spectrometry

HPLC-NMR.....High Pressure Liquid Chromatography-Nuclear Magnetic
Resonance Spectroscopy

HPLC-NMR-MS.....High Pressure Liquid Chromatography-Nuclear Magnetic
Resonance Spectroscopy-Mass Spectrometry

HRESILCMS High Resolution-Electrospray Ionisation-Liquid Chromatography-
Mass Spectrometry

HRESIMS.....High Resolution-Electrospray Ionisation-Mass Spectrometry

HSQCAD.....Heteronuclear Single Bond Coherence with Adiabatic pulses
 Hz.....hertz
 ID.....internal diameter
 IR.....Infrared
J.....coupling constant (Hz)
 LC.....Liquid Chromatography
 LOD.....limit of detection
 LRESIMS.....Low Resolution-Electrospray Ionisation-Mass Spectrometry
 LR/MS/MS.....Low Resolution Tandem Mass Spectrometry
m/z.....mass-to-charge-ratio (mass spectrometry)
 MATNAP.....Marine and Terrestrial Natural Products research group
 mg.....milligram
 MHz.....megahertz
 min.....minute
 mL.....millilitre
 mm.....millimetre
 MeOH.....methanol
 MS.....Mass Spectrometry
 NaCl.....sodium chloride

NCI.....National Cancer Institute (US)

ng.....nanogram

nm.....nanometre

NMR.....Nuclear Magnetic Resonance spectroscopy

NOE.....Nuclear Overhauser Enhancement

NOESY.....two dimensional Nuclear Overhauser Enhancement Spectroscopy

ORTEP.....Oak Ridge Thermal-Ellipsoid Plot Program

PDA.....Photo Diode Array detector

ppm.....parts per million

PTFE.....Poly Tetra Fluoro Ethylene (Teflon)

q.....quartet

ROESY.....Rotating Frame Overhauser Enhancement Spectroscopy

ROV.....Remotely Operated Vehicle

RP.....Reversed Phase

s.....singlet

S/N.....signal-to-noise

SCUBA.....Self-Contained Underwater Breathing Apparatus

sp.....species

t.....triplet

TLC.....Thin Layer Chromatography

TOCSY.....Total Correlation Spectroscopy

TOF.....Time of Flight (mass spectrometry)

UV.....Ultraviolet Spectroscopy

VLC.....Vacuum Liquid Chromatography

WET1D.....one dimensional Water Enhanced through Transverse gradients

Table of Contents

Declaration.....	ii
Acknowledgments.....	viii
Publications Resulting from PhD Thesis	x
Conference Proceedings.....	xiii
Abstract.....	xv
List of Abbreviations	xviii
Table of Contents.....	xxiv

Part A: Introduction.....1

Chapter 1: Overview and background on Natural Products, Chemical Profiling/Dereplication and Strategies Adopted.....2

Natural Products.....2

Terrestrial organisms.....3

Plants and Fungi.....5

Marine Invertebrates.....7

Marine Algae.....9

Conventional or Traditional Isolation and Identification of Natural Products.....11

Dereplication and Chemical Profiling.....12

Databases.....13

HPLC-MS.....	14
HPLC-NMR.....	15
Strategies Adopted.....	17
References.....	18
Chapter 2: NMR Spectroscopy for the Identification of Natural Products.....	25
Introduction.....	27
1-D NMR Experiments.....	30
<i>1-D NOE and 1-D TOCSY Experiments.....</i>	<i>30</i>
<i>DEPT and APT.....</i>	<i>32</i>
2-D NMR Experiments.....	33
<i>Homonuclear Approaches.....</i>	<i>33</i>
<i>Heteronuclear Approaches.....</i>	<i>34</i>
Hyphenation: HPLC-NMR.....	41
<i>Application to Organism Profiling and Structure Elucidation.....</i>	<i>42</i>
Summary.....	44
References.....	46
Chapter 3: HPLC-NMR for Chemical Profiling.....	48
Introduction.....	49
Microcoil HPLC-NMR and Capillary NMR (CapNMR).....	50

Cryogenically Cooled Probes.....	52
HPLC-SPE-NMR and Column Trapping.....	52
HPLC-NMR-MS.....	53
Natural Product Applications.....	54
On-Flow and Stop-Flow HPLC-NMR Analyses.....	55
Microcoil HPLC-NMR Analyses.....	57
CapNMR Analyses.....	58
HPLC-SPE-NMR Analyses.....	59
Column Trapping HPLC-NMR Analyses.....	59
HPLC-NMR-MS Analyses.....	59
Conclusion.....	60
References.....	60
Chapter 4: Limit of Detection in HPLC-NMR.....	63
Introduction.....	64
Materials and Methods.....	65
<i>Instrumentation.....</i>	<i>65</i>
<i>Reference Compounds and Solvents.....</i>	<i>65</i>
<i>Preparation of Reference Compound Solutions for HPLC-NMR LOD Studies.....</i>	<i>65</i>

<i>NMR Pulse Sequences</i>	65
<i>Marine Brown Alga Specimen</i>	65
<i>Marine Alga Extraction</i>	66
<i>HPLC-NMR Conditions for Marine Alga Analysis</i>	66
<i>HPLC-MS Conditions for Marine Alga Analysis</i>	66
Results and Discussion.....	66
<i>Limit of Detection (LOD) and Dynamic Linearity</i>	66
On-flow WET1D NMR Analysis.....	66
Stop-flow analysis – Wet1D.....	66
Stop-flow analysis – gCOSY.....	66
Stop-flow analysis – HSQCAD.....	67
Stop-flow analysis – gHMBCAD.....	67
Summary of Results.....	67
<i>LOD Case Study: Stop-flow HPLC-NMR Analysis of a Natural Product Crude Extract and Secondary Metabolite Identification</i>	69
Conclusions.....	70
Acknowledgments.....	70
References.....	70

<u>Part B: Terrestrial Organisms</u>	71
Chapter 5: Constituents from the Australian Plant <i>Macropidia fuliginosa</i>	73
Introduction.....	74
Results and Discussion.....	74
<i>On-line Phytochemical Profiling (HPLC-NMR and HPLC-MS)</i>	74
<i>Off-line Phytochemical Isolation</i>	75
<i>Biological Activity Studies</i>	78
Experimental.....	79
<i>General Experimental Procedures</i>	79
<i>Single Crystal X-ray Diffraction</i>	79
<i>Biological Evaluation</i>	79
<i>Plant Material</i>	80
<i>Phytochemical Profiling</i>	80
<i>Extraction and Isolation of Flowers</i>	80
<i>Extraction and Isolation of Bulbs</i>	80
<i>On-line (HPLC-NMR and HPLC-MS) Characterization of Compounds</i>	80
<i>Off-line Characterization of Compounds</i>	81
Acknowledgments.....	82
References.....	82

Chapter 6: Chemical Profiling and Isolation of Secondary Metabolites from <i>Haemodorum spicatum</i>	83
Introduction.....	84
Results and Discussion.....	84
Experimental Section.....	89
<i>General Experimental Procedures</i>	89
<i>Biological Evaluation</i>	90
<i>Plant Material</i>	90
<i>Chemical Profiling</i>	90
<i>Extraction and Isolation</i>	90
<i>On-line (HPLC-NMR and HPLC-MS) Characterization of Compounds</i>	90
<i>Off-line Characterization of Compounds</i>	91
Acknowledgments.....	91
References.....	92
Chapter 7: Secondary Metabolites of the Fungus <i>Leucocoprinus birnbaumii</i>	93
Introduction.....	94
Initial Analysis.....	94
Phytochemical Profiling.....	94
Off-line Isolation of Fatty Acids.....	95

Experimental.....	96
<i>General Experimental Procedures</i>	96
<i>Biological Evaluation</i>	96
<i>Terrestrial Fungus Material</i>	96
<i>Chemical Profiling</i>	96
<i>Extraction and Isolation</i>	97
<i>Ozonolysis</i>	97
<i>On-line (HPLC-NMR & HPLC-MS) Characterization of Compounds</i>	97
Acknowledgments.....	97
References.....	97
<u>Part C: Marine Organisms</u>	98
Chapter 8: Dereplication and Chemotaxonomical Profiling of Seven Marine Algae by HPLC-NMR & HPLC-MS	100
Introduction.....	101
Results and Discussion.....	102
<i>Chemical Profiling (HPLC-NMR & HPLC-MS)</i>	102
<i>Identification of Phenols, Phenolic Acids and Resorcinols</i>	106
<i>Identification of Xanthophylls</i>	107
<i>Identification of Halogenated C₁₅ Acetogenins</i>	108

<i>Identification of Phloroglucinols and Tocotrienols</i>	110
<i>Anti-microbial Activity</i>	112
Experimental Section.....	112
<i>Marine Alga Material</i>	112
<i>Extraction</i>	112
<i>Biological Evaluation</i>	114
<i>Chemical Profiling</i>	114
<i>HPLC-NMR & HPLC-MS Conditions</i>	114
<i>On-line (HPLC-NMR & HPLC-MS) Characterization of Compounds</i>	115
Conclusions.....	115
Acknowledgments.....	116
References.....	116
Chapter 9: Chemical Profiling and Isolation Studies of the Marine Brown Alga	
<i>Sargassum paradoxum</i>	119
Introduction.....	121
Results and Discussion.....	121
<i>Chemical Profiling (HPLC-NMR & HPLC-MS)</i>	123
<i>Off-line Bioassay-Guided isolation</i>	129
<i>Antimicrobial Studies</i>	134

Experimental Section.....	134
<i>General Experimental Procedures</i>	134
<i>Biological Evaluation</i>	136
<i>Marine Alga Material</i>	136
<i>Chemical Profiling</i>	136
<i>Extraction and Isolation</i>	138
<i>On-line (HPLC-NMR & HPLC-MS) Characterisation of Compounds</i>	138
<i>Off-line Characterisation of Compounds</i>	140
Conclusions.....	141
Acknowledgments.....	142
References.....	143
Chapter 10: Dereplication and Structural Identification Studies of Marine Algae of the Genus <i>Cystophora</i>	146
Introduction.....	147
Results and Discussion.....	147
<i>Chemical Profiling (HPLC-NMR & HPLC-MS)</i>	148
<i>Off-line Isolation of <i>C. monilifera</i> and <i>C. subfarcinata</i> Dichloromethane Crude Extract Secondary Metabolites</i>	149
<i>Biological Activity Studies</i>	151

Conclusions.....	152
Experimental.....	152
<i>General Experimental Procedures</i>	152
<i>Biological Evaluation</i>	152
<i>Alga Material</i>	152
<i>Chemical Profiling</i>	153
<i>Extraction and Isolation of C. monilifera</i>	153
<i>Extraction and Isolation of C. subfarcinata</i>	153
<i>On-line (HPLC-NMR & HPLC-MS) Characterization of Compounds</i>	153
<i>Off-line Characterization of Compounds</i>	154
Acknowledgments.....	154
References.....	155
Chapter 11: Relative Configuration Studies of the Marine Natural Product	
Elatenyne	156
Introduction.....	157
Results and Discussion.....	157
Concluding Remarks.....	159
Experimental.....	159
<i>General</i>	159

<i>Isolation and Purification of Elatenyne from L. elata</i>	159
<i>Derivatization of Elatenyne</i>	159
<i>HPLC Purification of the 1,2,3 triazole</i>	160
Acknowledgments.....	160
References.....	160
<u>Part D: Discussion and Conclusions</u>	161
Summary of Compounds Identified.....	167
References.....	182
<u>Appendix A</u>	183
<u>Appendix B</u>	207
<u>Appendix C</u>	292
<u>Appendix D</u>	328
<u>Appendix E</u>	404
<u>Appendix F</u>	471

PART A - Introduction

The chapters that encompass this section of the thesis (Chapters 1-4) include an overview of natural products, an outline and description of chemical profiling and dereplication, and the approaches adopted in this PhD thesis. Also included is the application of NMR to structurally identify natural products, recent advancements in HPLC-NMR and the limit of detection for a specific HPLC-NMR system.

This section of the thesis comprises two journal publications and one book section of a book chapter as listed below:

1. Brkljača, Robert, & Urban, Sylvia. (2014). Selected Applications of NMR Spectroscopy - Natural Products. In J. Fisher (Ed.), *Modern NMR Techniques for Synthetic Chemistry*. Florida, USA: CRC Press.
2. Brkljača, Robert, & Urban, Sylvia. (2011). Recent Advancements in HPLC-NMR and Applications for Natural Product Profiling and Identification. *Journal of Liquid Chromatography & Related Technologies*, 34(12), 1063-1076.
3. Brkljača, Robert, & Urban, Sylvia. (2015). Limit of Detection Studies for Application to Natural Product Identification using High Performance Liquid Chromatography Coupled to Nuclear Magnetic Resonance Spectroscopy. *Journal of Chromatography A*, 1375, 69-75.

CHAPTER 1

Overview and background on Natural Products, Chemical

Profiling/Dereplication and Strategies Adopted

Natural Products

Natural products, also known as secondary metabolites, are compounds produced by terrestrial and marine organisms. While it is not known exactly why these compounds are produced, it is thought that they may provide the organism with a possible chemical defence mechanism (Bennett & Wallsgrove, 1994; Pawlik, Chanas, Toonen, & Fenical, 1995) or to enhance the organisms overall fitness (reproduction, chemical communication, cell function) (Hay, 2009; Puglisi, Sneed, Sharp, Ritson-Williams, & Paul, 2014). Since historic times natural products have proved to be an important resource for the identification of potential new pharmaceuticals. Both terrestrial and marine sources have yielded a variety of compounds, displaying unique carbon skeletons and important therapeutic properties. Newman and Cragg reported that over the past 30 years (1981-2010), approximately 50% of the new drug entities have been discovered or are derived from a natural product origin (Newman & Cragg, 2012). Nature has the ability to create complex structural motifs which can also incorporate stereochemistry, which is difficult to recreate using synthetic and combinatorial chemistry. Natural products may also be used as drug leads, whereby an inactive or slightly active natural product is chemically modified to increase the potency or biological availability. Anti-cancer natural products represent the greatest number of new drug entities, however anti-bacterial and anti-viral natural products closely follow this

number (Newman & Cragg, 2012). In the area of anti-biotics, there is a pressing need for the discovery of new drugs. With the existence of drug resistant strains of bacteria, the discovery of new anti-biotics has never been more important. For instance the occurrence of resistant strains such as *Pseudomonas aeruginosa* and other multidrug resistant pathogens is well documented (Giamarellou & Poulakou, 2009; Igbinsosa et al., 2012), and there is a need to discover new drugs to target these strains. In addition, the emergence of new diseases also necessitates the need for new drugs. Natural product sources, particularly marine invertebrates, provide an ideal avenue for potential new drug discovery.

Terrestrial Organisms

Terrestrial organisms such as plants and fungi have been studied extensively and have a large precedence historically in drug discovery. Plants and fungi are generally easily accessible and larger amounts can usually be collected, making them ideal for natural product discovery. One of the earliest success stories of a terrestrial based natural product is penicillin G (**1**) (**Figure 1**) which was isolated and identified from the *Penicillium* bacterium in 1928 ("American Chemical Society International Historic Chemical Landmarks. Discovery and Development of Penicillin,"). Taxol (**2**), an approved anti-cancer drug, from the bark of *Taxus brevifolia*, was isolated in its pure form in 1967, but difficulty in determining its identity meant that the complete structure was not reported until 1971 (Wani, Taylor, Wall, Coggon, & McPhail, 1971). Silybin (**3**), is an example of a plant derived natural product currently undergoing clinical trials as an anti-cancer agent (Butler, 2008; Provinciali et al., 2007).

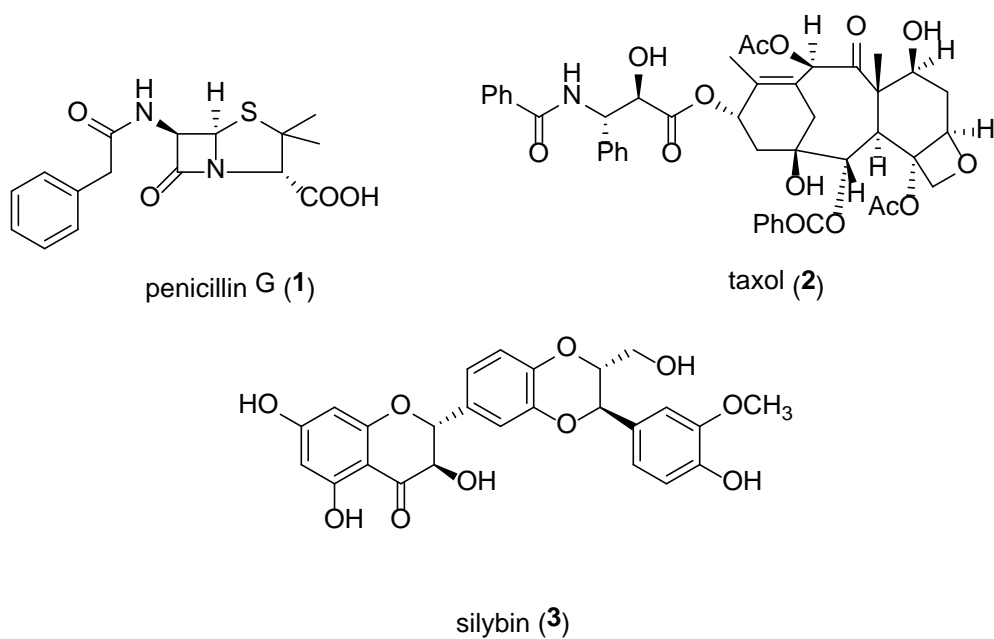


Figure 1: Chemical structures of penicillin (1), taxol (2) and silybin (3).

Ethnopharmacology is the study of plants traditionally used by native people to treat certain illnesses, such as the treatments used by the Australian Aborigines and in traditional Chinese medicines. The herb, *Artemisia annua* had been used for centuries as a traditional Chinese medicine to treat malaria, and during the investigation of this herb in 1971, the active component responsible for the anti-malarial activity was identified as artemisinin (4) (Klayman, 1985) (**Figure 2**).

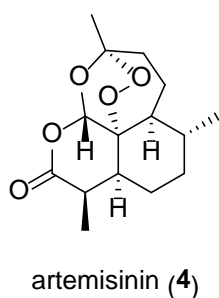
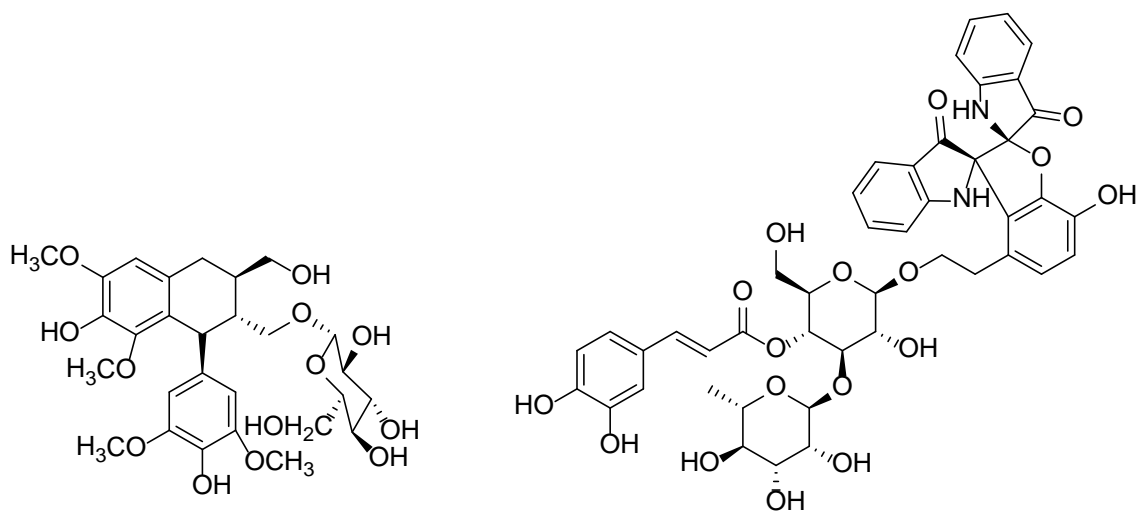


Figure 2: Chemical structure of artemisinin (4).

Terrestrial organisms generally produce different chemistry than their marine counterparts (Pietra, 2002), however there have been cases where natural products isolated from plants have also been isolated from marine sources, as in the case of δ -tocotrienol, which has been isolated from the plant *Cinnamosma fragrans* (Harinantenaina & Takaoka, 2006), and the alga *Cystophora siliquosa* (Laird et al., 2010). It is estimated that 5-15% of higher plants have been evaluated for the chemistry they produce (Cragg & Newman, 2005).

Plants and Fungi

Plants are composed of different components, such as the bulbs (or roots), stems, leaves, flowers and, at times, fruit. When undertaking an investigation of a plant, it is important to evaluate all parts of the plant individually, as each component/part may contain different chemistry, and therefore, different biological activity. For instance the roots of *Strobilanthes cusia* have been found to produce (+)-9-*O*- β -D-glucopyranosyl lariciresinol (Tanaka et al., 2004) whilst the leaves produce strobilanthoside A (**6**) (Gu et al., 2014) (**Figure 3**).



(+)-9- O - β -D-glucopyranosyl lariciresinol (**5**)

strobilantheside A (**6**)

Figure 3: Chemical structures of (+)-9- O - β -D-glucopyranosyl lariciresinol (**5**) and strobilantheside A (**6**).

Fungi can be classified into the micro- and the macro-fungi. The micro-fungi are most easily described as mould-type fungi, whereas the macro-fungi are described as mushrooms, or fungi that produce easily visible bodies. Chaetoviridin E (**7**) was identified from the micro-fungus *Chaetomium* sp. and displays anti-microbial activity (Kingsland & Barrow, 2009), while the triterpene lactone, ganodermalactone F (**8**) was identified from the macro-fungus *Ganoderma* sp., displaying anti-malarial activity (Lakornwong et al., 2014) (**Figure 4**).

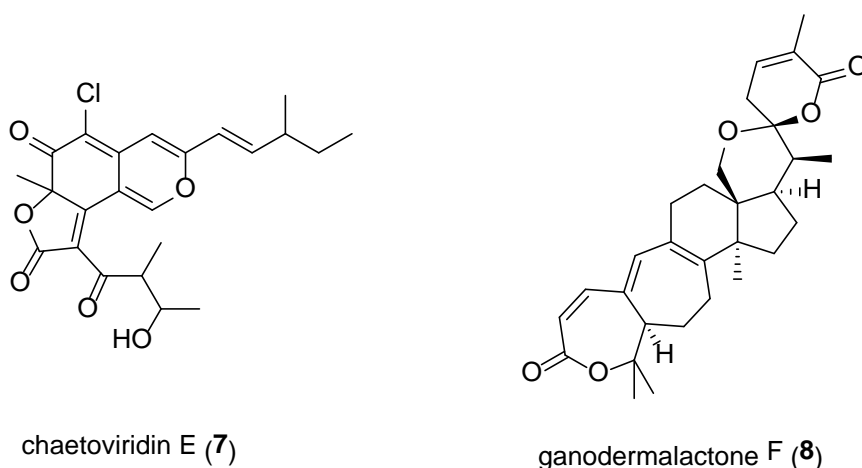
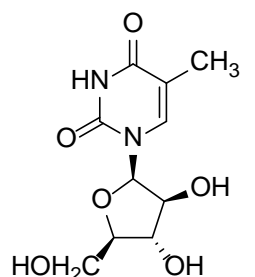


Figure 4: Chemical structures of chaetoviridin E (7) and ganodermalactone F (8).

Marine Invertebrates

Marine invertebrates have been studied less extensively than terrestrial organisms. This has been mainly attributed to the difficulty in obtaining the specimens and because marine organisms are generally less stable and more difficult to preserve than terrestrial species (Jha & Zi-rong, 2004). It was not until the advent of SCUBA (1970s) and then later the introduction of remotely operated vehicles (ROVs) that access to marine specimens became easier and more popular (Cragg & Newman, 2013). The marine environment is particularly suited to natural product discovery as 70% of the earth is covered by oceans, and the biodiversity observed in the marine environment greatly exceeds that seen on land (Jaume & Duarte, 2006). In recent years, extreme environments such as deep sea mounts and geothermal vents have provided a wealth of new chemistry which can be attributed to the unique biodiversity and the number of species in these locations (Skropeta & Wei, 2014). Like terrestrial species, many marine invertebrates are sessile, but any natural product produced by marine invertebrates as a chemical defence must be exponentially more potent, as it undergoes dilution into the surrounding seawater (Haefner, 2003). The first study of a marine invertebrate to yield biologically active compounds was in 1951, which reported the

isolation of a nucleoside, spongothymidine (**9**), from the sponge *Cryptotethia crypta* (Bergman & Feeney, 1951) (**Figure 5**).



spongothymidine (**9**)

Figure 5: Chemical structure of the nucleoside identified from *Cryptotethia crypta*.

Far fewer marine natural products have been approved as drugs. Research in this area has only been undertaken for the past 50 years, compared to natural products derived from terrestrial organisms which have been used for centuries across many civilisations and then studied extensively over the last century. The guidelines for drug approval (eg. FDA) have also changed significantly over the years, and in general have become more strict in approving a potential drug. This may have also affected the number of approved drugs in the recent decade/years. One of the first approved drugs from a marine organism was ziconotide (**10**) (**Figure 6**), a 25-amino acid peptide derived from the cone snail *Conus magus* (Mayer et al., 2010). Clinical studies continue to be carried out on marine natural products such as tetrodotoxin (**11**) (**Figure 6**) which is currently in phase 3 clinical trials to treat chronic pain ("About TTX," ; "Marine pharmaceuticals: the clinical pipeline,"). A review published in 2014 outlines other natural products in clinical trials (Butler, Robertson, & Cooper, 2014), which includes six compounds isolated or derived from marine invertebrates undergoing oncology trials, including plitidepsin (**12**) and bryostatin 1 (**13**).

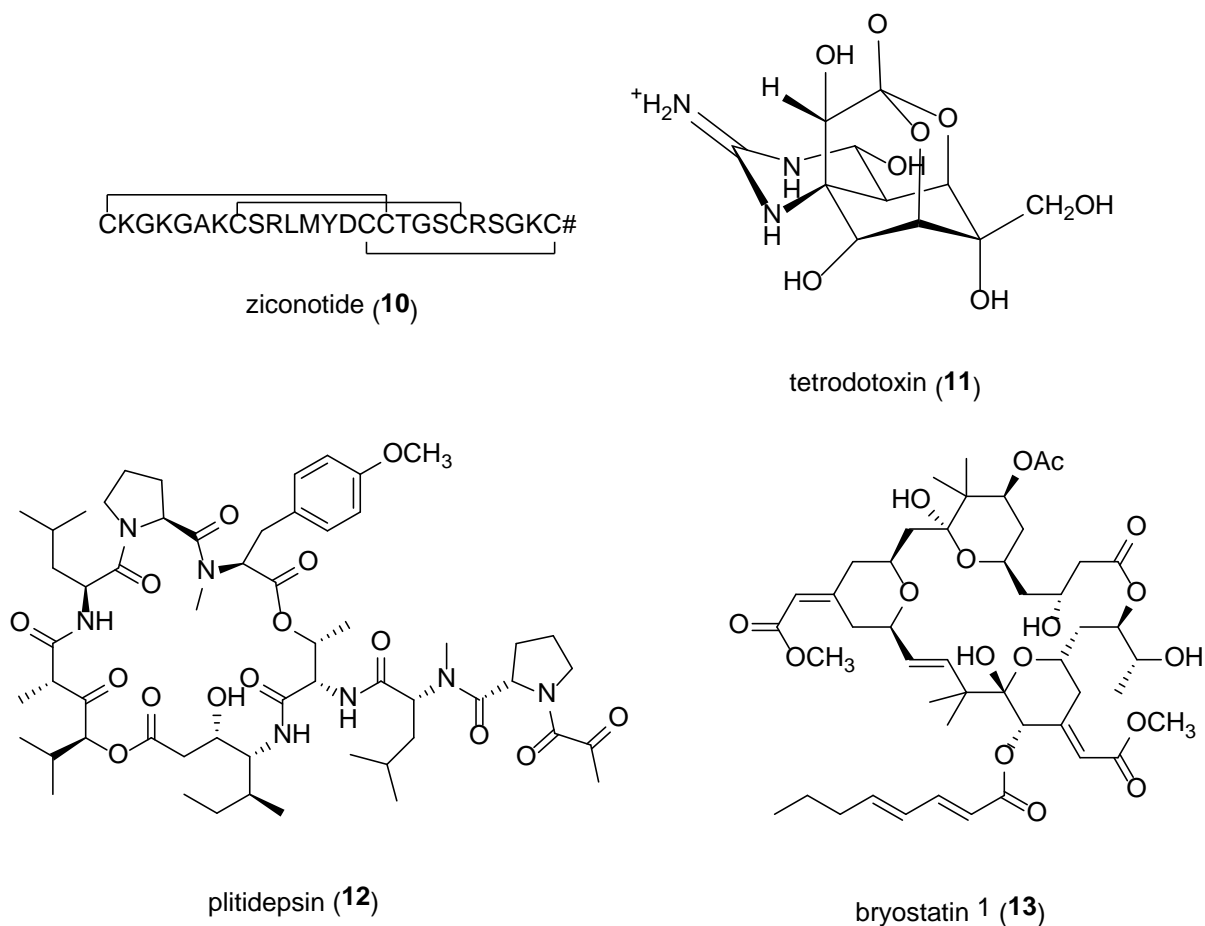


Figure 6: Chemical structures of ziconotide (10), tetrodotoxin (11), plitidepsin (12) and bryostatin 1 (13).

Marine Algae

Marine algae are comprised of four primary phyla; the red (Rhodophyta), green (Chlorophyta), brown (Phaeophyta) and the blue-green algae (Cyanobacteria) (Kornprobst, 2014). Each of these phyla displays unique features. Blue-green algae produce an abundant number of secondary metabolites containing nitrogen (approximately 80%) compared to the brown algae which display less than 5% of nitrogen containing secondary metabolites (Kornprobst, 2014). Terpenes constitute the largest chemical class present in marine

algae(Kornprobst, 2014), however the chemical classes present between different phyla of algae can vary significantly. Approximately 50% of the compounds reported from green algae are terpenes (Kornprobst, 2014), however the red algae produce a large number of halogen containing secondary metabolites (Choi, Pereira, & Gerwick, 2012). While each phylum of marine algae can display different chemistry, algae of the same phyla but from different genera, can also display different chemistry. *Sargassum* and *Caulocystis* represent two different genera belonging to the Phaeophyta (brown algae) phylum. The *Sargassum* genus is known to produce meroditerpenoid and phloroglucinol related compounds, while the *Caulocystis* genus produces acetogenin and resorcinol related compounds (MarinLit, 2015).

A recent review evaluated the number of new natural products reported from marine organisms. In 2013, a total of 40 (3.4%) of the new compounds were discovered from marine algae (Blunt, Copp, Keyzers, Munro, & Prinsep, 2015). **Figure 7** illustrates the number of new compounds per phyla, and clearly shows that the Chlorophyta have yielded the fewest number of new compounds. Interestingly the number of new compounds reported from Cyanobacteria and Rhodophyta had noticeably dropped compared to the previous year (Blunt, Copp, Keyzers, Munro, & Prinsep, 2014). Of the numerous bioactive compounds reported from marine algae, the cryptophycins represent a chemical class that displays potent anti-cancer activity (Smith, Zhang, Mooberry, Patterson, & Moore, 1994; Verma et al., 2015). Cryptophycin (**14**) (**Figure 8**) is an example of one of the members of the cryptophycin family, which is derived from the cyanobacteria *Nostoc* sp.(Smith et al., 1994; Verma et al., 2015).

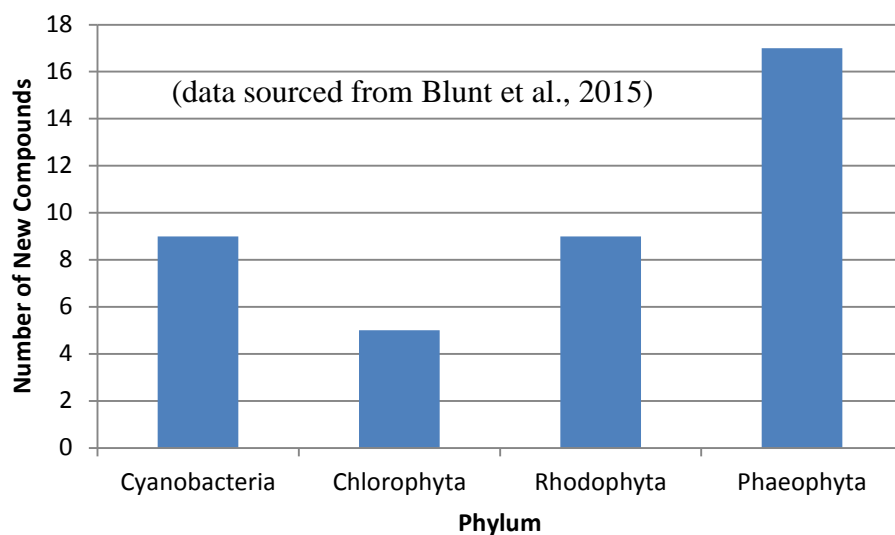
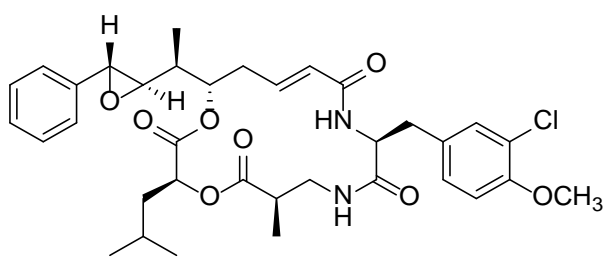


Figure 7: Number of new natural products identified in 2013 from the four main phyla of marine algae.



cryptophycin (**14**)

Figure 8: Chemical structure of cryptophycin (**14**).

Conventional or Traditional Isolation and Identification of Natural Products

Traditionally, the isolation and identification of natural products is carried out using fractionation steps involving various separation/purification methodologies followed by

characterisation using conventional solution state Nuclear Magnetic Resonance (NMR) spectroscopy in conjunction with mass spectrometric analyses. Bench column chromatography such as silica, C₁₈ and Sephadex LH-20 are commonly employed to fractionate crude extracts which are then typically further purified by reversed phase High Pressure Liquid Chromatography (RP-HPLC). This fractionation/isolation process can be quite a time consuming approach and can leave compounds susceptible to possible degradation or conversion to artifacts (Ghisalberti, 2007). It is also highly probable that following lengthy isolation procedures known compounds may be isolated. Once a pure compound is isolated it is identified using a range of 1D and 2D NMR spectroscopic experiments. An overview of these experiments and the approach taken to identify a range of natural products is outlined in **Chapter 2**. Isolated natural products (or secondary metabolites), often require further studies to deduce the complete structure and to characterise the compound. For instance to determine the absolute configuration, approaches including chemical degradation/derivatisation, circular dichroism (CD) or single crystal X-ray diffraction are available. For new compounds, mass spectrometry (MS), infra-red spectrometry (IR), ultra-violet spectrometry (UV) and specific rotation (in the case of chiral compounds) measurements need to be routinely carried out to undertake a complete characterisation.

Dereplication and Chemical Profiling

Chemical profiling or dereplication allows for the rapid identification of natural products without the need for lengthy off-line isolations and to attempt to minimise the risk of possible degradation. The aim is to identify the presence of known natural products as well as possible new compounds as rapidly as possible.

Dereplication generally refers to the identification of secondary metabolites in bioactive natural product extracts utilising a range of methodologies (Lang et al., 2008). Approaches in this area have involved the generation of fractions using various solid-phase chromatographic supports (eg. C₁₈, Sephadex LH-20 and ion-exchange) to ascertain the relative polarity, size and possible charge of the bioactive fractions. More recently a HPLC bioactivity profiling/microtitre plate technique was reported in conjunction with capillary NMR (CapNMR) (Lang et al., 2008). Finally, hyphenated spectrometric or spectroscopic techniques such as HPLC-MS or HPLC-NMR can also be used to assist in dereplication. The use of these techniques is often not sufficient for actual compound identification, but can greatly assist with structure class confirmation. Once information such as mass, UV chromophore, taxonomy or the presence of any unique NMR signals can be concluded, the use of chemical databases (eg. MarinLit, Dictionary of Natural Products or Scifinder) to assist the dereplication is mandatory.

Databases

Each chemical database has a separate set of parameters that can be searched, but generally, most contain the ability to search by taxonomy, UV and MS data. The ‘MarinLit’ and ‘Dictionary of Natural Products’ databases were the two databases used throughout these studies. Unique to the MarinLit database is the ability to search by NMR spectroscopic data. Dereplication of the components described in this thesis was generally achieved by searching a combination of the taxonomy, UV, proton/carbon NMR and MS data. In cases where multiple probable structures were identified, the NMR data obtained from HPLC-NMR was further reviewed to establish which of the structures was most likely. In cases where no match or a possible new compound was suggested, dereplication was carried out using a broader search regime. This generally involved using the taxonomy and UV data, to

assist in determining the nature of the structure class. Further evaluation of the MS and NMR data would then allow for a *tentative* structure to be proposed.

HPLC-MS

As indicated earlier, chemical profiling can involve the use of hyphenated spectrometric or spectroscopic methodologies. High Pressure Liquid Chromatography coupled to Mass Spectrometry (HPLC-MS) is a widely utilised profiling technique in the area of natural products. In this approach components within a crude extract can be easily separated, which allows for the acquisition of UV spectra (through PDA detection) and for potential molecular ions to be identified. Ideally an instrument capable of accurate mass (4 or 5 decimal places) is employed, which allows for the determination of molecular formulae, however low resolution instrumentation can also provide sufficient information to aid in possible compound identification. HPLC-MS is a sensitive technique making it suited to the area of natural product identification. However, molecular ions and molecular formulae alone are not always sufficient to unequivocally or *tentatively* identify components and additional data is needed, such as NMR spectroscopic data, especially in the case of structurally related isomers. In addition, a drawback of HPLC-MS is that it relies on the ability of compounds to ionise, whereby if a compound does not ionise, no molecular ion will be detected. HPLC-MS utilises soft ionisation techniques such as electrospray ionisation (ESI) and atmospheric pressure chemical ionisation (APCI). These soft ionisation techniques are perfectly suited for natural product analysis as it results in the observation of primarily the molecular ion and very few fragments, and, in this way it can easily allow for the determination of molecular formulae. Tandem mass spectrometry systems (MS/MS) allow for further fragmentation of the molecular ion and subsequent ions, yielding further information about the compound's structure.

HPLC-NMR

High Pressure Liquid Chromatography coupled to Nuclear Magnetic Resonance (HPLC-NMR) allows for the acquisition of important 1D and 2D NMR spectroscopic data that is vital for complete structure identification. HPLC-NMR still remains an underutilised technique, but it has seen the greatest application in the area of natural product identification. One of the limitations of HPLC-NMR when compared to HPLC-MS is the sensitivity. Recent advancements in probe design and suppression techniques have allowed the application of HPLC-NMR to become more widespread. A review outlining these advances and examples of the applications is provided in **Chapter 3**. Since the time of publication of this review in 2011, no further advancements have been made in the HPLC-NMR hardware. However, a number of publications reporting on the application of HPLC-NMR have appeared. For instance, the application of ultrafast 2D NMR was recently demonstrated for HPLC-NMR, whereby 2D NMR spectra, in this case COSY NMR spectra, were recorded in two scans (Queiroz Junior, Queiroz, Dhooghe, Ferreira, & Giraudeau, 2012). Between 2011-2014, HPLC-NMR has been most commonly used to profile natural product crude extracts but it has also been used for degradation and conformation studies. These have included the monitoring of titrations (Hentschel, Holtin, Steinhauser, & Albert, 2012), conformation studies (Haroune, Crowson, & Campbell, 2011), identification of degradation products (Narayanam, Sahu, & Singh, 2013; Shah, Sahu, & Singh, 2011), and for a variety of chemical profiling studies of marine and terrestrial organisms (De la Cruz et al., 2012; Kang et al., 2014; Schmidt, Nyberg, & Staerk, 2014; M. A. Timmers, Dias, & Urban, 2012; M. Timmers & Urban, 2013).

The limit of detection (LOD) of HPLC-NMR is well within the limits to easily identify multiple components within a natural product crude extract. In **Chapter 4** the LOD

for a 500 MHz HPLC-NMR system equipped with a 60 μ L conventional flowprobe is outlined for the HPLC-NMR system in the School of Applied Sciences at RMIT University in Melbourne, Australia. The LOD for five key 1D and 2D NMR spectroscopic experiments was established, using two reference compounds, including the on-flow (WET1D proton), stop-flow (WET1D proton), gCOSY, HSQCAD and gHMBCAD NMR experiments. Once established, application to a multiple component natural product crude extract was implemented to rapidly identify the components present. There has been a steady increase of the application of HPLC-NMR for the identification of compounds present in multiple component mixtures since 2011. Between the years 2011-2014, a total of 52 HPLC-NMR publications appeared (**Figure 9**). This represents the greatest number of HPLC-NMR publications within a four year period since the technique was first reported in 1987 (Laude Jr. & Wilkins, 1987).

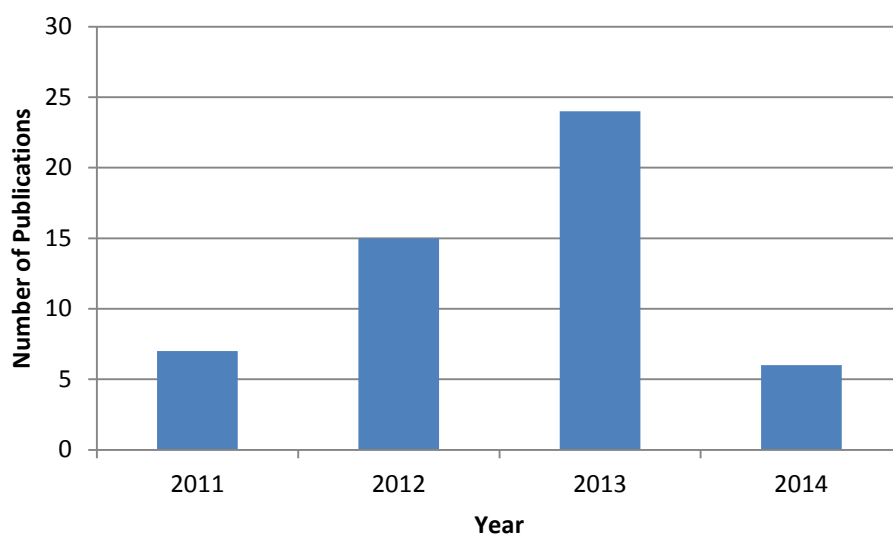


Figure 9: Number of publications featuring HPLC-NMR between the years 2011-2014.

HPLC-NMR and HPLC-MS (and HPLC-NMR-MS) can also be used in combination to rapidly dereplicate the structures of known natural products. Together, these two

techniques also have the ability to propose the identity of new natural products. While there are cases where a natural product can be completely identified on the basis of HPLC-NMR and HPLC-MS, in many instances this is not the case, and traditional off-line isolations become necessary. Off-line isolations are also necessary in order to deduce and evaluate the bioactive components present in a crude extract.

Strategies adopted

The aim of this thesis was to identify new natural products potentially displaying anti-microbial activity, which was accomplished by two separate approaches. Firstly a phytochemical profiling study of each organism utilising HPLC-NMR and HPLC-MS was conducted. This approach allowed for the identification of the structure classes present in each organism, along with the identity of the major, and some minor constituents. This step also enabled the identification of compounds that should be prioritised for further isolation on the basis that they may represent new structural derivatives.

The second approach involved the more traditional or conventional off-line isolation of the crude extract and in some cases, a bioassay-guided isolation approach. In this approach, crude extracts of the specimen were evaluated for anti-microbial activity. The crude extract was then fractionated using various solid-phase chromatographic supports (silica, C₁₈, Sephadex LH-20) and then, in general, approximately every third fraction was evaluated for anti-microbial activity. Fractions of interest were subsequently purified further by RP-HPLC, which resulted in pure compounds being obtained. This allowed for the confirmation of the structures as proposed by phytochemical profiling as well as unequivocally deducing the structures of new compounds. Importantly this approach enabled evaluation of the anti-microbial activity for the isolated compounds.

Reported in this thesis is the phytochemical profiling and off-line isolation studies of thirteen marine and terrestrial organisms.

References

- About TTX.). Retrieved 16 January 2015, from <http://www.wextech.ca/products.asp?m=1>
- American Chemical Society International Historic Chemical Landmarks. Discovery and Development of Penicillin.). Retrieved 16 January 2015, from <http://www.acs.org/content/acs/en/education/whatischemistry/landmarks/flemingpenicillin.html>
- Bennett, Richard N., & Wallsgrove, Roger M. (1994). Secondary metabolites in plant defence mechanisms. *New Phytologist*, 127(4), 617-633.
- Bergman, Werner, & Feeney, Robert J. (1951). Marine products. XXXII. The nucleosides of sponges. I. *Journal of Organic Chemistry*, 16, 981-987.
- Blunt, John W., Copp, Brent R., Keyzers, Robert A., Munro, Murray H. G., & Prinsep, Michele R. (2014). Marine natural products. *Nat. Prod. Rep.*, 31(2), 160-258.
- Blunt, John W., Copp, Brent R., Keyzers, Robert A., Munro, Murray H. G., & Prinsep, Michele R. (2015). Marine natural products. *Natural Product Reports*, 32(2), 116-211.
- Butler, Mark S. (2008). Natural products to drugs: natural product-derived compounds in clinical trials. *Natural Product Reports*, 25(3), 475-516.
- Butler, Mark S., Robertson, Avril A. B., & Cooper, Matthew A. (2014). Natural product and natural product derived drugs in clinical trials. *Natural Product Reports*, 31(11), 1612-1661.

- Choi, Hyukjae, Pereira, Alban R., & Gerwick, William H. (2012). The Chemistry of Marine Algae and Cyanobacteria. In E. Fattorusso, W. H. Gerwick & O. Tagliatalata-Scafati (Eds.), *Handbook of Marine Natural Products*. London, England: Springer.
- Cragg, Gordon M., & Newman, David J. (2005). Biodiversity: A continuing source of novel drug leads. *Pure Applied Chemistry*, 77(1), 7-24.
- Cragg, Gordon M., & Newman, David J. (2013). Natural products: A continuing source of novel drug leads. *Biochemica et Biophysica Acta, General Subjects*, 1830(6), 3670-3695.
- De la Cruz, Alexander Acevedo, Hilbert, Ghislaine, Riviere, Celine, Mengin, Virginie, Ollat, Nathalie, Bordenave, Louis, . . . Richard, Tristan. (2012). Anthocyanin identification and composition of wild *Vitis* spp. accessions by using LC-ms and LC-NMR. *Analytica Chimica Acta*, 732, 145-152.
- Ghisalberti, Emilio L. (2007). Detection and isolation of bioactive natural products. In R. J. Molyneux & S. M. Colegate (Eds.), *Bioactive Natural Products* (2nd ed., pp. 59-64): CRC Press.
- Giamarellou, Helen, & Poulakou, Garyphallia. (2009). Multidrug-resistant gram-negative infections: what are the treatment options? *Drugs*, 69(14), 1879-1901.
- Gu, Wei, Zhang, Yu, Hao, Xiao-Jiang, Yang, Fu-Mei, Sun, Qian-Yun, Morris-Natschke, Susan L., . . . Long, Chun-Lin. (2014). Indole alkaloid glycosides from the aerial parts of *Strobilanthes cusia*. *Journal of Natural Products*, 77(12), 2590-2594.
- Haefner, Burkhard. (2003). Drugs from the deep: marine natural products as drug candidates. *Drug Discovery Today*, 8(12), 536-544.
- Harinantenaina, Liva, & Takaoka, Shigeru. (2006). Cinnafagrins A-C, dimeric and trimeric drimane sesquiterpenoids from *Cinnamosma fragrans*, and structure revision of capsicodendrin. *Journal of Natural Products*, 69(8), 1193-1197.

- Haroune, Nicolas, Crowson, Andrew, & Campbell, Bill. (2011). Characterisation of triacetone triperoxide (TATP) conformers using LC-NMR. *Science and Justice*, 51, 50-56.
- Hay, Mark E. (2009). Marine chemical ecology: chemical signals and cues structure marine populations, communities, and ecosystems. *Annual Review of Marine Science*, 1, 193-212.
- Hentschel, Petra, Holtin, Karsten, Steinhauser, Lisa, & Albert, Klaus. (2012). Monitoring the on-line titration of enantiomeric omeprazole employing continuous-flow capillary microcoil ¹H NMR spectroscopy. *Chirality*, 24(12), 1074-1076.
- Igbinosa, Etinosa O., Odjadjare, Emmanuel E., Igbinosa, Isoken H., Orhue, Phillips O., Omoigberale, May N. O., & Amhanre, Napoleon I. (2012). Antibiotic synergy interaction against multidrug-resistant *Pseudomonas aeruginosa* isolated from an abattoir effluent environment. *Sci. World J.*
- Jaume, Damia, & Duarte, Carlos M. (2006). General aspects concerning marine and terrestrial biodiversity. In C. M. Duarte (Ed.), *The exploration of marine biodiversity: Scientific and technological challenges* (pp. 17-30). Bilbao, Spain: Fundacion BBVA.
- Jha, Rajeev Kumar, & Zi-rong, Xu. (2004). Biomedical compounds from marine organisms. *Marine Drugs*, 2(3), 123-146.
- Kang, Suk Woo, Kang, Kyungsu, Kim, Mi Ae, Jeon, Na Ra, Kim, Sang Min, Jeon, Je-Seung, . . . Um, Byung-Hun. (2014). Phytoestrogenic activity of *Aceriphyllum rossii* and rapid identification of phytoestrogens by LC-NMR/MS and bioassay-guided isolation. *European Food Research & Technology*, 239(2), 237-246.
- Kingsland, Sally R., & Barrow, Russell A. (2009). Identification of chaetoviridin E from a cultured microfungus, *Chaetomium* sp. and structural reassessment of chaetoviridins B and D. *Australian Journal of Chemistry*, 62(3), 269-274.

- Klayman, Daniel L. (1985). Qinghaosu (artemisinin): an antimalarial drug from China. *Science*, 228(4703), 1049-1055.
- Kornprobst, Jean-Michael (Ed.). (2014). *Encyclopedia of Marine Natural Products. Volume 1: General Aspects, Microorganisms, Algae and Fungi*. Weinheim, Germany: Wiley Blackwell.
- Laird, Damian W., Bennett, Sarah, Bian, Bao-Hong, Sauer, Benjamin, Wright, Kathleen, Hughes, Victoria, & van Altena, Ian A. (2010). Chemical investigation of seven Australian *Cystophora* species: New chemistry and taxonomic insights. *Biochemical Systematics and Ecology*, 38(2), 187-194.
- Lakornwong, Waranya, Kanokmedhakul, Kwanjai, Kanokmedhakul, Somdej, Kongsaree, Palangpon, Prabpai, Samran, Sibounnavong, Phoutthasone, & Soyong, Kasem. (2014). Triterpene lactones from cultures of *Ganoderma* sp. KM01. *Journal of Natural Products*, 77(7), 1545-1553.
- Lang, Gerhard, Mayhudin, Nor Ainy, Mitova, Maya I., Sun, Lin, van der Sar, Sonia, Blunt, John W., . . . Munro, Murray H. G. (2008). Evolving trends in the dereplication of natural product extracts: new methodology for rapid, small-scale investigation of natural products. *Journal of Natural Products*, 71(9), 1595-1599.
- Laude Jr., David A., & Wilkins, C. L. (1987). Reverse-phase high performance liquid chromatography/nuclear magnetic resonance spectrometry in protonated solvents. *Analytical Chemistry*, 59(4), 546-551.
- Marine pharmaceuticals: the clinical pipeline.). Retrieved 16 January 2015, from <http://marinepharmacology.midwestern.edu/clinPipeline.htm>
- MarinLit. (2015). Royal Society of Chemistry.

- Mayer, Alejandro M. S., Glaser, Keith B., Cuevas, Carmen, Jacobs, Robert S., Kem, William, Little, R. Daniel, . . . Shuster, Dale E. (2010). The odyssey of marine pharmaceuticals: a current pipeline perspective. *Trends in Pharmacological Sciences*, 31(6), 255-265.
- Narayanam, Mallikarjun, Sahu, Archana, & Singh, Saranjit. (2013). Characterization of stress degradation products of benazepril by using sophisticated hyphenated techniques. *Journal of Chromatography A*, 1271(1), 124-136.
- Newman, David J., & Cragg, Gordon M. (2012). Natural products as sources of new drugs over the 30 years from 1981 to 2010. *Journal of Natural Products*, 75(3), 311-335.
- Pawlik, Joseph R., Chanas, Brian, Toonen, Robert J., & Fenical, William. (1995). Defences of Caribbean sponges against predatory reef fish. I. Chemical deterrence. *Marine Ecology Progress Series*, 127, 183-194.
- Pietra, Francesco. (2002). Chapter 9 - Terrestrial vs marine natural product diversity. In F. Pietra (Ed.), *Biodiversity and Natural Product Diversity* (pp. 79-96). London, England: Pergamon.
- Provinciali, Mauro, Papalini, Francesca, Orlando, Fiorenza, Pierpaoli, Sara, Donnini, Alessia, Morazzoni, Paolo, . . . Smorlesi, Arianna. (2007). Effect of the silybin-phosphatidylcholine complex (IdB 1016) on the development of mammary tumors in HER-2/neu transgenic mice. *Cancer Research*, 67(5), 2022-2029.
- Puglisi, Melany P., Sneed, Jennifer M., Sharp, Koty H., Ritson-Williams, Raphael, & Paul, Valerie J. (2014). Marine chemical ecology in benthic environments. *Natural Product Reports*, 31(11), 1510-1553.
- Queiroz Junior, Luiz H. K., Queiroz, Darlene P. K., Dhooghe, Liene, Ferreira, Antonio G., & Giraudeau, Patrick. (2012). Real-time separation of natural products by ultrafast 2D NMR coupled to on-line HPLC. *Analyst*, 137(10), 2357-2361.

- Schmidt, Jeppe S., Nyberg, Nils T., & Staerk, Dan. (2014). Assesment of constituents in *Allium* by multivariate data analysis, high-resolution α -glucosidase inhibition assay and HPLC-SPE-NMR. *Food Chemistry*, 161, 192-198.
- Shah, Ravi Piyushkumar, Sahu, Archana, & Singh, Saranjit. (2011). Identification and characterization of geometrical isomeric photo degradation product of eprosartan using LC-MS and LC-NMR. *European Journal of Chemistry*, 2(2), 152-157.
- Skropeta, Danielle, & Wei, Liangqian. (2014). Recent advances in deep-sea natural products. *Natural Product Reports*, 31(8), 999-1025.
- Smith, Charles D., Zhang, Xinqun, Mooberry, Susan L., Patterson, Gregory M. L., & Moore, Richard E. (1994). Cryptophycin: A new antimicrotubule agent active against drug-resistant cells. *Cancer Research*, 54(14), 3779-3784.
- Tanaka, Tomonori, Ikeda, Tsuyoshi, Kaku, Miho, Zhu, Xing-Hua, Okawa, Masafumi, Yokomizo, Kazumi, . . . Nohara, Toshihiro. (2004). A new lignan glycoside and phenylethanoid glycosides from *Strobilanthes cusia* BREMEK. *Chemical & Pharmaceutical Bulletin*, 52(10), 1242-1245.
- Timmers, Michael Anthony, Dias, Daniel Anthony, & Urban, Sylvia. (2012). Application of HPLC-NMR in the identification of plocamenone and isoplocamenone from the marine red alga *Plocamium angustum*. *Marine Drugs*, 10(9), 2089-2102.
- Timmers, Michael, & Urban, Sylvia. (2013). HPLC-NMR chemical profiling and dereplication studies of the marine brown alga, *Cystophora torulosa*. *Natural Product Communications*, 8(6), 715-719.
- Verma, Vishal A., Pillow, Thomas H., DePalatis, Laura, Li, Guangmin, Lewis Phillips, Gail, Polson, Andrew G., . . . Zheng, Bing. (2015). The cryptophycins as potent payloads for antibody drug conjugates. *Bioorganic & Medical Chemistry Letters*, Ahead of Print.

Wani, Mansukhlal C., Taylor, Harold Lawrence, Wall, Monroe E., Coggon, Philip, & McPhail, Andrew T. (1971). Plant Antitumor agents. VI. Isolation and structure of taxol, a novel antileukemic and antitumor agent from *Taxus brevifolia*. *Journal of the American Chemical Society*, 93(9), 2325-2327.

CHAPTER 2

NMR Spectroscopy for the Identification of Natural Products

Chapter 2 describes the various NMR spectroscopic experiments which are used to elucidate the structures of secondary metabolites or natural products. This work has been published as outlined below.

Book section in book chapter publication resulting from this study:

Brkljača, Robert, & Urban, Sylvia. (2014). Selected Applications of NMR Spectroscopy - Natural Products. In J. Fisher (Ed.), *Modern NMR Techniques for Synthetic Chemistry*. Florida, USA: CRC Press.

Selected Applications of NMR Spectroscopy

*Robert Brkljača, Sylvia Urban,
Kristian Hollingsworth, W. Bruce Turnbull
and John A. Parkinson*

CONTENTS

Natural Products

Robert Brkljača and Sylvia Urban

- 1.1 Introduction
- 1.2 1-D NMR Experiments
 - 1.2.1 1-D NOE and 1-D TOCSY Experiments
 - 1.2.2 DEPT and APT
- 1.3 2-D NMR Experiments
 - 1.3.1 Homonuclear Approaches
 - 1.3.2 Heteronuclear Approaches
- 1.4 Hyphenation: HPLC-NMR
 - 1.4.1 Application to Organism Profiling and Structure Elucidation
- 1.5 Summary

NATURAL PRODUCTS

Robert Brkljača and Sylvia Urban

1.1 INTRODUCTION

For the last few centuries, natural products have played a pivotal role as a source of new pharmaceutical agents.¹ During the period 1981 to 2010, it has been documented that more than 40% of new chemical drug entities released were either a natural product or derived from a natural product.² While the total number of new drugs derived from a natural source decreased to only 12.2% in 1997, this figure soared to a new high of 50% in 2010.² This trend illustrates that, despite the efforts made in the combinatorial chemistry area, where potential new drug entities are systematically synthesised, natural products continue to play an important part in the future of drug discovery. This is especially important as new diseases emerge and the resistance to drugs, such as antibiotics, escalates.³

Many areas of the natural environment, including the marine and microbial environments, remain understudied. It is from these environments that natural product researchers are focussing their efforts to discover further new bioactive secondary metabolites possessing unique pharmacophores with pharmaceutical potential.⁴⁻⁶

In a natural product study, marine or terrestrial organisms are, first, solvent-extracted and then typically screened for potential biological activity. This can be achieved by screening the crude extract against a selected bioassay or, alternatively, against a variety of assays. If biological activity is detected, the crude extract is fractionated in an effort to isolate and then determine the structure of the active component(s) via a bioassay-directed approach. Any bioactive compounds identified are then further evaluated. The isolation and identification exercise can typically take a few short weeks or, in extreme cases, it can take years. Two important examples of anti-cancer natural products that took years to resolve include ecteinascidin 743 and taxol (Figure 1).

Selected Applications of NMR Spectroscopy

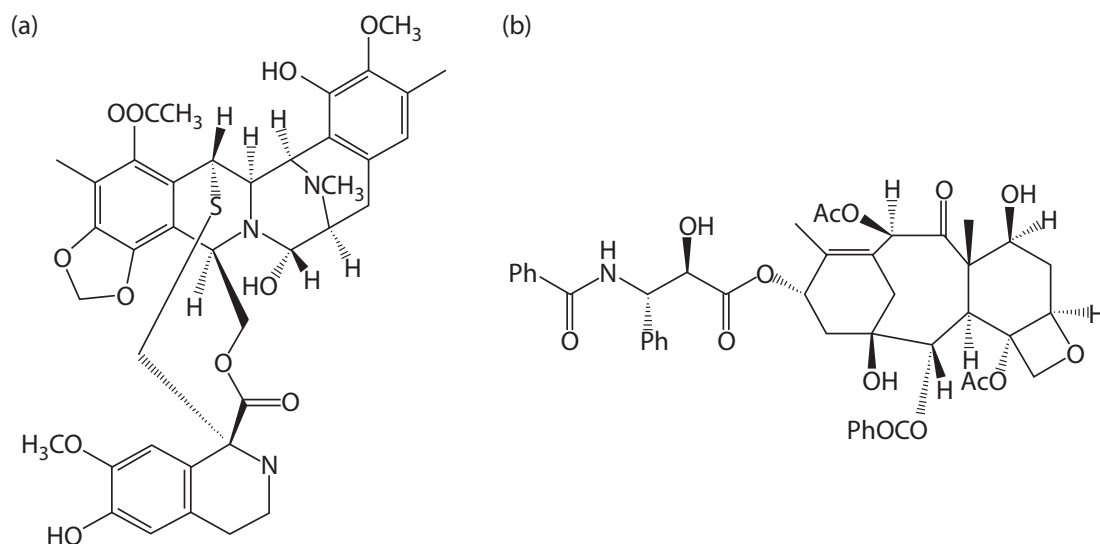


FIGURE 1 Structure of the anti-tumour agents ecteinascidin 743 (a) and taxol (paclitaxel) (b).

The tetrahydroisoquinoline alkaloid, ecteinascidin 743, is a potent anti-tumour natural product that was isolated from the Caribbean tunicate/ascidian *Ecteinascidia turbinata*.⁷ In 1970, it had been established that the crude extract derived from this ascidian displayed potent anti-tumour activity,⁸ but it was not until 1987 that the isolation and complete structure elucidation of the component responsible for this activity could be reported.⁷ Trabectedin (also known as ecteinascidin 743 or ET-743) is sold by Zeltia and Johnson and Johnson under the brand name YondelisTM. It is approved for use in Europe, Russia, and South Korea for the treatment of advanced soft tissue sarcoma. In the case of the anti-cancer natural product taxol, which was isolated from the Pacific yew tree *Taxus brevifolia*, the compound was isolated in its pure form in 1967, but its complete structure was not reported until 1971.⁹ When it was developed commercially by Bristol-Myers Squibb (BMS), the generic name was changed to paclitaxelTM, and the BMS compound is sold under the trademark TaxolTM. A newer formulation, in which paclitaxel is bound to albumin, is sold under the trademark AbraxaneTM. Taxol (paclitaxel) is used to treat a range of cancers, such as lung, ovarian, and breast cancers. Owing to a combination of the complexity in these structures, the low quantities isolated, and in the case of ET-743, the difficulty encountered with the isolation, it took many years and a tremendous effort to identify these important natural product drugs. Particularly, in the case of taxol (paclitaxel), it was the advances made in NMR spectroscopic techniques that enabled its structure to be finally elucidated.

The typical process for the isolation and identification of new bioactive natural products in a marine or terrestrial organism is summarised in Figure 2. Once an organism is collected and identified, a crude extract is generated by solvent extraction and evaluated for bioactivity against a panel of biological assays (e.g. anti-microbial and anti-tumour activities). Selection of an organism can be either random or targeted (e.g. a plant with known ethnopharmacological precedence or a

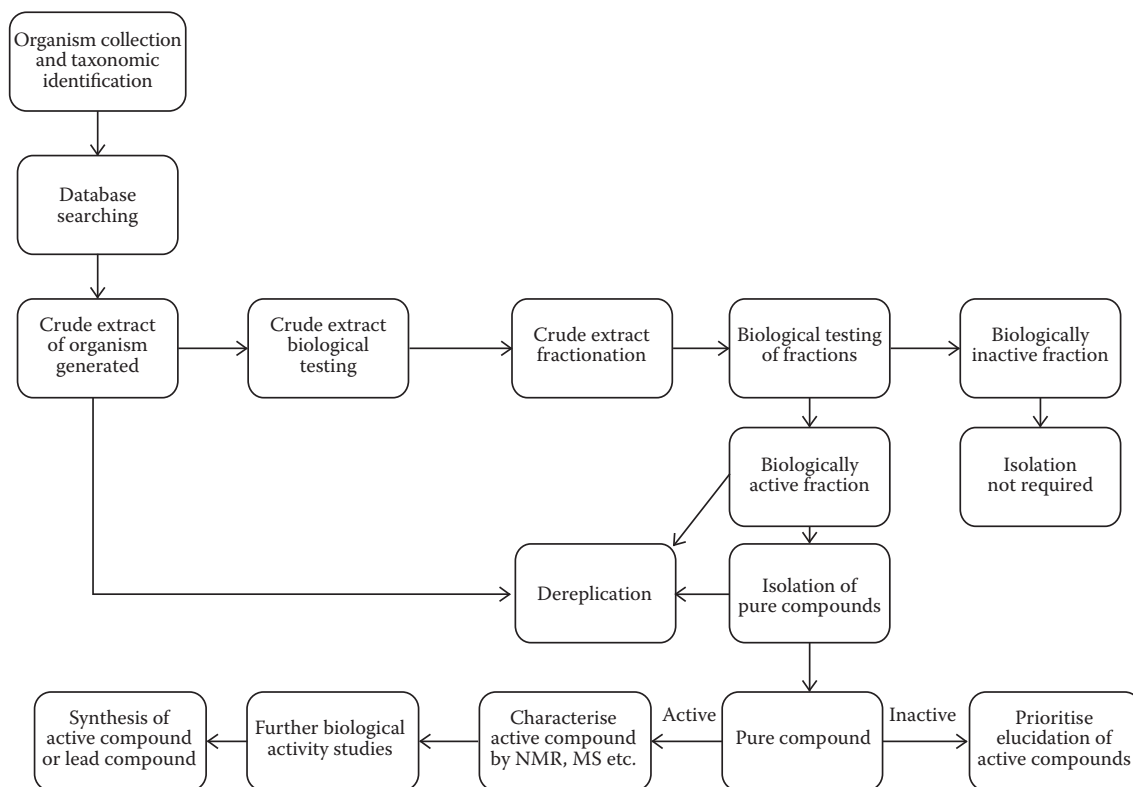


FIGURE 2 General process for the discovery of new bioactive natural products.

marine organism known for its chemical defense strategies). If biological activity is observed, the crude extract is further fractionated usually by column chromatography. In a bioassay-guided isolation, resulting fractions are tested against the particular biological assay(s) to confirm which fraction(s) contains the active component(s) of interest. Once a bioactive fraction(s) has been identified, each compound present is further fractionated and purified using high-performance liquid chromatography (HPLC). When a pure compound has been obtained, the structure of the natural product is elucidated and characterised using a variety of methodologies. These include infrared spectrometry, ultraviolet-visible (UV-VIS) spectroscopy, mass spectrometry (MS), X-ray diffraction, and most importantly, nuclear magnetic resonance (NMR) spectroscopy. The use of NMR spectroscopy for the structure determination of an unidentified natural product provides the greatest and most useful structure connectivity information. MS is used to confirm the molecular formula and weight. Once a natural product's structure has been elucidated, the compound can then be subjected to further biological evaluation, and if necessary/feasible, a total synthesis can be formulated to provide larger quantities for further studies. These further studies would include *in vivo* biological activity studies and, possibly, the determination of the mechanism of action, particularly for new bioactive natural products.

Since the isolation process can be lengthy and require considerable effort, it is important to recognise the presence of potential new secondary metabolites at the

earliest possible stage. The process known as ‘dereplication’ is vital to avoid the time-consuming process of isolating known and/or nuisance compounds. Combining both chemical and biological screening provides the quickest method to identify new lead compounds. Simple biological assays can be carried out to identify activity in crude extracts or fractions. These active extracts or fractions can then be chemically screened/profiled using techniques such as HPLC, UV-VIS spectroscopy, and NMR spectroscopy, or alternatively using hyphenated spectroscopic techniques such as HPLC-NMR or HPLC-MS.

Natural product structure elucidation studies have become increasingly easier over the last three to four decades due to the major advances that have occurred in a variety of NMR techniques. This is particularly evident when the introduction of higher magnetic field strengths and improved pulse sequences that became available is considered.¹⁰ There are many NMR experiments available for carrying out natural product structure elucidations. These can be broadly categorised into two main groups: the 1-D or the 2-D NMR experiments. Following an illustration of the utility of these two classes of experiment, we describe a high-throughput, hyphenated approach, HPLC-NMR, which is proving advantageous in the search for, and characterisation of, new natural products.

1.2 1-D NMR EXPERIMENTS

For natural product structure elucidations, ¹H and ¹³C are the most important nuclei, and several 1-D pulse sequences (some of which are discussed in the following) used for their observation are of fundamental importance. Together, they provide a detailed account of the number of protons and their associated coupling to other protons, the chemical environment, and an estimate of the number of carbons present. Experiments such as the 1-D single-irradiation (or steady-state) nuclear Overhauser enhancement (1-D NOE) and the distortionless enhancement by polarisation transfer (DEPT) NMR approach play a pivotal role in natural product characterisation.

1.2.1 1-D NOE and 1-D TOCSY Experiments

The steady-state NOE experiment involves the selected irradiation (or saturation) of a proton, which then relaxes via other protons that are close in space.¹¹ If the outcome of this experiment is subtracted from a control (off-resonance) experiment, the resultant difference spectrum will display a peak for the originally saturated resonance, which (for relatively low-molecular-weight species) will have a phase opposite to that for resonances of protons with which it shares a close spatial proximity. Typically, proton nuclei of up to 5 to 6 Å away will be detected via this through-space NMR experiment.¹² The strength of an observed NOE is greatly dependent on the combination of the molecular weight of the molecule and the saturation time.¹³ If the combination of these parameters is not optimised, no NOE will be observed. The 1-D NOE is favoured over the 2-D nuclear overhauser effect spectroscopy (NOESY) (transient NOE equivalent) for low- and medium-molecular-weight compounds primarily due to differing time demands.

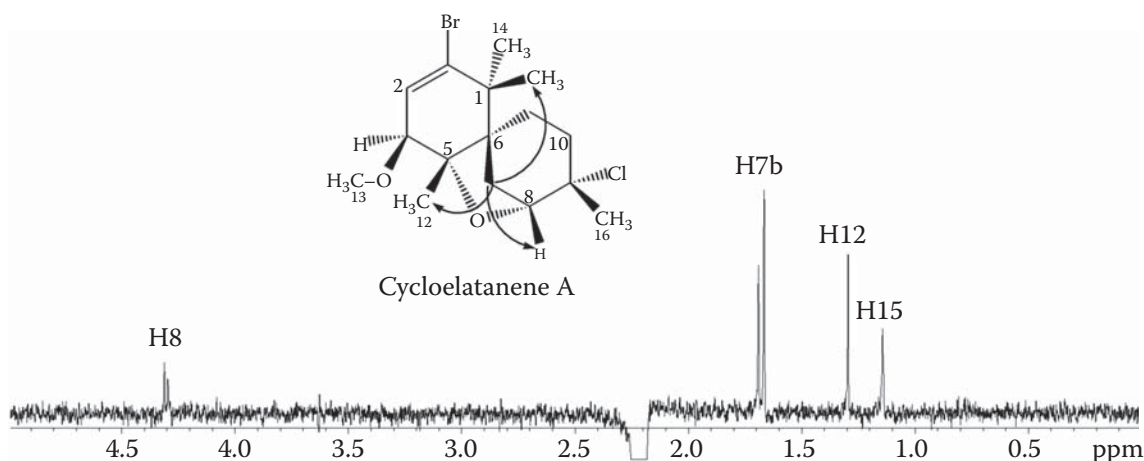


FIGURE 3 1-D NOE difference NMR spectrum of cycloelatanene A, illustrating the irradiation of the proton resonance at δ_{H} 2.21 (H7a).

A 1-D NOE NMR experiment was utilised to determine the relative configuration of the natural product cycloelatanene A, which was isolated from the Australian marine red alga *Laurencia elata*.¹⁴ The ^1H and ^{13}C NMR experiments confirmed this compound to be a C_{16} chamigrene, and the relative configuration was deduced through a series of 1-D NOE NMR experiments. Figure 3 illustrates the NOE difference spectrum for cycloelatanene A where the proton resonance at δ_{H} 2.21 (H7a) was irradiated. This irradiation resulted in four NOE enhancements being observed to the proton resonances at positions 7b, 8, 12 and 15 which concluded that these protons were all situated on the same face of the molecule.

The 1-D NOE NMR experiment only provides information on the protons connected through space. In contrast, the 1-D total correlation spectroscopy (1-D TOCSY) NMR experiment uses variable spin-locking times to allow for the determination of proton couplings along a compound chain.¹⁵ As the mixing time is changed, the polarisation energy is transferred through the bonds to other protons. Signals that appear with a shorter spin-locking time are closer (through-bonds) to the excited proton, and correspondingly, those appearing when longer spin-lock times are employed are further away from the selected proton. This NMR experiment is particularly useful for defining individual spin systems within a compound.

The natural product furospinosulin-1 was first isolated from the marine sponge *Ircinia spinosula*¹⁶ and recently re-isolated by the marine and terrestrial natural product (MATNAP) research group from *Dactylospongia* sp.¹⁷ Figure 4 shows the 1-D TOCSY spectra obtained for furospinosulin-1 using spin-lock times of 30, 70, 150 and 200 ms. The proton at δ_{H} 2.45 (H1) was selected, and by comparing the peak heights in each spectrum, it was possible to determine which protons were closer or further away in the covalently linked spin system.

This 1-D TOCSY NMR experiment indicated that the H2 and H3 protons were closest to the H1 proton and that the H18 and H3' protons were further away in terms of bonding from the H1 proton. The 2-D variant of the experiment provides a wealth of information, is not as easily interpreted as the 1-D experiment.

Selected Applications of NMR Spectroscopy

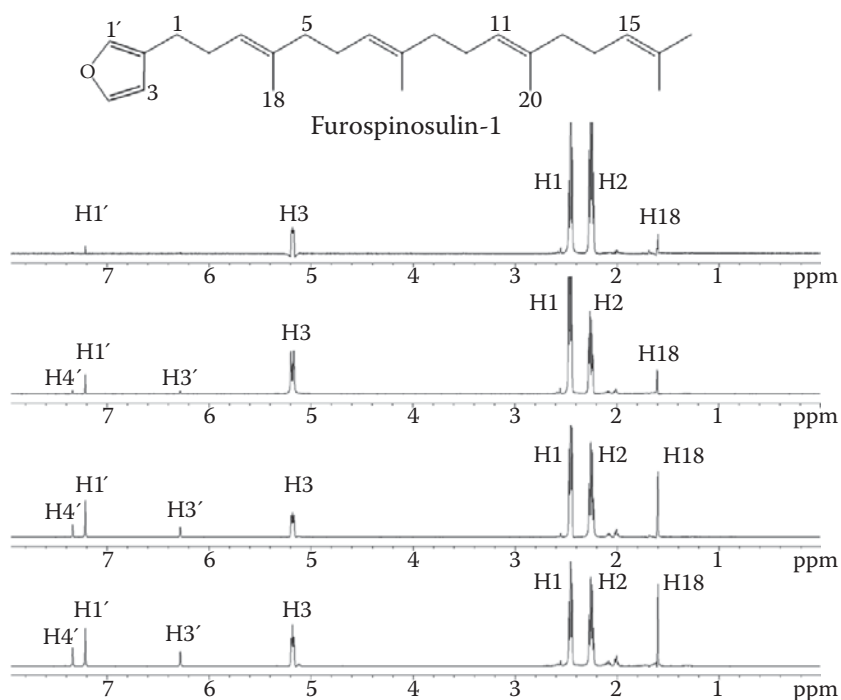


FIGURE 4 1-D TOCSY NMR spectra (spin-lock times [from top] of 30, 70, 150 and 200 ms) of furospinosulin-1.

1.2.2 DEPT and APT

The DEPT NMR experiment is a direct-detect heteronuclear experiment, in this case, ^{13}C detect, which provides information of the number of protons attached to the carbon nucleus. There are several versions of this experiment, which lead to slightly different data, but all of these reflect the attached-proton status of the ^{13}C atom. The DEPT45 NMR experiment shows all CH (methine), CH_2 (methylene), and CH_3 (methyl) carbons having the same (positive) phase.¹¹ Comparing the DEPT45 to the normal-broadband, proton-decoupled ^{13}C NMR spectrum, thus, enables quaternary carbons to be identified. The DEPT90 experiment is more selective and only displays CH (methine) carbons.¹¹ The DEPT135 shows all CH (methine), CH_2 (methylene), and CH_3 (methyl) carbons but with phase modulation. The CH (methine) and CH_3 (methyl) carbons appear with the same (positive) phase, and CH_2 (methylene) carbons appear with a 180° (negative) phase shift.¹¹ Combining a DEPT90 and DEPT135 NMR allows for all carbon-substitution types to be assigned. Another experiment similar to DEPT is the attached proton test (APT) experiment. The APT NMR experiment results in quaternary (C) and methylene (CH_2) carbons being positive and methyl (CH_3) and methine (CH) carbons being negative in their phasing.¹⁸ While these experiments still have their uses, they have been made almost redundant with the advent of the indirect-detection heteronuclear experiments (see in the following section).

Figure 5 shows the DEPT ^{13}C NMR spectrum as well as the APT NMR spectrum of the natural product furospinosulin-1. Comparison of the three different DEPT NMR spectra allows for each of the carbon multiplicities to be determined. Analysis of the APT will also allow for multiplicities to be determined; however, unlike in the DEPT NMR experiment, the quaternary carbons are observed.

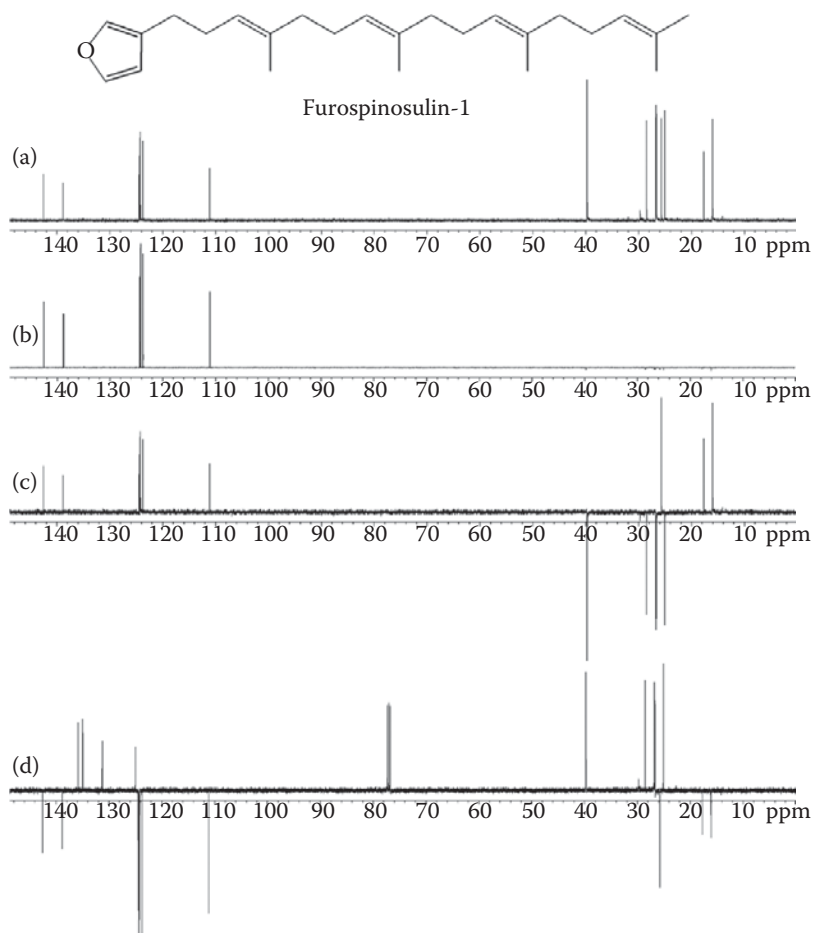


FIGURE 5 DEPT 45 (a), DEPT 90 (b), DEPT 135 (c) and APT (d) NMR spectra of furospinosulin-1, displaying selective carbon multiplicities.

1.3 2-D NMR EXPERIMENTS

In this section, we illustrate the application of 2-D NMR techniques to natural product characterisation. These are divided into two types. The homonuclear 2-D NMR experiments typically utilised include the correlation spectroscopy (COSY), NOESY, rotating frame Overhauser effect spectroscopy (ROESY), and TOCSY experiments. The heteronuclear 2-D NMR experiments (proton and carbon nuclei here) frequently implemented include the heteronuclear single quantum coherence (HSQC) and heteronuclear multiple quantum correlation (HMBC) NMR experiments. Most 2-D experiments come with non-gradient and gradient options (usually indicated by a 'g' in the name for the pulse sequence). The use of gradients typically increases the signal-to-noise as well as the quality of the spectra, and for this reason, it is very uncommon for gradient versions of the 2-D NMR experiments not to be used.

1.3.1 Homonuclear Approaches

1.3.1.1 Correlation Spectroscopy

The COSY NMR experiment provides information on which protons are immediate (bonding) neighbours, allowing for the spin systems of the natural product to

be determined.¹³ While coupling constants and splitting patterns observed in the 1-D ¹H NMR spectrum can be used to determine the number and geometric relationship of neighbouring protons, in complex systems, sometimes, this cannot be achieved. In these situations, 2-D COSY and related experiments are useful. The double-quantum-filtered COSY (DQFCOSY) NMR experiment, like the COSY NMR experiment, provides cross-peaks, indicating proton-proton coupling. However, unlike the COSY NMR experiment, the DQFCOSY is able to eliminate any peaks that do not have a double-quantum transition (i.e. singlets); this phase-sensitive spectrum has higher resolution and clearer-looking spectra, but the longer pulse sequence and quantum filter employed results in a loss of sensitivity.¹⁹

To illustrate the ability of the DQFCOSY to simplify and improve resolution, the natural product furospinosulin-1 was subjected to a gCOSY and a gDQFCOSY experiment. Figure 6 shows an expansion of the gCOSY and gDQFCOSY NMR experiments. It can be seen that the gCOSY NMR spectrum has regions where clear contours cannot be easily distinguished as well as the presence of long-range couplings. The gDQFCOSY NMR spectrum shows better resolution and a clearer-looking spectrum. In this NMR experiment, the long-range gCOSY correlations are not present.

1.3.1.2 NOESY and ROESY

The 2-D NOESY experiment provides the same type of information as the 1-D NOE spectrum except that all through-space connectivities within a molecule can be explored in a single experiment. Once again, proton-proton through-space relationships up to a distance of approximately 5 to 6 Å will be detected.

The compound 2,5,6-trimethoxy-9-phenyl-¹H-phenalen-1-one has been previously reported as being synthetically derived from a natural product.^{20,21} We have recently isolated this compound for the first time, arising as a naturally occurring pigment from the Australian plant *Haemodorum* sp.²² In the structure elucidation of this natural product, the point of attachment of the aromatic ring to either position 7 or 9 needed to be confirmed. The NOESY spectrum shown in Figure 7 clearly revealed a cross-peak between the aromatic proton at position 7 (δ_{H} 8.50) and the methoxy protons at position 6 (δ_{H} 4.10), demonstrating that the aromatic moiety must be attached at position 9. In this way, the NOESY spectrum could unequivocally confirm the structure of the natural pigment.

Just as the single-irradiation 1-D NOE NMR experiment requires the combination of the molecular weight and mixing time to be optimised to observe an NOE, the same criteria applies to the 2-D NOESY experiment. For intermediate-sized compounds or those that do not show strong NOESY correlations, the ROESY experiment is appropriate.^{15,23} While the ROESY NMR experiment may provide more information for intermediate-sized molecules compared to NOESY, the ROESY experiment is susceptible to also showing COSY- and TOCSY-type correlations, which adds complexity to the spectrum.¹¹

1.3.2 Heteronuclear Approaches

1.3.2.1 HSQC and HMBC

Earlier heteronuclear 2-D NMR experiments (pre-1990s) utilised the X nucleus, in this case, the carbon, as the observation frequency. These experiments were known

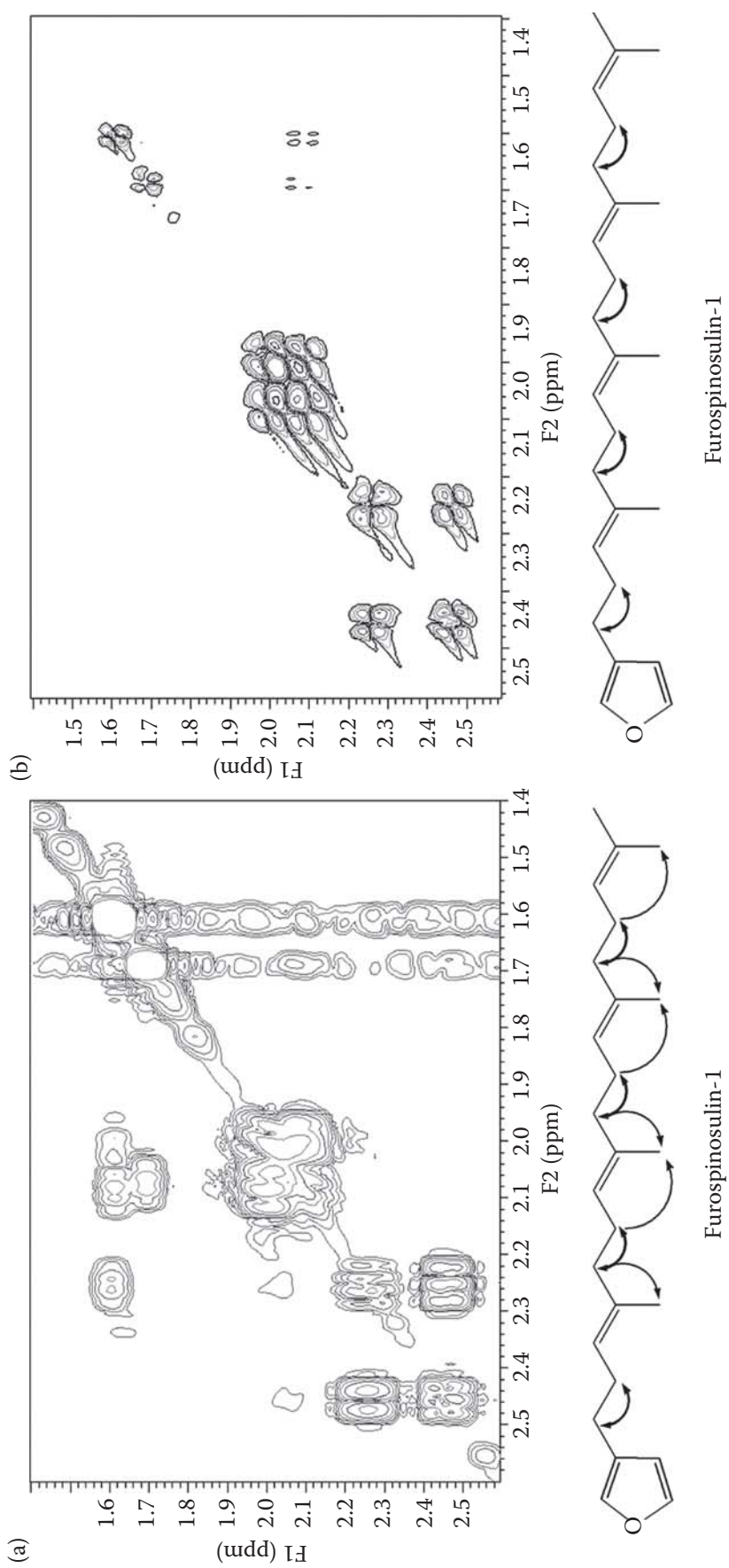


FIGURE 6 Expansion of gCOSY (a) and gDQFCOSY (b) NMR spectra, showing a selection of the observed ^1H – ^1H scalar (J) coupling connectivities in furospinosulin-1.

Selected Applications of NMR Spectroscopy

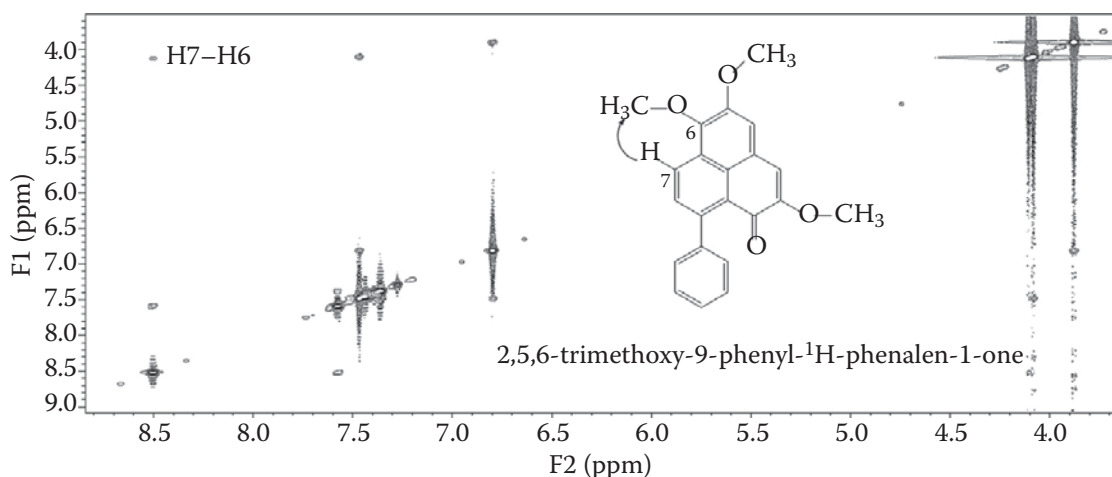


FIGURE 7 2-D NOESY NMR spectrum of 2,5,6-trimethoxy-9-phenyl-¹H-phenalen-1-one.

as the ‘heteronuclear shift correlation’ (HETCOR) and ‘correlation through long-range coupling’ (COLOC) approaches. The sensitivity of these experiments was dictated by that of the X nucleus and, thus, were not high. Subsequently, experiments have been implemented that employ the proton as the observation nucleus and carbon as the indirectly detected nucleus, therefore substantially increasing the sensitivity of these experiments. Thus, the indirect-detect equivalent of the HETCOR is the heteronuclear multiple quantum correlation (HMQC) NMR experiment, although the single-quantum equivalent (HSQC) is more frequently employed and the indirect equivalent of COLOC is the HMBC. These indirect-detection experiments are much more time efficient, and this is an imperative in the field of natural products, where frequently low to sub-milligram quantities are typically isolated.

In the past, assigning each proton to a specific carbon was almost exclusively done on the basis of the chemical shifts, and as such, sometimes, assignments were interchangeable or incorrectly applied. The HSQC NMR experiment has removed this ambiguity and determines which protons are directly attached to which carbon.¹⁸ The most basic HSQC NMR experiment will only correlate protons and carbons that are bonded to one another, and therefore, quaternary carbons do not appear in a HSQC NMR experiment. There are variants of the HSQC NMR experiment that offer spectra of improved quality with increased information. For example, the use of gradients along with adiabatic pulse versions during experiments offers increased sensitivity.^{24–26} There is also a version of the HSQC that provides carbon multiplicity information. In this experiment, methylene (CH₂) multiplicities are displayed in the negative phase, and methine/methyl (CH/CH₃) multiplicities are displayed in the positive phase.¹¹

While a COSY NMR experiment allows for the spin systems to be determined, the HMBC NMR experiment is the most important of the NMR experiments for natural product structure determination as it allows for the carbon skeleton of a natural product to be pieced together. This is achieved by formulating structure fragments on the basis of all the NMR (both 1-D and 2-D) information gathered and then forming connections of these structure fragments via through-bond connectivities observed in the HMBC NMR experiment. While the HSQC NMR experiment displays direct one-bond proton to carbon connectivities, the HMBC NMR experiment

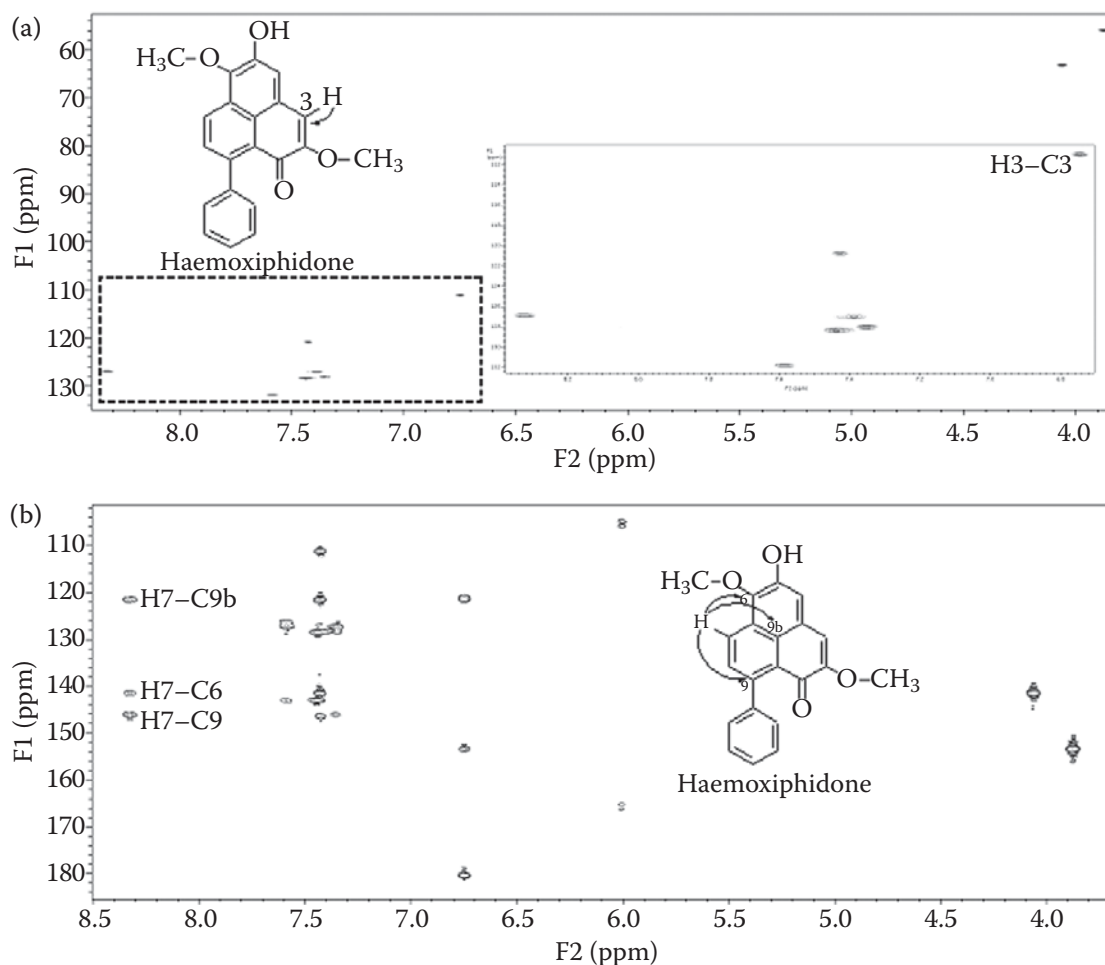


FIGURE 8 Sections of the 2-D gHSQCAD (a) and gHMBCAD (b) NMR spectra of haemoxiphidone.

provides proton to carbon connectivity usually up to two to three bonds removed²⁷ (in aromatic systems, four-bond correlations are also encountered). Unlike the HSQC NMR experiment, quaternary carbons are observed in the HMBC NMR experiment, thereby providing vital structure connectivity information.

The gradient heteronuclear single quantum coherence adiabatic (gHSQCAD) and gradient heteronuclear multiple-bond correlation adiabatic (gHMBCAD) NMR spectra of haemoxiphidone, a pigment isolated from the Australian plant *Haemodorum simulans*, are illustrated in Figure 8.²⁸ All the correlations observed in the gHSQCAD NMR spectrum were in the positive phase, indicating that the multiplicities of the carbons were either CH (methines) or CH₃ (methyls).

In the structure elucidation of this pigment, it was uncertain whether the aromatic moiety was attached at position 7 or 9 of the compound. Analysis of the HMBC NMR spectrum supported a position-9 attachment, which was also confirmed by 1-D NOE NMR experiments.²⁸

1.3.2.2 Coupled HSQC

In many natural products, it is common for proton signals to overlap, particularly, signals for those protons having complex splitting patterns. Some compounds require

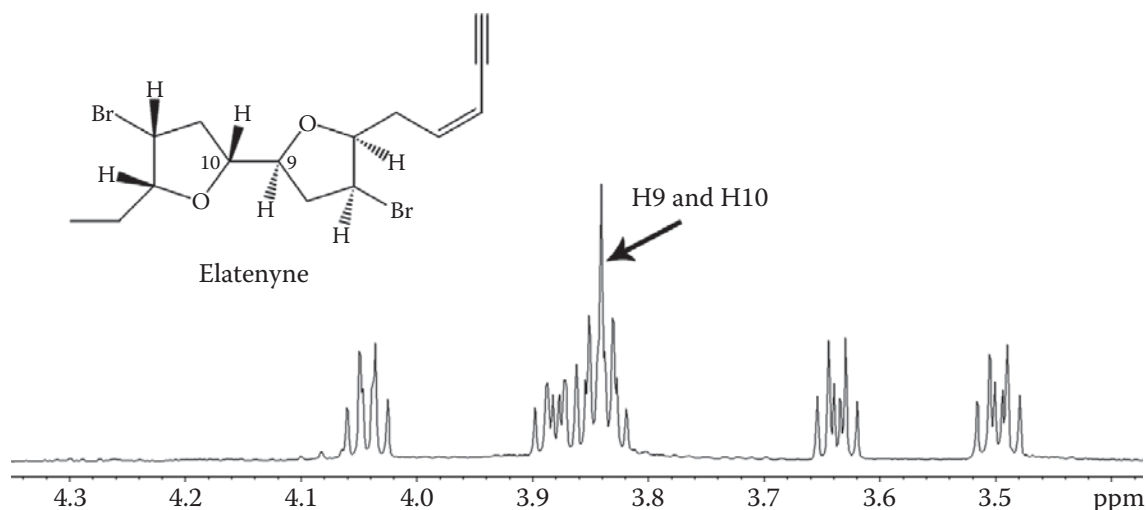


FIGURE 9 Expansion of the ^1H NMR spectrum (500 MHz, C_6D_6) of elatenyne.

the splitting patterns of protons to be clearly observed so that the structures may be deduced. The splitting patterns of overlapping protons may be observed by editing the standard HSQC experiment. The limiting factor is that the overlapping protons must be coupled to different carbons that do not overlap. In this variant of the HSQC NMR experiment, two parameters are changed. First, the number of data points collected in F2 (the acquisition dimension) is increased for greater resolution in the proton dimension. The second parameter that is changed is that the ^{13}C decoupling is turned off. This means that each proton signal will now be split by its H–C coupling constant. By extracting the 1-D traces from the 2-D HSQC, the splitting patterns of the overlapping protons may now be observed.^{29,30}

This particular problem was encountered in the structure of elatenyne, which was isolated from the Australian red alga *Laurencia elata*.^{14,31} The two protons at the ring junction (positions 9 and 10) were overlapped. It was vital to obtain the splitting pattern and coupling constant of these overlapped ring junction protons to propose a relative configuration for elatenyne. Figure 9 shows the region of the ^1H NMR spectrum for the overlapped protons at positions 9 and 10 (δ_{H} 3.86). Here, no splitting/coupling information about the overlapped protons could be deduced.

Figure 10 shows the edited gHSQCAD spectrum and extracted 1-D traces for the overlapped protons; the splitting pattern and coupling for the overlapped protons could be clearly observed. Each proton is split by their H–C coupling, and it is not uncommon for one mirrored splitting pattern to be clearer than the other. The splitting patterns were able to be deduced as a doublet of triplets and the coupling constant was measured, confirming that the two ring junction protons were in an axial–equatorial arrangement.³¹

1.3.2.3 CIGAR-HMBC

In rare instances, the HMBC NMR experiment will not be suited to particular compounds. The HMBC experiment uses fixed coupling constants to detect carbons correlating up to two to three bonds away. If expected correlations are not observed, the constant time inverse-detection gradient accordion rescaled (CIGAR)-HMBC may provide a better solution. The CIGAR-HMBC experiment is less sensitive than the

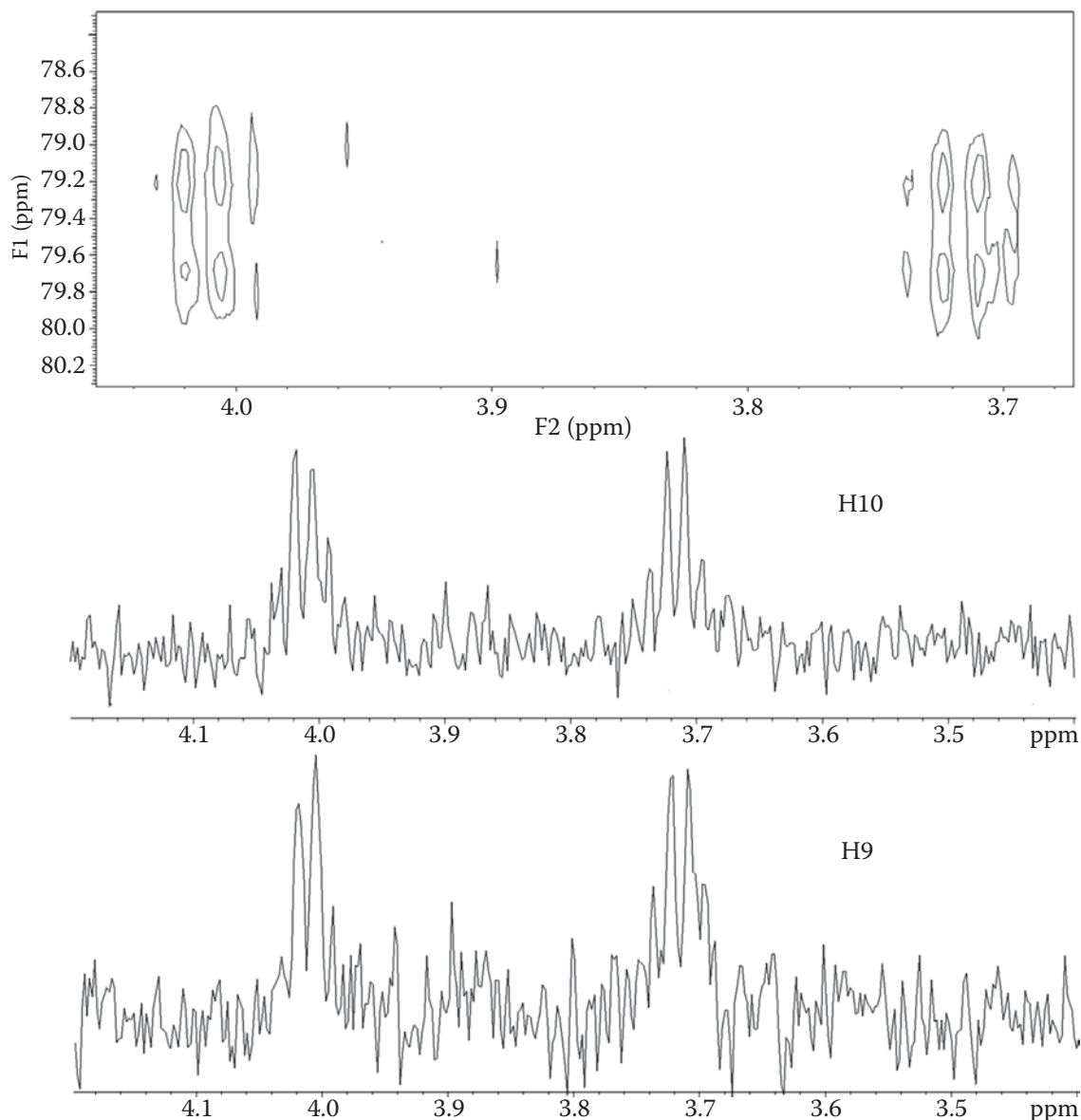


FIGURE 10 Expansion of coupled HSQC NMR spectrum and extracted 1-D traces of H9 and H10 (500 MHz, C_6D_6) of elatenyne.

HMBC experiment; however, the CIGAR-HMBC uses variable coupling constants.³² This experiment, therefore, provides a better opportunity to observe correlations further than three bonds away to detect situations where small coupling constants exist or instances where there might be a large range of coupling constants, as in the case of nitrogen-containing compounds.

1.3.2.4 HSQC-NOESY

In the previously discussed 2-D NOESY NMR experiment, one disadvantage is that, if two (or more) protons have the same chemical shift, it is difficult to distinguish which proton is, in fact, being detected. The band-selective HSQC-NOESY NMR experiment utilises both the NOESY and HSQC pulse sequences and can, therefore, be used to overcome the issues of overlapping proton chemical shifts.

For example, if a proton at δ_{H} 3.50 shows an NOE to a proton at δ_{H} 6.70 with an associated carbon chemical shift at δ_{C} 126.7 ppm, a cross-peak between δ_{H} 3.50 and δ_{C} 126.7 ppm will be observed. If another proton also co-occurs at δ_{H} 6.70 but with an associated carbon chemical shift at δ_{C} 130.5 ppm, this distinction would be evident in a band-selective HSQC-NOESY experiment.

1.3.2.5 Excitation-Sculptured Indirect-Detection Experiment

The HMBC experiment provides information about protons coupled to carbons two to three bonds away. However, this experiment does not provide any information about the magnitude of these coupling constants. The excitation-sculptured indirect-detection experiment (EXSIDE) is similar to the HMBC in that it shows proton-to-carbon coupling two to three bonds away but, unlike the HMBC, also displays the coupling constants.³³ This experiment displays a 2-D NMR spectrum similar to the HMBC, but each correlation appears as a doublet in the F1 dimension. By measuring the distance between each doublet and dividing by the J scaling factor, the coupling constants can be determined.

To illustrate the ability of the EXSIDE experiment to determine nJ C–H coupling constants, Figure 11 compares the results obtained in both the gHMBCAD and EXSIDE experiments for furospinosulin-1. In the gHMBCAD experiment, three distinct correlations can be observed for the proton at δ_{H} 7.21; however, no information about the coupling to the carbons can be deduced. The EXSIDE version still shows not only these three distinct correlations, but also the splitting of each carbon signal.

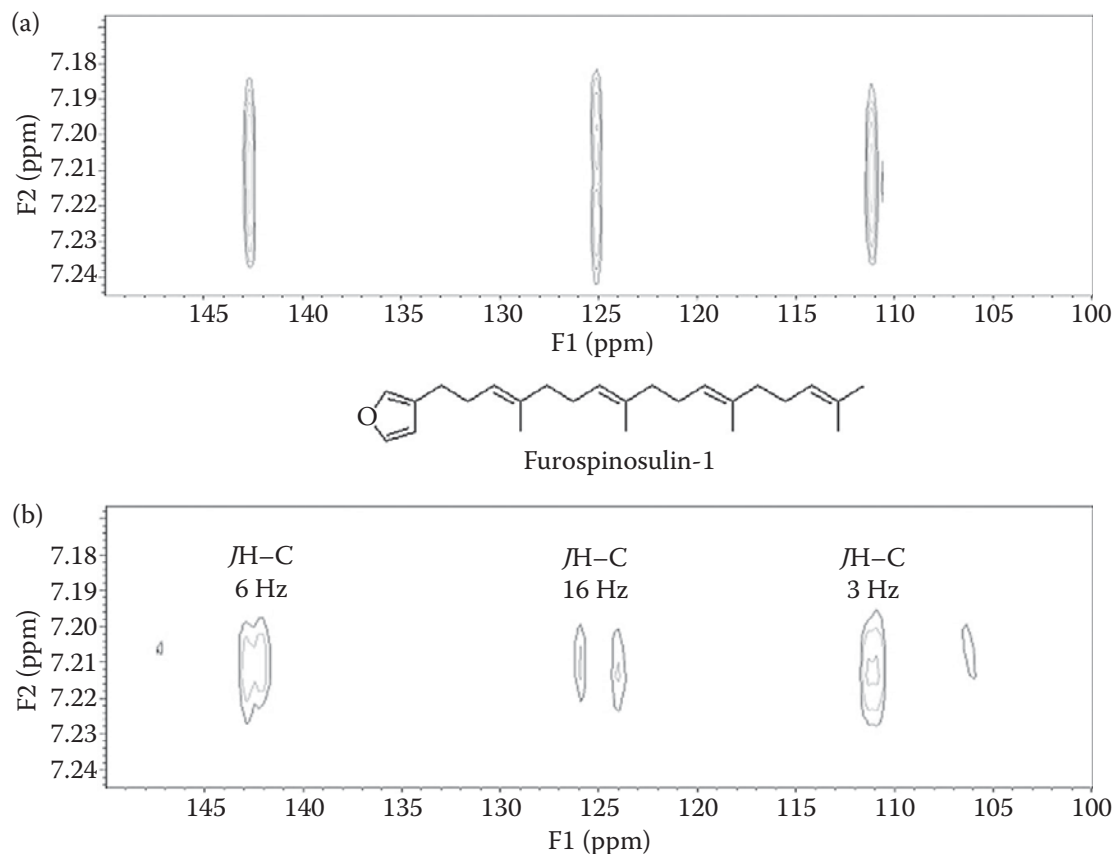


FIGURE 11 Expansions of the gHMBCAD and EXSIDE NMR spectra of furospinosulin-1.

By measuring the distance between each split carbon and dividing by the J factor, the coupling constants of these carbons were determined to be 6, 16 and 3 Hz.

1.4 HYPHENATION: HPLC-NMR

One of the more recent advancements and application of NMR spectroscopy has been the hyphenation to other separation and detection methodologies traditionally used separately in natural product isolation and characterisation. An example of such is the coupling of NMR to an HPLC system to yield the hyphenated spectroscopic technique known as 'HPLC-NMR'. This technique was developed in the 1970s;¹⁰ however, it has only recently taken over as a robust and powerful tool for chemical profiling, dereplication, and structure elucidation. Principally, the drawback for the hyphenated spectroscopic technique included the initial high costs and the lack of sensitivity. Developments in probe design, solvent suppression, loop collection, cold probes, column trapping, capillary NMR, and microcoils have allowed it to become the powerful technique that it is today and is now finding extensive use in the field of natural products.³⁴

HPLC-NMR operates in two main modes: on-flow and stop-flow.³⁴ On-flow mode utilises continuous ^1H NMR data acquisition for all components as they elute from the HPLC column and, for this reason, is a far less sensitive mode of operation. The on-flow mode is, therefore, useful in providing quick general structure class information that can be used to search various databases.

The more useful, stop-flow mode (Figure 12), allows for any one particular component to be trapped in the NMR flow cell at a time. By trapping one component, extended acquisitions are now possible, allowing for 2-D NMR experiments to be carried out.^{10,34} This increase in sensitivity is particularly important in natural

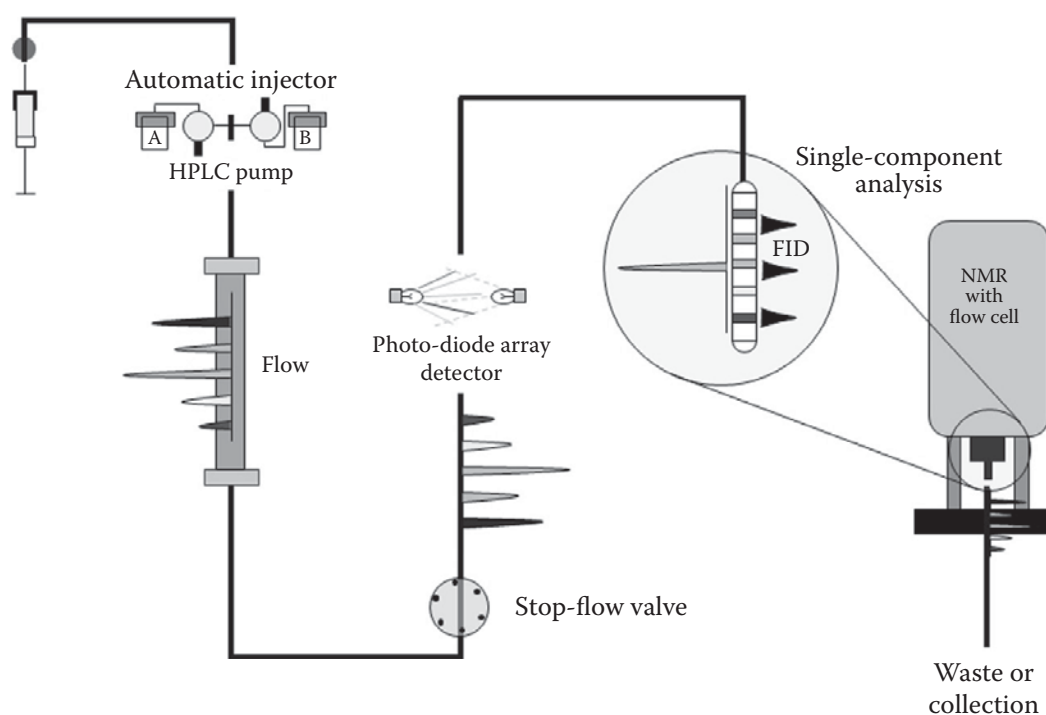


FIGURE 12 Schematic of stop-flow operation of HPLC-NMR.

product identification. In general, complete 2-D NMR data can be obtained for major components in crude extracts/enriched fractions, whereas usually, only ^1H NMR and COSY NMR data can be obtained for the minor components in the typical overnight time frame used to conduct conventional NMR experiments.

Other variants of HPLC-NMR utilise solid-phase extraction (SPE) columns to pre-concentrate analytes before NMR analysis to increase the signal-to-noise and experiment capability.³³ Loop collection allows for analytes to be separately collected and then either flushed into the flow cell one at a time or transferred into conventional NMR tubes for off-line analysis. Cold probes (or cryo probes) and microcoils have also allowed for increased sensitivity and, therefore, the NMR detection of smaller quantities of analytes.³⁴

HPLC-NMR can be further extended to include MS to yield HPLC-NMR-MS. This technique has two possible set-ups, namely 'parallel' and 'series'.³⁴ In a parallel set-up, a splitter is placed after the column and a small amount of the analyte is directed to the mass spectrometer, with the majority directed to the NMR spectrometer. In the series configuration, the mass spectrometer is placed after the NMR spectrometer. The latter set-up can sometimes be at a disadvantage since peaks can broaden and retention times can change by the time that the analytes reach the mass spectrometer.

1.4.1 Application to Organism Profiling and Structure Elucidation

We have conducted various studies utilising HPLC-NMR to chemically profile both marine and terrestrial natural product extracts and enriched fractions.^{14,35-41} Only recently, HPLC-NMR has been utilised to chemically profile the Australian brown alga *Sargassum paradoxum*.⁴² The crude dichloromethane extract of the alga was analysed, and a number of constituents were detected. The major constituent was identified using the stop-flow HPLC-NMR mode. This major constituent was present in sufficient abundance to allow for complete 2-D characterisation including gCOSY, gHSQCAD, and gHMBCAD analysis. The results obtained from the stop-flow HPLC-NMR analysis allowed the major constituent to be identified as isosargahydroquinic acid.⁴¹ The double bond geometry of this compound was secured by application of the 1-D NOE NMR experiment. The Wet1D (used to solvent suppress), gCOSY, gHSQCAD, and gHMBCAD NMR spectra are provided in Figures 13 to 16, respectively. This represents the first instance of a HMBC-NMR spectrum being obtained in the stop-flow HPLC-NMR mode on a system equipped with a 60 μL flow cell. The ability to obtain a HMBC NMR spectrum relies on the amount of analyte present, and the limitation is the ability to dissolve the fraction in a minimal amount of solvent. The mass limitation in HPLC-NMR analyses often remains a restriction for the technique since a reasonable signal-to-noise ratio for the compound must be achieved. However, as demonstrated by this example, it is possible to obtain HMBC data for main constituents in crude extracts without the need for pre-concentration, SPE cartridges, loop storage, or cold probes.

In the gHSQCAD NMR spectrum (Figure 15) of isosargahydroquinic acid obtained by stop-flow HPLC-NMR, the proton resonances between δ_{H} 3.00 and δ_{H} 4.50 ppm were attached to carbons that appeared in the negative phase (indicating methylene [CH_2] multiplicities) with all other carbon resonances appearing in the positive phase (indicating methine [CH] or methyl [CH_3] multiplicities).

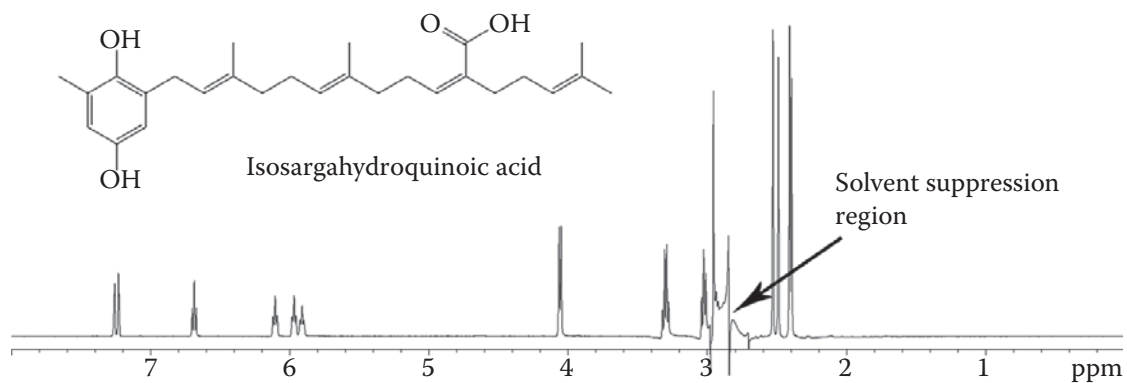


FIGURE 13 Wet 1-D HPLC-NMR spectrum of isosargahydroquinonic acid (500 MHz, 75% CH₃CN/D₂O).

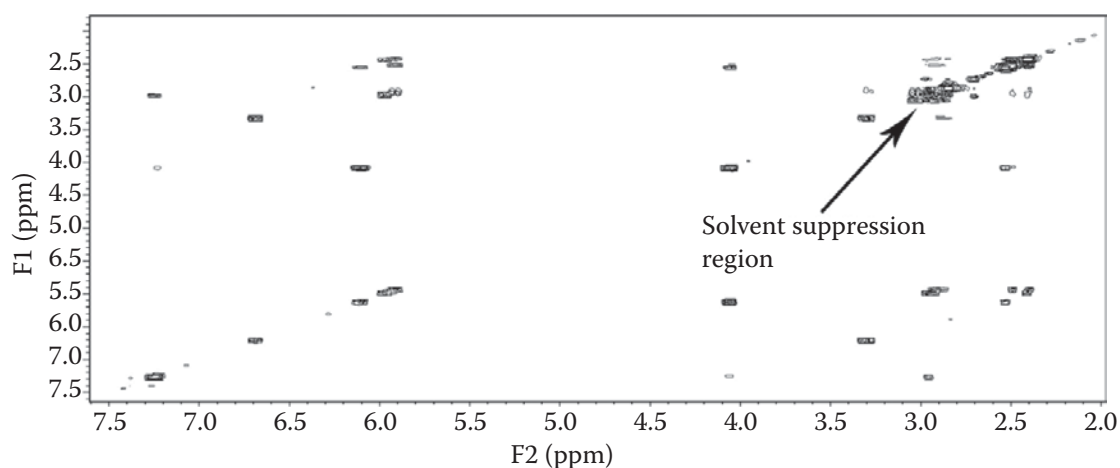


FIGURE 14 gCOSY NMR spectrum of isosargahydroquinonic acid (500 MHz, 75% CH₃CN/D₂O).

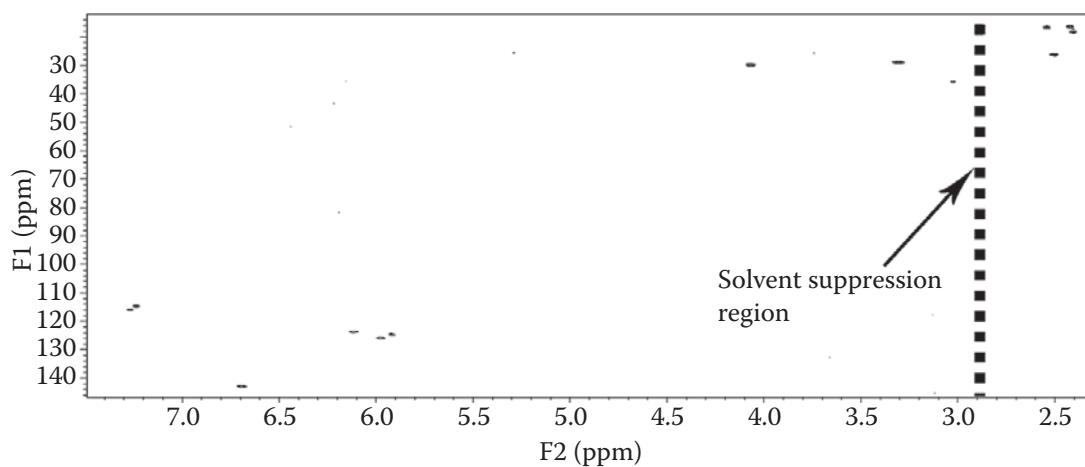


FIGURE 15 gHSQCAD NMR spectrum of isosargahydroquinonic acid (500 MHz, 75% CH₃CN/D₂O).

Selected Applications of NMR Spectroscopy

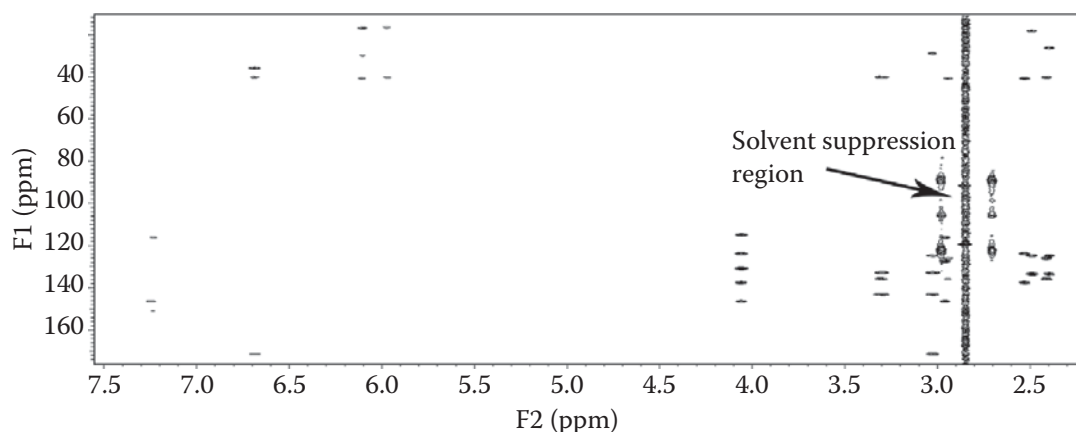


FIGURE 16 gHMBCAD NMR spectrum of isosargahydroquinic acid (500 MHz, 75% CH₃CN/D₂O).

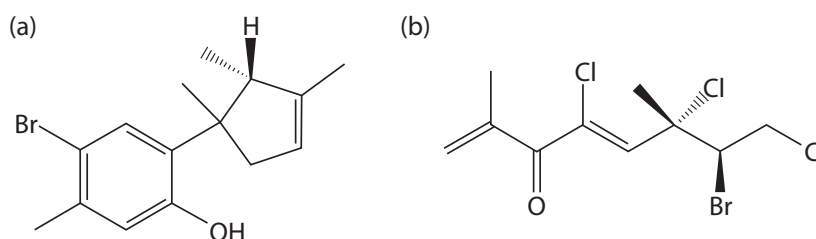


FIGURE 17 Structures of two new natural products (a, Isoallolaunterol [*Laurencia filiformis*] and b, Isoplocamenone [*Plocamium angustum*]), both of which are unstable and, hence, could only be elucidated *in situ*.

The importance of the application of HPLC-NMR was illustrated through two separate studies conducted by our research group. These included the investigation of two southern Australian red algae, namely *Laurencia filiformis*³⁶ and *Plocamium angustum*.³⁵ In both cases, new unstable natural products (Figure 17) were able to be identified by application of HPLC-NMR. Any attempted off-line isolation and characterisation of these two natural products could not be achieved, owing to their rapid degradation. HPLC-NMR analyses of the crude extracts of these two algae successfully established the structures *in situ*.

The unstable nature of natural products is a frequently encountered issue that is brought about by exposure to light, heat, or air oxidation, among other scenarios. The use of HPLC-NMR in such instances is invaluable in securing their structure.

1.5 SUMMARY

The use of NMR in natural product structure elucidation has continued to evolve. From its humble beginnings in 1-D proton and carbon spectra to the advanced methods such as 2-D experiments and hyphenated spectroscopic techniques, NMR has played a large and important role in the natural product field. Continuing efforts and progress in NMR spectroscopy with regard to new and improved pulse sequences, faster and more sensitive hardware, easier access to higher field strengths, and smaller

sample volumes will play an important role in natural product structure determination, allowing for the elucidation of ever-decreasing quantities. This is of vital importance in the field of natural product drug discovery where structure determination of sub-milligram quantities is now possible. The application of NMR spectroscopy in the hyphenated spectroscopic techniques such as HPLC-NMR will continue to evolve as more applications of the technique emerge, illustrating its strength and importance in chemical profiling/de-replication and in the rapid identification of natural products.

REFERENCES

1. Newman, D. J., G. M. Cragg and K. M. Snader. 2003. Natural products as sources of new drugs over the period 1981–2002. *Journal of Natural Products* 66, pp. 1022–1037.
2. Newman, D. J. and G. Cragg. 2012. Natural products as sources of new drugs over 30 years from 1981 to 2010. *Journal of Natural Products* 75, pp. 311–335.
3. Wright, G. D. 2012. Antibiotics: A new hope. *Chemistry and Biology* 19, pp. 3–10.
4. Colwell, R. R. 2002. Fulfilling the promise of biotechnology. *Biotechnology Advances* 20, pp. 215–228.
5. Hill, R. T. and W. Fenical. 2010. Pharmaceuticals from marine natural products: Surge or ebb? *Current Opinion in Biotechnology* 21, pp. 777–779.
6. Hughes, C. C. and W. Fenical. 2010. Antibacterials from the sea. *Chemistry: A European Journal* 16, pp. 12,512–12,525.
7. Rinehart, K. and T. G. Holt. 1987. *Purification and Characterisation of Ecteinascidins 729, 743, 745, 759a, 759b, and 770 Having Antibacterial and Anti-Tumour Properties*. Illinois: University of Illinois, pp. 1–32.
8. Sigel, M. M., L. L. Wellham, W. Lichter, L. E. Dudeck, J. Gargus and A. H. Lucas. 1969. In: *Food-Drugs from the Sea Proceedings*. Younghen H. W. Jr, ed. Washington, DC: Marine Technology Society, pp. 281–294.
9. Wani, M. C., H. L. Taylor, M. E. Wall, P. Coggon and A. T. McPhail. 1971. Plant anti-tumour agents: VI. Isolation and structure of taxol, a novel anti-leukemic and anti-tumour agent from *Taxus brevifolia*. *Journal of the American Chemical Society* 93, pp. 2325–2327.
10. Urban, S. and F. Separovic. 2005. Developments in hyphenated spectroscopic methods in natural product profiling. *Frontiers in Drug Design and Discovery* 1, pp. 113–166.
11. Claridge, T. D. W. 1999. *High-Resolution NMR Techniques in Organic Chemistry*. Oxford, United Kingdom: Elsevier Science, Ltd, pp. 139–146, 227–312 and 328–334.
12. Webb, G. A. 2008. *Modern Magnetic Resonance: Applications in Chemistry, Biological, and Marine Sciences*. Dordrecht, The Netherlands: Springer, pp. 409–412.
13. Keeler, J. 2005. *Understanding NMR Spectroscopy*. Chichester, United Kingdom: John Wiley & Sons, pp. 194–204 and 279–291.
14. Dias, D. A. and S. Urban. 2011. Phytochemical studies of the Southern Australian marine alga *Laurencia elata*. *Phytochemistry* 72, pp. 2081–2089.
15. Morris, G. A. and J. W. Emsley. 2010. *Multi-dimensional NMR Methods for the Solution State*. West Sussex, England: John Wiley & Sons, Ltd, pp. 205–219 and 233–258.
16. Cimino, G., S. de Stefano and L. Minale. 1972. Polyprenyl derivatives from the sponge *Ircinia spinosula*. *Tetrahedron* 28, pp. 1315–1324.
17. Brkljaca, R. and S. Urban. Phytochemical investigation of the sea sponge *Dactylospongia* sp. (unpublished results).
18. Jacobsen, N. E. 2007. *NMR Spectroscopy Explained*. New Jersey: John Wiley & Sons, Inc, pp. 220–222.
19. Becker, E. D. 2000. *High-Resolution NMR: Theory and Chemical Applications*. San Diego, California: Academic Press, pp. 330–334.
20. Cooke, R. G. and I. J. Rainbow. 1977. Coloring matters of Australian plants: XIX. Haemocorin: Unequivocal synthesis of the aglycone and some derivatives. *Australian Journal of Chemistry* 30, pp. 2241–2247.
21. Morrison, G. A. and B. Laundon. 1971. Naturally occurring compounds related to phenalenone: Part II. The synthesis of haemocorin aglycone. *Journal of the Chemical Society* 9, pp. 1694–1704.
22. Brkljaca, R. and S. Urban. Phytochemical investigation of the Australian plant *Haemodorium* sp. (unpublished results).
23. Friebolin, H. 2005. *Basic One- and Two-Dimensional NMR Spectroscopy*. Weinheim, Germany: Wiley-VCH, pp. 276–280 and 295–296.

24. Hadden, C. E. 2005. Adiabatic pulses in ^1H - ^{15}N direct and long-range heteronuclear correlations. *Magnetic Resonance in Chemistry* 43, pp. 330–333.
25. Hurd, R. E. 1990. Gradient-enhanced spectroscopy. *Journal of Magnetic Resonance* 87, pp. 422–428.
26. Ruiz-Cabello, J., G. W. Vuister, C. T. W. Moonen, P. van Gelderen, J. Cohen and P. C. M. van Zijl. 1992. Gradient-enhanced heteronuclear correlation spectroscopy: Theory and experimental aspects. *Journal of Magnetic Resonance* 100, pp. 282–302.
27. Bax, A. and M. F. Summers. 1986. ^1H and ^{13}C assignments from sensitivity-enhanced detection of heteronuclear multiple-bond connectivity by 2-D multiple quantum NMR. *Journal of the American Chemical Society* 108, pp. 2093–2094.
28. Urban, S., R. Brkljaca, J. M. White and M. A. Timmers. 2013. Phenylphenalenones and oxabenzochrysenones from the Australian plant *Haemodorum simulans*. *Phytochemistry* 95, pp. 351–359; 96, p. 465.
29. Mucci, A., F. Parenti and L. Schenetti. 2002. On the recovery of $^3J_{\text{H,H}}$ and the reduction of molecular symmetry by simple NMR inverse detection experiments. *European Journal of Organic Chemistry* 5, pp. 938–940.
30. Ryan, J. M. 2008. *Novel Secondary Metabolites from New Zealand Marine Sponges*. Wellington, New Zealand: Victoria University of Wellington, pp. 67–69.
31. Brkljača, R. and S. Urban. 2013. Relative configuration of the marine natural product elatenyne using NMR spectroscopic and chemical derivatisation methodologies. *Natural Product Communications* 8, pp. 729–732.
32. Hadden, C. E., G. E. Martin and V. V. Krishnamurthy. 2000. Constant time inverse-detection gradient accordion rescaled heteronuclear multiple-bond correlation spectroscopy: CIGAR-HMBC. *Magnetic Resonance in Chemistry* 38, pp. 143–147.
33. Krishnamurthy, V. V. 1996. Excitation-sculptured indirect-detection experiment (EXSIDE) for long-range CH coupling-constant Measurement. *Journal of Magnetic Resonance Series A* 121, pp. 33–41.
34. Brkljača, R. and S. Urban. 2011. Recent advancements in HPLC-NMR and applications for natural product profiling and identification. *Journal of Liquid Chromatography and Related Technologies* 34, pp. 1063–1076.
35. Timmers, M. A., D. A. Dias and S. Urban. 2012. Application of HPLC-NMR in the identification of plocamenone and isoplocamenone from the marine red alga *Plocamium angustum*. *Marine Drugs* 10, pp. 2089–2102.
36. Dias, D., J. M. White and S. Urban. 2009. *Laurencia filiformis*: Phytochemical profiling by conventional and HPLC-NMR approaches. *Natural Products Communication* 4, pp. 157–172.
37. Timmers, M. A., D. A. Dias and S. Urban. 2013. HPLC-NMR chemical profiling of the Australian carnivorous plant *Drosera erythroziza* subspecies magna. *Natural Products Journal* 3, pp. 35–41.
38. Dias, D. A. and S. Urban. 2009. Application of HPLC-NMR for the rapid chemical profiling of a Southern Australian sponge *Dactylospongia* sp. *Journal of Separation Science* 32, pp. 542–548.
39. Dias, D. A. and S. Urban. 2008. Phytochemical analysis of the Southern Australian marine alga *Plocamium mertensii* using HPLC-NMR. *Phytochemical Analysis* 19, pp. 453–470.
40. Urban, S. and M. Timmers. 2013. HPLC-NMR chemical profiling and dereplication studies of the marine brown alga *Cystophora torulosa*. *Natural Products Communication* 8, pp. 715–719.
41. Timmers, M. and S. Urban. 2011. Online (HPLC-NMR) and offline phytochemical profiling of the Australian plant *Lasiopetalum macrophyllum*. *Natural Products Communication* 6, pp. 1605–1616.
42. Brkljaca, R. and S. Urban. Phytochemical profiling and biological activity studies of the Southern Australian marine alga *Sargassum paradoxum* (unpublished results).

CHAPTER 3

HPLC-NMR for Chemical Profiling

Chapter 3 provides a review of the HPLC-NMR literature and details the recent advancements and applications of the technique. This work has been published as outlined below.

Journal publication resulting from this review:

Brkljača, Robert, & Urban, Sylvia. (2011). Recent Advancements in HPLC-NMR and Applications for Natural Product Profiling and Identification. *Journal of Liquid Chromatography & Related Technologies*, 34(12), 1063-1076.

RECENT ADVANCEMENTS IN HPLC-NMR AND APPLICATIONS FOR NATURAL PRODUCT PROFILING AND IDENTIFICATION

Robert Brkljača and Sylvia Urban

School of Applied Sciences, Health Innovations Research Institute (HIRi) RMIT University, Melbourne, Victoria, Australia

□ *This review provides a summary of the recent advances in high pressure liquid chromatography (HPLC) coupled to nuclear magnetic resonance (NMR) spectroscopy. Significant improvements have included the miniaturization of NMR components as well as the use of cryogenically cooled probes. Further hyphenated applications such as HPLC-SPE-NMR, column trapping and HPLC-NMR-MS are also discussed. Finally, an overview of the application of these methodologies to the profiling and dereplication of natural products is provided.*

Keywords advances, HPLC-NMR, hyphenated spectroscopy, natural products

INTRODUCTION

High pressure liquid chromatography (HPLC) coupled to nuclear magnetic resonance (NMR) spectroscopy (HPLC-NMR) was developed in 1978^[1] but has taken many years to evolve and become a more routine method for analysis. The initial draw-back for the hyphenated technique included the initial high costs and the lack of sensitivity.^[1] Over the years, developments in probe design and suppression techniques have enabled it to evolve into an effective method for principle component mixture analysis.^[1]

HPLC-NMR has various modes of operation, the two primary being on-flow and stop-flow, respectively.^[2] On-flow HPLC-NMR acquires solely ¹H NMR data and, as such, is most suitable for rapid identification of principle components. Stop-flow HPLC-NMR allows for longer acquisitions to

Address correspondence to Sylvia Urban, School of Applied Sciences, Health Innovations Research Institute (HIRi) RMIT University, GPO Box 2476V, Melbourne, Victoria 3001, Australia. E-mail: sylvia.urban@rmit.edu.au

be carried out on any one or more selected components, thereby resulting in improved spectra and the ability to also acquire 2D NMR data.^[2] Other HPLC-NMR modes such as time-slicing and loop collection are also becoming more commonly employed.^[3] Unfortunately, the lack of sensitivity remains somewhat of a drawback for the technique, with the limit of detection depending on a number of factors such as the magnetic field strength, the volume of the flow probe being used, and the mode of the experiment.^[4] However, in 2003 it was reported that for a 500 molecular weight analyte at a ¹H observation frequency of 600 MHz, the limit of detection was 100 ng for stop-flow and loop storage modes.^[5] This is a vast improvement in the detection limit of HPLC-NMR as compared to analyses conducted in the 1990s, which required anywhere between 150–500 ng.^[1] On-flow analyses rely heavily on sensitivity because analytes have short residence times in the NMR spectrometer. Providing that reasonable amounts of material are injected, stop-flow and loop collection make it possible for 2D NMR data such as COSY, TOCSY, and HSQC NMR spectra to be acquired. In spite of this, analyses such as natural product profiling require an improved detection limit and, therefore, efforts were focused on increasing the sensitivity of the technique.

This review discusses the more recent advancements in HPLC-NMR and how they have enhanced the sensitivity of the technique, enabling it to become a successful method for multicomponent analysis. The review also includes application of the various HPLC-NMR and related techniques to natural product analysis and identification.

MICROCOIL HPLC-NMR AND CAPILLARY NMR (CapNMR)

Undoubtedly the development of microcoil HPLC-NMR and capillary NMR (CapNMR) technologies have had a large impact on HPLC-NMR. Typically, NMR flow probes have volumes ranging from 40–120 μL .^[6] With the emergence of microcoil and CapNMR, which utilize active volumes of 2.5–5 μL ,^[7] the sensitivity of the technique dramatically increased. Both probes took advantage of reducing the flow cell diameter and the size of the receiver coils. By reducing the size of the cell and receiver coils, an increase in sensitivity resulted^[7] with a 5-fold increase in sensitivity being typically observed.^[8] The probes use a solenoid microcoil design^[9] compared to the traditional Helmholtz design that is achieved by wrapping a receiver coil directly around a capillary flow cell,^[7] with the cell and coil being placed in a magnetic susceptible fluid to reduce magnetic field inhomogeneities.^[7] The use of the solenoid receiver coils also allowed for the flow cell to be orientated horizontally in the NMR spectrometer. By

utilizing a horizontal orientation, a stronger coupling to the sample is observed that results in an increased sensitivity.^[7] Another advantage of the microcoil and CapNMR probes is in their ease of shimming, brought about from the smaller sample volumes and the coil design.^[7] In a similar fashion to conventional HPLC-NMR, microcoil HPLC-NMR can be run using different modes of operation such as on-flow and stop-flow.^[9]

Microcoil HPLC-NMR (Figure 1) is most suited for on-line HPLC-NMR analyses where components are separated and analyzed in a conventional HPLC-NMR system using either on-flow, stop-flow, or time slicing. CapNMR is used in off-line analyses whereby it is possible to inject single components or mixtures that have been previously isolated or fractionated. This can be achieved by either manually collecting the components and injecting them into the NMR spectrometer or alternatively by automatically injecting components that have been previously collected into a microtitre plate (Figure 1).^[10]

The CapNMR technique allows for the use of nondeuterated solvents in the off-line HPLC separation. This is attractive in that it reduces the analysis cost and it also allows for a wider range of solvents to be used. Previously isolated components are then redissolved in deuterated solvents and injected into the CapNMR flow probe. The advantage with this methodology is that very small amounts of deuterated solvents (approximately 6 μL) are needed.^[11] Using the CapNMR technique, ^1H NMR spectra can be obtained in minutes for samples in the 2–30 μg range.^[11]

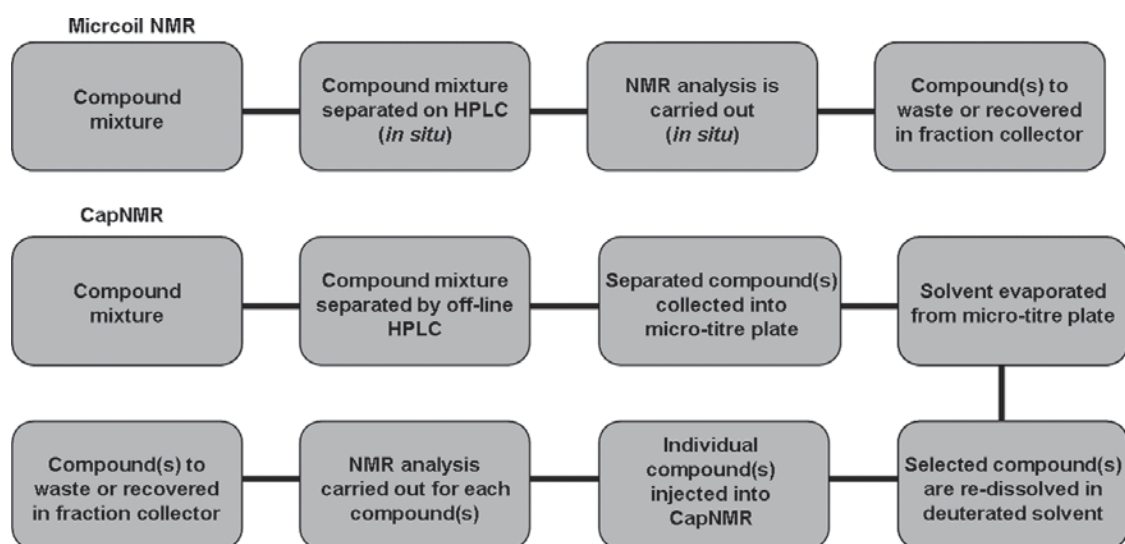


FIGURE 1 Flow chart variations of microcoil HPLC-NMR and CapNMR analyses.

CRYOGENICALLY COOLED PROBES

Noise observed in NMR spectra is created primarily by the receiver coils^[12] and a way to increase the signal-to-noise (S/N) ratio is to decrease the observed noise. This noise can be reduced by cryogenically cooling the receiver coils^[13] and other components such as the preamplifiers.^[12] The coils are cooled in a bath of liquid helium or with a stream of helium gas to a temperature of 15–30 K.^[13] The S/N ratios typically increase by a factor of 4^[12] compared to the same samples acquired with coils maintained at room temperature. Combining cryoprobe technology with microcoil technology has increased the sensitivity and detection limit of the technique by over 20 fold.^[14]

HPLC-SPE-NMR AND COLUMN TRAPPING

In recent years Solid Phase Extraction (SPE) has been included into the HPLC-NMR (Bruker NMR) set-up in an attempt to increase the amount of analyte in the flow cell. The SPE cartridge is placed after the HPLC separation and the technique allows for NMR data to be obtained for increased amounts of sample.^[15] Moreover, it allows for the use of non-deuterated solvents in the HPLC separation^[16] thereby reducing the cost for analysis dramatically and allowing for a wider range of solvents and higher gradients to be used in the separation.^[16] The SPE cartridges are kept in a nitrogen environment to avoid the risk of oxidation and a stream of nitrogen is used to dry the sample prior to washing the analyte off the cartridge.^[12] Repeated injections of the sample are made and the analyte of interest is collected on the SPE cartridge.^[12] Once sufficient quantities are collected, the cartridge is washed with a deuterated solvent which is then injected directly into the NMR flow cell (refer to Figure 2).^[12]

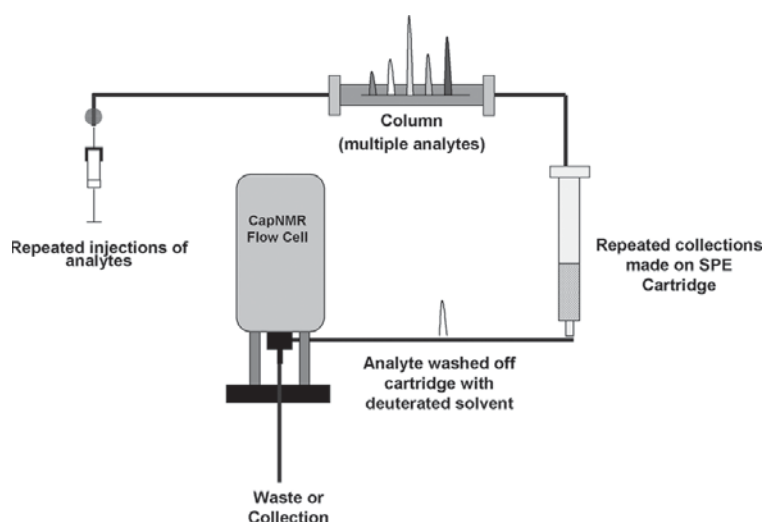


FIGURE 2 Schematic of HPLC-SPE-NMR (Bruker NMR) setup.

In this methodology it is important to ensure the analyte is eluted in a sharp band to maximize the amount of the analyte in the active volume of the flow cell.^[16] One final advantage of this set-up is that because a deuterated solvent is used in the analysis, suppression is generally unnecessary during the NMR acquisition.^[12]

A similar and parallel technique to HPLC-SPE-NMR is the use of automated column trapping. Unlike the SPE technique, this utilizes a C18 guard column to trap the analyte and is used for Varian HPLC-NMR systems.^[17] The HPLC-NMR is set up to automatically collect the analyte on the guard column and once collected, the system automatically back flushes the analyte as a sharp band into the flow probe.^[17] By placing a C18 guard column after the HPLC it is possible for the analyte to be collected and preconcentrated before it enters the flow probe.^[17] Using this technique, an increase in the S/N ratio of 14 fold was obtained^[17] and the advantage lies in the fact that it is faster than the SPE method described earlier as no drying of the samples or column washing is required. Both techniques provide a robust way to increase the amount of analyte and produce a higher quality NMR spectrum.

The HPLC-SPE-NMR technique can be extended to include mass spectrometry (MS), creating the hyphenated system HPLC-SPE-NMR-MS. The HPLC-SPE-NMR-MS technique diverts the eluant from the HPLC column to both the MS and SPE cartridge, which is split in a ratio of 95%/5% to the SPE cartridge and MS, respectively.^[18] Once the eluant has been diverted to both the MS and SPE cartridge, the technique follows the same principles as the HPLC-SPE-NMR technique.

HPLC-NMR-MS

HPLC-NMR provides invaluable spectroscopic data (UV profiles and NMR spectra), which is crucial in identifying compounds. Unfortunately, in many instances, NMR data alone (in conjunction with the UV data obtained from the HPLC) is insufficient to completely identify a compound, especially for new chemical entities. Further information such as mass spectrometry (MS) can assist further in compound identification. Previously MS had to be conducted off-line and separately from the HPLC-NMR process. However, in recent years, successful hyphenation of HPLC-NMR-MS has been achieved whereby all of the NMR and MS data is obtained in a single acquisition.^[19] The HPLC-NMR-MS hyphenation technique utilizes a splitter to divert the eluant from the HPLC column to both the NMR flow probe and to the MS [2] and this set-up is known as a parallel configuration (Figure 3).^[20]

Owing to the vast differences in the sensitivities of MS and NMR, the splitter is set-up to divert considerably higher amounts of the analyte to

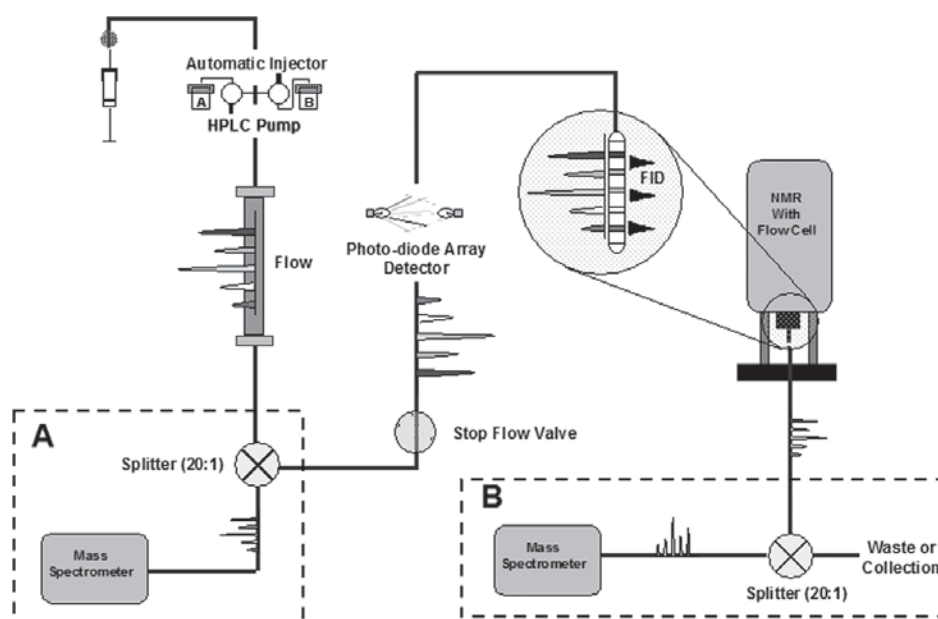


FIGURE 3 Schematic of HPLC-NMR-MS showing parallel (A) and series (B) configurations.

the NMR than the MS. Using a splitting ratio of 20:1 allows for the MS to operate at optimal conditions and for sufficient amounts of the analyte to be detected by the NMR spectrometer.^[20]

HPLC-NMR-MS can also be run in the series configuration (Figure 3) whereby the splitter and MS are placed after the NMR spectrometer.^[20] This set up has the advantage of being a simpler system which can be easily disconnected to allow for separate NMR and MS analyses to be conducted.^[20] The disadvantage of the series configuration in HPLC-NMR-MS is that it introduces the opportunity for the peaks to disperse or for the retention times of the peaks to drift as they reach the MS.^[20] Despite which configuration is employed, HPLC-NMR-MS is unquestionably a powerful and valuable technique for both rapid compound identification/profiling and for complex mixture analysis.

NATURAL PRODUCT APPLICATIONS

The application of HPLC-NMR to assist in natural product profiling and identification has been attracting more interest in recent years, particularly in the analysis of marine natural products.^[21–23] As a result of the advancements made in HPLC-NMR, many publications have appeared in the literature, which have taken advantage of these improvements. A brief overview of some of these more recent analyses is provided in the following sections.

On-Flow and Stop Flow HPLC-NMR Analyses

In 2009, on-flow and stop-flow HPLC-NMR, utilizing a 60 μL (active volume) flow probe, was used to profile the crude extract of a southern Australian marine alga, *Laurencia filiformis*. This resulted in the identification of two new compounds, cycloisoallolaurinterol (1) and isoallolaurinterol (2), together with the ability to monitor on-line chemical conversions (Figures 4 and 5).^[23]

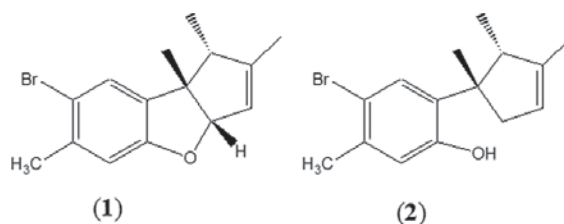


FIGURE 4 Chemical structures of cycloisoallolaurinterol (1) and isoallolaurinterol (2).

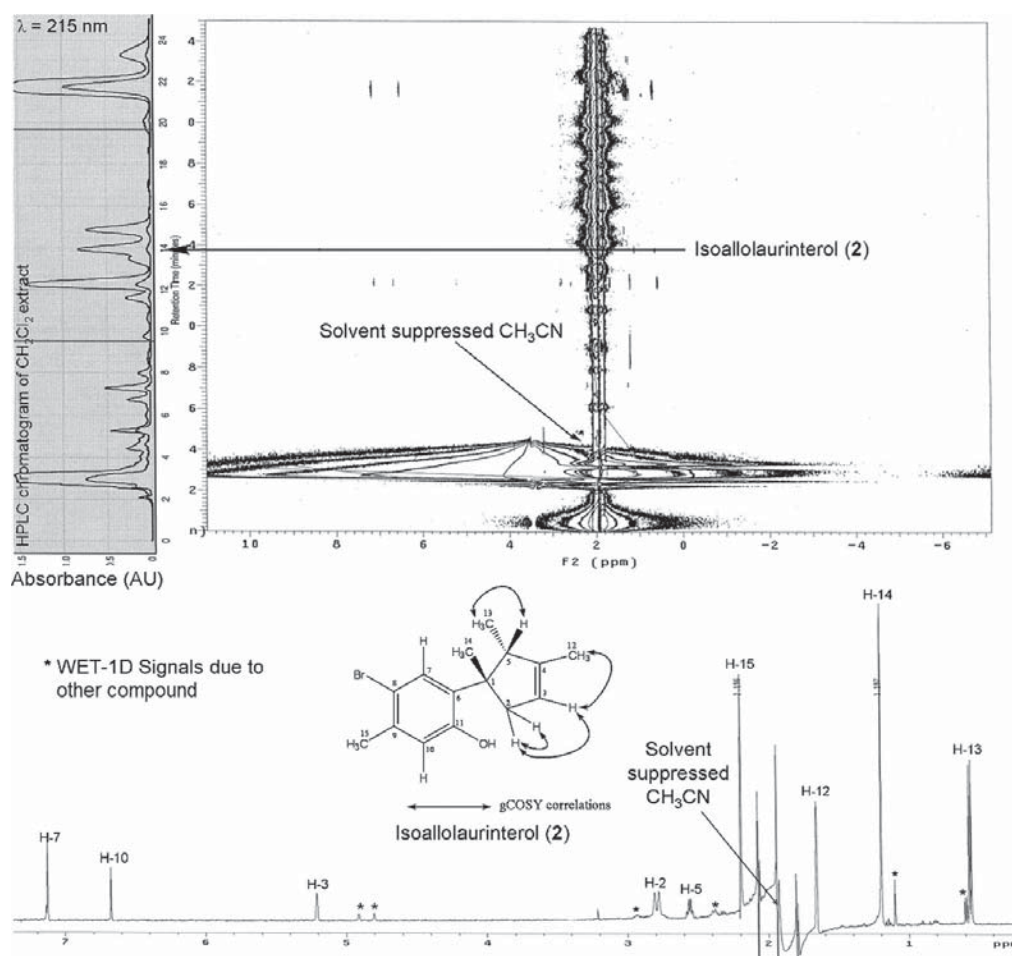


FIGURE 5 2D-HPLC-NMR contour plot with extracted WET-1D ^1H NMR of isoallolaurinterol (2).

This application of HPLC-NMR was also able to demonstrate the importance of using the technique to identify unstable, inter-converting secondary metabolites.

Other studies conducted by the same research group have focused on rapidly profiling the crude extract of a southern Australian marine sponge, *Dactylospongia* sp.^[22] and an Australian marine alga, *Plocamium mertensii*.^[21] The study of the marine red alga, *Plocamium mertensii* resulted in the partial identification of several polyhalogenated monoterpenes (3)–(6) using both on-flow and stop-flow HPLC-NMR (Figures 6 and 7). Subsequent off-line characterization studies also led to a number of chemical shift re-assignment for (5).^[21] Time-slicing was also employed in the HPLC-NMR analysis to resolve the two closely eluting secondary metabolites (5) and (6).^[21]

These analyses were able to demonstrate successful natural product profiling using crude extracts for the HPLC-NMR analyses, whereas others have demonstrated the use of enriched fractions in their HPLC-NMR studies.^[24]

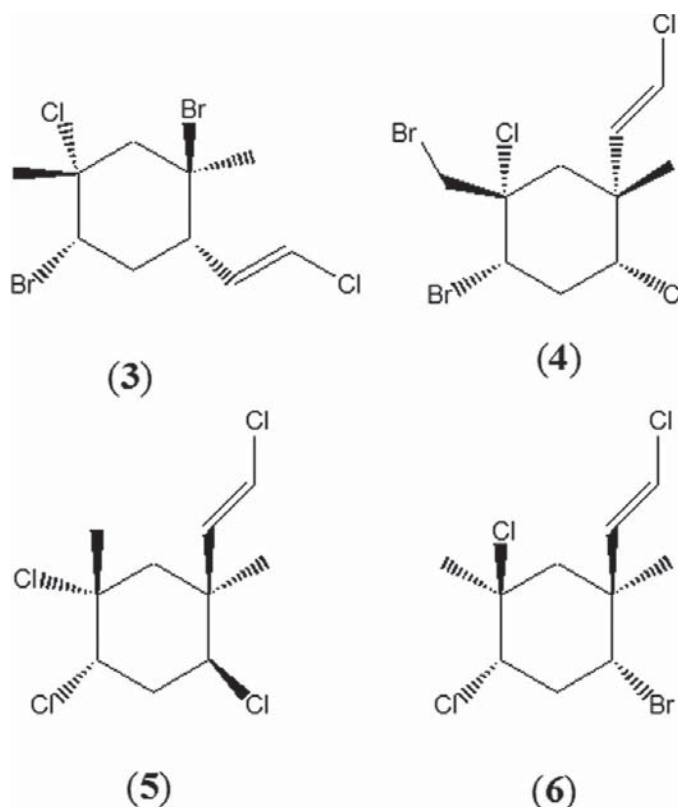


FIGURE 6 Chemical structures of compounds identified from *Plocamium mertensii*.

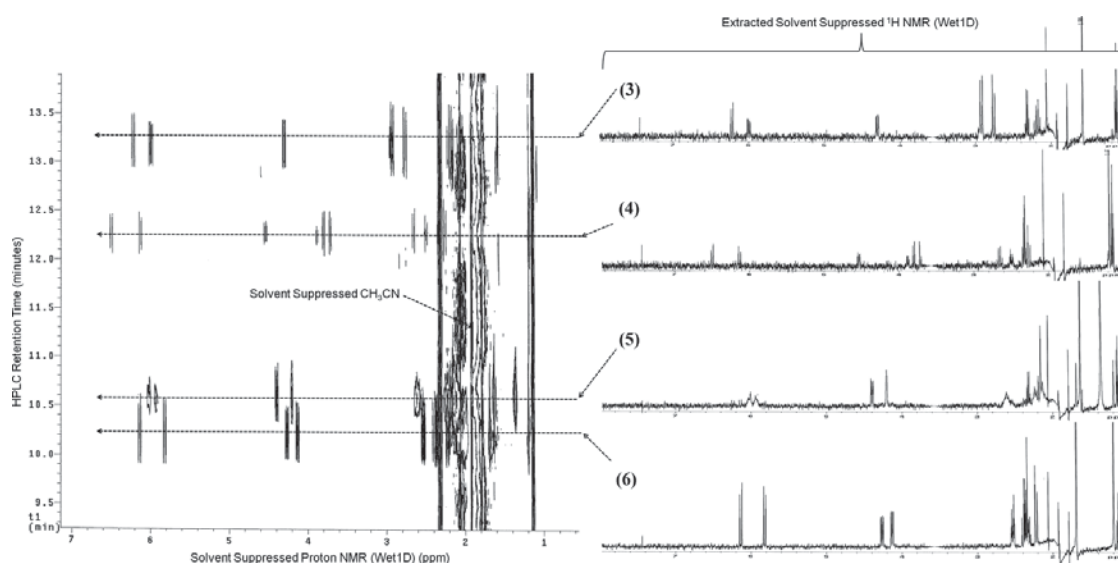
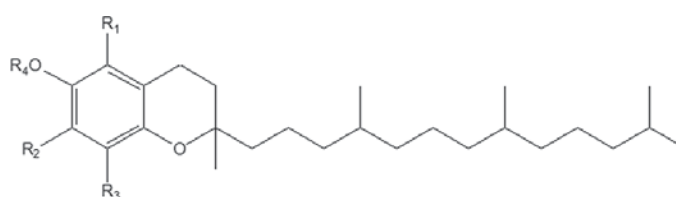


FIGURE 7 2D-HPLC-NMR contour plot of compounds (3)–(6) from *Plocamium mertensii*.

Microcoil HPLC-NMR Analyses

In 2005, a 1.5 μL (active volume) microcoil flow probe was employed to identify three compounds in a rosemary extract using the stop-flow mode.^[25] The retention times and UV data of the three compounds was sufficient for identification, but NMR data was also acquired to further confirm their identities.^[25] In 2004, another study dealt with the application of the microcoil HPLC-NMR technique for the separation of six tocopherol homologues (7)–(12) from a standard solution mixture (Figure 8). These compounds were subsequently identified using a microcoil flow probe with an active volume of 1.5 μL using on-flow and stop-flow modes.^[26]



- (7) $R_1 = \text{H}$, $R_2 = \text{H}$, $R_3 = \text{H}$, $R_4 = \text{H}$
- (8) $R_1 = \text{H}$, $R_2 = \text{H}$, $R_3 = \text{CH}_3$, $R_4 = \text{H}$
- (9) $R_1 = \text{H}$, $R_2 = \text{CH}_3$, $R_3 = \text{CH}_3$, $R_4 = \text{H}$
- (10) $R_1 = \text{CH}_3$, $R_2 = \text{H}$, $R_3 = \text{CH}_3$, $R_4 = \text{H}$
- (11) $R_1 = \text{CH}_3$, $R_2 = \text{CH}_3$, $R_3 = \text{CH}_3$, $R_4 = \text{H}$
- (12) $R_1 = \text{CH}_3$, $R_2 = \text{CH}_3$, $R_3 = \text{CH}_3$, $R_4 = \text{COCH}_3$

FIGURE 8 Chemical structures of the six tocopherol derivatives identified.

CapNMR Analyses

In 2005, CapNMR was successful in identifying thirteen new steroids from fireflies such as compound (13) (Figure 9).^[27] Using this methodology, 2D NMR data could be acquired for each fraction of interest.^[27]

CapNMR has also been used successfully to identify new halichondrin derivatives from a New Zealand marine sponge, *Lissodendoryx* sp.^[28] This particular sponge had previously been investigated, but as a result of the improvements in NMR sensitivity (acquisition of the CapNMR probe), the sponge extract was re-examined. This resulted in four new halichondrin derivatives (14)–(17) being identified which displayed different structural features to halichondrin B (18) on the left-hand side of the compound (Figure 10).^[28]

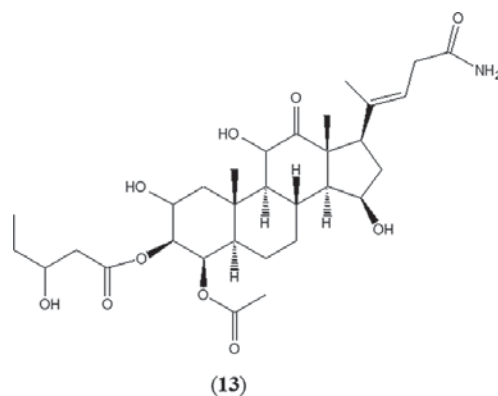


FIGURE 9 Chemical structure of one of the steroids identified from fireflies.

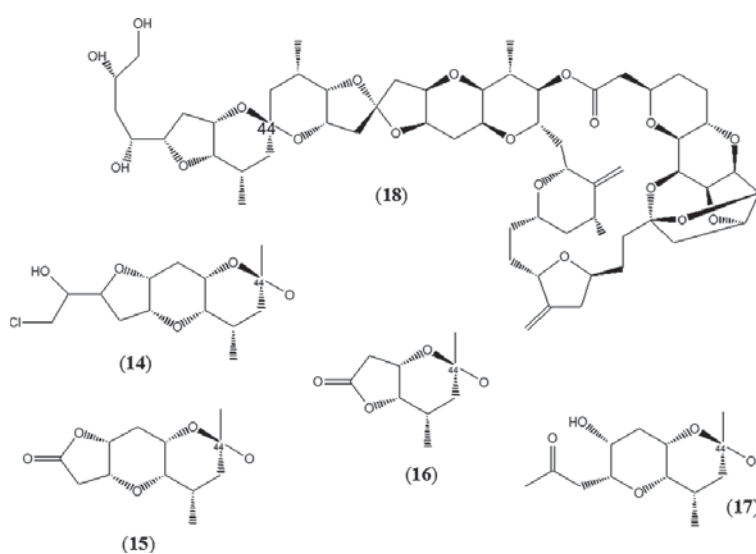


FIGURE 10 Chemical structures of halichondrin B (18) and the new halichondrin derivatives (14–17).

HPLC-SPE-NMR Analyses

In 2007 HPLC-SPE-NMR was applied for the rapid identification of the major constituents in the plant *Hubertia* sp., including three new quinic acids (19), (20), and (21) (Figure 11).^[15]

Also in 2007, it was demonstrated that the HPLC-SPE-NMR technique was able to identify and determine structures of compounds comprising <0.5% of the extract.^[29]

A 2008 study, which focused on the metabolism of a synthesized compound, was able to successfully demonstrate the use of a HPLC-SPE-NMR-MS system. New compounds formed after metabolism were identified using the HPLC-SPE-NMR-MS set-up.^[30]

Column Trapping HPLC-NMR Analyses

In 2006 the use of a HPLC-NMR system with automated column trapping was demonstrated.^[17] A mixture of three nonsteroidal anti-inflammatory drugs were separated and preconcentrated on a C18 guard column prior to injection into the NMR flow probe.^[17] It was reported that the automated column trapping technique yielded gains of up to 14-fold in the sensitivity of the analytes.^[17]

HPLC-NMR-MS Analyses

In 2008, a parallel HPLC-NMR-MS system was utilized to identify active metabolites in *Fischerella ambigua*, a strain of cyanobacteria.^[10] A bioactive

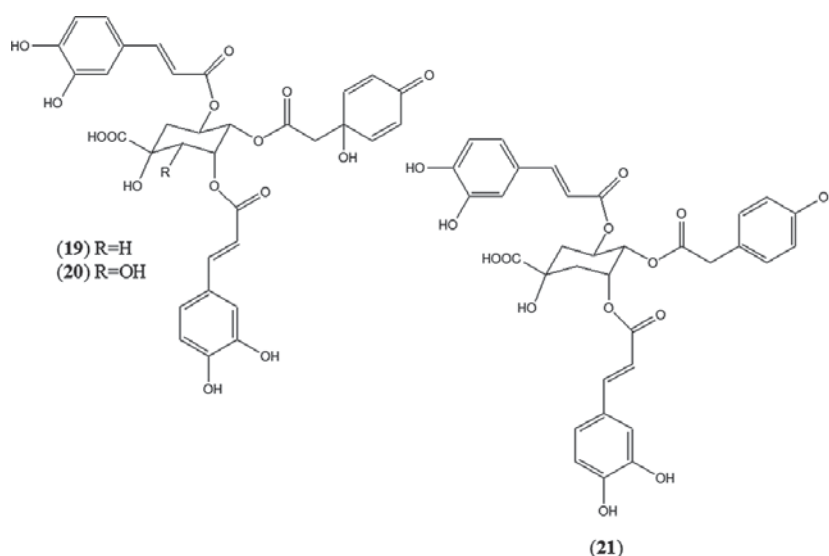


FIGURE 11 Chemical structures of the three new quinic acids (19–21) identified from the plant *Hubertia* sp.

extract was fractionated using silica gel chromatography which yielded a bioactive fraction showing anti-bacterial activity against *Mycobacterium tuberculosis*.^[10] The bioactive fraction was then separated on a HPLC column and the eluant split between the MS and a microtitre plate fraction collector. The fractions in the microtitre plate were evaporated and then resuspended in deuterated NMR solvent and sequentially injected into the flow probe.^[10] Once the MS and NMR data were obtained, both sets of data were compared and correlated to identify the metabolites in the Cyanobacteria.^[10] Several known compounds were identified as well as one unknown compound, which was later identified after a scaled-up growth and re-extraction of the organism.^[10,31,32]

CONCLUSION

The incorporation of the advancements in HPLC-NMR have enabled the methodology to become a robust and powerful technique for rapidly profiling and dereplicating mixtures such as natural product extracts and enriched fractions. It is now possible to determine chemical structures from much smaller quantities and this, in turn, has resulted in the identification of a number of new compounds. The recent advancements have also reduced analysis time, allowing for faster throughput of samples. HPLC-NMR is an especially relevant methodology to employ in the study of unstable or light sensitive compounds. A search conducted in the Scifinder database clearly indicates that the number of publications utilizing HPLC-NMR and closely related hyphenated spectroscopic techniques, as discussed in this review, have steadily increased since its development and implementation. A review of the application of HPLC-NMR methodologies tends to suggest that interest peaked in approximately 2003, but has not shown any signs of abating. It is expected that further future advancements in the hyphenated technique will also have a large impact on the ability to employ the methodology even more successfully, with further improvements to the limits of detection anticipated.

REFERENCES

1. Urban, S.; Separovic, F. Developments in Hyphenated Spectroscopic Methods in Natural Product Profiling. *Front. Drug Des. Discovery* **2005**, *1*, 113–166.
2. Cazes, J. *Encyclopedia of Chromatography*, 3rd ed., CRC Press: Boca Raton, 2010.
3. Urban, S. LC-NMR: Profiling and Dereplication of Natural Product Extracts. *Chem. Aust.* **2006**, *73* (8), 15–17.
4. Wolfender, J.-L.; Marti, G.; Queiroz, E. F. Advances in Techniques for Profiling Crude Extracts and for the Rapid Identification of Natural Products: Dereplication, Quality Control and Metabolomics. *Curr. Org. Chem.* **2010**, *14* (16), 1808–1832.
5. Corcoran, O.; Spraul, M. LC-NMR-MS in Drug Discovery. *Drug Discovery Today* **2003**, *8* (14), 624–631.

6. Wolfender, J.-L.; Queiroz, E. F.; Hostettmann, K. The Importance of Hyphenated Techniques in the Discovery of New Lead Compounds from Nature. *Expert Opin. Drug Discovery* **2006**, *1* (3), 237–260.
7. Schroeder, F. C.; Gronquist, M. Extending the Scope of NMR Spectroscopy with Microcoil Probes. *Angew. Chem. Int. Ed.* **2006**, *45* (43), 7122–7131.
8. Lewis, R. J.; Bernstein, M. A.; Duncan, S. J.; Sleight, C. J. A Comparison of Capillary-Scale LC-NMR with Alternative Techniques: Spectroscopic and Practical Considerations. *Magn. Reson. Chem.* **2005**, *43* (9), 783–789.
9. Kuehnle, M.; Holtin, K.; Albert, K. Capillary NMR Detection in Separation Science. *J. Sep. Sci.* **2009**, *32* (5–6), 719–726.
10. Lin, Y.; Schiavo, S.; Orjala, J.; Vouros, P.; Kautz, R. Microscale LC-MS-NMR Platform Applied to the Identification of Active Cyanobacterial Metabolites. *Anal. Chem.* **2008**, *80* (21), 8045–8054.
11. Sun Lin, J.; Mahyudin, N. A.; Chamyuang, S.; Blunt, J. W.; Cole, T.; Lang, G.; Mitova, M. I.; van der Sar, S.; Munro, M. H. G. Less is More: Dereplication and Discovery Using CapNMR Techniques, Mannapro XII: 12th International Symposium on Marine Natural Products, Queenstown, New Zealand, Feb. 4–9, 2007.
12. Staerk, D.; Lambert, M.; Jaroszewski, J. W. HPLC-NMR Techniques for Plant Extract Analysis. *Med. Plant Biotech.* **2007**, *1*, 29–48.
13. Martin, G. E. Small-Volume and High-Sensitivity NMR Probes. *Ann. Rep. NMR Spectrosc.* **2005**, *56*, 1–96.
14. Molinski, T. F. Nanomole-Scale Natural Products Discovery. *Curr. Opin. Drug Discovery* **2009**, *12* (2), 197–206.
15. Sprogoe, K.; Staerk, D.; Jaeger, A. K.; Adersen, A.; Hansen, S. H.; Witt, M.; Landbo, A.-K. R.; Meyer, A. S.; Jaroszewski, J. W. Targeted Natural Product Isolation Guided by HPLC-SPE-NMR: Constituents of *Hubertia* Species. *J. Nat. Prod.* **2007**, *70* (9), 1472–1477.
16. Jaroszewski, J. W. Hyphenated NMR Methods in Natural Products Research, Part 2: HPLC-SPE-NMR and Other New Trends in NMR Hyphenation. *Planta Med.* **2005**, *71* (9), 795–802.
17. Djukovic, D.; Liu, S.; Henry, I.; Tobias, B.; Raftery, D. Signal Enhancement in HPLC/Microcoil NMR Using Automated Column Trapping. *Anal. Chem.* **2006**, *78* (20), 7154–7160.
18. Schlotterbeck, G.; Ceccarelli, S. M. LC-SPE-NMR-MS: A Total Analysis System for Bioanalysis. *Bioanalysis* **2009**, *1* (3), 549–559.
19. Down, S. LC-NMR/MS. *Spectrosc. Eur.* **2004**, *16* (3), 8, 10, 12, 14.
20. Yang, Z. Online Hyphenated Liquid Chromatography-Nuclear Magnetic Resonance Spectroscopy-Mass Spectrometry for Drug Metabolite and Nature Product Analysis. *J. Pharm. Biomed. Anal.* **2006**, *40* (3), 516–527.
21. Dias, D. A.; Urban, S. Phytochemical Analysis of the Southern Australian Marine Alga, *Plocamium mertensii* Using HPLC-NMR. *Phytochem. Anal.* **2008**, *19*, 453–470.
22. Dias, D. A.; Urban, S. Application of HPLC-NMR for the Rapid Chemical Profiling of a Southern Australian Sponge, *Dactylospongia* sp. *J. Sep. Sci.* **2009**, *32* (4), 542–548.
23. Dias, D. A.; White, J. M.; Urban, S. *Laurencia filiformis*: Phytochemical Profiling by Conventional and HPLC-NMR Approaches. *Nat. Prod. Comm.* **2009**, *4* (2), 157–172.
24. Wolfender, J.-L.; Ndjoko, K.; Hostettmann, K. The Potential of LC-NMR in Phytochemical Analysis. *Phytochem. Anal.* **2001**, *12*, 2–22.
25. Exarchou, V.; Krucker, M.; van Beek, T. A.; Vervoort, J.; Gerothanassis, I. P.; Albert, K. LC-NMR Coupling Technology: Recent Advancements and Applications in Natural Products Analysis. *Magn. Reson. Chem.* **2005**, *43* (9), 681–687.
26. Krucker, M.; Lienau, A.; Putzbach, K.; Grynbaum, M. D.; Schuler, P.; Albert, K. Hyphenation of Capillary HPLC to Microcoil ¹H NMR Spectroscopy for the Determination of Tocopherol Homologues. *Anal. Chem.* **2004**, *76* (9), 2623–2628.
27. Gronquist, M.; Meinwald, J.; Eisner, T.; Schroeder, F. C. Exploring Uncharted Terrain in Nature's Structure Space Using Capillary NMR Spectroscopy: 13 Steroids from 50 Fireflies. *J. Amer. Chem. Soc.* **2005**, *127* (31), 10810–10811.
28. Hickford, S. J. H.; Blunt, J. W.; Munro, M. H. G. Antitumour Polyether Macrolides: Four New Halichondrins from the New Zealand Deep-Water Marine Sponge *Lissodendoryx* sp. *Bioorg. Med. Chem.* **2009**, *17*, 2199–2203.

29. Lambert, M.; Wolfender, J. -L.; Strk, D.; Christensen, S. B.; Hostettmann, K.; Jaroszewski, J. W. Identification of Natural Products Using HPLC-SPE Combined with CapNMR. *Anal. Chem.* **2007**, *79* (2), 727–735.
30. Ceccarelli, S. M.; Schlotterbeck, G.; Boissin, P.; Binder, M.; Buettelmann, B.; Hanlon, S.; Jaeschke, G.; Kolczewski, S.; Kupfer, E.; Peters, J.-U.; Porter, R. H. P.; Prinssen, E. P.; Rueher, M.; Ruf, I.; Spooren, W.; Stampfli, A.; Vieira, E. Metabolite Identification via LC-SPE-NMR-MS of the *in vitro* Biooxidation Products of a Lead mGlu5 Allosteric Antagonist and Impact on the Improvement of Metabolic Stability in the Series. *Chem. Med. Chem.* **2008**, *3* (1), 136–144.
31. Mo, S.; Kronic, A.; Chlipala, G.; Orjala, J. Antimicrobial Ambiguine Isonitriles from the Cyanobacterium *Fischerella ambigua*. *J. Nat. Prod.* **2009**, *72* (5), 894–899.
32. Mo, S.; Kronic, A.; Santarsiero, B.; Franzblau, S.; Orjala, J. Hapalindole-Related Alkaloids from the Cultured Cyanobacterium *Fischerella ambigua*. *Phytochemistry* **2010**, *71* (17–18), 2116–2123.

CHAPTER 4

Limit of Detection in HPLC-NMR

Chapter 4 describes the limit of detection (LOD) of HPLC-NMR, as applied to a 500 MHz NMR spectrometer, equipped solely with a 60 μ L flow cell. The LOD was established for five key NMR experiments and the results have been published as outlined below. Appendix A contains supplementary information relevant to this study.

Journal publication resulting from this study:

Brkljača, Robert, & Urban, Sylvia. (2015). Limit of Detection Studies for Application to Natural Product Identification using High Performance Liquid Chromatography Coupled to Nuclear Magnetic Resonance Spectroscopy. *Journal of Chromatography A*, 1375, 69-75.



Limit of detection studies for application to natural product identification using high performance liquid chromatography coupled to nuclear magnetic resonance spectroscopy



Robert Brkljača, Sylvia Urban*

School of Applied Sciences, Health Innovations Research Institute (HIRI), RMIT University, GPO Box 2476V, Melbourne, Victoria 3001, Australia

ARTICLE INFO

Article history:

Received 20 August 2014
Received in revised form 16 October 2014
Accepted 27 November 2014
Available online 4 December 2014

Keywords:

HPLC–NMR
Limit of detection (LOD)
Natural products
Hyphenated spectroscopy
Cystophora subfarcinata

ABSTRACT

In the pursuit of new natural products, the demand to rapidly identify compounds present, in ever decreasing amounts, in complex crude extracts has become a limiting factor. Despite improvements in HPLC–NMR hardware and pulse sequences, no extensive limit of detection (LOD) investigations have been reported for the acquisition of 2D NMR spectroscopic experiments acquired through HPLC–NMR. In this study the LOD for five key 1D and 2D NMR spectroscopic experiments have been established, using two reference compounds, including the on-flow (WET 1D proton), stop-flow (WET1D proton), gCOSY, HSQCAD and gHMBCAD NMR experiments. The LOD for all of the NMR experiments were within the range of 700 ng to 1 mg for the set of fixed experimental parameters implemented. For principle components in a complex multi-component mixture, this would allow for in situ compound identification. HPLC–NMR analysis was employed to investigate the principle components present in a marine brown alga crude extract, *Cystophora subfarcinata*.

Crown Copyright © 2014 Published by Elsevier B.V. All rights reserved.

1. Introduction

HPLC–NMR remains an underutilised technique particularly in the identification of natural products. The technique was developed in the 1970s [1] but has only recently become a more routine method for analysis. Developments in suppression methodologies and probe design have largely overcome the initial drawbacks of the insensitivity that is so widely attributed to the instrumental technique [1,2]. HPLC–NMR is now becoming recognised as being pivotal for the on-line identification of natural products [3], particularly those that are unstable and in its ability to resolve closely eluting compounds. While HPLC–MS offers increased sensitivity and is frequently employed for structure identification, for unknown compounds with isobaric masses, HPLC–NMR is the only method that provides structural information such as the ability to differentiate between structural isomers such as compounds with varying substitution patterns.

There are two primary modes of operation for HPLC–NMR. These include the on-flow and stop-flow HPLC–NMR methodologies respectively [4]. Rapid identification of general structure class(es) for principle components is frequently possible in the

on-flow mode [1,2]. Unlike on-flow HPLC–NMR, which acquires continuous ^1H NMR data as the sample is separated, in the stop-flow HPLC–NMR mode the HPLC pumps are paused to allow for the analysis of a single component in the NMR flow cell for an indefinite period. This allows for extended NMR acquisition times to be implemented and therefore results in improved signal to noise (S/N) NMR spectra as well as permitting 2D NMR experiments to be acquired [4].

The sensitivity of HPLC–NMR is influenced by the magnetic field strength, the volume of the flow probe being used and the mode of the HPLC–NMR experiment [5]. In 2002, a limit of detection (LOD) of 100 ng was reported for a 600 MHz system using either the stop-flow or loop storage modes for proton observations for a compound of molecular weight of 500 g/mol [6]. While a range of NMR experiments including ^1H , COSY, NOESY, ROESY, HSQC and HMBC NMR experiments have been carried out using various HPLC–NMR systems, no LOD has been reported for these experiments [2]. In the case of HMBC NMR spectra, these experiments have been acquired on HPLC–NMR systems, equipped with cold probes, microcoils or after pre-concentration steps [2]. A study recently conducted by the Marine and Terrestrial Natural Product (MATNAP) research group has resulted in the first acquisition of a gHMBCAD NMR spectrum, acquired on a 500 MHz HPLC–NMR system solely equipped with a 60 μL flow cell (active volume) without the use of any pre-concentration or cold probes [7]. We have also reported several

* Corresponding author. Tel.: +61 3 9925 3376; fax: +61 3 9925 3747.
E-mail address: sylvia.urban@rmit.edu.au (S. Urban).

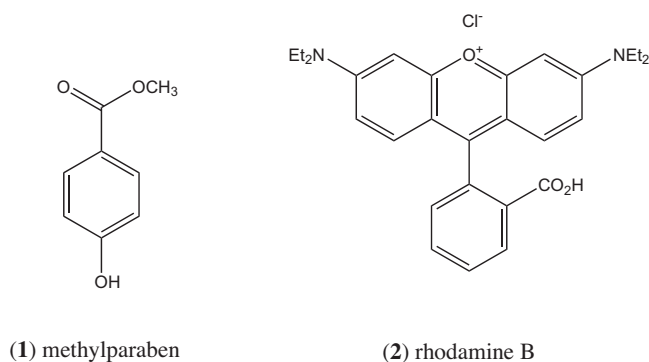


Fig. 1. Structures of the reference compounds employed for the determination of the LOD for the 1D and 2D NMR spectroscopic experiments acquired via HPLC–NMR.

instances where HPLC–NMR has been successful in identifying new, unstable compounds that could not be isolated by conventional off-line approaches [2,7–9].

The current study established the LOD for various common 1D and 2D NMR experiments using two reference compounds (Fig. 1), and found that the LOD was well within the range that is typically observed for components occurring within natural product crude extracts.

2. Materials and methods

2.1. Instrumentation

The HPLC–NMR analyses were carried out on a 500 MHz Agilent DD2 NMR spectrometer equipped with a Varian ^1H [^{13}C] pulsed field gradient flow probe with a 60 μL active volume flow cell coupled to a Varian Prostar 210 solvent delivery system, a Prostar 430 Autosampler and a Prostar 335 PDA detector. The HPLC–NMR analyses were carried out using a CORBA communication and operated with Vnmrj software. The 2H resonance observed from the D_2O was used to obtain field-frequency lock. The resonances from the HOD and the methyl of the acetonitrile were suppressed using the WET solvent suppression experiment [10]. The residual HOD resonance of D_2O was referenced to 4.64 ppm. Indirectly detected ^{13}C NMR shifts were referenced to the unified TMS scale with a frequency ratio of 25.15 [11]. For both on-flow and stop-flow HPLC–NMR modes 50 μL injections of the two reference compounds (methylparaben and rhodamine B) were injected onto an Agilent Eclipse Plus C_{18} (150 \times 4.6) 5 μm HPLC column using a solvent composition of 50% $\text{CH}_3\text{CN}/\text{D}_2\text{O}$ at a flow rate of 0.8 mL/min.¹

2.2. Reference compounds and solvents

Speciality solvents were used for the HPLC–NMR analyses to minimise the need for solvent suppression. Reversed phase HPLC–NMR was carried out using a $\text{CH}_3\text{CN}/\text{D}_2\text{O}$ HPLC solvent system. Acetonitrile (HPLC–NMR grade) was purchased from Fluka Analytical, which had been purified (glass distilled) to ensure only trace amounts of propionitrile were present. D_2O (99.9%) was purchased from Cambridge Isotope Laboratories, Inc. To determine the LOD for the various NMR experiments conducted via HPLC–NMR, two reference compounds were selected that would

¹ It is important to note that this particular HPLC–NMR system utilises solely D_2O and CH_3CN as mobile phase solvents. The use of methanol as an eluent is found to irreversibly stick to the HPLC tubing and flow cell, and is therefore not recommended for HPLC–NMR use. In addition samples must be dissolved in either D_2O or HPLC–NMR grade CH_3CN or a combination of the two solvents for similar reasons.

readily dissolve in CH_3CN and D_2O . One of the standard compounds selected was of low molecular weight, namely methylparaben (152.15 g/mol) (Ajax) and the other compound was of a medium to high molecular weight, namely rhodamine B (479.01 g/mol) (Gurr). These compounds were selected as they were readily available, highly soluble in acetonitrile, display a variety of chemical shift environments and multiplicities/coupling constants, together with the fact that they represent the typical range of molecular weights frequently encountered in small molecule natural product isolation and identification studies.

2.3. Preparation of reference compound solutions for HPLC–NMR LOD studies

Standards of the methylparaben reference compound were prepared so that these would yield injected amounts of 1000, 500, 200, 50, 25, 15, 10, 5, 2.5, 1, 0.7 and 0.5 μg per 50 μL injection respectively. Based on the S/N observed in the NMR spectra obtained for the methylparaben reference compound, the rhodamine B reference compound standards were increased since a higher molecular weight compound would require a greater amount to be injected to achieve a reasonable S/N . Therefore rhodamine B was prepared so that injected amounts of 1000, 500, 250, 100 and 50 μg per 50 μL injection respectively were achieved.

2.4. NMR pulse sequences

The NMR pulse sequences used for this study included the on-flow WET 1D and in the stop-flow mode the WET1D, gCOSY, HSQCAD and gHMBCAD NMR experiments. All NMR experiments were carried out at 25 $^\circ\text{C}$ and utilised the standard experimental parameters supplied by the Vnmrj software unless otherwise stated. During the WET suppression, decoupling of the ^{13}C satellites was enabled. In the on-flow WET1D NMR experiment, WET suppression was utilised followed by acquisition of four scans (and two steady state scans) for each subsequent spectrum. The stop-flow WET1D NMR experiment utilised suppression sequences for both the CH_3CN and HDO resonances (suppression at 2.82 and 4.64 ppm respectively, and was acquired for 64 scans (ns) for a total acquisition time of 3 min 12 s (fn = 32,768, at = 1.81939, np = 32,960, lb = 0.5). Each of the two dimensional NMR experiments utilised the WET solvent suppression pulse sequence prior to acquisition. The gCOSY NMR experiment was acquired for four scans (ns) and 256 increments (ni), for a total acquisition time of 20 min 59 s (fn = 4096, fn1 = 4096, at = 0.148378, np = 2688, weighting = sqsinebell). The HSQCAD NMR experiment utilised a delay time (d1) of 1.5 s, and was acquired for 16 scans (ns) and 256 increments (ni), for a total acquisition time of 4 h 7 min (fn = 4096, fn1 = 2048, at = 0.150034, np = 2718, $^1\text{J}_{\text{HC}}$ = 146 Hz, weighting = Gaussian). The gHMBCAD NMR experiment utilised a delay time (d1) of 0.8 s, and was acquired for 64 scans (ns) and 512 increments (ni), for a total acquisition time of 20 h 50 min (fn = 4096, fn1 = 4096, at = 0.132701, np = 2404, $^1\text{J}_{\text{HC}}$ = 8 Hz, weighting = Gaussian). Each of the pulse sequences contained the WET solvent suppression procedure developed by Smallcombe et al., commonly employed on Varian (Agilent) HPLC–NMR systems, which selectively suppresses the residual signals of D_2O and CH_3CN , to substantially increase the detection sensitivity of the analytes.

2.5. Marine brown alga specimen

The marine brown alga (*Cystophora subfarinata*) was collected at low tide on 22 January, 2006 from the Borough of Queenscliff, near Point Lonsdale, Victoria, Australia. The alga was identified by Dr G. Kraft (The University of Melbourne, Victoria, Australia) and a voucher specimen designated the code number 2006-11 is

deposited at the School of Applied Sciences (Discipline of Chemistry), RMIT University.

2.6. Marine alga extraction

The frozen marine alga (20.3 g, wet weight) was extracted with 3:1 methanol/dichloromethane (1 L). The crude extract was then decanted and concentrated under reduced pressure and sequentially solvent partitioned (triturated) into dichloromethane and methanol soluble extracts respectively. HPLC–NMR and HPLC–MS was carried out on the dichloromethane soluble extract of the alga. The dichloromethane extract (741.9 mg) was dissolved in HPLC–NMR grade CH₃CN and filtered through a 0.45 PTFE membrane filter, whereby each injection (50 μL) represented 3520 μg of the crude extract.

2.7. HPLC–NMR conditions for marine alga analysis

For both the on-flow and stop-flow HPLC–NMR analyses 50 μL injections (representing 3520 μg) of the dichloromethane crude extract of the alga were injected onto an Agilent Eclipse Plus C₁₈ (150 × 4.6) 5 μm HPLC column using a solvent composition of 75% CH₃CN/D₂O at a flow rate of 1.0 mL/min.

2.8. HPLC–MS conditions for marine alga analysis

HRESI LC–MS was carried out on an Agilent 6540 Series Q-TOF system (ESI operation conditions of 12 L/min N₂, 325 °C drying gas temperature and 3500 V capillary voltage) equipped with an Agilent 1260 Series LC solvent delivery module (75% CH₃OH at a flow rate of 1.0 mL/min) in both the negative and positive ionisation modes using an Agilent Eclipse Plus C₁₈ (4.6 × 150) 5 μm HPLC column. The instrument was calibrated using the 'Agilent Tuning Mix' with purine as the reference compound and the Hewlett–Packard standard HP0921.

3. Results and discussion

3.1. Limit of detection (LOD) and dynamic linearity

Several approaches exist for determining the detection limit depending on whether the procedure is non-instrumental or instrumental. For hyphenated methods, the limit of detection (LOD) is generally defined by the performance of the less-sensitive detector. In analytical procedures that exhibit baseline noise such as NMR spectroscopy, determination of the *S/N* ratio is performed. A *S/N* ratio of 3 is generally considered acceptable for estimating the detection limit [12]. For the structural elucidation of unknown compounds it is necessary to observe all signals in the NMR spectrum and so the *S/N* of the smallest peak must be detected and used for the LOD determination.

The LOD was found to vary for each NMR experiment conducted. The LOD for the on-flow and stop-flow WET1D NMR experiments was established based on a *S/N* of 3 for the smallest peak in the ¹H NMR spectrum for the reference compound (δ 8.30 ppm for methylparaben and δ 8.41 ppm for rhodamine B respectively). For HPLC–NMR in natural product applications, the LOD would appropriately be the amount of a minor component necessary to obtain an interpretable NMR spectrum, suitable for dereplication under typical acquisition conditions. To achieve an interpretable ¹H NMR spectrum, the integration, multiplicity and coupling constants for the signals must be easily determined.

Visual evaluation may also be used for non-instrumental or instrumental methods as an approach for determining the LOD. Here the detection limit is determined by the analysis of samples with known concentrations (or in this case, the known amount

injected) of the reference compound and by establishing the minimum level at which the reference compound can be reliably detected [12]. This LOD approach was adopted for all of the 2D NMR experiments which were acquired in the stop-flow HPLC–NMR mode.

The LOD for the gCOSY NMR experiment was defined as the minimum amount injected of the sample that would enable cross peaks or correlations to be observed between each coupled proton. The LOD for the HSQCAD NMR experiment was defined as the minimum injectable amount required to observe all of the correlations arising from protonated carbons. Lastly, the LOD for the gHMBCAD NMR experiment was defined as the minimum required amount injected that would result in sufficient two and three bond proton to carbon correlations to be observed that would permit an unequivocal structural elucidation of the component to be established. Together with the LOD, the linear dynamic range for the on-flow and stop-flow WET1D NMR experiments of the reference compounds were recorded (Figs. 2 and 3). Linearity of the NMR *S/N* was observed for the lower amounts injected of the two reference compounds. For the 2D NMR experiments the dynamic linear range was not determined because the LOD for these experiments is based on a visual evaluation rather than determination of the *S/N*.

NMR experiments for each of the two reference compounds were evaluated beginning with the highest amount injected. NMR experiments were re-acquired for each of the amounts injected until the smallest peak for the two reference compounds could no longer be observed with a *S/N* of 3 or until the expected 2D correlations were no longer observed.

3.1.1. On-flow WET1D NMR analysis

The on-flow HPLC–NMR experiment estimated LOD values at the 2.3 and 85 μg levels respectively for each of the two reference compounds, methylparaben and rhodamine B. The increase in the *S/N* for the smallest peak resulting for the methylparaben reference compound from each injection corresponding to a higher amount injected can be seen in Fig. 2. These LODs are only accurate for a flow rate of 0.8 mL/min and a block size of four scans. Changes in the flow rate and block size would affect the LOD for the on-flow WET1D NMR experiment. These detection limits would be easily achieved for principle components within a natural product crude extract.

3.1.2. Stop-flow analysis – WET1D

The stop-flow WET1D NMR experiment was the most sensitive of the NMR experiments evaluated. This was not surprising in that this mode permits single component analysis to be achieved by trapping the compound in the NMR flow cell for an indefinite period, resulting in an approximately 200% increase in the sensitivity compared to the data obtained from the on-flow WET1D NMR analysis. A LOD at the 700 ng level was estimated for methylparaben while a LOD at the 20 μg level was estimated for rhodamine B. The increase in *S/N* for methylparaben and for rhodamine B resulting from higher amounts of the reference compounds injected is evident in Fig. 3. These LODs would allow for not only principle component, but also minor component analysis and identification in a complex mixture. Only 64 scans were utilised in these experiments so increasing the number of scans would easily allow for lower amounts of the compounds to be detected.

3.1.3. Stop-flow analysis – gCOSY

The gCOSY NMR experiment acquired in the stop-flow HPLC–NMR mode estimated LODs of 5 and 250 μg for methylparaben and rhodamine B respectively. One of the drawbacks of proton NMR spectra acquired via the stop-flow WET1D NMR experiment, is that for the very low amounts injected, signals that closely reside in the suppression regions of the D₂O and CH₃CN are often

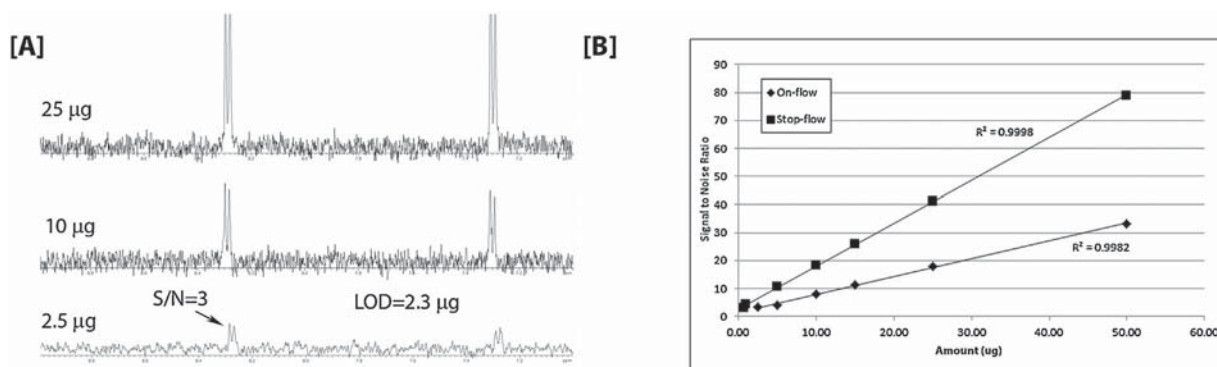


Fig. 2. (A) On-flow WET1D NMR spectra of a selection of amounts injected for methylparaben and (B) the dynamic linear range illustrating the LOD of methylparaben for on-flow and stop-flow WET1D NMR experiments based on achieving a S/N of 3 for the smallest peak (8.30 ppm).

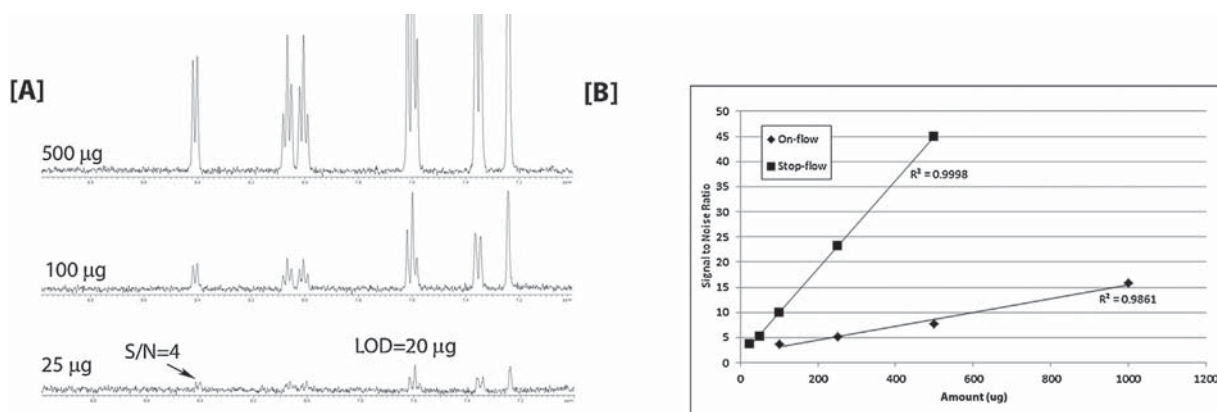


Fig. 3. (A) Stop-flow WET1D NMR spectra of a selection of amounts injected for rhodamine B and (B) the dynamic linear range illustrating the LOD of rhodamine B for on-flow and stop-flow WET1D NMR experiments based on achieving a S/N of 3 for the smallest peak (8.41 ppm).

difficult to observe as they are inadvertently also suppressed. The advantage of the gCOSY NMR experiment is that, as long as the proton NMR signals that reside in the suppression region are coupled, valuable proton-to-proton coupling can still be observed and hence protons in this region can still be identified.

3.1.4. Stop-flow analysis – HSQCAD

Only limited studies have been reported for some of the 2D heteronuclear NMR experiments. For instance HSQC and HMBC NMR spectra have been published for basic HPLC–NMR systems together with systems equipped with pre-concentration abilities such as guard columns or SPE cartridges [8,13–15]. The LOD for methylparaben and rhodamine B for the HSQCAD NMR experiment were estimated as 50 and 500 µg respectively. These LOD values fall within the range that typify components occurring within natural product crude extracts. If these LOD values are not achieved, partial HSQCAD NMR data can still be obtained.

3.1.5. Stop-flow analysis – gHMBCAD

The last of the 2D NMR experiments evaluated was the gHMBCAD NMR experiment. Depending on the molecular weight as well as the solubility of the analyte(s), gHMBCAD NMR spectra acquired through the stop-flow HPLC–NMR mode may only be acquired successfully for major or principle components. LOD values of 250 µg and 1000 µg were estimated for methylparaben and rhodamine B respectively. The LOD of rhodamine B clearly illustrates that when higher molecular weight compounds are analysed, difficulties may be encountered in obtaining quality gHMBCAD NMR spectra that permit sufficient through bond correlations to be observed. The other problem is that many compounds do not possess the

solubility that is required to analyse them via HPLC–NMR. As the gHMBCAD NMR experiment is the definitive experiment required to link structural fragments assembled from other NMR experiments, the ability to acquire this experiment successfully will be the determining factor as to whether a complete structure (particularly a de novo structure determination) can be elucidated.

3.1.6. Summary of results

A comparison of the LOD established for the two reference compounds (methylparaben and rhodamine B) in each of the NMR experiments is illustrated in Figs. 2–4. As the NMR pulse sequence becomes more complex, as in the case for the HSQCAD and gHMBCAD NMR experiments, the amount of compound required for low compared to medium to high molecular weight compound

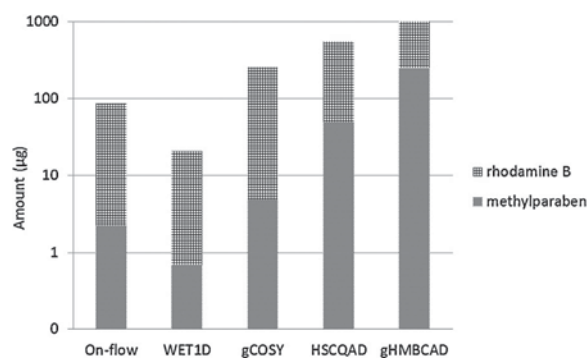


Fig. 4. LOD for 1D and 2D NMR experiments for the reference compounds methylparaben and rhodamine B.

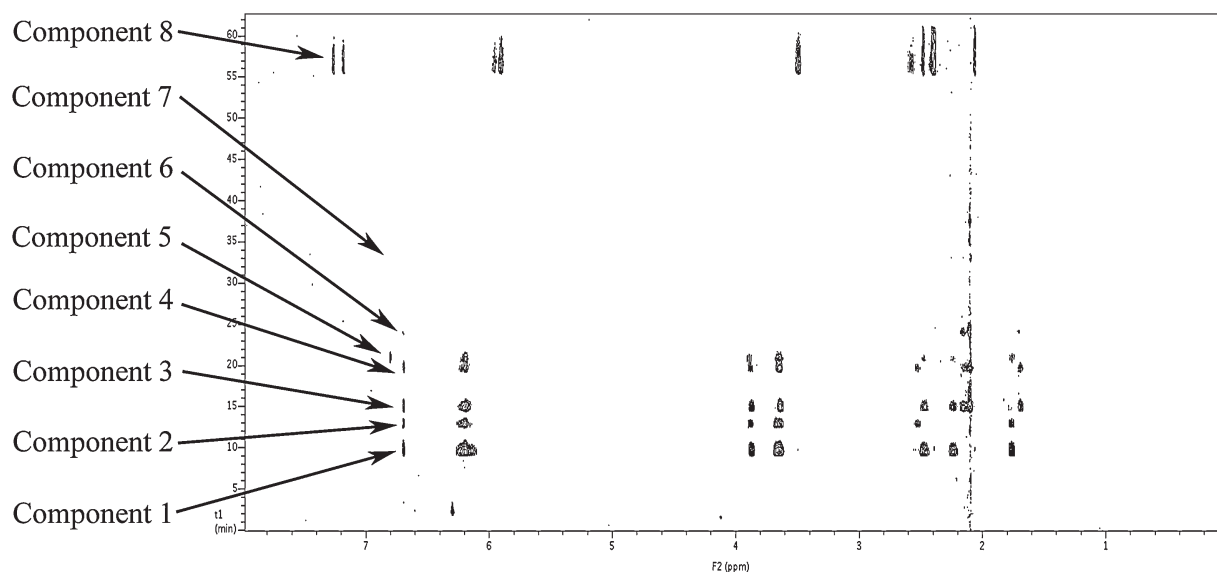


Fig. 5. On-flow 2D HPLC–NMR contour plot resulting from the analysis of the dichloromethane crude extract of the marine alga, *C. subfarcinata* showing the detection of components 1–8 (note: components 6 and 7 could only be detected via stop-flow HPLC–NMR analyses).

identifications becomes more apparent, whereby the latter will require exceedingly more amounts injected to obtain interpretable results. Previous 2D NMR spectra acquired via various HPLC–NMR studies have only provided LOD values for stop-flow WET1D and gCOSY NMR experiments. This therefore represents the first

report of the LOD (for a set of fixed parameters) for the gCOSY, HSQCAD and gHMBCAD NMR experiments acquired on a 500 MHz HPLC–NMR system equipped with a 60 μ L active volume flow cell. In defining the LOD an important factor that needs to be considered is the chromatographic peak width. To obtain NMR

Table 1

NMR data (500 MHz, 75% $\text{CH}_3\text{CN}/\text{D}_2\text{O}$) for 1-(2,4,6-trihydroxyphenyl)-6,9,12,15-octadecatetraen-1-one (**3**) and 1-(2,4,6-trihydroxyphenyl)-5,8,11,14,17-eicosapentaen-1-one (**4**) obtained via stop-flow HPLC–NMR.

1-(2,4,6-Trihydroxyphenyl)-6,9,12,15-octadecatetraen-1-one (3)					1-(2,4,6-Trihydroxyphenyl)-5,8,11,14,17-eicosapentaen-1-one (4)		
Position	δ_{C} , ^a mult.	δ_{H} (J in Hz)	gCOSY	gHMBCAD	δ_{C} , ^a mult.	δ_{H} (J in Hz)	gCOSY
1	207.2, C				ND		
2	44.3, CH_2	3.88, t (7.5)	3	1, 3, 4	ND	3.90, t (7.5)	3
3	25.1, CH_2	2.48, p (7.5)	2, 4	1, 2	ND	2.53, p (7.5)	2
4	30.0, CH_2	2.24, p (7.5)	3, 5	6	ND	SS	
5	ND	2.95, m ^b			129.0, CH	6.20, m	
6	130.9, CH	6.20, m	5	8	129.0, CH	6.20, m	7
7	128.8, CH	6.20, m	8	8	26.1, CH_2	3.66, m	6, 8
8	26.1, CH_2	3.66, m	7, 9	7, 9, 10	129.0, CH	6.20, m	7
9	128.8, CH	6.20, m	8	8, 11	129.0, CH	6.20, m	10
10	128.8, CH	6.20, m	11	8, 11	26.1, CH_2	3.66, m	9, 11
11	26.1, CH_2	3.66, m	10, 12	9, 10, 12, 13	129.0, CH	6.20, m	10
12	128.8, CH	6.20, m	11	11, 14	129.0, CH	6.20, m	13
13	128.8, CH	6.20, m	14	11, 14	26.1, CH_2	3.66, m	12, 14
14	26.1, CH_2	3.66, m	13, 15	12, 13, 15	129.0, CH	6.20, m	13
15	128.8, CH	6.20, m	14	14	129.0, CH	6.20, m	16
16	132.7, CH	6.20, m		14	26.1, CH_2	3.66, m	15, 17
17	21.1, CH_2	SS			129.0, CH	6.20, m	16
18	14.5, CH_3	1.77, t (8.0)		16, 17	129.0, CH	6.20, m	
19					ND	SS	
20					ND	1.77, t (8.0)	
1'	105.1, C				ND		
2'	164.9, C*				ND		
3'	95.6, CH	6.70, s		1', 2', 5'	95.8, CH	6.71, s	
4'	ND*				ND		
5'	95.6, CH	6.70, s		1', 3', 6'	95.8, CH	6.71, s	
6'	164.9, C*				ND		
1'-OH		ND				ND	
4'-OH		ND				ND	
6'-OH		ND				ND	

Referenced to D_2O (δ_{H} 4.64 ppm).

SS, signal suppressed.

ND, not detected.

* Signals interchangeable.

^a Carbon assignments based on HSQCAD and gHMBCAD NMR experiments

^b Proton chemical shift based on correlation observed in gCOSY NMR experiment

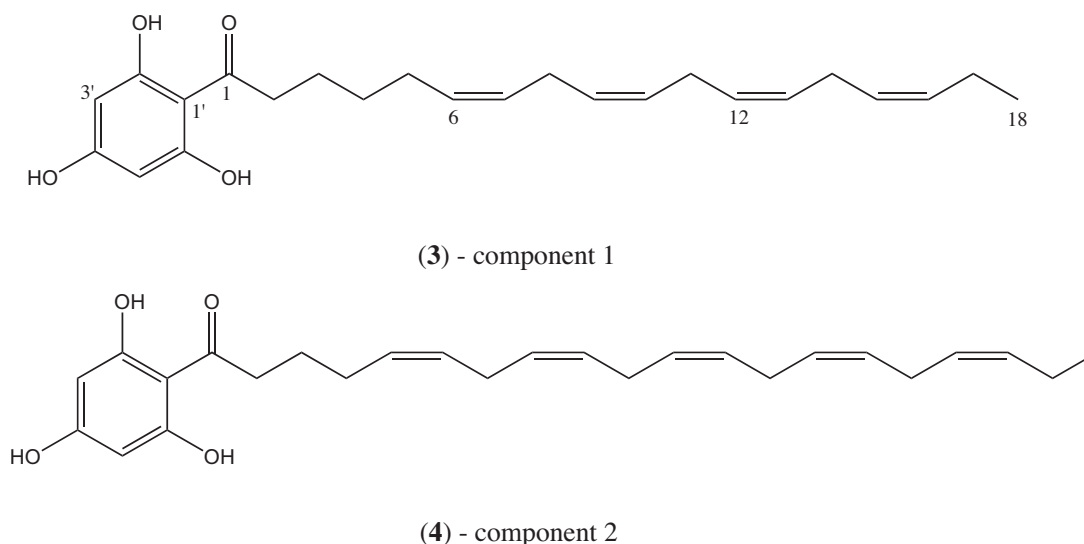


Fig. 6. Structures of the previously reported phloroglucinols (components **1** and **2**) identified based on the HPLC–NMR and HPLC–MS analyses of the dichloromethane crude extract of the marine alga, *C. subfarcinata*.

spectra with the necessary S/N of 3, it is important that the chromatographic peaks eluting from the HPLC are contained within the active volume of the HPLC–NMR flow cell. The compromise to this scenario is that in HPLC–NMR analyses it is often a requirement to overload the HPLC column in an effort to achieve a higher injectable amount and therefore have a better chance to detect the component, particularly in the acquisition of the heteronuclear 2D NMR experiments. However, at the lower amounts injected chromatographic peak shape is generally not an issue as components tend to typically show a sharp peak shape.

The LOD for methylparaben and rhodamine B analyses concluded that it is possible to carry out complete on-line 1D and 2D NMR acquisition for structure identification. The intention was to then extend the LOD HPLC–NMR study to the analysis of a multi-component mixture (i.e. a natural product extract).

3.2. LOD case study: stop-flow HPLC–NMR analysis of a natural product crude extract and secondary metabolite identification

A natural product crude extract was selected as a case study following the LOD study. The crude extract of the marine brown alga (*C. subfarcinata*) was analysed by HPLC–NMR and HPLC–MS in an attempt to ascertain the ability of HPLC–NMR in combination with HPLC–MS to completely characterise and identify components in situ within a multi-component mixture. HPLC–NMR was implemented in an effort to rapidly establish the nature of the structure class(es) and to attempt to identify the components present in the dichloromethane crude extract of the marine alga, *C. subfarcinata*. A combination of on-flow and stop-flow HPLC–NMR analyses detected the presence of eight components (Fig. 5) of which two could be rapidly identified. Analysis of the extracted stop-flow WET1D NMR spectra suggested that almost all of the compounds were structurally related with characteristic proton NMR signals in the aromatic and olefinic regions, together with various upfield proton NMR signals. By direct comparison of the S/N for each of the compounds it could be concluded that component **1** represented the main constituent of the dichloromethane crude extract of the marine alga. Component **1** was completely characterised by 1D and 2D NMR experiments acquired through the stop-flow HPLC–NMR mode. This illustrated that the established LODs for the selected NMR experiments acquired via stop-flow HPLC–NMR were

achievable within a multi-component mixture using the fixed set of experimental parameters.

Dereplication and identification of component **1** was achieved using the MarinLit database using the molecular weight (obtained by high resolution HPLC–MS), taxonomy of the alga, several of the distinct carbon NMR signals and analysis of both the 1D and 2D NMR data. This suggested the identity of component **1** to be a previously reported phloroglucinol (**3**) (Fig. 6) [16]. The stop-flow HPLC–NMR WET 1D proton NMR spectrum of component **1** supported this structure with the presence of two distinct proton signals in the downfield region of the spectrum at δ_H 6.70 and 6.20 respectively, a triplet methyl (δ_H 1.77, t, $J=8.0$ Hz, H-18) and various other upfield signals. Due to the suppression of the acetonitrile signal, no signals were observed in the 2.65–3.00 ppm region of the spectrum. However analysis of the gCOSY NMR spectrum showed the presence of a correlation within the HDO suppression region, thereby confirming the presence of a proton signal at δ_H 2.95. A set of methylene protons at δ_H 3.88 and 2.48 (H-2 and H-3 respectively) showed HMBC NMR correlations to a carbon at δ_C 207.2 (C-1), confirming the position of the carbonyl group. Complete analysis of the 1D and 2D NMR data obtained via stop-flow HPLC–NMR (Table 1), along with the observed UV chromophore at 285 nm, which supported the presence of a phloroglucinol moiety [17], allowed the complete structure of component **1** to be deduced as the previously described phloroglucinol, 1-(2,4,6-trihydroxyphenyl)-6,9,12,15-octadecatetraen-1-one (**3**) [18].

Stop-flow HPLC–NMR analysis of component **2** allowed for the acquisition of a WET1D proton NMR spectrum, gCOSY and partial HSQCAD NMR data (Table 1). This data alone was not sufficient to completely identify component **2**, however searches conducted in the MarinLit database using the taxonomy, UV data, molecular mass, and key carbon NMR chemical shifts, permitted dereplication. Component **2** could be identified as the previously reported phloroglucinol 1-(2,4,6-trihydroxyphenyl)-5,8,11,14,17-eicosapentaen-1-one (**4**) (Fig. 6) [19]. On the basis of the HPLC–NMR and HPLC–MS studies conducted on the remaining components (**3–8**) in the crude extract of *C. subfarcinata*, in consultation with the MarinLit database, these most likely represented new structural variants of the phloroglucinol structure class. However, insufficient structural information was obtained via HPLC–NMR since these components were present in much lower amounts in the crude extract. In summary the extracted UV profiles for each of the

components, the stop-flow WET1D NMR spectra and the use of the MarinLit database were able to conclude two distinct structure classes (phloroglucinols and a meroditerpenoid). An estimate of the amounts of the two main components present in the crude extract was proposed. Component **1** was present at approximately 0.8–1.0 mg since complete 2D NMR data was easily achieved in the stop-flow HPLC–NMR mode within the fixed time restrictions and parameters. Component **2** was present at less than 0.5 mg as complete 2D NMR data could not be obtained within the fixed parameter set. The LODs of the HSQCAD and gHMBCAD NMR experiments require that approximately 0.5–1.0 mg of a component be present for sufficient correlations to be observed in these two NMR experiments.

4. Conclusions

The LOD for various 1D and 2D NMR experiments acquired via on-flow and stop-flow HPLC–NMR has been extensively reported for the first time. This was achieved using a low and a medium to high molecular weight reference compound with fixed NMR experimental acquisition times, on a 500 MHz HPLC–NMR system equipped with a 60 μ L active volume flow cell. The LOD HPLC–NMR study was extended to include the analysis of a complex natural product crude extract (representing a multi-component mixture) which, providing that there is sufficient solubility in water and acetonitrile, enables rapid on-line structure elucidation to be achieved. To improve the LOD of HPLC–NMR on this system higher capacity columns could be considered.

Acknowledgments

The Marine And Terrestrial Natural Product (MATNAP) research group thanks Dr G. Kraft (The University of Melbourne) for the taxonomic identification of the marine alga; Dr J. Niere (RMIT University) for her useful NMR discussions and guidance; Dr R. Tinker for providing advice and for proof reading this manuscript; and Dr J. Ryan (Agilent Australia) for his useful NMR insight and technical support. R. Brkljača acknowledges his Australian Postgraduate Award (APA) scholarship that supported these studies.

Appendix A. Supplementary data

Supplementary data associated with this article can be found, in the online version, at <http://dx.doi.org/10.1016/j.chroma.2014.11.074>.

References

- [1] S. Urban, F. Separovic, Developments in hyphenated spectroscopic methods in natural product profiling, *Front. Drug Des. Discov.* 1 (2005) 113–166.
- [2] R. Brkljača, S. Urban, Recent advancements in HPLC–NMR and applications for natural product profiling and identification, *J. Liq. Chromatogr. Relat. Technol.* 34 (2011) 1063–1076.
- [3] S.C. Bobzin, S. Yang, T.P. Kasten, Application of liquid chromatography–nuclear magnetic resonance spectroscopy to the identification of natural products, *J. Chromatogr. B: Biomed. Sci. Appl.* 748 (2000) 259–267.
- [4] J. Cazes, in: J. Cazes (Ed.), *Encyclopaedia of Chromatography*, CRC Press, Boca Raton, 2010, pp. 1337–1351.
- [5] J.-L. Wolfender, G. Marti, E.F. Queiroz, Advances in techniques for profiling crude extracts and for the rapid identification of natural products: dereplication, quality control and metabolomics, *Curr. Org. Chem.* 14 (2010) 1808–1832.
- [6] O. Corcoran, M. Spraul, LC–NMR–MS in drug discovery, *Drug Discov. Today* 8 (2003) 624–631.
- [7] R. Brkljača, S. Urban, Chemical profiling (HPLC–NMR & HPLC–MS), isolation and identification of bioactive meroditerpenoids from the southern Australian marine brown alga *Sargassum Paradoxum*, *Mar. Drugs* (submitted).
- [8] M.A. Timmers, D.A. Dias, S. Urban, Application of HPLC–NMR in the identification of plocamenone and isoplocamenone from the marine red alga *Plocamium angustum*, *Mar. Drugs* 10 (2012) 2089–2102.
- [9] D.A. Dias, J.M. White, S. Urban, *Laurencia filiformis*: phytochemical profiling by conventional and HPLC–NMR approaches, *Nat. Prod. Commun.* 4 (2009) 157–172.
- [10] S.H. Smallcombe, S.L. Patt, P.A. Keifer, WET solvent suppression and its applications to LC NMR and high-resolution NMR spectroscopy, *J. Magn. Reson. Ser. A* 117 (1995) 295–303.
- [11] R.K. Harris, E.D. Becker, S.M. Cabral de Menezes, R. Goodfellow, P. Granger, NMR nomenclature. Nuclear spin properties and conventions for chemical shifts. IUPAC recommendations 2001, *Magn. Reson. Chem.* 40 (2002) 489–505.
- [12] ICH, *Validation of Analytical Procedures: Text and Methodology Q2(R1)*, 1996.
- [13] J.R. Kesting, D. Staerk, M.V. Tejesvi, K.R. Kini, H.S. Prakash, J.W. Jaroszewski, HPLC–SPE–NMR identification of a novel metabolite containing the benzo[c]oxepin skeleton from the endophytic fungus *Pestalotiopsis virgatula* culture, *Planta Med.* 75 (2009) 1104–1106.
- [14] D.L. Norwood, J.O. Mullis, M. Davis, S. Pennino, T. Egert, N.C. Gonnella, Automated solid phase extraction (SPE) LC/NMR applied to the structural analysis of extractable compounds from a pharmaceutical packaging material of construction, *PDA J. Pharm. Sci. Technol.* 67 (2013) 267–287.
- [15] T. Richard, H. Temsamani, E. Cantos-Villar, J.-P. Monti, Application of LC–MS and LC–NMR techniques for secondary metabolite identification, *Adv. Bot. Res.* 67 (2013) 67–98.
- [16] *MarinLit Database*, Royal Chemical Society, 2014.
- [17] A.I. Scott, *Interpretation of the Ultraviolet Spectra of Natural Products*, Pergamon Press Ltd, London, 1964.
- [18] R. Kazlauskas, L. King, P.T. Murphy, R.G. Warren, R.J. Wells, New Metabolites from the Brown Algal Genus *Cystophora*, *Aust. J. Chem.* 34 (1981) 439–447.
- [19] V. Amico, R. Currenti, G. Oriente, M. Piattelli, C. Tringali, A phloroglucinol derivative from the brown alga *Zonaria tournefortii*, *Phytochemistry* 20 (1981) 1451–1453.

PART B – Terrestrial Organisms

The chapters that make up this section (Chapters 5-7) of the thesis highlight the investigations conducted on two Australian plants from the Haemodoraceae family and one fungus. The studies conducted include application of phytochemical profiling (HPLC & HPLC-MS) to rapidly dereplicate the structure classes and the identity of the compounds present in the crude extracts of these organisms. This was conducted in conjunction with the use of traditional off-line isolation methodologies in order to explore the nature of the bioactive secondary metabolites present. This section of the thesis describes the identification of a total of ten new and twenty previously reported secondary metabolites and is comprised of three journal publications as listed below:

1. Brkljača, Robert, White, Jonathan M., & Urban, Sylvia. (2015). Phytochemical Investigation of the Constituents Derived from the Australian Plant *Macropidia fuliginosa*. *Journal of Natural Products*, 78(7), 1600-1608.
2. Brkljača, Robert, & Urban, Sylvia. (2015). HPLC-NMR & HPLC-MS profiling and bioassay-guided identification of secondary metabolites from the Australian plant *Haemodorum spicatum*. *Journal of Natural Products*, 78(7), 1486-1494.

3. **Brkljača, Robert, & Urban, Sylvia.** (2015). Rapid Dereplication and Identification of the Bioactive Constituents from the Fungus, *Leucocoprinus birnbaumii*. *Natural Product Communications*, 10(1), 95-98.

CHAPTER 5

*Constituents from the Australian Plant *Macropidia fuliginosa**



Kingdom: Plantae

Phylum: Charophyta

Class: Equisetopsida

Order: Commelinales

Family: Haemodoraceae

Genus: *Macropidia*

Species: *fuliginosa*

Purchased from Garden World Nursery (Braeside, Victoria, Australia) in October 2012 and also from the Kurunga Native Nursery (Mount Evelyn, Victoria, Australia) in January 2011 and again in November 2012.

Chapter 5 details the isolation of various new and known compounds from the flowers and bulbs of *Macropidia fuliginosa*. This work has been published in the *Journal of Natural Products*. Appendix B contains supplementary information relevant to this study.

Journal publication resulting from this study:

Brkljača, Robert, White, Jonathan M., & Urban, Sylvia. (2015). Phytochemical investigation of the constituents derived from the Australian plant *Macropidia fuliginosa*. *Journal of Natural Products*, 78(7), 1600-1608.

Phytochemical Investigation of the Constituents Derived from the Australian Plant *Macropidia fuliginosa*

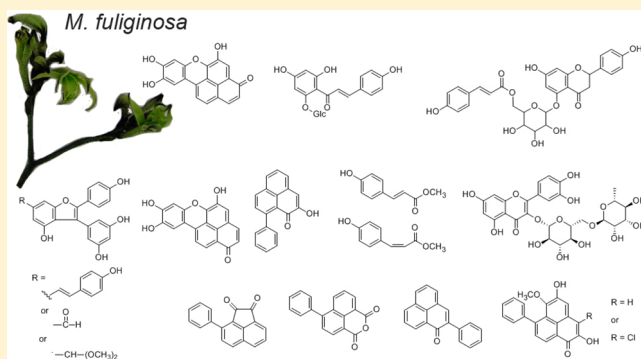
Robert Brkljača,[†] Jonathan M. White,[‡] and Sylvia Urban^{*,†}

[†]School of Applied Sciences (Discipline of Chemistry), Health Innovations Research Institute (HIRi), RMIT University, GPO Box 2476 V, Melbourne, Victoria 3001, Australia

[‡]School of Chemistry and Bio21 Institute, The University of Melbourne Melbourne, Victoria 3010, Australia

S Supporting Information

ABSTRACT: A phytochemical study of the flowers and bulbs derived from the Australian plant *Macropidia fuliginosa*, involving hyphenated spectroscopic methodologies (HPLC-NMR and HPLC-MS), together with conventional isolation strategies, resulted in the identification of 16 constituents (1, 2, 4–17) representative of six different structural classes. Six new compounds (12–17) were identified from the bulbs of the plant. The isolated compounds were assessed for antimicrobial activity, and compound 8 was found to be more potent against *P. aeruginosa* than ampicillin.



Plants commonly known as kangaroo paw comprise a number of species belonging to two genera of the family Hemodoraceae, which are endemic to the southwest corner of Western Australia. There are 11 different species of kangaroo paw, 10 of which belong to the *Anigozanthos* genus and one to the *Macropidia* genus.¹ Various species of the *Anigozanthos* genus have been studied and have yielded a range of secondary metabolites including phenylphenalenones, dimeric phenylphenalenones, resveratrol analogues, and oxabenzochrysenones.^{2–7} By contrast, *Macropidia fuliginosa*, commonly known as black kangaroo paw, which is classified separately from the other kangaroo paw species, has not been extensively studied. The flowers of *M. fuliginosa* have been reported to produce the two oxabenzochrysenones hemofluorones A (1) and B (2).⁸ Initially hemofluorone B was reported to have the structure as depicted by 3,⁸ but this was subsequently revised to 2.³ Other plants belonging to the family Hemodoraceae, such as *Hemodorum simulans* and *Xiphidium caeruleum*, also produce oxabenzochrysenones as well as phenylphenalenones,^{9,10} which are typical secondary metabolites of many of the species derived from this family.

As part of our continuing efforts to study the chemical diversity of Australian plants, we recently conducted phytochemical studies of two different *Hemodorum* species, one of which is used for the treatment of dysentery.^{10,11} Motivated by the limited studies that have been conducted on *M. fuliginosa*, together with our interest in the constituents derived from the Hemodoraceae family of plants, specimens of *M. fuliginosa* were purchased and subjected to a phytochemical study. Investigation of the flowers and bulbs of *M. fuliginosa* yielded six new (12–17) and 10 known compounds (1, 2, 4–

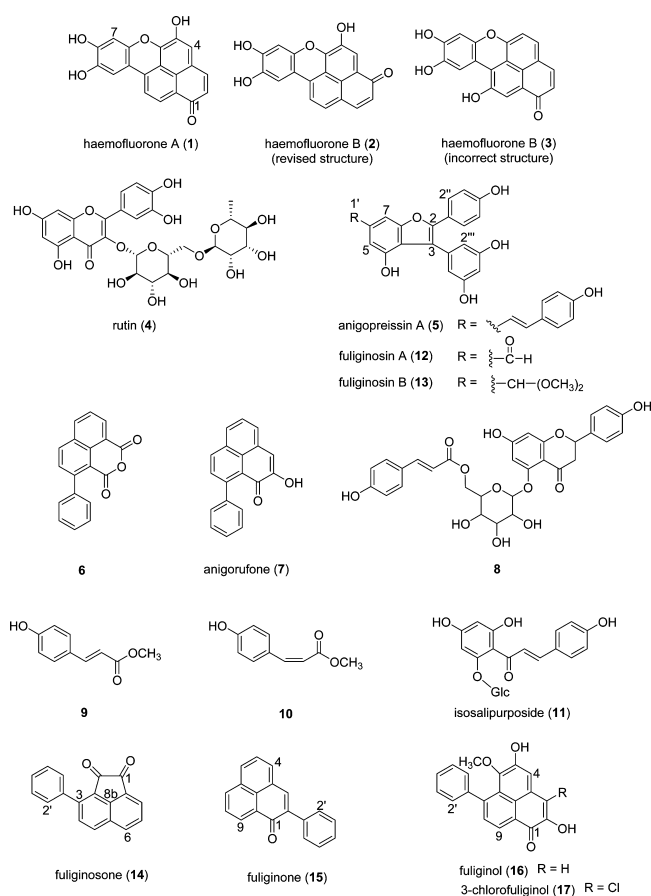
11). The structures of three of these compounds (14, 16, and 17) were defined by single-crystal X-ray diffraction in combination with detailed spectroscopic methods, while the complete 2D NMR spectroscopic characterization of 1, 6, and 11 is reported herein for the first time.

RESULTS AND DISCUSSION

The flowers and bulbs of *M. fuliginosa* were separately extracted with 3:1 MeOH/CH₂Cl₂, and the solvent was evaporated under reduced pressure and sequentially solvent-partitioned (trituated) into CH₂Cl₂- and MeOH-soluble fractions, respectively. The crude CH₂Cl₂ extract of the flowers was found to be more active than the MeOH crude extract and was selected for phytochemical profiling. While both the CH₂Cl₂- and MeOH-soluble fractions of the bulbs displayed antimicrobial activity, only the CH₂Cl₂ extract was subjected to an on-line phytochemical profiling study. This selection was made on the basis of preliminary analytical HPLC and ¹H NMR analyses, which indicated the presence of more secondary metabolites in the CH₂Cl₂ crude extract. The CH₂Cl₂ crude extract showed better separation of the secondary metabolites present. Both the CH₂Cl₂ and MeOH crude extracts derived from the bulbs of *M. fuliginosa* were subjected to an off-line phytochemical investigation.

On-line Phytochemical Profiling (HPLC-NMR and HPLC-MS). The CH₂Cl₂ extracts of the bulbs and flowers were subjected to HPLC-NMR and HPLC-MS chemical profiling with a total of 10 peaks detected (see Supporting

Received: February 16, 2015



Information). While the CH_2Cl_2 crude extract of the bulbs displayed reasonable solubility in MeCN and D_2O , the CH_2Cl_2 crude extract of the flowers did not. This meant that HPLC-NMR data could not be obtained for the crude extract derived from the flowers and that dereplication of the constituents present in this extract relied solely on the interpretation of the HPLC-MS and UV spectroscopic data. The process known as dereplication aims to rapidly deduce the chemical classes or compounds present in a crude extract and involves the use of chemical databases such as the Dictionary of Natural Products, MarinLit, or SciFinder. These databases can be utilized to search characteristic UV, MS, and NMR data.

HPLC-MS of the CH_2Cl_2 crude extract of the flowers showed the presence of four compounds, each displaying unique UV absorbance maxima. The molecular formula of the compound eluting at $t_R = 2.45$ min was determined as $\text{C}_{27}\text{H}_{30}\text{O}_{16}$ [observed m/z at 609.1453 $[\text{M} - \text{H}]^-$ (calcd for $\text{C}_{27}\text{H}_{29}\text{O}_{16}$: m/z 609.1456)], and the compound displayed UV absorbance maxima above 350 nm. A search conducted in the Dictionary of Natural Products using the molecular formula and consideration of the UV absorbance maxima allowed the tentative identification of the compound eluting at $t_R = 2.45$ min as rutin (4). Similar analyses of the data and literature searches conducted for the compounds eluting at $t_R = 3.74$ and 4.44 min resulted in these constituents being tentatively identified as hemofluorones A (1) and B (2), respectively. The fourth compound eluting at $t_R = 15.05$ min could not be identified, but based on the characteristic UV absorbance at 368 nm it was concluded to be a flavonoid,^{12,13} a common chemical class of the Hemodoraceae.¹⁴

The HPLC-NMR and HPLC-MS of the CH_2Cl_2 crude extract derived from the bulbs displayed the presence of six

compounds, of which three ($t_R = 4.11$, 12.35, and 19.18 min) were identified as the known compounds 5–7, respectively, based on a dereplication strategy involving the use of the Dictionary of Natural Products to search the molecular formulas and characteristic UV absorbance maxima in combination with the taxonomy of the plant. The WET1D ^1H NMR spectrum and extracted UV profile of the two compounds eluting at $t_R = 3.28$ min (coeluting peaks) showed close similarity to 5, suggesting these compounds were structural analogues containing a formyl (δ_{H} 10.25, s) and a methoxy (δ_{H} 4.18, s) moiety. The WET1D NMR spectrum of the compound eluting at $t_R = 11.31$ min suggested an unsubstituted phenylphenalenone; however the extracted UV profile was not in agreement, displaying an absorbance below 400 nm. Phenylphenalenones typically display an absorbance at 450 nm,² suggesting that the compound eluting at $t_R = 11.31$ min was of a closely related structural class.

Off-line Phytochemical Isolation. The off-line isolation and fractionation of the crude extracts derived from the flowers and bulbs of *M. fuliginosa* yielded a total of 16 compounds (1, 2, 4–17). The identities of the four compounds ($t_R = 3.28$, 11.31, and 15.05 min) dereplicated in the on-line chemical profiling approach were subsequently confirmed as 12, 13, 14, and 8, respectively. In total the off-line phytochemical isolation approach resulted in the identification of seven known secondary metabolites from the flowers (1, 2, 4, 8–11) and three from the bulbs (5–7), and their NMR and MS data were in accordance with literature values.^{2–5,8,15–18}

Fuliginosins A (12) and B (13) were isolated as brown oils from the bulbs of *M. fuliginosa*. Comparison of the ^1H NMR spectra of 12 and 13 supported the fact that these compounds were structural analogues and that they were closely related to anigopreissin A (5) except that the resonances for the *trans*-phenylvinyl system in anigopreissin A (5) were absent in both 12 and 13. The ^1H NMR spectrum of fuliginosin A (12) showed the presence of a formyl moiety (δ_{H} 9.91, s) which showed key gHMBCAD NMR correlations to the adjacent aromatic ring (C-5 and C-7, respectively), confirming its attachment to position C-6. Complete analyses of the 1D and 2D NMR data (Table 1) allowed for 12 to be identified as the new benzofuran 3-(3,5-dihydroxyphenyl)-4-hydroxy-2-(4-hydroxyphenyl)benzofuran-6-carbaldehyde and given the trivial name fuliginosin A. Inspection of the ^1H and HSQCAD NMR spectra of fuliginosin B (13) indicated the presence of two methoxy moieties (δ_{H} 3.23, s, (6H); δ_{C} 52.9) as well as a characteristic deshielded methine [δ_{H} 5.36, s, (1H); δ_{C} 103.1]. Key gHMBCAD NMR correlations indicated that these methoxy moieties and the deshielded methine were attached to an aromatic ring. Specifically, the deshielded methine proton showed correlations to the carbons at positions C-5 and C-7 together with correlations to the two methoxy moieties, which confirmed the attachment of this structural unit to C-6. Analyses of the 1D and 2D NMR data (Table 1) allowed for 13 to be identified as the new benzofuran 5-[6-dimethoxymethyl-4-hydroxy-2-(4-hydroxyphenyl)benzofuran-3-yl]benzene-1,3-diol and given the trivial name fuliginosin B. Fuliginosin B (13) is the dimethyl acetal of fuliginosin A (12), and it was suspected that 13 could be an artifact produced from 12 as a result of the extraction with MeOH. An attempt to convert fuliginosin A (12) to fuliginosin B (13), whereby the former was stored in MeOH as well as in a mixture of 3:1 MeOH/ CH_2Cl_2 , showed no conversion after a period of approximately 1 week. This

Table 1. ^1H and ^{13}C NMR Data (500 MHz, $\text{DMSO-}d_6$) for Fuliginosins A (12) and B (13)

position	fuliginosin A (12)				fuliginosin B (13)			
	δ_{C} , mult	δ_{H} (J in Hz)	gCOSY	gHMBCAD	δ_{C} , ^a mult	δ_{H} (J in Hz)	gCOSY	gHMBCAD
2	152.9, C				149.8, C			
3	116.1, C				115.8, C			
3a	116.1, C				118.3, C			
4	152.8, C				154.9, C ^d			
5	107.3, CH	7.07, s		1', 3a, ^c 4, ^c 6, 7	107.2, CH	6.63, s		1', 3a, 7, 7a
6	124.0, C				ND			
7	106.2, CH	7.61, s		1', 5, 6, 7a	100.9, CH	6.98, s		1', 3a, 4b, ^c 5
7a	154.5, C				152.3, C ^d			
1'	192.6, CH	9.91, s		7, 5	103.1, CH	5.36, s		7, 5, 2a'-OCH ₃ , 2b'-OCH ₃
1''	120.9, C				121.7, C			
2''	128.7, CH	7.35, d (9.0)	3''	2, 4'', 6''	128.4, CH	7.27, d (8.5)	3''	2, 4''
3''	116.0, CH	6.73, d (9.0)	2''	1'', 4'', 5''	115.9, CH	6.69, d (8.5)	2''	1'', 4''
4''	158.7, C				158.2, C			
5''	116.0, CH	6.73, d (9.0)	6''	1'', 3'', 4''	115.9, CH	6.69, d (8.5)	6''	1'', 4''
6''	128.7, CH	7.35, d (9.0)	5''	2, 2'', 4''	128.4, CH	7.27, d (8.5)	5''	2, 4''
1'''	133.9, C				ND			
2'''	109.0, CH	6.22, d (2.0)		3, 3''', 4''', 6'''	109.1, CH	6.20, d (2.0)	4'''	3, 3''', 4''', 5''', 6'''
3'''	158.5, C				158.6, C			
4'''	102.4, CH	6.20, dd (2.0, 2.0)		2''', 3''', 5''', 6'''	102.3, CH	6.16, dd (2.0, 2.0)	2''', 6'''	2''', 3''', 5''', 6'''
5'''	158.5, C				158.6, C			
6'''	109.0, CH	6.22, d (2.0)		3, 2''', 4''', 5'''	109.1, CH	6.20, d (2.0)	4'''	3, 2''', 3''', 4''', 5'''
4-OH		ND ^b				ND ^b		
4''-OH		ND ^b				ND ^b		
3'''-OH		ND ^b				ND ^b		
5'''-OH		ND ^b				ND ^b		
2a'-OCH ₃					52.9, CH ₃	3.23, s		1'
2b'-OCH ₃					52.9, CH ₃	3.23, s		1'

^aCarbon assignments based on HSQCAD and gHMBCAD NMR experiments. ^bSignal not detected. ^cIndicates weak or long-range signal. ^dSignals interchangeable.

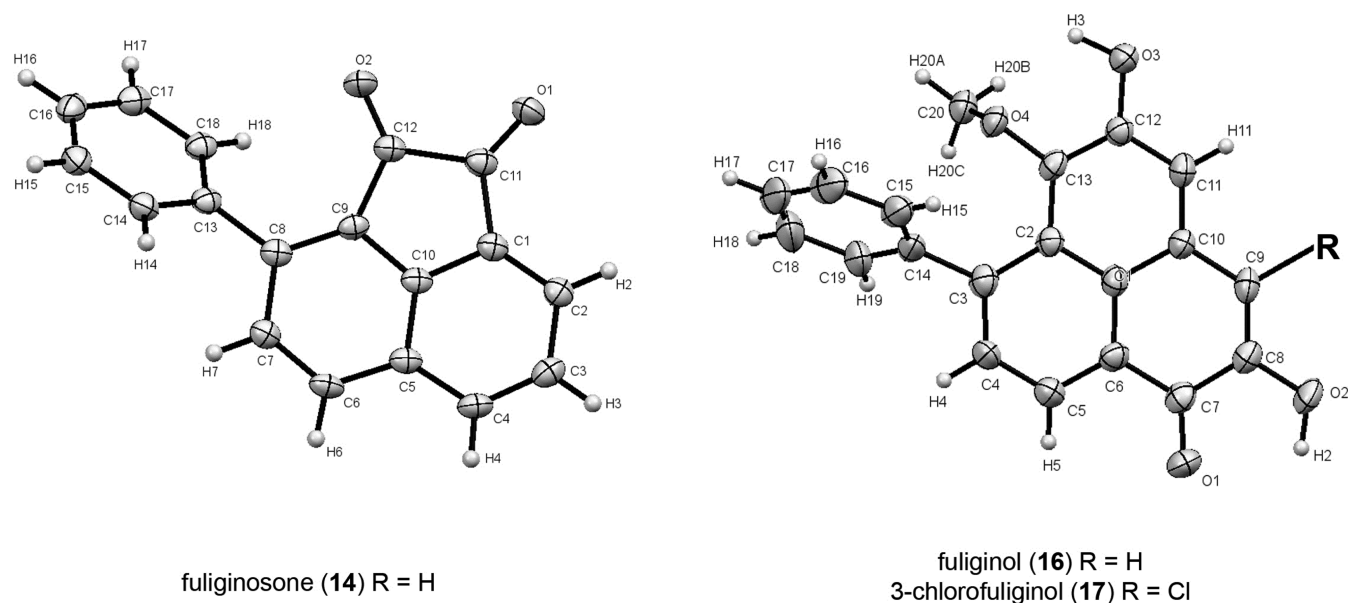


Figure 1. Single-crystal X-ray diffraction structures (ORTEP) of fuliginosone (14), fuliginol (16), and 3-chlorofuliginol (17).

suggested that fuliginosin B (13) may be a natural product, but the possibility of it being an artifact cannot be excluded.

Fuliginosone (14) was isolated as bright yellow needles. The ^1H NMR spectrum showed the presence of eight discrete aromatic/olefinic signals (δ_{H} 8.30 (1H), 8.29 (1H), 8.15 (1H), 7.87 (1H), 7.85 (1H), 7.72 (2H), 7.55 (2H), and 7.52 (1H),

respectively). Inspection of the UV spectrum of 14 showed an absorbance at 323 nm, which is not consistent with a phenylphenalenone skeleton (typically >400 nm).² In addition the ^{13}C NMR spectrum showed the presence of two diagnostic carbonyl signals (δ_{C} 187.7 and 186.9), which also was not in accordance with typical phenylphenalenones.^{9,10,19} HRESIMS

revealed the molecular formula of **14** to be $C_{18}H_{10}O_2$ (observed m/z at 259.0752 $[M + H]^+$ (calcd for $C_{18}H_{10}O_2$: m/z 259.0759). The presence of 18 carbons, as compared to phenylphenalenones, which typically contain 19 carbons, also supported a deviation to that structure class. It was proposed that **14** contained a “dione” moiety in a five-membered ring, rather than containing a “dione” moiety in a six-membered ring. This would account for the reduction in the number of carbons that is typically observed in the phenylphenalenones. A pendant aromatic ring substituted at C-3 or C-5 was established by analysis of the NMR data. Predicted carbon chemical shifts for the two possible structures were compared using Advanced Chemistry Development (ACD) laboratories and ChemDraw software.^{20,21} Substitution of the pendant aromatic ring at C-3 showed carbon chemical shifts of δ_C 126 and 138 for C-4 and C-5, respectively. The alternative C-5-substituted structure showed carbon chemical shifts of δ_C 122 and 130 for C-3 and C-4, respectively. Two of the predicted carbon chemical shifts (δ_C 138 and 130) differ significantly, and on the basis of a comparison of the observed and calculated carbon chemical shifts, the pendant aromatic ring was placed at C-3. A single-crystal X-ray diffraction (Figure 1) study of **14** enabled the structure to be unequivocally deduced as 3-phenylacenaphthylene-1,2-dione and given the trivial name fuliginosone. Analyses of the 1D and 2D NMR data (Table 2) also supported the structure of fuliginosone (**14**).

Table 2. 1H and ^{13}C NMR Data (500 MHz, $CDCl_3$) of Fuliginosone (**14**)

position	δ_C , mult	δ_H (J in Hz)	gCOSY	gHMBCAD
1	187.7, C			
2	186.9, C			
2a	130.1, C			
3	136.4, C			
4	131.1, CH	7.87, d (8.5)	5	2, ^b 2a, 3, 5a
5	132.6, CH ^a	8.30, d (8.5)	4	2a, ^b 4, ^b 5a, 8b, 1 ^b
5a	123.9, C			
6	132.5, CH ^a	8.29, d (8.0)	7	5, 5a, 7, ^b 8, 8b
7	128.0, CH	7.85, ddd (8.0, 7.0, 1.0)	6, 8	5a, 8a
8	122.3, CH	8.15, dd (7.0, 1.0)	7	1, 6, 7, ^b 8b
8a	128.1, C			
8b	146.9, C			
1'	139.8, C			
2'	128.5, CH	7.55, m	3'	3, 6'
3'	129.7, CH	7.72, ddd (8.0, 8.0, 1.5)	2'	1', 2', 4'
4'	129.2, CH	7.52, m		3', 5'
5'	129.7, CH	7.72, ddd (8.0, 8.0, 1.5)	6'	1', 4', 6'
6'	128.5, CH	7.55, m	5'	3, 2'

^aSignals interchangeable. ^bIndicates weak or long-range correlation.

Fuliginone (**15**) was isolated as a brown solid. The UV spectrum showed a diagnostic absorbance at 430 nm, confirming a phenylphenalenone-type structure.² Two spin systems were evident from H-4 to H-6 and from H-7 to H-9 on the basis of gCOSY and gHMBCAD NMR data. An aromatic proton (δ_H 7.17) and a pendant aromatic ring could be located at either C-2 or C-3, respectively. Key NOE enhancements were observed between H-4 (δ_H 7.72) and the proton at δ_H 7.17. This secured the position of the aromatic proton (δ_H

7.17) at C-3 and, therefore, the aromatic ring at C-2. Thus, the structure of compound **15** was defined as 2-phenyl-1H-phenalen-1-one. A literature review indicated that this compound was obtained as a synthetic analogue;²² however the UV and NMR data provided in that study do not support this structure. All reported phenylphenalenones display a diagnostic UV absorbance between 430 and 450 nm;^{2,5,9,10,19} however, the product obtained in the synthetic study showed an absorbance at 403 nm.²² Second, several NMR signals were not observed in the synthetic compound reported, in particular the proton signal at δ_H 7.17 and the carbon signals at δ_C 149.5 and 113.8.²² Thus, this represents the first isolation and characterization of compound **15**, and it was given the trivial name fuliginone.

Fuliginol (**16**) was isolated as a brown solid, and analysis of the UV spectrum revealed an absorption at 463 nm, which was supportive of a phenylphenalenone.² The 1H and ^{13}C NMR spectra indicated the presence of a methoxy moiety (δ_H 3.10 (3H); δ_C 61.5), and the IR spectrum supported the presence of a hydroxy group (3369 cm^{-1}). The molecular formula was obtained via ESIMS and deduced as $C_{20}H_{14}O_4$ (observed m/z at 317.0814 $[M - H]^-$ (calcd for $C_{20}H_{13}O_4$: m/z 317.0814). This indicated the presence of two hydroxy groups. Analysis of the gHMBCAD NMR data for H-4 revealed correlations to two deshielded oxygenated tertiary carbons (δ_C 142.8 and 147.8). The methoxy moiety (δ_H 3.10) also showed an HMBC correlation to the carbon at δ_C 142.8, indicating that the methoxy moiety was at C-6. Comparison of the NMR data with those of structurally related phenylphenalenones showed that the C-6 methoxy resonances are deshielded (approximately at δ_H 4.00) compared to their C-5 counterparts (approximately at δ_H 3.00) due to the shielding effect of the aromatic ring.¹⁹ The assignment of the methoxy group at C-6 allowed for subsequent assignment of the C-5 and C-6 chemical shifts at δ_C 147.8 and 142.8 ppm, respectively. A single-crystal X-ray diffraction study (Figure 1) provided the unequivocal identification for **16** as 2,5-dihydroxy-6-methoxy-7-phenyl-1H-phenalen-1-one, and it was given the trivial name fuliginol (Table 4).

Fuliginol (**16**) was isolated as a pure compound prior to the crystallization process, and NMR, UV, and IR data were acquired on the single compound. During the process of crystallization and in the single-crystal X-ray diffraction study the presence of a cocrystal occurring with **16** (in a ratio of approximately 1:1) was noted. This cocrystal (Figure 1), a chlorinated derivative of **16**, was identified as 3-chloro-2,5-dihydroxy-6-methoxy-7-phenyl-1H-phenalen-1-one (**17**) and given the trivial name 3-chlorofuliginol. It is believed that the $CHCl_3$ used during the IR analysis was responsible for the introduction of the chlorine substituent. Upon completion of the X-ray analysis, the crystals were resuspended in the same batch of $CHCl_3$ in an attempt to convert all of **16** to **17**; however after 4 weeks the two compounds remained present in a ratio of approximately 1:1. HPLC purification was attempted on the mixture; however, **16** and **17** were inseparable. Complete 1D and 2D NMR, together with MS analysis, were done on the mixture (Table 4). While fuliginol (**16**) was isolated from the bulbs of the plant, 3-chlorofuliginol (**17**) may represent an artifact of the isolation process.

The absolute configuration of rutin (**4**) was established by comparison of the specific rotation with an authentic standard. The absolute configurations of compounds **8** and **11** remain

Table 3. ^1H and ^{13}C NMR Data (500 MHz, CDCl_3) of Fuliginone (15)

position	δ_{C} , ^a mult	δ_{H} (J in Hz)	gCOSY	gHMBCAD	1D NOE
1	180.5, C				
2	149.5, C				
3	113.8, CH	7.17, s		1, 2, 4, 9b	4, 2', 6'
3a	128.4, C				
4	130.5, CH	7.72, d (7.5)	5	3, 6, 9b	3
5	127.2, CH	7.59, dd (7.5, 8.0)	4, 6	3a, 6a	
6	129.8, CH	7.94, d (8.0)	5	4, 7, 9b	5, 7
6a	132.0, C				
7	136.6, CH	8.28, d (7.5)	8	6, 9, 9b	6, 8
8	126.8, CH	7.81, t (7.5)	7, 9	6a, 9a	
9	131.1, CH	8.74, d (7.5)	8	1, 7, 9b	
9a	127.5, C				
9b	124.4, C				
1'	142.9, C				
2'	128.1, CH	7.49, m	3'	1', 6'	
3'	127.8, CH	7.39, m	2'	4', 5'	
4'	127.3, CH	7.44, m		3', 5'	
5'	127.8, CH	7.39, m	6'	3', 4'	
6'	128.1, CH	7.49, m	5'	1', 2'	

^aCarbon assignments based on HSQCAD and gHMBCAD NMR experiments.

unassigned. Insufficient quantities of these compounds precluded a specific rotation from being obtained.

Biological Activity Studies. Of the compounds isolated from *M. fuliginosa*, rutin (4) possesses a range of properties including antioxidant,^{23,24} antihypertensive,²⁵ and antiviral²⁶ activities, while anigopreissin A (5) has been reported to prevent wrinkles that are caused by muscular contractions.²⁷ Anigorufone (7) inhibits the growth of the casual agent of

Panama's disease,²⁸ antifungal activity against *Mycosphaerella fijiensis*,^{29,30} and activities as a nematostatic and nematocidal compound.³¹ Methyl *trans-p*-coumarate (9) displays antimelanogenic,³² antiadipogenic,³³ anti-inflammatory,³⁴ and antioxidant activities,¹⁶ along with α -glucosidase inhibitory effects.¹⁶ Methyl *cis-p*-coumarate (10) has been reported as an antiradical compound.³⁵ Isosalipurposide (11) shows a range of activity including cytotoxicity against CaCo-2³⁶ and L929 cells³⁷ and antileishmanial,³⁸ anticarcinogenic,³⁹ and anticancer activities.⁴⁰

Antimicrobial evaluation of the crude extracts and the isolated compounds was carried out against five bacteria and one fungus. Crude extracts and mixtures were tested at 50, 25, or 1 mg/mL, while pure compounds, together with a commercially available antibiotic and antifungal agent, were tested between 1639 and 5230 μM (Table 5). Compared to the antibiotic ampicillin, the isolated compounds were less active; however compound 8 was more potent against *Pseudomonas aeruginosa* than ampicillin. In recent years concern has grown around *P. aeruginosa* with regard to its prevalence and multidrug resistance;⁴¹ thus the identification of possible drug leads against this bacteria is important.

Thus, on-line phytochemical profiling studies conducted via HPLC-NMR and HPLC-MS were successful in dereplicating the structures of several known compounds, as well as identifying the presence of new compounds in the crude extract of the bulbs of *M. fuliginosa*. This approach, in combination with the off-line phytochemical isolation, led to the identification of a total of 16 compounds representative of six different structure classes, including the identification of six new compounds (12–17). The isolated compounds were evaluated for antimicrobial activity, with only one compound (8) showing promising activity.

Table 4. ^1H and ^{13}C NMR Data (500 MHz, CDCl_3) for Fuliginol (16) and 3-Chlorofuliginol (17)

position	fuliginol (16)				3-chlorofuliginol (17)			
	δ_{C} , mult	δ_{H} (J in Hz)	gCOSY	gHMBCAD	δ_{C} , mult	δ_{H} (J in Hz)	gCOSY	gHMBCAD
1	180.4, C				178.2, C			
2	148.8, C				146.1, C			
3	114.0, CH	7.07, s		1, 2, 4, 9b	121.3, C ^b			
3a	127.6, C				124.4, C ^b			
4	122.0, CH	7.49, s		3, 3a, 5, 6, 9b	120.7, CH	8.10, s		3, 3a, 5, 6, 9b
5	147.8, C				147.9, C			
6	142.8, C				143.7, C			
6a	127.0, C				127.7, C			
7	145.7, C				146.2, C			
8	131.1, CH	7.63, d (7.5)	9	6a, 7, 9, 9a, 1'	131.1, CH	7.65, d (7.5)	9	6a, 1'
9	128.4, CH	8.61, d (7.5)	8	1, 7, 8, 9a, 9b	129.0, CH	8.62, d (7.5)	8	1, 7, 9b
9a	124.9, C				125.9, C			
9b	121.2, C				120.7, C			
1'	141.7, C				141.6, C			
2'	129.5, CH	7.50, m	3'	7, 1', 3', 4'	129.3, CH	7.50, m	3'	3', 4'
3'	127.3, CH	7.44, m	2'	1', 2', 4', 5'	127.3, CH	7.45, m	2'	1', 2'
4'	127.3, CH	7.44, m		2', 3', 5', 6'	127.3, CH	7.45, m		2', 6'
5'	127.3, CH	7.44, m	6'	1', 3', 4', 6'	127.3, CH	7.45, m	6'	1', 6'
6'	129.5, CH	7.50, m	5'	7, 1', 4', 5'	129.3, CH	7.50, m	5'	4', 5'
2-OH		ND ^a			ND ^a			
5-OH		ND ^a			ND ^a			
6-OCH ₃	61.5, CH ₃	3.10, s		6	61.6, CH ₃	3.14, s		6

^aSignal not detected. ^bSignals interchangeable.

Table 5. Antimicrobial Activity of the Crude Extracts and Pure Compounds Obtained from *M. fuliginosa*, Together with Commercial Standard Antibiotic and Antifungal Compounds, Showing Zones of Inhibition (mm)

	concentration	microorganism					
		<i>E. coli</i> ^a ATCC 25922	<i>S. aureus</i> ^b ATCC 25923	<i>S. aureus</i> MRSA ^c 344/2-32	<i>P. aeruginosa</i> ^d ATCC 27853	<i>S. pyogenes</i> ^e 345/1	<i>C. albicans</i> ^f ATCC 10231
CH ₂ Cl ₂ extract of flowers	25 mg/mL	ND ^g	1	ND ^g	3	1	ND ^g
MeOH extract of flowers	50 mg/mL	ND ^g	ND ^g	ND ^g	ND ^g	ND ^g	ND ^g
CH ₂ Cl ₂ extract of bulbs	50 mg/mL	ND ^g	1	ND ^g	2	3	1
MeOH extract of bulbs	50 mg/mL	ND ^g	1	2	1	4	1
mixture of hemofluorones A (1) and B (2)	1 mg/mL	ND ^g	ND ^g	ND ^g	1	ND ^g	ND ^g
rutin (4)	1639 μM	ND ^g	ND ^g	ND ^g	ND ^g	ND ^g	ND ^g
anigopreissin A (5)	2211 μM	ND ^g	2	ND ^g	ND ^g	1	ND ^g
2-phenylnaphthalic anhydride (6)	3649 μM	ND ^g	ND ^g	ND ^g	2	ND ^g	ND ^g
anigorufone (7)	3675 μM	ND ^g	ND ^g	ND ^g	ND ^g	ND ^g	ND ^g
compound 8	1724 μM	1	ND ^g	ND ^g	10	1	ND ^g
mixture of compounds 9 and 10	1 mg/mL	ND ^g	1	ND ^g	ND ^g	1	ND ^g
isosalipurposide (11)	3030 μM	ND ^g	ND ^g	ND ^g	2	ND ^g	ND ^g
fuliginosin A (12)	2762 μM	ND ^g	1	ND ^g	ND ^g	1	ND ^g
fuliginosin B (13)	2450 μM	ND ^g	ND ^g	ND ^g	ND ^g	ND ^g	ND ^g
fuliginosone (14)	3875 μM	ND ^g	2	ND ^g	1	ND ^g	ND ^g
fuliginone (15)	3905 μM	ND ^g	ND ^g	ND ^g	ND ^g	2	ND ^g
mixture of fuliginol (16) and 3-chlorofuliginol (17)	1 mg/mL	ND ^g	ND ^g	ND ^g	ND ^g	3	ND ^g
ampicillin (antibiotic)	2862 μM	ND ^g	15	3	2	20	NT ^h
carbendazim (antifungal)	5230 μM	NT ^h	NT ^h	NT ^h	NT ^h	NT ^h	ND ^g

^a*Escherichia coli*. ^b*Staphylococcus aureus*. ^cMethicillin-resistant *Staphylococcus aureus*. ^d*Pseudomonas aeruginosa*. ^e*Streptococcus pyogenes*. ^f*Candida albicans*. ^gIndicates no zone of inhibition detected. ^hIndicates not tested.

EXPERIMENTAL SECTION

General Experimental Procedures. All organic solvents used were analytical reagent (AR or GR), UV spectroscopic, or HPLC grade with Milli-Q water also being used. Optical rotations were carried out using a 1.5 mL cell on a Rudolph Research Analytical Autopol IV automatic polarimeter, set to the Na 589 nm wavelength. UV/vis spectra were recorded on an Agilent Cary 60 spectrophotometer, using EtOH. FTIR spectra were recorded as a film using NaCl disks on a PerkinElmer Spectrum One FTIR spectrometer. Uncorrected melting points were recorded on a Gallenkamp melting point apparatus. ¹H (500 MHz), ¹³C (125 MHz), and 1D NOE spectra were acquired in CDCl₃ and DMSO-*d*₆ on a 500 MHz Agilent DD2 NMR spectrometer with referencing to solvent signals (δ_{H} 7.26; δ_{C} 77.0 and δ_{H} 2.50; δ_{C} 39.5 ppm, respectively). Two-dimensional NMR experiments recorded included gradient correlation spectroscopy (gCOSY), heteronuclear single-quantum correlation spectroscopy with adiabatic pulses (HSQCAD), and gradient heteronuclear multiple-bond spectroscopy with adiabatic pulses (gHMBCAD). Silica gel flash chromatography was carried out using Davisil LC35 Å silica gel (40–60 mesh) with a 20% stepwise solvent elution from 100% petroleum ether (60–80 °C) to 100% CH₂Cl₂ to 100% EtOAc and finally to 100% MeOH. C₁₈ vacuum liquid chromatography (VLC) was carried out on silica gel 60 RP-18 (40–63 μm) using a 20% stepwise solvent elution from 100% H₂O to 100% MeOH, and, finally, to 100% CH₂Cl₂ or a 20% stepwise elution from 30% CH₃CN/H₂O to 90% CH₃CN/H₂O and a final elution of 100% CH₃CN. ESI mass spectra were obtained on a Micromass Platform II mass spectrometer equipped with an LC-10AD Shimadzu solvent delivery module (50% CH₃CN/H₂O at a flow rate of 0.2 mL/min) in both the positive and negative ionization modes using cone voltages between 20 and 30 V. HRESIMS was carried out on an Agilent 6200 Series TOF system (ESI operation conditions of 8 L/min N₂, 325 °C drying gas temperature, and 3500 V capillary voltage) equipped with an Agilent 1200 Series LC solvent delivery module (100% MeOH at a flow rate of 0.3 mL/min) in either the positive or negative ionization modes. The instrument was calibrated using the “Agilent Tuning Mix” with purine as the reference compound and the Hewlett–Packard standard

HP0921. HRMS was also carried out on a Waters Xevo QToF mass spectrometer, with an atmospheric solids analysis probe (ASAP) source (probe temperature set to 300 °C; source temperature set to 80 °C; sampling cone voltage of 20.0 V). Accurate mass was obtained by lockmass using leucine enkephalin as the reference compound. All analytical HPLC analyses and method development were performed on a Dionex P680 solvent delivery system equipped with a PDA100 UV detector (operated using Chromeleon software). Analytical HPLC analyses were carried out using either a gradient method (0–2 min 10% CH₃CN/H₂O; 14–24 min 75% CH₃CN/H₂O; 26–30 min 100% CH₃CN; and 32–40 min 10% CH₃CN/H₂O or 0–3.5 min 30% CH₃CN/H₂O; 8.5–40 min 50% CH₃CN/H₂O) or an isocratic method (either 70, 50, 45, 40, 30, or 25% CH₃CN/H₂O) on an Alltech Alltima HP C₁₈ (250 × 4.6) 5 μm column at a flow rate of 1.0 mL/min. Semipreparative HPLC was carried out on a Varian Prostar 210 solvent delivery system equipped with a Prostar 335 PDA detector (operated using Star Workstation software) using either a gradient method (0–2 min 10% CH₃CN/H₂O; 14–24 min 75% CH₃CN/H₂O; 26–30 min 100% CH₃CN; and 32–40 min 10% CH₃CN/H₂O or 0–3.5 min 30% CH₃CN/H₂O; 8.5–40 min 50% CH₃CN/H₂O) or an isocratic method (either 70, 50, 45, 40, 30, or 25% CH₃CN/H₂O) using an Alltech Alltima C₁₈ (250 × 10) 5 μm column at a flow rate of 3.5 mL/min.

Single-Crystal X-ray Diffraction. Crystals of fuliginosone (14), fuliginol (16), and 3-chlorofuliginol (17) were obtained by dissolving the compounds in CH₂Cl₂ and allowing the solvent to evaporate at room temperature. Crystallographic diffraction data were collected with an Oxford SuperNova diffractometer using Cu radiation ($k = 1.54184 \text{ \AA}$). Data were reduced using the CrystalPRO software. The temperature of the data collection was maintained at 130 K, using an Oxford Cryostream cooling device. The structure was solved by direct methods and difference Fourier synthesis and was refined on F^2 (SHELXL-97).⁴² A thermal ellipsoid plot was generated using the program ORTEP-3⁴³ integrated within the WINGX program suite.⁴⁴

Biological Evaluation. For the biological evaluation procedure, refer to Brkljajča and Urban.⁴⁵

Plant Material. Several specimens of the plant (*M. fuliginosa*) were purchased from Kuranga Native Nursery (Mount Evelyn, Victoria, Australia) and from Gardenworld Nursery (Braeside, Victoria, Australia) in January 2011, October 2012, and November 2012. The bulbs of the plants purchased in 2011 and 2012 were used in this study, while the flowers were harvested from the plants purchased in 2012. The bulbs and flowers were separated and then stored at -80°C until extraction. Voucher specimens were designated with the code numbers 2011-01a (bulbs), 2011-02a (bulbs), 2012-01a (bulbs), and 2012_05a (flowers), respectively, and are deposited in the School of Applied Sciences (Discipline of Applied Chemistry), RMIT University.

Phytochemical Profiling. Chemical profiling was carried out on the CH_2Cl_2 -soluble extracts of the bulbs and flowers using HPLC-NMR and HPLC-MS methodologies. Details of these analyses are provided in the General Experimental Procedures section and in Brkljača and Urban.⁴⁵ The CH_2Cl_2 extract of the bulbs (157.9 mg) was dissolved in HPLC-NMR grade CH_3CN (1580 μL) and filtered through a 0.45 PTFE membrane filter (Grace Davison Discovery Sciences) for HPLC-NMR analysis. Owing to the poor solubility of the CH_2Cl_2 crude extract of the flowers in CH_3CN , no HPLC-NMR was conducted. HPLC-MS analyses were carried out on the CH_2Cl_2 crude extracts of both the bulbs and flowers.

Extraction and Isolation of Flowers. The flowers of the plant (31 g, wet weight) were extracted with 3:1 MeOH/ CH_2Cl_2 (2 L). The crude extract was decanted and concentrated under reduced pressure and sequentially solvent partitioned (trituated) into CH_2Cl_2 - and MeOH-soluble extracts, respectively. A portion of the MeOH extract of the flowers (200 mg) was subjected to Sephadex LH-20 column chromatography (100% MeOH) to yield seven fractions. The fourth fraction was subjected to RP-HPLC (using a gradient of 0–3.5 min 30% $\text{CH}_3\text{CN}/\text{H}_2\text{O}$; 8.5–40 min 50% $\text{CH}_3\text{CN}/\text{H}_2\text{O}$) to yield isosalipurposide (**11**) (0.7 mg, 0.01%). Another portion of the MeOH extract of the flowers (244 mg) was subjected to Sephadex LH-20 column chromatography (100% MeOH) to yield six fractions. The fourth fraction yielded a mixture (13.6 mg, 0.2%) of hemofluorones A (**1**) and B (**2**). The second fraction was subjected to RP-HPLC (25% $\text{CH}_3\text{CN}/\text{H}_2\text{O}$) to yield rutin (**4**) (4.6 mg, 0.08%). The third fraction was subjected to reversed-phase HPLC (30% $\text{CH}_3\text{CN}/\text{H}_2\text{O}$) to yield the *p*-hydroxycinnamate of salipurposide (**8**) (0.4 mg, 0.007%), a mixture of methyl *trans*- and *cis*-*p*-coumarate (**9** and **10**) (0.1 mg, 0.002%), and isosalipurposide (**11**) (0.1 mg, 0.002%). Another portion of the MeOH extract (83.4 mg) was subjected to C_{18} VLC (20% stepwise elution from 30% $\text{CH}_3\text{CN}/\text{H}_2\text{O}$ to 90% $\text{CH}_3\text{CN}/\text{H}_2\text{O}$ and finally to 100% CH_3CN) to yield 11 fractions. The first fraction (50% $\text{CH}_3\text{CN}/\text{H}_2\text{O}$) was subjected to Sephadex LH-20 column chromatography (100% MeOH) to yield rutin (**4**) (6.4 mg, 0.1%). The second VLC fraction (50% $\text{CH}_3\text{CN}/\text{H}_2\text{O}$) was subjected to Sephadex LH-20 column chromatography (100% MeOH) to yield 11 fractions. Fractions 5–8 were combined to yield the *p*-hydroxycinnamate of salipurposide (**8**) (2.1 mg, 0.04%). The percentage yields are reported on the basis of the dry mass of the flowers extracted.

Extraction and Isolation of Bulbs. The bulbs of the plant (77 g, wet weight) were extracted with 3:1 MeOH/ CH_2Cl_2 (2 L). The crude extract was decanted and concentrated under reduced pressure and sequentially solvent partitioned (trituated) into CH_2Cl_2 - and MeOH-soluble extracts, respectively. The CH_2Cl_2 extract was subjected to flash silica gel column chromatography (20% stepwise elution from petroleum ether (60–80 $^{\circ}\text{C}$) to CH_2Cl_2 to EtOAc and, finally, to MeOH). The 100% CH_2Cl_2 fraction yielded anigorufone (**7**) (35.8 mg, 0.05%). The 80% CH_2Cl_2 /EtOAc fraction (first eluting band) was subjected to RP-HPLC (70% $\text{CH}_3\text{CN}/\text{H}_2\text{O}$) to yield 2-phenyl-naphthalic anhydride (**6**) (0.8 mg, 0.001%), anigorufone (**7**) (6.0 mg, 0.009%), and fuliginosone (**14**) (1.6 mg, 0.002%). The 80% CH_2Cl_2 /EtOAc fraction (second eluting band) was subjected to Sephadex LH-20 column chromatography (100% MeOH) to yield four fractions. The third fraction was subjected to reversed-phase HPLC (70% $\text{CH}_3\text{CN}/\text{H}_2\text{O}$) to yield anigorufone (**7**) (4.5 mg, 0.007%), fuliginosone (**14**) (1.5 mg, 0.002%), 2-phenyl-1*H*-phenalen-1-one (**15**) (1.9 mg, 0.003%), and fuliginol (**16**) (6.5 mg, 0.01%). A portion

of the MeOH extract (150 mg) was subjected to RP-HPLC (50% $\text{CH}_3\text{CN}/\text{H}_2\text{O}$) to yield anigopreissin A (**5**) (12.2 mg, 0.02%) and fuliginosin A (**12**) (4.0 mg, 0.006%). Another portion of the MeOH extract (220 mg) was subjected to C_{18} VLC (20% stepwise elution from H_2O to MeOH and finally to CH_2Cl_2) to yield 10 fractions. The 20% $\text{H}_2\text{O}/\text{MeOH}$ fraction was subjected to reversed-phase HPLC (50% $\text{CH}_3\text{CN}/\text{H}_2\text{O}$) to yield anigopreissin A (**5**) (17.1 mg, 0.03%) and fuliginosin A (**12**) (5.6 mg, 0.008%). One of the fractions from the HPLC purification was further subjected to RP-HPLC (50% $\text{CH}_3\text{CN}/\text{H}_2\text{O}$) to yield fuliginosin A (**12**) (0.6 mg, 0.001%) and fuliginosin B (**13**) (0.7 mg, 0.001%). The percentage yields are reported on the basis of the dry mass of the bulbs extracted.

On-line (HPLC-NMR and HPLC-MS) Characterization of Compounds. Compounds Derived from the Flowers of *M. fuliginosa*. Hemofluorone A (5,8,9-trihydroxy-1*H*-naphtho[2,1,8-*mna*]xanthen-1-one) (**1**): $t_{\text{R}} = 3.74$ min; UV (extracted from PDA) (30% $\text{CH}_3\text{CN}/\text{D}_2\text{O}$) $\lambda_{\text{max}} 572$ nm; HPLC-MS m/z 317.0453 (calcd for $\text{C}_{19}\text{H}_9\text{O}_5$, 317.0450).

Hemofluorone B (5,8,9-trihydroxy-3*H*-naphtho[2,1,8-*mna*]xanthen-3-one) (**2**): $t_{\text{R}} = 4.44$ min; UV (extracted from PDA) (30% $\text{CH}_3\text{CN}/\text{D}_2\text{O}$) $\lambda_{\text{max}} 551$ nm; HPLC-MS m/z 317.0453 (calcd for $\text{C}_{19}\text{H}_9\text{O}_5$, 317.0450).

Rutin (**4**): $t_{\text{R}} = 2.45$ min; UV (extracted from PDA) (30% $\text{CH}_3\text{CN}/\text{D}_2\text{O}$) $\lambda_{\text{max}} 353$ nm; HPLC-MS m/z 609.1453 (calcd for $\text{C}_{27}\text{H}_{29}\text{O}_{16}$, 609.1456).

p-Hydroxycinnamate of salipurposide (**8**): $t_{\text{R}} = 15.05$ min; UV (extracted from PDA) (30% $\text{CH}_3\text{CN}/\text{D}_2\text{O}$) $\lambda_{\text{max}} 317, 368$ nm; HPLC-MS m/z 579.1503 (calcd for $\text{C}_{30}\text{H}_{27}\text{O}_{12}$, 579.1503).

Compounds Derived from the Bulbs of *M. fuliginosa*. Anigopreissin A (5-[4-hydroxy-2-(4-hydroxyphenyl)-6- $\{(1E)-2-(4-hydroxyphenyl)ethenyl\}-3-benzofuranyl\}-1,3-benzenediol$) (**5**): $t_{\text{R}} = 4.11$ min; UV (extracted from PDA) (50% $\text{CH}_3\text{CN}/\text{D}_2\text{O}$) $\lambda_{\text{max}} 263, 303, 355$ nm; HPLC-NMR WET1D NMR (500 MHz, 50% $\text{CH}_3\text{CN}/\text{D}_2\text{O}$) obtained from stop-flow HPLC-NMR mode δ 7.82 (2H, d, $J = 9.0$ Hz, H-2a/H-6a*), 7.77 (2H, d, $J = 9.0$ Hz, H-3a/H-5a*), 7.59 (1H, d, $J = 1.0$ Hz, H-10b $^{\circ}$), 7.52 (1H, d, $J = 16.0$ Hz, H-7b $^{\wedge}$), 7.42 (1H, d, $J = 16.0$ Hz, H-8b $^{\wedge}$), 7.22 (2H, d, $J = 8.0$ Hz, H-2b/H-6b $^{\#}$), 7.20 (1H, s, H-12a), 7.15 (2H, d, $J = 8.0$ Hz, H-3b/H-5b $^{\#}$), 6.83 (1H, d, $J = 1.0$ Hz, H-14b $^{\circ}$), 6.78 (2H, s, H-10a/H-14a), * $^{\wedge}$ signals interchangeable; HPLC-MS m/z 451.1189 (calcd for $\text{C}_{28}\text{H}_{19}\text{O}_6$, 451.1182).

2-Phenyl-naphthalic anhydride (**6**): $t_{\text{R}} = 12.35$ min; UV (extracted from PDA) (50% $\text{CH}_3\text{CN}/\text{D}_2\text{O}$) $\lambda_{\text{max}} 240, 323$ nm; HPLC-NMR WET1D NMR (500 MHz, 50% $\text{CH}_3\text{CN}/\text{D}_2\text{O}$) obtained from stop-flow HPLC-NMR mode δ 8.80 (2H, d, $J = 8.5$ Hz, H-4/H-5 $^{\#}$), 8.52 (1H, d, $J = 8.0$ Hz, H-7 $^{\#}$), 8.29 (1H, dd, $J = 8.0, 8.5$ Hz, H-6), 8.27 (1H, d, $J = 8.5$ Hz, H-3), 8.10 (2H, d, $J = 7.5$ Hz, H-2'/H-6'), 7.94 (2H, m, H-3'/H-5'), 7.92 (1H, m, H-4'), $^{\#}$ signals interchangeable; HPLC-NMR ^{13}C NMR (125 MHz, 50% $\text{CH}_3\text{CN}/\text{D}_2\text{O}$) obtained from stop-flow HPLC-NMR mode δ 134.0 (CH, C-4/C-5 $^{\#}$), 131.6 (CH, C-3), 130.4 (CH, C-2'/C6'), 129.8 (CH, C-4'), 129.2 (CH, C-3'/C-5'), 129.1 (CH, C-6), 123.1 (CH, C-7 $^{\#}$), $^{\#}$ signals interchangeable; HPLC-MS m/z 275.0700 (calcd for $\text{C}_{18}\text{H}_{11}\text{O}_3$, 275.0708).

Anigorufone (2-hydroxy-9-phenyl-1*H*-phenalen-1-one) (**7**): $t_{\text{R}} = 19.18$ min; UV (extracted from PDA) (50% $\text{CH}_3\text{CN}/\text{D}_2\text{O}$) $\lambda_{\text{max}} 410$ nm; HPLC-NMR WET1D NMR (500 MHz, 50% $\text{CH}_3\text{CN}/\text{D}_2\text{O}$) obtained from stop-flow HPLC-NMR mode δ 8.73 (1H, d, $J = 8.0$ Hz, H-7 $^{\#}$), 8.44 (1H, d, $J = 8.0$ Hz, H-4*), 8.22 (1H, d, $J = 7.0$ Hz, H-6*), 8.06 (1H, dd, $J = 7.0, 8.0$ Hz, H-5), 7.97 (1H, d, $J = 8.0$ Hz, H-8 $^{\#}$), 7.84 (2H, m, H-3'/H-5'), 7.82 (1H, m, H-4'), 7.75 (2H, d, $J = 7.5$ Hz, H-2'/H-6'), 7.59 (1H, s, H-3), * $^{\#}$ signals interchangeable; HPLC-NMR ^{13}C NMR (125 MHz, 50% $\text{CH}_3\text{CN}/\text{D}_2\text{O}$) obtained from stop-flow HPLC-NMR mode δ 136.5 (CH, C-7 $^{\#}$), 132.0 (CH, C-8 $^{\#}$), 131.8 (CH, C-6*), 130.8 (CH, C-4*), 129.1 (CH, C-3'/C-5'), 128.5 (CH, C-2'/C-6'), 128.2 (CH, C-4'), 128.0 (CH, C-5), 114.7 (CH, C-3), * $^{\#}$ signals interchangeable; HPLC-MS m/z 271.0765 (calcd for $\text{C}_{19}\text{H}_{11}\text{O}_2$, 271.0759).

Fuliginosin A [3-(3,5-dihydroxyphenyl)-4-hydroxy-2-(4-hydroxyphenyl)benzofuran-6-carbaldehyde] (**12**) and B [5-(6-dimethoxymethyl)-4-hydroxy-2-(4-hydroxyphenyl)benzofuran-3-

yl)benzene-1,3-diol] (13): $t_R = 3.28$ min; UV (extracted from PDA) (50% CH₃CN/D₂O) λ_{max} 238, 268, 322, 362 nm; HPLC-NMR WET1D NMR (500 MHz, 50% CH₃CN/D₂O) obtained from stop-flow HPLC-NMR mode δ 10.25 (s), 8.01 (s), 7.82 (d, $J = 8.5$ Hz), 7.79 (s), 7.51 (s), 7.17 (d, $J = 8.5$ Hz), 7.02 (s), 6.77 (s), 6.74 (s), 4.18 (s), 4.15 (s).

Fuliginosone (3-phenylacenaphthylene-1,2-dione) (14): $t_R = 11.31$ min; UV (extracted from PDA) (50% CH₃CN/D₂O) λ_{max} 240, 345 nm; HPLC-NMR WET1D NMR (500 MHz, 50% CH₃CN/D₂O) obtained from stop-flow HPLC-NMR mode δ 9.02 (1H, d, $J = 8.0$ Hz, H-4*), 8.88 (1H, d, $J = 8.0$ Hz, H-5*), 8.83 (1H, d, $J = 8.0$ Hz, H-6*), 8.29 (1H, dd, $J = 8.0, 8.0$ Hz, H-7), 8.07 (1H, d, $J = 8.0$ Hz, H-8*), 7.80–7.96 (5H, m, H-2'/H-3'/H-4'/H-5'/H-6'), *signals interchangeable; HPLC-MS m/z 259.0766 (calcd for C₁₈H₉O₂, 259.0759).

Off-line Characterization of Compounds. Hemofluorone A (5,8,9-trihydroxy-1H-naphtho[2,1,8-mna]xanthen-1-one) (1): purple, amorphous solid; all off-line NMR and MS data were identical to literature data;⁸ ¹³C NMR (125 MHz, DMSO-*d*₆) δ 181.8 (C, C-1), 158.1 (C, C-6a), 148.1 (C, C-9*), 146.6 (C, C-8*), 141.6 (C, C-5*), 140.0 (C, C-5a*), 139.3 (CH, C-3), 135.5 (C, C-10b), 131.4 (CH, C-12), 126.9 (CH, C-2), 124.5 (C, C-12a), 122.6 (CH, C-4), 121.8 (C, C-3a), 121.5 (C, C-12b), 118.3 (C, C-12c), 113.6 (CH, C-11), 107.0 (C, C-10a), 105.4 (CH, C-10), 102.5 (CH, C-7), *signals interchangeable.

Hemofluorone B (5,8,9-trihydroxy-3H-naphtho[2,1,8-mna]xanthen-3-one) (2): purple, amorphous solid; all off-line NMR and MS data were identical to literature data.^{3,8}

Rutin: brown oil; all off-line NMR, MS, and specific rotation data were identical to literature data¹⁷ and compared to an authentic standard of rutin.

Anigopreissin A (5-[4-hydroxy-2-(4-hydroxyphenyl)-6-((1E)-2-(4-hydroxyphenyl)ethenyl)-3-benzofuran-1-yl]-1,3-benzenediol) (5): brown oil; all off-line NMR and MS data were identical to literature data.⁴

2-Phenyl-naphthalic anhydride (6): yellow, amorphous solid; all off-line UV and MS data were identical to literature data;² ¹H NMR (500 MHz, CDCl₃) δ 8.71 (1H, dd, $J = 7.5, 1.5$ Hz, H-7), 8.34 (1H, dd ($J = 8.5, 1.5$ Hz, H-5), 8.29 (1H, d, $J = 8.5$ Hz, H-4), 7.85 (1H, dd, $J = 8.5, 7.5$ Hz, H-6), 7.69 (1H, d, $J = 8.5$ Hz, H-3), 7.42–7.57* (5H, m, H-2', H-3', H-4', H-5', H-6'); ¹³C NMR (125 MHz, CDCl₃) δ 161.0 (C, C-9), 150.2 (C, C-2), 140.3 (C, C-1'), 135.4 (CH, C-5), 134.2 (CH, C-4), 133.7 (CH, C-7), 131.8 (CH, C-3), 131.2 (C, C-4a), 131.1 (C, C-8a), 128.2–128.4* (CH, C-2', C-3', C-4', C-5', C-6'), 127.1 (CH, C-6), 119.2 (C, C-8), 115.5 (C, C-1), ND (C, C-10), * indicates signals overlapped.

Anigorufone (2-hydroxy-9-phenyl-1H-phenalen-1-one) (7): orange, amorphous solid; all off-line NMR and MS data were identical to literature data.⁵

p-Hydroxycinnamate of salipurposide (2,3-dihydro-7-hydroxy-2-(4-hydroxyphenyl)-5-[[6-O-[3-(4-hydroxyphenyl)-1-oxo-2-propen-1-yl]- β -D-glucopyranosyl]oxy]-4H-1-benzopyran-4-one) (8): light brown, amorphous solid; all off-line NMR and MS data were identical to literature data.¹⁸

Mixture of methyl *trans*-*p*-coumarate (9) and methyl *cis*-*p*-coumarate (10): amorphous, brown solid; *trans* to *cis* ratio was 1:0.17, respectively; all off-line NMR and MS data were identical to literature data.^{16,46,47}

Isoalipurposide (11): yellow, amorphous solid; all off-line NMR and MS data were identical to literature data;¹⁵ ¹H NMR (500 MHz, CD₃OD) δ 8.05 (1H, d, $J = 15.5$ Hz, H-8), 7.65 (1H, d, $J = 15.5$ Hz, H-7), 7.61 (2H, d, $J = 9.0$ Hz, H-2/H-6), 6.83 (2H, d, $J = 9.0$ Hz, H-3/H-5), 6.17 (1H, brs, H-14*), 5.95 (1H, brs, H-12*), 5.15 (1H, d, $J = 7.0$ Hz, H-16), 3.92 (1H, d, $J = 12.0$ Hz, H-21a), 3.75 (1H, dd, $J = 4.5, 12.0$ Hz, H-21b), 3.55 (1H, m, H-17), 3.52 (1H, m, H-19*), 3.48 (1H, m, H-20), 3.46 (1H, m, H-18*), *signals interchangeable; ¹³C NMR (125 MHz, CD₃OD) δ 192.9 (C, C-9), 160.5 (C, C-13), 159.7 (C, C-4), 142.3 (CH, C-7), 130.4 (CH, C-2/C-6), 127.1 (C, C-1), 124.8 (CH, C8), 115.5 (CH, C-3/C-5), 105.6 (C, C-10), 100.4 (CH, C-16), 97.6 (CH, C-12*), 95.1 (CH, C14*), 73.6 (CH, C-17), 77.2 (CH, C-

19#/C-20), 69.7 (CH, C-18*), 60.9 (CH₂, C-21), ND (C-11/C-15), *signals interchangeable.

Fuliginosin A [3-(3,5-dihydroxyphenyl)-4-hydroxy-2-(4-hydroxyphenyl)benzofuran-6-carbaldehyde] (12): dark yellow oil; UV (EtOH) λ_{max} (log ϵ) 285 (3.75), 324 (3.77), 367 (3.79) nm; IR ν_{max} 3208, 2926, 1682, 1607, 1515, 1443, 1397, 1324, 1276 cm⁻¹; ¹H NMR (500 MHz, DMSO-*d*₆) see Table 1; ¹³C NMR (125 MHz, DMSO-*d*₆) see Table 1; HRESIMS m/z 361.0715 (calcd for C₂₁H₁₃O₆, 361.0712).

Fuliginosin B [5-(6-(dimethoxymethyl)-4-hydroxy-2-(4-hydroxyphenyl)benzofuran-3-yl)benzene-1,3-diol] (13): brown oil; UV (EtOH) λ_{max} (log ϵ) 303 (3.08), 313 (4.08), 369 (3.53) nm; IR ν_{max} 3419, 2923, 2131, 1645 cm⁻¹; ¹H NMR (500 MHz, DMSO-*d*₆) see Table 1; ¹³C NMR (125 MHz, DMSO-*d*₆) see Table 1; HRESIMS m/z 407.1138 (calcd for C₂₃H₁₉O₇, 407.1131).

Fuliginosone (3-phenylacenaphthylene-1,2-dione) (14): bright yellow needles (CH₂Cl₂); mp 217–222 °C; C₁₈H₁₀O₂, $M = 258.26$, $T = 130.0(2)$ K, $\lambda = 1.5418$ Å, orthorhombic, space group *Pbca*, $a = 8.4671(4)$ Å, $b = 7.3151(4)$ Å, $c = 39.179(2)$ Å, $V = 2426.7(2)$ Å³, $Z = 8$, $D_c = 1.414$ Mg/m³ $\mu(\text{Cu K}\alpha) 0.736$ mm⁻¹, $F(000) = 1072$, crystal size $0.27 \times 0.07 \times 0.02$ mm, 6910 reflections measured, 2188 independent reflections ($R_{int} = 0.052$), the final R was 0.0493 [$I > 2\sigma(I)$] and $wR(F^2)$ was 0.1255 (all data). Crystallographic data for 14 have been deposited at the Cambridge Crystallographic Data Centre (CCDC 1044045), 12 Union Road, Cambridge, CB2 1EZ, UK (www.ccdc.cam.ac.uk/data_request/cif); UV (EtOH) λ_{max} (log ϵ) 244 (4.43), 324 (3.76) nm; IR ν_{max} 1719, 1590 cm⁻¹; ¹H NMR (500 MHz, CDCl₃) see Table 2; ¹³C NMR (125 MHz, CDCl₃) see Table 2; HRESIMS m/z 259.0752 (calcd for C₁₈H₁₁O₂, 259.0759).

Fuliginone (2-phenyl-1H-phenalen-1-one) (15): brown, amorphous solid; UV (EtOH) λ_{max} (log ϵ) 333 (3.63), 368 (3.65), 431 (3.59) nm; IR ν_{max} 3350, 2925, 2854, 1622, 1574, 1510, 1491, 1409, 1274, 1214 cm⁻¹; ¹H NMR (500 MHz, CDCl₃) see Table 3; ¹³C NMR (125 MHz, CDCl₃) see Table 3; HRASAPMS m/z 257.0856 (calcd for C₁₉H₁₃O, 257.0966).

Fuliginol (2,5-dihydroxy-6-methoxy-7-phenyl-1H-phenalen-1-one) (16): cocrystal with 3-chlorofuliginol, orange needles (CHCl₃); did not melt below 360 °C; 0.57(C₂₀H₁₂ClO₄) 0.43(C₂₀H₁₄O₄), $M = 337.79$, $T = 130.0(2)$ K, $\lambda = 1.5418$ Å, triclinic, space group *P1*, $a = 7.1864(15)$ Å, $b = 10.074(2)$ Å, $c = 10.803(3)$ Å, $\alpha = 89.17(2)^\circ$, $\beta = 77.53(2)^\circ$, $\gamma = 82.260(18)^\circ$, $V = 756.6(3)$ Å³, $Z = 2$, $D_c = 1.483$ Mg/m³, $\mu(\text{Cu K}\alpha) 1.732$ mm⁻¹, $F(000) = 350$, crystal size $0.14 \times 0.04 \times 0.02$ mm, 3885 reflections measured, 2213 independent reflections ($R_{int} = 0.057$), the final R was 0.0704 [$I > 2\sigma(I)$] and $wR(F^2)$ was 0.200 (all data). Crystallographic data for 16 and 17 have been deposited at the Cambridge Crystallographic Data Centre (CCDC 1044044), 12 Union Road, Cambridge, CB2 1EZ, UK (www.ccdc.cam.ac.uk/data_request/cif); UV (EtOH) λ_{max} (log ϵ) 275 (4.10), 375 (3.91), 463 (3.54) nm; IR ν_{max} 3369, 1618, 1569, 1393, 1215 cm⁻¹; ¹H NMR (500 MHz, CDCl₃) see Table 4; ¹³C NMR (125 MHz, CDCl₃) see Table 4; HRESIMS m/z 317.0814 (calcd for C₂₀H₁₃O₄, 317.0814).

3-Chlorofuliginol (3-chloro-2,5-dihydroxy-6-methoxy-7-phenyl-1H-phenalen-1-one) (17): cocrystal data (see fuliginol (16)); ¹H NMR (500 MHz, CDCl₃) see Table 4; ¹³C NMR (125 MHz, CDCl₃) see Table 4; HRESIMS m/z 351.0427 (calcd for C₂₀H₁₂³⁵ClO₄, 351.0424).

■ ASSOCIATED CONTENT

📄 Supporting Information

Supporting Information including the on-line HPLC-NMR and HPLC-MS analyses from the phytochemical profiling together with the off-line NMR and high-resolution MS data associated with this study. The Supporting Information is available free of charge on the ACS Publications website at DOI: 10.1021/acs.jnatprod.5b00161.

AUTHOR INFORMATION

Corresponding Author

*Tel: +61-3-9925-3376. Fax: +61-3-9925-3747. E-mail: sylvia.urban@rmit.edu.au.

Notes

The authors declare no competing financial interest.

ACKNOWLEDGMENTS

The Marine and Terrestrial Natural Product (MATNAP) research group would like to thank Mrs. N. Thurbon (School of Applied Sciences (Discipline of Biotechnology and Biological Sciences), Science Engineering and Health, RMIT University) for providing access to the microorganisms to conduct the antimicrobial assays and for her invaluable technical support; Ms. S. Duck (School of Chemistry, Faculty of Science, Monash University) for conducting the HRMS analyses along with access to the HPLC-MS instrument; and Dr. J. Niere for NMR discussions and guidance. R.B. would also like to acknowledge his Australian Postgraduate Award (APA) scholarship that has supported his Ph.D. studies.

REFERENCES

- (1) FloraBase—the Western Australian Flora. Department of Parks and Wildlife; <https://florabase.dpaw.wa.gov.au/>, 1998.
- (2) Cooke, R. G.; Thomas, R. L. *Aust. J. Chem.* **1975**, *28*, 1053–1057.
- (3) Chaffee, A. L.; Cooke, R. G.; Dagley, I. J.; Perlmutter, P.; Thomas, R. L. *Aust. J. Chem.* **1981**, *34*, 587–598.
- (4) Holscher, D.; Schneider, B. *Phytochemistry* **1996**, *43*, 471–473.
- (5) Holscher, D.; Schneider, B. *Phytochemistry* **1997**, *45*, 87–91.
- (6) Holscher, D.; Schneider, B. *Phytochemistry* **1999**, *50*, 155–161.
- (7) Otalvaro, F.; Gorls, H.; Holscher, D.; Schmitt, B.; Echeverri, F.; Quinones, W.; Schneider, B. *Phytochemistry* **2002**, *60*, 61–66.
- (8) Cooke, R. G.; Dagley, I. J. *Aust. J. Chem.* **1979**, *32*, 1841–1847.
- (9) Opitz, S.; Holscher, D.; Oldham, N. J.; Bartram, S.; Schneider, B. *J. Nat. Prod.* **2002**, *65*, 1122–1130.
- (10) Urban, S.; Timmers, M. A.; Brkljaca, R.; White, J. M. *Phytochemistry* **2013**, *95*, 351–359.
- (11) Brkljaca, R.; Urban, S. *J. Nat. Prod.* **2015**, 150619083902008.
- (12) Sisa, M.; Bonnet, S. L.; Ferreira, D.; Van der Westhuizen, J. H. *Molecules* **2010**, *15*, 5196–5245.
- (13) Tsimogiannis, D.; Samiotaki, M.; Panayotou, G.; Oreopoulou, V. *Molecules* **2007**, *12*, 593–606.
- (14) *Dictionary of Natural Products (CHEMnetBASE)*, 2015.
- (15) Gujer, R.; Magnolato, D.; Self, R. *Phytochemistry* **1986**, *25*, 1431–1436.
- (16) Wan, C.; Yuan, T.; Cirello, A. L.; Seeram, N. P. *Food Chem.* **2012**, *135*, 1929–1937.
- (17) Li, Y.-L.; Li, J.; Wang, M.-L.; Yao, X.-S. *Molecules* **2008**, *13*, 1931–1941.
- (18) Freischmidt, A.; Jurgenliemk, G.; Kraus, B.; Okpanyi, S. N.; Muller, J.; Kelber, O.; Weiser, D.; Heilmann, J. *Phytomedicine* **2012**, *19*, 245–252.
- (19) Dias, D. A.; Goble, D. J.; Silva, C. A.; Urban, S. *J. Nat. Prod.* **2009**, *72*, 1075–1080.
- (20) *ACD/Labs*, version 8.0; Advanced Chemistry Development, Inc.: Toronto, Canada, 2014.
- (21) *ChemBioDraw Ultra*, version 13.0; PerkinElmer Inc.: Cambridge, MA, USA, 2012.
- (22) Asscher, Y.; Agranat, I. *J. Org. Chem.* **1980**, *45*, 3364–3366.
- (23) Ivanov, I. G.; Vrancheva, R. Z.; Marchev, A. S.; Petkova, N. T.; Aneva, I. Y.; Denev, P. P.; Georgiev, V. G.; Pavlov, A. I. *Int. J. Curr. Microbiol. Appl. Sci.* **2014**, *3*, 296–306.
- (24) de Franca Ferreira, E. L.; Mascarenhas, T. S.; de Carvalho Oliveira, J. P.; Chaves, M. H.; Araujo, B. Q.; Cavalheiro, A. J. *J. Med. Plants Res.* **2014**, *8*, 353–360.
- (25) Olaleye, M. T.; Crown, O. O.; Akinmoladun, A. C.; Akindahunsi, A. A. *Hum. Exp. Toxicol.* **2014**, *33*, 602–608.
- (26) Zandi, K.; Teoh, B.-T.; Sam, S.-S.; Wong, P.-F.; Mustafa, M. R.; Abubakar, S. *J. Med. Plants Res.* **2014**, *8*, 307–312.
- (27) Fructus, A. E. France Patent FR 2867977 2005.
- (28) Luis, J. G.; Fletcher, W. Q.; Echeverri, F.; Abad, T.; Kishi, M. P.; Perales, A. *Nat. Prod. Lett.* **1995**, *6*, 23–30.
- (29) Quinones, W.; Escobar, G.; Echeverri, F.; Torres, F.; Rosero, Y.; Arango, V.; Cardona, G.; Gallego, A. *Molecules* **2000**, *5*, 974–980.
- (30) Otalvaro, F.; Nanclares, J.; Vasquez, L. E.; Quinones, W.; Echeverri, F.; Arango, R.; Schneider, B. *J. Nat. Prod.* **2007**, *70*, 887–890.
- (31) Holscher, D.; Dhakshinamoorthy, S.; Alexandrov, T.; Becker, M.; Bretschneider, T.; Buerkert, A.; Crecelius, A. C.; De Waele, D.; Elsen, A.; Heckel, D. G.; Heklau, H.; Hertweck, C.; Kai, M.; Knop, K.; Krafft, C.; Maddula, R. K.; Matthaus, C.; Popp, J.; Schneider, B.; Schubert, U. S.; Sikora, R. A.; Svatos, A.; Swennen, R. L. *Proc. Natl. Acad. Sci. U. S. A.* **2014**, *111*, 105–110.
- (32) Cho, J.-G.; Huh, J.; Jeong, R.-H.; Cha, B.-J.; Shrestha, S.; Lee, D.-G.; Kang, H.-C.; Kim, J.-Y.; Baek, N.-I. *Nat. Prod. Res.* **2015**, *29*, 1–3.
- (33) Lee, M.; Lee, H. H.; Lee, J.-K.; Ye, S.-K.; Kim, S. H.; Sung, S. H. *Bioorg. Med. Chem. Lett.* **2013**, *23*, 3170–3174.
- (34) Cho, J.-Y.; Hwang, T.-L.; Chang, T.-H.; Lim, Y.-P.; Sung, P.-J.; Lee, T.-H.; Chen, J.-J. *Food Chem.* **2012**, *135*, 17–23.
- (35) Skalicka-Wozniak, K.; Melliou, E.; Gortzi, O.; Glowniak, K.; Chinou, I. B. *Z. Naturforsch., C: J. Biosci.* **2007**, *62*, 797–800.
- (36) Tofighi, Z.; Asgharian, P.; Goodarzi, S.; Hadjiakhoondi, A.; Ostad, S. N.; Yassa, N. *Med. Chem. Res.* **2014**, *23*, 1718–1724.
- (37) Morikawa, T.; Wang, L.-B.; Nakamura, S.; Ninomiya, K.; Yokoyama, E.; Matsuda, H.; Muraoka, O.; Wu, L.-J.; Yoshikawa, M. *Chem. Pharm. Bull.* **2009**, *57*, 361–367.
- (38) Kayser, O.; Kiderlen, A. F. *Phytother. Res.* **2001**, *15*, 148–152.
- (39) Yagura, T.; Motomiya, T.; Ito, M.; Honda, G.; Iida, A.; Kiuchi, F.; Tokuda, H.; Nishino, H. *J. Nat. Med.* **2008**, *62*, 174–178.
- (40) Aljancic, I. S.; Vuckovic, I.; Jadrantin, M.; Pesic, M.; Dordevic, I.; Podolski-Renic, A.; Stojkovic, S.; Menkovic, N.; Vajs, V. E.; Milosavljevic, S. M. *Phytochemistry* **2014**, *98*, 190–196.
- (41) Master, R. N.; Clark, R. B.; Karlowsky, J. A.; Ramirez, J.; Bordon, J. M. *Int. J. Antimicrob. Agents* **2011**, *38*, 291–295.
- (42) Sheldrick, G. M. *Acta Crystallogr., Sect. A: Found. Crystallogr.* **2008**, *64*, 112–122.
- (43) Farrugia, L. J. *J. Appl. Crystallogr.* **1997**, *30*, 565.
- (44) Farrugia, L. J. *J. Appl. Crystallogr.* **1999**, *32*, 837–838.
- (45) Brkljaca, R.; Urban, S. *Mar. Drugs* **2015**, *13*, 102–127.
- (46) Speranza, G.; Martignoni, A.; Manitto, P. *J. Nat. Prod.* **1988**, *51*, 588–590.
- (47) Lee, Y. G.; Cho, J.-Y.; Kim, C.-M.; Lee, S.-H.; Kim, W.-S.; Jeon, T.-I.; Park, K.-H.; Moon, J.-H. *Food Sci. Biotechnol.* **2013**, *22*, 803–810.

CHAPTER 6

Chemical Profiling and Isolation of Secondary Metabolites from

Haemodorum spicatum



Kingdom: Plantae

Phylum: Charophyta

Class: Equisetopsida

Order: Commelinales

Family: Haemodoraceae

Genus: *Haemodorum*

Species: *spicatum*

Collected from the Arrowsmith River
Region, Eneabba, Western Australia,
Australia in October 2010.

Chapter 6 outlines the phytochemical profiling and bioassay guided isolation of the constituents from the bubs of the Australian plant *Haemodorum spicatum*. This work has been published in the *Journal of Natural Products*. Appendix C contains supplementary information relevant to this study.

Journal publication resulting from this study:

Brkljača, Robert, & Urban, Sylvia. (2015). Chemical Profiling/HPLC-NMR and HPLC-MS profiling and bioassay-guided identification of secondary metabolites from the Australian plant *Haemodorum spicatum*. *Journal of Natural Products*, 78(7), 1486-1494.

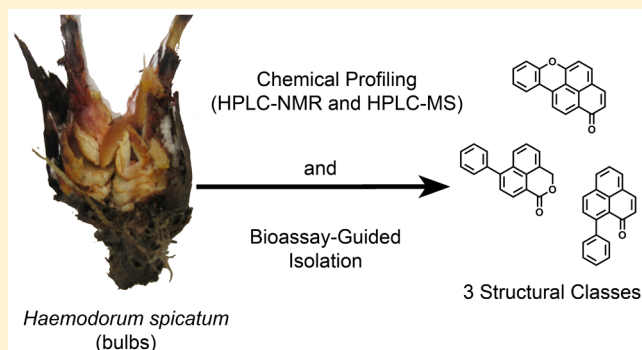
HPLC-NMR and HPLC-MS Profiling and Bioassay-Guided Identification of Secondary Metabolites from the Australian Plant *Haemodorum spicatum*

Robert Brkljača and Sylvia Urban*

School of Applied Sciences (Discipline of Chemistry), Health Innovations Research Institute (HIRi), RMIT University, GPO Box 2476 V Melbourne, Victoria 3001, Australia

S Supporting Information

ABSTRACT: Phytochemical dereplication was undertaken on the bioactive crude CH_2Cl_2 extract of the bulbs of the Australian plant *Haemodorum spicatum* employing HPLC-NMR and HPLC-MS methodologies. Subsequent bioassay-guided isolation resulted in the identification of two new phenylphenalenones [haemoxiphidone (**8**) and haemodoronol (**17**)] and two new chromenes [haemordione (**13**) and haemordiol (**16**)], together with seven previously described compounds. Antimicrobial testing showed that the compounds displayed selective antibacterial activity. Most noteworthy were the activities displayed by several of the compounds against multi-drug-resistant *Pseudomonas aeruginosa*.



The *Haemodorum* genus (Haemodoraceae family) consists of 20 different species.¹ Various studies have reported that the Haemodoraceae family contains chemotaxonomic markers made up of three distinct secondary metabolite structural classes including the phenylphenalenones, the oxabenzochrysenones, and the chromenes.^{2–4} Altogether, 30 phenylphenalenones have been reported from the family Haemodoraceae, including four from the *Haemodorum* genus, of which 15 possess a 9-substituted aromatic moiety, while the others display a 4-, 6-, or 7-substituted aromatic ring.^{2–24} Phenylphenalenones containing sugar moieties appear to favor the 7-substituted aromatic position. Only six oxabenzochrysenones have been reported from the family Haemodoraceae, half of which occur in the *Haemodorum* genus, and, unlike the phenylphenalenones, the oxabenzochrysenones contain no terminal aromatic ring.^{2,3,7,11,15,19,25–29} The final structural class associated with the family Haemodoraceae is the chromenes, which can contain either one or two carbonyl functional groups in the lower right ring system. Twenty-three chromenes have been reported from the family Haemodoraceae, of which five occur within the genus *Haemodorum*.^{2,3,5–11,18,19,26,30,31} All but one of the chromenes have a 7-substituted aromatic ring.

Biosynthetically, the phenylphenalenones are derived from a diarylheptanoid intermediate formed from phenylalanine and tyrosine.^{14,32–36} The chromenes are produced by the same diarylheptanoid intermediate pathway, but this most likely undergoes oxidative rearrangement and decarboxylation to incorporate the additional oxygen into the ring system.³⁷ No in-depth studies have been conducted to conclude the biosynthetic pathway of the oxabenzochrysenones. However,

two reports have suggested that oxidative cyclization may be involved in converting phenylphenalenones to oxabenzochrysenones.^{27,28}

As part of continuing efforts to study the chemical diversity and ethnopharmacology of Australian plants, particularly of the family Haemodoraceae, the chemistry of *Haemodorum spicatum* R. Br. was investigated. Of significance is the fact that the bulbs of *H. spicatum* are reported to have been used as a traditional medicine by the Australian Aborigines to treat dysentery.³⁸ The present investigation on the bulbs of *H. spicatum* has yielded two new [(haemoxiphidone (**8**) and haemodoronol (**17**)] and two previously reported phenylphenalenones (**2** and **15**), four known oxabenzochrysenones (**1**, **5**, **11**, and **12**), and two new [haemordione (**13**) and haemordiol (**16**)] chromenes as well as a reported (**3**) chromene. For three (**2**, **5**, and **11**) of the known compounds identified, this represents their first occurrence as natural products. The complete 2D NMR spectroscopic characterization of **2**, **5**, and **11** is also reported herein for the first time. All isolated compounds were evaluated for their selective antibacterial activity.

RESULTS AND DISCUSSION

The bulbs and stems of *H. spicatum* were extracted with 3:1 MeOH/ CH_2Cl_2 , evaporated under reduced pressure, and then sequentially and exhaustively solvent partitioned into CH_2Cl_2 - and MeOH-soluble fractions, respectively. Antimicrobial testing was carried out on both the CH_2Cl_2 - and MeOH-soluble crude

Received: November 12, 2014

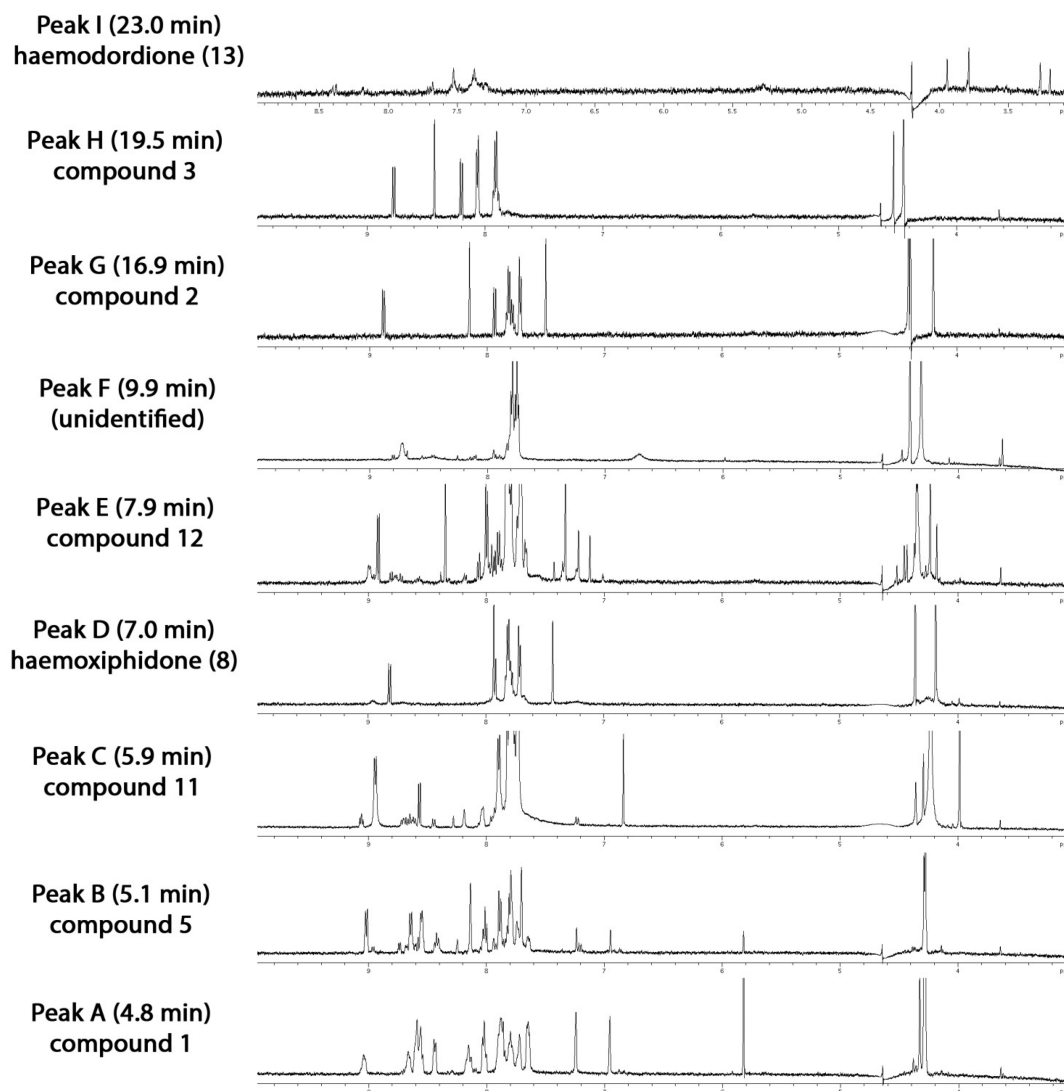


Figure 1. Stop-flow Wet1D proton NMR spectra (500 MHz, 50% CH₃CN/D₂O, suppression of HDO and CH₃CN at δ_{H} 4.64 and 2.38 ppm, respectively) of peaks A–I resulting from analysis of the CH₂Cl₂ crude extract of *H. spicatum*.

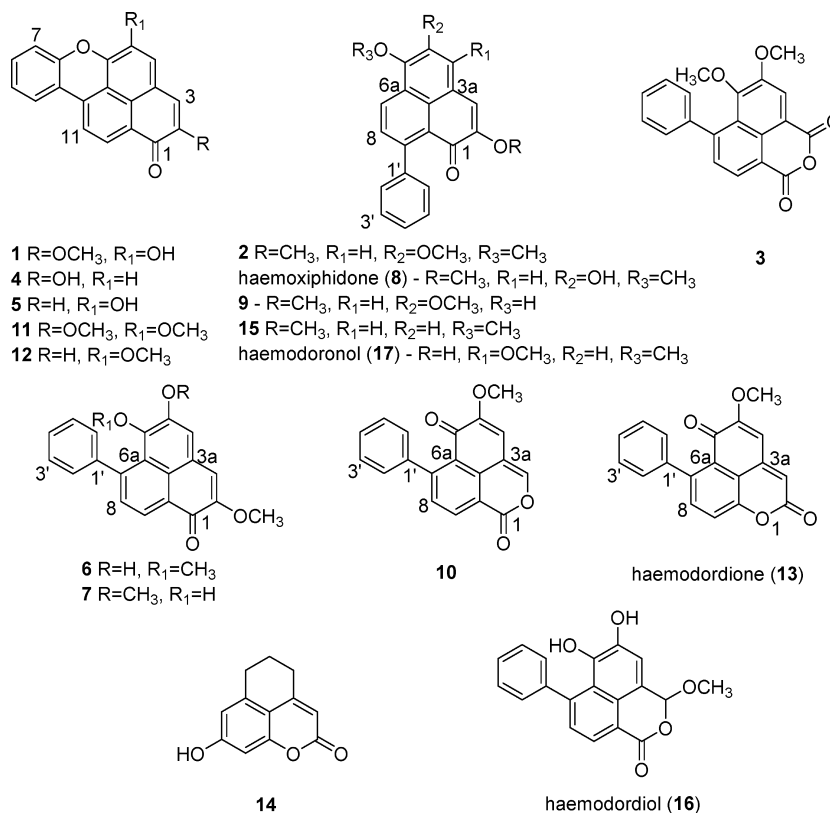
extracts of the bulbs and the aerial parts of the plant. It was found that the CH₂Cl₂-soluble extract of the bulbs displayed significant antibacterial activity. On the basis of the observed activity along with the known ethnopharmacology associated with the crude extract derived from the bulbs, the CH₂Cl₂ crude extract was prioritized for further chemical investigation.

Dereplication of the secondary metabolites present in the bioactive CH₂Cl₂ crude extract was achieved using HPLC-NMR and HPLC-MS in combination with the use of selected databases. Nine peaks (peaks A–I in Figure 1) were detected by HPLC-NMR and HPLC-MS. Analysis of the HPLC-NMR data showed the presence of characteristic proton NMR signals that suggested the presence of aromatic and methoxy moieties, and further examination of the UV profiles obtained (as detected by PDA) confirmed the presence of three distinct chemical classes. These were the phenylphenalenones ($\lambda > 400$ nm),¹⁸ oxabenzochrysenones ($\lambda > 500$ nm),²⁷ and chromenes ($\lambda < 400$ nm),² which are all known to occur within the family Haemodoraceae.^{2,3}

An important requirement for HPLC-NMR analysis is that the sample to be analyzed is at least moderately soluble in acetonitrile. It is important to note that this particular HPLC-

NMR system utilizes only D₂O and CH₃CN as mobile-phase solvents. MeOH as a solvent for elution is found to stick irreversibly to the HPLC tubing and flow cell and therefore is not recommended for HPLC-NMR use. In addition, samples must be dissolved in either D₂O or HPLC-NMR grade CH₃CN or a combination of the two solvents for similar reasons. The CH₂Cl₂ crude extract of the bulbs of *H. spicatum* displayed poor solubility in acetonitrile. In terms of HPLC-NMR chemical profiling this meant that only WET1D (stop-flow proton NMR) and gCOSY NMR spectra could be obtained for the compounds present, given the small amounts that could be loaded onto the HPLC column. These two NMR experiments alone are not sufficient for an unequivocal structure identification; however by adopting the use of chemical databases such as the *Dictionary of Natural Products* (www.dnp.chemnetbase.com) and SciFinder (<https://scifinder.cas.org>), dereplication may assist in concluding the structure classes present and often the most likely identity for some of the compounds detected. During HPLC-MS analysis it was noted that some of the compounds (11 and 12) displayed an inability to ionize or would only ionize on the low-resolution

Chart 1



instrument ion source (3). In these instances, the chemical profiling/dereplication identification process was hindered.

Peaks A, G, and H (Figure 1) were dereplicated and identified based on examination of the WET1D (stop-flow proton NMR), gCOSY NMR, the molecular mass obtained from either low- or high-resolution HPLC-ESIMS together with the extracted UV profile/spectrum (obtained from PDA detection). On the basis of these analyses and data, the most likely structure was deduced for these three peaks. Peak A was proposed to be the known oxabenzochrysenone 5-hydroxy-2-methoxy-1*H*-naphtho[2,1,8-*mna*]xanthen-1-one (1), peak G was proposed to be the previously reported phenylphenalenone 2,5,6-trimethoxy-9-phenyl-1*H*-phenalen-1-one (2), and peak H was suggested to be the previously described chromene 5,6-dimethoxy-7-phenyl-1*H*,3*H*-naphtho[1,8-*cd*]pyran-1,3-dione (3).

Peak B closely eluted with peak A (Figure 1), which displayed a characteristic UV chromophore at 540 nm, consistent with an oxabenzochrysenone-type structure.²⁷ A SciFinder (<https://scifinder.cas.org>) database search using the HPLC-NMR and UV (which supported a oxabenzochrysenone structure) data was refined using the molecular ion (m/z 287.0705 [M + H]⁺) observed in the high-resolution HPLC-MS analysis. This resulted in two possible structures being proposed for peak B, namely, 2-hydroxy-1*H*-naphtho[2,1,8-*mna*]xanthen-1-one (4) and 5-hydroxy-1*H*-naphtho[2,1,8-*mna*]xanthen-1-one (5). It was not possible to establish which isomer could be attributed to peak B based on the WET1D (stop-flow proton NMR) and gCOSY NMR data alone.

Peaks C and E (Figure 1) could not be identified, but analysis of their UV profiles confirmed an oxabenzochrysenone-type structure for both.

Peaks D and F (Figure 1) displayed UV chromophores at 460 and 438 nm, respectively, consistent with those observed for phenylphenalenones.¹⁸ Both peaks also displayed isobaric molecular ions at m/z 333.1123 [M + H]⁺. Unlike peak F, which showed only two large aromatic multiplets (δ_{H} 7.78, m; 7.75, m), peak D exhibited various resolved signals (δ_{H} 8.81, d, $J = 8.5$ Hz; 7.92, d, $J = 8.5$ Hz; 7.71, d, $J = 7.5$ Hz; 7.43, s). The mass of peaks D and F (332 Da) and the family Haemodoraceae were used to search the *Dictionary of Natural Products* (www.dnp.chemnetbase.com) database. Four possible phenylphenalenone structures were suggested, including 5-hydroxy-2,5-dimethoxy-7-phenylphenalen-1-one (6), 6-hydroxy-2,5-dimethoxy-7-phenylphenalen-1-one (7), 5-hydroxy-2,5-dimethoxy-9-phenylphenalen-1-one (8), and 6-hydroxy-2,5-dimethoxy-9-phenylphenalen-1-one (9). Of these possibilities, compound 8 represents a new phenylphenalenone. On the basis of literature precedence, which shows that 9-substituted phenylphenalenones tend to be favored, either compound 8 or 9 would be the most likely structure for peak D.

The identify of peak F, which displayed only two large aromatic multiplets, was not represented by any of the structures as depicted for compounds 6–9. Peak F was therefore concluded to represent an unidentified phenylphenalenone, warranting further off-line isolation and identification.

A characteristic UV profile (345 and 388 nm) was observed for peak I (Figure 1). Typically chromenes display one absorbance at <400 nm, but, in this case, peak I showed two distinct absorbances of <400 nm, suggesting an analogue of the chromene skeleton.² In reviewing compounds that have been reported from the family Haemodoraceae, a structural analogue (10) of the chromene structure was noted.² Chromenes isolated from the Haemodoraceae family typically contain one

Table 1. ¹H (500 MHz) and ¹³C (125 MHz) NMR Data for Haemodordione (13), Haemodordioli (16), and Haemodoronol (17) Recorded in CDCl₃

position	haemodordione (13)			haemodordioli (16)			haemodoronol (17)			
	δ_H (J in Hz)	δ_C^a type	gCOSY	δ_H (J in Hz)	δ_C^a type	gCOSY	δ_H (J in Hz)	δ_C^a type	gCOSY	gHMBCAD
1					163.4, C					
2		160.2, C						184.8, C		
3	6.62, s	114.4, CH	2, 4, 9b	6.54, s	102.0, CH	1, OCH ₃ -3	8.39, s	148.2, C		
3a		142.7, C			ND ^b , C			114.9, CH		1, 2, 3a, 9b
4	6.50, s	106.0, CH	3, 5, 6, 9b	8.09, s	119.8, CH	3, 6, 9b		121.3, C		
5		156.6, C			138.1, C			143.8, C		
6		178.2, C			146.3, C			103.3, CH		6, 3a, 6a
6a		125.4, C			119.6, C ^c			166.1, C		
7		141.7, C			143.0, C			123.7, C		
8	7.56, d (9.0)	135.7, CH	9	7.74, d (7.0)	129.8, CH	9	8.20, d (7.5)	125.1, CH	8	6, 9, 9b
9	7.62, d (9.0)	120.9, CH	8	8.61, d (7.0)	129.8, CH	8	7.37, d (7.5)	128.8, CH	7	6a, 9a, 1'
9a		151.5, C			118.2, C ^c			143.3, C		
9b		116.0, C			127.0, C			119.3, C		
1'		140.3, C			139.8, C			124.2, C		
2'	7.26, m	128.2, CH	7, 3', 4', 6'	7.51–7.55, m	129.2, CH ^d	4'	7.44, m	142.7, C		1', 3', 4', 6'
3'	7.42, m	128.2, CH	1', 2', 5'	7.51–7.55, m	128.3, CH ^{e,d}		7.44, m	127.4–128.8, CH		1', 2', 4', 5'
4'	7.41, m	127.5, CH	2, 3', 5', 6'	7.51–7.55, m	128.5, CH		7.44, m	127.4–128.8, CH		2', 3', 5', 6'
5'	7.42, m	128.2, CH	1', 3', 6'	7.51–7.55, m	128.3, CH ^d		7.44, m	127.4–128.8, CH		1', 3', 4', 6'
6'	7.26, m	128.2, CH	7, 2', 4', 5'	7.51–7.55, m	129.2, CH ^d	4'	7.44, m	127.4–128.8, CH		1', 2', 4', 5'
OH-2							ND ^b			
OCH ₃ -3				3.80, s	56.8, CH ₃	3	4.08, s			4
OCH ₃ -4								57.0, CH ₃		
OCH ₃ -5	3.92, s	56.3, CH ₃	5							
OH-5				8.05, s		5				
OCH ₃ -6										
OH-6				8.05, s		6	4.03, s	56.0, CH ₃	5	6

^aCarbon NMR assignments based on gHSQCAD and gHMBCAD experiments. ^bSignal not detected. ^{c,d}Signals interchangeable.

or two carbonyl groups in the lower ring system. While compound **10** contains two carbonyl groups, these are now located in two separate aromatic ring systems. It is expected that such a structural analogue would give rise to two slightly different UV absorbances. The two observed UV absorbances for peak I were not in agreement with those reported for compound **10** (243 and 390 nm), which suggested a possible isomer.² Unfortunately, no clear molecular ion was observed in the HPLC-MS analysis, and so no conclusive structure could be proposed for peak I.

An off-line bioassay-guided isolation approach was conducted to determine which compounds were responsible for the observed antibacterial activity of the crude extract of the plant, to identify unequivocally each of the components, and to isolate and confirm the structures of the putative new compounds suggested by the chemical profiling methodology adopted. The bioassay-guided isolation approach resulted in a total of 10 compounds (**1**, **2**, **5**, **8**, **11–13**, and **15–17**) being isolated. Off-line isolation confirmed that peaks B and D corresponded to compounds **5** and **8**, respectively. The structures for peaks C, E, and I were found to correspond to the previously reported oxabenzochrysenones **11** and **12** and the new chromene **13**, respectively. Compound **3** and peak F were not obtained by the off-line bioassay-guided isolation approach. It is uncertain whether these components degraded or if they had converted into other compounds.

Six previously identified oxabenzochrysenone and phenylphenalenone compounds (**1**, **2**, **5**, **11**, **12**, and **15**) were identified by comparison of their NMR spectroscopic and mass spectrometric data to values reported in the literature.^{2,17,27–29,39,40}

Off-line isolation and subsequent characterization of peak D (Figure 1) confirmed this component to be the new phenylphenalenone haemoxiphidone (**8**), which was isolated as an orange solid. This particular compound was concurrently isolated within the research group from a separate *Haemodorum* species.³ Unequivocal identification of haemoxiphidone (**8**) was ultimately achieved by consideration of the data obtained in both studies. While the earlier study established a C-9 substitution for the aromatic moiety by HMBC NMR correlations,³ the present investigation was able to assign the point of attachment utilizing single-irradiation 1D NOE NMR experiments. Specifically, a key NOE NMR enhancement was observed between the proton at δ_{H} 8.32 (d, $J = 8.5$ Hz) and the methoxy moiety at position H-6 (δ_{H} 4.06, s), which confirmed that the aromatic ring is substituted at the C-9 position in compound **8**.³

Haemodordione (**13**) displayed characteristic UV absorbances at 313 and 373 nm, which were attributed to the chromene structure class.² Comparison of the off-line NMR data obtained for haemodordione (**13**) and compound **10** showed similarities, although two principal differences were noted. These included the H-3 proton in compound **10**, which appeared significantly downfield (δ_{H} 8.09) when compared to that observed for **13** (δ_{H} 6.62). In addition, the C-3 resonance was dramatically different between **10** and **13** (δ_{C} 145.7 and 114.4, respectively), suggesting **13** to be an isomer of **10** whereby the lactone moiety is reversed. Further literature searches of compounds containing the substructure present in **13** with the lactone moiety reversed⁴¹ provided support for the structure of the chromene **14**. A comparison of the proton and carbon chemical shifts at positions H-3 and C-3 for **13** and **14** (δ_{H} 6.62 and 5.98 and δ_{C} 114.4 and 105.9, respectively) showed a closer

agreement than the chemical shifts between **10** and **13**. This provided confirmation that in **13** the carbonyl group is located at position C-2. The HRESIMS of **13** displayed a $[M + H]^+$ peak at m/z 305.0809 (calcd for $\text{C}_{19}\text{H}_{13}\text{O}_4$, m/z 305.0814), consistent with 14 degrees of unsaturation and a molecular formula of $\text{C}_{19}\text{H}_{12}\text{O}_4$. Complete analysis of the NMR (Table 1) and MS data allowed **13** to be identified as the new chromene 5-methoxy-7-phenylbenzo[*de*]chromene-2,6-dione, to which was accorded the trivial name haemodordione.

Haemodordiol (**16**) displayed a characteristic UV absorbance at 326 nm, which was consistent with the chromene structural class.² Analysis of the NMR data of haemodordiol (**16**) (Table 1) supported the presence of a single carbonyl group. A characteristic proton chemical shift at δ_{H} 6.54 (s) suggested that one of the carbonyl groups had been replaced by a methine group. This proton displayed gHMBC NMR correlations to the carbonyl at position C-1 (δ_{C} 163.4) as well as to a methoxy moiety (δ_{C} 56.8, δ_{H} 3.80, s). The HRMS of haemodordiol (**16**) yielded a molecular formula of $\text{C}_{19}\text{H}_{14}\text{O}_5$ (observed m/z 345.0749 $[M + \text{Na}]^+$ (calcd for $\text{C}_{19}\text{H}_{14}\text{O}_5\text{Na}$, m/z 345.0739)). This supported the fact that two hydroxy groups are retained in this structure. On the basis of the proton coupling and splitting observed for the remaining protons, it was proposed that the two hydroxy groups are located at positions C-4, C-5, or C-6. The singlet proton at δ_{H} 8.09 showed key gHMBC NMR correlations to carbons δ_{C} 102.0 (C-3), 146.3 (C-6), and 127.0 (C-9b), enabling the hydroxy group moieties to be placed at positions C-4 and C-5. All but one of the previously reported chromenes display a 7-substituted terminal aromatic moiety. The observed gHMBC NMR correlations from the proton at position H-9 (δ_{H} 8.61, d, $J = 7.0$ Hz) to the carbon at position C-1 (δ_{C} 163.4) permitted the location of substitution of the terminal aromatic ring to be established for **16**, since only a 7-substituted terminal aromatic ring would enable such a correlation to be observed. Analysis of the remaining NMR and MS data allowed **16** (haemodordiol) to be proposed as the new compound 5,6-dihydroxy-3-methoxy-7-phenyl-1*H*,3*H*-benzo[*de*]isochromen-1-one. The absolute configuration of the C-3 stereogenic center remains undefined.

Haemodoronol (**17**) was isolated as a brown solid. The proton NMR and UV spectroscopic data (Table 1) of haemodoronol (**17**) showed similarities to analogous data for compounds **8** and **15**, indicating the presence of a phenylphenalenone skeleton. HRMS yielded a molecular ion at m/z 333.1120 $[M + H]^+$ (calcd for $\text{C}_{21}\text{H}_{17}\text{O}_4$, m/z 333.1127), supporting a molecular formula of $\text{C}_{21}\text{H}_{16}\text{O}_4$. Characteristic of this phenylphenalenone was the presence of a considerably deshielded ^1H NMR singlet at δ_{H} 8.39 (s). This suggested a different substitution pattern from the other phenylphenalenones isolated in this investigation. This proton showed key gHMBC NMR correlations to the carbons at δ_{C} 184.8 (C-1), 148.2 (C-2), 121.3 (C-3a), and 124.2 (C-9b), indicating that it is located on the ring containing the carbonyl moiety and situated at position C-3.

The carbon signal at δ_{C} 148.2 was located at position C-2 and substituted with a hydroxy group. Another singlet was observed at δ_{H} 6.16, s, which is usually positioned on the upper aromatic moiety, typically at position H-4. However, the significant deshielding observed for the H-3 proton (δ_{H} 8.39, s) suggested the proton at δ_{H} 6.16 (s) to be located at either position H-5 or H-6, rather than at position H-4. Two methoxy moieties were also observed (δ_{H} 4.03, s and 4.08, s), and it was rationalized that one of these is substituted at position C-4. To

Table 2. Antimicrobial Activity of the Plant Crude Extracts and Pure Compounds Isolated from *H. spicatum* Together with Commercial Standard Antibiotic and Antifungal Compounds, Showing Zones of Inhibition (mm)

	concentration (mg/mL)	microorganism					
		<i>E. coli</i> ATCC 25922	<i>S. aureus</i> ATCC 25923	<i>S. aureus</i> MRSA 344/2-32	<i>P. aeruginosa</i> ATCC 27853	<i>S. pyogenes</i> 345/1	<i>C. albicans</i> ATCC 10231
CH ₂ Cl ₂ extract (bulbs)	50	ND ^a	1	1	3	2	ND ^a
MeOH extract (bulbs)	50	ND ^a	ND ^a	ND ^a	ND ^a	ND ^a	ND ^a
CH ₂ Cl ₂ extract (stems)	50	ND ^a	3	3	ND ^a	ND ^a	ND ^a
MeOH extract (stems)	50	ND ^a	ND ^a	1	ND ^a	1	ND ^a
compound 1	1	1	ND ^a	ND ^a	5	2	ND ^a
compound 2	1	1	ND ^a	1	1	1	ND ^a
compound 5	1	ND ^a	ND ^a	ND ^a	3	1	ND ^a
haemoxiphidone (8)	1	1	1	ND ^a	1	1	ND ^a
compound 11	1	ND ^a	ND ^a	ND ^a	4	2	ND ^a
compound 12	1	ND ^a	1	1	3	3	ND ^a
haemodordione (13)	1	1	ND ^a	ND ^a	ND ^a	ND ^a	ND ^a
compound 15	1	1	ND ^a	ND ^a	3	1	ND ^a
haemodordioid (16)	1	1	ND ^a	ND ^a	1	1	ND ^a
haemodoronol (17)	1	1	1	1	5	1	ND ^a
ampicillin (antibiotic)	1	ND ^a	15	3	2	20	NT ^b
carbendazim (antifungal)	1	NT ^b	NT ^b	NT ^b	NT ^b	NT ^b	ND ^a

^aIndicates no zone of inhibition detected. ^bIndicates not tested.

establish the locations for the terminal aromatic ring and methoxy moieties, a NOESY NMR experiment was conducted. The signal at δ_{H} 8.20 (d, $J = 7.5$ Hz, H-7) showed a NOE enhancement to one of the methoxy signals (δ_{H} 4.03, s), which confirmed the terminal aromatic moiety to be substituted at position C-9 and the methoxy group at δ_{H} 4.03 to occur at position C-6. In addition, the signal at δ_{H} 8.39 (s, H-3) showed a NOE enhancement to the other methoxy signal (δ_{H} 4.08, s), confirming that this second methoxy group is located at C-4. Complete analysis of the NMR data allowed 17 (haemodoronol) to be identified as the new compound 2-hydroxy-4,6-dimethoxy-9-phenyl-1*H*-phenalen-1-one. This compound represents a new variation of the substitution pattern seen usually in the phenylphenalenones, where typically the methoxy moieties occur on adjacent carbons.

Each of the new compounds identified in this study (8, 13, 16, and 17) contain methoxy substituents. A review of the literature provides evidence that methoxy substituents present at the C-4, C-5, and C-6 positions occur in natural product molecules of compounds of the family Haemodoraceae, even when solvents such as acetone are used.² However, the same study concluded that a methoxy group moiety at position C-3 in the chromenes may be artifactual, arising from the use of MeOH during solvent extraction.² This indicates that compound 16 may be an artifact produced due to the isolation procedure that was used.

In the bioassay-guided isolation procedure implemented, the plant crude extracts, selected silica gel column fractions, each of the compounds isolated (1, 2, 5, 8, 11–13 and 15–17), a commercially available standard antibiotic (ampicillin), and an antifungal agent (carbendazim) were assessed for antimicrobial activity. Antimicrobial assays were conducted against five bacteria, *E. coli*, *S. aureus*, *S. aureus* MRSA, *P. aeruginosa*, and *S. pyogenes*, and a yeast, *C. albicans*. Crude extracts and enriched

fractions were tested at a concentration of 25 or 50 mg/mL, while pure compounds and the standards were tested at 1 mg/mL. Each of the isolated compounds showed selective and varying degrees of antimicrobial activity.

Previous reports indicate that 15 showed no reportable antialgal activity⁴² and that haemoxiphidone (8) displayed no significant activity in the P388 murine lymphocytic leukemia cytotoxicity assay.³

This represents the first instance where all three co-occurring structure classes have been assessed for antimicrobial activity in a single study. The 10 compounds tested showed only antibacterial properties (against both Gram-positive and Gram-negative bacteria), but no antifungal activity (Table 2). For each of the compounds isolated, the greatest activity was observed against *P. aeruginosa* and *S. pyogenes*. Three of the compounds (2, 12, and 17) slightly inhibited the growth of the resistant *S. aureus* MRSA. Of significance is that compounds 1, 5, 11, 12, 15, and 17 all inhibited the growth of *P. aeruginosa* in a more potent manner than ampicillin. In recent years concern has increased for *P. aeruginosa* in relation to its prevalence and multidrug resistance.⁴¹ The importance of identifying compounds that can inhibit this bacterium remains important and highly relevant. No significant differences in activity were observed for the phenylphenalenones and the oxabenzochrysenones, irrespective of the substitution pattern of the aromatic ring.

■ EXPERIMENTAL SECTION

General Experimental Procedures. All organic solvents used were analytical reagent (AR or GR), UV spectroscopic, or HPLC grade, with Milli-Q water also being used. UV/vis spectra were recorded on an Agilent Cary 60 spectrophotometer, using ethanol. FTIR spectra were recorded as a film using NaCl disks on a PerkinElmer Spectrum One FTIR spectrometer. ¹H (500 MHz), ¹³C

(125 MHz), and 1D NOE spectra were acquired in CDCl₃ on a 500 MHz Agilent DD2 NMR spectrometer with referencing to solvent signals (δ 7.26 and 77.0 ppm). Two-dimensional NMR experiments recorded included gCOSY, HSQCAD, gHMBCAD, and NOESY NMR experiments. Low-resolution ESI mass spectra were obtained on a Micromass Platform II mass spectrometer equipped with an LC-10AD Shimadzu solvent delivery module (50% CH₃CN/H₂O at a flow rate of 0.2 mL/min) in both the positive and negative ionization modes using cone voltages between 20 and 30 V. Silica gel flash chromatography was carried out using Davisil LC35 Å silica gel (40–60 mesh) with a 20% stepwise solvent elution from 100% petroleum spirits (60–80 °C) to 100% CH₂Cl₂, to 100% EtOAc, and finally to 100% MeOH. HRMS was also analyzed using a Waters Xevo QTOF mass spectrometer, with an atmospheric solids analysis probe (ASAP) source (probe temperature set to 300 °C; source temperature set to 80 °C; sampling cone voltage of 20.0 V). Accurate mass was obtained by lockmass using leucine enkephalin as the reference compound. All analytical HPLC analyses and method development were performed on a Dionex P680 solvent delivery system equipped with a PDA100 UV detector (operated using “Chromleon” software). Analytical HPLC analysis was carried out using either a gradient method of 0–2 min 10% CH₃CN/H₂O; 14–24 min 75% CH₃CN/H₂O; 26–30 min 100% CH₃CN; and 32–40 min 10% CH₃CN/H₂O or else an isocratic method (either 70% or 60% CH₃CN/H₂O) on an Alltech Alltima HP C₁₈ (250 × 4.6) 5 μm column at a flow rate of 1.0 mL/min. Semipreparative HPLC was carried out on a Varian Prostar 210 solvent delivery system equipped with a Prostar 335 PDA detector (operated using “Star Workstation” software) using an isocratic method (either 70% or 60% CH₃CN/H₂O) and an Alltech Alltima C₁₈ (250 × 10) 5 μm column at a flow rate of 3.5 mL/min.

Biological Evaluation. Crude extracts, enriched fractions, compounds isolated from the bulbs, and the commercially available standard antibiotic (ampicillin, Sigma-Aldrich (Castle Hill, NSW, Australia)) and antifungal (carbendazim, Sigma-Aldrich (Castle Hill, NSW, Australia)) compounds were evaluated against six microorganisms (five bacteria and one fungus) at concentrations of 50, 25, or 1 mg/mL. Each microorganism was prepared by creating a 0.5 McFarlane solution suspension. Lawn cultures were prepared on either Mueller-Hinton or brain heart infusion agar (BHIA) (used for *S. pyogenes*). Then, 20 μL of the crude extracts, enriched fractions, pure compounds, or the standard compounds (ampicillin and carbendazim) were pipetted onto 6 mm diameter filter paper disks, and their solvents evaporated. These disks were then placed onto the prepared lawn cultures and incubated at 37 °C overnight. Active antimicrobial samples displayed a zone of inhibition outside the disk, which was measured in millimeters as the radius of inhibition for each bacterium/fungus. The six test organisms used were *Escherichia coli* (ATCC 25922), *Staphylococcus aureus* (ATCC 25923), *Staphylococcus aureus* MRSA (344/2-32), *Pseudomonas aeruginosa* (ATCC 27853) *Streptococcus pyogenes* (345/1), and *Candida albicans* (ATCC 10231).

Plant Material. The plant (*H. spicatum*) was collected in October 2010 from the Arrowsmith River Region, close to the Western Flora Caravan Park, near Eneabba in Western Australia. The plant was collected and identified by M_r Allan Tinker (plant license SW008335). Voucher specimens designated with the codes 2010-20a (bulbs) and 2010-20b (aerial parts), respectively, were deposited at the School of Applied Sciences (Discipline of Applied Chemistry), RMIT University. In this study, only the bulbs (2010-20a) of *H. spicatum* were investigated.

Chemical Profiling. Chemical profiling was carried out on the CH₂Cl₂-soluble extract of the bulbs of *H. spicatum* employing HPLC-NMR and HPLC-MS techniques. HPLC-NMR was carried out on a 500 MHz Agilent DD2 NMR spectrometer equipped with a Varian ¹H[¹³C] pulsed field gradient flow probe with a 60 μL active volume flow cell coupled to a Varian Prostar 210 solvent delivery system, a Prostar 430 autosampler, and a Prostar 335 PDA detector. HPLC-NMR analysis was carried out using CORBA communication and operated with Vnmrj software. The 2H resonance observed from the D₂O was used to obtain field-frequency lock. The signals from the HOD and the methyl of the acetonitrile were suppressed using the

WET solvent suppression experiment.⁴³ The residual HOD signal of D₂O was referenced to 4.64 ppm. For both the on-flow and stop-flow HPLC-NMR modes, 50 μL injections (approximately 2500 μg) of the CH₂Cl₂ extract were injected onto an Agilent Zorbax Eclipse Plus C₁₈ (150 × 4.6) 5 μm column using a solvent composition of 50% CH₃CN/D₂O at a flow rate of 0.8 mL/min. In the stop-flow HPLC-NMR mode, WET1D and gCOSY NMR experiments were acquired. HRESIMS was carried out on an Agilent 6200 Series TOF system (ESI operation conditions of 8 L/min N₂, 325 °C drying gas temperature, and 3500 V capillary voltage) equipped with an Agilent 1200 Series LC solvent delivery module (100% CH₃OH at a flow rate of 0.3 mL/min) in either the positive or negative ionization modes. The instrument was calibrated using the “Agilent Tuning Mix” with purine as the reference compound and the Hewlett–Packard standard HP0921. High-resolution electrospray liquid chromatography mass spectrometry (LC-HRESIMS) was carried out on the same system and conditions using an Agilent Zorbax Eclipse Plus C₁₈ (150 × 4.6) 5 μm column using a solvent composition of 50% CH₃CN/H₂O at a flow rate of 0.8 mL/min. Low-resolution electrospray liquid chromatography mass spectrometry (LC-LRESIMS) was carried out on an Applied Biosystems MDS Sciex Q Trap LC/MS/MS system (3500 V capillary voltage) equipped with an Agilent 1200 Series LC solvent delivery module using a solvent composition of 50% CH₃CN/H₂O at a flow rate of 0.2 mL/min using an Agilent Zorbax Eclipse Plus C₁₈ (150 × 2.1) 5 μm column. Formic acid and ammonium acetate buffers were also evaluated during LC-MS analysis. However, no improvement in ionization of the molecular ions was observed; therefore no buffers were utilized. The CH₂Cl₂-soluble extract (123.6 mg) was dissolved in HPLC-NMR grade CH₃CN (2500 μL) and filtered through a 0.45 PTFE membrane filter (Grace Davison Discovery Sciences).

Extraction and Isolation. The stems of the *H. spicatum* (252.5 g, wet weight) were extracted with 3:1 MeOH/CH₂Cl₂ (2 L). The crude extract was then decanted and concentrated under reduced pressure and finally sequentially solvent partitioned (triturated) into CH₂Cl₂- and MeOH-soluble extracts, respectively. The bulbs of *H. spicatum* (121.6 g, wet weight) were extracted with 3:1 MeOH/CH₂Cl₂ (2 L). The crude extract was then decanted and concentrated under reduced pressure and sequentially triturated exhaustively into CH₂Cl₂- and MeOH-soluble extracts, respectively. The CH₂Cl₂ extract was subjected to flash silica gel column chromatography (20% stepwise elution from petroleum spirits (60–80 °C) to CH₂Cl₂ to EtOAc, and finally to MeOH). The first of the 60% CH₂Cl₂/EtOAc silica gel column fractions collected was subjected to reversed-phase HPLC (70% CH₃CN/H₂O) to yield 2,5,6-trimethoxy-9-phenyl-1H-phenalen-1-one (**2**) (9.8 mg, 0.033%), haemodordione (**13**) (1.0 mg, 0.003%), 2,6-dimethoxy-9-phenyl-1H-phenalen-1-one (**15**) (0.7 mg, 0.002%), and haemodordioldiol (**16**) (0.9 mg, 0.003%). The second of the 60% CH₂Cl₂/EtOAc silica gel column fractions collected was further purified by reversed-phase HPLC (70% CH₃CN/H₂O) to yield haemoxiphidone (**8**) (0.9 mg, 0.003%). The 20% CH₂Cl₂/EtOAc to 80% EtOAc/MeOH silica gel fractions were combined and subjected to reversed-phase HPLC (60% CH₃CN/H₂O) to yield 5-hydroxy-2-methoxy-1H-naphtho[2,1,8-*mna*]xanthen-1-one (**1**) (0.9 mg, 0.003%), 5-hydroxy-1H-naphtho[2,1,8-*mna*]xanthen-1-one (**5**) (0.7 mg, 0.002%), 2,5-dimethoxy-1H-naphtho[2,1,8-*mna*]xanthen-1-one (**11**) (0.4 mg, 0.001%), 5-methoxy-1H-naphtho[2,1,8-*mna*]xanthen-1-one (**12**) (0.6 mg, 0.002%), and haemodoronol (**17**) (1.3 mg, 0.004%). The percentage yields are reported on the basis of the dry mass of the bulbs extracted.

Online (HPLC-NMR and HPLC-MS) Characterization of Compounds. 5-Hydroxy-2-methoxy-1H-naphtho[2,1,8-*mna*]xanthen-1-one (**1**): UV (50% CH₃CN/D₂O) λ_{\max} 540 nm; HPLC-MS *m/z* 317.0809 (calcd for C₂₀H₁₃O₄, 317.0814).

2,5,6-Trimethoxy-9-phenyl-1H-phenalen-1-one (**2**): UV (50% CH₃CN/D₂O) λ_{\max} 464 nm; HPLC-NMR WET 1D NMR (500 MHz, 50% CH₃CN/D₂O) obtained from stop-flow HPLC-NMR mode δ 8.88 (1H, d, *J* = 8.5 Hz, H-7*), 8.15 (1H, s, H-4[#]), 7.93 (1H, d, *J* = 8.5 Hz, H-8*), 7.80 (3H, m, H-3'/H-4'/H-5'), 7.71 (2H, d, *J* = 7.0 Hz, H-2'/H-6'), 7.50 (1H, s, H-3[#]), 4.41 (3H, s, OCH₃-2'), 4.39

(3H, s, OCH₃-5[^]), 4.20 (3H, s, OCH₃-6[^]) (*[#]signals interchangeable); HPLC-MS *m/z* 347.1277 (calcd for C₂₂H₁₉O₄, 347.1283).

5,6-Dimethoxy-7-phenyl-1H,3H-naphtho[1,8-cd]pyran-1,3-dione (3): UV (50% CH₃CN/D₂O) λ_{max} 360 nm; HPLC-NMR WET 1D NMR (500 MHz, 50% CH₃CN/D₂O) obtained from stop-flow HPLC-NMR mode δ 8.77 (1H, d, *J* = 8.5 Hz, H-8*), 8.43 (1H, s, H-4), 8.19 (1H, d, *J* = 8.5, H-9*), 8.06 (2H, d, *J* = 7.0 Hz, H-2'/H-6), 7.90 (3H, m, H-3'/H-4'/H-5'), 4.53 (3H, s, OCH₃-5[#]), 4.44 (3H, s, OCH₃-6[#]) (*[#]signals interchangeable); HPLC-MS *m/z* 357 [M + Na]⁺.

5-Hydroxy-1H-naphtho[2,1,8-mna]xanthen-1-one (5): UV (50% CH₃CN/D₂O) λ_{max} 540 nm; HPLC-MS *m/z* 287.0705 (calcd for C₂₉H₁₀O₃, 287.0708).

Haemoxiphidone (5-hydroxy-2,6-dimethoxy-9-phenyl-1H-phenalen-1-one) (8): UV (50% CH₃CN/D₂O) λ_{max} 460 nm; HPLC-NMR WET 1D NMR (500 MHz, 50% CH₃CN/D₂O) obtained from stop-flow HPLC-NMR mode δ 8.81 (1H, d, *J* = 8.5 Hz, H-8), 7.93 (1H, s, H-3*), 7.92 (1H, d, *J* = 8.5 Hz, H-7), 7.80 (3H, m, H-3'/H-4'/H-5'), 7.71 (2H, d, *J* = 7.5 Hz, H-2'/H-6'), 7.43 (1H, s, H-4*), 4.36 (3H, s, OCH₃-2[#]), 4.18 (3H, s, OCH₃-6[#]), ND (OH-5) (*[#]signals interchangeable); HPLC-MS *m/z* 333.1123 (calcd for C₂₁H₁₇O₄, 333.1127).

2,5-Dimethoxy-1H-naphtho[2,1,8-mna]xanthen-1-one (11): UV (50% CH₃CN/D₂O) λ_{max} 535 nm; HPLC-NMR WET 1D NMR (500 MHz, 50% CH₃CN/D₂O) obtained from stop-flow HPLC-NMR mode δ 8.94 (d, *J* = 8.0 Hz), 8.56 (d, *J* = 7.0 Hz), 7.89 (d, *J* = 8.0 Hz), 7.72–7.83 (m), 6.84 (s), 3.98 (s).

5-Methoxy-1H-naphtho[2,1,8-mna]xanthen-1-one (12): UV (50% CH₃CN/D₂O) λ_{max} 510 nm; HPLC-NMR WET 1D NMR (500 MHz, 50% CH₃CN/D₂O) obtained from stop-flow HPLC-NMR mode δ 8.91 (d, *J* = 8.0 Hz), 8.35 (s), 7.99 (d, *J* = 8.0 Hz), 7.67–7.84 (m), 7.33 (s), 4.23 (s).

Off-line Characterization of Compounds: 5-Hydroxy-2-methoxy-1H-naphtho[2,1,8-mna]xanthen-1-one (1): purple solid; the UV, NMR spectroscopic and mass spectrometric data were identical to those reported in the literature.²

2,5,6-Trimethoxy-9-phenyl-1H-phenalen-1-one (2): orange solid; the UV, NMR spectroscopic and mass spectrometric data were identical to those reported in the literature;¹⁷ ¹H NMR (500 MHz, CDCl₃) δ 8.50 (1H, d, *J* = 8.5 Hz, H-7), 7.58 (1H, d, *J* = 8.5 Hz, H-8), 7.46 (1H, s, H-4), 7.44 (2H, m, H-3', H-5'), 7.39 (1H, m, H-4'), 7.36 (2H, m, H-2', H-6'), 6.80 (1H, s, H-3), 4.10 (3H, s, OCH₃-6), 4.08 (3H, s, OCH₃-5), 3.88 (3H, s, OCH₃-2); ¹³C NMR (500 MHz, CDCl₃) δ 179.9 (s, C-1), 153.1 (s, C-2), 148.7 (s, C-5), 146.7 (s, C-9), 144.4 (s, C-6), 142.8 (s, C-1'), 131.6 (d, C-8), 128.2 (d, C-3', C-5'), 128.1 (d, C-7), 127.9 (d, C-2', C-6'), 127.7 (s, C-9a), 127.0 (d, C-4'), 125.6 (s, C-6a), 125.2 (s, C-9b), 121.1 (s, C-3a), 118.1 (d, C-4), 111.1 (d, C-3), 62.0 (q, OCH₃-6), 57.0 (q, OCH₃-5), 55.5 (q, OCH₃-2); ESIMS *m/z* 347 [M + H]⁺.

5-Hydroxy-1H-naphtho[2,1,8-mna]xanthen-1-one (5): purple solid; the UV, NMR spectroscopic and mass spectrometric data were identical to those reported in the literature;³⁹ ¹H NMR (500 MHz, *d*₆-DMSO) δ 8.46 (1H, d, *J* = 8.0 Hz, H-12), 8.41 (1H, d, *J* = 8.0 Hz, H-10), 8.34 (1H, d, *J* = 8.0 Hz, H-11), 8.03 (1H, d, *J* = 10.0 Hz, H-3), 7.87 (1H, s, H-4), 7.63 (1H, dd, *J* = 7.0, 8.0 Hz, H-8), 7.51 (1H, d, *J* = 8.0 Hz, H-7), 7.41 (1H, dd, *J* = 7.0, 8.0 Hz, H-9), 6.69 (1H, d, *J* = 10.0 Hz, H-2); ¹³C NMR (500 MHz, *d*₆-DMSO) δ 183.2 (s, C-1), 151.8 (s, C-6a), 141.1 (d, C-3), 140.3 (s, C-5*) 132.7 (d, C-8, C-10b), 129.9 (d, C-12), 127.6 (s, C-12a), 127.2 (d, C-2), 125.2 (d, C-9), 124.9 (d, C-10), 124.6 (d, C-4), 121.1 (s, C-12b), 120.4 (s, C-12c), 120.1 (s, C-3a), 119.3 (s, C-10a), 118.2 (d, C-7), 116.8 (d, C-11), ND (s, C-5a*) (*signals interchangeable); ESIMS *m/z* 285 [M - H]⁻.

Haemoxiphidone (5-hydroxy-2,6-dimethoxy-9-phenyl-1H-phenalen-1-one) (8): orange solid; UV (EtOH) λ_{max} (log ϵ) 275 (4.10), 375 (3.70), 468 (3.48) nm; IR ν_{\max} 3246, 2928, 2854, 1730, 1627, 1556, 1466, 1359, 1212 cm⁻¹; ¹H NMR (500 MHz, CDCl₃) and ¹³C NMR (125 MHz, CDCl₃) see ref 3; ESIMS *m/z* 333 [M + H]⁺; HRESIMS *m/z* 333.1125 (calcd for C₂₁H₁₇O₄, 333.1127).

2,5-Dimethoxy-1H-naphtho[2,1,8-mna]xanthen-1-one (11): purple solid; the UV, NMR spectroscopic and mass spectrometric data

were identical to those reported in the literature;²⁸ ¹H NMR (500 MHz, CDCl₃) δ 8.89 (1H, d, *J* = 8.0 Hz, H-12), 8.22 (1H, d, *J* = 8.5 Hz, H-10), 8.14 (1H, d, *J* = 8.0 Hz, H-11), 7.72 (1H, s, H-4), 7.57 (2H, m, H-7, H-8), 7.39 (1H, m, H-9), 7.12 (1H, s, H-3), 4.18 (3H, s, OCH₃-5), 4.02 (3H, s, OCH₃-2); ¹³C NMR (500 MHz, *d*₆-CDCl₃) δ 178.1 (s, C-1), 153.2 (s, C-2), 151.9 (s, C-6a), 142.3 (s, C-5), 139.9 (s, C-5a) 133.8 (s, C-10b), 132.2 (d, C-12), 131.8 (d, C-8), 127.5 (s, C-12c), 124.7 (d, C-9), 123.8 (d, C-10), 119.7 (s, C-10a), 118.5 (s, C-12b), 118.1 (d, C-3, C-7), 117.7 (d, C-4), 115.5 (d, C-11), 57.4 (q, OCH₃-5), 55.9 (q, OCH₃-2), ND (s, C-12a*) (*signals interchangeable); ESIMS *m/z* 331 [M + H]⁺.

5-Methoxy-1H-naphtho[2,1,8-mna]xanthen-1-one (12): purple solid; the UV, NMR spectroscopic and mass spectrometric data were identical to those reported in the literature.^{27,39}

Haemodordione (5-methoxy-7-phenylbenzo[de]chromene-2,6-dione) (13): orange solid; UV (EtOH) λ_{max} (log ϵ) 255 (3.83), 313 (3.51), 373 (3.41) nm; IR ν_{\max} 2925, 2854, 1724, 1670, 1626, 1598, 1465, 1279, 1197, 1139 cm⁻¹; ¹H NMR (500 MHz, CDCl₃) and ¹³C NMR (125 MHz, CDCl₃) see Table 1; ESIMS *m/z* 305 [M + H]⁺, 327 [M + Na]⁺; HRESIMS *m/z* 305.0809 (calcd for C₁₉H₁₃O₄, 305.0814).

2,6-Dimethoxy-9-phenyl-1H-phenalen-1-one (15): orange solid; the UV, NMR spectroscopic and mass spectrometric data were identical to those reported in the literature.⁴⁰

Haemodordioli (5,6-dihydroxy-3-methoxy-7-phenyl-1H,3H-benzo[de]isochromen-1-one) (16): purple solid; [α]_D²² +16 (c 0.00025, CHCl₃); UV (EtOH) λ_{max} (log ϵ) 261 (5.74), 326 (5.20) nm; IR ν_{\max} 3419, 2925, 2854, 1730, 1634, 1460 cm⁻¹; ¹H NMR (500 MHz, CDCl₃) and ¹³C NMR (125 MHz, CDCl₃) see Table 1; HRASAPMS *m/z* 345.0749 (calcd for C₁₉H₁₄O₅Na, 345.0739).

Haemodoronol (2-hydroxy-4,6-dimethoxy-9-phenyl-1H-phenalen-1-one) (17): brown solid; UV (EtOH) λ_{max} (log ϵ) 275 (4.69), 295, (4.77), 400 (4.16), 519 (4.38) nm; IR ν_{\max} 3368, 2925, 2853, 1736, 1615, 1582, 1492, 1464, 1403, 1375, 1337, 1305, 1267 cm⁻¹; ¹H NMR (500 MHz, CDCl₃) and ¹³C NMR (125 MHz, CDCl₃) see Table 1; ESIMS *m/z* 333 [M + H]⁺; HRESIMS *m/z* 333.1120 (calcd for C₂₁H₁₇O₄, 333.1127).

■ ASSOCIATED CONTENT

■ Supporting Information

Supporting Information including off-line NMR and high-resolution MS data associated with this study. The Supporting Information is available free of charge on the ACS Publications website at DOI: 10.1021/np500905g.

■ AUTHOR INFORMATION

Corresponding Author

*Tel: +61-3-9925-3376. Fax: +61-3-9925-3747. E-mail: sylvia.urban@rmit.edu.au.

Notes

The authors declare no competing financial interest.

■ ACKNOWLEDGMENTS

The Marine and Terrestrial Natural Product (MATNAP) research group would like to thank Mr. A. Tinker for the collection and taxonomic identification of the plant; Mrs. N. Thurbon [School of Applied Sciences (Discipline of Biotechnology and Biological Sciences), Science Engineering and Health, RMIT University] for providing access to the microorganisms to conduct the antimicrobial assays and for her invaluable technical support; Ms. S. Duck (School of Chemistry, Faculty of Science, Monash University) for conducting the high-resolution mass spectrometric analyses; and Dr. J. Niere for her useful NMR discussions and guidance. R.B. would like to acknowledge an Australian Postgraduate Award (APA) scholarship that has supported his Ph.D. studies.

■ REFERENCES

- (1) *Species 2000 & ITIS Catalogue of Life, 2015 Annual Checklist*. www.catalogueoflife.org/col/, 2015.
- (2) Opitz, S.; Holscher, D.; Oldham, N. J.; Bartram, S.; Schneider, B. *J. Nat. Prod.* **2002**, *65*, 1122–1130.
- (3) Urban, S.; Timmers, M. A.; Brkljaca, R.; White, J. M. *Phytochemistry* **2013**, *95*, 351–359.
- (4) Holscher, D.; Schneider, B. *Phytochemistry* **1997**, *45*, 87–91.
- (5) Fang, J.; Kai, M.; Schneider, B. *Phytochemistry* **2012**, *81*, 144–152.
- (6) Fang, J.; Hoelscher, D.; Schneider, B. *Phytochemistry* **2012**, *82*, 143–148.
- (7) Fang, J.-J.; Paetz, C.; Hoelscher, D.; Munde, T.; Schneider, B. *Phytochem. Lett.* **2011**, *4*, 203–208.
- (8) Dias, D. A.; Goble, D. J.; Silva, C. A.; Urban, S. *J. Nat. Prod.* **2009**, *72*, 1075–1080.
- (9) Schneider, B.; Hoelscher, D. *Planta* **2007**, *225*, 763–770.
- (10) Schneider, B.; Paetz, C.; Hoelscher, D.; Opitz, S. *Magn. Reson. Chem.* **2005**, *43*, 724–728.
- (11) Opitz, S.; Schneider, B. *Phytochemistry* **2002**, *61*, 819–825.
- (12) Holscher, D.; Schneider, B. *Phytochemistry* **1998**, *50*, 155–161.
- (13) Dora, G.; Xie, X. Q.; Edwards, J. M. *J. Nat. Prod.* **1993**, *56*, 2029–2033.
- (14) Beecher, C. W. W.; Sarg, T. M.; Edwards, J. M. *J. Nat. Prod.* **1983**, *46*, 932–933.
- (15) Chaffee, A. L.; Cooke, R. G.; Dagley, I. J.; Perlmutter, P.; Thomas, R. L. *Aust. J. Chem.* **1981**, *34*, 587–598.
- (16) Cooke, R. G.; Dagley, I. J. *Aust. J. Chem.* **1978**, *31*, 193–197.
- (17) Cooke, R. G.; Rainbow, I. J. *Aust. J. Chem.* **1977**, *30*, 2241–2247.
- (18) Cooke, R. G.; Thomas, R. L. *Aust. J. Chem.* **1975**, *28*, 1053–1057.
- (19) Edwards, J. M.; Weiss, U. *Phytochemistry* **1974**, *13*, 1597–1602.
- (20) Edwards, J. M. *Phytochemistry* **1974**, *13*, 290–291.
- (21) Bick, I. R. C.; Blackman, A. J. *Aust. J. Chem.* **1973**, *26*, 1377–1380.
- (22) Kornfeld, J. M.; Edwards, J. M. *Biochim. Biophys. Acta, Gen. Subj.* **1972**, *286*, 88–90.
- (23) Edwards, J. M.; Weiss, U. *Phytochemistry* **1970**, *9*, 1653–1657.
- (24) Cooke, R. G.; Segal, W. *Aust. J. Chem.* **1955**, *8*, 107–113.
- (25) Brand, S.; Hoelscher, D.; Schierhorn, A.; Svatos, A.; Schroeder, J.; Schneider, B. *Planta* **2006**, *224*, 413–428.
- (26) Opitz, S.; Schnitzler, J. P.; Hause, B.; Schneider, B. *Planta* **2003**, *216*, 881–889.
- (27) Opitz, S.; Otalvaro, F.; Echeverri, F.; Quinones, W.; Schneider, B. *Nat. Prod. Lett.* **2002**, *16*, 335–338.
- (28) Cooke, R. G.; Dagley, I. J. *Aust. J. Chem.* **1979**, *32*, 1841–1847.
- (29) Weiss, U.; Edwards, J. M. *Tetrahedron Lett.* **1969**, *49*, 4325–4328.
- (30) Bazan, A. C.; Edwards, J. M. *Phytochemistry* **1976**, *15*, 1413–1415.
- (31) Cooke, R. G. *Phytochemistry* **1970**, *9*, 1103–1106.
- (32) Schmitt, B.; Schneider, B. *Phytochemistry* **1999**, *52*, 45–53.
- (33) Harmon, A. D.; Edwards, J. M. *Tetrahedron Lett.* **1977**, 4471–4474.
- (34) Thomas, R. *J. Chem. Soc. D* **1971**, 739–740.
- (35) Schmitt, R. C.; Edwards, J. M.; Weiss, U. *Phytochemistry* **1972**, *11*, 1717–1720.
- (36) Hoelscher, D.; Schneider, B. *J. Chem. Soc. D* **1995**, 525–526.
- (37) Opitz, S.; Schneider, B. *Phytochemistry* **2003**, *62*, 307–312.
- (38) Webb, L. J. *Guide to the Medicinal and Poisonous Plants of Queensland*; Council for Scientific and Industrial Research: Melbourne, 1948.
- (39) Cooke, R. G.; Merrett, B. K.; O’Loughlin, G. J.; Pietersz, G. A. *Aust. J. Chem.* **1980**, *33*, 2317–2324.
- (40) DellaGreca, M.; Previtiera, L.; Zarrelli, A. *Tetrahedron* **2009**, *65*, 8206–8208.
- (41) Master, R. N.; Clark, R. B.; Karlowsky, J. A.; Ramirez, J.; Bordon, J. M. *Int. J. Antimicrob. Agents* **2011**, *38*, 291–295.
- (42) DellaGreca, M.; Lanzetta, R.; Molinaro, A.; Monaco, P.; Previtiera, L. *Bioorg. Med. Chem. Lett.* **1992**, *2*, 311–314.
- (43) Smallcombe, S. H.; Patt, S. L.; Keifer, P. A. *J. Magn. Reson., Ser. A* **1995**, *117*, 295–303.

CHAPTER 7

Secondary Metabolites of the fungus *Leucocoprinus*

birnbaumii



Kingdom: Fungi
Phylum: Basidiomycota
Class: Agaricomycetes
Order: Agaricales
Family: Agaricaceae
Genus: *Leucocoprinus*
Species: *birnbaumii*

Collected from Eltham, Victoria, Australia
in January 2006.

Chapter 7 describes the compounds identified from the terrestrial fungus *Leucocoprinus birnbaumii*. This work has been published, the details of which are outlined below.

Journal publication resulting from this study:

Brkljača, Robert, & Urban, Sylvia. (2015). Rapid Dereplication and Identification of the Bioactive Constituents from the Fungus, *Leucocoprinus birnbaumii*. *Natural Product Communications*, 10(1), 95-98.

Rapid Dereplication and Identification of the Bioactive Constituents from the Fungus, *Leucocoprinus birnbaumii*

Robert Brkljača^a and Sylvia Urban^{a,*}

^aSchool of Applied Sciences, Health Innovations Research Institute (HIRI) RMIT University, GPO Box 2476V Melbourne, Victoria 3001, Australia

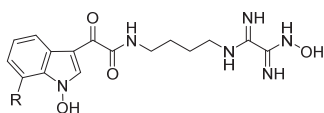
sylvia.urban@rmit.edu.au

Received: May 1st, 2014; Accepted: May 13th, 2014

A series of fatty acids were rapidly dereplicated and partially identified from the flowerpot fungus, *Leucocoprinus birnbaumii* using HPLC-NMR and HPLC-MS. Subsequent off-line isolation unequivocally established the structures, and anti-microbial testing concluded that the fatty acids displayed moderate but selective anti-microbial activity. This represents the first report of these compounds occurring in this particular terrestrial fungus.

Keywords: *Leucocoprinus birnbaumii*, HPLC-NMR, Fungus, Biological Activity, Dereplication, Fatty Acids.

The bright yellow fungus, *Leucocoprinus birnbaumii* (Agaricaceae), is a species of gilled mushroom. It is also known as the “flowerpot parasol and the plantpot dapperling” as it is commonly found growing in flowerpots and greenhouses [1]. The fungus has been reported to be poisonous, and ingestion can cause symptoms such as vomiting, nausea and diarrhea [2]. As yet, there has been no reported biological activity study conducted on either the crude extract or any of the compounds previously reported from the fungus. One of the first studies of *L. birnbaumii* established the content of crude protein, amino acids, sugars and minerals present in the fungus [3]. A second and more in depth study, reported on the isolation and identification of the two hydroxyindole pigments, birnbaumin A (**1**) and B (**2**), which are responsible for the bright yellow color associated with the fungus [4].



(**1**) birnbaumin A R = H
(**2**) birnbaumin B R = OH

Figure 1: Structures of the pigments identified from *L. birnbaumii*.

As part of the continuing bioactive natural product discovery activities of the Marine and Terrestrial Natural Product (MATNAP) research group at RMIT University, a sample of *L. birnbaumii* that was found growing in a flowerpot was harvested and subjected to a chemical investigation. In this study we report the first biological activity evaluation of the crude extract and for three of the compounds isolated from the fungus.

Initial analysis

The dichloromethane crude extract of the fungus displayed no anti-microbial activity while the methanol crude extract showed only minimal anti-microbial activity against *Streptococcus pyogenes*. Based on subsequent proton NMR and analytical HPLC analyses, only the dichloromethane extract showed the presence of compounds that warranted further investigation. Despite this, C₁₈ Vacuum Liquid Chromatography (VLC) was carried out on the methanol crude extract in an effort to deduce if this extract could be deconvoluted and whether it warranted further chemical investigation. Subsequent analysis of the resulting C₁₈ fractions concluded that birnbaumin A (**1**) and B (**2**), which have characteristic UV chromophores at λ_{\max} 322 and 356 nm respectively, could not be detected in any of the fractions on the basis of the HPLC contour plot obtained via PDA. Only very polar compounds present in minor quantities were observed and so only the dichloromethane crude extract was further investigated. No previous studies have focused on evaluating the secondary metabolites present in the dichloromethane extract of this fungus.

Phytochemical profiling

The dichloromethane crude extract was subjected to phytochemical profiling and dereplication using HPLC-NMR and HPLC-MS. A total of three components were detected, and comparison of the on-flow HPLC-NMR proton NMR data indicated that these differed vastly to the data reported for birnbaumin A (**1**) and B (**2**) [4], immediately indicating the presence of a different structural class.

Analysis of the WETID proton NMR spectra (extracted from the on-flow HPLC-NMR experiment) for each of the components,



Dr Sylvia Urban leads the Marine and Terrestrial Natural Product (MATNAP) research group at RMIT University. She was awarded the Gerald Blunden Award for the best research article for 2011 in *Natural Product Communications*, was the recipient of the Ronald Riseborough prize in chemistry, and has also been awarded the American Society of Pharmacognosy Research Starter Grant for a project entitled “*Investigation into the Chemistry and Biological Activity of the Orange-Rot Fungus, Pycnoporus cinnabarinus*”. Dr Urban has been researching in the field of natural products chemistry for in excess of 20 years. Her interests include marine and terrestrial natural products chemistry; isolation and structural characterization; NMR spectroscopy and analytical separation and profiling methodologies for natural product discovery.

clearly showed that they were structurally related. The presence of olefinic signals and signals in the upfield region of the spectra suggested the presence of alkenes, such as those observed in fatty acids. This was further supported by the UV profile observed for these components which indicated very little conjugation since no UV chromophores were observed above 212 nm. Due to the small quantity of the dichloromethane crude extract available, only one stop flow HPLC-NMR experiment was conducted, which allowed for a WET1D proton NMR spectrum and gCOSY NMR data to be obtained for component 1.

Analysis of the WET1D proton NMR spectrum of component 1 showed the presence of four olefinic protons (δ_{H} 6.77, m, 4H). In addition, an observed molecular ion of m/z 279.2338 [M-H]⁻ was observed for this component for which a molecular formula of C₁₈H₃₂O₂ could be deduced. This particular formula has three degrees of unsaturation, two of which are confirmed by the presence of the four olefinic protons, thereby confirming the presence of two double bonds, and the remaining degree of unsaturation is due to the presence of a carbonyl bond which is typically present as a carboxylic acid in fatty acids. However, the position of the two double bonds could not be unequivocally placed. In this way component 1 could only be partially identified as a variant of octadecadienoic acid with unspecified double bond placement. Component 2 exhibited the same characteristic UV and NMR features as component 1. The HPLC-MS showed the presence of a molecular ion at m/z 281.2493 [M-H]⁻, which is two mass units higher than for component 1. This is attributed to the loss of one of the double bonds. As in the case of component 1, the double bond positions in component 2 could not be unequivocally located. This allowed component 2 to be partially identified as a variant of octadecenoic acid with unspecified double bond placement. Lastly, component 3 also showed the characteristic features of a fatty acid. However, the extracted WET1D proton NMR spectrum also showed the presence of a methoxy moiety (δ_{H} 5.03, s, 3H). Component 3 did not ionize in either positive or negative ESI modes during the HPLC-MS analyses due to methylation of the carboxylic acid preventing ionization from occurring. Based on the two previously identified components and on biosynthetic grounds, it was assumed that component 3 contained the same number of carbons in the alkene side chain. Integration of the extracted WET1D proton NMR spectrum, and comparison of the methoxy and olefinic resonances, supported the presence of four olefinic protons (δ_{H} 6.77, m, 4H) and, therefore, two double bonds. On this basis, component 3 was partially identified as a variant of methyl octadecadienoate with unspecified double bond placement.

Off-line isolation of fatty acids

In an attempt to unambiguously identify the fatty acids present in *L. birnbaumii*, and to possibly identify the presence of any other minor compounds, an off-line isolation was implemented. The dichloromethane crude extract was subjected to reversed phase HPLC and the HPLC chromatogram showed the presence of the same three components as those observed in the off-line study. These components were separated and collected based on their retention time and peak height/area using an automatic fraction collector.

Component 1 was isolated as yellow oil. The proton NMR spectrum showed the presence of four olefinic protons (δ_{H} 5.36, m, 4H), along with five methylene functionalities (δ_{H} 2.78, dd, $J = 6.5, 7.0$ Hz; 2.35, t, $J = 8.0$ Hz; 2.05, dt, $J = 6.5, 7.0$ Hz; 1.64, p, $J = 8.0$ Hz; and 1.33, m) and one methyl group (δ_{H} 0.90, t, $J = 7.0$ Hz, 3H). The carbon NMR spectrum showed the presence of an ester functional group (δ_{C} 179.7), four olefinic carbons (δ_{C} 130.2, 130.0, 128.0 and

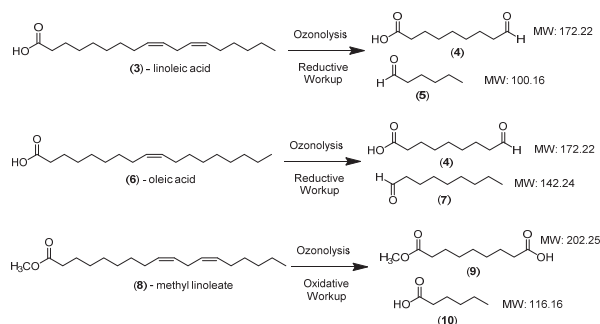


Figure 2: Identity and possible structures of components 1, 2 and 3, with expected fragments resulting from the ozonolysis with reductive and oxidative workups.

127.8) and various methylene and methyl carbons. Complete analysis of the 2D NMR spectroscopic data obtained (gCOSY, HSQCAD and gHMBCAD) allowed for the overall structure to be determined as a fatty acid. However, despite the ability to obtain comprehensive 2D NMR data, the position of the double bonds could not be unequivocally placed due to the overlapped nature of the proton and carbon NMR chemical shifts. In order to determine the position of the double bonds, a chemical derivatization would be necessary.

It is well established that the location of olefinic bonds in fatty acids can be secured by ozonolysis and mass spectrometry whereby fragments are converted either into aldehydes, ketones or acids, depending on the subsequent work up used [5, 6]. Ozonolysis of component 1 was carried out with a reductive workup. In this reaction, dimethyl sulfide was used as the reducing agent, which results in the production of aldehydes [7, 8]. Subsequent mass spectrometric analysis of the fragment showed a molecular ion at m/z 171 [M-H]⁻ for the ozonoid aldehyde product. Analysis of the gCOSY and gHMBCAD NMR data supported five possible positions for the location of the double bonds.

Comparing the mass of each of the aldehydes produced that could result from the five possible structures with the actual observed mass, allowed the position of the double bonds to be secured. The position of the two double bonds was, therefore, established as commencing at position 9, as the resulting fragment would yield an observed ion at m/z 171.0 [M-H]⁻ (Figure 2). Therefore, component 1 was identified as the previously reported fatty acid octadeca-9,12-dienoic acid, also known as linoleic acid (3) [9].

Component 2 was identified in a similar manner. Initial analysis of the proton NMR spectrum showed that there were only two olefinic protons (δ_{H} 5.36, m, 2H). A reductive workup of the ozonolysis reaction, followed by mass spectrometric analysis of the fragment indicated the presence of a molecular ion at m/z 171.0 (Figure 2). Considering all possible structures, component 2 was identified as the previously reported fatty acid octadec-9-enoic acid, also known as oleic acid (6) [9].

Lastly, component 3 did not ionize in either positive or negative ESI-MS modes, but a molecular ion was observed at m/z 294, which was obtained via GC-MS analysis. Component 3 also had very similar proton and carbon NMR data to the other two components, but contained a methoxy moiety (δ_{H} 3.67, s; δ_{C} 51.5). Ozonolysis was also carried out on component 3 using a reductive workup, but this was unsuccessful. Instead, an oxidative workup of the ozonolysis reaction using Jones' reagent was implemented, and this was successful. Unlike the reductive workup, oxidative workups produce acids [7, 8]. Mass spectrometry carried out after ozonolysis

showed the presence of a molecular ion at m/z 201, which confirmed that the double bonds were also located at position 9 (Figure 2). The identity of this compound was concluded to be the methyl ester of the fatty acid octadeca-9,12-dienoic acid methyl ester, also known as methyl linoleate (**8**) [9].

Most naturally occurring fatty acids possess a *cis* or *Z* double bond geometry [10, 11]. On biosynthetic grounds this was concluded to also be the case for the fatty acids identified in this study

Biological evaluation of the three fatty acids (**3**, **6** and **8**) was carried out against six microorganisms (*Escherichia coli*, *Staphylococcus aureus*, *S. aureus* MRSA, *Streptococcus pyogenes*, *Pseudomonas aeruginosa* and *Candida albicans*). Each of the three fatty acids (**3**, **6** and **8**) showed moderate anti-bacterial activity with some selectivity and the fatty acids were able to inhibit the growth of both Gram-positive and Gram-negative bacteria. The observed activity (measured as a zone of inhibition) against the six organisms tested for each of the three fatty acids (**3**, **6** and **8**), which were tested at a concentration of 1 mg/mL, is given in Table 1. The observed activity for the three acids is in agreement with that previously reported, with fatty acids known to display various antibacterial activity [12-16].

Table 1: Anti-microbial activity (reported as measured zones of inhibition in mm) of the isolated fatty acids.

Compound	Linoleic acid (3)	Oleic acid (6)	Methyl linoleate (8)
Microorganism			
<i>E. coli</i>	ND	ND	ND
<i>S. aureus</i>	1	ND	1
MRSA	ND	ND	ND
<i>P. aeruginosa</i>	ND	3	2
<i>S. pyogenes</i>	3	ND	1
<i>C. albicans</i>	ND	ND	ND

ND Indicates no zone of inhibition was detected

Experimental

General experimental procedures: All organic solvents used were analytical reagent (AR or GR), UV spectroscopic, or HPLC grades with milli-Q water also being used. ^1H (500 MHz) and ^{13}C (125 MHz) NMR spectra were acquired in CDCl_3 on a 500 MHz Agilent DD2 NMR spectrometer with referencing to solvent signals (δ 7.26 and 77.0 ppm). Two-dimensional NMR experiments recorded included gCOSY, HSQCAD, and gHMBCAD experiments. ESI mass spectra were obtained on a Micromass Platform II mass spectrometer equipped with a LC-10AD Shimadzu solvent delivery module (50% $\text{CH}_3\text{CN}/\text{H}_2\text{O}$ at a flow rate of 0.2 mL/min) in both the positive and negative ionization modes using cone voltages between 20 and 30 V. GCMS was carried out on a Varian CP-3800 gas chromatograph equipped with a Varian CP-8410 autoinjector and Varian Saturn 2200 GC/MS/MS detector. The injector port temperature was set to 280°C; the column oven was set to 150°C and was ramped at a rate of 5°C/min to 225°C, which was held for 8 min. The carrier gas flow rate was 1.0 mL/min. HPLC-NMR was carried out on a 500 MHz Agilent DD2 NMR spectrometer equipped with a Varian $^1\text{H}/^{13}\text{C}$ pulsed field gradient flow probe with a 60 μL active volume flow cell coupled to a Varian Prostar 210 solvent delivery system, a Prostar 430 Autosampler and a Prostar 335 PDA detector. THE HPLC-NMR analyses were carried out using the CORBA communication and operated with VnmrJ software. The 2H resonance observed from the D_2O was used to obtain field-frequency lock. The resonances from the HOD and the methyl of the acetonitrile were suppressed using the WET solvent suppression experiment [17]. The residual HOD resonance of D_2O was referenced to 4.79 ppm. For both on-flow and stop-flow HPLC-NMR analyses, 50 μL (2,500 μg) of the dichloromethane extract

was injected onto an Agilent Eclipse Plus C_{18} (150 x 4.6) 5 μm HPLC column using a solvent composition of 90% $\text{CH}_3\text{CN}/\text{D}_2\text{O}$ at a flow rate of 1 mL/min. In the stop-flow HPLC-NMR mode WET1D and gCOSY NMR experiments were acquired. HRESILCMS was carried out on an Agilent 6540 Series Q-TOF system (ESI operation conditions of 12 L/min N_2 , 325°C drying gas temperature and 3500 V capillary voltage) equipped with an Agilent 1260 Series LC solvent delivery module (90% CH_3OH at a flow rate of 1.0 mL/min) in negative and positive ionization modes using an Agilent Eclipse Plus C_{18} (4.6 x 150) 5 μm HPLC column. The instrument was calibrated using the 'Agilent Tuning Mix' using purine as the reference compound and the Hewlett-Packard standard HP0921. Analytical HPLC analyses were carried out using either a gradient HPLC method 0–2 min 10% $\text{CH}_3\text{CN}/\text{H}_2\text{O}$; 14–24 min 75% $\text{CH}_3\text{CN}/\text{H}_2\text{O}$; 26–30 min 100% CH_3CN and 32–40 min 10% $\text{CH}_3\text{CN}/\text{H}_2\text{O}$ or an isocratic HPLC method (90% $\text{CH}_3\text{CN}/\text{H}_2\text{O}$) on an Alltech Alltima HP C_{18} (250 x 4.6) 5 μm column at a flow rate of 1.0 mL/min. Semi-preparative HPLC was carried out on a Dionex P680 (solvent delivery module) equipped with a Dionex UVD340U PDA detector and a Foxy Jr. automated fraction collector. An isocratic HPLC method (90% $\text{CH}_3\text{CN}/\text{H}_2\text{O}$) was employed using a Phenomenex Luna (2) 100 Å C_{18} 250 x 10 mm (5 μm) HPLC column. The automatic fraction collector was programmed to collect the 3 fatty acids based on their retention times (12.89, 18.81 and 26.02 min, respectively) and a peak threshold value at a flow rate of 3.5 mL/min. Vacuum flash chromatography (VLC) was carried out using C_{18} on the methanol crude extract of the fungus. The VLC separation began with a solvent system comprised of 100% H_2O which, in 20% stepwise increments, made its way through to MeOH and finally DCM.

Biological evaluation: Crude extracts of the fungus (dichloromethane and methanol extract) were evaluated against 6 micro-organisms (5 bacteria and one test fungi) at concentrations of 25 and 50 mg/mL respectively. Pure compounds were tested at a concentration of 1 mg/mL. Each micro-organism was prepared by creating a 0.5 McFarlane solution suspension. Lawn cultures were prepared on either Mueller-Hinton or Brain Heart Infusion Agar (BHIA) (used for the *S. pyogenes*). Then 20 μL of the crude extracts or pure compounds were pipetted onto 6 mm diameter filter paper disks and their solvents evaporated. These disks were then placed onto the prepared lawn cultures and incubated at 37°C overnight. Active anti-microbial samples displayed a zone of inhibition outside the disk, which was measured in mm as the radius of inhibition for each bacteria/fungi. The 6 test organisms were *Escherichia coli* (ATCC 25922), *Staphylococcus aureus* (ATCC 25923), *S. aureus* MRSA (344/2-32), *Pseudomonas aeruginosa* (ATCC 27853) *Streptococcus pyogenes* (345/1) and *Candida albicans* (ATCC 10231).

Terrestrial fungus material: The bright yellow fungus (*L. birnbaumii*) was collected on 29 January, 2006 in Eltham North, Victoria, Australia by Dr S. Urban. The fungus was growing in a pot alongside a palm. The fungus was identified by Prof A. Lawrie (School of Applied Sciences, Discipline of Biotechnology and Biological Sciences, RMIT University). A voucher specimen (designated the code number 2006_15) is deposited at the School of Applied Sciences (Discipline of Applied Chemistry), RMIT University.

Chemical profiling: Chemical profiling was carried out on the dichloromethane soluble extract of the fungus employing HPLC-NMR and HPLC-MS methodologies. Details of these analyses are provided in the Experimental Details section. The dichloromethane extract (29.5 mg) was dissolved in HPLC-NMR grade CH_3CN (590

μL) and filtered through a 0.45 PTFE membrane filter (Grace Davison Discovery Sciences).

Extraction and solution: The fungus (8.5 g, wet weight) was extracted with 3:1 methanol/dichloromethane (1 L). The crude extract was then decanted and concentrated under reduced pressure and sequentially solvent partitioned (trituated) into dichloromethane and methanol soluble extracts, respectively. The dichloromethane crude extract was subjected to reversed phase HPLC (90% CH₃CN/H₂O) to yield linoleic acid (**3**) (17.8 mg, 0.40%), oleic acid (**6**) (6.9 mg, 0.15%) and methyl linoleate (**8**) (4.4 mg, 0.10%), respectively. The percentage yields are reported on the basis of the dry mass of the fungus extracted.

Ozonolysis: (Reductive workup) - Linoleic acid (**3**) (8.0 mg) and oleic acid (**6**) (3.0 mg) were individually dissolved in 25 mL of dichloromethane. The samples were then placed into an acetone/dry ice bath and ozone bubbled through at a rate of 19 mg/L for 5 min. The ozonides were quenched with dimethyl sulfide and then 40 mL of water was added. The ozonolysis products were extracted by washing with dichloromethane (3 x 50 mL) and subsequently analyzed by LRESIMS.

(Oxidative workup) - Methyl linoleate (**8**) (2.0 mg) was subjected to the same ozonolysis conditions as described above, with the exception that the ozonide was quenched using Jones' reagent. The extraction of the product was also carried out as specified above.

On-line (HPLC-NMR & HPLC-MS) characterization of compounds:

Component 1 (variant of octadecadienoic acid with unspecified double bond positions).

¹H NMR (500 MHz, 90% CH₃CN/D₂O) (Stop-flow mode): 6.77 (4H, m), 4.20 (2H, dd, *J* = 6.5, 7.0 Hz), 3.66 (m), 2.96 (2H, m), 2.71 (16H, m), 2.30 (3H, m).

HPLC-HR-ESI-MS (negative mode): *m/z* at 279.2338 [M-H]⁻ (calcd. for C₁₈H₃₁O₂: *m/z* 279.2324).

Component 2 (variant of octadecenoic acid with unspecified doubled bond position).

¹H NMR (500 MHz, 90% CH₃CN/D₂O) (On-flow mode): 6.77 (2H, m), 3.67 (2H, m), 2.96 (4H, m), 2.69 (22H, m), 2.30 (3H, m).
HPLC-HR-ESI-MS (negative mode): *m/z* at 281.2493 [M-H]⁻ (calcd. for C₁₈H₃₃O₂: *m/z* 281.2481).

Component 3 (variant of methyl octadecadienoate with unspecified double bond positions).

¹H NMR (500 MHz, 90% CH₃CN/D₂O) (On-flow mode): 6.77 (4H, m), 5.03 (3H, s), 4.20 (2H, m), 3.70 (2H, m), 2.98 (2H, m), 2.71 (m), 2.30 (3H, m).
LRESIMS: no molecular ion observed in either positive or negative ionization modes.

Acknowledgments -The Marine and Terrestrial Natural Product (MATNAP) research group would like to thank Prof A. Lawrie (School of Applied Sciences, Discipline of Biotechnology and Biological Sciences, RMIT University) for the taxonomic identification of the fungus; Mrs N. Thurbon (School of Applied Sciences, Discipline of Biotechnology and Biological Sciences, RMIT University) for providing access to the micro-organisms to conduct the anti-microbial assays and for other invaluable technical support; Ms S. Duck (School of Chemistry, Faculty of Science, Monash University) for conducting the high resolution HPLC-MS analyses; Dr J. Niere for her useful NMR discussions and guidance; Prof M. Rizzacasa (School of Chemistry, Bio21 Molecular Science and Biotechnology Institute, University of Melbourne) for providing access to the ozone generator. Mr R. Brkljača would like to acknowledge his Australian Postgraduate Award (APA) scholarship that has supported his PhD studies.

References

- [1] Arora D. (1986) *Mushrooms Demystified*. Ten Speed Press, California.
- [2] Hall IR, Stephenson SC, Buchanan PK, Yun W, Cole ALJ. (2003) *Edible and Poisonous Mushrooms of the World*. Timber Press, Cambridge, UK.
- [3] Goyal R, Misra PS, Pathak NC. (1990-1991) Cultivation and nutritive value of *Leucocoprinus birnbaumii*. *Acta Botanica Hungarica*, **36**, 181-185.
- [4] Bartsch A, Bross M, Spitteller P, Spitteller M, Steglich W. (2005) Birnbaumia A and B: Two unusual 1-hydroxyindole pigments from the "flower pot parasol" *Leucocoprinus birnbaumii*. *Angewandte Chemie, International Edition*, **44**, 2957-2959.
- [5] Privett OS, Nickell C. (1962) Determination of structure of unsaturated fatty acids via reductive ozonolysis. *Journal of the American Oil Chemists' Society*, **39**, 414-419.
- [6] Sun C, Curtis JM. (2013) Locating double bonds in lipids - New approaches to the use of ozonolysis. *Lipid Technology*, **25**, 279-282.
- [7] Furniss BS, Hannaford AJ, Smith PWG, Tatchell AR. (1989) *Vogel's Textbook of Practical Organic Chemistry*. Longman Group UK Limited, Essex, UK
- [8] Smith MB, March J. (2001) *March's Advanced Organic Chemistry: Reactions, Mechanisms, and Structure*. Wiley, New York.
- [9] SDBSWeb : <http://sdbs.riondb.aist.go.jp> (National Institute of Advanced Industrial Science and Technology).
- [10] Rustan AC, Drevon CA. (2001) *Fatty acids: Structures and properties*, eLS. John Wiley & Sons, Ltd, Chichester, UK.
- [11] Ledoux M, Juaneda P, Sebedio J-L. (2007) *Trans* fatty acids: definition and occurrence in foods. *European Journal of Lipid Science and Technology*, **109**, 891-900.
- [12] Kabara JJ, Swieczkowski DM, Conley AJ, Truant JP. (1972) Fatty acids and derivatives as antimicrobial agents. *Antimicrobial Agents and Chemotherapy*, **2**, 23-28.
- [13] Dilika F, Bremner PD, Meyer JJM. (2000) Antibacterial activity of linoleic and oleic acids isolated from *Helichrysum pedunculatum*: a plant used during circumcision rites. *Fitoterapia*, **71**, 450-452.
- [14] Mishra PM, Sree A, Baliarsingh S. (2009) Antibacterial study and fatty acid analysis of lipids of the sponge *Myrmekioderma granulata*. *Chemistry of Natural Compounds*, **45**, 621-624.
- [15] Suliman MB, Nour AH, Yusoff MM, Nour AH, Kuppusamy P, Yuvaraj AR, Adam MS. (2013) Fatty acid composition and antibacterial activity of *Swietenia macrophylla* King seed oil. *African Journal of Plant Science*, **7**, 300-303.
- [16] Desbois AP, Lawlor KC. (2013) Antibacterial activity of long-chain polyunsaturated fatty acids against *Propionibacterium acnes* and *Staphylococcus aureus*. *Marine Drugs*, **11**, 4544-4557.
- [17] Smallcombe SH, Patt SL, Keifer PA. (1995) WET solvent solvent suppression and its application to LC NMR and high-resolution NMR spectroscopy. *Journal of Magnetic Resonance, Series A*, **117**, 295-303.

PART C – Marine Organisms

The chapters that encompass this section of the thesis (Chapters 8-11) include studies conducted on various marine algae derived from the Phaeophyta (eight species) and Rhodophyta (2 species) phyla. The application of phytochemical profiling (HPLC-NMR & HPLC-MS) to rapidly dereplicate and identify the structure classes and the identities of the compounds present in a variety of algae is presented. In total this section of the thesis describes the identification of thirteen new and twenty two previously reported secondary metabolites. The acquisition of a gHMBCAD NMR experiment without the use of pre-concentration, cold probes or microcoils is also documented for the first time. Finally the application of NMR (nOe experiments) and circular dichroism (CD) spectroscopy were implemented to either deduce or propose the relative and absolute configuration for some of the compounds identified from these marine organisms.

This section of the thesis is comprised of four journal publications as detailed below:

1. Brkljača, Robert, Göker, Emrehan S., & Urban, Sylvia. (2015). Dereplication and Chemotaxonomical Studies of Marine Algae of the Ochrophyta and Rhodophyta Phyla. *Marine Drugs*, 13(5), 2714-2731.
2. Brkljača, Robert, & Urban, Sylvia. (2015). Chemical Profiling (HPLC-NMR & HPLC-MS), Isolation and Identification of Bioactive Meroditerpenoids from the Southern Australian Marine Brown Alga *Sargassum paradoxum*. *Marine Drugs*, 13(1), 102-127.

3. Brkljača, Robert, & Urban, Sylvia. (2015). HPLC-NMR and HPLC-MS investigation of antimicrobial constituents in *Cystophora monilifera* and *Cystophora subfarcinata*. *Phytochemistry*, 117, 200-208.

4. Brkljača, Robert, & Urban, Sylvia. (2013). Relative Configuration of the Marine Natural Product Elatenyne using NMR Spectroscopic and Chemical Derivatization Methodologies. *Natural Product Communications*, 8(6), 729-732.

CHAPTER 8

Dereplication and Chemotaxonomical Profiling of Seven Marine

Algae by HPLC-NMR & HPLC-MS.



Genus: *Halopteris*
Species: *pseudospicata*



Genus: *Sargassum*
Species: *cf fallax*



Genus: *Sargassum*
Species: *vestitum*



Genus: *Sargassum*
Species: *decipiens*



Genus: *Cystophora*
Species: *retroflexa*



Genus: *Cystophora*
Species: *subfarcinata*



Genus: *Laurencia*
Species: *sp.*

Chapter 8 describes the rapid dereplication of sixteen compounds from six marine algae from the Phaeophyceae and one from the Rhodophyceae phyla, which was achieved by HPLC-NMR and HPLC-MS. This work has been published (see details as given below). Appendix D contains supplementary information relevant to the study.

Brkljača, Robert, Göker, Emrehan S., & Urban, Sylvia. (2015). Dereplication and Chemotaxonomical Studies of Marine Algae of the Ochrophyta and Rhodophyta Phyla. *Marine Drugs*, 13(5), 2714-2731.

Article

Dereplication and Chemotaxonomical Studies of Marine Algae of the Ochrophyta and Rhodophyta Phyla

Robert Brkljača, Emrehan Semih Göker and Sylvia Urban *

School of Applied Sciences (Discipline of Chemistry), Health Innovations Research Institute (HIRi), RMIT University, GPO Box 2476V Melbourne, Victoria 3001, Australia;
E-Mails: robert.brkljaca@rmit.edu.au (R.B.); emrehan_goker@hotmail.com (E.S.G.)

* Author to whom correspondence should be addressed; E-Mail: sylvia.urban@rmit.edu.au;
Tel.: +61-3-9925-3376.

Academic Editor: Alejandro M. Mayer

Received: 6 March 2015 / Accepted: 21 April 2015 / Published: 30 April 2015

Abstract: Dereplication and chemotaxonomic studies of six marine algae of the Ochrophyta and one of the Rhodophyta phyla resulted in the detection of 22 separate compounds. All 16 secondary metabolites, including four new compounds (**16–19**), could be rapidly dereplicated using HPLC-NMR and HPLC-MS methodologies in conjunction with the MarinLit database. This study highlights the advantages of using NMR data (acquired via HPLC-NMR) for database searching and for the overall dereplication of natural products.

Keywords: ochrophyta; rhodophyta; dereplication; profiling; algae; HPLC-NMR; HPLC-MS

1. Introduction

The Ochrophyta phylum contains in excess of 1800 species [1]. Recently, 17 new compounds, mostly terpenoids, were reported from the Ochrophyta phylum [2]. In contrast, marine algae belonging to the Rhodophyta phylum, are represented by over 6500 species [1] and produce a large number of halogenated secondary metabolites [3]. For example, nine new compounds were recently reported from the Rhodophyta phylum, a majority representative of bromophenols [2].

The intention of this study was to select a range of marine algae and conduct a dereplication/chemotaxonomical investigation as a means to rapidly differentiate the secondary metabolites present across different genera and between species of the same genera. For instance, marine algae of the Ochrophyta phylum such as *Cystophora retroflexa* have been reported to produce carotenoids,

phlorethols and fucophlorethols [4–6] while *Cystophora subfarcinata* is known to produce tocotrienols and phloroglucinols [7]. The remaining Ochrophyta phylum genera and species investigated included, *Sargassum decipiens*, *Sargassum vestitum*, *Sargassum cf. fallax*, and *Halopteris pseudospicata* and importantly these have not had any marine secondary metabolites reported. However, the *Sargassum* genus is known to produce meroditerpenoid, tocotrienol and terpenoid type compounds [8]. The only marine alga of the Rhodophyta phylum studied was of the *Laurencia* genus which is known to produce very different secondary metabolites from the marine brown algae [9–12].

In this study, we examined six specimens of marine brown algae belonging to the Ochrophyta phylum (*Sargassum cf. fallax*, *Sargassum decipiens* (R.Brown ex Turner) J.Agardh, *Sargassum vestitum* (R.Brown ex Turner) C.Agardh, *Cystophora retroflexa* (Labillardière) J.Agardh, *Cystophora subfarcinata* (Mertens) J.Agardh and *Halopteris pseudospicata* Sauvageau) and one marine red alga from the Rhodophyta phylum (*Laurencia* sp.), all of which were collected from Port Phillip Bay, Victoria, Australia. These marine algae were selected for phytochemical evaluation on the basis of three criteria, but in all three instances the intention was to rapidly dereplicate the secondary metabolites present and to avoid lengthy isolations. The marine algae were either selected on the basis of the observed biological activity of the crude extracts, or due to the fact that no previous secondary metabolites had been described from the species of marine alga. The final motivation for the selection was based upon the fact that our research group has previously conducted studies on other closely related *Sargassum*, *Cystophora* and *Laurencia* species and so the intention was to compare the secondary metabolites in closely related species.

Herein, we report the chemical profiling/dereplication conducted using HPLC-NMR and HPLC-MS leading to the identification of seven different structure classes. In total, 22 compounds were detected in the dichloromethane crude extracts of the marine algae studied, of which 16 could be dereplicated.

2. Results and Discussion

The frozen marine algae were extracted with 3:1 methanol/dichloromethane, evaporated under reduced pressure and sequentially solvent partitioned (trituated) into dichloromethane and methanol soluble fractions, respectively. The dichloromethane and methanol crude extracts were initially analysed by off-line analytical HPLC and ¹H-NMR analyses and this established that the majority of the secondary metabolites were present in the dichloromethane crude extracts. Based on this, only the dichloromethane extracts were further examined by chemical profiling methodologies (HPLC-NMR & HPLC-MS).

2.1. Chemical Profiling (HPLC-NMR & HPLC-MS)

The dichloromethane crude extracts were subjected to both HPLC-NMR and HPLC-MS chemical profiling and a total of 22 compounds were detected from the seven separate marine algae. Identical HPLC-NMR and HPLC-MS conditions were employed to probe the dichloromethane crude extracts of each alga to allow for comparison between each genera and/or species. Analysis of the stop-flow WET1D proton NMR spectra and extracted UV profiles for each of the compounds concluded the presence of seven distinct chemical structure classes including phenolic acids, phenols, resorcinols, phloroglucinols, xanthophylls, tocotrienols and C₁₅ halogenated acetogenins, which are known to occur in these genera or species of algae [6–8,13–17].

Twelve known (**1–5**, **11–15**, **20** and **21**) and four new (**16–19**) compounds (Figure 1) were dereplicated from the dichloromethane crude extracts of the algae. Compounds were dereplicated by analysis of the HPLC-NMR acquired data (WET1D and various combinations of gCOSY, HSQCAD, and gHMBCAD), high resolution HPLC-MS data, and use of the MarinLit database by searching parameters such as the taxonomy (usually genus), UV, MS and NMR data. While some structure classes are unique to certain genera or species, some can be present across various genera or species of algae (Table 1). For instance, in this study, phloroglucinols were detected in *S. cf. fallax*, *C. subfarcinata* and *C. retroflexa* while tocotrienols were exclusive to *S. cf. fallax*. The xanthophylls, which are known to occur in many marine brown algae [8,18], were found in high abundance in *S. vestitum* and *H. pseudospicata*. The specimen of *S. decipiens* was concluded to produce phenolic acids, phenols, and resorcinols while the specimen of *Laurencia* sp. could be deduced as containing C₁₅ halogenated acetogenins. Table 2 summarises each of the components detected in the seven marine algae studied together with the search criteria used to dereplicate the structures present in the dichloromethane crude extracts. The amount of compound present in each of the crude extracts was estimated on the basis of the limit of detection (LOD) methodology recently reported for our HPLC-NMR system [19]. In this study, the LOD for five key NMR experiments was established for a given set of parameters. These LODs and the parameters utilized were reviewed, and on this basis, the approximate amount of each compound present in the crude extract for each of the HPLC-NMR analyses undertaken was estimated (see Table 2). In HPLC-NMR analyses, it is imperative to suppress signals arising from the HPLC solvents (HDO signal arising from D₂O and the CH₃CN peak) in order to maximise signal intensity and obtain better quality NMR spectra. Unfortunately, during this process NMR signals of the compound of interest which occur within this suppression region are also inadvertently suppressed.

Table 1. Chemotaxonomic comparison of the seven marine algae studied and the chemical classes present in each.

Alga	Chemical Class(es) Present	Compounds Present *
<i>C. subfarcinata</i>	Phloroglucinols	18, 19
<i>C. retroflexa</i>	Phloroglucinols	11-13, 16, 18, 20, 21
<i>S. cf. fallax</i>	Phloroglucinols, tocotrienols	12, 14, 15, 17, 20, 21
<i>S. decipiens</i>	Phenols, phenolic acids, resorcinols	1–4
<i>S. vestitum</i>	Xanthophylls	5
<i>H. pseudospicata</i>	Xanthophylls	5
<i>Laurencia</i> sp.	Polyhalogenated C ₁₅ acetogenins	-

* Retention times for compounds present are provided in Table 2.

Table 2. Identification of chemical structure classes present in seven marine algae studied (ordered on the basis of HPLC-NMR retention time, R_t).

Peak #	R_t (min)	Compound	Structure Class	Marine Alga (~Amount Present in μg)	UV (nm)	MarinLit Search Parameters	New/Known
1	2.29	(2)	Phenolic acid	<i>S. decipiens</i> (500–1000)	240, 302	Compound not in MarinLit database	Known
2	2.44	(3)	Phenol	<i>S. decipiens</i> (500–1000)	236, 301	Compound not in MarinLit database	Known
3	3.42	(11)	Phloroglucinol	<i>C. retroflexa</i> (750–1000)	235, 285	Molecular formula, UV ± 5	Known
4	3.55	(1)	Phenolic acid	<i>S. decipiens</i> (<100)	235, 301	Molecular formula, UV ± 10	Known
5	4.45	(16)	Phloroglucinol	<i>C. retroflexa</i> (750–1000)	235, 285	Compound not in MarinLit database	New
6	5.00	n.a.	C ₁₅ acetogenin	<i>Laurencia</i> sp. (<25)	220, 237	Genus, UV ± 5 , 1 triplet methyl group	Not Identified
7	6.05	n.a.	Unknown	<i>Laurencia</i> sp. (500–1000)	220, 240, 255	Unable to dereplicate using any parameters	Not Identified
8	6.70	n.a.	C ₁₅ acetogenin	<i>Laurencia</i> sp. (<25)	220, 237	Genus, UV ± 5 , 1 triplet methyl group	Not Identified
9	7.87	(4)	Resorcinol	<i>S. decipiens</i> (<10)	229, 276, 281	Compound not in MarinLit database	Known
10	9.98	(12)	Phloroglucinol	<i>C. retroflexa</i> (500–1000), <i>S. cf. fallax</i> (<250)	230, 285	Molecular formula, UV ± 5	Known
11	12.95	(13)	Phloroglucinol	<i>C. retroflexa</i> (250–750)	230, 285	Molecular formula, UV ± 5	Known
12	13.65	(17)	Phloroglucinol	<i>S. cf. fallax</i> (<250)	215, 228, 285	Compound not in MarinLit database	New
13	14.53	(5)	Xanthophyll	<i>S. vestitum</i> (<100), <i>H. pseudospicata</i> (<100)	450	Molecular formula	Known
14	15.50	(20)	Phloroglucinol	<i>C. retroflexa</i> (<500), <i>S. cf. fallax</i> (<100)	212, 228, 285	Compound not in MarinLit database	Known [13]

Table 2. Cont.

15	20.15	(21)	Phloroglucinol	<i>C. retroflexa</i> (<250), <i>S. cf. fallax</i> (<50)	230, 285	Compound not in MarinLit database	Known [13]
16	21.62	(14)	Phloroglucinol	<i>S. cf. fallax</i> (<100)	212, 228, 285	Molecular formula, UV \pm 5	Known
17	22.96	(18)	Phloroglucinol	<i>C. retroflexa</i> (<100), <i>C. subfarcinata</i> (<50)	228, 285	Compound not in MarinLit database	New
18	23.16	n.a.	Phloroglucinol	<i>C. retroflexa</i> (<100)	238, 288	Genus, UV \pm 5	Not Identified
19	26.71	n.a.	Xanthophyll	<i>S. vestitum</i> (<5), <i>H. pseudospicata</i> (<5)	450	Insufficient data to search MarinLit Database	Not Identified
20	30.27	n.a.	Xanthophyll	<i>S. vestitum</i> (<5), <i>H. pseudospicata</i> (<5)	450	Insufficient data to search MarinLit Database	Not Identified
21	33.40	(19)	Phloroglucinol	<i>C. subfarcinata</i> (<50)	213, 228, 285	Compound not in MarinLit database	New
22	60.80	(15)	Tocotrienol	<i>S. cf. fallax</i> (<10)	212, 300	Class, UV \pm 5, contains only singlet aromatic/vinyl CH ₃ groups, aromatic ring	Known

n.a. indicates that a structure could not be concluded.

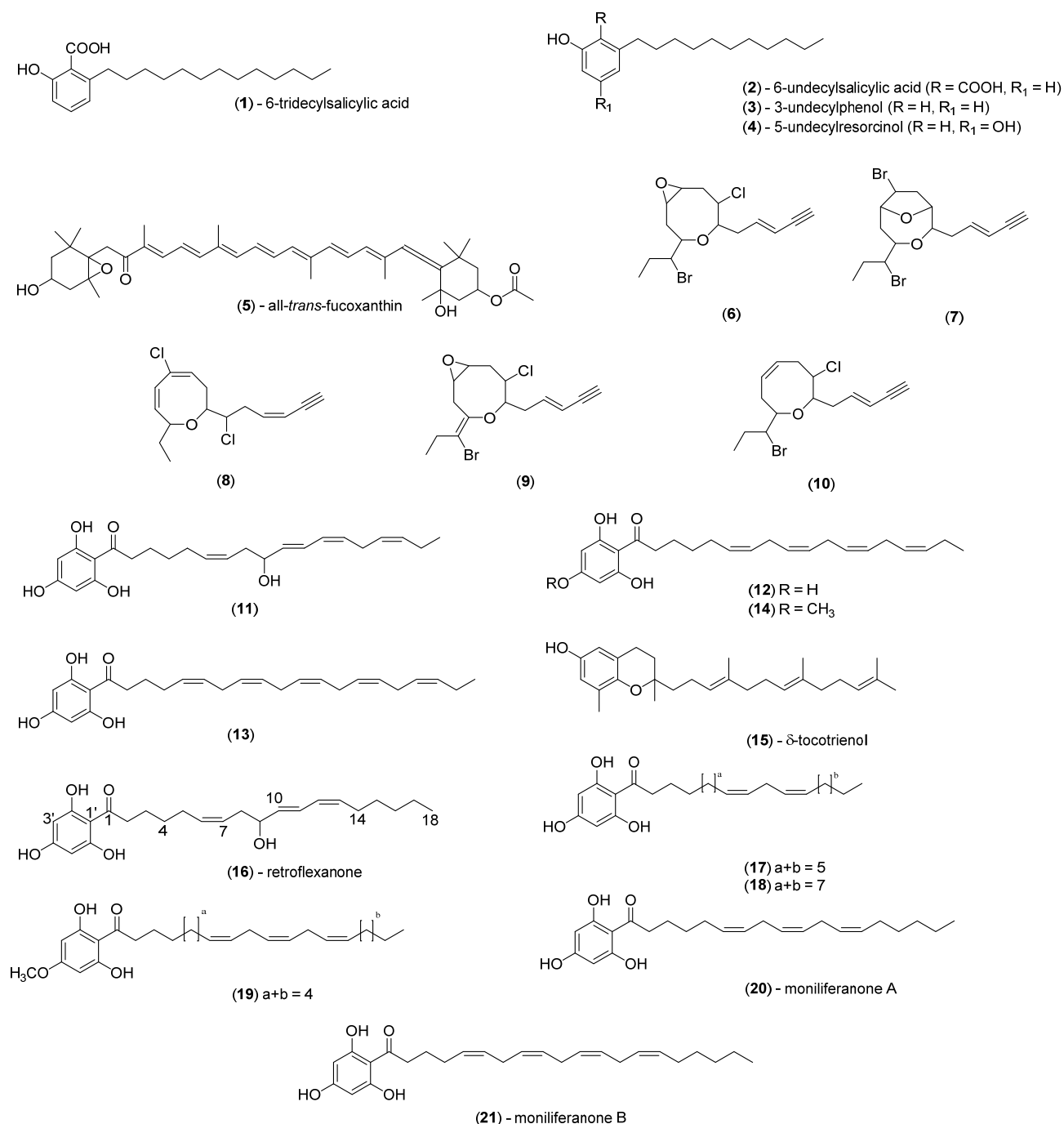


Figure 1. Compounds and range of structure classes as dereplicated by HPLC-NMR and HPLC-MS in conjunction with the MarinLit database.

2.2. Identification of Phenols, Phenolic Acids and Resorcinols

The specimen of *S. decipiens* was concluded to contain compounds 1–4, which represent three different structure classes (phenols, phenolic acids and resorcinols). While the phenols and phenolic acids displayed similar UV absorbances (300 nm), the resorcinol exhibited unique UV absorbances (276 and 281 nm). The compound eluting at $R_t = 3.55$ min was dereplicated from the MarinLit database using the molecular formula and UV absorbances as search parameters. This yielded four possible compounds, but analysis of the NMR data obtained from HPLC-NMR supported only one of these

structures. In this way, the compound eluting at $R_t = 3.55$ min could be identified as 6-tridecylsalicylic acid (**1**) which had been previously reported from the marine brown alga *Caulocystis cephalornithos* [20].

The remaining compounds eluting at $R_t = 2.29$, 2.44 and 7.87 min did not yield any matches in the MarinLit database when using various combinations of UV, mass and molecular formulae, and, when only UV data was searched this resulted in far too many possible structure classes. On the basis of the WET1D NMR spectra and UV profiles of the remaining three compounds ($R_t = 2.29$, 2.44 and 7.87 min) it could be concluded that they were closely related to 6-tridecylsalicylic acid (**1**). The marine brown alga *C. cephalornithos*, which is known to produce 6-tridecylsalicylic acid (**1**), also produces a variety of structurally related analogues [20,21]. Comparison of the data obtained from HPLC-NMR and HPLC-MS to the data for the compounds reported from *C. cephalornithos*, allowed for the compounds eluting at $R_t = 2.29$, 2.44 and 7.87 min to be identified as undecylsalicylic acid (**2**), 3-undecylphenol (**3**) and 5-undecylresorcinol (**4**) respectively. It is important to point out that these compounds do not appear separately in the MarinLit database and care must be taken in such dereplication exercises. This is the first study conducted on *S. decipiens* and compounds **1–4** have not been reported from the *Sargassum* genus. This highlights the importance of profiling different genera and species as a means of extending knowledge on marine biodiversity. The HPLC-NMR and HPLC-MS data of the compounds identified were consistent with the data reported previously [20–23].

2.3. Identification of Xanthophylls

The dichloromethane crude extracts of *S. vestitum* and *H. pseudospicata* were found to contain an abundance of xanthophylls. The main compound in the dichloromethane crude extract of each of these two algae (compound eluting at $R_t = 14.53$ min) was identified as all-*trans*-fucoxanthin (**5**), the main pigment found in marine brown algae. This pigment was identified using the MarinLit database by searching the molecular formula obtained by high resolution HPLC-MS, which yielded only one structure. The UV profile, WET1D, gCOSY and HSQCAD NMR spectra of **5** were found to be in agreement with the structure of all-*trans*-fucoxanthin [24,25] A ROESYAD NMR experiment conducted in stop-flow HPLC-NMR mode confirmed that the configuration for all of the double bonds was *trans* (Figure 2).

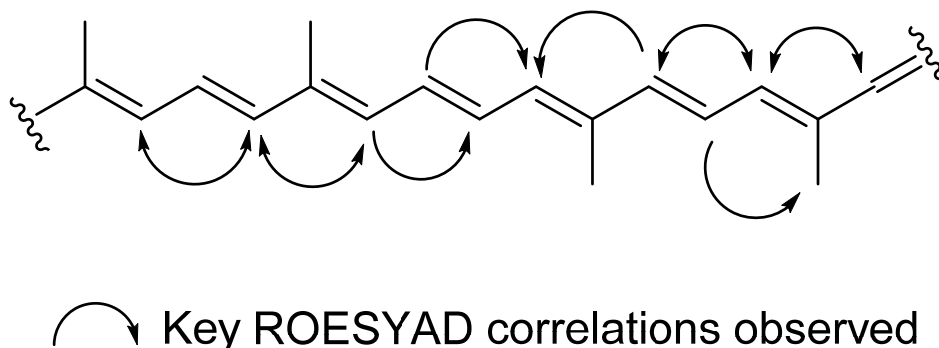


Figure 2. key ROESYAD correlations confirming the all *trans* configuration in all-*trans*-fucoxanthin (**5**).

A further two structurally related compounds eluting at $R_t = 26.71$ and 30.27 min were also detected in the dichloromethane crude extract of both *S. vestitum* and *H. pseudospicata*, but in much lower quantities. Identification was not possible due to the insufficient quantities present to obtain HPLC-NMR data, and due to the fact that the compounds did not ionize in either positive or negative ESI high resolution HPLC-MS. However, these compounds could be deduced to be two xanthophyll structural analogues based upon comparison of their UV profiles to all-*trans*-fucoxanthin (**5**) (Figure 3). This is the first report of all-*trans*-fucoxanthin (**5**) and other xanthophylls occurring in the *Halopteris* genus [8].

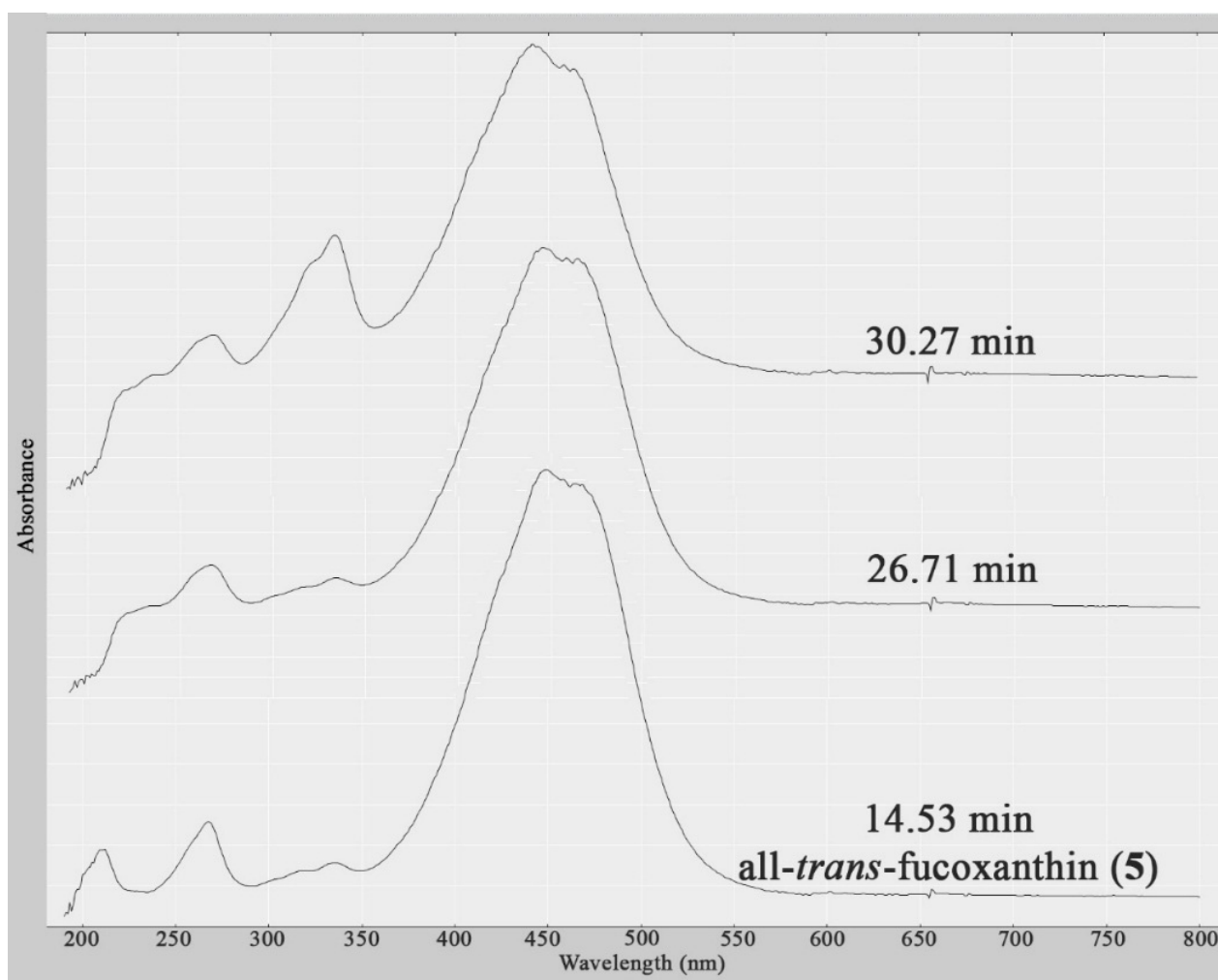


Figure 3. UV profiles (obtained from HPLC-NMR) of the three related xanthophylls present in the dichloromethane crude extracts of *H. pseudospicata* and *S. vestitum* showing their similarity.

2.4. Identification of Halogenated C_{15} Acetogenins

Profiling of a specimen of *Laurencia* sp. yielded three compounds (eluting at $R_t = 5.00$, 6.05 and 6.70 min), which displayed similar WET1D NMR spectra (Figure 4) confirming that they were structurally related. WET1D and gCOSY NMR data were obtained for the compounds eluting at $R_t = 5.00$ and 6.70 min, while WET1D, gCOSY, HSQCAD and gHMBCAD NMR data was obtained for the compound eluting at $R_t = 6.05$ min.

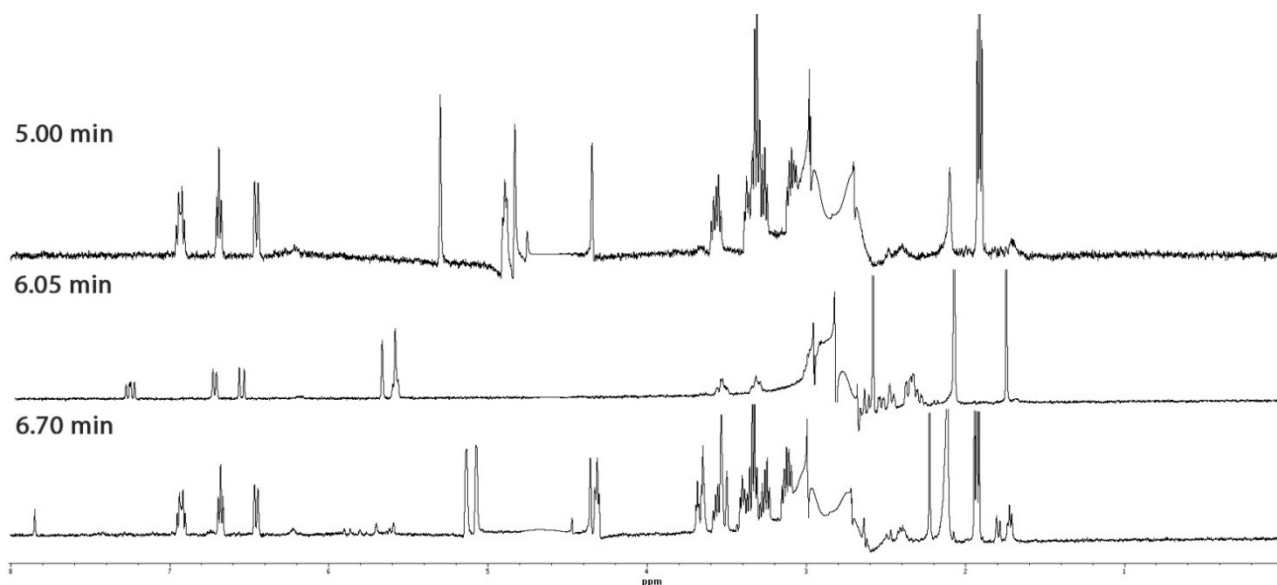


Figure 4. WET1D NMR spectra (75% CH₃CN/D₂O, 500 MHz) of compounds eluting at $R_t = 5.00$, 6.05 and 6.70 min from the dichloromethane crude extract of *Laurencia* sp.

Based upon the HPLC-NMR WET1D spectra (Figure 4), it was clear that the compounds eluting at $R_t = 5.00$ and 6.70 min were structural analogues, whereas the compound eluting at $R_t = 6.05$ min was a closely related structural derivative. A MarinLit search was conducted for the compound eluting at $R_t = 5.00$ min using the genus, UV and the presence of a single triplet methyl in the WET1D proton NMR spectrum obtained from stop-flow HPLC-NMR. This yielded nine possible structures including five polyhalogenated C₁₅ acetogenins (**6–10**) (Figure 1). The WET1D NMR data for the compound eluting at $R_t = 5.00$ min supported the presence of olefinic protons (δ 6.93, dt, $J = 7.5, 10.0$ Hz; 6.69, t, $J = 8.0$ Hz; 6.46, d, $J = 10.0$ Hz), and the presence of halogens was deduced based on the presence of several deshielded methines (δ 5.30, s; 4.90, m; 4.84, s; 4.76, s; 4.35, s). Unfortunately, due to suppression of the methine signals in the D₂O suppression region, it was not possible to confirm the total number of halogens present. Furthermore, the compound eluting at $R_t = 5.00$ min did not ionize in either positive or negative ESI high resolution HPLC-MS, making it impossible to determine a molecular formula. It could only be proposed that the compounds eluting at $R_t = 5.00$ min and $R_t = 6.70$ min are of the polyhalogenated C₁₅ acetogenin structure class, but the exact nature of the ring size could not be concluded.

The WET1D NMR spectrum for the compound eluting at $R_t = 6.05$ min showed slight differences suggesting it was a structural variant, further supported by the UV profile (220, 237 nm for the compounds eluting at $R_t = 5.00$ and 6.70 min), which also differed, and the absence of any absorbances in the UV profile suggested very little conjugation (220, 240 and 255 nm). Only partial HSQCAD and gHMBCAD NMR data could be obtained for this component and this hindered the ability to dereplicate the compound. Similar to the compounds eluting at $R_t = 5.00$ and 6.70 min, the compound eluting at $R_t = 6.05$ min did not ionize in either positive or negative ESI high resolution HPLC-MS. Various searches conducted of the MarinLit database using different combinations of data (taxonomy, UV and NMR) did not aid in dereplicating a general structure class, and so the compound eluting at $R_t = 6.05$ min

remains unidentified. Off-line isolation would be necessary to unequivocally deduce the structures of these three compounds.

2.5. Identification of Phloroglucinols and Tocotrienols

The dichloromethane crude extracts of *S. cf. fallax*, *C. subfarcinata* and *C. retroflexa* yielded a total of eleven phloroglucinols (**11–14**, **16–21**) and one tocotrienol (**15**). These two structure classes display similar UV absorbances, with the phloroglucinols typically displaying an absorbance at 285 nm and the tocotrienols at 300 nm, however, differences are observed in the WET1D NMR spectra. This represents the first instance of phloroglucinols and tocotrienols being reported from *C. retroflexa* and *S. cf. fallax*. The known phloroglucinols (**11–14**) and tocotrienol (**15**) were all dereplicated with use of the MarinLit database utilising the search parameters as indicated in Table 2, and by comparison of the NMR data obtained by HPLC-NMR. One of the phloroglucinols (compound eluting at $R_t = 23.16$ min) could not be identified due to insufficient quantities present to permit sufficient HPLC-NMR data acquisition and also due to there being no observed molecular ion in the high resolution HPLC-MS. However, based on the similarities of the UV absorbances and WET1D NMR data to **11**, it was concluded to represent a phloroglucinol containing an alcohol substituent in the terpene side chain. δ -tocotrienol (**15**) did not ionize in the high resolution HPLC-MS analysis, but a search of the MarinLit database together with consideration of the WET1D NMR data, resulted in δ -tocotrienol (**15**) being identified. The HPLC-NMR and HPLC-MS data of the known compounds was consistent with the data previously reported [26–29].

As well as compounds **11–15**, a series of new phloroglucinols were also determined. A MarinLit search conducted on these phloroglucinols using combinations of taxonomy, UV, molecular formulae and NMR data did not result in any confirmed structures, supporting the fact that these represented new phloroglucinols.

High resolution HPLC-MS yielded a molecular formula of $C_{24}H_{34}O_5$ for **16** (observed 401.2337 [M – H][–], calcd. for $C_{24}H_{33}O_5$, 401.2328) and stop-flow HPLC-NMR enabled for WET1D proton, gCOSY, HSQCAD and gHMBCAD NMR data to be obtained (Table 3). Three double bonds were concluded to be present based on the degrees of unsaturation and inspection of the WET1D NMR spectrum (δ_H 7.30, 1H; 6.80, 1H; 6.48, 1H; 6.32, 1H; 6.28, 1H; 6.23, 1H). A diagnostic methine at δ_H 4.96 was observed which suggested the presence of an alcohol substituent, together with a diagnostic methylene at δ_H 3.89, which is typical of the methylene group attached adjacent to the ketone functionality. The gCOSY and gHMBCAD NMR data was able to secure the spin system from this diagnostic methylene (δ_H 3.89, H-2) to the first olefinic proton (δ_H 6.32, H-6). Further interpretation of the gCOSY NMR data secured the spin system from H-6 (δ_H 6.32) to H-14 (δ_H 3.00). The proton at position H-14 lies on the edge of the suppression region of the acetonitrile signal, which prevented any gCOSY NMR correlations from the proton being observed. Fortunately, in the gHMBCAD NMR spectrum, key correlations were observed from this methylene which allowed for the carbon at position C-15 to be assigned (δ_C 29.9). The terminal methyl group (δ_H 1.72, H-18) displayed a key gHMBCAD NMR correlation to the carbon at position C-16 (δ_C 32.0), confirming its assignment. The protons at positions H-5, H-15 and H-16 could not be assigned as these signals resided in the acetonitrile suppression region. The configuration of the double bonds was established by consideration of the NMR coupling constants and on biosynthetic grounds. Compound **16** represents a structure analogue of the

known phloroglucinol **11**, which is known to have a 6Z configuration [28]. The co-occurrence of **11** and **16** led to the conclusion that their double bond configuration about position 6/7 would be the same when considering their biosynthesis. As such, the structure for **16** was proposed as 9-hydroxy-1-(2,4,6-trihydroxyphenyl)octadeca-6Z,10E,12Z-trien-1-one, attributed the trivial name retroflexanone (**16**). The configuration of the single stereogenic center at position C-9 remains undefined.

Table 3. NMR data (500 MHz, 75% CH₃CN/D₂O, suppression of HDO and CH₃CN at δ_{H} 4.64 and 2.82 ppm, respectively) for retroflexanone (**16**) obtained via stop-flow HPLC-NMR.

Retroflexanone (16)				
Position	δ_{H} (J in Hz)	δ_{C} ^a , Type	gCOSY	gHMBCAD
1		207.2, s		
2	3.89, t (7.0)	44.2, t	3	1, 3, 4
3	2.48, p (7.0)	25.1, t	2, 4	1, 2, 4, 5
4	2.23, m	29.9, t	3	2, 3, 5, 6
5	SS	27.8, t		
6	6.32, m	132.6, d	7	
7	6.23, m	126.2, d	6, 8	
8	3.12, m	35.8, t	7 ^w , 9	6, 7, 9
9	4.96, dt (6.5, 7.0)	72.6, d	8, 10	11
10	6.48, dd (7.0, 15.0)	136.6, d	9, 11	12
11	7.30, dd (15.0, 11.0)	126.4, d	10, 12	
12	6.80, t (11.0)	128.8, d	11, 13 ^w	
13	6.28, m	133.3, d	12, 14	
14	3.00, m ^b	ND		12, 13, 15
15	SS	29.9, t		
16	SS	32.0, t		
17	2.13, m	23.0, t	18	16
18	1.72, t (6.5)	14.3, q	17	16, 17
1'		105.2, s		
2'		165.0, s*		
3'	6.72, s	95.7, d		1', 2', 5'
4'		ND*		
5'	6.72, s	95.7, d		1', 3', 6'
6'		165.0, s*		
2'-OH	ND			
4'-OH	ND			
6'-OH	ND			

^a carbon assignments based on HSQCAD and gHMBCAD NMR experiments; ^b signal assigned based on correlations in gCoSY experiment; * signals for C-2' and C-6' are interchangeable with C4'; ^w indicates weak or long range correlation; SS Signal suppressed; ND Not Detected.

Based upon the molecular formula of the phloroglucinols eluting at $R_t = 13.65, 22.96$ and 33.40 min, the number of double bonds present in each compound could be concluded. Unfortunately, NMR and MS data alone is not sufficient to determine the placement of the double bond within the structures. This meant that only *tentative* structures could be proposed, which are represented as **17–19**, respectively. To

establish the position of the double bonds in the terpene side chain, off-line approaches such as chemical derivatization or degradation are required. The double bonds were assigned on the basis that olefinic protons that correspond to a *cis* geometry appear as a narrow multiplet in the proton NMR spectrum [28] which was also observed for the known compounds (**12–14**) during this study.

Phloroglucinols **20** and **21** (compounds eluting at $R_t = 20.15$ and 15.50 min) do not appear in the MarinLit database, however, a recent study conducted by the research group describes the first report of these phloroglucinols occurring in *C. monilifera* and *C. subfarcinata* [13].

2.6. Anti-Microbial Activity

The crude extracts of *S. cf. fallax*, *S. vestitum*, *C. subfarcinata*, *H. pseudospicata* and *C. retroflexa* were assessed for their anti-microbial activity against six bacteria and three fungi (Table 4). The crude extracts of the algae showed varying selectivity and activity across the micro-organisms tested, with *S. vestitum*, *C. subfarcinata* and *C. retroflexa* showing the most promising activity. The crude extracts of the two marine algae specimens containing the xanthophylls (*S. vestitum* and *H. pseudospicata*) displayed different biological activity suggesting that the active component(s) was unlikely to be the xanthophylls but other chemical component(s). However, all-*trans*-fucoxanthin (**5**) has been reported to display anti-inflammatory, anti-oxidant and anti-tumor activity [30–33]. The crude extracts of *S. cf. fallax*, *C. subfarcinata*, *C. retroflexa* all showed similar anti-microbial activities which can potentially be attributed to the presence of the phloroglucinols. Phloroglucinols have been demonstrated to possess various anti-microbial activities [34–36]. The crude extracts of *S. decipiens* and *Laurencia* sp. were not evaluated for their biological activity.

3. Experimental Section

3.1. Marine Alga Material

S. cf. fallax was collected at low tide on January 3, 2003 from St Paul's Beach, Sorrento, Port Phillip Bay, Victoria, Australia. *C. subfarcinata*, *S. vestitum* and *H. pseudospicata* were collected at low tide on January 22, 2006 from the Borough of Queenscliff (near Point Lonsdale), Port Phillip Bay, Victoria, Australia. *Laurencia* sp., *S. decipiens* and *C. retroflexa* were collected by SCUBA on 21 April 2010 from Governor Reef (near Indented Head), Port Phillip Bay, Victoria, Australia. The marine algae were identified by Dr. Gerald Kraft (The University of Melbourne) and voucher specimens (designated the code numbers 2003-06, 2006-11, 2006-12, 2006-13, 2010-04, 2010-08 and 2010-09, respectively) are deposited at the School of Applied Sciences (Discipline of Applied Chemistry), RMIT University, Melbourne, Australia.

3.2. Extraction

Each of the frozen marine algae were extracted with 3:1 methanol/dichloromethane (1 L). The crude extracts were then decanted and concentrated under reduced pressure and sequentially solvent partitioned (trituated) into dichloromethane and methanol soluble extracts, respectively.

Table 4. Anti-microbial activity of the crude extracts obtained from *S. cf. fallax*, *C. subfarcinata*, *C. retroflexa*, *S. vestitum* and *H. pseudospicata* showing zones of inhibition (mm).

Crude	Microorganism Concentration (mg/mL)	<i>E. coli</i>		<i>S. aureus</i>		<i>S. aureus</i>		<i>S. aureus</i>		<i>P. aeruginosa</i>		<i>S. pyogenes</i>		<i>B. subtilis</i>		<i>C. albicans</i>		<i>T. mentagrophytes</i>		<i>C. resinae</i>		
		ATCC	25922	ATCC	25923	ATCC	25923	MRSA	344/2-32	ATCC	27853	345/1	19659	ATCC 10231	or 14053*	ATCC 28185						
<i>S. vestitum</i> (3:1 MeOH/DCM)	50	ND ^a	ND ^a	NT ^b	NT ^b	NT ^b	NT ^b	3	NT ^b	ND ^a	3*	2	ND ^a	ND ^a								ND ^a
	50	ND ^a	ND ^a	NT ^b	NT ^b	NT ^b	NT ^b	ND ^a	NT ^b	ND ^a	ND ^a	ND ^a	ND ^a	ND ^a	ND ^a							ND ^a
<i>S. cf. fallax</i> (3:1 MeOH/DCM)	50	ND ^a	ND ^a	NT ^b	NT ^b	NT ^b	NT ^b	ND ^a	NT ^b	ND ^a	2	ND ^a	ND ^a	ND ^a	2	ND ^a	ND ^a	ND ^a				ND ^a
	50	ND ^a	ND ^a	NT ^b	NT ^b	NT ^b	NT ^b	1	NT ^b	ND ^a	3*	ND ^a	ND ^a	ND ^a	ND ^a	ND ^a	ND ^a	ND ^a				ND ^a
<i>C. retroflexa</i> (DCM)	50	ND ^a	ND ^a	2	4	3	6	5	ND ^a	NT ^b	ND ^a	NT ^b	NT ^b	NT ^b	NT ^b	NT ^b	NT ^b	NT ^b				NT ^b
	50	1	1	4	6	1	1	1	ND ^a	NT ^b	ND ^a	NT ^b	NT ^b	NT ^b	NT ^b	NT ^b	NT ^b	NT ^b				NT ^b

^a indicates no zone of inhibition detected; ^b indicates not tested; * indicates tested against ATCC 14053. Please note: *S. decipiens* and *Laurentia* sp. were not evaluated for biological activity.

3.3. Biological Evaluation

For details on the biological evaluation of the dichloromethane and methanol crude extracts of *C. retroflexa* please refer to [37]. The 3:1 MeOH/DCM crude extracts of *S. cf. fallax*, *C. subfarcinata*, *S. vestitum* and *H. pseudospicata* were assessed for anti-microbial activity at the University of Canterbury, Christchurch, New Zealand. A standardized inoculum was prepared by transferring a loop of bacterial/fungal cells, from a freshly grown stock slant culture, into a 10 mL vial of sterile water. This was vortexed and compared to a 5% BaCl₂ in water standard to standardize the cell density. This gave a cell density of 10⁸ colony-forming units per millilitre. Ten millilitres of the standardized inoculum was then added to 100 mL of Mueller Hinton or potato dextrose agar (at between 40 and 50 °C) and mixed by swirling, giving a final cell density of 10⁷ colony forming units per millilitre. Five millilitres of this was poured into sterile 85 mm petri dishes. The suspensions were allowed to cool and solidify on a level surface to give a “lawn” of bacteria/fungi over the dish. The crude extract was pipetted onto 6 millimeter diameter filter paper disks and the solvent evaporated. These disks were then placed onto the prepared seeded agar dishes (with appropriate solvent and positive controls) and incubated. Active anti-microbial samples displayed a zone of inhibition outside the disk, which was measured in mm as the radius of inhibition for each bacteria/fungi. The six organisms were *Escherichia coli* (ATCC 25922), *Bacillus subtilis* (ATCC 19659) and *Pseudomonas aeruginosa* (ATCC27853) for the bacteria and, *Candida albicans* (ATCC 14053), *Trichophyton mentagrophytes* (ATCC 28185) and *Cladosporium resinae* for the fungi.

3.4. Chemical Profiling

Chemical profiling was carried out on the dichloromethane soluble extracts of the marine algae employing HPLC-NMR and HPLC-MS methodologies. The dichloromethane extracts were dissolved in HPLC-NMR grade CH₃CN and filtered through a 0.45 PTFE membrane filter (Grace Davison Discovery Sciences, Columbia, MD, USA). *S. decipiens*: 109.1 mg dissolved in 1090 µL (5005 µg per HPLC-NMR injection); *C. retroflexa*: 185.6 mg dissolved in 2230 µL (4161 µg per HPLC-NMR injection); *S. cf. fallax*: 166.5 mg dissolved in 1665 µL (5000 µg per HPLC-NMR injection); *S. vestitum*: 342.8 mg dissolved in 3430 µL (4997 µg per HPLC-NMR injection); *H. pseudospicata*: 61.6 mg dissolved in 615 µL (5008 µg per HPLC-NMR injection); *Laurencia* sp.: 216.2 mg dissolved in 2160 µL (5005 µg per HPLC-NMR injection); *C. subfarcinata*: 741.9 mg dissolved in 7420 µL (4999 µg per HPLC-NMR injection).

3.5. HPLC-NMR & HPLC-MS Conditions

For details of the HPLC-NMR conditions please refer to [37]. For both on-flow and stop-flow HPLC-NMR modes, 50 µL injections of the dichloromethane extracts were injected onto an Agilent Eclipse Plus C₁₈ (150 × 4.6) 5 µ column using a solvent composition of 75% CH₃CN/D₂O at a flow rate of 1 mL/min. During HPLC-NMR analyses, the HDO and CH₃CN signals are suppressed at 4.64 and 2.82 ppm, respectively. In the stop-flow HPLC-NMR mode, WET1D, gCOSY, HSQCAD and gHMBCAD NMR experiments were acquired. HRESILCMS was carried out on an Agilent 6540 Series TOF system in either the positive or negative ionization mode (ESI operation conditions of 12 L/min

N2, 325 °C drying gas temperature, and 3500 V capillary voltage) equipped with an Agilent 1260 Infinity Binary Pump, Agilent 1290 Infinity Autosampler and Agilent 1260 DAD detector (Agilent, Santa Clara, CA, USA). The instrument was calibrated using the “Agilent Tuning Mix” with purine as the reference compound and the Hewlett-Packard standard HP0921. The separations were carried out using an Agilent Eclipse Plus C₁₈ (4.6 × 150) 5 μ column using a solvent composition of 75% CH₃CN/H₂O at a flow rate of 1 mL/min.

3.6. On-Line (HPLC-NMR & HPLC-MS) Partial Characterization of Compounds

1-(2,4,6-trihydroxyphenyl)-hexadecadien-1-one (unknown double bond positions) (**17**): HPLC-NMR WET1D NMR (500 MHz, 75% CH₃CN/D₂O, suppression of HDO and CH₃CN at t δ_H 4.64 and 2.82 ppm, respectively) obtained from stop-flow mode δ 6.71 (2H, s, H-3'/H-5'), 6.22 (4H, m, CHCH), 3.89 (2H, t, *J* = 8.0, H-2), 3.62 (2H, m, CHCH₂CH), 2.11 (m, CH₂)*, 1.77 (3H, t, *J* = 8.0 ; HRESILCMS; *m/z* 359.2226 (calcd for C₂₂H₃₁O₄, 359.2222).

1-(2,4,6-trihydroxyphenyl)-octadecadien-1-one (unknown double bond positions) (**18**): HPLC-NMR WET1D NMR (500 MHz, 75% CH₃CN/D₂O, suppression of HDO and CH₃CN at t δ_H 4.64 and 2.82 ppm, respectively) obtained from stop-flow mode δ 6.70 (2H, s, H-3'/H-5'), 6.20 (4H, m, CHCH), 3.87 (2H, t, *J* = 7.5, H-2), 3.61 (2H, dd, *J* = 6.0, 7 Hz, CHCH₂CH), 2.46 (2H, m, H-3), 2.11 (m, CH₂)*, 1.71 (3H, t, *J* = 7.0 ; HRESILCMS; *m/z* 387.2539 (calcd for C₂₄H₃₅O₄, 387.2535).

1-(2,6-dihydroxy-4-methoxyphenyl)-octadecatrien-1-one (unknown double bond positions) (**19**): HPLC-NMR WET1D NMR (500 MHz, 75% CH₃CN/D₂O, suppression of HDO and CH₃CN at t δ_H 4.64 and 2.82 ppm, respectively) obtained from stop-flow mode δ 6.82 (2H, s, H-3'/H-5'), 6.21 (6H, m, CHCH), 3.91 (2H, t, *J* = 7.0, H-2), 3.66 (4H, m, CHCH₂CH), 2.49 (2H, m, H-3), 2.25 (2H, m, H-4), 2.10 (m, CH₂)*, 1.70 (3H, t, *J* = 6.5 ; HRESILCMS; *m/z* 399.2539 (calcd for C₂₅H₃₅O₄, 399.2535).

Please refer to the supplementary information file containing UV profiles, HPLC-NMR data including tabulated NMR data and the high resolution HPLC-MS chromatograms for all remaining compounds (these are listed in order of retention time).

4. Conclusions

This study has demonstrated the importance and ability of HPLC-NMR in conjunction with high resolution HPLC-MS and databases such as MarinLit to rapidly dereplicate the identity of secondary metabolites from a range of marine algae. The chemical diversity between, and within, marine algae genera was highlighted (See Tables 1 and 2). The phloroglucinols (**11–14**, **16–21**) are an example of compounds that can be found occurring across different species of the same genus (*Cystophora*), while the xanthophylls (**15**) provide an example of compounds that can extend over different genera (*Halopteris* and *Sargassum*). The application of HPLC-NMR to investigate either genera or species of marine algae which were previously not studied (*S. decipiens*, *S. vestitum*, *S. cf. fallax*, and *H. pseudospicata*) and to rapidly identify structure classes present, without the need for traditional and lengthy isolation procedures is noteworthy. Finally, this study also highlights the advantage of using HPLC-NMR over HPLC-MS data for dereplication, especially when compounds do not easily ionize during HPLC-MS analyses. In such cases, crucial NMR data, which can be acquired via HPLC-NMR, provides important

structural features and connectivity, which can enable a compound to be dereplicated. Unlike HPLC-MS, HPLC-NMR also allows for the differentiation of structural isomers.

Acknowledgments

The Marine And Terrestrial Natural Product (MATNAP) research group would like to thank Roderick Watson (MAFRI), Rick Tinker, Daniel Dias and Priyanka Reddy for their assistance with the collection of the marine algae; Gerald Kraft (The University of Melbourne) for the taxonomic identification of the marine algae; Nerida Thurbon (School of Applied Sciences (Discipline of Biotechnology and Biological Sciences), Science Engineering and Health, RMIT University) for providing access to the micro-organisms to conduct the anti-microbial assays and for her invaluable technical support; Gill Ellis (University of Canterbury, Christchurch, New Zealand) for conducting some of the anti-microbial biological testing; Sally Duck (School of Chemistry, Faculty of Science, Monash University) for conducting the high resolution mass spectrometric analyses (HPLC-MS). Robert Brkljača would like to acknowledge his Australian Postgraduate Award (APA) scholarship that has supported his studies. Emrehan Göker was a recipient of the School of Applied Sciences Vacation scholarship that supported his BSc (AppSc) (honours) studies on *C. retroflexa*.

Author Contributions

Experimental work for *S. cf. fallax*, *C. subfarcinata*, *S. vestitum*, *H. pseudospicata*, *Laurencia* sp., and *S. decipiens* was conducted by R. Brkljača. Experimental work for *C. retroflexa* was conducted by E. S. Göker. Manuscript was prepared by R. Brkljača and S. Urban.

Supplementary Information

HPLC-NMR and HPLC-MS data and UV profiles for the crude extracts of the seven marine algae are included (these are listed in order of retention time). This material is available free of charge via MDPI Website.

Conflicts of Interest

The authors declare no conflict of interest.

References

1. Guiry, M.D.; Guiry, G.M. AlgaeBase. Available online: <http://www.algaebase.org> (accessed on 6 March 2015).
2. Blunt, J.W.; Copp, B.R.; Keyzers, R.A.; Munro, M.H.; Prinsep, M.R. Marine natural products. *Nat. Prod. Rep.* **2015**, *32*, 116–211.
3. Choi, H.; Pereira, A.R.; Gerwick, W.H. The Chemistry of Marine Algae and Cyanobacteria. In *Handbook of Marine Natural Products*; Fattorusso, E., Gerwick, W.H., Tagliatela-Scafati, O., Eds.; Springer: London, England, UK, 2012.
4. Sailler, B.; Glombitza, K.-W. Halogenated phlorethols and fucophlorethols from the brown alga *Cystophora retroflexa*. *Nat. Toxins* **1999**, *7*, 57–62.

5. Sailer, B.; Glombitza, K.-W. Phlorethols and fucophlorethols from the brown alga *Cystophora retroflexa*. *Phytochemistry* **1999**, *50*, 869–881.
6. Czczuga, B.; Taylor, F.J. Carotenoid content in some species of the brown and red algae from the coastal area of New Zealand. *Biochem. Syst. Ecol.* **1986**, *15*, 5–8.
7. Laird, D.W.; Bennett, S.; Bian, B.; Sauer, B.; Wright, K.; Hughes, V.; van Altena, I.A. Chemical investigation of seven Australasian *Cystophora* species: New chemistry and taxonomic insights. *Biochem. Syst. Ecol.* **2010**, *38*, 187–194.
8. MarinLit Database. Available online: <http://pubs.rsc.org/marinlit/> (accessed on 6 March 2015).
9. Kazlauskas, R.; Murphy, P.T.; Wells, R.J.; Daly, J.J.; Oberhansli, W.E. Heterocladol, a halogenated selinane sesquiterpene of biosynthetic significance from the red alga *Laurencia filiformis*: Its isolation, crystal structure and absolute configuration. *Aust. J. Chem.* **1977**, *30*, 2679–2687.
10. Capon, R.; Ghisalberti, E.L.; Jefferies, P.R.; Skelton, B.W.; White, A.H. Sesquiterpene metabolites from *Laurencia filiformis*. *Tetrahedron* **1981**, *37*, 1613–1621.
11. Capon, R.J.; Ghisalberti, E.L.; Mori, T.A.; Jefferies, P.R. Sesquiterpenes from *Laurencia* spp. *J. Nat. Prod.* **1988**, *51*, 1302–1304.
12. Dias, D.A.; White, J.M.; Urban, S. *Laurencia filiformis*: Phytochemical profiling by conventional and HPLC-NMR approaches. *Nat. Prod. Commun.* **2009**, *4*, 157–172.
13. Brkljača, R.; Urban, S. Dereplication (HPLC-NMR & HPLC-MS) and structural identification studies of marine brown algae of the genus *Cystophora*. *Phytochemistry* **2015**, submitted for publication.
14. Suzuki, M.; Takahashi, Y.; Matsuo, Y.; Guiry, M.D.; Masuda, M. Scanlonenyne, a novel halogenated C₁₅ acetogenin from the red alga *Laurencia obtusa* in Irish waters. *Tetrahedron* **1997**, *53*, 4271–4278.
15. San-Martin, A.; Darias, J.; Soto, H.; Contreras, C.; Herrera, J.S.; Roviroso, J. A new C₁₅ acetogenin from the marine alga *Laurencia claviformis*. *Nat. Prod. Lett.* **1997**, *10*, 303–311.
16. Suzuki, M.; Nakano, S.; Takahashi, Y.; Abe, T.; Masuda, M. Bisezakyne-A and -B, halogenated C₁₅ acetogenins from a Japanese *Laurencia* species. *Phytochemistry* **1999**, *51*, 657–662.
17. Aydogmus, Z.; Imre, S.; Ersoy, L.; Wray, V. Halogenated secondary metabolites from *Laurencia obtusa*. *Nat. Prod. Res.* **2004**, *18*, 43–49.
18. Takaichi, S. Carotenoids in Algae: Distributions, Biosyntheses and Functions. *Mar. Drugs* **2011**, *9*, 1101–1118.
19. Brkljača, R.; Urban, S. Limit of detection studies for application to natural product identification using high performance liquid chromatography coupled to nuclear magnetic resonance spectroscopy. *J. Chromatogr. A* **2015**, *1375*, 69–75.
20. Kazlauskas, R.; Mulder, J.; Murphy, P.T.; Wells, R.J. New metabolites from the brown alga *Caulocystis cephalornithos*. *Aust. J. Chem.* **1980**, *33*, 2097–2101.
21. Narkowicz, C.K.; Blackman, A.J. Further acetogenins from Tasmanian collections of *Caulocystis cephalornithos* demonstrating chemical variability. *Biochem. Syst. Ecol.* **2006**, *34*, 635–641.
22. Spencer, G.F.; Tjarks, L.W.; Kleiman, R. Alkyl and phenylalkyl anacardic acids from *Knema elegans* seed oil. *J. Nat. Prod.* **1980**, *43*, 724–730.
23. Asakawa, Y.; Masuya, T.; Tori, M.; Campbell, E.O. Long chain alkyl phenols from the liverwort *Schistochila appendiculata*. *Phytochemistry* **1987**, *26*, 735–738.

24. Englert, G.; Bjornland, T.; Liaaen-Jensen, S. 1D and 2D NMR studies of some allenic carotenoids of the fucoxanthin series. *Magn. Reson. Chem.* **1990**, *28*, 519–528.
25. Haugan, J.A.; Englert, G.; Glinz, E.; Liaaen-Jensen, S. Algal carotenoids. 48. Structural assignments of geometrical isomers of fucoxanthin. *Acta Chem. Scand.* **1992**, *46*, 389–395.
26. Ohnmacht, S.; West, R.; Simionescu, R.; Atkinson, J. Assignment of the ¹H and ¹³C NMR of tocotrienols. *Magn. Reson. Chem.* **2008**, *46*, 287–294.
27. Gregson, R.P.; Kazlauskas, R.; Murphy, P.T.; Wells, R.J. New metabolites from the brown alga *Cystophora torulosa*. *Aust. J. Chem.* **1977**, *30*, 2527–2532.
28. Kazlauskas, R.; King, L.; Murphy, P.T.; Warren, R.G.; Wells, R.J. New metabolites from the Brown Algal Genus *Cystophora*. *Aust. J. Chem.* **1981**, *34*, 439–447.
29. Amico, V.; Currenti, R.; Oriente, G.; Piatelli, M.; Tringali, C. A phloroglucinol derivative from the brown alga *Zonaria tournefortii*. *Phytochemistry* **1981**, *20*, 1451–1453.
30. Kim, S.-K.; Pangestuti, R. Biological activities and potential health benefits of fucoxanthin derived from marine brown algae. *Adv. Food Nutr. Res.* **2011**, *64*, 111–128.
31. Tan, C.-P.; Hou, Y.-H. First evidence for the anti-inflammatory activity of fucoxanthin in high-fat-diet-induced obesity in mice and the antioxidant functions in PC12 cells. *Inflammation* **2014**, *37*, 443–450.
32. Kim, K.-N.; Heo, S.-J.; Kang, S.-M.; Ahn, G.; Jeon, Y.-J. Fucoxanthin induces apoptosis in human leukemia HL-60 cells through a ROS-mediated Bel-xL pathway. *Toxicol. Vitro* **2010**, *24*, 1648–1654.
33. Xia, S.; Wang, K.; Wan, L.; Li, A.; Hu, Q.; Zhang, C. Production, characterization, and antioxidant activity of fucoxanthin from the marine diatom *Odontella aurita*. *Mar. Drugs* **2013**, *11*, 2667–2681.
34. Wisespongpan, P.; Kuniyoshi, M. Bioactive phloroglucinols from the brown alga *Zonaria diesingiana*. *J. Appl. Phycol.* **2003**, *15*, 225–228.
35. Gerwick, W.; Fenical, W. Phenolic lipids from the related marine algae of the order Dictyotales. *Phytochemistry* **1982**, *21*, 633–637.
36. Ravi, B.N.; Murphy, P.T.; Lidgard, R.O.; Warren, R.G.; Wells, R.J. C₁₈ terpenoid metabolites of the brown alga *Cystophora moniliformis*. *Aust. J. Chem.* **1982**, *35*, 171–182.
37. Brkljača, R.; Urban, S. Chemical profiling (HPLC-NMR & HPLC-MS), isolation, and identification of bioactive meroditerpenoids from the southern Australian marine brown alga *Sargassum paradoxum*. *Mar. Drugs* **2015**, *13*, 102–127.

© 2015 by the authors; licensee MDPI, Basel, Switzerland. This article is an open access article distributed under the terms and conditions of the Creative Commons Attribution license (<http://creativecommons.org/licenses/by/4.0/>).

CHAPTER 9

Chemical Profiling and Isolation Studies of the Marine Brown

Alga Sargassum paradoxum



Kingdom: Chromista

Phylum: Ochrophyta

Class: Phaeophyceae

Order: Fucales

Family: Sargassaceae

Genus: *Sargassum*

Species: *paradoxum*

Collected by SCUBA from Governor Reef, near indented Heads at a depth of 3 m from Port Phillip Bay, Victoria, Australia in April 2010.

Chapter 9 describes the chemical profiling and isolation methodologies adopted in the identification of the constituents present in the crude extract of the marine brown alga *Sargassum paradoxum*. The results of this study have been published as outlined below. Supplementary information relevant to the study is provided in Appendix E.

Journal publication resulting from this study:

Brkljača, Robert, & Urban, Sylvia. (2015). Chemical Profiling (HPLC-NMR & HPLC-MS), Isolation and Identification of Bioactive Meroditerpenoids from the Southern Australian Marine Brown Alga *Sargassum paradoxum*. *Marine Drugs*, 13(1), 102-127.

Article

Chemical Profiling (HPLC-NMR & HPLC-MS), Isolation, and Identification of Bioactive Meroditerpenoids from the Southern Australian Marine Brown Alga *Sargassum paradoxum*

Robert Brkljača and Sylvia Urban *

School of Applied Sciences (Discipline of Chemistry), Health Innovations Research Institute (HIRi)
RMIT University, GPO Box 2476V Melbourne, Victoria 3001, Australia;
E-Mail: robert.brkljaca@rmit.edu.au

* Author to whom correspondence should be addressed; E-Mail: sylvia.urban@rmit.edu.au;
Tel.: +61-3-9925-3376.

Academic Editor: Orazio Tagliatela-Scafati

Received: 7 November 2014 / Accepted: 15 December 2014 / Published: 29 December 2014

Abstract: A phytochemical investigation of a southern Australian marine brown alga, *Sargassum paradoxum*, resulted in the isolation and identification of four new (**5**, **9**, **10**, and **15**) and nine previously reported (**1**, **2**, **6–8**, and **11–14**) bioactive meroditerpenoids. HPLC-NMR and HPLC-MS were central to the identification of a new unstable compound, sargahydroquinal (**9**), and pivotal in the deconvolution of eight (**1**, **2**, **5–7**, and **10–12**) other meroditerpenoids. In particular, the complete characterization and identification of the two main constituents (**1** and **2**) in the crude dichloromethane extract was achieved using stop-flow HPLC-NMR and HPLC-MS. This study resulted in the first acquisition of gHMBCAD NMR spectra in the stop-flow HPLC-NMR mode for a system solely equipped with a 60 µL HPLC-NMR flow cell without the use of a cold probe, microcoil, or any pre-concentration.

Keywords: *Sargassum*; profiling; dereplication; HPLC-NMR; HPLC-MS; bioassay-guided; biological activity; meroditerpenoid

1. Introduction

Terpenoids and phenolic compounds represent the largest group of secondary metabolites reported from marine brown algae [1]. Marine brown algae belonging to the *Sargassum* genus (Sargassaceae, Fucales) number in excess of 300 species [2] located throughout most regions of the world [3,4], and are known to produce secondary metabolites such as meroterpenoids [1,5]. Meroditerpenoids are metabolites of mixed biogenesis containing terpenoid and non-terpenoid derived fragments. Meroditerpenoids derived from algae of the genus *Sargassum* are comprised of a polyprenyl chain attached to either a *p*-benzoquinone or hydroquinone moiety [6–8]. Variations of the meroditerpenoid structures occur mainly in the terpene side chain and include the addition of exocyclic double bonds, carboxylic acids, alcohols, or aldehyde functional groups [1,7,9]. Meroditerpenoids have been reported to display a range of biological activities including antibacterial, antioxidant, and antitumor activities [6,7,10–12].

We recently examined a specimen of the marine brown alga *Sargassum paradoxum* (R. Brown ex Turner) Hooker and Harvey, collected from Port Phillip Bay, Victoria, Australia. This alga was selected for chemical investigation on the basis of the crude extract antimicrobial activity and that no previous chemistry had been reported from this particular *Sargassum* species [1,13]. Previous studies conducted by our research group on another closely related *Sargassum* species (*S. fallax*) resulted in the isolation of three new meroditerpenoids [7]. This also provided the motivation for studying this *Sargassum* species in that a comparison of the two species could potentially allow for chemotaxonomic markers to be identified. Herein we report the chemical profiling study conducted using HPLC-NMR and HPLC-MS together with the bioassay-guided isolation and structure determination of one new meroditerpenoid with a hydroquinone moiety paradoxhydroquinone (**5**) and two new meroditerpenoids possessing a *p*-benzoquinone moiety, paradoxquinol (**10**) and paradoxquinone (**15**). A new unstable meroditerpenoid, sargahydroquinol (**9**), was identified on the basis of the HPLC-NMR and HPLC-MS studies conducted. Revisions in the proton and/or carbon NMR chemical shift assignments for three of the meroditerpenoids (**1**, **2**, and **13**) have also been documented. In all, 14 meroditerpenoids (Figure 1) were detected in the crude extract of *S. paradoxum* and, of these, 13 could be identified using a combination of on-line (HPLC-NMR and HPLC-MS) and off-line (conventional isolation and structure elucidation) methodologies.

2. Results and Discussion

The frozen marine alga was extracted with 3:1 methanol/dichloromethane, evaporated under reduced pressure, and sequentially solvent partitioned (trituated) into dichloromethane- and methanol-soluble fractions, respectively. While both the dichloromethane- and methanol-soluble fractions displayed some antimicrobial activity, the dichloromethane extract was slightly more selective in its activity (Section 2.3). ¹H NMR and analytical HPLC analyses indicated that the dichloromethane extract contained a series of structurally related compounds. On the basis of these observations, only the dichloromethane extract was further examined.

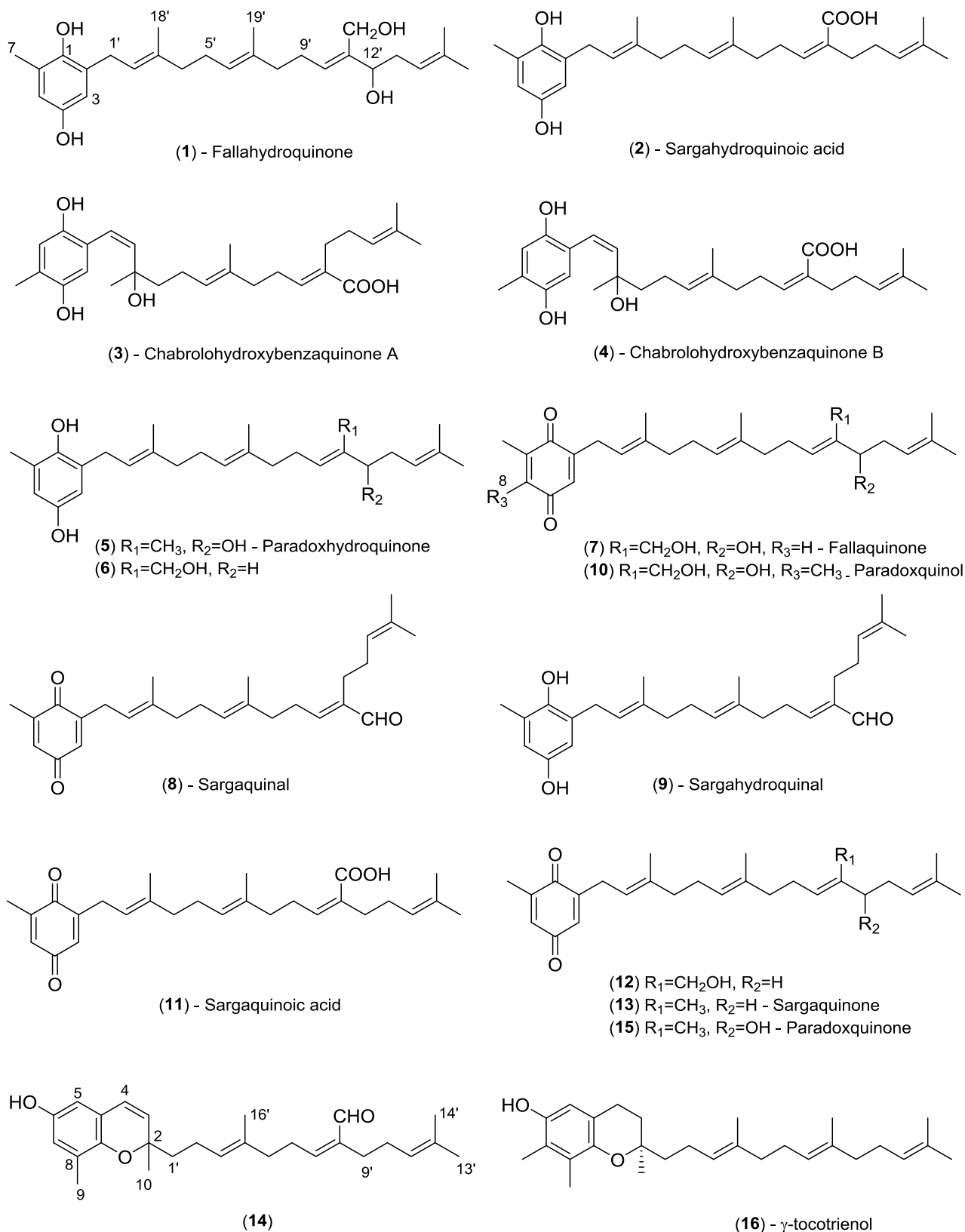


Figure 1. Structures of meroditerpenoids.

2.1. Chemical Profiling (HPLC-NMR & HPLC-MS)

The dichloromethane extract was subjected to both HPLC-NMR and HPLC-MS chemical profiling and a total of 10 peaks (A–J) were detected (Figure 2). Analysis of the stop-flow WET1D proton NMR spectra showed the presence of characteristic proton NMR signals in the aromatic and olefinic regions, together with various upfield proton NMR signals (Figure 2). Examination of the UV profile extracted for each of the peaks detected by PDA showed the presence of two distinct UV chromophores at λ_{max} 255 and 290 nm, typical of *p*-benzoquinones and hydroquinones that are known to occur in this genera of algae [1,13].

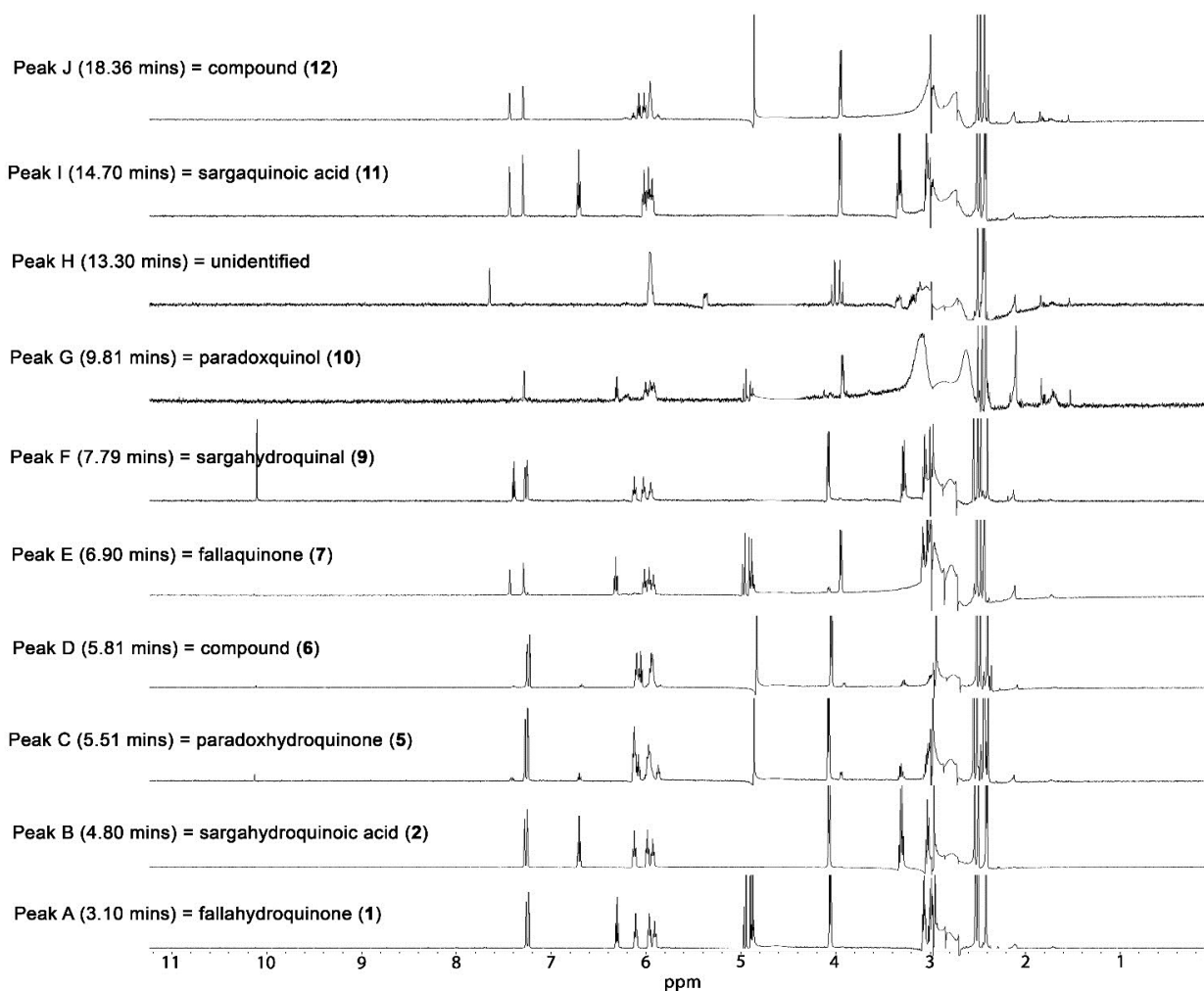


Figure 2. Stop-flow Wet1D proton NMR spectra (500 MHz, 75% CH₃CN/D₂O, suppression of HDO and CH₃CN at $t_{\delta\text{H}}$ 4.64 and 2.82 ppm, respectively) of peaks A–J resulting from analysis of the dichloromethane crude extract of *S. paradoxum*.

The two main peaks that were present in the dichloromethane crude extract of *S. paradoxum* (peaks A and B in Figure 2) were completely identified and characterized by HPLC-NMR and HPLC-MS. Both compounds displayed a UV maxima at 290 nm, supporting the presence of a hydroquinone moiety [14].

The HPLC-NMR stop-flow WET1D proton NMR spectrum of peak A (Figure 2) showed two *meta*-coupled protons at δ_{H} 7.22 and 7.25, indicating the presence of an aromatic moiety displaying an

AB splitting pattern as well as deshielded proton signals at δ_{H} 4.95, 4.88, and 4.87. Complete analysis of the 1D and 2D NMR data (Table 1) obtained via stop-flow HPLC-NMR, and the high resolution ESI MS obtained for this peak via HPLC-MS analysis (m/z 427.2846 $[\text{M} - \text{H}]^-$), allowed for the structure to be unequivocally elucidated as the previously described meroditerpenoid fallahydroquinone (**1**) [7].

The HPLC-NMR stop-flow WET1D proton NMR spectrum of peak B (Figure 2) supported the presence of a *meta*-coupled aromatic AB system (δ_{H} 7.23 and 7.26). Also present was a deshielded olefinic proton resonance (δ_{H} 6.69). The gHMBCAD NMR spectrum obtained in the stop-flow HPLC-NMR mode showed a signal at δ_{C} 170.9 ppm, confirming a carboxylic acid functional group (Table 1). Complete analysis of the 1D and 2D NMR data obtained via stop-flow HPLC-NMR and the high-resolution ESI MS obtained via HPLC-MS (m/z 425.2694 $[\text{M} - \text{H}]^-$) suggested the previously described meroditerpenoid sargahydroquinoic acid (**2**) [8]. While a direct comparison of the proton NMR chemical shifts obtained via stop-flow HPLC-NMR to the NMR data reported in the literature is impeded by the expected chemical shifts differences that occur for spectra acquired using off-line conventional deuterated NMR solvents compared to HPLC-NMR solvents, the majority of the proton NMR signals for this compound varied from the literature data by a consistent factor. However, the proton chemical shift for position H-10' (δ_{H} 6.69) differed to that reported for sargahydroquinoic acid (**2**) (δ_{H} 6.02) [8]. To confirm the 10'/11' double bond configuration, single irradiation nOe NMR experiments were carried out whilst in the stop-flow HPLC-NMR mode. The proton at δ_{H} 6.69 was irradiated and a key nOe enhancement observed to the methylene protons at δ_{H} 3.02 (H-12'). This provided confirmation that peak B (Figure 2) has a 10'*Z* double bond configuration, which corresponds to the structure assigned to sargahydroquinoic acid. Further confirmation of the 10'*Z* double bond configuration came from comparison to the meroditerpenoids chabrolohydroxybenzaquinone A (**3**) and C (**4**), which were isolated as co-occurring double bond isomers from the soft coral *Nephtea charoli* [15]. These compounds show that there is a characteristic difference in the carbon chemical shift of the C-12' methylene (δ_{C} 26.7 ppm and 34.5 ppm for the 10'*E* and 10'*Z* isomers, respectively) [15]. This γ effect is particularly valuable for distinguishing *E* and *Z* isomers of trisubstituted alkenes. Since the carbon for the C-12' methylene in (**2**) displayed a carbon chemical shift at δ_{C} 35.3, this provided further confirmation for the 10'*Z* configuration.

Table 1. NMR data (500 MHz, 75% CH₃CN/D₂O, suppression of HDO and CH₃CN at δ_H 4.64 and 2.82 ppm, respectively) for fallahydroquinone (1) and sargahydroquinone acid (2) obtained via stop-flow HPLC-NMR.

Position	Fallahydroquinone (1)				Sargahydroquinone Acid (2)				
	δ_C^a , Type	δ_H (J in Hz)	gCOSY	gHMBCAD	δ_C^a , Type	δ_H (J in Hz)	gCOSY	gHMBCAD	nOe
1	146.0, C				146.0, C				
2	ND ^b				130.4, C				
3	114.4, CH	7.22, d (3.0)			114.4, CH	7.23, d (3.0)	1'	1, 4, 5	
4	ND ^b				150.6, C				
5	115.6, CH	7.25, d (3.0)	7		115.6, CH	7.26, d (3.0)	7	1, 3	
6	126.9, C				126.9, C				
7	ND ^b	2.96, s	5	1, 5, 6	ND ^b	2.96, s		1, 5, 6	
1'	29.3, CH ₂	4.05, d (7.5)	2', 18'	1, 3, 2', 3'	29.3, CH ₂	4.06, d (7.0)	3, 2', 18'	1, 2, 3, 2', 3'	
2'	123.4, CH	6.10, t (7.5)	1', 18'		123.4, CH	6.10, t (7.0)	1', 18'	1', 4', 18'	
3'	137.0, C				137.1, C				
4'	40.2, CH ₂	SS ^c			40.2, CH ₂	2.91, m			
5'	ND ^b	2.94, m			ND ^b	2.94, m	6', 19'	3', 4', 6', 7'	
6'	125.4, CH	5.96, t (7.0)	5', 19'		125.6, CH	5.97, t (7.0)	5', 19'	8', 19'	
7'	135.6, C				135.4, C				
8'	40.1, CH ₂	SS ^c			39.6, CH ₂	2.91, m	9'		
9'	ND ^b	3.01, m	10'	10', 11'	28.4, CH ₂	3.30, dt (7.0, 7.5)	10'	7', 8', 10', 11'	
10'	130.7, CH	6.30, t (7.0)	9'		142.6, CH	6.69, t (7.5)	9'	8', 12', 20'	9', 12'
11'	140.3, C				132.5, C				
12'	75.7, CH	4.87, t (7.5)	13'	10', 11'	35.3, CH ₂	3.02, m		10', 11', 13', 14', 20'	
13'	35.4, CH ₂	3.06, dd (7.0, 7.5)	12', 14', 16', 17'	12', 14', 15'	28.3, CH ₂	2.91, m	17'		

Table 1. Cont.

14'	121.6, CH	5.90, dd (7.0)	13'	124.3, CH	5.91, t (7.0)	13', 16', 17'	16'
15'	134.1, C			133.1, C			
16'	18.0, CH ₃	2.41, s		17.7, CH ₃	2.39, s	14'	14', 15', 17'
17'	25.9, CH ₃	2.49, s	13'	25.7, CH ₃	2.49, s	14'	14', 15', 16'
18'	16.2, CH ₃	2.52, s	1'	16.2, CH ₃	2.53, s	1', 2'	1', 2', 3', 4'
19'	16.1, CH ₃	2.41, s		15.9, CH ₃	2.41, s	6'	6', 7', 8'
20a'		4.95, d (12.5)		170.9, C			
20b'	57.8, CH ₂	4.88, d (12.0)					
1-OH		ND ^b			ND ^b		
4-OH		ND ^b			ND ^b		
12'-OH		ND ^b			ND ^b		
20'-OH		ND ^b			ND ^b		

^a Carbon NMR assignments made on the basis of gHSQCAD and gHMBCAD NMR experiments; ^b Signal not detected due to signal suppression; ^c Signal suppressed.

The HPLC-NMR stop-flow WET1D proton NMR spectra of peaks C and D resembled that of peak A [fallahydroquinone (**1**)] (Figure 2), both of which eluted closely. Upon closer examination, it was evident that peak D was a meroditerpenoid that contained one alcohol functional group, due to the presence of a deshielded methylene proton at δ_{H} 4.84. Examination of the high resolution-ESI MS obtained via HPLC-MS for peaks C and D indicated that these were isobaric and that they both possessed a UV maxima at 290 nm, supportive of a hydroquinone moiety [14]. On the basis of the mass difference and the proton NMR differences it was proposed that peak D contained a terminal alcohol moiety but, unlike fallahydroquinone (**1**), did not contain a secondary alcohol functional group; this led to peak D being identified as the previously reported compound 2-[11-(hydroxymethyl)-3,7,15-trimethyl-2,6,10,14-hexadecatetraen-1-yl]-6-methyl-1,4-benzenediol (**6**) [16]. This represents the first report of **6** occurring as a natural product. Due to suppression of the HDO peak, no deshielded proton resonances could be observed for peak C; however, in consideration of the slight elution time difference, and the identical molecular masses, it was suspected that peak C contained an oxymethine group. While in stop-flow HPLC-NMR, the closely eluting compounds showed diffusion, and the oxymethine signal at δ_{H} 4.84 could clearly be distinguished via on-flow HPLC-NMR as being present in peak D and absent in peak C (see Supplementary Information file). The structure of peak C was proposed to be the new meroditerpenoid 2-[12-hydroxy-3,7,11,15-tetramethyl-2,6,10,14-hexadecatetraen-1-yl]-6-methyl-1,4-benzenediol, attributed the trivial name paradoxhydroquinone (**5**). Although subsequent off-line isolation of peaks C and D afforded an inseparable mixture, identification of these peaks was possible via the chemical profiling approach since individual WET1D proton and gCOSY NMR data could be obtained separately for each peak. This highlights an important feature of HPLC-NMR: typically co-eluting secondary metabolites that are difficult to obtain separately by conventional off-line isolation approaches can be obtained as separate entities via stop-flow HPLC-NMR.

Peak E was determined to be the previously described meroditerpenoid fallaquione (**7**) [7], based on the observed UV maxima, together with the stop-flow WET1D proton NMR spectrum and the high-resolution ESI MS obtained via HPLC-MS, which showed the presence of an ion at m/z 425.2694 $[M - H]^-$.

On the basis of the HPLC-NMR stop-flow WET1D proton NMR spectrum of peak F and the UV profile (λ_{max} 290 nm), this compound also possessed a hydroquinone moiety [14]. The high-resolution ESI MS ion m/z of 409.2745 $[M - H]^-$ obtained via HPLC-MS suggested a molecular formula of $\text{C}_{27}\text{H}_{38}\text{O}_3$. The stop-flow WET1D proton NMR spectrum showed a distinct proton signal at δ_{H} 10.07, s, confirming the presence of an aldehyde moiety. The MarinLit database indicated that sargaquinal (**8**), which possesses a *p*-benzoquinone moiety and an aldehyde functional group, had been previously reported from the *Sargassum* genus [17]. Peak F was proposed as being the new meroditerpenoid (possessing a hydroquinone moiety), attributed the name sargahydroquinal (**9**). During subsequent off-line bioassay-guided isolation, sargahydroquinal (**9**) oxidized into sargaquinal (**8**) before any off-line data could be obtained. Owing to the low abundance of sargahydroquinal (**9**) in the crude dichloromethane extract, only the stop-flow WET1D proton NMR and gCOSY data were obtained in the HPLC-NMR mode for sargahydroquinal (**9**) and are provided in Table 2. By comparison of the off-line data for sargaquinal (**8**) to peak F, the structure of sargahydroquinal (**9**) could be established. The configuration of the double bonds for sargaquinal (**8**) have been reported as 2'E, 6'E, and 10'E [17].

A bsNOESY NMR experiment carried out for sargaquinal (**8**) revealed nOe enhancements between the olefinic protons at positions H-2' and H-6' to the methylene protons at positions H-4' and H-8', along with the olefinic proton at position H-10' showing a nOe enhancement to the aldehyde proton at position H-20'. On biosynthetic grounds, the same configuration was attributed to the double bonds in sargahydroquinal (**9**).

Table 2. NMR data (500 MHz, 75% CH₃CN/D₂O, suppression of HDO and CH₃CN at δ_{H} 4.64 and 2.82 ppm, respectively) for sargahydroquinal (**9**) obtained via stop-flow HPLC-NMR.

Sargahydroquinal (9)		
Position	δ_{H} (<i>J</i> in Hz)	gCOSY
1		
2		
3	7.23, d (2.5)	
4		
5	7.25, d (2.5)	
6		
7	2.94, s	
1'	4.05, d (7.5)	2', 18'
2'	6.10, t (7.5)	1'
3'		
4'	2.70-3.00, m	
5'	2.96, m	6'
6'	6.00, t (7.0)	5'
7'		
8'	2.98, m	9'
9'	3.26, dt (7.0, 8.0)	8', 10'
10'	7.37, t (7.0)	9'
11'		
12'	2.70-3.00, m	
13'	2.70-3.00, m	
14'	5.92, t (7.0)	16'
15'		
16'	2.37, s	14'
17'	2.48, s	
18'	2.52, s	1', 2'
19'	2.35, s	
20'	10.07, s	
1-OH	ND ^a	
4-OH	ND ^a	

^a Signal not detected.

The UV profile (λ_{max} 255 nm) observed for peak G in the HPLC-NMR and HPLC-MS analyses confirmed a *p*-benzoquinone moiety [14]. The HPLC-NMR stop-flow WET1D proton NMR spectrum of peak G showed close resemblance to fallaquinone (**7**), except that an aromatic proton NMR resonance was absent. Comparison of the mass of peak G to fallaquinone (**7**), observed from ESI MS

obtained via HPLC-MS analysis, showed a difference of 14 mass units, indicating that one of the aromatic proton signals had been replaced by a methyl substituent. The structure of peak G was therefore proposed to be the new meroditerpenoid 5-[12*R*-hydroxy-11-(hydroxymethyl)-3,7,15-trimethyl-2,6,10,14-hexadecatetraen-1-yl]-2,3-dimethyl-1,4-benzoquinone, attributed the trivial name paradoxquinol (**10**).

Peak I showed close similarities to sargahydroquinic acid (**2**) and was identified as the previously reported sargahydroquinic acid (**11**) [7,17], the benzoquinone counter part of **2**.

Peak J possessed a *p*-benzoquinone moiety from the UV chromophore at 263 nm [14]. Analysis of the HPLC-NMR stop-flow WET1D NMR data showed close resemblance to **6**. On the basis of the molecular ion deduced from the high-resolution ESI MS (409.2742 [M – H][–]) obtained via HPLC-MS, in consultation with a SciFinder search, peak J was identified as previously described meroditerpenoid 2-[11-(hydroxymethyl)-3,7,15-trimethyl-2,6,10,14-hexadecatetraen-1-yl]-6-methyl-1,4-benzoquinone (**12**) [16,17]. Although subsequent off-line isolation afforded **12** and **15** as an inseparable mixture, identification of these compounds was possible via the chemical profiling approach since individual WET1D and gCOSY NMR data could be obtained separately for **12**, which could then be related back to the mixture.

2.2. Off-Line Bioassay-Guided Isolation

Following the chemical profiling (HPLC-NMR and HPLC-MS) conducted on the dichloromethane crude extract, a bioassay-guided isolation approach was undertaken to deduce the nature of the bioactive constituent(s) responsible for the crude extract bioactivity. The off-line isolation also allowed for any further identification and characterization of the meroditerpenoids concluded on the basis of the chemical profiling analysis as well as identifying any additional minor constituents not detected by HPLC-NMR.

A portion of the dichloromethane extract was fractionated by silica gel flash chromatography and selected fractions were evaluated for antimicrobial activity. Fractions for further purification were selected based on the observed antimicrobial activity, analysis of the ¹H NMR spectra, and the analytical HPLC chromatograms. Purification was conducted using reversed phase HPLC resulting in the isolation of 12 meroditerpenoids, eight (**1**, **2**, **5–7**, and **10–12**) of which were previously detected by HPLC-NMR and HPLC-MS analyses, and four of which were additional meroditerpenoids (**8** and **13–15**) that were not observed in the chemical profiling. Nine known meroditerpenoids (**1**, **2**, **6–8**, and **11–14**) were isolated and identified by direct comparison of their NMR spectroscopic and mass spectrometry data with that reported in the literature [7,8,16–19]. The off-line study also confirmed the structures of **1**, **2**, **5–7**, and **9–12** as deduced by HPLC-NMR and HPLC-MS.

Fallahydroquinone (**1**) was isolated as an unstable yellow oil. Analysis of the 2D NMR data showed that the carbon NMR chemical shifts for positions C-2 and C-6, reported as occurring at δ_c 125.4 and 127.8, respectively, should be reassigned to δ_c 127.8 (C-2) and δ_c 125.4 (C-6), respectively. In addition, the proton NMR signals for the position H-4' and H-8' protons reported at δ_H 2.01 and 2.08, respectively, should also be reversed. The specific rotations of the previously reported meroditerpenoids fallahydroquinone (**1**) and fallaquinone (**7**) were compared to literature values [7]. While the specific rotation for fallahydroquinone (**1**) was comparable in sign and magnitude, the

specific rotation of fallaquinone (**7**) differed to that reported. The purity of fallaquinone (**7**) in this study was higher than that obtained in the original isolation. It was concluded that the impurities present were sufficient to cause the specific rotation to vary in sign and magnitude. The accuracy of the specific rotations was considered given the low quantities isolated. The relevant compounds isolated in this study were of high purity, and did not display small specific rotations. That both the specific rotation of both fallahydroquinone (**1**) and fallaquinone (**7**) are of the same sign and magnitude is consistent with the fact that the former oxidizes to the latter with retention of configuration.

Sargahydroquinoic acid (**2**) was isolated as an unstable oil. Analysis of the 2D NMR data showed that the carbon NMR chemical shifts for positions C-9' and C-13', reported as occurring at δ_c 27.8 and 28.3, respectively, should be reassigned to δ_c 28.3 (C-9') and δ_c 27.8 (C-13'), respectively.

Comparison of the 2D NMR data of sargaquinone (**13**) with the literature data indicated discrepancies with some of the carbon NMR chemical shift assignments. The carbon NMR chemical shifts for positions C-3, C-5, C-3', and C-15' were either incorrectly assigned or not assigned. These carbon NMR chemical shifts have been unequivocally established as occurring at δ_c 132.3, 133.2, 140.0 and 131.3, respectively.

Sargahydroquinol (**9**) and one other unidentified peak (peak H) (Figure 2) degraded during the off-line isolation, which meant that it was not possible to conduct a complete 2D NMR or antimicrobial activity evaluation on these constituents.

Paradoxhydroquinone (**5**) was isolated off-line as an inseparable mixture with 2-[11-(hydroxymethyl)-3,7,15-trimethyl-2,6,10,14-hexadecatetraen-1-yl]-6-methyl-1,4-benzenediol (**6**) in a ratio of approximately 3:5. While complete 2D NMR characterization was conducted on the mixture, these components were obtained as separate entities via stop-flow HPLC-NMR. By analysis of the data obtained from both chemical profiling and off-line isolation, the compounds could be identified. In the first instance, the previously reported compound 2-[11-(hydroxymethyl)-3,7,15-trimethyl-2,6,10,14-hexadecatetraen-1-yl]-6-methyl-1,4-benzenediol (**6**) could be confirmed [16]. The comparison of the aromatic proton signals of **5** with those of the known meroditerpenoids isolated supported the presence of a hydroquinone moiety. The structure of **5** as proposed by chemical profiling was confirmed by analysis of the gHMBCAD NMR spectrum, which indicated that the proton signal at δ_H 3.97 (H-12') showed correlations with the carbons at δ_c 126.2 (C-10'), 120.2 (C-14'), and 11.7 (C-20') (Table 3). The oxymethine group was concluded to be located at position 12' on the basis of the HMBC NMR correlation observed from the singlet methyl group at position H-20' (δ_H 1.61, s) to the carbon at δ_c 77.3 (C-12'), which is directly coupled to the signal at δ_H 3.97. The compound was identified as the new meroditerpenoid 2-[12-hydroxy-3,7,11,15-tetramethyl-2,6,10,14-hexadecatetraen-1-yl]-6-methyl-1,4-benzenediol, and attributed the trivial name paradoxhydroquinone (**5**). Unfortunately, **5** and **6** oxidized to **15** and **12** before any NOESY NMR experiments could be carried out. Therefore a bsNOESY NMR experiment was carried out on **15** and **12**, respectively, and the results related back to **5** and **6**. On biosynthetic grounds, the configuration of the double bonds was therefore confirmed as 2'*E*, 6'*E*, and 10'*E* for **5**, and 2'*E*, 6'*E*, and 10'*Z* for **6**.

Table 3. ^1H and ^{13}C NMR data (500 MHz, CDCl_3) data for paradoxhydroquinone (**5**).

Paradoxhydroquinone (5)				
Position	δC^a , Type	δH (J in Hz)	gCOSY	gHMBCAD
1	146.4, C			
2	127.6, C			
3	114.0, CH	6.46, d (2.5)	5, 1'	1, 4, 5, 1'
4	149.0, C			
5	115.5, CH	6.50, d (2.5)	3, 7	1, 3, 4, 7
6	125.5, C			
7	16.0, CH_3	2.18, s	5	1, 5, 6
8				
1'	30.0, CH_2	3.28, d (7.0)	3, 2', 4' _w , 18' _w	1, 2, 3, 2', 3'
2'	122.0, CH	5.26, t (7.0)	1', 4', 18'	1', 4', 18'
3'	138.1, C			
4'	39.5, CH_2	2.08, m	1' _w	5', 18'
5'	26.1, CH_2	2.13, m		4', 7'
6'	124.4, CH	5.09, m		4', 5', 19'
7'	135.1, C			
8'	39.2, CH_2	2.01, m		6', 7', 9', 19'
9'	26.1, CH_2	2.10, m	8'	7', 10', 11'
10'	126.2, CH	5.37, t (6.5)	9', 20'	12', 20'
11'	136.6, C			
12'	77.3, CH	3.97, dd (6.0, 7.0)	13a', 13b'	10', 14', 20'
13a'	34.2, CH_2	2.20, m	12', 16', 17'	
13b'		2.28, ddd (7.0, 8.0, 14.0)	12', 16', 17'	12', 14', 15'
14'	120.2, CH	5.09, m	16', 17'	
15'	134.7, C			
16'	18.0, CH_3	1.63, s	14'	14', 15', 17'
17'	25.9, CH_3	1.72, s	13b', 14'	14', 15', 16'
18'	16.2, CH_3	1.75, s	1', 2'	2', 3', 4'
19'	16.1, CH_3	1.59, s	5', 6'	7', 8'
20'	11.7, CH_3	1.61, s	10'	10', 11', 12'
1-OH		ND ^b		
4-OH		ND ^b		
12'-OH		ND ^b		

^a Carbon NMR assignments made on the basis of gHSQCAD and gHMBCAD NMR experiments. ^b Signal not detected.

Paradoxquinol (**10**), unlike many of the previously isolated meroditerpenoids, which show the presence of an AB aromatic system, only displayed a single aromatic proton NMR signal at δ 6.46, s (H-3), suggesting further substitution of the *p*-benzoquinone ring. The gHMBCAD NMR spectrum confirmed the structure of **10** as proposed by chemical profiling. The two deshielded methyl groups [δ_{H} 2.03 (s, H-7) and 2.00 (s, H-8)] showed correlations to carbons at δ_{C} 140.6 (C-5), 141.5 (C-6), and 187.7 (C-1), and δ 140.6 (C-5), 141.5 (C-6), and 187.9 (C-4), respectively (Table 4). Further analysis of the HMBC NMR data confirmed the position of attachment for the terminal and the secondary alcohol moieties as positions 20' and 12', respectively, and confirmed **10** as the new meroditerpenoid 5-[12*R*-hydroxy-11-

(hydroxymethyl)-3,7,15-trimethyl-2,6,10,14-hexadecatetraen-1-yl]-2,3-dimethyl-1,4-benzoquinone, attributed the trivial name paradoxquinol (**10**). A single irradiation nOe NMR experiment confirmed the configuration of the double bond at position C-10' as 10'*E* (irradiation of H-10' showed a key enhancement to H-12'). Although this represents the first occurrence in a marine alga of a meroditerpenoid containing the position 8 methyl, this biosynthetic feature has been reported in terrestrial natural products [20,21]. It is suggested that the biosynthetic pathway of **10** is reminiscent to that of γ -tocotrienol (**16**).

Paradoxquinone (**15**) was isolated off-line as an inseparable mixture with 2-[11-(hydroxymethyl)-3,7,15-trimethyl-2,6,10,14-hexadecatetraen-1-yl]-6-methyl-1,4-benzoquinone (**12**) in a ratio of approximately 3:5. While complete NMR characterization was conducted on the mixture, the latter of these was identified as a separate entity via stop-flow HPLC-NMR. By analysis of the data obtained from both chemical profiling and off-line isolation, the latter of these compounds could be identified as the known meroditerpenoid 2-[11-(hydroxymethyl)-3,7,15-trimethyl-2,6,10,14-hexadecatetraen-1-yl]-6-methyl-1,4-benzoquinone (**12**). This compound had previously been reported as a derivative of a natural product; however, this represents the first report of its natural occurrence [17]. The ¹H NMR spectrum of paradoxquinone (**15**) was similar to that of paradoxhydroquinone (**5**). Minor differences were observed for the aromatic protons (6.46, bs and 6.54, bs) and the terminal methyl group at position H-7 (δ_{H} 2.05, s) (Table 4). Complete analysis of the 2D NMR spectra resulted in the compound being identified as the new meroditerpenoid 2-[12-hydroxy-3,7,11,15-tetramethyl-2,6,10,14-hexadecatetraen-1-yl]-6-methyl-1,4-benzoquinone, attributed the trivial name paradoxquinone (**15**). For compound **12**, nOe enhancements were observed from each of the olefinic protons at positions H-2', H-6', and H-10' to the methylene protons at H-4', H-8', and H-12'. For compound **15**, nOe enhancements were observed from the olefinic protons at positions H-2' and H-6' to the methylene protons at H-4' and H-8', together with an enhancement from the olefinic proton at H-10' to the oxymethine proton at H-12'. The configuration of the double bonds was therefore confirmed as 2'*E*, 6'*E*, and 10'*E* for **15**, and 2'*E*, 6'*E*, and 10'*Z* for **12**.

The chirality of secondary allylic alcohols can be elucidated via the exciton chirality method (usually by preparation of a benzoate derivative) or by NMR spectroscopy of the diastereoisomeric Mosher or modified Mosher esters [22–25]. In the former methodology, the absolute configuration of acyclic secondary alcohols have been assigned by interpretation of the Cotton effects observed at two wavelength regions (~220 and ~240–260 nm, respectively) [22,24].

The CD spectra of fallahydroquinone (**1**), fallaquinone (**7**), and paradoxquinol (**10**) were recorded and Cotton effects observed in the circular dichroism spectra noted. The CD spectra of fallahydroquinone (**1**), fallaquinone (**7**), and paradoxquinol (**10**) all showed the presence of positive Cotton effects at 260, 247, and 245 nm, respectively, of $\Delta\epsilon$ +2.0, +2.3, and +2.4 as well as at 224, 220, and 220 nm of $\Delta\epsilon$ +1.8, +1.0, and +6.4, respectively. On the basis of the similarities in the CD spectra, these compounds were concluded to have the same (undefined) absolute configuration. Subsequent to these analyses, fallahydroquinone (**1**), fallaquinone (**7**), and paradoxquinol (**10**) completely degraded, which precluded any further attempts to address the absolute configuration by conversion to the corresponding Mosher esters.

Table 4. ¹H and ¹³C NMR data (500 MHz, CDCl₃) data for paradoxinol (10) and paradoxquinone (15).

Position	Paradoxinol (10)				Paradoxquinone (15)			
	δC ^a , Type	δH (J in Hz)	gCOSY	gHMBCAD	δC ^a , type	δH (J in Hz)	gCOSY	gHMBCAD
1	187.7, C				188.0, C			
2	148.1, C				148.5, C			
3	132.1, CH	6.46, s	1'		132.3, CH	6.46, bs	5, 1'	1, 4, 5
4	187.9, C				188.0, C			
5	140.6, C*				133.2, CH	6.54, bs	3, 7	1, 3, 4
6	141.5, C*				145.9, C			
7	12.4, CH ₃	2.03, s		1, 5, 6	16.0, CH ₃	2.05, s	5	1, 5, 6
8	12.1, CH ₃	2.00, s		4, 5, 6			3, 2', 18'	1, 2, 3, 2', 3'
1'	27.4, CH ₂	3.12, d (7.0)	3, 2', 18'	1, 2, 3, 2', 3'	27.5, CH ₂	3.13, d (7.5)	1', 18	1', 4', 18'
2'	118.2, CH	5.15, t (7.0)	1', 18'	4'	118.1, CH	5.15, t (7.5)		
3'	139.5, C				139.8, C			2', 3', 5', 18'
4'	39.5, CH ₂	2.06, m		2', 5', 6', 18'	39.6, CH ₂	2.07, m	6', 18' ^w , 19' ^w	3', 4', 6', 7'
5'	26.3, CH ₂	2.12, m	6'	4', 6'	26.2, CH ₂	2.11, m	5'	4', 5', 19'
6'	124.4, CH	5.11, m	5', 19'	4', 8'	124.2, CH	5.10, m		
7'	134.7, C				135.1, C			6', 7', 10'
8'	39.5, CH ₂	2.06, m		19'	39.3, CH ₂	2.02, m	10', 20' ^w	7', 10', 11'
9'	26.0, CH ₂	2.21, m	10'		26.2, CH ₂	2.11, m	9', 20'	9', 12', 20'
10'	130.5, CH	5.53, t (7.0)	9'	12', 20'	126.1, CH	5.38, t (7.0)		
11'	138.9, C				136.7, C		13a'	10', 11', 13', 14', 20'
12'	76.9, CH	4.16, dd (5.5, 7.5)	13a', 13b'	10'	77.2, CH	3.97, dd (5.5, 7.5)	12', 17'	
13a'	35.1, CH ₂	2.26, m	12', 14'		34.2, CH ₂	2.20, m	12', 17'	11', 12', 14', 15'
13b'	119.9, CH	2.43, ddd (7.5, 8.5, 14.5)	12', 13a', 14'	12', 14'	120.3, CH	2.27, m	17'	
14'	135.4, C	5.11, m	16', 17'		134.6, C	5.09, m		
15'	18.1, CH ₃	1.65, s	13a', 13b'	14', 15', 17'	18.0, CH ₃	1.63, s		14', 15'
17'	25.9, CH ₃	1.73, s	13a', 13b', 14'	14', 15', 16'	25.9, CH ₃	1.72, s		14', 15', 16'
18'	16.1, CH ₃	1.62, s	1', 2'	2', 3', 4'	16.1, CH ₃	1.61, s		2', 3'
19'	16.1, CH ₃	1.60, s	5', 6'	6', 7', 8'	16.1, CH ₃	1.61, s		7'
20'	58.5, CH ₂	4.26, d (3.5)		10', 11', 12'	11.7, CH ₃	1.61, s		10', 11'
12'-OH		ND ^b				ND ^b		
20'-OH		ND ^b				ND ^b		

^a Carbon NMR assignments made on the basis of gHSQCAD and gHMBCAD NMR experiments. ^b Signal not detected. * Indicates signals interchangeable

The compounds isolated from *S. paradoxum* in this study also occur in many other *Sargassum* species. However, two of the compounds—fallahydroquinone (**1**) and fallaquinone (**7**)—have only been reported from one other *Sargassum* species (*S. fallax*) [7]. On this basis, it is proposed that the presence of these two compounds could potentially be used as chemotaxonomic biomarkers for *S. paradoxum* and *S. fallax*.

2.3. Antimicrobial Studies

Fallahydroquinone (**1**) and fallaquinone (**7**) have been previously reported to display slight antitumor activity [7]. Sargahydroquinoic acid (**2**) and sargaquinoic acid (**11**) display similar antitumor [7,26] and peroxy-nitrite-scavenging activity [27], as well as antiplasmodial activity against malaria parasites [28]. Sargahydroquinoic acid (**2**) also shows insecticidal activity [29], selective vasodilatation effects [30], the ability to stimulate adipocyte differentiation [31], and radical scavenging activity [6]. Sargaquinoic acid (**11**) shows weak antimicrobial activity [7], the ability to promote neurite outgrowth [32], the ability to induce cell apoptosis [33], antioxidant activity [34], and cholinesterase inhibition activity [35]. Sargaquinal (**8**) displays antiplasmodial activity against malaria parasites [28]. A range of activities have been reported for sargaquinone (**13**) including radical scavenging [36], anti-inflammatory activity [37], activity against P-388 cells [7,38], and ichthyotoxicity to certain species of fish [39]. Antileishmanial activity has been reported for 9-(6-hydroxy-2,8-dimethyl-2*H*-1-benzopyran-2-yl)-6-methyl-2-(4-methyl-3-penten-1-yl)-2,6-nonadienal (**14**) [19].

Antimicrobial evaluation of the crude extracts, selected silica column fractions, and the isolated meroditerpenoids was carried out against five bacteria and one fungus. Eleven of the isolated meroditerpenoids (**1–2**, **5–7**, **9–13**, and **15**), together with a commercially available antibiotic and antifungal agent, were tested at 1 mg/mL, with all displaying varying degrees of zones of inhibition in the antimicrobial assays (Table 5). Compared to the antibiotic ampicillin, the isolated compounds were far less potent against *S. aureus* and *S. pyogenes*. However, compounds **2**, **7**, **8**, and **13** were more potent against *P. aeruginosa* than ampicillin. In recent years, concern has grown around *P. aeruginosa* with regards to its prevalence and multidrug resistance [40]; therefore, the importance of identifying possible drug leads against these bacteria remains highly relevant. There was no difference in activity between compounds with the hydroquinone or the *p*-benzoquinone moieties. The activity observed for sargaquinone (**13**), the simplest of the meroditerpenoids isolated, suggests that the unsubstituted meroditerpenoid skeleton is responsible for the activity against *P. aeruginosa*. The addition of an alcohol group at position 12' or 20' (**1**, **5**, **6**, **12**, and **15**) appears to reduce the activity against *P. aeruginosa*, but increases the activity against *S. pyogenes*. Finally, incorporation of a carboxylic acid at position C-20' (**2** and **11**) gives rise to activity against *S. aureus* and *S. aureus* MRSA.

3. Experimental Section

3.1. General Experimental Procedures

All organic solvents used were analytical reagent (AR or GR), UV spectroscopic, or HPLC grades with milli-Q water also being used. Optical rotations were carried out using a 1.5-mL cell on a Rudolph Research Analytical Autopol IV automatic polarimeter, set to the Na 589 nm wavelength.

UV/VIS spectra were recorded on an Agilent CARY 60 spectrophotometer, using ethanol. CD spectra were obtained on a Jasco 815 Circular Dichroism spectrometer in ethanol. FTIR spectra were recorded as a film using a NaCl disk on a Perkin-Elmer Spectrum One FTIR spectrometer. ^1H (500 MHz), ^{13}C (125 MHz), and 1D nOe spectra were acquired in CDCl_3 on a 500 MHz Agilent DD2 NMR spectrometer with referencing to solvent signals (δ 7.26 and 77.0 ppm). Two-dimensional NMR experiments recorded included gradient correlation spectroscopy (gCOSY), heteronuclear single-quantum correlation spectroscopy with adiabatic pulses (HSQCAD), gradient heteronuclear multiple-bond spectroscopy with adiabatic pulses (gHMBCAD), and band selective 2D nuclear overhauser enhancement spectroscopy (bsNOESY) experiments. ESI mass spectra were obtained on a Micromass Platform II mass spectrometer equipped with a LC-10AD Shimadzu solvent delivery module (50% $\text{CH}_3\text{CN}/\text{H}_2\text{O}$ at a flow rate of 0.2 mL/min) in both the positive and negative ionization modes using cone voltages between 20 and 30 V. Silica gel flash chromatography was carried out using Davisil LC35Å silica gel (40–60 mesh) with a 20% stepwise solvent elution from 100% petroleum spirits (60–80 °C) to 100% dichloromethane to 100% ethyl acetate and finally to 100% methanol. HPLC-NMR was carried out on a 500 MHz Agilent DD2 NMR spectrometer equipped with a Varian $^1\text{H}[^{13}\text{C}]$ pulsed field gradient flow probe with a 60- μL active volume flow cell coupled to a Varian Prostar 210 solvent delivery system, a Prostar 430 Autosampler, and a Prostar 335 PDA detector. The HPLC-NMR analyses were carried out using CORBA communication and operated with VnmrJ software. The 2H resonance observed from the D_2O was used to obtain a field-frequency lock. The resonances from the HOD and the methyl of the acetonitrile were suppressed using the water enhanced through transverse gradients (WET) solvent suppression experiment [41]. The residual HOD resonance of D_2O was referenced to 4.64 ppm. For both on-flow and stop-flow HPLC-NMR modes, 50- μL injections (4995 μg) of the dichloromethane extract were injected onto an Agilent Eclipse Plus C_{18} (150 \times 4.6) 5- μ column using a solvent composition of 75% $\text{CH}_3\text{CN}/\text{D}_2\text{O}$ at a flow rate of 1 mL/min. In the stop-flow HPLC-NMR mode WET1D, gCOSY, HSQCAD, gHMBCAD, and 1D nOe NMR experiments were acquired. HRESIMS was carried out on an Agilent 6200 Series TOF system (ESI operation conditions of 8 L/min N_2 , 325 °C drying gas temperature, and 3500 V capillary voltage) equipped with an Agilent 1200 Series LC solvent delivery module (100% CH_3OH at a flow rate of 0.3 mL/min) in either the positive or negative ionization modes. The instrument was calibrated using the “Agilent Tuning Mix” with purine as the reference compound and the Hewlett–Packard standard HP0921. HRESILCMS was carried out on the same system and conditions using an Agilent Eclipse Plus C_{18} (4.6 \times 150) 5- μ column using a solvent composition of 75% $\text{CH}_3\text{CN}/\text{H}_2\text{O}$ at a flow rate of 1 mL/min. All analytical HPLC analyses and method development were performed on a Dionex P680 solvent delivery system equipped with a PDA100 UV detector (operated using “Chromeleon” software). Analytical HPLC analyses were carried out using either a gradient method 0–2 min 10% $\text{CH}_3\text{CN}/\text{H}_2\text{O}$; 14–24 min 75% $\text{CH}_3\text{CN}/\text{H}_2\text{O}$; 26–30 min 100% CH_3CN ; and 32–40 min 10% $\text{CH}_3\text{CN}/\text{H}_2\text{O}$ or an isocratic method (either 100%, 95%, 90%, or 85% $\text{CH}_3\text{CN}/\text{H}_2\text{O}$) on an Alltech Alltima HP C_{18} (250 \times 4.6) 5- μ column at a flow rate of 1.0 mL/min. Semi-preparative HPLC was carried out on a Varian Prostar 210 solvent delivery system equipped with a Prostar 335 PDA detector (operated using “Star Workstation” software) using an isocratic method (either 100%, 95%, 90%, or 85% $\text{CH}_3\text{CN}/\text{H}_2\text{O}$) and an Alltech Alltima C_{18} (250 \times 10) 5- μ column at a flow rate of 3.5 mL/min.

3.2. Biological Evaluation

Crude extracts, enriched fractions, and compounds isolated from the marine alga, together with the standard antibiotic (ampicillin, Sigma-Aldrich, Castle Hill, Australia) and antifungal (carbendazim, Sigma-Aldrich, Castle Hill, Australia) compounds, were evaluated against six microorganisms (five bacteria and one fungus) at concentrations of 50, 25, or 1 mg/mL (see Table 5). Each microorganism was prepared by creating a 0.5 McFarlane solution suspension. Lawn cultures were prepared on either Mueller–Hinton or Brain Heart Infusion Agar (BHIA) (used for *S. pyogenes*). Then 20 µL of the crude extracts, enriched fractions, pure compounds or the standard compounds (ampicillin and carbendazim) were pipetted onto 6 mm diameter filter paper disks and their solvents evaporated. These disks were then placed onto the prepared lawn cultures and incubated at 37 °C overnight. Active antimicrobial samples displayed a zone of inhibition outside the disk, which was measured in mm as the radius of inhibition for each bacteria/fungi. The five test bacteria were *Escherichia coli* (ATCC 25922), *Staphylococcus aureus* (ATCC 25923), *Staphylococcus aureus* MRSA (344/2-32), *Pseudomonas aeruginosa* (ATCC 27853), and *Streptococcus pyogenes* (345/1). The test fungus was *Candida albicans* (ATCC 10231).

3.3. Marine Alga Material

The marine brown alga was collected by SCUBA at a depth of 3 m on 21 April 2010 from Governor Reef near Indented Head, Port Phillip Bay, Victoria, Australia and then stored at –80 °C. The alga was identified as *Sargassum paradoxum* (R. Brown ex Turner) Hooker and Harvey by Dr. Gerald Kraft (Honorary Principal Fellow), Faculty of Science, School of Botany, The University of Melbourne, Australia. A voucher specimen (designated the code number 2010–12) is deposited at the School of Applied Sciences (Discipline of Applied Chemistry), RMIT University.

3.4. Chemical Profiling

Chemical profiling was carried out on the dichloromethane soluble extract of the alga employing HPLC-NMR and HPLC-MS methodologies. Details of these analyses are provided in Section 3.1. The dichloromethane extract (77 mg) was dissolved in HPLC-NMR grade CH₃CN (771 µL) and filtered through a 0.45 PTFE membrane filter (Grace Davison Discovery Sciences).

Table 5. Antimicrobial activity of the crude extract, selected silica column fractions, and pure compounds obtained from *S. paradoxum*, together with commercial standard antibiotic and antifungal compounds, showing zones of inhibition (mm).

	Microorganism					
	<i>E. coli</i>	<i>S. aureus</i>	<i>S. aureus MRSA</i>	<i>P. aeruginosa</i>	<i>S. pyogenes</i>	<i>C. albicans</i>
Concentration (mg/mL)	ATCC 25922	ATCC 25923	344/2-32	ATCC 27853	345/1	ATCC 10231
Dichloromethane extract	ND ^g	2	1	ND ^g	5	ND ^g
Methanol extract	ND ^g	1	1	10	3	4
Silica fraction 1 ^a	ND ^g	ND ^g	ND ^g	ND ^g	ND ^g	ND ^g
Silica fraction 4 ^b	ND ^g	ND ^g	ND ^g	ND ^g	1	ND ^g
Silica fraction 6 ^c	ND ^g	ND ^g	1	ND ^g	1	ND ^g
Silica fraction 10 ^d	ND ^g	ND ^g	1	4	3	ND ^g
Silica fraction 13 ^e	ND ^g	ND ^g	1	ND ^g	3	ND ^g
Silica fraction 17 ^f	ND ^g	ND ^g	ND ^g	ND ^g	ND ^g	ND ^g
Fallahydroquinone (1)	ND ^g	ND ^g	ND ^g	ND ^g	1	ND ^g
Sargahydroquinone acid (2)	ND ^g	1	1	2	3	ND ^g
Paradoxhydroquinone (5) & compound (6)	ND ^g	ND ^g	ND ^g	ND ^g	3	ND ^g
Fallaquinone (7)	ND ^g	ND ^g	ND ^g	4	ND ^g	ND ^g
Sargaquinol (8)	ND ^g	ND ^g	ND ^g	3	1	ND ^g
Paradoxquinol (10)	ND ^g	ND ^g	ND ^g	ND ^g	1	ND ^g
Sargaquinone acid (11)	ND ^g	1	1	1	3	ND ^g
Paradoxquinone (15) & compound (12)	ND ^g	ND ^g	ND ^g	ND ^g	2	ND ^g
Sargaquinone (13)	ND ^g	ND ^g	ND ^g	5	ND ^g	ND ^g
Ampicillin (antibiotic)	ND ^g	15	3	2	20	NT ^h
Carbendazim (antifungal)	NT ^h	NT ^h	NT ^h	NT ^h	NT ^h	ND ^g

^a 100% to 80% petroleum spirits (60–80 °C)/dichloromethane; ^b 20% petroleum spirits (60–80 °C)/dichloromethane; ^c 80% dichloromethane/ethyl acetate; ^d 20% dichloromethane/ethyl acetate; ^e 80% ethyl acetate/methanol; ^f 100% methanol; ^g Indicates no zone of inhibition detected; ^h Indicates not tested.

3.5. Extraction and Isolation

The frozen marine alga (88 g, wet weight) was extracted with 3:1 methanol/dichloromethane (2 L). The crude extract was then decanted and concentrated under reduced pressure and sequentially solvent partitioned (trituated) into dichloromethane- and methanol-soluble extracts, respectively. Approximately 450 mg of the dichloromethane extract was subjected to flash silica gel column chromatography (20% stepwise elution from petroleum spirits (60–80 °C) to dichloromethane to ethyl acetate and finally to methanol). The 40% petroleum spirits/dichloromethane silica gel column fraction was subjected to reversed phase HPLC (100% CH₃CN) to yield sargaquinone (**13**) (2.5 mg, 0.02%). The 80% dichloromethane/ethyl acetate silica gel fraction was subjected to reversed-phase HPLC (95% CH₃CN/H₂O) to yield paradoxquinone (**15**) and 2-[11-(hydroxymethyl)-3,7,15-trimethyl-2,6,10,14-hexadecatetraen-1-yl]-6-methyl-1,4-benzoquinone (**12**) as an inseparable mixture (6.0 mg, 0.04%), and sargaquinal (**8**) (3.0 mg, 0.02%). The 40% dichloromethane/ethyl acetate to 60% dichloromethane/ethyl acetate silica gel column fractions were combined and subjected to Sephadex LH-20 size exclusion column chromatography using 100% methanol. The third fraction resulting from this analysis was subjected to reversed phase HPLC (85% CH₃CN/H₂O) to yield fallaquinone (**7**) (1.3 mg, 0.01%) and paradoxquinol (**10**) (0.2 mg, 0.001%). The remaining half of the dichloromethane extract was purified separately using reversed-phase HPLC (90% CH₃CN/H₂O) to yield fallahydroquinone (**1**) (7.3 mg, 0.05%), sargahydroquinoic acid (**2**) (17.6 mg, 0.11%), paradoxhydroquinone (**5**) and 2-[11-(hydroxymethyl)-3,7,15-trimethyl-2,6,10,14-hexadecatetraen-1-yl]-6-methyl-1,4-benzenediol (**6**) as an inseparable mixture (6.5 mg, 0.04%), sargaquinoic acid (**11**) (13.1 mg, 0.08%), and 9-(6-hydroxy-2,8-dimethyl-2*H*-1-benzopyran-2-yl)-6-methyl-2-(4-methyl-3-penten-1-yl)-2,6-nonadienal (**14**) (0.4 mg, 0.005%). The percentage yields are reported on the basis of the dry mass of the alga extracted (refer to the supporting information for details of the bioassay-guided isolation scheme adopted).

3.6. On-Line (HPLC-NMR & HPLC-MS) Characterization of Compounds

2-[12*S*-Hydroxy-11-(hydroxymethyl)-3,7,15-trimethyl-2,6,10,14-hexadecatetraen-1-yl]-6-methyl-1,4-benzenediol (fallahydroquinone) (**1**): HPLC-NMR WET1D NMR (500 MHz, 75% CH₃CN/D₂O, suppression of HDO and CH₃CN at $t_{\delta H}$ 4.64 and 2.82 ppm, respectively) obtained from stop-flow mode (see Table 1); HRESILCMS m/z 427.2846 (calcd for C₂₇H₃₉O₄, 427.2849).

12-(2,5-Dihydroxy-3-methylphenyl)-6,10-dimethyl-2-(4-methyl-3-penten-1-yl)-(2*Z*,6*E*,10*E*)-2,6,10-dodecatrienoic acid (sargahydroquinoic acid) (**2**): HPLC-NMR WET1D NMR (500 MHz, 75% CH₃CN/D₂O, suppression of HDO and CH₃CN at $t_{\delta H}$ 4.64 and 2.82 ppm respectively) obtained from stop-flow mode (see Table 1); HRESILCMS m/z 425.2694 (calcd for C₂₇H₃₇O₄, 425.2692).

2-[12-Hydroxy-3,7,11,15-tetramethyl-2,6,10,14-hexadecatetraen-1-yl]-6-methyl-1,4-benzenediol (paradoxhydroquinone) (**5**): HPLC-NMR WET1D NMR (500 MHz, 75% CH₃CN/D₂O, suppression of HDO and CH₃CN at $t_{\delta H}$ 4.64 and 2.82 ppm, respectively) obtained from stop-flow mode δ 7.26 (1H, d, $J = 3.0$, H-5), 7.22 (1H, d, $J = 3.0$, H-3), 6.11 (1H, t, $J = 7.0$, H-2'), 6.06 (1H, t, $J = 7.0$, H-10'), 5.96 (2H, m, H-6'/H-14'), 4.06 (2H, d, $J = 7.0$, H-1'), 3.30 (1H, dd, $J = 7.0, 7.0$, H-12'), 2.95–3.04 (m), 2.96 (3H, s, H-7), 2.94 (2H, m, H-5'/H-13'*), 2.53 (3H, s, H-18'), 2.49 (3H, s, H-17'), 2.42 (3H, s, H-16'), 2.41 (3H, s,

H-20'*), 2.37 (3H, s, H-19'*), ND (1-OH, 4-OH, 12'-OH) *signals interchangeable; HRESILCMS m/z 411.2899 (calcd for C₂₇H₃₉O₃, 411.2899).

2-[11-(Hydroxymethyl)-3,7,15-trimethyl-2,6,10,14-hexadecatetraen-1-yl]-6-methyl-1,4-benzenediol (**6**): HPLC-NMR WET1D NMR (500 MHz, 75% CH₃CN/D₂O, suppression of HDO and CH₃CN at $t_{\delta H}$ 4.64 and 2.82 ppm, respectively) obtained from stop-flow mode δ 7.25 (1H, d, $J = 3.0$, H-5), 7.22 (1H, d, $J = 3.0$, H-3), 6.10 (1H, t, $J = 7.0$, H-2'), 6.06 (1H, t, $J = 7.5$, H-10'), 5.95 (2H, m, H-6'/H-14'), 4.84 (2H, s, H-20'), 4.05 (2H, d, $J = 7.0$, H-1'), 2.95–3.04 (m), 2.97 (3H, s, H-7), 2.95 (2H, m, H-9'), 2.93 (2H, m, H-5'/H-13'*), 2.52 (3H, s, H-18'), 2.48 (3H, s, H-17'), 2.41 (6H, s, H-16'/H19') ND (1-OH, 4-OH, 20'-OH) *signals interchangeable; HRESILCMS m/z 411.2899 (calcd for C₂₇H₃₉O₃, 411.2899).

5-[12S-Hydroxy-11-(hydroxymethyl)-3,7,15-trimethyl-2,6,10,14-hexadecatetraen-1-yl]-6-methyl-1,4-benzoquinone (fallaquinone) (**7**): HPLC-NMR WET1D NMR (500 MHz, 75% CH₃CN/D₂O, suppression of HDO and CH₃CN at $t_{\delta H}$ 4.64 and 2.82 ppm, respectively) obtained from stop-flow mode δ 7.42 (1H, bs, H-5), 7.28 (1H, bs, H-3), 6.30 (1H, t, $J = 7.5$, H-10'), 6.00 (1H, t, $J = 7.0$, H-2'), 5.95 (1H, t, $J = 6.5$, H-6'), 5.91 (1H, t, $J = 6.5$, H-14'), 4.95 (1H, d, $J = 12.0$, H-20a'), 4.89 (1H, d, $J = 12.5$, H-20b'), 4.87 (1H, dd, $J = 6.0, 7.0$, H-12'), 3.93 (2H, d, $J = 7.0$, H-1'), 2.95–3.10 (m), 3.08 (2H, m, H-13'), 3.03 (2H, m, H-9'), 2.96 (2H, m, H-5'), 2.50 (3H, s, H-17'), 2.46 (3H, s, H-18'), 2.42 (6H, s, H-16'/H-19') ND (12'-OH, 20'-OH); HRESILCMS m/z 425.2694 (calcd for C₂₇H₃₇O₄, 425.2692).

6,10-dimethyl-12-(5-methyl-3,6-dihydroxy-1,4-cyclohexadien-1-yl)-2-(4-methyl-3-pentenyl)-(2E, 6E,10E)-2,6,10-dodecatrienal (sargahydroquinal) (**9**): UV (75% CH₃CN/D₂O) λ_{max} 238, 292; HPLC-NMR WET1D NMR (500 MHz, 75% CH₃CN/D₂O, suppression of HDO and CH₃CN at $t_{\delta H}$ 4.64 and 2.82 ppm, respectively) obtained from stop-flow mode (see Table 2); HRESILCMS m/z 409.2745 (calcd for C₂₇H₃₇O₃, 409.2743).

5-[12S-Hydroxy-11-(hydroxymethyl)-3,7,15-trimethyl-2,6,10,14-hexadecatetraen-1-yl]-2,3-dimethyl-1,4-benzoquinone (paradoxquinol) (**10**): HPLC-NMR WET1D NMR (500 MHz, 75% CH₃CN/D₂O, suppression of HDO and CH₃CN at $t_{\delta H}$ 4.64 and 2.82 ppm, respectively) obtained from stop-flow mode δ 7.27 (1H, s, H-3), 6.29 (1H, t, $J = 7.0$, H-10'), 5.99 (1H, m, H-2'), 5.92 (2H, m, H-6'/H-14'), 4.95 (1H, d, $J = 12.0$, H-20a'), 4.88 (1H, d, $J = 13.0$, H-20b'), 4.87 (1H, dd, $J = 6.0, 7.5$, H-12'), 3.92 (2H, d, $J = 7.5$, H-1'), 2.95–3.10 (m), 2.49 (3H, s, H-18'), 2.45 (3H, s, H-17'), 2.41 (6H, s, H-16'/H-19') ND (12'-OH, 20'-OH); HRESILCMS m/z 439.2850 (calcd for C₂₈H₃₉O₄, 439.2849).

6,10-Dimethyl-12-(5-methyl-3,6-dioxo-1,4-cyclohexadien-1-yl)-2-(4-methyl-3-pentenyl)-(2Z,6E, 10E)-2,6,10-dodecatrienoic acid (sargaquinoic acid) (**11**): HPLC-NMR WET1D NMR (500 MHz, 75% CH₃CN/D₂O, suppression of HDO and CH₃CN at $t_{\delta H}$ 4.64 and 2.82 ppm, respectively) obtained from stop-flow mode δ 7.42 (1H, d, $J = 1.5$, H-5), 7.28 (1H, d, $J = 1.5$, H-3), 6.69 (1H, t, $J = 7.5$, H-10'), 6.00 (1H, t, $J = 7.0$, H-2'), 5.95 (1H, t, $J = 6.5$, H-6'), 5.91 (1H, t, $J = 6.5$, H-14'), 3.93 (2H, d, $J = 7.0$, H1'), 3.31 (2H, dt, $J = 7.5, 8.0$, H-9'), 3.02 (2H, m, H-12'), 2.95–3.10 (m), 2.97 (2H, m, H-5'), 2.49 (3H, s, H-17'), 2.46 (3H, s, H-18'), 2.41 (3H, s, H-19'), 2.40 (3H, s, H-16') ND (20'-OH); HRESILCMS m/z 423.2542 (calcd for C₂₇H₃₅O₄, 423.2536).

2-[11-(Hydroxymethyl)-3,7,15-trimethyl-2,6,10,14-hexadecatetraen-1-yl]-6-methyl-1,4-benzoquinone (**12**): HPLC-NMR WET1D NMR (500 MHz, 75% CH₃CN/D₂O, suppression of HDO and CH₃CN at

t δ_{H} 4.64 and 2.82 ppm, respectively) obtained from stop-flow mode δ 7.41 (1H, bs, H-5), 7.27 (1H, bs, H-3), 6.05 (1H, t, $J = 7.5$, H-10'), 6.00 (1H, t, $J = 7.5$, H-2'), 5.94 (2H, m, H-6'/H-14'), 4.84 (2H, s, H-20'), 3.93 (2H, d, $J = 7.5$, H1'), 2.95–3.10 (m), 2.49 (3H, s, H-17'), 2.46 (3H, s, H-18'), 2.41 (6H, s, H-16'/H-19') ND (20'-OH); HRESILCMS m/z 409.2742 (calcd for $\text{C}_{27}\text{H}_{37}\text{O}_3$, 409.2743).

3.7. Off-Line Characterization of Compounds

(2'E,6'E,10'Z)-2-[12S-Hydroxy-11-(hydroxymethyl)-3,7,15-trimethyl-2,6,10,14-hexadecatetraen-1-yl]-6-methyl-1,4-benzenediol (fallahydroquinone) (**1**): unstable yellow oil; $[\alpha]_{\text{D}}^{25} +45.1$ (c 0.035, CHCl_3); CD (EtOH) λ_{max} ($\Delta\epsilon$) 202 (+6.1), 221 (+1.6), 224 (1.8), 243 (−0.2), 260 (+2.0), 275 (+0.5), 290 (+0.6); UV (EtOH) λ_{max} ($\log \epsilon$) 252 (3.60), 288 (3.58); IR ν_{max} 3391, 2925, 2855, 1652, 1607, 1470, 1381, 1197, 1037 cm^{-1} . All off-line NMR spectroscopic and mass spectrometric data were identical to those reported in the literature; however, some carbon and proton NMR chemical shift reassignments have been made [7].

(2'E,6'E,10'Z)-12-(2,5-Dihydroxy-3-methylphenyl)-6,10-dimethyl-2-(4-methyl-3-penten-1-yl)-2,6,10-dodecatrienoic acid (sargahydroquinonic acid) (**2**): yellow oil which darkened with time. All off-line NMR spectroscopic and mass spectrometric data were identical to those reported in the literature [7,8].

(2'E,6'E,10'Z)-2-[12-Hydroxy-3,7,11,15-tetramethyl-2,6,10,14-hexadecatetraen-1-yl]-6-methyl-1,4-benzenediol (paradoxhydroquinone) (**5**): dark yellow oil; ^1H and ^{13}C NMR (500 MHz, CDCl_3) (see Table 3); ESIMS m/z 411 $[\text{M} - \text{H}]^-$; HRESIMS m/z 411.2898 (calcd for $\text{C}_{27}\text{H}_{39}\text{O}_3$, 411.2899).

(2'E,6'E,10'Z)-2-[11-(Hydroxymethyl)-3,7,15-trimethyl-2,6,10,14-hexadecatetraen-1-yl]-6-methyl-1,4-benzenediol (**6**): dark yellow oil. All off-line NMR spectroscopic and mass spectrometric data were identical to those reported in the literature [16]. Acquisition of the 1D and 2D NMR data has resulted in the first complete assignment of this compound and is provided in the supporting information.

(2'E,6'E,10'Z)-5-[12S-Hydroxy-11-(hydroxymethyl)-3,7,15-trimethyl-2,6,10,14-hexadecatetraen-1-yl]-6-methyl-1,4-benzoquinone (fallaquinone) (**7**): unstable yellow oil which darkened with time; $[\alpha]_{\text{D}}^{25} +31.4$ (c 0.065, CHCl_3); CD (EtOH) λ_{max} ($\Delta\epsilon$) 206 (+1.8), 220 (+1.0), 238 (+2.1), 247 (+2.3), 262 (+1.6), 270 (+1.9), 286 (+0.1), 294 (+0.3); UV (EtOH) λ_{max} ($\log \epsilon$) 254 (4.10); IR ν_{max} 3392, 2924, 2855, 1652, 1614, 1510, 1436, 1378, 1295, 1195, 1156 cm^{-1} . All off-line NMR spectroscopic and mass spectrometric data were identical to those reported in the literature [7].

(2'E,6'E,10'Z)-6,10-Dimethyl-12-(5-methyl-3,6-dioxo-1,4-cyclohexadien-1-yl)-2-(4-methyl-3-pentenyl)-2,6,10-dodecatrienal (sargaquinal) (**8**): yellow oil which darkened with time; ^1H NMR (500 MHz, CDCl_3) δ 9.34 (1H, s, H-20'), 6.54 (1H, bs, H-5), 6.45 (1H, bs, H-3), 6.43 (1H, t, $J = 7.5$, H-10'), 5.15 (2H, t, $J = 7.5$, H-2', H-6'), 5.09 (1H, m, H-14'), 3.12 (2H, d, $J = 7.5$, H1'), 2.45 (2H, dt, $J = 7.0, 7.5$, H-9'), 2.26 (2H, t, $J = 7.5$ Hz, H-12'), 2.17 (2H, m, H-8'), 2.14 (2H, m, H-5'), 2.07 (2H, m, H-4'), 2.06 (3H, s, H-7), 2.03 (2H, m, H-13'), 1.66 (3H, s, H-16'), 1.63 (3H, s, H-18'), 1.62 (3H, s, H-19'), 1.57 (3H, s, H-17'); ^{13}C NMR (125 MHz, CDCl_3) δ 195.2 (CH, C-20'), 188.0 (C, C-1, C-4), 155.0 (CH, C-10'), 148.4 (C, C-2), 146.0 (C, C-6), 143.2 (C, C-11'), 139.7 (C, C-3'), 133.9 (C, C-7'), 133.2 (CH, C-5), 132.4 (C, C-15'), 132.2 (CH, C-3), 125.1 (CH, C-6'), 123.6 (CH, C-14'), 118.2 (CH, C-2'),

39.5 (CH₂, C-4'), 38.3 (CH₂, C-8'), 27.5 (CH₂, C-1'), 27.4 (CH₂, C-9'), 27.0 (CH₂, C-13'), 26.4 (CH₂, C-5'), 25.7 (CH₃, C-16'), 24.3 (CH₂, C-12'), 17.7 (CH₃, C-17'), 16.0 (CH₃, C-7, C-18', C-19').

(2'E,6'E,10'Z)-5-[12S-Hydroxy-11-(hydroxymethyl)-3,7,15-trimethyl-2,6,10,14-hexadecatetraen-1-yl]-2,3-dimethyl-1,4-benzoquinone (paradoxquinol) (**10**): unstable yellow oil which darkened with time; $[\alpha]_D^{25} +48.5$ (*c* 0.0125, CHCl₃); CD (EtOH) λ_{\max} ($\Delta\epsilon$) 218 (+6.2), 220 (+6.4), 235 (−4.2), 245 (+2.4), 255 (+1.2); UV (EtOH) λ_{\max} (log ϵ) 232 (4.17), 254 (4.32); IR ν_{\max} 3401, 2924, 2853, 1652, 1511, 1456, 1249 cm^{−1}; ¹H and ¹³C NMR (500 MHz, CDCl₃) (see Table 4); ESIMS *m/z* 439 [M − H][−]; HRESIMS *m/z* 439.2850 (calcd for C₂₈H₃₉O₄, 439.2849).

(2'E,6'E,10'Z)-6,10-Dimethyl-12-(5-methyl-3,6-dioxo-1,4-cyclohexadien-1-yl)-2-(4-methyl-3-pentenyl)-2,6,10-dodecatrienoic acid (sargaquinoic acid) (**11**): yellow oil which darkened with time. All off-line NMR spectroscopic and mass spectrometric data were identical to those reported in the literature [7,17].

(2'E,6'E,10'Z)-2-[11-(Hydroxymethyl)-3,7,15-trimethyl-2,6,10,14-hexadecatetraen-1-yl]-6-methyl-1,4-benzoquinone (**12**): dark yellow oil. All off-line NMR spectroscopic and mass spectrometric data were identical to those reported in the literature [16,17]. Acquisition of the 1D and 2D NMR data has resulted in the first complete assignment of this compound and is provided in the supporting information.

(2'E,6'E,10'Z)-2-Methyl-6-(3,7,11,15-tetramethyl-2,6,10,14-hexadecatetraenyl)-1,4-benzoquinone (sargaquinone) (**13**): dark yellow oil. All off-line NMR spectroscopic and mass spectrometric data were identical to those reported in the literature; however, some carbon NMR chemical shift reassignments have been made [18].

(3'E,7'Z)-9-(6-Hydroxy-2,8-dimethyl-2H-1-benzopyran-2-yl)-6-methyl-2-(4-methyl-3-penten-1-yl)-2,6-nonadienal (**14**): dark yellow oil; UV (90% CH₃CN/H₂O) λ_{\max} 232, 273s, 334; IR ν_{\max} 3351, 2961, 2925, 2853, 2718, 1725, 1684, 1640, 1610, 1508, 1456, 1376, 1250 cm^{−1}. All off-line NMR spectroscopic and mass spectrometric data were identical to those reported in the literature [19].

(2'E,6'E,10'Z)-2-[12-Hydroxy-3,7,11,15-tetramethyl-2,6,10,14-hexadecatetraen-1-yl]-6-methyl-1,4-benzoquinone (paradoxquinone) (**15**): yellow oil which darkened with time; ¹H and ¹³C NMR (500 MHz, CDCl₃) (see Table 4); ESIMS *m/z* 409 [M − H][−]; HRESIMS *m/z* 409.2755 (calcd for C₂₇H₃₇O₃, 409.2743).

4. Conclusions

The study of the marine brown alga *S. paradoxum* successfully implemented the use of HPLC-NMR and HPLC-MS, in combination with the use of databases, to rapidly dereplicate, identify, and deduce the structures of nine meroditerpenoids (**1**, **2**, **5–7**, and **9–12**). In particular, chemical profiling was an invaluable tool for the on-line identification of sargahydroquinal (**9**), which rapidly degraded when an off-line bioassay-guided isolation was employed, as well as for the meroditerpenoids **5**, **6**, and **12**, which could be resolved and identified as individual components via stop-flow HPLC-NMR. This study reports, for the first time, the complete 1D and 2D NMR characterization and identification of two known (**1** and **2**) natural products via stop-flow HPLC-NMR and HPLC-MS. The bioassay-guided isolation approach confirmed the identity of the compounds responsible for the dichloromethane crude

extract antimicrobial activity. Subsequent biological evaluation of the isolated meroditerpenoids indicated that there were no significant differences in antimicrobial activity for 11 of the meroditerpenoids isolated. Off-line bioassay-guided isolation also permitted the first complete NMR characterization of 2-[11-(hydroxymethyl)-3,7,15-trimethyl-2,6,10,14-hexadecatetraen-1-yl]-6-methyl-1,4-benzenediol (**6**) and 2-[11-(hydroxymethyl)-3,7,15-trimethyl-2,6,10,14-hexadecatetraen-1-yl]-6-methyl-1,4-benzoquinone (**12**) to be carried out. It is proposed that the presence of fallahydroquinone (**1**) and fallaquinone (**7**) could be used as potential chemotaxonomic markers for both *S. paradoxum* and *S. fallax*, which have only been reported from these two species of *Sargassum*.

Acknowledgments

The Marine and Terrestrial Natural Product (MATNAP) research group would like to thank G. Kraft (The University of Melbourne, Victoria, Australia) for the taxonomic identification of the marine alga; R. Watson from the Victorian Marine Sciences Consortium (VMSC) for the collection of the specimen; N. Thurbon (School of Applied Sciences (Discipline of Biotechnology and Biological Sciences)), RMIT University for providing access to the microorganisms for the antimicrobial assays as well as for her invaluable technical support; S. Duck (School of Chemistry, Faculty of Science, Monash University) for conducting the high-resolution mass spectrometric and HPLC-MS analyses; J. Niere for her useful NMR discussions and guidance; and D. Giang for his assistance with some of the preliminary fractionations and isolation. Robert Brkljača would also like to acknowledge his Australian Postgraduate Award (APA) scholarship that supported his PhD studies.

Author Contributions

All experimental work was conducted by R. Brkljača. Manuscript was prepared by R. Brkljača and S. Urban.

Supplementary Information

Complete HPLC-NMR and HPLC-MS analysis profiles of the crude extract of *S. paradoxum* are included. NMR spectroscopic and mass spectrometric data obtained from the HPLC-NMR and HPLC-MS analyses have been provided for the meroditerpenoids (**1**, **2**, **5–7**, and **9–12**). The off-line NMR spectroscopic and mass spectrometric data obtained for the new meroditerpenoids (**5**, **10**, and **15**) and for compounds **6** and **12**, which have been characterized completely for the first time, have also been made available. This material is available free of charge via the Internet at <http://pubs.acs.org>.

Conflicts of Interest

The authors declare no conflict of interest.

References

1. *MarinLit Database*; Royal Society of Chemistry: Cambridge, UK, 2014.
2. Guiry, M.D.; Guiry, G.M. *AlgaeBase*; World-Wide Electronic Publication: National University of Ireland, Galway, Ireland, 2014. Available online: <http://www.algaebase.org> (accessed on 1 December 2014).
3. Phillips, N. Biogeography of *Sargassum* (Phaeophyta) in the Pacific basin. *Taxon. Economic Seaweeds* **1995**, *5*, 107–144.
4. Dixon, R.R.M.; Mattio, L.; Huisman, J.M.; Payri, C.E.; Bolton, J.J.; Gurgel, C.F.D. North meets south—Taxonomic and biogeographic implications of a phylogenetic assessment of *Sargassum* subgenera *Arthrophyucus* and *Bactrophyucus* (Fucales, Phaeophyceae). *Phycologia* **2014**, *53*, 15–22.
5. Liu, L.; Heinrich, M.; Myers, S.; Dworjanyn, S.A. Towards a better understanding of medicinal uses of the brown seaweed *Sargassum* in traditional chinese medicine: A phytochemical and pharmacological review. *J. Ethnopharmacol.* **2012**, *142*, 591–619.
6. Jung, M.; Jang, K.H.; Kim, B.; Lee, B.H.; Choi, B.W.; Oh, K.-B.; Shin, J. Meroditerpenoids from the brown alga *Sargassum siliquastrum*. *J. Nat. Prod.* **2008**, *71*, 1714–1719.
7. Reddy, P.; Urban, S. Meroditerpenoids from the southern australian marine brown alga *Sargassum fallax*. *Phytochemistry* **2009**, *70*, 250–255.
8. Segawa, M.; Shirahama, H. New plastoquinones from the brown alga *Sargassum sagamianum* var. *yezoense*. *Chem. Lett.* **1987**, *16*, 1365–1366.
9. Kim, M.C.; Kwon, H.C.; Kim, S.N.; Kim, H.S.; Um, B.H. Plastoquinones from *Sargassum yezoense*; chemical structures and effects of the activation of peroxisome proliferator-activated receptor gamma. *Chem. Pharm. Bull.* **2011**, *59*, 834–838.
10. Horie, S.; Tsutsumi, S.; Takada, Y.; Kimura, J. Antibacterial quinone metabolites from the brown alga, *Sargassum sagamianum*. *Bull. Chem. Soc. Jpn.* **2008**, *81*, 1125–1130.
11. Culioli, G.; Ortalo-Magne, A.; Valls, R.; Hellio, C.; Clare, A.S.; Piovetti, L. Antifouling activity of meroditerpenoids from the marine brown alga *Halidrys siliquosa*. *J. Nat. Prod.* **2008**, *71*, 1121–1126.
12. Foti, M.; Piattelli, M.; Amico, V.; Ruberto, G. Antioxidant activity of phenolic meroditerpenoids from marine algae. *J. Photochem. Photobiol. B* **1994**, *26*, 159–164.
13. *SciFinder*; American Chemical Society: Washington, DC, USA, 2014.
14. Scott, A.I. *Interpretation of the Ultraviolet Spectra of Natural Products*; Pergamon Press Ltd.: London, UK, 1964.
15. Sheu, J.-H.; Su, J.-H.; Sung, P.-J.; Wang, G.-H.; Dai, C.-F. Novel meroditerpenoid-related metabolites from the formosan soft coral *Nephthea chabrolii*. *J. Nat. Prod.* **2004**, *67*, 2048–2052.
16. Sato, A.; Shindo, T.; Hasegawa, K.; Ushiyama, S. Preparation of 2-(11-Hydroxymethyl-3,7,15-Trimethyl-2,6,10,14-Hexadecatetraenyl)-6-Methyl-1,4-Benzoquinone or -1,4-Benzenediol or Their Acyl Derivatives as 5-Lipoxygenase Inhibitors. Kokai Tokkyo Koho, Japan H02-290826, 1990.
17. Kusumi, T.; Shibata, Y.; Ishitsuka, M.; Kinoshita, T.; Kakisawa, H. Structures of new plastoquinones from the brown alga *Sargassum serratifolium*. *Chem. Lett.* **1979**, *8*, 277–278.
18. Amico, V.; Cunsolo, F.; Piattelli, M.; Ruberto, G. Tetraprenyltoluquinols from the brown alga *Cystoseira jabukae*. *Phytochemistry* **1985**, *24*, 1047–1050.

19. Kimura, J.; Horie, C.; Marushima, H.; Matsumoto, Y.; Sanjoba, C.; Osada, Y. Antileishmanial Agents Containing p-Benzoquinone Derivative. JP 2012-502793, 2012.
20. Silva, D.H.S.; Pereira, F.C.; Zanoni, M.V.B.; Yoshida, M. Lipophyllic antioxidants from *Iryanthera juruensis* fruits. *Phytochemistry* **2001**, *57*, 437–442.
21. Barr, R.; Crane, F.L. Comparative studies on plastoquinones. III. Distribution of plastoquinones in higher plants. *Plant Physiol.* **1967**, *42*, 1255–1263.
22. Gonnella, N.C.; Nakanishi, K. General method for determining absolute configurations of acyclic allylic alcohols. *J. Am. Chem. Soc.* **1982**, *104*, 3775–3776.
23. Kobayashi, M.; Ito, M.; Koyama, T.; Ogura, K. Stereochemistry of the carbon to carbon bond formation in the biosynthesis of polyprenyl chains with *Z* double bonds. Studies with undecaprenyl-pyrophosphate synthetase. *J. Am. Chem. Soc.* **1985**, *107*, 4588–4589.
24. Lamshoft, M.; Schmickler, H.; Marner, F.-J. Determination of the absolute configuration of hydroxyiridals by chiroptical and NMR spectroscopic methods. *Eur. J. Org. Chem.* **2003**, *2003*, 727–733.
25. Sunazuka, T.; Shirahata, T.; Yoshida, K.; Yamamoto, D.; Harigaya, Y.; Nagai, T.; Kiyohara, H.; Yamada, H.; Kuwajima, I.; Omura, S. Total synthesis of pinellic acid, a potent oral adjuvant for nasal influenza vaccine. Determination of the relative and absolute configuration. *Tetrahedron Lett.* **2002**, *43*, 1265–1268.
26. De la Mare, J.-A.; Lawson, J.C.; Chiwakata, M.T.; Beukes, D.R.; Edkins, A.L.; Blatch, G.L. Quinones and halogenated monoterpenes of algal origin show anti-proliferative effects against breast cancer cells *in vitro*. *Investig. New Drugs* **2012**, *30*, 2187–2200.
27. Seo, Y.; Lee, H.-J.; Park, K.E.; Kim, Y.A.; Ahn, J.W.; Yoo, J.S.; Lee, B.-J. Peroxynitrite-scavenging constituents from the brown alga *Sargassum thunbergii*. *Biotechnol. Bioprocess Eng.* **2004**, *9*, 212–216.
28. Afolayan, A.F.; Bolton, J.J.; Lategan, C.A.; Smith, P.J.; Beukes, D.R. Fucoxanthin, tetraprenylated toluquinone, and toluhydroquinone metabolites from *Sargassum heterophyllum* inhibit the *in vitro* growth of the malaria parasite *Plasmodium falciparum*. *J. Biosci.* **2008**, *63*, 848–852.
29. Cespedes, C.L.; Torres, P.; Marin, J.C.; Arciniegas, A.; de Vivar, A.R.; Perez-Castorena, A.L.; Aranda, E. Insect growth inhibition by tocotrienols and hydroquinones from *Roldana barba-johannis*. *Phytochemistry* **2004**, *65*, 1963–1975.
30. Park, B.-G.; Shin, W.-S.; Um, Y.; Cho, U.; Park, G.-M.; Yeon, D.-S.; Kwon, S.-C.; Ham, J.; Choi, B.W.; Lee, S. Selective vasodilatation effect of sargahydroquinonic acid, an active constituent of *Sargassum micracanthum*, on the basilar arteries of rabbits. *Bioorg. Med. Chem. Lett.* **2008**, *18*, 2624–2627.
31. Kim, S.-N.; Choi, H.Y.; Lee, W.; Park, G.-M.; Shin, W.-S.; Kim, Y.K. Sargaquinoic acid and sargahydroquinonic acid from *Sargassum yezoense* stimulate adipocyte differentiation through PPAR α/γ activation in 3T3-L1 cells *FEBS Lett.* **2008**, *582*, 3465–3472.
32. Kamei, Y.; Tsang, C.K. Sargaquinoic acid promotes neurite outgrowth via protein kinase A and MAP kinases-mediated signaling pathways in PC12D cells. *Int. J. Dev. Neurosci.* **2003**, *21*, 255–262.

33. Hur, S.; Lee, H.; Kim, Y.; Lee, B.-H.; Shin, J.; Kim, T.-Y. Sargaquinoic acid and sargachromenol, extracts of *Sargassum sagamianum*, induce apoptosis in HaCaT cells and mice skin: Its potentiation of UVB-induced apoptosis. *Eur. J. Pharmacol.* **2008**, *582*, 1–11.
34. Silva, D.H.S.; Zhang, Y.; Santos, L.A.; Bolzani, V.S.; Nair, M.G. Lipoperoxidation and cyclooxygenases 1 and 2 inhibitory compounds from *Iryanthera juruensis*. *J. Agric. Food Chem.* **2007**, *55*, 2569–2574.
35. Choi, B.W.; Ryu, G.; Park, S.H.; Kim, E.S.; Shin, J.; Roh, S.S.; Shin, H.C.; Lee, B.-H. Anticholinesterase activity of plastoquinones from *Sargassum sagamianum*: Lead compounds for Alzheimer's disease therapy. *Phytother. Res.* **2007**, *21*, 423–426.
36. Nahas, R.; Abatis, D.; Anagnostopoulou, M.A.; Kefalas, P.; Vagias, C.; Roussis, V. Radical-scavenging activity of aegean sea marine algae. *Food Chem.* **2007**, *102*, 577–581.
37. Tziveleka, L.-A.; Abatis, D.; Paulus, K.; Bauer, R.; Vagias, C.; Roussis, V. Marine polyprenylated hydroquinones, quinones and chromenols with inhibitory effects on leukotriene formation. *Chem. Biodivers.* **2005**, *2*, 901–909.
38. Voutquenne, L.; Lavaud, C.; Massiot, G.; Sevenet, T.; Hadi, H.A. Cytotoxic polyisoprenes and glycosides of long-chain fatty alcohols from *Dimocarpus fumatus*. *Phytochemistry* **1999**, *50*, 63–69.
39. Gerwick, W.H.; Fenical, W.; Norris, J.N. Chemical variation in the tropical seaweed *Styopodium zonale* (dictyotaceae). *Phytochemistry* **1985**, *24*, 1279–1283.
40. Master, R.N.; Clark, R.B.; Karlowsky, J.A.; Ramirez, J.; Bordon, J.M. Analysis of resistance, cross-resistance and antimicrobial combinations for *Pseudomonas aeruginosa* isolates from 1997 to 2009. *Int. J. Antimicrob. Agents* **2011**, *38*, 291–295.
41. Smallcombe, S.H.; Patt, S.L.; Keifer, P.A. WET solvent suppression and its applications to LC NMR and high-resolution NMR spectroscopy. *J. Magn. Reson. Ser. A* **1995**, *117*, 295–303.

© 2014 by the authors; licensee MDPI, Basel, Switzerland. This article is an open access article distributed under the terms and conditions of the Creative Commons Attribution license (<http://creativecommons.org/licenses/by/4.0/>).

CHAPTER 10

*Dereplication and Structural Identification Studies of Marine Algae
of the Genus Cystophora*



Kingdom: Chromista, Phylum: Ochrophyta, Class: Phaeophyceae, Order: Fucales, Family:
Sargassaceae

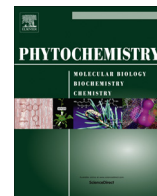
Genus: *Cystophora*
Species: *monilifera*

Genus: *Cystophora*
Species: *subfarcinata*

Chapter 10 describes the dereplication and structural identification studies of two marine algae of the *Cystophora* genus. This work has been published in *Phytochemistry*. Appendix F contains supplementary information relevant to this study.

Journal publication resulting from this study:

Brkljača, Robert, & Urban, Sylvia. (2015). HPLC-NMR and HPLC-MS investigation of antimicrobial constituents in *Cystophora monilifera* and *Cystophora subfarcinata*. *Phytochemistry*, 117, 200-208.



HPLC–NMR and HPLC–MS investigation of antimicrobial constituents in *Cystophora monilifera* and *Cystophora subfarcinata*



Robert Brkljača, Sylvia Urban*

School of Applied Sciences (Discipline of Chemistry), Health Innovations Research Institute (HIRI), RMIT University, GPO Box 2476V, Melbourne, Victoria 3001, Australia

ARTICLE INFO

Article history:

Received 20 February 2015

Received in revised form 3 June 2015

Accepted 8 June 2015

Keywords:

Cystophora

Brown alga

Phloroglucinol

HPLC–NMR

HPLC–MS

Dereplication

Antimicrobial activity

ABSTRACT

The crude dichloromethane extracts of the marine brown algae *Cystophora monilifera* and *Cystophora subfarcinata* were subjected to phytochemical profiling. This enabled the structures of both new and known phloroglucinols to be dereplicated and proposed using HPLC–NMR and HPLC–MS. Subsequent isolation confirmed the presence of four new and eight previously reported compounds. Five of the isolated phloroglucinols displayed selective antimicrobial activity.

Crown Copyright © 2015 Published by Elsevier Ltd. All rights reserved.

1. Introduction

Marine brown algae of the *Cystophora* genus are comprised of 28 known species (Guiry and Guiry, 2015) and phytochemical studies have been carried out on approximately 14 of these species (MarinLit Database, 2015). Brown algae are known to produce phlorotannins or phloroglucinols which display various biological properties including antioxidant, anticancer, antidiabetic, anti-inflammatory and antimicrobial activities (Ryu and Kim, 2013). Only recently, seven new phloroglucinol and phlorotannins were reported which display a variety of biological activities including radical scavenging activity and antioxidant activities (Blunt et al., 2014). Of these compounds one was identified as a potential antidiabetic lead compound (Blunt et al., 2014).

To date, two separate reports have described the chemistry of *Cystophora monilifera* and *Cystophora subfarcinata* respectively. These include the discovery of two new phloroglucinols (Kazlauskas et al., 1981) from *C. monilifera* and a phloroglucinol and a tocotrienol (Laird et al., 2010) from *C. subfarcinata*, respectively. As part of our on-going efforts to evaluate the chemistry and biological activity of southern Australian marine algae, we examined the crude extracts of the marine brown algae *C. monilifera* J. Agardh and *C. subfarcinata* (Mertens) J. Agardh. These studies were motivated by the fact that these species of *Cystophora* have

not been extensively studied. This resulted in the identification of four new (**8**, **9**, **11** and **12**) and six known phloroglucinols (**1–6**) together with two previously described tocotrienols (**7** and **10**). Compounds **4–9** and **11** were present in both of the crude extracts of the marine algae specimens studied.

2. Results and discussion

The marine algae (*C. monilifera* and *C. subfarcinata*) were extracted with 3:1 methanol/dichloromethane, evaporated under reduced pressure, and sequentially solvent partitioned (trituated) into dichloromethane and methanol soluble fractions respectively. The dichloromethane crude extract of *C. monilifera* displayed greater antimicrobial activity than the corresponding methanol extract, and so was selected for further analysis. The 3:1 methanol/dichloromethane extract of *C. subfarcinata* displayed selective antimicrobial activity, however it was not further established which of the dichloromethane or methanol crude extracts displayed greater activity. Subsequent off-line analytical HPLC and ¹H NMR analyses on the dichloromethane and methanol extracts of *C. subfarcinata* indicated that the dichloromethane extract contained a greater diversity and range of compounds. Since the antimicrobial activity of the dichloromethane extract of *C. monilifera* was greater, this was also presumed to be the case for the dichloromethane crude extract of *C. subfarcinata* and on this basis was selected for phytochemical evaluation.

* Corresponding author.

E-mail address: sylvia.urban@rmit.edu.au (S. Urban).

2.1. Chemical profiling (HPLC–NMR & HPLC–MS)

Dereplication of the components present in the dichloromethane crude extracts of *C. monilifera* and *C. subfarcinata* was achieved using HPLC–NMR & HPLC–MS in conjunction with database searching. Examination of the UV profiles extracted (see Supporting file) for each of the components (Fig. 1) detected by PDA showed the presence of a distinct UV chromophore at 280 nm supporting the presence of phloroglucinols (Scott, 1964) and another chromophore at 300 nm supporting the presence of tocotrienols (MarinLit Database, 2015). Both of these structural classes are known to occur within the *Cystophora* genus (MarinLit Database, 2015). The dichloromethane crude extract of *C. monilifera* and *C. subfarcinata* showed the presence of seven peaks (A–G) and six peaks (D–F, H–J) respectively (Fig. 1). This represented a total of ten different compounds (peaks A–J) being detected, three of which were found to co-occur in the dichloromethane crude extracts of the two algae (peaks D–F).

Seven of the peaks (A–E, I and J) (Fig. 1) present in the dichloromethane crude extracts of *C. monilifera* and *C. subfarcinata* could be identified as the previously reported phloroglucinols 9-hydroxy-1-(2,4,6-trihydroxyphenyl)-6Z,10E,12Z,15Z-octadecate-traen-1-one (1) (Kazlauskas et al., 1981), 15-hydroxy-1-(2,4,6-trihydroxyphenyl)-5Z,8Z,11Z,13E,17Z-eicosapentaen-1-one (2) (Amico et al., 1982), 9-hydroxy-1-(2,6-dihydroxy-4-methoxyphenyl)-6Z,10Z,12Z,15Z-octadecatetraen-1-one (3) (Kazlauskas et al., 1981), 1-(2,4,6-trihydroxyphenyl)-6Z,9Z,12Z,15Z-octadecatetraen-1-one (4) (Kazlauskas et al., 1981), 1-(2,4,6-trihydroxyphenyl)-5Z,8Z,11Z,14Z,17Z-eicosapentaen-1-one (5) (Amico et al., 1981),

1-(2,6-dihydroxy-4-methoxyphenyl)-6Z,9Z,12Z,15Z-octadecate-traen-1-one (6) (Gregson et al., 1977), and δ -tocotrienol (7) (Ohnmacht et al., 2008) respectively (Fig. 2). The identities of these peaks could be dereplicated based on examination of a combination of the NMR spectra obtained via stop-flow HPLC–NMR (WET1D proton, gCOSY, gHSQCAD, gHMBCAD NMR data), the molecular formula identified from the high-resolution HPLC–MS data, the UV absorbances and taxonomy, in conjunction with the use of the MarinLit or SciFinder databases. In addition to these known compounds, three new phloroglucinols (peaks F, G and H) were likely based on the unique masses established by high-resolution HPLC–MS and the proton NMR data obtained via HPLC–NMR, which did not correspond to any of the known phloroglucinols.

In the dichloromethane crude extract of *C. monilifera*, peaks F and G co-eluted, which made it difficult to interpret the NMR data. However, in the dichloromethane crude extract of *C. subfarcinata*, peak F (compound 8) was also present, and importantly, it did not co-elute with any other secondary metabolite. High resolution HPLC–MS yielded a molecular formula of $C_{24}H_{34}O_4$ for 8 (observed 385.2384 [M–H][−], calcd for $C_{24}H_{33}O_4$, 385.2384). Stop-flow HPLC–NMR enabled for WET1D proton, gCOSY, 1D TOCSY and partial HSQCAD NMR data to be obtained. A diagnostic methylene at δ_H 3.90 was observed which corresponds to the methylene adjacent to the ketone functionality. The gCOSY NMR data was able to secure the spin system and connectivity from this methylene at position H-2 through to H-4. The proton at H-4 (δ_H 2.26, pentet) did not show any gCOSY NMR correlations, however the multiplicity of this signal indicated the presence of an additional methylene

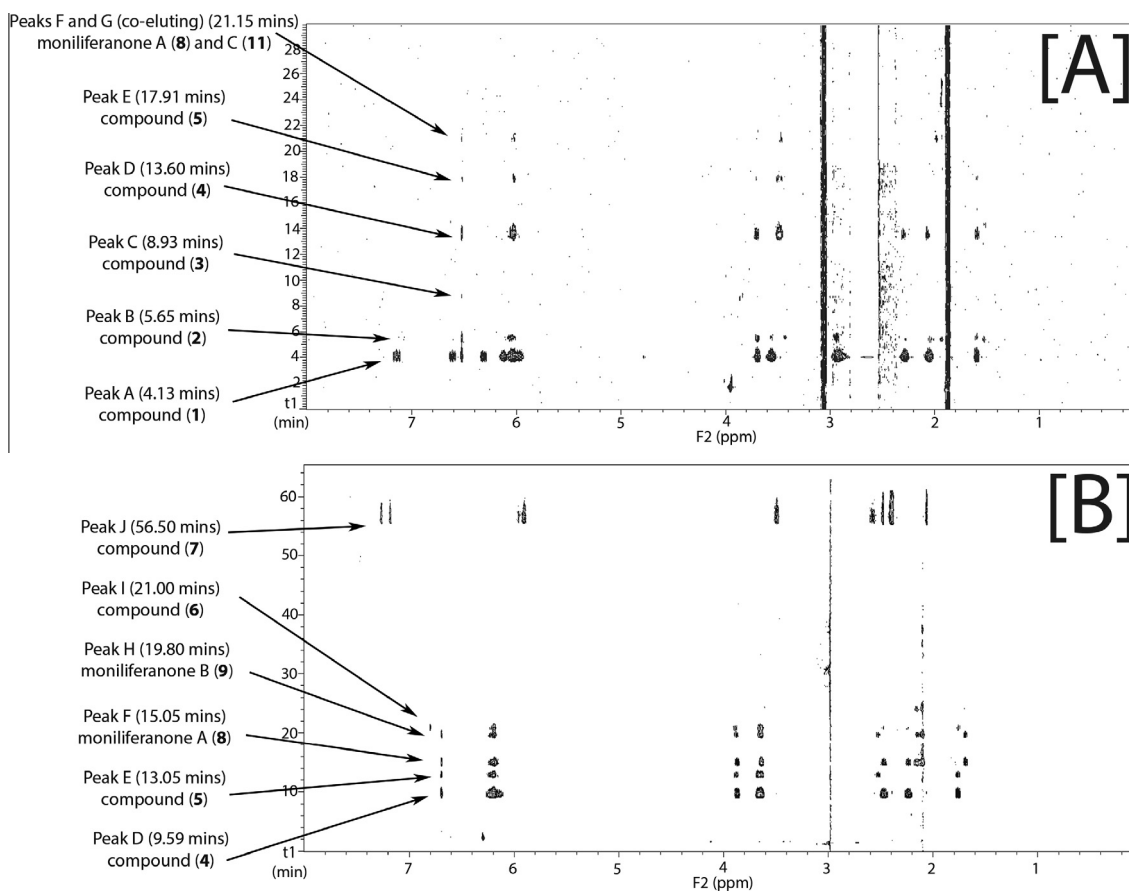


Fig. 1. (A) On-flow HPLC–NMR 2D contour plot (500 MHz, 70% CH_3CN/D_2O) of the dichloromethane crude extract of *C. monilifera* and (B) On-flow HPLC–NMR 2D contour plot (500 MHz, 75% CH_3CN/D_2O) of the dichloromethane crude extract of *C. subfarcinata* illustrating the presence of ten different chemical components (A–J) and three components (D–F) occurring in both crude dichloromethane extracts.

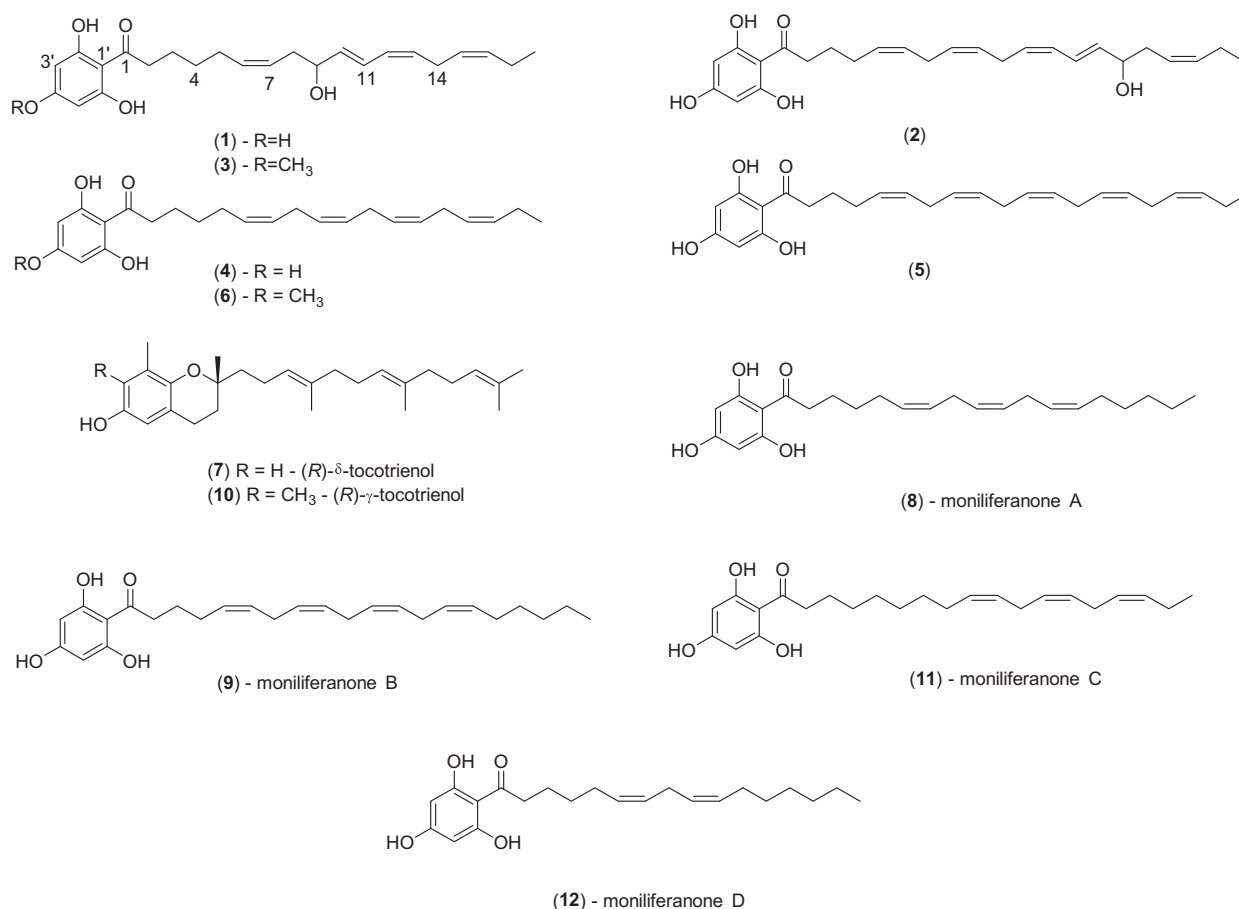


Fig. 2. Structures of the phloroglucinols and tocotrienols identified in *C. monilifera* and *C. subfarcinata*.

group at position 5. To confirm the connectivity from H-4, a 1D TOCSY was acquired whereby excitation of the proton at H-2 showed a transfer of magnetization to H-3 and H-4, and four other protons. A transfer of magnetization to δ_{H} 2.99 was observed, which corresponds to the methylene at position H-5. This particular signal occurs close to the suppression region of the acetonitrile signal, which explains why a correlation between H-4 and H-5 was not observed in the gCOSY NMR spectrum obtained via HPLC–NMR. The proton at H-2 also showed a transfer of magnetization to the olefinic protons at δ_{H} 6.20, confirming the double bond placement at C-6/C-7. Lastly, a transfer of magnetization was observed to another methylene at δ_{H} 3.66 which was assigned to position H-8. The HSQCAD NMR spectrum indicated that the methylene at δ_{H} 3.66 was associated with a carbon at δ_{C} 26.2, which is diagnostic of a methylene located between two double bonds, as in the case of the phloroglucinols (Amico et al., 1981, 1982; Blackman et al., 1988; Gerwick and Fenical, 1982; Gregson et al., 1977; Kazlauskas et al., 1981), and that each of the three double bonds in **8** are separated by one methylene group. These features allowed the structure for **8** to be proposed as 1-(2,4,6-trihydroxyphenyl)-octadeca-6Z,9Z,12Z-trien-1-one, attributed the trivial name moniliferanone A. No structure could be proposed for peak G due to the limited NMR data that could be obtained via HPLC–NMR, but based on the similarity of the NMR and mass spectrometric data, it was known to represent a structural isomer.

Similarly, peak H displayed characteristic phloroglucinol signals (δ_{H} 6.72, s, (2H); 6.27–6.20, m (8H); 3.90, t, (2H); 3.67, m (6H)) in the on-flow HPLC–NMR analysis and stop-flow HPLC–NMR allowed for the acquisition of WET1D proton and gCOSY NMR data. Analysis of the gCOSY NMR spectrum allowed for the spin system

between H-2 and H-5 to be secured. Analysis of the high resolution HPLC–MS of **9** yielded the molecular formula C₂₆H₃₆O₄ (observed 411.2540 [M–H][–], calcd for C₂₆H₃₅O₄[–], 411.2541) which supported nine degrees of unsaturation, four of which were attributed to the olefinic bonds (δ_{H} 6.27 (1H), 6.21 (8H)) in the side chain and the remaining five due to the aromatic ring. Examination of the gCOSY NMR data indicated that the first double bond was located at C-5/C-6, and the diagnostic methylene at δ_{H} 3.67 confirmed that each of the four double bonds was separated by a single methylene group. This allowed for the identity of **9** to be proposed as 1-(2,4,6-trihydroxyphenyl)-eicosa-5Z,8Z,11Z,14Z-tetraen-1-one, attributed the trivial name moniliferanone B.

2.2. Off-line isolation of *C. monilifera* and *C. subfarcinata* dichloromethane crude extract secondary metabolites

An off-line isolation approach was carried out on the dichloromethane crude extracts of *C. monilifera* and *C. subfarcinata* to establish which compounds were responsible for the antimicrobial activity and to confirm the structures of the suspected new phloroglucinols identified by phytochemical profiling. This yielded eleven compounds (**1**, **2**, **4–12**) of which compounds **1**, **2**, **4–12** were isolated from *C. monilifera* and compounds **4–9** and **11** were isolated from *C. subfarcinata*.

Of the eleven compounds isolated in the off-line isolation study, seven have been previously reported (**1**, **2**, **4–7**, and **10**) while four are new (**8**, **9**, **11** and **12**). Compound **3** was not isolated in the off-line studies. In addition five of the previously reported phloroglucinols (**1**, **2**, **4–6**) have been completely characterized by 2D NMR for the first time, which resulted in carbon chemical shift

assignments for these compounds. Finally two carbon chemical shift revisions are reported for **2**.

All of the off-line NMR and MS data for the known compounds **1** (Kazlauskas et al., 1981), **2** (Amico et al., 1982), **4** (Kazlauskas et al., 1981), **5** (Gerwick and Fenical, 1982), **6** (Gregson et al., 1977), **7** (Ohnmacht et al., 2008), and **10** (Ohnmacht et al., 2008) was in accordance with that reported in the literature.

Analysis of the 1D and 2D NMR data of compound **2** led to a carbon chemical shift revision. Previously, the carbons at positions C-3 and C-4 had been reported as δ_C 27.0 and 24.8 respectively (Amico et al., 1982), but these carbon assignments have now been revised and should be reversed.

Moniliferanone A (**8**) corresponding to peak F in the chemical profiling, was obtained from *C. monilifera* and *C. subfarcinata*. The structure as proposed for **8** by chemical profiling was confirmed by off-line analysis (Table 1) and the position of the double bonds was confirmed by correlations observed in the gHMBC NMR spectrum. Moniliferanone A (**8**) was obtained in an inseparable mixture with moniliferanone C (**11**), however identification was possible because the HPLC–NMR data could be obtained separately for moniliferanone A (**8**) from the crude extract of *C. subfarcinata* since it did not co-occur as a mixture with **11**.

Moniliferanone B (**9**), corresponding to peak H in the chemical profiling, was isolated as an oil from *C. monilifera* and *C. subfarcinata*. The structure proposed for **9** by chemical profiling was confirmed by the off-line analysis (Table 1).

Moniliferanone C (**11**), corresponding to peak G from the photochemical profiling (Fig. 1), was isolated as an oil in a mixture with moniliferanone A (**8**) from *C. monilifera* (in a ratio of approximately 0.45–1) and *C. subfarcinata* (in a ratio of 0.25–1). Identification of moniliferanone C (**11**) within the mixture was made possible since HPLC–NMR provided the ability to resolve and therefore assign the signals belonging solely to moniliferanone A (**8**). The triplet methyl

at δ_H 0.98 is diagnostic for phloroglucinols which have the side chain terminating with an ethyl group, as in the case of compounds **1**, **2**, **4–6** (Amico et al., 1982; Gerwick and Fenical, 1982; Kazlauskas et al., 1981; Wisespongpan and Kuniyoshi, 2003). Subsequent interpretation of the gHMBC NMR spectrum of **11** indicated that the triplet methyl (δ_H 0.98) displayed correlations to two carbons, δ_C 132.0 and 20.6 (C-16 and C-17 respectively). The deshielded methylene (δ_H 2.82; δ_C 25.6) is diagnostic of a methylene between two double bonds, confirming that the double bonds are sequential in their placement. The positions of the remaining double bonds were confirmed to occur at C-9/10, C-12/13 and C-15/16. Complete analysis of the NMR data allowed the compound to be deduced as 1-(2,4,6-trihydroxyphenyl)-octadeca-9Z,12Z,15Z-trien-1-one (**11**), which has been attributed the trivial name moniliferanone B. During the phytochemical profiling of *C. monilifera*, moniliferanone A (**8**) was detected with moniliferanone C (**11**) in a ratio of 1–0.50. This relative ratio is consistent with the ratio obtained for the mixture of **8** and **11** when isolated off-line. However, in the phytochemical profiling *C. subfarcinata*, moniliferanone A (**8**) was detected with moniliferanone C (**11**) in a ratio of 1–0.07. This supported the fact that **11** was essentially absent from the crude extract of *C. subfarcinata*. The ratios suggest that in the time it took to extract and analyze the *C. monilifera* crude extract by HPLC–NMR, moniliferanone A (**8**) and C (**11**) had sufficient time to form an equilibrium mixture. However, in the case of *C. subfarcinata*, the relative proportions of moniliferanone A (**8**) and C (**11**) changed dramatically between the time it took to complete the chemical profiling by HPLC–NMR and the off-line isolation. For this reason it is suspected that moniliferanone C (**11**) may represent an artifact arising from a double bond migration.

Moniliferanone D (**12**) was isolated from *C. monilifera* and *C. subfarcinata* as an oil. A molecular formula of $C_{22}H_{32}O_4$ was determined by HRESIMS (359.2221 [M–H][−] (calcd for $C_{22}H_{31}O_4$,

Table 1
NMR data (500 MHz, CDCl₃) for moniliferanone A (**8**) and B (**9**).

Position	Moniliferanone A (8)				Moniliferanone B (9)			
	δ_C^a , type	δ_H (J in Hz)	gCOSY	gHMBC	δ_C^a , type	δ_H (J in Hz)	gCOSY	gHMBC
1	205.9, C				205.9, C			
2	43.8, CH ₂	3.11, t (7.5)	3	1, 3, 4	43.6, CH ₂	3.13, t (7.5)	3	1, 3
3	24.4, CH ₂	1.72, m	2, 4	4	24.8, CH ₂	1.78, m	2, 4	1, 2, 4, 5
4	29.5, CH ₂	1.46, m	3, 5	3, 6	27.2, CH ₂	2.18, dt (7.0, 7.0)	3, 5	2, 3, 5, 6
5	27.2, CH ₂	2.12, dt (7.5, 7.5)	4, 6	3, 4, 6, 7	130.0, CH	5.44, m	4	
6	130.0, CH	5.41, m	5		128.2, CH	5.37, m	7	7
7	128.0, CH	5.37, m	8	8, 9	25.9, CH ₂	2.83, m	6, 8	8, 9
8	25.6, CH ₂	2.82, m	7, 9	7, 9	128.6, CH	5.37, m	7	7, 10
9	128.1, CH	5.37, m	8	8, 10, 11	128.6, CH	5.37, m	10	7, 10
10	128.1, CH	5.37, m	11	8, 9, 11	25.9, CH ₂	2.83, m	9, 11	8, 9, 11, 12
11	25.6, CH ₂	2.82, m	10, 12	10	128.6, CH	5.37, m	10	10, 13
12	127.7, CH	5.37, m	11	11	128.6, CH	5.37, m	13	10, 13
13	130.5, CH	5.39, m			25.9, CH ₂	2.83, m	12, 14	11, 12
14	27.2, CH ₂	2.06, dt (7.5, 7.5)	13, 15	12, 13, 15, 16	128.1, CH	5.37, m	13	13
15	29.5, CH ₂	1.34, m	14	13, 14	130.8, CH	5.40, m	16	
16	31.5, CH ₂	1.29, m			27.5, CH ₂	2.05, dt (7.0, 7.0)	15, 17	14, 15, 17
17	22.6, CH ₂	1.30, m	18	16	29.6, CH ₂	1.34, m	16	
18	14.1, CH ₃	0.89, t (7.0)	17	16, 17	31.8, CH ₂	1.27, m		
19					22.9, CH ₂	1.29, m	20	18
20					14.3, CH ₃	0.89, t (6.5)	19	18, 19
1'	104.8, C				105.0, C			
2'	161.0, C				ND ^b			
3'	95.5, CH	5.90, bs		1', 4', 5'	95.7, CH	5.91, s		1'
4'	163.4, C				ND ^b			
5'	95.5, CH	5.90, bs		1', 3', 4'	95.7, CH	5.91, s		1'
6'	161.0, C				ND ^b			
2'-OH		13.47, bs				12.00, bs		
4'-OH		13.49, bs				12.00, bs		
6'-OH		13.47, bs				12.00, bs		

^a Carbon assignment based on gHSQCAD and gHMBC NMR experiments.

^b Indicates signal not detected.

Table 2
NMR data (500 MHz, CDCl₃) for moniliferanone C (**11**) and moniliferanone D (**12**).

Position	Moniliferanone C (11)				Moniliferanone D (12)			
	δ_c^a , type	δ_H (J in Hz)	gCOSY	gHMBC	δ_c^a , type	δ_H (J in Hz)	gCOSY	gHMBC
1	205.9, C				206.0, C			
2	43.8, CH ₂	3.09, t (7.5)	1.72	1, 3, 4	43.8, CH ₂	3.13, t (7.5)	3	1, 3
3	24.4, CH ₂	1.72, m	3.11, 1.46	4	24.5, CH ₂	1.73, m	2, 4	
4	29.5, CH ₂	1.48, m	1.72, 1.36	3	29.5, CH ₂	1.45, tt (7.0, 8.0)	3, 5	
5	29.4, CH ₂	1.36, m			27.2, CH ₂	2.12, dt (7.0, 7.5)	4, 6	3, 4, 6, 7
6	29.4, CH ₂	1.36, m			130.2, CH	5.39, m	5	
7	29.4, CH ₂	1.36, m		6	128.2, CH	5.36, m		
8	27.2, CH ₂	2.12, dt (7.5, 7.5)	5.41, 1.46	7, 9, 10	25.6, CH ₂	2.79, dd (6.0, 7.5)	7	7, 10
9	130.0, CH	5.41, m	2.12		128.2, CH	5.36, m		
10	128.1, CH	5.37, m	2.82	11, 12	130.2, CH	5.39, m	11	
11	25.6, CH ₂	2.82, m	5.37	10, 12, 13	27.2, CH ₂	2.04, dt (6.5, 7.0)	10, 12	9, 10, 12
12	128.1, CH	5.37, m	2.82	10, 11, 13, 14	29.4, CH ₂	1.29, m	11	
13	128.1, CH	5.37, m	2.82	11, 12, 14, 15	29.4, CH ₂	1.29, m		
14	25.6, CH ₂	2.82, m	5.37	12, 13, 15	31.6, CH ₂	1.26, m		
15	128.1, CH	5.37, m	2.82	13, 14	22.6, CH ₂	1.29, m	16	14
16	132.0, CH	5.40, m	2.09		14.1, CH ₃	0.87, m	15	14, 15
17	20.6, CH ₂	2.09, m	0.98, 5.40					
18	14.3, CH ₃	0.98, t (7.5)	2.09	16, 17				
1'	104.8, C				ND ^b			
2'	161.0, C				ND ^b			
3'	95.5, CH	5.90, bs		1', 4', 5'	95.4, CH	5.92, bs		
4'	163.4, C				ND ^b			
5'	95.5, CH	5.90, bs		1', 3', 4'	95.4, CH	5.92, bs		
6'	161.0, C				ND ^b			
2'-OH		13.47, bs				ND ^b		
4'-OH		13.49, bs				ND ^b		
6'-OH		13.47, bs				ND ^b		

^a Carbon assignment based on gHSQCAD and gHMBC NMR experiments.

^b Indicates signal not detected.

359.2228) possessing seven degrees of unsaturation, indicating that only two double bonds (δ_H 5.39, 5.36; 4H) were present. The side chain for moniliferanone D (**12**) was also shorter than that observed for moniliferanone C (**11**), consisting of a total of 16 carbons. Analysis of the gCOSY NMR correlations was vital in positioning the double bonds. The spin system from H-2 to H-6 could be secured and allowed placement of the double bonds at positions C-6/7 and C-9/10 respectively. Complete analysis of the NMR data (Table 2) allowed for the identity to be deduced as 1-(2,4,6-trihydroxyphenyl)-hexadeca-6Z,9Z-tetraen-1-one (**12**), attributed the trivial name moniliferanone D.

The configuration of the double bonds for each of the compounds isolated was determined by comparison to literature data, if available, and by consideration of ¹H NMR and IR data. The absence of significant absorptions between 800 and 900 cm⁻¹ in the IR spectrum, is supportive of a Z double bond configuration (Gerwick and Fenical, 1982). In addition Z double bond geometries show a narrow multiplet for the chemical shift corresponding to the olefinic proton signals (Kazlauskas et al., 1981). Also methylenes adjacent to the double bonds display carbon chemical shifts in the region δ_C 25–26 ppm, which is typical of methylenes shielded by two cis-double bonds (Amico et al., 1982). The E double bond geometries were concluded on the basis of ¹H NMR coupling constants. The absolute configuration of the secondary alcohol in **1** and **2** remains undefined, since these compounds underwent rapid degradation and no specific rotations could be obtained prior to their decomposition. The absolute configuration of the secondary alcohol compound **3**, which was not isolated by the off-line approach, also remains unassigned. All naturally occurring tocotrienols reported to date display an R configuration at the stereogenic centre at position 2 (Drotleff and Ternes, 1999, 2001). On this basis the absolute configuration of the single stereogenic centre in δ -tocotrienol (**7**) and γ -tocotrienol (**10**) was concluded to most likely be R, and the measured specific rotation of δ -tocotrienol (**7**) was in agreement with that reported in the literature

(Couladouros et al., 2007). This would represent the first report of R- γ -tocotrienol (**10**) being isolated from a marine source.

2.3. Biological activity studies

All eleven of the compounds isolated in the off-line phytochemical profiling of *C. monilifera* and *C. subfarinata* were assessed for antimicrobial activity against nine organisms. The isolated compounds (**1**, **2**, **4–12**), together with a commercially available antibacterial and antifungal agent, were tested at 1 mg/mL and all displayed varying degrees of zones of inhibition in the antimicrobial assays (Table 3).

Biological activities have been previously reported for **2**, **4** and **6**, which have been shown to inhibit the growth of *Bacillus subtilis* and *Staphylococcus aureus* (Gerwick and Fenical, 1982; Wisespongpan and Kuniyoshi, 2003). R- δ -Tocotrienol (**7**) and R- γ -tocotrienol (**10**) display broad biological activities including the ability to induce cell cycle arrest and apoptosis in various cells such as adipocytes, colon carcinoma, pancreatic cancer and lung cancer (Hodul et al., 2013; Ji et al., 2011; Wu et al., 2013; Zhang et al., 2013).

Five of the phloroglucinols (**1**, **4**, **6**, **9** and **12**) isolated displayed selective antibacterial properties, against both gram positive and gram negative bacteria. Four of the compounds (**1**, **4**, **9** and **12**) only showed activity against *Streptococcus pyogenes*, which is responsible for various ear, eye and sinus infections, along with septic arthritis (Ryan and Ray, 2010). Compound **6** inhibited the growth of both gram positive and gram negative bacteria, such as *S. aureus* and *Pseudomonas aeruginosa*. Interest in obtaining drug leads to target *P. aeruginosa* has increased because of the prevalence and multidrug resistance this micro-organism has shown (Master et al., 2011). All of the active phloroglucinols (**1**, **4**, **6**, **9** and **12**) were noticeably less active than a commercially available antibacterial agent (ampicillin).

Table 3

Antimicrobial activity of the crude extracts and pure compounds obtained from *C. monilifera* and *C. subfarcinata*, together with commercial standard antibacterial and antifungal compounds, showing zones of inhibition (mm).

	Microorganism Concentration (mg/mL)	<i>E. coli</i> ATCC 25922	<i>S. aureus</i> ATCC 25923	<i>S. aureus</i> MRSA 344/2-32	<i>P. aeruginosa</i> ATCC 27853	<i>S. pyogenes</i> 345/1	<i>B. subtilis</i> ATCC 19659	<i>C. albicans</i> ATCC 10231 or 14053*	<i>T. mentagrophytes</i> ATCC 28185	<i>C. resinae</i>
Dichloromethane extract of <i>C. monilifera</i>	50	ND ^a	1	2	ND ^a	6	NT ^b	ND ^a	NT ^b	NT ^b
Methanol extract of <i>C. monilifera</i>	50	ND ^a	ND ^a	ND ^a	ND ^a	ND ^a	NT ^b	ND ^a	NT ^b	NT ^b
3:1 MeOH/DCM extract of <i>C. subfarcinata</i>	50	ND ^a	NT ^b	NT ^b	1	NT ^b	ND ^a	ND ^{a*}	3	ND ^a
Compound 1	1	ND ^a	ND ^a	ND ^a	ND ^a	1	NT ^b	ND ^a	NT ^b	NT ^b
Compound 2	1	ND ^a	ND ^a	ND ^a	ND ^a	ND ^a	NT ^b	ND ^a	NT ^b	NT ^b
Compound 4	1	ND ^a	ND ^a	ND ^a	ND ^a	1	NT ^b	ND ^a	NT ^b	NT ^b
Compound 5	1	ND ^a	ND ^a	ND ^a	ND ^a	ND ^a	NT ^b	ND ^a	NT ^b	NT ^b
Compound 6	1	ND ^a	1	ND ^a	1	ND ^a	NT ^b	ND ^a	NT ^b	NT ^b
<i>R</i> - δ -Tocotrienol (7)	1	ND ^a	ND ^a	ND ^a	ND ^a	ND ^a	NT ^b	ND ^a	NT ^b	NT ^b
Mixture of moniliferanone A (8) and C (11)	1	ND ^a	ND ^a	ND ^a	ND ^a	ND ^a	NT ^b	ND ^a	NT ^b	NT ^b
Moniliferanone B (9)	1	ND ^a	ND ^a	ND ^a	ND ^a	1	NT ^b	ND ^a	NT ^b	NT ^b
<i>R</i> - γ -Tocotrienol (10)	1	ND ^a	ND ^a	ND ^a	ND ^a	ND ^a	NT ^b	ND ^a	NT ^b	NT ^b
Moniliferanone D (12)	1	ND ^a	ND ^a	ND ^a	ND ^a	1	NT ^b	ND ^a	NT ^b	NT ^b
Ampicillin (antibacterial)	1	ND ^a	15	3	2	20	NT ^b	NT ^b	NT ^b	NT ^b
Carbendazim (antifungal)	1	NT ^b	NT ^b	NT ^b	NT ^b	NT ^b	NT ^b	ND ^a	NT ^b	NT ^b

^a Indicates no zone of inhibition detected.

^b Indicates not tested.

* Indicates tested against ATCC 14053.

3. Conclusions

Phytochemical profiling and dereplication employing HPLC–NMR and HPLC–MS methodologies was successful in identifying six known (**1**–**6**) phloroglucinols along with one known tocotrienol (**7**), and three suspected new (**8**, **9** and **11**) phloroglucinols. Subsequent off-line isolation yielded five phloroglucinols (**1**, **4**, **6**, **9**, and **12**) displaying slight but selective antibacterial activity.

4. Experimental section

4.1. General experimental procedures

For details on the general experimental procedures please refer to (Brkljača and Urban, 2015). For both on-flow and stop-flow HPLC–NMR modes 50 μ L injections of *C. monilifera* and *C. subfarcinata* (4971 and 4999 μ g, respectively) of the dichloromethane extracts were injected onto an Agilent Eclipse Plus C₁₈ (150 \times 4.6) 5 μ column using a solvent composition of 70% or 75% CH₃CN/D₂O (*C. monilifera* and *C. subfarcinata*, respectively) at a flow rate of 1 mL/min. In the stop-flow HPLC–NMR mode WET1D, gCOSY, HSQCAD, gHMBCAD and 1D TOCSY NMR experiments were acquired. HRESILCMS was carried out using an Agilent Eclipse Plus C₁₈ (4.6 \times 150) 5 μ column using a solvent composition of 70% or 75% CH₃CN/H₂O (*C. monilifera* and *C. subfarcinata*, respectively) at a flow rate of 1 mL/min. Analytical HPLC analyses were carried out using either a gradient method 0–2 min 10% CH₃CN/H₂O; 14–24 min 75% CH₃CN/H₂O; 26–30 min 100% CH₃CN and 32–40 min 10% CH₃CN/H₂O or an isocratic method (either 100%, 90% or 80% CH₃CN/H₂O) on an Alltech Alltima HP C₁₈ (250 \times 4.6) 5 μ column at a flow rate of 1.0 mL/min. Semi-preparative HPLC analysis were carried out using an isocratic method (either 100%, 90%, 85% or 80% CH₃CN/H₂O) and an Alltech Alltima C₁₈ (250 \times 10) 5 μ column at a flow rate of 3.5 or 4.0 mL/min.

4.2. Biological evaluation

For details on the biological evaluation please refer to (Brkljača and Urban, 2015). The crude extract of *C. subfarcinata*

was also assessed for antimicrobial activity at the University of Canterbury, Christchurch, New Zealand. A standardized inoculum was prepared by transferring a loop of bacterial/fungal cells, from a freshly grown stock slant culture, into a 10 mL vial of sterile water. This was vortexed and compared to a 5% BaCl₂ in water standard to standardize the cell density. This gave a cell density of 108 colony-forming units per mL. Ten milliliters of the standardized inoculum was then added to 100 mL of Mueller Hinton or potato dextrose agar (at between 40 and 50 °C) and mixed by swirling, giving a final cell density of 107 colony forming units per mL. Five milliliters of this was poured into sterile 85 mm petri dishes. The suspensions were allowed to cool and solidify on a level surface to give a 'lawn' of bacteria/fungi over the dish (for further information see www.clsi.org). The crude extract was pipetted onto 6 mm diameter filter paper disks and the solvent evaporated. This disks were then placed onto the prepared seeded agar dishes (with appropriate solvent and positive controls) and incubated. Active antimicrobial samples displayed a zone of inhibition outside the disk, which was measured in mm as the radius of inhibition for each bacteria/fungi. The six organisms were *Escherichia coli* (ATCC 25922), *B. subtilis* (ATCC 19659) and *P. aeruginosa* (ATCC27853) for the bacteria and, *Candida albicans* (ATCC 14053), *Trichophyton mentagrophytes* (ATCC 28185) and *Cladosporium resinae* for the fungi. Since the completion of these studies the University of Canterbury has phased out these antimicrobial assays.

4.3. Alga material

C. monilifera was collected via SCUBA on 21 April, 2010 from Governor Reef (near indented head), Port Phillip Bay, Victoria, Australia. *C. subfarcinata* was collected by hand intertidally on 22 January, 2006 from the Borough of Queenscliffe (near Point Lonsdale), Port Phillip Bay, Victoria, Australia. The algae were identified by Dr. Gerry Kraft (The University of Melbourne) and voucher specimens (designated the code number 2010–14 and 2006–11, respectively) are deposited at the School of Applied Sciences (Discipline of Applied Chemistry), RMIT University.

4.4. Chemical profiling

Chemical profiling was carried out on the dichloromethane soluble extracts of the algae employing HPLC–NMR and HPLC–MS. Details of these analyses are provided in the general experimental procedures section and (Brkljača and Urban, 2015). The dichloromethane extracts of *C. monilifera* and *C. subfarcinata* (170.0 and 741.9 mg, respectively) were dissolved in HPLC–NMR grade CH₃CN (1710 and 7420 μL, respectively) and filtered through a 0.45 PTFE membrane filter (Grace Davison Discovery Sciences).

4.5. Extraction and isolation of *C. monilifera*

C. monilifera (58 g, wet weight) was extracted with 3:1 methanol/dichloromethane (2 L). The crude extract was then decanted and concentrated under reduced pressure and sequentially solvent partitioned (trituated) into dichloromethane and methanol soluble extracts respectively. The dichloromethane extract was subjected to flash silica gel column chromatography (20% stepwise elution from petroleum spirits (60–80 °C) to dichloromethane to ethyl acetate and finally to methanol). The 100% dichloromethane and 80% dichloromethane (first fraction) silica gel column fraction were further purified by reversed phase HPLC (100% CH₃CN) to yield *R*-δ-tocotrienol (**7**) (3.0 mg, 0.03%) and *R*-γ-tocotrienol (**10**) (2.1 mg, 0.02%). The 80% dichloromethane (second fraction) silica gel column fraction was further fractionated by Sephadex LH-20 chromatography (100% methanol) to yield 6 fractions. The second fraction was further purified using reversed phase HPLC (90% CH₃CN) to yield **1** (1.6 mg, 0.01%) and **2** (1.3 mg, 0.01%). The third fraction from the Sephadex LH-20 column was further fractionated by VLC C₁₈ column chromatography (20% stepwise elution from water to methanol and finally to dichloromethane) to yield 12 fractions. The 100% methanol and 80% methanol fractions were combined. The combined fraction was subjected to reversed phase HPLC (90% CH₃CN) in which the compounds eluting between 0 and 14 min were collected into one flask and the compounds eluting from 14 to 40 min were collected into another flask. The compounds which eluted between 0 and 14 min were subjected to reversed phase HPLC purification (90% CH₃CN) to yield **4** (2.7 mg, 0.03%) and **5** (1.4 mg, 0.01%). The compounds eluting between 14 and 40 min were subjected to further purification by reversed phase HPLC (90% CH₃CN) to yield 3 compounds; moniliferanone D (**12**) (0.6 mg, 0.002%) and a mixture of moniliferanone A and C (**8** and **11**) (2.6 mg, 0.02%). One of the peaks from the reversed phase HPLC purification of 14–40 min was further purified by reversed phase HPLC (80% CH₃CN) to yield **6** (0.3 mg, 0.003%) and moniliferanone B (**9**) (0.7 mg, 0.01%). The percentage yields are reported on the basis of the dry mass of the alga extracted.

4.6. Extraction and isolation of *C. subfarcinata*

C. subfarcinata (20 g, wet weight) was extracted with 3:1 methanol/dichloromethane (2 L). The crude extract was then decanted and concentrated under reduced pressure and sequentially solvent partitioned (trituated) into dichloromethane and methanol soluble extracts respectively. The dichloromethane extract was subjected to reversed phase HPLC (85% CH₃CN) to yield **4** (18.4 mg, 0.2%), **5** (5.3 mg, 0.06%), a mixture of **6** and moniliferanone B (**9**) (6.8 mg, 0.08%), *R*-δ-tocotrienol (**7**) (14.9 mg, 0.2%) and a mixture of moniliferanone A and C (**8** and **11**) (7.5 mg, 0.09%). The percentage yields are reported on the basis of the dry mass of the alga extracted.

4.7. On-line (HPLC–NMR & HPLC–MS) characterization of compounds

9-Hydroxy-1-(2,4,6-trihydroxyphenyl)-6Z,10E,12Z,15Z-octadecatetraen-1-one (**1**): HPLC–NMR WET 1D NMR (500 MHz, 70% CH₃CN/D₂O) obtained from stop-flow mode δ 7.21 (1H, dd, *J* = 11.0, 15.0, H-11), 6.67 (1H, t, *J* = 11.0 Hz, H-12), 6.59 (2H, s, H-3', H-5'), 6.38 (1H, dd, *J* = 6.5, 15.0 Hz, H-10), 6.18 (1H, m, H-6), 6.18–6.10 (2H, m, H-15, H-16), 6.10 (2H, m, H-7, H-13), 4.84 (1H, dt, *J* = 6.5, 7.0 Hz, H-9), 3.76 (2H, t, *J* = 7.0 Hz, H-2), 3.62 (2H, q, *J* = 7.5 Hz, H-14), 2.99 (2H, m, H-8), 2.34 (2H, p, *J* = 7.0 Hz, H-3), 2.10 (2H, p, *J* = 7.0 Hz, H-4), 1.66 (3H, t, *J* = 7.5 Hz, H-18); HPLC–NMR ¹³C NMR (125 MHz, 70% CH₃CN/D₂O) obtained from a HSQC experiment in stop-flow mode δ 207.4 (C, C-1), 165.0 (C, C-2', C-4', C-6'), 137.2 (CH, C-10), 133.1 (CH, C-16), 132.8 (CH, C-6), 131.1 (CH, C-13), 128.9 (CH, C-12), 127.5 (CH, C-15), 126.2 (CH, C-7), 126.1 (CH, C-11), 105.2 (C, C-1'), 95.7 (CH, C-3', C-5'), 72.7 (CH, C-9), 44.3 (CH₂, C-2), 35.8 (CH₂, C-8), 29.9 (CH₂, C-4), 27.8 (CH₂, C-5), 26.5 (CH₂, C-14), 25.1 (CH₂, C-3), 21.1 (CH₂, C-17), 14.6 (CH₃, C-18); HRESILCMS *m/z* 399.2177 (calcd for C₂₄H₃₁O₅, 399.2177).

15-Hydroxy-1-(2,4,6-trihydroxyphenyl)-5Z,8Z,11Z,13E,17Z-eicosapentaen-1-one (**2**): HPLC–NMR WET 1D NMR (500 MHz, 70% CH₃CN/D₂O) obtained from stop-flow mode δ 7.17 (1H, dd, *J* = 11.0, 14.5 Hz, H-13), 6.67 (1H, dd, *J* = 11.0, 11.0 Hz, H-12), 6.35 (1H, dd, *J* = 6.0, 14.5 Hz, H-14), 6.25–6.05 (6H, m, H-5, H-6, H-8, H-9, H-17, H-18), 6.15 (1H, m, H-11), 4.83 (1H, dt, *J* = 6.0, 7.5 Hz, H-15), 3.76 (2H, t, *J* = 7.5 Hz, H-2), 2.88 (2H, m, H-10), 2.35 (2H, p, *J* = 7.5 Hz, H-3), 2.11 (2H, m, H-4), 2.01 (2H, m, H-19), 1.59 (3H, t, *J* = 6.5 Hz, H-20); HRESILCMS *m/z* 425.2334 (calcd for C₂₆H₃₃O₅, 425.2333).

9-Hydroxy-1-(2,6-dihydroxy-4-methoxyphenyl)-6Z,10Z,12Z,15Z-octadecatetraen-1-one (**3**): HPLC–NMR WET 1D NMR (500 MHz, 70% CH₃CN/D₂O) obtained from stop-flow mode δ 7.25 (1H, dd, *J* = 11.5, 15.0, H-11), 6.70 (1H, t, *J* = 10.5 Hz, H-12), 6.59 (2H, s, H-3', H-5'), 6.24–6.05 (6H, m, H-6, H-7, H-10, H-13, H-15, H-16), 4.39 (1H, dt, *J* = 6.5, 8.0 Hz, H-9), 3.93 (3H, s, H-4'-OCH₃), 3.75 (2H, t, *J* = 7.5 Hz, H-2), 3.63 (2H, dd, *J* = 7.0, 8.0 Hz, H-14), 2.99 (2H, m, H-8), 2.34 (2H, m, H-3), 2.10 (2H, m, H-4), 1.66 (3H, t, *J* = 7.5 Hz, H-18); HRESILCMS *m/z* 413.2333 (calcd for C₂₅H₃₃O₅, 413.2333).

1-(2,4,6-Trihydroxyphenyl)-6Z,9Z,12Z,15Z-octadecatetraen-1-one (**4**): HPLC–NMR WET 1D NMR (500 MHz, 70% CH₃CN/D₂O) obtained from stop-flow mode δ 6.60 (2H, s, H-3', H-5'), 6.10 (8H, m, H-6, H-7, H-9, H-10, H-15, H-16), 3.77 (2H, t, *J* = 7.5 Hz, H-2), 3.55 (6H, m, H-8, H-11, H-14), 2.83 (2H, m, H-5), 2.37 (2H, p, *J* = 7.5 Hz, H-3), 2.13 (2H, p, *J* = 7.5 Hz, H-4), 1.66 (3H, t, *J* = 7.5 Hz, H-18); HRESILCMS *m/z* 383.2222 (calcd for C₂₄H₃₁O₄, 383.2228).

1-(2,4,6-Trihydroxyphenyl)-5Z,8Z,11Z,14Z,17Z-eicosapentaen-1-one (**5**): HPLC–NMR WET 1D NMR (500 MHz, 70% CH₃CN/D₂O) obtained from stop-flow mode δ 6.59 (2H, s, H-3', H-5'), 6.08 (10H, m, H-5, H-6, H-8, H-9, H-11, H-12, H-14, H-15, H-17, H-18), 3.77 (2H, t, *J* = 7.0 Hz, H-2), 3.53 (8H, m, H-7, H-10, H-13, H-16), 2.41 (4H, m, H-3, H-4), 1.65 (3H, t, *J* = 8.0 Hz, H-20); HRESILCMS *m/z* 409.2385 (calcd for C₂₆H₃₃O₄, 409.2384).

1-(2,6-Dihydroxy-4-methoxyphenyl)-6Z,9Z,12Z,15Z-octadecatetraen-1-one (**6**): HPLC–NMR WET 1D NMR (500 MHz, 75% CH₃CN/D₂O) obtained from stop-flow mode δ 6.82 (2H, s, H-3', H-5'), 6.20 (8H, m, H-6, H-7, H-9, H-10, H-12, H-13, H-15, H-16), 3.90 (2H, t, *J* = 7.0 Hz, H-2), 3.66 (6H, m, H-8, H-11, H-14), 2.49 (2H, p, *J* = 7.0 Hz, H-3), 2.25 (2H, p, *J* = 7.0 Hz, H-4), 2.11 (2H, m, H-17), 1.77 (3H, t, *J* = 7.5 Hz, H-18); HRESILCMS *m/z* 397.2381 (calcd for C₂₅H₃₃O₄, 397.2384).

R-δ-tocotrienol (**7**): HPLC–NMR WET 1D NMR (500 MHz, 75% CH₃CN/D₂O) obtained from stop-flow mode δ 7.28 (1H, s, H-7), 7.20 (1H, s, H-5), 5.97 (1H, t, *J* = 7.0 Hz, H-3'), 5.92 (2H, m, H-7', H-11'), 3.51 (2H, t, *J* = 7.0 Hz, H-4), 3.38 (4H, m, H-5', H-9'), 2.95

(6H, m, H-2', H-6', H-10'), 2.60 (2H, m, H-3), 2.49 (3H, s, 12b'-CH₃), 2.42 (3H, s, 8'-CH₃), 2.41 (3H, s, 4'-CH₃), 2.40 (3H, s, 12a'-CH₃), 2.08 (3H, s, 2-CH₃). *Signals interchangeable.

1-(2,4,6-Trihydroxyphenyl)-octadeca-6Z,9Z,12Z-trien-1-one (**8**): HPLC-NMR WET 1D NMR (500 MHz, 70% CH₃CN/D₂O) obtained from stop-flow mode δ 6.73 (2H, s, H-3', H-5'), 6.20 (6H, m, H-6, H-7, H-9, H-10, H-12, H-13), 3.90 (2H, t, J = 7.5 Hz, H-2), 3.66 (4H, m, H-8, H-11), 2.99 (2H, m, H-5), 2.50 (2H, p, J = 7.5 Hz, H-3), 2.26 (2H, p, J = 7.5 Hz, H-4), 2.18 (4H, m, H-15, H-16), 2.13 (2H, m, H-17), 1.72 (3H, t, J = 7.0 Hz, H-18); HPLC-NMR ¹³C NMR (125 MHz, 75% CH₃CN/D₂O) obtained from a HSQC experiment in stop-flow mode δ 128.8 (CH, C-6, C-7, C-9, C-10, C-12, C-13), 95.7 (CH, C-3', C-5'), 26.2 (CH₂, C-8, C-11); HRESILCMS m/z 385.2384 (calcd for C₂₄H₃₃O₄, 385.2384).

1-(2,4,6-Trihydroxyphenyl)-eicosa-5Z,8Z,11Z,14Z-tetraen-1-one (moniliferanone B) (**9**): HPLC-NMR WET 1D NMR (500 MHz, 75% CH₃CN/D₂O) obtained from stop-flow mode δ 6.72 (2H, s, H-3', H-5'), 6.21 (8H, m, H-5, H-6, H-8, H-9, H-11, H-12, H-14, H-15), 3.90 (2H, t, J = 7.0 Hz, H-2), 3.67 (6H, m, H-7, H-10, H-13), 2.98 (2H, m, H-4), 2.55 (2H, p, J = 7.0 Hz, H-3), 2.17 (4H, m, H-17, H-18), 2.13 (2H, m, H-19), 1.71 (3H, t, J = 6.5 Hz, H-20); HRESILCMS m/z 411.2540 (calcd for C₂₆H₃₅O₄, 411.2541).

4.8. Off-line characterization of compounds

9-Hydroxy-1-(2,4,6-trihydroxyphenyl)-6Z,10E,12Z,15Z-octadecatetraen-1-one (**1**): unstable pale yellow oil; All off-line NMR spectroscopic and mass spectrometric data was identical to that reported in the literature (Kazlauskas et al., 1981). ¹³C NMR (125 MHz, CDCl₃) obtained from HSQC and HMBC NMR experiments δ 135.1 (CH, C-10), 133.6 (CH, C-6), 132.5 (CH, C-16), 131.0 (CH, C-13), 127.7 (CH, C-12), 126.4 (CH, C-15), 125.9 (CH, C-11), 124.5 (CH, C-7), 94.5 (CH, C-3', C-5'), 72.4 (CH, C-9), 43.4 (CH₂, C-2), 35.2 (CH₂, C-8), 29.2 (CH₂, C-4), 26.8 (CH₂, C-5), 26.0 (CH₂, C-14), 24.5 (CH₂, C-3), 20.6 (CH₂, C-17), 14.3 (CH₃, C-18).

15-Hydroxy-1-(2,4,6-trihydroxyphenyl)-5Z,8Z,11Z,13E,17Z-eicosapentaen-1-one (**2**): unstable pale yellow oil; All off-line NMR spectroscopic and mass spectrometric data was identical to that reported in the literature (Amico et al., 1982). ¹³C NMR (125 MHz, CDCl₃) obtained from HSQC and HMBC NMR experiments δ 206.0 (C, C-1), 134.6 (CH, C-14), 133.5 (CH, C-11), 132.6 (CH, C-18), 131.8 (CH, C-6*), 129.7 (CH, C-5), 128.2 (CH, C-8*), 127.5 (CH, C-12), 126.4 (CH, C-9), 126.3 (CH, C-13), 124.4 (CH-C-17), 95.4 (CH, C-3', C-5'), 72.6 (CH, C-15), 43.8 (CH₂, C-2), 35.1 (CH₂, C-16), 27.5 (CH₂, C-4), 26.0 (CH₂, C-10), 25.9 (CH₂, C-7), 24.7 (CH₂, C-3), 20.6 (CH₂, C-19), 14.3 (CH₃, C-20). *Signals interchangeable.

1-(2,4,6-Trihydroxyphenyl)-6Z,9Z,12Z,15Z-octadecatetraen-1-one (**4**): unstable pale yellow oil; All off-line NMR spectroscopic and mass spectrometric data was identical to that reported in the literature (Kazlauskas et al., 1981). ¹³C NMR (125 MHz, CDCl₃) obtained from HSQC and HMBC NMR experiments δ 205.9 (C, C-1), 132.1 (CH, C-16), 130.1 (CH, C-6), 128.2 (CH, C-7, C-9, C-10, C-12, C-13), 127.1 (CH, C-15), 95.5 (CH, C-3', C-5'), 43.7 (CH₂, C-2), 29.5 (CH₂, C-4), 27.7 (CH₂, C-5), 25.6 (CH₂, C-8, C-11, C-14), 24.3 (CH₂, C-3), 20.5 (CH₂, C-17), 14.3 (CH₃, C-18).

1-(2,4,6-Trihydroxyphenyl)-5Z,8Z,11Z,14Z,17Z-eicosapentaen-1-one (**5**): unstable pale yellow oil; All off-line NMR spectroscopic and mass spectrometric data was identical to that reported in the literature (Gerwick and Fenical, 1982). ¹³C NMR (125 MHz, CDCl₃) obtained from HSQC and HMBC NMR experiments δ 205.8 (C, C-1), 163.5 (C, C-2', C-4', C-6'), 132.1 (CH, C-18), 129.9 (CH, C-5), 128.3 (CH, C-6, C-8, C-9, C-11, C-12, C-14, C-15), 127.0 (CH, C-17), 104.8 (C, C-1'), 95.5 (CH, C-3', C-5'), 43.4 (CH₂, C-2), 26.9 (CH₂, C-4), 25.6 (CH₂, C-7, C-10, C-13, C-16), 24.5 (CH₂, C-3), 20.4 (CH₂, C-19), 14.2 (CH₃, C-20).

1-(2,6-Dihydroxy-4-methoxyphenyl)-6Z,9Z,12Z,15Z-octadecatetraen-1-one (**6**): unstable pale yellow oil; All off-line NMR spectroscopic and mass spectrometric data was identical to that reported in the literature (Gregson et al., 1977); ¹³C NMR (125 MHz, CDCl₃) obtained from HSQC and HMBC NMR experiments δ 206.7 (C, C-1), 165.4 (C, C-4'), 132.1 (CH, C-16), 130.1 (CH, C-6), 128.1 (CH, C-9, C-10, C-12, C-13), 127.9 (CH, C-7), 127.0 (CH, C-15), 105.3 (C, C-1'), 93.9 (CH, C-3', C-5'), 55.4 (CH₃, 4'-OCH₃), 44.1 (CH₂, C-2), 29.5 (CH₂, C-4), 27.2 (CH₂, C-5), 25.5 (CH₂, C-8, C-11, C-14), 24.2 (CH₂, C-3), 20.6 (CH₂, C-17), 14.3 (CH₃, C-18).

R- δ -Tocotrienol (**7**): light yellow, unstable oil; $[\alpha]_D^{24}$ +12.4 (c 0.00476, CHCl₃)¹; All off-line NMR spectroscopic, mass spectrometric and specific rotation data was in agreement to that reported in the literature (Couladouros et al., 2007; Ohnmacht et al., 2008).

R- γ -Tocotrienol (**10**): light yellow, unstable oil; no specific rotation could be recorded prior to decomposition. All off-line NMR spectroscopic and mass spectrometric data was identical to that reported in the literature (Ohnmacht et al., 2008).

Mixture of 1-(2,4,6-trihydroxyphenyl)-octadeca-6Z,9Z,12Z-trien-1- (moniliferanone A) (**8**) and 1-(2,4,6-trihydroxyphenyl)-octadeca-9Z,12Z,15Z-trien-1-one (moniliferanone C) (**11**): isolated in a ratio of 1–0.45, respectively in *C. monilifera* and in a ratio of 1–0.25, respectively in *C. subfarinata*; unstable oil, which darkened over time; UV (EtOH) $\lambda_{\max}(\log \epsilon)$ 229 (3.85), 289 (3.99); IR ν_{\max} 3290, 3012, 2927, 2856, 1635, 1521, 1456, 1394, 1251 cm⁻¹; ¹H NMR (500 MHz, CDCl₃) and ¹³C NMR (125 MHz, CDCl₃) see Tables 1 and 2; ESIMS m/z 385 [M-H]⁻; HRESIMS m/z 385.2385 (calcd for C₂₄H₃₃O₄, 385.2384).

1-(2,4,6-Trihydroxyphenyl)-eicosa-5Z,8Z,11Z,14Z-tetraen-1-one (moniliferanone B) (**9**): unstable oil, which darkened over time; UV (EtOH) $\lambda_{\max}(\log \epsilon)$ 228 (3.98), 290 (3.96); IR ν_{\max} 3283, 3012, 2956, 2926, 2855, 1622, 1513, 1456, 1261 cm⁻¹; ¹H NMR (500 MHz, CDCl₃) and ¹³C NMR (125 MHz, CDCl₃) see Table 1; ESIMS m/z 411 [M-H]⁻; HRESIMS m/z 411.2536 (calcd for C₂₆H₃₅O₄, 411.2541).

1-(2,4,6-Trihydroxyphenyl)-hexadeca-6Z,9Z-tetraen-1-one (moniliferanone D) (**12**): unstable oil, which darkened over time; UV (EtOH) $\lambda_{\max}(\log \epsilon)$ 226 (3.37), 289 (3.36); IR ν_{\max} 3351, 3010, 2926, 2855, 1711, 1626, 1457, 1257 cm⁻¹; ¹H NMR (500 MHz, CDCl₃) and ¹³C NMR (125 MHz, CDCl₃) see Table 2; ESIMS m/z 359 [M-H]⁻; HRESIMS m/z 359.2221 (calcd for C₂₂H₃₁O₄, 359.2228).

Acknowledgments

The Marine And Terrestrial Natural Product (MATNAP) research group would like to thank Mr. Roderick Watson (MAFRI), Dr. Rick Tinker, Dr. Daniel Dias and Ms. Priyanka Reddy for their assistance with the collection of the two marine algae; Dr. Gerry Kraft (School of Biological Sciences, The University of Melbourne) for the taxonomic identification of the marine algae; Mrs. Nerida Thurbon (School of Applied Sciences (Discipline of Biotechnology and Biological Sciences), Science Engineering and Health, RMIT University) for providing access to the micro-organisms to conduct the antimicrobial assays and for her invaluable technical support; Ms. Gill Ellis (University of Canterbury, Christchurch, New Zealand) for conducting some of the antimicrobial biological testing of *C. subfarinata*; Ms. Sally Duck (School of Chemistry, Faculty of Science, Monash University) for conducting the high resolution mass spectrometric analyses (ESI-MS) and HPLC-MS; Dr. Julie Niere for her useful NMR discussions and guidance.

¹ Specific rotation in the literature is small. Trace amounts of contaminants/impurities present can affect the overall value.

Mr. Robert Brkljača would also like to acknowledge his Australian Postgraduate Award (APA) scholarship that has supported his PhD studies.

Appendix A. Supplementary data

Supplementary data associated with this article can be found, in the online version, at <http://dx.doi.org/10.1016/j.phytochem.2015.06.014>.

References

- Amico, V., Currenti, R., Oriente, G., Piattelli, M., Tringali, C., 1981. A phloroglucinol derivative from the brown alga *Zonaria tournefortii*. *Phytochemistry* 20, 1451–1453.
- Amico, V., Nicolosi, G., Oriente, G., Piattelli, M., Tringali, C., 1982. A novel acylphloroglucinol from the brown alga *Zonaria tournefortii*. *Phytochemistry* 21, 739–741.
- Blackman, A.J., Rogers, G.I., Volkman, J.K., 1988. Phloroglucinol derivatives from three Australian marine algae of the genus *Zonaria*. *J. Nat. Prod.* 51, 158–160.
- Blunt, J.W., Copp, B.R., Keyzers, R.A., Munro, M.H.G., Prinsep, M.R., 2014. Marine natural products. *Nat. Prod. Rep.* 31, 160.
- Brkljača, R., Urban, S., 2015. Chemical profiling (HPLC–NMR & HPLC–MS), isolation, and identification of bioactive meroditerpenoids from the southern Australian marine brown alga *Sargassum paradoxum*. *Mar. Drugs* 13, 102–127.
- Couladouros, E.A., Moutsos, V.I., Lampropoulou, M., Little, J.L., Hyatt, J.A., 2007. A short and convenient chemical route to optically pure 2-methyl chromanmethanols. Total asymmetric synthesis of β -, γ -, and δ -tocotrienols. *J. Org. Chem.* 72, 6735–6741.
- Drotleff, A.M., Ternes, W., 1999. *Cis/trans* isomers of tocotrienols – occurrence and bioavailability. *Eur. Food Res. Technol.* 210, 1–8.
- Drotleff, A.M., Ternes, W., 2001. Determination of RS, E/Z-tocotrienols by HPLC. *J. Chromatogr. A* 909, 215–223.
- Gerwick, W., Fenical, W., 1982. Phenolic lipids from the related marine algae of the order Dictyotales. *Phytochemistry* 21, 633–637.
- Gregson, R.P., Kazlauskas, R., Murphy, P.T., Wells, R.J., 1977. New metabolites from the brown alga *Cystophora torulosa*. *Aust. J. Chem.* 30, 2527–2532.
- Guiry, M.D., Guiry, G.M., 2015. AlgaeBase. Available online: <<http://www.algaebase.org>> (accessed on 17 February 2015).
- Hodul, P.J., Dong, Y., Husain, K., Pimiento, J.M., Chen, J., Zhang, A., Francois, R., Pledger, W.J., Coppola, D., Sebti, S.M., Chen, D.-T., Malafa, M.P., 2013. Vitamin E δ -tocotrienol induces p27Kip1-dependant cell-cycle arrest in pancreatic cancer cells via an E2F-1-dependant mechanism. *PLoS One* 8.
- Ji, X., Wang, Z., Geamanu, A., Sarkar, F.H., Gupta, S.V., 2011. Inhibition of cell growth and induction of apoptosis in non-small cell lung cancer cells by delta-tocotrienol is associated with Notch-1 down-regulation. *J. Cell. Biochem.* 112, 2773–2783.
- Kazlauskas, R., King, L., Murphy, P.T., Warrem, R.G., Wells, R.J., 1981. New metabolites from the brown algal genus *Cystophora*. *Aust. J. Chem.* 34, 439–447.
- Laird, D.W., Bennett, S., Bian, B., Sauer, B., Wright, K., Hughes, V., van Altena, I.A., 2010. Chemical investigation of seven Australasian *Cystophora* species: new chemistry and taxonomic insights. *Biochem. Syst. Ecol.* 38, 187–194.
- MarinLit Database, 2015. Available online: <<http://pubs.rsc.org/marinlit/>> (accessed on 17 February 2015).
- Master, R.N., Clark, R.B., Karlowsky, J.A., Ramirez, J., Bordon, J.M., 2011. Analysis of resistance, cross-resistance and antimicrobial combinations for *Pseudomonas aeruginosa* isolates from 1997 to 2009. *Int. J. Antimicrob. Agents* 38, 291–295.
- Ohnmacht, S., West, R., Simionescu, R., Atkinson, J., 2008. Assignment of the ^1H and ^{13}C NMR of tocotrienols. *Magn. Reson. Chem.* 46, 287–294.
- Ryan, K.J., Ray, C.G., 2010. *Sherris Medical Microbiology*. The McGraw-Hill Companies Inc., USA.
- Ryu, B., Kim, S.-K., 2013. Pharmacological potential of phlorotannis from marine brown algae. In: Kim, S.-K. (Ed.), *Mar. Pharmacogn.* CRC Press, Florida, USA.
- Scott, A.I., 1964. *Interpretation of the Ultraviolet Spectra of Natural Products*. Pergamon Press Ltd., London.
- Wisespongpan, P., Kuniyoshi, M., 2003. Bioactive phloroglucinols from the brown alga *Zonaria diesingiana*. *J. Appl. Phycol.* 15, 225–228.
- Wu, S.-J., Huang, G.-Y., Ng, L.-T., 2013. γ -Tocotrienol induced cell cycle arrest and apoptosis via activating the bax-mediated mitochondrial and AMPK signaling pathways in 3T3-L1 adipocytes. *Food Chem. Toxicol.* 59, 501–513.
- Zhang, J.-S., Li, D.-M., Ma, Y., He, N., Gu, Q., Wang, F.-C., Jiang, S.-Q., Chen, B.-Q., Liu, J.-R., 2013. γ -Tocotrienol induces paraptosis-like cell death in human colon carcinoma SW620 cells. *PLoS ONE* 8, e57779.

CHAPTER 11

Relative Configuration Studies of the Marine Natural Product

Elatenyne



Kingdom: Plantae
Phylum: Rhodophyta
Class: Florideophyceae
Order: Ceramiales
Family: Rhodomelaceae
Genus: *Laurencia*
Species: *elata*

Collected at low tide at St. Paul's Beach,
Sorrento, Port Phillip Bay, Victoria,
Australia in January 2003.

Chapter 11 details the chemical derivatisation and relative configuration studies carried out on elatenyne, a marine natural product isolated from *Laurencia elata*. This work has been published as outlined below.

Journal publication resulting from this study:

Brkljača, Robert, & Urban, Sylvia. (2013). Relative Configuration of the Marine Natural Product Elatenyne using NMR Spectroscopic and Chemical Derivatization Methodologies. *Natural Product Communications*, 8(6), 729-732.

Relative Configuration of the Marine Natural Product Elatenyne using NMR Spectroscopic and Chemical Derivatization Methodologies

Robert Brkljača and Sylvia Urban*

School of Applied Sciences, Health Innovations Research Institute (HIRI) RMIT University,
GPO Box 2476V Melbourne, Victoria 3001, Australia

sylvia.urban@rmit.edu.au

Received: May 2nd, 2013; Accepted: May 7th, 2013

NMR spectroscopic methodologies used to characterize and elucidate the structure of the marine natural product elatenyne were also applied to the characterization of a new triazole structural derivative of elatenyne, obtained by “Click” chemistry. The two most probable relative configurations assigned to naturally occurring elatenyne were concluded on the basis of key single irradiation nOe NMR enhancements, in combination with the use of a variant of the HSQC NMR experiment that permitted NMR coupling constants to be measured for the overlapped ring junction protons. This study represents the first application of “Click” chemistry to chemically derivatize an unmodified natural product.

Keywords: *Laurencia elata*, Elatenyne, Relative configuration, “Click” chemistry, nOe NMR enhancements, Natural products.

Elatenyne was first reported in 1986 from the marine red alga, *Laurencia elata* and the structure was originally assigned as having a pyrano[3,2-*b*]pyran (**1**) (Figure 1) carbon skeleton on the basis of a detailed spectroscopic investigation [1]. In 2006 the pyrano[3,2-*b*]pyran (**1**) structure was successfully synthesized and the NMR data found to differ from the natural product. Further investigations of synthetic model compounds ultimately supported the correct structure of elatenyne as possessing the 2,2'-bifuranyl structure (**2**) (Figure 1) [2,3]. The structure of elatenyne consists of six stereocentres (Figure 1), giving a total of thirty-two possible diastereoisomers. To date, computational methods have been used to establish which of these possible diastereoisomers would be the closest match to the NMR data. The use of these GIAO ¹³C NMR calculations concluded that the four most likely diastereoisomers (**3-6**) of elatenyne were those depicted in Figure 1 with compound **3** deemed to be the most likely structure of elatenyne [4].

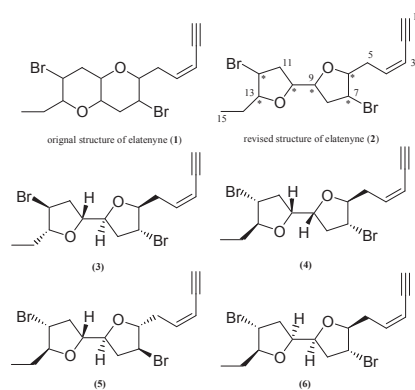


Figure 1: Incorrect and revised structures of elatenyne (**1** and **2**, respectively) and the four most likely diastereoisomers (**3-6**) as concluded by GIAO ¹³C NMR calculations [4].

In addition to the use of computational methods, total synthesis of the revised structure of elatenyne (**2**) was undertaken to establish which of the four proposed diastereoisomers corresponded to the most probable structure of elatenyne. Two separate syntheses were successful in obtaining elatenyne, but the absolute configuration could only be proposed as that depicted in compound **3** [5].

The Marine and Terrestrial Natural Product (MATNAP) research group at RMIT University recently published results from an investigation conducted on the Australian red alga *Laurencia elata* [6]. In this study chemical profiling of the crude extract employing HPLC-NMR and subsequent off-line isolation resulted in the isolation of five chemical constituents, one of which was elatenyne [6]. At that time an attempt to address the relative configuration of elatenyne was undertaken and two diastereoisomers (**6** and **7**) were proposed (Figures 1 and 2) [6]. One of these (**6**) was in accordance with one of the four concluded on the basis of GIAO ¹³C NMR calculations. The other diastereoisomer (**7**) was tentatively proposed on the basis of single irradiation nOe NMR enhancements and by comparison of the ¹H NMR data and coupling constants with a structurally related natural product, notoryne (**8**) (Figure 2), whose absolute configuration had been established [7].

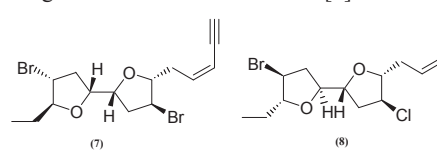


Figure 2: Additional diastereoisomer (**7**) proposed by comparisons with notoryne (**8**).

Elatenyne was isolated as an unstable, colorless oil which darkened over time. In the first report of the isolation and structure determination of elatenyne, a specific rotation of +19° was recorded at the sodium wavelength 589 nm [1]. The NMR and mass spectrometric data for elatenyne isolated in our study was identical to that previously published, except that a specific optical rotation of -10° was recorded at the sodium wavelength 589 nm. This anomaly had also been noted by Burton and co-workers in their studies of elatenyne [3,5]. Given the small specific rotation displayed by elatenyne, minor contaminants present and/or operator/instrumental error could easily affect the final measurement. In our study of elatenyne the specific rotation was also recorded at a number of Hg wavelengths (365, 405, 436 and 546 nm), but only the 365 nm wavelength resulted in a measurable specific rotation of -20°. The specific rotations obtained for elatenyne in our study were in close agreement and in accordance with those recently reported for synthetic elatenyne (-10° at 365 nm) [5].

In an effort to deduce the relative configuration of elatenyne, our previous investigations involved conducting a series of single irradiation 1D nOe NMR experiments in CDCl_3 [6]. Despite proposing two likely diastereoisomers for elatenyne (**6** and **7**) (Figures 1 and 2), this study was by no means conclusive due to the poor resolution observed for some of the signals [6]. In an attempt to obtain improved resolution of the ^1H NMR signals, a range of NMR solvents were explored to determine which would offer the greatest signal dispersion and coupling information. These NMR solvents included CDCl_3 , C_6D_6 , CD_3OD , $\text{DMSO}-d_6$ and acetone- d_6 . It was evident that C_6D_6 (Table 1) and $\text{DMSO}-d_6$ provided the best resolution in the upfield region of the ^1H NMR spectrum. Only specific protons of interest were irradiated in the single irradiation nOe NMR experiments conducted in these two NMR solvents.

Table 1: ^1H (500 MHz, C_6D_6) and selected single irradiation 1D nOe NMR spectroscopic data of elatenyne (**2**)

Position	δ_{H} (J in Hz)	nOe
1	2.77, d (1.8)	
2	-	
3	5.36, dd (11.0, 1.8)	
4	5.72, dt (11.0, 7.5)	
5a	2.41, ddd (14.5, 7.5, 7.5)	
5b	2.49, ddd (14.5, 6.5, 6.5)	
6	4.06, dt (5.5, 5.5)	H4, H5a, H5b, H7, H8b, H9*
7	3.66, dt (7.5, 5.5)	H4, H5a, H5b, H6, H8a, H8b, H9*
8a	1.91, ddd (14.0, 7.5, 7.5)	H7, H9*
8b	1.98, m	H6, H7, H9*
9	3.86, dt (7.5, 6.5) ^a	H6, H7, H8a, H8b
10	3.86, dt (7.0, 6.5) ^a	H11a, H11b, H12
11a	2.03, m	H10*, H12
11b	1.98, m	H10*, H12
12	3.53, dt (7.0, 5.5)	H10, H11a, H11b, H13, H14a, H14b, H15
13	3.89, dt (7.5, 5.0)	H11a, H12, H14b, H15
14a	1.23, ddq (14.0, 7.5, 7.5)	
14b	1.37, ddq (14.0, 7.5, 5.0)	
15	0.81, t (7.5)	

^a Coupling constants determined on the basis of an edited HSQCAD NMR experiment

* Signal overlapped

In an effort to resolve the multiplicity for the ring junction protons in the ^1H NMR spectrum of elatenyne, a variation of the standard HSQC NMR experiment that allows for the splitting patterns ($^3J_{\text{HH}}$ coupling values) of overlapping protons to be deduced was carried out [8,9]. Experimentally, a HSQC experiment is set up with the absence of ^{13}C decoupling and with an acquisition time of approximately 1 second. This extended acquisition time allows for increased resolution in the F_2 dimension, which allows for the measurement of $^3J_{\text{HH}}$ values. Turning off the ^{13}C decoupler removes the strong coupling normally observed between the two overlapping protons. It is important for the overlapping protons to be adjoined to two resolved carbons for this experiment to be successful. This variation of the HSQC NMR experiment (Figure 3) showed that the splitting pattern of the two overlapping ring junction protons (in C_6D_6) were in fact doublets of triplets with coupling constants of 7.5 and 6.5 Hz for the position 9 proton and 7.0 and 6.5 Hz for the position 10 proton. These coupling constants were compared with those for the ring junction protons in nortoryne (**8**), for which the absolute configuration had been established [7]. This enabled an axial-equatorial relationship for the ring junction protons in elatenyne to be concluded.

Single irradiation 1D nOe NMR experiments were then carried out and enhancements from the four key ^1H NMR resonances (positions 6, 7, 12, 13) were studied closely in an effort to deduce a possible favored diastereoisomer. It was evident that certain ^1H NMR chemical shifts were overlapped in either C_6D_6 or $\text{DMSO}-d_6$. Therefore, both sets of ^1H NMR data obtained in each solvent were closely examined. In C_6D_6 the protons at positions 6 and 7 (δ 4.06 and 3.66, respectively) on one side of the molecule showed an nOe NMR enhancement with the proton at position 9 (δ 3.86) confirming that these protons are positioned on the same face of the molecule. Similarly in $\text{DMSO}-d_6$, the protons at positions 12 and 13

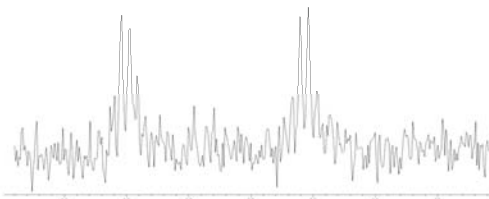


Figure 3: Extracted 1D trace of the proton signal at δ 3.86 coupled to the carbon at 79.5 ppm of a 2D HSQC NMR experiment illustrating a dt (7.0, 6.5 Hz) coupling.

(δ 4.24 and 3.91, respectively) also showed a nOe NMR enhancement with the proton at position 10 (δ 4.11), confirming that these protons also all lie in the same orientation. The nOe NMR enhancement observed from the position 13 proton at δ 3.91 to the ring junction proton at position 10 (δ 4.11) in $\text{DMSO}-d_6$ was crucial for establishing the relative configuration of the left hand side of the structure of elatenyne. In CDCl_3 this nOe NMR enhancement could not be observed due to the close proximity of the position 13 and 10 proton chemical shifts at δ 3.89 and 3.86, respectively. These nOe NMR enhancements, together with the axial-equatorial orientation of the ring junction protons established from the variant HSQC NMR experiment, were able to conclude two likely diastereoisomers (**9** and **10**) for elatenyne (Figure 4). These diastereoisomers are different from the proposed absolute configuration of elatenyne (**3**), as well to the other three most likely diastereoisomers that have been recently proposed (**4-6**) [4,5]. The nOe NMR enhancements observed were able to rule out the other proposed diastereoisomers when bond distances were also considered.

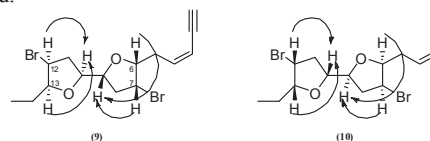


Figure 4: Diastereoisomers **9** and **10** proposed for elatenyne showing key nOe NMR enhancements observed in C_6D_6 and $\text{DMSO}-d_6$.

Following the proposal of the relative configurations of elatenyne, Circular Dichroism (CD) analysis was also carried out. No closely related model compounds with CD spectra could be sourced from the literature, which prevented any comparison and possible absolute configuration being proposed. Despite this, the CD spectrum of elatenyne was recorded in ethanol in order to document it for future reference. This was deemed to be particularly important as a means of comparison for when the absolute configuration of natural elatenyne might be established.

Attempts to crystallize elatenyne for possible X-ray diffraction analysis were also carried out using various methods and solvents; however, none was successful. It was rationalized that a chemical derivatization of elatenyne would be the only method that might aid in crystallization. In the selection of the most appropriate chemical derivatization method for elatenyne, two important criteria were considered. First, the chemical derivatization method must not result in racemization of elatenyne and secondly, the reaction must provide a high recovery. It was concluded that the terminal alkyne was the ideal moiety for derivatization in the structure of elatenyne, as this position would have the lowest probability of altering the absolute configuration. Consultation of the chemical literature indicated that 'Click' chemistry would be an ideal reaction for derivatizing elatenyne. Click' chemistry typically involves reactions between alkynes and azides. A 1,3-dipolar cycloaddition occurs between the alkyne and azide to form a 1,2,3 triazole in the presence of a metal catalyst [10]. Rigid molecular systems or those containing stackable pi systems, typically display the ability to

crystallize. Therefore an azide with a terminal aromatic group (**11**) was selected for the derivatization. The presence of the 1,2,3 triazole, along with the aromatic system, would hopefully increase the chances of crystallization. The reaction of elatenyne with the selected azide is outlined in Figure 5.

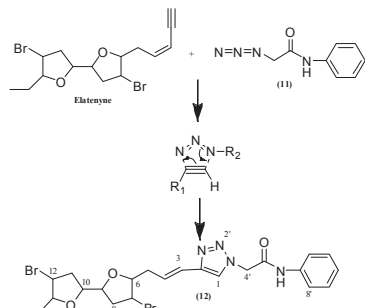


Figure 5: Derivatization of elatenyne to yield the new 1,2,3 triazole derivative (**12**) using 'Click' Chemistry.

The 'Click' reaction was successful in derivatizing elatenyne to produce the 1,2,3 triazole (**12**). This triazole derivative is new to the scientific literature and was purified and then subjected to 1D and 2D NMR spectroscopic (Table 2) and mass spectrometric analyses. Single irradiation nOe NMR enhancement experiments were also carried out on key selected protons at positions 6, 7, 12 and 13 in order to confirm that the derivatization process did not alter the relative configuration of the original elatenyne structure. On the basis of the nOe NMR enhancements and coupling constants observed, it was concluded that the relative configuration of the derivative had not changed from that of elatenyne. Specific rotations of the triazole derivative were recorded at 589 and 365

nm. The specific rotations were recorded as 0° and +16.4° at 589 and 365 nm, respectively. This meant that although the magnitude of the specific rotation remained consistent with that observed for elatenyne, the sign of the optical rotation had changed at the mercury wavelength. Although the triazole was purified by HPLC, NMR spectroscopy clearly showed the presence of an unknown minor impurity. For a compound such as elatenyne that is known to have such a small optical rotation, any impurity present is expected to drastically effect the optical rotation measurement, as was observed with the triazole derivative. Attempts to crystallize the triazole were unsuccessful. A range of solvents and crystallization methods were investigated, but each attempt resulted in the recovery of an amorphous solid.

Concluding remarks: Two relative configurations of natural elatenyne were tentatively proposed on the basis of a range of NMR spectroscopic experiments. Attempts to ascertain the absolute configuration of elatenyne via crystallization were not fruitful. However, the first application of 'Click' chemistry to a marine natural product was implemented, resulting in a new structural derivative. The concluded relative configurations of naturally occurring elatenyne are not in accordance with the proposed absolute configuration, nor with the four likely relative configurations of elatenyne recently proposed. Since the possible diastereoisomers of elatenyne do not show distinct chemical shift differences in their NMR spectra, this makes it difficult to establish the relative configuration unequivocally for naturally occurring elatenyne by either synthetic or computational methods. Ultimately the absolute configuration of elatenyne should be secured by X-ray crystallography on a suitable derivative.

Table 2: ¹H (500 MHz) and ¹³C (125 MHz) NMR spectroscopic data of the triazole derivative (**12**) in CDCl₃.

Position	δ _H (J in Hz)	δ _C ^a , mult	gCOSY	gHMBCAD	nOe
1	7.82 s	123.8, CH	-	C2	-
2	-	145.6, C	-	-	-
3	6.56 d, J = 11.5 Hz	119.3, CH	H4	C1, C2, C5	-
4	5.91 dt, J = 6.5, 11.5 Hz	129.2, CH	H3, H5a, H5b	C5, C6	-
5a	2.77 ddd, J = 7.0, 7.0, 14.5 Hz	33.5, CH ₂	H4, H5b, H6	C3, C4, C6, C7	-
5b	2.91 ddd, J = 5.5, 7.0, 13.5 Hz	-	H4, H5a, H6	C3, C4, C6, C7	-
6	4.27 dt, J = 5.5, 6.5 Hz	86.7, CH	H5a, H5b, H7	C4, C7, C8	H4, H5a, H5b, H7, H9
7	4.10 dt, J = 5.5, 6.5 Hz	48.5, CH	H6, H8a, H8b	C5, C9	H6, H8b, H9
8a	2.34 m	38.4, CH ₂	H7, H8b, H9	C6 (w), C7, C9, C10	-
8b	2.41 m	-	H7, H8a, H9	C6, C7, C9, C10	-
9	4.17 dt, J = 6.5, 7.0 Hz ^b	79.7, CH	H8a, H8b	C8	-
10	4.16 dt, J = 6.0, 8.0 Hz ^b	79.2, CH	H11	C11	-
11	2.28 dd J = 5.5, 6.5 Hz	38.8, CH ₂	H10, H12	C9, C10, C12, C13	-
12	3.94 dt, J = 6.0, 6.0 Hz	48.9, CH	H11, H13	C10, C14	H10, H11, H14a, H14b, H15
13	4.02 dt, J = 6.0, 6.0 Hz	88.7, CH	H12, H14a, H14b	C12, C15	H10, H11, H14b, H15
14a	1.50 ddq, J = 7.0, 7.0, 14.0 Hz	26.8, CH ₂	H13, H14b, H15	C12, C13, C15	-
14b	1.65 m ^c	-	H13, H14a, H15	C12, C13, C15	-
15	0.98 t, J = 6.5 Hz	10.1, CH ₃	H14a, H14b	C13, C14	-
1'	-	-	-	-	-
2'	-	-	-	-	-
3'	-	-	-	-	-
4'	5.20 s	53.7, CH ₂	-	C1, C5'	-
5'	-	162.8, C	-	-	-
6'	8.03 bs	-	-	-	-
7'	-	136.5, C	-	-	-
8'	7.48 d, J = 8.0 Hz	120.2, CH	H9', H10'(w)	C7', C9', C10', C12'	-
9'	7.34 dd, J = 7.0, 8.0 Hz	129.1, CH	H8', H10'	C7', C8', C10', C11'	-
10'	7.16 dd, J = 7.0, 8.0 Hz	125.3, CH	H9', H11'	C8', C9', C11', C12'	-
11'	7.34 dd, J = 7.0, 8.0 Hz	129.1, CH	H10', H12'	C7', C9', C10', C12'	-
12'	7.48 d, J = 8.0 Hz	120.2, CH	H10'(w), H11'	C7', C8', C10', C11'	-

^aCarbon assignments based on HSQCAD and gHMBCAD NMR experiments. ^bCoupling extracted from edited HSQCAD NMR experiment. ^cSignal obscured by solvent peak. ^wweak correlation

Experimental

General: For detailed information on the general experimental procedures please see references [6,11]. 1D and 2D NMR, 500 MHz Varian INOVA NMR; CD, Jasco J-815 spectrometer in ethanol over a range of 200-600 nm using 3 accumulations.

Isolation and purification of elatenyne from *L. elata*: For details regarding the fractionation and subsequent purification of elatenyne (**2**) (7.1mg, 0.14%) see reference [6] (% based on the mass of the dried weight of the marine alga).

Derivatization of elatenyne: Elatenyne (7.1 mg), DMSO (1.7 mL) and deionised water (850 µL) were placed into a vial. 2-azido-N-phenylacetamide (9.8 mg) was then dissolved in DMSO (1015 µL) and 500 µL of this solution was added to the vial containing elatenyne, together with ascorbic acid (5.7 mg), CuSO₄ (4.0 mg) and additional deionised water (255 µL). The reaction was stirred for 2 days after which time the 1,2,3 triazole (90% yield) was recovered by solvent-solvent extraction (3 x 20 mL of *n*-hexane) followed by evaporation of *n*-hexane under reduced pressure.

HPLC purification of the 1,2,3 triazole (4,4'-dibromo-5-ethyl-5'-(Z)-pent-2-en-4-ynyl)octahydro[2,2']-bifuran (12): Following the derivatization of elatenyne, semi-preparative HPLC was carried out to purify the triazole from the remaining excess azide. Reversed phased semi-preparative HPLC was carried out on a Dionex P680 (solvent delivery module) equipped with a Dionex UVD340U PDA detector and a Foxy Jr. automated fraction collector. An isocratic method (75% CH₃CN/H₂O) was employed using a Phenomenex Luna (2) 100 Å C₁₈ 250 x 10 mm (5 µm) column. The automatic fraction collector was programmed to collect the triazole based on the elution time (7.10 min) and peak threshold. This resulted in 5.4 mg of the derivative being recovered.

Elatenyne (2), isolated as a colorless oil, which darkened over time. $[\alpha]_D^{25}$: -10.0 (*c* 0.0498, CH₂Cl₂) and $[\alpha]_{365}^{25}$: -20.1 (*c* 0.0498, CH₂Cl₂).

CD (EtOH): 215 nm ($\Delta\epsilon$ +50.8), 235 nm ($\Delta\epsilon$ +121.5), 256 nm ($\Delta\epsilon$ -22.0), 287 nm ($\Delta\epsilon$ +13.2).

¹H NMR (500 MHz, C₆D₆): Table 1.

¹H NMR (500 MHz, CD₃OD): 6.06 (1H, dt, *J* = 7.0, 11.0 Hz, H4), 5.60 (1H, dd, *J* = 2.0, 11.0 Hz, H3), 4.17 (4H, m, H6, H7, H9, H10), 4.10 (1H, dt, *J* = 5.5, 7.5 Hz, H12), 3.98 (1H, dt, *J* = 5.5, 7.5 Hz, H13), 3.52 (1H, d, *J* = 2.0 Hz, H1), 2.64 (1H, m, H5b), 2.55 (1H, m, H5a), 2.36 (2H, m, H8b, H11b), 2.29 (2H, m, H8a, H11a), 1.65 (1H, m, H14b), 1.50 (1H, ddq, *J* = 7.5, 8.0, 15.0 Hz, H14a), 0.98 (3H, t, *J* = 7.5 Hz, H15); ¹³C NMR (CD₃OD): 139.5 (CH, C4), 110.6 (CH, C3), 88.9 (CH, C13), 86.6 (CH, C6), 79.8* (CH, C9), 79.3* (CH, C10), 48.9 (CH, C12), 48.5 (CH, C7), 38.2 (CH₂, C8 and C11), 34.1 (CH₂, C5), 26.4 (CH₂, C14), 9.1 (CH₃, C15), ND (CH, C1), ND (C, C2) *signals interchangeable

¹H NMR (DMSO-*d*₆): 6.05 (1H, dt, *J* = 7.5, 10.5 Hz, H4), 5.61 (1H, d, *J* = 11.0 Hz, H3), 4.28 (1H, dt, *J* = 4.5, 7.0 Hz, H7), 4.24 (1H, dt, *J* = 4.5, 7.0 Hz, H12), 4.11 (2H, m, H9, H10), 4.09 (1H, m, H6), 3.91 (1H, dt, *J* = 5.0, 7.0 Hz, H13), 2.53 (1H, ddd, *J* = 6.5, 6.5, 14.0 Hz, H5b), 2.42 (1H, ddd, *J* = 7.5, 7.5, 14.0 Hz, H5a), 2.30 (2H, ddd, *J* = 7.0, 7.5, 14.0 Hz, H8b, H11b), 2.20 (2H, m, H8a, H11a), 1.53 (1H, m, H14b), 1.38 (1H, ddq, *J* = 7.5, 8.0, 15.0 Hz, H14a), 0.87 (3H, t, *J* = 7.5 Hz, H15), ND* (H1); *Solvent overlap; ¹³C NMR (500 MHz, DMSO-*d*₆): 140.7 (CH, C4), 111.2 (CH, C3), 88.5 (CH, C13), 86.2 (CH, C6), 79.7* (CH, C9), 79.2* (CH, C10), 51.2 (CH, C12), 50.8 (CH, C7), 38.3 (CH₂, C8 and C11), 34.8 (CH₂, C5), 26.8 (CH₂, C14), 10.4 (CH₃, C15), ND (CH, C1), ND (C, C2) * signals interchangeable.

¹H NMR (500 MHz, (acetone-*d*₆): 6.14 (1H, dt, *J* = 7.5, 11.0 Hz, H4), 5.63 (1H, dd, *J* = 2.0, 11.0 Hz, H3), 4.25 (1H, dt, *J* = 5.0, 7.0

Hz, H7), 4.17 (4H, m, H6, H9, H10, H12), 3.96 (1H, dt, *J* = 5.5, 8.0 Hz, H13), 3.67 (1H, d, *J* = 2.0 Hz, H1), 2.68 (1H, ddd, *J* = 6.0, 7.0, 14.0 Hz, H5b), 2.55 (1H, ddd, *J* = 7.5, 7.0, 14.5 Hz, H5a), 2.42 (2H, ddd, *J* = 7.0, 7.5, 14.0 Hz, H8b, H11b), 2.31 (2H, ddd, *J* = 6.0, 6.0, 14.0 Hz, H8a, H11a), 1.66 (1H, m, H14b), 1.50 (1H, ddq, *J* = 7.5, 8.0, 15.0 Hz, H14a), 0.96 (3H, t, *J* = 7.5 Hz, H15); ¹³C NMR (500 MHz, acetone-*d*₆): 140.1 (CH, C4), 110.6 (CH, C3), 88.6 (CH, C13), 86.3 (CH, C6), 79.8* (CH, C9), 79.3* (CH, C10), 49.7 (CH, C12), 49.4 (CH, C7), 38.5 (CH₂, C8 and C11), 34.3 (CH, C5), 26.5 (CH₂, C14), 9.47 (CH₃, C15), ND (CH, C1), ND (C, C2) * signals interchangeable

Elatenyne triazole derivative (12), isolated as an amorphous green solid.

$[\alpha]_D^{25}$: ±0 (*c* 0.0044, CH₂Cl₂) and $[\alpha]_{365}^{25}$: +16.4 (*c* 0.0044, CH₂Cl₂).

IR (film): 3292, 2925, 2854, 1667, 1602, 1557, 1499, 1446, 1312, 1255 cm⁻¹.

UV/VIS) λ_{\max} (EtOH) nm (log ϵ): 236 (4.21).

¹H NMR and ¹³C NMR (CDCl₃): Table 2.

ESIMS (positive mode): *m/z* 487 [M-Br⁸¹]⁺, 489 [M-Br⁷⁹]⁺, 569 [M+H]⁺, 591 [M+Na]⁺.

HR-ESI-MS (positive mode): *m/z* at 567.0609 [M+H]⁺ (calcd. For C₂₃H₂₈O₃N₄⁷⁹Br₂: *m/z* 567.0508); *m/z* at 569.0596 [M+H]⁺ (calcd. For C₂₃H₂₈O₃N₄⁸⁰Br₂: *m/z* 568.0508); *m/z* at 571.0573 [M+H]⁺ (calcd. For C₂₃H₂₈O₃N₄⁸¹Br₂: *m/z* 571.0508); *m/z* at 591.0409 [M+Na]⁺ (calcd. For C₂₃H₂₈O₃N₄⁸⁰Br₂Na: *m/z* 591.0426).

Acknowledgments - The Marine and Terrestrial Natural Product (MATNAP) research group would like to thank: Dr Daniel Dias for his original isolation of elatenyne; Dr Paul Donnelly University of Melbourne) for providing the azide used in the derivatization of elatenyne; Dr Jonathan White (Melbourne University) for important discussions and recommendations regarding the use of "Click" chemistry for the derivatization of elatenyne; Ms Sally Duck (Monash University) for providing high resolution mass spectrometry; Dr John Ryan (Agilent Australia) for his informative discussions and recommendations regarding the variation of the HSQC NMR experiment used in this study; Dr Jonathan Burton (Oxford University) for his constant and useful correspondence and for recommending the recording of specific rotations for elatenyne at various mercury wavelengths; and Dr Julie Niere for her useful NMR guidance and discussions.

References

- Hall JG, Reiss JA. (1986) Elatenyne - a pyrano[3,2-*b*]pyranyl vinyl acetylene from the red alga *Laurencia elata*. *Australian Journal of Chemistry*, **39**, 1401-1409.
- Sheldrake HM, Jamieson C, Burton JW. (2006) The changing faces of halogenated marine natural products: Total synthesis of the reported structures of elatenyne and an enyne from *Laurencia majuscula*. *Angewandte Chemie*, **45**, 7199-7202.
- Sheldrake HM, Jamieson C, Pascu SI, Burton JW. (2009) Synthesis of the originally proposed structures of elatenyne and an enyne from *Laurencia majuscula*. *Organic and Biomolecular Chemistry*, **7**, 238-252.
- Smith SG, Paton RS, Burton JW, Goodman JM. (2008) Stereostructure assignment of flexible five-membered rings by GIAO ¹³C NMR calculations: Prediction of the stereochemistry of elatenyne. *Journal of Organic Chemistry*, **73**, 4053-4062.
- Dyson BS, Burton JW, Sohn T-i, Kim B, Bae H, Kim D. (2012) Total synthesis and structure confirmation of elatenyne: Success of computational methods for NMR prediction with highly flexible diastereomers. *Journal of the American Chemical Society*, **134**, 11781-11790.
- Dias DA, Urban S. (2011) Phytochemical studies of the southern Australian marine alga, *Laurencia elata*. *Phytochemistry*, **72**, 2081-2089.
- Kikuchi H, Suzuki T, Kurosawa E, Suzuki M. (1991) The structure of notoryne, a halogenated C15 nonterpenoid with a novel carbon skeleton from the red alga *Laurencia nipponica* Yamada. *Bulletin of the Chemical Society of Japan*, **64**, 1763-1775.
- Mucci A, Parenti F, Schenetti L. (2002) On the recovery of ³J_{H,H} and the reduction of molecular symmetry by simple NMR inverse detection experiments. *European Journal of Organic Chemistry*, 938-940.
- Ryan JM. (2008) PhD thesis. Novel secondary metabolites from New Zealand marine sponges. Victoria University of Wellington, Wellington, New Zealand.
- Binder WH, Sachsenhofer R. (2008) 'Click' chemistry in polymer and material science: An update. *Macromolecular Rapid Communications*, **29**, 952-981.
- Reddy P, Urban S. (2008) Linear and cyclic C18 terpenoids from the Southern Australian marine brown alga *Cystophora moniliformis*. *Journal of Natural Products*, **71**, 1441-1446.

PART D – Discussion & Conclusions

Discussion and Concluding Remarks

A total of sixty five secondary metabolites were identified from the thirteen marine and terrestrial organisms investigated (**Figure 1**). HPLC-NMR was pivotal for the successful dereplication of the secondary metabolites in the chemical profiling approach adopted. In particular, HPLC-NMR was instrumental in the identification of an unstable compound that could not be isolated by off-line approaches. A comprehensive HPLC-NMR LOD study, whereby a gHMBCAD NMR spectrum was acquired on a HPLC-NMR system solely equipped with a 60 μ L flow cell, was also achieved.

Of the sixty five compounds identified, fifty four were also isolated by off-line approaches. A total of twenty two new natural products and one new natural product derivative were identified (**Figure 1**). Seventeen distinct structure classes were identified during the course of these studies. The new compounds reported in this thesis are representative of seven different structure classes. Five previously known compounds are now reported as natural products for the first time.

Of the fifty compounds assessed for their biological activity forty two displayed some anti-microbial activity (**Figure 2**), but none of the compounds displayed anti-fungal activity.

Nine compounds were completely characterised by 2D NMR spectroscopy for the first time. A total of five carbon and one proton NMR chemical shift reassignments were also made for four of the compounds isolated.

Total Compounds Identified

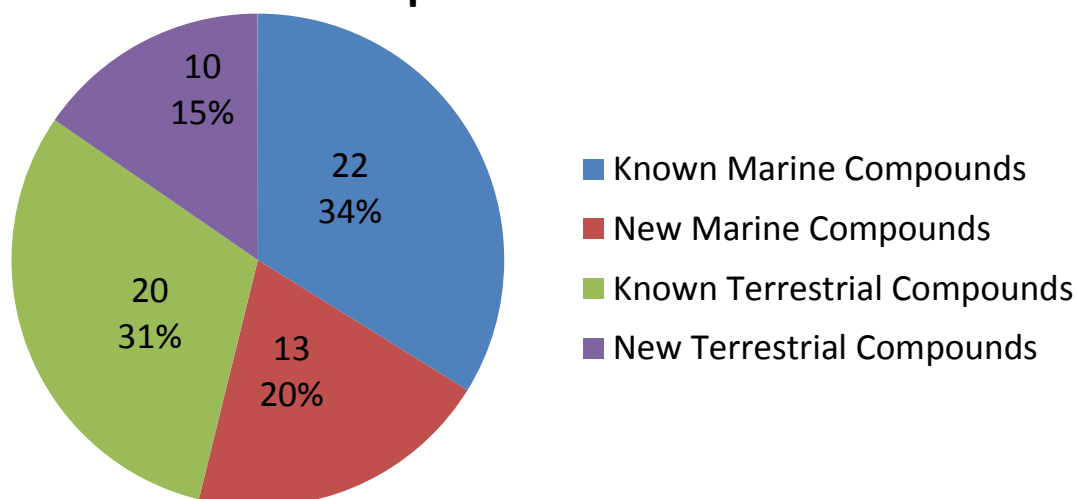


Figure 1: Total number of compounds identified.

Compounds Displaying Anti-Microbial Activity

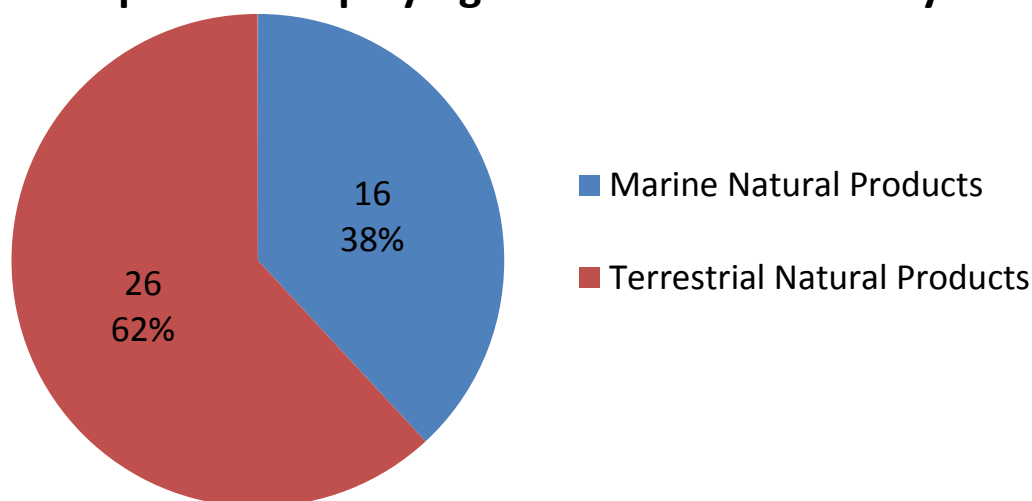


Figure 2: Number of marine and terrestrial compounds displaying anti-biotic activity.

While the aim of the thesis was to discover new natural products, rather than to explore why these compounds are produced, it can be assumed that the secondary metabolites isolated would serve a particular function. However, it is not known whether this would be for a chemical defence or to promote reproduction or cell function.

The overall chemical diversity displayed between marine and terrestrial specimens was extensive. Two plant specimens studied were of the same family (Haemodoraceae), which

produced different chemistry. Whilst the phenylphenalenones, oxabenzochrysenones and chromenes were common structural classes, the kangaroo paw (*Macropidia fuliginosa*) specimen produced several different structural classes including chalcones, resveratrol dimers and flavonoids. Likewise in Chapter 8, which detailed the chemical profiling of seven marine algae, three of the marine algae were of the *Sargassum* genus and two were of the *Cystophora* genus. Whilst the two *Cystophora* species produced similar chemistry, each of the three species of *Sargassum* produced unique chemistry. Both of these examples highlight the importance of investigating unstudied species, despite the amount of knowledge that may be known for the genus or family of the organism.

The disk diffusion assay used in this thesis was employed to ascertain whether a particular natural product may display anti-microbial activity. While this particular method is suitable to establish whether a particular crude extract or compound may display anti-microbial activity, the methodology does have limitations. In particular, the compounds being tested must be able to diffuse within the agar medium, otherwise no zone of inhibition will be observed. Furthermore, despite ampicillin being used as a general positive control in some of the assays conducted, no direct comparison of the potency can be made between the isolated compounds tested and ampicillin. Future work should involve further anti-microbial testing of compounds that displayed promising activity using a more sophisticated assay method. Modern methods such as a tetrazolium or similar colorimetric cell proliferation assay would be ideal as the diffusion characteristic of the isolated compounds would not be an issue, and the potency of compound could be expressed as an MIC₅₀ value, which in turn could be directly compared to other available anti-microbial drugs (Chand, Lusunzi, Veal, Williams, & Karuso, 1994; Mann & Markham, 1998).

Many of the compounds identified in this thesis conform to Lipinski's Rule of 5 (Lipinski, Lombardo, Dominy, & Feeney, 1997), in that they contain properties which may suggest they could be converted into an orally available drug. Whilst the water-octanol partition co-efficient was not measured for any of the compounds identified, it can be determined which of the compounds conform to Lipinski's three remaining rules. Providing

any of the compounds conforms to all of the three remaining rules, it could potentially be considered as a suitable orally available drug. Of all of the 65 compounds identified, 60 conform to all three of Lipinski's remaining rules, which include having a molecular weight less than 500 Da, containing no more than ten oxygen or nitrogen atoms, and having no more than five nitrogen-hydrogen or oxygen-hydrogen bonds. These compounds should be subjected to further biological activity studies, from which any compounds displaying potent activity could be prioritised as a drug lead. Compounds **1**, **38** and **61** (see table below) either have a molecular weight greater than 500 Da, contain more than ten oxygen or nitrogen atoms, or contain more than five nitrogen-hydrogen or oxygen-hydrogen bonds. If the water-octanol partition co-efficient of these compounds is less than five, these compounds still conform to Lipinski's rules, however if the co-efficient is greater than five, these compounds must be excluded. Compounds **39** and **40** (see table below) do not conform to Lipinski's rules and must also be excluded.

A variant of Lipinski's Rule of 5 exists, known as The Rule of 3, which determines whether a compound is a suitable drug-lead (Congreve, Carr, Murray, & Jhoti, 2003). The Rule of 3 dictates that a drug-lead compound should have a molecular weight less than 300 Da, contain no more than three oxygen or nitrogen atoms, no more than three nitrogen-hydrogen or oxygen-hydrogen bonds, and display a water-octanol partition co-efficient of less than three. Again whilst the water-octanol partition co-efficients were not measured, it can be determined which of the compounds comply with the remaining rules. Fourteen of the compounds identified (**2-4**, **10**, **24**, **25**, **30**, **31**, **44-46**, **62**, **64** and **65**-see table below) comply with the remaining rules and therefore represent potential drug-leads. Twelve other compounds (**5-11**, **17-19**, **32** and **63**-see table below) do not conform to one of the remaining rules. Providing these compounds display a water-octanol partition co-efficient of less than three, they would also represent potential drug-leads.

The meroditerpenoids (**5-16**) were the most unstable structure class isolated in this thesis, in particular the hydroquinones which oxidised within a few days, even when stored at -80 °C. The phloroglucinols (**47-60**) which were isolated from several algae degraded after

approximately two weeks at -20 °C. The majority of the terrestrial natural products isolated were stable when stored at -20 °C and did not show any signs of degradation even after one year post isolation. In terms of bioavailability, it could be proposed that, once again, the meroditerpenoids and phloroglucinols would be the most unstable. This is attributed to the fact that they often contain functional groups such as alcohols and ketones, along with double bonds, which could be rapidly metabolised *in vivo*.

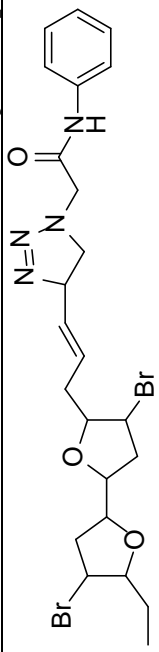



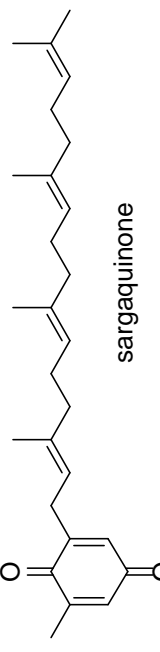
This thesis has illustrated that for the dereplication of natural products, the use of HPLC-NMR should be implemented in more instances. While the use of UV and MS data, from hyphenated techniques such as HPLC-MS in particular, has been widely adopted to prioritise and dereplicate samples, the use of these two pieces of data may, in more instances than not, fail to provide key structural information which can be used to determine if a particular crude extract or fraction contains a possible new compound. The information obtained from HPLC-NMR analysis provides a wealth of structural knowledge and should be widely implemented, in conjunction with a complementary technique such as HPLC-MS. In most chapters in this thesis, dereplication using HPLC-NMR together with HPLC-MS was able to deduce the identity of many components. However, if HPLC-MS had solely been used, as is the case for many dereplication studies, the identity of these components would have not been possible.

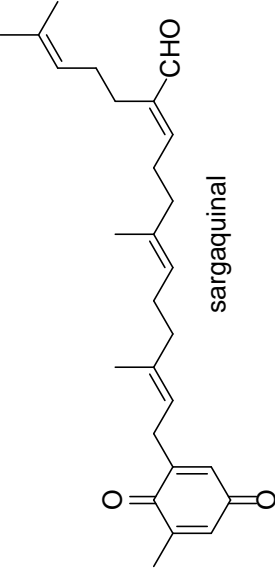
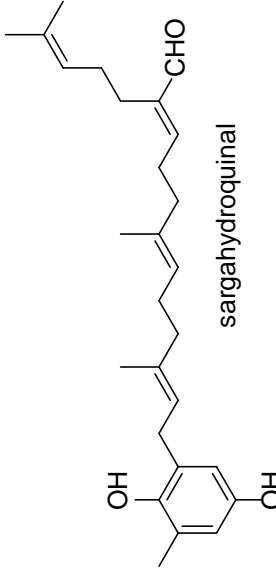
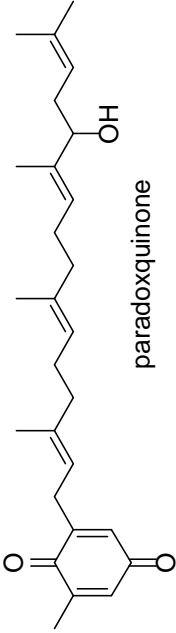
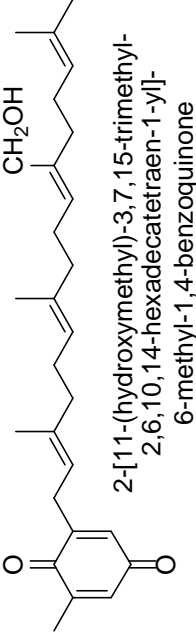
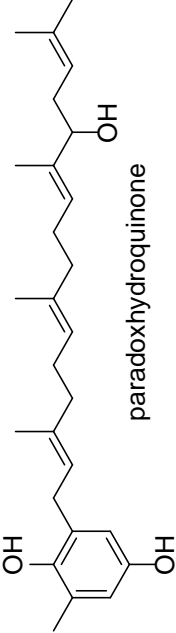
This thesis has also identified particular areas that should be prioritised for future research. Compounds which showed promising anti-bacterial activity, in particular the oxabenzochrysenones, phenylphenalenones, and compound **39**, should be further evaluated using more a sophisticated assay method such as a colorimetric cell proliferation assay. Many of the species investigated represent members of the *Sargassum* and *Cystophora* genera which produced an abundance of new chemical entities. This highlights the fact that these two genera should continue to be evaluated for further new chemistry. Two of the Australian plants studied are endemic to Western Australia which is an area of Australia with high biodiversity and remains understudied by natural product chemists. This should become an area for targeted research as should the study of Australian plants which may have been used

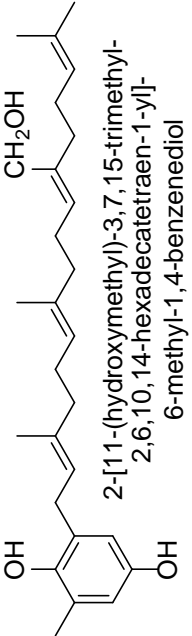
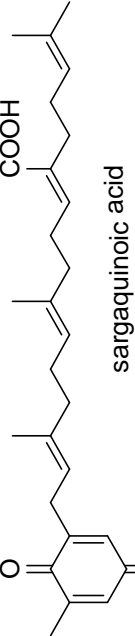
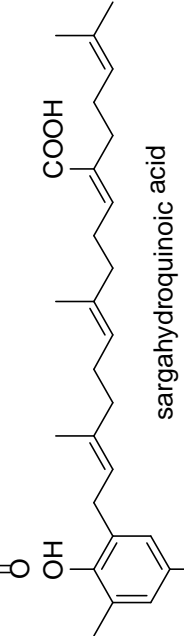
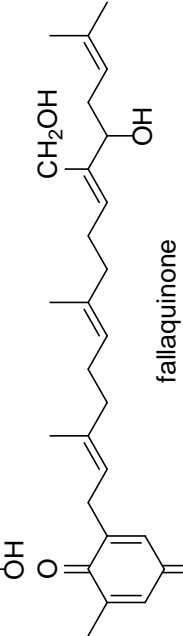
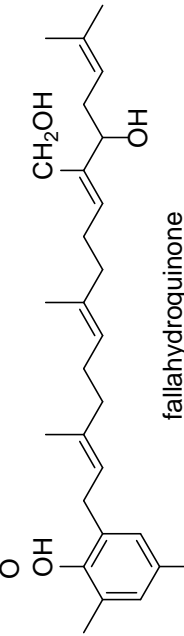
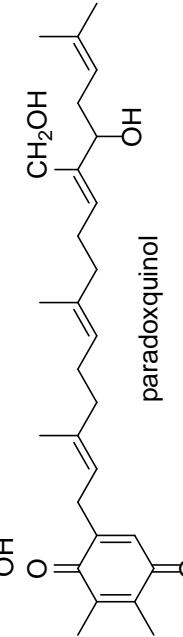
by the Australian Aborigines. The diversity present in the oceans and in marine invertebrates was exemplified in the study of a number of marine algae in this thesis and so the study of southern Australian marine invertebrates should also continue utilising efficient dereplication strategies such as those employed in this thesis. The MeOH crude extract of the bulbs of the kangaroo paw specimen (*Macropidia fuliginosa*) should be re-investigated as it displayed inhibitory activity against the MRSA bacterium. None of the compounds isolated from the MeOH extract described in this thesis displayed activity against MRSA. Either a synergistic effect is operating, or the compound responsible for the activity was not isolated. For this reason, this should be re-explored in an effort to deduce which of the two possibilities accounts for the activity displayed by the crude extract.

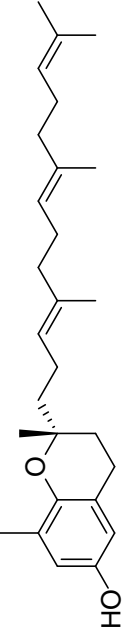
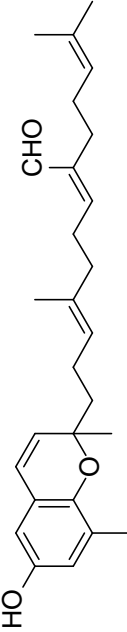
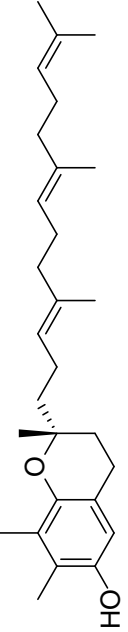
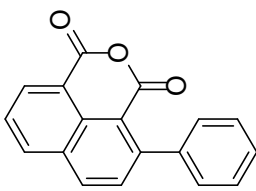
The table that follows provides a summary for each of the compounds identified. Compounds are arranged by chemical structure class and by molecular weight and also provided are the details of the source organism.

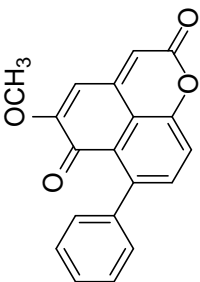
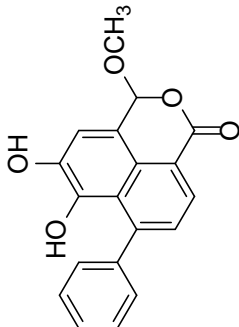
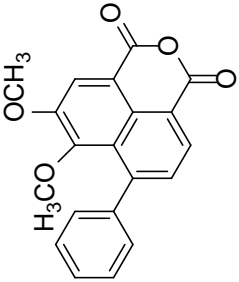
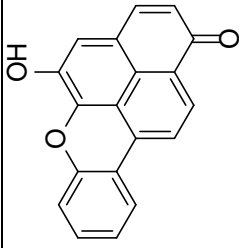
Summary of Compounds Identified

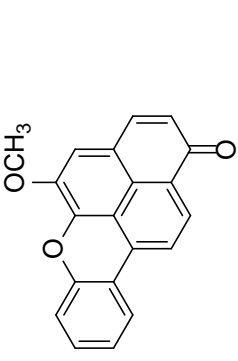
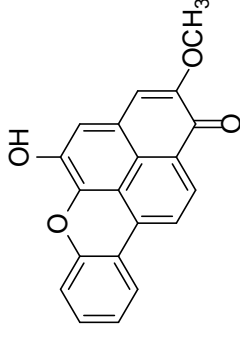
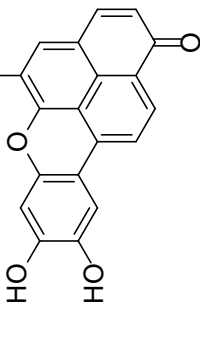
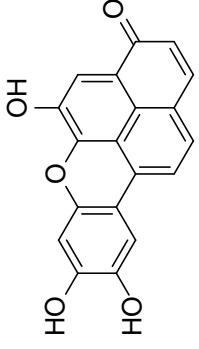
#	Structure and Name	Properties	Source	Activity	Comment	Chapter
Pyrano[3,2-b]pyranyl Vinyl Acetylenes						
1	 <p>(4,4'-dibromo-5-ethyl-5'-(Z)-pent-2-en-4-ynyl)octahydro[2,2']-bifuran</p>	MW 570 [α] ₃₆₅ ²⁵ +16.4	<i>L. elata</i>	-	New derivative	11
Fatty Acids						
2	 <p>linoleic acid</p>	MW 280	<i>L. birnbaumii</i>	<i>S. aureus</i> , <i>S. pyogenes</i>	Known	7
3	 <p>oleic acid</p>	MW 282	<i>L. birnbaumii</i>	<i>P. aeruginosa</i>	Known	7
4	 <p>methyl linoleate</p>	MW 294	<i>L. birnbaumii</i>	<i>S. aureus</i> , <i>P. aeruginosa</i> , <i>S. pyogenes</i>	Known	7
Meroditerpenoids						
5	 <p>sargaquinone</p>	MW 394	<i>S. paradoxum</i>	<i>P. aeruginosa</i>	Known, carbon NMR reassignment	9

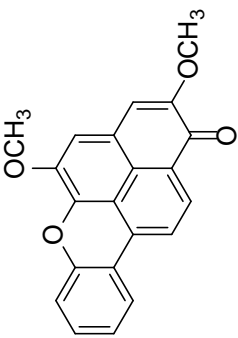
#	Structure and Name	Properties	Source	Activity	Comment	Chapter
Meroditerpenoids (cont.)						
6	 <p style="text-align: center;">sargaquinal</p>	MW 408	<i>S. paradoxum</i>	<i>P. aeruginosa</i> , <i>S. pyogenes</i>	Known	9
7	 <p style="text-align: center;">sargahydroquinal</p>	MW 410	<i>S. paradoxum</i>	-	New, identified by HPLC-NMR	9
8	 <p style="text-align: center;">paradoxquinone</p>	MW 410	<i>S. paradoxum</i>	<i>S. pyogenes</i>	New	9
9	 <p style="text-align: center;">2-[11-(hydroxymethyl)-3,7,15-trimethyl- 2,6,10,14-hexadecatetraen-1-yl]- 6-methyl-1,4-benzoquinone</p>	MW 410	<i>S. paradoxum</i>	<i>S. pyogenes</i>	Known, first isolation	9
10	 <p style="text-align: center;">paradoxhydroquinone</p>	MW 412	<i>S. paradoxum</i>	<i>S. pyogenes</i>	New	9

#	Structure and Name	Properties	Source	Activity	Comment	Chapter
Meroditerpenoids (cont.)						
11	 <p>2-[11-(hydroxymethyl)-3,7,15-trimethyl-2,6,10,14-hexadecatetraen-1-yl]-6-methyl-1,4-benzenediol</p>	MW 412	<i>S. paradoxum</i>	<i>S. pyogenes</i>	Known, first isolation	9
12	 <p>sargaquinoic acid</p>	MW 424	<i>S. paradoxum</i>	<i>S. aureus</i> , <i>S. aureus</i> MRSA, <i>P. aeruginosa</i> , <i>S. pyogenes</i>	Known	9
13	 <p>sargahydroquinoic acid</p>	MW 426	<i>S. paradoxum</i>	<i>S. aureus</i> , <i>S. aureus</i> MRSA, <i>P. aeruginosa</i> , <i>S. pyogenes</i>	Known, carbon NMR reassignment	9
14	 <p>fallaquinone</p>	MW 426 [α] _D ²⁵ +31.4	<i>S. paradoxum</i>	<i>P. aeruginosa</i>	Known	9
15	 <p>fallahydroquinone</p>	MW 428 [α] _D ²⁵ +45.1	<i>S. paradoxum</i>	<i>S. pyogenes</i>	Known, carbon and proton NMR reassignment	9
16	 <p>paradoxquinol</p>	MW 440 [α] _D ²⁵ +48.5	<i>S. paradoxum</i>	<i>S. pyogenes</i>	New	9

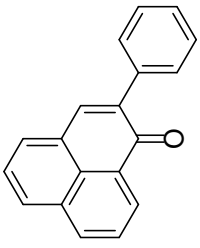
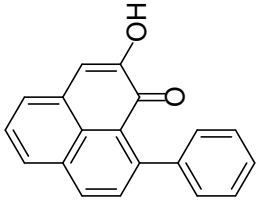
#	Structure and Name	Properties	Source	Activity	Comment	Chapter
Tocotrienols						
17	 (R) - δ -tocotrienol	MW 396	<i>C. monilifera</i> , <i>C. subfarcinata</i> , <i>S. cf fallax</i>	-	Known	8, 10
18	 (R) - γ -tocotrienol 9-(6-hydroxy-2,8-dimethyl-2H-1-benzopyran-2-yl)-6-methyl-2-(4-methyl-3-penten-1-yl)-2,6-nonadienal	MW 408	<i>S. paradoxum</i>	-	Known	9
19	 (R) - α -tocotrienol	MW 410	<i>C. monilifera</i>	-	Known, first isolation from marine source	10
Chromenes						
20	 2-phenylnaphthalic anhydride	MW 274	<i>M. fuliginosa</i>	<i>P. aeruginosa</i>	Known, first 2D NMR characterisation	5

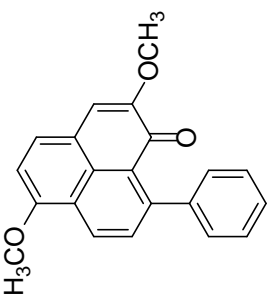
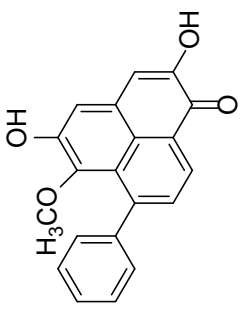
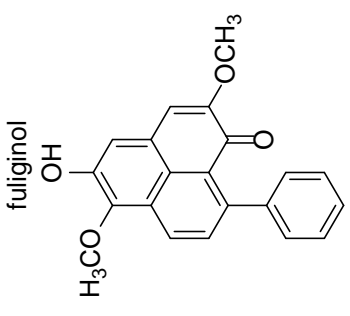
#	Structure and Name	Properties	Source	Activity	Comment	Chapter
Chromenes (cont.)						
21	 <p>haemodordione</p>	MW 304	<i>H. spicatum</i>	<i>E. coli</i>	New	6
22	 <p>haemodordiol</p>	MW 322	<i>H. spicatum</i>	<i>E. coli</i> , <i>S. aeruginosa</i> , <i>S. pyogenes</i>	New	6
23	 <p>5,6-dimethoxy-7-phenyl-1H,3H-naphtho[1,8-cd]pyran-1,3-dione</p>	MW 334	<i>H. spicatum</i>	-	Known	6
Oxabenzochrysenones						
24	 <p>5-hydroxy-1H-naphtho[2,1,8-mna]xanthen-1-one</p>	MW 286	<i>H. spicatum</i>	<i>P. aeruginosa</i> , <i>S. pyogenes</i>	Known, first isolation, first 2D NMR characterisation	6

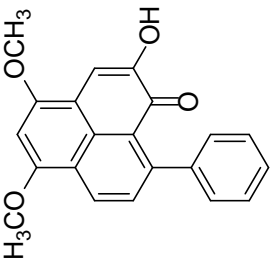
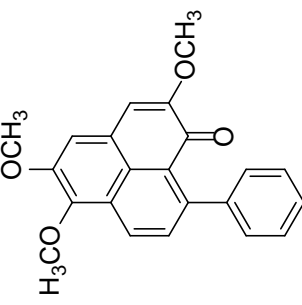
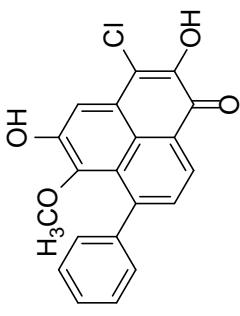
#	Structure and Name	Properties	Source	Activity	Comment	Chapter
Oxabenzochrysenones (cont.)						
25	 <p>5-methoxy-1H-naphtho[2,1,8-mna]xanthen-1-one</p>	MW 300	<i>H. spicatum</i>	<i>S. aureus</i> , <i>S. aureus</i> MRSA, <i>P. aeruginosa</i> , <i>S. pyogenes</i>	Known	6
26	 <p>5-hydroxy-2-methoxy-6-oxabenzodefchrysen-1-one</p>	MW 316	<i>H. spicatum</i>	<i>E. coli</i> , <i>P. aeruginosa</i> , <i>S. pyogenes</i>	Known	6
27	 <p>haemofluorone A</p>	MW 318	<i>M. fuliginosa</i>	<i>P. aeruginosa</i>	Known	5
28	 <p>haemofluorone B</p>	MW 318	<i>M. fuliginosa</i>	<i>P. aeruginosa</i>	Known	5

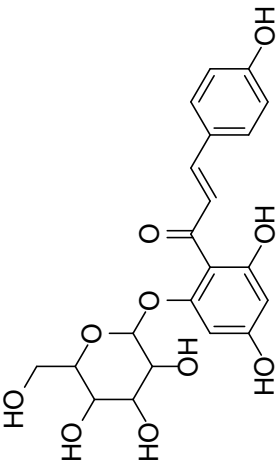
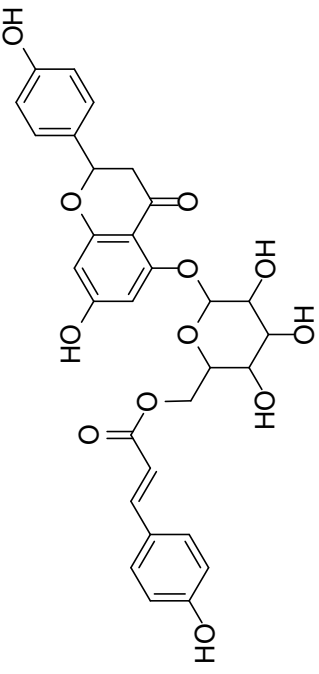
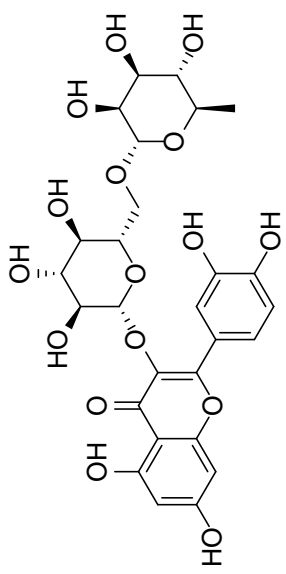
#	Structure and Name	Properties	Source	Activity	Comment	Chapter
Oxabenzochrysenones (cont.)						
29	 <p>2,5-dimethoxy-1H-naphtho[2,1,8-mna]xanthen-1-one</p>	MW 330	<i>H. spicatum</i>	<i>P. aeruginosa</i> , <i>S. pyogenes</i>	Known, first isolation, first 2D NMR characterisation	6

Phenylphenalenones

30	 <p>fuliginone</p>	MW 256	<i>M. fuliginosa</i>	<i>S. pyogenes</i>	New	5
31	 <p>anigorufone</p>	MW 272	<i>M. fuliginosa</i>	-	Known	5

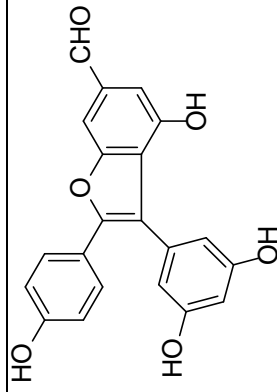
#	Structure and Name	Properties	Source	Activity	Comment	Chapter
Phenylphenalenones (cont.)						
32	 <p>2,6-dimethoxy-9-phenyl-1H-phenalen-1-one</p>	MW 316	<i>H. spicatum</i>	<i>E. coli</i> , <i>P. aeruginosa</i> , <i>S. pyogenes</i>	Known	6
33	 <p>fuliginol</p>	MW 318	<i>M. fuliginosa</i>	<i>S. pyogenes</i>	New	5
34	 <p>haemoxiphidone</p>	MW 332	<i>H. spicatum</i>	<i>E. coli</i> , <i>S. aureus</i> , <i>P. aeruginosa</i> , <i>S. pyogenes</i>	New	6

#	Structure and Name	Properties	Source	Activity	Comment	Chapter
Phenylphenalenones (cont.)						
35	 <p>haemodoronol</p>	MW 332	<i>H. spicatum</i>	<i>E. coli</i> , <i>S. aureus</i> , <i>S. aureus</i> MRSA, <i>P. aeruginosa</i> , <i>S. pyogenes</i>	New	6
36	 <p>2,5,6-trimethoxy-9-phenyl-1H-phenalen-1-one</p>	MW 346	<i>H. spicatum</i>	<i>E. coli</i> , <i>S. aureus</i> MRSA, <i>P. aeruginosa</i> , <i>S. pyogenes</i>	Known, first isolation, first 2D NMR characterisation	6
37	 <p>chlorofuliginol</p>	MW 352	<i>M. fuliginosa</i>	<i>S. pyogenes</i>	New	5

#	Structure and Name	Properties	Source	Activity	Comment	Chapter
Chalcones						
38	 <p>isosalipurposide</p>	MW 434	<i>M. fuliginosa</i>	<i>P. aeruginosa</i>	Known	5
Flavonoids						
39	 <p>6''-(<i>p</i>-hydroxycinnamate) salipurposide</p>	MW 580	<i>M. fuliginosa</i>	<i>E. coli</i> , <i>P. aeruginosa</i> , <i>S. pyogenes</i>	Known	5
40	 <p>rutin</p>	MW 610 [α] _D ²² +1.4	<i>M. fuliginosa</i>	-	Known	5

#	Structure and Name	Properties	Source	Activity	Comment	Chapter
---	--------------------	------------	--------	----------	---------	---------

Resveratrol Dimers



41

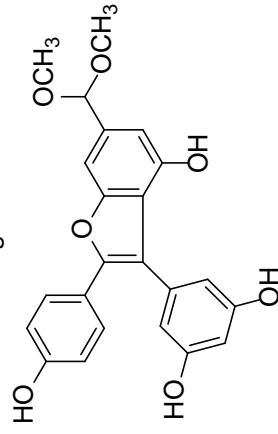
S. aureus,
S. pyogenes

M. fuliginosa

MW 362

5

fuliginosin A



42

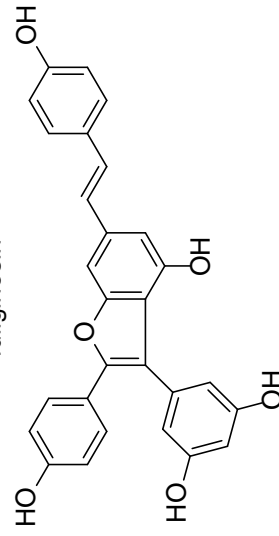
-

M. fuliginosa

MW 408

5

fuliginosin B



43

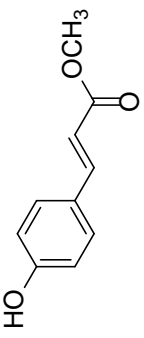
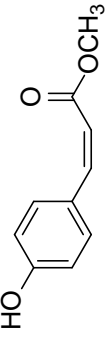
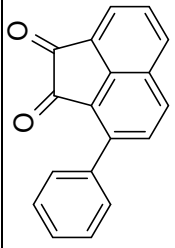
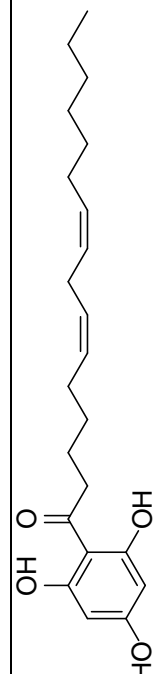
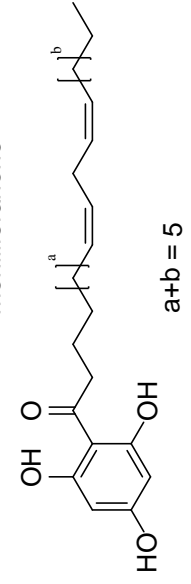
S. aureus,
S. pyogenes

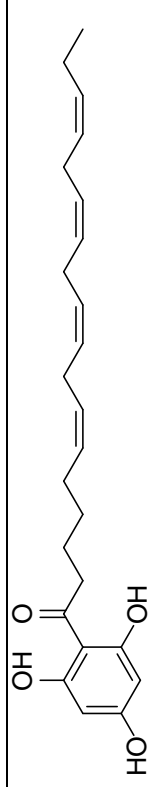
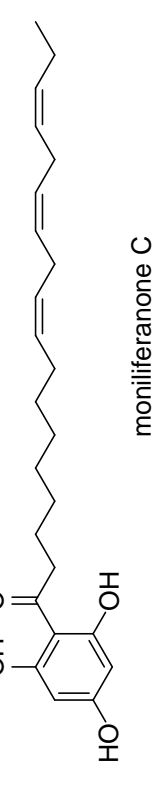
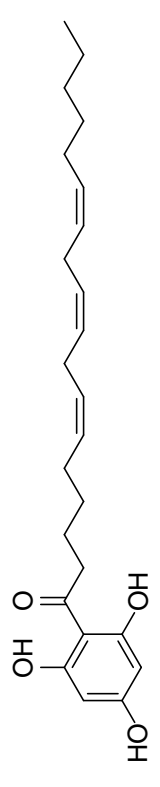
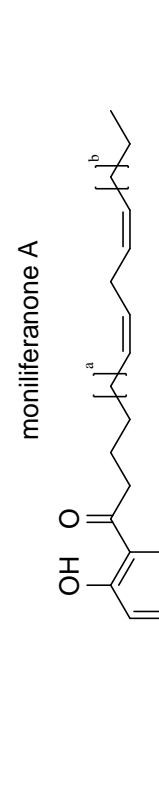
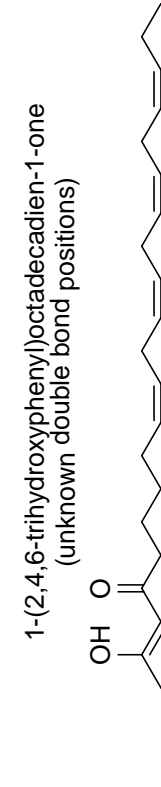
M. fuliginosa

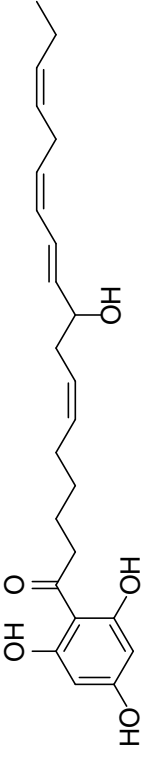
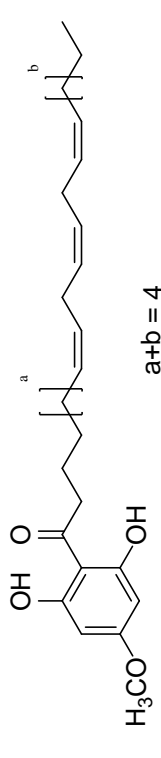
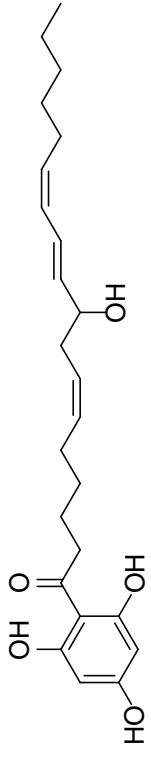
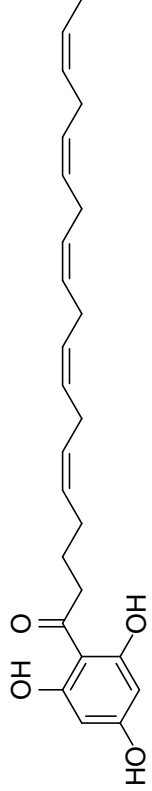
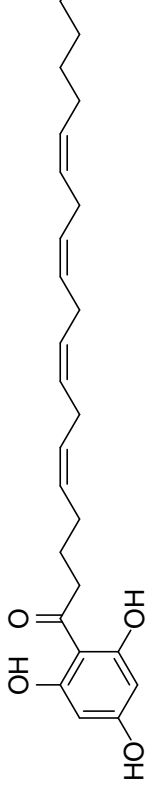
MW 452

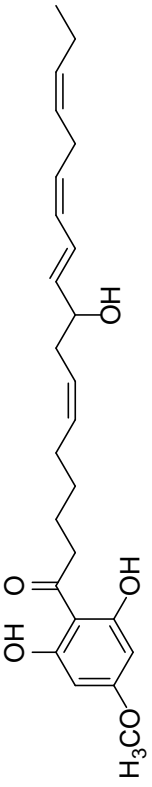
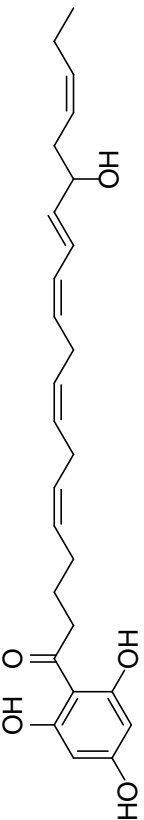
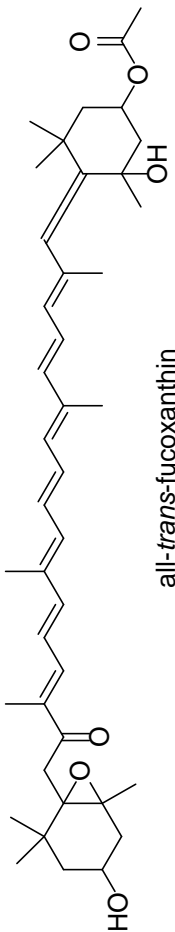
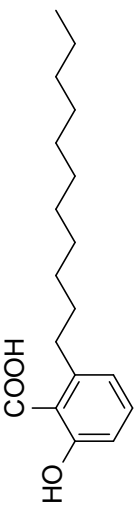
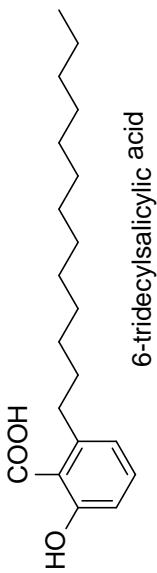
5

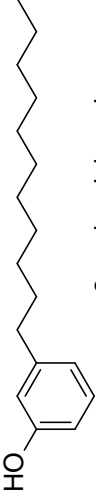
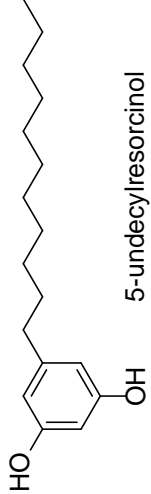
anigopreissin A

#	Structure and Name	Properties	Source	Activity	Comment	Chapter
Cinnamic Acid Derivatives						
44	 methyl <i>trans</i> <i>p</i> -coumarate	MW 178	<i>M. fuliginosa</i>	<i>S. aureus</i> , <i>S. pyogenes</i>	Known	5
45	 methyl <i>cis</i> <i>p</i> -coumarate	MW 178	<i>M. fuliginosa</i>	<i>S. aureus</i> , <i>S. pyogenes</i>	Known	5
Acenaphthylenes						
46	 fuliginosone	MW 258	<i>M. fuliginosa</i>	<i>S. aureus</i> , <i>P. aeruginosa</i>	New	5
Phloroglucinols						
47	 moniliferanone D	MW 360	<i>C. monilifera</i>	<i>S. pyogenes</i>	New	10
48	 1-(2,4,6-trihydroxyphenyl)hexadecadien-1-one (unknown double bond positions)	MW 360	<i>S. cf fallax</i>	-	New	8

#	Structure and Name	Properties	Source	Activity	Comment	Chapter
Phloroglucinols (cont.)						
49	 <p>1-(2,4,6-trihydroxyphenyl)-6Z,9Z,12Z,15Z-octadecatetraen-1-one</p>	MW 384	<i>C. monilifera</i> , <i>C. subfarcinata</i> , <i>C. retroflexa</i> , <i>S. cf fallax</i>	<i>S. pyogenes</i>	Known, first 2D NMR characterisation	8, 10
50	 <p>moniliferanone C</p>	MW 386	<i>C. monilifera</i> , <i>C. subfarcinata</i>	-	New	10
51	 <p>moniliferanone A</p>	MW 386	<i>C. monilifera</i> , <i>C. subfarcinata</i> , <i>C. retroflexa</i> , <i>S. cf fallax</i>	-	New	8, 10
52	 <p>1-(2,4,6-trihydroxyphenyl)octadecadien-1-one (unknown double bond positions)</p> <p>a+b = 7</p>	MW 388	<i>C. retroflexa</i> , <i>C. subfarcinata</i>	-	New	8
53	 <p>1-(2,6-dihydroxy-4-methoxyphenyl)- 6Z,9Z,12Z,15Z-octadecatetraen-1-one</p>	MW 398	<i>C. monilifera</i> , <i>C. subfarcinata</i> , <i>S. cf fallax</i>	<i>S. aureus</i> , <i>P. aeruginosa</i>	Known, first 2D NMR characterisation	8, 10

#	Structure and Name	Properties	Source	Activity	Comment	Chapter
Phloroglucinols (cont.)						
54	 <p>9-hydroxy-1-(2,4,6-trihydroxyphenyl)-6Z,10E,12Z,15Z-octadecatetraen-1-one</p>	MW 400	<i>C. monilifera</i> <i>C. retroflexa</i>	<i>S. pyogenes</i>	Known, first 2D NMR characterisation	8, 10
55	 <p>1-(2,6-dihydroxy-4-methoxyphenyl)octadecatrien-1-one (unknown double bond positions)</p>	MW 400	<i>C. subfarcinata</i>	-	New	8
56	 <p>retroflexanone</p>	MW 402	<i>C. retroflexa</i>	-	New	8
57	 <p>1-(2,4,6-trihydroxyphenyl)-5Z,8Z,11Z,14Z,17Z-eicosapentaen-1-one</p>	MW 410	<i>C. monilifera</i> , <i>C. subfarcinata</i> , <i>C. retroflexa</i>	-	Known, first 2D NMR characterisation	8, 10
58	 <p>moniliferanone B</p>	MW 412	<i>C. monilifera</i> , <i>C. subfarcinata</i> , <i>C. retroflexa</i> , <i>S. cf fallax</i>	<i>S. pyogenes</i>	New	8, 10

#	Structure and Name	Properties	Source	Activity	Comment	Chapter
Phloroglucinols (cont.)						
59	 <p>9-hydroxy-1-(2,6-dihydroxy-4-methoxyphenyl)-6Z,10Z,12Z,15Z-octadecatetraen-1-one</p>	MW 414	<i>C. monilifera</i>	-	Known	10
60	 <p>15-hydroxy-1-(2,4,6-trihydroxyphenyl)-5Z,8Z,11Z,13E,17Z-eicosapentaen-1-one</p>	MW 426	<i>C. monilifera</i>	-	Known, first 2D NMR characterisation, carbon reassignment	10
Xanthophylls						
61	 <p>all-trans-fucoxanthin</p>	MW 658	<i>S. vestitum</i> , <i>H. pseudospicata</i>	-	Known	8
Phenolic Acids						
62	 <p>6-undecylsalicylic acid</p>	MW 292	<i>S. decipiens</i>	-	Known	8
63	 <p>6-tridecylsalicylic acid</p>	MW 320	<i>S. decipiens</i>	-	Known	8

#	Structure and Name	Properties	Source	Activity	Comment	Chapter
Phenols						
64	 3-undecylphenol	MW 248	<i>S. decipiens</i>	-	Known	8
Resorcinols						
65	 5-undecylresorcinol	MW 264	<i>S. decipiens</i>	-	Known	8

References

- Chand, S., Lusunzi, I., Veal, D. A., Williams, L. R., & Karuso, P. (1994). Rapid screening of the antimicrobial activity of extracts and natural products. *Journal of Antibiotics*, 47(11), 1295-1304.
- Congreve, Miles, Carr, Robin, Murray, Chris, & Jhoti, Harren. (2003). A 'Rule of Three' for fragment-based lead discovery? *Drug Discovery Today*, 8(19), 876-877.
- Lipinski, Christopher A., Lombardo, Franco, Dominy, Beryl W., & Feeney, Paul J. (1997). Experimental and computational approaches to estimate solubility and permeability in drug discovery and development settings. *Advanced Drug Delivery Reviews*, 23(1-3), 3-25.
- Mann, C.M., & Markham, J. L. (1998). A new method for determining the minimum inhibitory concentration of essential oils. *Journal of Applied Microbiology*, 84(4), 538-544.

APPENDIX A

Supplementary Information for HPLC-NMR Limit of Detection Studies

This appendix contains further information relevant to the HPLC-NMR limit of detection studies as outlined in Chapter 4.

Limit of Detection Studies for Application to Natural Product Identification using High Performance Liquid Chromatography coupled to Nuclear Magnetic Resonance Spectroscopy

*Robert Brkljača and Sylvia Urban**

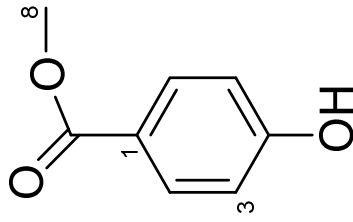
School of Applied Sciences (Discipline of Chemistry), Health Innovations Research Institute (HIRi) RMIT University, GPO Box 2476V Melbourne, Victoria 3001, Australia).

Supporting Information

- S1.** NMR data of methylparaben acquired by stop-flow HPLC-NMR and by conventional off-line NMR analyses.
- S2.** WET1D Proton NMR spectra (obtained from stop-flow HPLC-NMR mode) of methylparaben (amounts of 0.5, 0.7, 1, 5, 10, 15, 25, 50, 200, 500 and 1000 µg injected, 500 MHz, 50% CH₃CN/D₂O).
- S3.** WET1D Proton NMR spectrum (obtained from stop-flow HPLC-NMR mode) of methylparaben (5 µg injected, 500 MHz, 50% CH₃CN/D₂O).
- S4.** WET1D Proton NMR spectrum (obtained from conventional off-line NMR mode) of methylparaben (500 MHz, 50% CH₃CN/D₂O).
- S5.** gCOSY NMR spectrum (obtained from stop-flow HPLC-NMR mode) of methylparaben (5 µg injected, 500 MHz, 50% CH₃CN/D₂O).
- S6.** gCOSY NMR spectrum (obtained from conventional off-line NMR mode) of methylparaben (500 MHz, 50% CH₃CN/D₂O).
- S7.** HSQCAD NMR spectrum (obtained from stop-flow HPLC-NMR mode) of methylparaben (50 µg injected, 500 MHz, 50% CH₃CN/D₂O).
- S8.** HSQCAD NMR spectrum (obtained from conventional off-line NMR mode) of methylparaben (500 MHz, 50% CH₃CN/D₂O).
- S9.** gHMBCAD NMR spectrum (obtained from stop-flow HPLC-NMR mode) of methylparaben (250 µg injected, 500 MHz, 50% CH₃CN/D₂O).
- S10.** gHMBCAD NMR spectrum (obtained from conventional off-line NMR mode) of methylparaben (500 MHz, 50% CH₃CN/D₂O).
- S11.** NMR data of rhodamine B acquired by stop-flow HPLC-NMR and by conventional off-line NMR analyses.
- S12.** WET1D Proton NMR spectra (obtained from stop-flow HPLC-NMR mode) of rhodamine B (amounts of 25, 50, 100, 250, 500 and 1000 µg injected, 500 MHz, 50% CH₃CN/D₂O).
- S13.** WET1D Proton NMR spectrum (obtained from stop-flow HPLC-NMR mode) of rhodamine B (50 µg injected, 500 MHz, 50% CH₃CN/D₂O).
- S14.** WET1D Proton NMR spectrum (obtained from conventional off-line NMR mode) of rhodamine B (500 MHz, 50% CH₃CN/D₂O).

- S15.** gCOSY NMR spectrum (obtained from stop-flow HPLC-NMR mode) of rhodamine B (250 µg injected, 500 MHz, 50% CH₃CN/D₂O).
- S16.** gCOSY NMR spectrum (obtained from conventional off-line NMR mode) of rhodamine B (500 MHz, 50% CH₃CN/D₂O).
- S17.** HSQCAD NMR spectrum (obtained from stop-flow HPLC-NMR mode) of rhodamine B (500 µg injected, 500 MHz, 50% CH₃CN/D₂O).
- S18.** HSQCAD NMR spectrum (obtained from conventional off-line NMR mode) of rhodamine B (500 MHz, 50% CH₃CN/D₂O).
- S19.** gHMBCAD NMR spectrum (obtained from stop-flow HPLC-NMR mode) of rhodamine B (1000 µg injected, 500 MHz, 50% CH₃CN/D₂O).
- S20.** gHMBCAD NMR spectrum (obtained from conventional off-line NMR mode) of rhodamine B (500 MHz, 50% CH₃CN/D₂O).
- S21.** WET1D Proton NMR spectrum (obtained from stop-flow HPLC-NMR mode) of component 1 at 9.59 mins (3520 µg of the crude extract of *C. subfarcinata* injected, 500 MHz, 75% CH₃CN/D₂O).
- S22.** gCOSY NMR spectrum (obtained from stop-flow HPLC-NMR mode) of component 1 at 9.59 mins (500 MHz, 75% CH₃CN/D₂O).
- S23.** HSQCAD NMR spectrum (obtained from stop-flow HPLC-NMR mode) of component 1 at 9.59 mins (500 MHz, 75% CH₃CN/D₂O).
- S24.** gHMBCAD NMR spectrum (obtained from stop-flow HPLC-NMR mode) of component 1 at 9.59 mins (500 MHz, 75% CH₃CN/D₂O).
- S25.** High resolution negative ESI-MS of component 1 at 9.59 mins obtained from HRESILC-MS.
- S26.** WET1D Proton NMR spectrum (obtained from stop-flow HPLC-NMR mode) of component 2 at 13.05 mins (3520 µg of the crude extract of *C. subfarcinata* injected, 500 MHz, 75% CH₃CN/D₂O).
- S27.** gCOSY NMR spectrum (obtained from stop-flow HPLC-NMR mode) of component 2 at 13.05 mins (500 MHz, 75% CH₃CN/D₂O).
- S28.** HSQCAD NMR spectrum (obtained from stop-flow HPLC-NMR mode) of component 2 at 13.05 mins (500 MHz, 75% CH₃CN/D₂O).
- S29.** High resolution negative ESI-MS of component 2 at 13.05 mins obtained from HRESILC-MS.

*Corresponding author. Tel: +61 3 9925 3376; Fax: +61 3 9925 3747
E-mail address: sylvia.urban@rmit.edu.au (S. Urban).



S1. NMR data of methylparaben acquired by stop-flow HPLC-NMR and by conventional off-line NMR analyses.

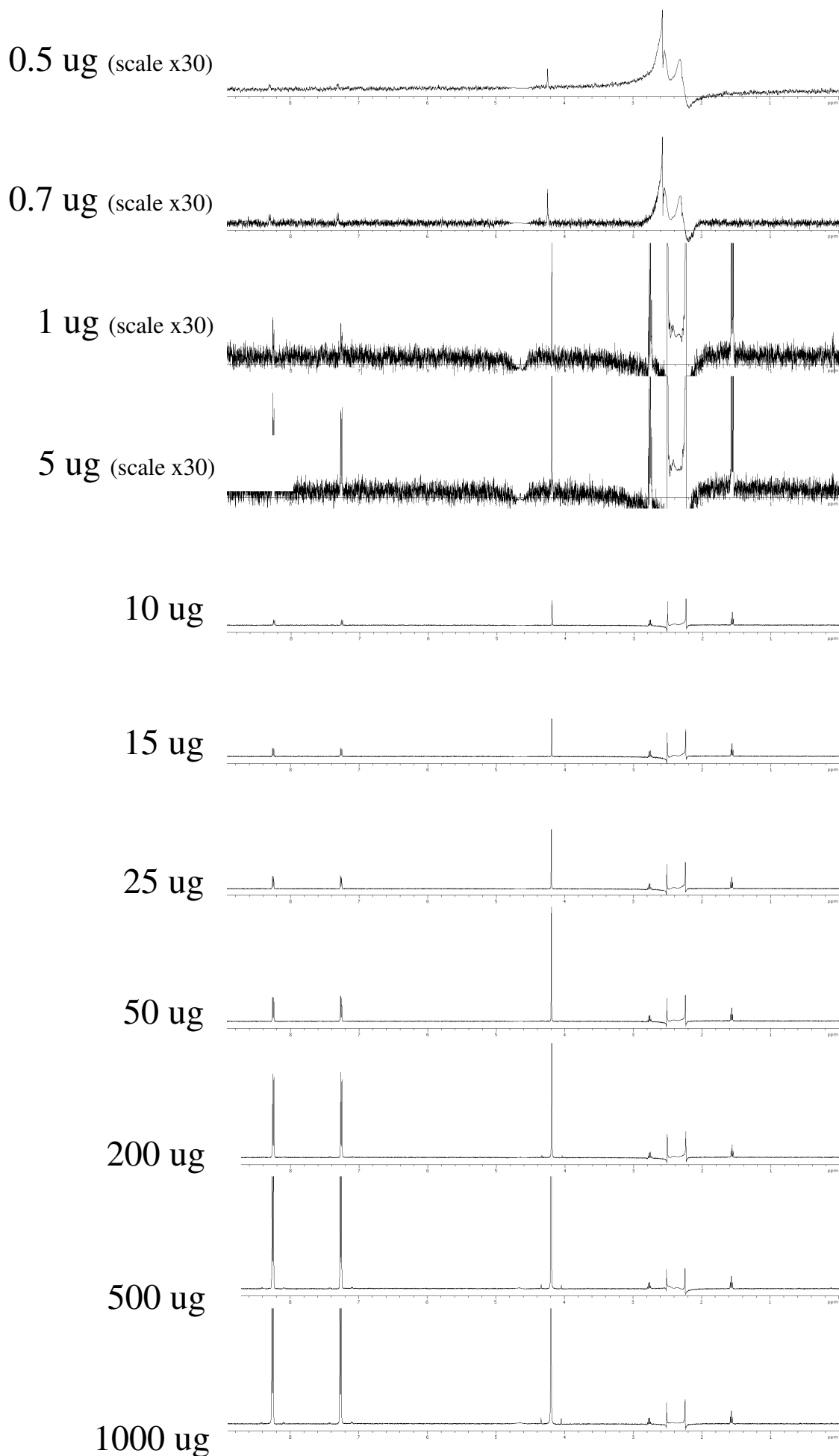
methyl paraben (HPLC-NMR) (500 MHz, 50% CH₃CN/D₂O)		methyl paraben (conventional NMR) (500 MHz, 50% CH₃CN/D₂O)						
Position	Proton (<i>J</i> in Hz) ^a	gCOSY ^a	HSQCAD (mult.) ^b	gHMBCAD ^c	Proton (<i>J</i> in Hz)	gCOSY	HSQCAD (mult.)	gHMBCAD
2	8.30, d (9.0)	H-3	132.3, d	C-4, C-6, C-7	8.26, d (9.0)	H-3	132.2, d	C-1 ^w , C-3 ^w , C-4, C-6, C-7
3	7.31, d (9.0)	H-2	115.8, d	C-1, C-4 ^w , C-5	7.28, d(9.0)	H-2	115.8, d	C1, C-2 ^w , C-4, C-5, C-7
5	7.31, d (9.0)	H-6	115.8, d	C-1, C-3, C-4 ^w	7.28, d(9.0)	H-6	115.8, d	C-1, C-3, C-4, C-6 ^w , C-7
6	8.30, d (9.0)	H-5	132.3, d	C-2, C-4, C-7	8.26, d(9.0)	H-5	132.2, d	C-1 ^w , C-2, C-4, C-5 ^w , C-7
8	4.24, s	-	52.4, q	C-7	4.21, s	-	52.4, q	C-7

^a Data obtained at 5 µg.

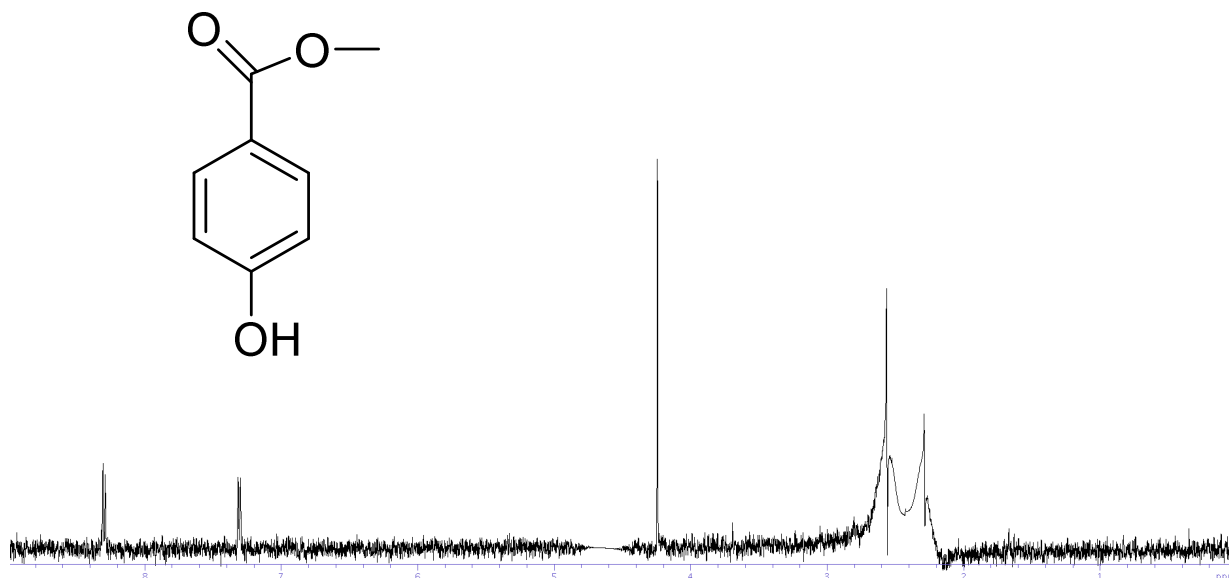
^b Data obtained at 50 µg.

^c Data obtained at 250 µg.

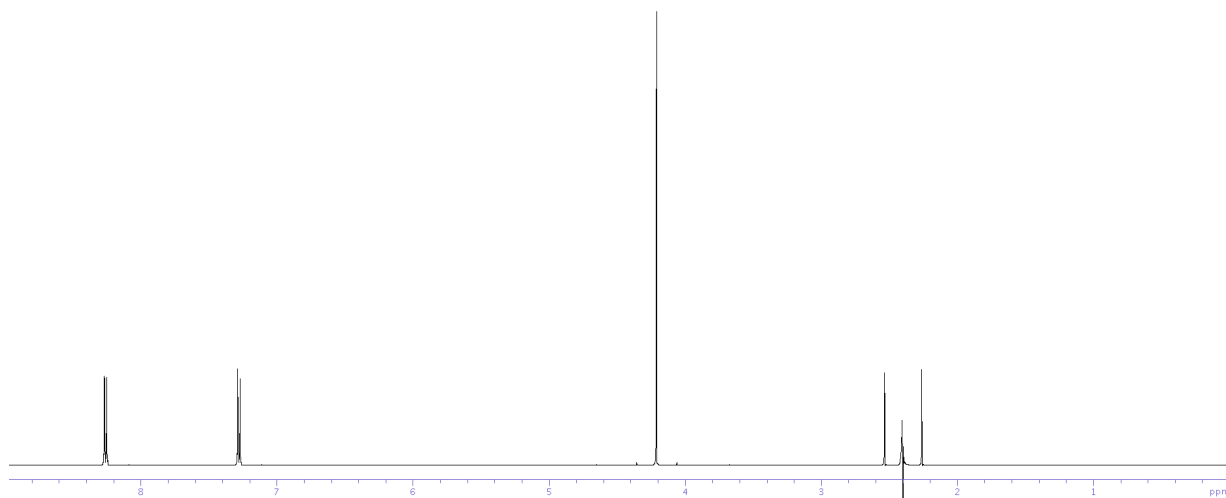
^w Indicates weak or long range correlation



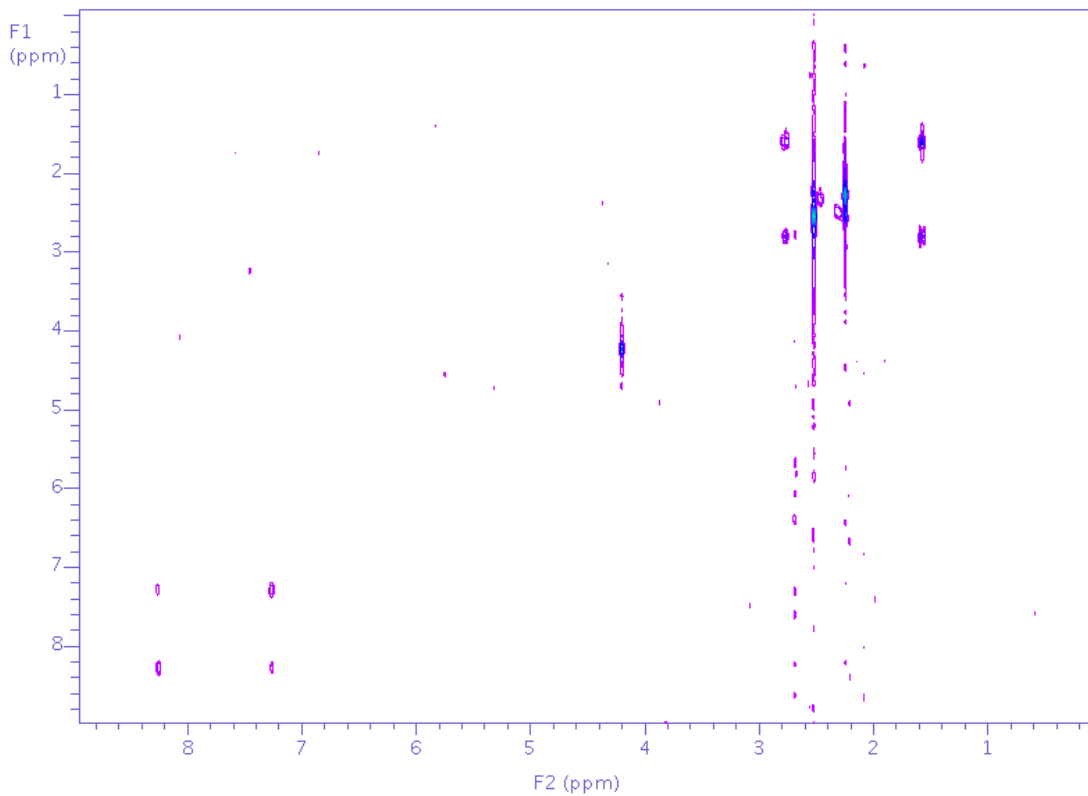
S2. WET1D Proton NMR spectra (obtained from stop-flow HPLC-NMR mode) of methylparaben (amounts of 0.5, 0.7, 1, 5, 10, 15, 25, 50, 200, 500 and 1000 µg injected, 500 MHz, 50% CH₃CN/D₂O).



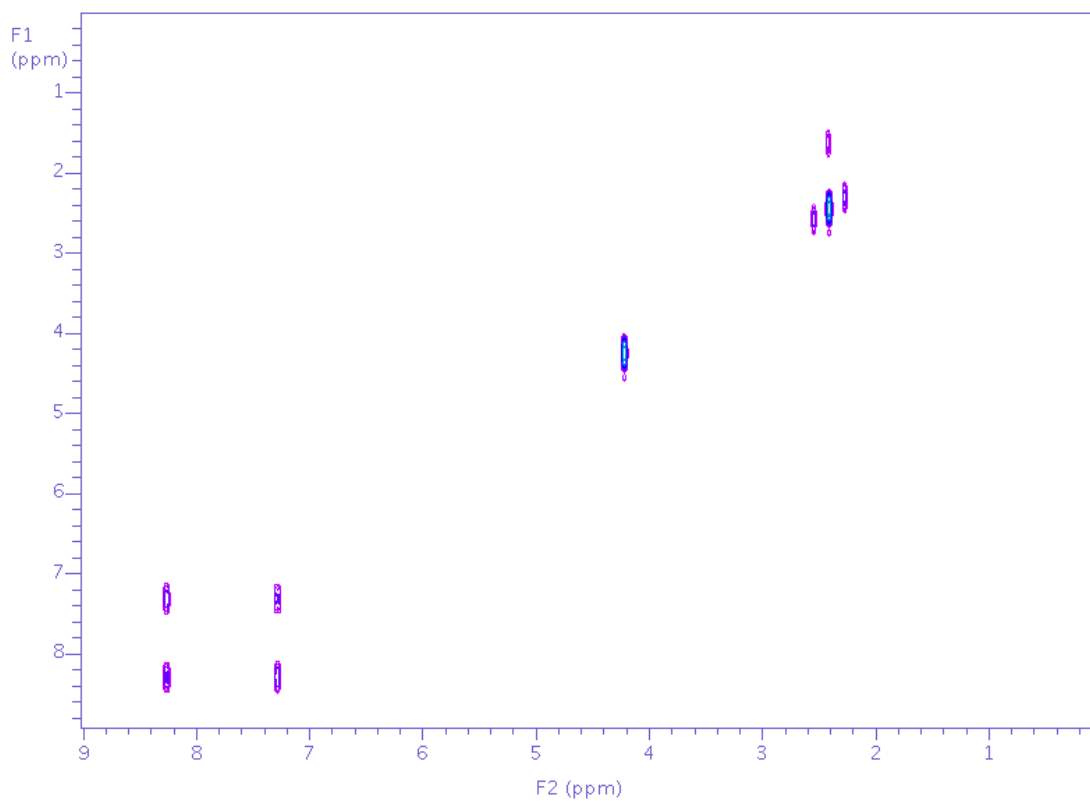
S3. WET1D Proton NMR spectrum (obtained from stop-flow HPLC-NMR mode) of methylparaben (5 μ g injected, 500 MHz, 50% CH₃CN/D₂O).



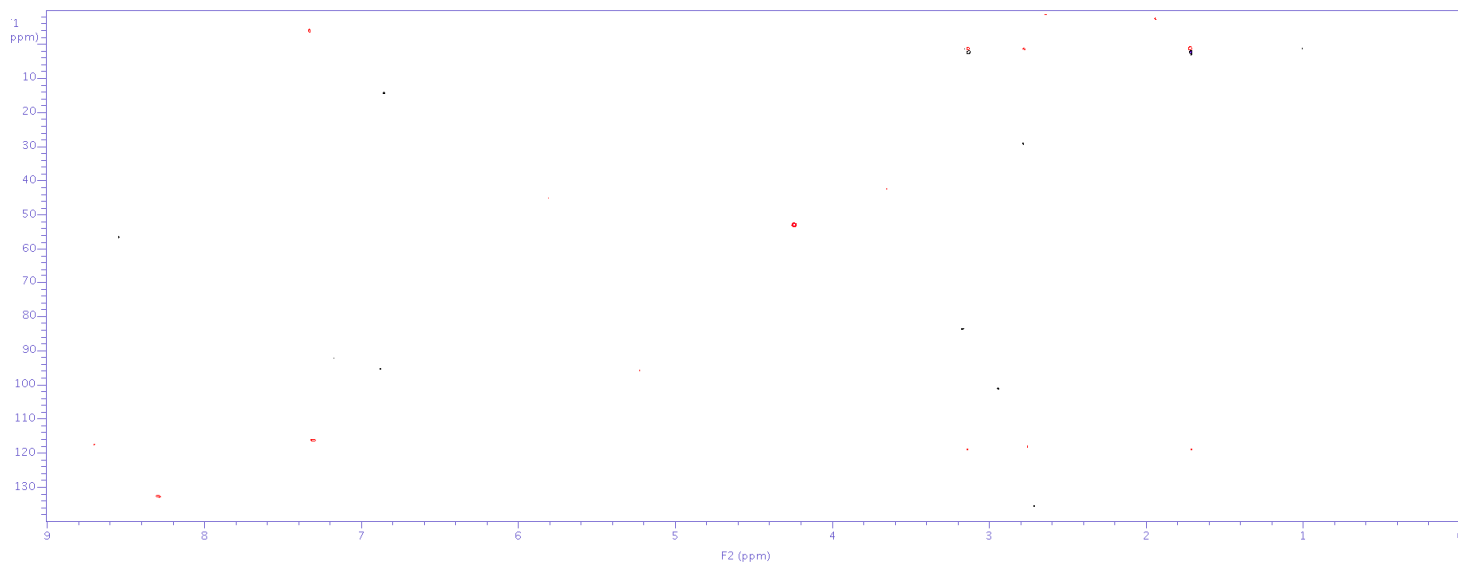
S4. WET1D Proton NMR spectrum (obtained from conventional off-line NMR mode) of methylparaben (500 MHz, 50% CH₃CN/D₂O).



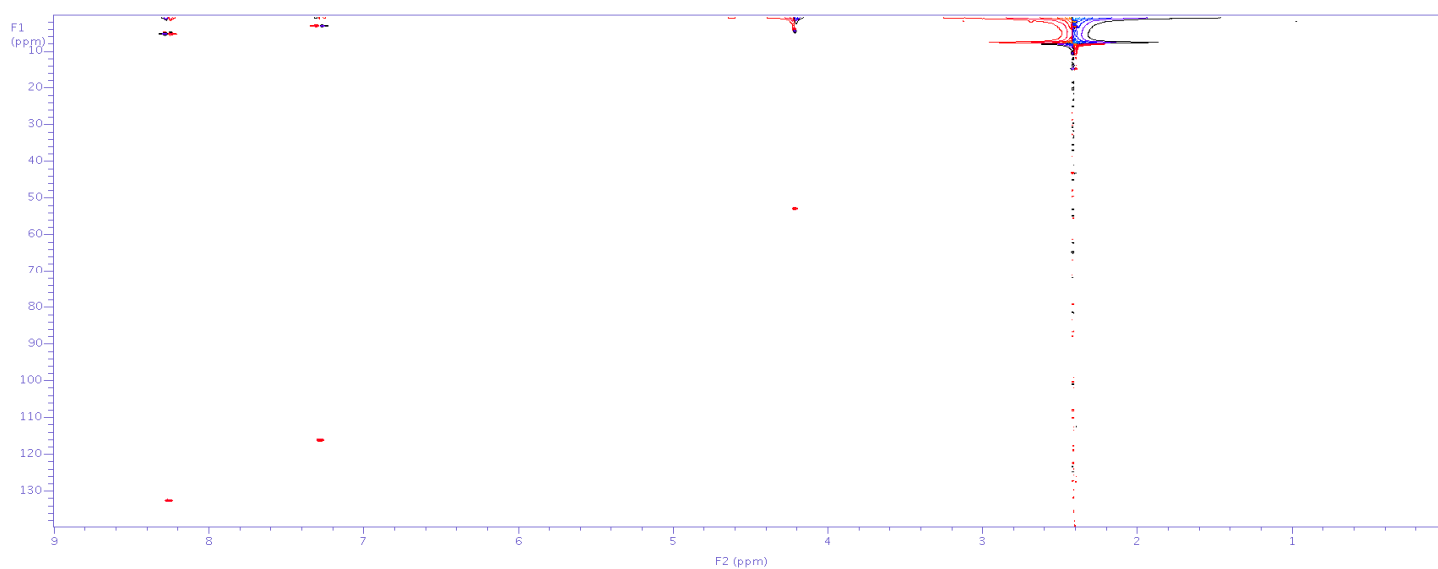
S5. gCOSY NMR spectrum (obtained from stop-flow HPLC-NMR mode) of methylparaben (5 μ g injected, 500 MHz, 50% CH₃CN/D₂O).



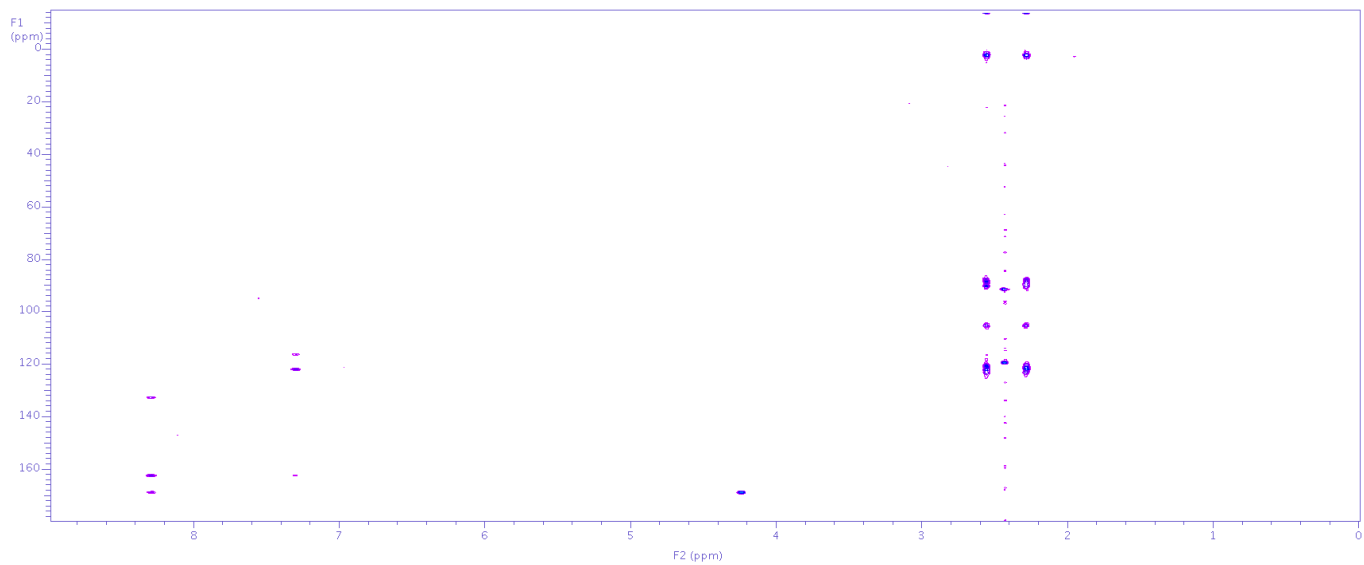
S6. gCOSY NMR spectrum (obtained from conventional off-line NMR mode) of methylparaben (500 MHz, 50% CH₃CN/D₂O).



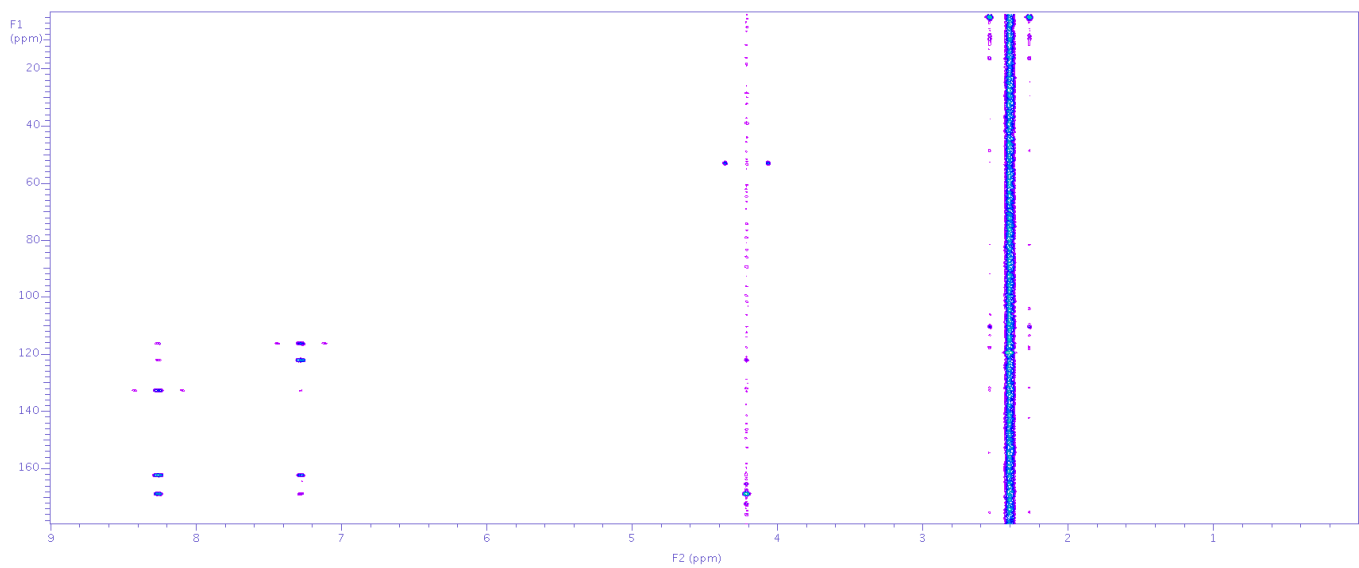
S7. HSQCAD NMR spectrum (obtained from stop-flow HPLC-NMR mode) of methylparaben (50 μg injected, 500 MHz, 50% $\text{CH}_3\text{CN}/\text{D}_2\text{O}$).



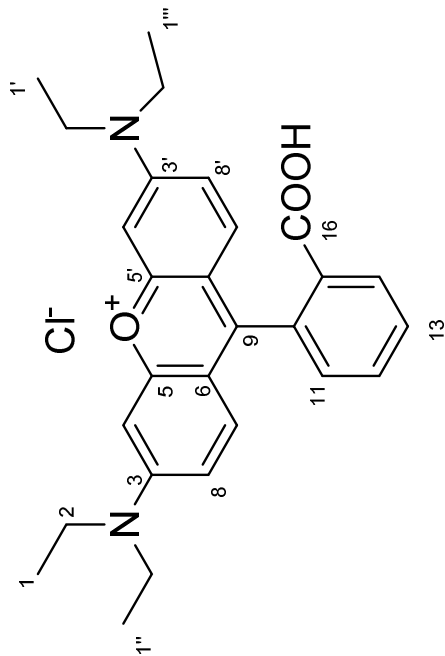
S8. HSQCAD NMR spectrum (obtained from conventional off-line NMR mode) of methylparaben (500 MHz, 50% $\text{CH}_3\text{CN}/\text{D}_2\text{O}$).



S9. gHMBCAD NMR spectrum (obtained from stop-flow HPLC-NMR mode) of methylparaben (250 μg injected, 500 MHz, 50% $\text{CH}_3\text{CN}/\text{D}_2\text{O}$).



S10. gHMBCAD NMR spectrum (obtained from conventional off-line NMR mode) of methylparaben (500 MHz, 50% $\text{CH}_3\text{CN}/\text{D}_2\text{O}$).



S11. NMR data of rhodamine B acquired by stop-flow HPLC-NMR and by conventional off-line NMR analyses.

rhodamine B (HPLC-NMR) (500 MHz, 50% CH ₃ CN/D ₂ O)				rhodamine B (conventional NMR) (500 MHz, 50% CH ₃ CN/D ₂ O)				
Position	Proton (<i>J</i> in Hz) ^a	gCOSY ^b	HSQCAD (mult.) ^c	gHMBCAD ^d	Proton (<i>J</i> in Hz) ^b	gCOSY ^b	HSQCAD (mult.) ^b	gHMBCAD ^b
1	1.66, t (7.0)	H-2	12.3, q	C-2	1.64, t (7.0)	H-2	12.3, q	C-2
2	4.00, q (7.0)	H-1	46.1, t	C-1, C-3, C-2''	4.00, q (7.0)	H-1	46.1, t	C-1, C-3, C-2''
4	7.25, bs	-	96.3, d	5, 6, 8	7.26, bs	H-8	96.4, d	C-5, C-6, C-8
7	7.61, d (10.0)	H-8	131.6, d	C-3, C-5, C-6 ^w , C-8, C-9	7.48, d (9.5)	H-8	131.6, d	C-3, C-4, C-5, C-6, C-8, C-9
8	7.36, dd (10.0, 1.0)	H-7	114.6, d	C-4, C-6	7.33, bd (9.5)	H-4, H-7	114.6, d	C-4, C-6, C-7
11	7.59, m	H-12	130.5, d	C-13	7.74, d (7.5)	H-12	130.5, d	C-9, C-13, C-15
12	8.08, dd (7.5, 8.0)	H-11	133.3, d	C-10, C-13	8.24, dd (7.5, 7.5)	H-11	133.4, d	C-10, C-16 ^w
13	8.02, dd (7.0, 7.5)	H-14	130.8, d	C-15	8.19, dd (7.5, 7.5)	H-14	130.8, d	C-10, C-12, C-14
14	8.41, d (7.0)	H-13	131.8, d	C-10, C-12, C-16	8.70, d (7.5)	H-13	131.8, d	C-11, C-13, C-15
1'	1.66, t (7.0)	H-2'	12.3, q	C-2'	1.64, t (7.0)	H-2'	12.3, q	C-2'
2'	4.00, q (7.0)	H-1'	46.1, t	C-1', C-3', C-2'''	4.00, q (7.0)	H-1'	46.1, t	C-1', C-3', C-2'''
4'	7.25, bs	-	96.3, d	C-5', C-6', C-8'	7.26, bs	H-8'	96.4, d	C-5', C-6', C-8'
7'	7.61, d (10.0)	H-8'	131.6, d	C-9, C-3', C-5', C-6 ^w , C-8'	7.48, d (9.5)	H-8'	131.6, d	C-9, C-3', C-4', C-5', C-6', C-8'
8'	7.36, dd (10.0, 1.0)	H-7'	114.6, d	C-4', C-6'	7.33, bd (9.5)	H-4', H-7'	114.6, d	C-4', C-6', C-7'
1''	1.66, t (7.0)	H-2''	12.3, q	C-2''	1.64, t (7.0)	H-2''	12.3, q	C-2''
2''	4.00, q (7.0)	H-1''	46.1, t	C-2, C-3, C-1''	4.00, q (7.0)	H-1''	46.1, t	C-2, C-3, C-1''
1'''	1.66, t (7.0)	H-2'''	12.3, q	C-2'''	1.64, t (7.0)	H-2'''	12.3, q	C-2'''
2'''	4.00, q (7.0)	H-1'''	46.1, t	C-2', C-3', C-1'''	4.00, q (7.0)	H-1'''	46.1, t	C-2', C-3', C-1'''

^a Data obtained at 50 µg (please note that chemical shifts vary with concentration).

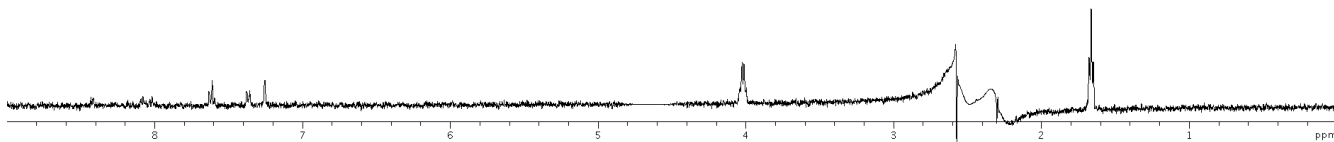
^b Data obtained at 250 µg.

^c Data obtained at 500 µg.

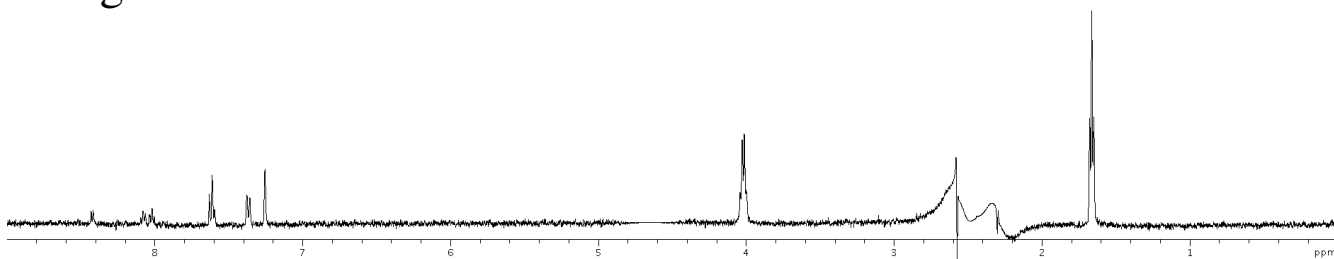
^d Data obtained at 1000 µg.

^w Indicated weak or long range correlation

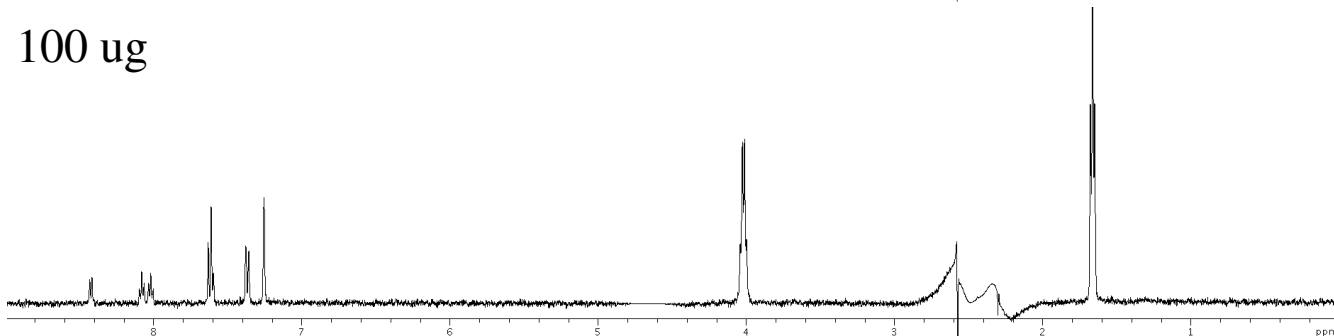
25 ug



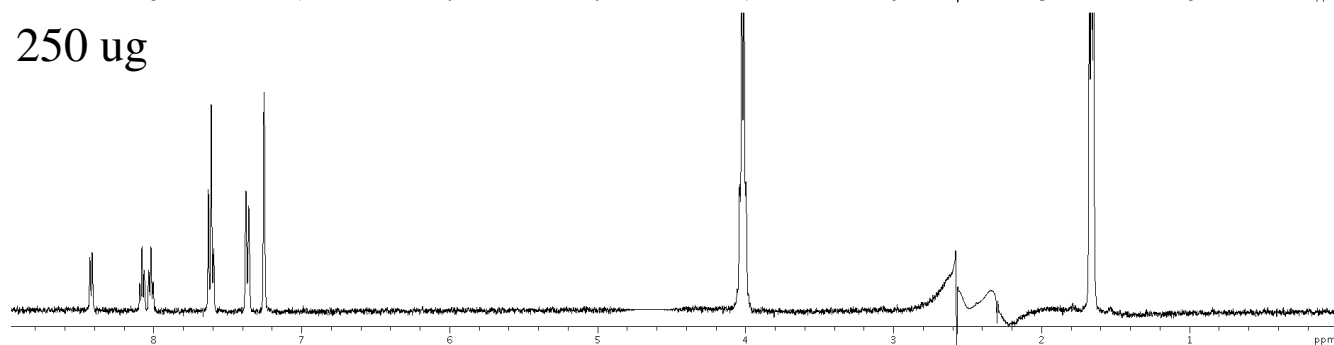
50 ug



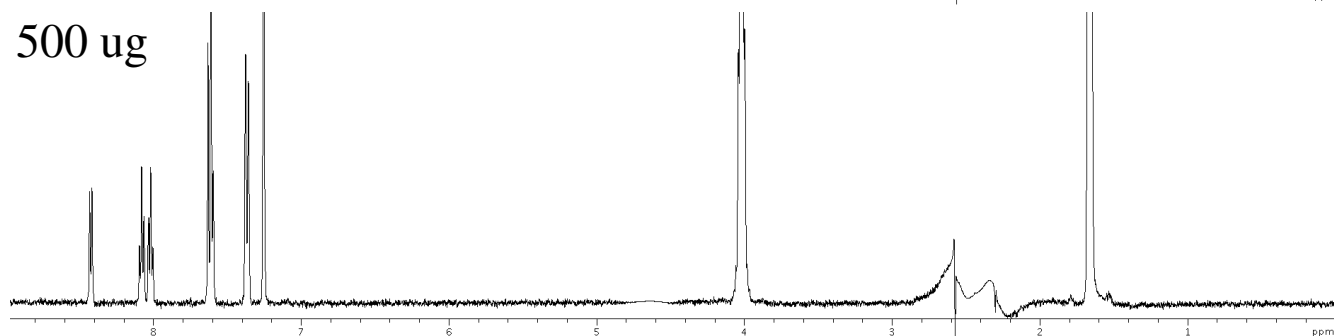
100 ug



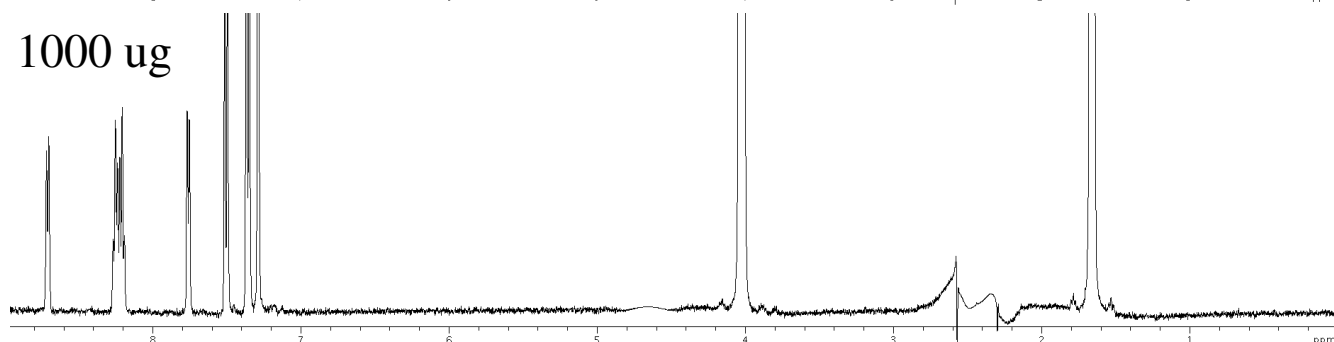
250 ug



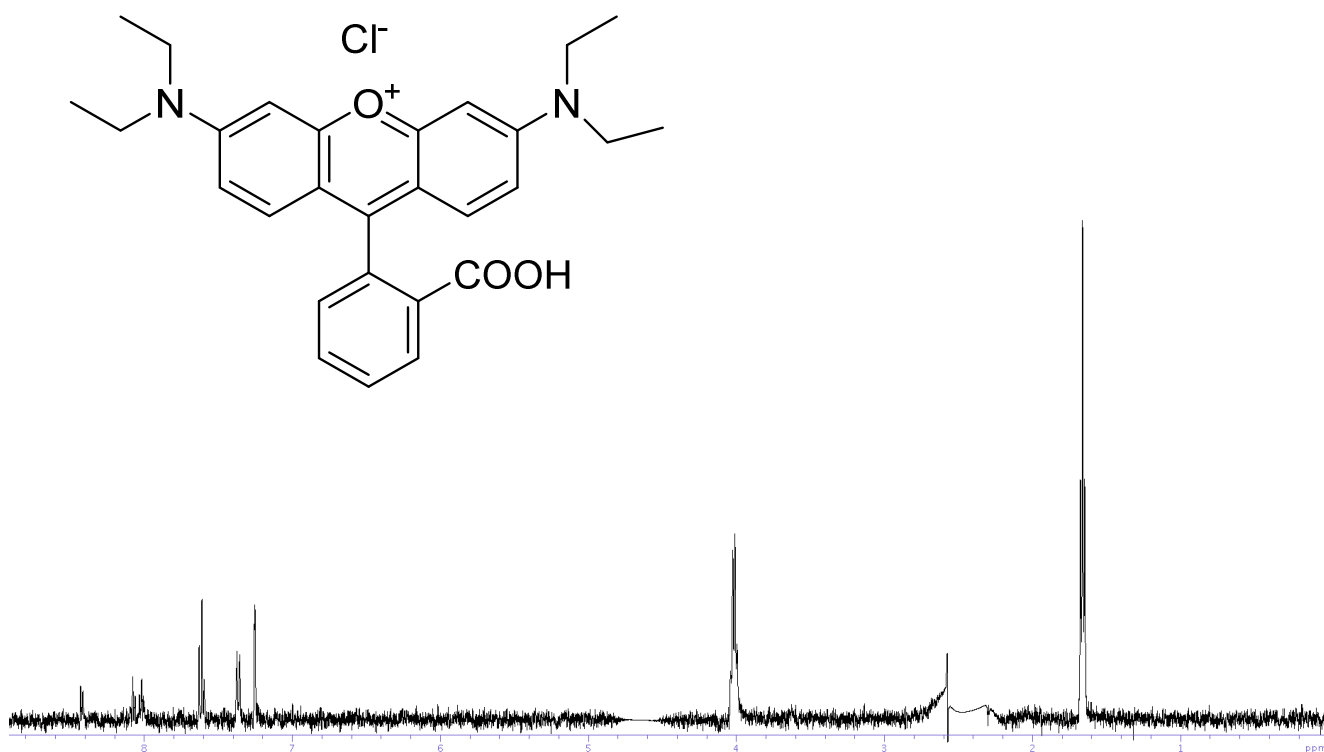
500 ug



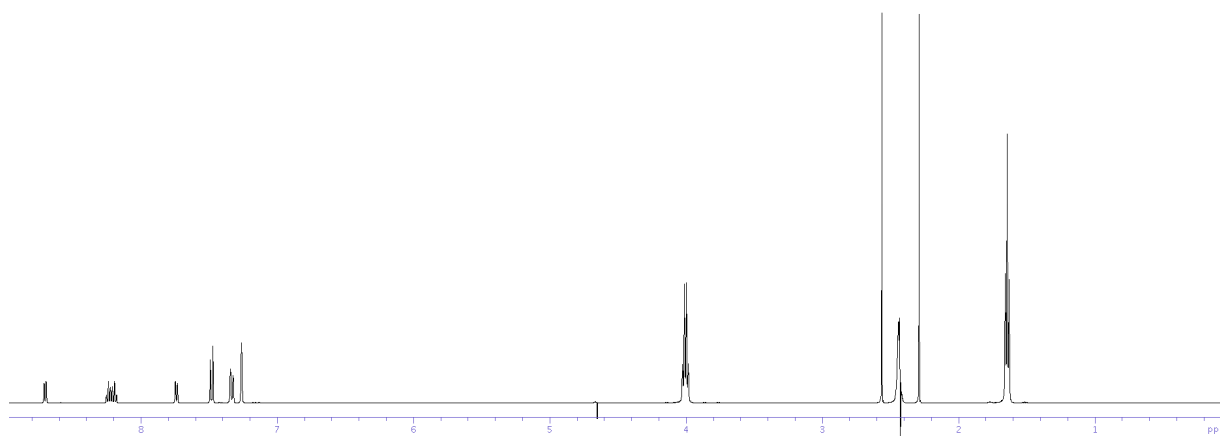
1000 ug



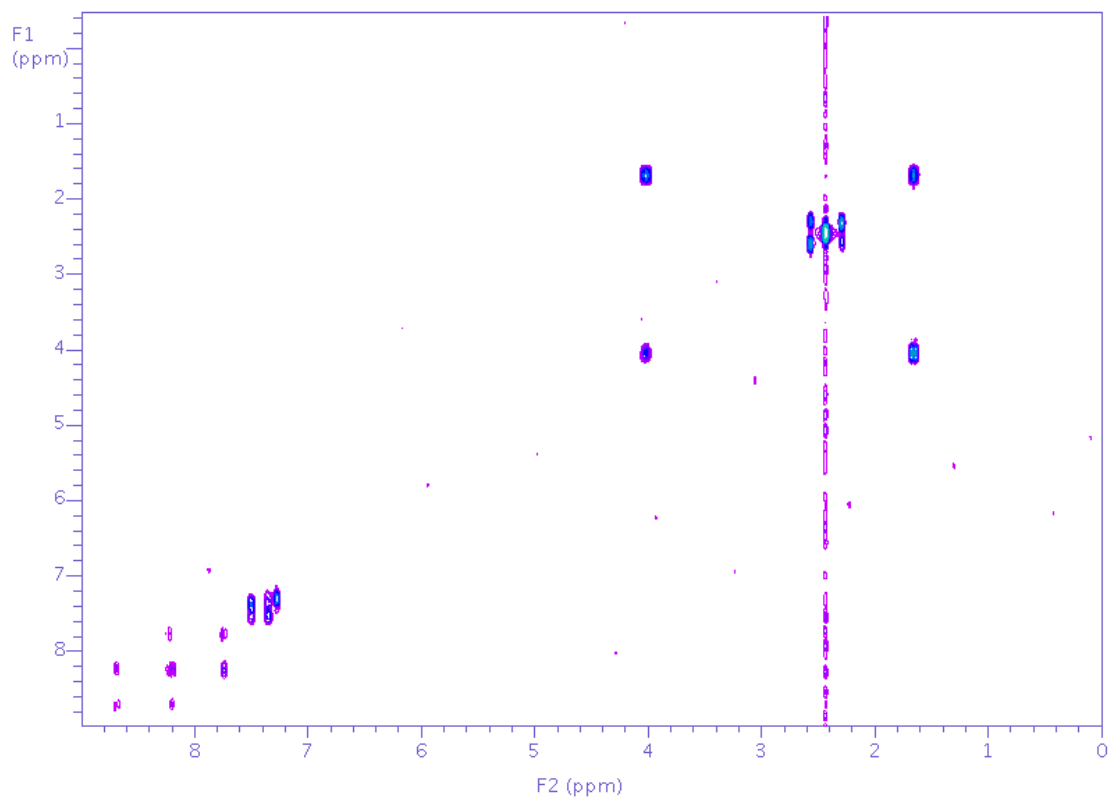
S12. WET1D Proton NMR spectra (obtained from stop-flow HPLC-NMR mode) of rhodamine B (amounts of 25, 50, 100, 250, 500 and 1000 μg injected, 500 MHz, 50% $\text{CH}_3\text{CN}/\text{D}_2\text{O}$).



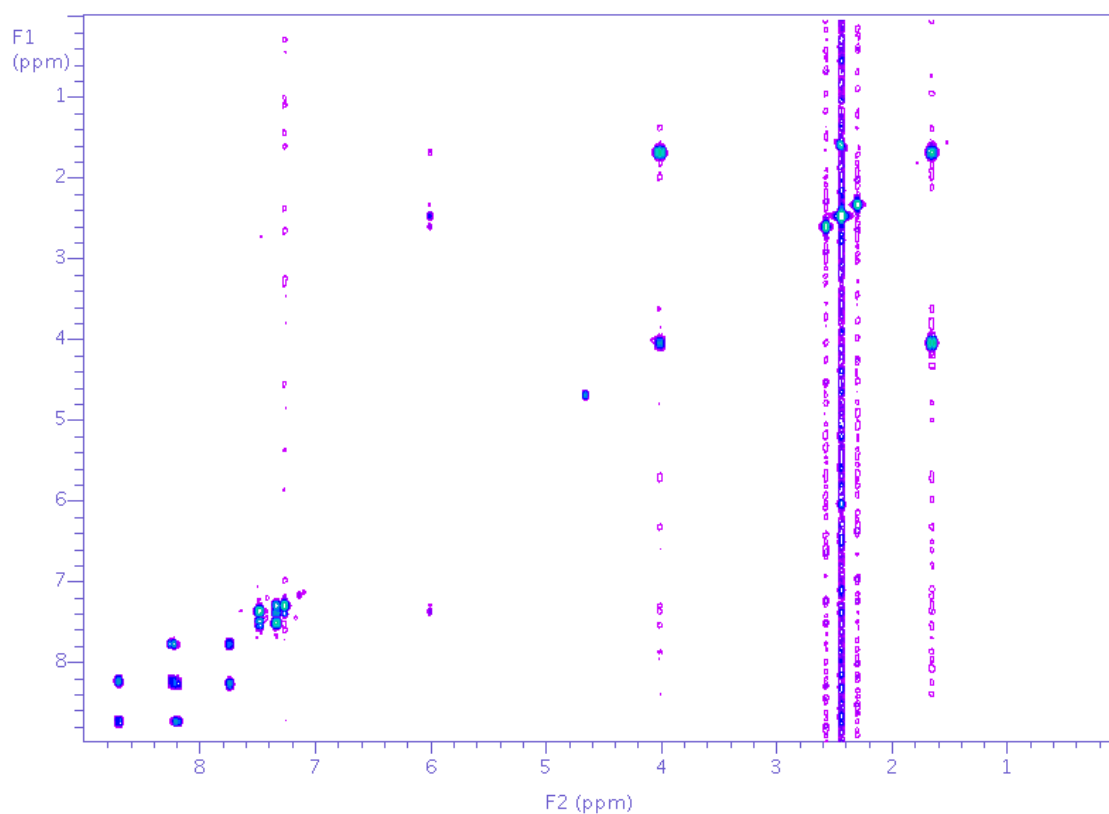
S13. WET1D Proton NMR spectrum (obtained from stop-flow HPLC-NMR mode) of rhodamine B (50 μg injected, 500 MHz, 50% $\text{CH}_3\text{CN}/\text{D}_2\text{O}$).



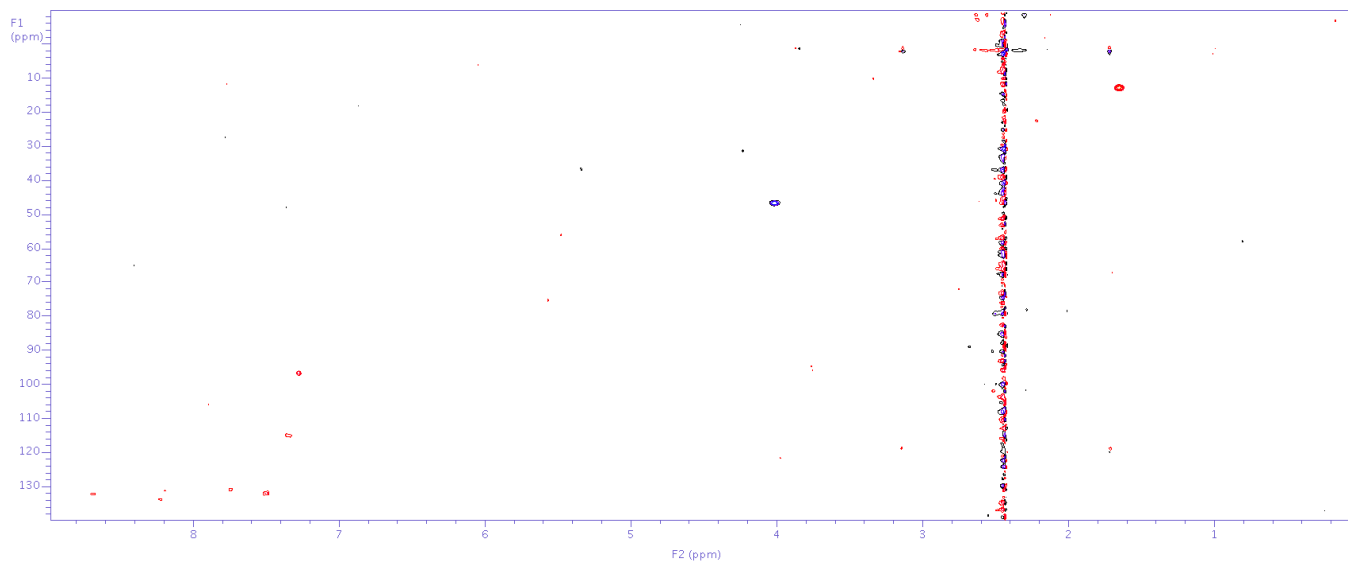
S14. WET1D Proton NMR spectrum (obtained from conventional off-line NMR mode) of rhodamine B (500 MHz, 50% $\text{CH}_3\text{CN}/\text{D}_2\text{O}$).



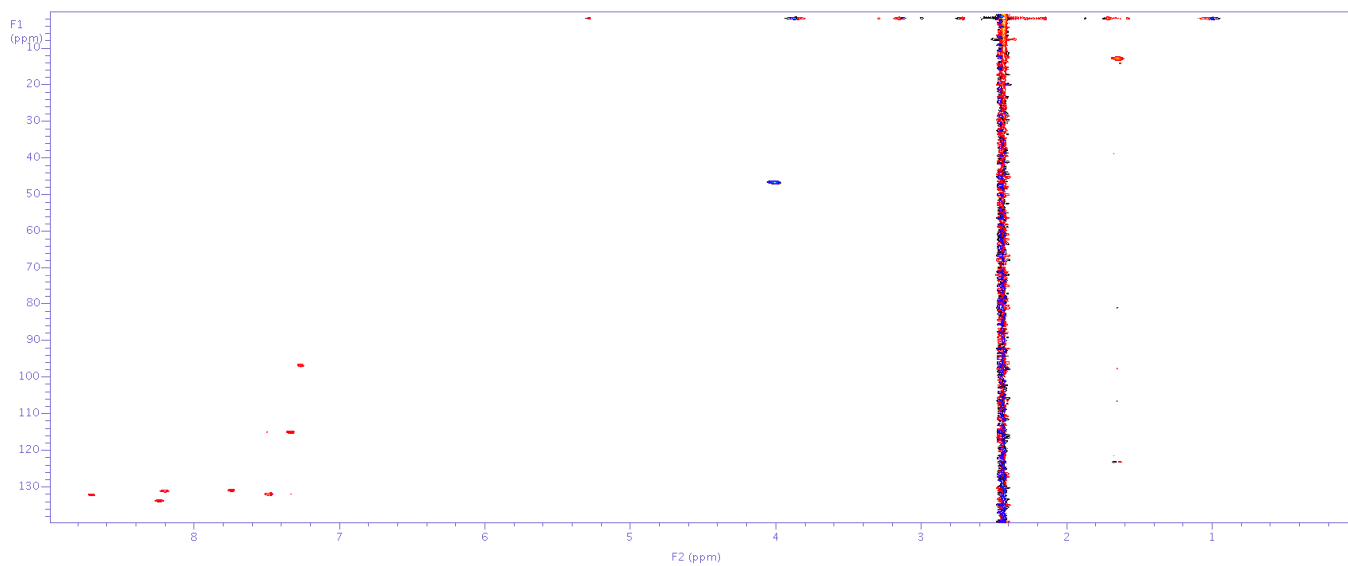
S15. gCOSY NMR spectrum (obtained from stop-flow HPLC-NMR mode) of rhodamine B (250 μg injected, 500 MHz, 50% $\text{CH}_3\text{CN}/\text{D}_2\text{O}$).



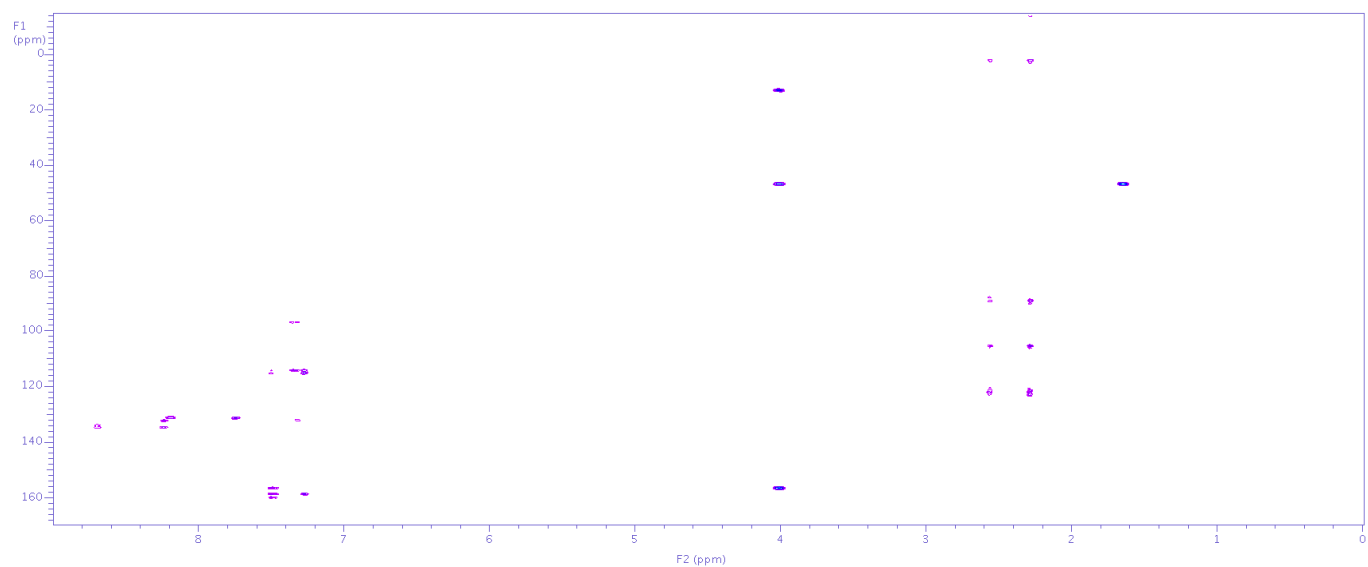
S16. gCOSY NMR spectrum (obtained from conventional off-line NMR mode) of rhodamine B (500 μg injected, 500 MHz, 50% $\text{CH}_3\text{CN}/\text{D}_2\text{O}$).



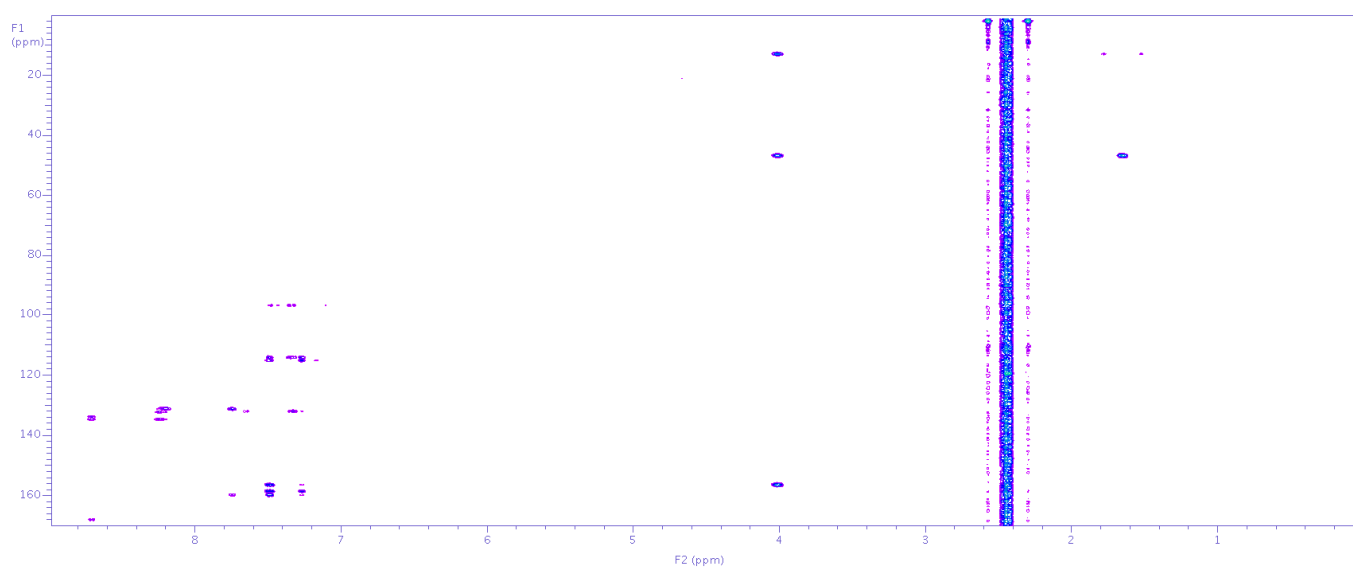
S17. HSQCAD NMR spectrum (obtained from stop-flow HPLC-NMR mode) of rhodamine B (500 μg injected, 500 MHz, 50% $\text{CH}_3\text{CN}/\text{D}_2\text{O}$).



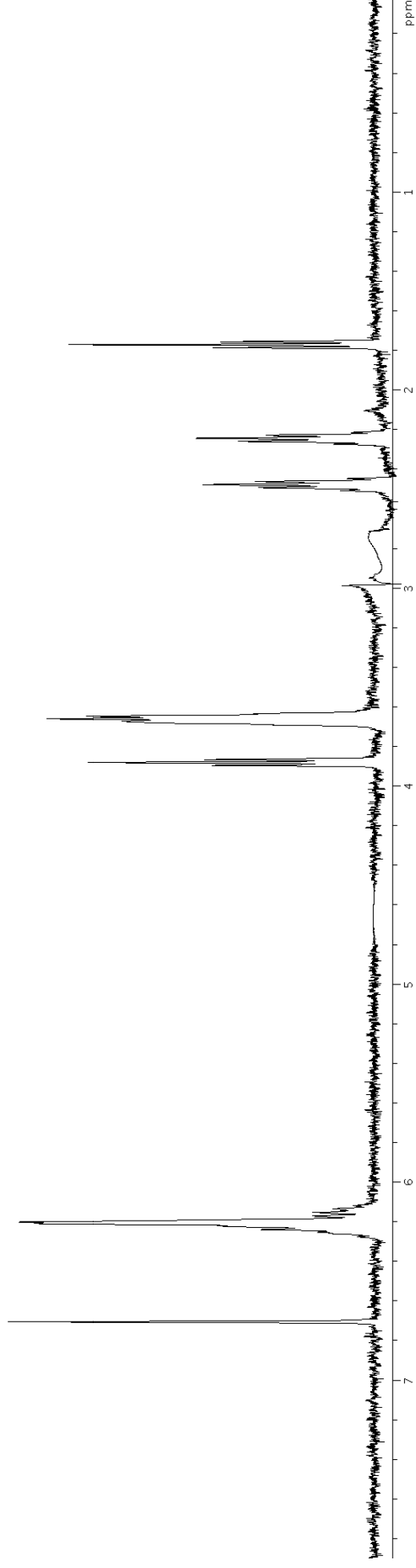
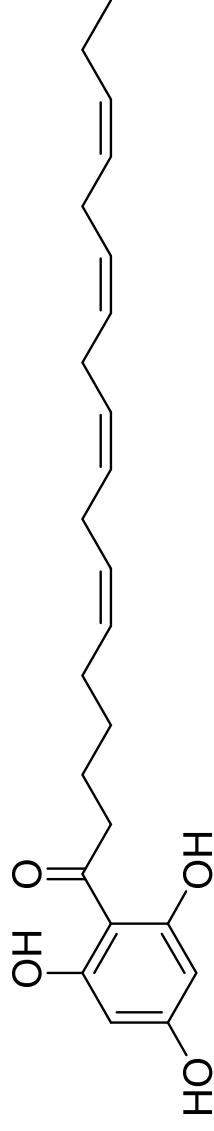
S18. HSQCAD NMR spectrum (obtained from conventional off-line NMR mode) of rhodamine B (500 MHz, 50% $\text{CH}_3\text{CN}/\text{D}_2\text{O}$).



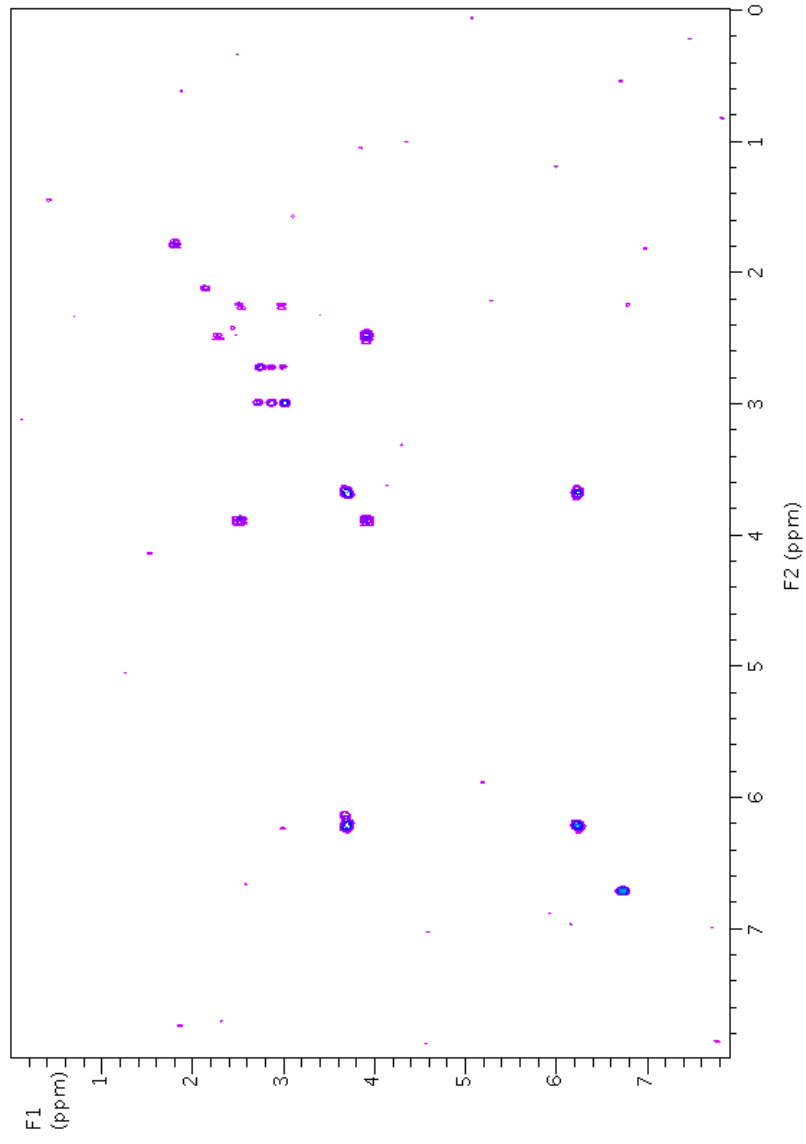
S19. gHMBCAD NMR spectrum (obtained from stop-flow HPLC-NMR mode) of rhodamine B (1000 µg injected, 500 MHz, 50% CH₃CN/D₂O).



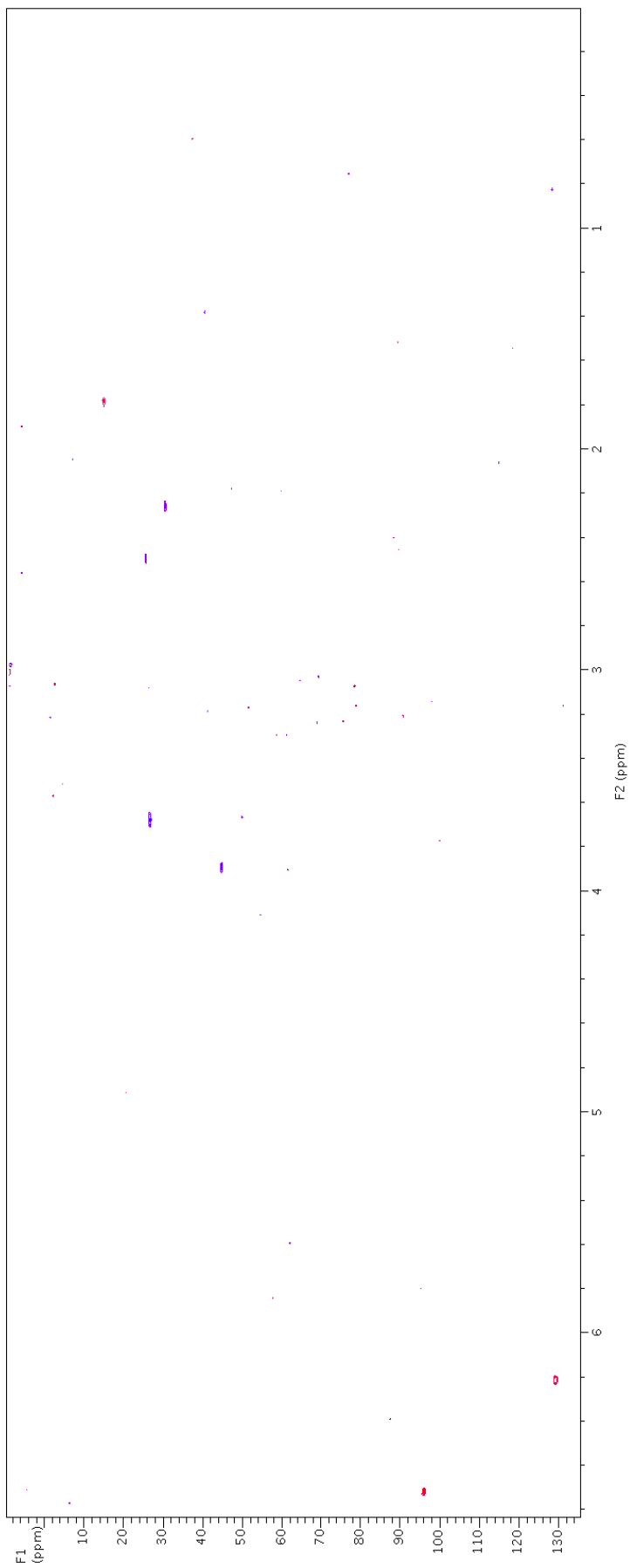
S20. gHMBCAD NMR spectrum (obtained from conventional off-line NMR mode) of rhodamine B (500 µg injected, 500 MHz, 50% CH₃CN/D₂O).



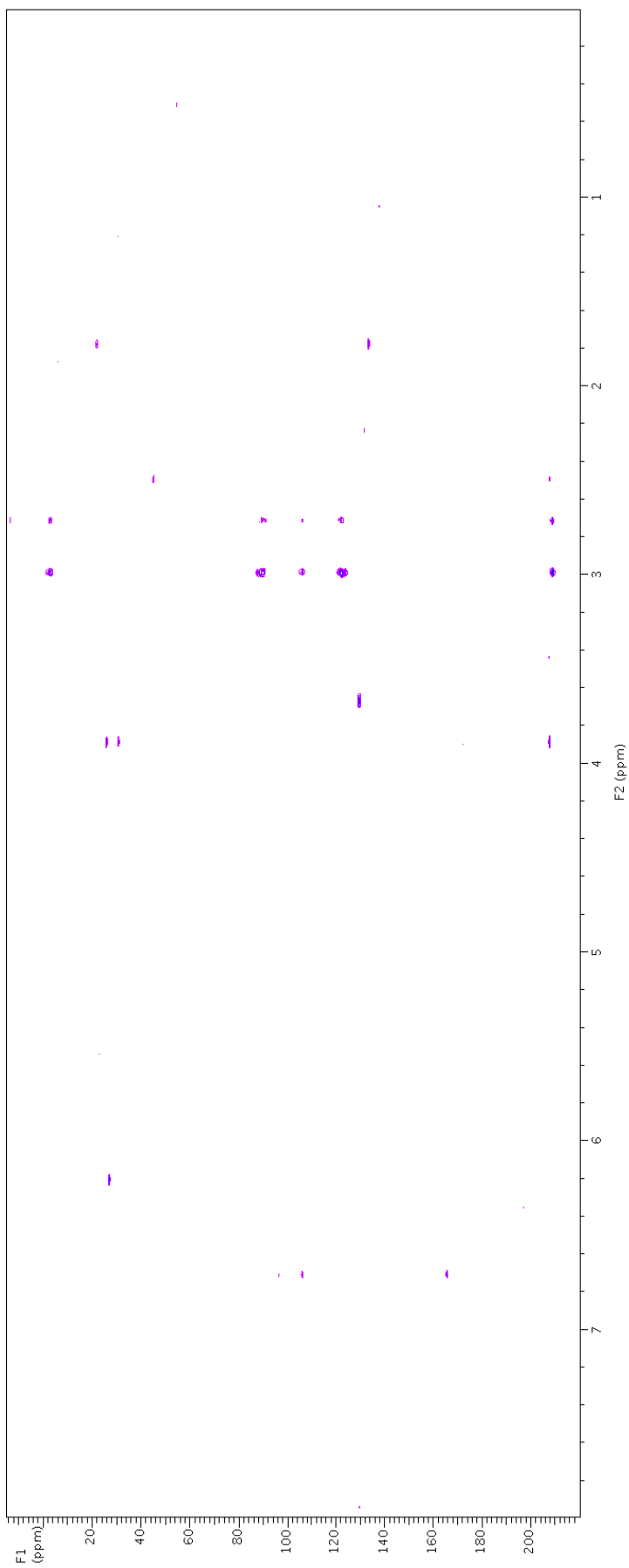
S21. WET1D Proton NMR spectrum (obtained from stop-flow HPLC-NMR mode) of component 1 at 9.59 mins (3520 μg of the crude extract of *C. subfarcinata* injected, 500 MHz, 75% $\text{CH}_3\text{CN}/\text{D}_2\text{O}$).



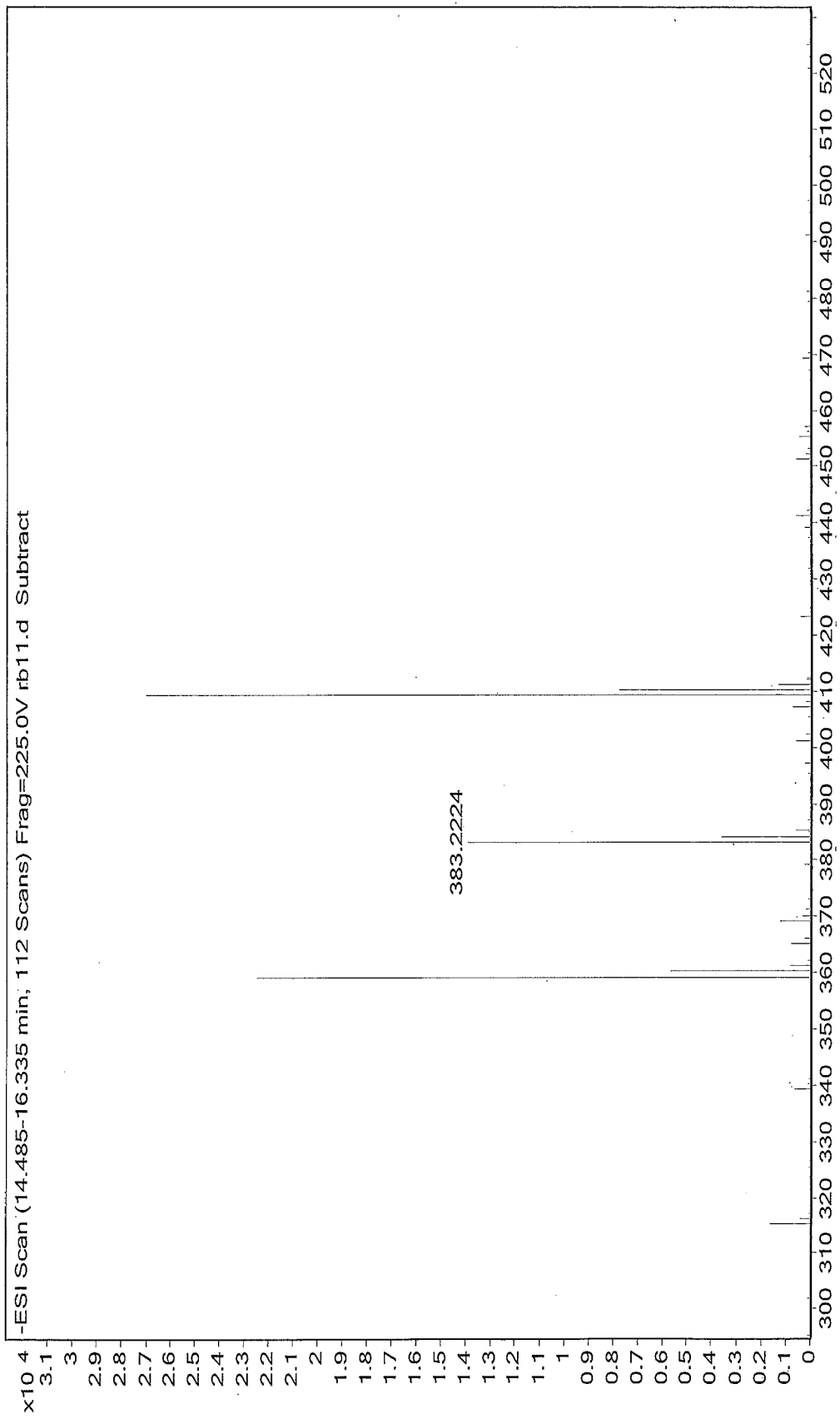
S22. gCOSY NMR spectrum (obtained from stop-flow HPLC-NMR mode) of component 1 at 9.59 mins (500 MHz, 75% CH₃CN/D₂O).



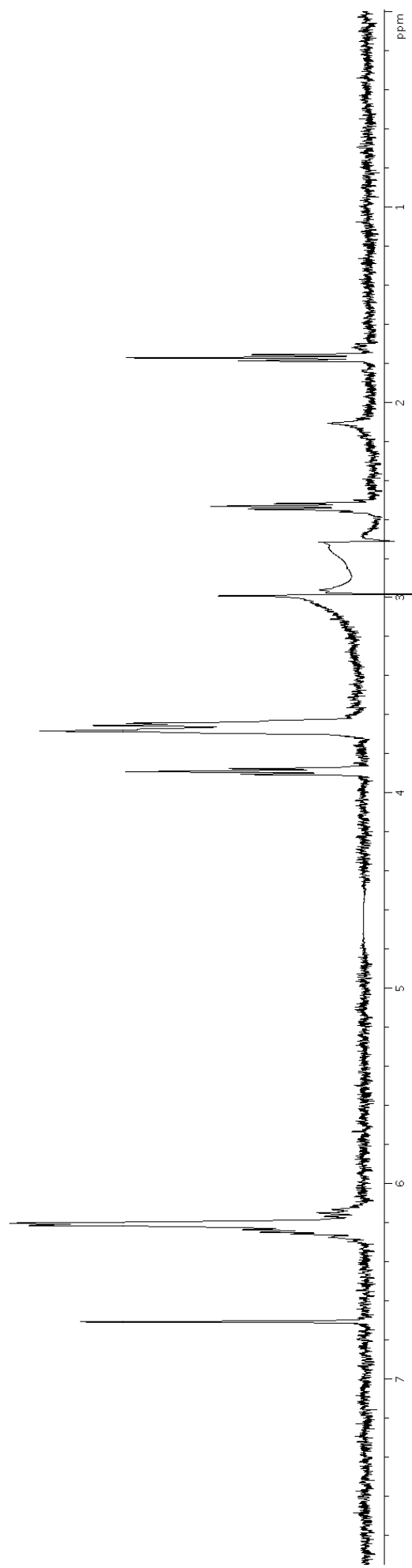
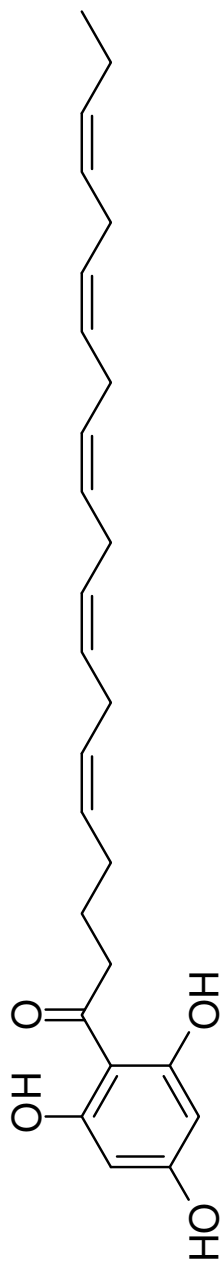
S23. HSQCAD NMR spectrum (obtained from stop-flow HPLC-NMR mode) of component 1 at 9.59 mins (500 MHz, 75% CH₃CN/D₂O).



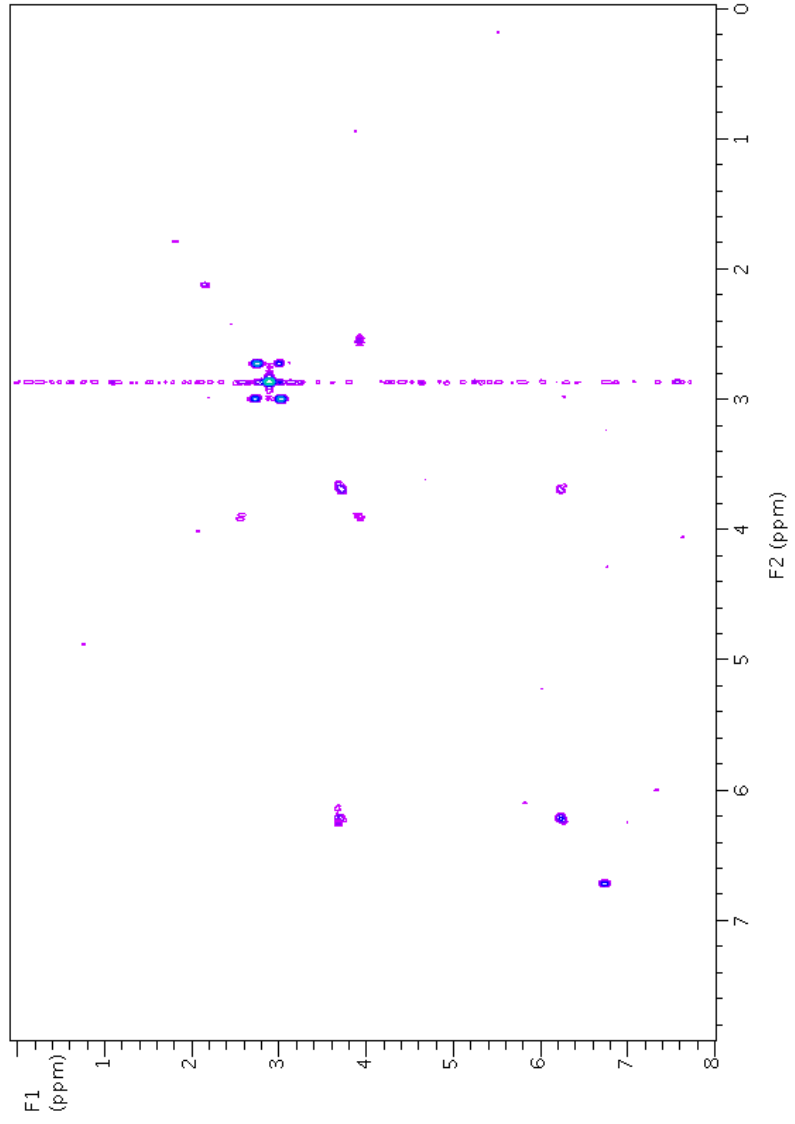
S24. gHMBCAD NMR spectrum (obtained from stop-flow HPLC-NMR mode) of component 1 at 9.59 mins (500 MHz, 75% CH₃CN/D₂O).



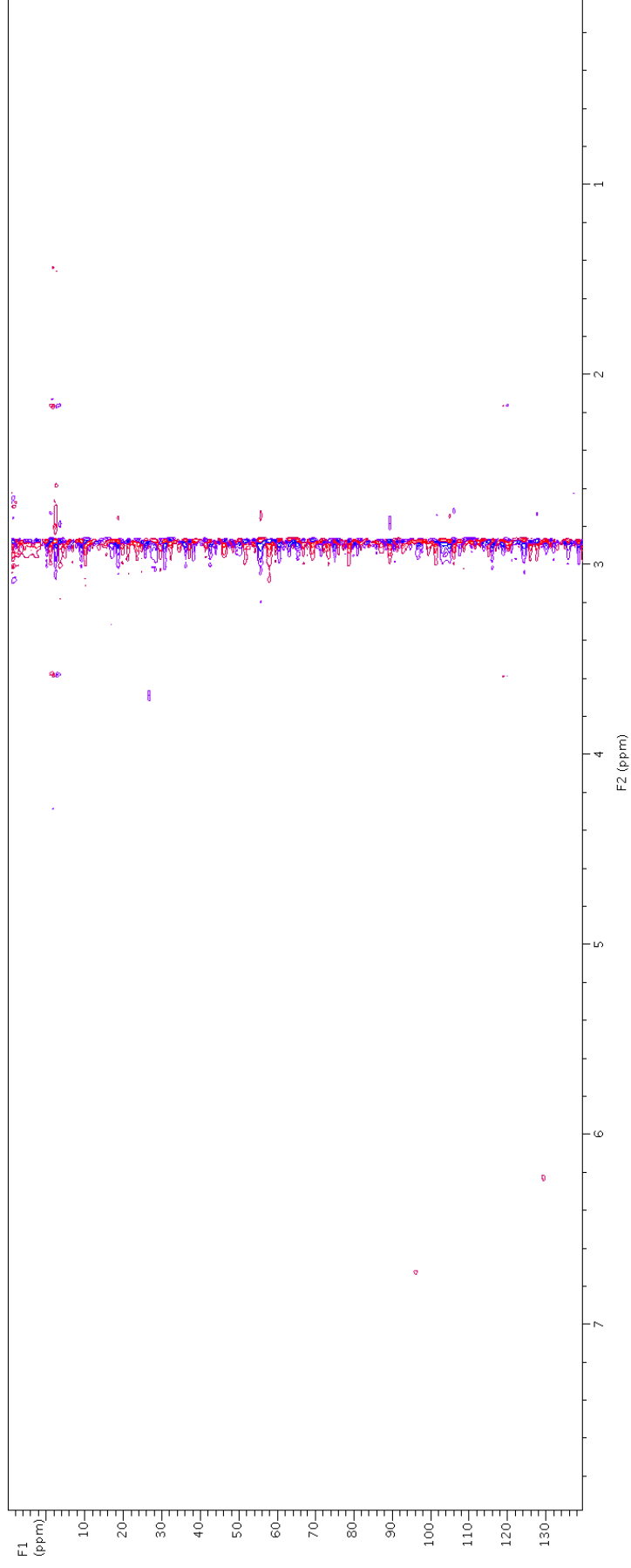
S25. High resolution negative ESI-MS of component 1 at 9.59 mins obtained from HRESILC-MS.



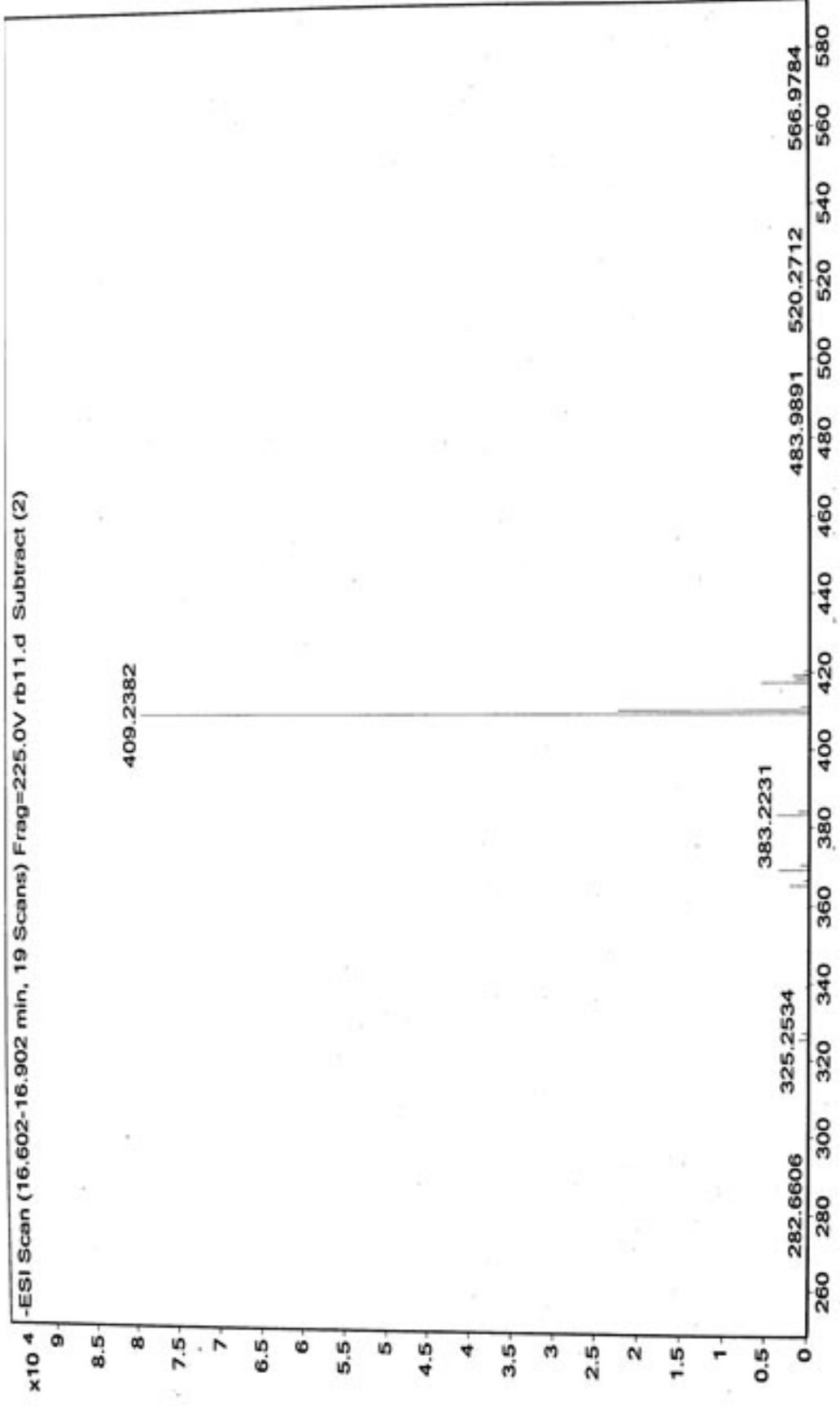
S26. WET1D Proton NMR spectrum (obtained from stop-flow HPLC-NMR mode) of component 2 at 13.05 mins (3520 μg of the crude extract of *C. subfarcinata* injected, 500 MHz, 75% $\text{CH}_3\text{CN}/\text{D}_2\text{O}$).



S27. gCOSY NMR spectrum (obtained from stop-flow HPLC-NMR mode) of component 2 at 13.05 mins (500 MHz, 75% CH₃CN/D₂O).



S28. HSQCAD NMR spectrum (obtained from stop-flow HPLC-NMR mode) of component 2 at 13.05 mins (500 MHz, 75% CH₃CN/D₂O).



S29. High resolution negative ESI-MS of component 2 at 13.05 mins obtained from HRESILC-MS.

APPENDIX B

Supplementary Information for the Study of the Australian plant

Macropidia fuliginosa

This appendix contains further information relevant to the chemical investigation conducted on the flowers and bulbs of the Australian plant *Macropidia fuliginosa* as outlined in Chapter 5.

PHYTOCHEMICAL INVESTIGATION OF THE CONSTITUENTS DERIVED FROM THE AUSTRALIAN PLANT *MACROPIDIA FULIGINOSA*

Robert Brkljača[†], *Jonathan M. White*[§] and *Sylvia Urban*^{†*}

[†]School of Applied Sciences (Discipline of Chemistry), Health Innovations Research Institute (HIRi) RMIT University, GPO Box 2476V Melbourne, Victoria 3001, Australia.

[§] School of Chemistry and Bio21 Institute, The University of Melbourne, Victoria 3010, Australia

Supporting Information

S1. Extracted UV profile of compound eluting at 2.45 mins (rutin (**4**)) from HPLC.

S2. High resolution negative ESI-MS of compound eluting at 2.45 mins (rutin (**4**)) from HPLC-MS.

S3. Extracted UV profile of compound eluting at 3.74 mins (haemofluorone A (**1**)) from HPLC.

S4. High resolution negative ESI-MS of compound eluting at 3.74 mins (haemofluorone A (**1**)) from HPLC-MS.

S5. Extracted UV profile of compound eluting at 4.44 mins (haemofluorone B (**2**)) from HPLC.

S6. High resolution negative ESI-MS of compound eluting at 4.44 mins (haemofluorone B (**2**)) from HPLC-MS.

S7. Extracted UV profile of compound eluting at 15.05 mins (compound **8**) from HPLC.

S8. High resolution negative ESI-MS of compound eluting at 15.05 mins (compound **8**) from HPLC-MS.

S9. Stop-flow WET1D Proton NMR spectrum of compounds eluting at (3.28 mins) (fuliginosin A (**12**) and B (**13**)).

S10. On-flow WET1D Proton NMR spectrum of compound eluting at 4.11 mins (anigopreissin A (**5**)).

S11. On-flow WET1D Proton NMR spectrum of compound eluting at 4.11 mins (anigopreissin A (**5**)).

S12. High resolution negative ESI-MS of compound eluting at 4.11 mins (anigopreissin A (**5**)) from HPLC-MS.

S13. Stop-flow WET1D Proton NMR spectrum of compound eluting at 11.31 mins (fuliginosone (**14**)).

S14. Expansion of Stop-flow WET1D Proton NMR spectrum of compound eluting at 11.31 mins (fuliginosone (**14**)).

- S15.** High resolution negative ESI-MS of compound eluting at 11.31 mins (fuliginosone (**14**)) from HPLC-MS.
- S16.** Stop-flow WET1D Proton NMR spectrum of compound eluting at 12.35 mins (compound **6**).
- S17.** Expansion of Stop-flow WET1D Proton NMR spectrum of compound eluting at 12.35 mins (compound **6**).
- S18.** gCOSY NMR spectrum (from stop-flow HPLC-NMR) of compound eluting at 12.35 mins (compound **6**).
- S19.** HSQCAD NMR spectrum (from stop-flow HPLC-NMR) of compound eluting at 12.35 mins (compound **6**).
- S20.** Expansion of HSQCAD NMR spectrum (from stop-flow HPLC-NMR) of compound eluting at 12.35 mins (compound **6**).
- S21.** High resolution negative ESI-MS of compound eluting at 12.35 mins (compound **6**) from HPLC-MS.
- S22.** Stop-flow WET1D Proton NMR spectrum of compound eluting at 19.11 mins (anigorufone (**7**)).
- S23.** Expansion of Stop-flow WET1D Proton NMR spectrum of compound eluting at 19.11 mins (anigorufone (**7**)).
- S24.** gCOSY NMR spectrum (from stop-flow HPLC-NMR) of compound eluting at 19.11 mins (anigorufone (**7**)).
- S25.** HSQCAD NMR spectrum (from stop-flow HPLC-NMR) of compound eluting at 19.11 mins (anigorufone (**7**)).
- S26.** Expansion of HSQCAD NMR spectrum (from stop-flow HPLC-NMR) of compound eluting at 19.11 mins (anigorufone (**7**)).
- S27.** High resolution negative ESI-MS of compound eluting at 19.11 mins (anigorufone (**7**)) from HPLC-MS.
- S28.** ^1H NMR spectrum (500 MHz, d_6 -DMSO) of fuliginosin A (**12**).
- S29.** gCOSY NMR spectrum (500 MHz, d_6 -DMSO) of fuliginosin A (**12**).
- S30.** HSQCAD NMR spectrum (500 MHz, d_6 -DMSO) of fuliginosin A (**12**).
- S31.** Expansion of HSQCAD NMR spectrum (500 MHz, d_6 -DMSO) of fuliginosin A (**12**).

- S32.** gHMBCAD NMR spectrum (500 MHz, d_6 -DMSO) of fuliginosin A (**12**).
- S33.** Expansion of gHMBCAD NMR spectrum (500 MHz, d_6 -DMSO) of fuliginosin A (**12**).
- S34.** High resolution negative ESI-MS of fuliginosin A (**12**).
- S35.** ^1H NMR spectrum (500 MHz, d_6 -DMSO) of fuliginosin B (**13**).
- S36.** Expansion of ^1H NMR spectrum (500 MHz, d_6 -DMSO) of fuliginosin B (**13**).
- S37.** gCOSY NMR spectrum (500 MHz, d_6 -DMSO) of fuliginosin B (**13**).
- S38.** HSQCAD NMR spectrum (500 MHz, d_6 -DMSO) of fuliginosin B (**13**).
- S39.** Expansion of HSQCAD NMR spectrum (500 MHz, d_6 -DMSO) of fuliginosin B (**13**).
- S40.** gHMBCAD NMR spectrum (500 MHz, d_6 -DMSO) of fuliginosin B (**13**).
- S41.** Expansion of gHMBCAD NMR spectrum (500 MHz, d_6 -DMSO) of fuliginosin B (**13**).
- S42.** High resolution negative ESI-MS of fuliginosin B (**13**).
- S43.** ^1H NMR spectrum (500 MHz, CDCl_3) of fuliginosone (**14**).
- S44.** Expansion of ^1H NMR spectrum (500 MHz, CDCl_3) of fuliginosone (**14**).
- S45.** ^{13}C NMR spectrum (500 MHz, CDCl_3) of fuliginosone (**14**).
- S46.** gCOSY NMR spectrum (500 MHz, CDCl_3) of fuliginosone (**14**).
- S47.** HSQCAD NMR spectrum (500 MHz, CDCl_3) of fuliginosone (**14**).
- S48.** Expansion of HSQCAD NMR spectrum (500 MHz, CDCl_3) of fuliginosone (**14**).
- S49.** gHMBCAD NMR spectrum (500 MHz, CDCl_3) of fuliginosone (**14**).
- S50.** Expansion of gHMBCAD NMR spectrum (500 MHz, CDCl_3) of fuliginosone (**14**).
- S51.** High resolution negative ESI-MS of fuliginosone (**14**).
- S52.** Atomic coordinates ($\times 10^4$) and equivalent isotropic displacement parameters ($\text{\AA}^2 \times 10^3$) for fuliginosone (**14**). $U(\text{eq})$ is defined as one third of the trace of the orthogonalized U^{ij} tensor.
- S53.** ^1H NMR spectrum (500 MHz, CDCl_3) of fuliginone (**15**).
- S54.** Expansion of ^1H NMR spectrum (500 MHz, CDCl_3) of fuliginone (**15**).
- S55.** gCOSY NMR spectrum (500 MHz, CDCl_3) of fuliginone (**15**).

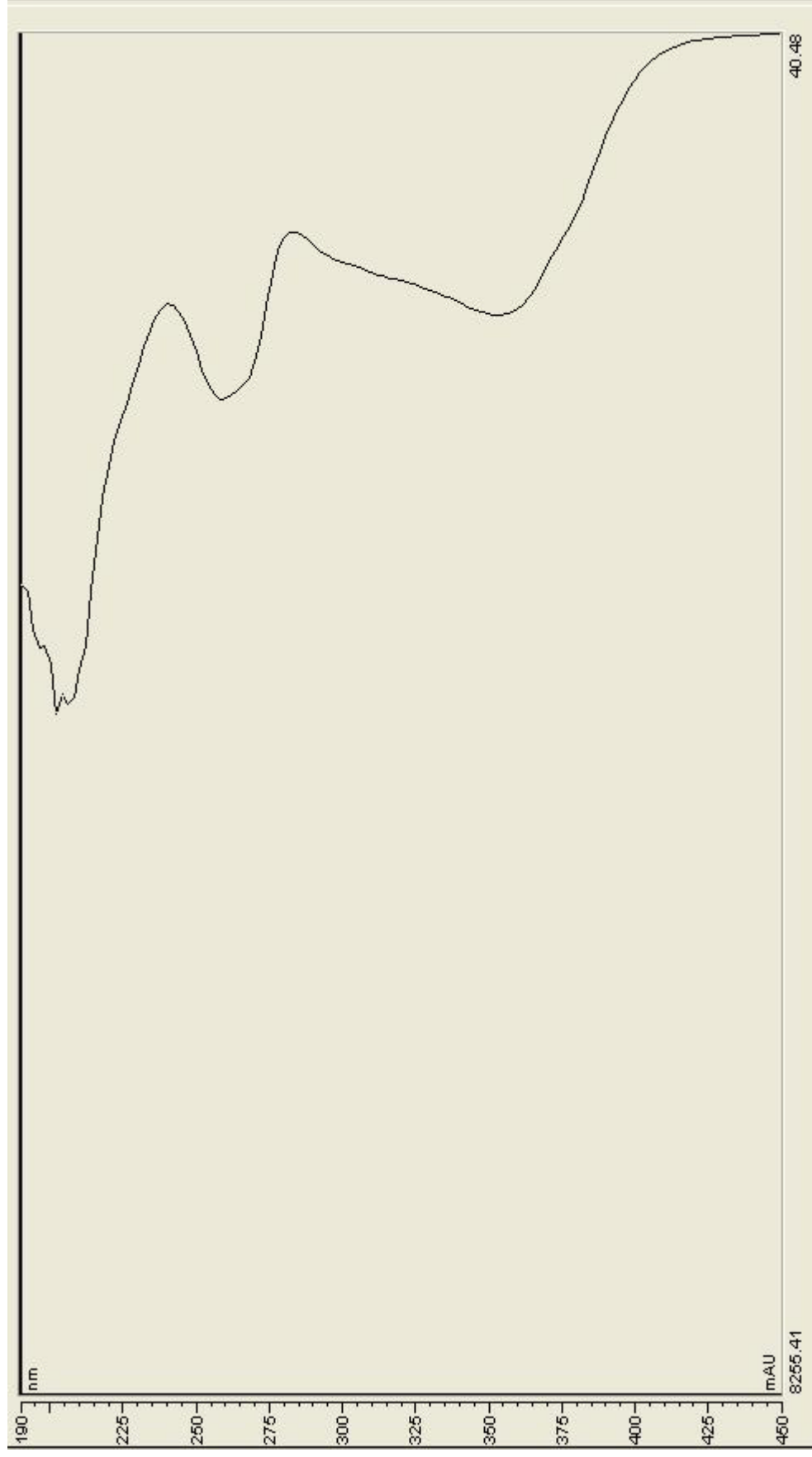
- S56.** HSQCAD NMR spectrum (500 MHz, CDCl₃) of fuliginone (**15**).
- S57.** Expansion of HSQCAD NMR spectrum (500 MHz, CDCl₃) of fuliginone (**15**).
- S58.** gHMBCAD NMR spectrum (500 MHz, CDCl₃) of fuliginone (**15**).
- S59.** Expansion of gHMBCAD NMR spectrum (500 MHz, CDCl₃) of fuliginone (**15**).
- S60.** Single irradiation nOe NMR spectrum (500 MHz, CDCl₃) of fuliginone (**15**) showing the irradiation of δ_{H} 7.17 (H-3).
- S61.** Single irradiation nOe NMR spectrum (500 MHz, CDCl₃) of fuliginone (**15**) showing the irradiation of δ_{H} 7.72 (H-4).
- S62.** High resolution positive ASAP-MS of fuliginone (**15**).
- S63.** ¹H NMR spectrum (500 MHz, CDCl₃) of fuliginol (**16**).
- S64.** Expansion of ¹H NMR spectrum (500 MHz, CDCl₃) of fuliginol (**16**).
- S65.** ¹³C NMR spectrum (500 MHz, CDCl₃) of fuliginol (**16**).
- S66.** gCOSY NMR spectrum (500 MHz, CDCl₃) of fuliginol (**16**).
- S67.** HSQCAD NMR spectrum (500 MHz, CDCl₃) of fuliginol (**16**).
- S68.** Expansion of HSQCAD NMR spectrum (500 MHz, CDCl₃) of fuliginol (**16**).
- S69.** gHMBCAD NMR spectrum (500 MHz, CDCl₃) of fuliginol (**16**).
- S70.** Expansion of gHMBCAD NMR spectrum (500 MHz, CDCl₃) of fuliginol (**16**).
- S71.** ¹H NMR spectrum (500 MHz, CDCl₃) of fuliginol (**16**) and chlorofuliginol (**17**).
- S72.** Expansion of ¹H NMR spectrum (500 MHz, CDCl₃) of fuliginol (**16**) and chlorofuliginol (**17**).
- S73.** gCOSY NMR spectrum (500 MHz, CDCl₃) of fuliginol (**16**) and chlorofuliginol (**17**).
- S74.** HSQCAD NMR spectrum (500 MHz, CDCl₃) of fuliginol (**16**) and chlorofuliginol (**17**).
- S75.** Expansion of HSQCAD NMR spectrum (500 MHz, CDCl₃) of fuliginol (**16**) and chlorofuliginol (**17**).
- S76.** gHMBCAD NMR spectrum (500 MHz, CDCl₃) of fuliginol (**16**) and chlorofuliginol (**17**).
- S77.** Expansion of gHMBCAD NMR spectrum (500 MHz, CDCl₃) of fuliginol (**16**) and chlorofuliginol (**17**).

S78. High resolution negative ESI-MS of fuliginol (**16**) and chlorofuliginol (**17**).

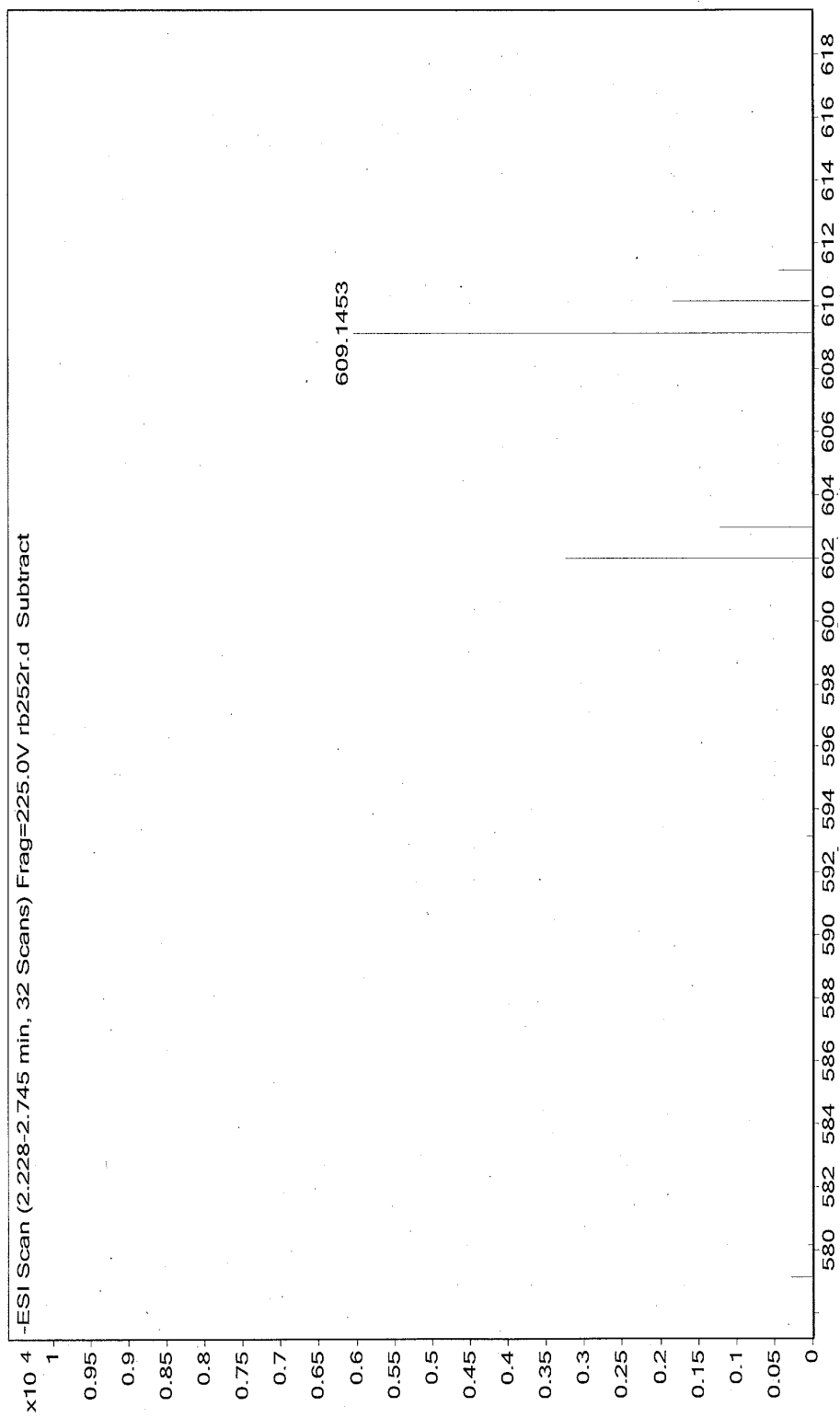
S79. Atomic coordinates ($\times 10^4$) for fuliginol (**16**) and chlorofuliginol (**17**) and equivalent isotropic displacement parameters ($\text{\AA}^2 \times 10^3$) for fuliginol (**16**) and chlorofuliginol (**17**). $U(\text{eq})$ is defined as one third of the trace of the orthogonalized U_{ij} tensor.

*Corresponding author. Tel: +61 3 9925 3376; Fax: +61 3 9925 3747

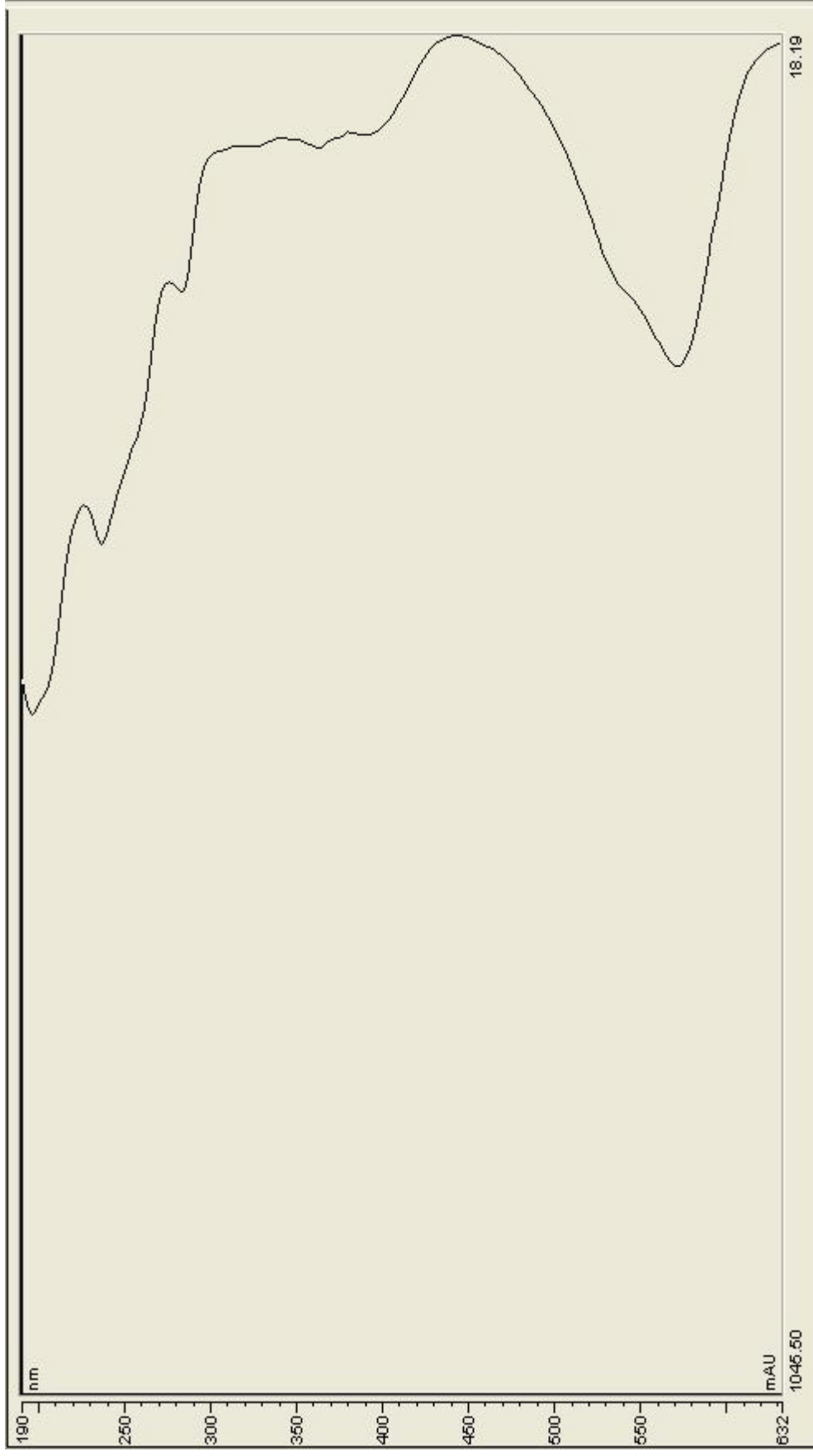
E-mail address: sylvia.urban@rmit.edu.au (S. Urban).



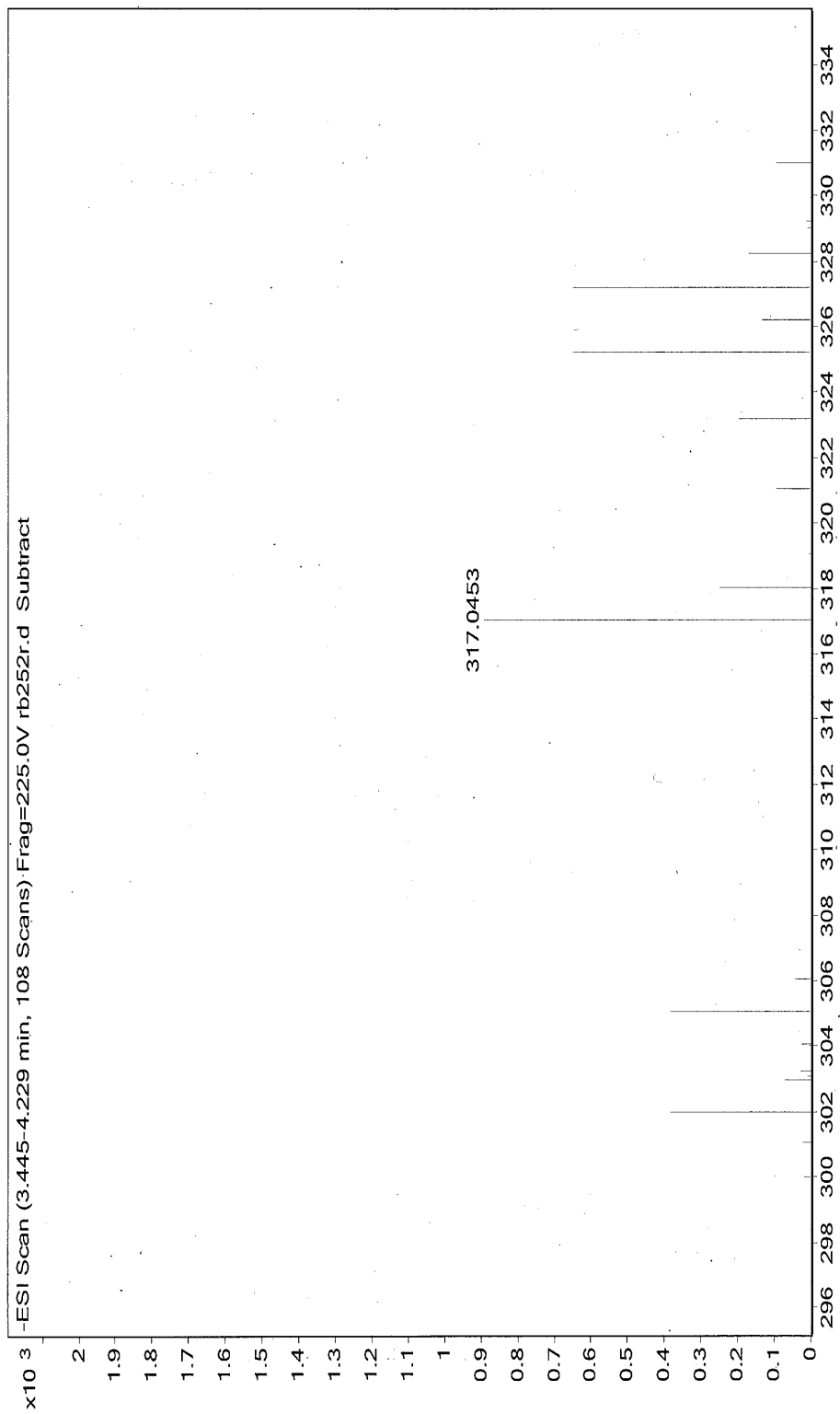
S1. Extracted UV profile of compound eluting at 2.45 mins (rutin (**4**)) from HPLC.



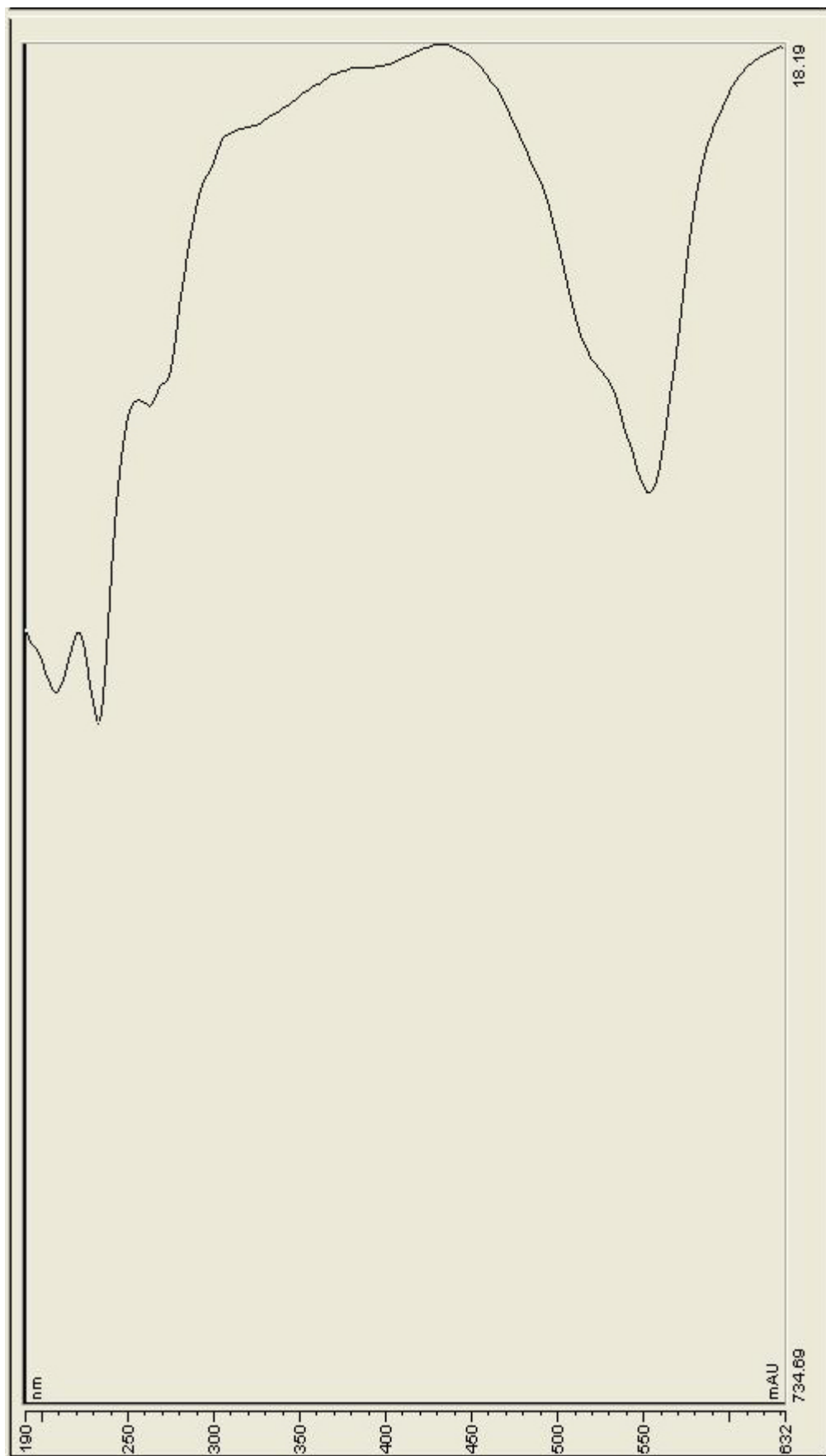
S2. High resolution negative ESI-MS of compound eluting at 2.45 mins (rutin (4)) from HPLC-MS.



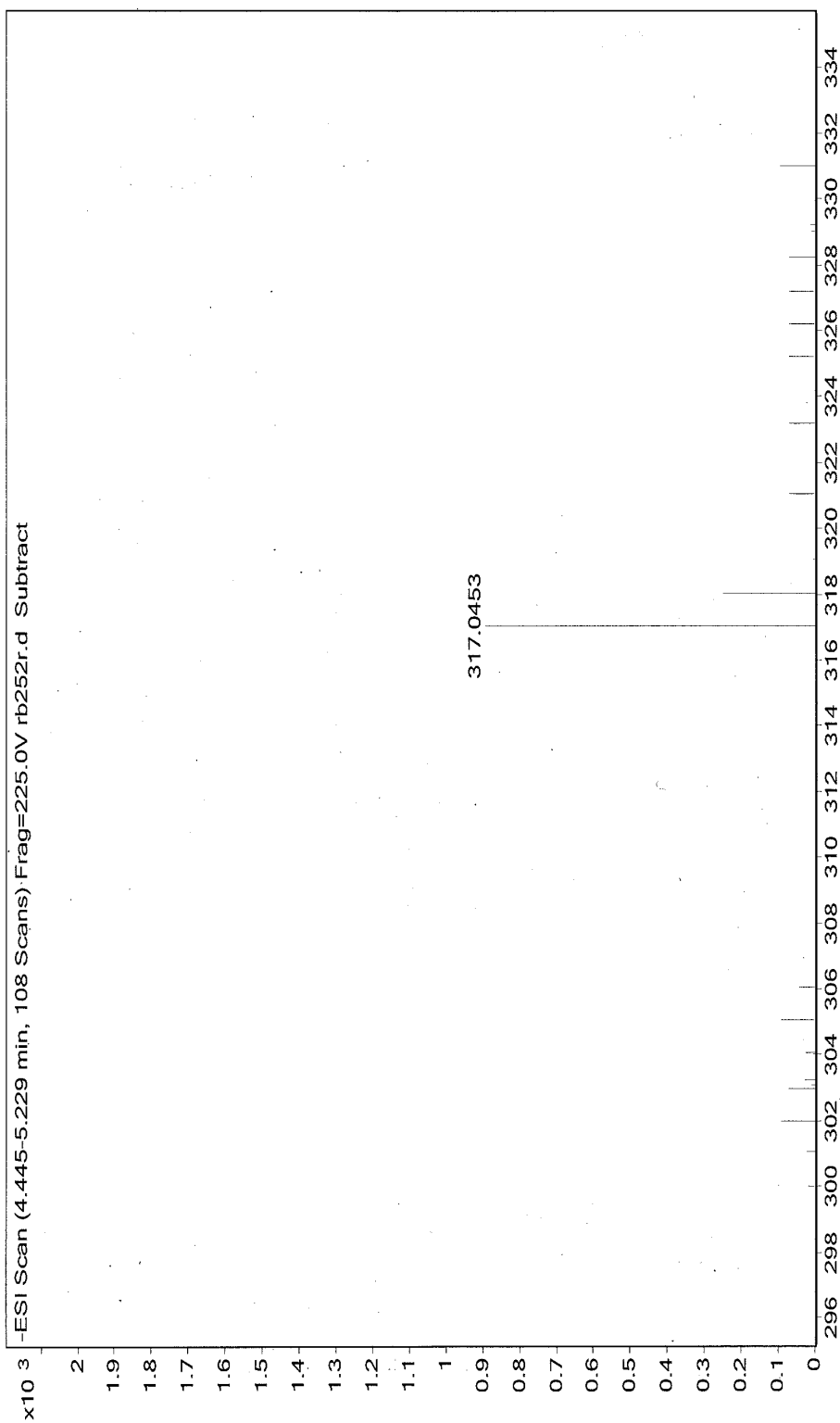
S3. Extracted UV profile of compound eluting at 3.74 mins (haemofluorone A (1)) from HPLC.



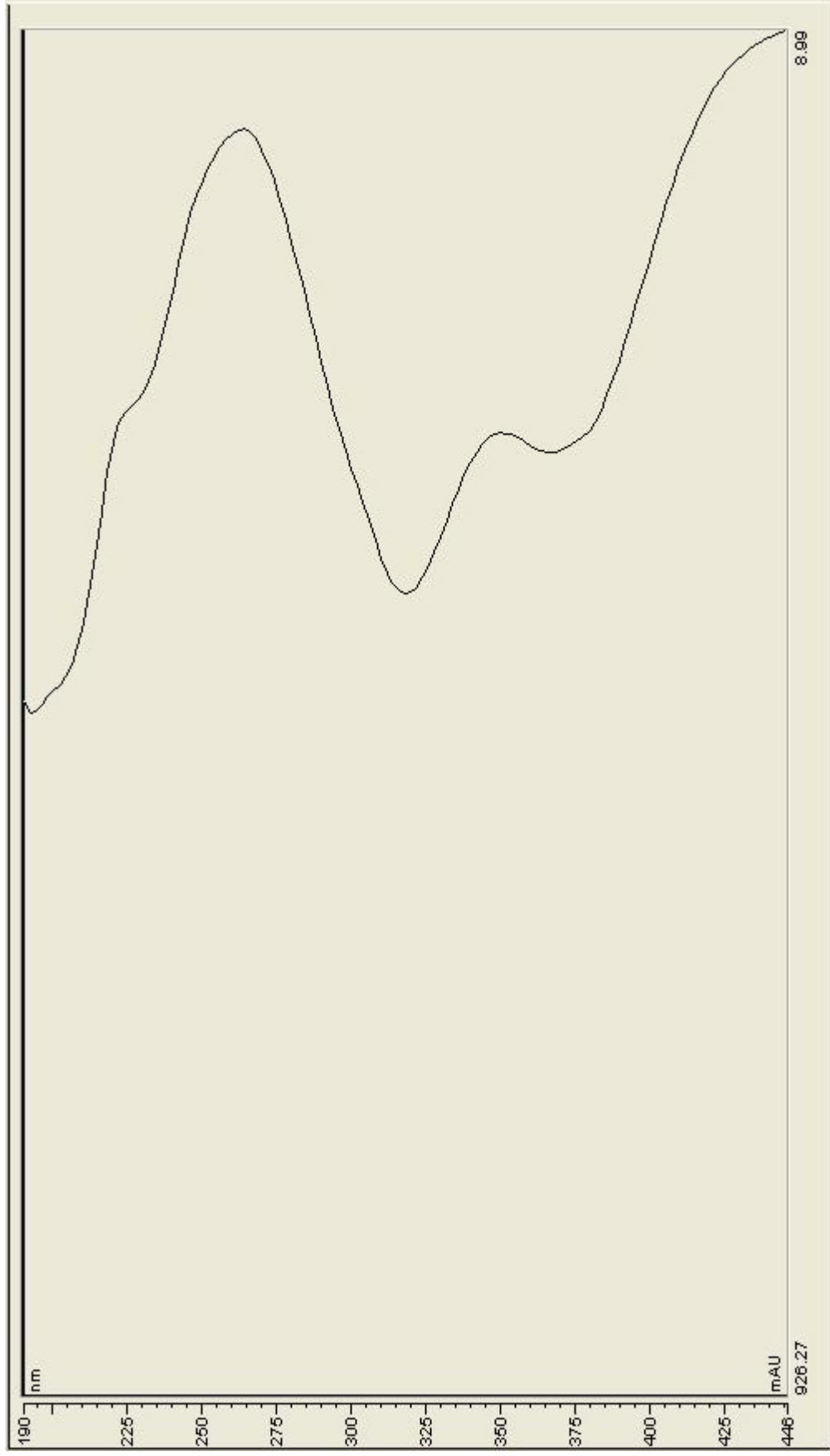
S4. High resolution negative ESI-MS of compound eluting at 3.74 mins (haemofluorone A (1)) from HPLC-MS.



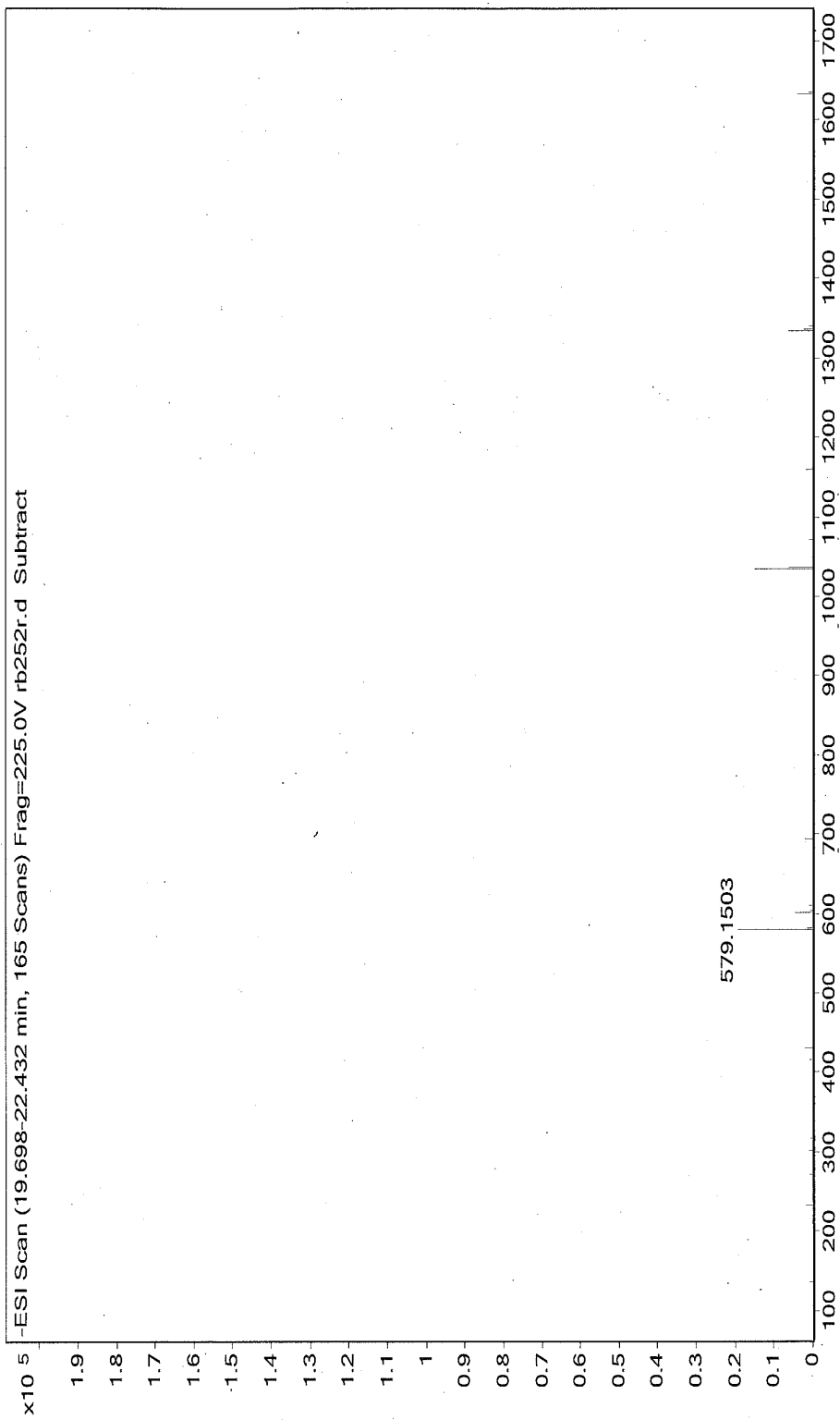
S5. Extracted UV profile of compound eluting at 4.44 mins (haemofluorone B (2)) from HPLC.



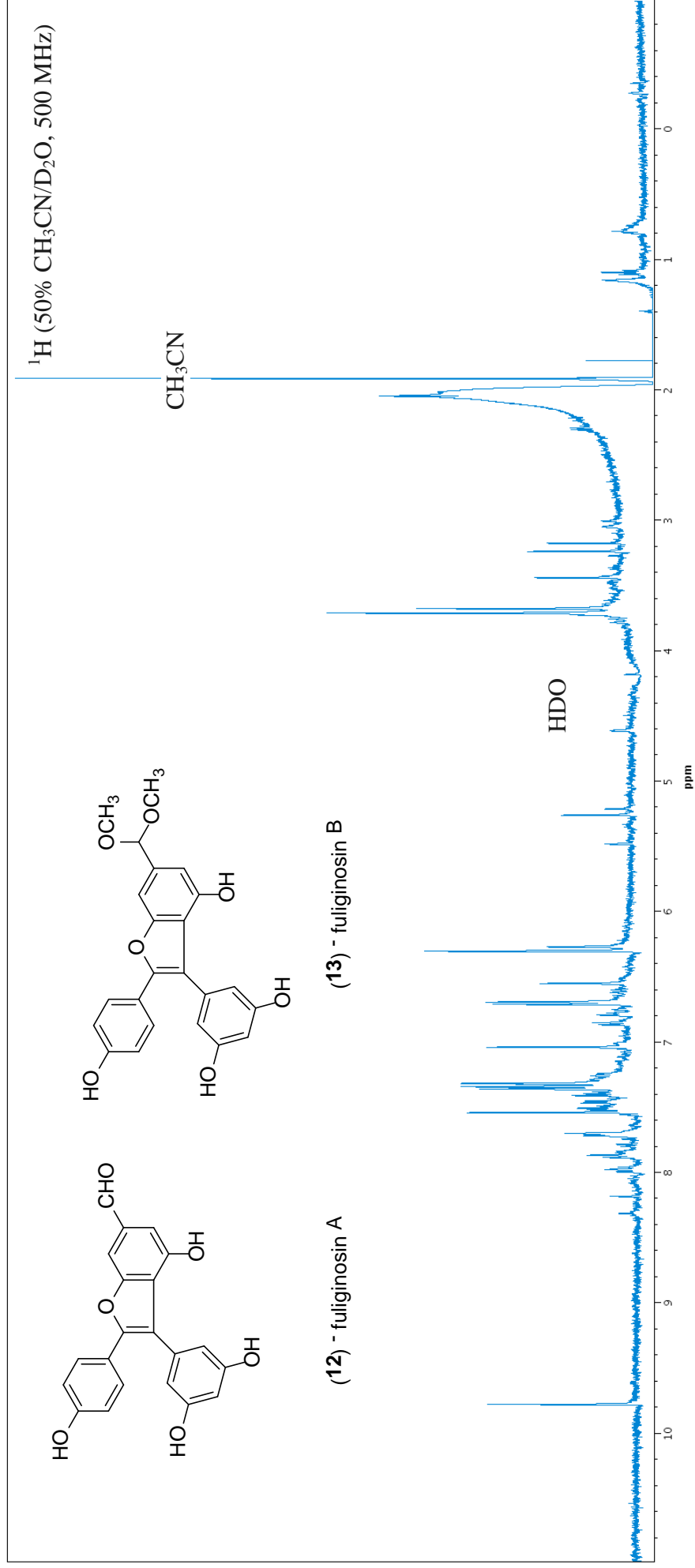
S6. High resolution negative ESI-MS of compound eluting at 4.44 mins (haemofluorone B (2)) from HPLC-MS.



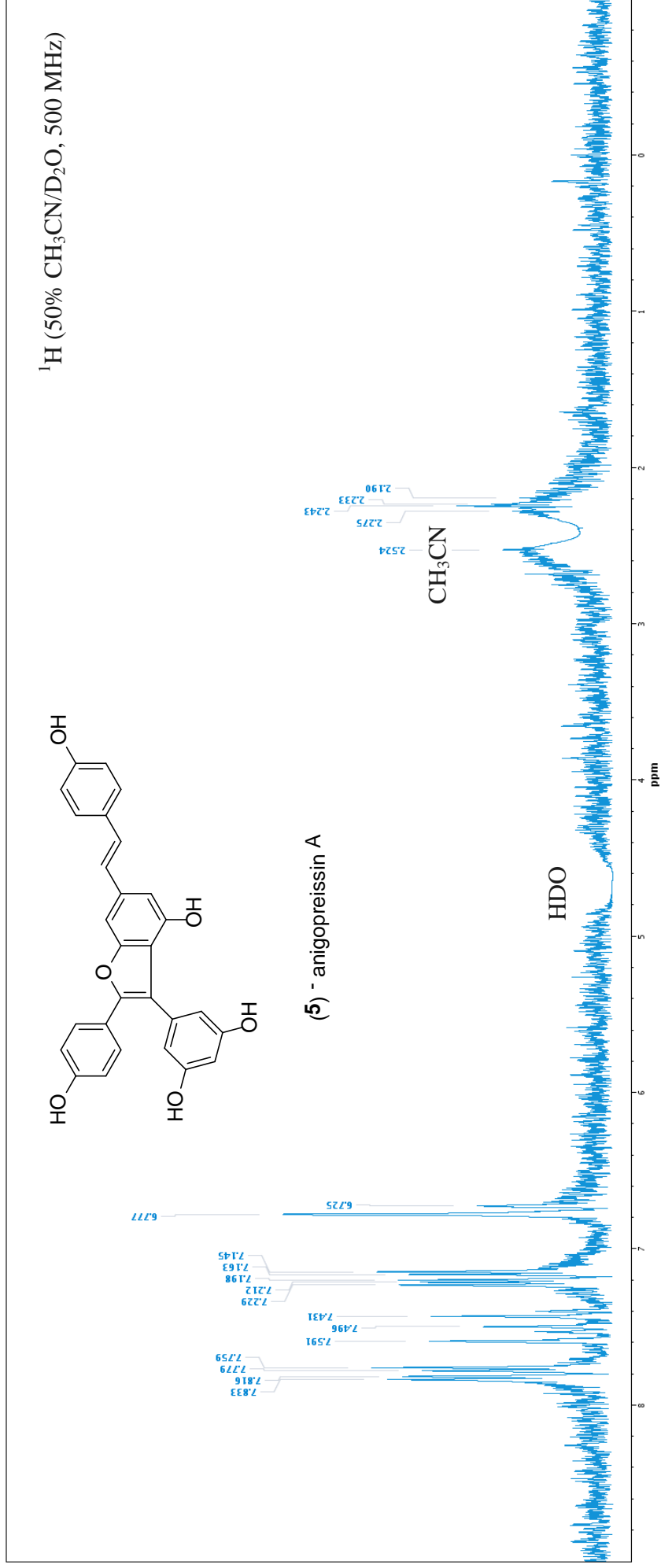
S7. Extracted UV profile of compound eluting at 15.05 mins (compound **8**) from HPLC.



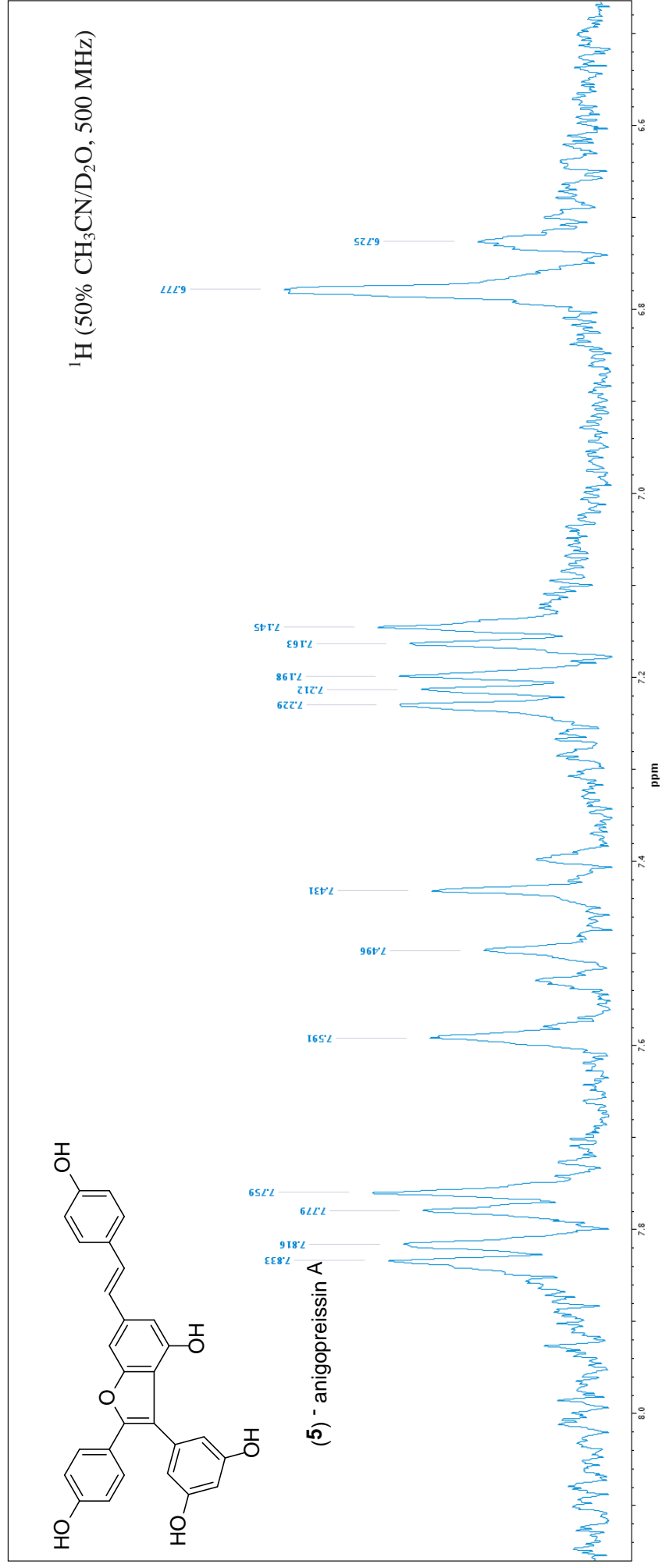
S8. High resolution negative ESI-MS of compound eluting at 15.05 mins (compound **8**) from HPLC-MS.



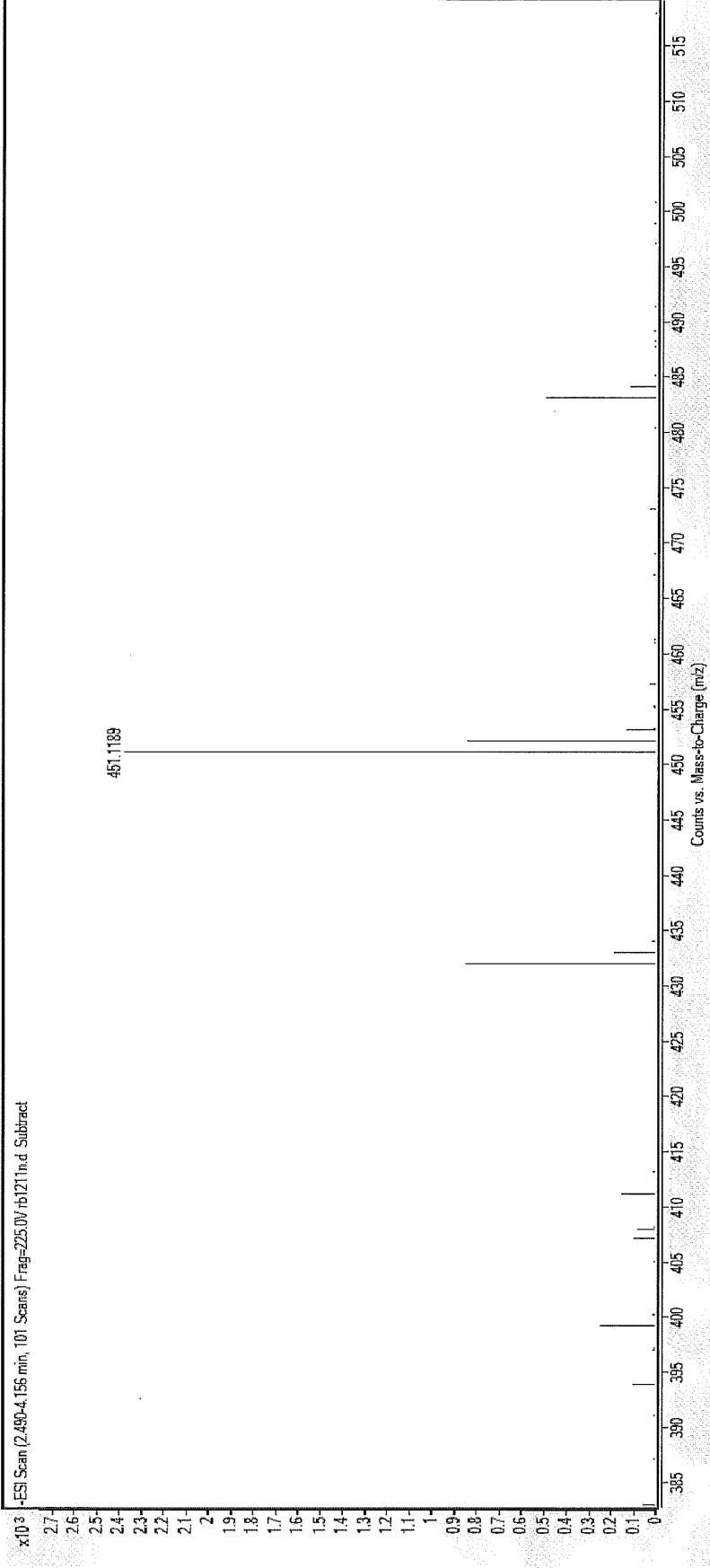
S9. Stop-flow WET1D Proton NMR spectrum of compounds eluting at (3.28 mins) (fuliginosin A (**12**) and B (**13**)).



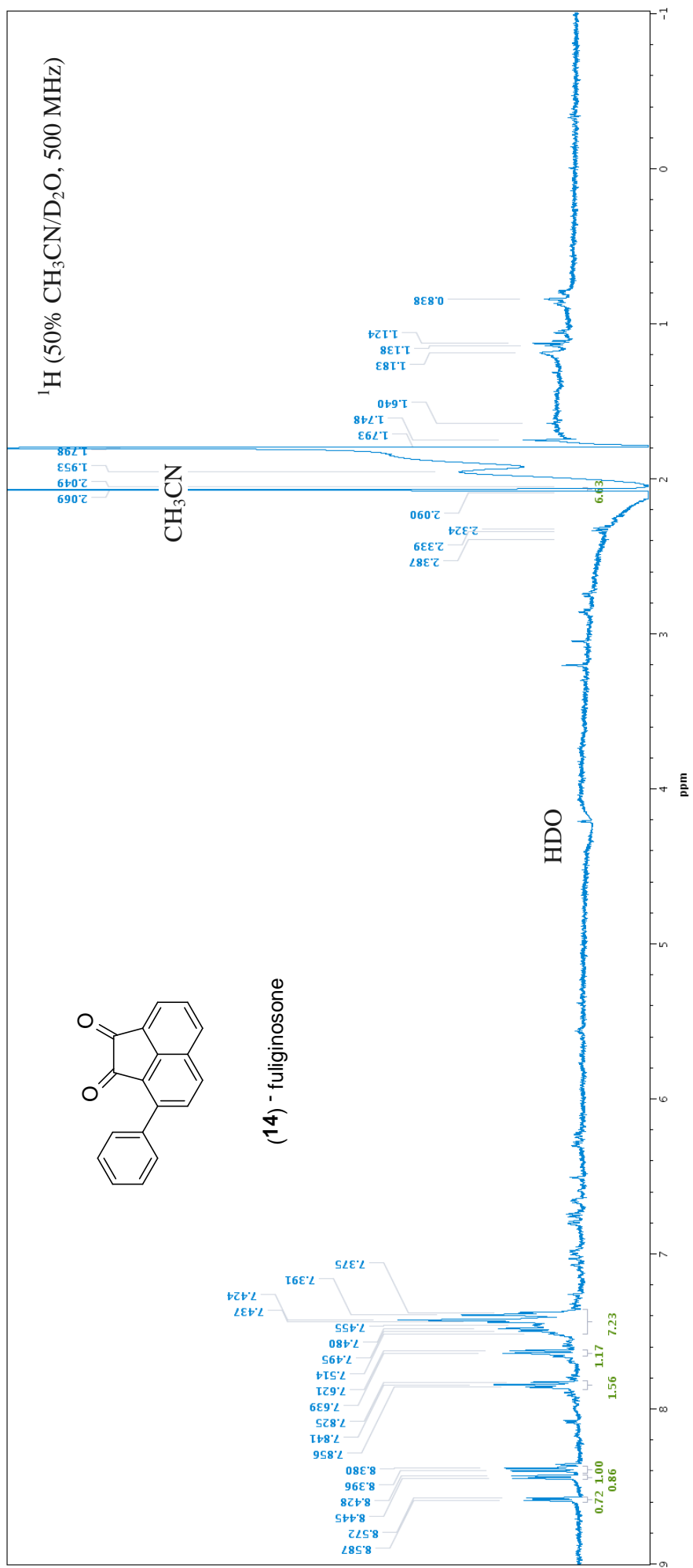
S10. On-flow WETID Proton NMR spectrum of compound eluting at 4.11 mins (anigopreissin A (5)).



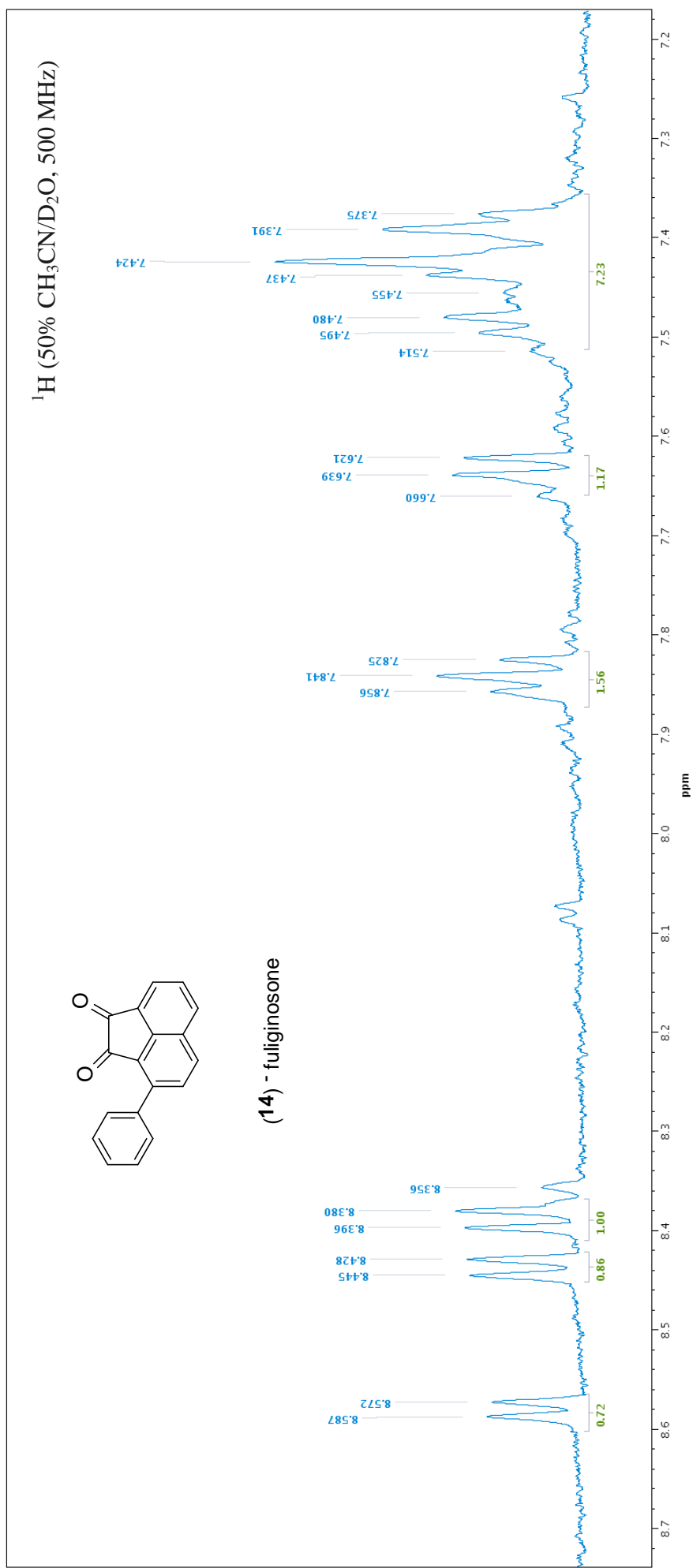
S11. On-flow WETID Proton NMR spectrum of compound eluting at 4.11 mins (anigopreissin A (**5**)).



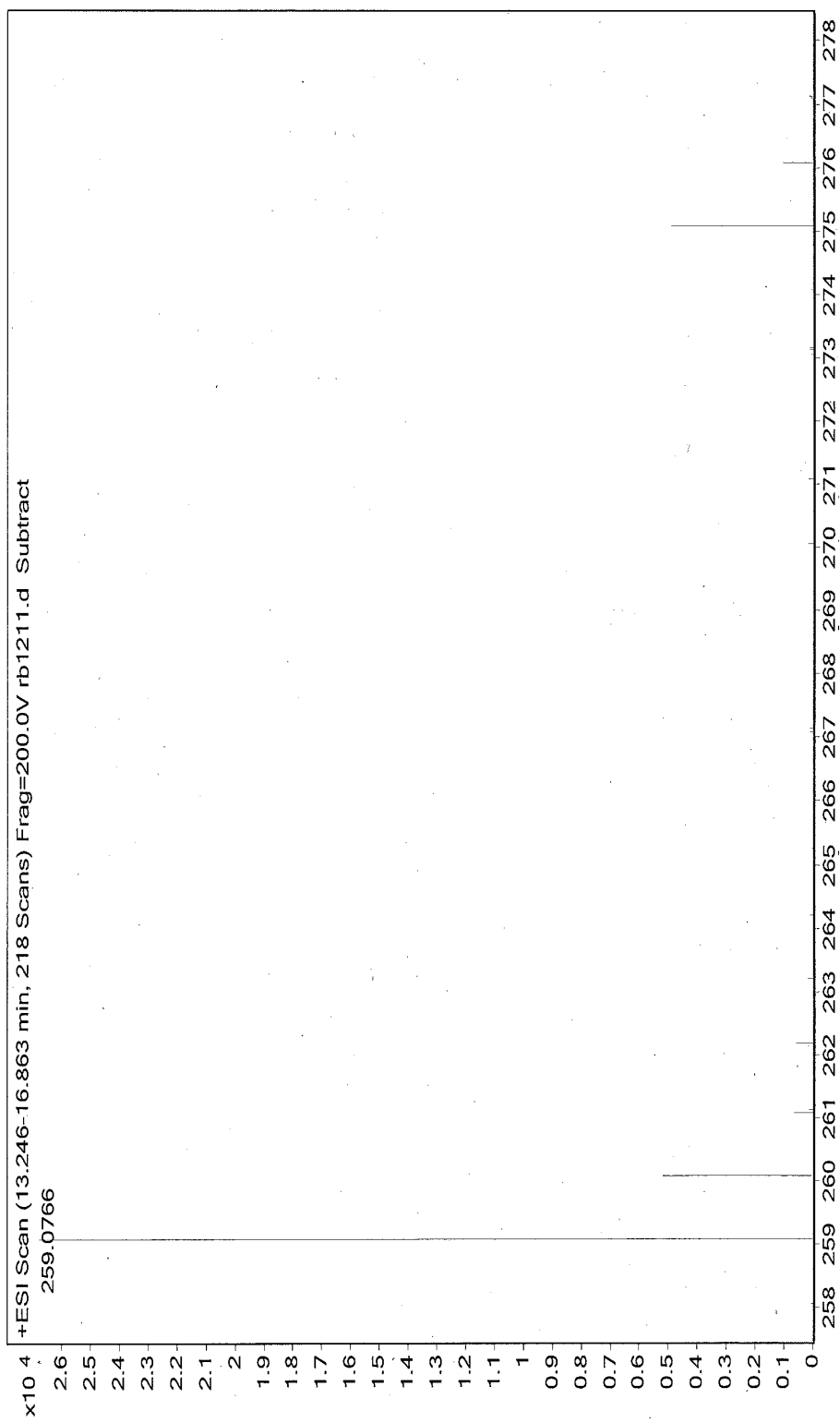
S12. High resolution negative ESI-MS of compound eluting at 4.11 mins (anigopreissin A (5)) from HPLC-MS.



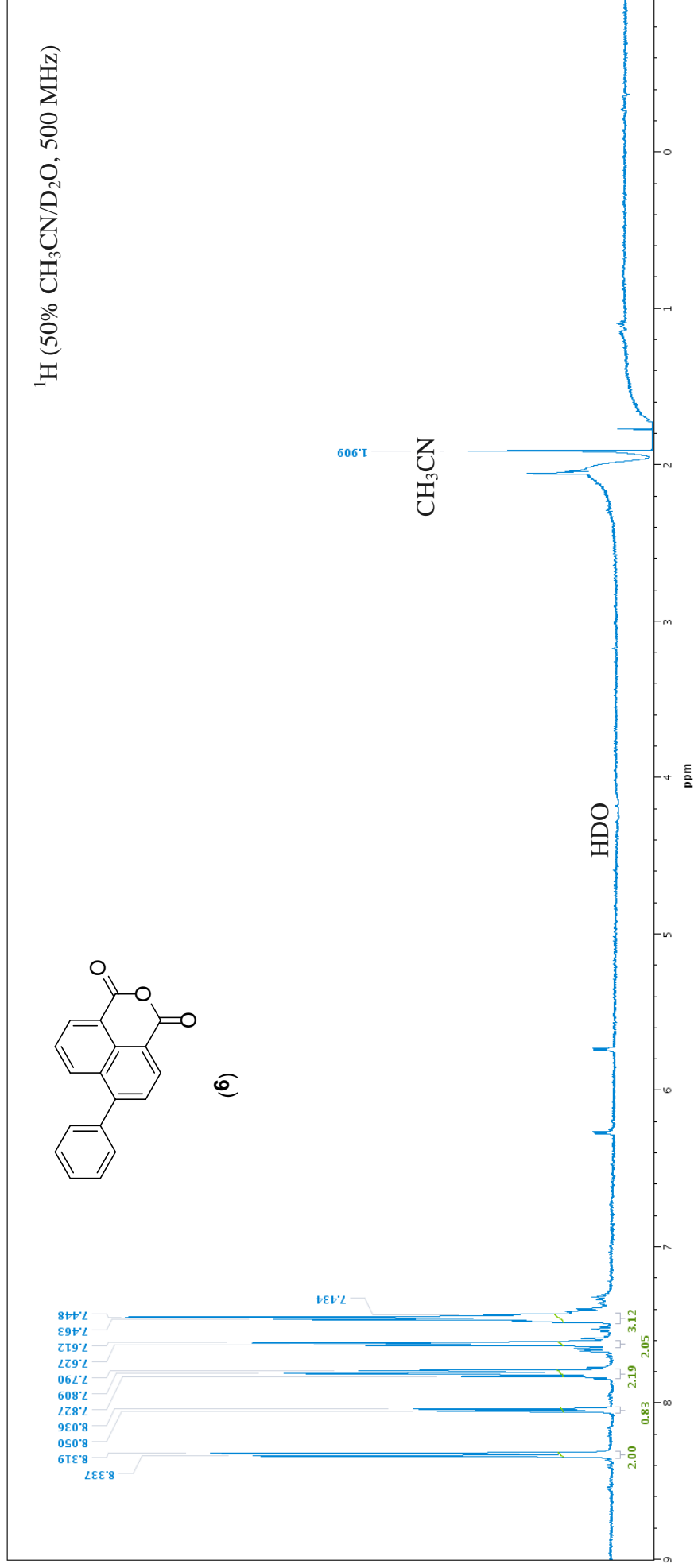
S13. Stop-flow WETID Proton NMR spectrum of compound eluting at 11.31 mins (fuliginosone (**14**)).



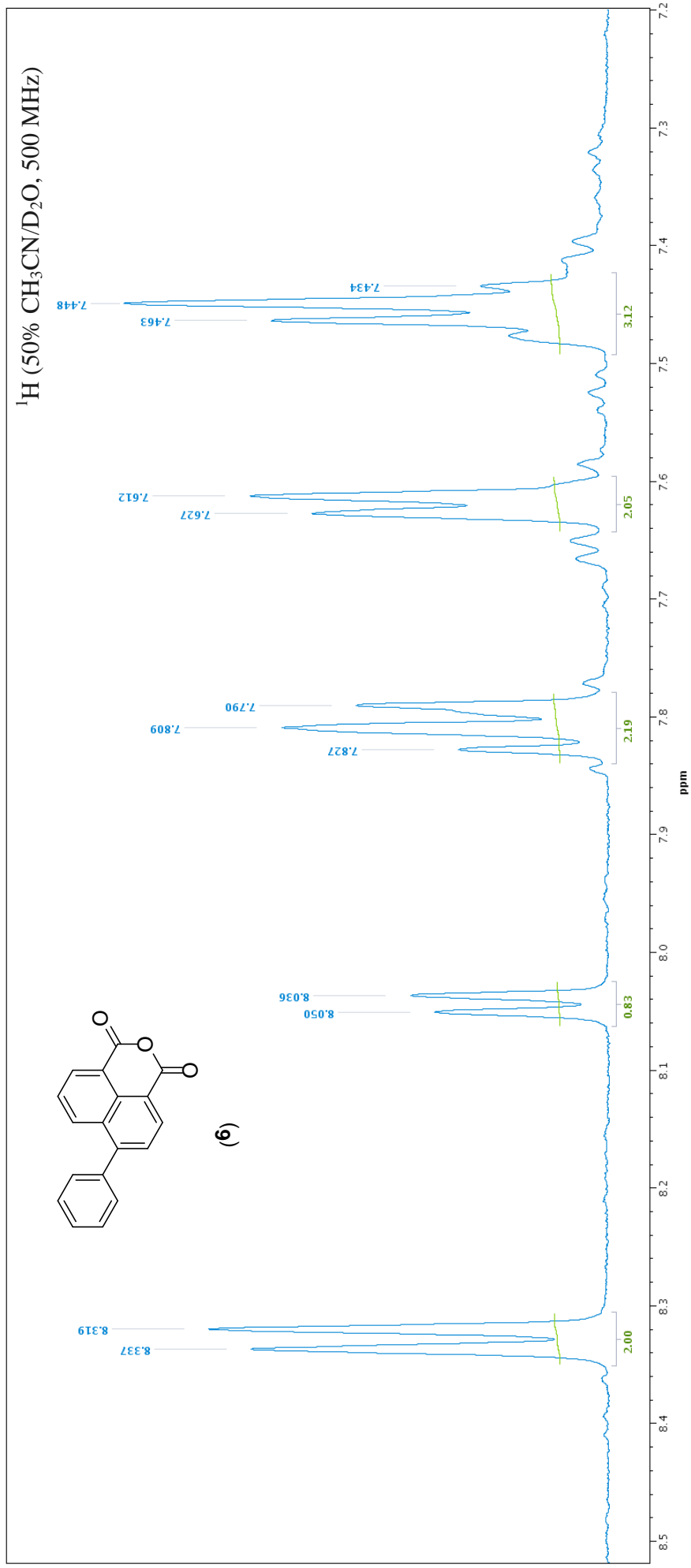
S14. Expansion of Stop-flow WET1D Proton NMR spectrum of compound eluting at 11.31 mins (fuliginosone (**14**)).



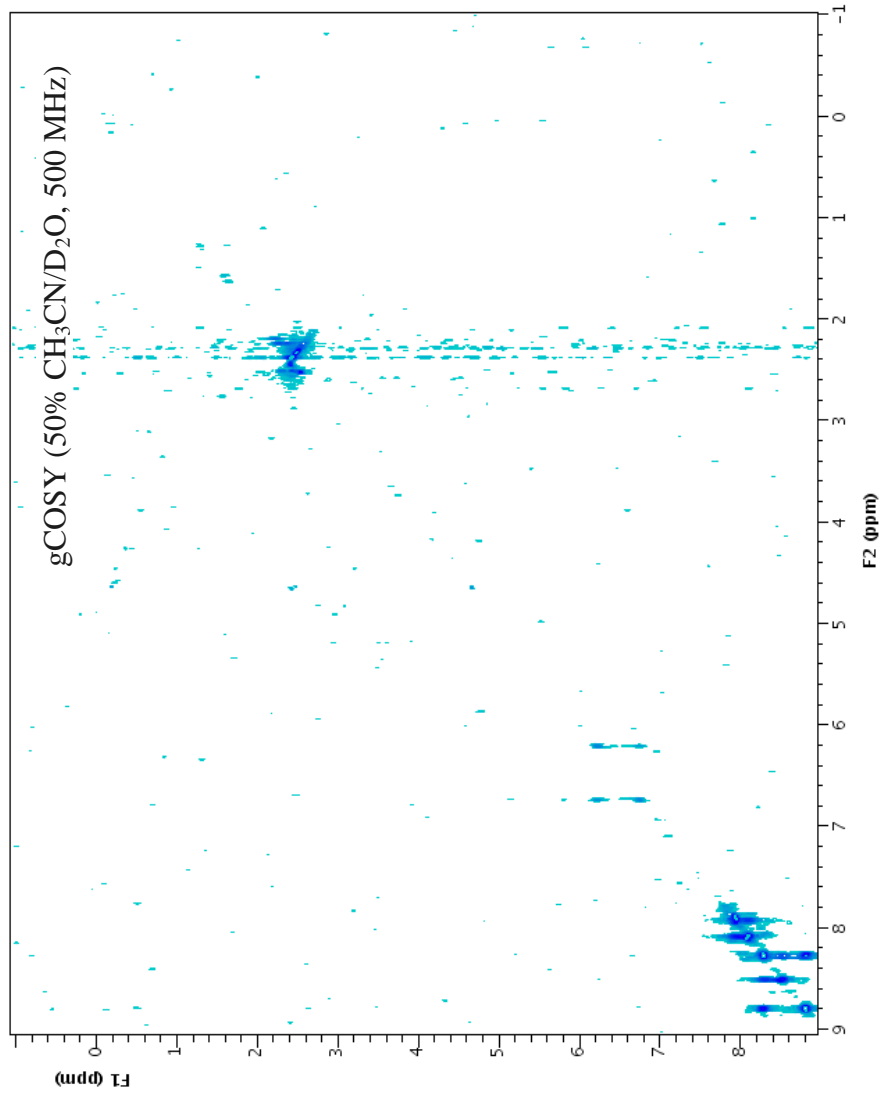
S15. High resolution negative ESI-MS of compound eluting at 11.31 mins (fuliginosone (**14**)) from HPLC-MS.



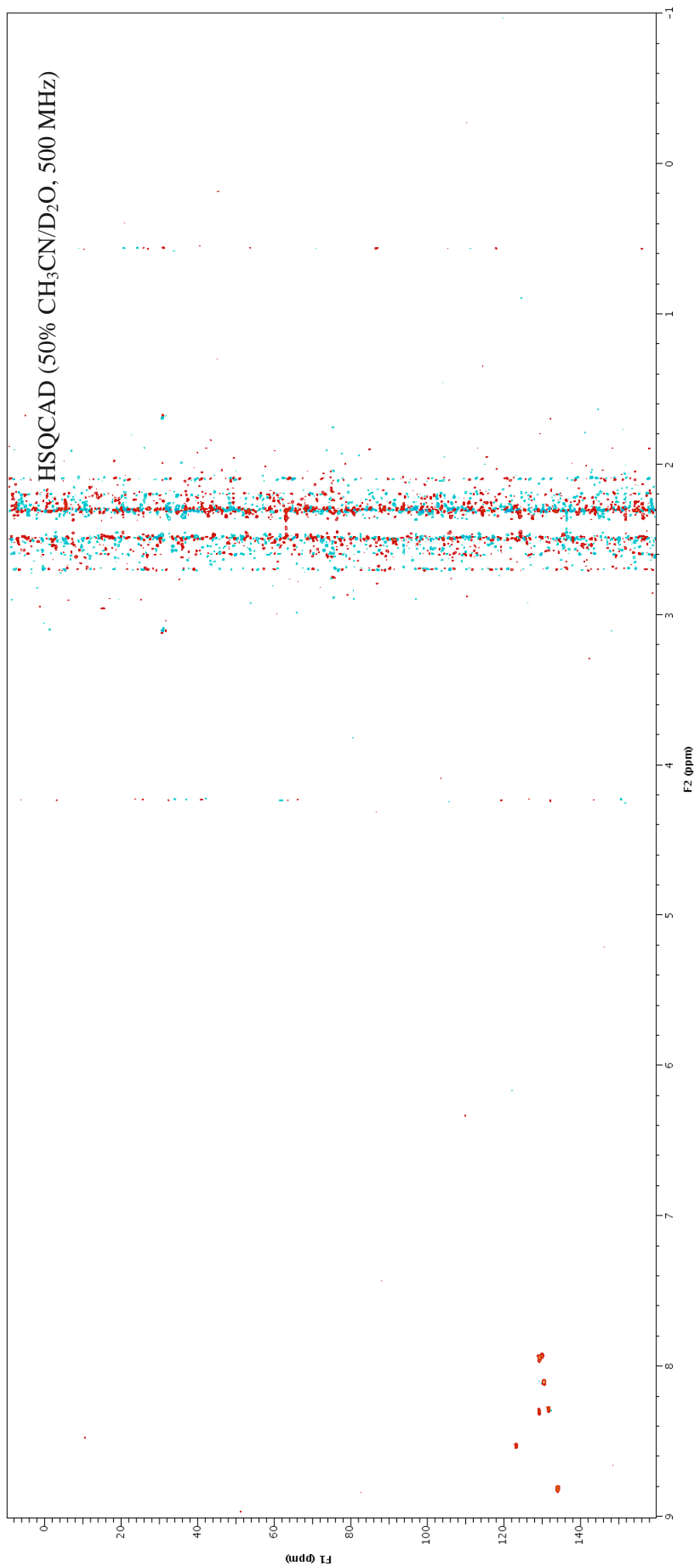
S16. Stop-flow WET1D Proton NMR spectrum of compound eluting at 12.35 mins (compound **6**).



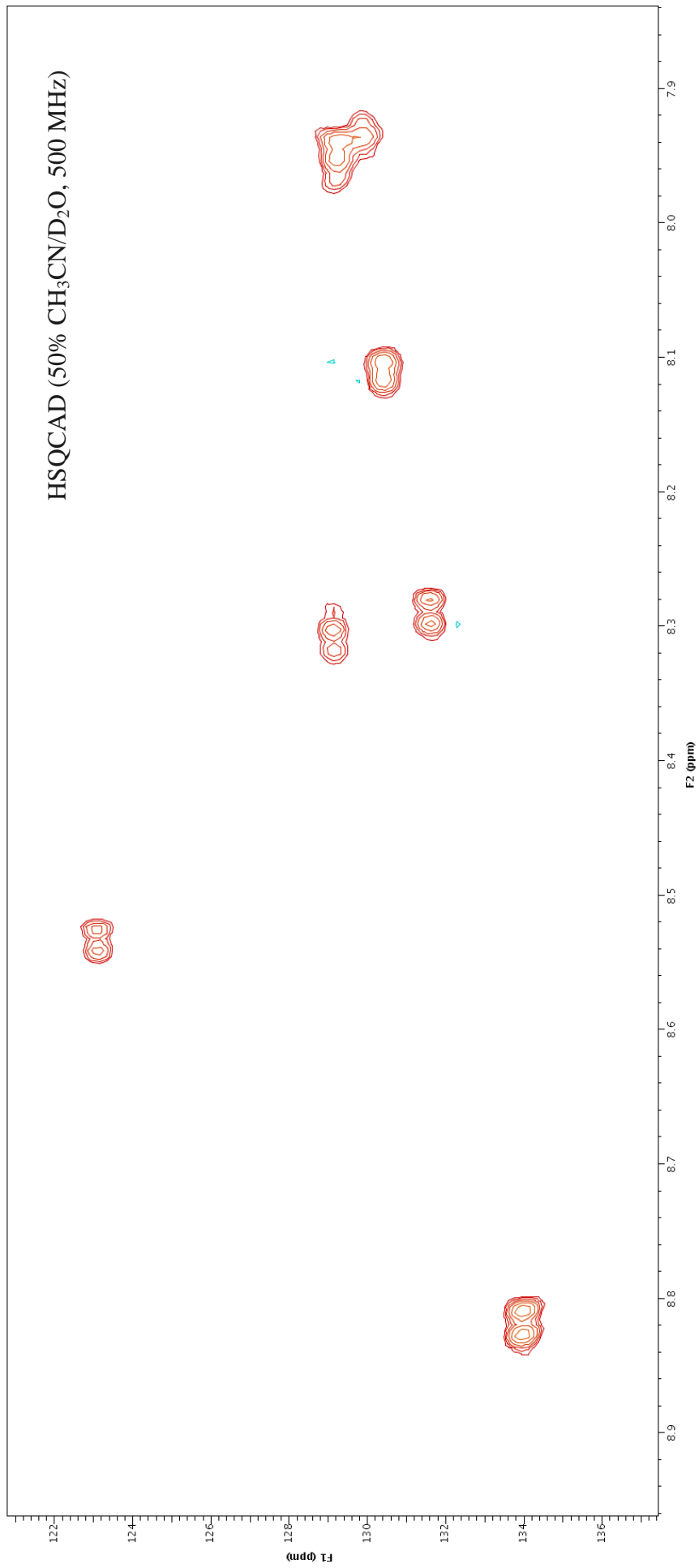
S17. Expansion of Stop-flow WET1D Proton NMR spectrum of compound eluting at 12.35 mins (compound **6**).



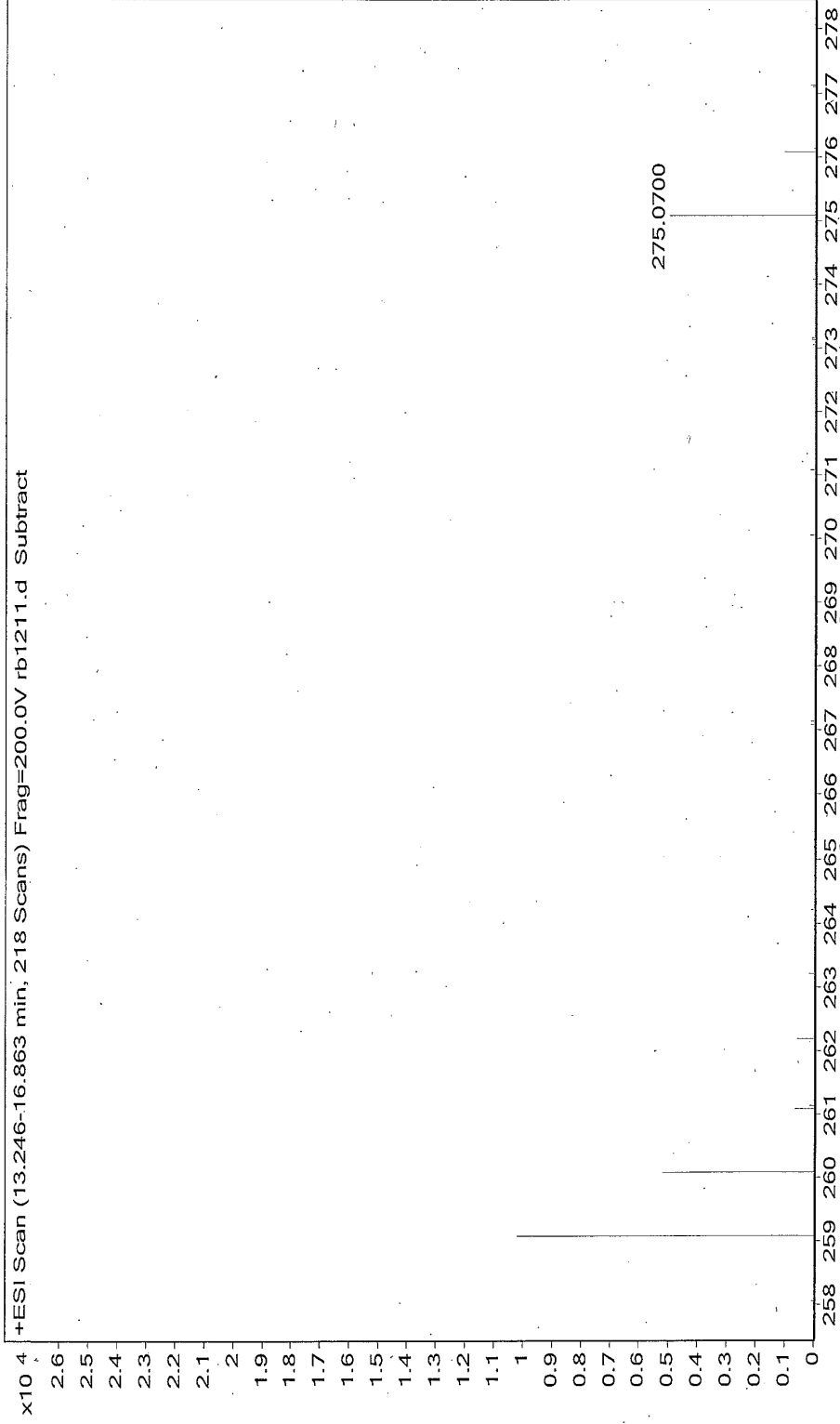
S18. gCOSY NMR spectrum (from stop-flow HPLC-NMR) of compound eluting at 12.35 mins (compound **6**).



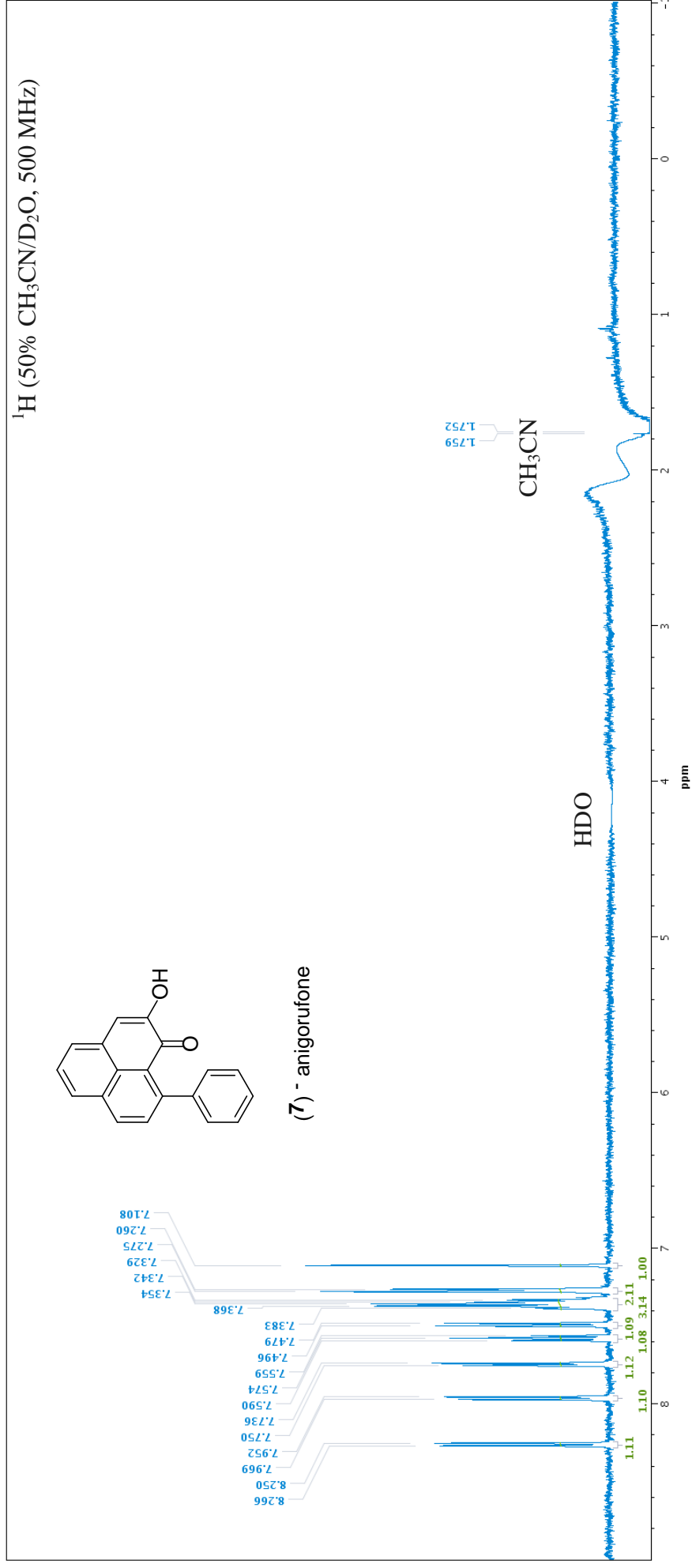
S19. HSQCAD NMR spectrum (from stop-flow HPLC-NMR) of compound eluting at 12.35 mins (compound **6**).



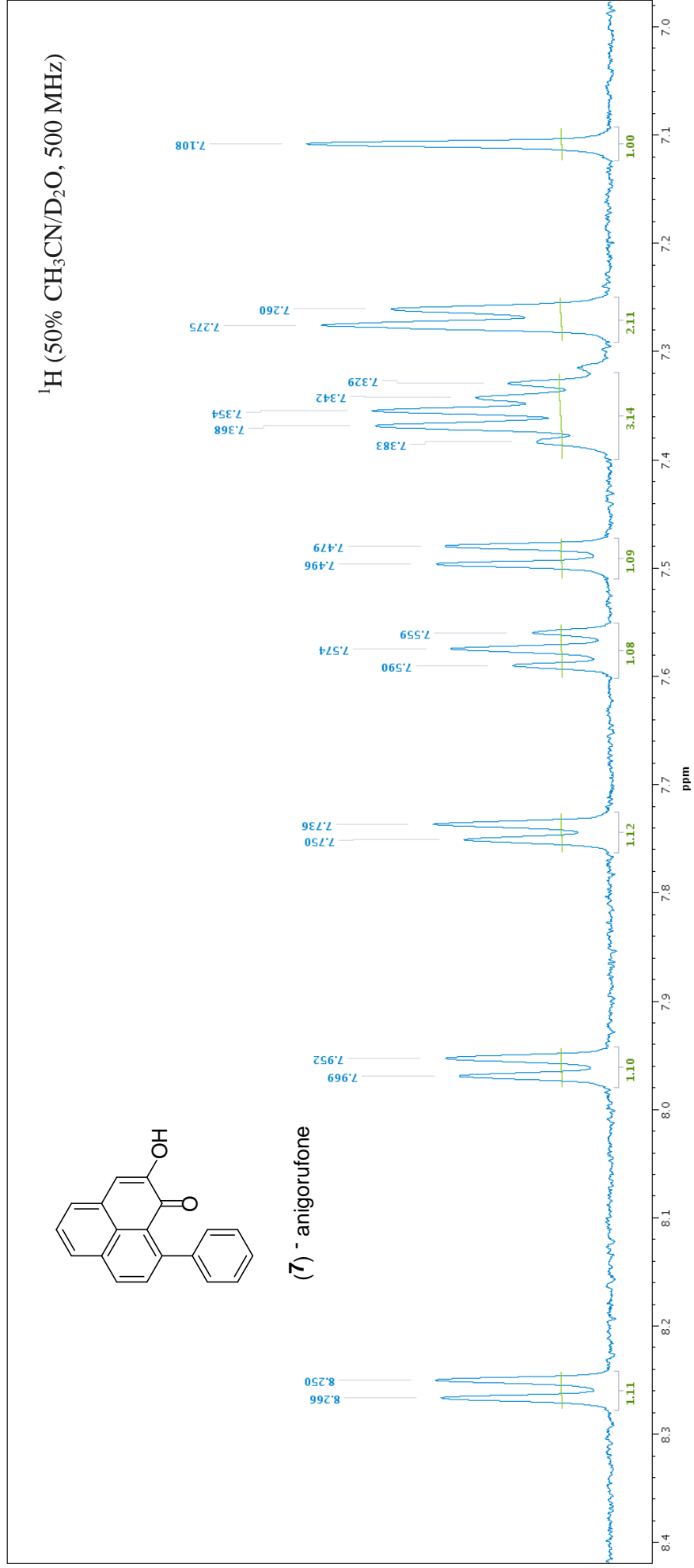
S20. Expansion of HSQCAD NMR spectrum (from stop-flow HPLC-NMR) of compound eluting at 12.35 mins (compound **6**).



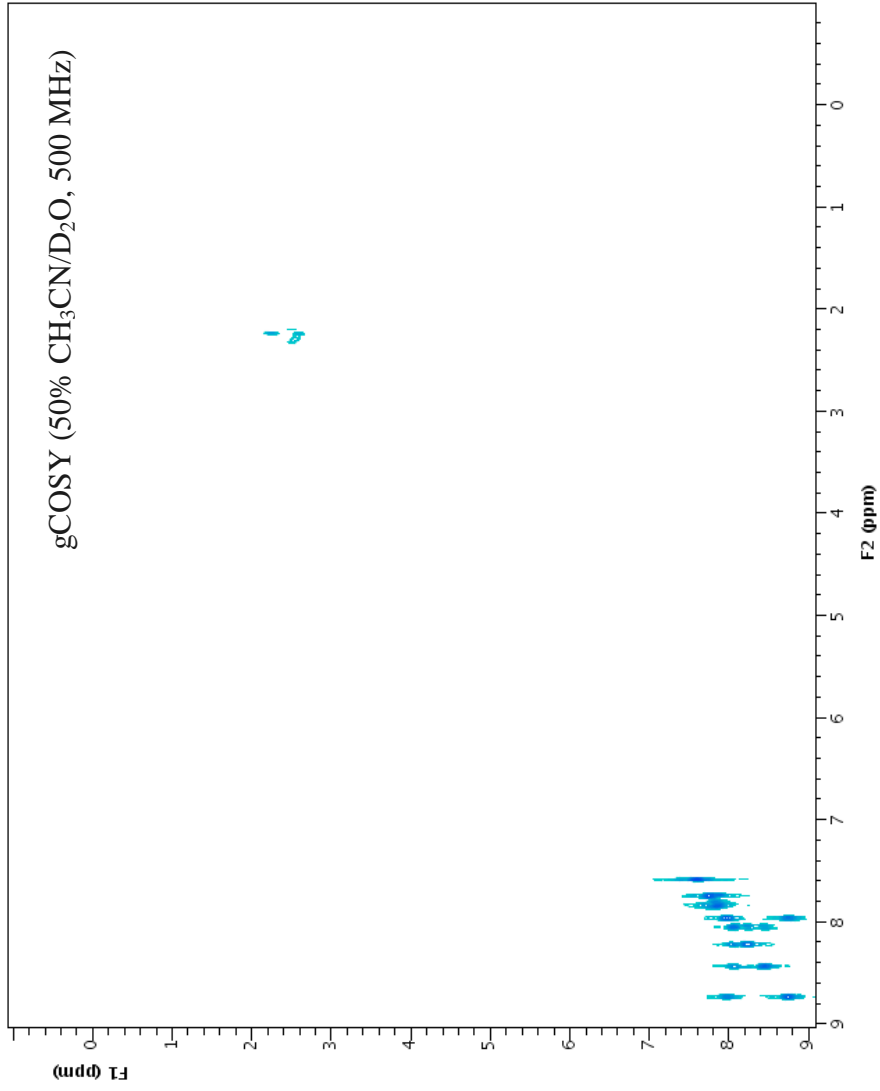
S21. High resolution negative ESI-MS of compound eluting at 12.35 mins (compound **6**) from HPLC-MS.



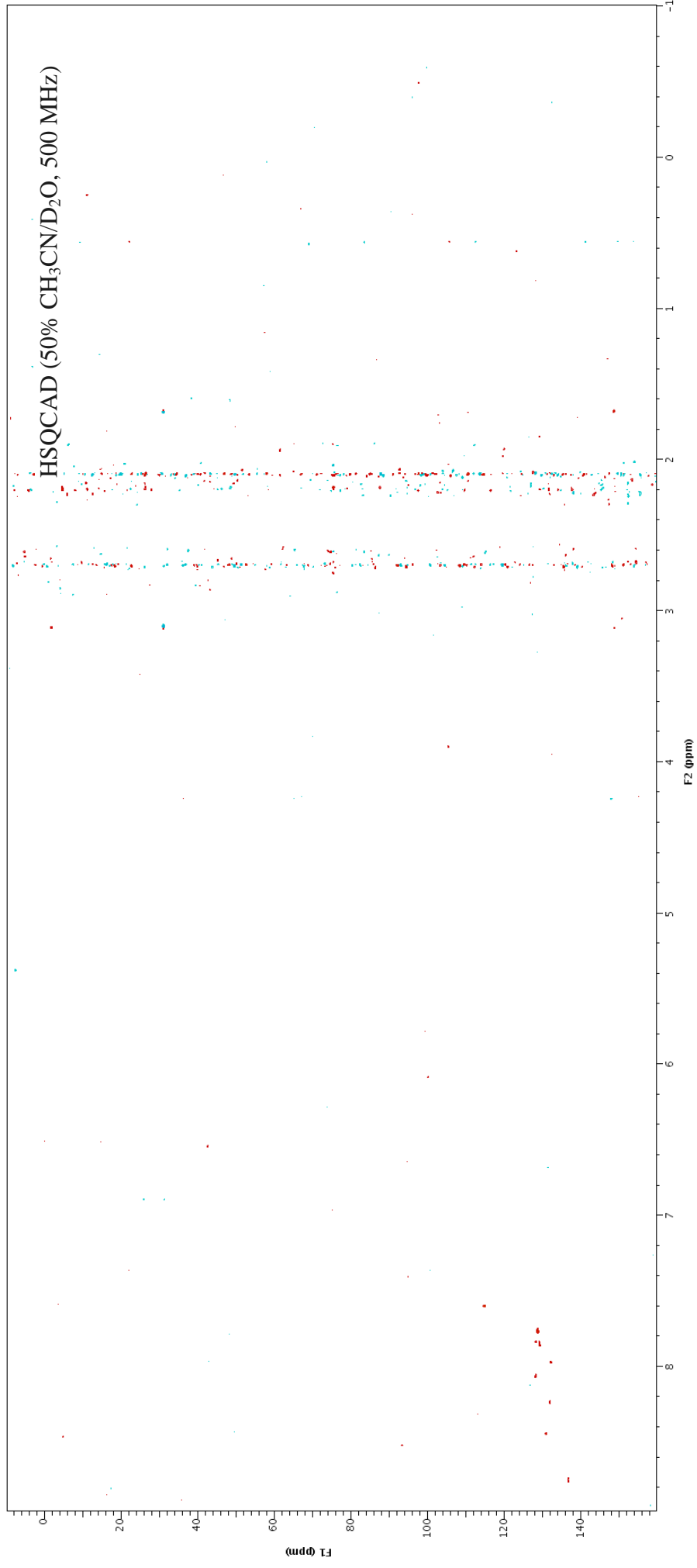
S22. Stop-flow WET1D Proton NMR spectrum of compound eluting at 19.11 mins (anigorufone (7)).



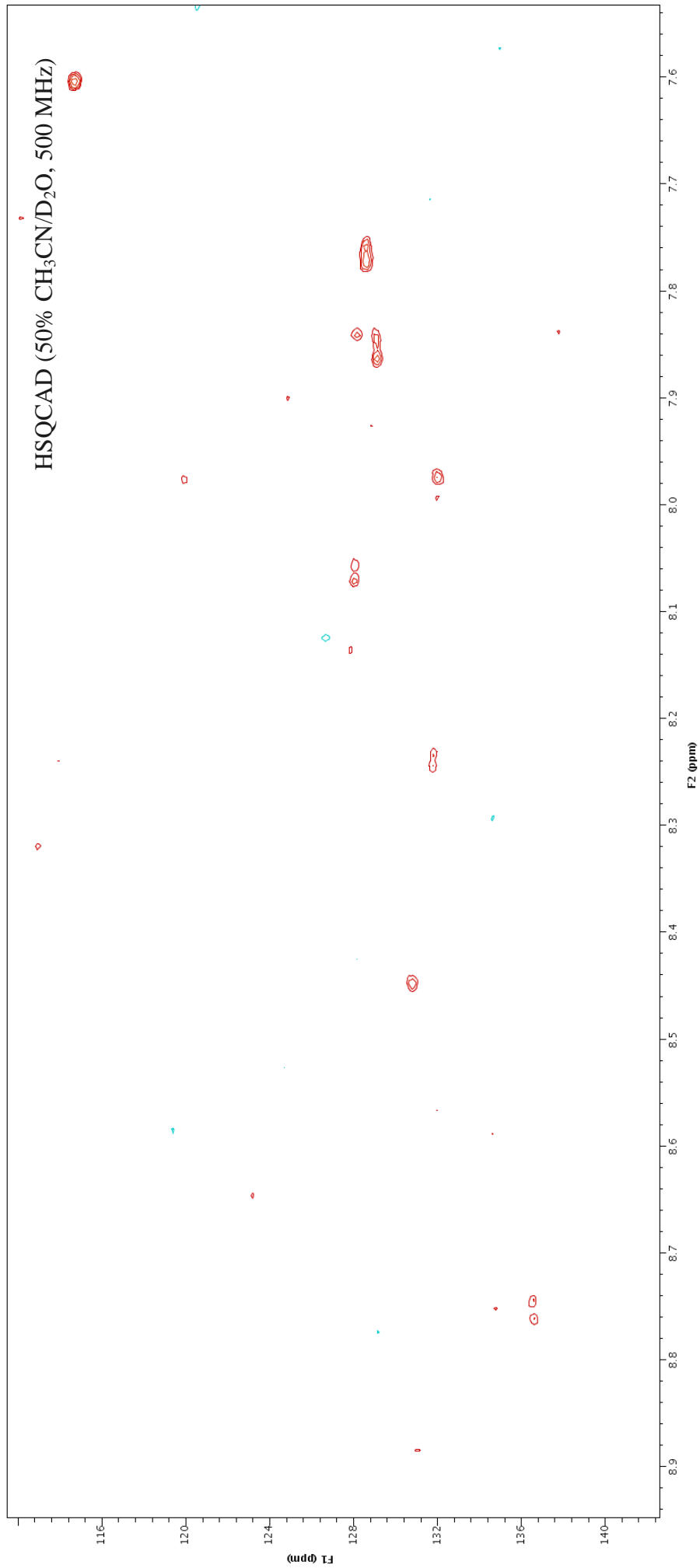
S23. Expansion of Stop-flow WET1D Proton NMR spectrum of compound eluting at 19.11 mins (anigorufone (7)).



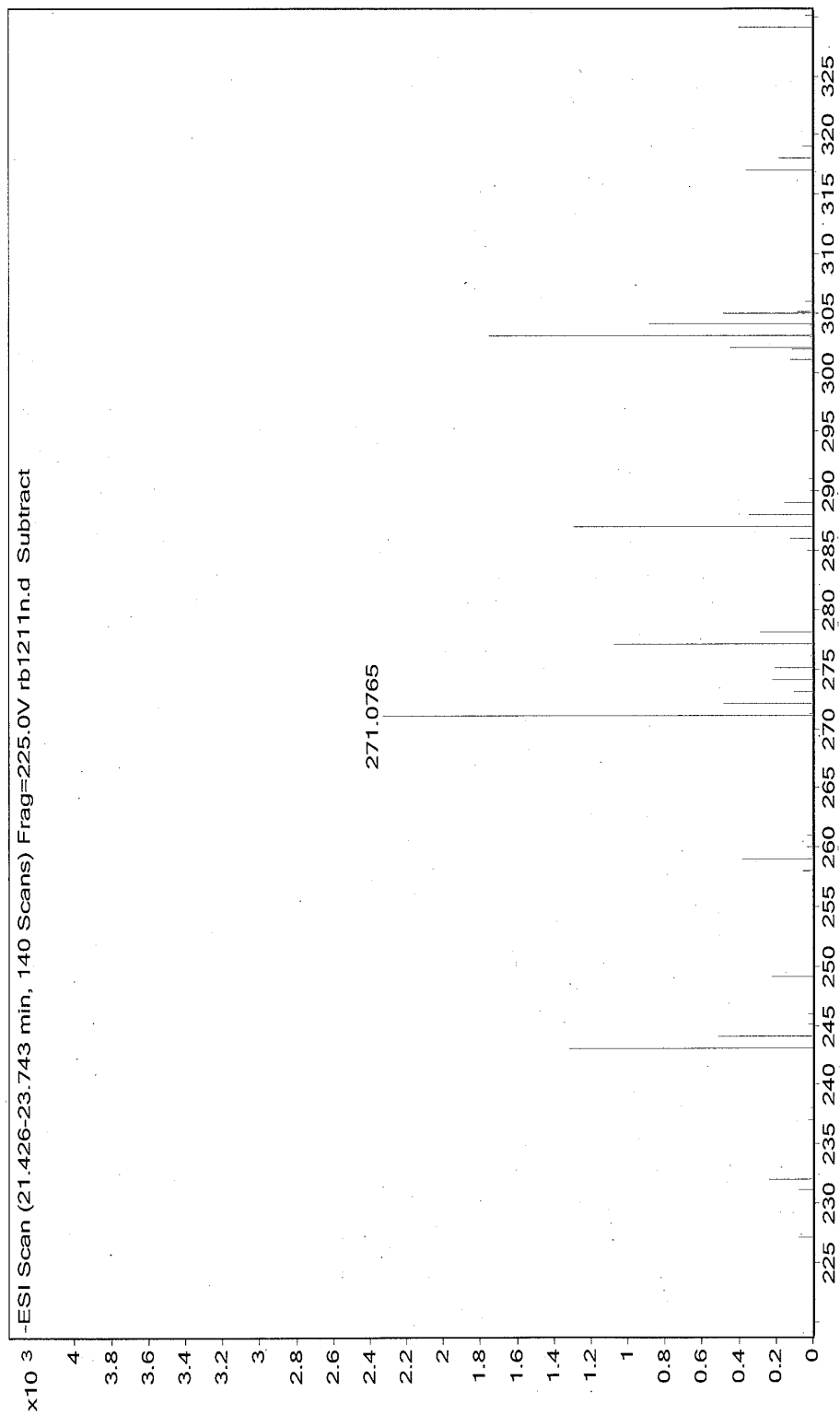
S24. gCOSY NMR spectrum (from stop-flow HPLC-NMR) of compound eluting at 19.11 mins (anigorufone (**7**)).



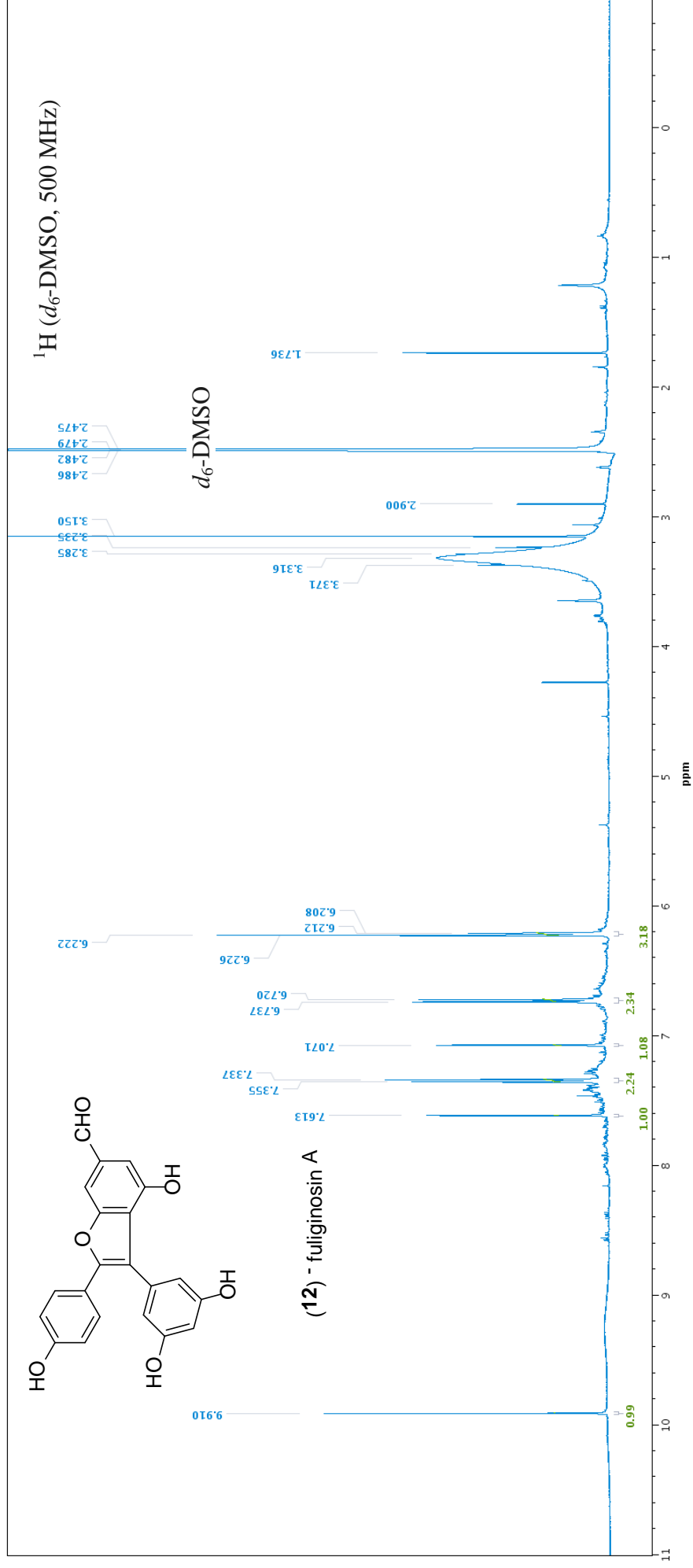
S25. HSQCAD NMR spectrum (from stop-flow HPLC-NMR) of compound eluting at 19.11 mins (anigorufone (7)).



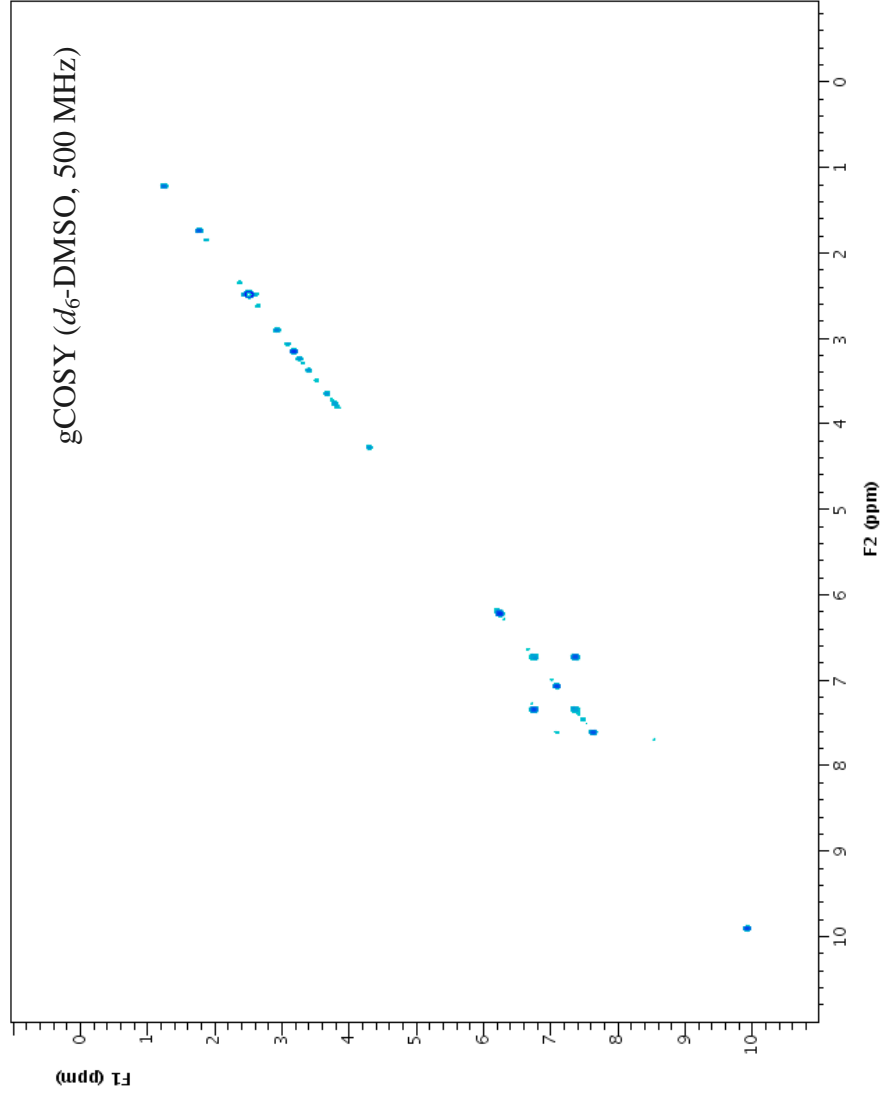
S26. Expansion of HSQCAD NMR spectrum (from stop-flow HPLC-NMR) of compound eluting at 19.11 mins (anigorufone (7)).



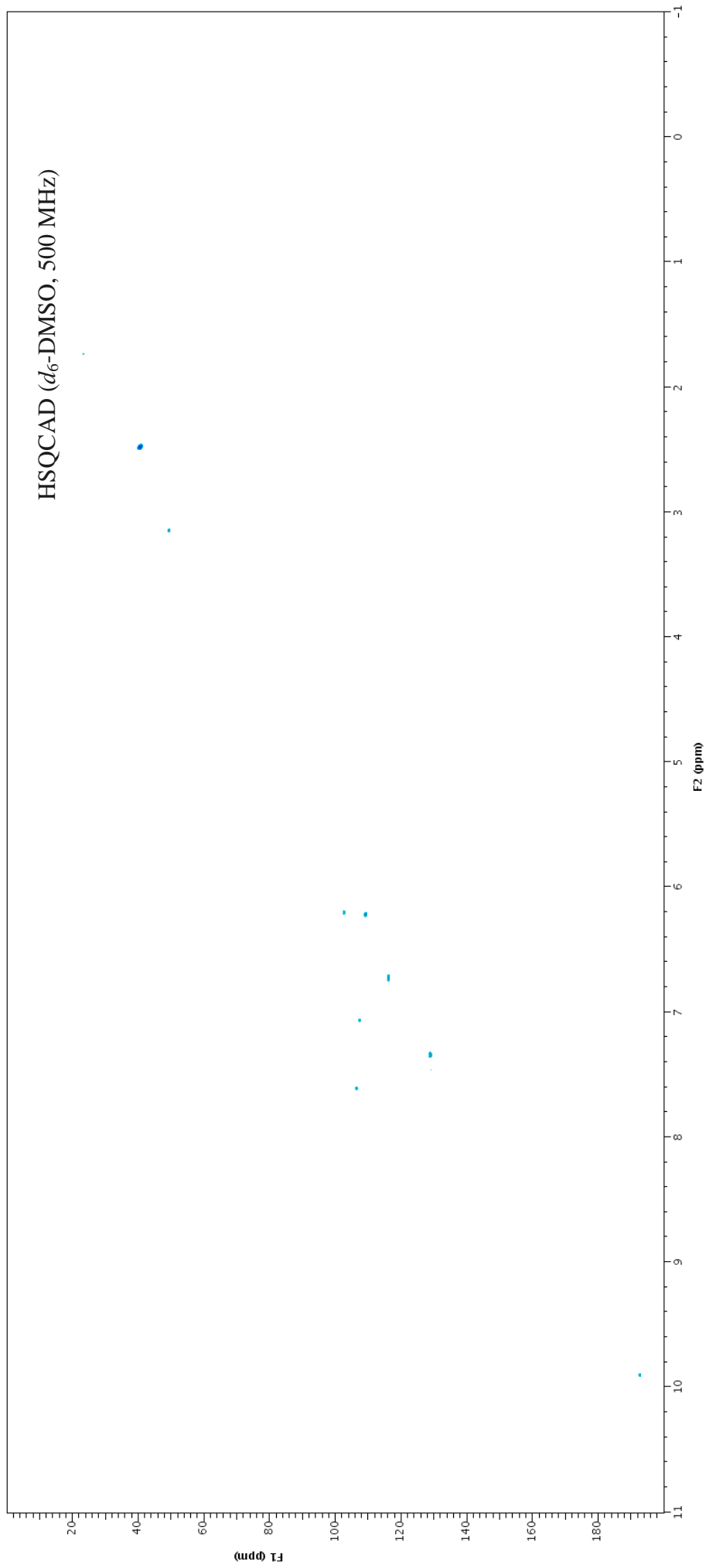
S27. High resolution negative ESI-MS of compound eluting at 19.11 mins (anigorufone (7)) from HPLC-MS.



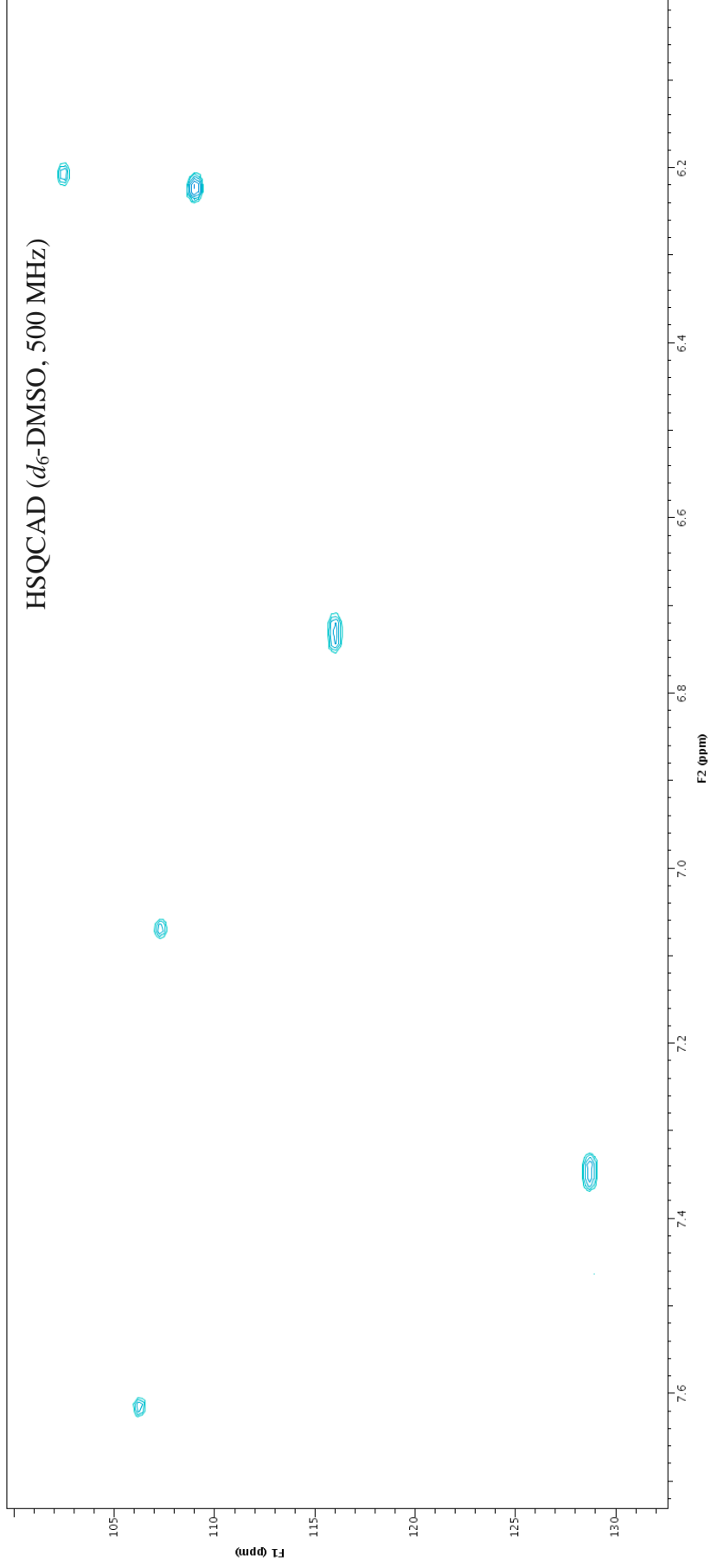
S28. ¹H NMR spectrum (500 MHz, d₆-DMSO) of fuliginosin A (12).



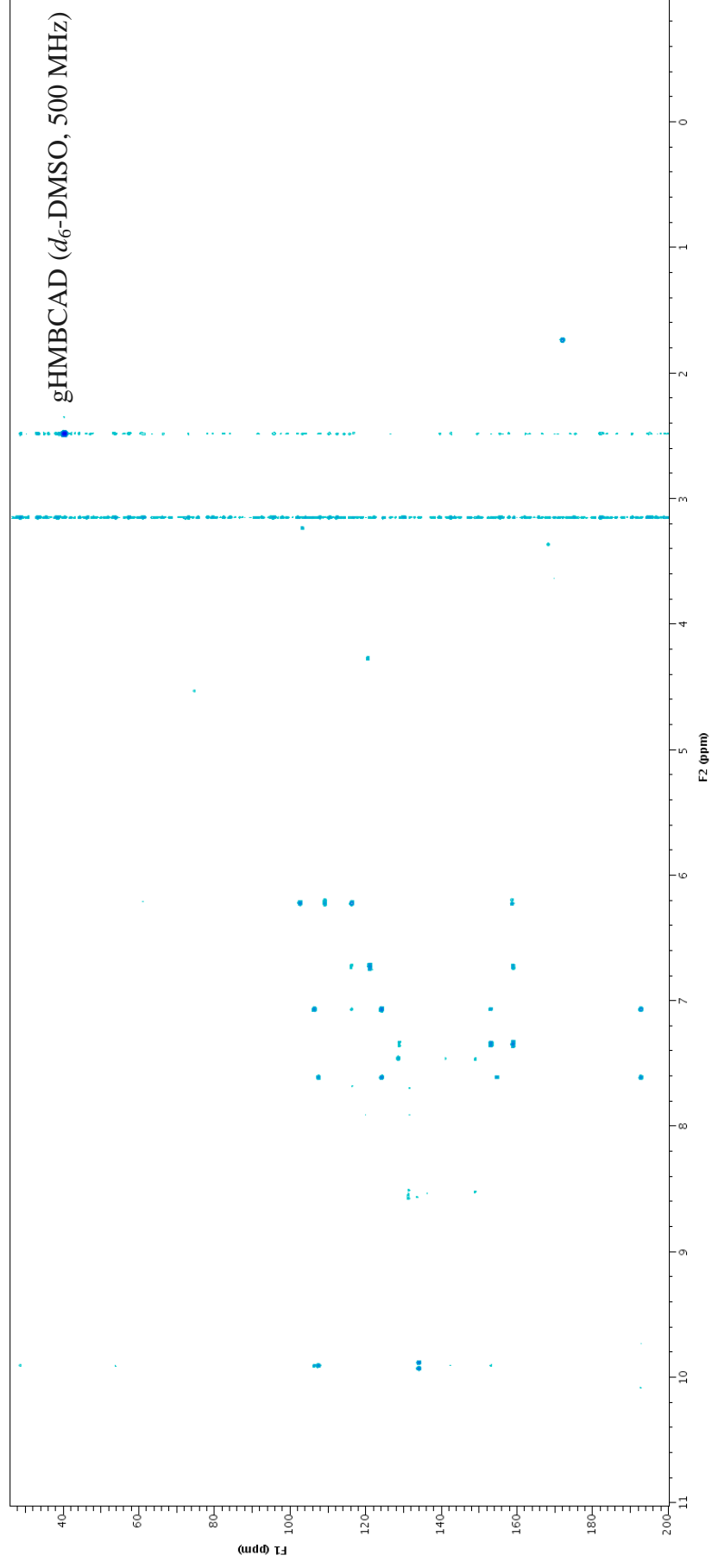
S29. gCOSY NMR spectrum (500 MHz, d_6 -DMSO) of fuliginosin A (**12**).



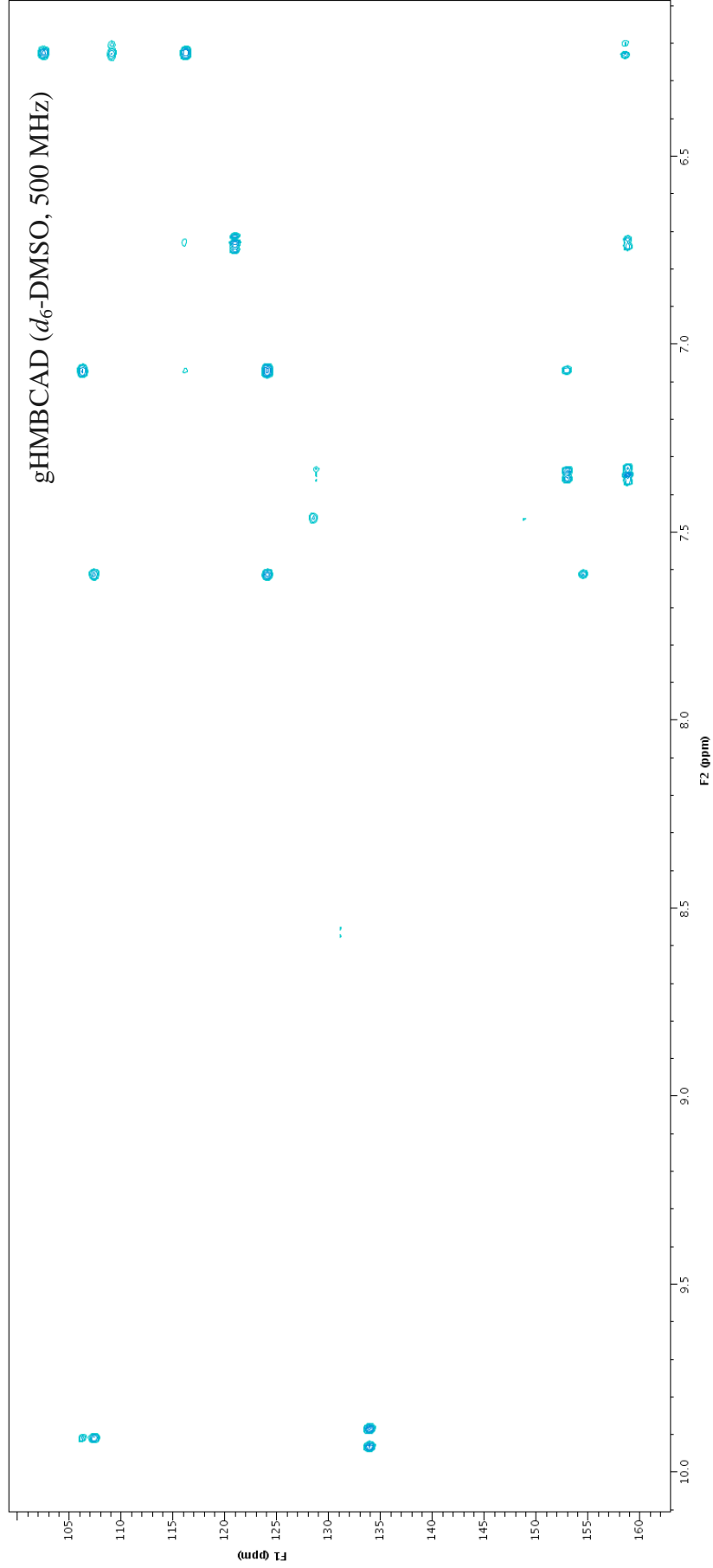
S30. HSQCAD NMR spectrum (500 MHz, d_6 -DMSO) of fuliginosin A (**12**).



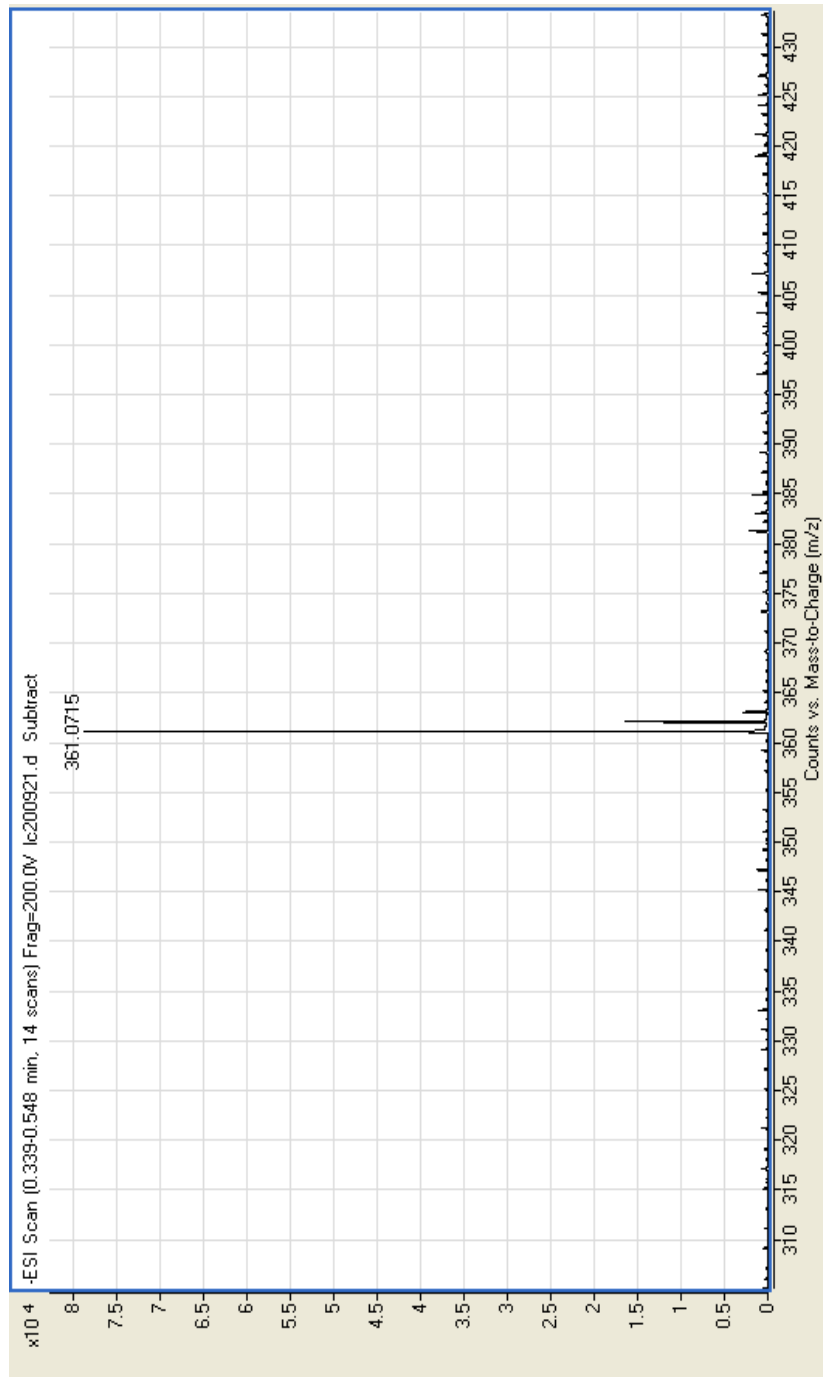
S31. Expansion of HSQCAD NMR spectrum (500 MHz, d_6 -DMSO) of fuliginosin A (**12**).



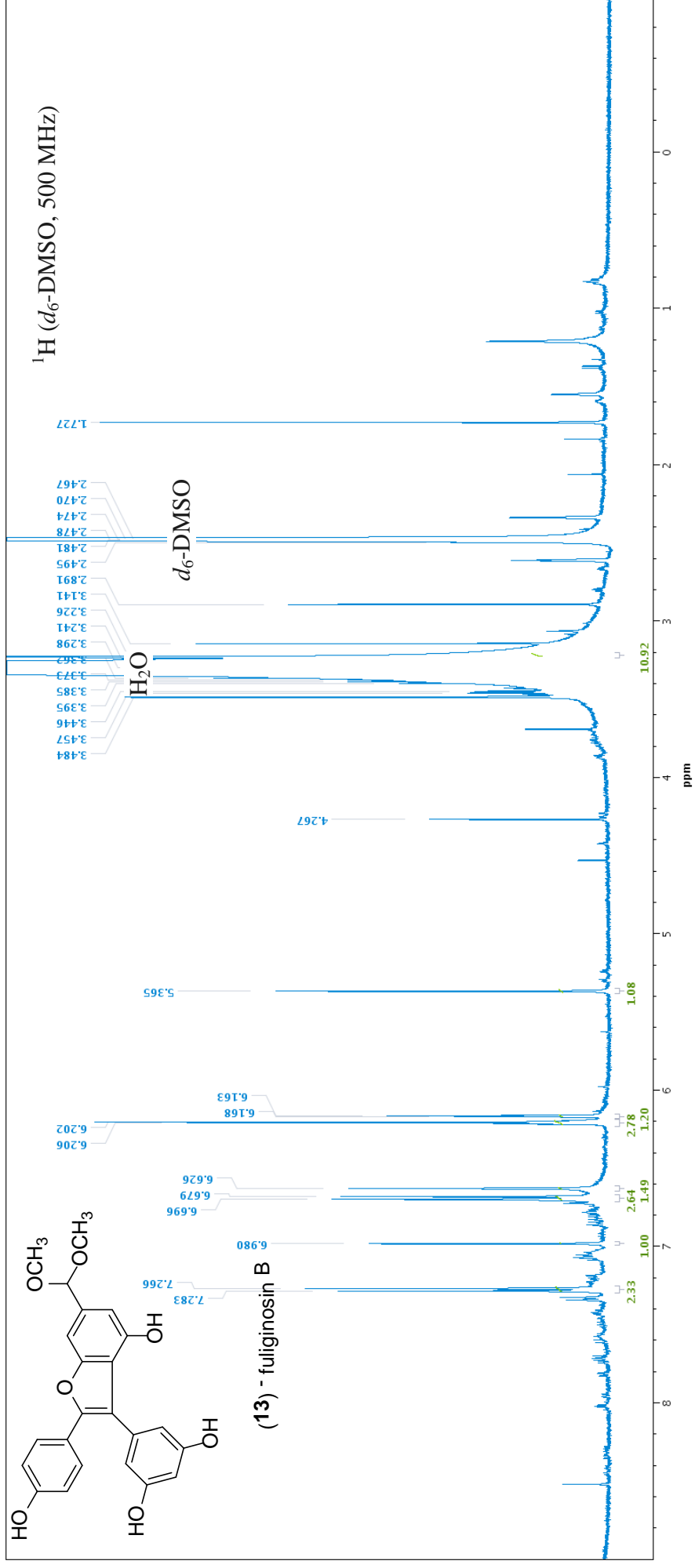
S32. gHMBCAD NMR spectrum (500 MHz, d_6 -DMSO) of fuliginosin A (**12**).



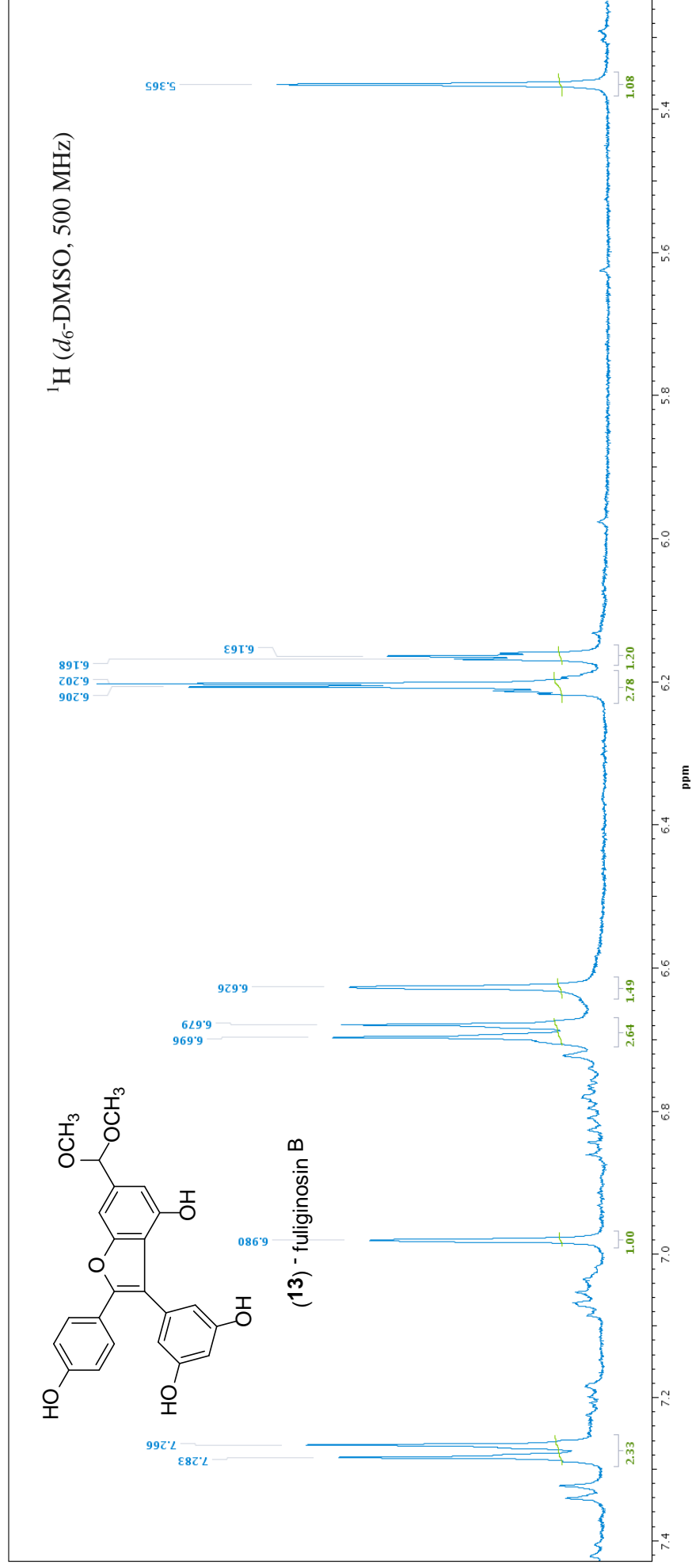
S33. Expansion of gHMBCAD NMR spectrum (500 MHz, d_6 -DMSO) of fuliginosin A (**12**).



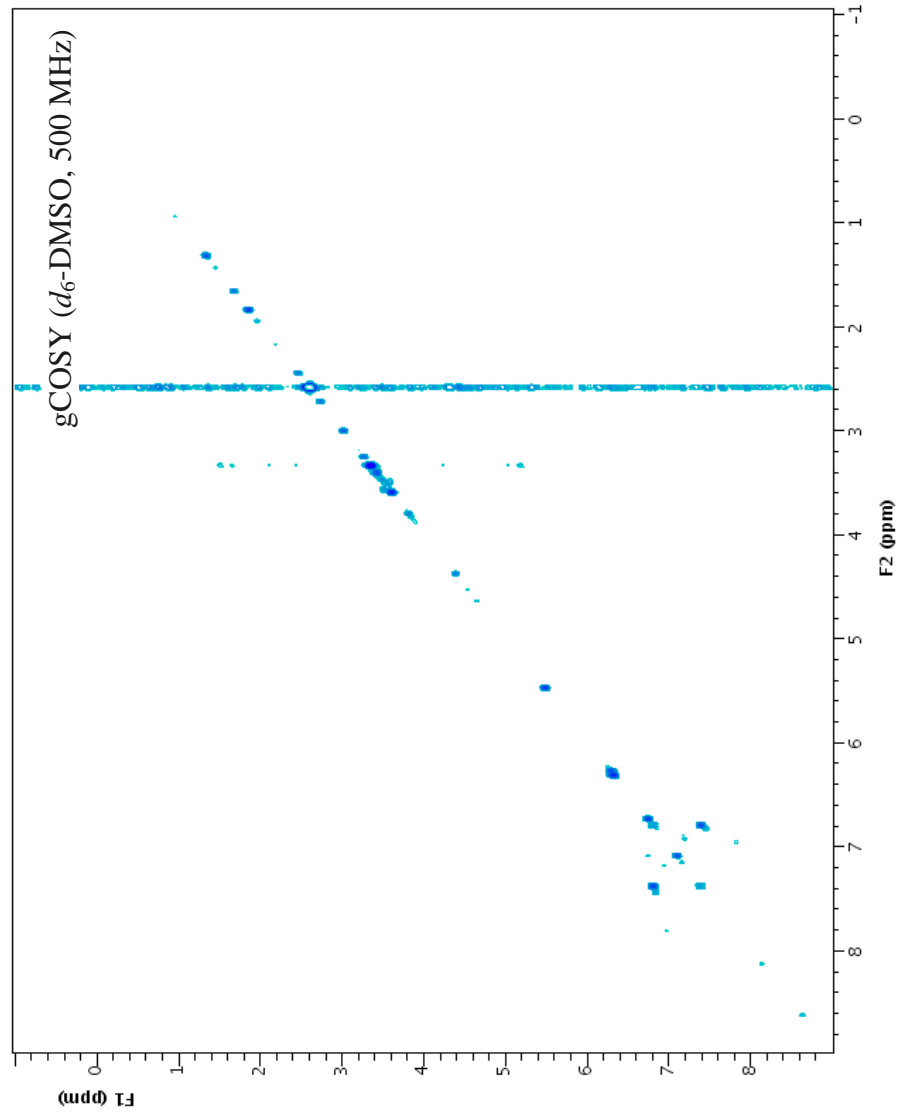
S34. High resolution negative ESI-MS of fuliginosin A (12).



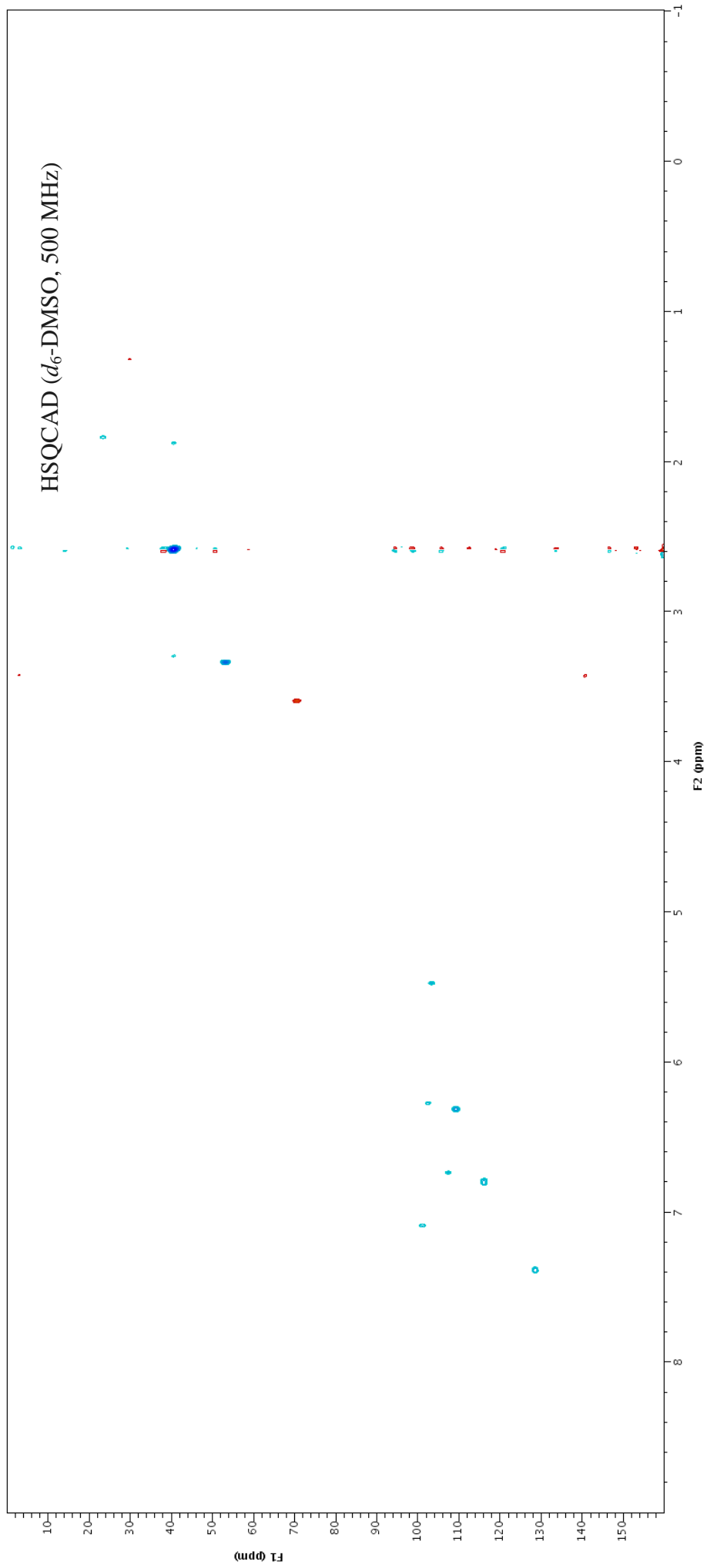
S35. ¹H NMR spectrum (500 MHz, *d*₆-DMSO) of fuliginosin B (**13**).



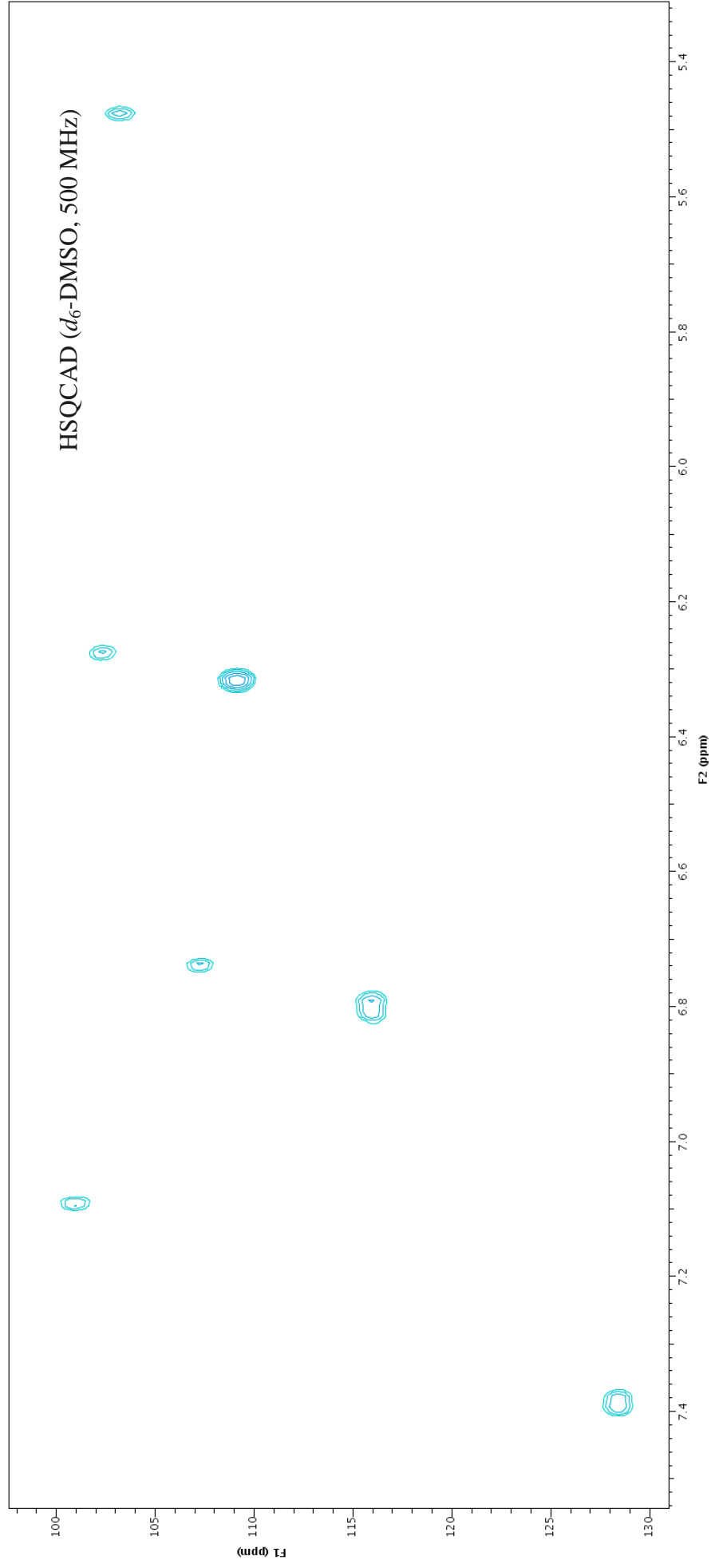
S36. Expansion of ¹H NMR spectrum (500 MHz, d₆-DMSO) of fuliginosin B (**13**).



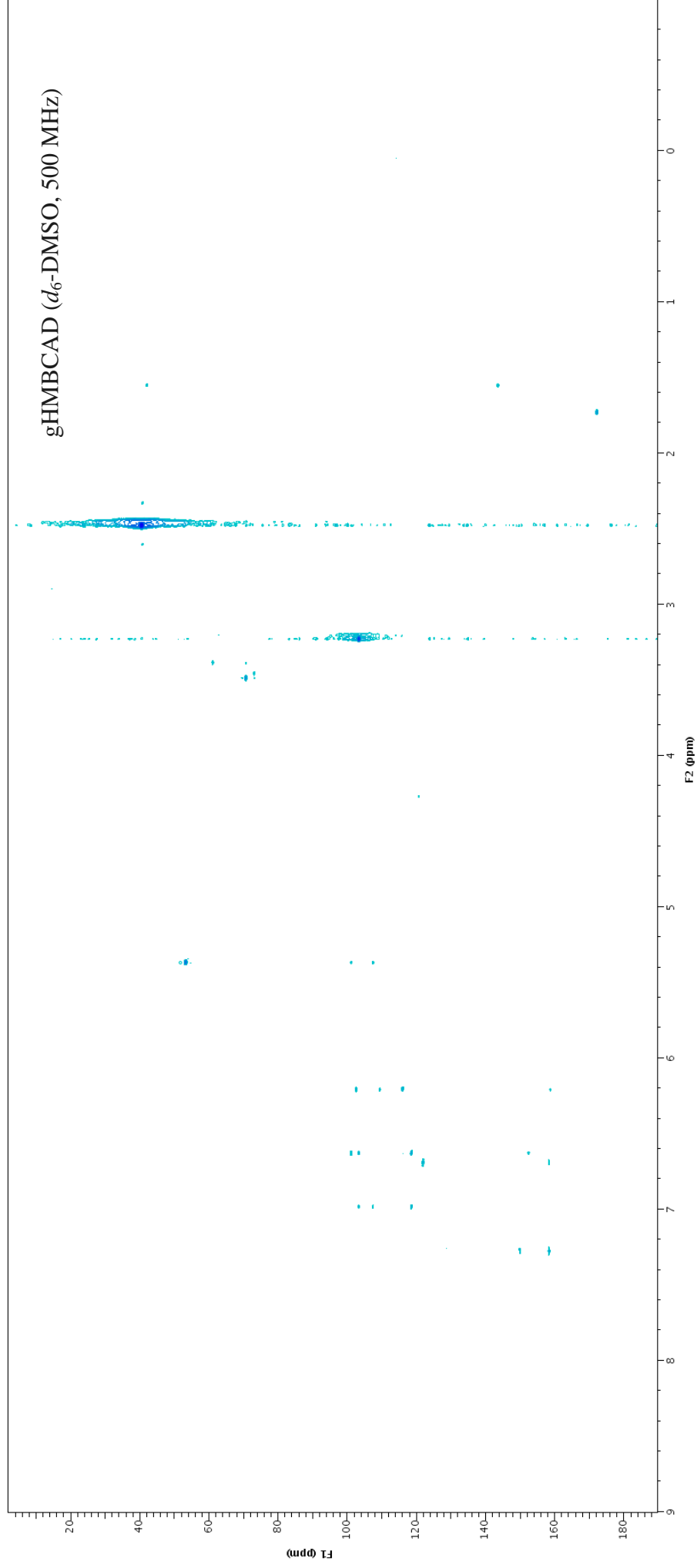
S37. gCOSY NMR spectrum (500 MHz, d_6 -DMSO) of fuliginosin B (**13**).



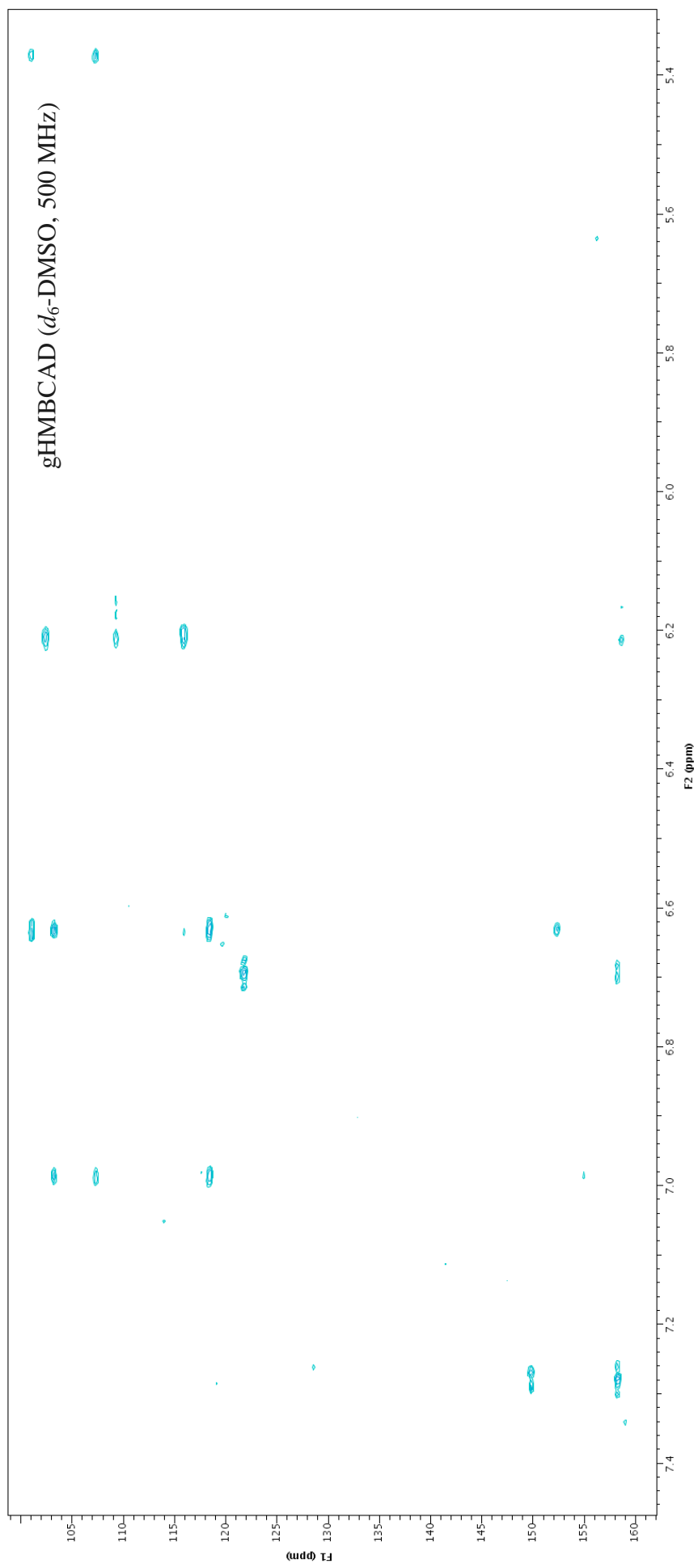
S38. HSQCAD NMR spectrum (500 MHz, d_6 -DMSO) of fuliginosin B (**13**).



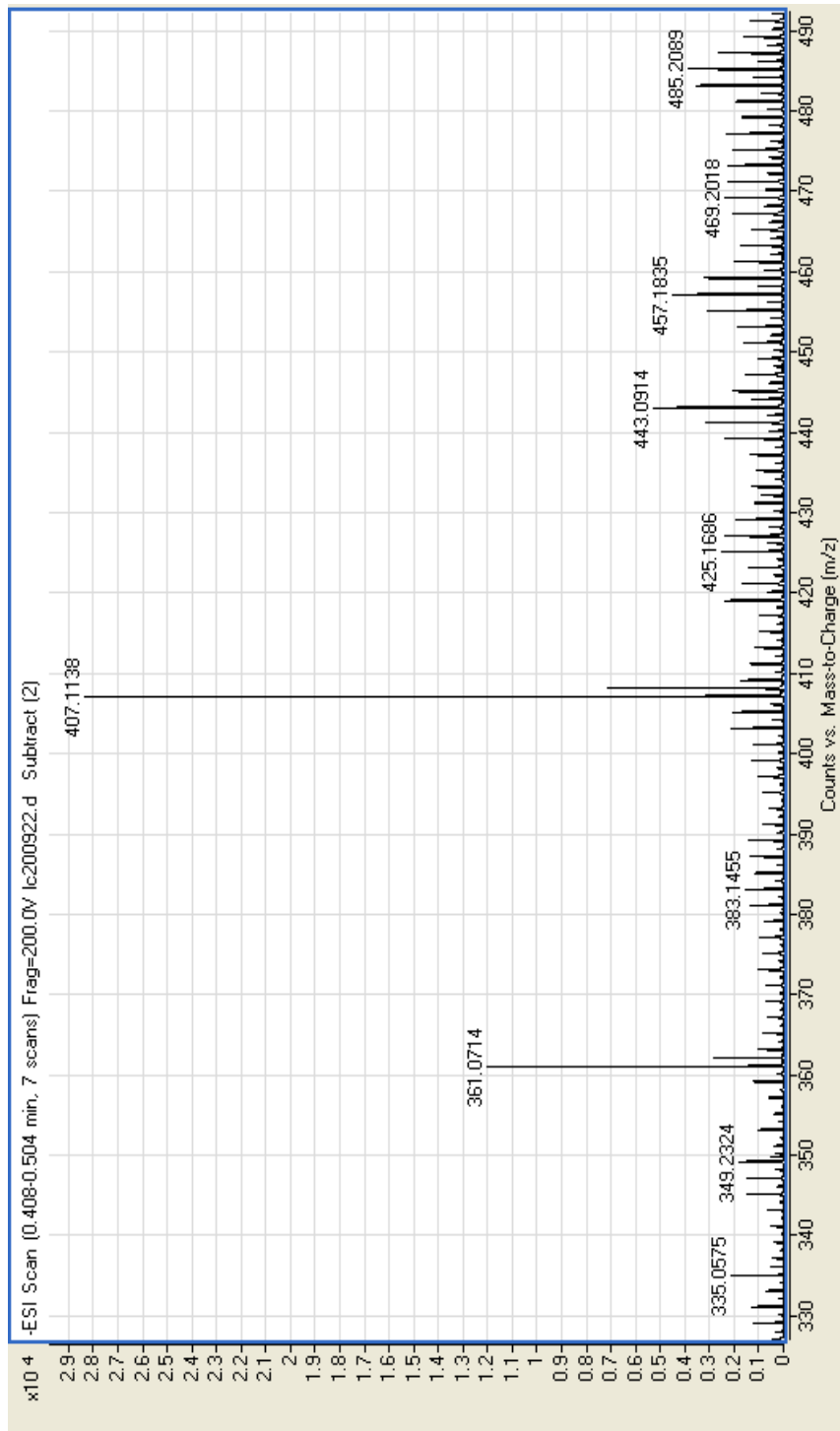
S39. Expansion of HSQCAD NMR spectrum (500 MHz, d_6 -DMSO) of fuliginosin B (**13**).



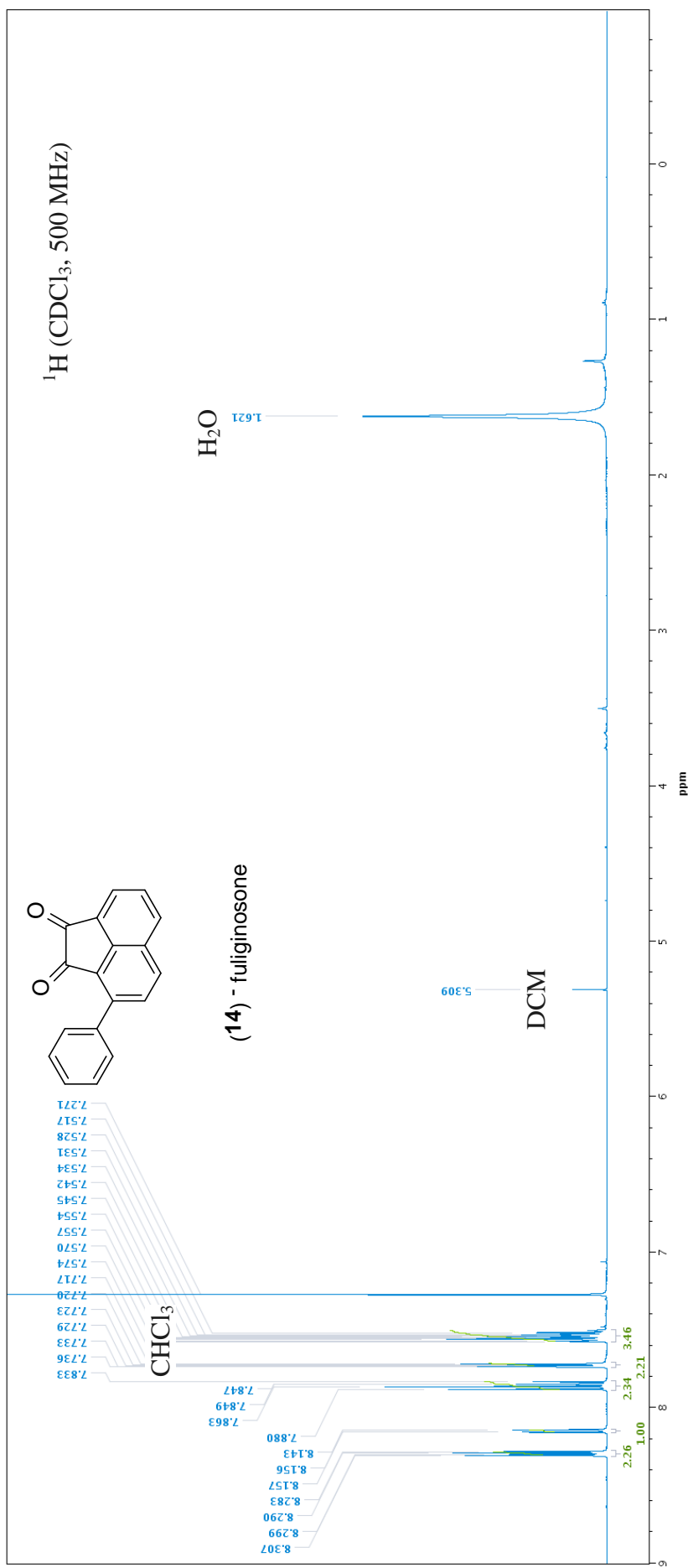
S40. gHMBCAD NMR spectrum (500 MHz, d_6 -DMSO) of fuliginosin B (**13**).



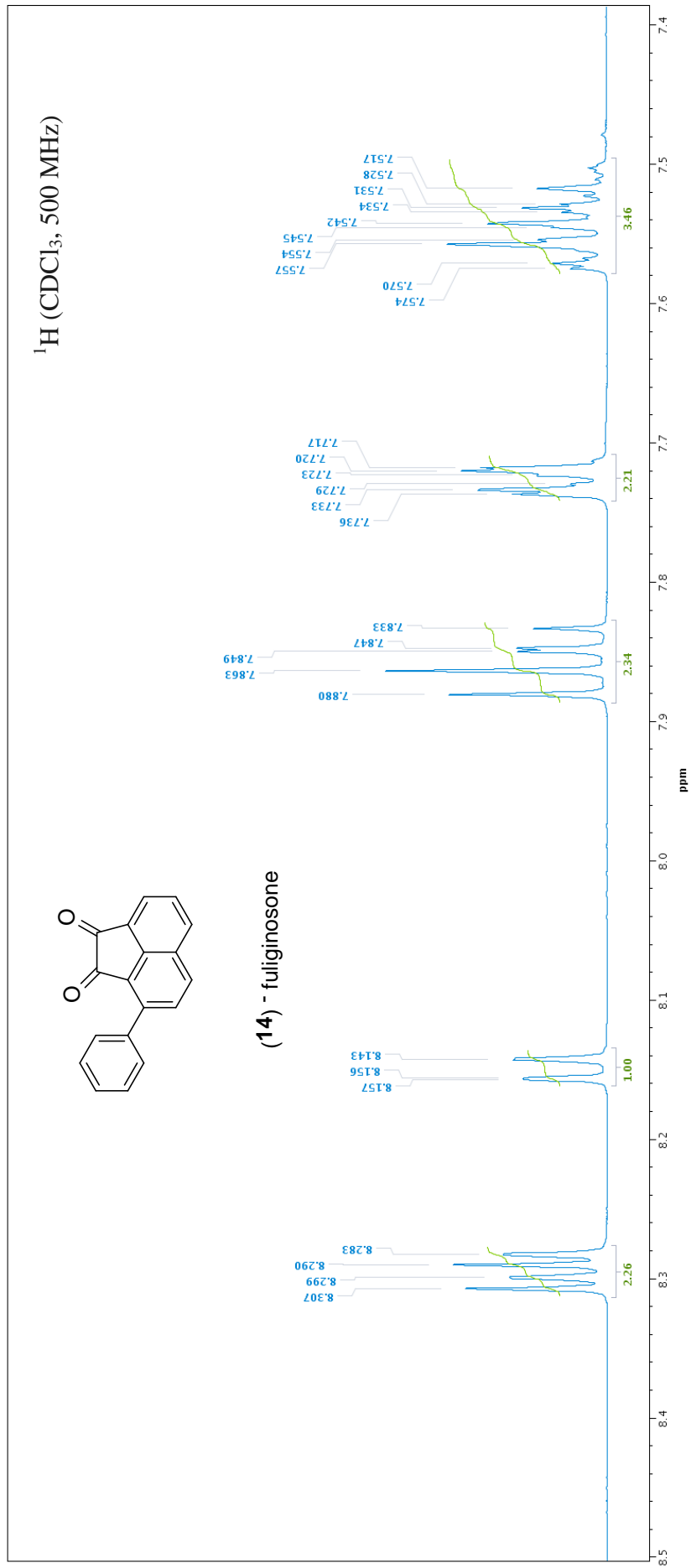
S41. Expansion of gHMBCAD NMR spectrum (500 MHz, d_6 -DMSO) of fuliginosin B (**13**).



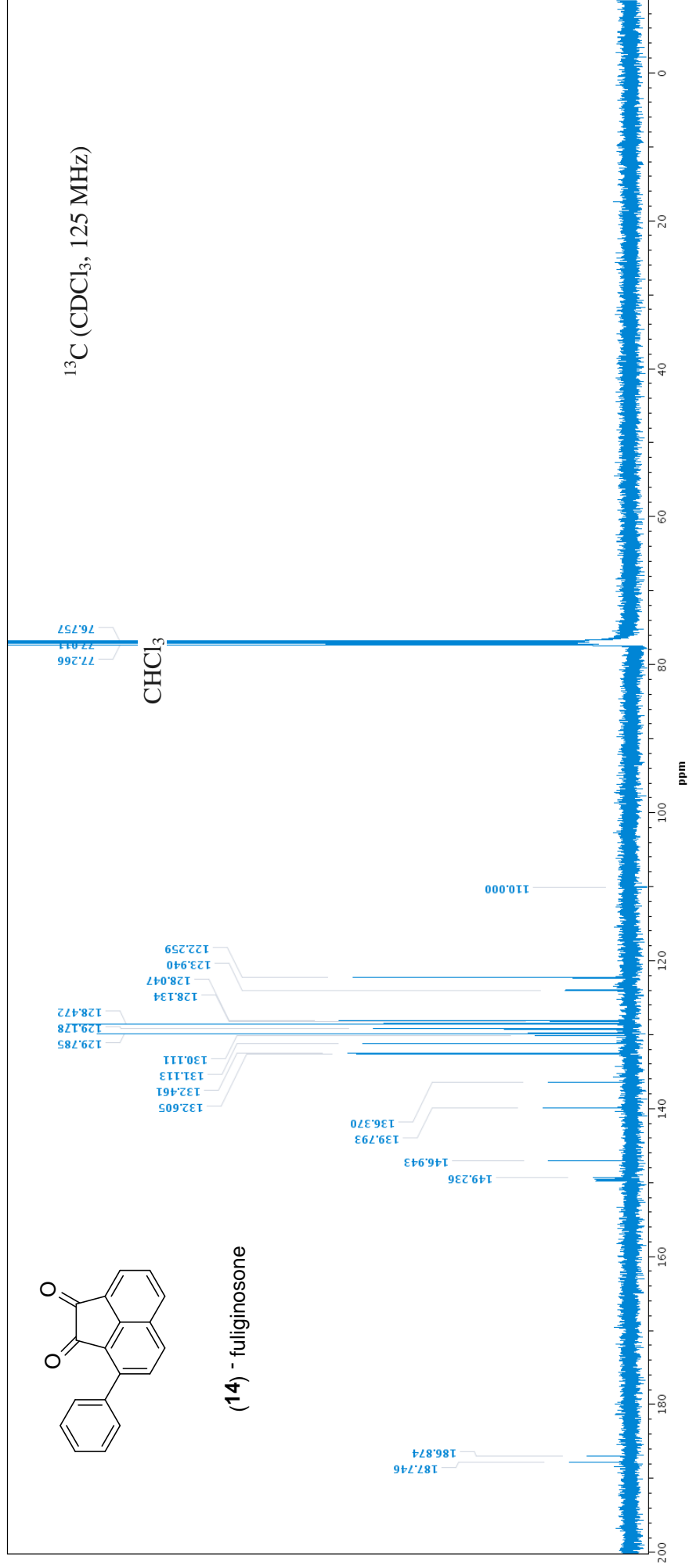
S42. High resolution negative ESI-MS of fuliginosin B (**13**).



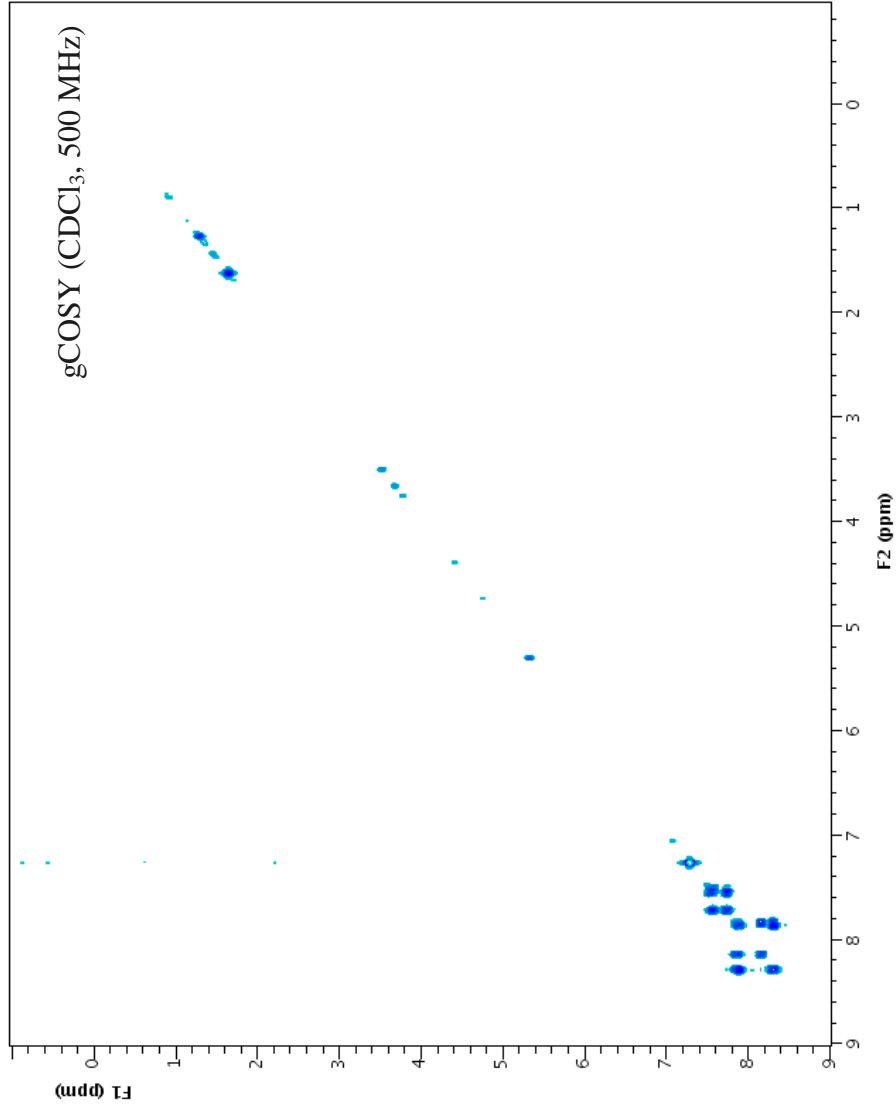
S43. ¹H NMR spectrum (500 MHz, CDCl₃) of fuliginosone (**14**).



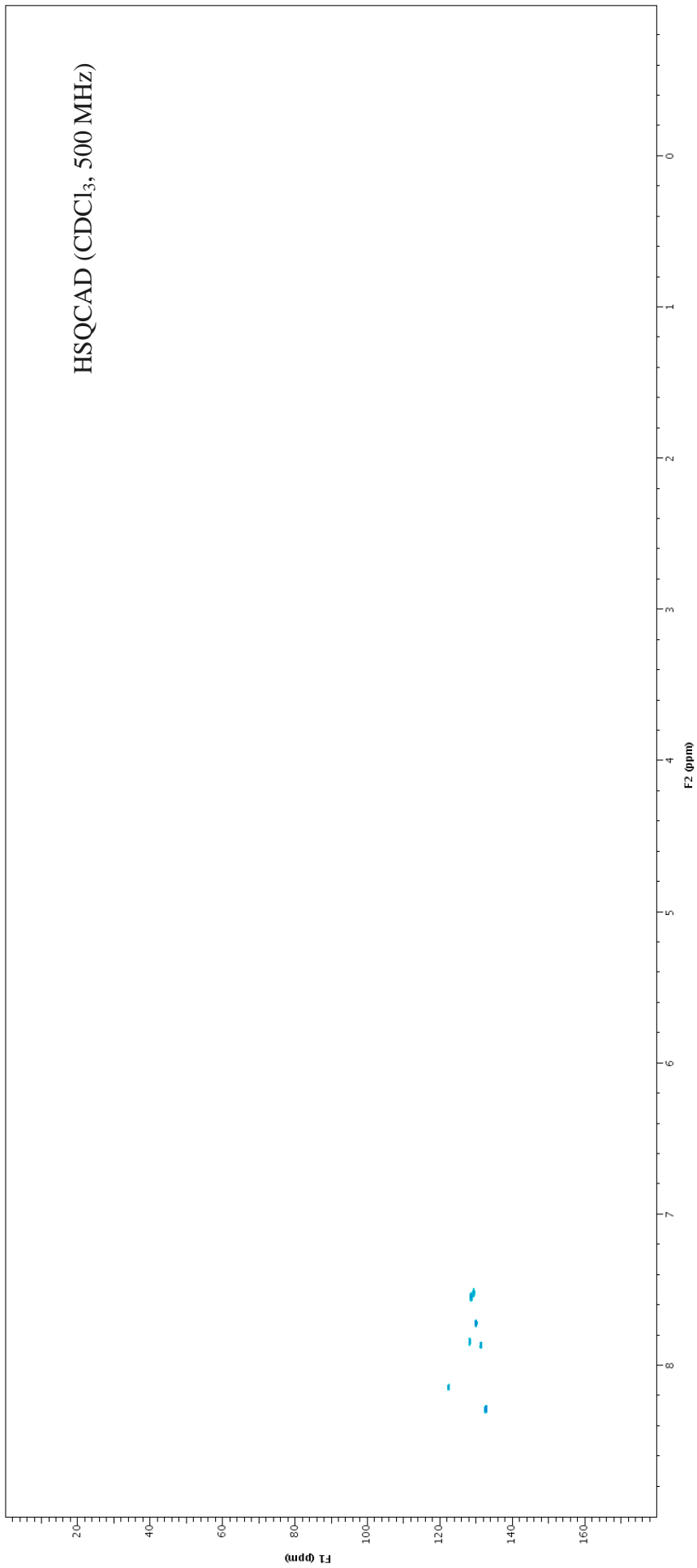
S44. Expansion of ¹H NMR spectrum (500 MHz, CDCl₃) of fuliginosone (**14**).



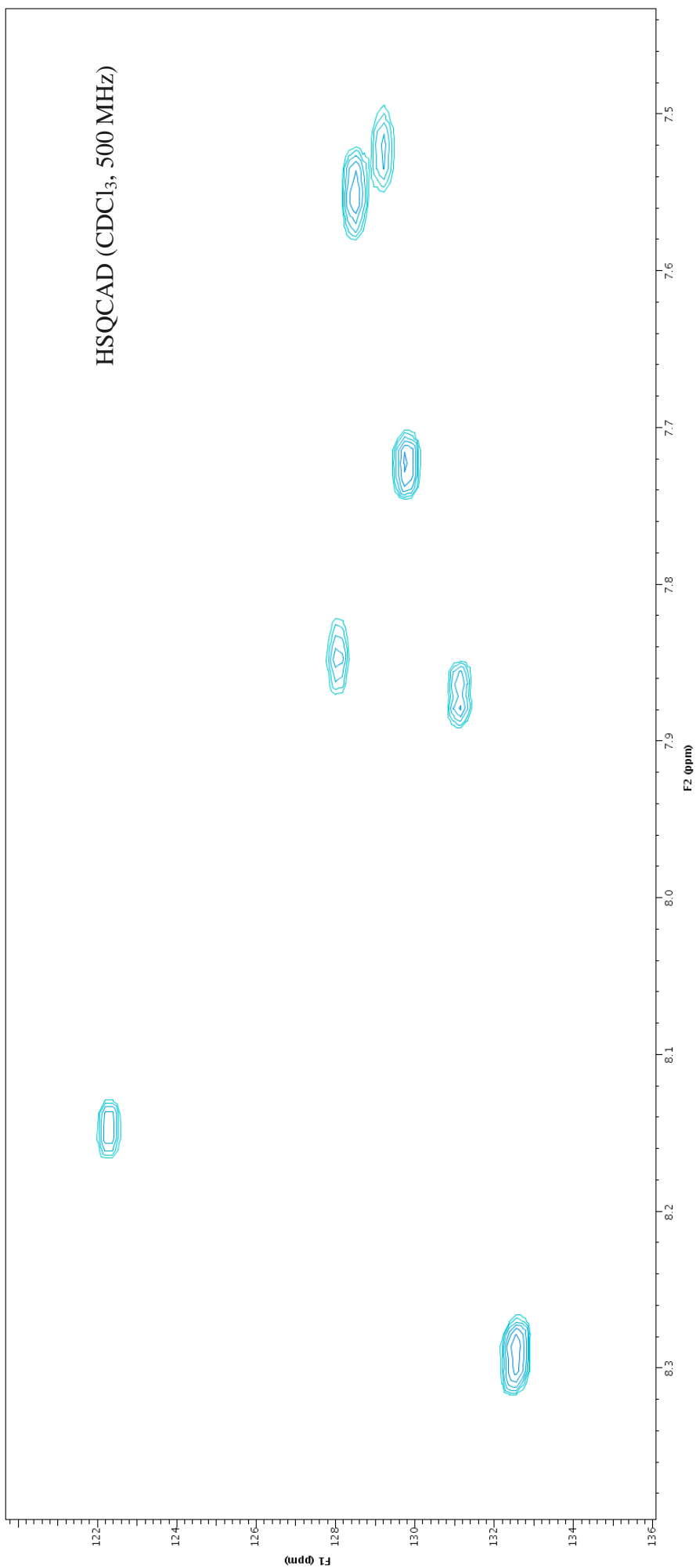
S45. ^{13}C NMR spectrum (500 MHz, CDCl₃) of fuliginosone (**14**).



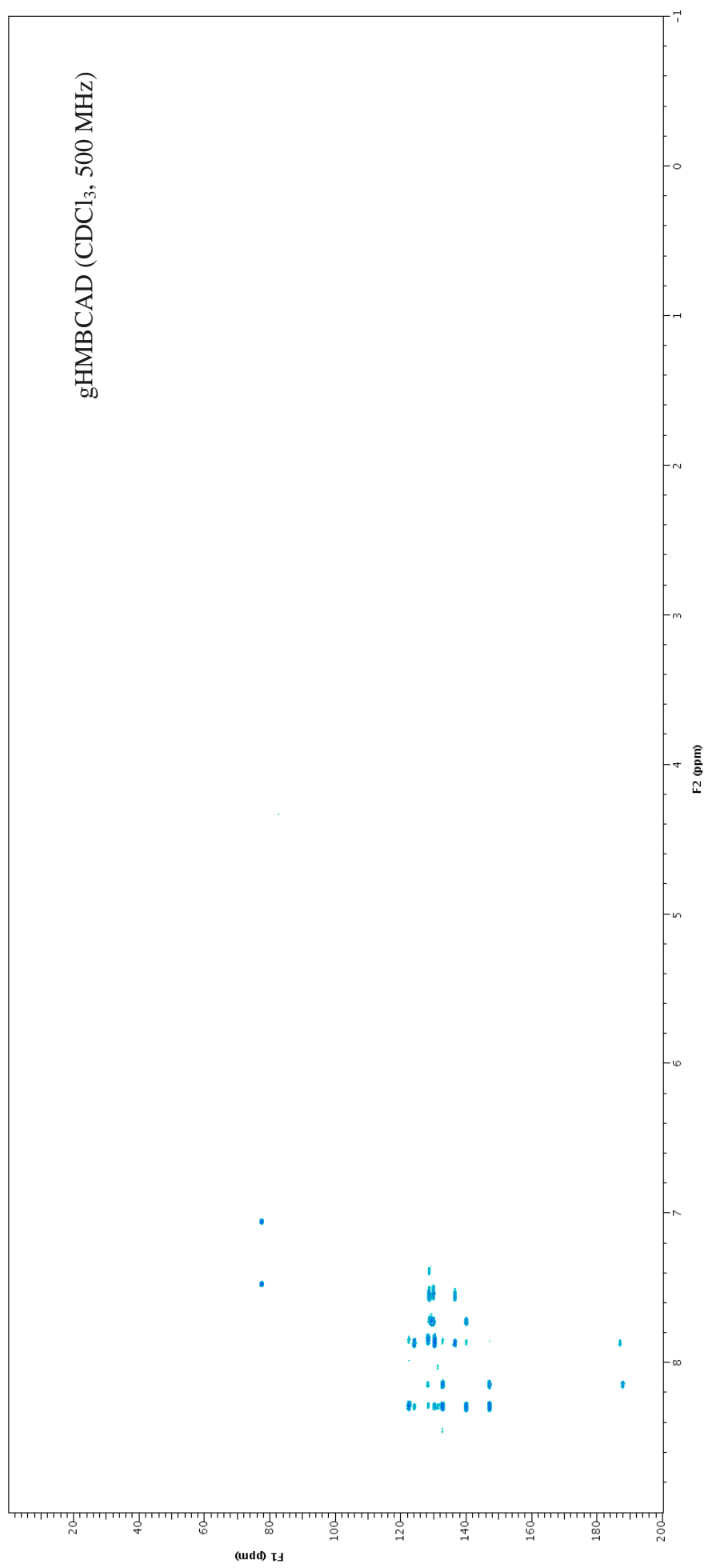
S46. gCOSY NMR spectrum (500 MHz, CDCl₃) of fuliginosone (**14**).



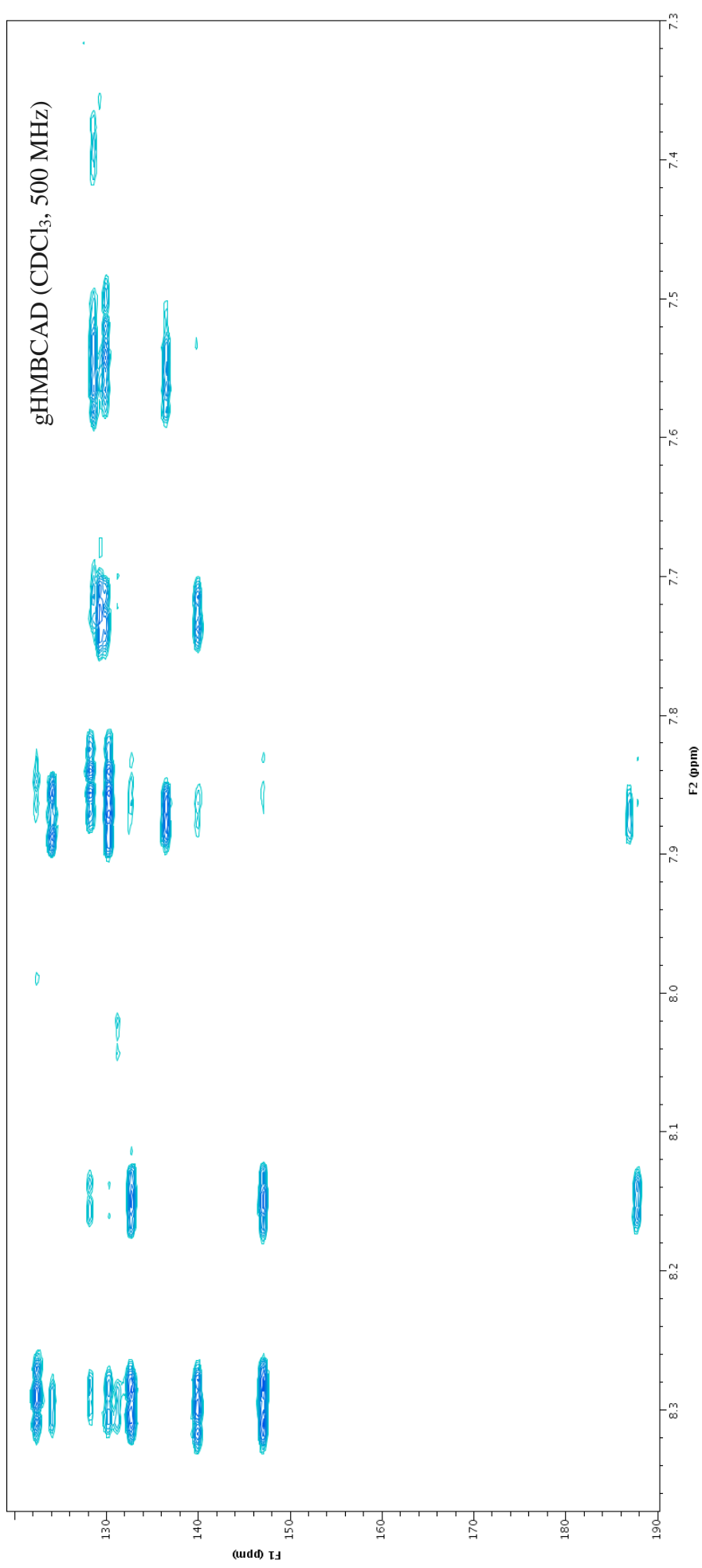
S47. HSQCAD NMR spectrum (500 MHz, CDCl₃) of fuliginosone (**14**).



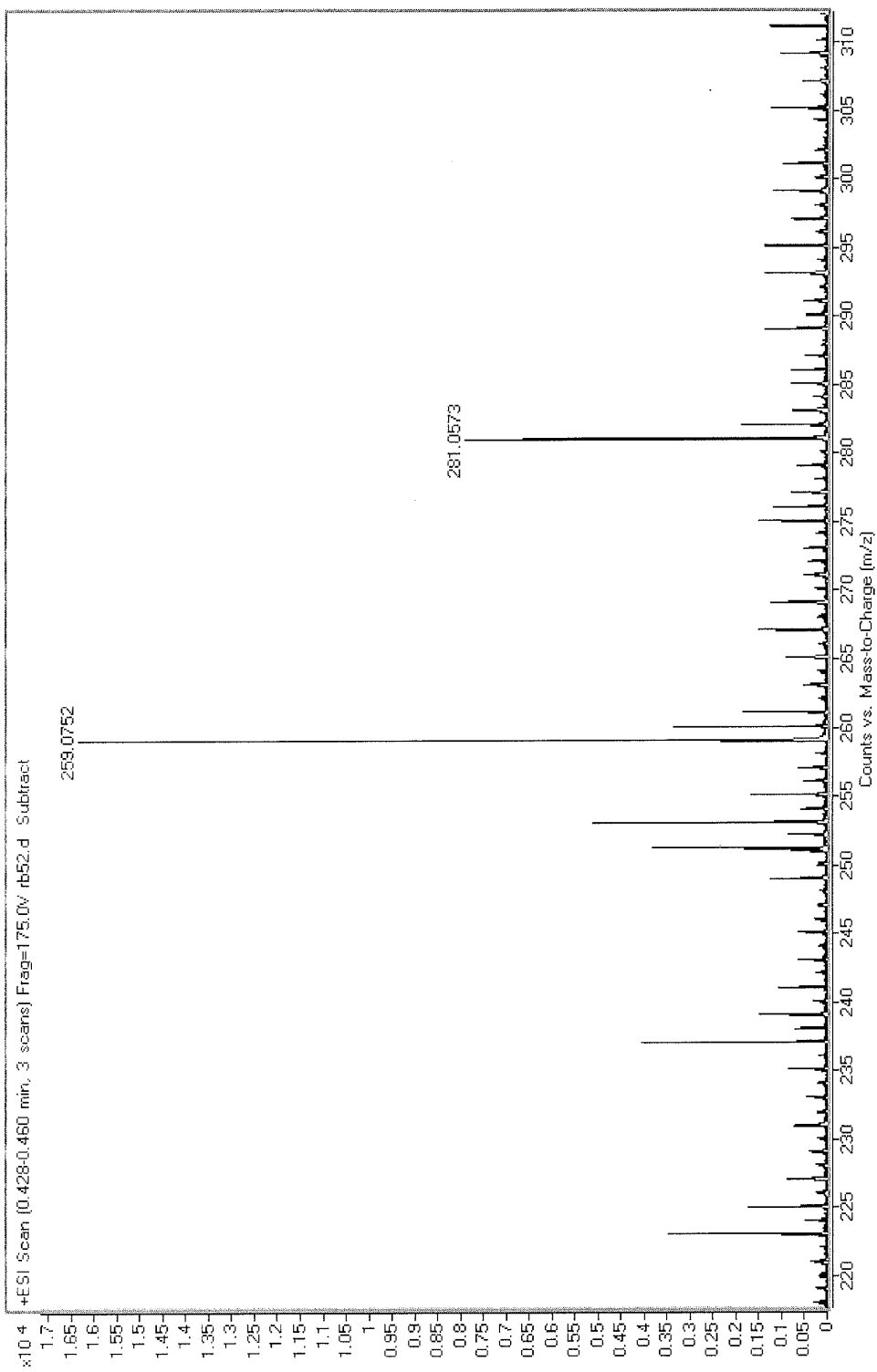
S48. Expansion of HSQCAD NMR spectrum (500 MHz, CDCl₃) of fuliginosone (**14**).



S49. gHMBCAD NMR spectrum (500 MHz, CDCl₃) of fuliginosone (**14**).



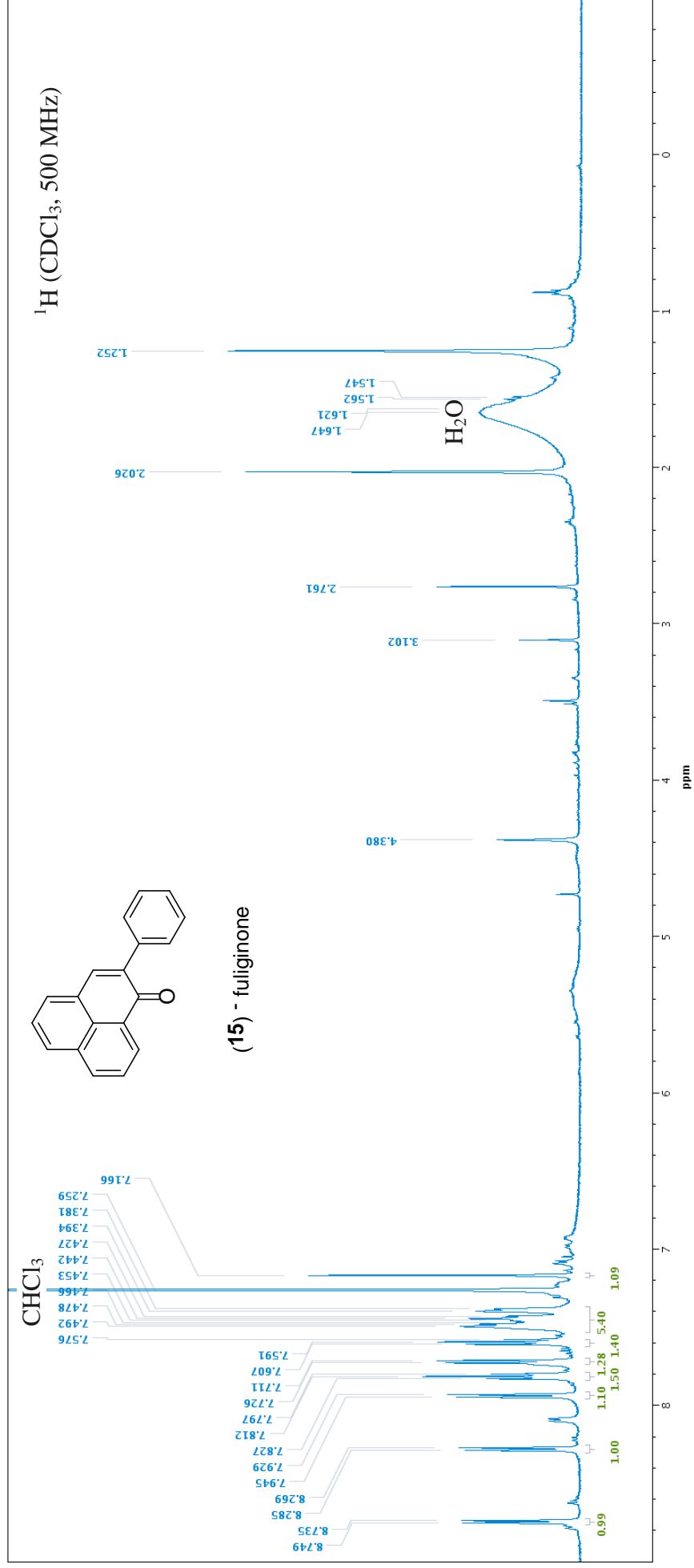
S50. Expansion of gHMBCAD NMR spectrum (500 MHz, CDCl₃) of fuliginosone (**14**).



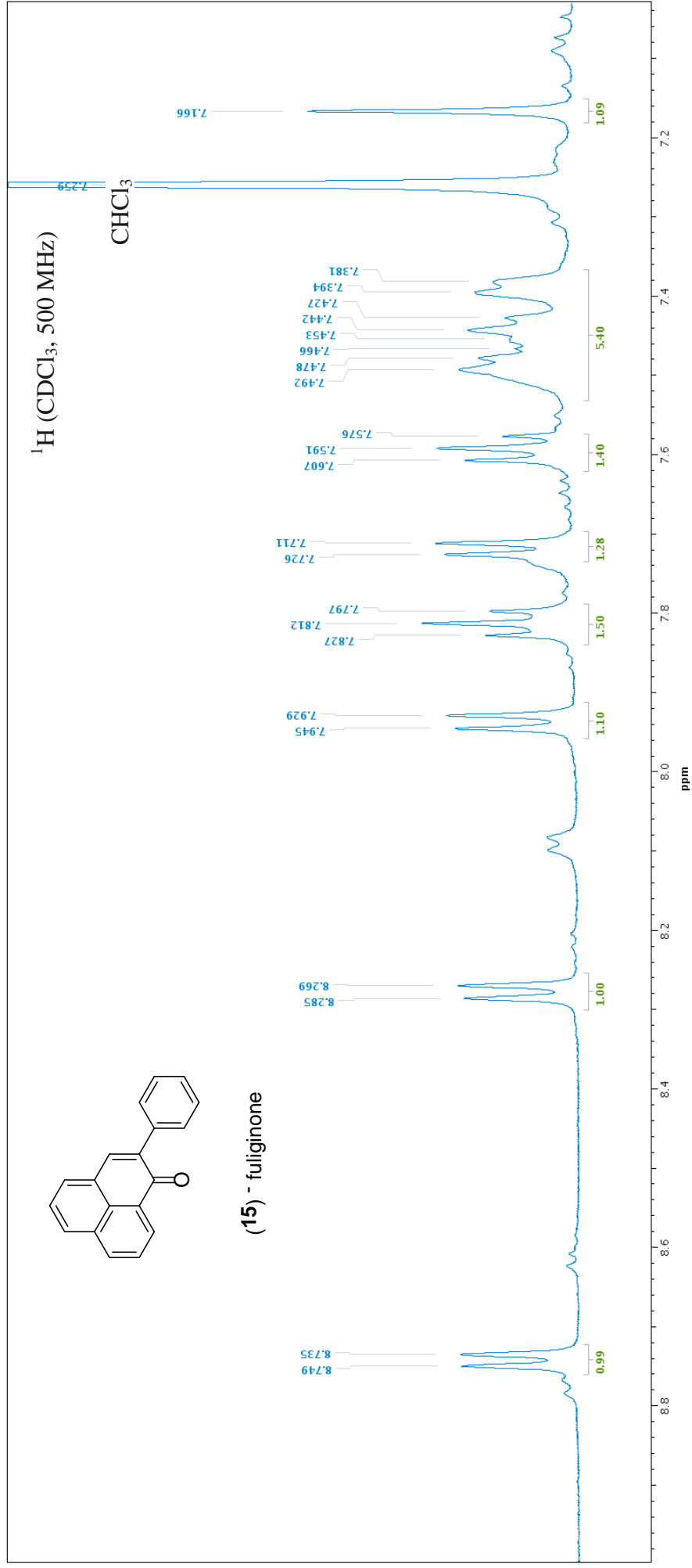
S51. High resolution negative ESI-MS of fuliginosone (**14**).

S52. Atomic coordinates ($\times 10^4$) and equivalent isotropic displacement parameters ($\text{\AA}^2 \times 10^3$) for fuliginosone (**14**). $U(\text{eq})$ is defined as one third of the trace of the orthogonalized U^{ij} tensor.

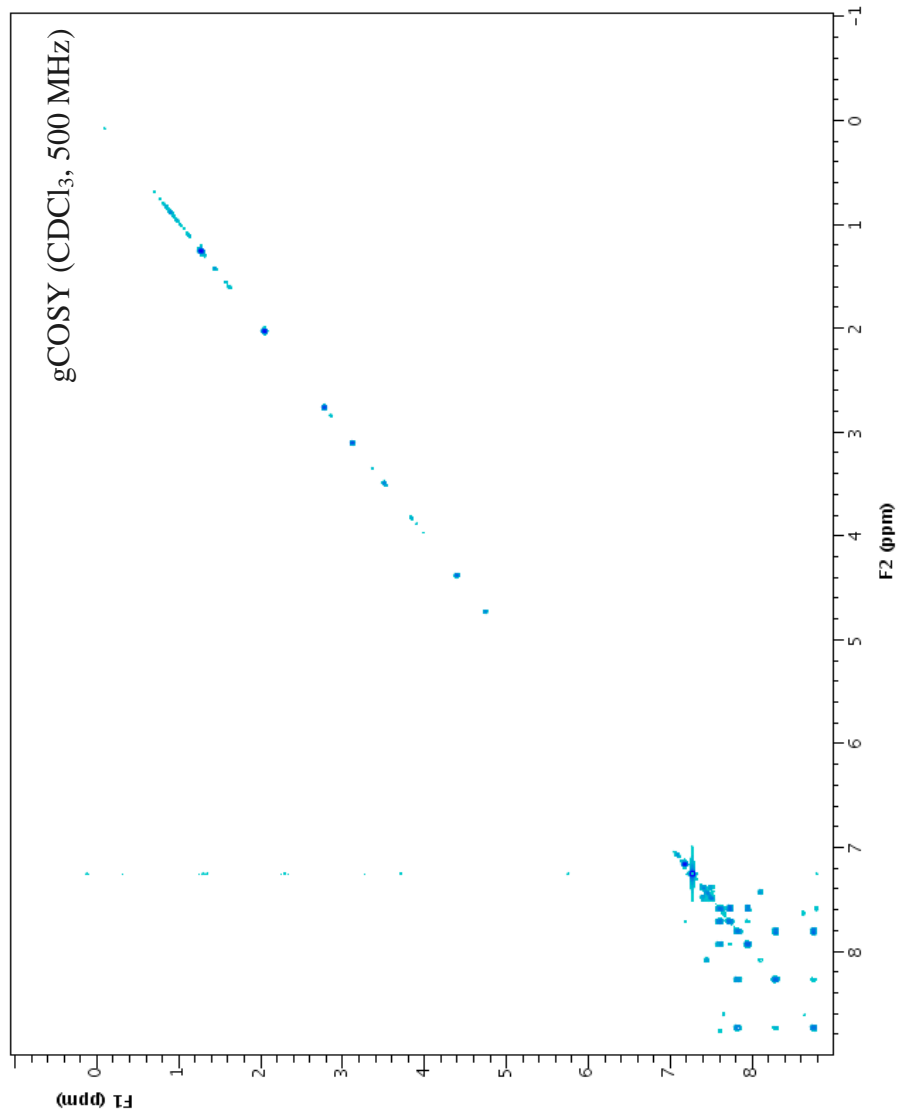
	x	y	z	U(eq)
C(1)	6572(3)	-827(3)	4452(1)	25(1)
C(2)	7571(3)	-1319(3)	4710(1)	27(1)
C(3)	9216(3)	-1187(3)	4652(1)	29(1)
C(4)	9827(3)	-560(3)	4351(1)	27(1)
C(5)	8819(2)	-25(3)	4078(1)	24(1)
C(6)	9260(2)	632(3)	3753(1)	26(1)
C(7)	8145(3)	1018(3)	3509(1)	25(1)
C(8)	6493(2)	822(3)	3566(1)	23(1)
C(9)	6029(2)	232(3)	3887(1)	23(1)
C(10)	7182(2)	-181(3)	4138(1)	22(1)
C(11)	4830(3)	-864(3)	4417(1)	27(1)
C(12)	4479(2)	-250(3)	4041(1)	25(1)
C(13)	5370(3)	1239(3)	3286(1)	24(1)
C(14)	5701(3)	686(3)	2952(1)	28(1)
C(15)	4688(3)	1130(3)	2685(1)	32(1)
C(16)	3349(3)	2150(3)	2749(1)	33(1)
C(17)	2993(3)	2697(3)	3079(1)	30(1)
C(18)	3993(3)	2241(3)	3346(1)	26(1)
O(1)	3821(2)	-1277(2)	4619(1)	35(1)
O(2)	3174(2)	-301(2)	3918(1)	34(1)



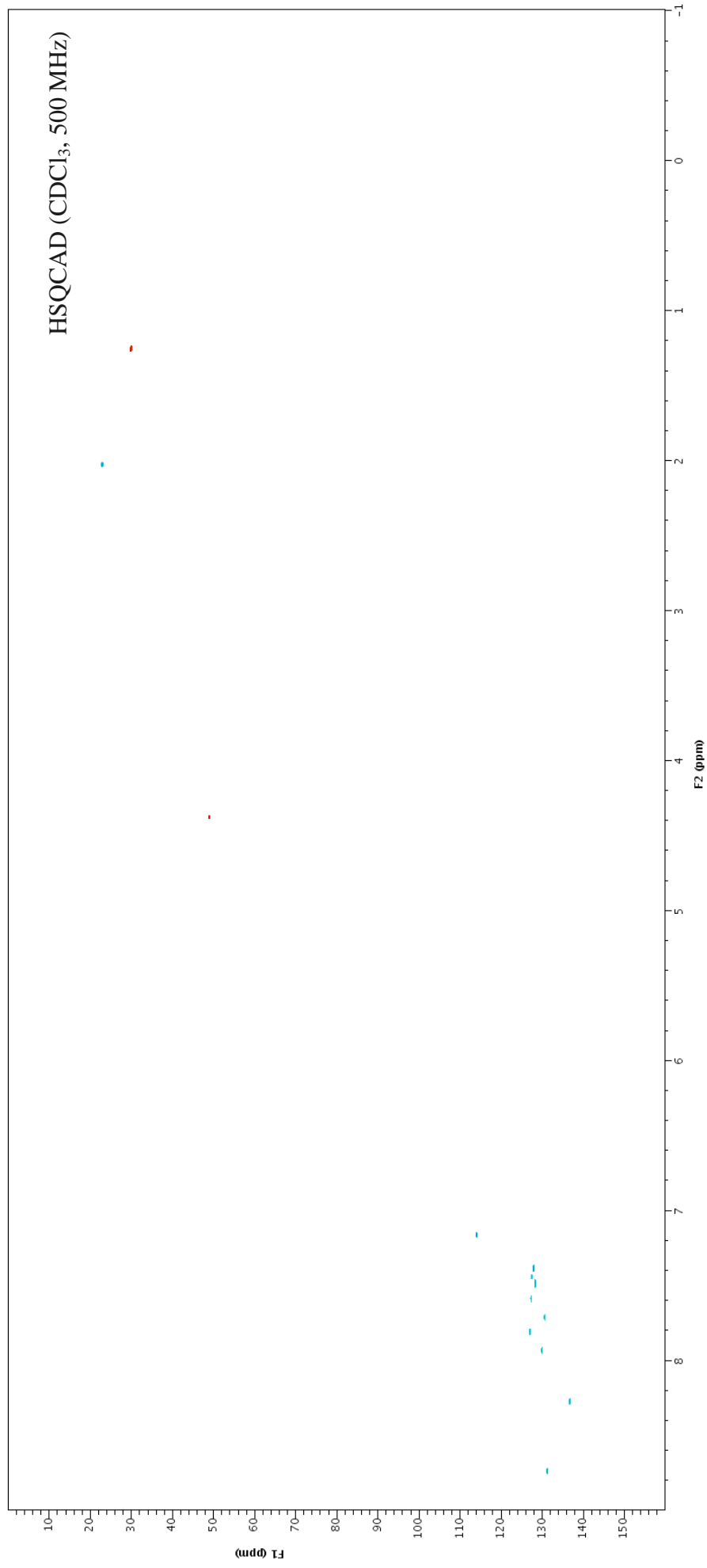
S53. ¹H NMR spectrum (500 MHz, CDCl₃) of fuliginone (**15**).



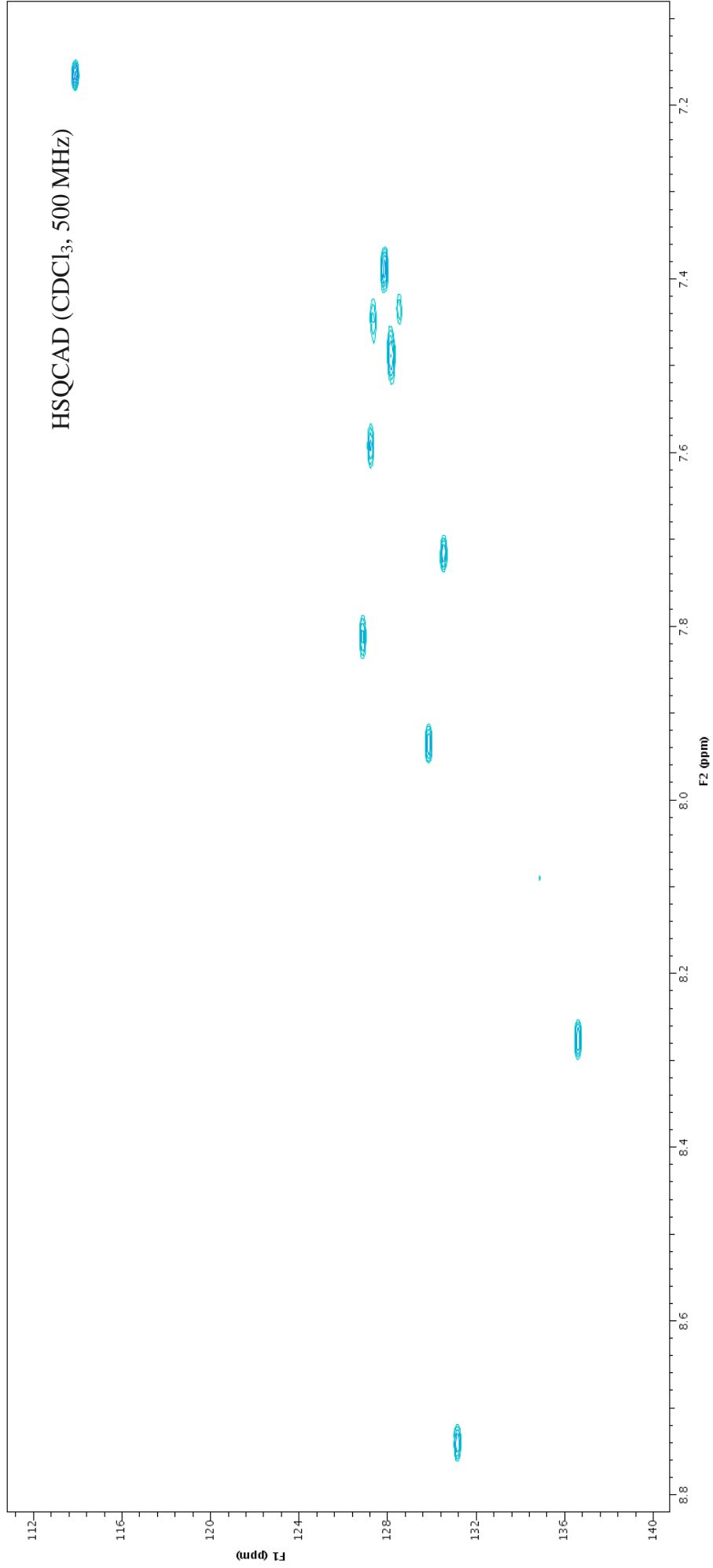
S54. Expansion of ¹H NMR spectrum (500 MHz, CDCl₃) of fuliginone (**15**).



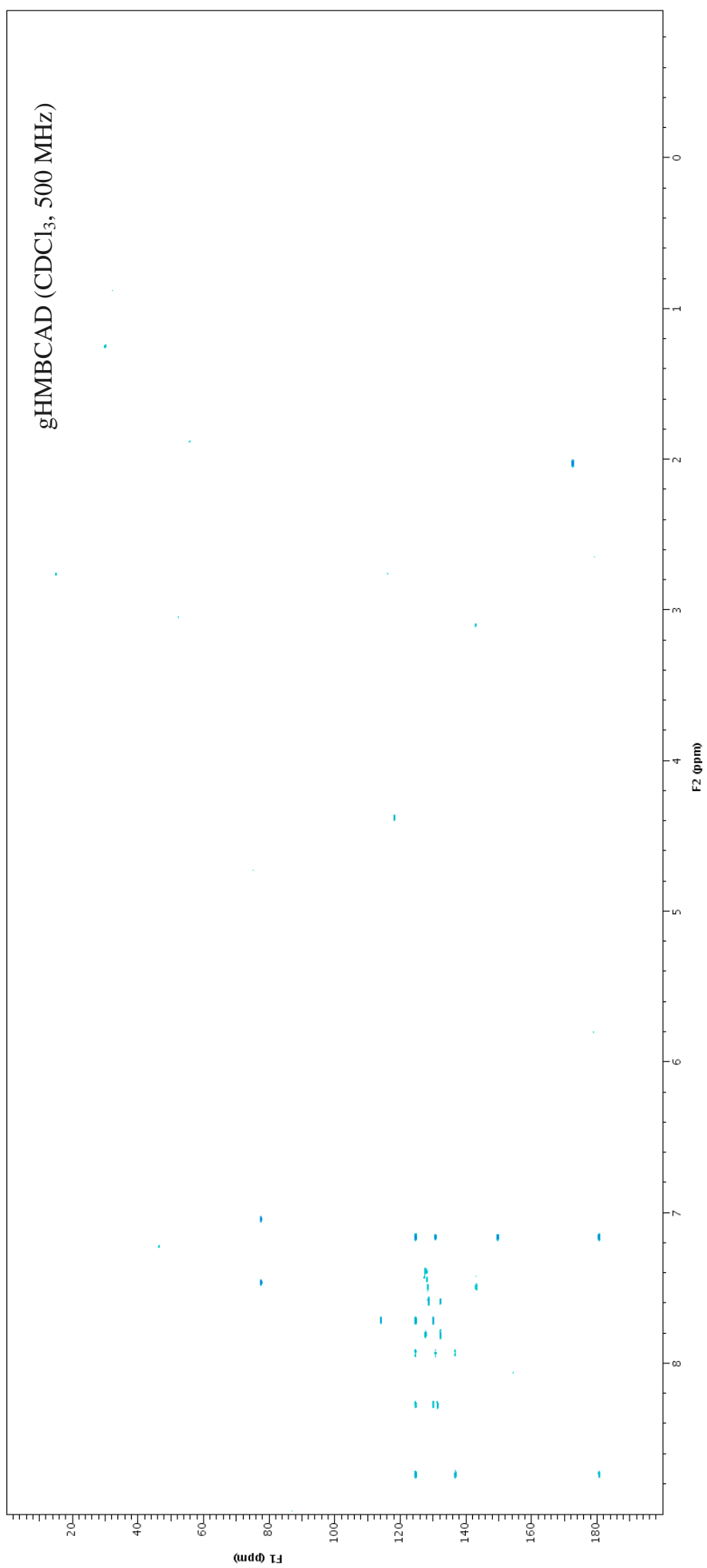
S55. gCOSY NMR spectrum (500 MHz, CDCl₃) of fuliginone (**15**).



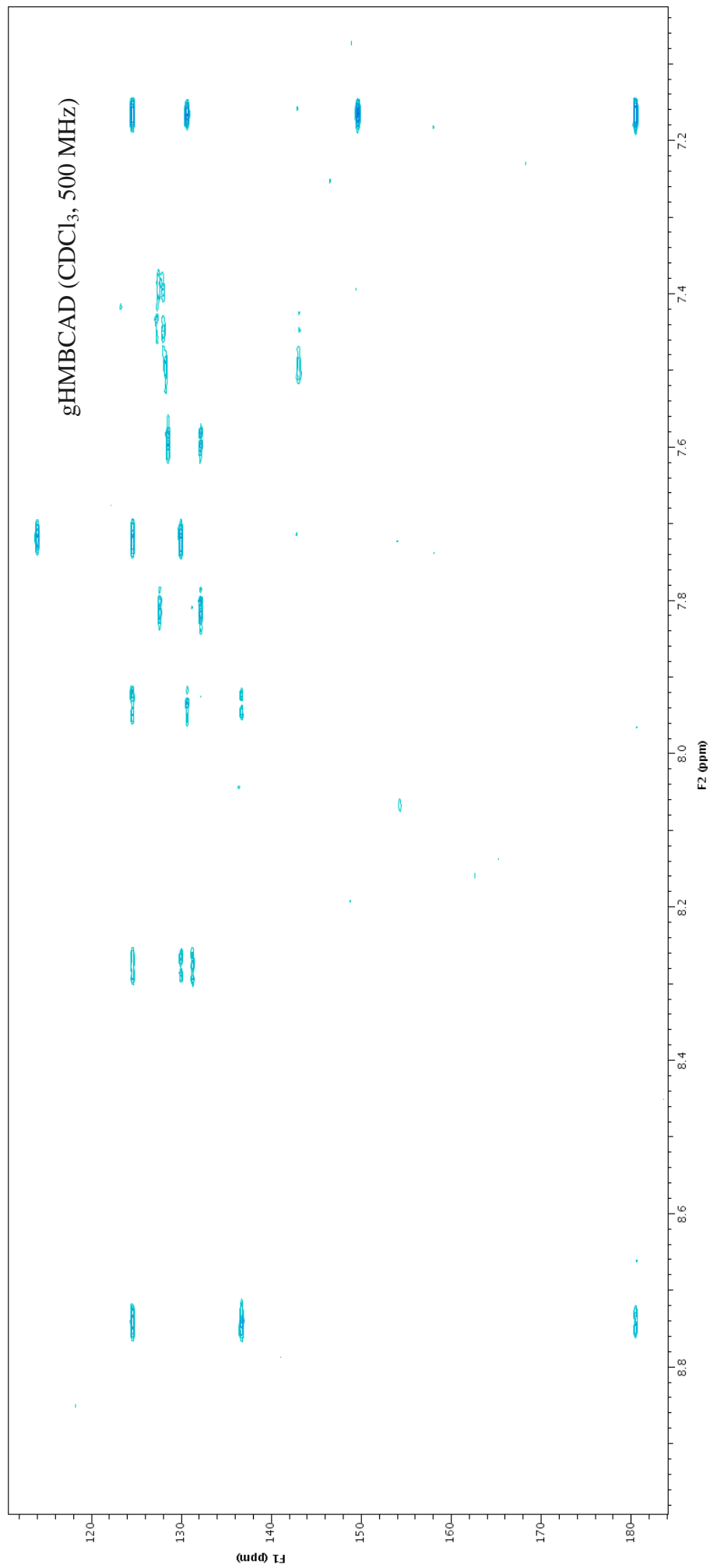
S56. HSQCAD NMR spectrum (500 MHz, CDCl₃) of fuliginone (**15**).



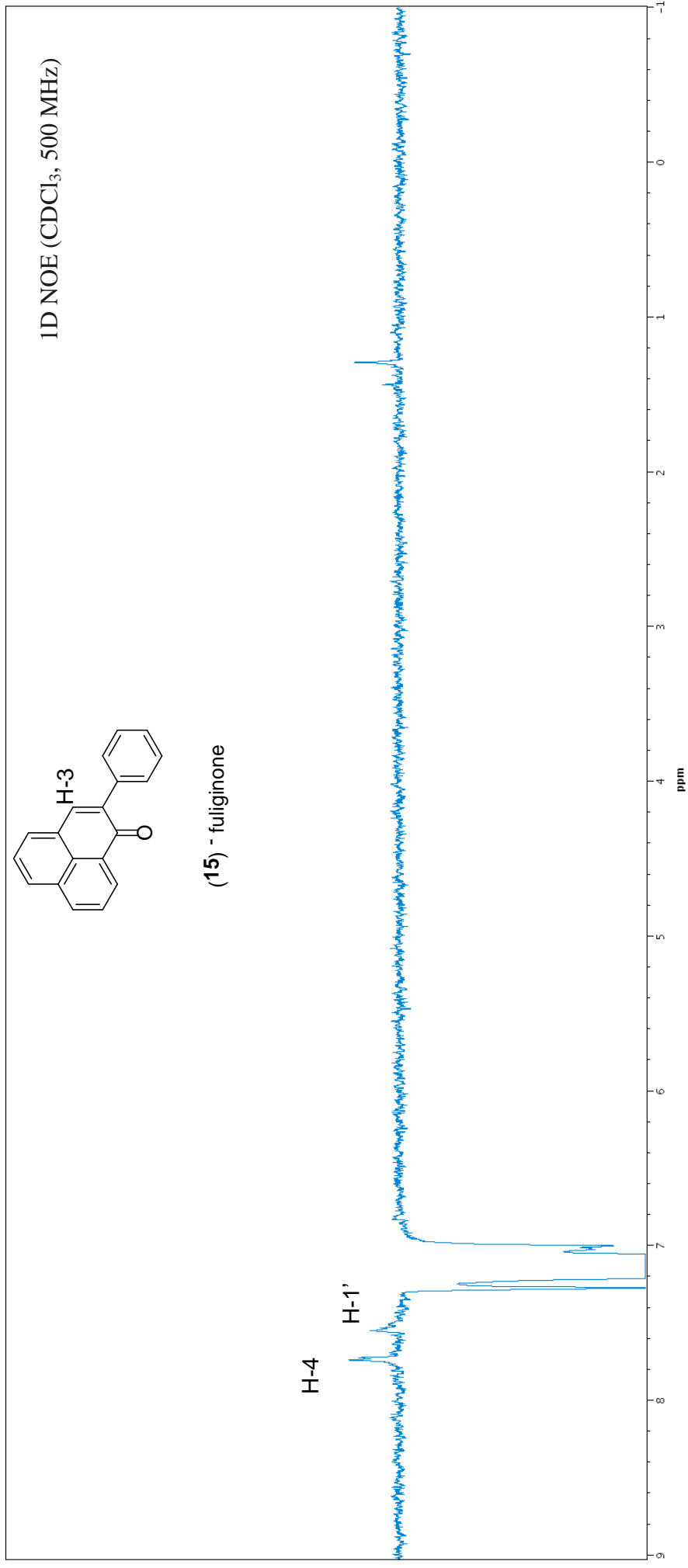
S57. Expansion of HSQCAD NMR spectrum (500 MHz, CDCl₃) of fuliginone (**15**).



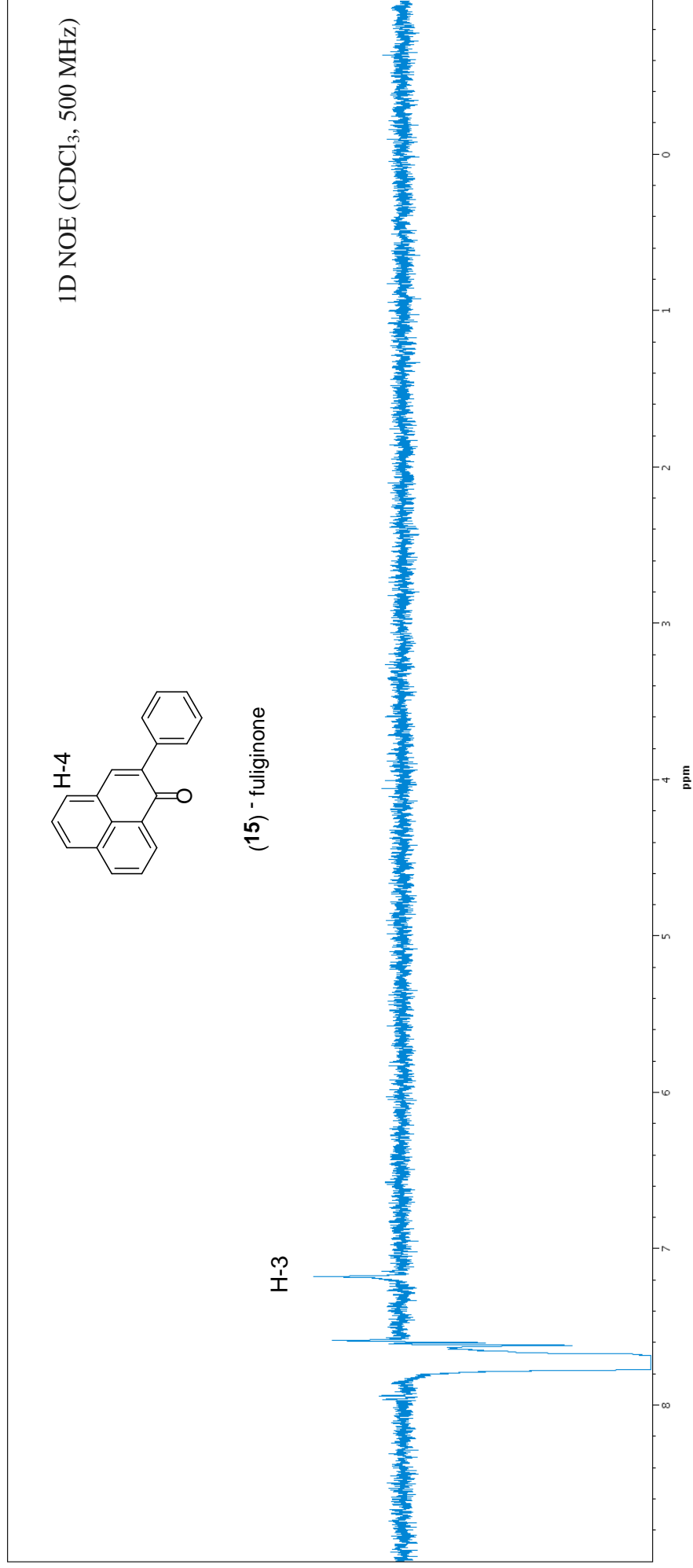
S58. gHMBCAD NMR spectrum (500 MHz, CDCl₃) of fuliginone (**15**).



S59. Expansion of gHMBCAD NMR spectrum (500 MHz, CDCl₃) of fuliginone (**15**).

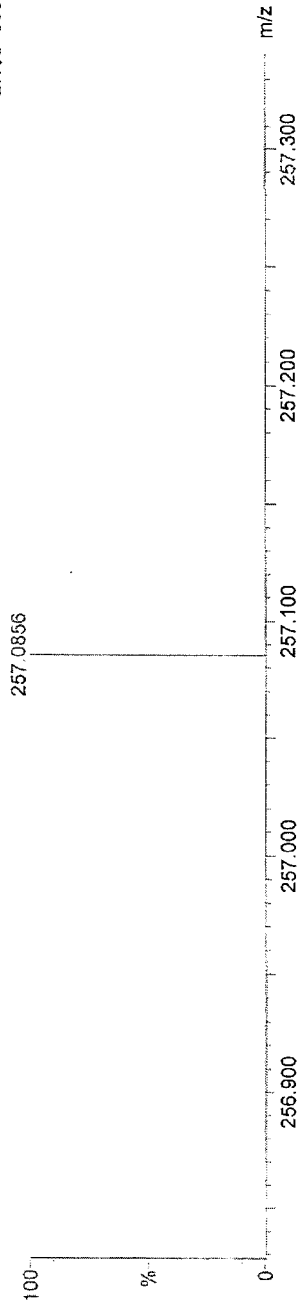


S60. Single irradiation nOe NMR spectrum (500 MHz, CDCl₃) of fuliginone (**15**) showing the irradiation of δ_{H} 7.17 (H-3).

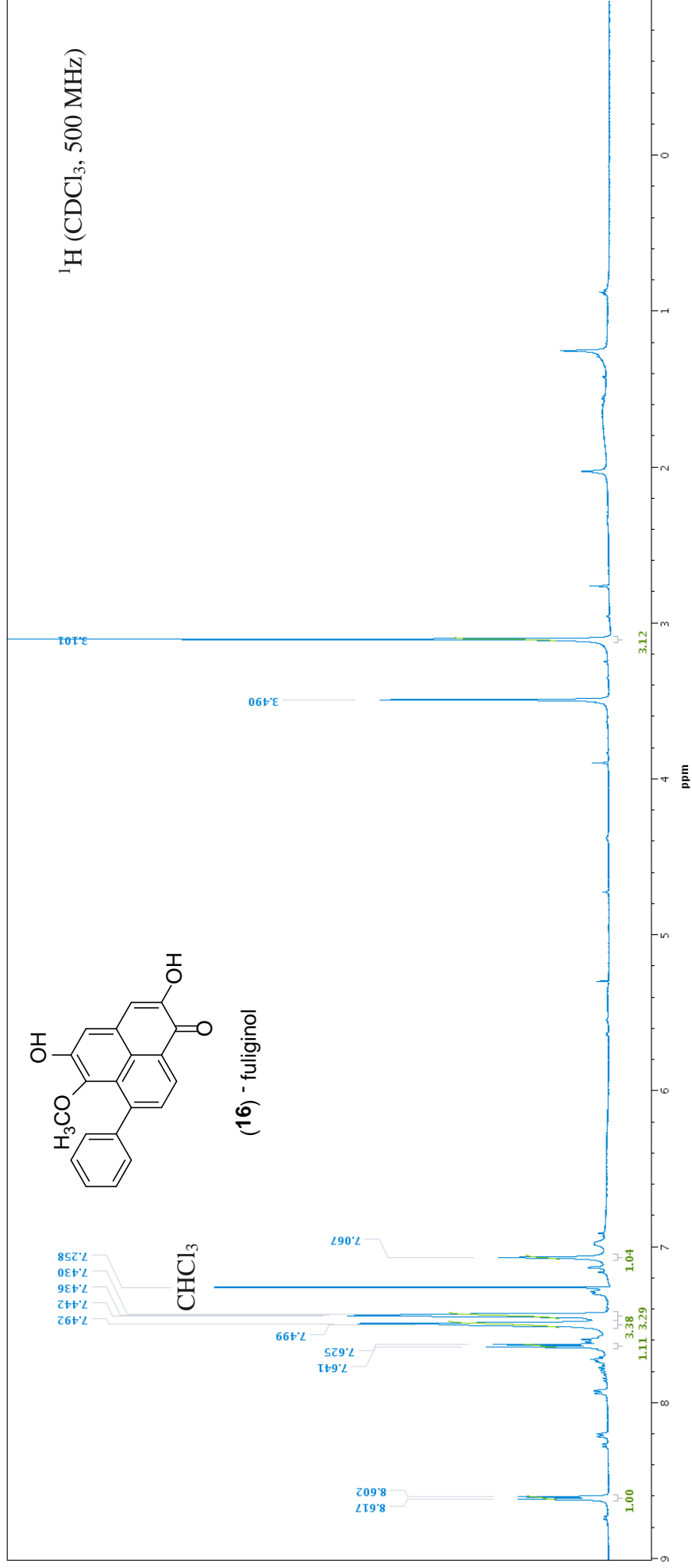


S61. Single irradiation nOe NMR spectrum (500 MHz, CDCl₃) of fuliginone (**15**) showing the irradiation of δ_{H} 7.72 (H-4).

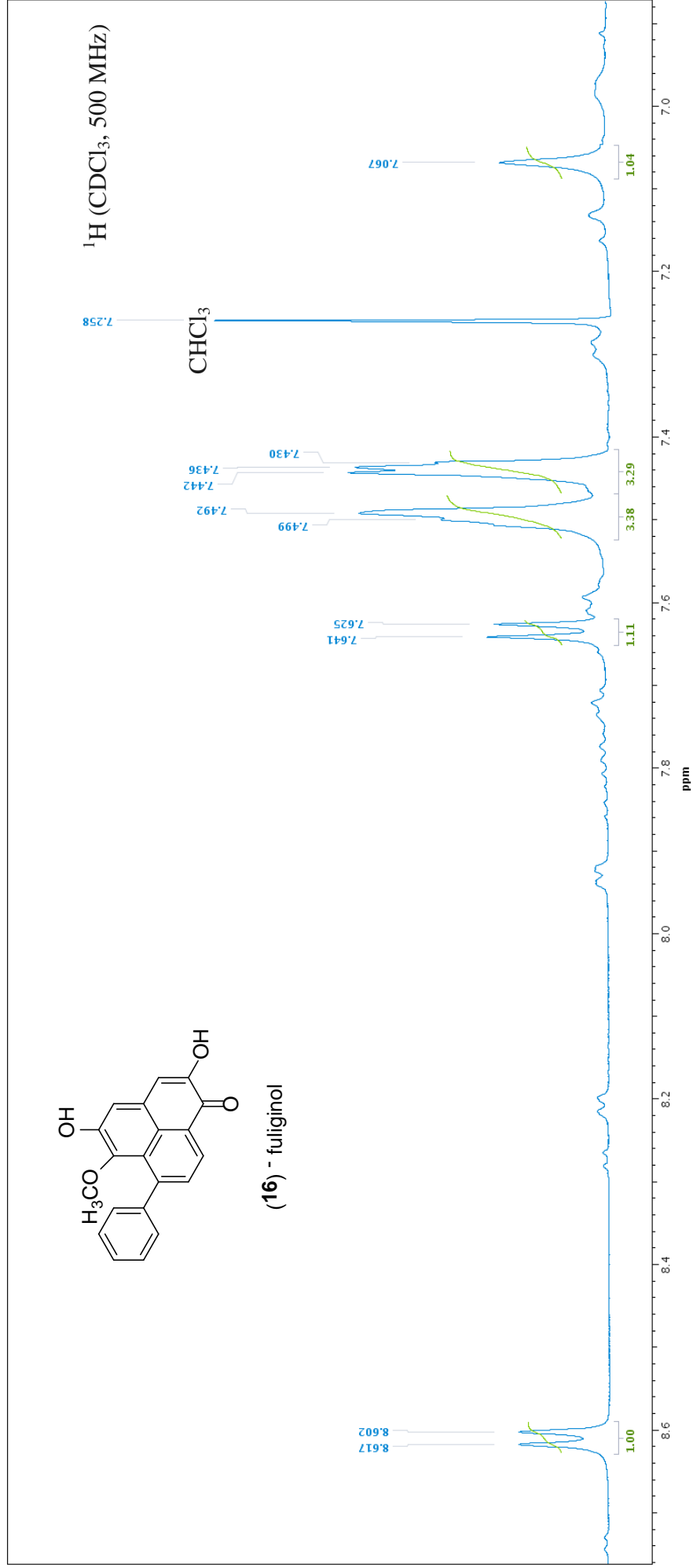
1: TOF MS AP+
2.10e+003



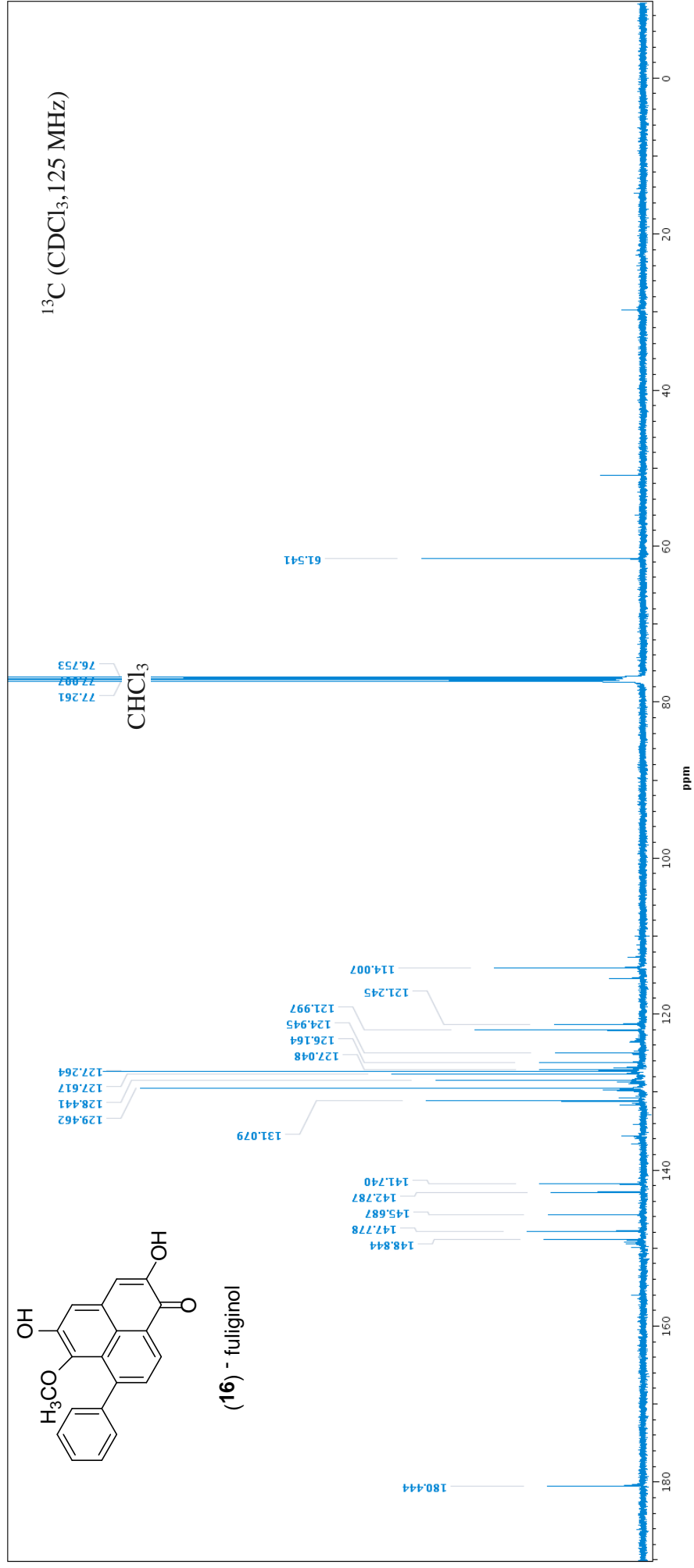
S62. High resolution positive ASAP-MS of fuliginone (**15**).



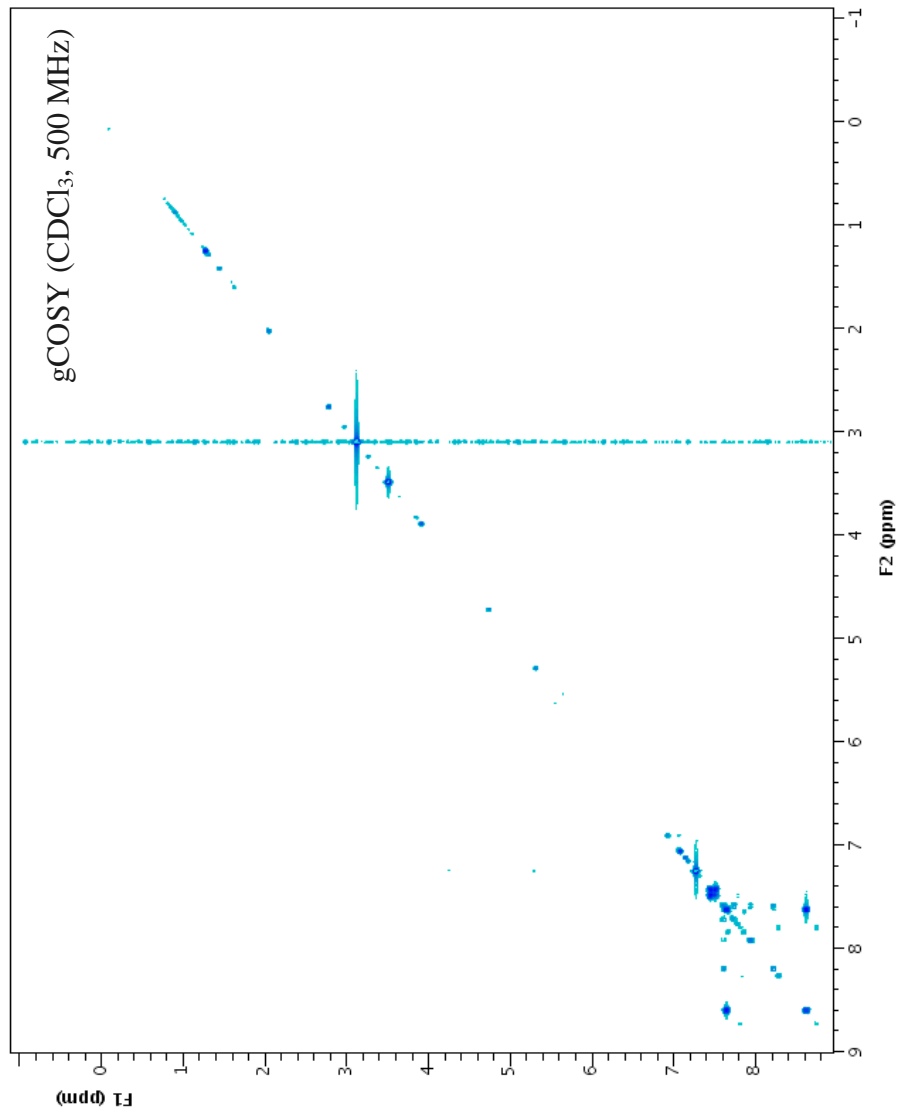
S63. ¹H NMR spectrum (500 MHz, CDCl₃) of fuliginol (**16**).



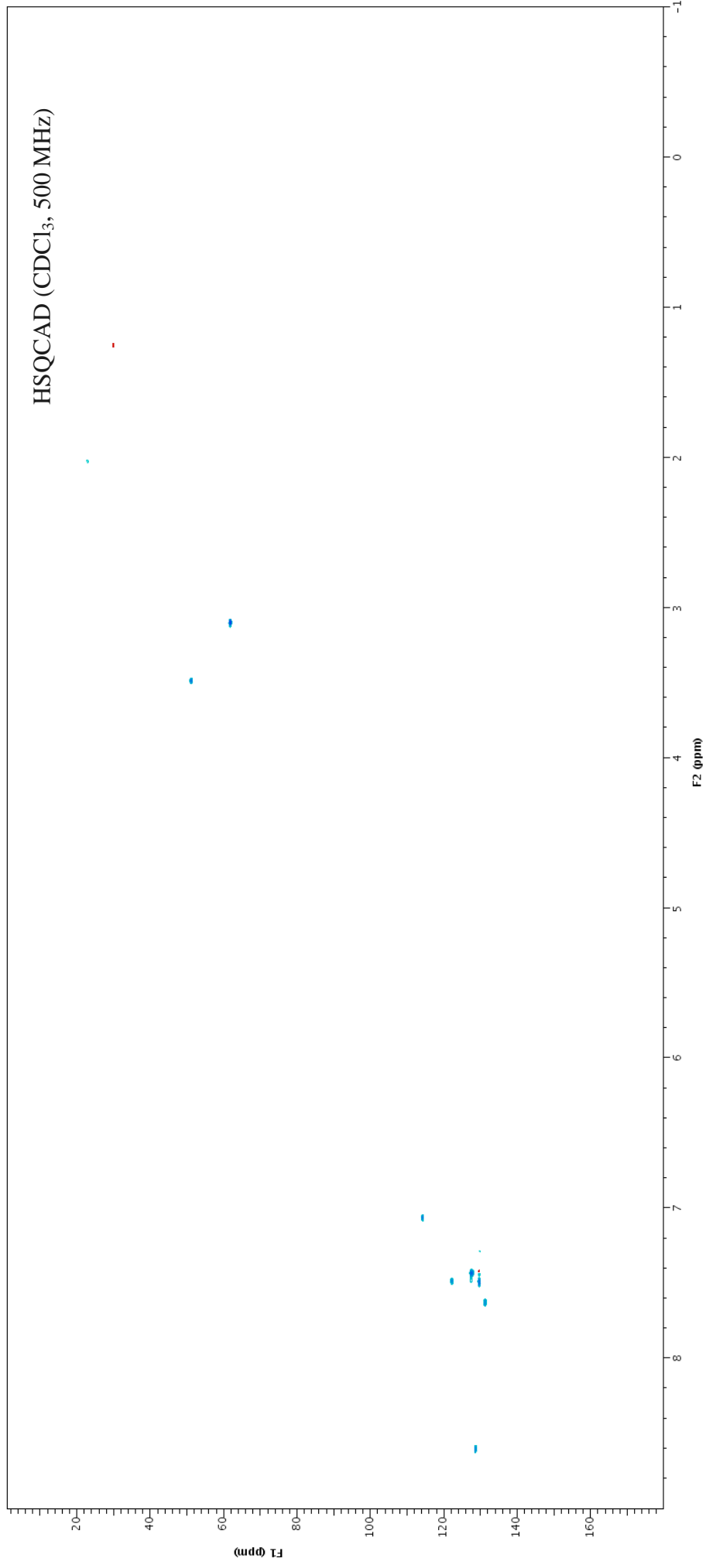
S64. Expansion of ¹H NMR spectrum (500 MHz, CDCl₃) of fuliginol (**16**).



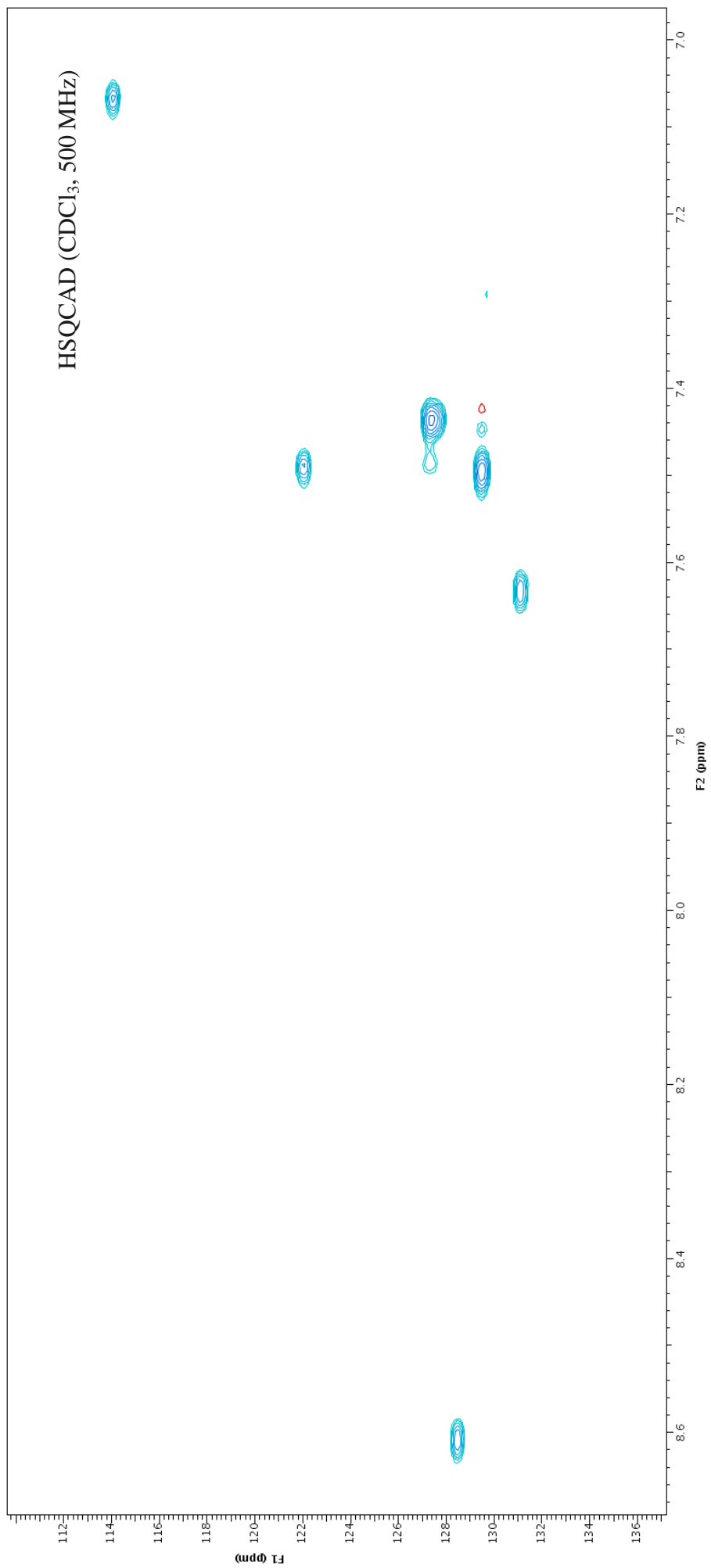
S65. ¹³C NMR spectrum (500 MHz, CDCl₃) of fuliginol (**16**).



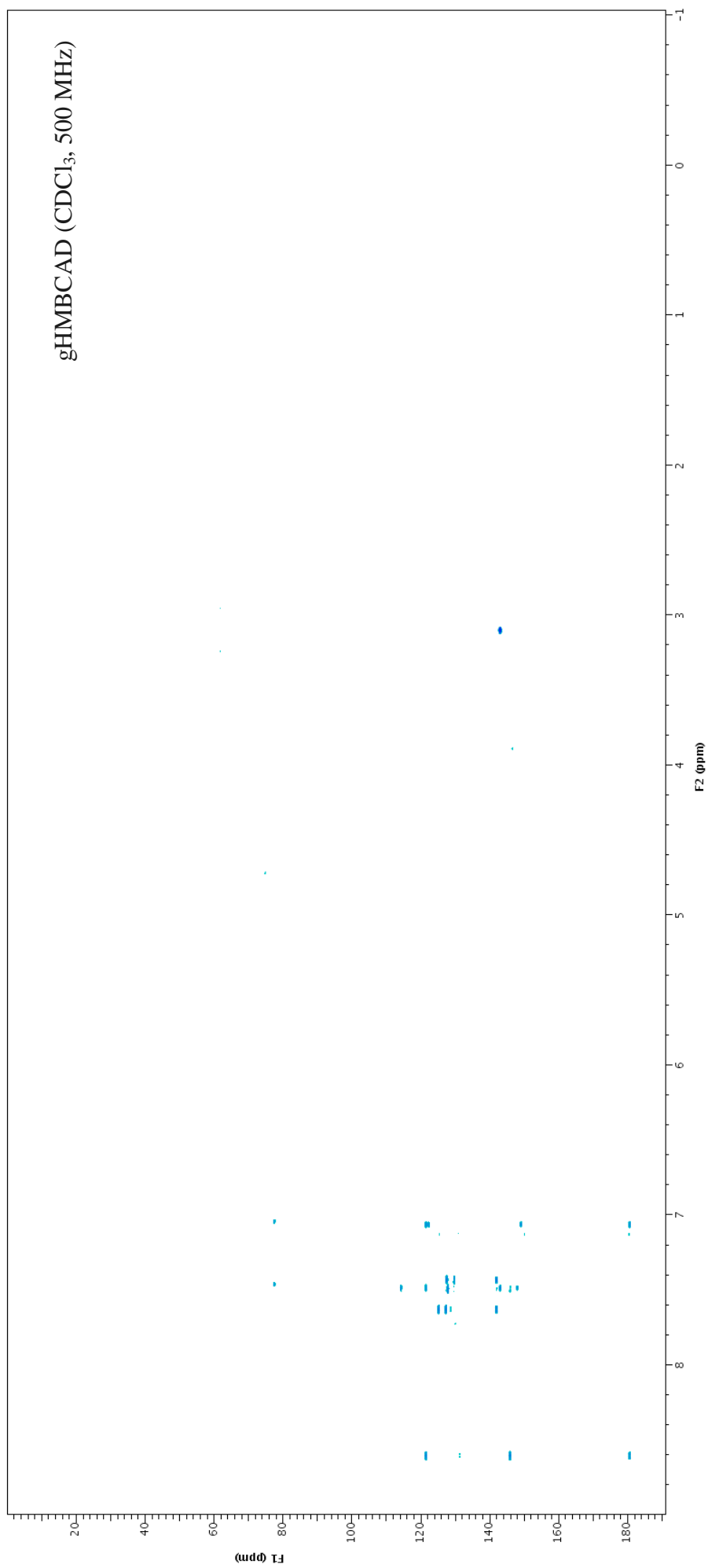
S66. gCOSY NMR spectrum (500 MHz, CDCl₃) of fuliginol (**16**).



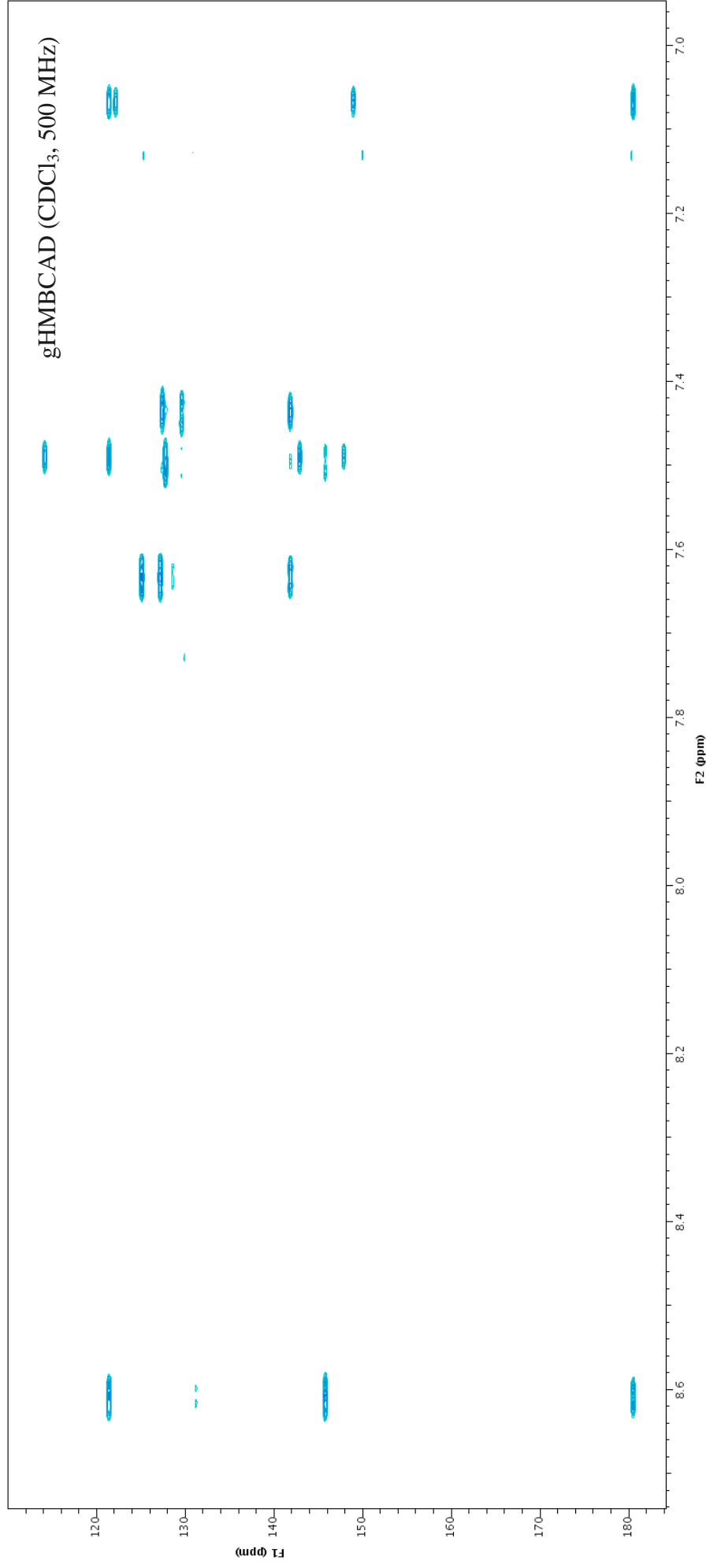
S67. HSQCAD NMR spectrum (500 MHz, CDCl₃) of fuliginol (**16**).



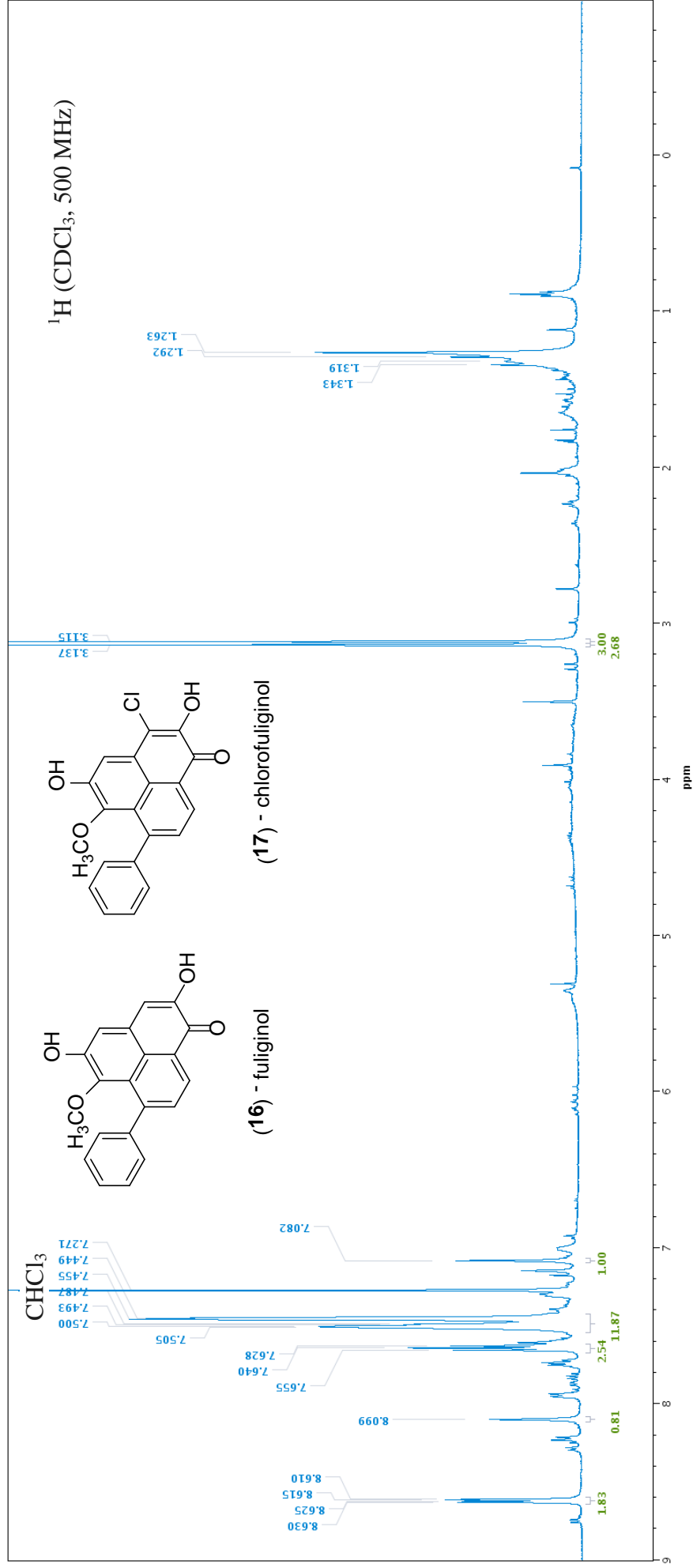
S68. Expansion of HSQCAD NMR spectrum (500 MHz, CDCl₃) of fuliginol (**16**).



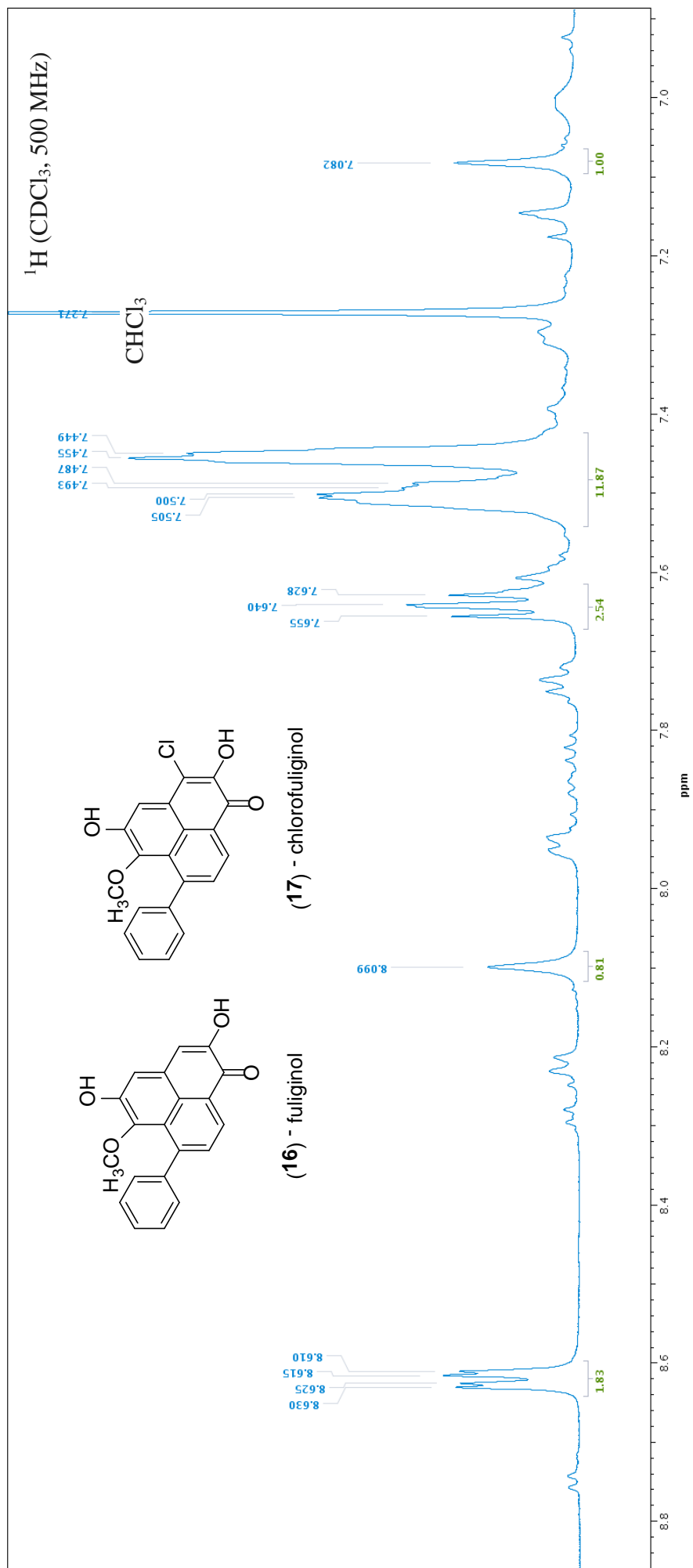
S69. gHMBCAD NMR spectrum (500 MHz, CDCl₃) of fuliginol (**16**).



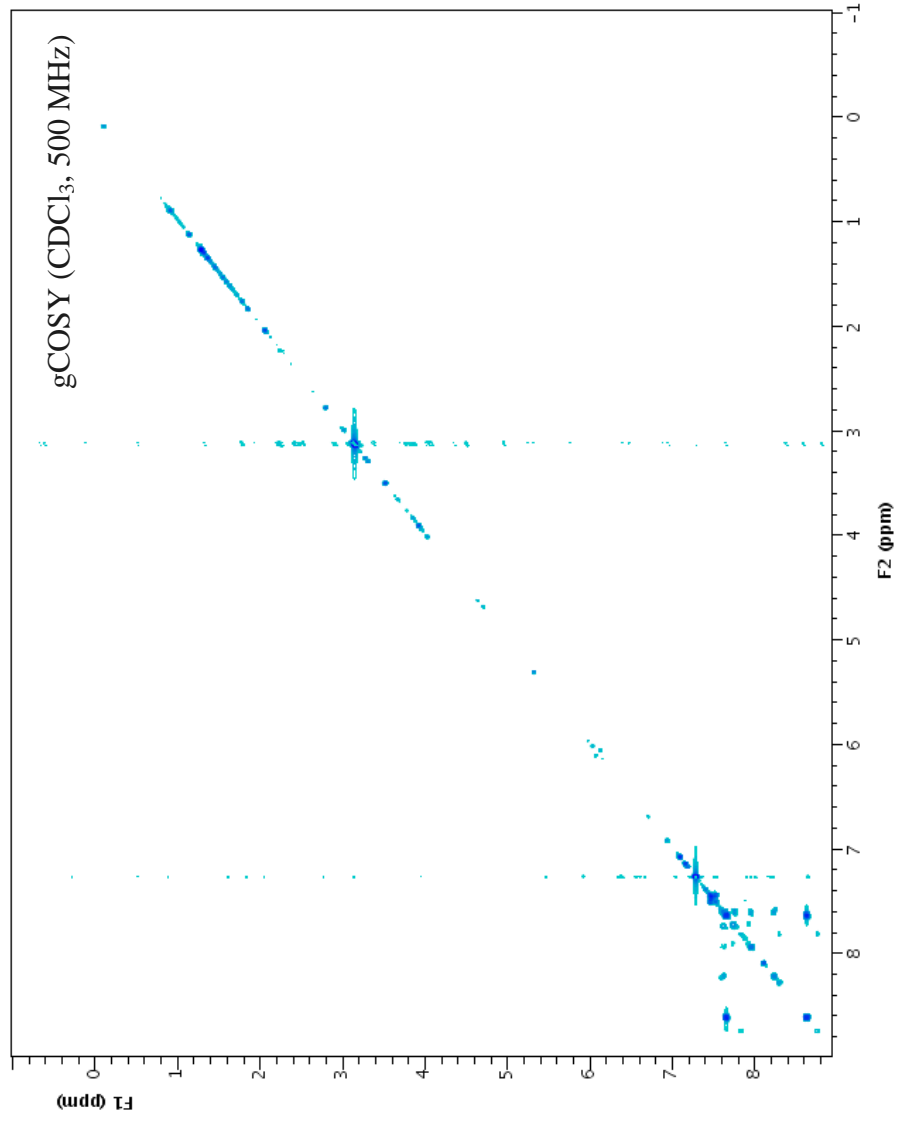
S70. Expansion of gHMBCAD NMR spectrum (500 MHz, CDCl₃) of fuliginol (**16**).



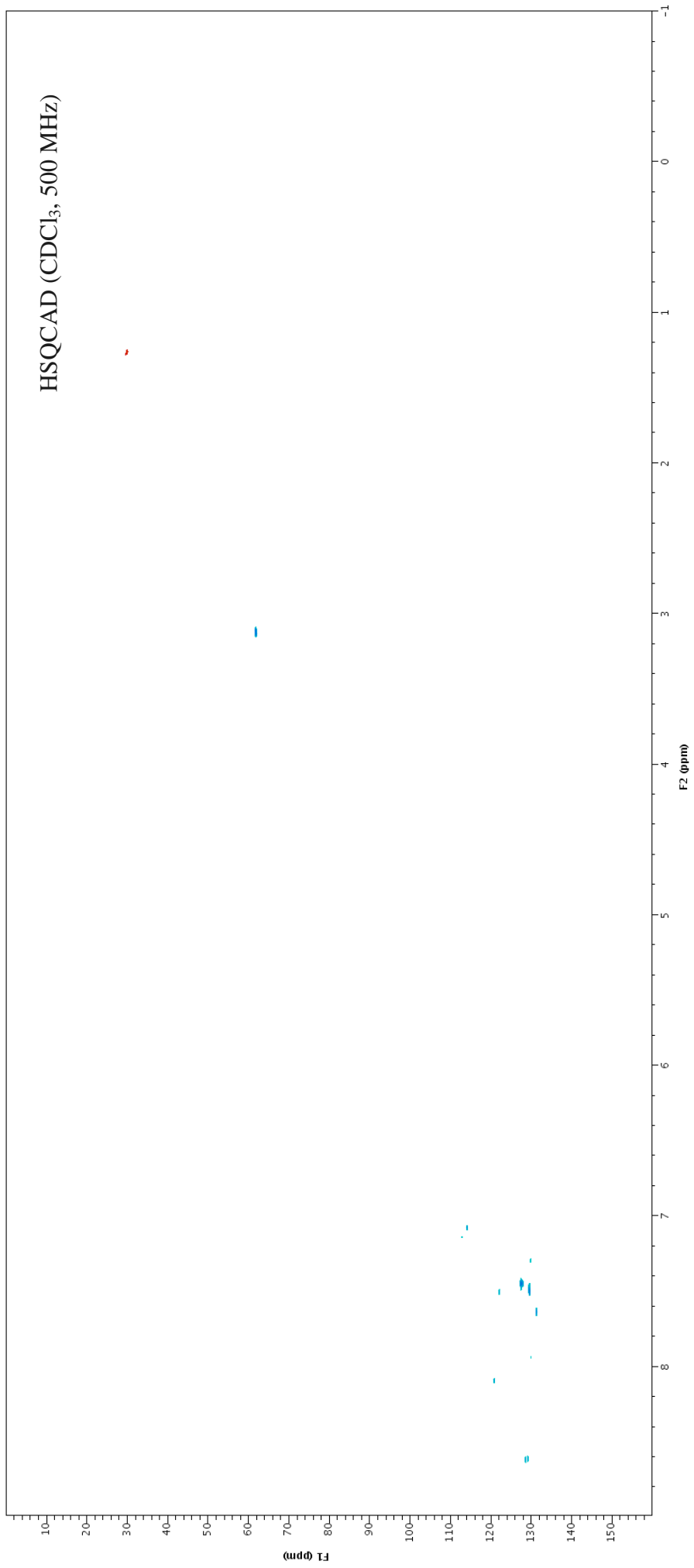
S71. ¹H NMR spectrum (500 MHz, CDCl₃) of fuliginol (**16**) and chlorofuliginol (**17**).



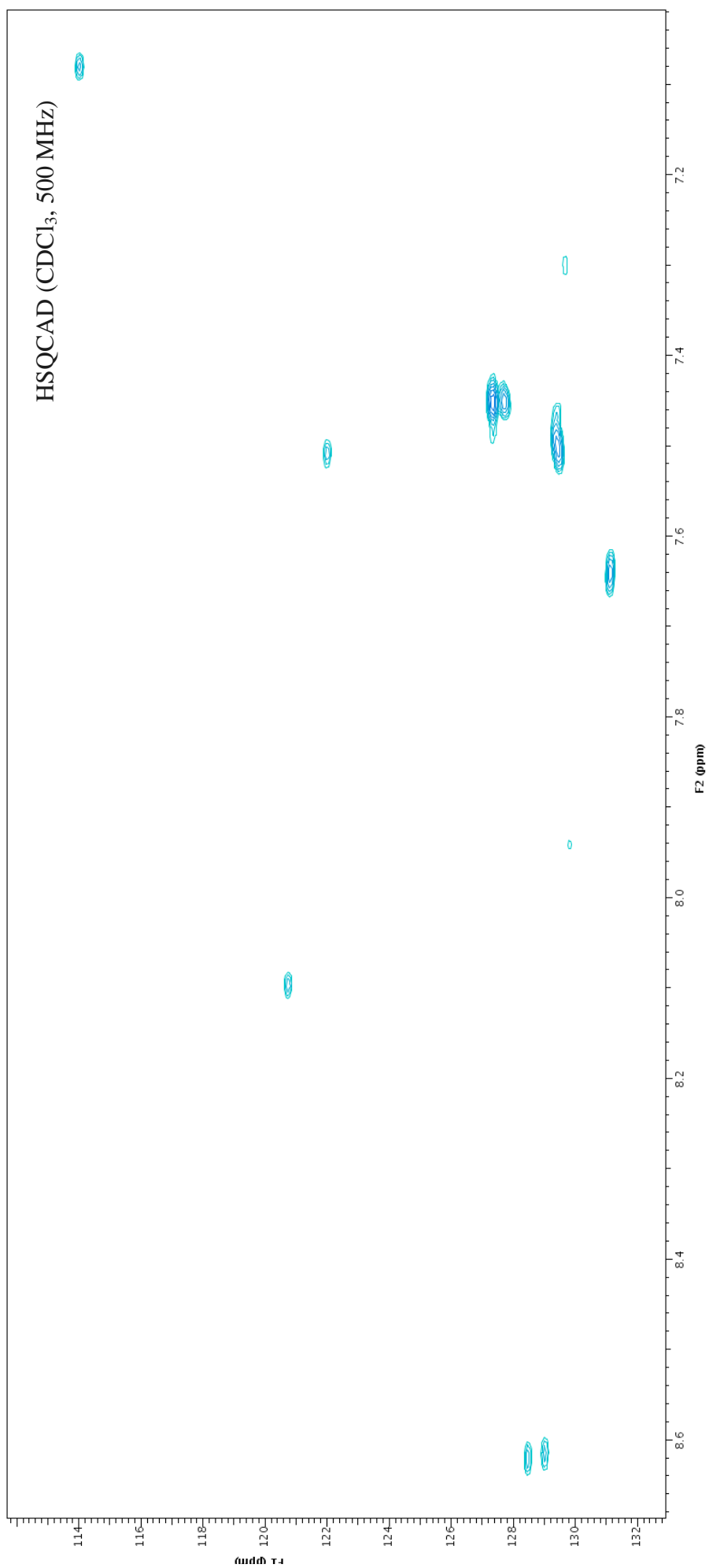
S72. Expansion of ¹H NMR spectrum (500 MHz, CDCl₃) of fuliginol (**16**) and chlorofuliginol (**17**).



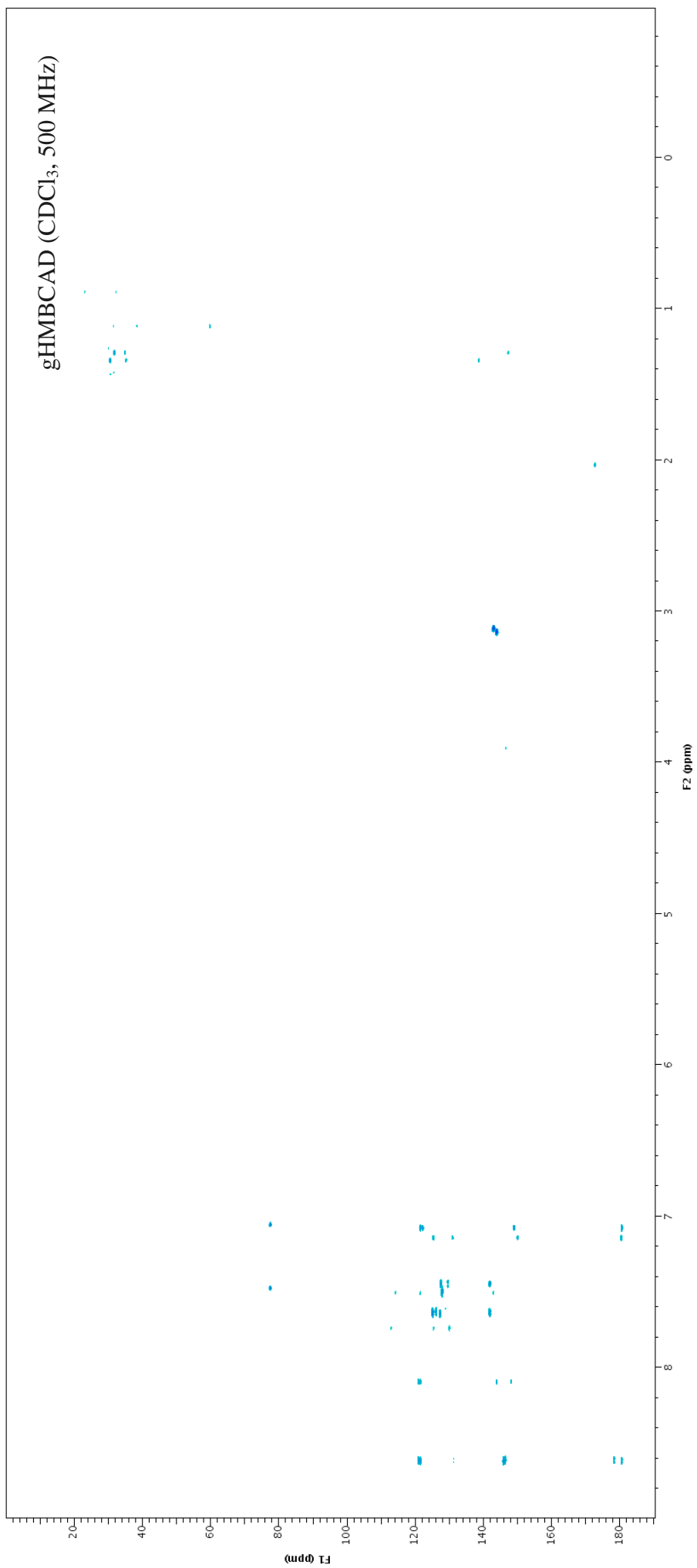
S73. gCOSY NMR spectrum (500 MHz, CDCl₃) of fuliginol (**16**) and chlorofuliginol (**17**).



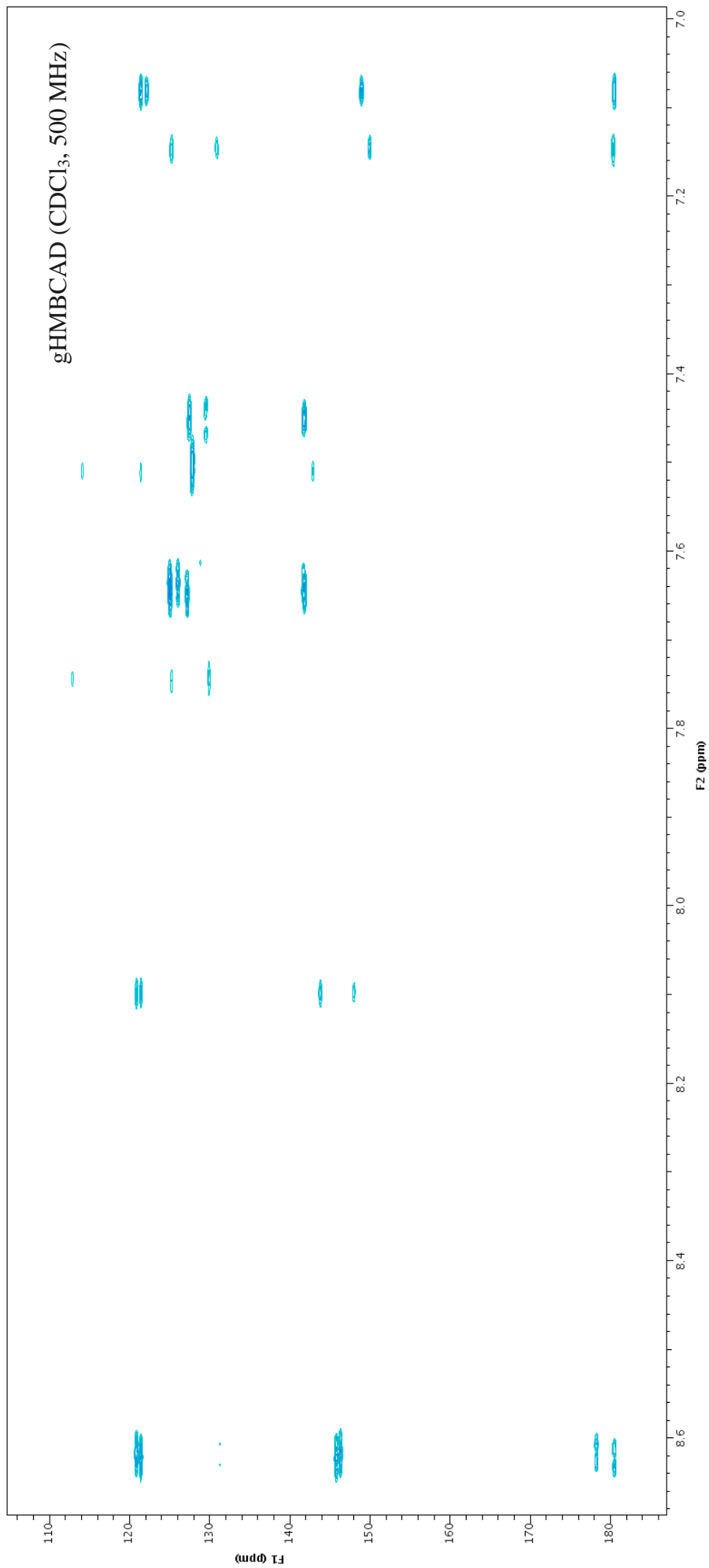
S74. HSQCAD NMR spectrum (500 MHz, CDCl₃) of fuliginol (**16**) and chlorofuliginol (**17**).



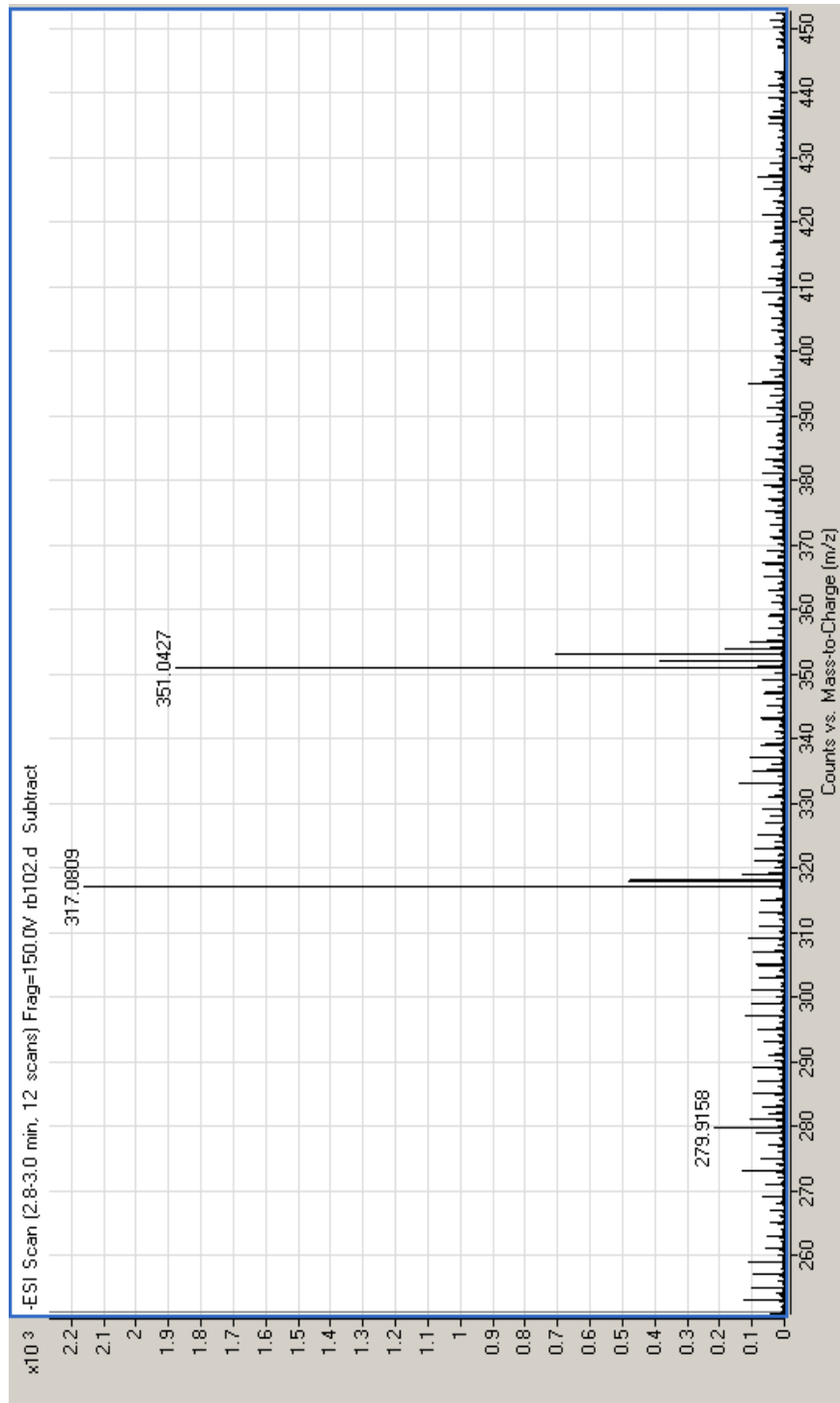
S75. Expansion of HSQCAD NMR spectrum (500 MHz, CDCl₃) of fuliginol (**16**) and chlorofuliginol (**17**).



S76. gHMBCAD NMR spectrum (500 MHz, CDCl₃) of fuliginol (**16**) and chlorofuliginol (**17**).



S77. Expansion of gHMBCAD NMR spectrum (500 MHz, CDCl₃) of fuliginol (**16**) and chlorofuliginol (**17**).



S78. High resolution negative ESI-MS of fuliginol (**16**) and chlorofuliginol (**17**).

S79. Atomic coordinates ($\times 10^4$) for fuliginol (**16**) and chlorofuliginol (**17**) and equivalent isotropic displacement parameters ($\text{\AA}^2 \times 10^3$) for fuliginol (**16**) and chlorofuliginol (**17**). $U(\text{eq})$ is defined as one third of the trace of the orthogonalized U^{ij} tensor.

	x	y	z	U(eq)
C(1)	7429(6)	4440(4)	5709(4)	33(1)
C(2)	7287(6)	3404(4)	6613(4)	31(1)
C(3)	7335(6)	3718(4)	7906(4)	38(1)
C(4)	7600(7)	5004(4)	8186(4)	41(1)
C(5)	7738(7)	6007(4)	7304(4)	40(1)
C(6)	7612(6)	5762(4)	6070(4)	34(1)
C(7)	7691(6)	6845(4)	5159(4)	36(1)
C(8)	7599(6)	6522(4)	3860(4)	36(1)
C(10)	7324(6)	4181(4)	4422(4)	34(1)
C(11)	7081(6)	2913(4)	4076(4)	37(1)
C(12)	6971(6)	1879(4)	4946(4)	32(1)
C(13)	7105(6)	2088(4)	6194(4)	33(1)
C(14)	7054(7)	2761(4)	8990(4)	43(1)
C(15)	5285(8)	2303(5)	9402(4)	50(1)
C(16)	5002(10)	1505(5)	10464(5)	67(2)
C(17)	6447(12)	1160(6)	11109(5)	77(2)
C(18)	8166(12)	1615(6)	10702(5)	75(2)
C(19)	8483(9)	2431(5)	9643(4)	55(1)
C(20)	8800(7)	289(4)	7047(4)	44(1)
O(1)	7787(5)	8022(3)	5423(3)	47(1)
O(2)	7662(5)	7548(3)	3033(3)	45(1)
O(3)	6748(5)	646(3)	4543(3)	40(1)
O(4)	6982(4)	996(3)	6974(3)	38(1)
C(9)	7451(6)	5270(4)	3524(4)	37(1)
Cl	7444(3)	4912(2)	1958(2)	41(1)
C(9')	7451(6)	5270(4)	3524(4)	37(1)

APPENDIX C

Supplementary Information for the Study of the Australian Plant

Haemodorum spicatum

This appendix contains further information relevant to study of the Australian plant *Haemodorum spicatum* as described in Chapter 6.

HPLC-NMR and HPLC-MS Profiling and Bioassay-Guided Identification of Secondary Metabolites from the Australian Plant *Haemodorum spicatum*

Robert Brkljača and Sylvia Urban*

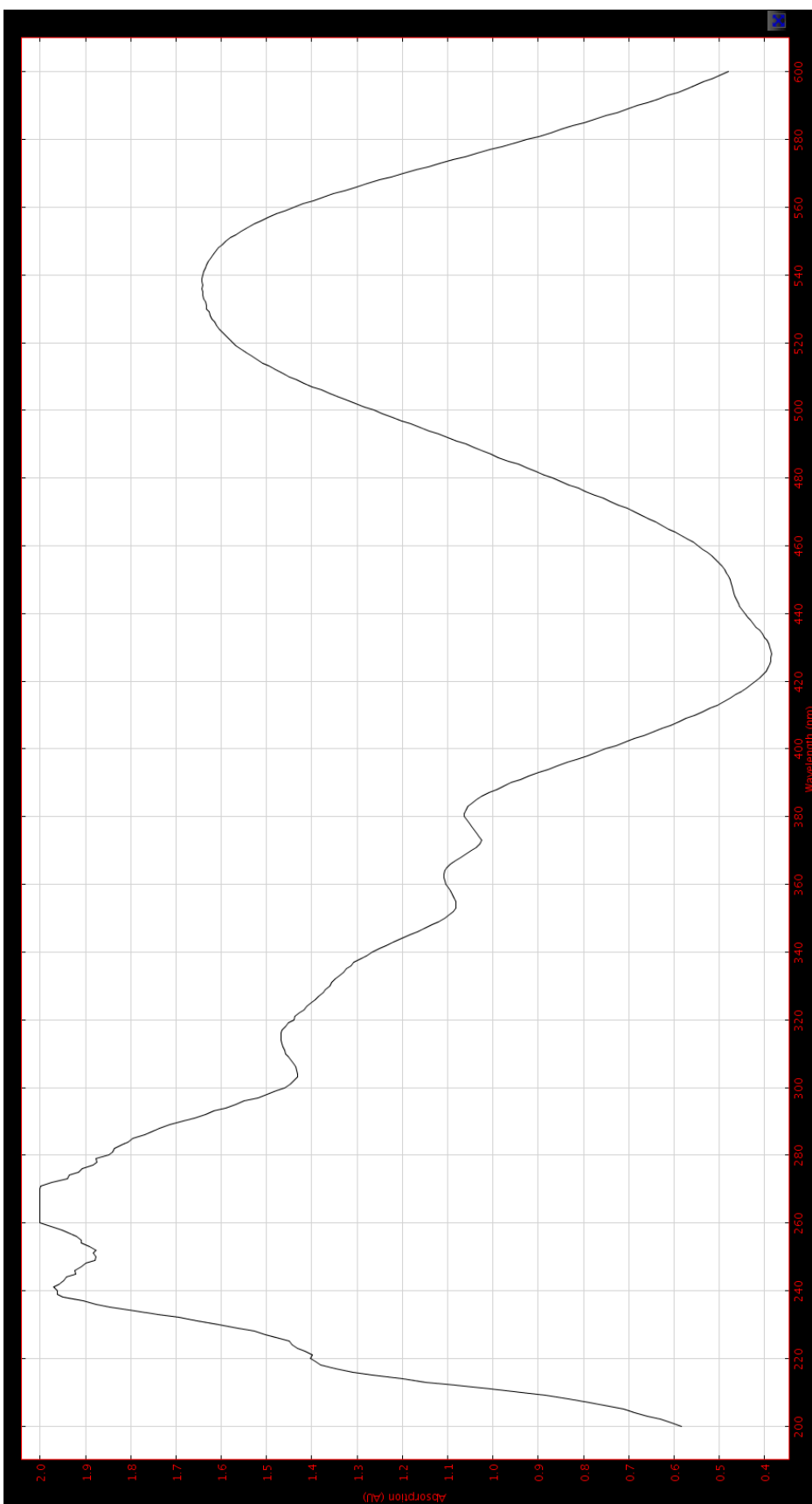
School of Applied Sciences (Discipline of Chemistry), Health Innovations Research Institute (HIRi) RMIT University, GPO Box 2476V Melbourne, Victoria 3001, Australia).

Supporting Information

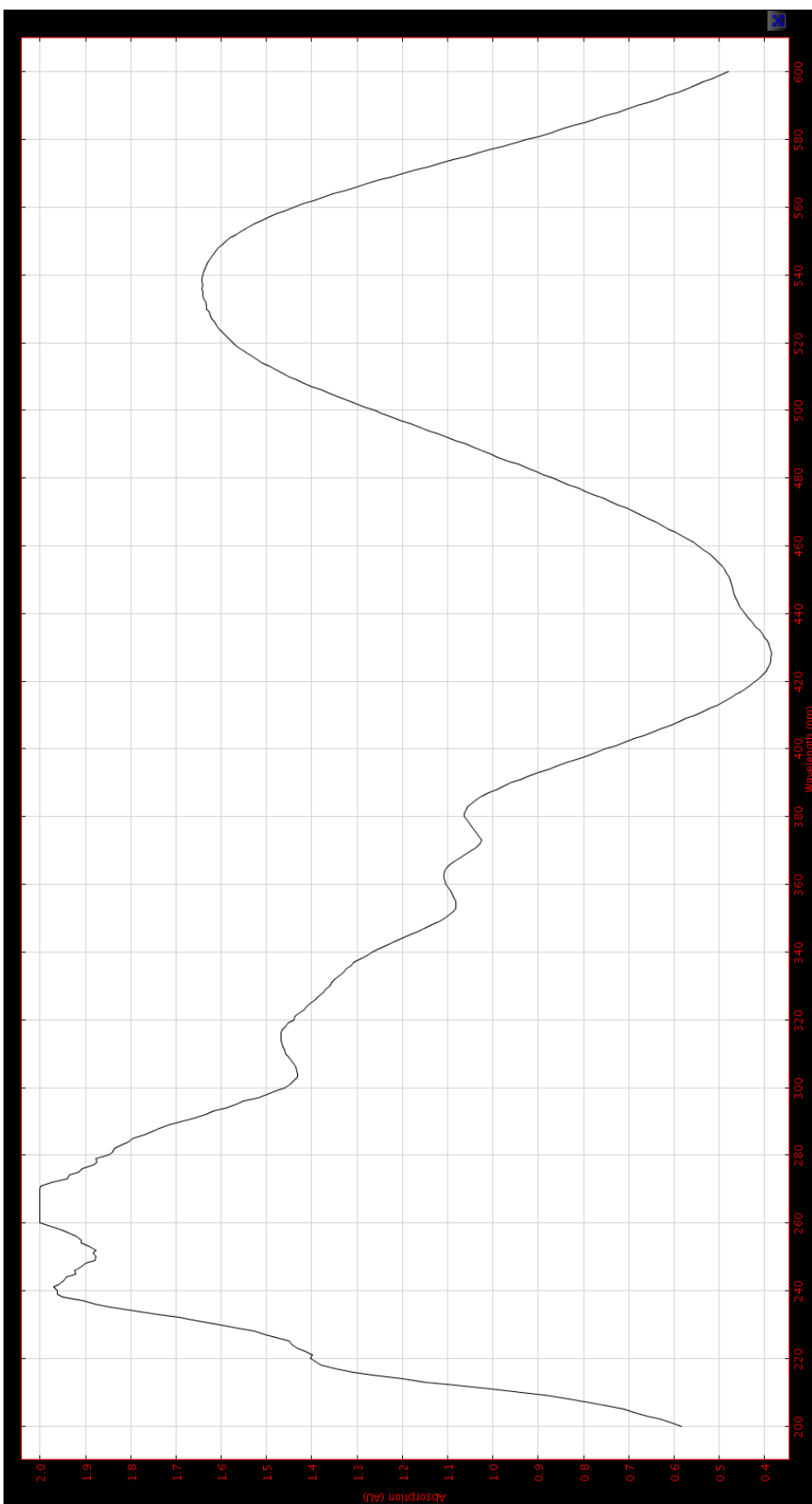
- S1. Extracted UV trace from HPLC-NMR for peak A ($R_t = 4.8$ min) (1).
- S2. Extracted UV trace from HPLC-NMR for peak B ($R_t = 5.1$ min) (5).
- S3. Extracted UV trace from HPLC-NMR for peak C ($R_t = 5.9$ min)(11).
- S4. Extracted UV trace from HPLC-NMR for peak D ($R_t = 7.0$ min) (8).
- S5. Extracted UV trace from HPLC-NMR for peak E ($R_t = 7.9$ min) (12).
- S6. Extracted UV trace from HPLC-NMR for peak F ($R_t = 9.9$ min).
- S7. Extracted UV trace from HPLC-NMR for peak G ($R_t = 16.9$ min) (2).
- S8. Extracted UV trace from HPLC-NMR for peak H ($R_t = 19.5$ min) (3).
- S9. Extracted UV trace from HPLC-NMR for peak I ($R_t = 23.0$ min) (13).
- S10. ^1H NMR spectrum (500 MHz, CDCl_3) of haemoxiphidone (8).
- S11. gCOSY NMR spectrum (500 MHz, CDCl_3) of haemoxiphidone (8).
- S12. gHSQCAD NMR spectrum (500 MHz, CDCl_3) of haemoxiphidone (8).
- S13. gHMBC NMR spectrum (500 MHz, CDCl_3) of haemoxiphidone (8).
- S14. Single irradiation nOe NMR spectrum (500 MHz, CDCl_3) of haemoxiphidone (8).showing the irradiation of δ_{H} 8.32 (H-7).
- S15. High resolution positive ESI-MS of haemoxiphidone (8).
- S16. ^1H NMR spectrum (500 MHz, CDCl_3) of haemodordione (13).
- S17. ^{13}C NMR spectrum (125 MHz, CDCl_3) of haemodordione (13).
- S18. gCOSY NMR spectrum (500 MHz, CDCl_3) of haemodordione (13).
- S19. gHSQCAD NMR spectrum (500 MHz, CDCl_3) of haemodordione (13).
- S20. gHMBC NMR spectrum (500 MHz, CDCl_3) of haemodordione (13).

- S21.** High resolution positive ESI-MS of haemodordione (**13**).
- S22.** ¹H NMR spectrum (500 MHz, CDCl₃) of haemodordioid (**16**).
- S23.** gCOSY NMR spectrum (500 MHz, CDCl₃) of haemodordioid (**16**).
- S24.** gHSQCAD NMR spectrum (500 MHz, CDCl₃) of haemodordioid (**16**).
- S25.** gHMBC NMR spectrum (500 MHz, CDCl₃) of haemodordioid (**16**).
- S26.** High resolution ASAP-MS of haemodordioid (**16**).
- S27.** ¹H NMR spectrum (500 MHz, CDCl₃) of haemodoronol (**17**).
- S28.** gCOSY NMR spectrum (500 MHz, CDCl₃) of haemodoronol (**17**).
- S29.** gHSQCAD NMR spectrum (500 MHz, CDCl₃) of haemodoronol (**17**).
- S30.** gHMBC NMR spectrum (500 MHz, CDCl₃) of haemodoronol (**17**).
- S31.** NOESY NMR spectrum (500 MHz, CDCl₃) of haemodoronol (**17**).
- S32.** Expansion of NOESY NMR spectrum (500 MHz, CDCl₃) of haemodoronol (**17**).
- S33.** High resolution positive ESI-MS of haemodoronol (**17**).

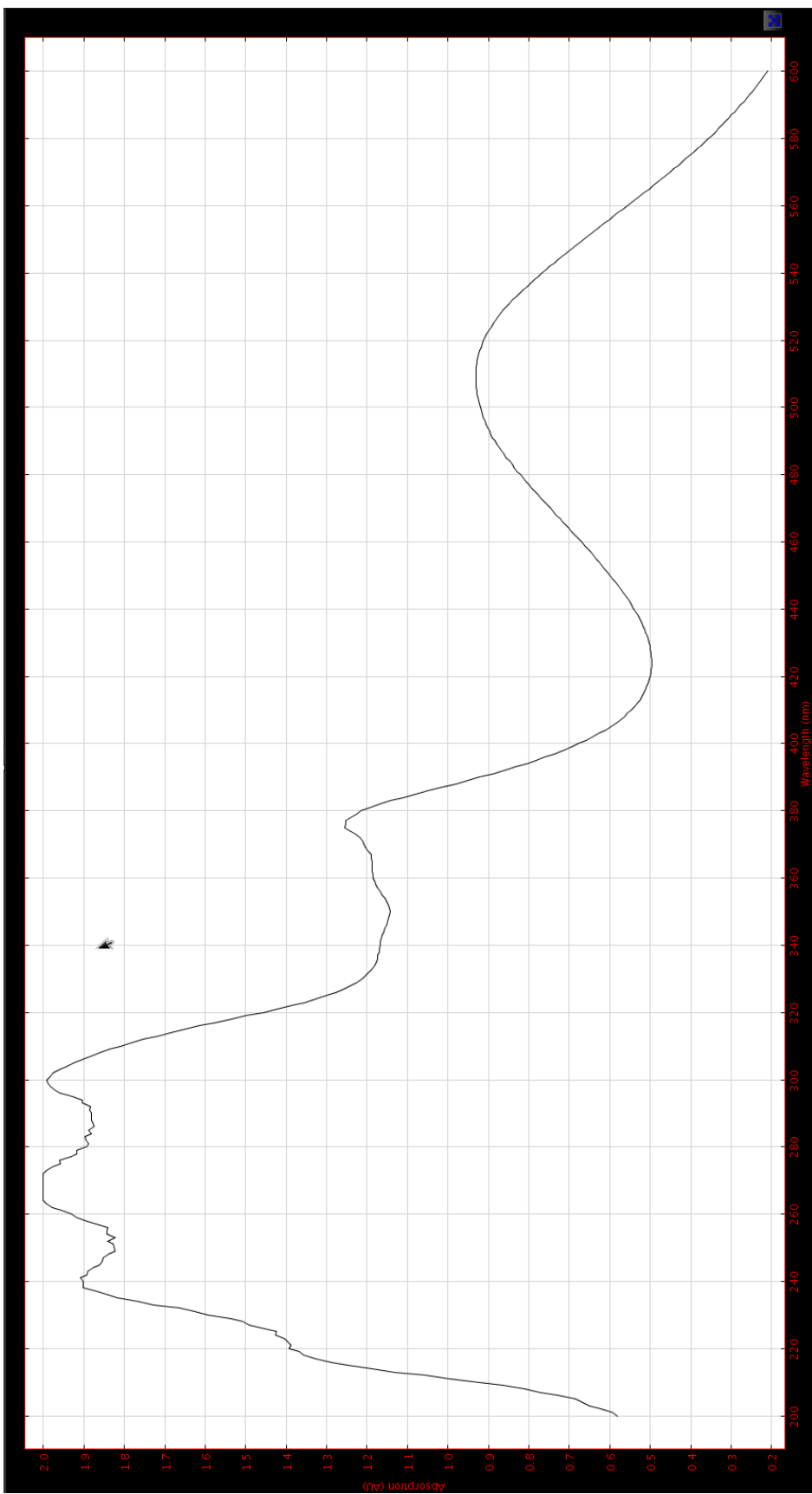
*Corresponding author. Tel: +61 3 9925 3376; Fax: +61 3 9925 3747
E-mail address: sylvia.urban@rmit.edu.au (S. Urban).



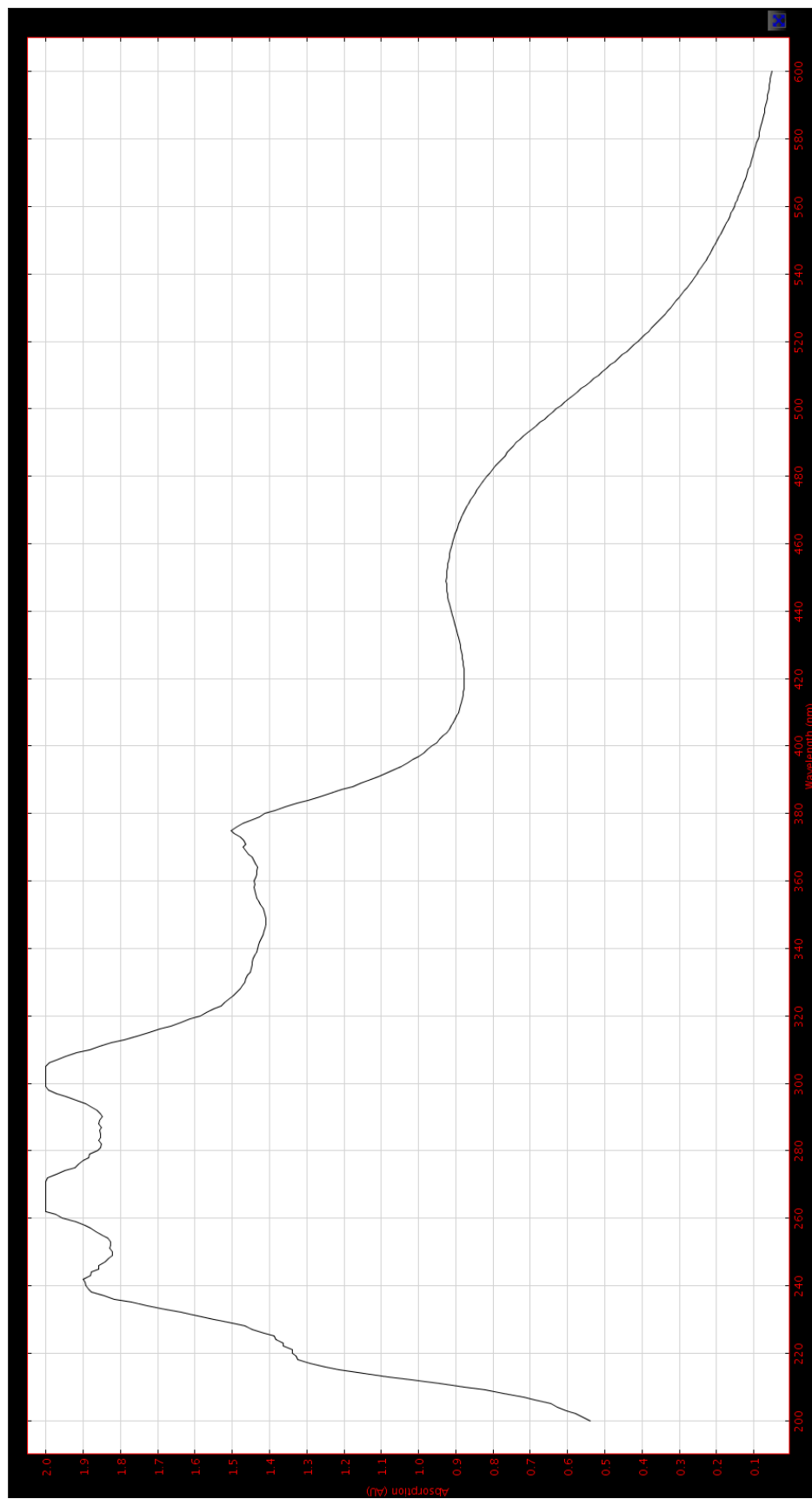
S1. Extracted UV trace from HPLC-NMR for peak A ($R_t = 4.8$ min) (**1**).



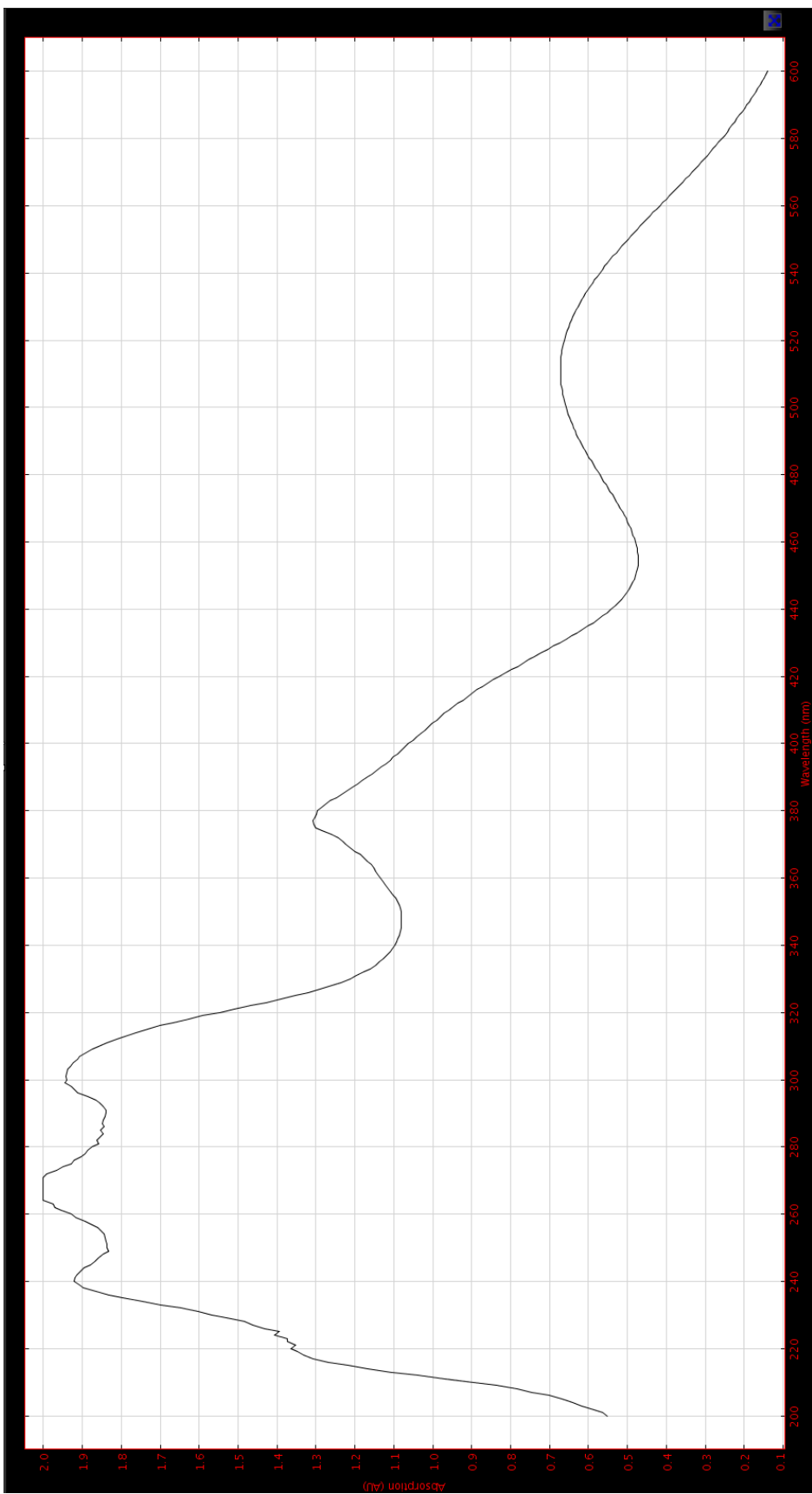
S2. Extracted UV trace from HPLC-NMR for peak B ($R_t = 5.1$ min) (5).



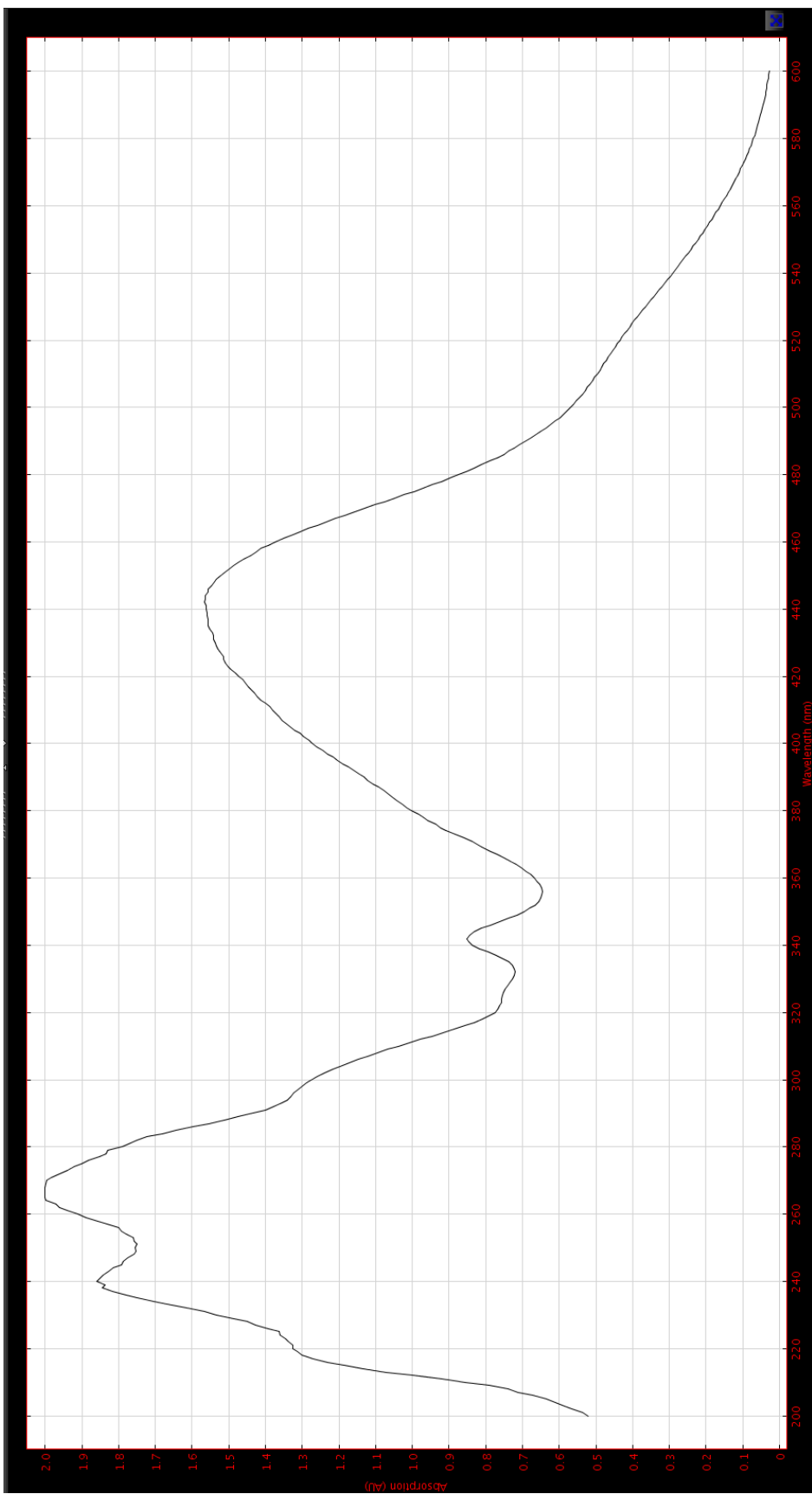
S3. Extracted UV trace from HPLC-NMR for peak C ($R_t = 5.9$ min) (**11**).



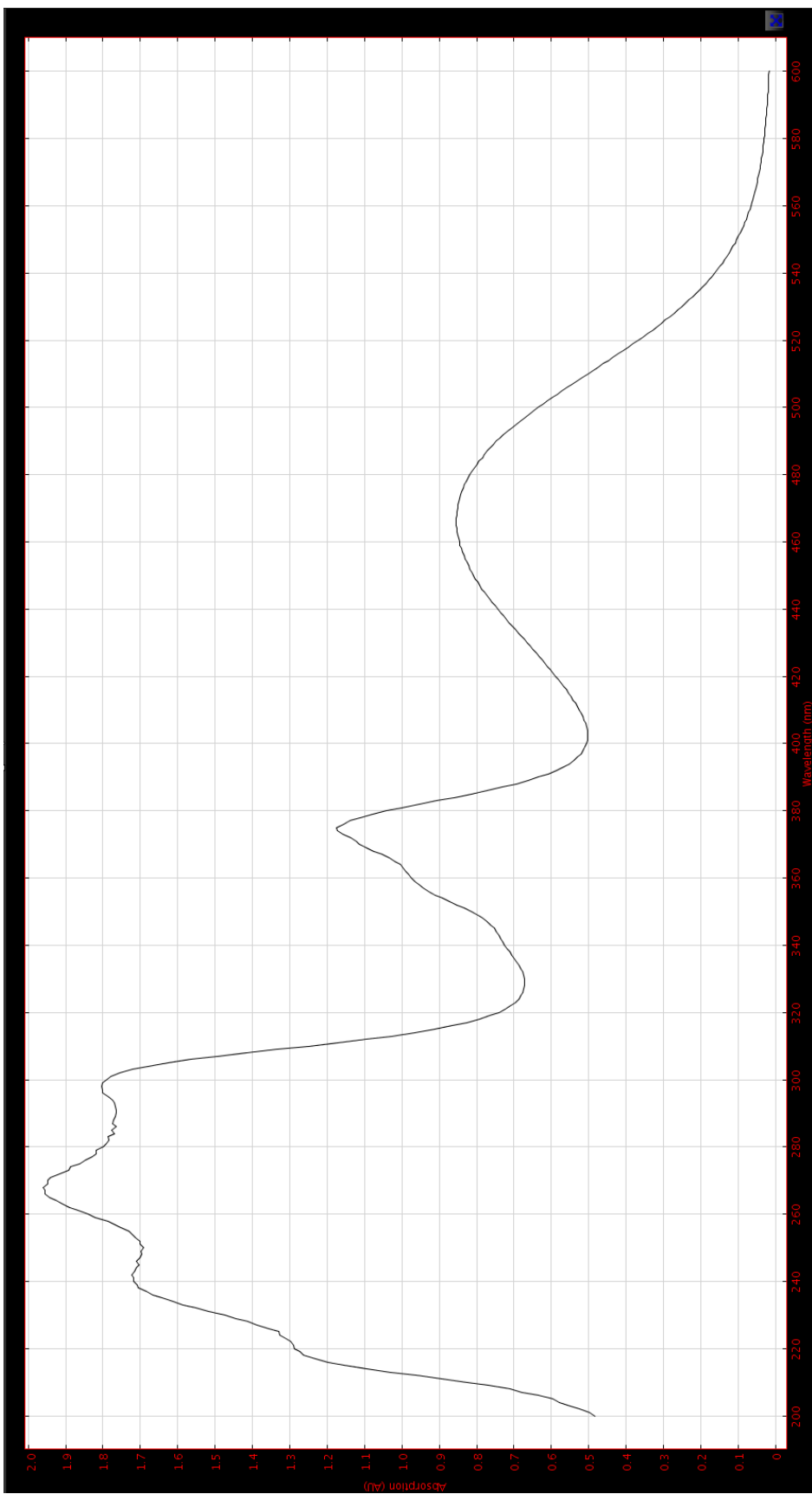
S4. Extracted UV trace from HPLC-NMR for peak D ($R_t = 7.0$ min) **(8)**.



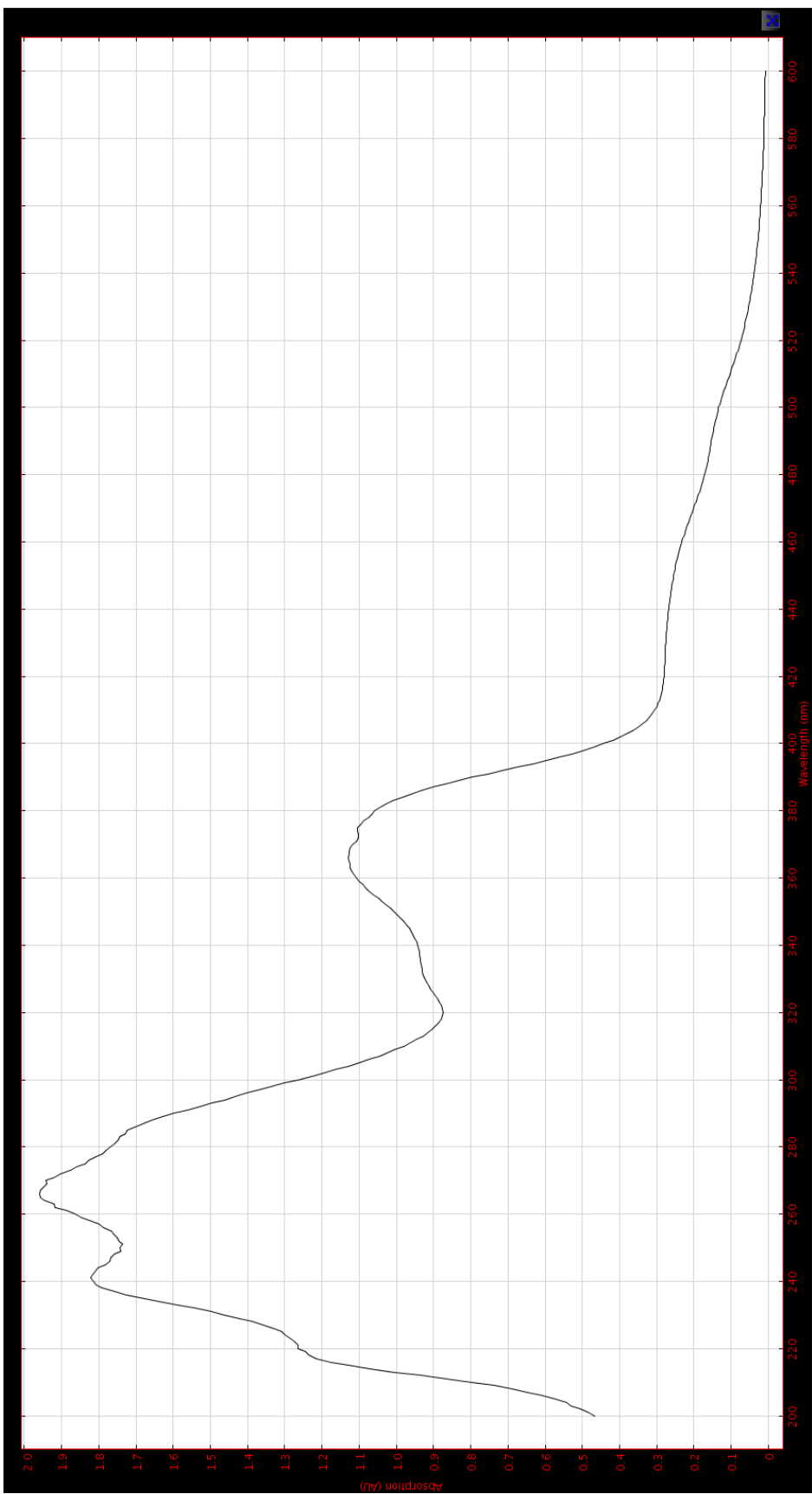
S5. Extracted UV trace from HPLC-NMR for peak E ($R_t = 7.9$ min) (**12**).



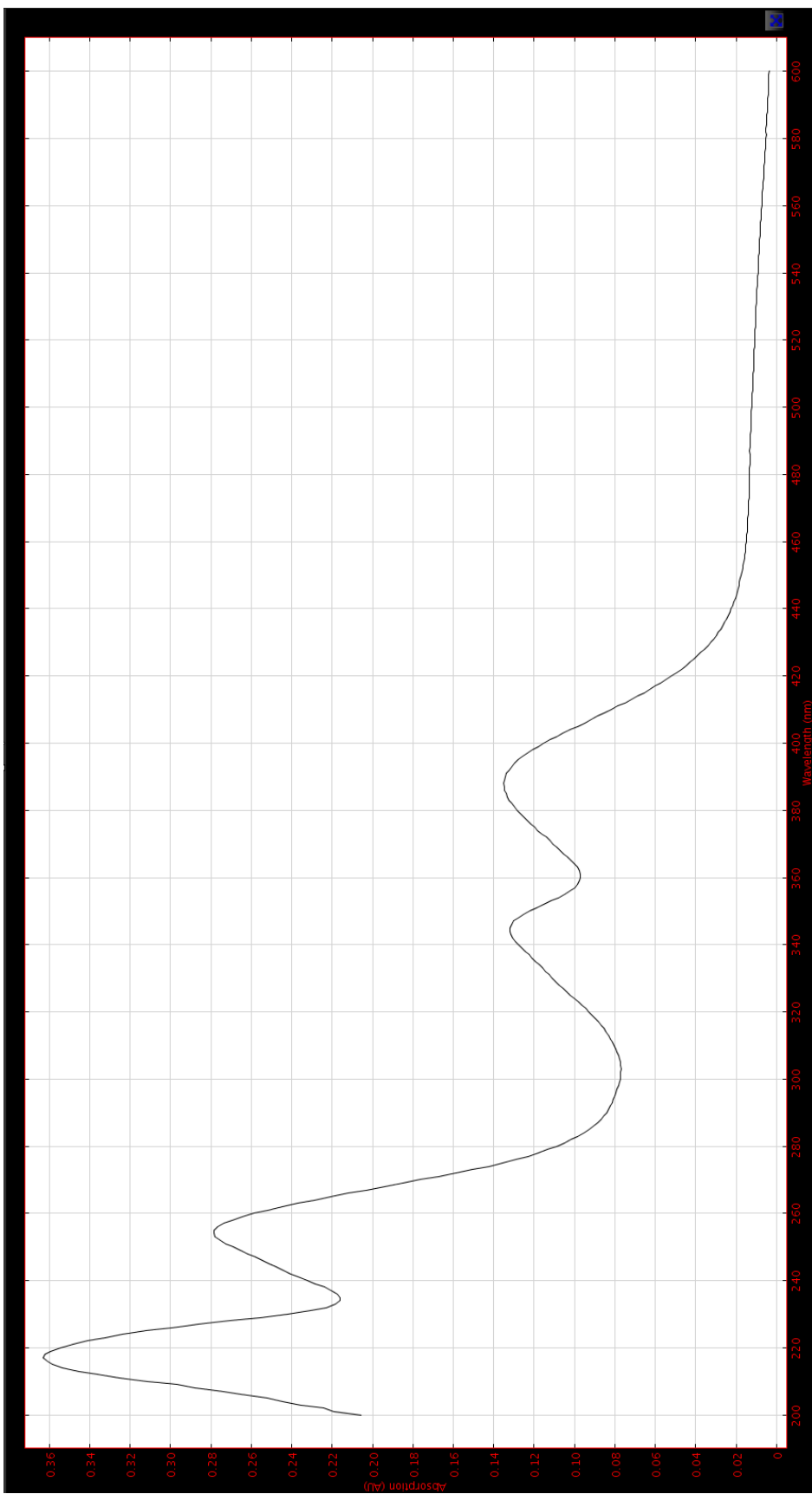
S6. Extracted UV trace from HPLC-NMR for peak F ($R_t = 9.9$ min).



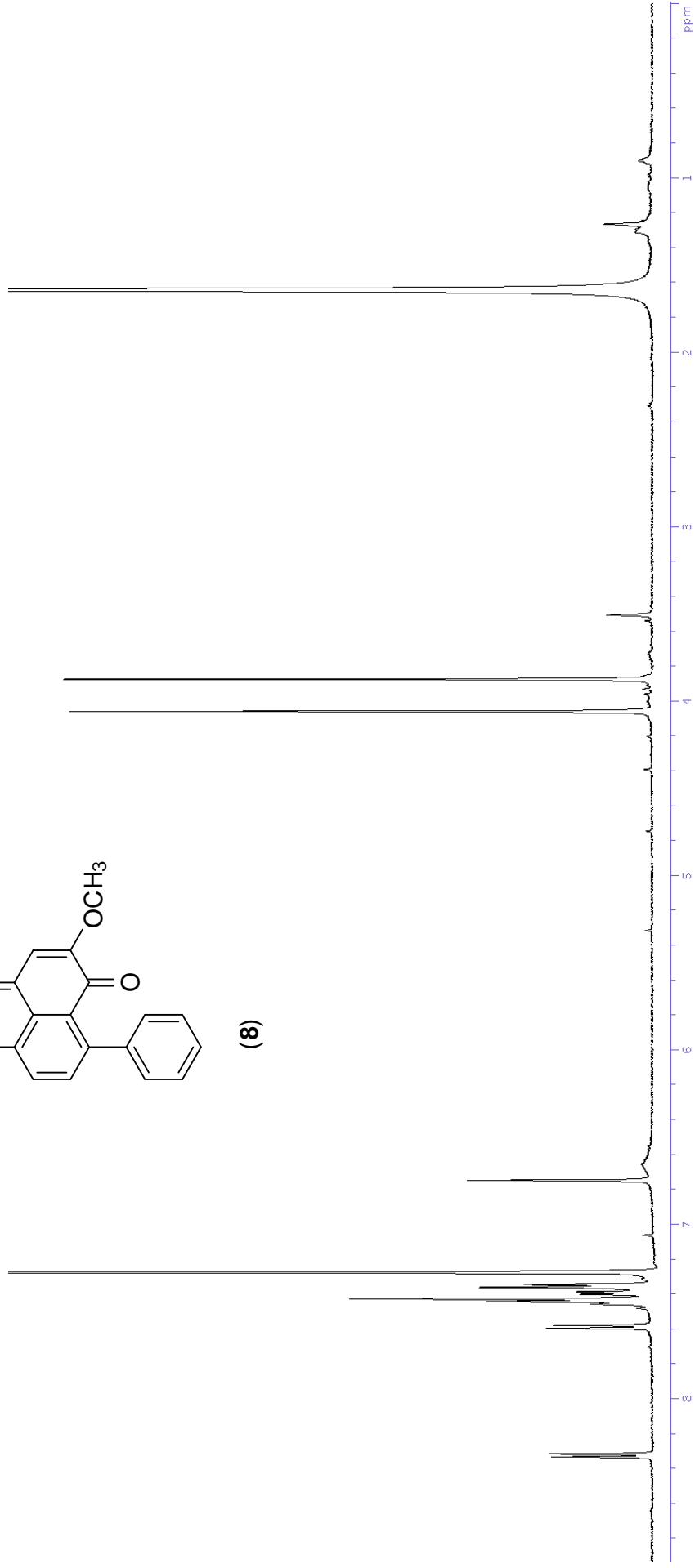
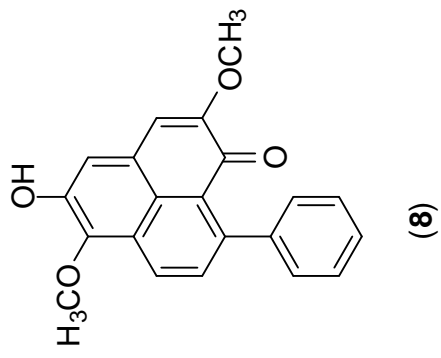
S7. Extracted UV trace from HPLC-NMR for peak G ($R_t = 16.9$ min) (2).



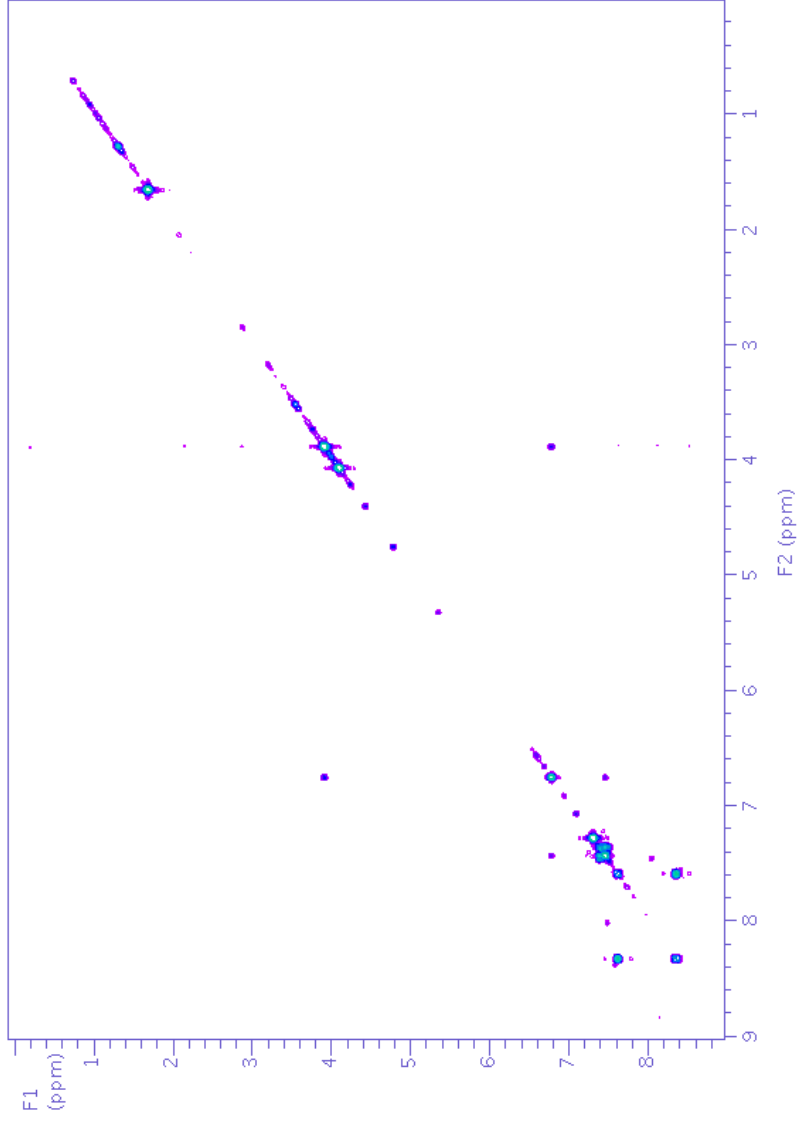
S8. Extracted UV trace from HPLC-NMR for peak H ($R_t = 19.5$ min) (3).



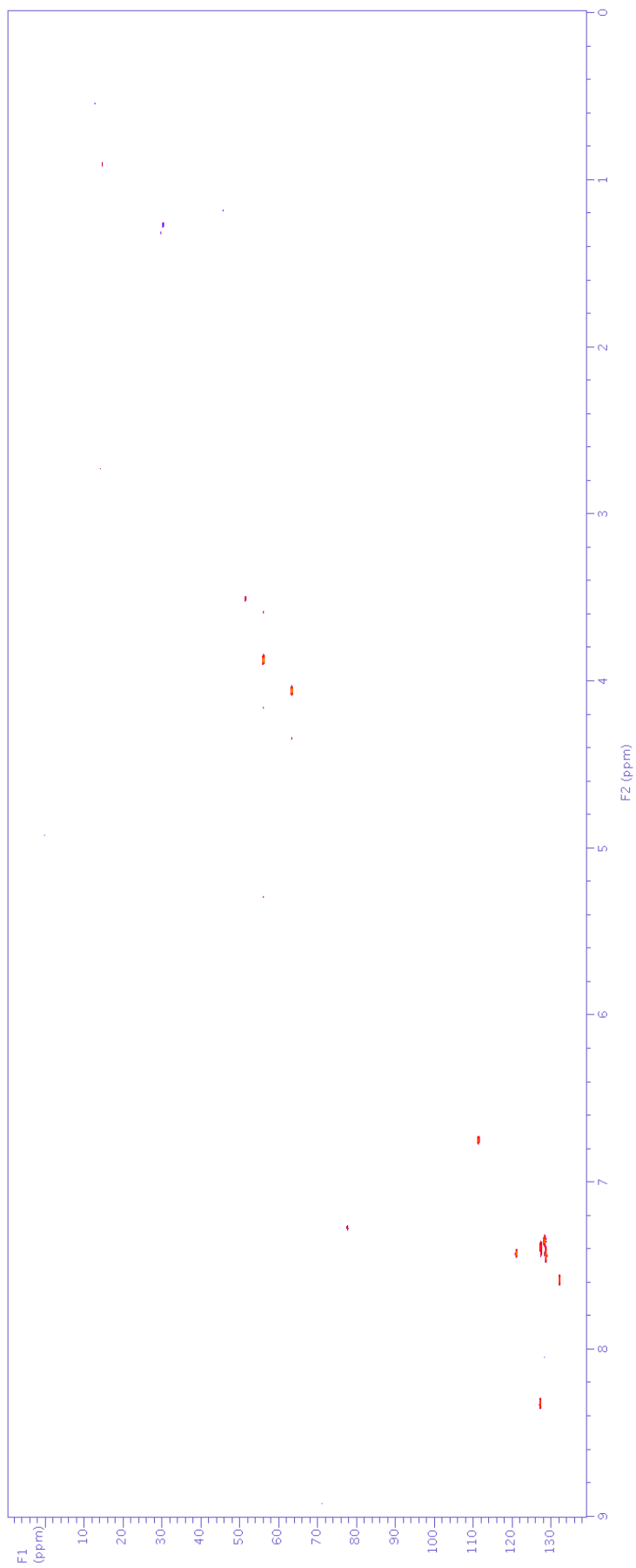
S9. Extracted UV trace from HPLC-NMR for peak I ($R_t = 23.0$ min) (**13**).



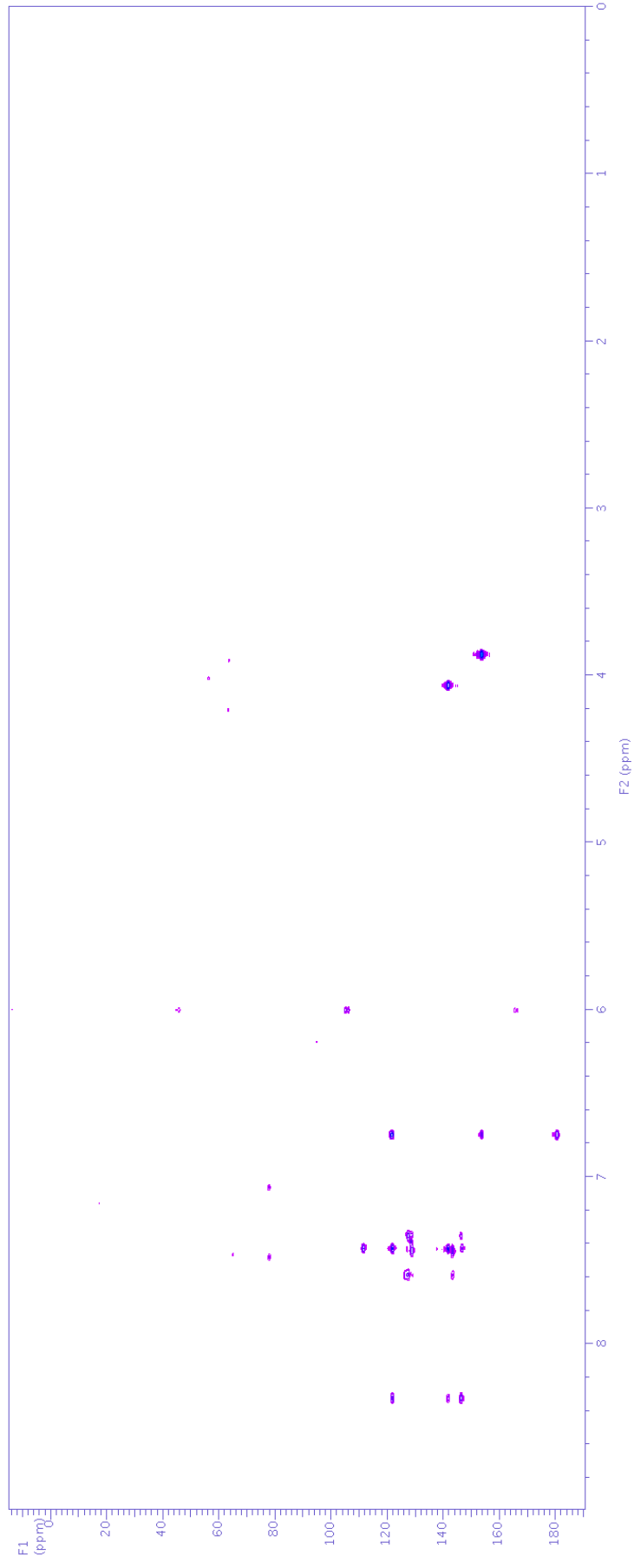
S10. ¹H NMR spectrum (500 MHz, CDCl₃) of haemoxiphidone (8).



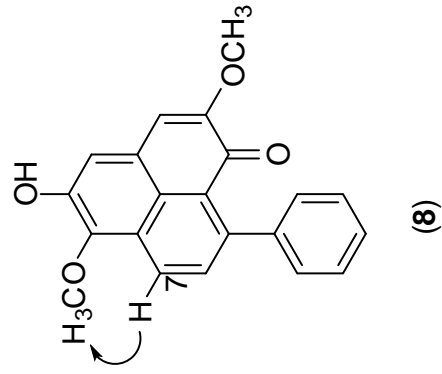
S11. gCOSY NMR spectrum (500 MHz, CDCl₃) of haemoxiphidone (**8**).



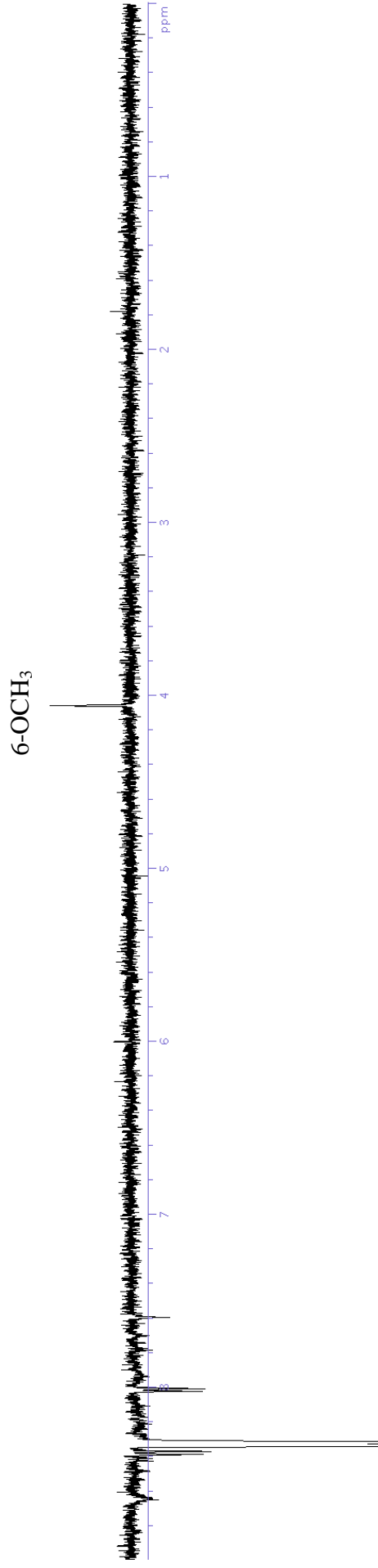
S12. gHSQCAD NMR spectrum (500 MHz, CDCl₃) of haemoxiphidone (**8**).



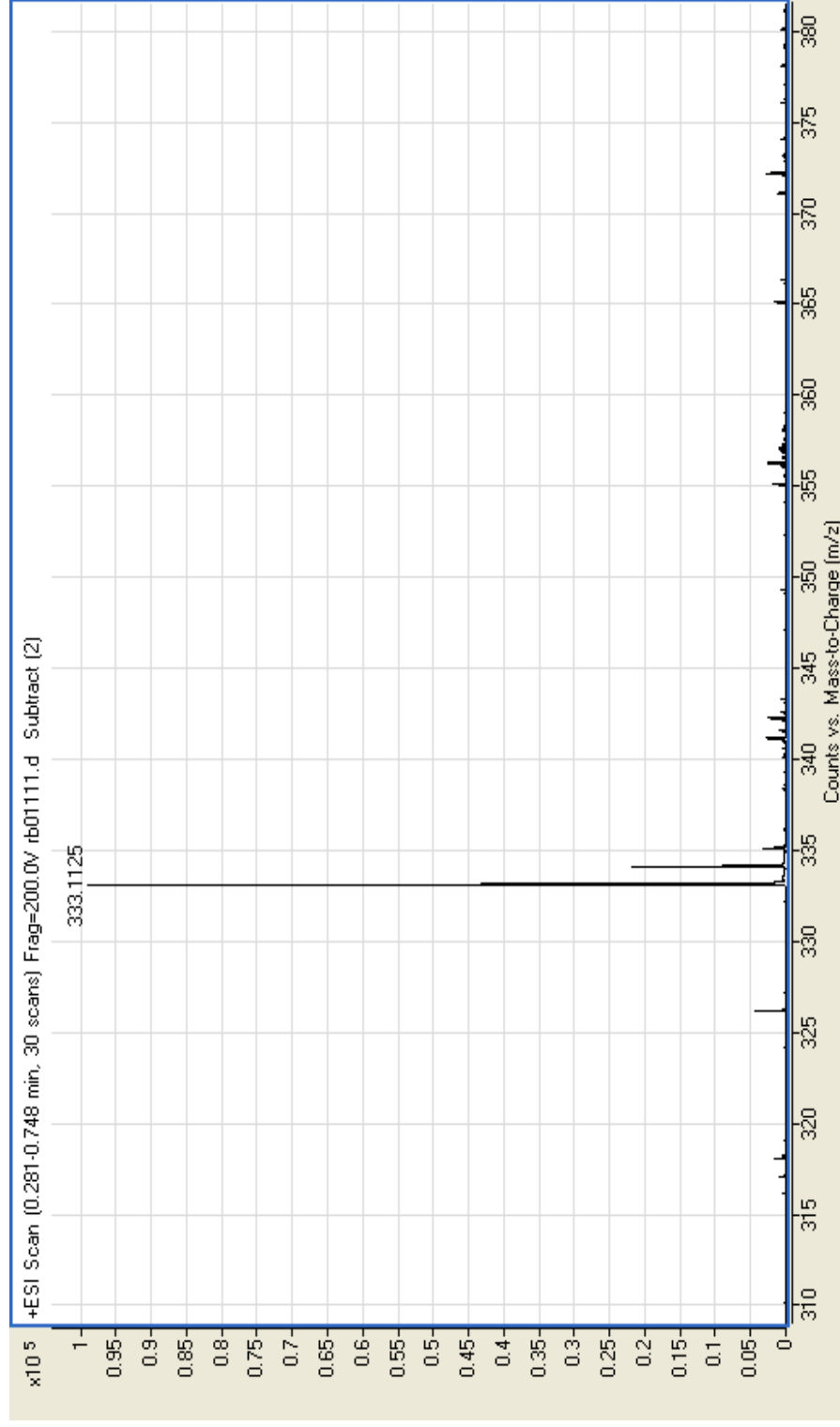
S13. gHMBC NMR spectrum (500 MHz, CDCl₃) of haemoxiphidone (**8**).



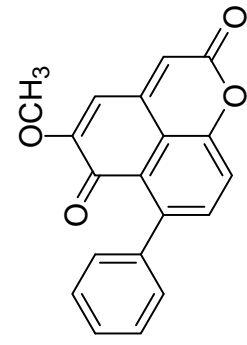
(8)



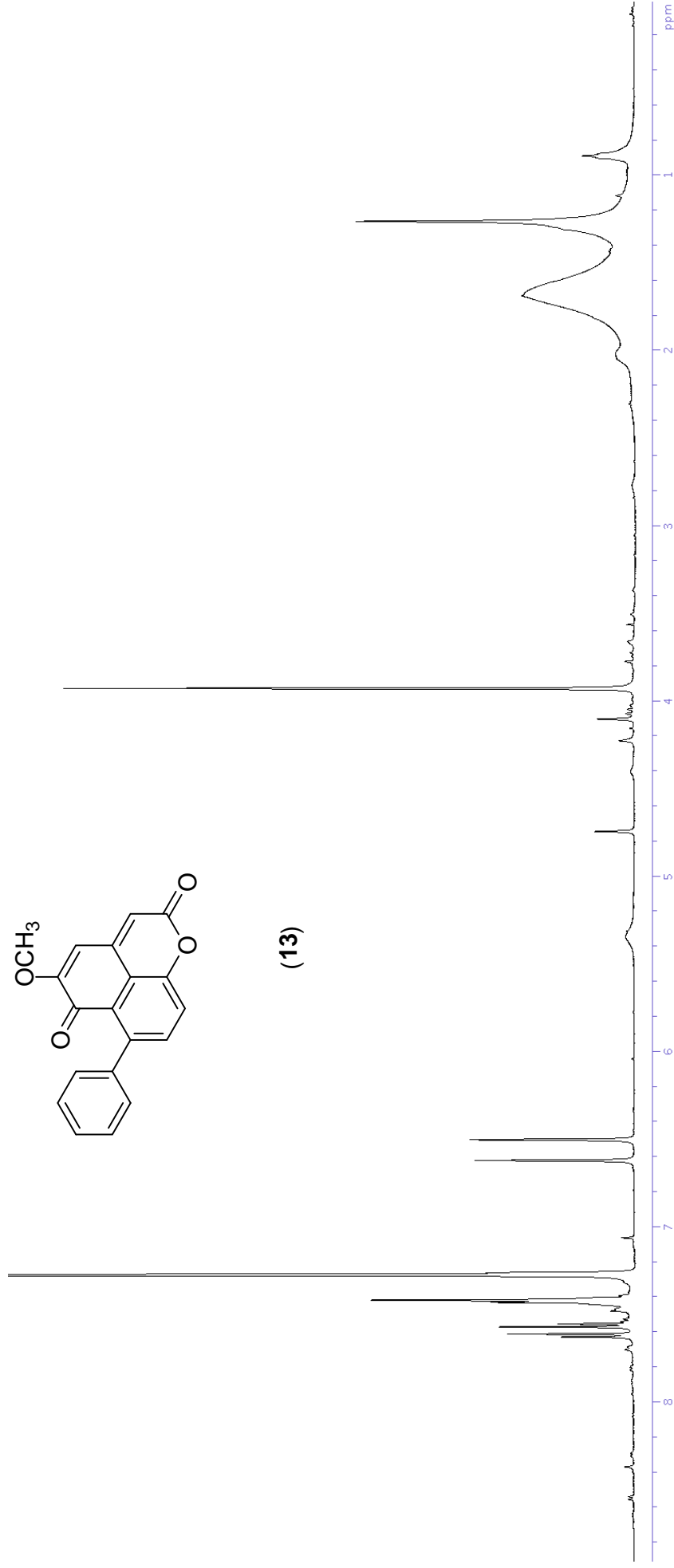
S14. Single irradiation nOe NMR spectrum (500 MHz, CDCl₃) of haemoxiphidone (8) showing the irradiation of δ_{H} 8.32 (H-7).



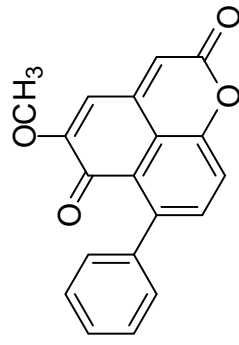
S15. High resolution positive ESI-MS of haemoxiphidone (**8**).



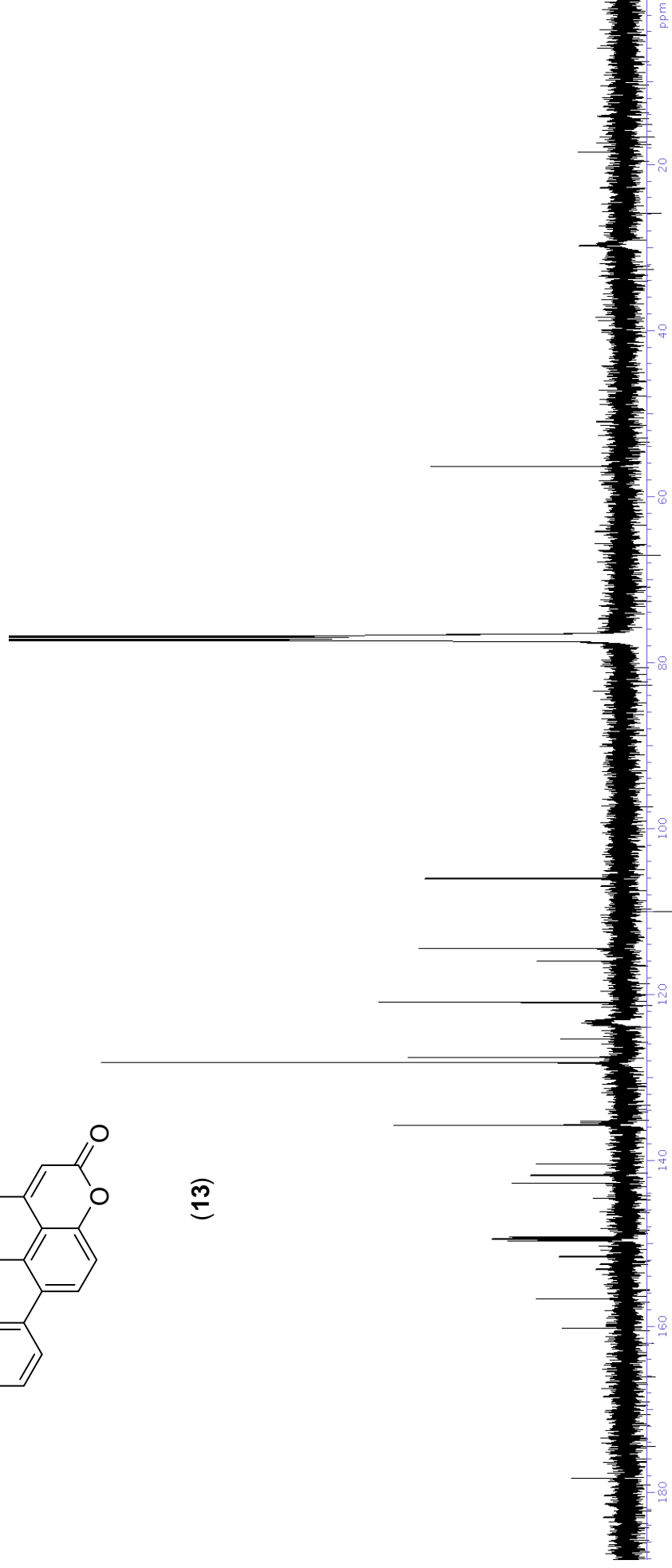
(13)



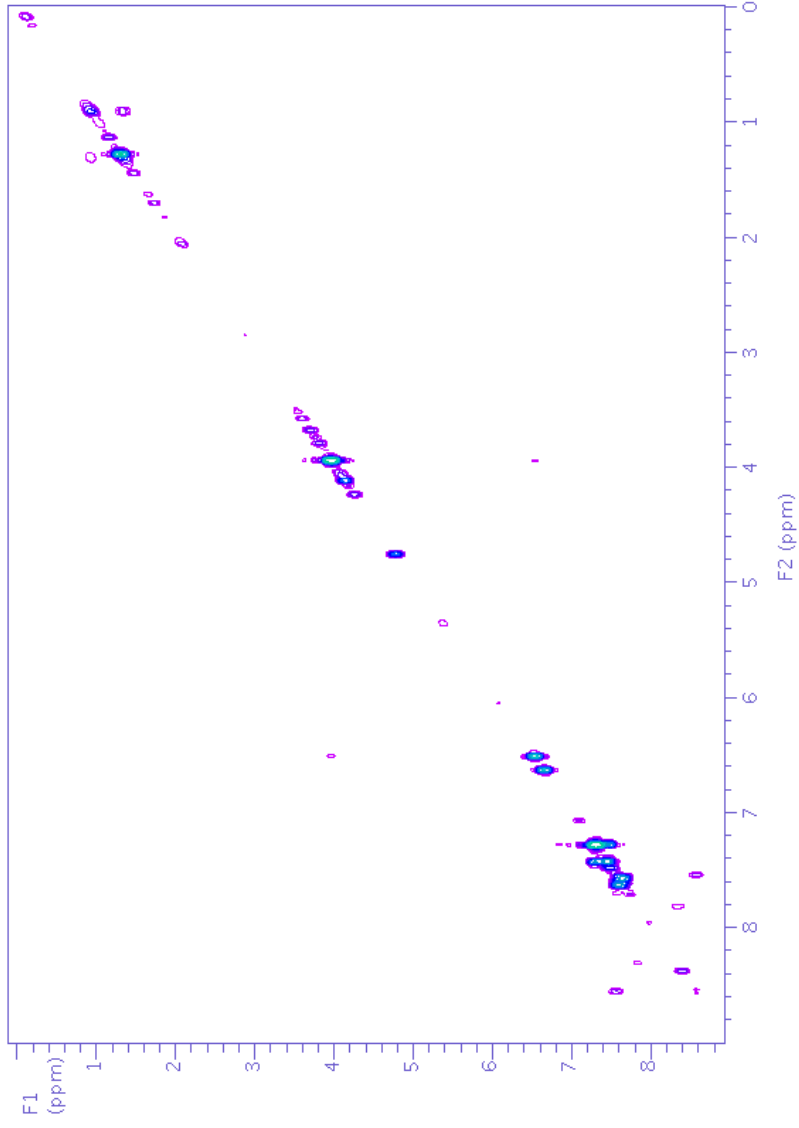
S16. ^1H NMR spectrum (500 MHz, CDCl_3) of haemodordione (**13**).



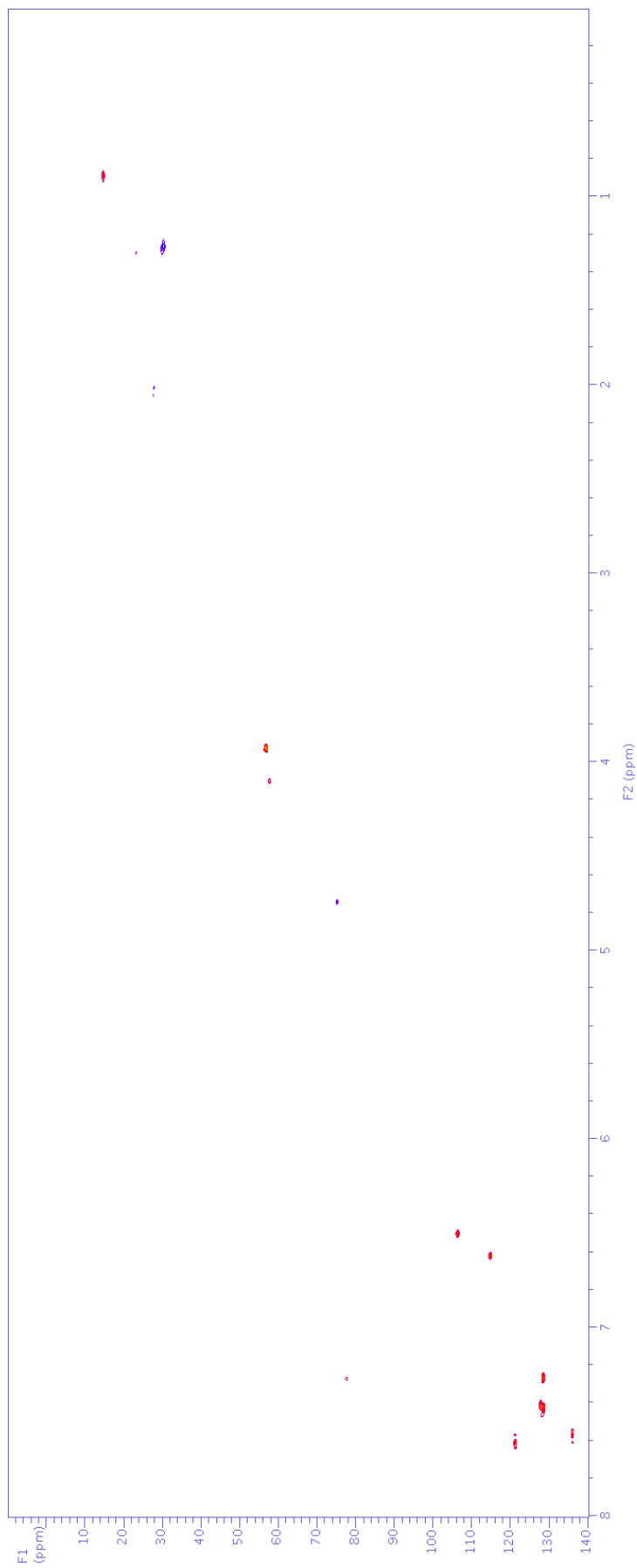
(13)



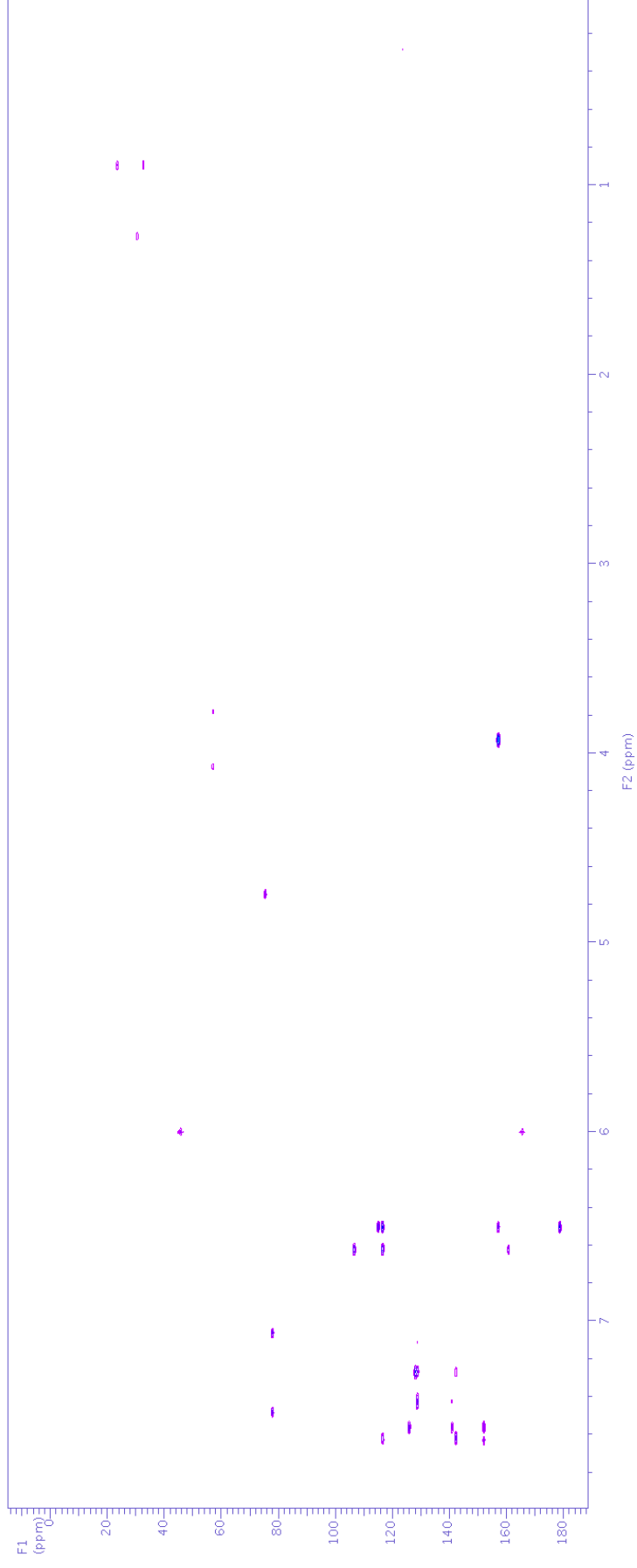
S17. ¹³C NMR spectrum (125 MHz, CDCl₃) of haemodordione (13).



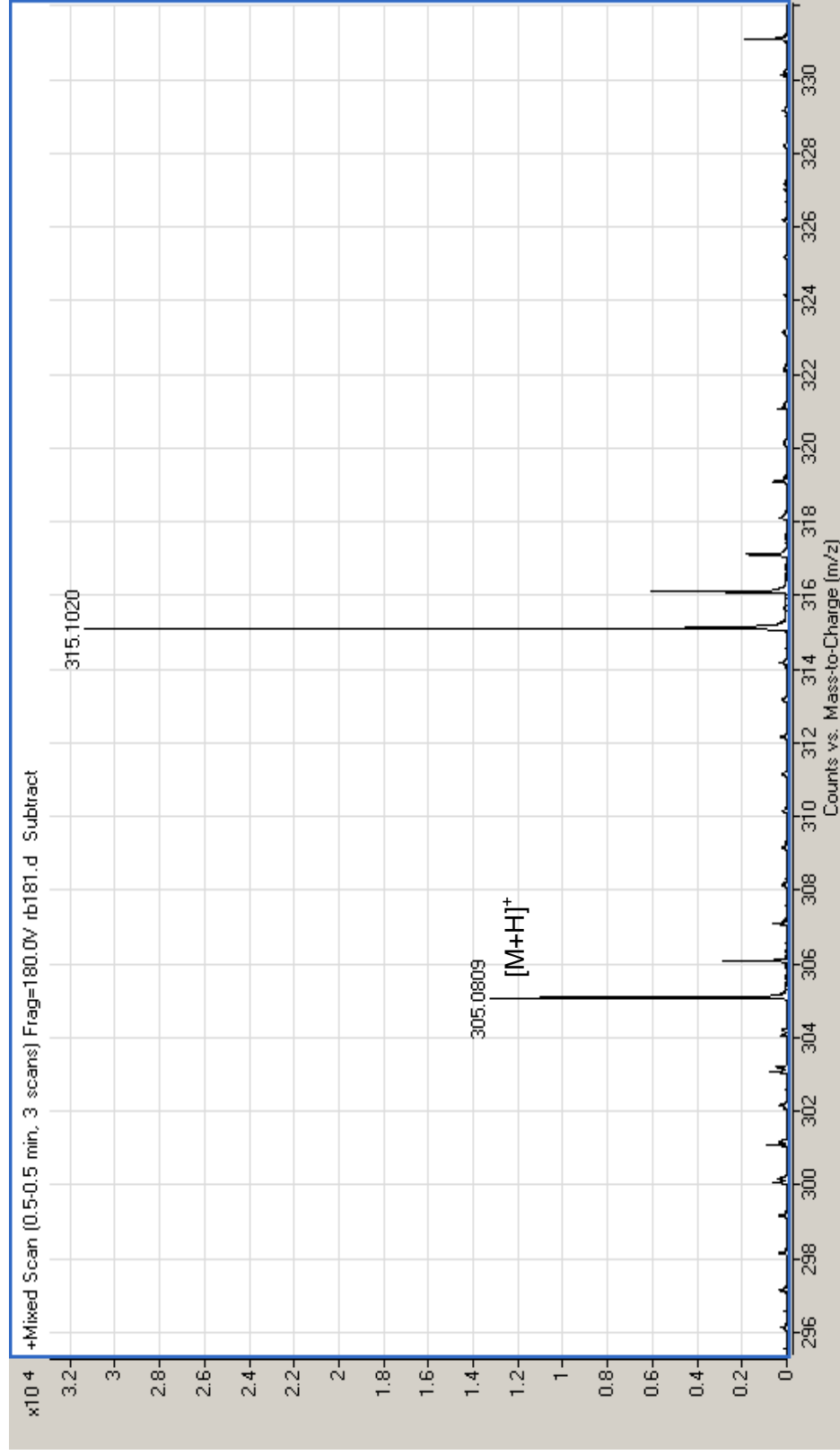
S18. gCOSY NMR spectrum (500 MHz, CDCl_3) of haemodordione (**13**).



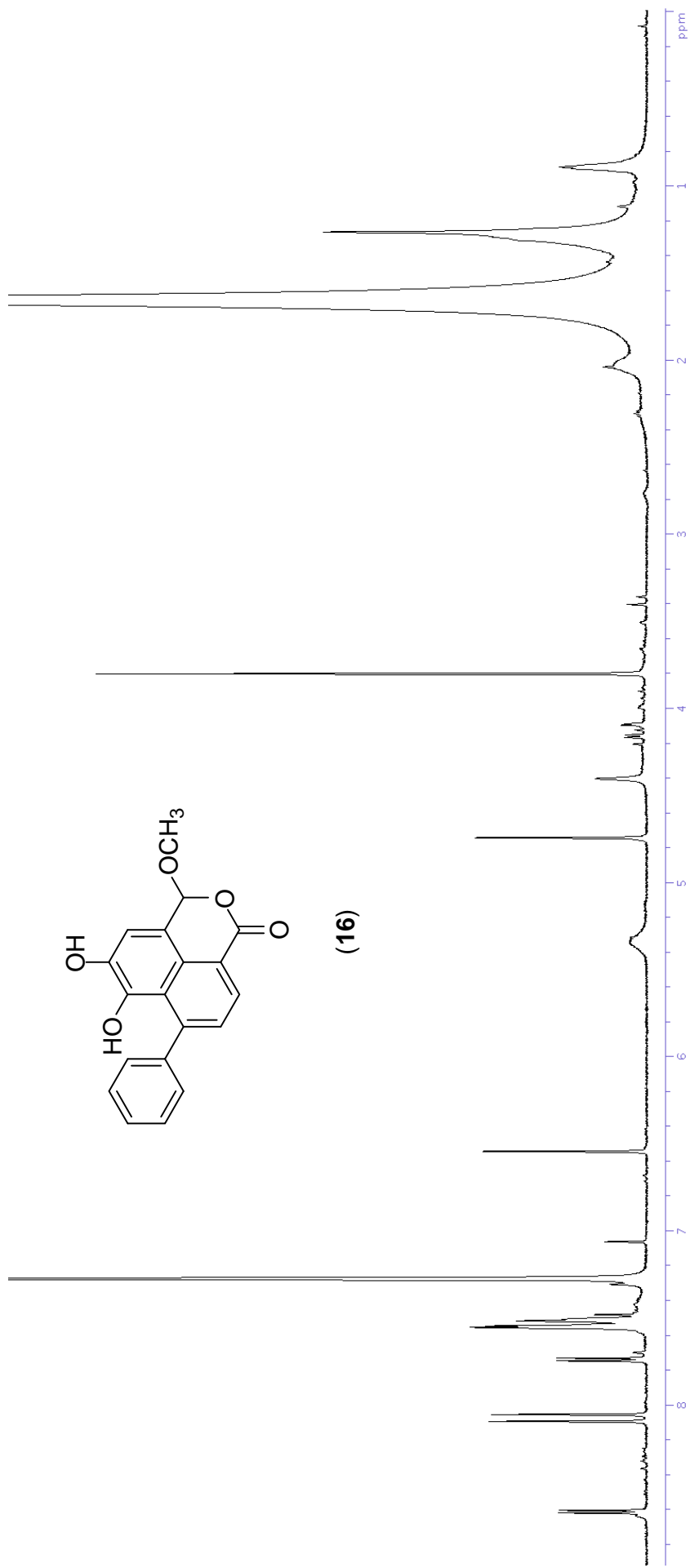
S19. gHSQCAD NMR spectrum (500 MHz, CDCl₃) of haemodordione (**13**).



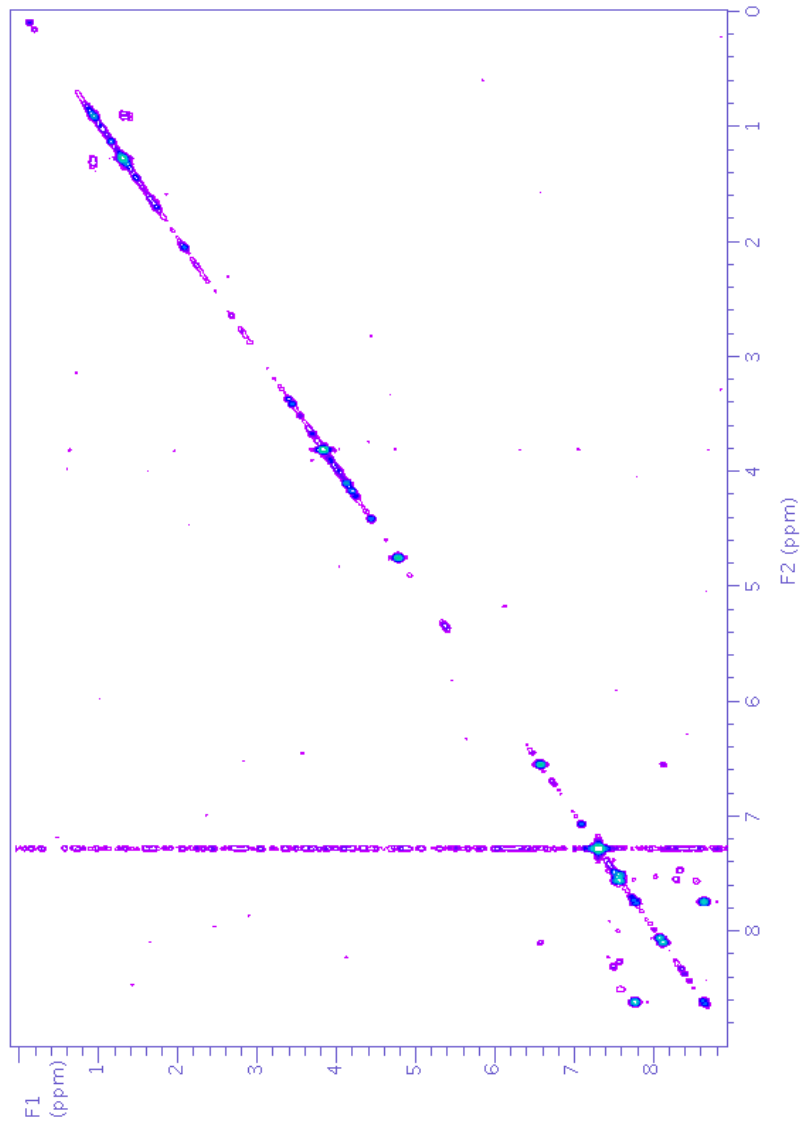
S20. gHMBC NMR spectrum (500 MHz, CDCl₃) of haemodordione (**13**).



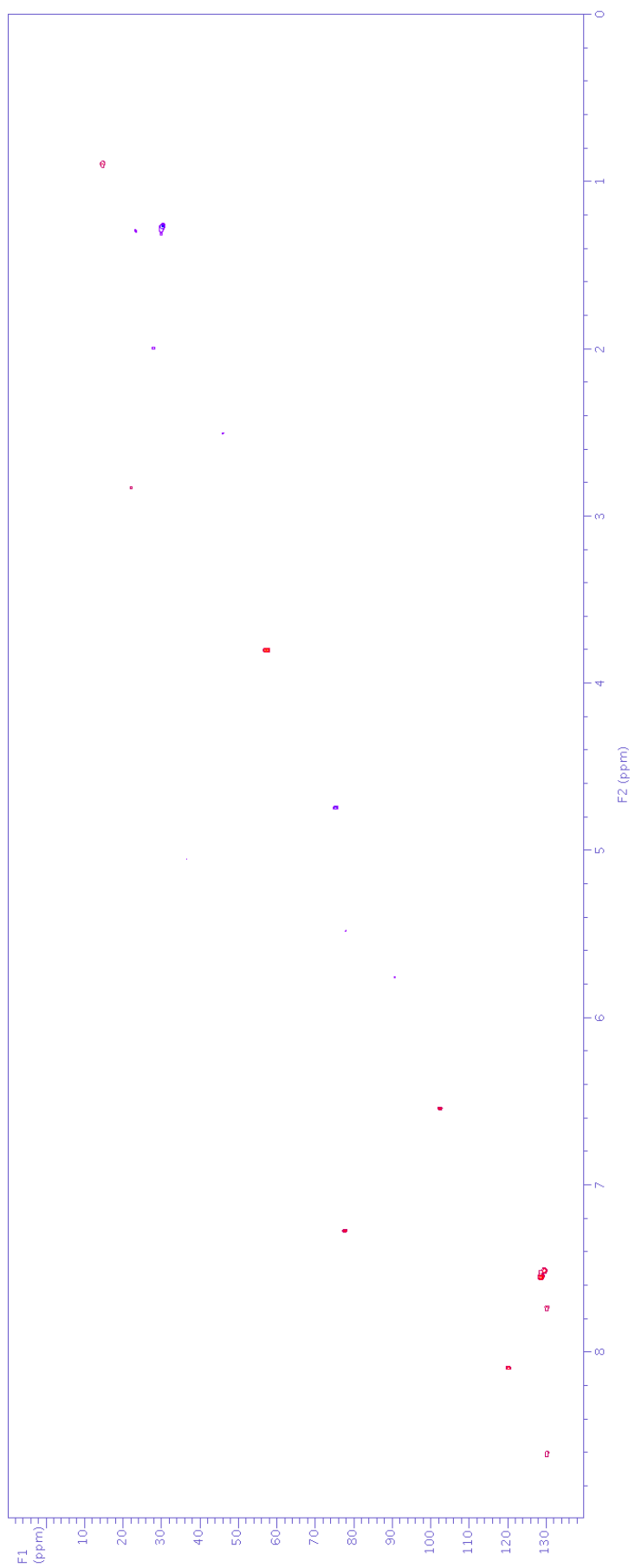
S21. High resolution positive ESI-MS of haemodione (**13**).



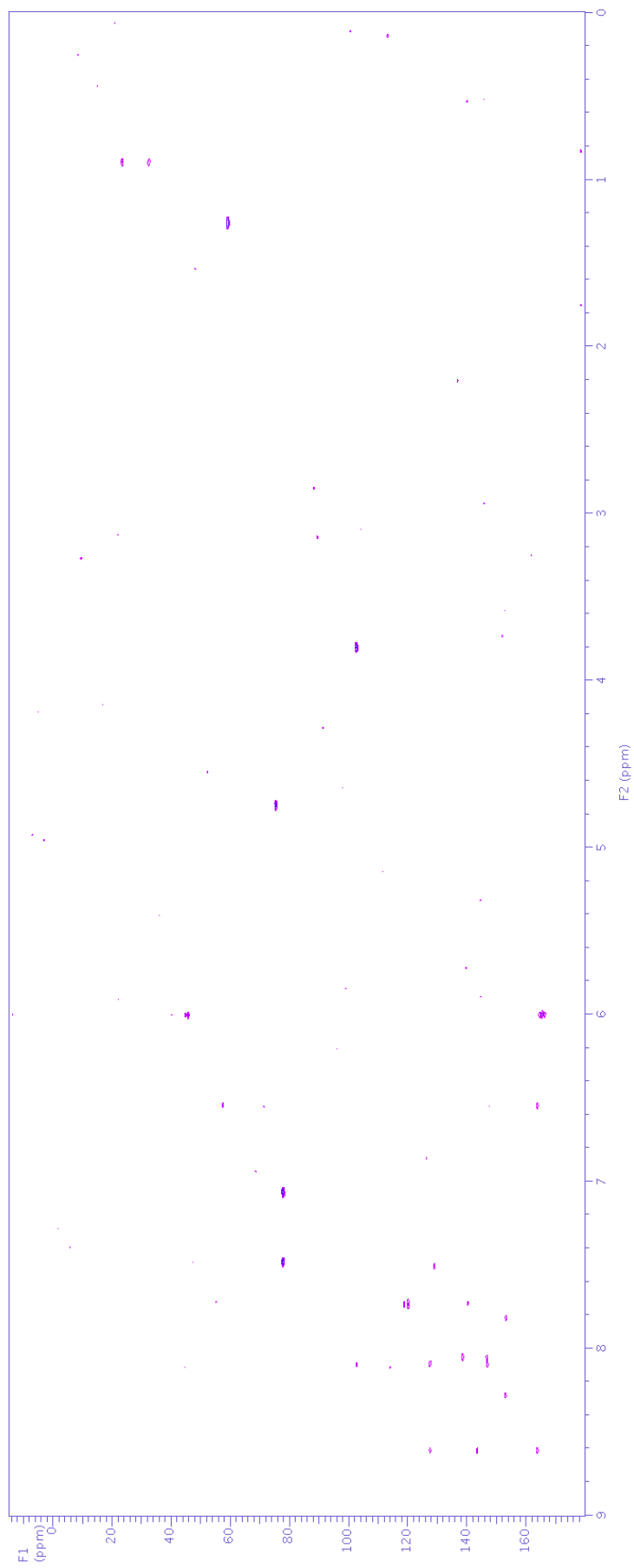
S22. ¹H NMR spectrum (500 MHz, CDCl₃) of haemodordiol (**16**).



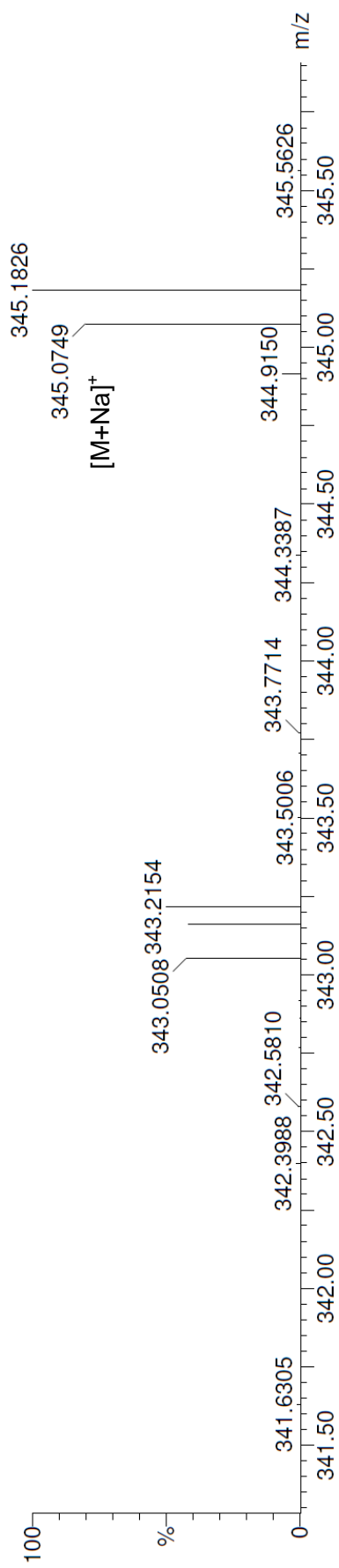
S23. gCOSY NMR spectrum (500 MHz, CDCl₃) of haemodordiol (**16**).



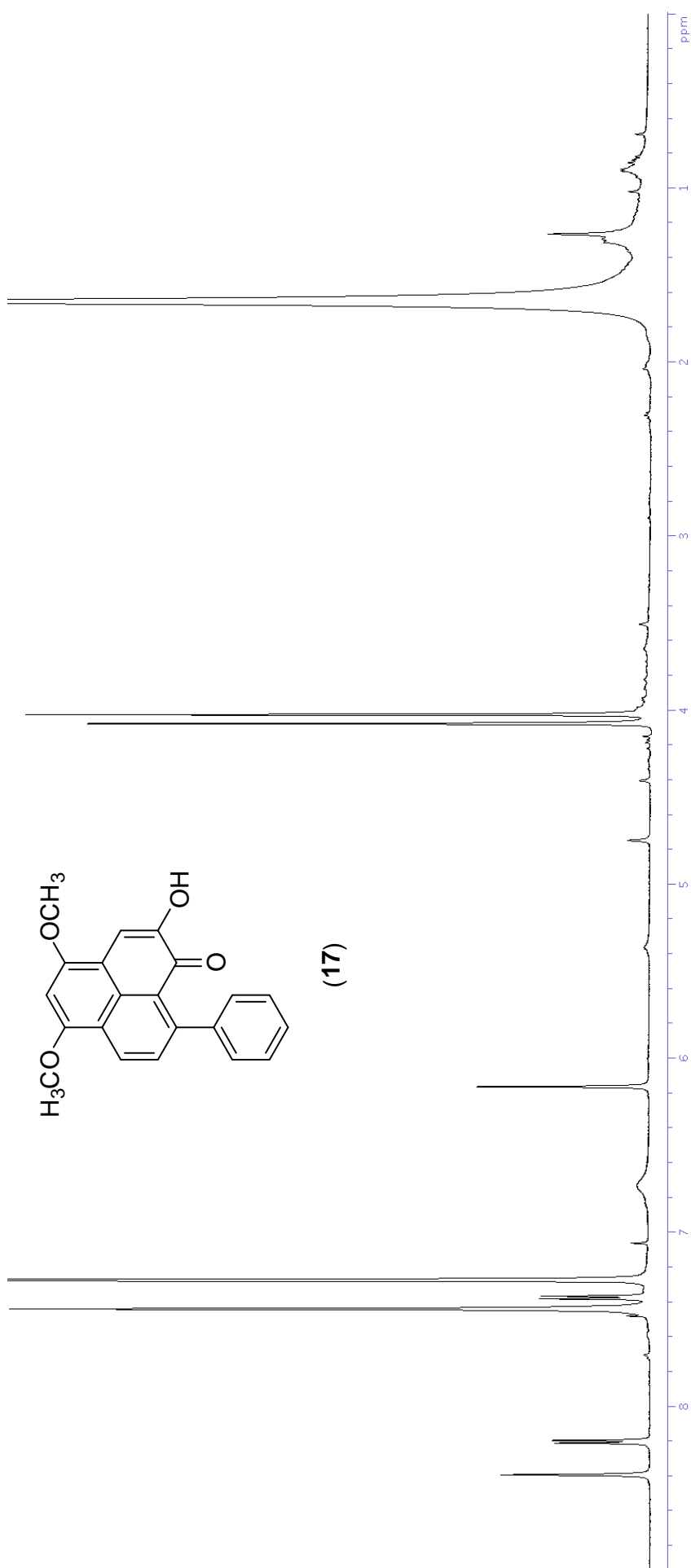
S24. gHSQCAD NMR spectrum (500 MHz, CDCl₃) of haemodordiol (**16**).



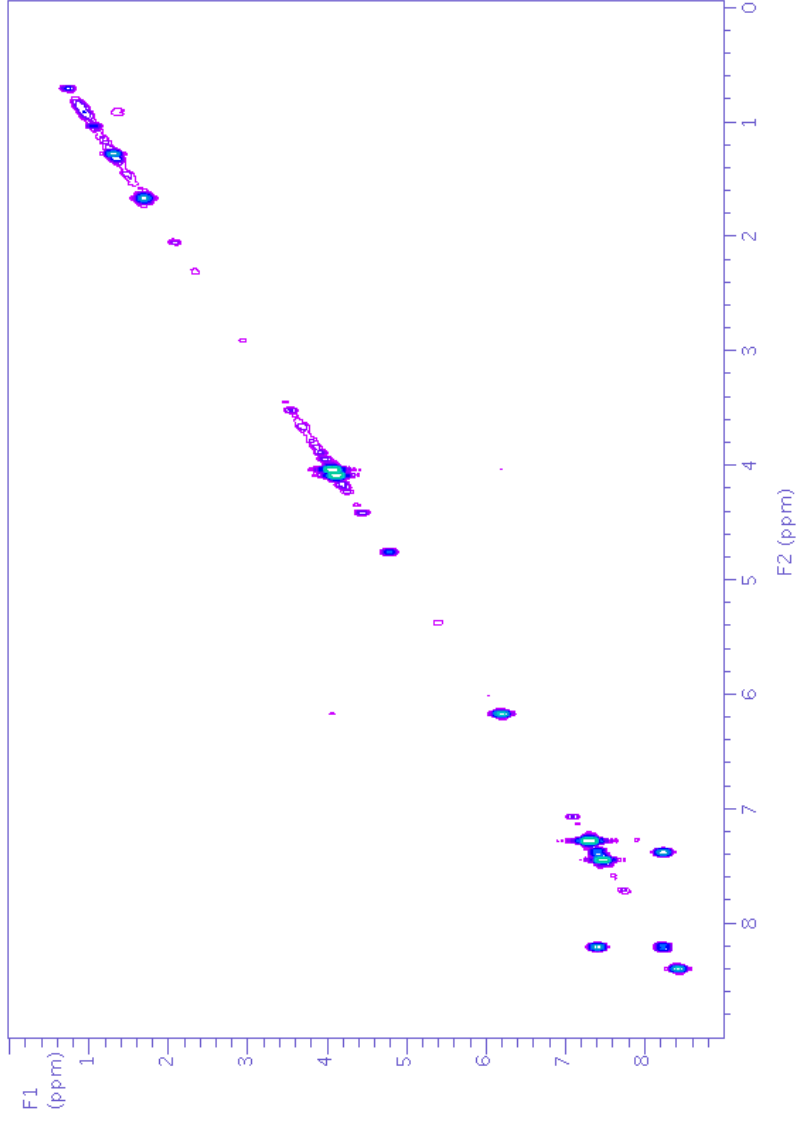
S25. gHMBC NMR spectrum (500 MHz, CDCl₃) of haemodordiol (**16**).



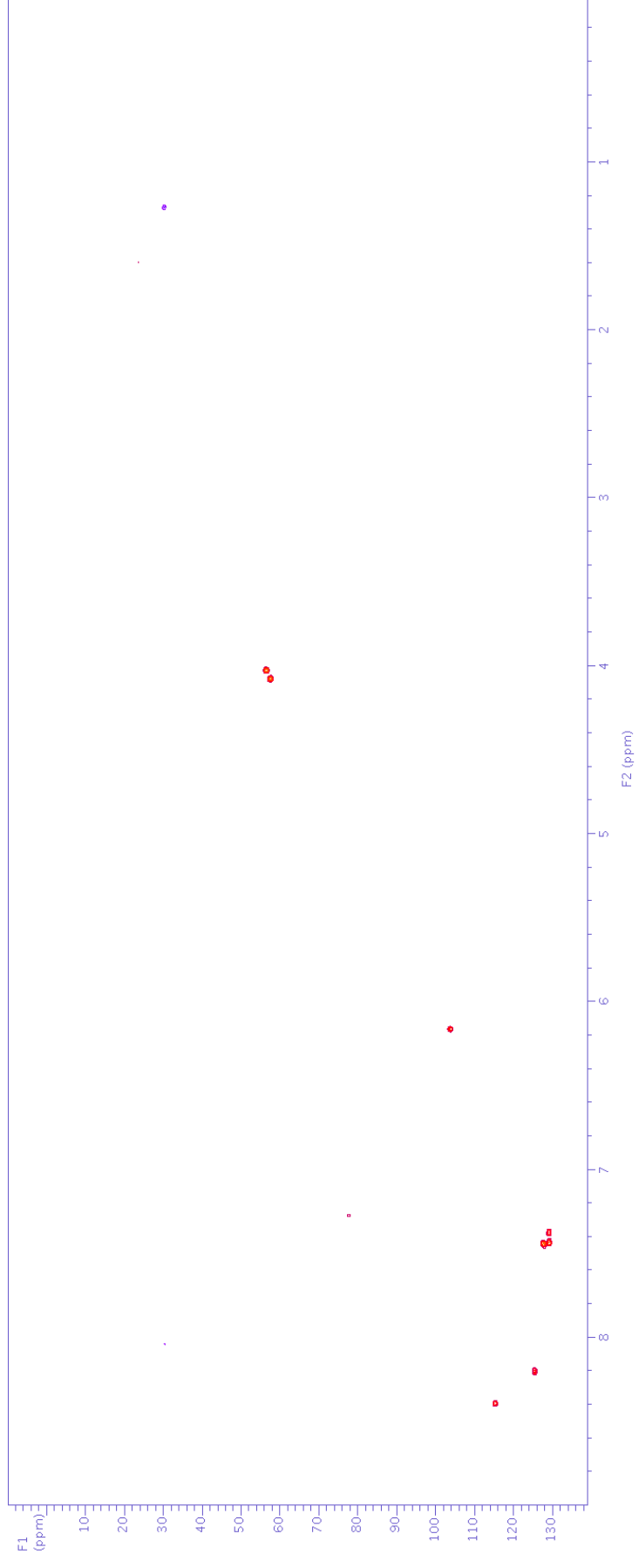
S26. High resolution ASAP-MS of haemodordiol (**16**).



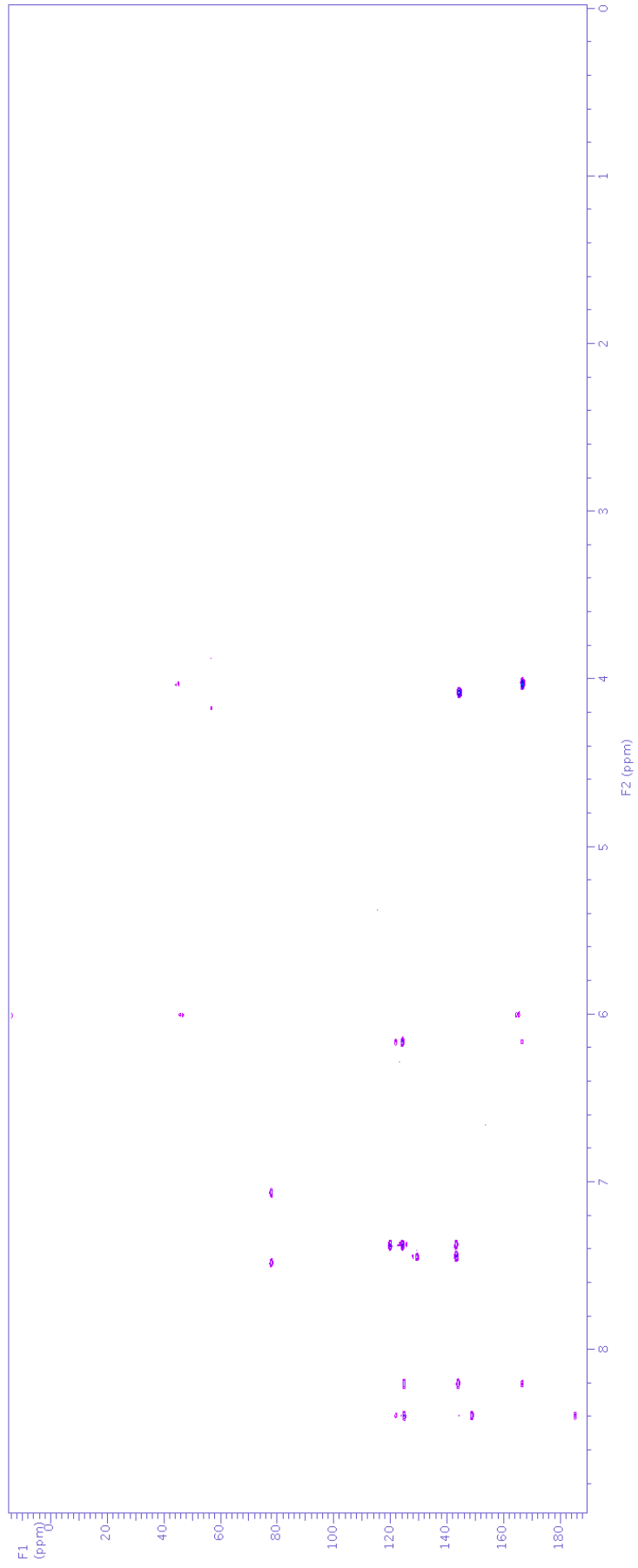
S27. ^1H NMR spectrum (500 MHz, CDCl_3) of haemodoronol (**17**).



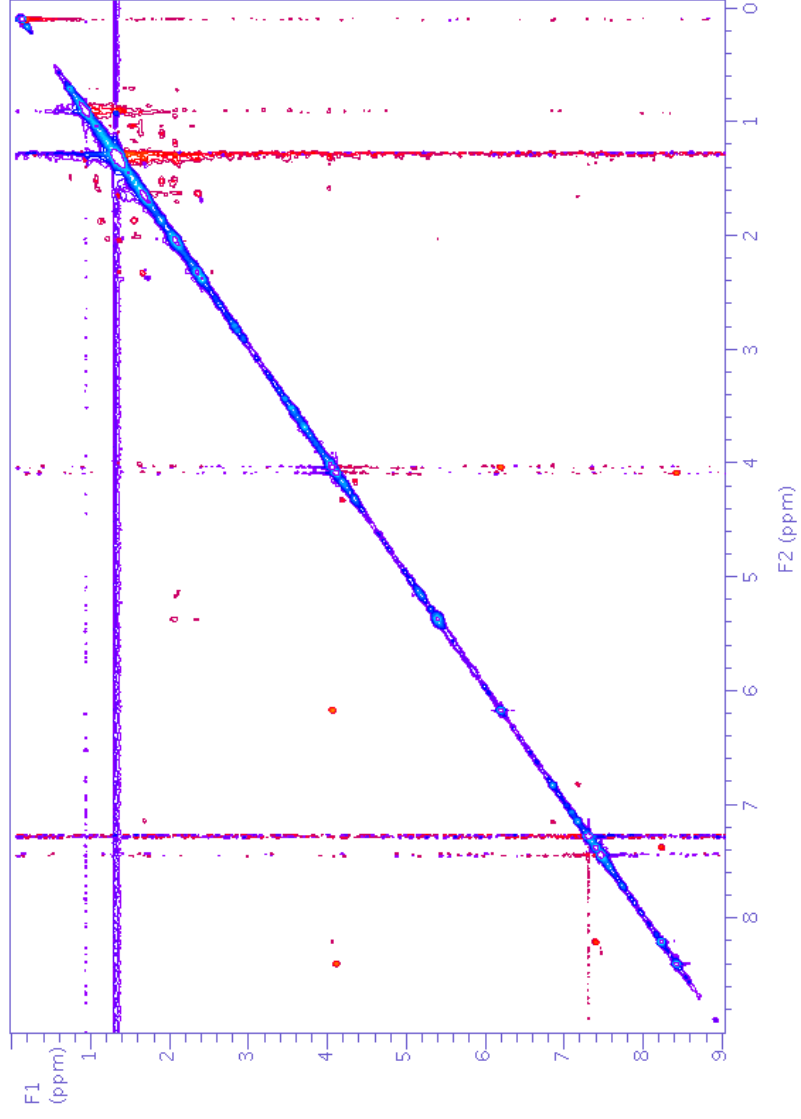
S28. gCOSY NMR spectrum (500 MHz, CDCl₃) of haemodoronol (**17**).



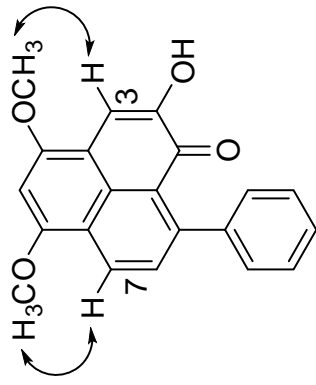
S29. gHSQC NMR spectrum (500 MHz, CDCl₃) of haemodoronol (**17**).



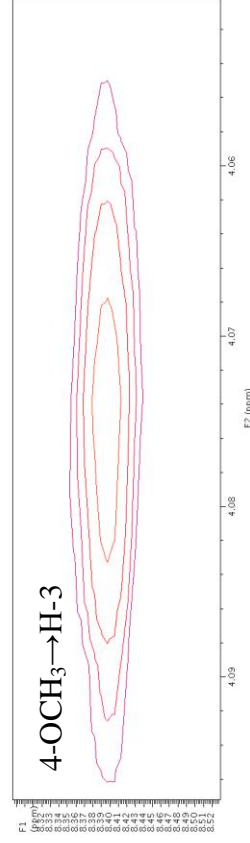
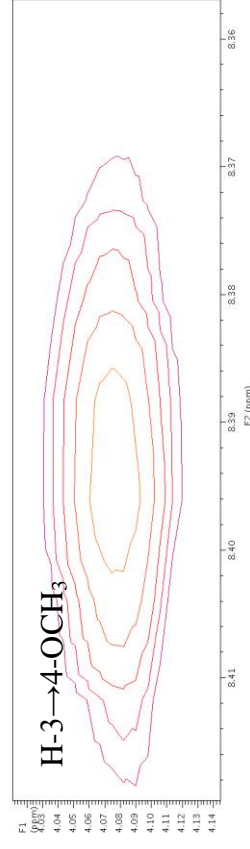
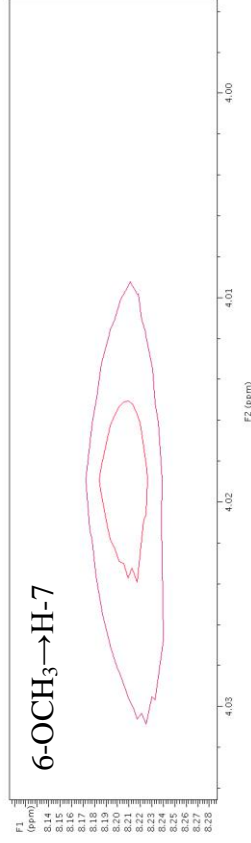
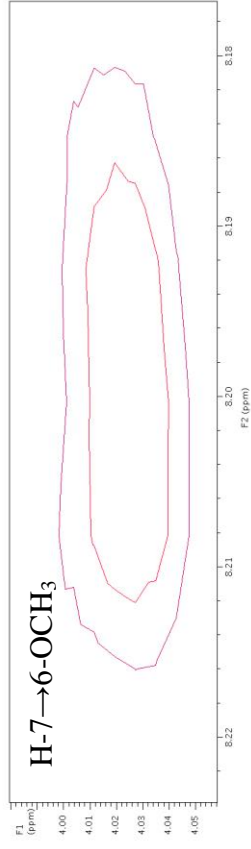
S30. gHMBC NMR spectrum (500 MHz, CDCl₃) of haemodoronol (**17**).



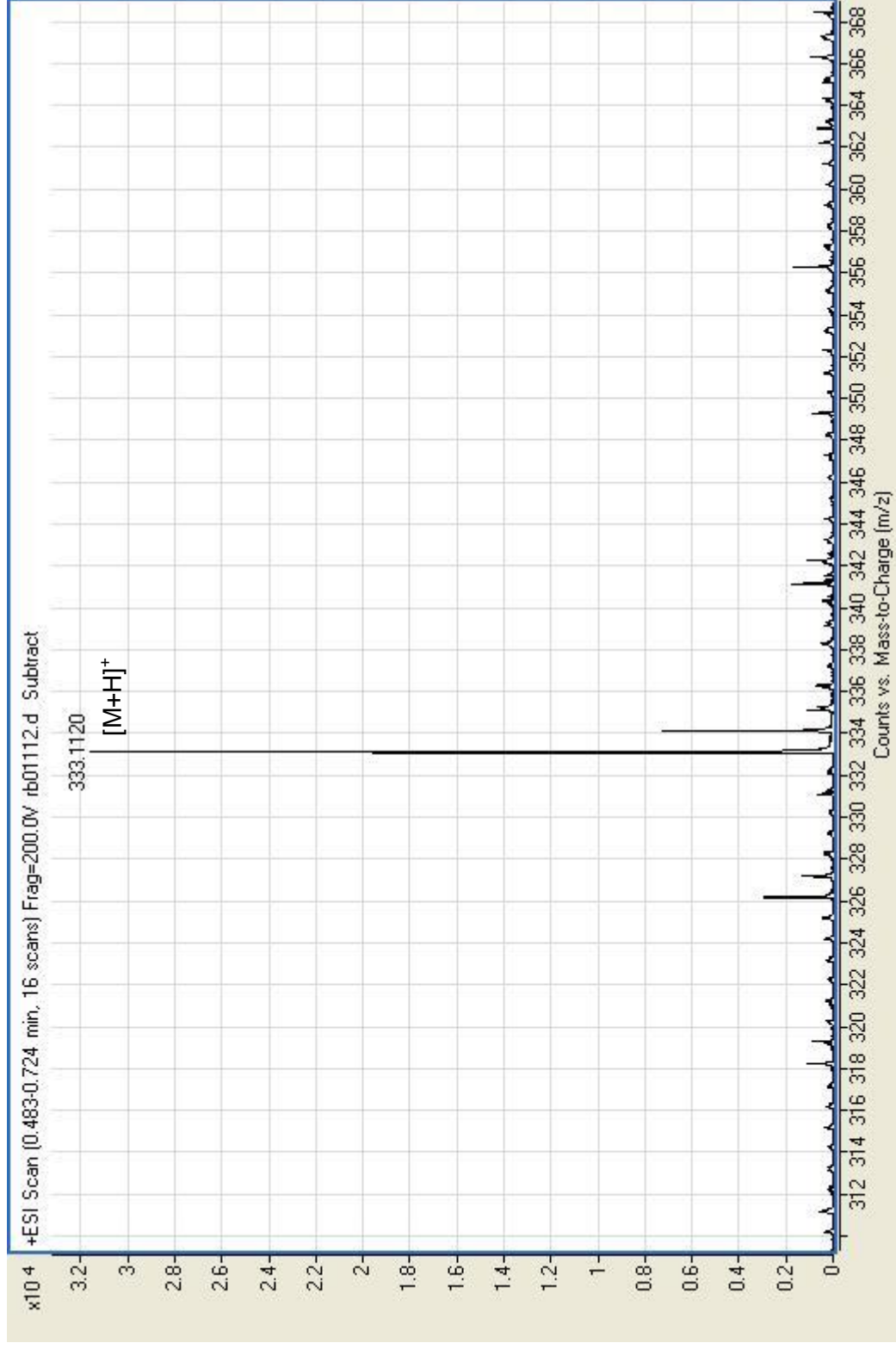
S31. NOESY NMR spectrum (500 MHz, CDCl_3) of haemodoronol (**17**).



(17)



S32. Expansion of NOESY NMR spectrum (500 MHz, CDCl₃) of haemodoronol (17).



S33. High resolution positive ESI-MS of haemodoronol (**17**).

APPENDIX D

Supplementary Information for the Dereplication Studies

Conducted on Seven Marine Algae

This appendix contains further information relevant to the dereplication studies (HPLC-NMR & HPLC-MS) conducted on seven marine algae as given in Chapter 8.

Supplementary Information

Order Based on Retention Time

Figure S1. Extracted UV profile of compound eluting at 2.29 min (**2**) from HPLC-NMR (*S. decipiens*).

Figure S2. WET1D Proton NMR spectrum (500 MHz, 75% CH₃CN/D₂O) of compound eluting at 2.29 min (**2**) (*S. decipiens*).

Figure S3. gCOSY NMR spectrum (500 MHz, 75% CH₃CN/D₂O) of compounds eluting at 2.29 (**2**) and 2.44 min (**3**) (peaks diffused during stop-flow analysis) (*S. decipiens*).

Figure S4. HSQCAD NMR spectrum (500 MHz, 75% CH₃CN/D₂O) of compounds eluting at 2.29 (**2**) and 2.44 min (**3**) (peaks diffused during stop-flow analysis) (*S. decipiens*).

Figure S5. gHMBCAD NMR spectrum (500 MHz, 75% CH₃CN/D₂O) of compounds eluting at 2.29 (**2**) and 2.44 min (**3**) (peaks diffused during stop-flow analysis) (*S. decipiens*).

Figure S6. High resolution negative ESI-MS of compound eluting at 2.29 min (**2**) from HPLC-MS (*S. decipiens*).

Figure S7. NMR data for compound eluting at 2.29 min (**2**) (*S. decipiens*).

Figure S8. Extracted UV profile of compound eluting at 2.44 min (**3**) from HPLC-NMR (*S. decipiens*).

Figure S9. WET1D Proton NMR spectrum (500 MHz, 75% CH₃CN/D₂O) of compound eluting at 2.44 min (**3**) (*S. decipiens*).

Figure S10. High resolution negative ESI-MS of compound eluting at 2.44 min (**3**) from HPLC-MS (*S. decipiens*).

Figure S11. NMR data for compound eluting at 2.44 min (**3**) (*S. decipiens*).

Figure S12. Extracted UV profile of compound eluting at 3.42 min (**11**) from HPLC-NMR (*C. retroflexa*).

Figure S13. WET1D Proton NMR spectrum (500 MHz, 75% CH₃CN/D₂O) of compound eluting at 3.42 min (**11**) (*C. retroflexa*).

Figure S14. High resolution negative ESI-MS of compound eluting at 3.42 min (**11**) from HPLC-MS (*C. retroflexa*).

Figure S15. NMR data for compound eluting at 3.42 min (**11**) (*C. retroflexa*).

Figure S16. Extracted UV profile of compound eluting at 3.55 min (**1**) from HPLC-NMR (*S. decipiens*).

Figure S17. WET1D Proton NMR spectrum (500 MHz, 75% CH₃CN/D₂O) of compound eluting at 3.55 min (**1**) (*S. decipiens*).

Figure S18. gCOSY NMR spectrum (500 MHz, 75% CH₃CN/D₂O) of compound eluting at 3.55 min (**1**) (*S. decipiens*).

Figure S19. High resolution negative ESI-MS of compound eluting at 3.55 min (**1**) from HPLC-MS (*S. decipiens*).

Figure S20. NMR data for compound eluting at 3.55 min (**1**) (*S. decipiens*).

Figure S21. Extracted UV profile of compound eluting at 4.45 min (**16**) from HPLC-NMR (*C. retroflexa*).

Figure S22. WET1D Proton NMR spectrum (500 MHz, 75% CH₃CN/D₂O) of compound eluting at 4.45 min (**16**) (*C. retroflexa*).

Figure S23. gCOSY NMR spectrum (500 MHz, 75% CH₃CN/D₂O) of compound eluting at 4.45 min (**16**) (*C. retroflexa*).

Figure S24. HSQCAD NMR spectrum (500 MHz, 75% CH₃CN/D₂O) of compound eluting at 4.45 min (**16**) (*C. retroflexa*).

Figure S25. gHMBCAD NMR spectrum (500 MHz, 75% CH₃CN/D₂O) of compound eluting at 4.45 min (**16**) (*C. retroflexa*).

Figure S26. High resolution negative ESI-MS of compound eluting at 4.45 min (**16**) from HPLC-MS (*C. retroflexa*).

Figure S27. Extracted UV profile of compound eluting at 5.00 min from HPLC-NMR (*Laurencia* sp.).

Figure S28. WET1D Proton NMR spectrum (500 MHz, 75% CH₃CN/D₂O) of compound eluting at 5.00 min (*Laurencia* sp.).

Figure S29. gCOSY NMR spectrum (500 MHz, 75% CH₃CN/D₂O) of compound eluting at 5.00 min (*Laurencia* sp.).

Figure S30. Extracted UV profile of compound eluting at 6.05 min from HPLC-NMR (*Laurencia* sp.).

Figure S31. WET1D Proton NMR spectrum (500 MHz, 75% CH₃CN/D₂O) of compound eluting at 6.05 min (*Laurencia* sp.).

Figure S32. gCOSY NMR spectrum (500 MHz, 75% CH₃CN/D₂O) of compound eluting at 6.05 min (*Laurencia* sp.).

Figure S33. HSQCAD NMR spectrum (500 MHz, 75% CH₃CN/D₂O) of compound eluting at 6.05 min (*Laurencia* sp.).

Figure S34. gHMBCAD NMR spectrum (500 MHz, 75% CH₃CN/D₂O) of compound eluting at 6.05 min (*Laurencia* sp.).

Figure S35. Extracted UV profile of compound eluting at 6.70 min from HPLC-NMR (*Laurencia* sp.).

Figure S36. WET1D Proton NMR spectrum (500 MHz, 75% CH₃CN/D₂O) of compound eluting at 6.70 min (*Laurencia* sp.).

Figure S37. gCOSY NMR spectrum (500 MHz, 75% CH₃CN/D₂O) of compound eluting at 6.70 min (*Laurencia* sp.).

Figure S38. Extracted UV profile of compound eluting at 7.87 min (**4**) from HPLC-NMR (*S. decipiens*).

Figure S39. WET1D Proton NMR spectrum (500 MHz, 75% CH₃CN/D₂O) of compound eluting at 7.87 min (**4**) (*S. decipiens*).

Figure S40. gCOSY NMR spectrum (500 MHz, 75% CH₃CN/D₂O) of compound eluting at 7.87 min (**4**) (*S. decipiens*).

Figure S41. High resolution negative ESI-MS of compound eluting at 7.87 min (**4**) from HPLC-MS (*S. decipiens*).

Figure S42. NMR data for compound eluting at 7.87 min (**4**) (*S. decipiens*).

Figure S43. Extracted UV profile of compound eluting at 9.98 min (**12**) from HPLC-NMR (*C. retroflexa*).

Figure S44. WET1D Proton NMR spectrum (500 MHz, 75% CH₃CN/D₂O) of compound eluting at 9.98 min (**12**) (*C. retroflexa*).

Figure S45. gCOSY NMR spectrum (500 MHz, 75% CH₃CN/D₂O) of compound eluting at 9.98 min (**12**) (*C. retroflexa*).

Figure S46. HSQCAD NMR spectrum (500 MHz, 75% CH₃CN/D₂O) of compound eluting at 9.98 min (**12**) (*C. retroflexa*).

Figure S47. gHMBCAD NMR spectrum (500 MHz, 75% CH₃CN/D₂O) of compound eluting at 9.98 min (**12**) (*C. retroflexa*).

Figure S48. High resolution negative ESI-MS of compound eluting at 9.98 min (**12**) from HPLC-MS (*C. retroflexa*).

Figure S49. NMR data for compound eluting at 9.98 min (**12**) (*C. retroflexa*).

Figure S50. Extracted UV profile of compound eluting at 12.95 min (**13**) from HPLC-NMR (*C. retroflexa*).

Figure S51. WET1D Proton NMR spectrum (500 MHz, 75% CH₃CN/D₂O) of compound eluting at 12.95 min (**13**) (*C. retroflexa*).

Figure S52. gCOSY NMR spectrum (500 MHz, 75% CH₃CN/D₂O) of compound eluting at 12.95 min (**13**) (*C. retroflexa*).

Figure S53. HSQCAD NMR spectrum (500 MHz, 75% CH₃CN/D₂O) of compound eluting at 12.95 min (**13**) (*C. retroflexa*).

Figure S54. High resolution negative ESI-MS of compound eluting at 12.95 min (**13**) from HPLC-MS (*C. retroflexa*).

Figure S55. NMR data for compound eluting at 12.95 min (**13**) (*C. retroflexa*).

Figure S56. Extracted UV profile of compound eluting at 13.65 min (**17**) from HPLC-NMR (*S. cf. fallax*).

Figure S57. WET1D Proton NMR spectrum (500 MHz, 75% CH₃CN/D₂O) of compound eluting at 13.65 min (**17**) (*S. cf. fallax*).

Figure S58. gCOSY NMR spectrum (500 MHz, 75% CH₃CN/D₂O) of compound eluting at 13.65 min (**17**) (*S. cf. fallax*).

Figure S59. High resolution negative ESI-MS of compound eluting at 13.65 min (**17**) from HPLC-MS (*S. cf. fallax*).

Figure S60. Extracted UV profile of compound eluting at 14.53 min (**5**) from HPLC-NMR (*H. pseudospicata*).

Figure S61. WET1D Proton NMR spectrum (500 MHz, 75% CH₃CN/D₂O) of compound eluting at 14.53 min (**5**) (*H. pseudospicata*).

Figure S62. gCOSY NMR spectrum (500 MHz, 75% CH₃CN/D₂O) of compound eluting at 14.53 min (**5**) (*H. pseudospicata*).

Figure S63. HSQCAD NMR spectrum (500 MHz, 75% CH₃CN/D₂O) of compound eluting at 14.53 min (**5**) (*H. pseudospicata*).

Figure S64. ROESYAD NMR spectrum (500 MHz, 75% CH₃CN/D₂O) of compound eluting at 14.53 min (**5**) (*H. pseudospicata*).

Figure S65. High resolution negative ESI-MS of compound eluting at 14.53 min (**5**) from HPLC-MS (*H. pseudospicata*).

Figure S66. High resolution positive ESI-MS of compound eluting at 14.53 min (**5**) from HPLC-MS (*H. pseudospicata*).

Figure S67. NMR data for compound eluting at 14.53 min (**5**) (*H. pseudospicata*).

Figure S68. Extracted UV profile of compound eluting at 15.50 min (**20**) from HPLC-NMR (*S. cf. fallax*).

Figure S69. WET1D Proton NMR spectrum (500 MHz, 75% CH₃CN/D₂O) of compound eluting at 15.50 min (**20**) (*S. cf. fallax*).

Figure S70. High resolution negative ESI-MS of compound eluting at 15.50 min (**20**) from HPLC-MS (*S. cf. fallax*).

Figure S71. NMR data for compound eluting at 15.50 min (**20**) (*S. cf. fallax*).

Figure S72. Extracted UV profile of compound eluting at 20.15 min (**21**) from HPLC-NMR (*C. retroflexa*).

Figure S73. WET1D Proton NMR spectrum (500 MHz, 75% CH₃CN/D₂O) of compound eluting at 20.15 min (**21**) (*C. retroflexa*).

Figure S74. High resolution negative ESI-MS of compound eluting at 20.15 min (**21**) from HPLC-MS (*C. retroflexa*).

Figure S75. NMR data for compound eluting at 20.15 min (**21**) (*C. retroflexa*).

Figure S76. Extracted UV profile of compound eluting at 21.62 min (**14**) from HPLC-NMR (*S. cf. fallax*).

Figure S77. WET1D Proton NMR spectrum (500 MHz, 75% CH₃CN/D₂O) of compound eluting at 21.62 min (**14**) (*S. cf. fallax*).

Figure S78. High resolution negative ESI-MS of compound eluting at 21.62 min (**14**) from HPLC-MS (*S. cf. fallax*).

Figure S79. NMR data for compound eluting at 21.62 min (**14**) (*S. cf. fallax*).

Figure S80. Extracted UV profile of compound eluting at 22.96 min (**18**) from HPLC-NMR (*C. subfarcinata*).

Figure S81. WET1D Proton NMR spectrum (500 MHz, 75% CH₃CN/D₂O) of compound eluting at 22.96 min (**18**) (*C. subfarcinata*).

Figure S82. High resolution negative ESI-MS of compound eluting at 22.96 min (**18**) from HPLC-MS (*C. subfarcinata*).

Figure S83. Extracted UV profile of compound eluting at 23.16 min from HPLC-NMR (*C. retroflexa*).

Figure S84. WET1D Proton NMR spectrum (500 MHz, 75% CH₃CN/D₂O) of compound eluting at 23.16 min (*C. retroflexa*).

Figure S85. Extracted UV profile of compound eluting at 26.71 min from HPLC-NMR (*H. pseudospicata*).

Figure S86. Extracted UV profile of compound eluting at 30.27 min from HPLC-NMR (*H. pseudospicata*).

Figure S87. Extracted UV profile of compound eluting at 33.40 min (**19**) from HPLC-NMR (*C. subfarcinata*).

Figure S88. WET1D Proton NMR spectrum (500 MHz, 75% CH₃CN/D₂O) of compound eluting at 33.40 min (**19**) (*C. subfarcinata*).

Figure S89. High resolution negative ESI-MS of compound eluting at 33.40 min (**19**) from HPLC-MS (*C. subfarcinata*).

Figure S90. Extracted UV profile of compound eluting at 60.80 min (**15**) from HPLC-NMR (*S. cf. fallax*).

Figure S91. WET1D Proton NMR spectrum (500 MHz, 75% CH₃CN/D₂O) of compound eluting at 60.80 min (**15**) (*S. cf. fallax*).

Figure S92. NMR data for compound eluting at 60.80 min (**15**) (*S. cf. fallax*).

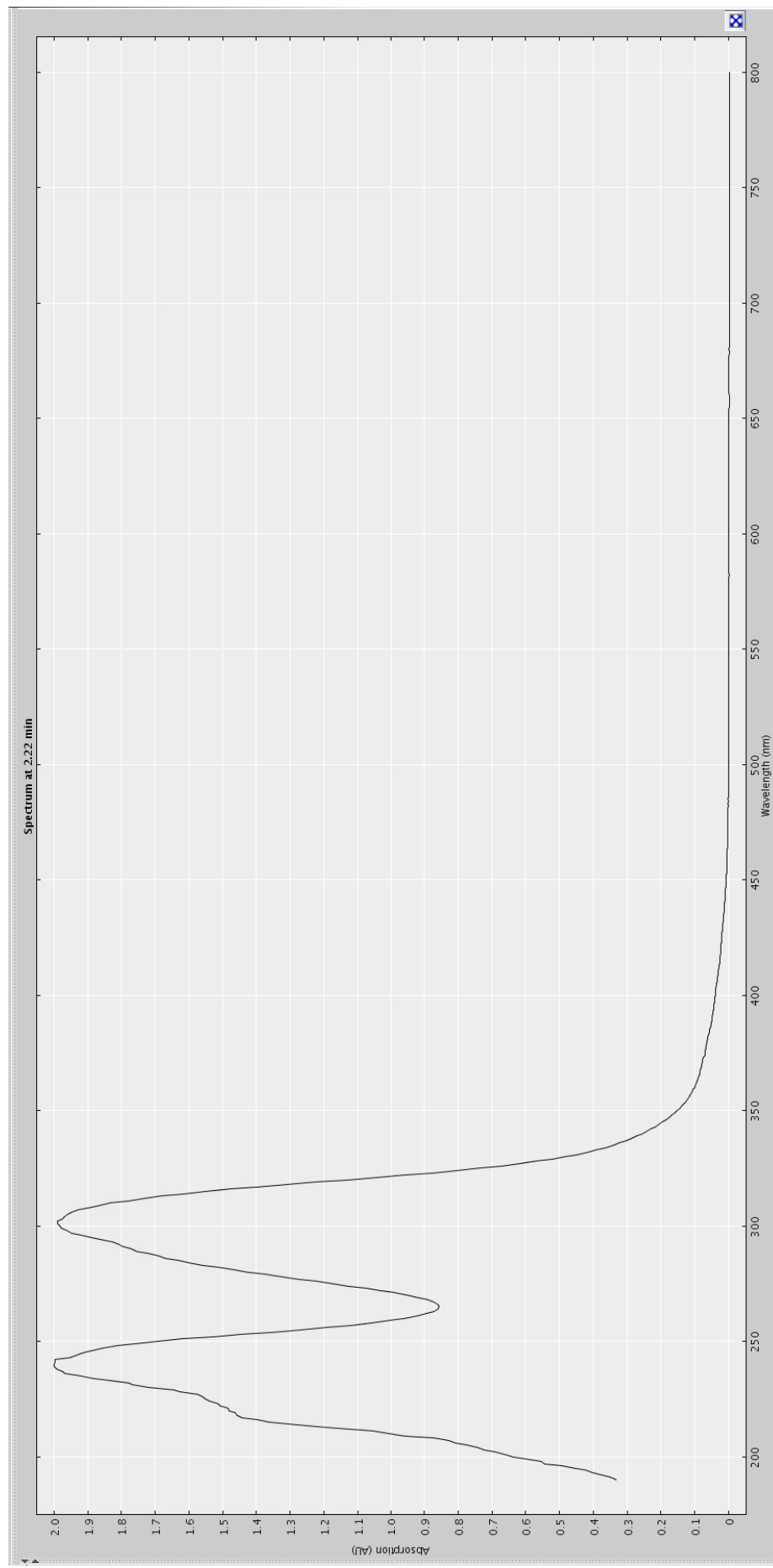


Figure S1. Extracted UV profile of compound eluting at 2.29 min (2) from HPLC-NMR (*S. decipiens*).

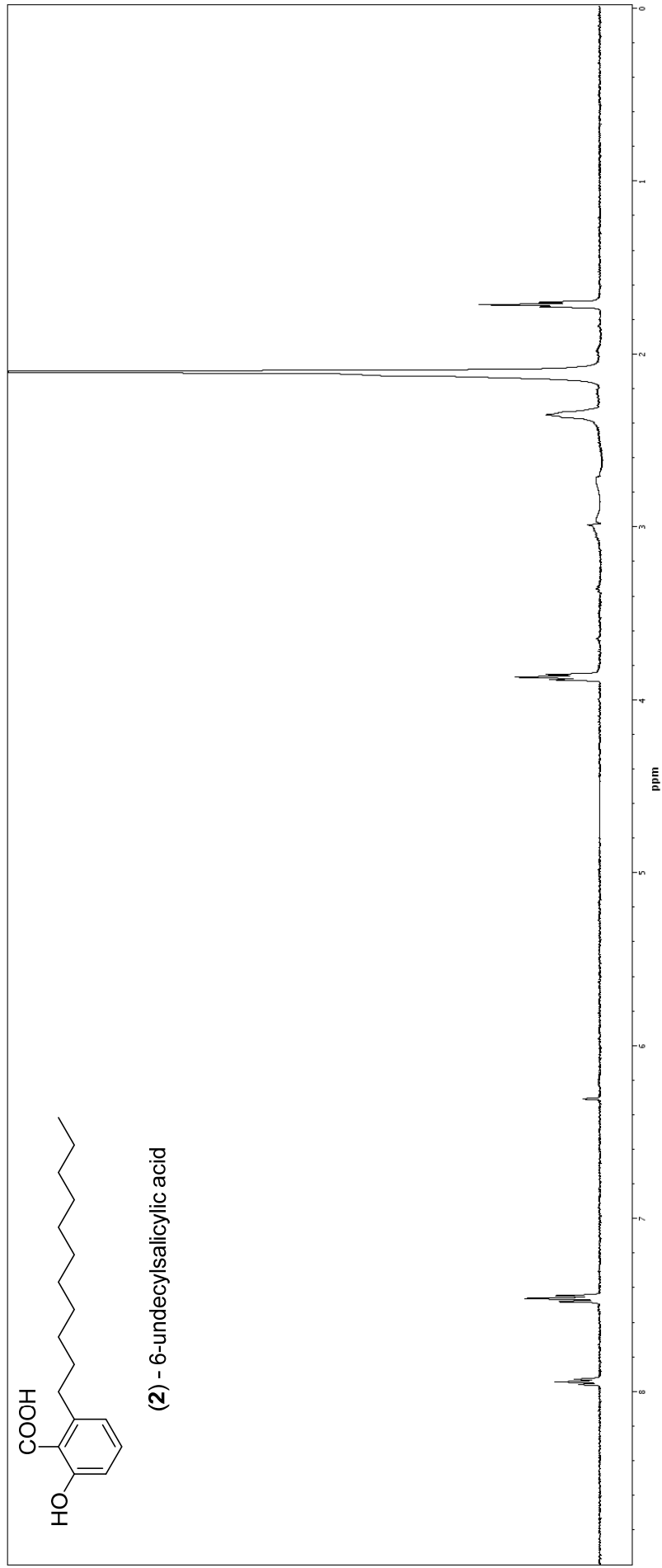


Figure S2. WET1D Proton NMR spectrum (500 MHz, 75% CH₃CN/D₂O) of compound eluting at 2.29 min (**2**) (*S. decipiens*).

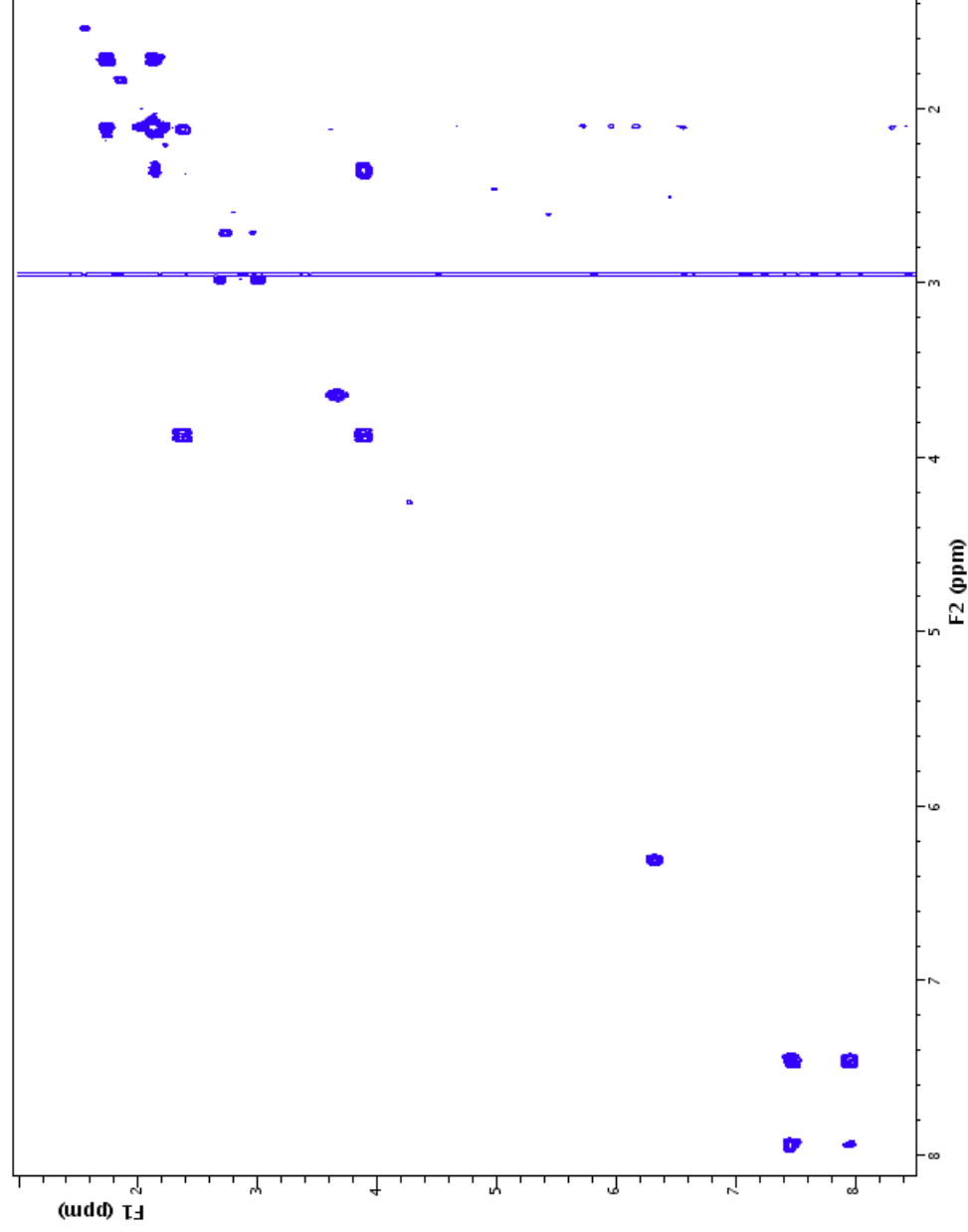


Figure S3. gCOSY NMR spectrum (500 MHz, 75% CH₃CN/D₂O) of compounds eluting at 2.29 (2) and 2.44 min (3) (peaks diffused during stop-flow analysis) (*S. decipiens*).

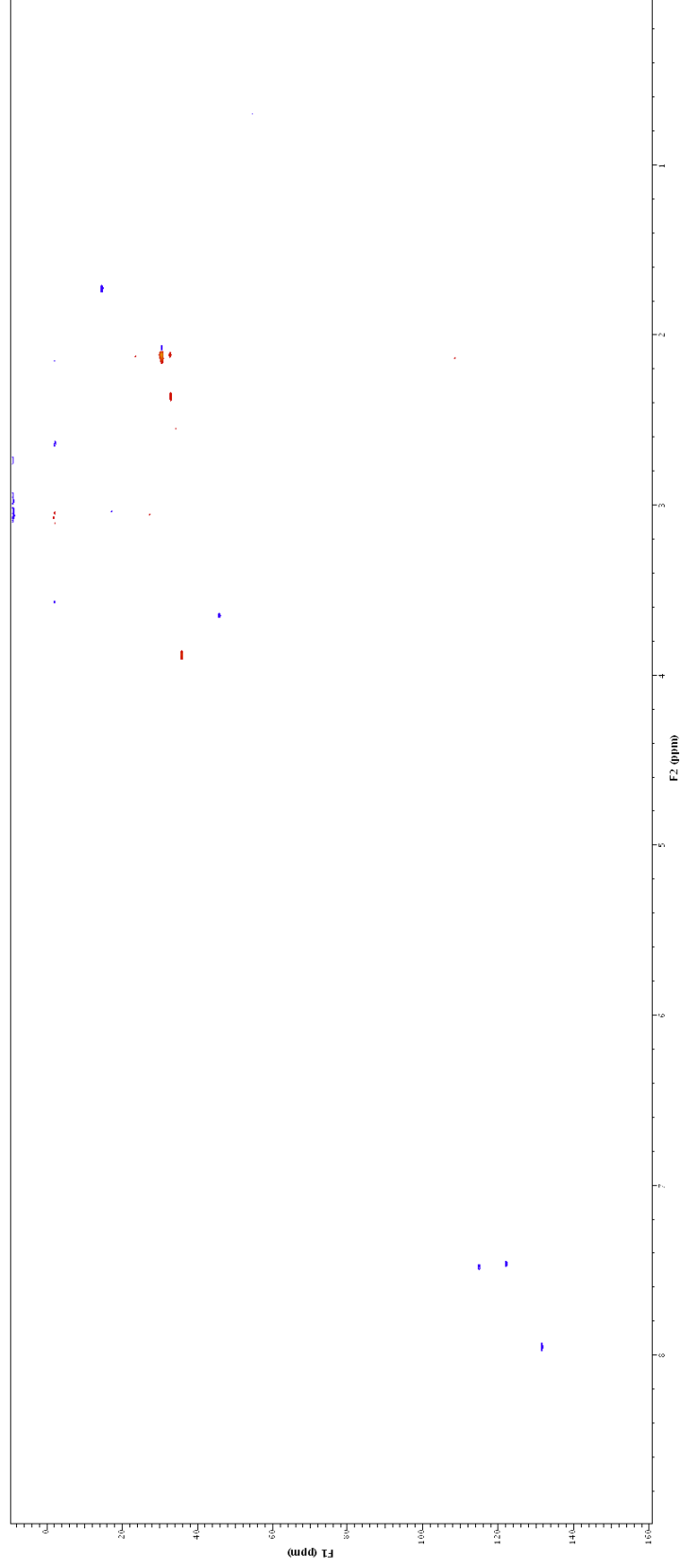


Figure S4. HSQCAD NMR spectrum (500 MHz, 75% CH₃CN/D₂O) of compounds eluting at 2.29 (2) and 2.44 min (3) (peaks diffused during stop-flow analysis) (*S. decipiens*).

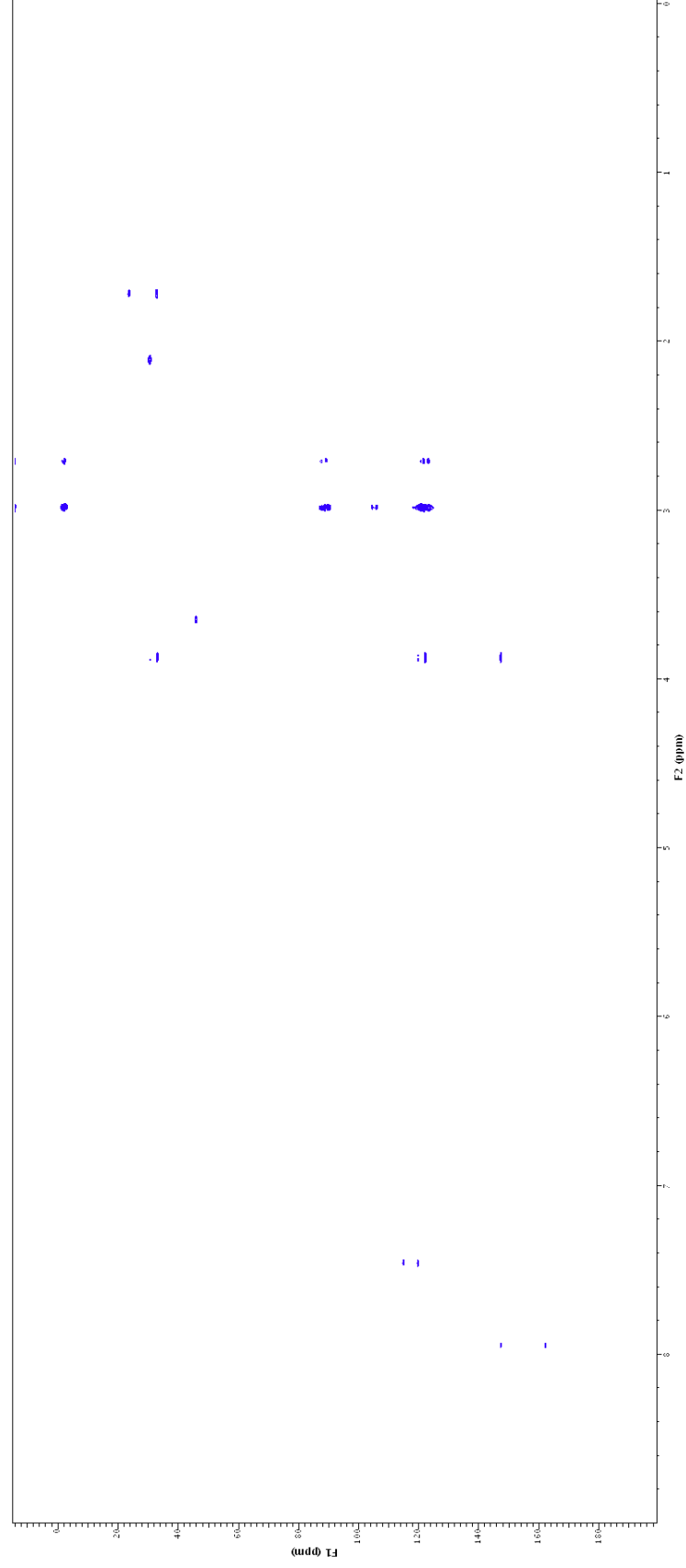


Figure S5. gHMBCAD NMR spectrum (500 MHz, 75% CH₃CN/D₂O) of compounds eluting at 2.29 (**2**) and 2.44 min (**3**) (peaks diffused during stop-flow analysis) (*S. decipiens*).

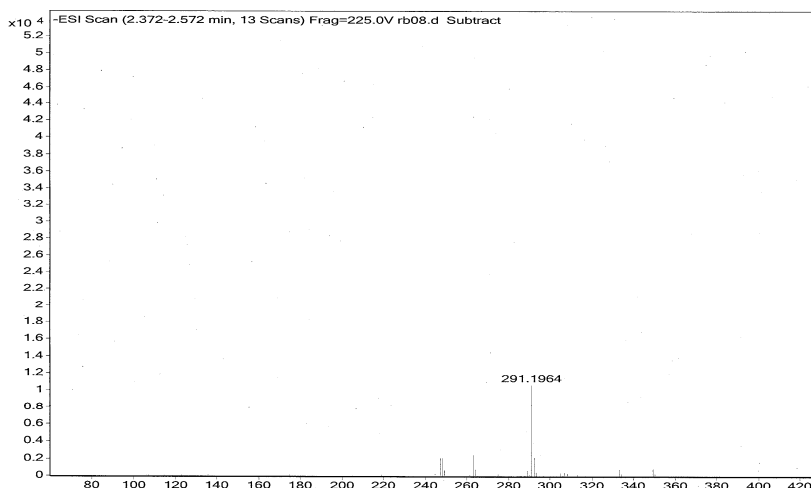
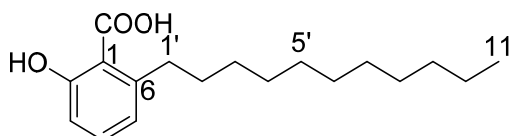


Figure S6. High resolution negative ESI-MS of compound eluting at 2.29 min (**2**) from HPLC-MS (*S. decipiens*).



(2) - 6-undecylsalicylic acid

Position	δ_C^a , mult.	δ_H (J in Hz)	gCOSY	gHMBCAD
1	119.6, s			
2	162.0, s			
3	114.7, d	7.47, d (8.0)	4	-
4	131.4, d	7.94, dd (8.0, 8.0)	3, 5	2, 6
5	121.9, d	7.45, d (8.0)	4	1, 3
6	147.2, s			
7	ND			
1'	35.5, t	3.87, t (7.5)	2'	1, 5, 6, 2', 3'
2'	32.7, t	2.35, m	1'	3', 4'
3'	30.2, t	2.10, m		4', 5'
4'	30.2, t	2.10, m		3', 5', 6'
5'	30.2, t	2.10, m		3', 4', 6', 7'
6'	30.2, t	2.10, m		4', 5', 7', 8'
7'	30.2, t	2.10, m		5', 6', 8'
8'	30.2, t	2.10, m		6', 7'
9'	32.5, t	2.10, m		7', 8'
10'	23.2, t	2.10, m	11'	8'
11'	14.3, q	1.71, t (6.0)	10'	9', 10'
2-OH		ND		
7-OH		ND		

Referenced to 75% CH₃CN/D₂O; ^a Carbon assignments based on HSQCAD and gHMBCAD NMR experiments; ND Not Detected.

Figure S7. NMR data for compound eluting at 2.29 min (**2**) (*S. decipiens*).

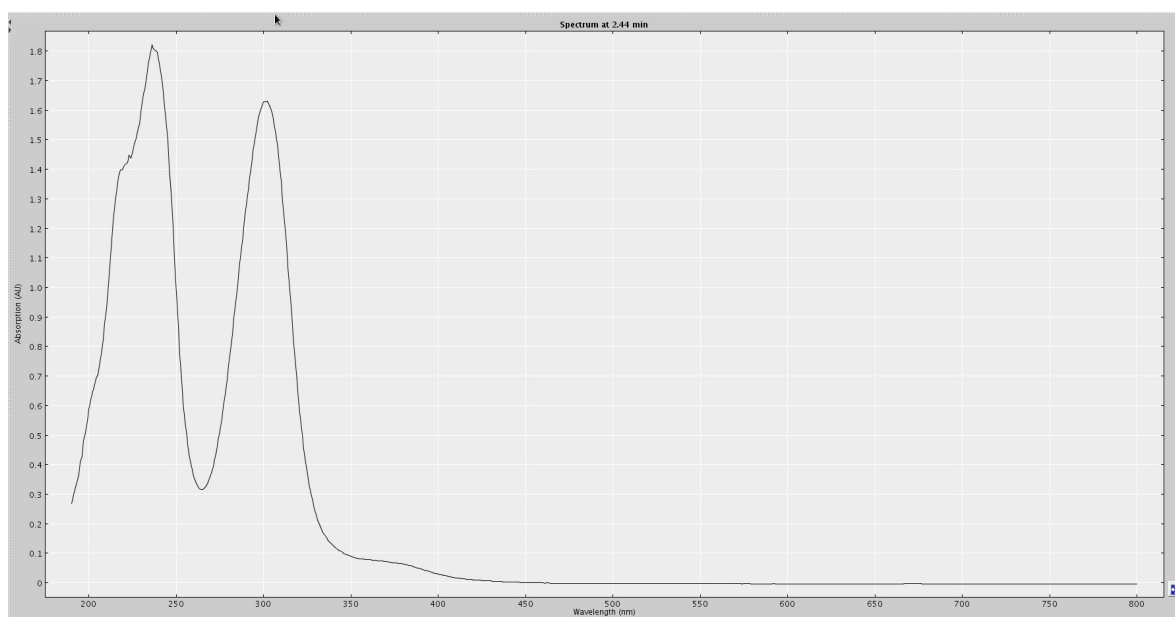


Figure S8. Extracted UV profile of compound eluting at 2.44 min (**3**) from HPLC-NMR (*S. decipiens*).

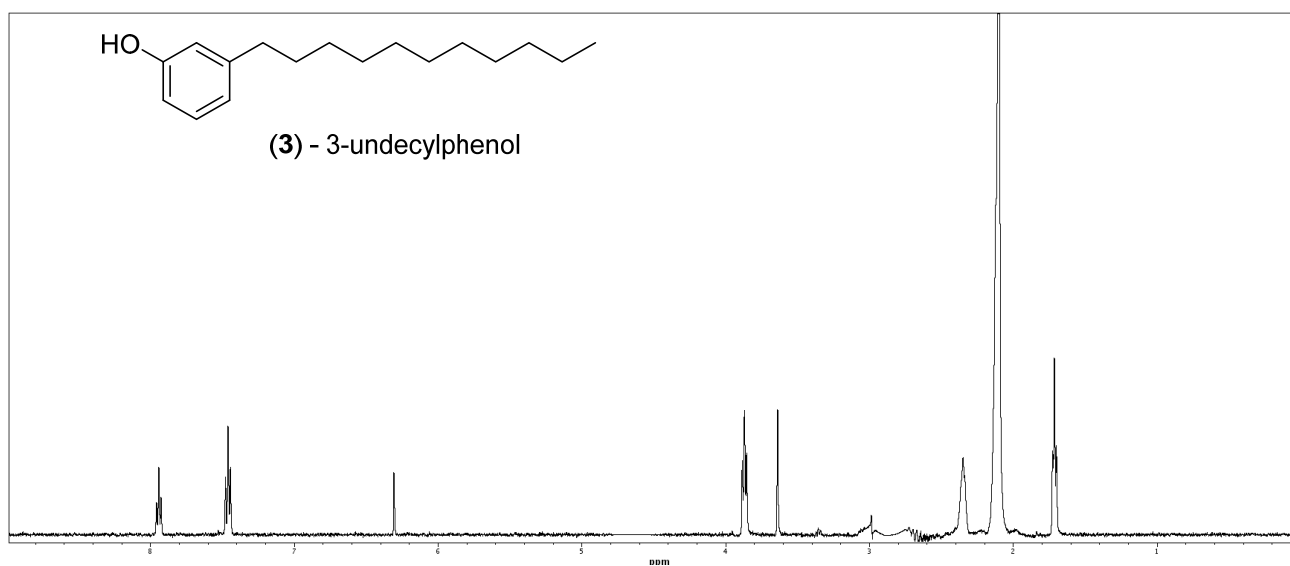


Figure S9. WET1D Proton NMR spectrum (500 MHz, 75% CH₃CN/D₂O) of compound eluting at 2.44 min (**3**) (*S. decipiens*).

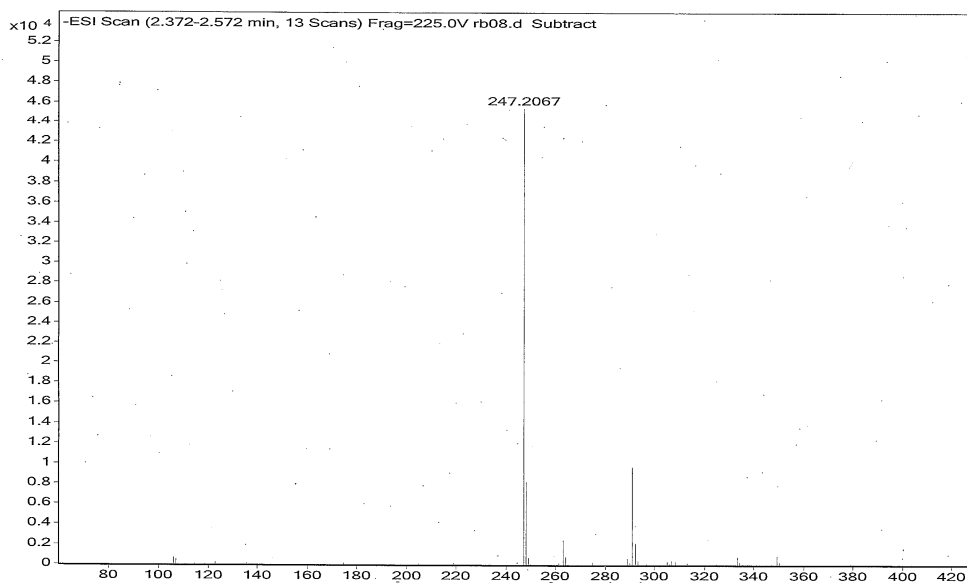
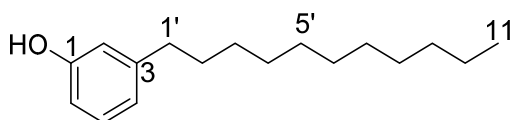


Figure S10. High resolution negative ESI-MS of compound eluting at 2.44 min (**3**) from HPLC-MS (*S. decipiens*).



(3) - 3-undecylphenol

Position	δ_C^a , mult.	δ_H (J in Hz)	gCOSY	gHMBCAD
1	162.0, s			
2	ND	6.31, s		
3	147.2, s			
4	121.9, d	7.45, d (8.5)	5	6
5	131.5, d	7.94, dd (8.5, 9.0)	4, 6	1, 3
6	114.7, d	7.47, d (9.0)*	5	
1'	35.5, t	3.87, t (7.5)	2'	3, 4, 2', 3'
2'	32.7, t	2.35, m	1'	3', 4'
3'	30.2, t	2.10, m		4', 5'
4'	30.2, t	2.10, m		3', 5', 6'
5'	30.2, t	2.10, m		3', 4', 6', 7'
6'	30.2, t	2.10, m		4', 5', 7', 8'
7'	30.2, t	2.10, m		5', 6', 8'
8'	30.2, t	2.10, m		6', 7'
9'	32.5, t	2.10, m		7', 8'
10'	23.2, t	2.10, m	11'	8'
11'	14.3, q	1.71, t (6.0)	10'	9', 10'
1-OH		ND		

Referenced to 75% CH₃CN/D₂O; ^a Carbon assignments based on HSQCAD and gHMBCAD NMR experiments; ND Not Detected; * Signals overlapped.

Figure S11. NMR data for compound eluting at 2.44 min (**3**) (*S. decipiens*).

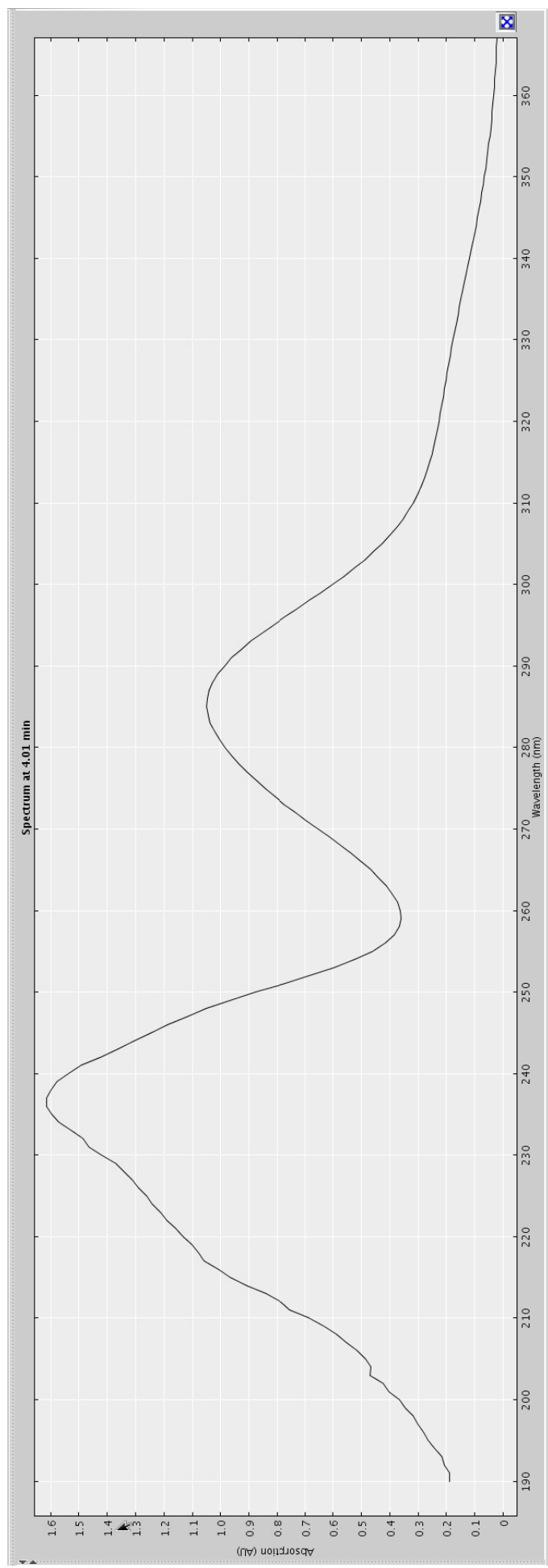


Figure S12. Extracted UV profile of compound eluting at 3.42 min (**11**) from HPLC-NMR (*C. retroflexa*).

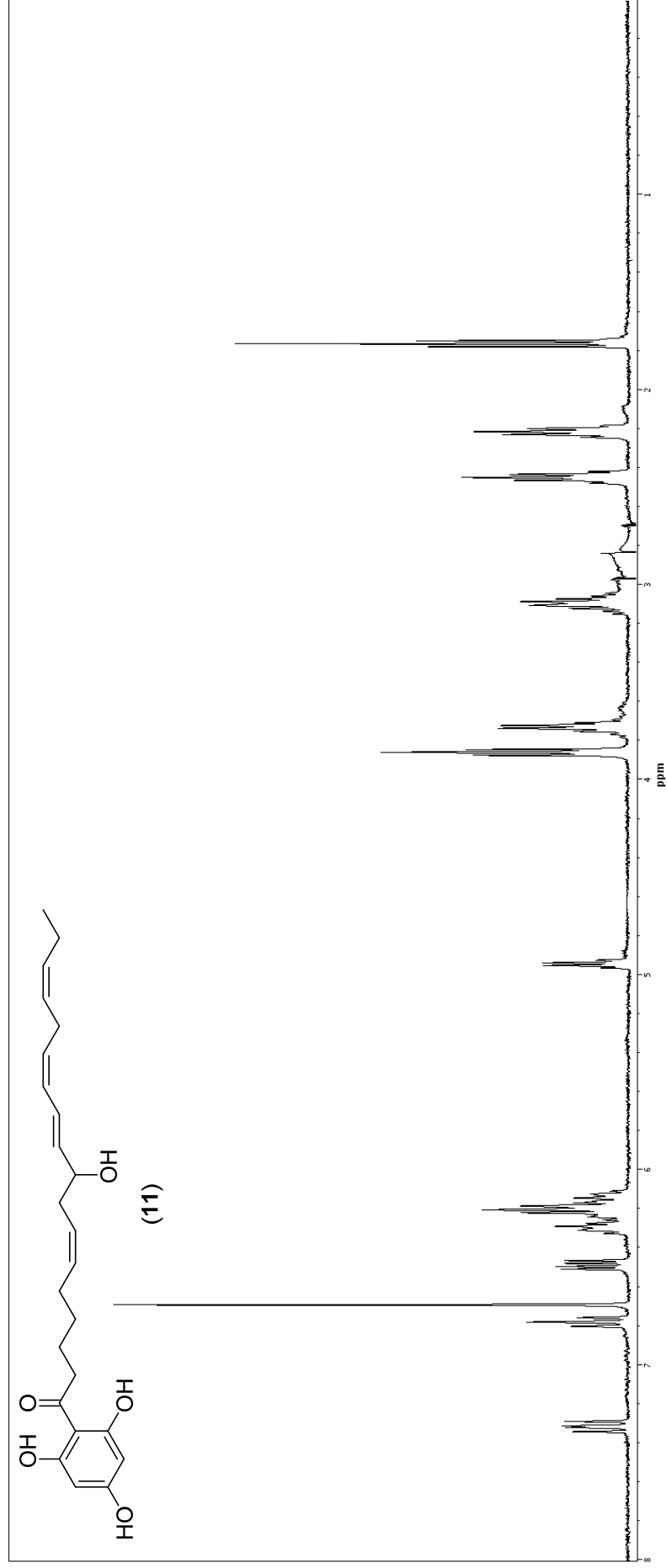


Figure S13. WET1D Proton NMR spectrum (500 MHz, 75% CH₃CN/D₂O) of compound eluting at 3.42 min (**11**) (*C. retroflexa*).

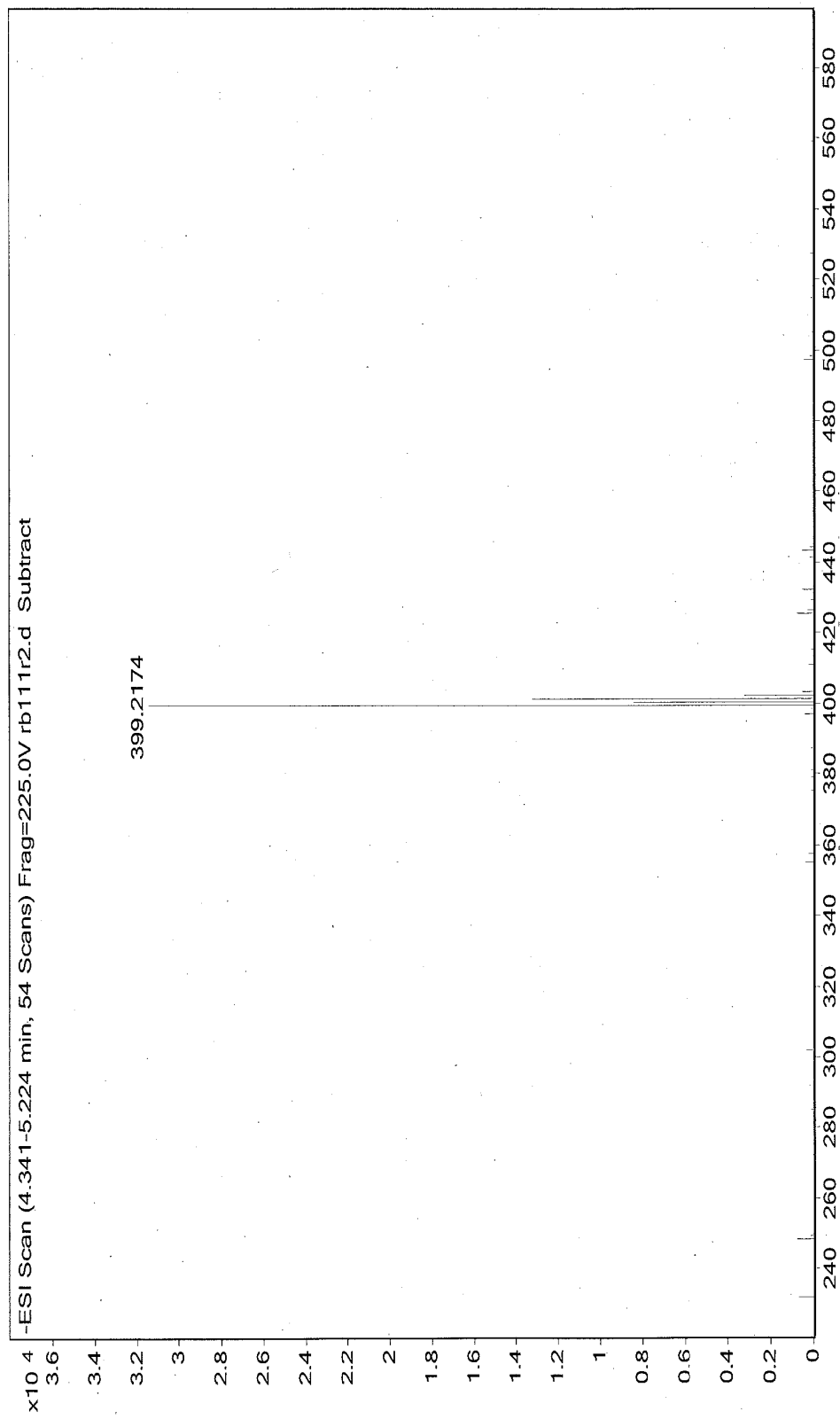
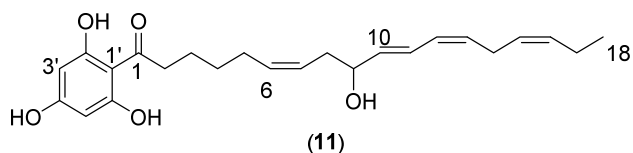


Figure S14. High resolution negative ESI-MS of compound eluting at 3.42 min (**11**) from HPLC-MS (*C. retroflexa*).



Position	δ_H (J in Hz)
1	
2	3.86, t (7.5)
3	2.45, p (7.5)
4	2.21, p (7.5)
5	3.10, dt (7.5, 9.5)
6	6.10–6.34, m
7	6.10–6.34, m
8	3.73, dd (7.0, 7.5)
9	4.95, dt (14.0, 7.0)
10	6.48, dd (15.0, 7.0)
11	7.32, dd (15.0, 11.0)
12	6.78, dd (11.0, 10.5)
13	6.10–6.34, m
14	SS
15	6.10–6.34, m
16	6.10–6.34, m
17	SS
18	1.76, t (7.5)
1'	
2'	
3'	6.69, s
4'	
5'	6.69, s
6'	
9-OH	ND
2'-OH	ND
4'-OH	ND
6'-OH	ND

Referenced to D₂O (δ_H 4.64 ppm); SS Signal suppressed; ND Not Detected.

Figure S15. NMR data for compound eluting at 3.42 min (11) (*C. retroflexa*).

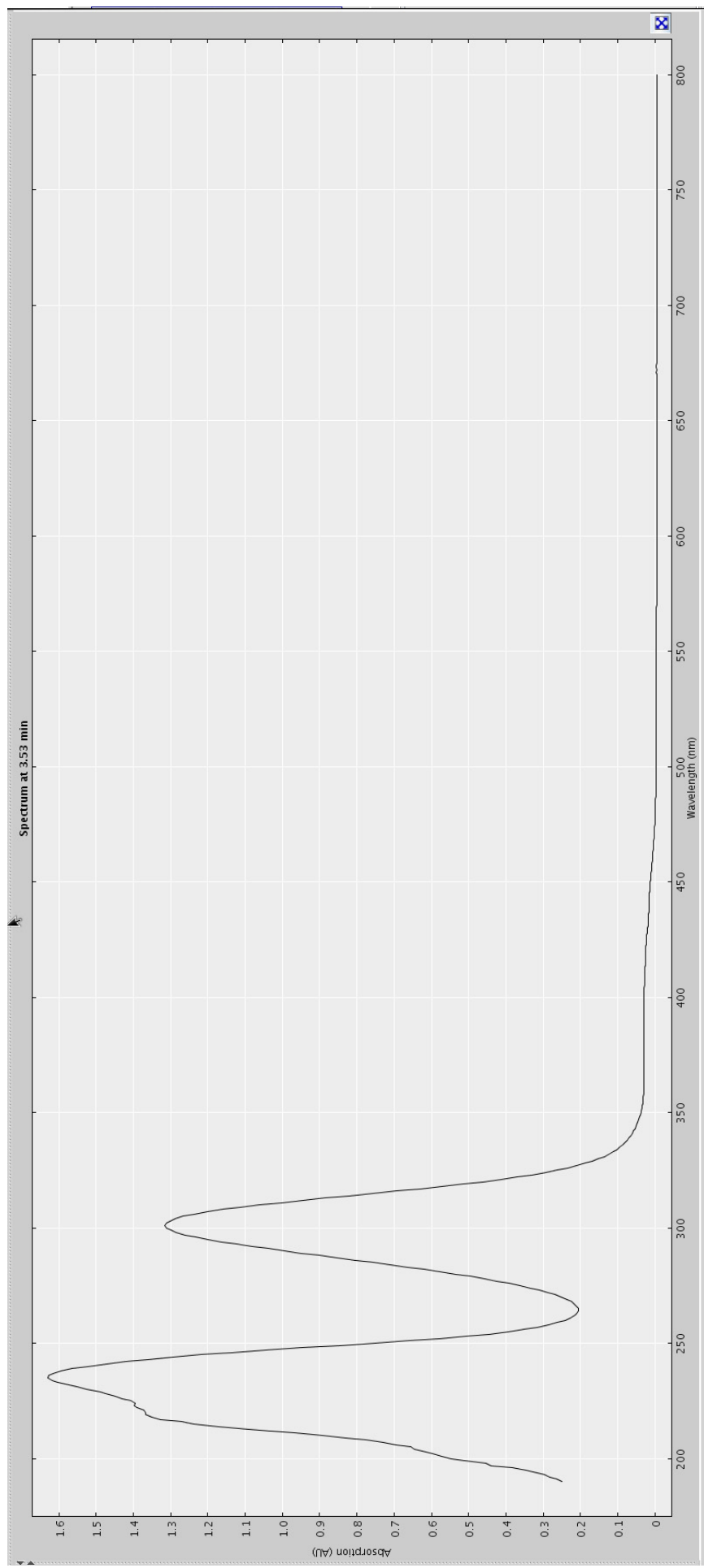


Figure S16. Extracted UV profile of compound eluting at 3.55 min (**1**) from HPLC-NMR (*S. decipiens*).

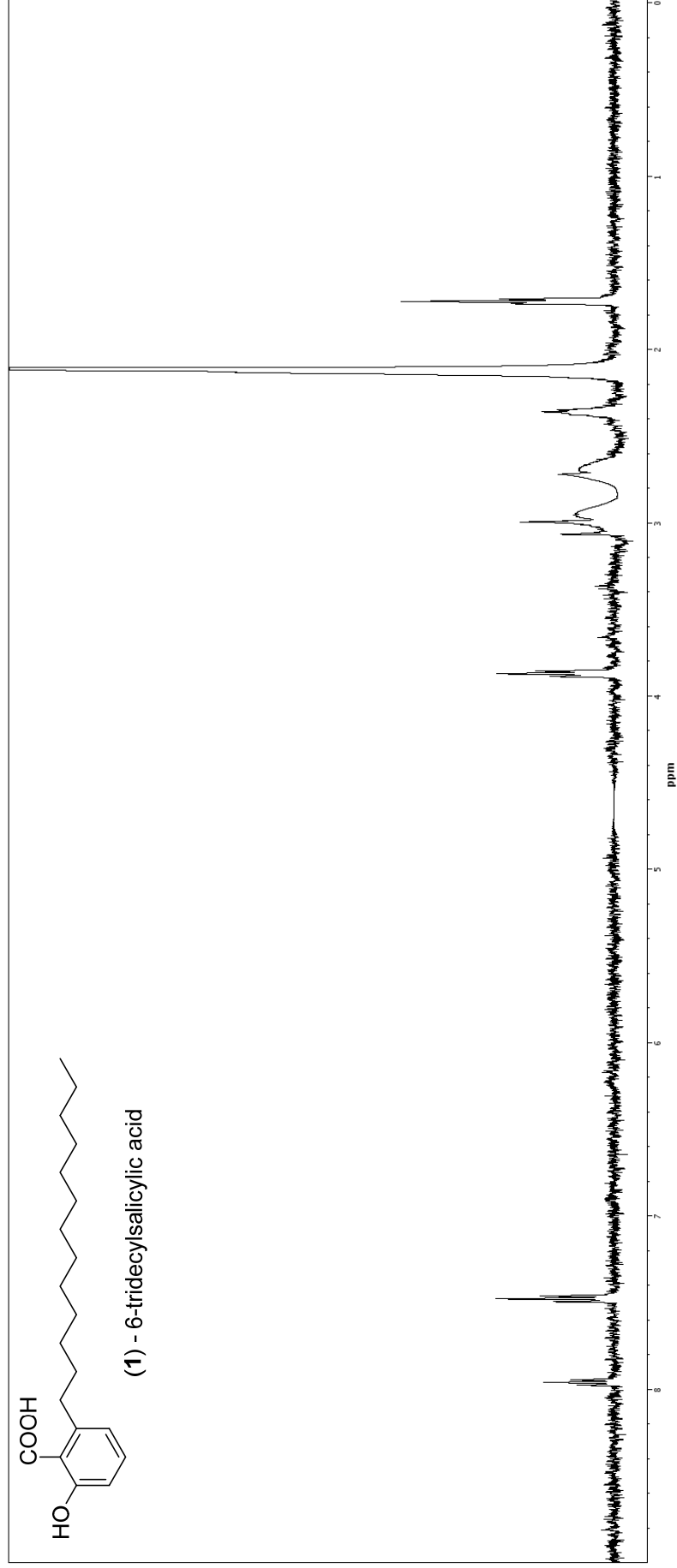


Figure S17. WETID Proton NMR spectrum (500 MHz, 75% CH₃CN/D₂O) of compound eluting at 3.55 min (**1**) (*S. decipiens*).

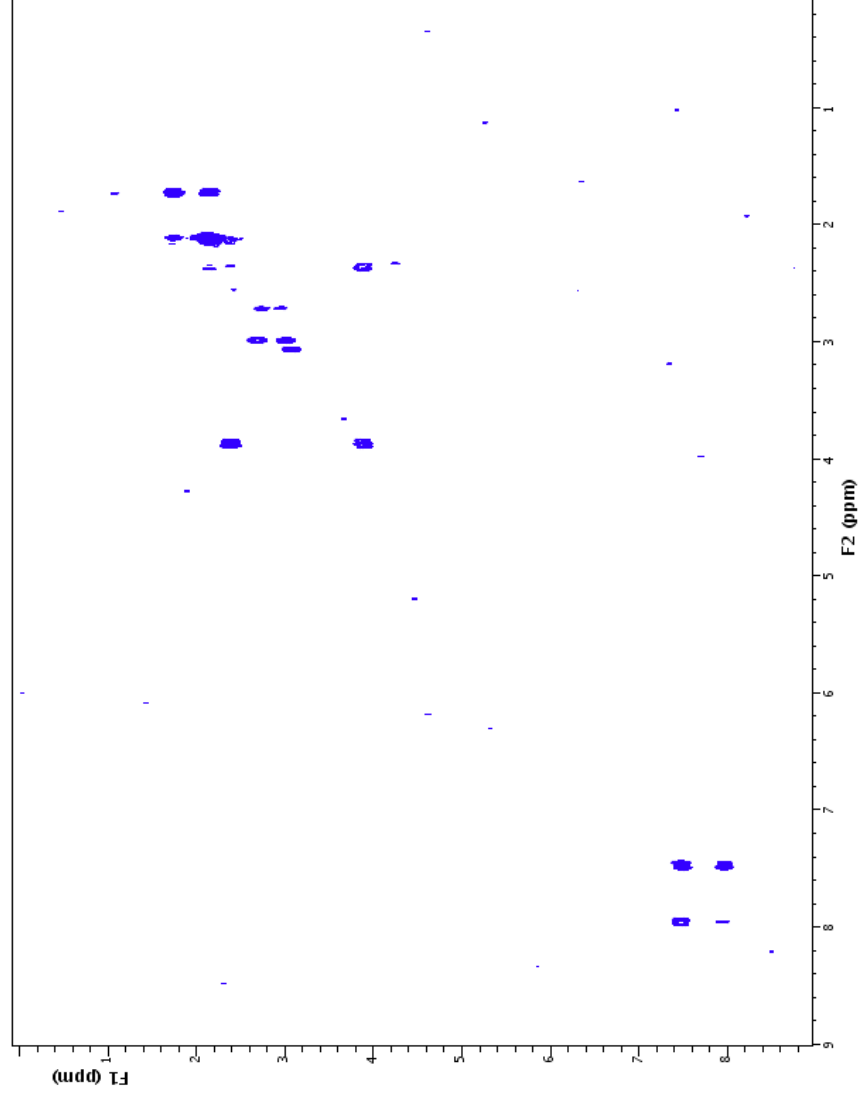


Figure S18. gCOSY NMR spectrum (500 MHz, 75% CH₃CN/D₂O) of compound eluting at 3.55 min (**1**) (*S. decipiens*).

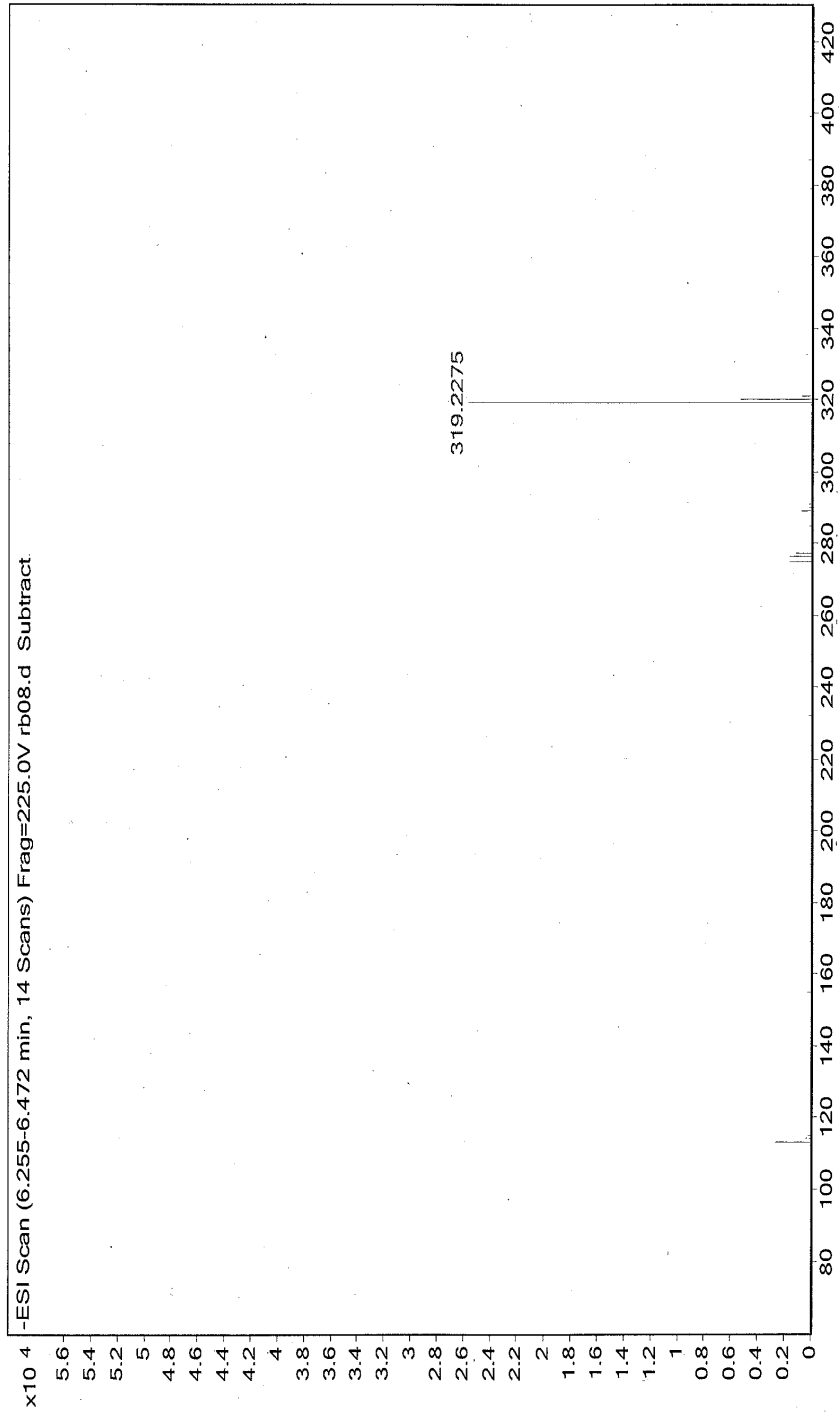
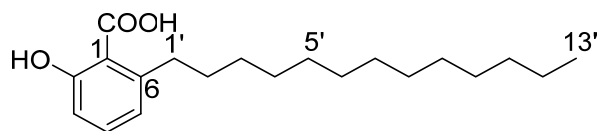


Figure S19. High resolution negative ESI-MS of compound eluting at 3.55 min (**1**) from HPLC-MS (*S. decipiens*).



(1) - 6-tridecylsalicylic acid

Position	δ_H (J in Hz)	gCOSY
1		
2		
3	7.48, d (8.0)	4
4	7.96, dd (7.5, 8.0)	3, 5
5	7.47, d (7.5)	4
6		
7		
1'	3.87, t (8.5)	2'
2'	2.36, m	1'
3'	2.11, m	
4'	2.11, m	
5'	2.11, m	
6'	2.11, m	
7'	2.11, m	
8'	2.11, m	
9'	2.11, m	
10'	2.11, m	
11'	2.11, m	
12'	2.11, m	13'
13'	1.72, t (7.5)	12'
2-OH	ND	
7-OH	ND	

Referenced to 75% CH₃CN/D₂O; ND Not Detected.

Figure S20. NMR data for compound eluting at 3.55 min (1) (*S. decipiens*).

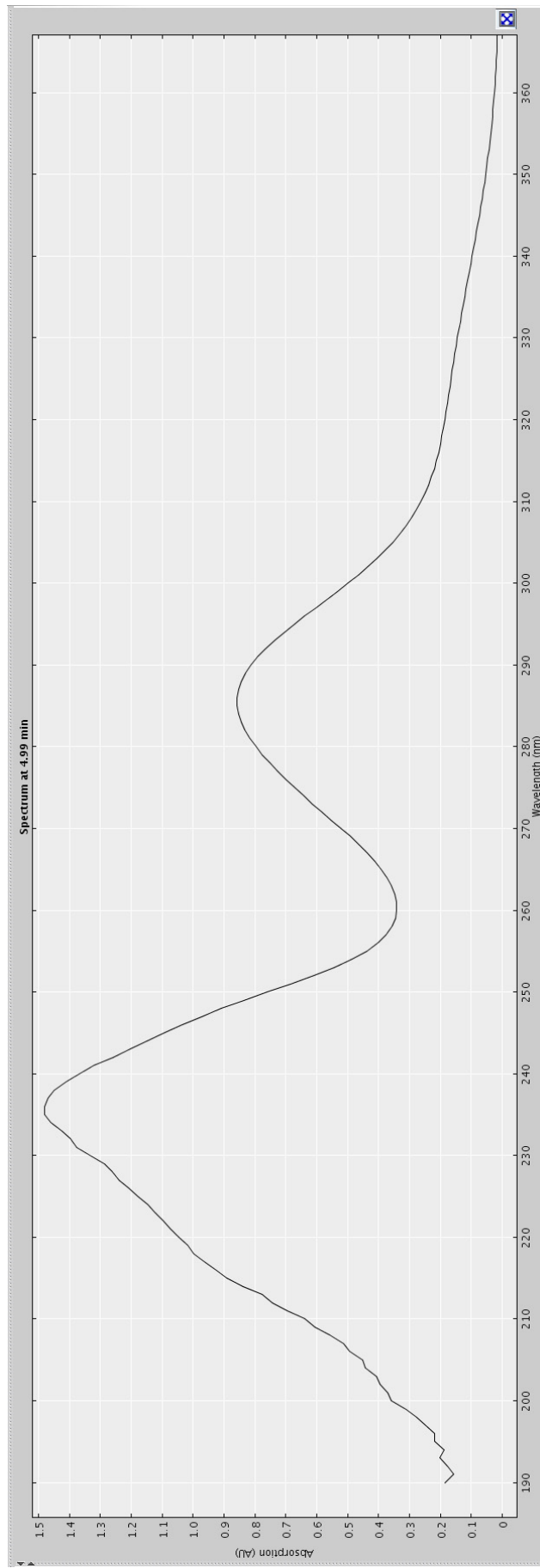


Figure S21. Extracted UV profile of compound eluting at 4.45 min (**16**) from HPLC-NMR (*C. retroflexa*).

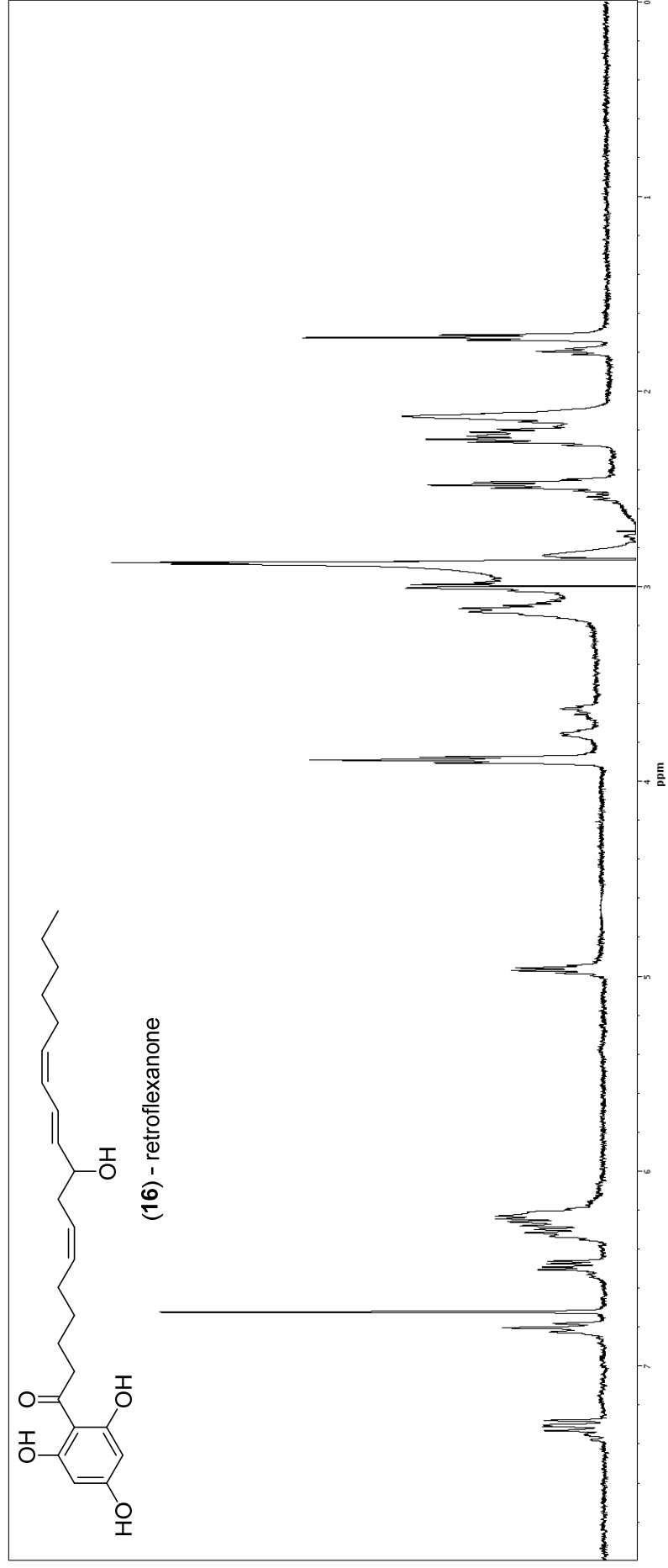


Figure S22. WET1D Proton NMR spectrum (500 MHz, 75% CH₃CN/D₂O) of compound eluting at 4.45 min (**16**) (*C. retroflexa*).

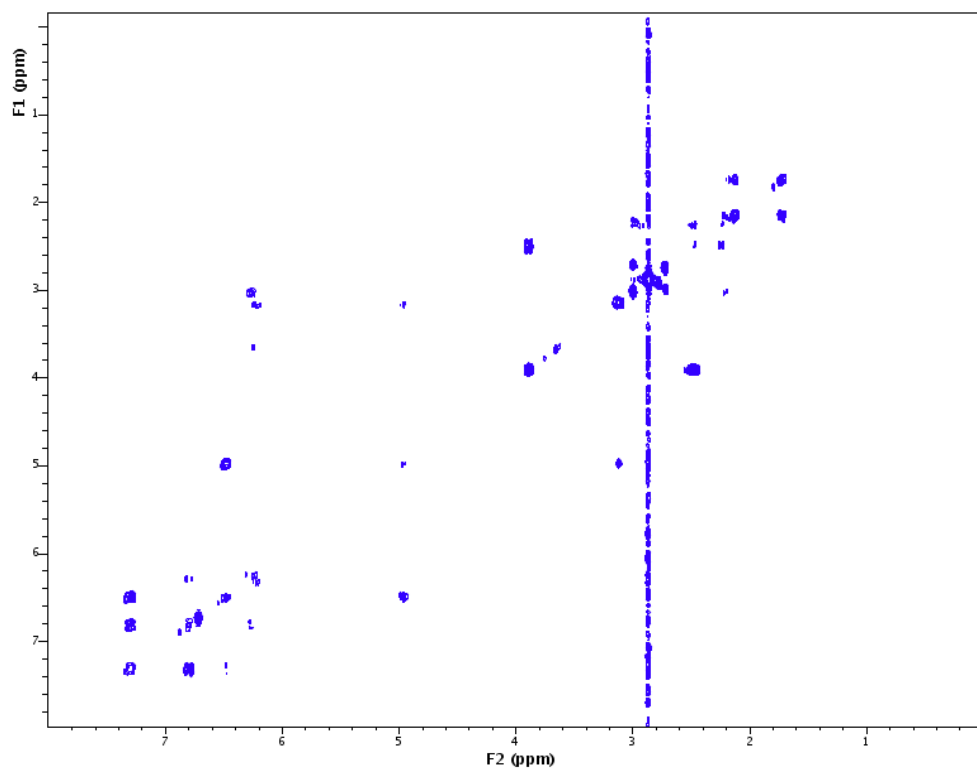


Figure S23. gCOSY NMR spectrum (500 MHz, 75% CH₃CN/D₂O) of compound eluting at 4.45 min (**16**) (*C. retroflexa*).

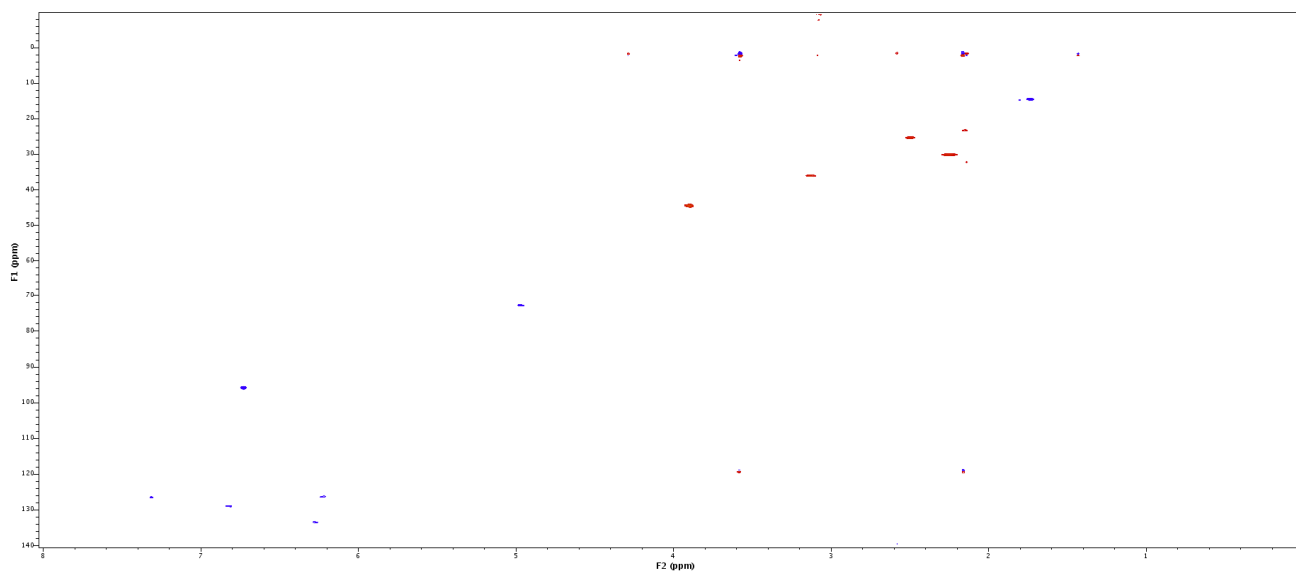


Figure S24. HSQCAD NMR spectrum (500 MHz, 75% CH₃CN/D₂O) of compound eluting at 4.45 min (**16**) (*C. retroflexa*).

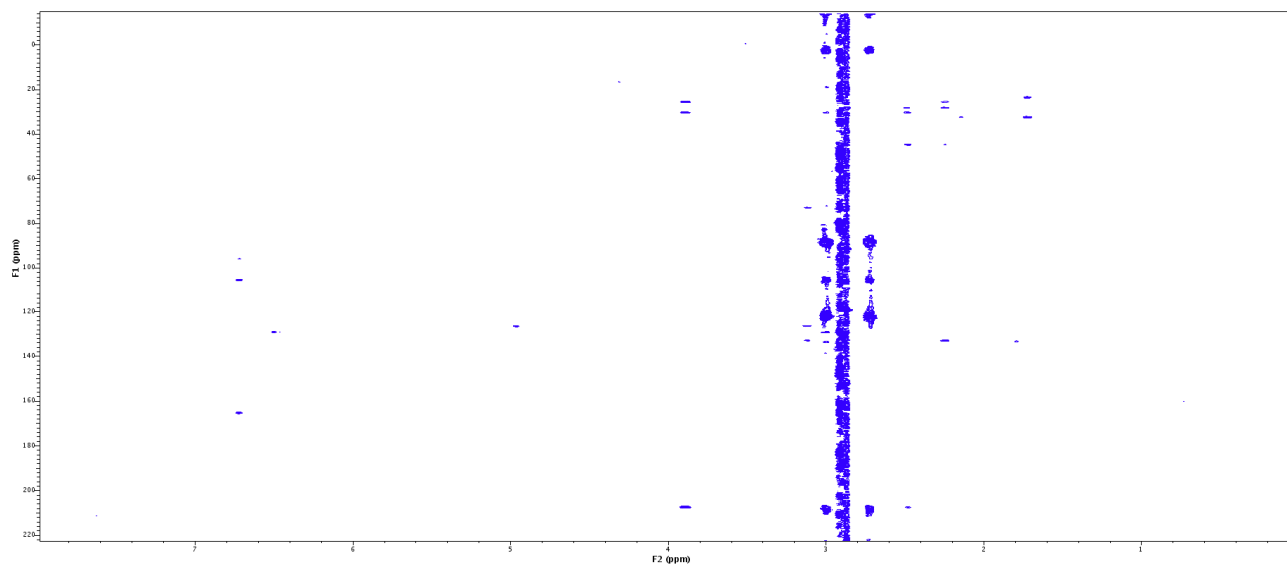


Figure S25. gHMBCAD NMR spectrum (500 MHz, 75% CH₃CN/D₂O) of compound eluting at 4.45 min (**16**) (*C. retroflexa*).

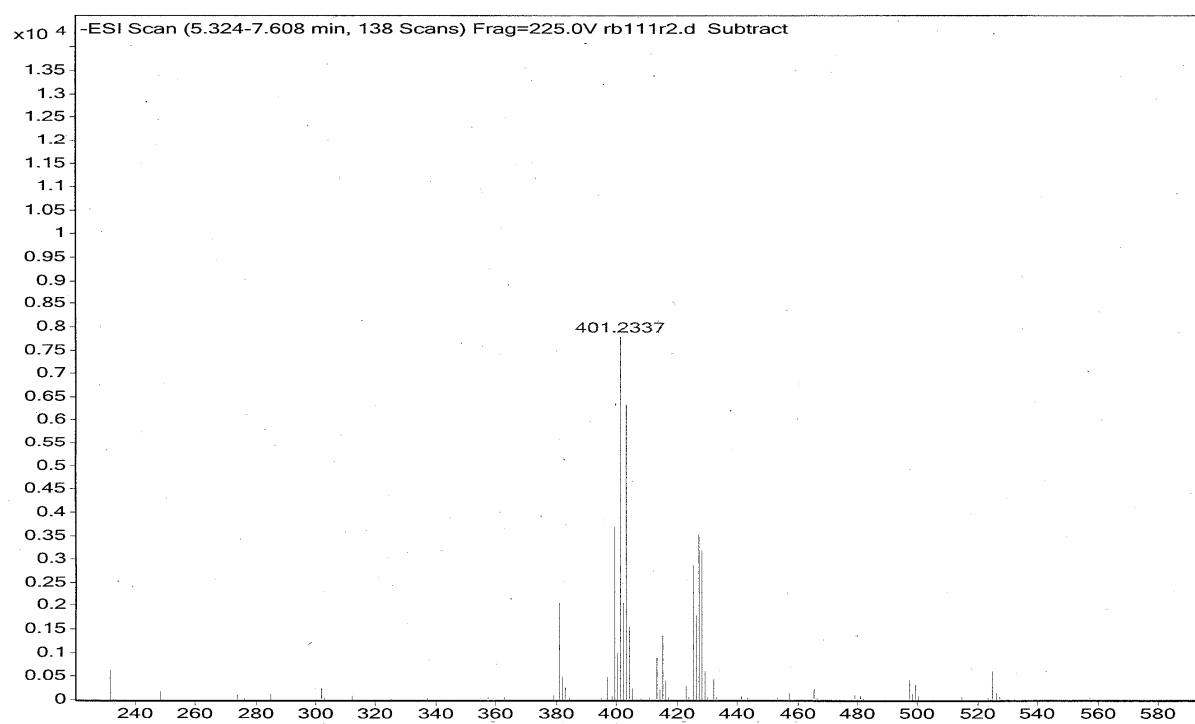


Figure S26. High resolution negative ESI-MS of compound eluting at 4.45 min (**16**) from HPLC-MS (*C. retroflexa*).

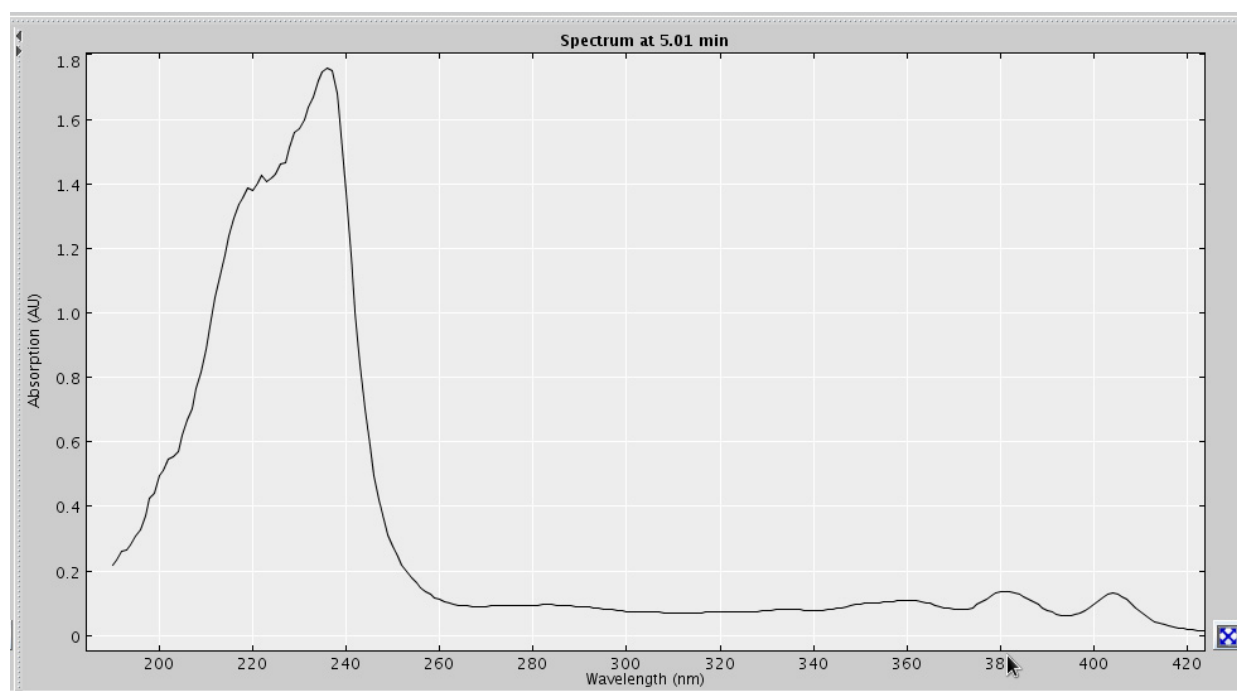


Figure S27. Extracted UV profile of compound eluting at 5.00 min from HPLC-NMR (*Laurencia* sp.).

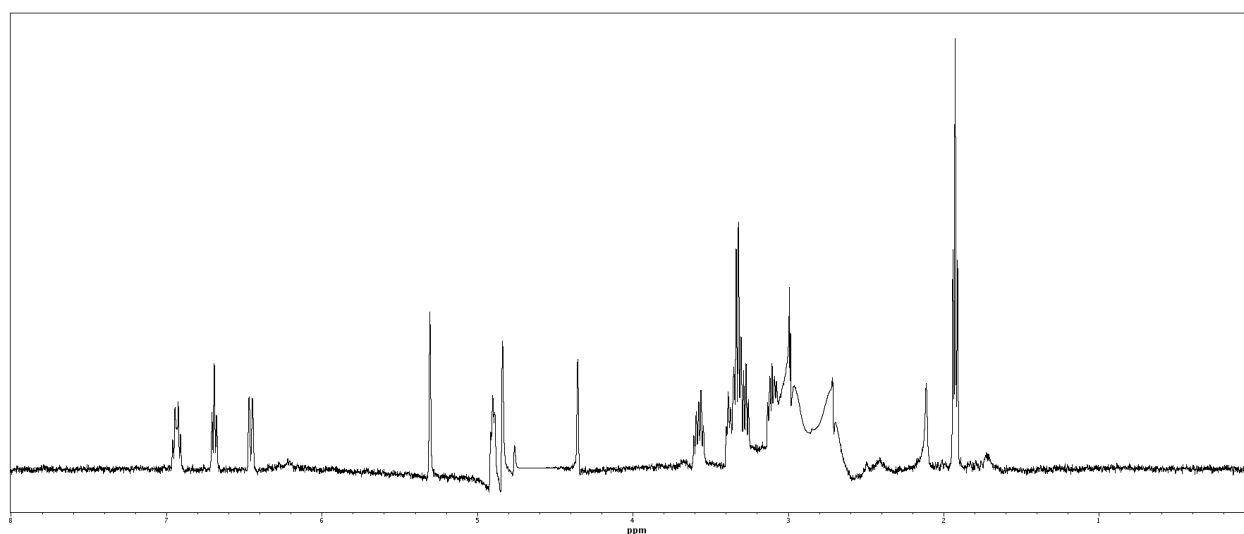


Figure S28. WET1D Proton NMR spectrum (500 MHz, 75% CH₃CN/D₂O) of compound eluting at 5.00 min (*Laurencia* sp.).

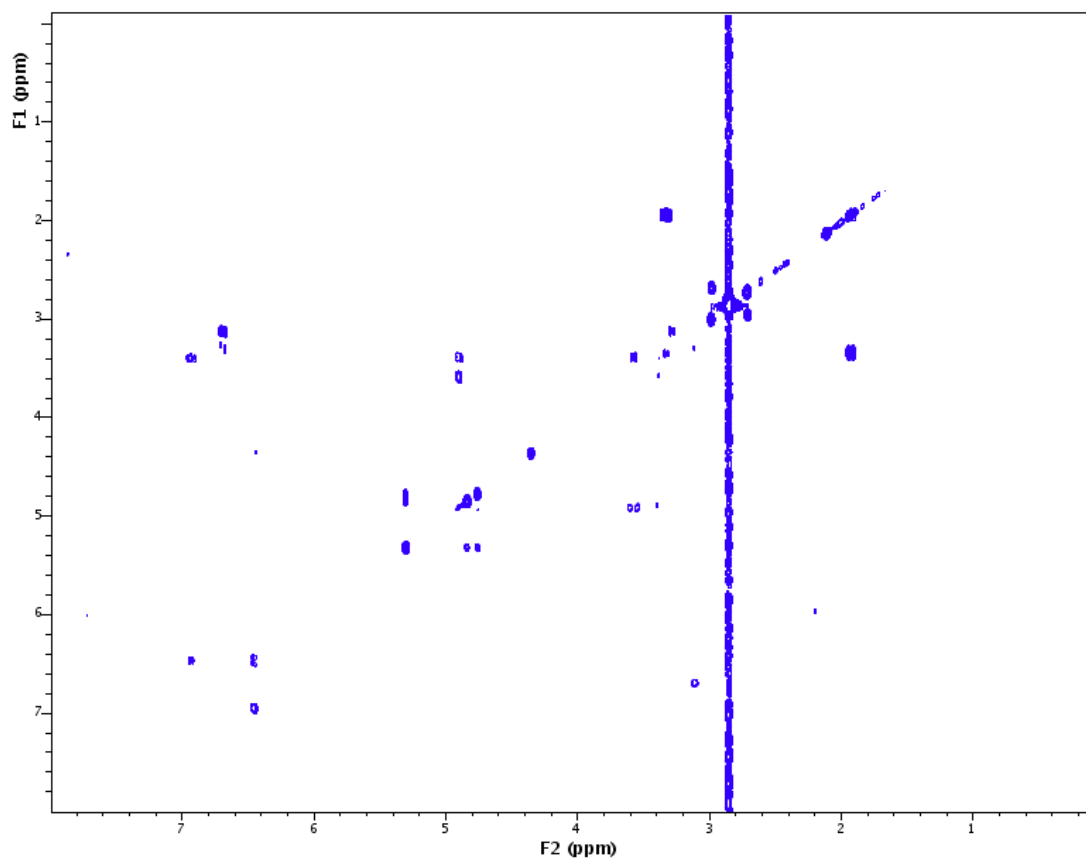


Figure S29. gCOSY NMR spectrum (500 MHz, 75% CH₃CN/D₂O) of compound eluting at 5.00 min (*Laurencia* sp.).

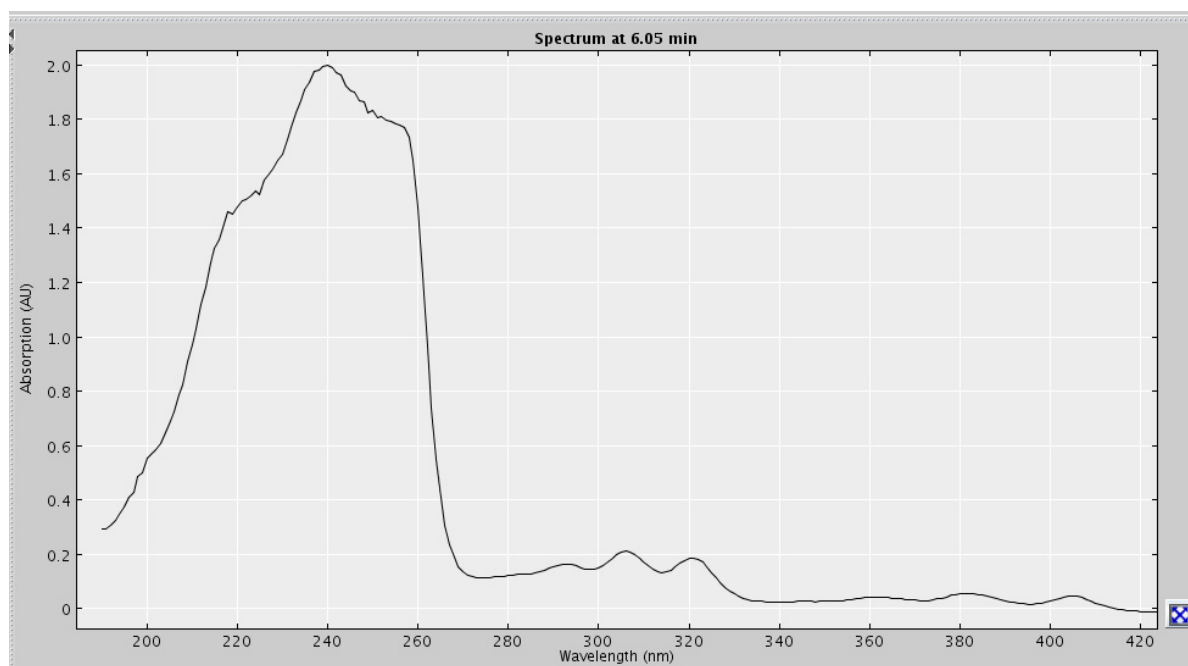


Figure S30. Extracted UV profile of compound eluting at 6.05 min from HPLC-NMR (*Laurencia* sp.).

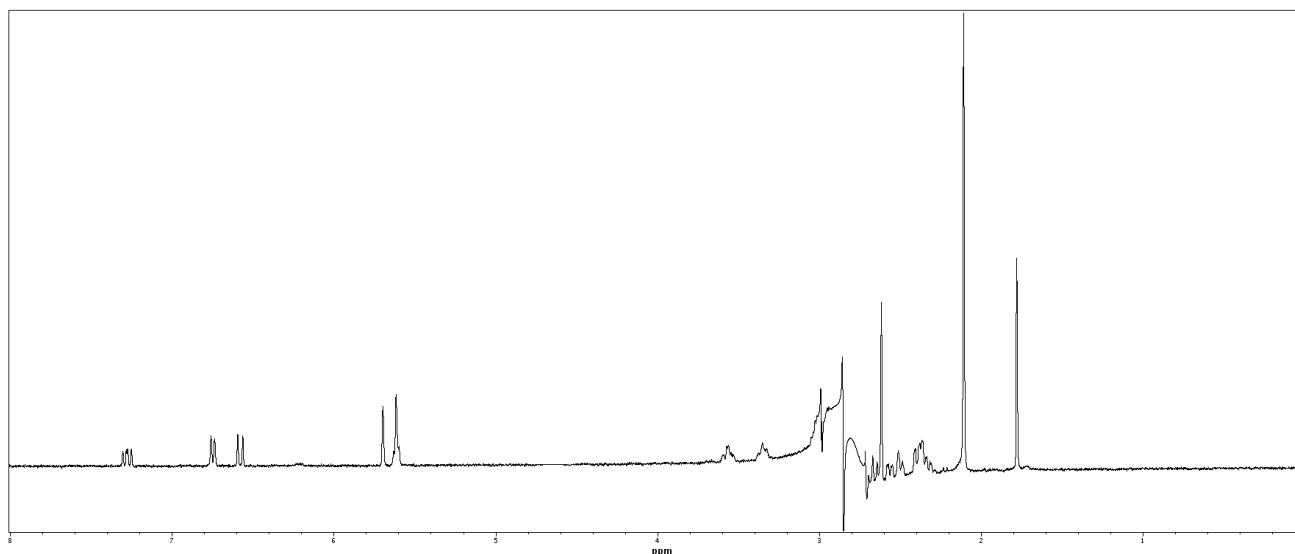


Figure S31. WET1D Proton NMR spectrum (500 MHz, 75% CH₃CN/D₂O) of compound eluting at 6.05 min (*Laurencia* sp.).

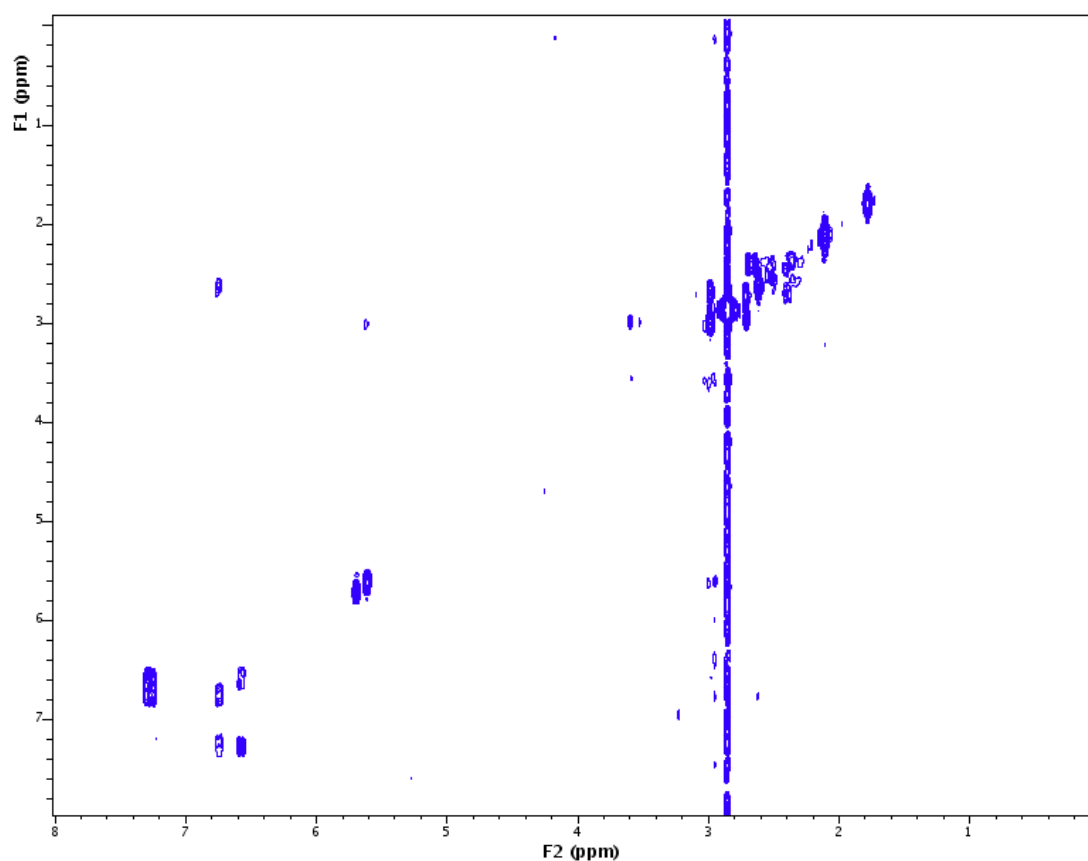


Figure S32. gCOSY NMR spectrum (500 MHz, 75% CH₃CN/D₂O) of compound eluting at 6.05 min (*Laurencia* sp.).

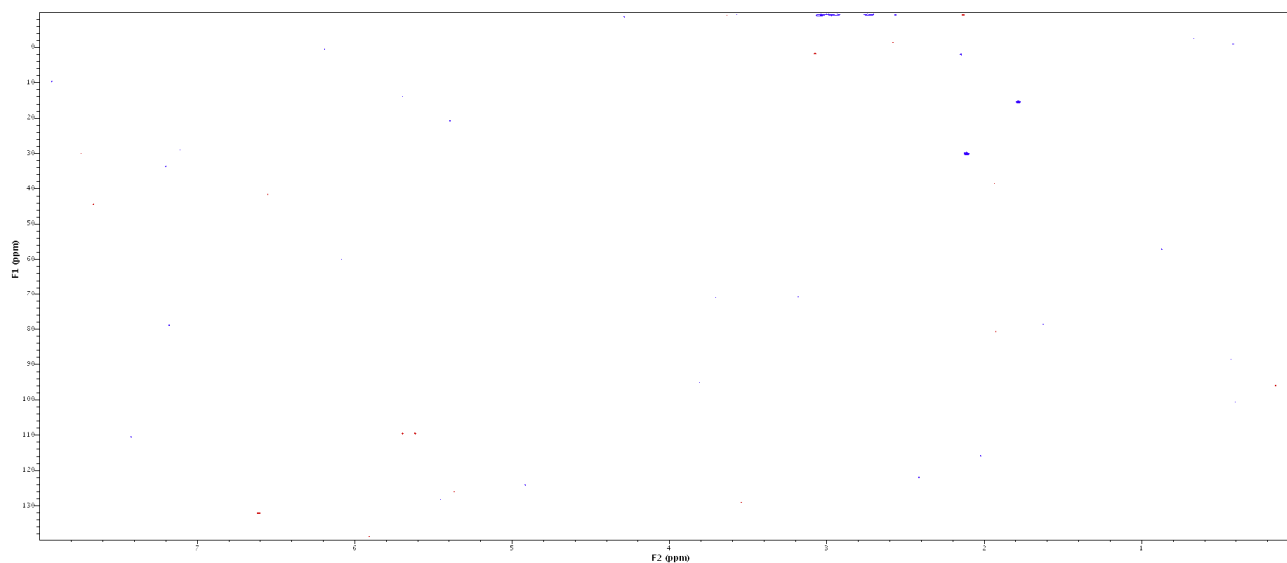


Figure S33. HSQCAD NMR spectrum (500 MHz, 75% CH₃CN/D₂O) of compound eluting at 6.05 min (*Laurencia* sp.).

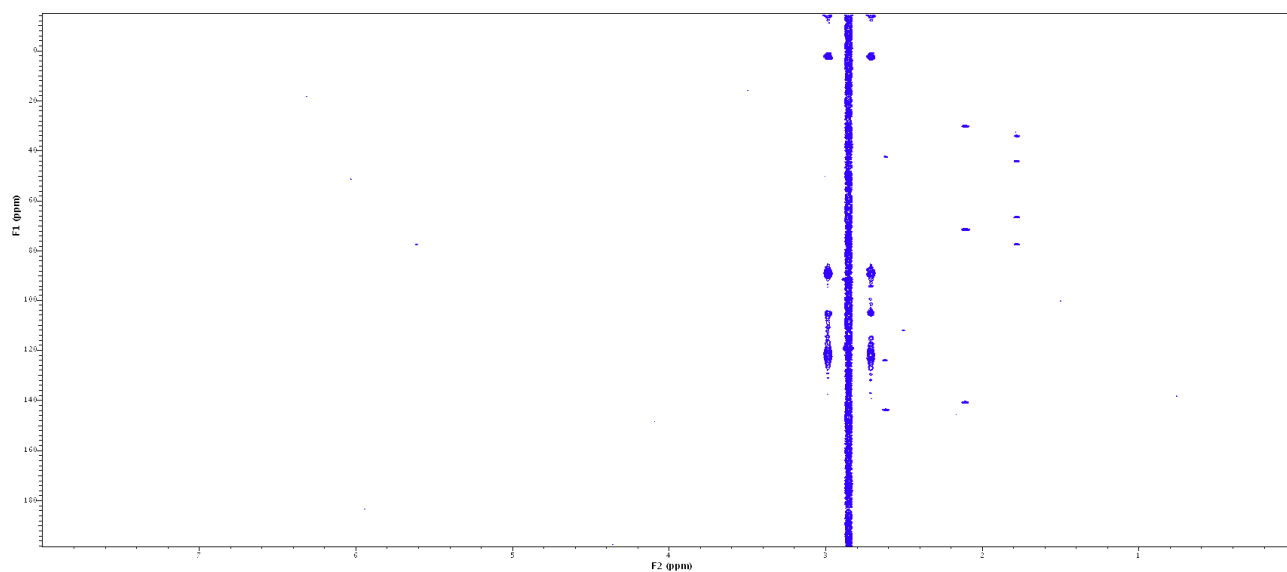


Figure S34. gHMBCAD NMR spectrum (500 MHz, 75% CH₃CN/D₂O) of compound eluting at 6.05 min (*Laurencia* sp.).

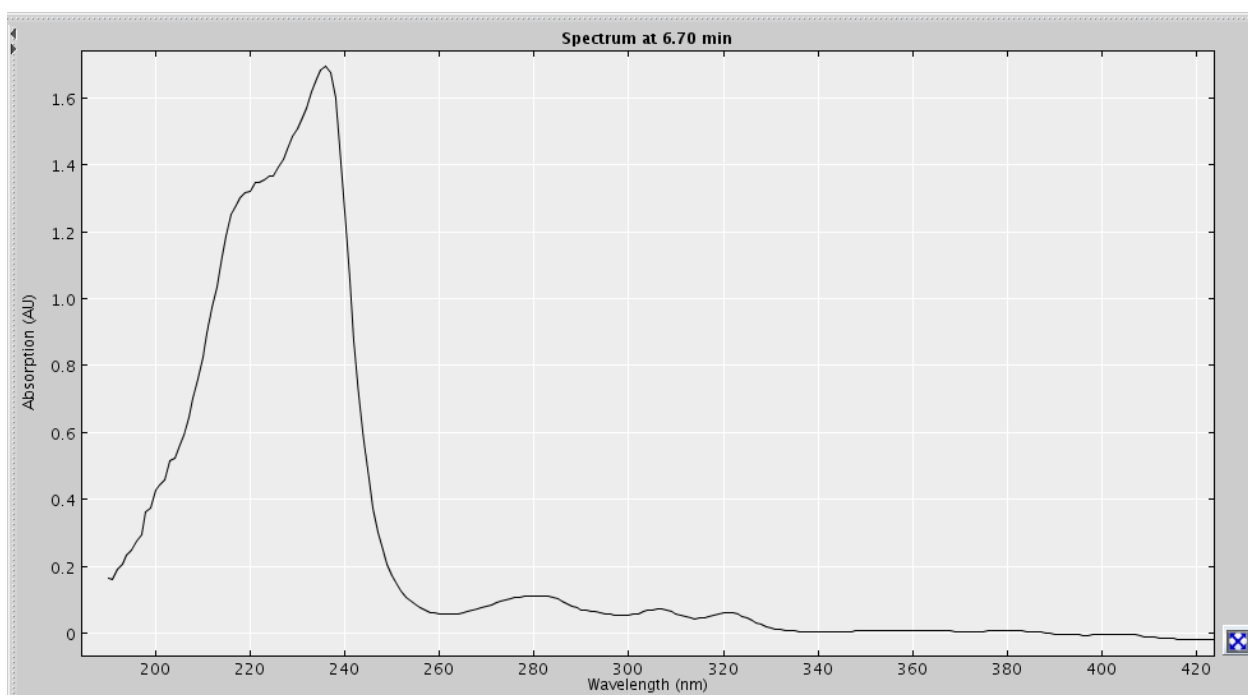


Figure S35. Extracted UV profile of compound eluting at 6.70 min from HPLC-NMR (*Laurencia* sp.).

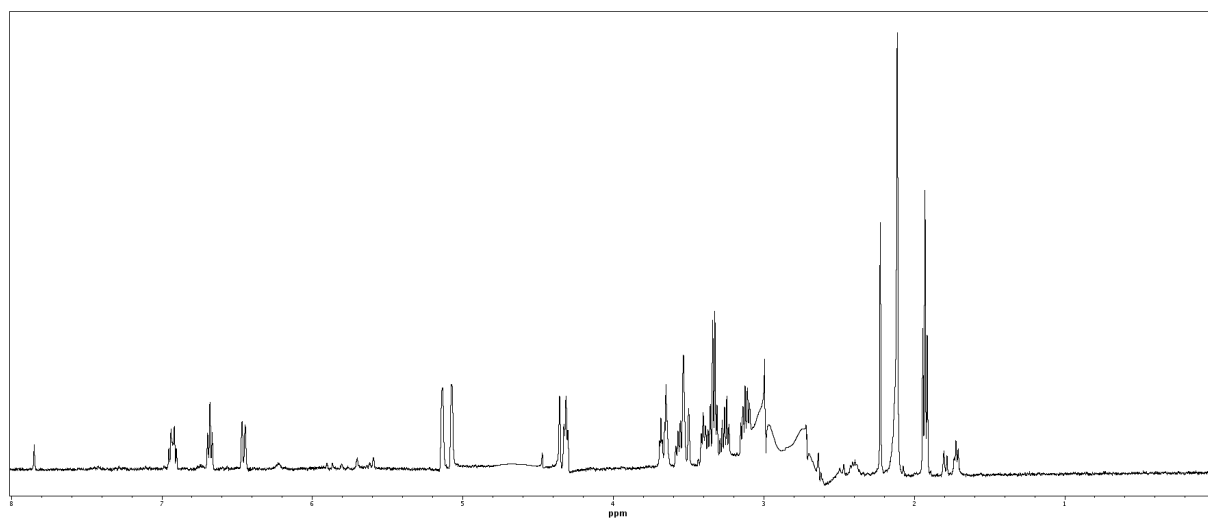


Figure S36. WET1D Proton NMR spectrum (500 MHz, 75% CH₃CN/D₂O) of compound eluting at 6.70 min (*Laurencia* sp.).

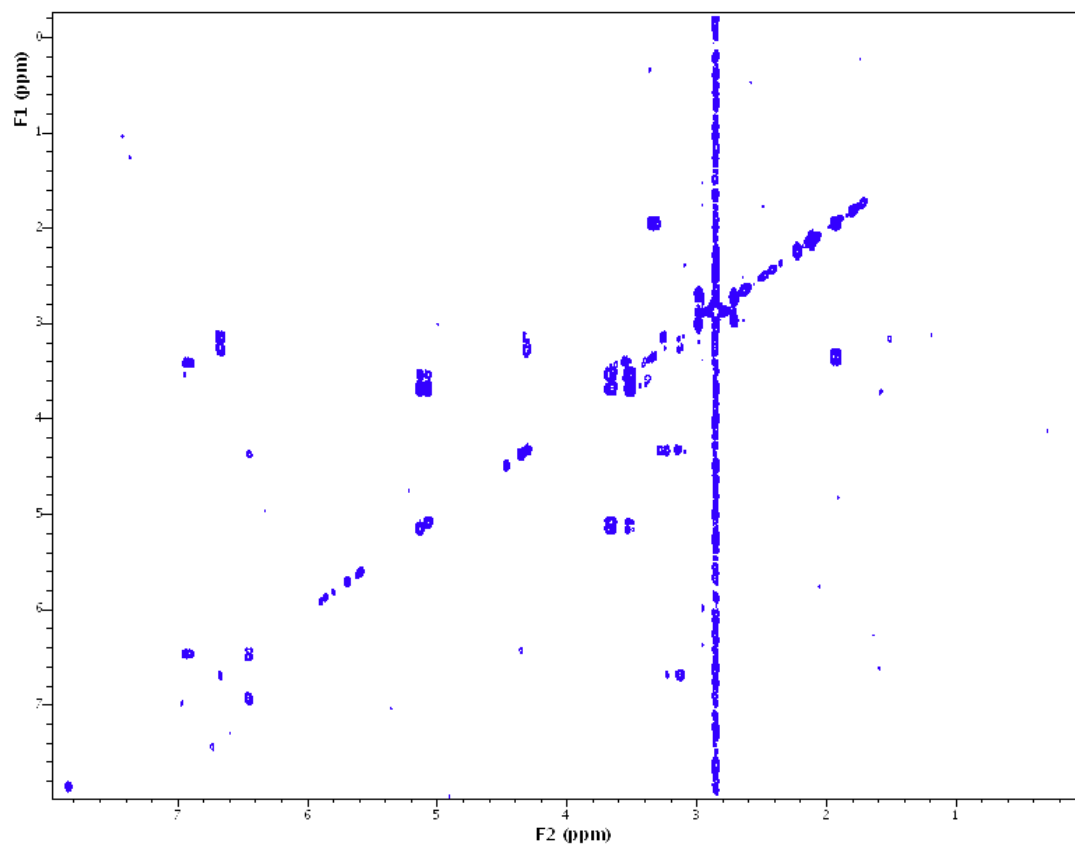


Figure S37. gCOSY NMR spectrum (500 MHz, 75% CH₃CN/D₂O) of compound eluting at 6.70 min (*Laurencia* sp.).

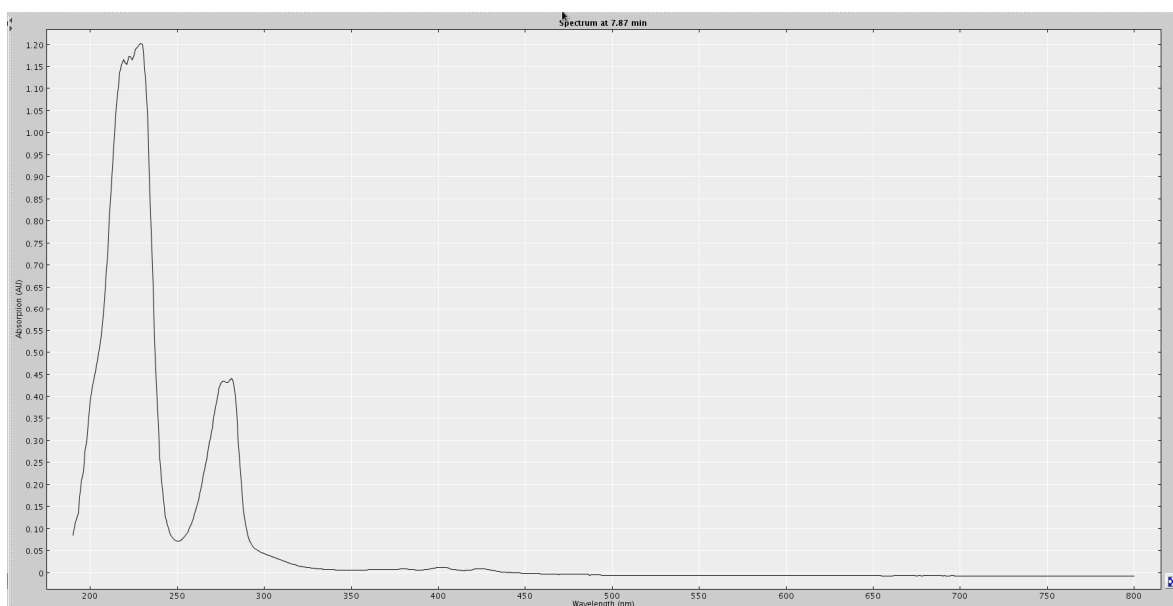


Figure S38. Extracted UV profile of compound eluting at 7.87 min (**4**) from HPLC-NMR (*S. decipiens*).

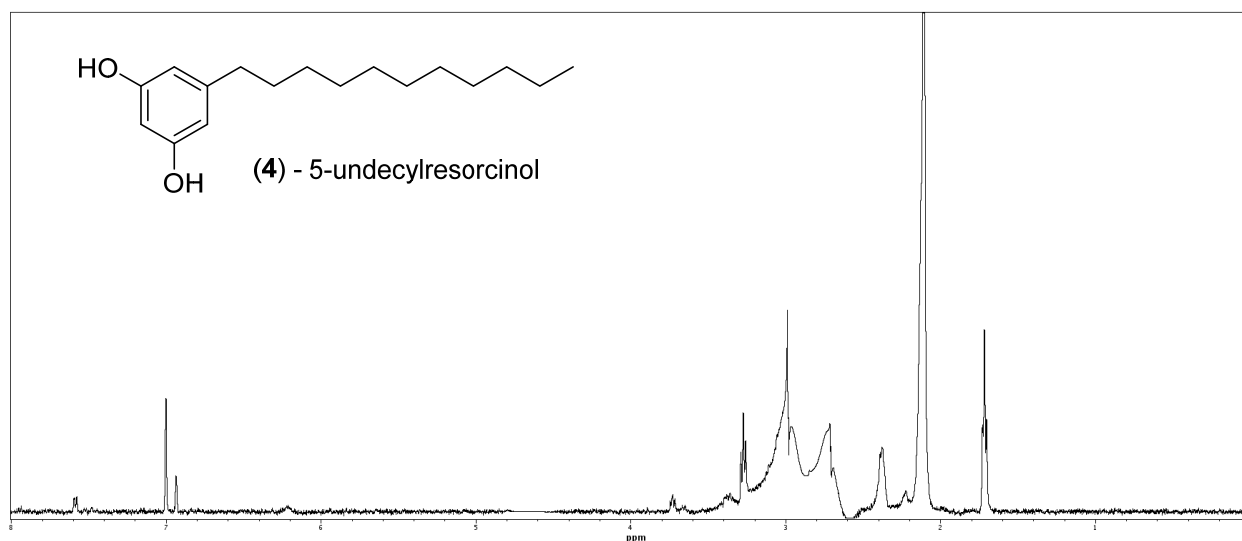


Figure S39. WET1D Proton NMR spectrum (500 MHz, 75% CH₃CN/D₂O) of compound eluting at 7.87 min (4) (*S. decipiens*).

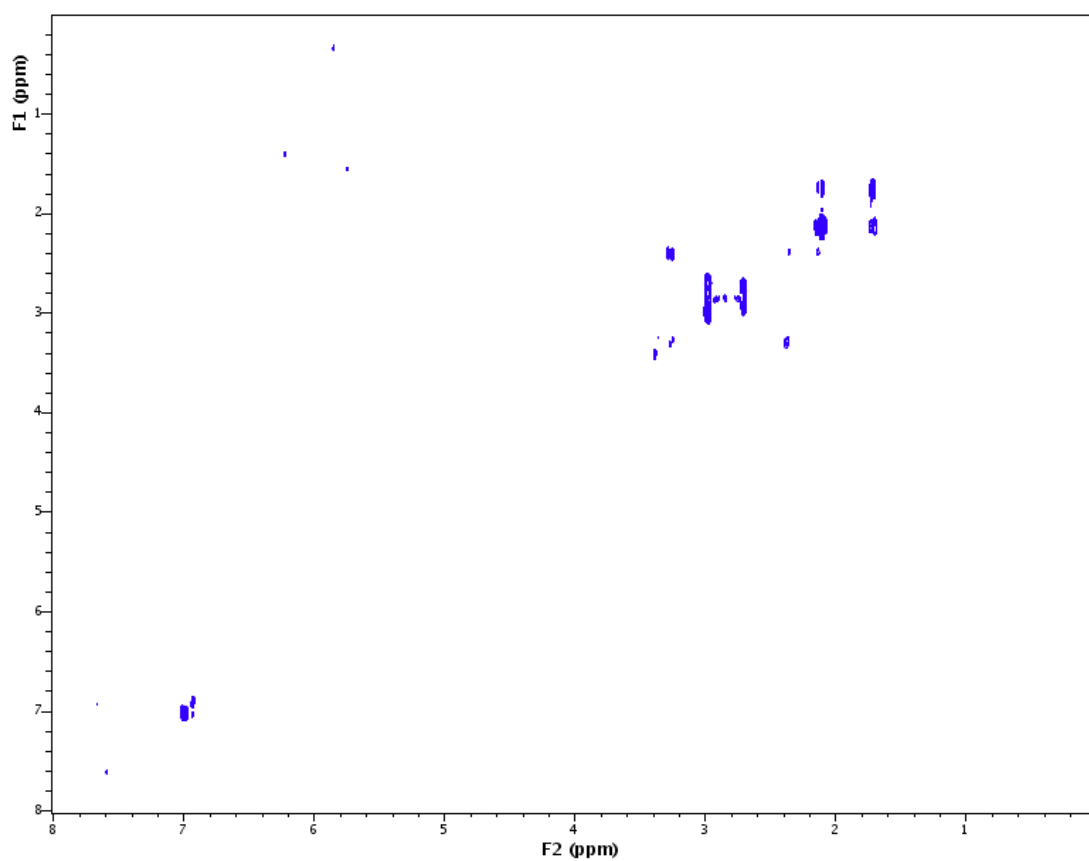


Figure S40. gCOSY NMR spectrum (500 MHz, 75% CH₃CN/D₂O) of compound eluting at 7.87 min (4) (*S. decipiens*).

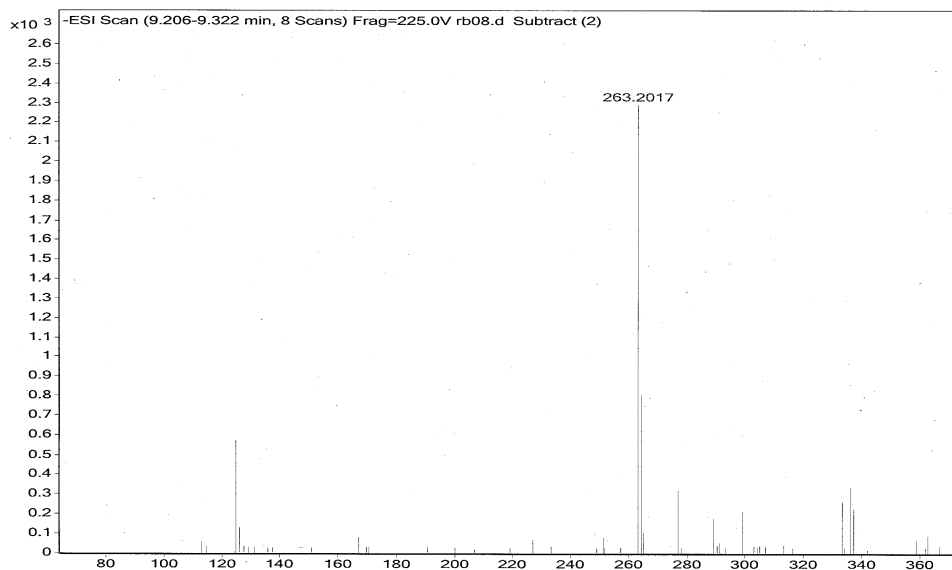
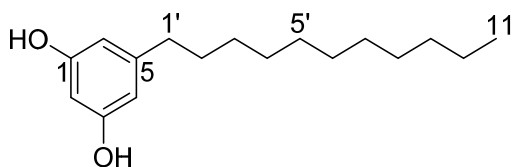


Figure S41. High resolution negative ESI-MS of compound eluting at 7.87 min (**4**) from HPLC-MS (*S. decipiens*).



(4) - 5-undecylresorcinol

Position	δ_H (J in Hz)	gCOSY
1		
2	6.93, s	
3		
4	7.00, s	
5		
6	7.00, s	
1'	3.27, t (7.5)	2'
2'	2.38, m	1'
3'	2.11, m	
4'	2.11, m	
5'	2.11, m	
6'	2.11, m	
7'	2.11, m	
8'	2.11, m	
9'	2.11, m	
10'	2.11, m	11'
11'	1.72, t (6.5)	10'
1-OH	ND	
3-OH	ND	

Referenced to 75% CH₃CN/D₂O; ND Not Detected.

Figure S42. NMR data for compound eluting at 7.87 min (**4**) (*S. decipiens*).

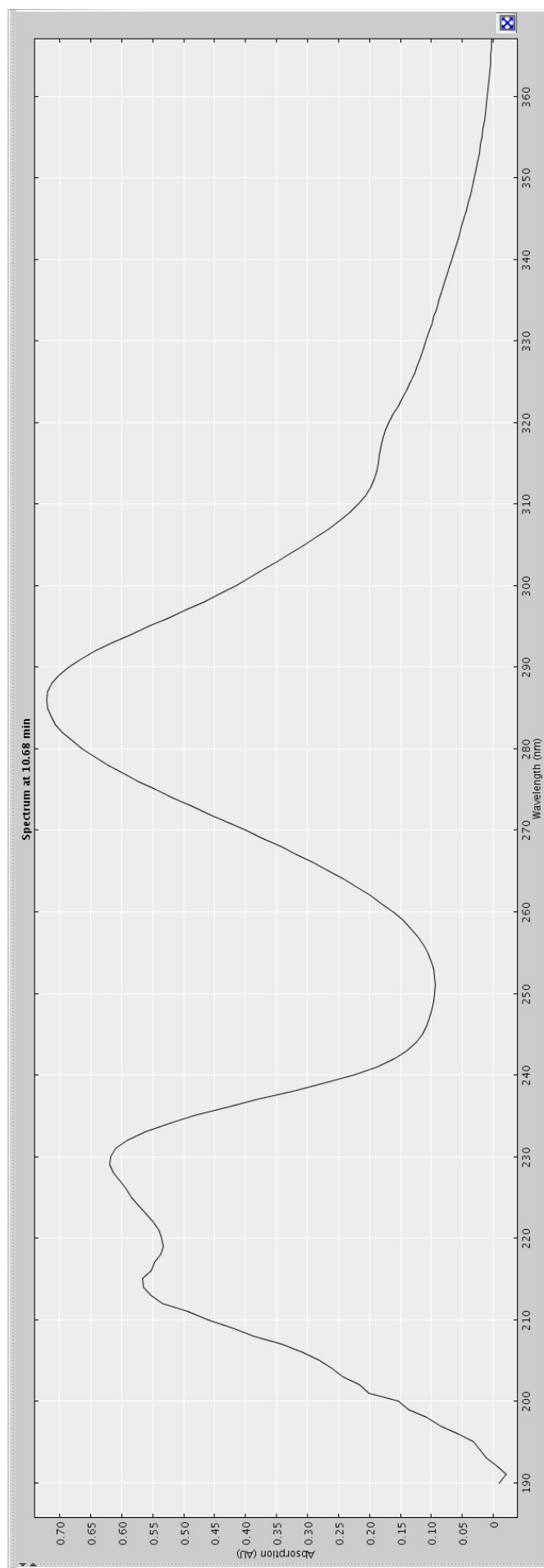


Figure S43. Extracted UV profile of compound eluting at 9.98 min (**12**) from HPLC-NMR (*C. retroflexa*).

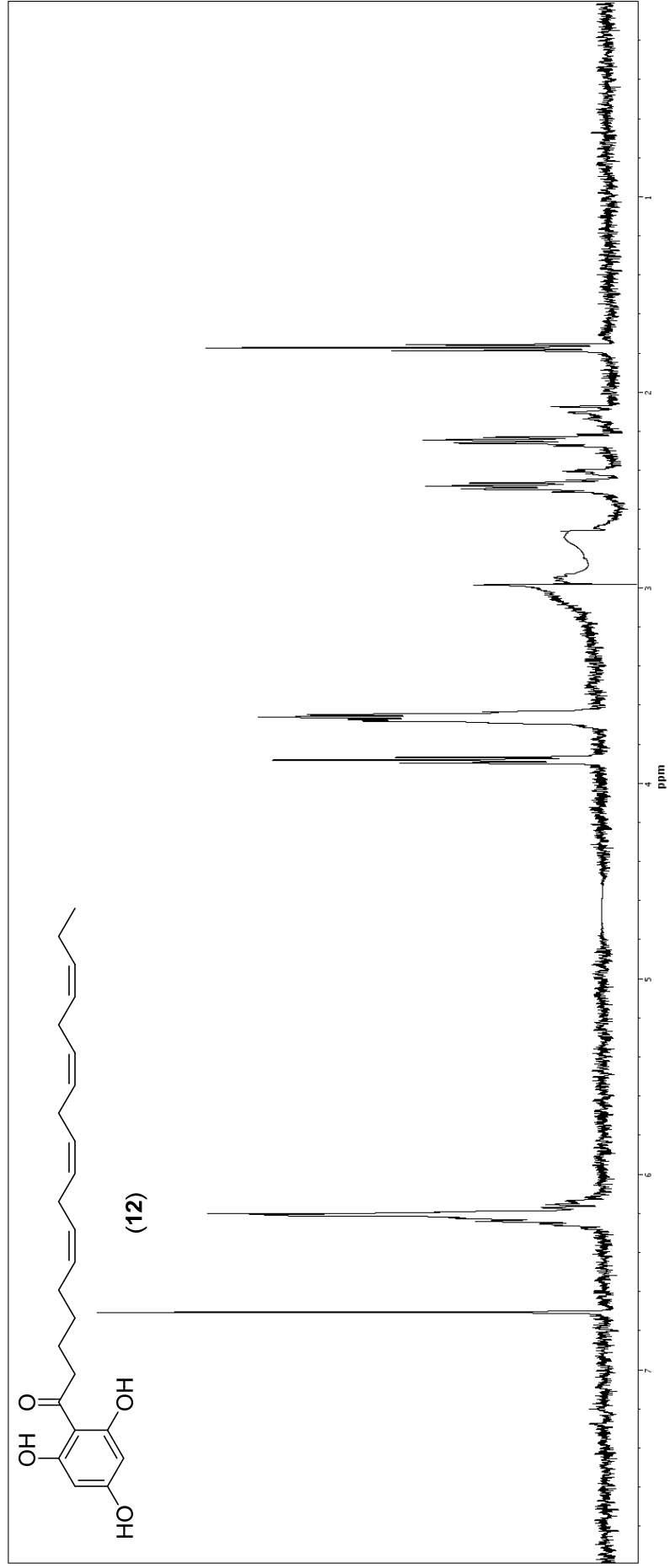


Figure S44. WET1D Proton NMR spectrum (500 MHz, 75% CH₃CN/D₂O) of compound eluting at 9.98 min (12) (*C. retroflexa*).

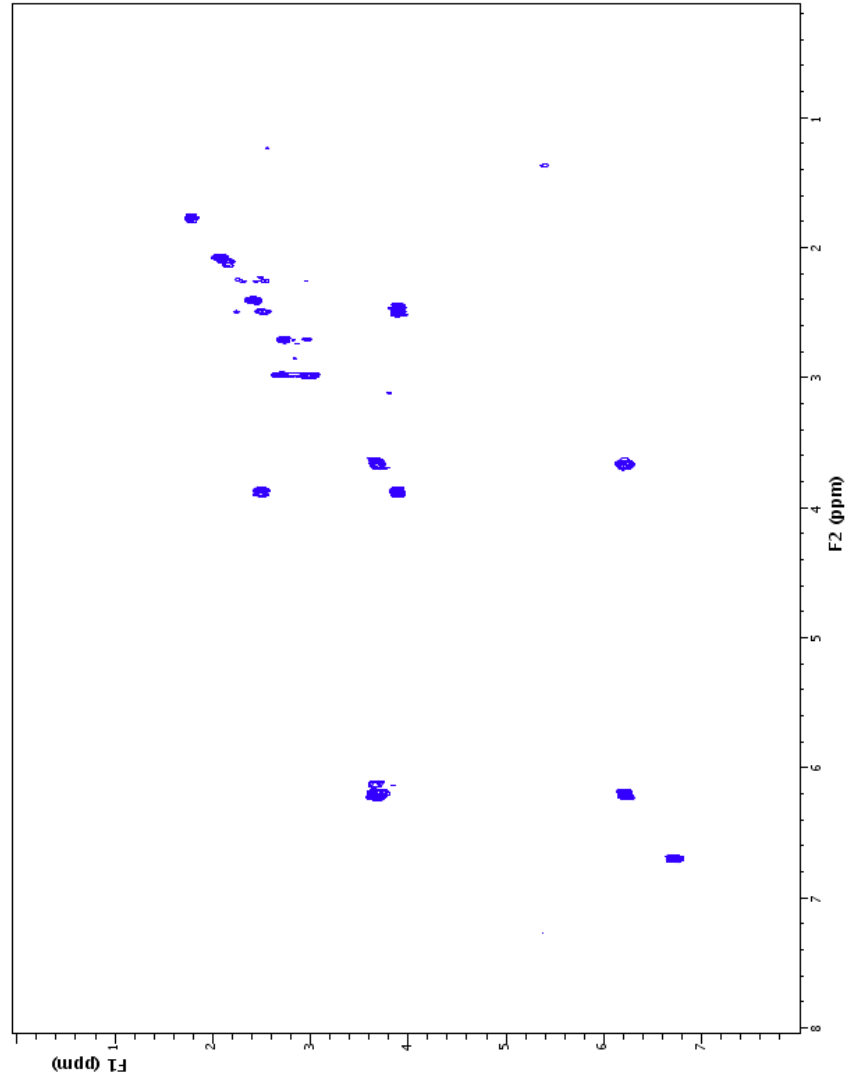


Figure S45. gCOSY NMR spectrum (500 MHz, 75% CH₃CN/D₂O) of compound eluting at 9.98 min (**12**) (*C. retroflexa*).

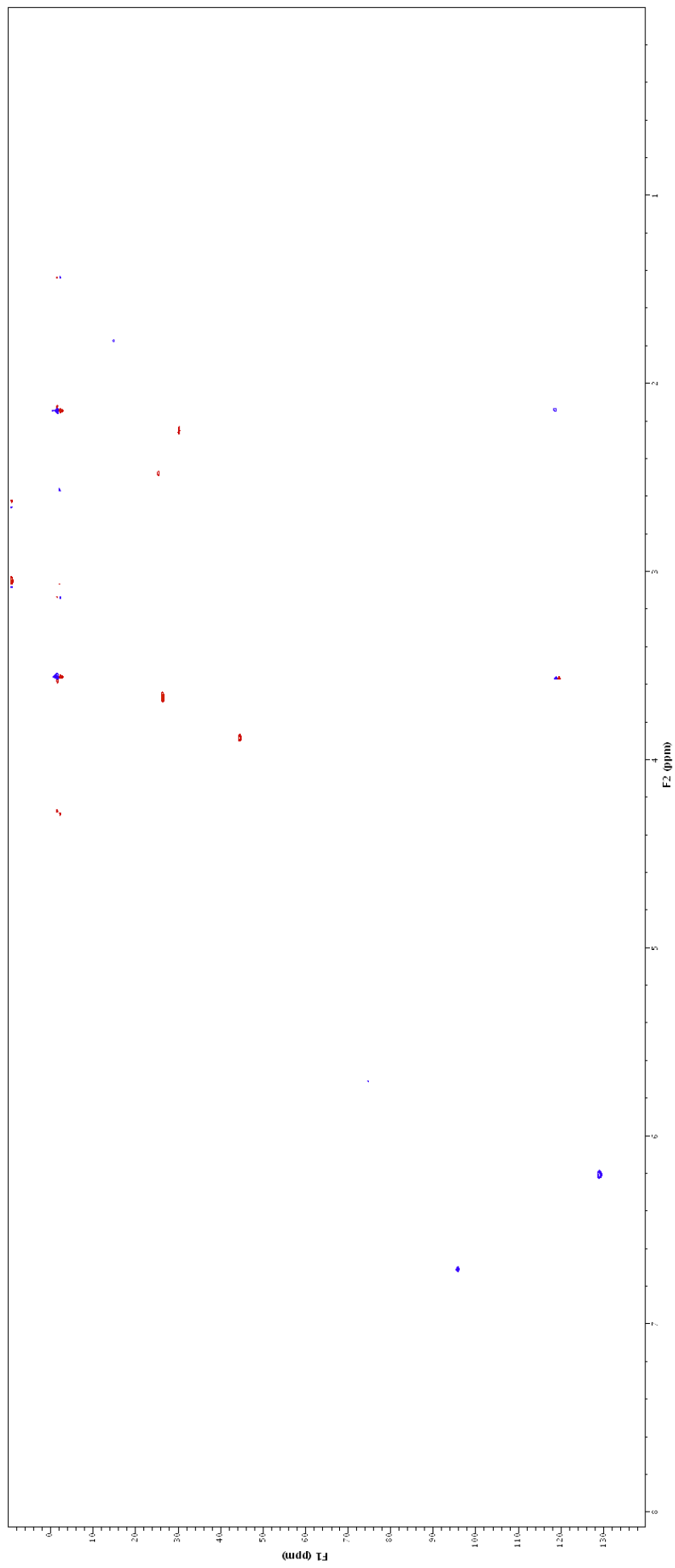


Figure S46. HSQCAD NMR spectrum (500 MHz, 75% CH₃CN/D₂O) of compound eluting at 9.98 min (**12**) (*C. retroflexa*).

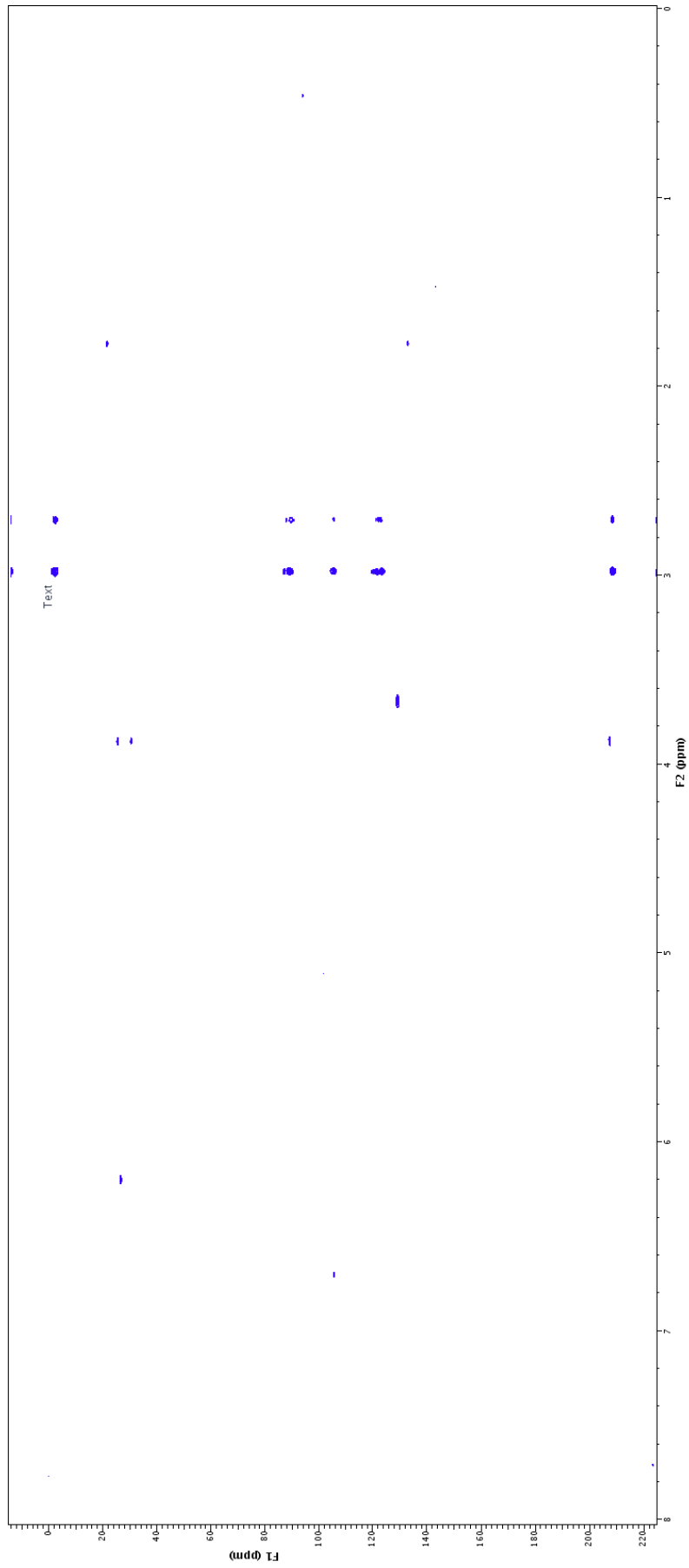


Figure S47. gHMBCAD NMR spectrum (500 MHz, 75% CH₃CN/D₂O) of compound eluting at 9.98 min (**12**) (*C. retroflexa*).

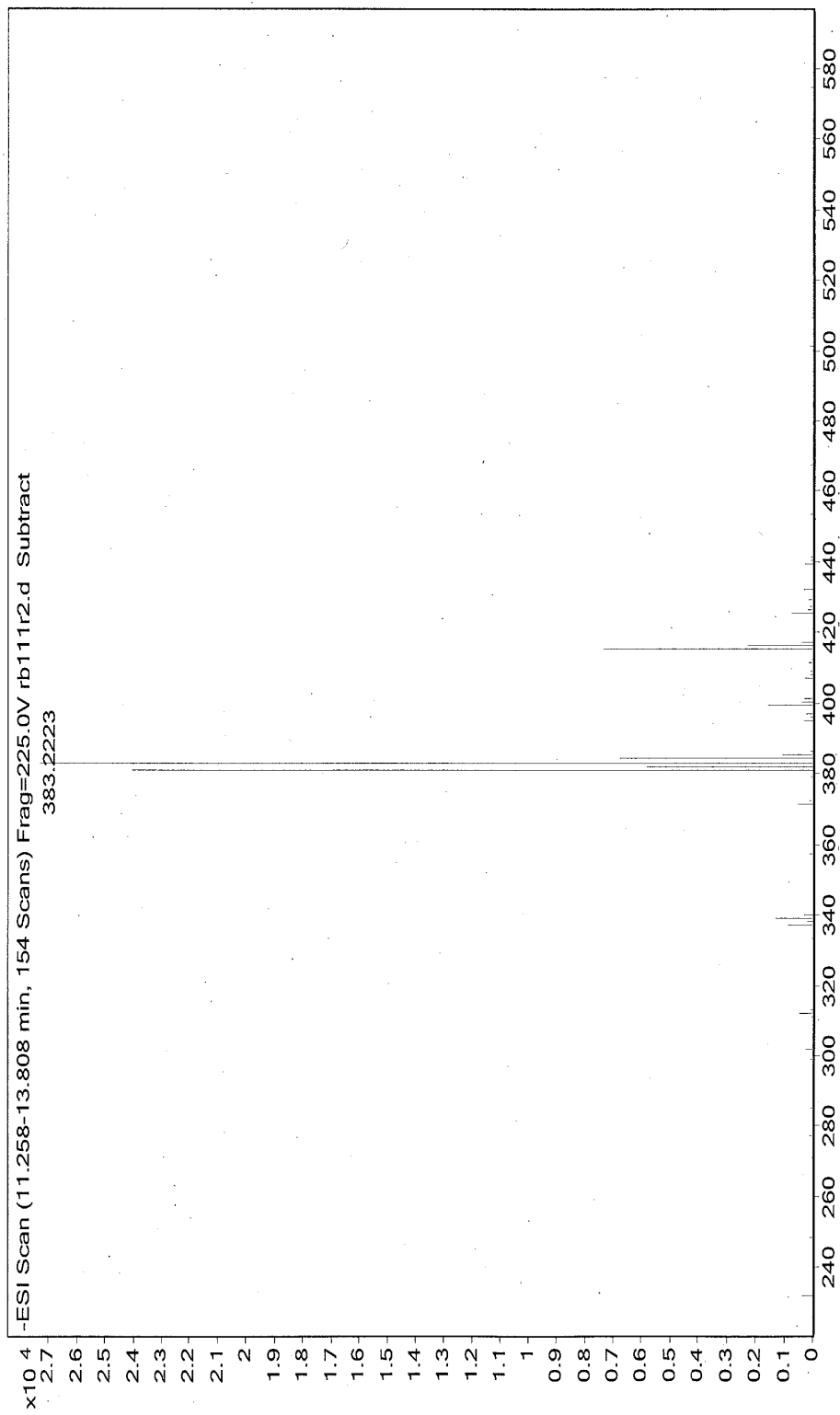
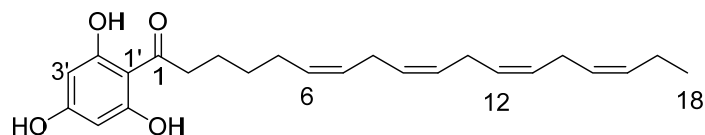


Figure S48. High resolution negative ESI-MS of compound eluting at 9.98 min (**12**) from HPLC-MS (*C. retroflexa*).



(12)

Position	δ_{H} (J in Hz)	δ_{C} , mult. ^a	gCOSY	gHMBCAD
1		207.2, s		
2	3.87, t (7.5)	44.3, t	3	1, 3, 4
3	2.46, p (7.5)	25.1, t	2, 4	5 ^w
4	2.23, p (7.5)	30.0, t	3	
5	SS	30.4, t		
6	6.18–6.28, m	128.9, d		8
7	6.18–6.28, m	128.9, d	8	
8	3.64, m	26.2, t	7, 9	6, 10
9	6.18–6.28, m	128.9, d	8	11
10	6.18–6.28, m	128.9, d	11	8
11	3.64, m	26.2, t	10, 12	9, 13
12	6.18–6.28, m	128.9, d	11	14
13	6.18–6.28, m	128.9, d	14	11
14	3.64, m	26.2, t	13, 15	12
15	6.18–6.28, m	128.9, d	14	
16	6.18–6.28, m	132.7, d		14
17	SS	21.1, t		
18	1.76, t (7.0)	14.6, q		16, 17
1'		105.0, s		
2'		164.9, s		
3'	6.69, s	95.7, d		1', 2', 4', 6'
4'		164.9, s		
5'	6.69, s	95.7, d		
6'		164.9, s		
2'-OH	ND			
4'-OH	ND			
6'-OH	ND			

Referenced to D₂O (δ_{H} 4.64 ppm); ^a carbon assignments based on HSQCAD and gHMBCAD NMR experiments; ^w indicates weak or long range correlation; SS Signal suppressed; ND Not Detected.

Figure S49. NMR data for compound eluting at 9.98 min (12) (*C. retroflexa*).

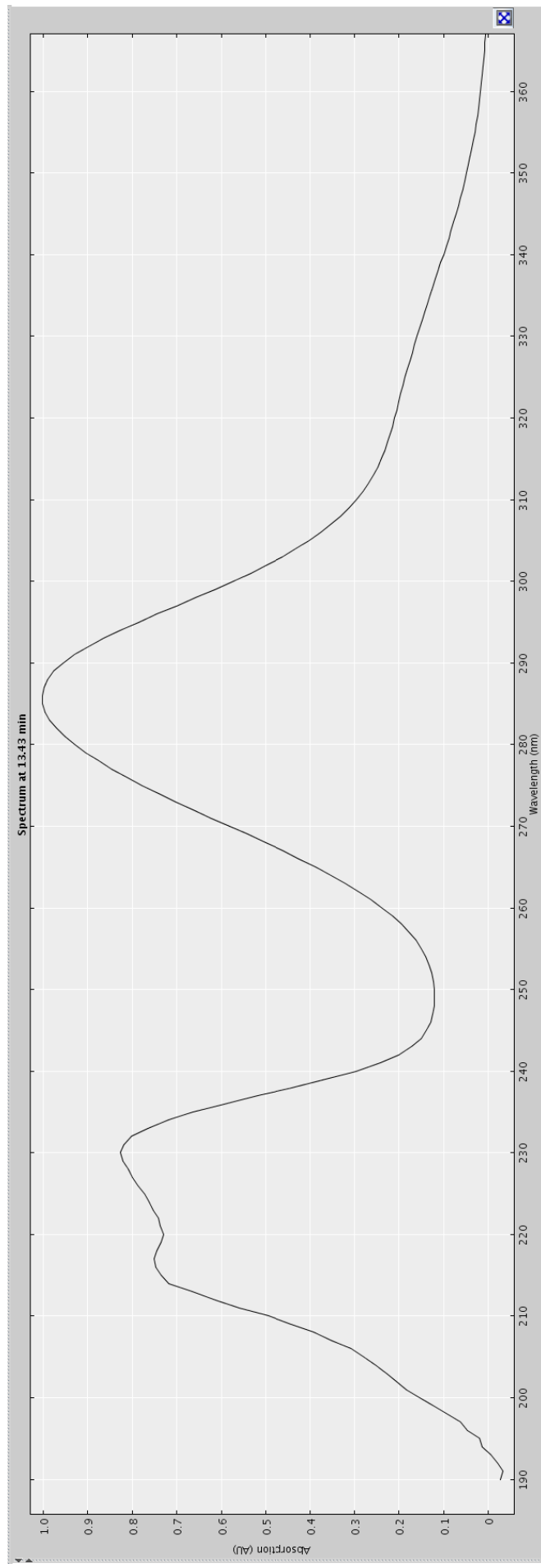


Figure S50. Extracted UV profile of compound eluting at 12.95 min (**13**) from HPLC-NMR (*C. retroflexa*).

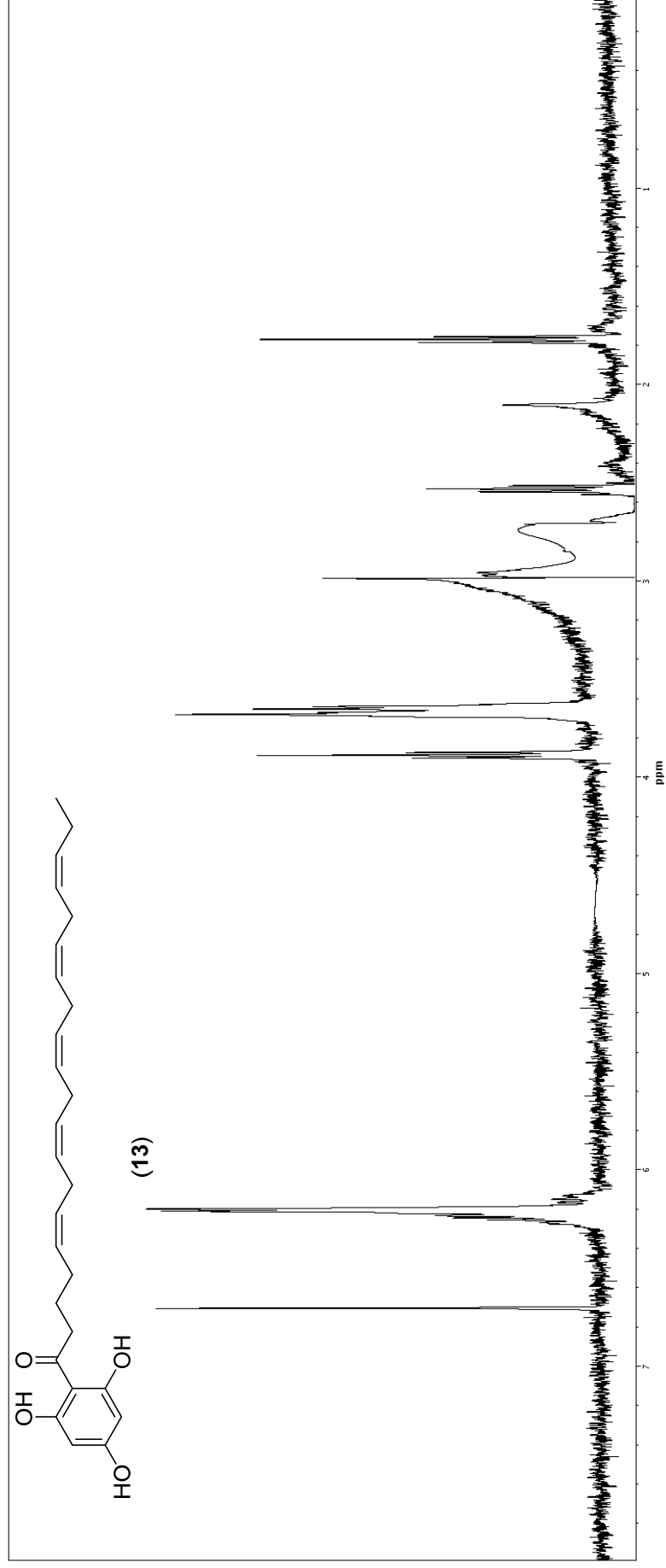


Figure S51. WET1D Proton NMR spectrum (500 MHz, 75% CH₃CN/D₂O) of compound eluting at 12.95 min (**13**) (*C. retroflexa*).

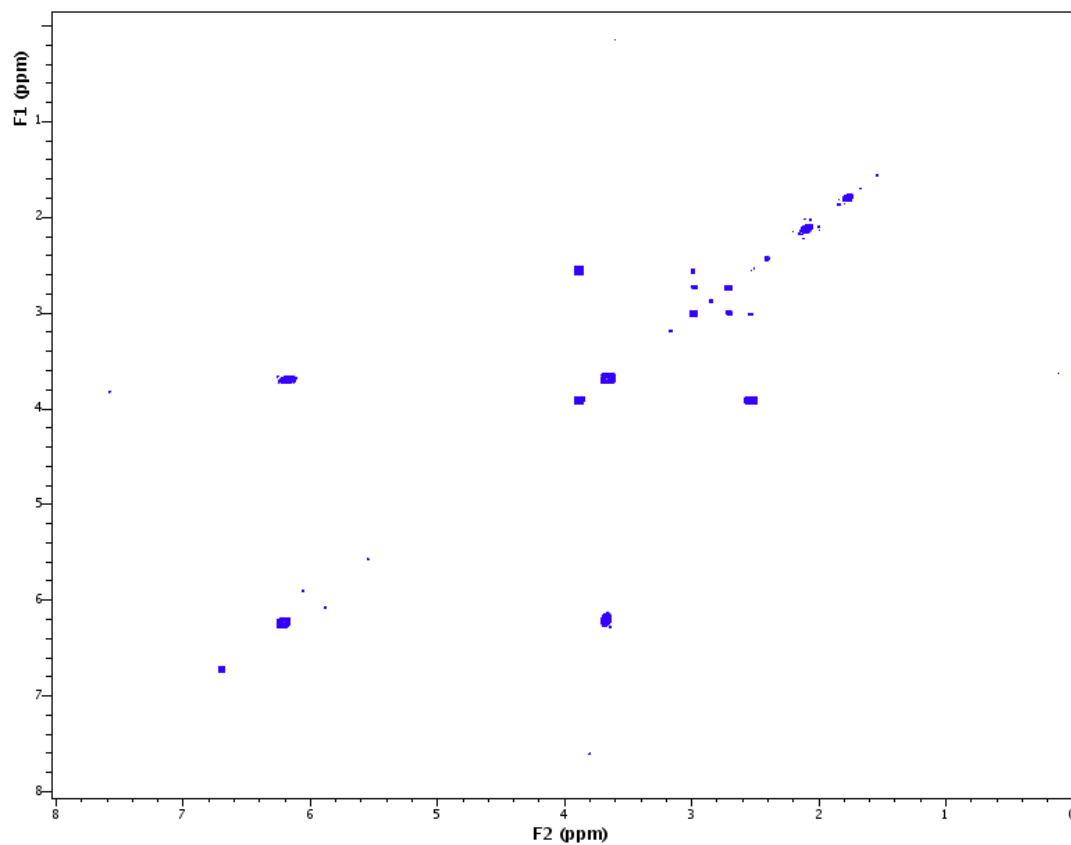


Figure S52. gCOSY NMR spectrum (500 MHz, 75% CH₃CN/D₂O) of compound eluting at 12.95 min (**13**) (*C. retroflexa*).

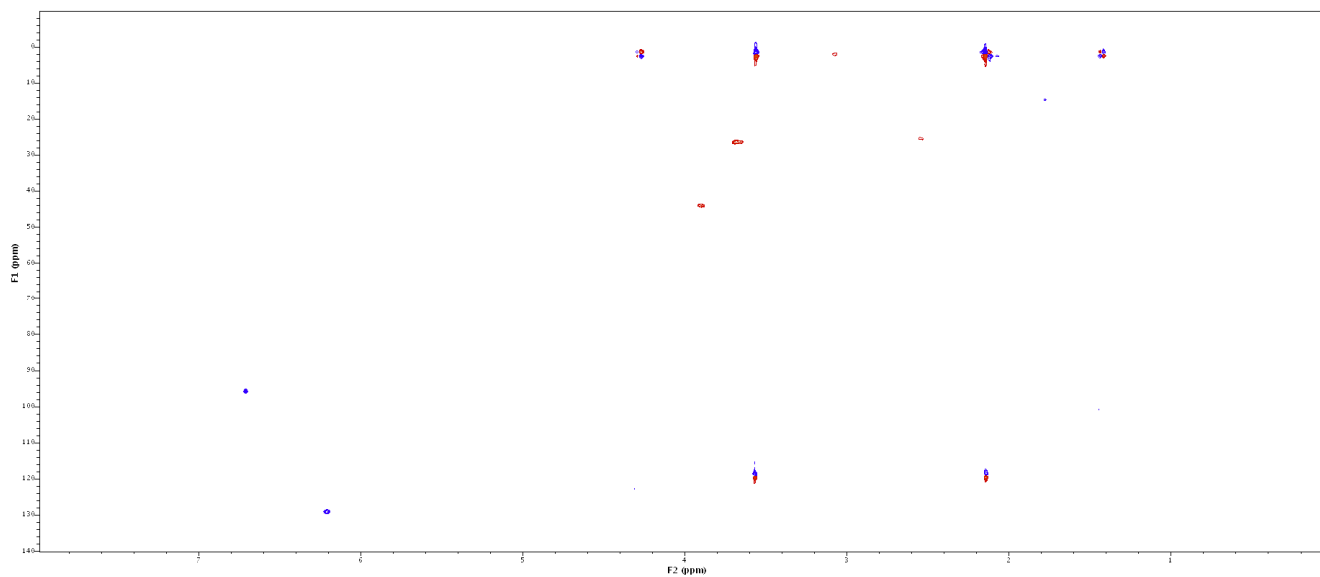


Figure S53. HSQCAD NMR spectrum (500 MHz, 75% CH₃CN/D₂O) of compound eluting at 12.95 min (**13**) (*C. retroflexa*).

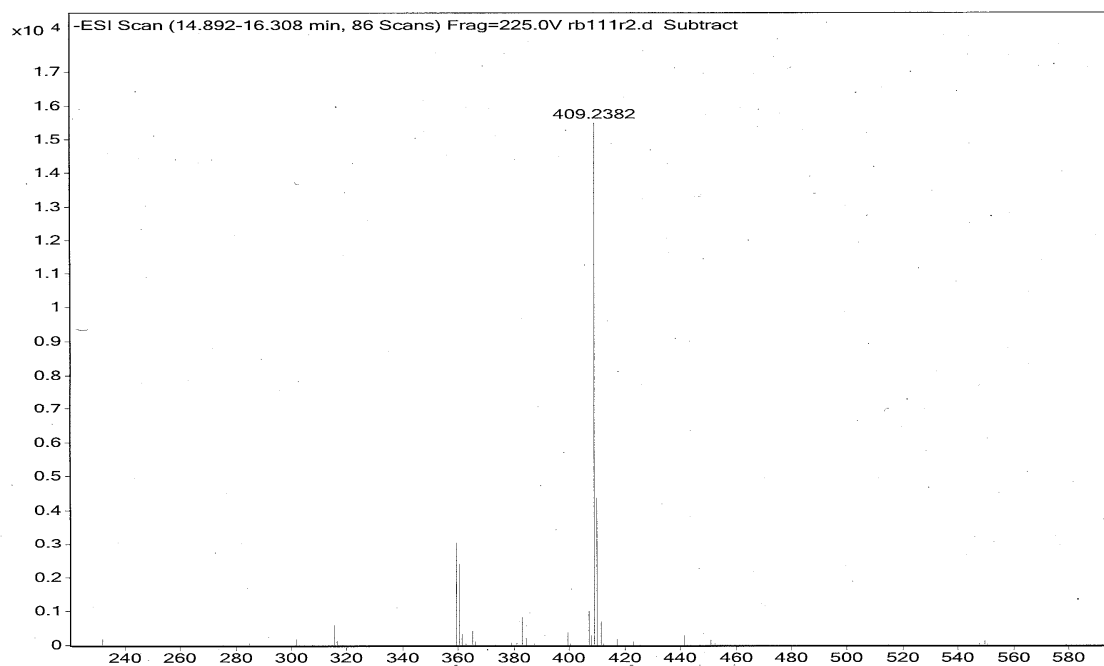
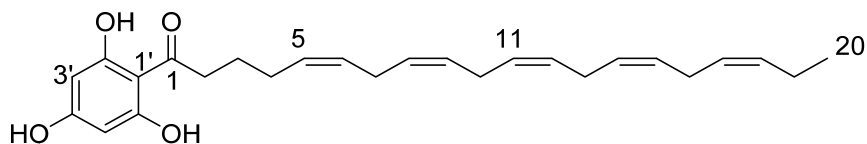


Figure S54. High resolution negative ESI-MS of compound eluting at 12.95 min (**13**) from HPLC-MS (*C. retroflexa*).



(13)

Position	δ_{H} (J in Hz)	δ_{C} , mult. ^a	gCOSY
1			
2	3.88, t (7.0)	43.8, t	3
3	2.55, m	25.3, t	2, 4
4	3.00, m	ND	3
5	6.19, m	128.9, d	
6	6.19, m	128.9, d	7
7	3.60–3.70, m	26.2, t	6, 8
8	6.19, m	128.9, d	7
9	6.19, m	128.9, d	10
10	3.60–3.70, m	26.2, t	9, 11
11	6.19, m	128.9, d	10
12	6.19, m	128.9, d	13
13	3.60–3.70, m	26.2, t	12, 14
14	6.19, m	128.9, d	13
15	6.19, m	128.9, d	16
16	3.60–3.70	26.2, t	15, 17
17	6.19, m	128.9, d	16
18	6.19, m	128.9, d	
19	SS	ND	
20	1.76, t (7.5)	14.4, q	
1'		ND	
2'		ND	
3'	6.69, s	95.6, d	
4'		ND	
5'	6.69, s	95.6, d	
6'		ND	
2'-OH	ND		
4'-OH	ND		
6'-OH	ND		

Referenced to D₂O (δ_{H} 4.64 ppm); ^a carbon assignments based on HSQCAD NMR experiments; SS Signal suppressed; ND Not Detected.

Figure S55. NMR data for compound eluting at 12.95 min (13) (*C. retroflexa*).

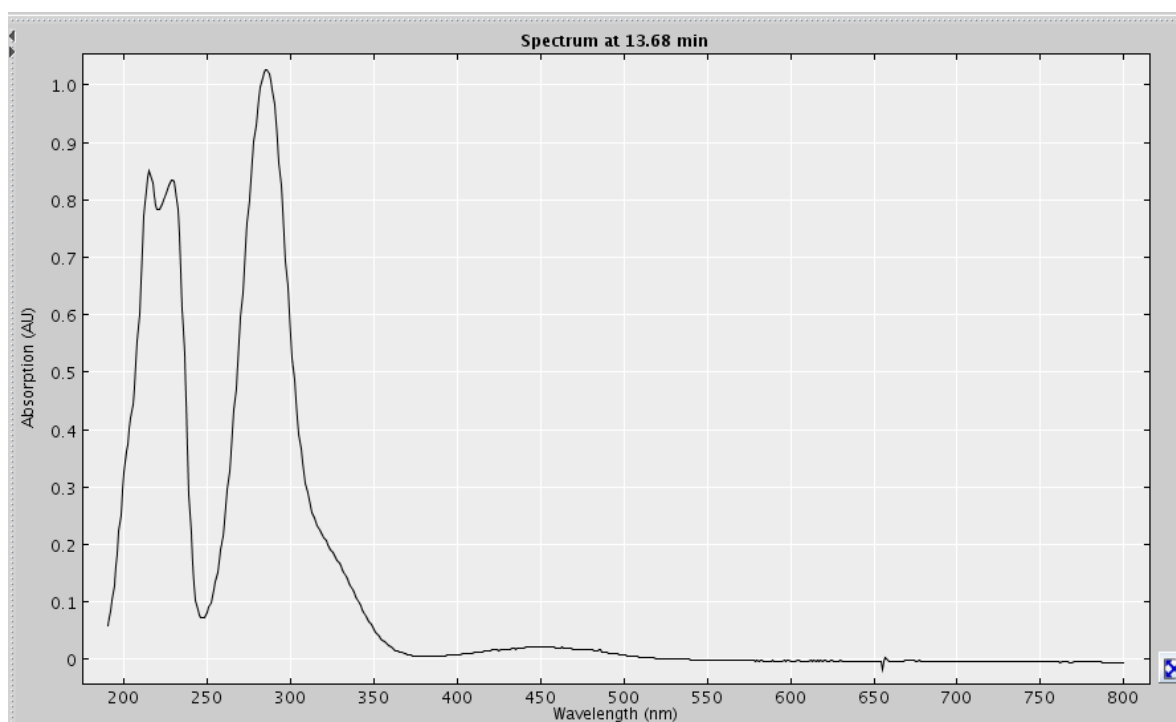


Figure S56. Extracted UV profile of compound eluting at 13.65 min (**17**) from HPLC-NMR (*S. cf. fallax*).

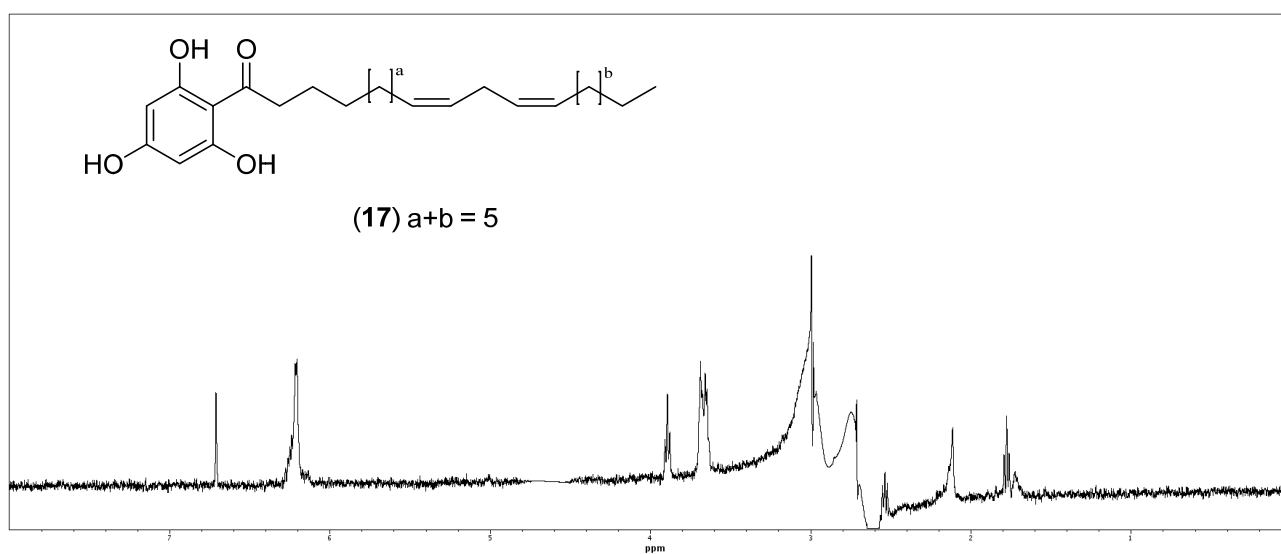


Figure S57. WET1D Proton NMR spectrum (500 MHz, 75% CH₃CN/D₂O) of compound eluting at 13.65 min (**17**) (*S. cf. fallax*).

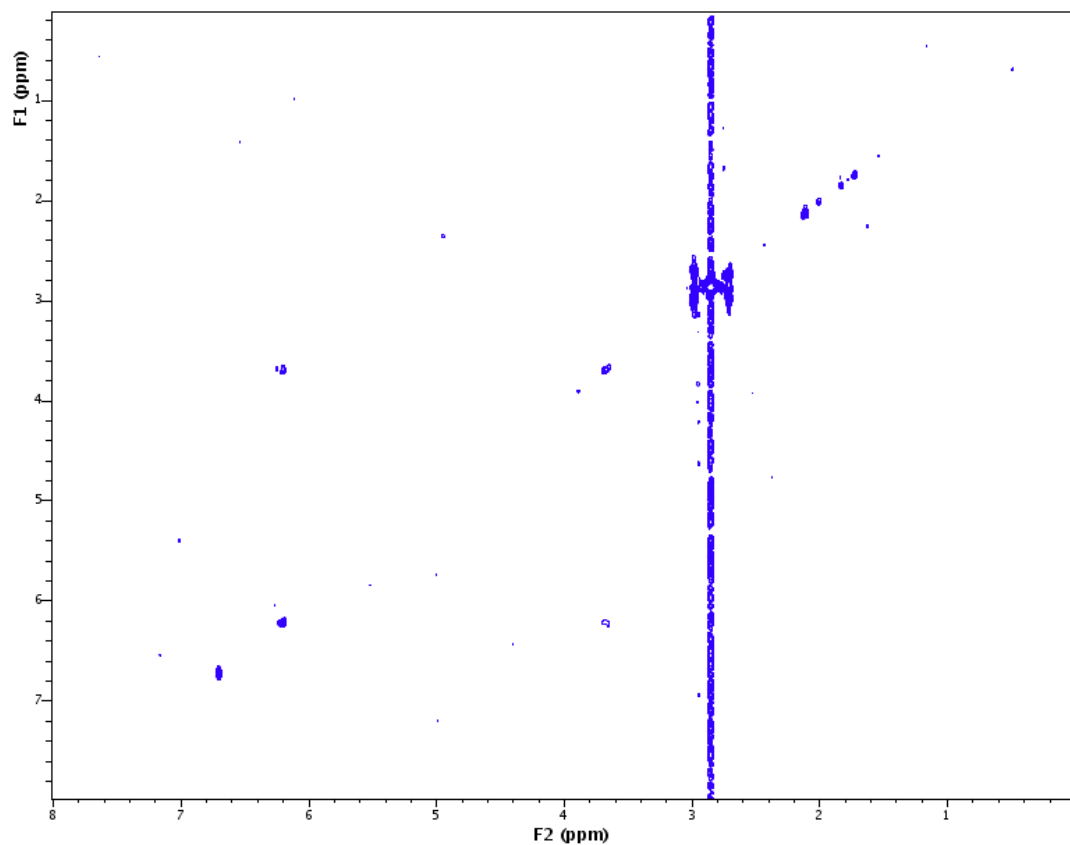


Figure S58. gCOSY NMR spectrum (500 MHz, 75% CH₃CN/D₂O) of compound eluting at 13.65 min (**17**) (*S. cf. fallax*).

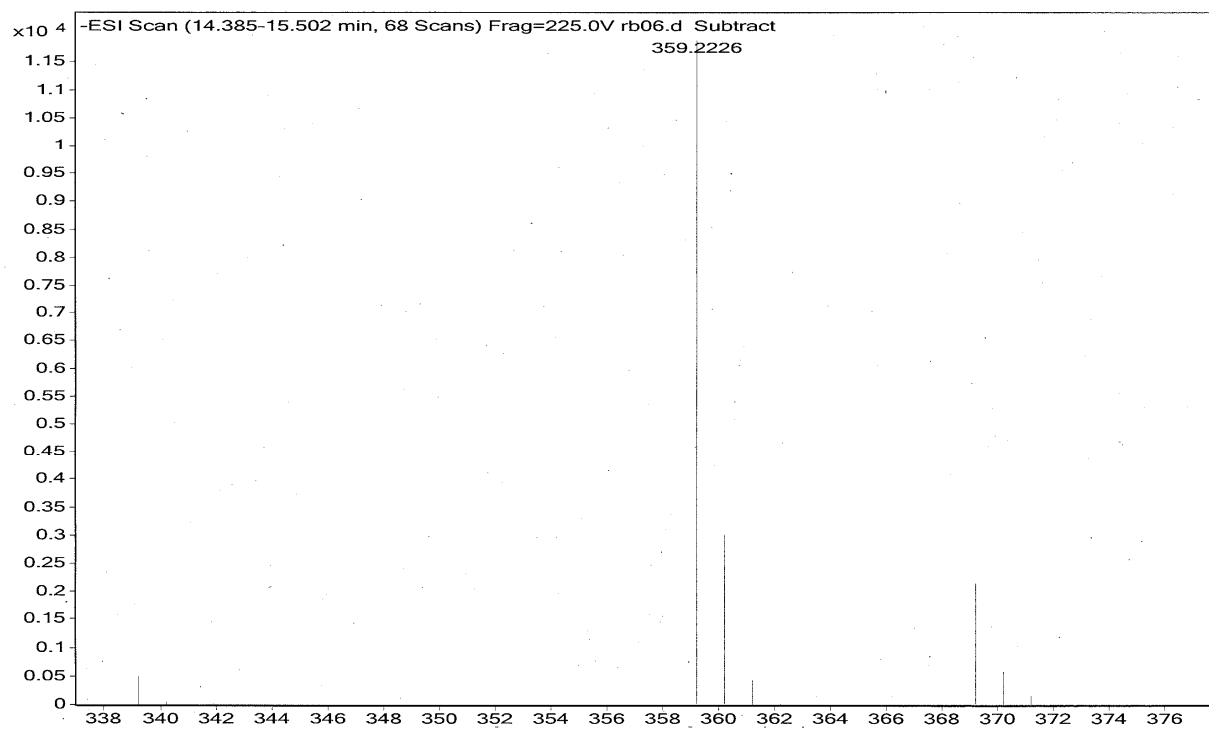


Figure S59. High resolution negative ESI-MS of compound eluting at 13.65 min (**17**) from HPLC-MS (*S. cf. fallax*).

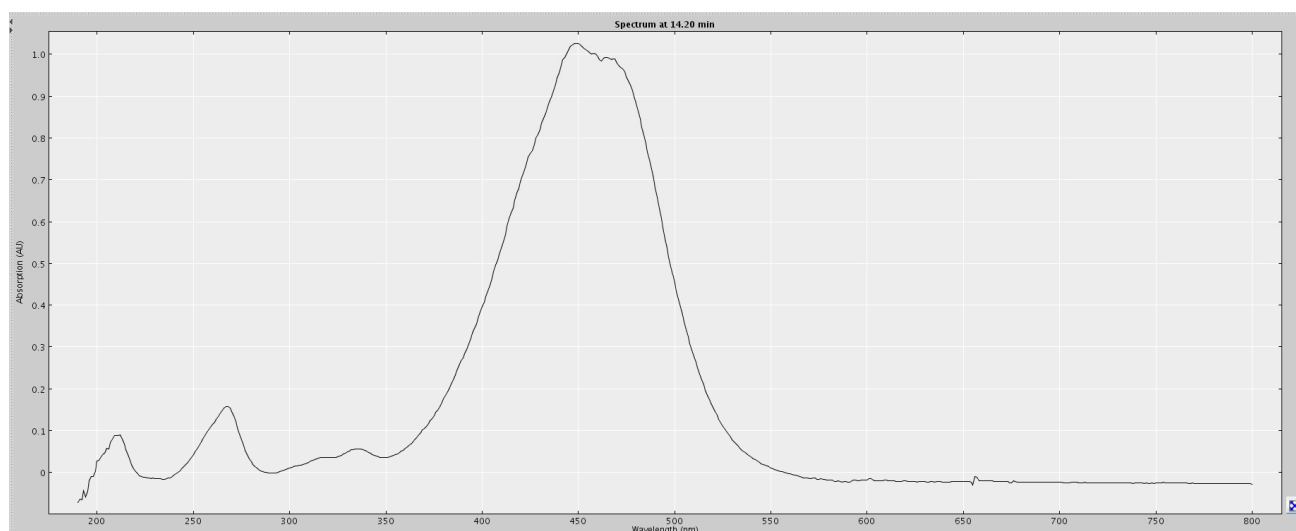


Figure S60. Extracted UV profile of compound eluting at 14.53 min (**5**) from HPLC-NMR (*H. pseudospicata*).

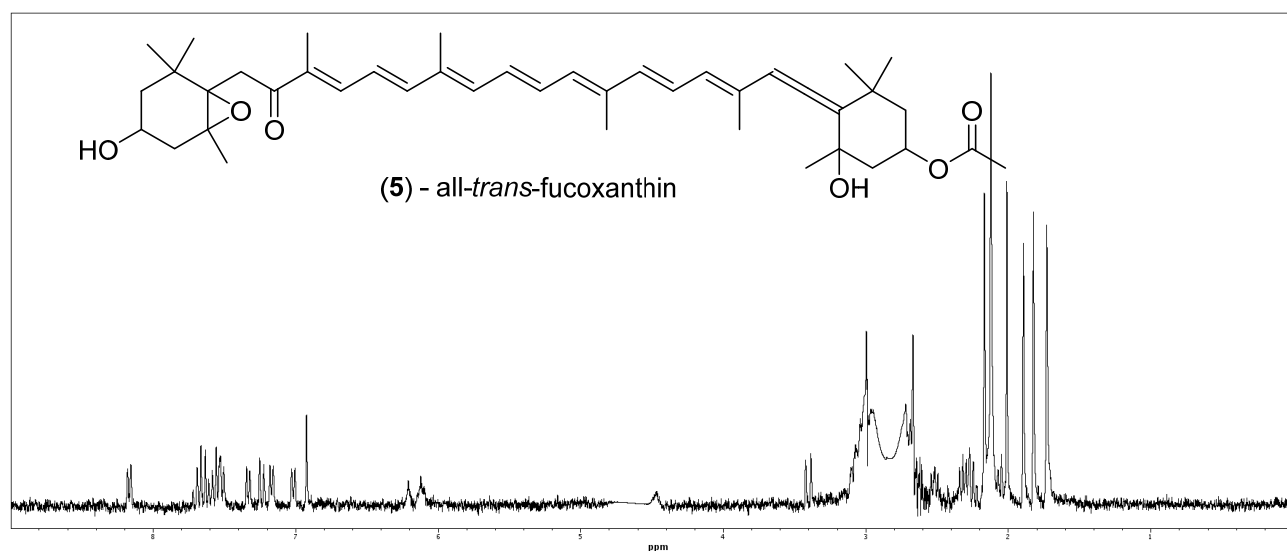


Figure S61. WET1D Proton NMR spectrum (500 MHz, 75% CH₃CN/D₂O) of compound eluting at 14.53 min (**5**) (*H. pseudospicata*).

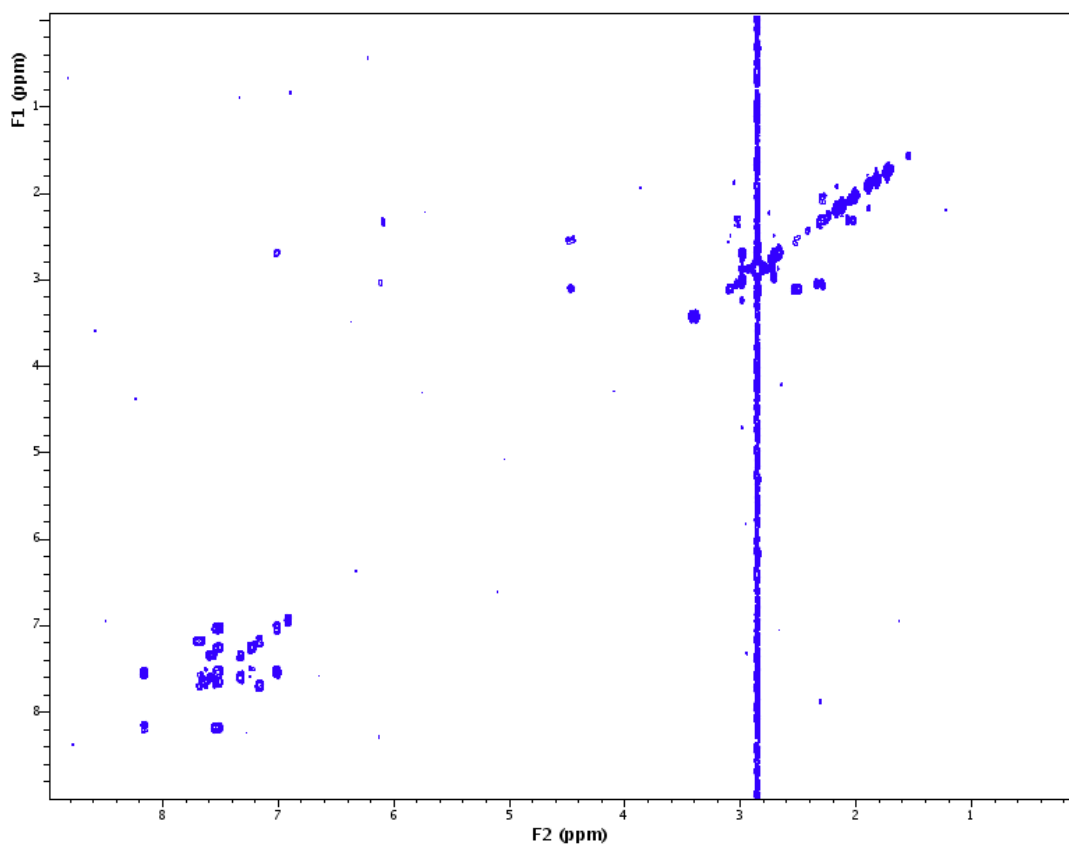


Figure S62. gCOSY NMR spectrum (500 MHz, 75% CH₃CN/D₂O) of compound eluting at 14.53 min (**5**) (*H. pseudospicata*).

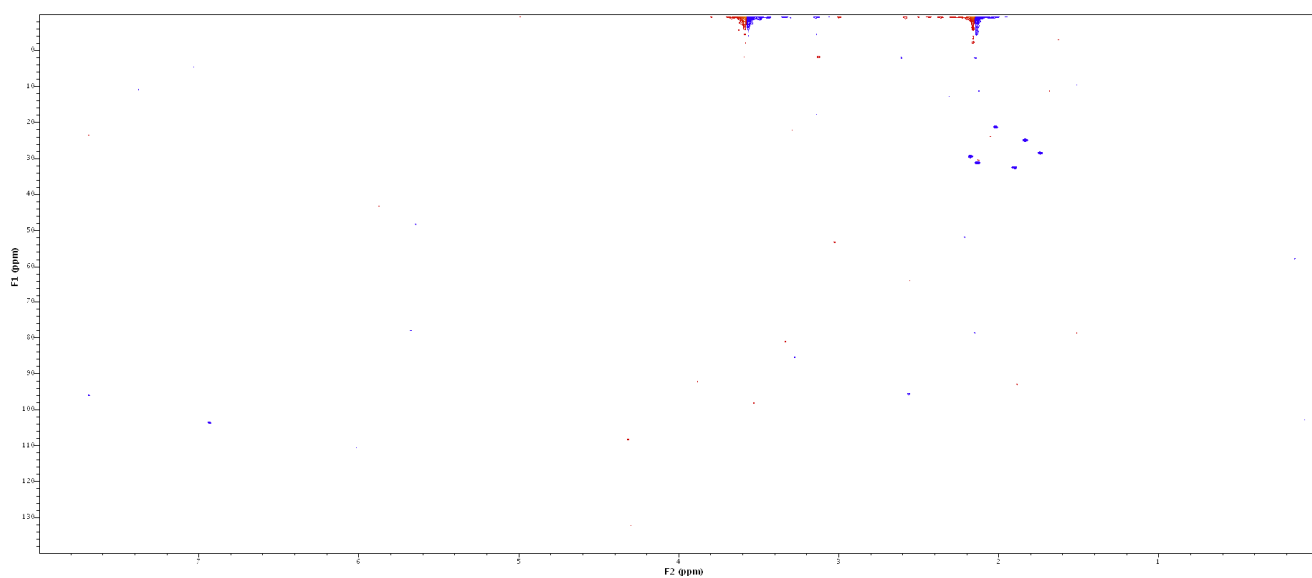


Figure S63. HSQCAD NMR spectrum (500 MHz, 75% CH₃CN/D₂O) of compound eluting at 14.53 min (**5**) (*H. pseudospicata*).

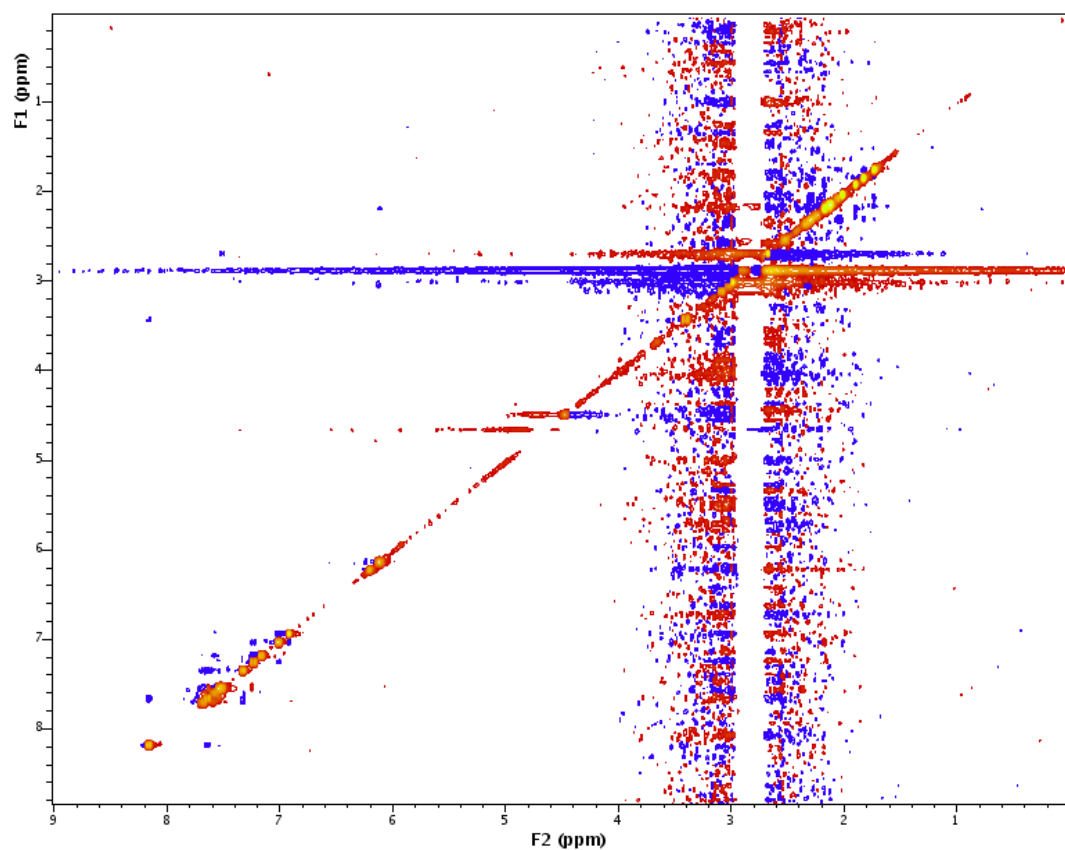


Figure S64. ROESYAD NMR spectrum (500 MHz, 75% CH₃CN/D₂O) of compound eluting at 14.53 min (**5**) (*H. pseudospicata*).

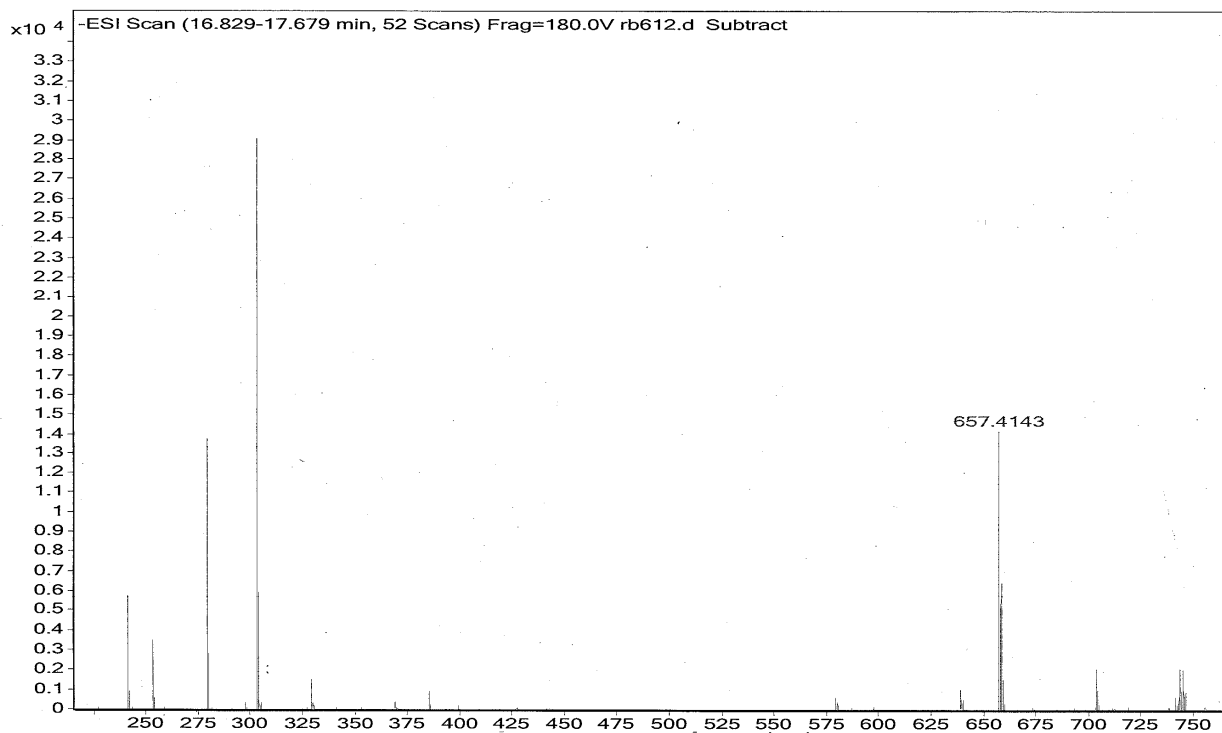


Figure S65. High resolution negative ESI-MS of compound eluting at 14.53 min (**5**) from HPLC-MS (*H. pseudospicata*).

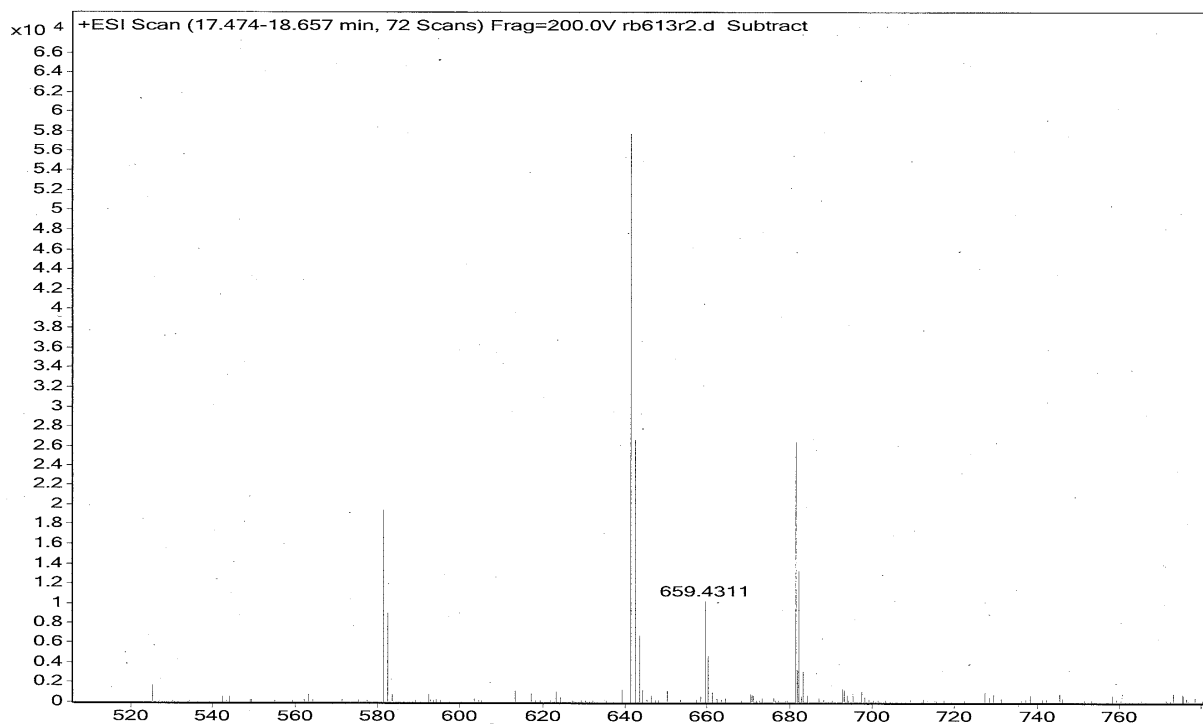
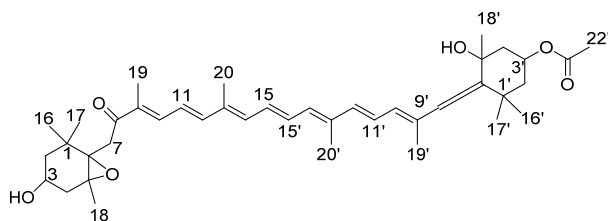


Figure S66. High resolution positive ESI-MS of compound eluting at 14.53 min (**5**) from HPLC-MS (*H. pseudospicata*).



Position	δ_C^a , mult.	δ_H (J in Hz)	gCOSY	Roesyad
1	ND			
2a	ND	SS		
2b	ND	SS		
3	ND	4.46, m		
4a	ND	SS		
4b	ND	SS		
5	ND			
6	ND			
7a	ND	3.40, d (18.5)		
7b	ND	SS		
8	ND			
9	ND			
10	ND	8.16, d (10.5)	11	7a, 12

Figure S67. Cont.

11	ND	7.54, m	10, 12	
12	ND	7.65, m		10, 14
13	ND			
14	ND	7.33, d (10.5)	15	12, 15'
15	ND	7.58, m	14	14'
16	24.7, CH ₃	1.82, s		
17	28.2, CH ₃	1.73, s		
18	21.0, CH ₃	2.01, s		
19	ND	SS		
20	ND	SS		
1'	ND			
2a'	ND	2.29, m	2b'	16'
2b'		2.04 ^b		
3'	ND	6.12, m	2a', 4b'	
4a'	ND	2.51, m	4b'	
4b'		3.02 ^b		
5'	ND			
6'	ND			
7'	ND			
8'	103.4, CH	6.92, s		10'
9'	ND			
10'	ND	7.01, d (11.5)	11', 19'	8', 12'
11'	ND	7.53, m	10', 12'	19'
12'	ND	7.23, d (15.0)		10', 14'
13'	ND			
14'	ND	7.16, d (12.0)	15'	
15'	ND	7.69, m	14'	
16'	29.2, CH ₃	2.16, s		
17'	32.3, CH ₃	1.89, s		
18'	30.9, CH ₃	2.12, s		
19'	ND	2.67 ^b		
20'	ND	SS		
21'	ND			
22'	ND	SS		
3-OH		ND		
5'-OH		ND		

Referenced to 75% CH₃CN/D₂O; ^a Carbon assignments based on HSQCAD NMR experiment; ^b Proton assignment based on gCOSY experiment; ND Not Detected; SS Signal suppressed.

Figure S67. NMR data for compound eluting at 14.53 min (**5**) (*H. pseudospicata*).

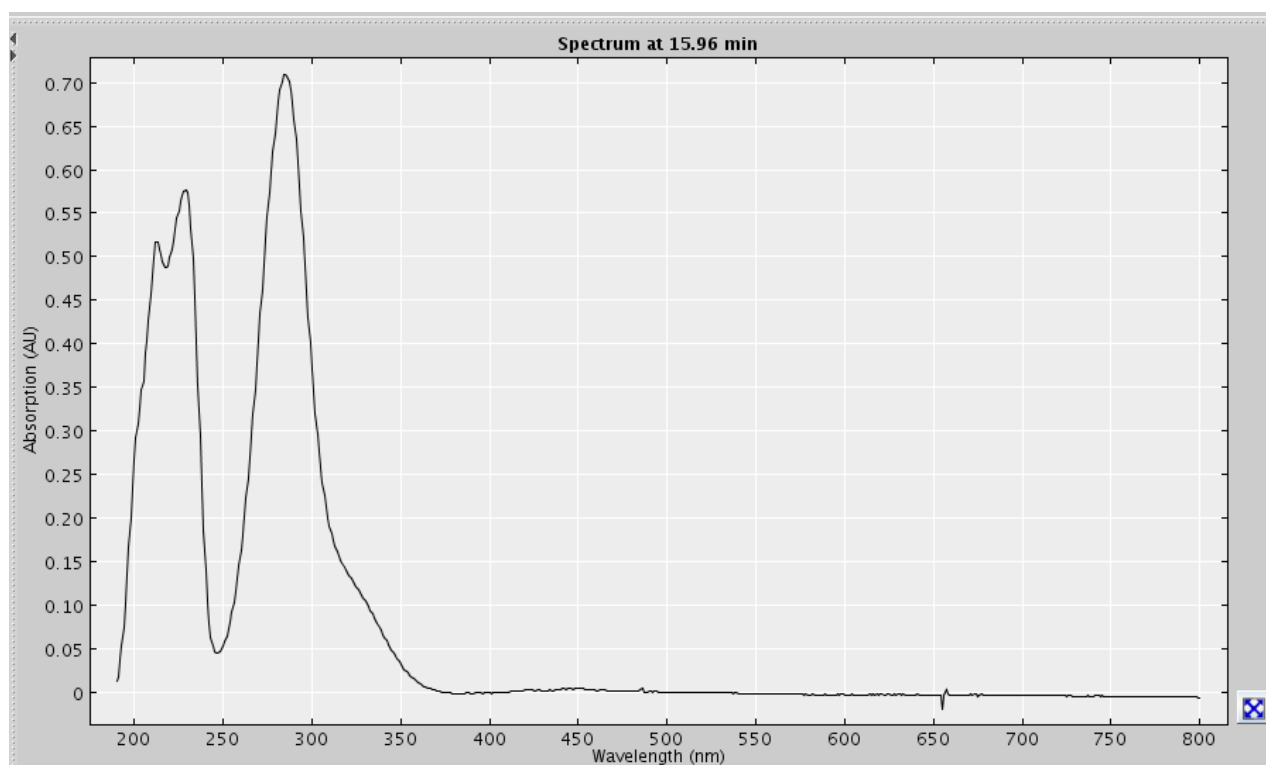


Figure S68. Extracted UV profile of compound eluting at 15.50 min (**20**) from HPLC-NMR (*S. cf. fallax*).

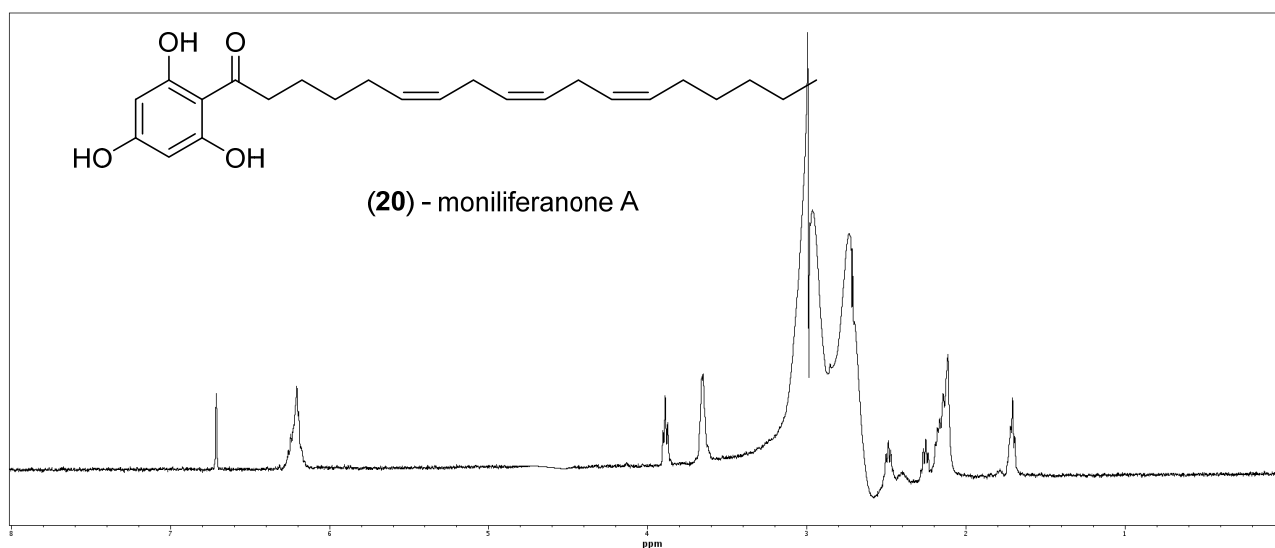


Figure S69. WET1D Proton NMR spectrum (500 MHz, 75% CH₃CN/D₂O) of compound eluting at 15.50 min (**20**) (*S. cf. fallax*).

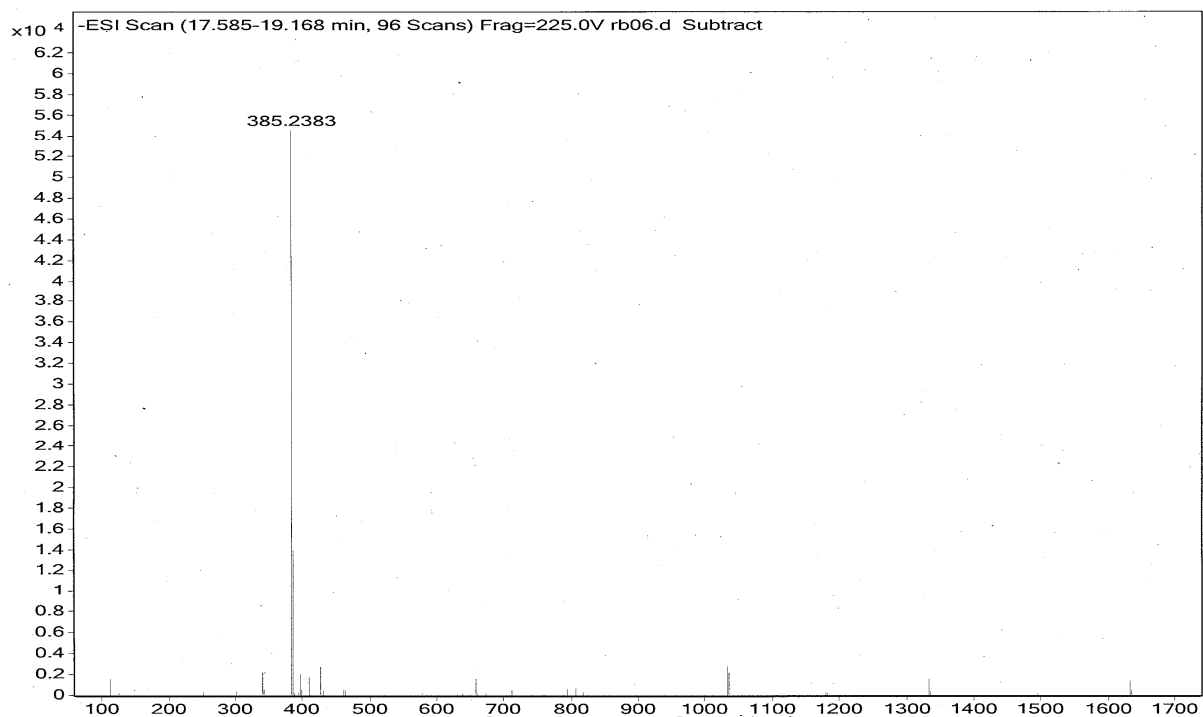
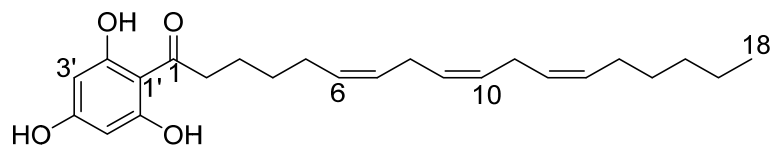


Figure S70. High resolution negative ESI-MS of compound eluting at 15.50 min (**20**) from HPLC-MS (*S. cf. fallax*).



(20) - moniliferanone A

Position	δ_H (J in Hz)
1	
2	3.88, t (7.5)
3	2.48, p (7.5)
4	2.25, p (7.5)
5	SS
6	6.20, m
7	6.20, m
8	3.65, m
9	6.20, m
10	6.20, m
11	3.65, m
12	6.20, m
13	6.20, m
14	SS
15	2.11–2.16, m
16	2.11–2.16, m
17	2.11–2.16, m
18	1.71, t (7.0)
1'	
2'	
3'	6.71, s
4'	
5'	6.71, s
6'	
1'-OH	ND
4'-OH	ND
6'-OH	ND

Referenced to 75% CH₃CN/D₂O; SS Signal suppressed; ND Not Detected.

Figure S71. NMR data for compound eluting at 15.50 min (**20**) (*S. cf. fallax*).

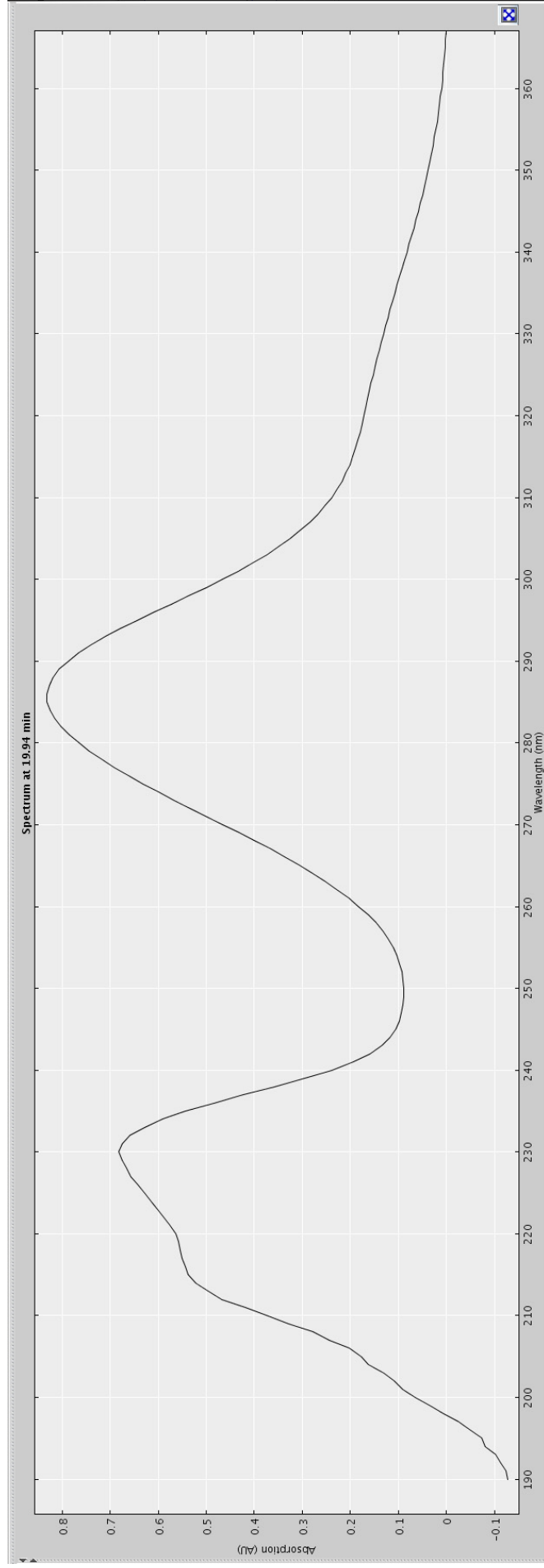


Figure S72. Extracted UV profile of compound eluting at 20.15 min (**21**) from HPLC-NMR (*C. retroflexa*).

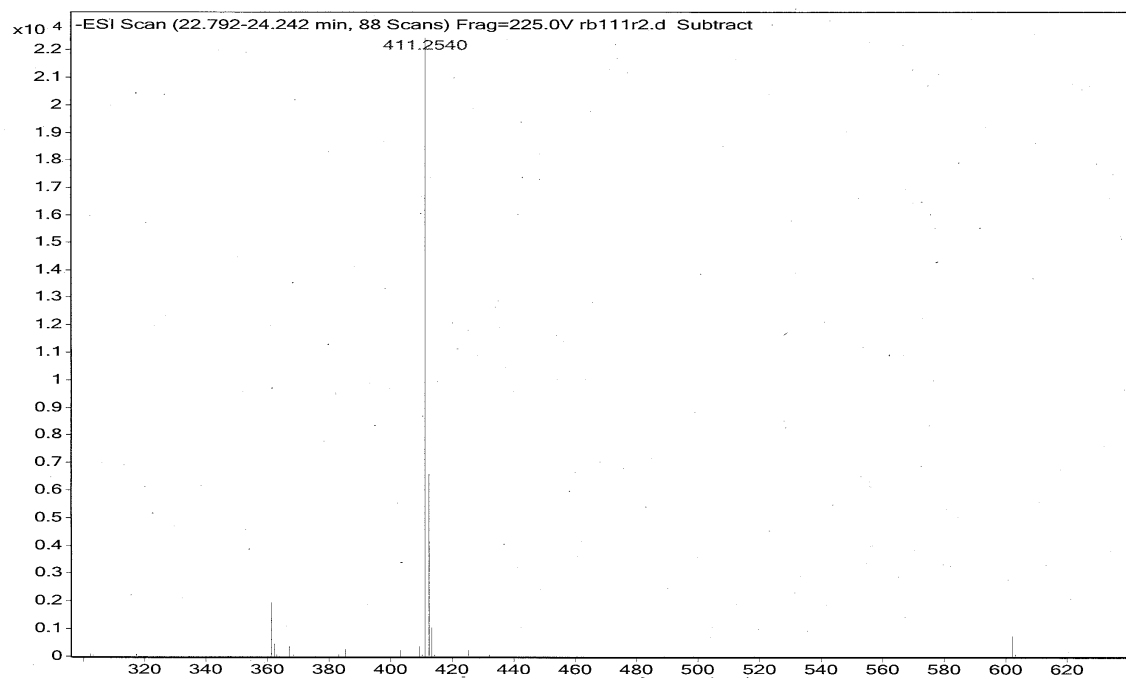
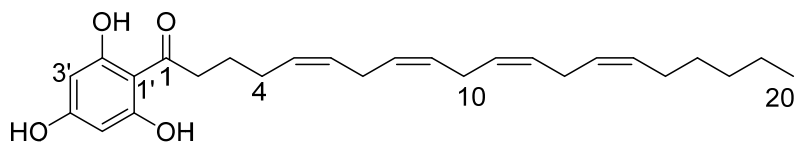


Figure S74. High resolution negative ESI-MS of compound eluting at 20.15 min (**21**) from HPLC-MS (*C. retroflexa*).



(21) - moniliferanone B

Position	δ_H (J in Hz)
1	
2	3.91, t (7.0)
3	2.55, m
4	SS
5	6.16–6.24, m
6	6.16–6.24, m
7	3.66, m
8	6.16–6.24, m
9	6.16–6.24, m
10	3.66, m
11	6.16–6.24, m
12	6.16–6.24, m
13	3.66, m
14	6.16–6.24, m
15	6.16–6.24, m
16	SS
17	SS
18	SS
19	SS
20	1.72, t (7.0)
1'	
2'	
3'	6.72, s
4'	
5'	6.72, s
6'	
2'-OH	ND
4'-OH	ND
6'-OH	ND

Referenced to D₂O (δ_H 4.64 ppm); SS Signal suppressed; ND Not Detected.

Figure S75. NMR data for compound eluting at 20.15 min (21) (*C. retroflexa*).

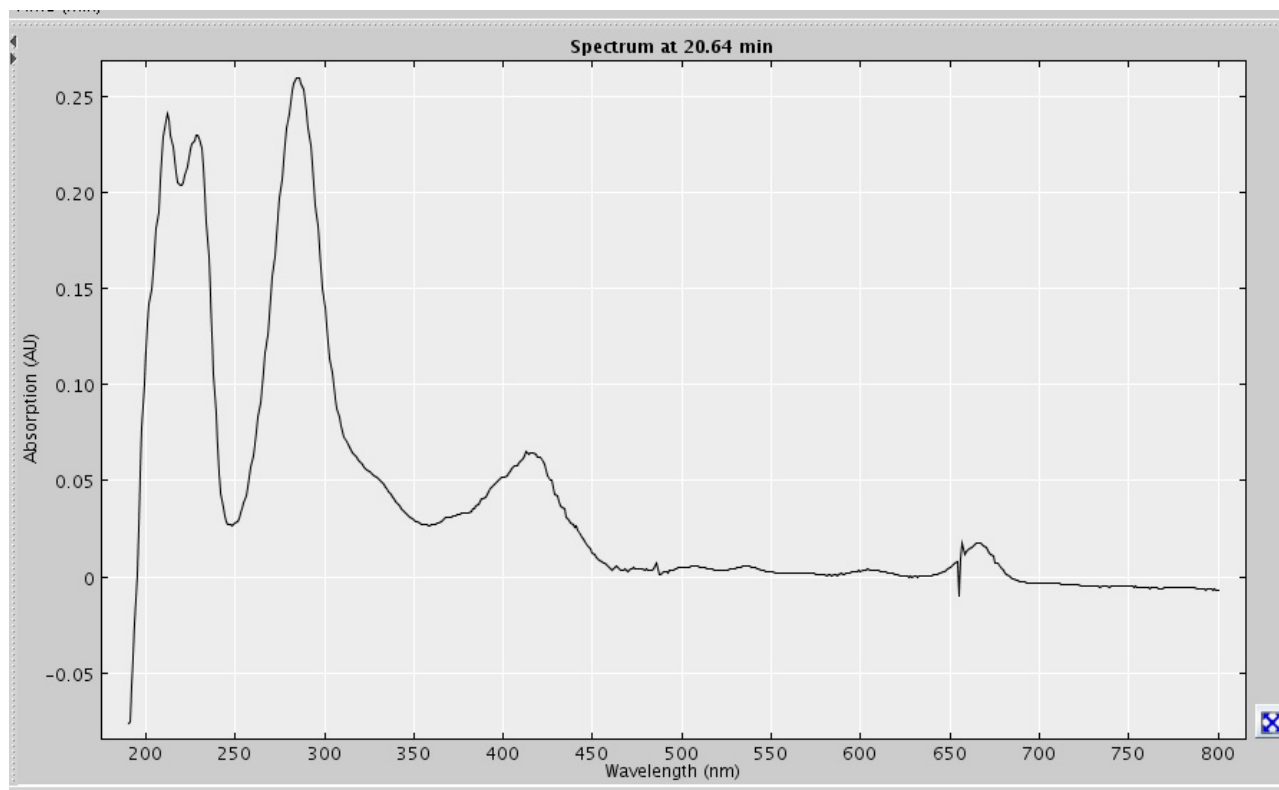


Figure S76. Extracted UV profile of compound eluting at 21.62 min (**14**) from HPLC-NMR (*S. cf. fallax*).

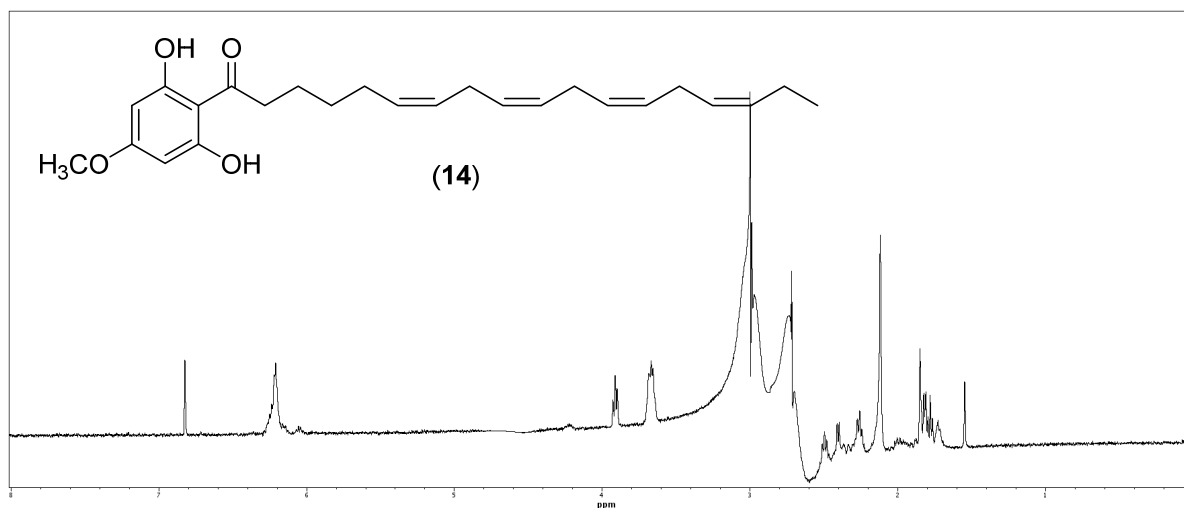


Figure S77. WET1D Proton NMR spectrum (500 MHz, 75% CH₃CN/D₂O) of compound eluting at 21.62 min (**14**) (*S. cf. fallax*).

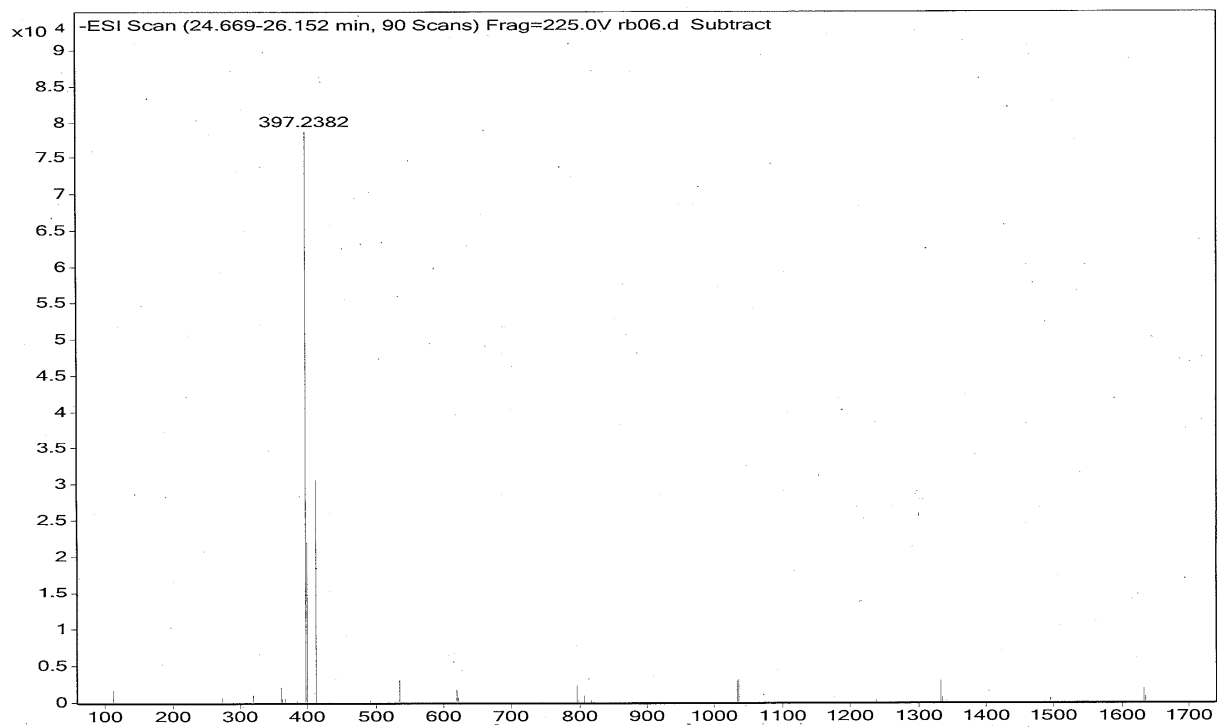
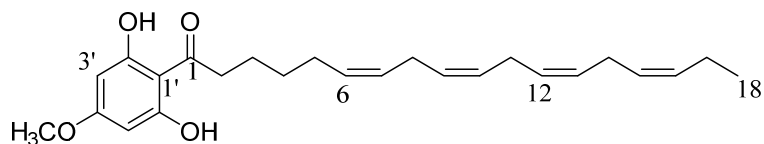


Figure S78. High resolution negative ESI-MS of compound eluting at 21.62 min (**14**) from HPLC-MS (*S. cf. fallax*).



(14)

Position	δ_H (J in Hz)
1	
2	3.91, t (8.0)
3	2.49, m
4	2.25, m
5	2.40, m *
6	6.21, m
7	6.21, m
8	3.66, m
9	6.21, m
10	6.21, m
11	3.66, m
12	6.21, m
13	6.21, m
14	3.66, m
15	6.21, m
16	6.21, m
17	SS *
18	1.78, t (7.5)
1'	
2'	
3'	6.81, s
4'	
5'	6.81, s
6'	
1'-OH	ND
4'-OCH ₃	SS
6'-OH	ND

Referenced to 75% CH₃CN/D₂O; * signals interchangeable; SS Signal suppressed; ND Not Detected.

Figure S79. NMR data for compound eluting at 21.62 min (14) (*S. cf. fallax*).

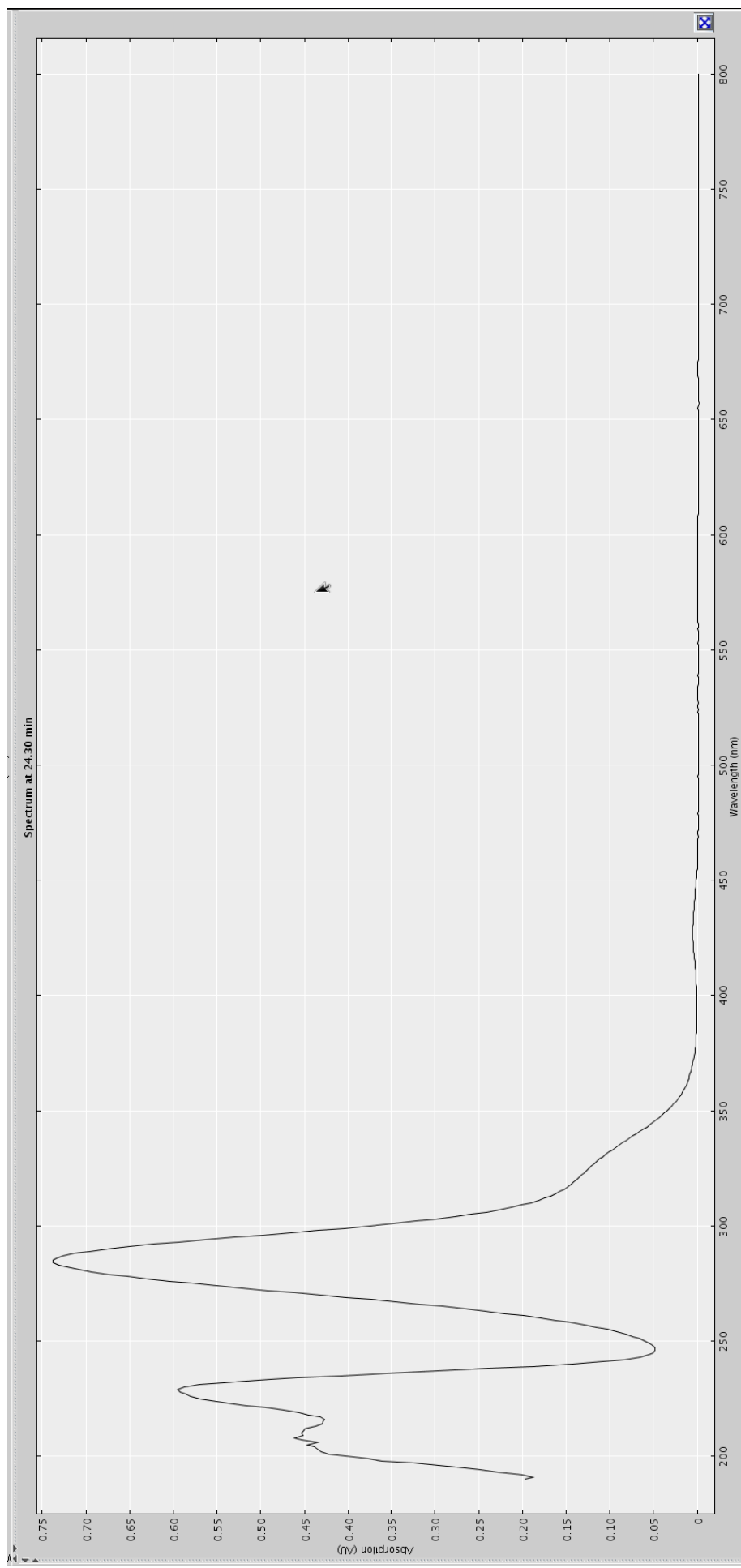


Figure S80. Extracted UV profile of compound eluting at 22.96 min (**18**) from HPLC-NMR (*C. subfarcinata*).

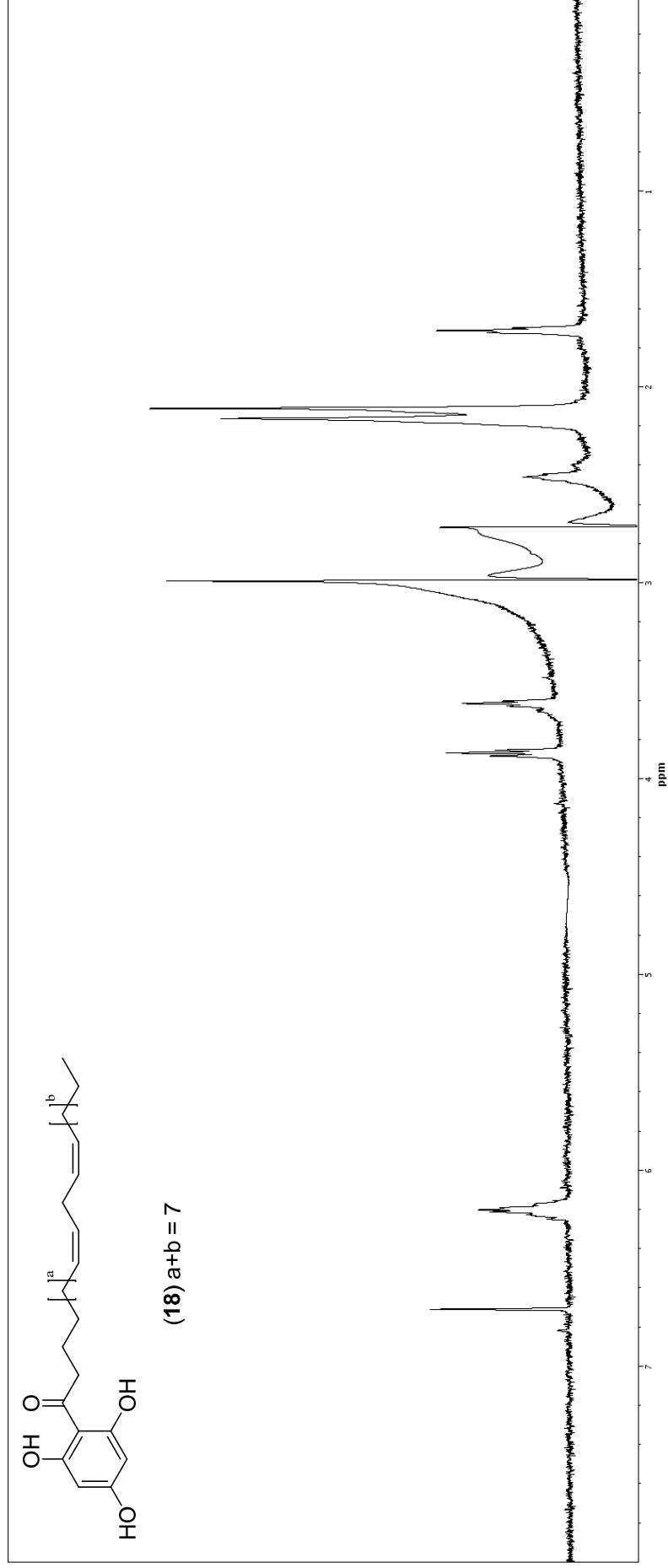


Figure S81. WET1D Proton NMR spectrum (500 MHz, 75% CH₃CN/D₂O) of compound eluting at 22.96 min (18) (*C. subfarcinata*).

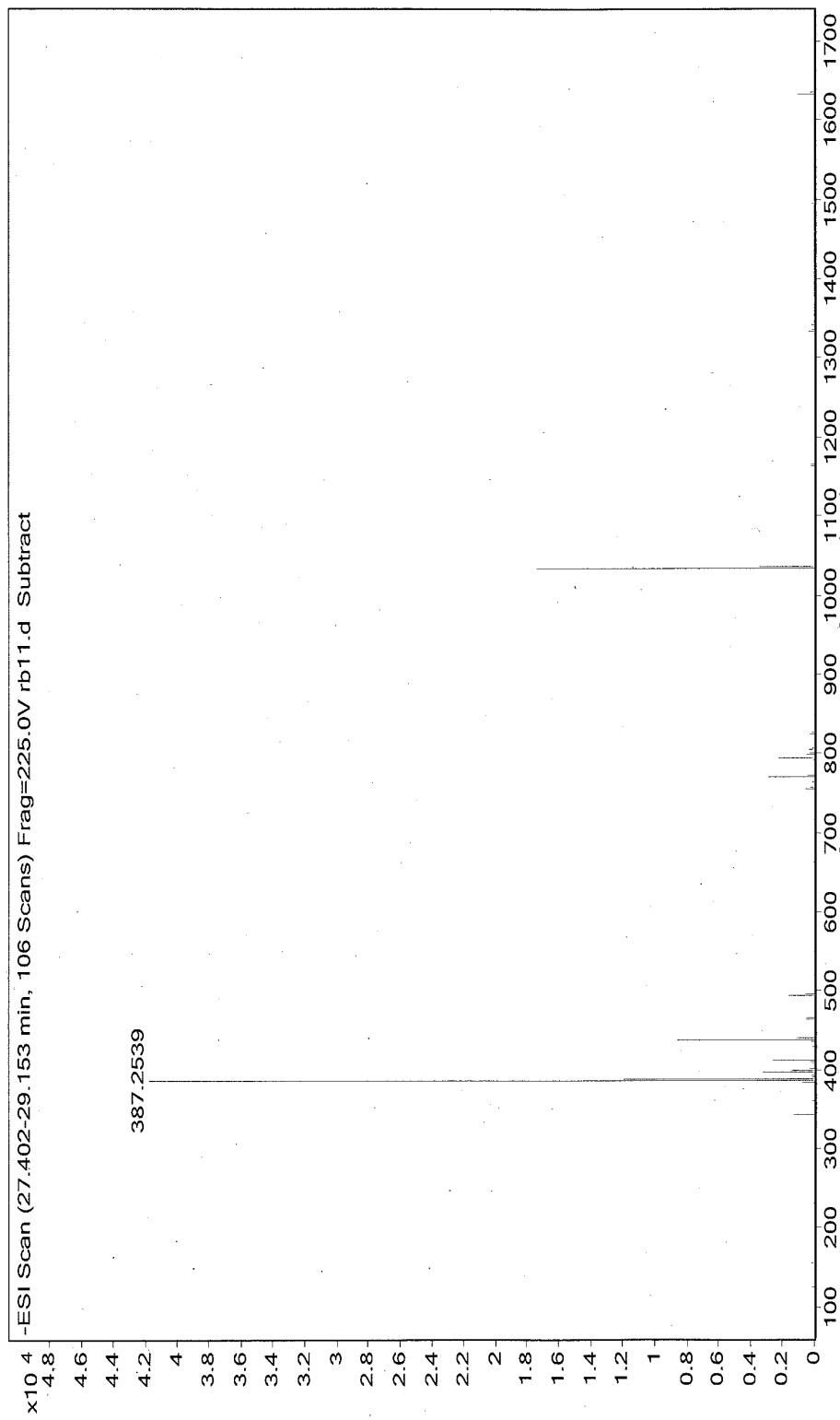


Figure S82. High resolution negative ESI-MS of compound eluting at 22.96 min (**18**) from HPLC-MS (*C. subfarcinata*).

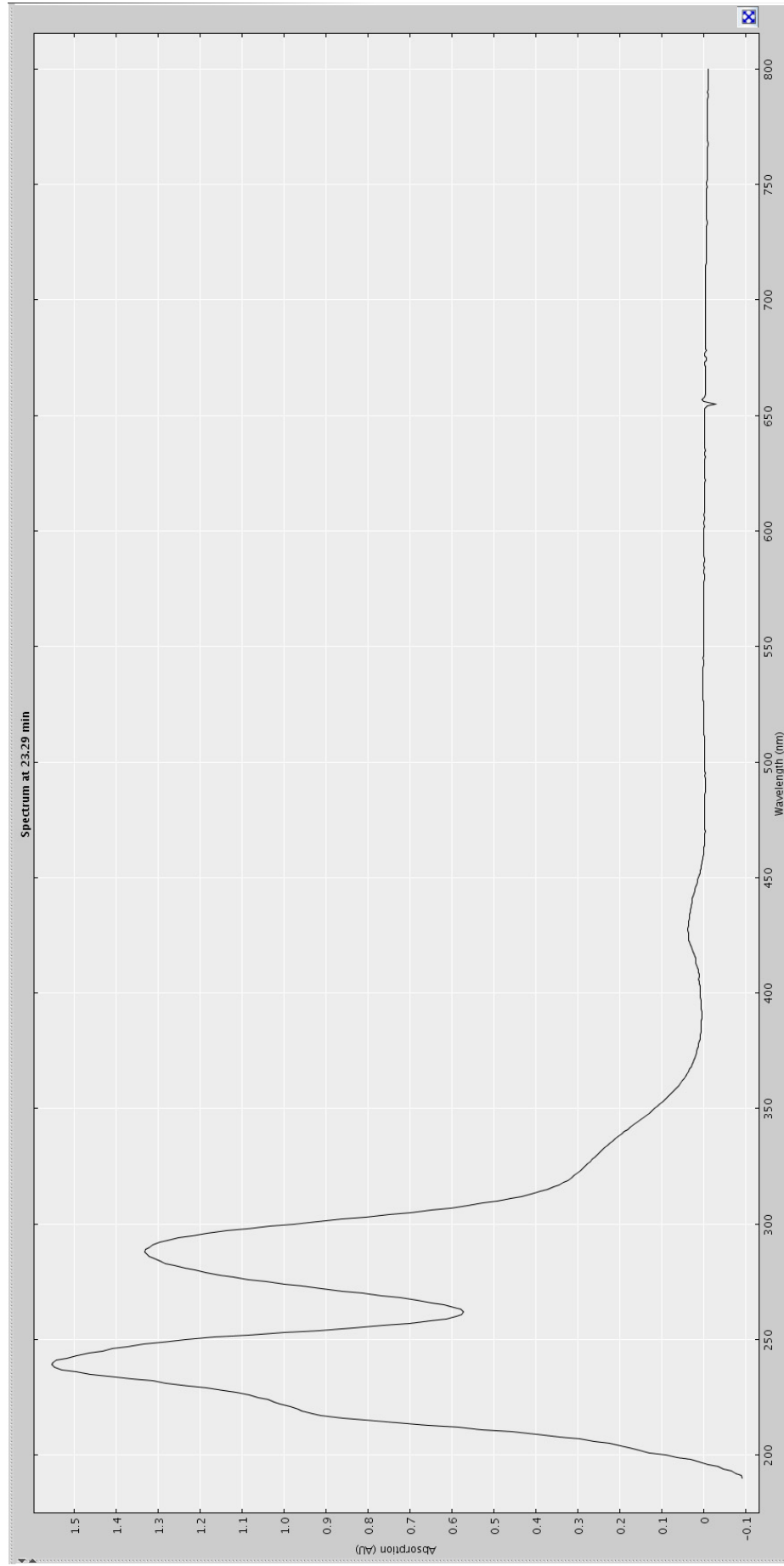


Figure S83. Extracted UV profile of compound eluting at 23.16 min from HPLC-NMR (*C. retroflexa*).

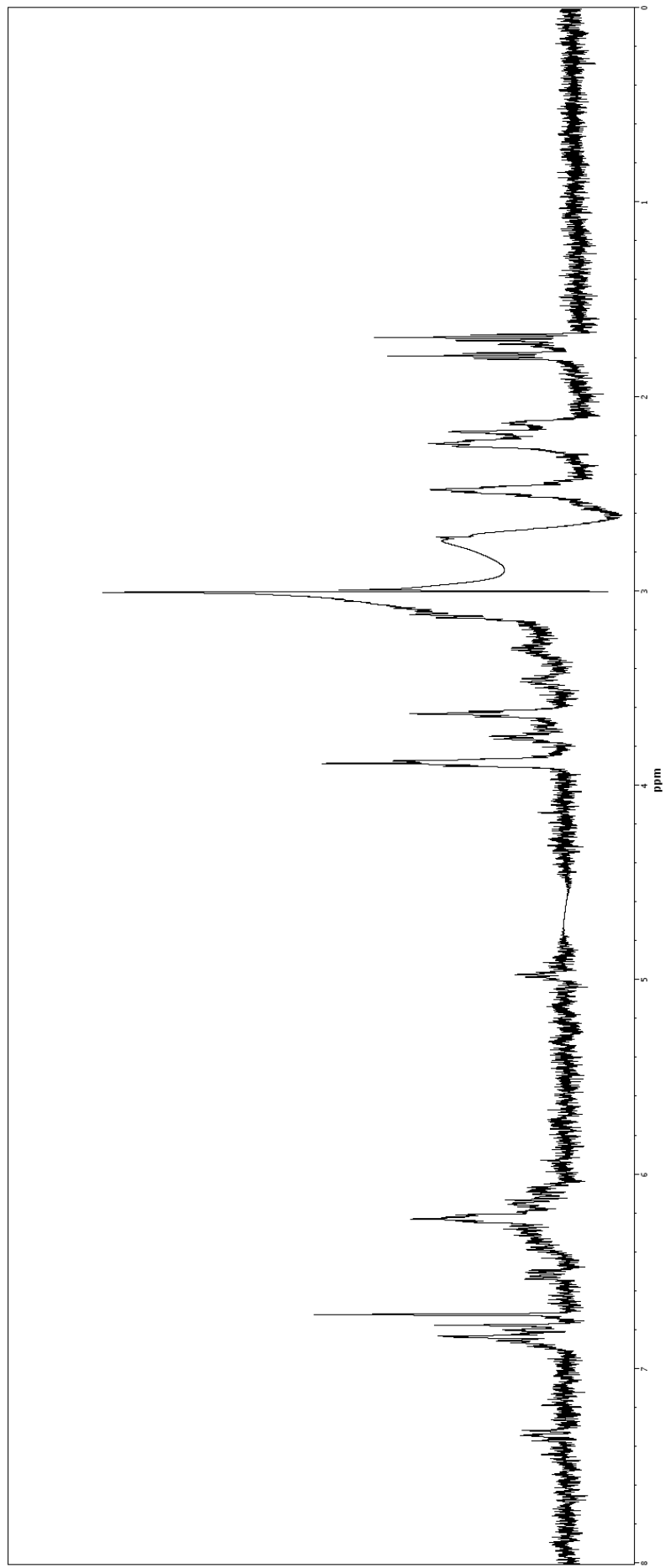


Figure S84. WET1D Proton NMR spectrum (500 MHz, 75% CH₃CN/D₂O) of compound eluting at 23.16 min (*C. retroflexa*).

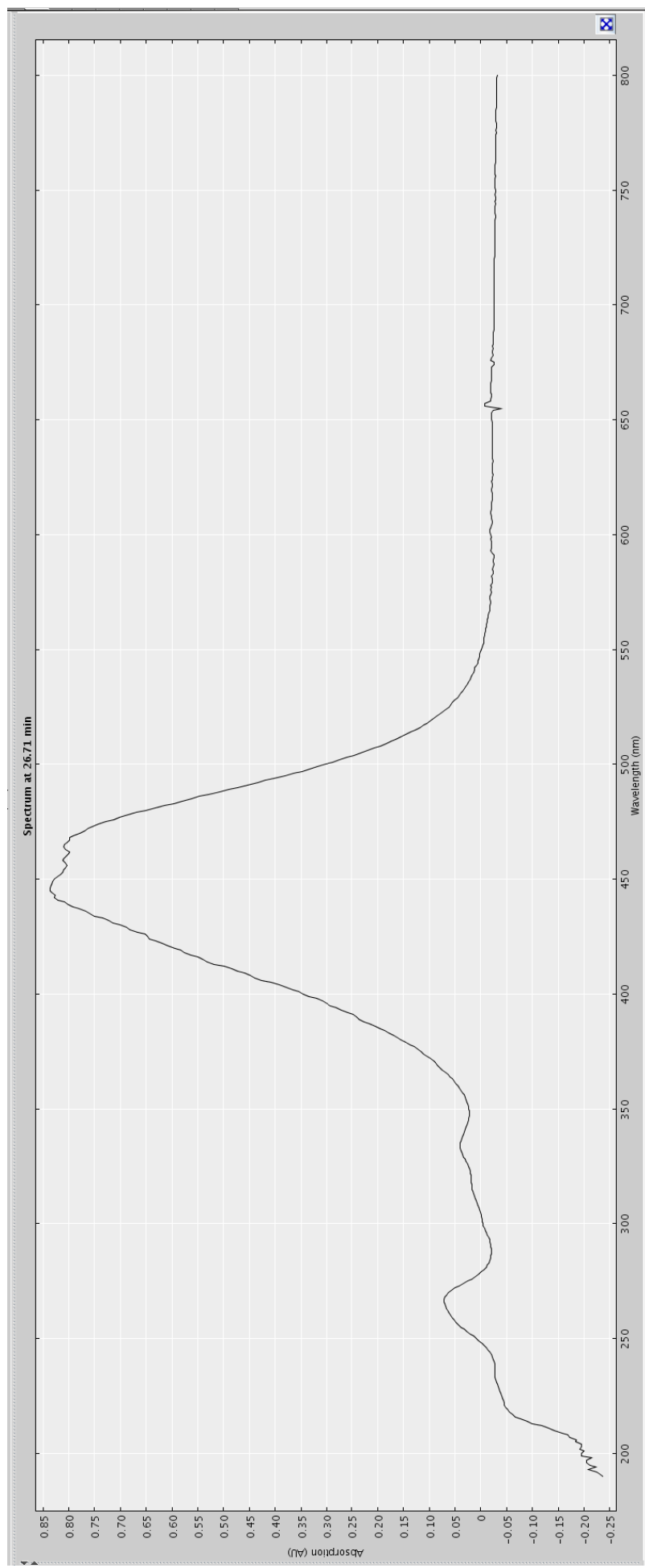


Figure S85. Extracted UV profile of compound eluting at 26.71 min from HPLC-NMR (*H. pseudospicata*).

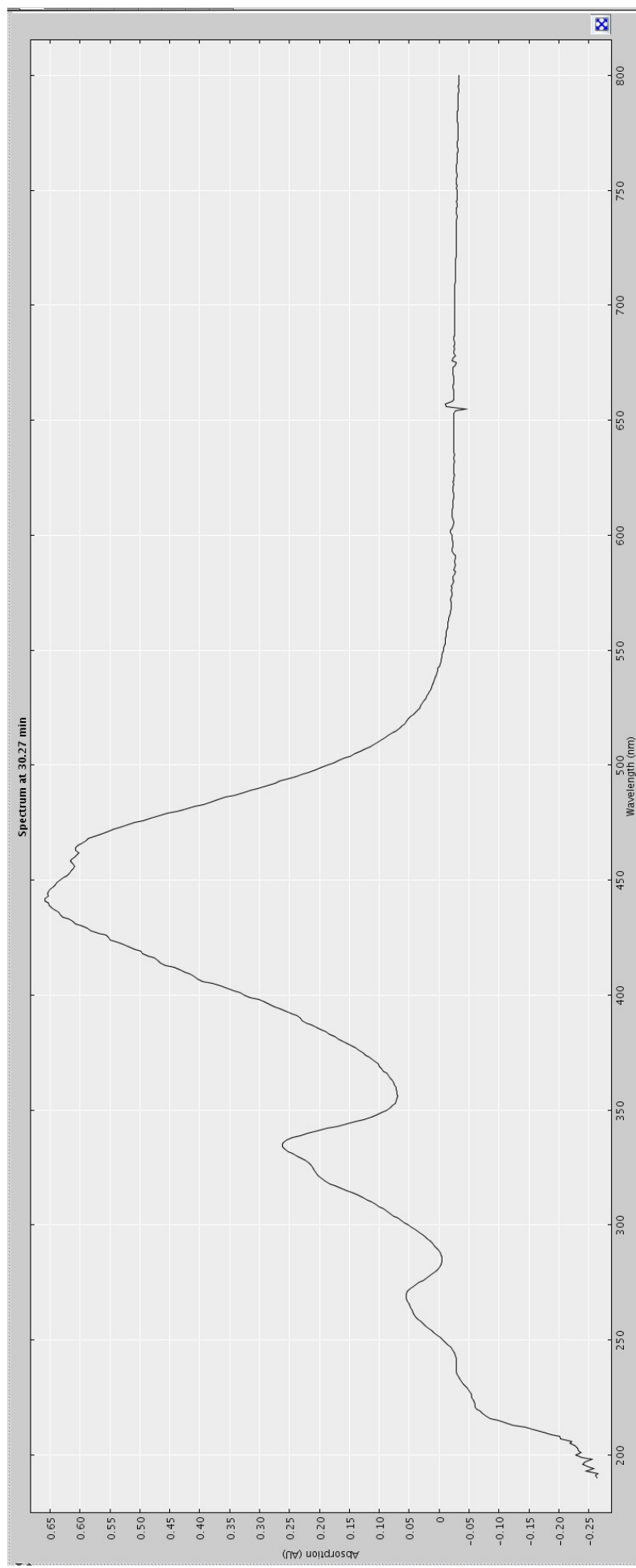


Figure S86. Extracted UV profile of compound eluting at 30.27 min from HPLC-NMR (*H. pseudospicata*).

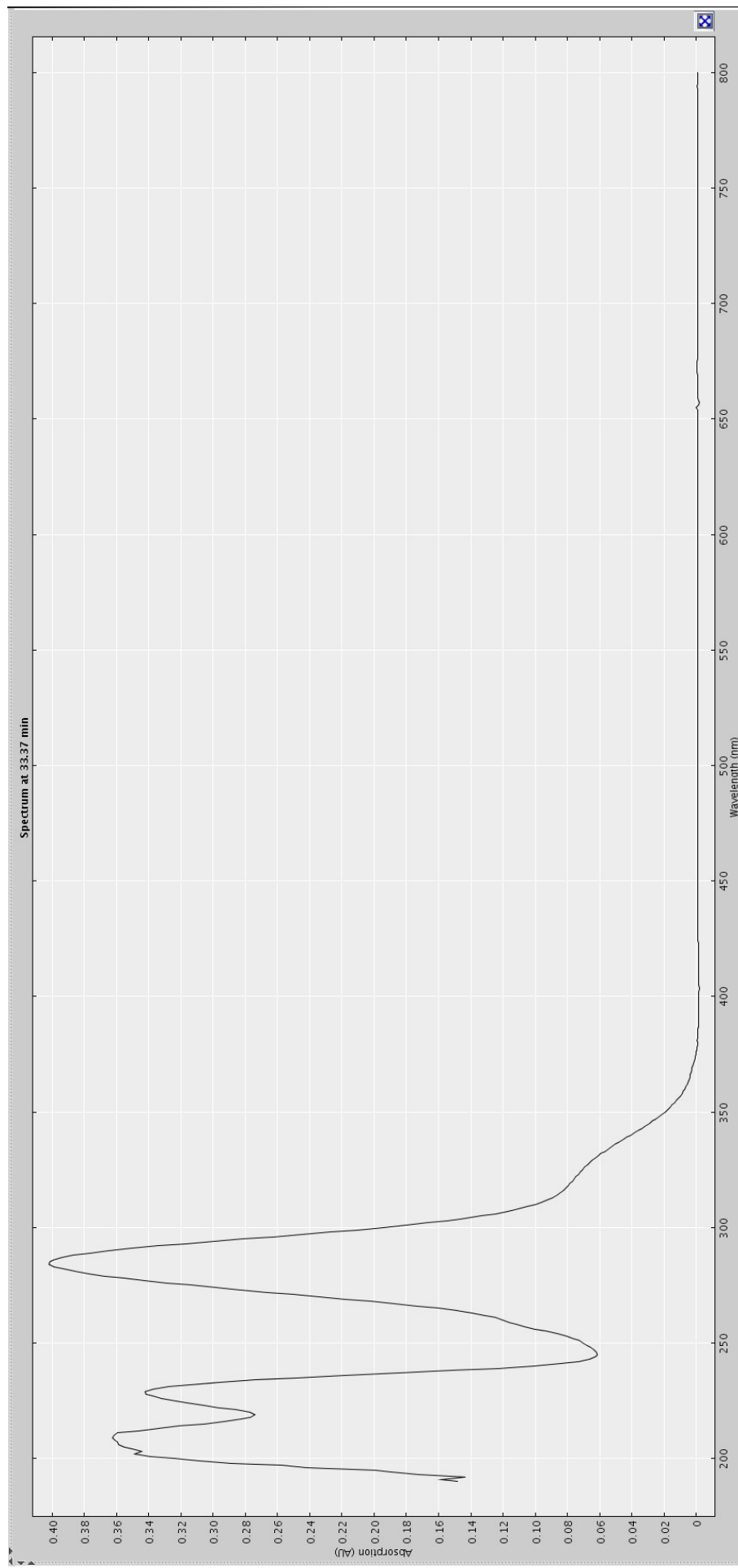


Figure S87. Extracted UV profile of compound eluting at 33.40 min (**19**) from HPLC-NMR (*C. subfarcinata*).

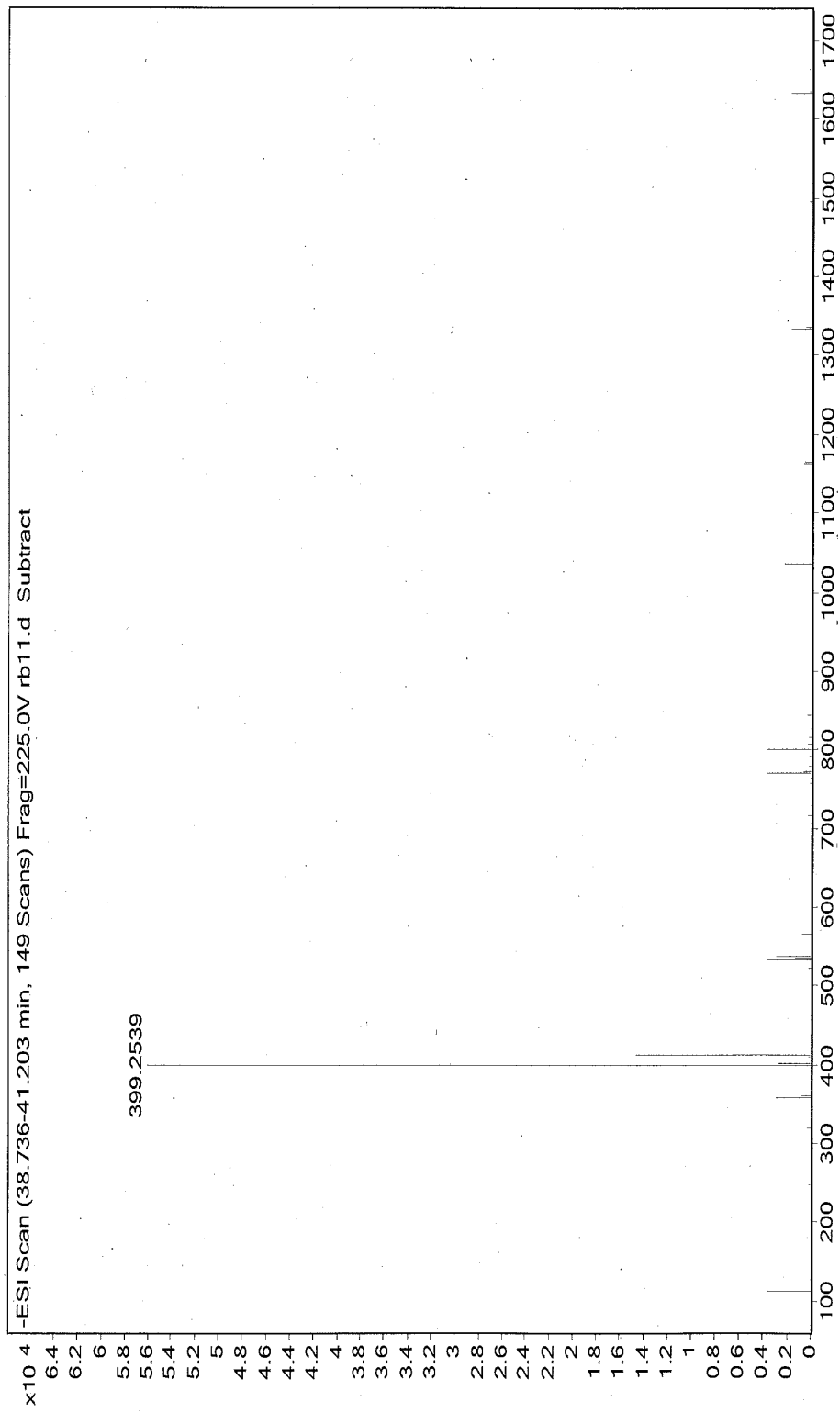


Figure S89. High resolution negative ESI-MS of compound eluting at 33.40 min (**19**) from HPLC-MS (*C. subfarcinata*).

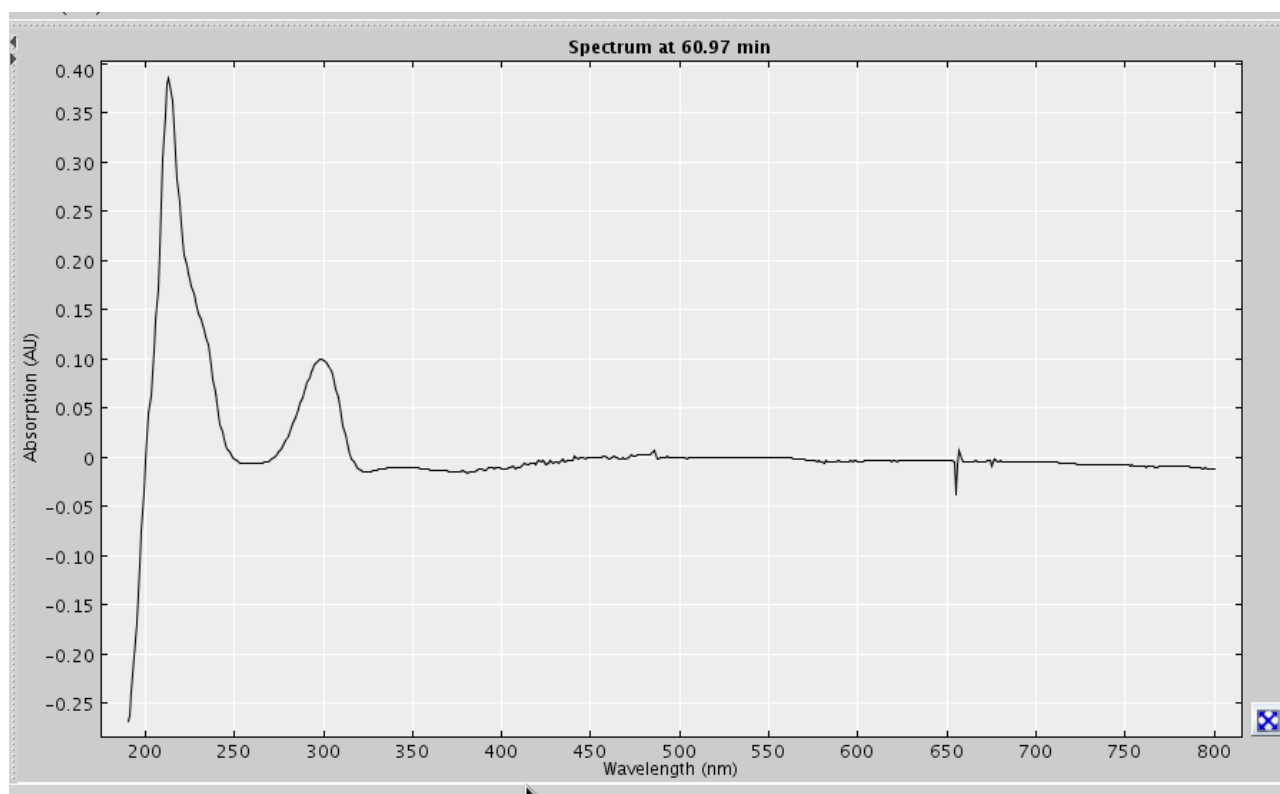


Figure S90. Extracted UV profile of compound eluting at 60.80 min (**15**) from HPLC-NMR (*S. cf. fallax*).

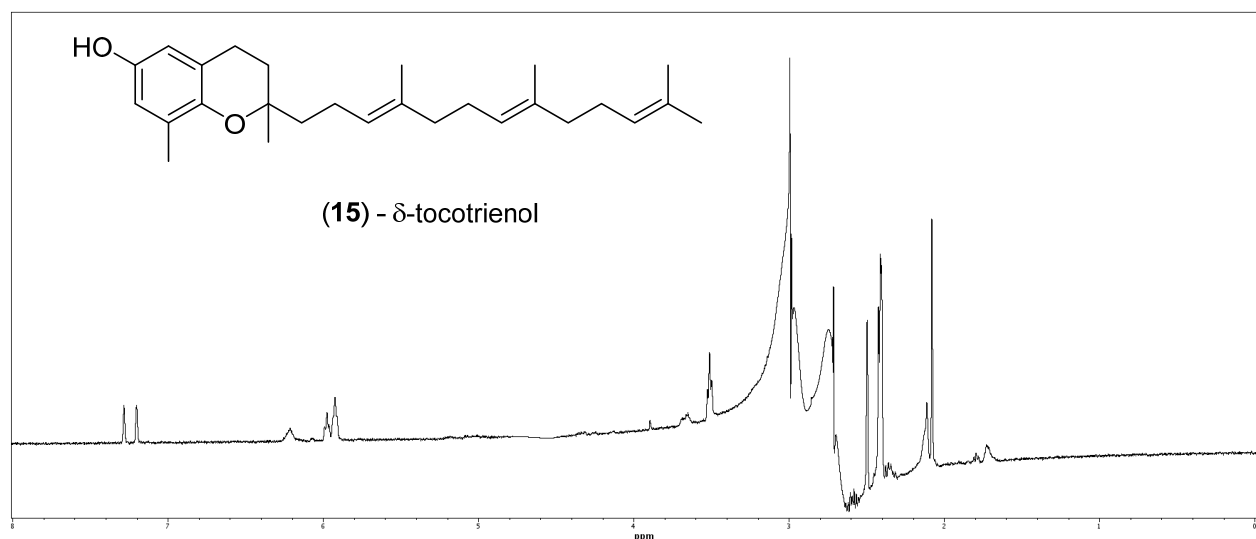
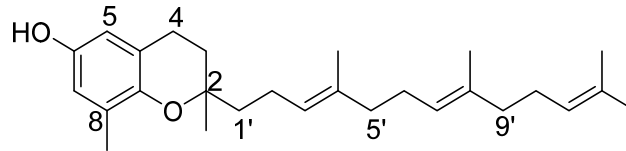


Figure S91. WET1D Proton NMR spectrum (500 MHz, 75% CH₃CN/D₂O) of compound eluting at 60.80 min (**15**) (*S. cf. fallax*).



(15) - δ -tocotrienol

Position	δ_H (J in Hz)
1	
2	
3	SS
4	3.51, t (7.0)
5	7.20, s
6	
7	7.28, s
8	
9	
10	
1'	SS
2'	SS
3'	5.97, t (7.0)
4'	
5'	SS
6'	SS
7'	5.92, m
8'	
9'	SS
10'	SS
11'	5.92, m
12'	
2-CH ₃	2.08, s
8-CH ₃	SS
4'-CH ₃	2.41, s
8'-CH ₃	2.42, s*
12a'-CH ₃	2.40, s*
12b'-CH ₃	2.49, s
6-OH	ND

Referenced to 75% CH₃CN/D₂O; * Signals interchangeable.

Figure S92. NMR data for compound eluting at 60.80 min (15) (*S. cf. fallax*).

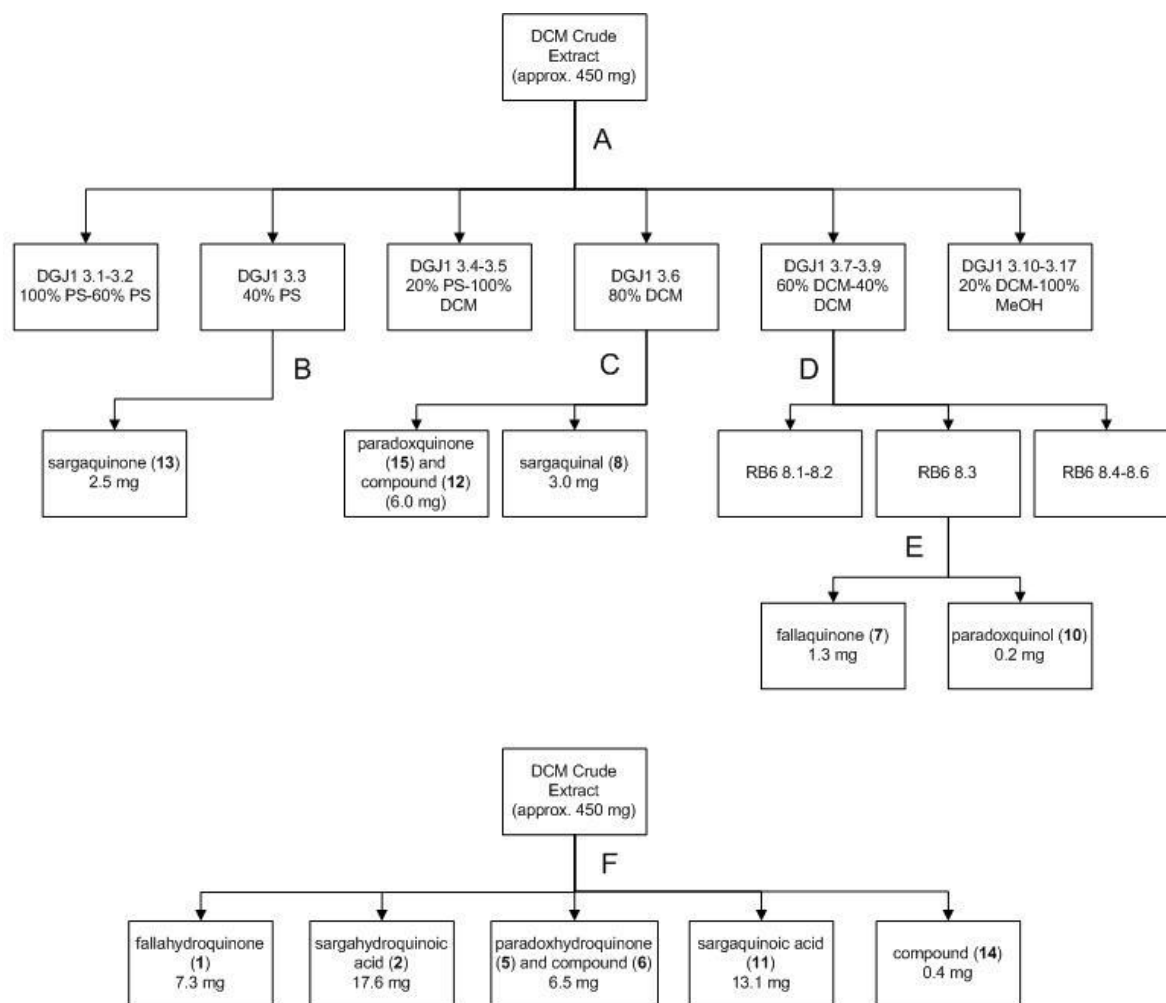
© 2015 by the authors; licensee MDPI, Basel, Switzerland. This article is an open access article distributed under the terms and conditions of the Creative Commons Attribution license (<http://creativecommons.org/licenses/by/4.0/>).

APPENDIX E

Supplementary Information for the Study of the Australian Marine Brown Alga *Sargassum paradoxum*

This appendix contains further information relevant to the study of the Australian marine brown alga *Sargassum paradoxum* as outlined in Chapter 9.

Supplementary Information



A – Flash silica gel column (20% stepwise elution from PS → DCM → EtOAc → MeOH)

B – RP-HPLC (100% CH₃CN)

C – RP-HPLC (95% CH₃CN/H₂O)

D – fractions combined, Sephadex LH-20 column (100% MeOH)

E – RP-HPLC (85% CH₃CN/H₂O)

F – RP-HPLC (90% CH₃CN/H₂O)

PS – petroleum spirits (60-80°C)

DCM – dichloromethane

EtOAc -ethyl acetate

MeOH - methanol

Figure S1. Bioassay-guided isolation scheme for *S. paradoxum*.

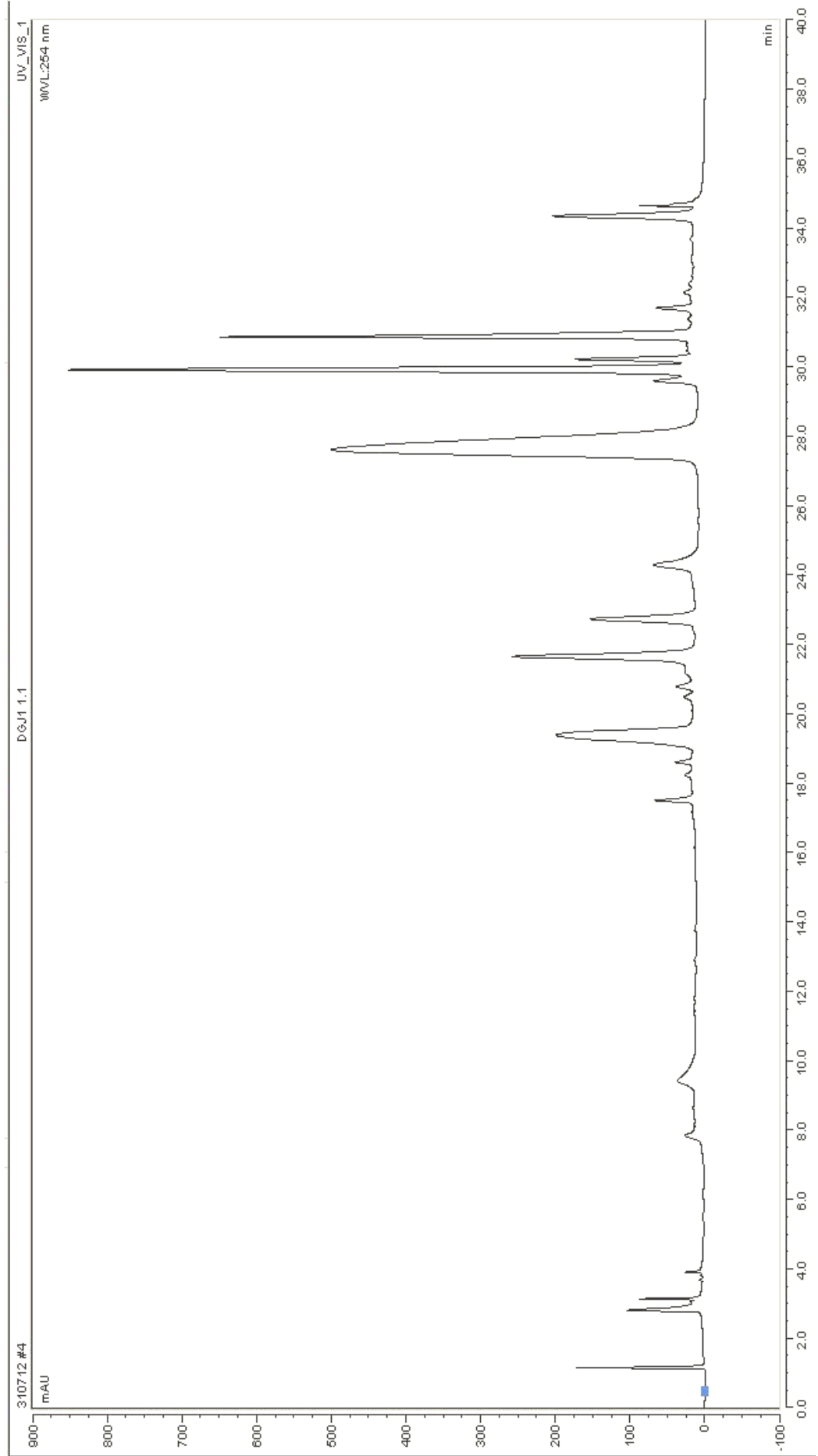


Figure S2. Analytical HPLC chromatogram of DCM crude extract of *S. paradoxum*.

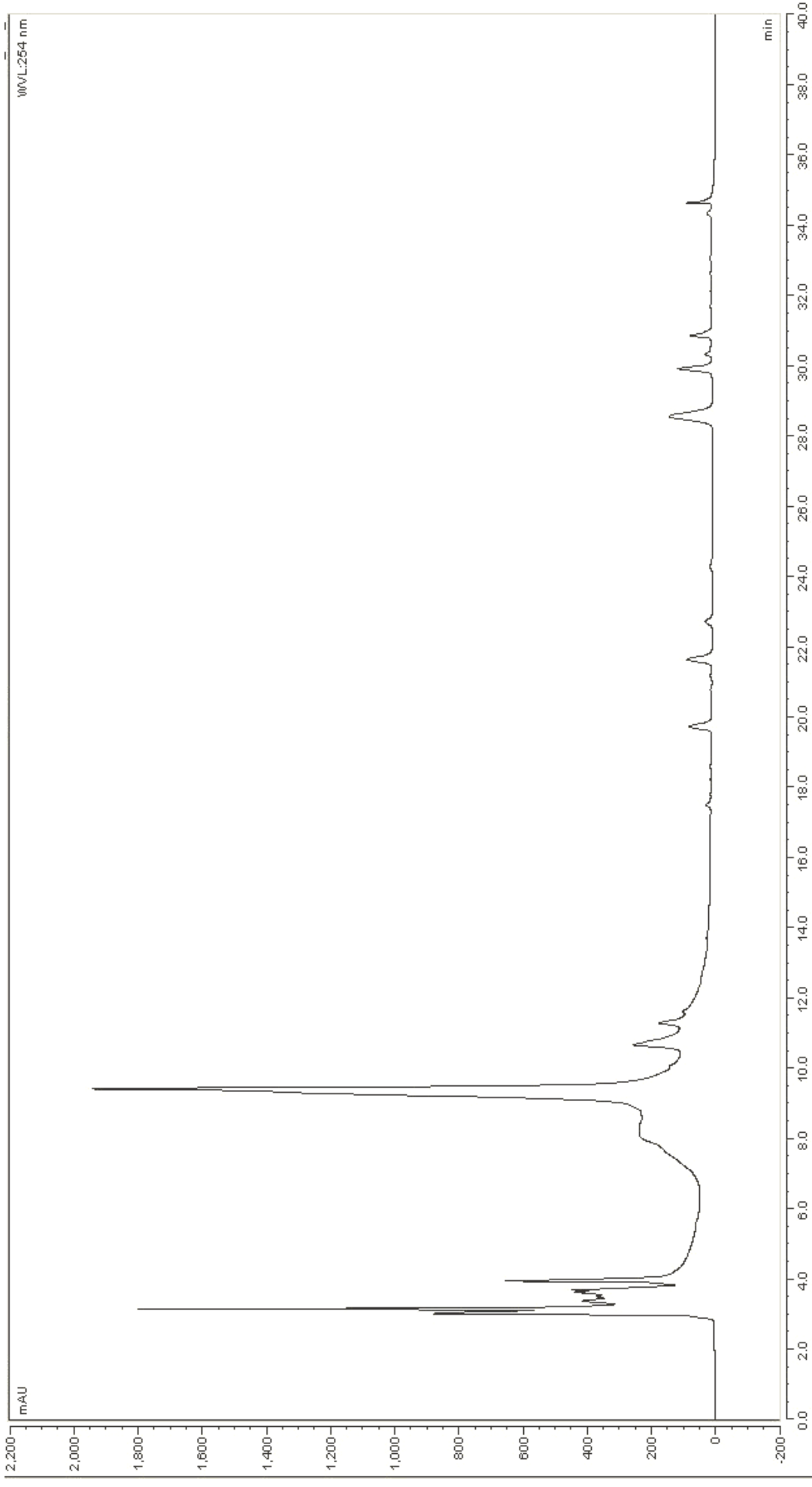


Figure S3. Analytical HPLC chromatogram of MeOH crude extract of *S. paradoxum*.

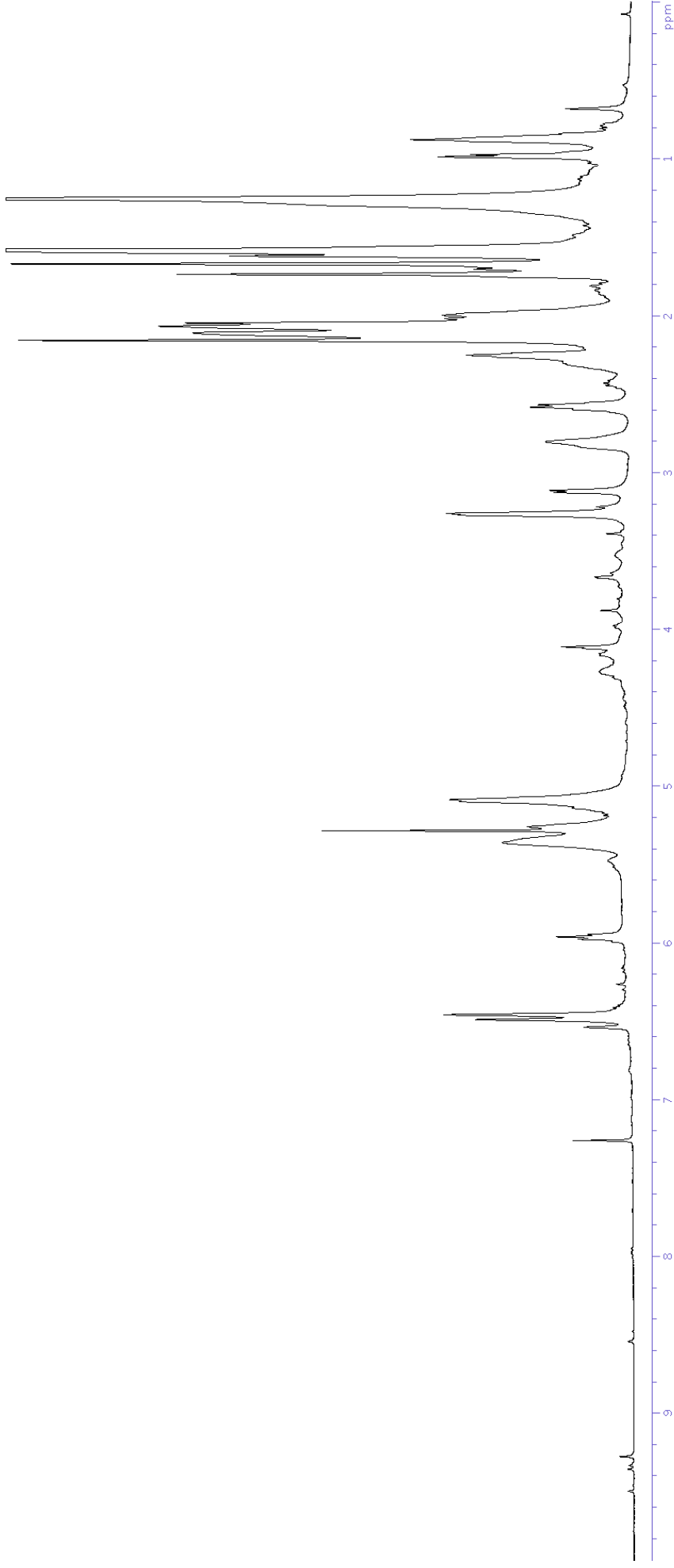


Figure S4. ¹H NMR spectrum (500 MHz, CDCl₃) of DCM crude extract of *S. paradoxum*.

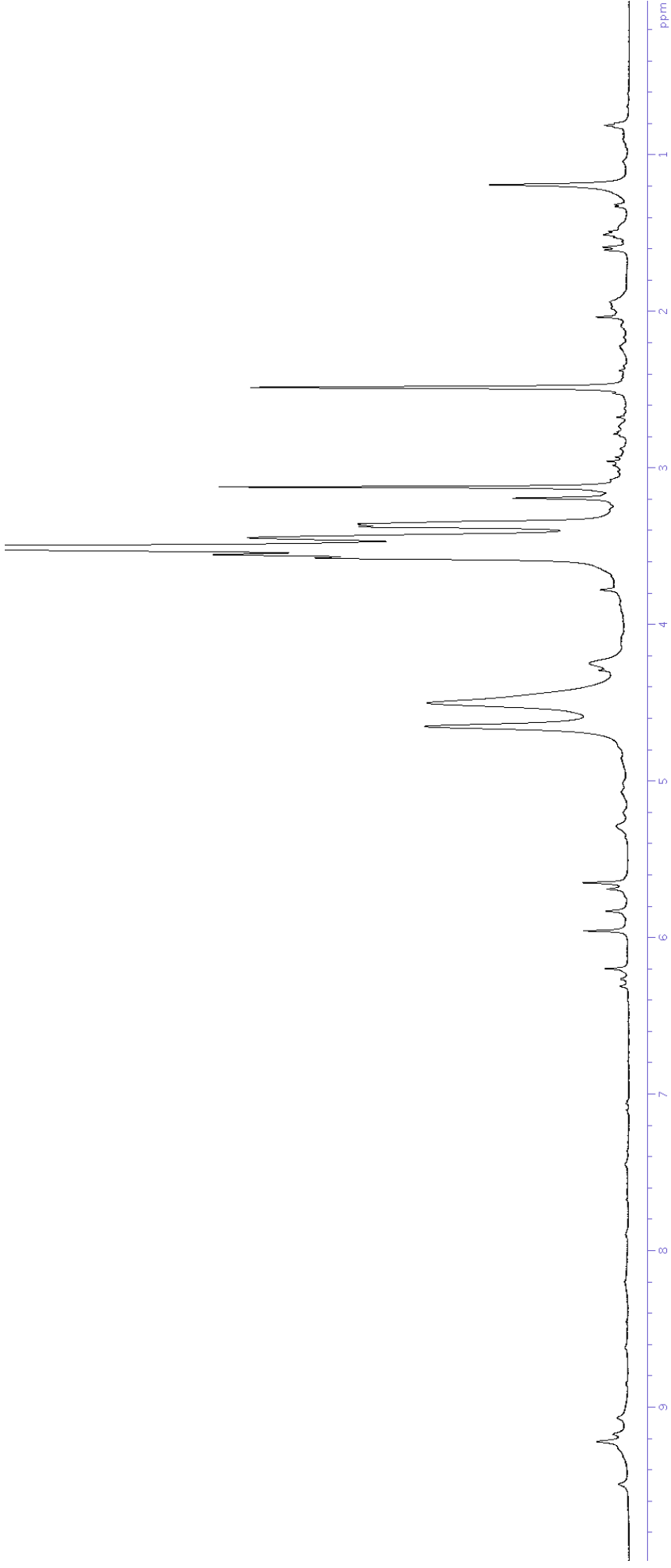


Figure S5. ^1H NMR spectrum (500 MHz, d_6 -DMSO) of MeOH crude extract of *S. paradoxum*.

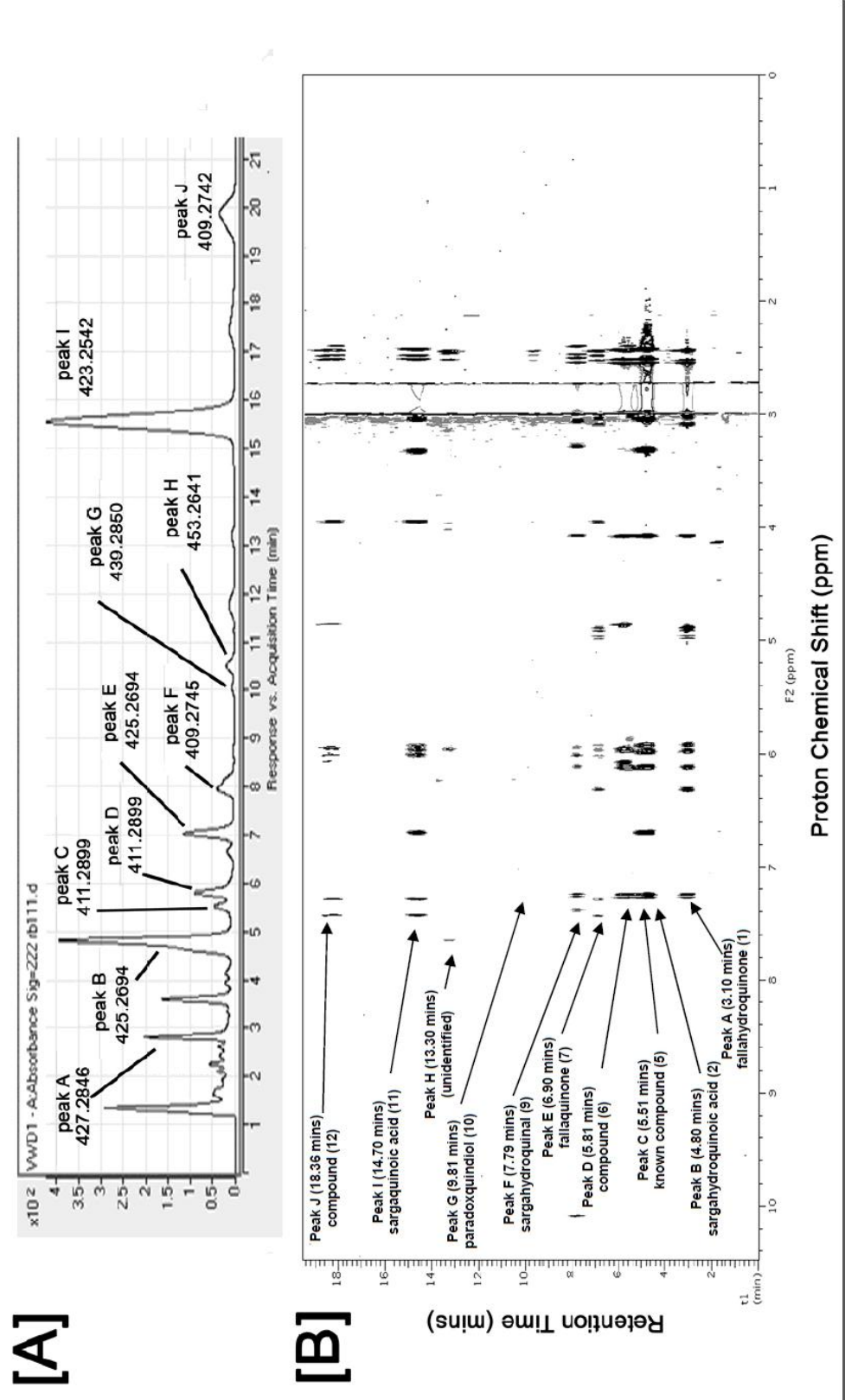


Figure S6. [A] HPLC-MS chromatographic trace showing the corresponding high resolution m/z ions of peaks A–J (Negative mode ESI MS with UV detection at 222 nm) and [B] On-flow 2D HPLC-NMR contour plot resulting from the analysis of the dichloromethane crude extract of *Sargassum paradoxum* showing the detection of peaks A–J.

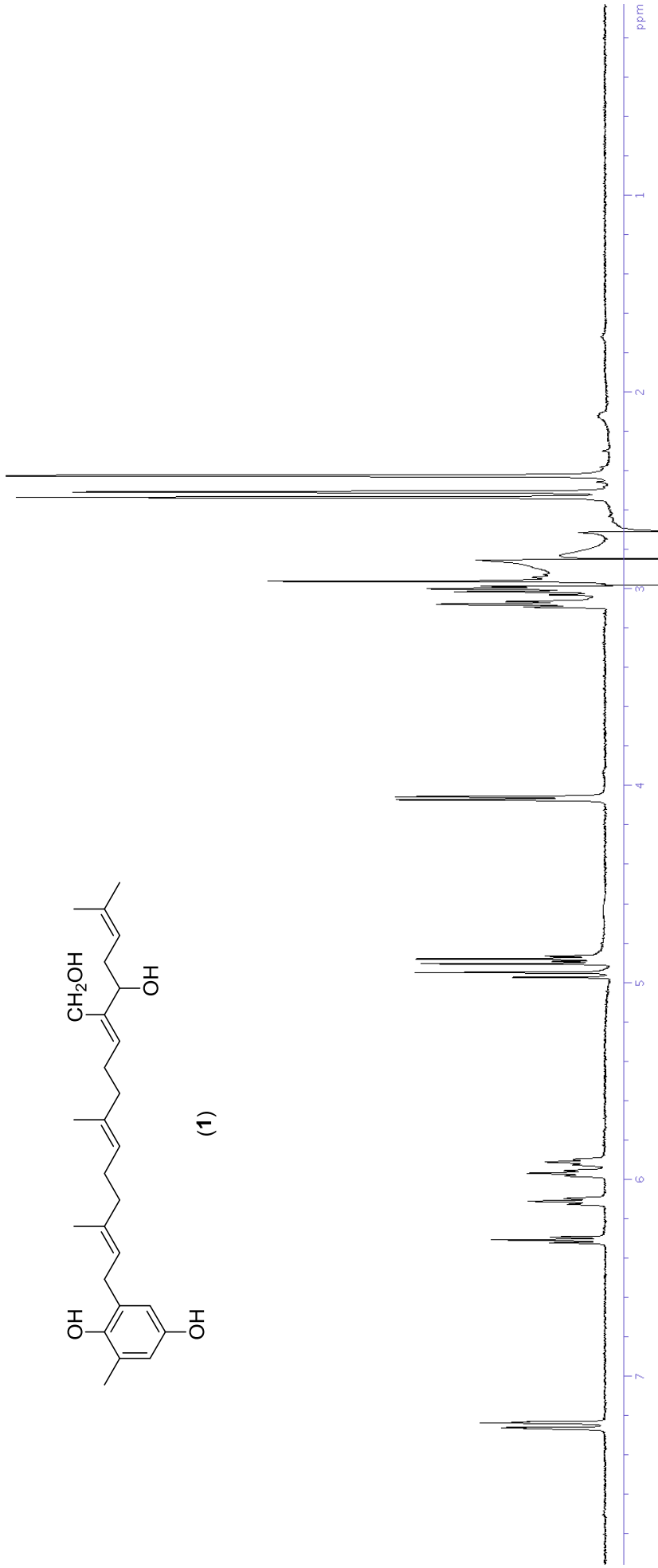


Figure S7. Stop-flow WETID Proton NMR spectrum of peak A (3.10 min) (compound **1**).

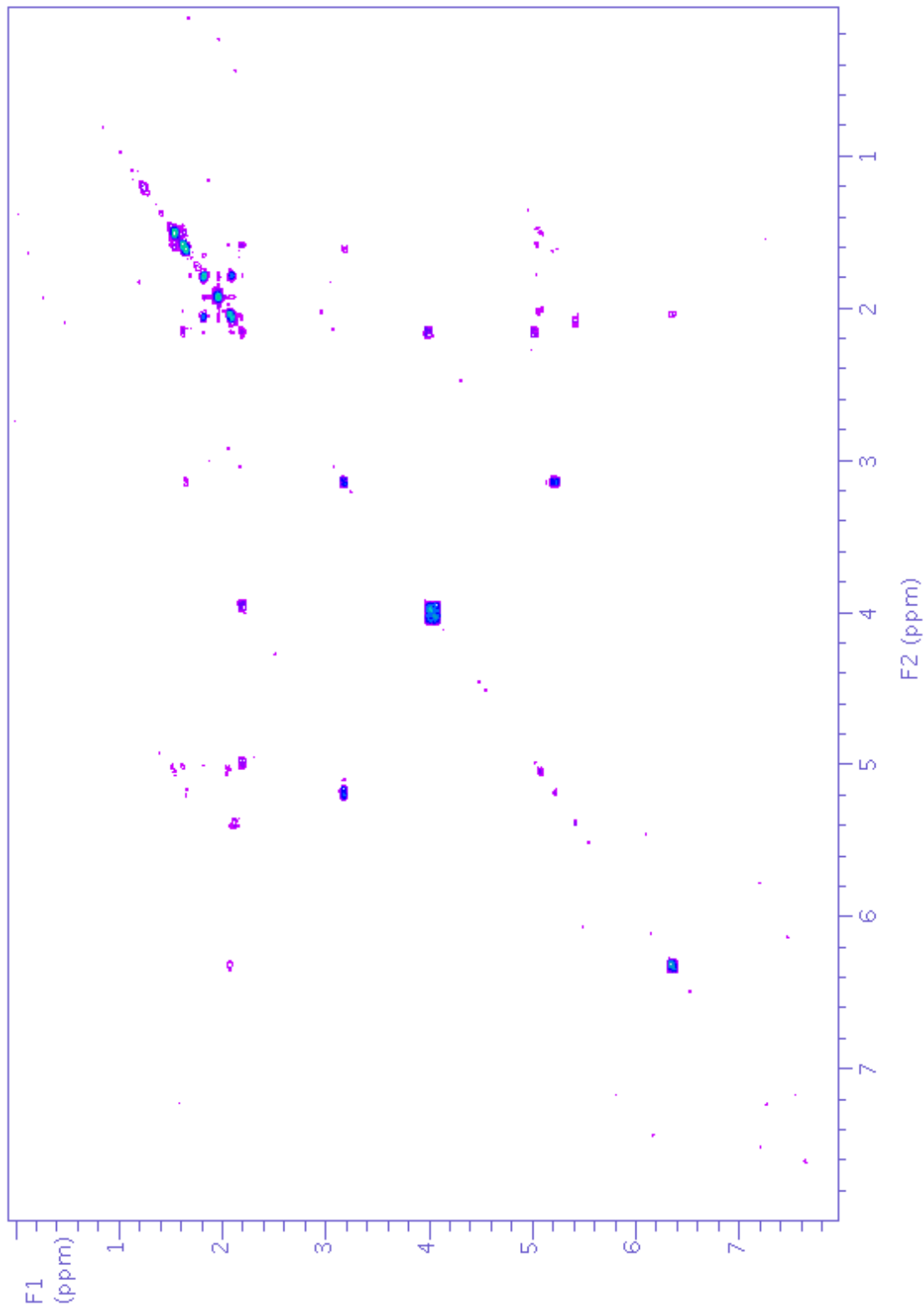


Figure S8. gCOSY NMR spectrum (from stop-flow HPLC-NMR) of peak A (3.10 min) (compound **1**).

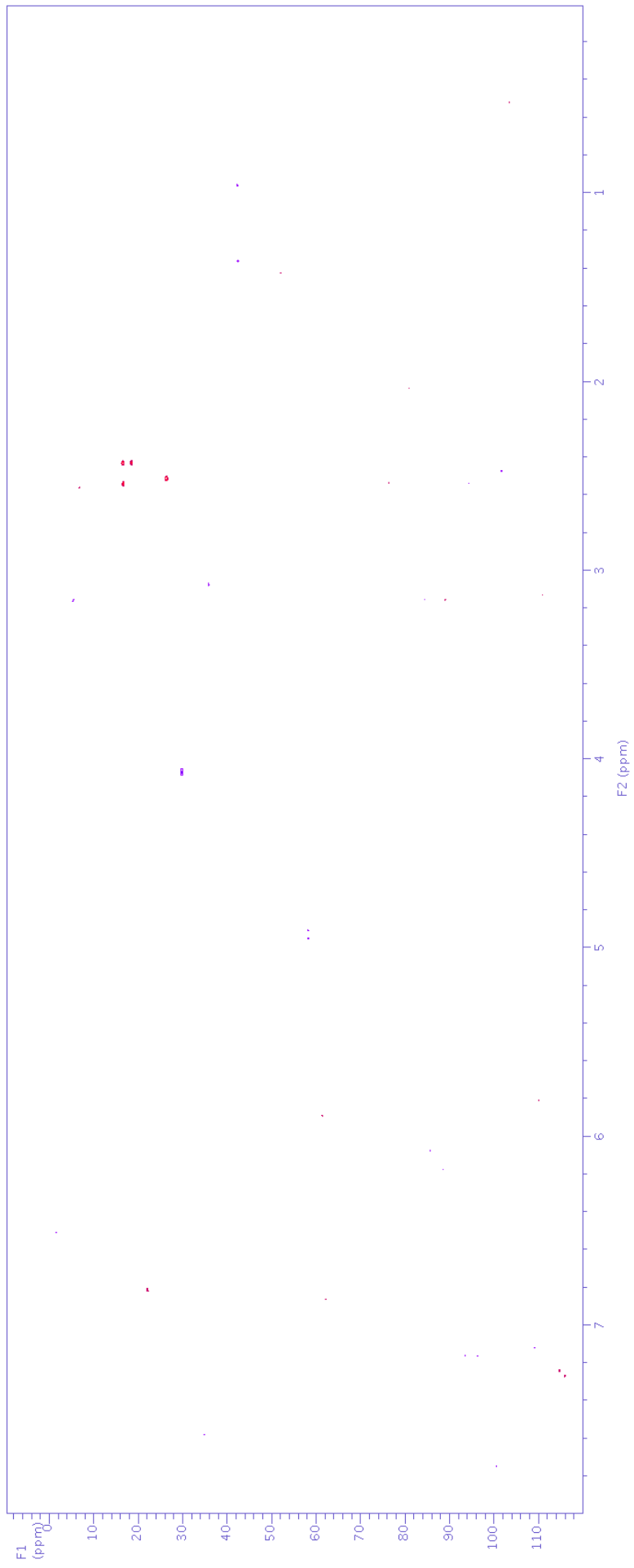


Figure S9. gHSQCAD NMR spectrum (from stop-flow HPLC-NMR) of peak A (3.10 min) (compound **1**).

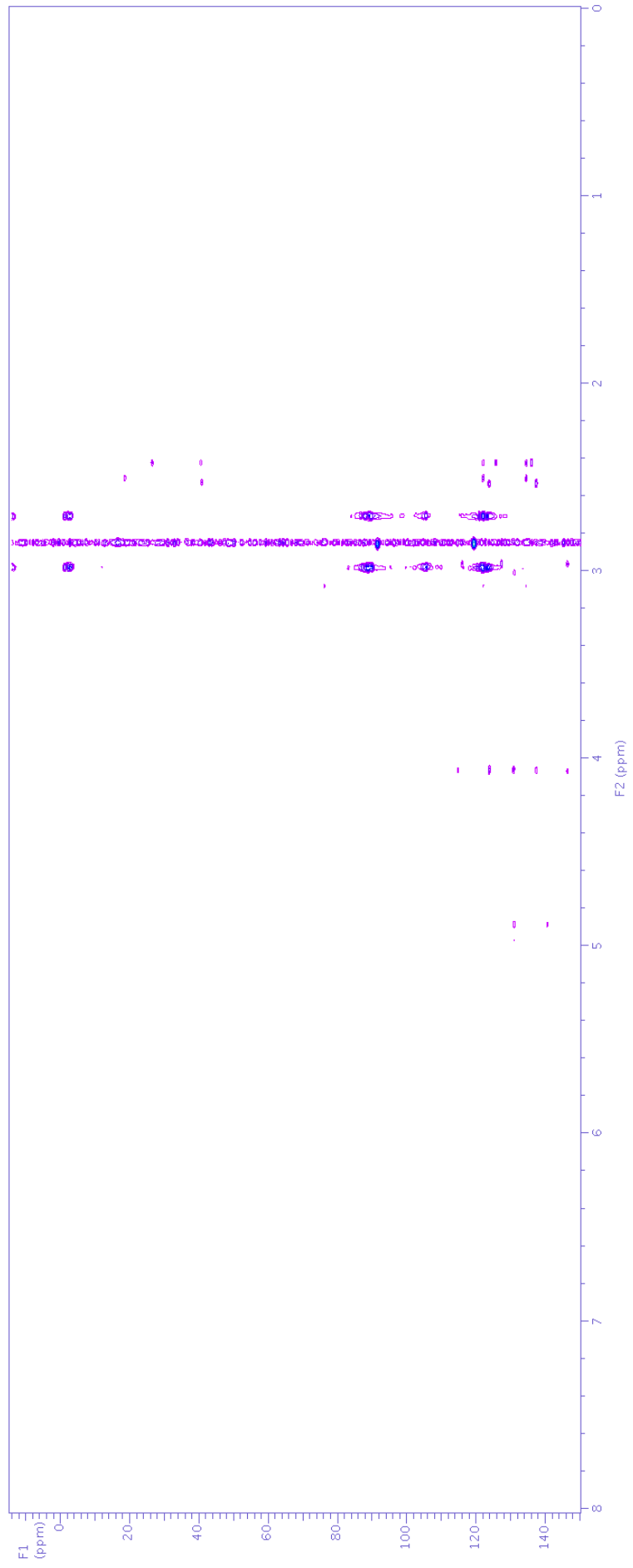


Figure S10. gHMBCAD NMR spectrum (from stop-flow HPLC-NMR) of peak A (3.10 min) (compound **1**).

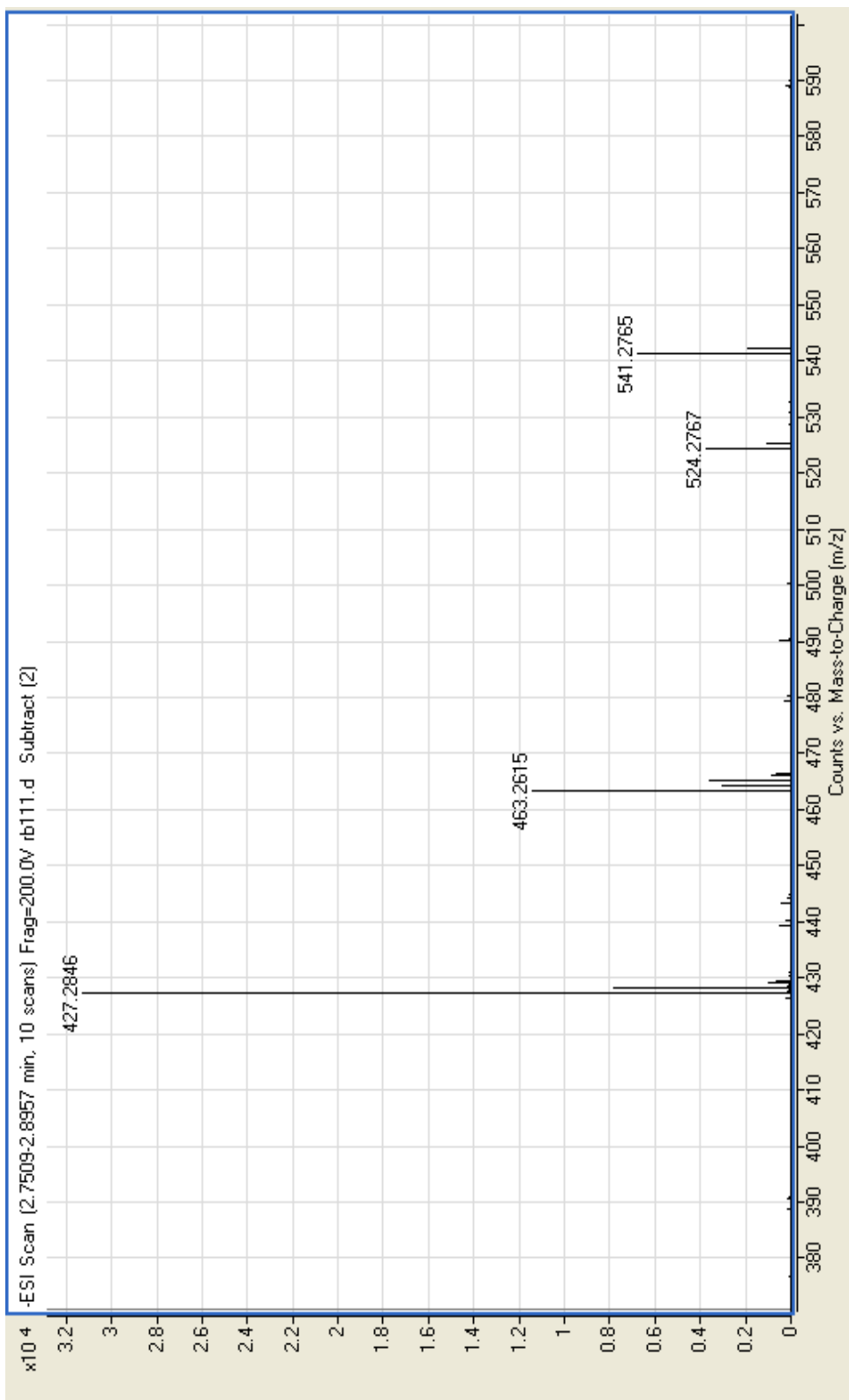


Figure S11. High resolution negative ESI-MS of peak A (3.10 min) (compound **1**) from HPLC-MS.

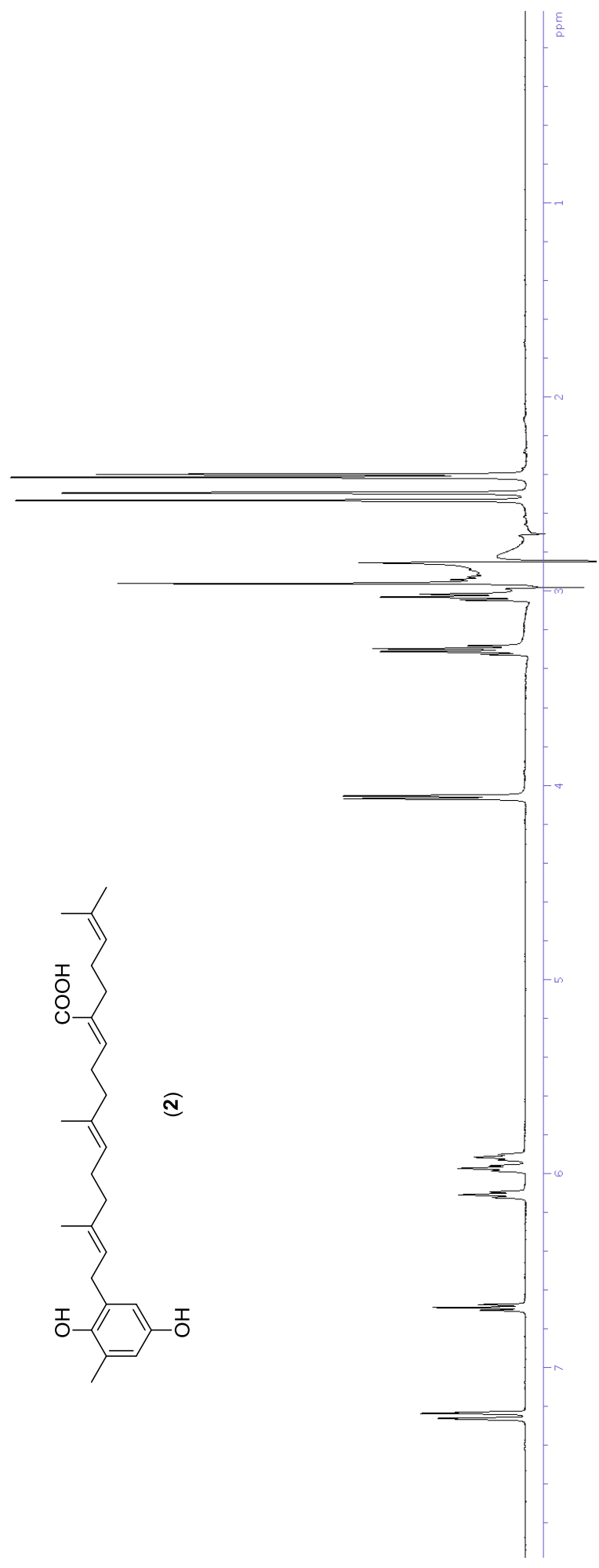


Figure S12. Stop-flow WET1D Proton NMR spectrum of peak B (4.80 min) (compound **2**).

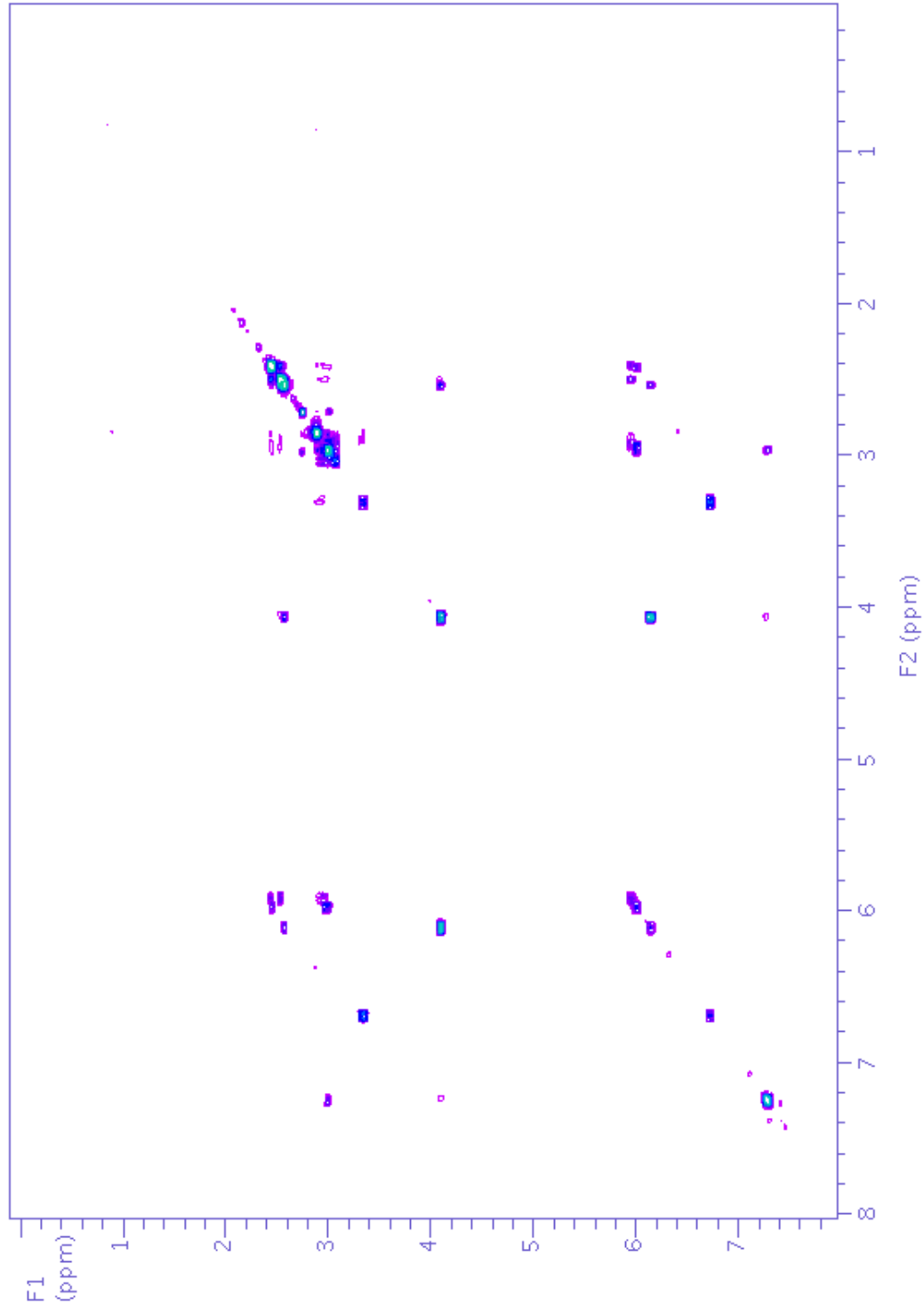


Figure S13. gCOSY NMR spectrum (from stop-flow HPLC-NMR) of peak B (4.80 min) (compound 2).

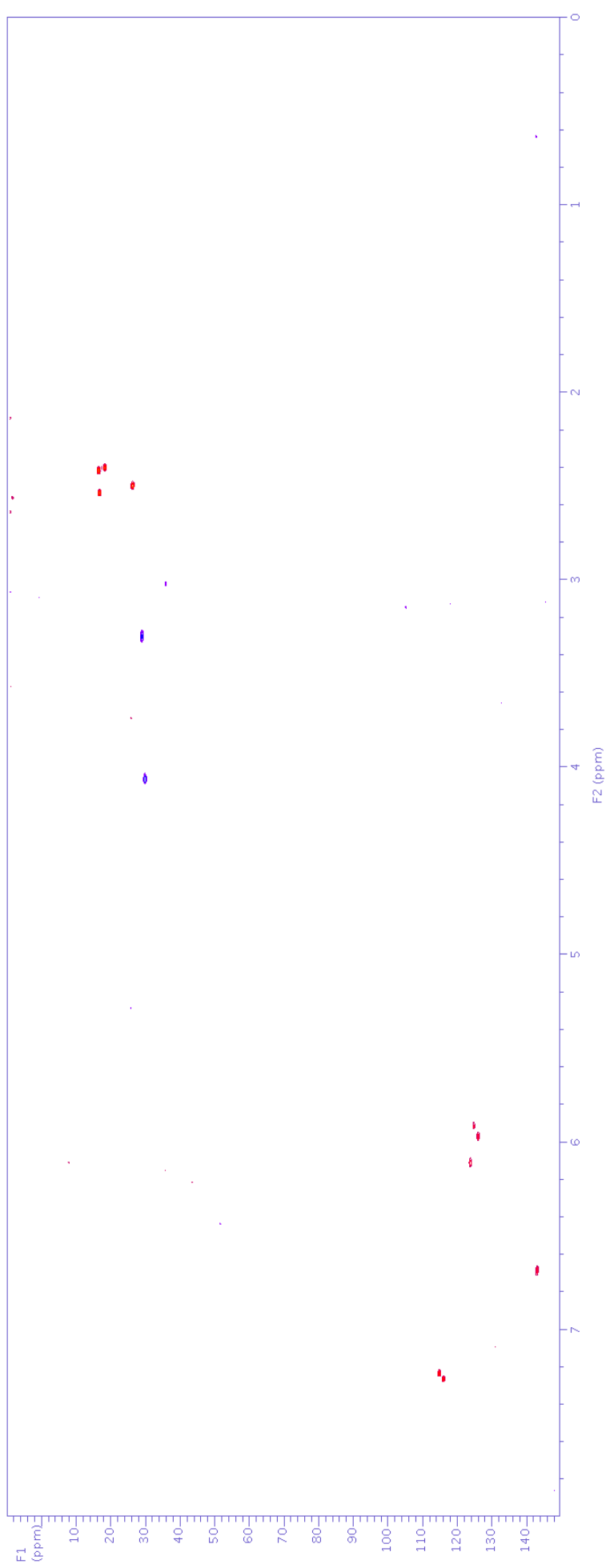


Figure S14. gHSQCAD NMR spectrum (from stop-flow HPLC-NMR) of peak B (4.80 min) (compound **2**).

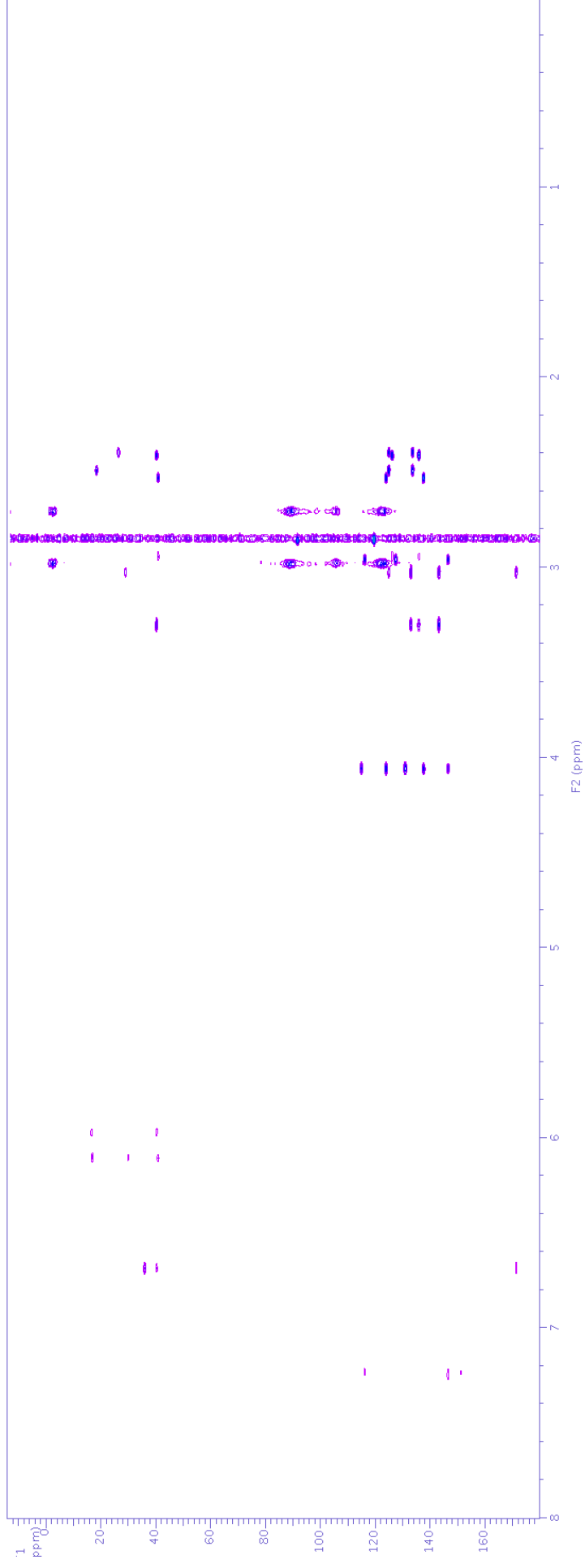


Figure S15. gHMBCAD NMR spectrum (from stop-flow HPLC-NMR) of peak B (4.80 min) (compound 2).

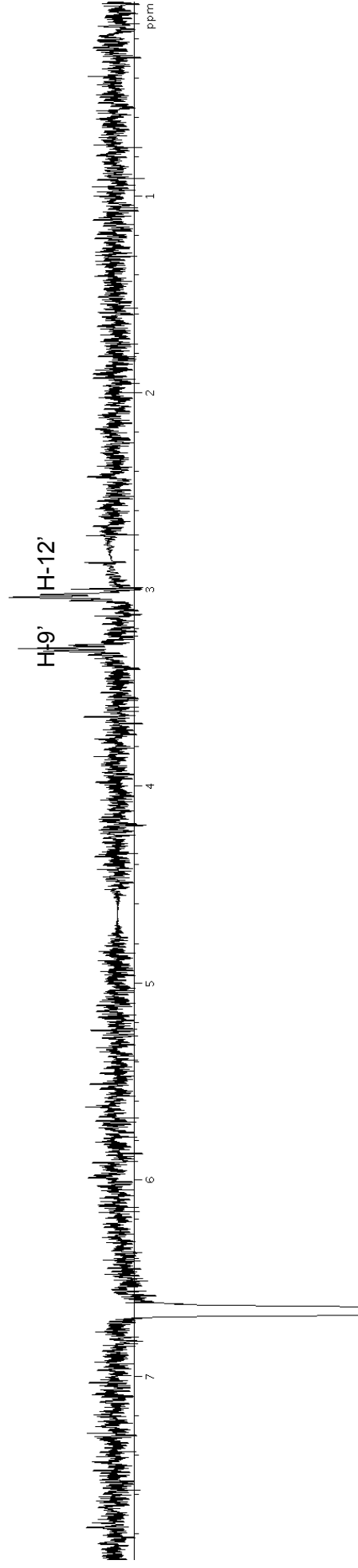
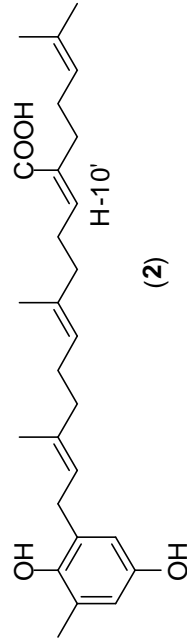


Figure S16. Single irradiation nOe NMR spectrum (from stop-flow HPLC-NMR) of peak B (compound **2**) showing the irradiation of δ_{H} 6.69 (H-10').

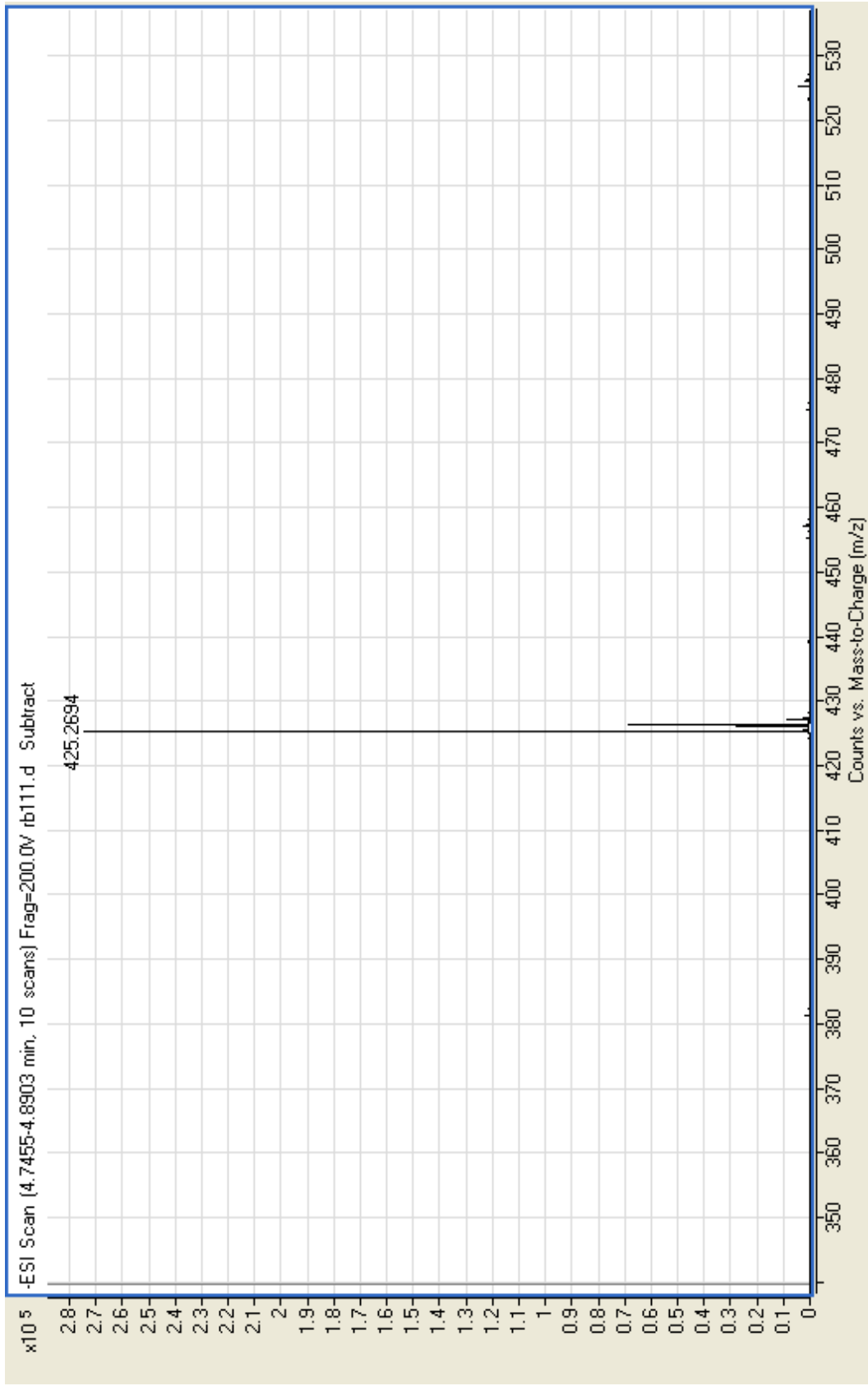


Figure S17. High resolution negative ESI-MS of peak B (4.80 min) (compound 2) from HPLC-MS.

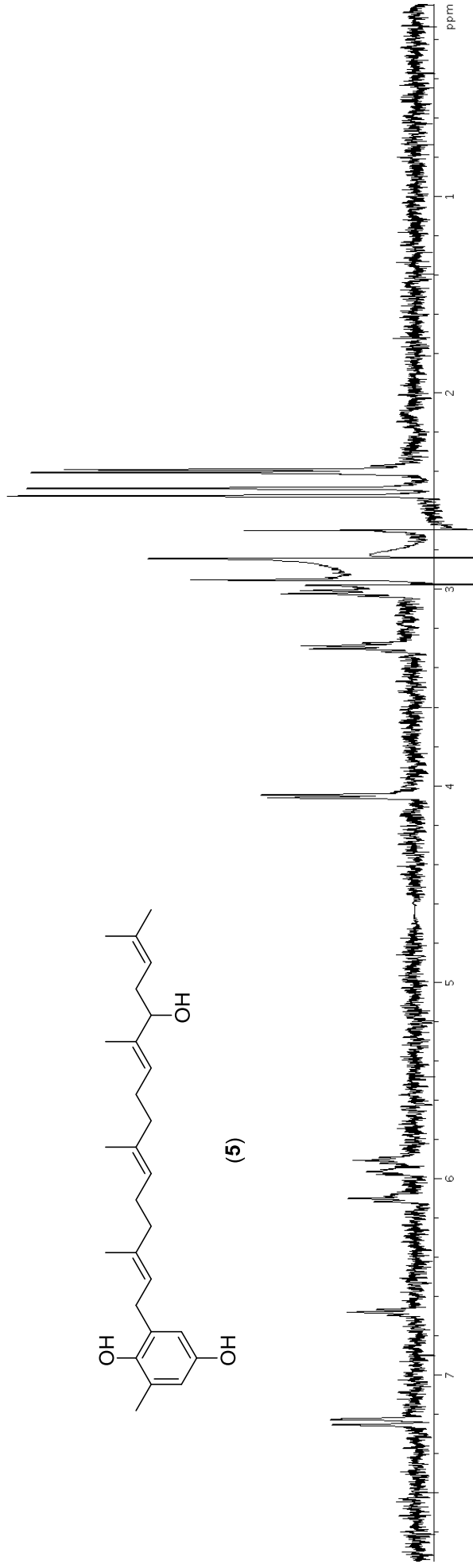
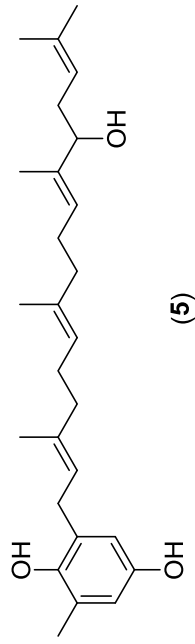


Figure S18. On-flow WETID Proton NMR spectrum of peak C (5.51 min) (compound 5).

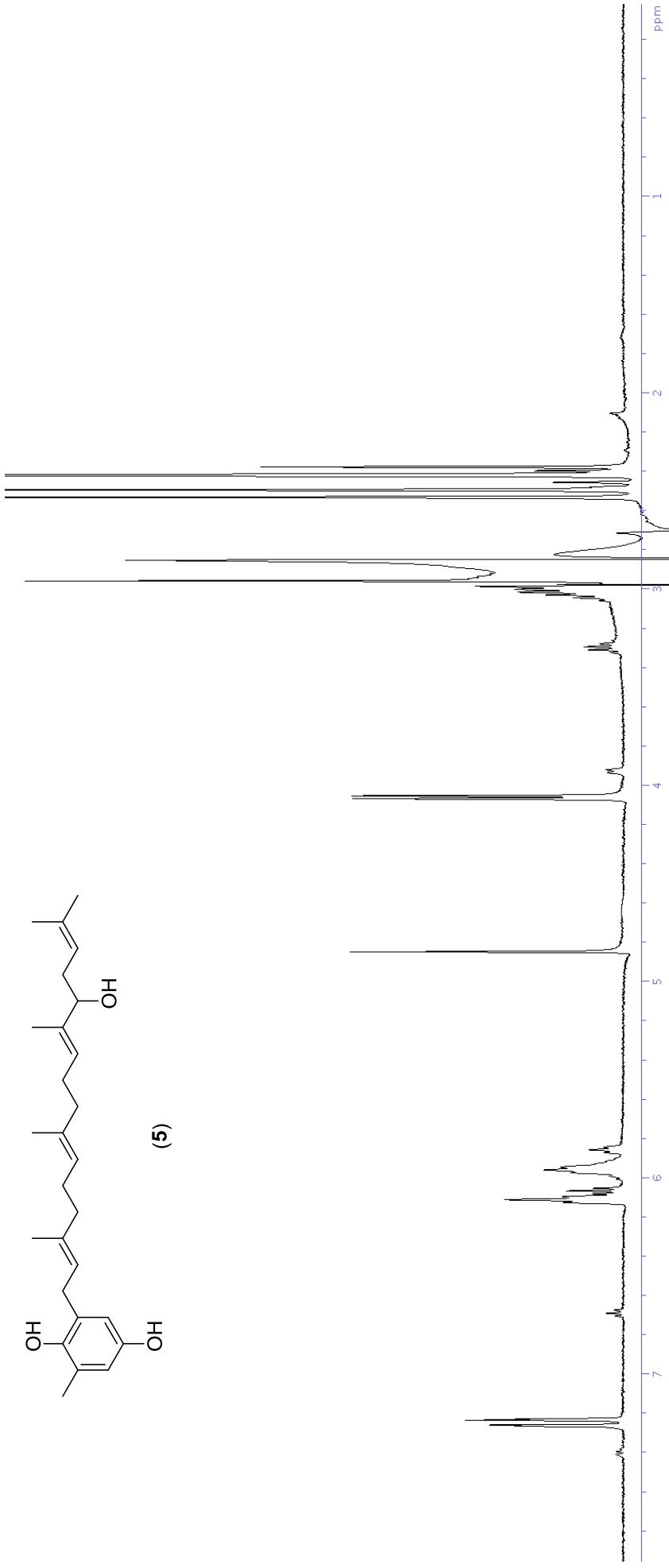
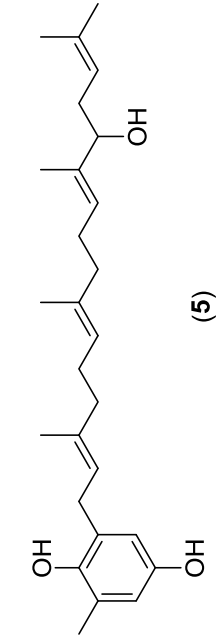


Figure S19. Stop-flow WETID Proton NMR spectrum of peak C (5.51 min) (compound 5).

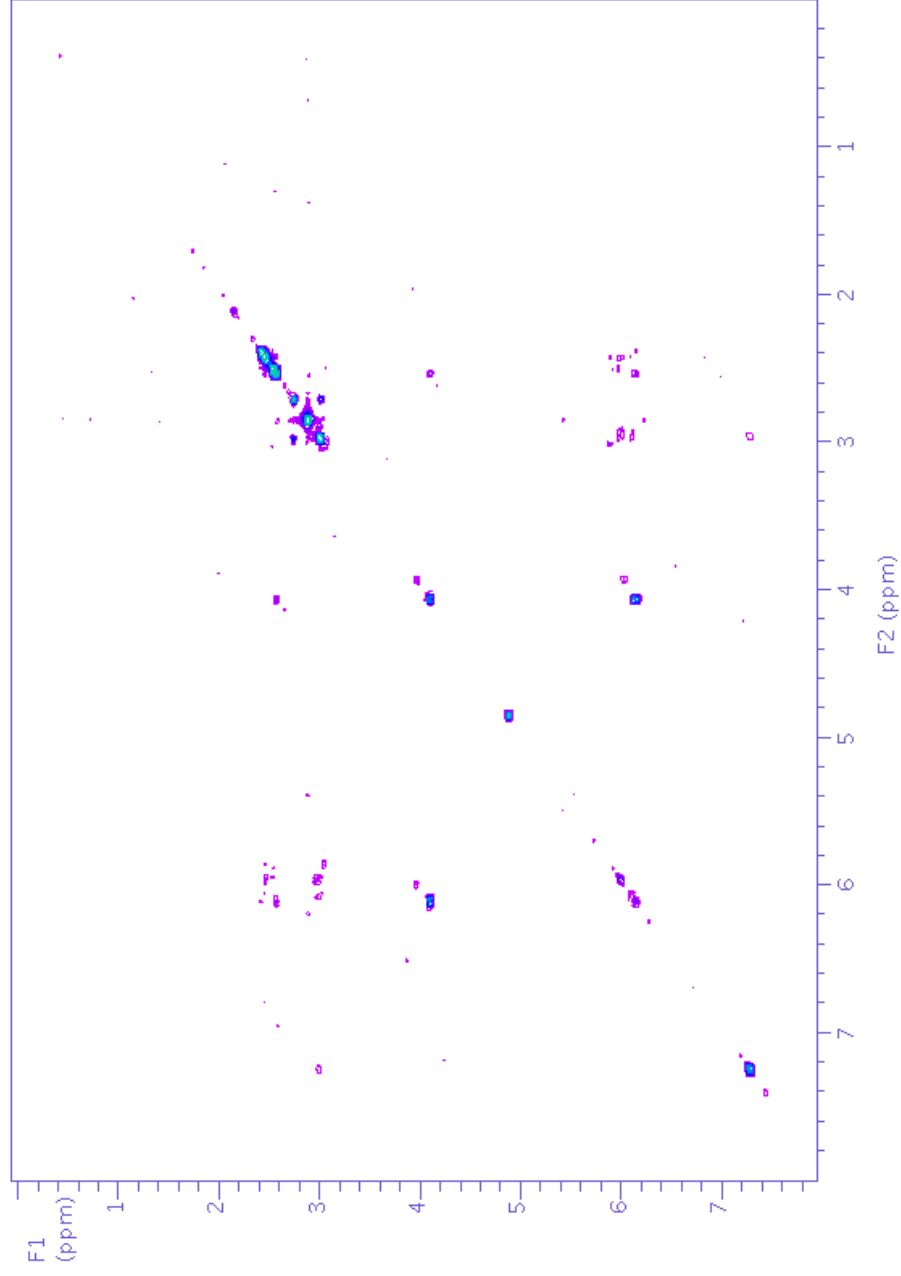


Figure S20. gCOSY NMR spectrum (from stop-flow HPLC-NMR) of peak C (5.51 min) (compound 5).

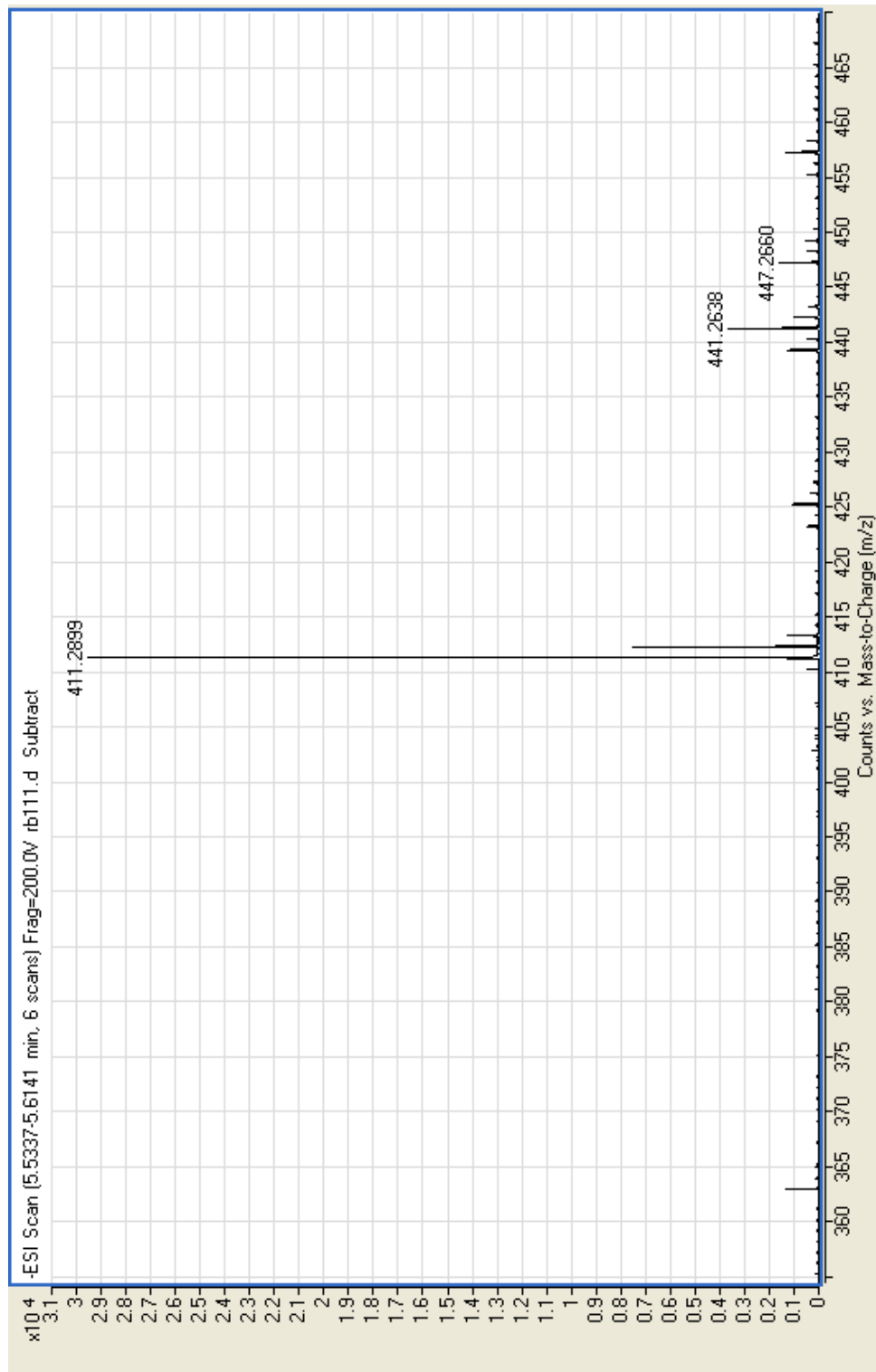


Figure S21. High resolution negative ESI-MS of peak C (5.51 min) (compound 5) from HPLC-MS.

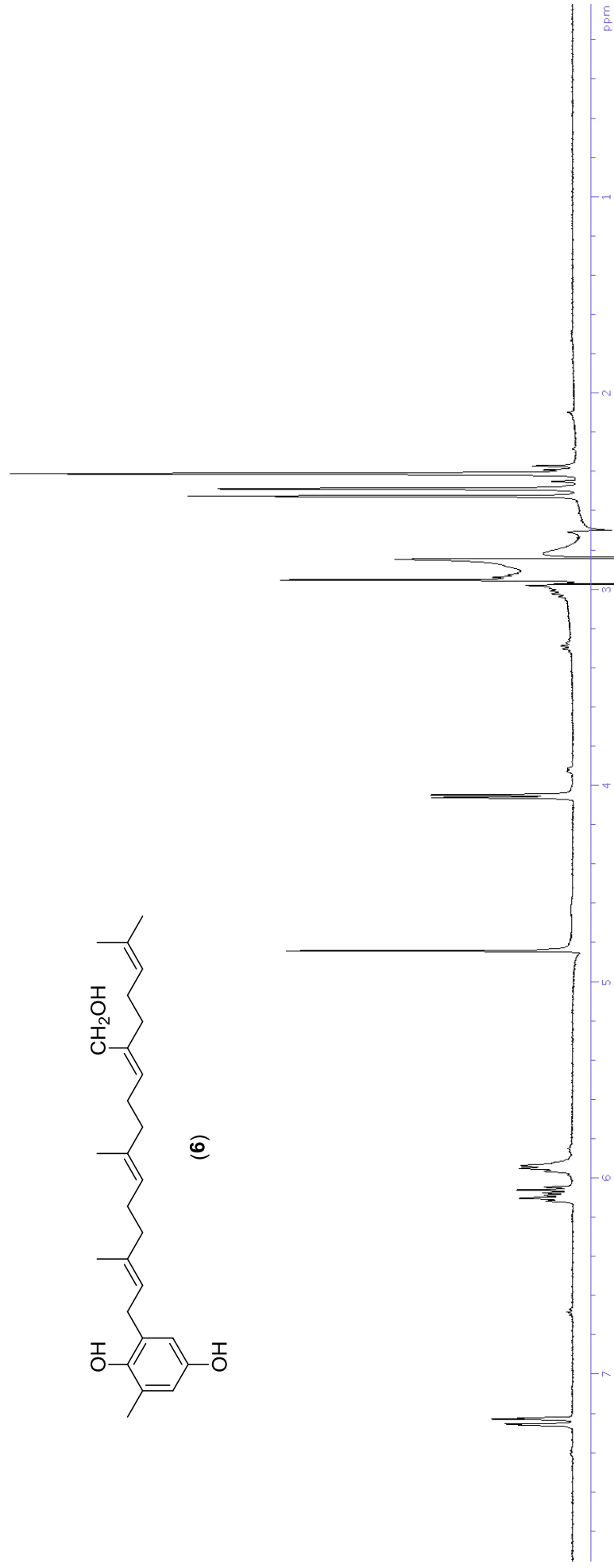


Figure S23. Stop-flow WET1D Proton NMR spectrum of peak D (5.81 min) (compound 6).

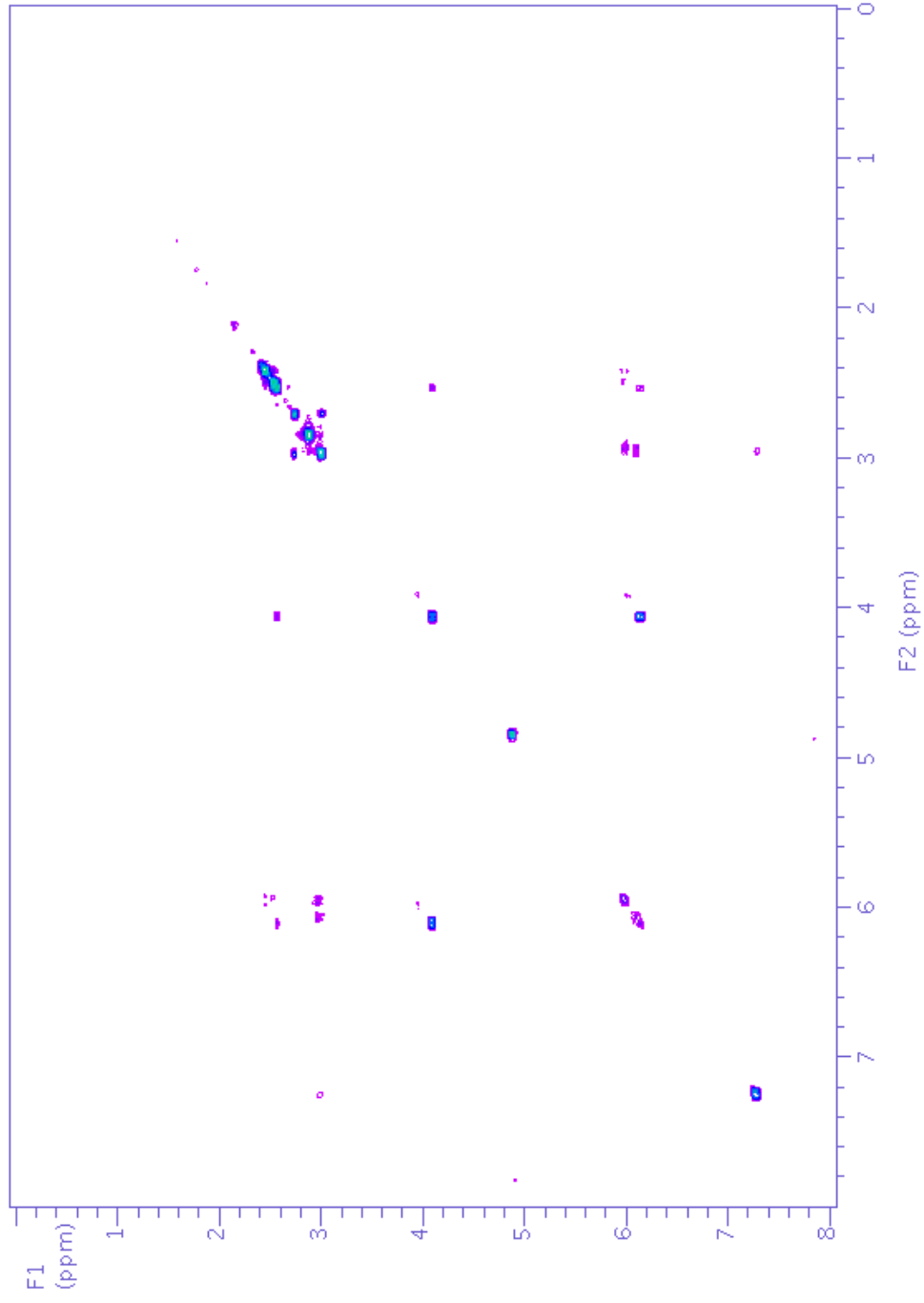


Figure S24. gCOSY NMR spectrum (from stop-flow HPLC-NMR) of peak D (5.81 min) (compound **6**).

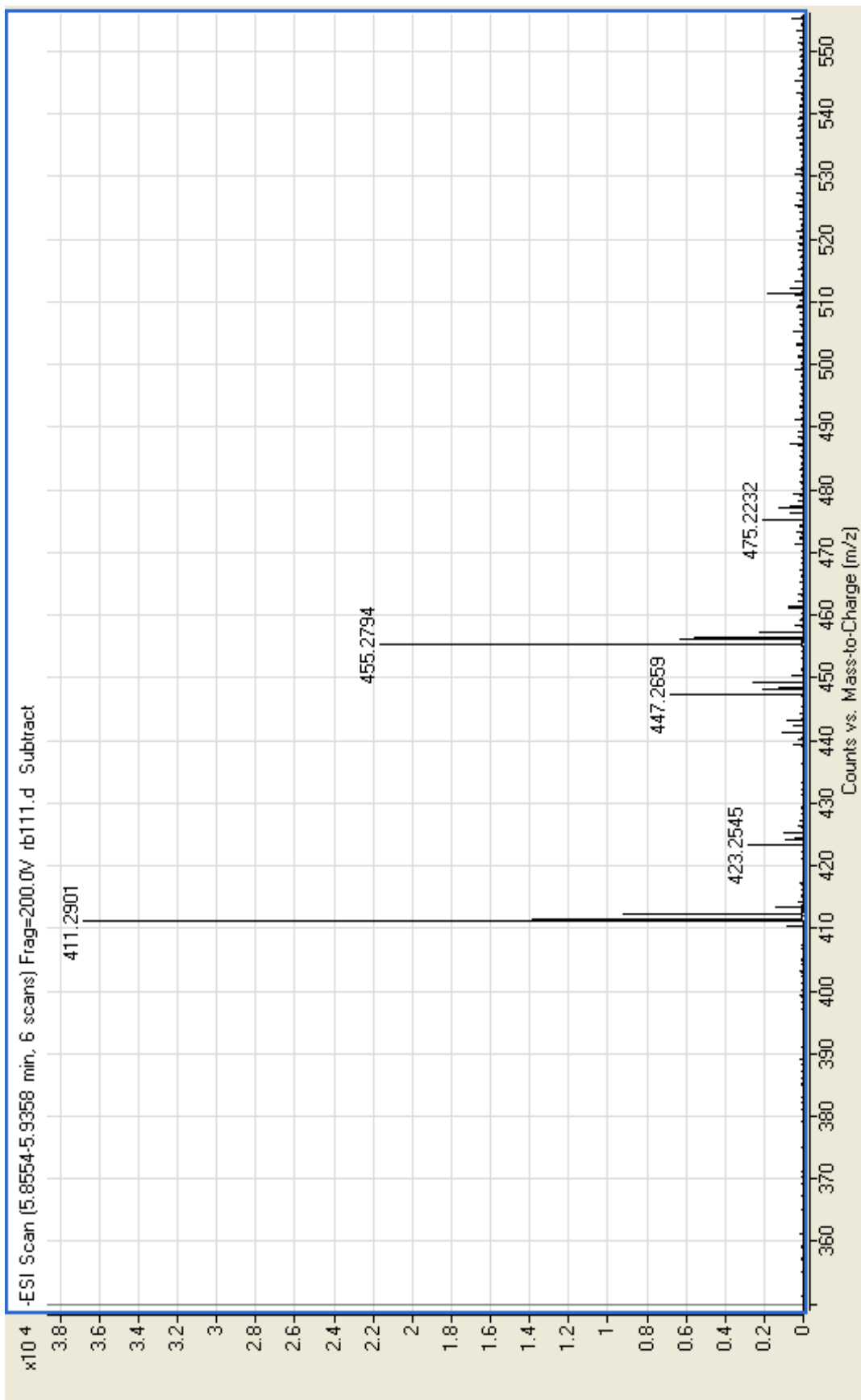


Figure S25. High resolution negative ESI-MS of peak D (5.81 mins) (compound 6) from HPLC-MS.

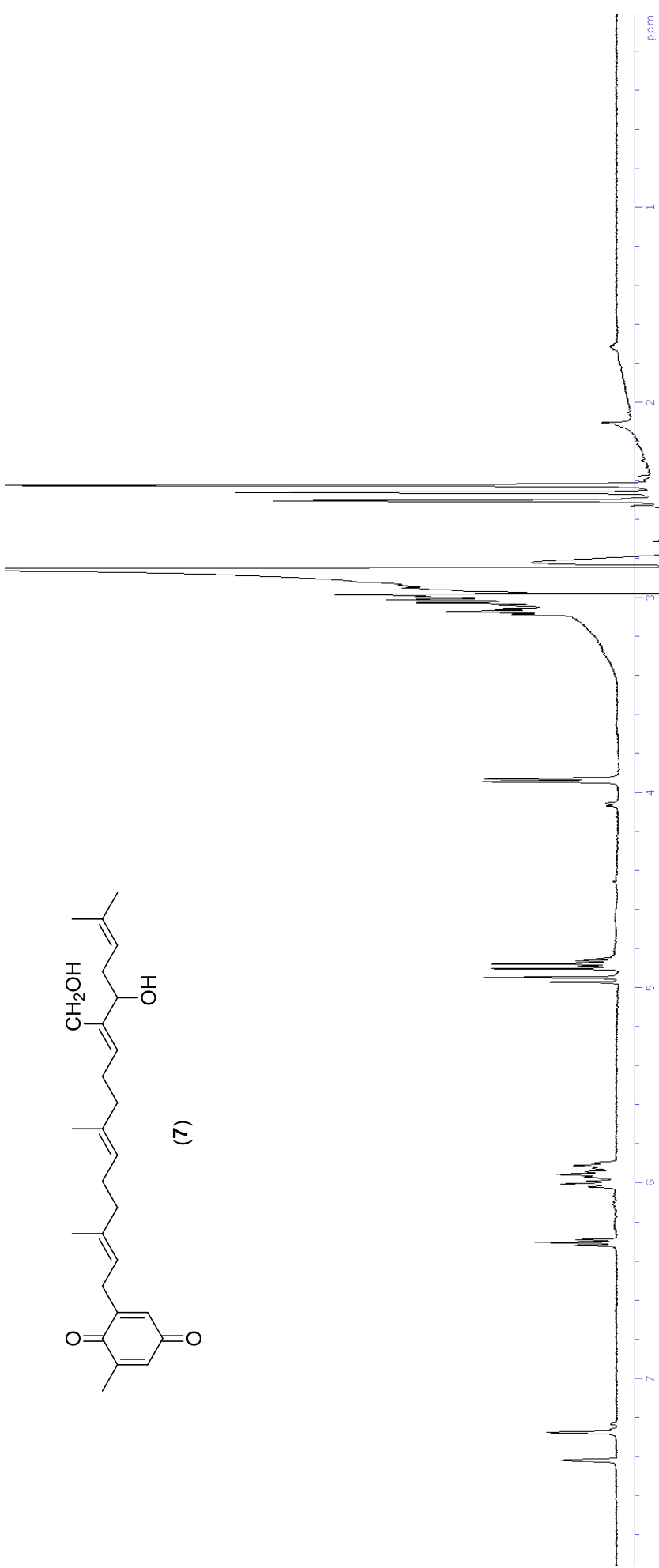


Figure S26. Stop-flow WET1D Proton NMR spectrum of peak E (6.90 mins) (compound 7).

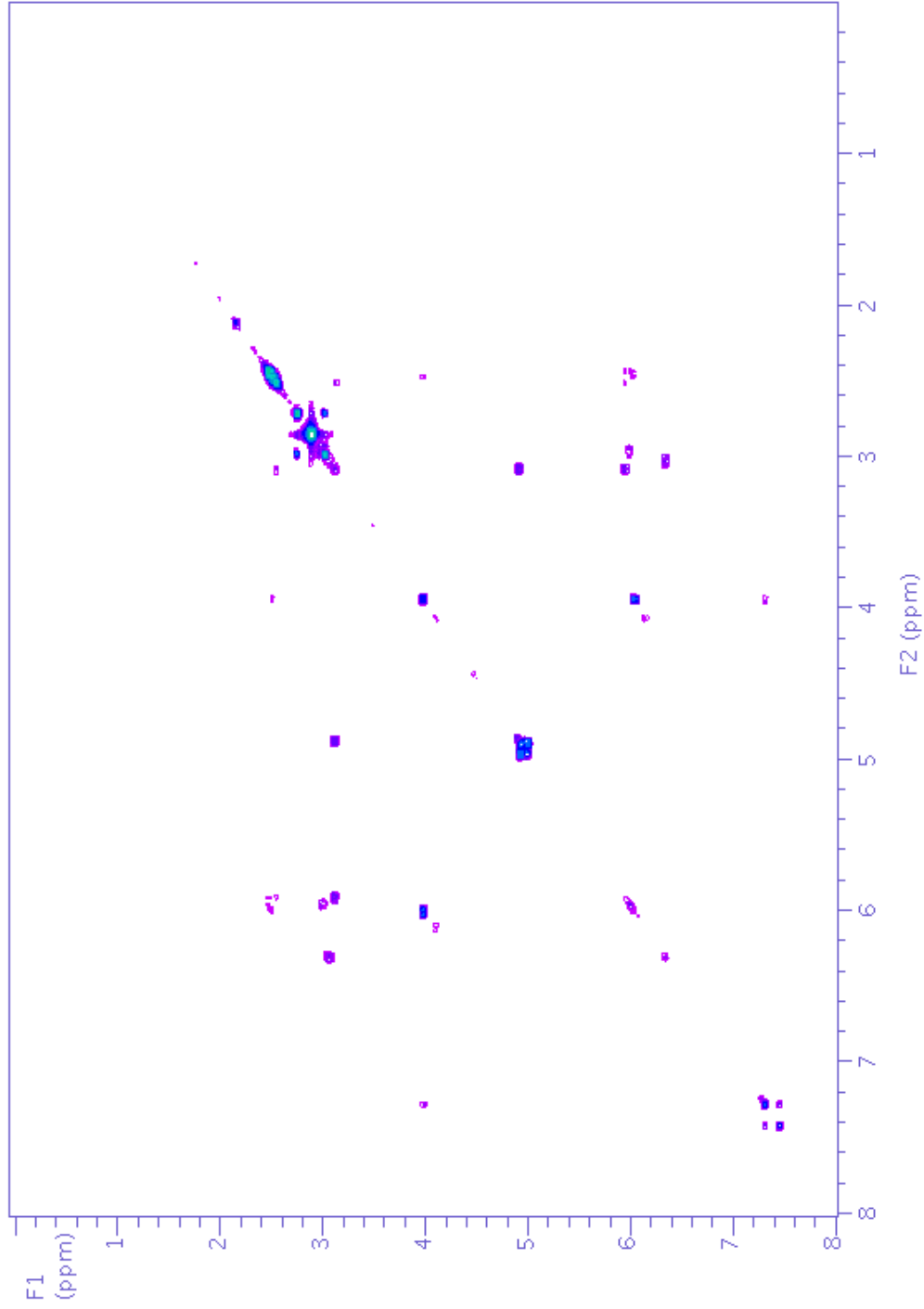


Figure S27. gCOSY NMR spectrum (from stop-flow HPLC-NMR) of peak E (6.90 min) (compound **7**).

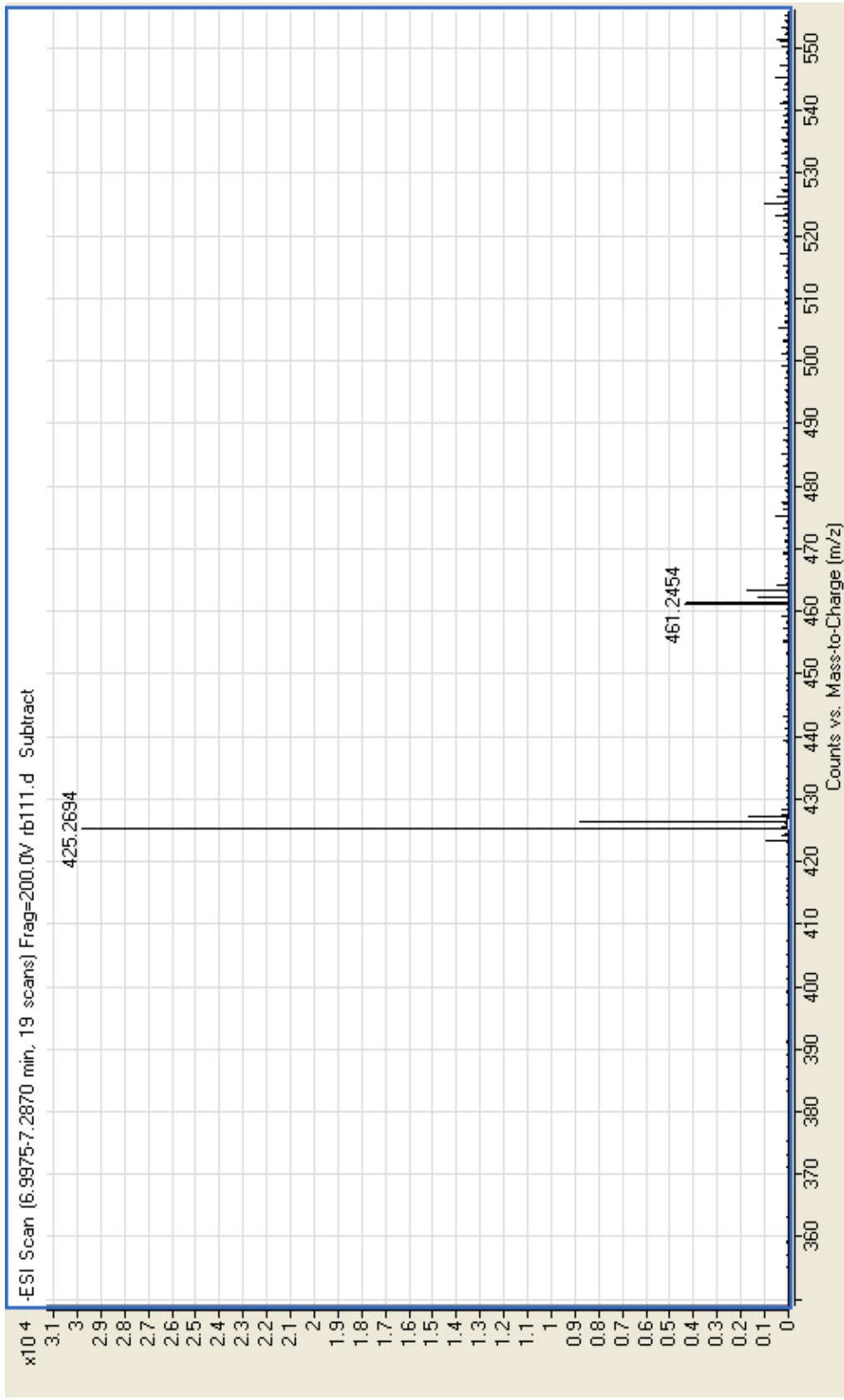


Figure S28. High resolution negative ESI-MS of peak E (6.90 min) (compound 7) from HPLC-MS.

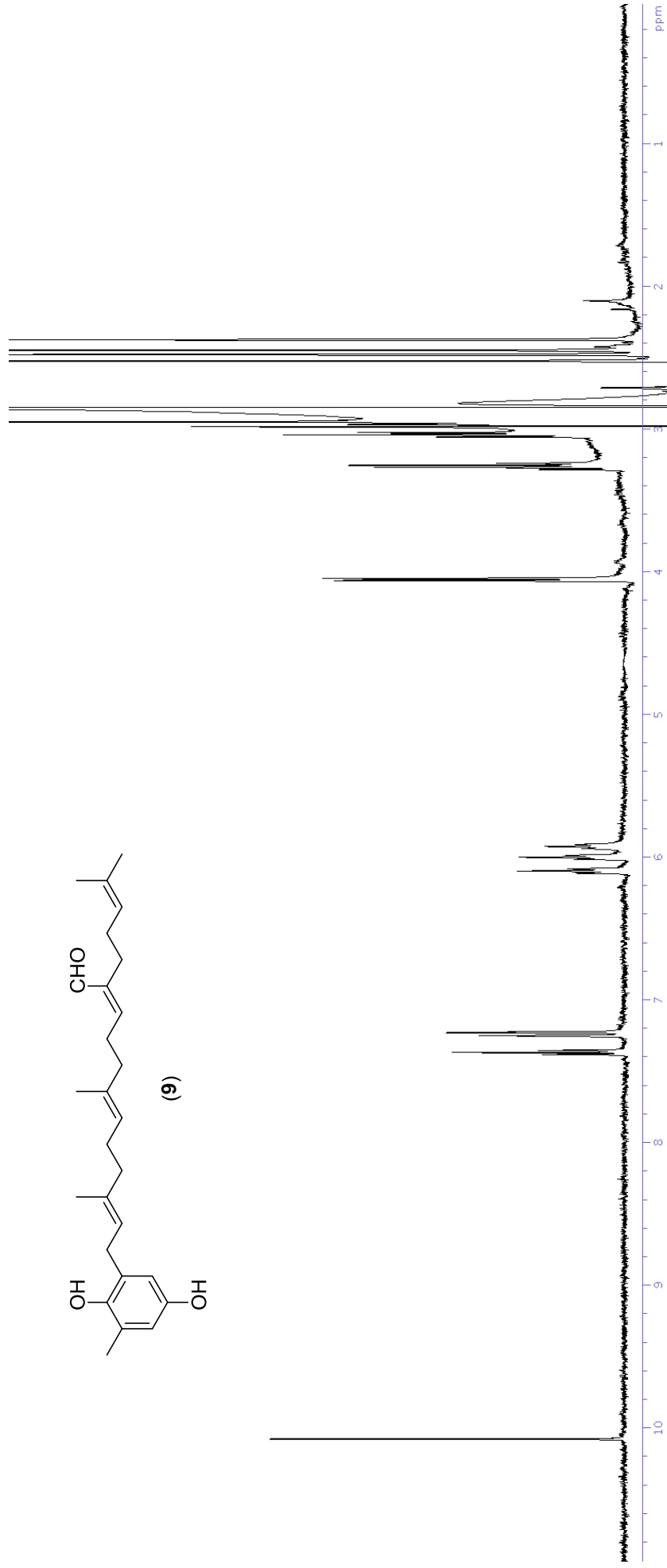


Figure S29. Stop-flow WET1D Proton NMR spectrum of peak F (7.79 min) (compound **9**).

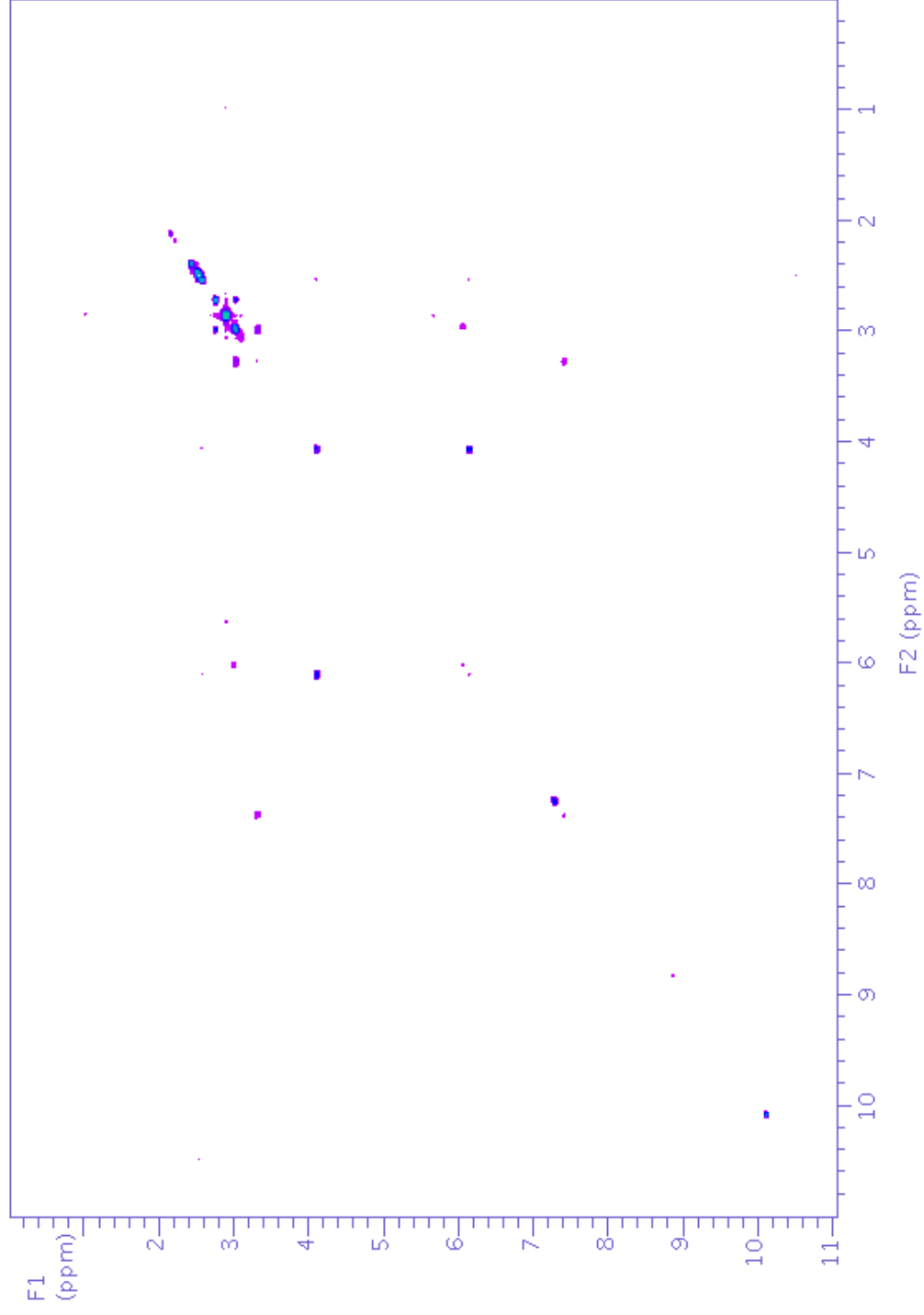


Figure S30. gCOSY NMR spectrum (from stop-flow HPLC-NMR) of peak F (7.79 min) (compound **9**).

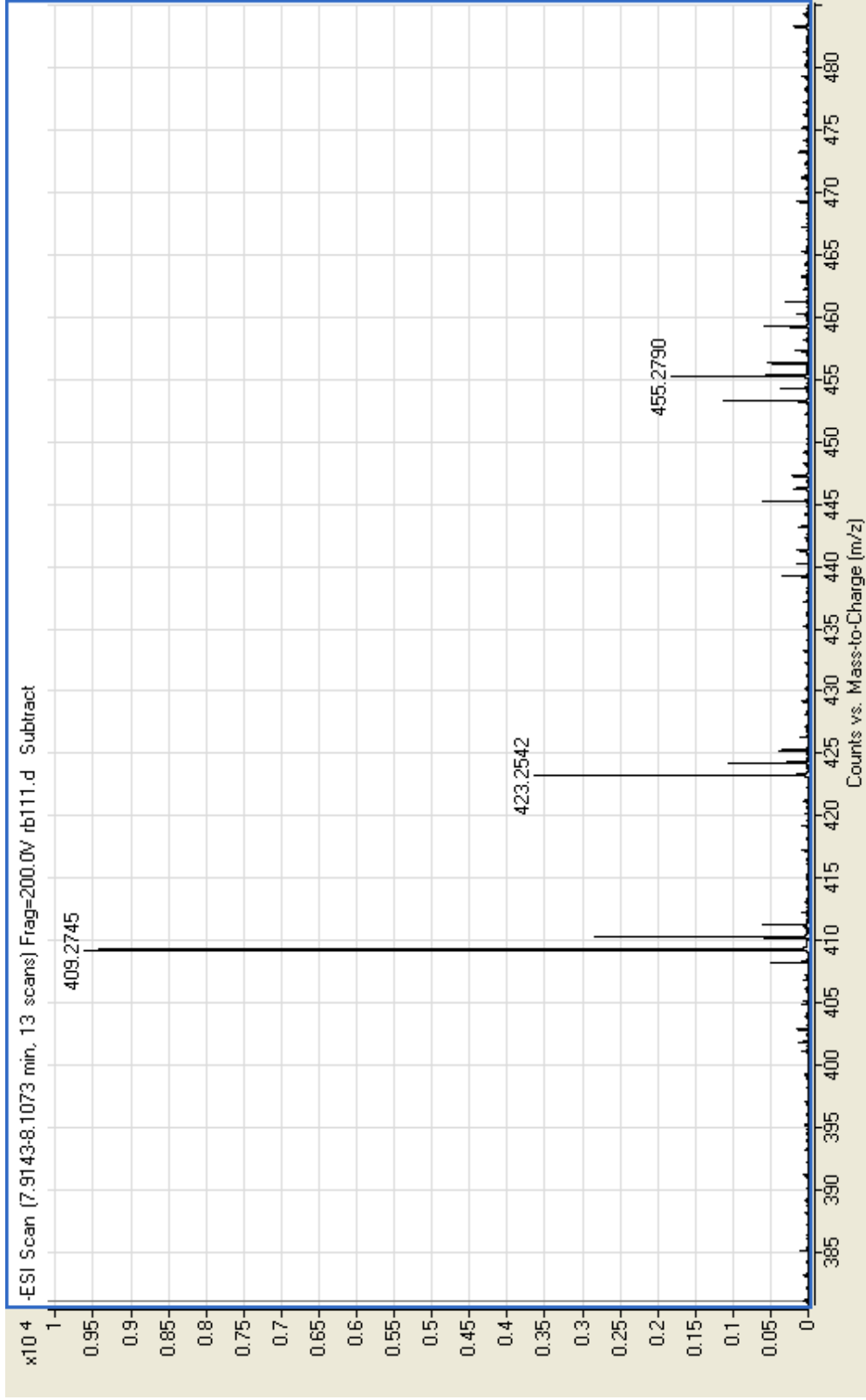


Figure S31. High resolution negative ESI-MS of peak F (7.79 min) (compound **9**) from HPLC-MS.

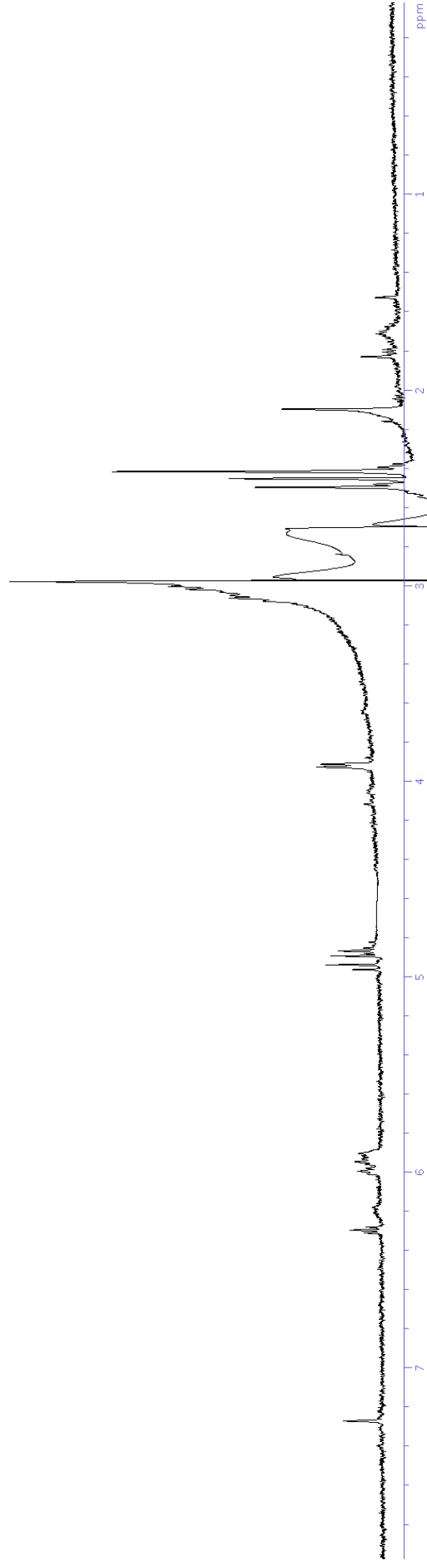


Figure S32. Stop-flow WETID Proton NMR spectrum of peak G (9.81 min) (compound **10**).

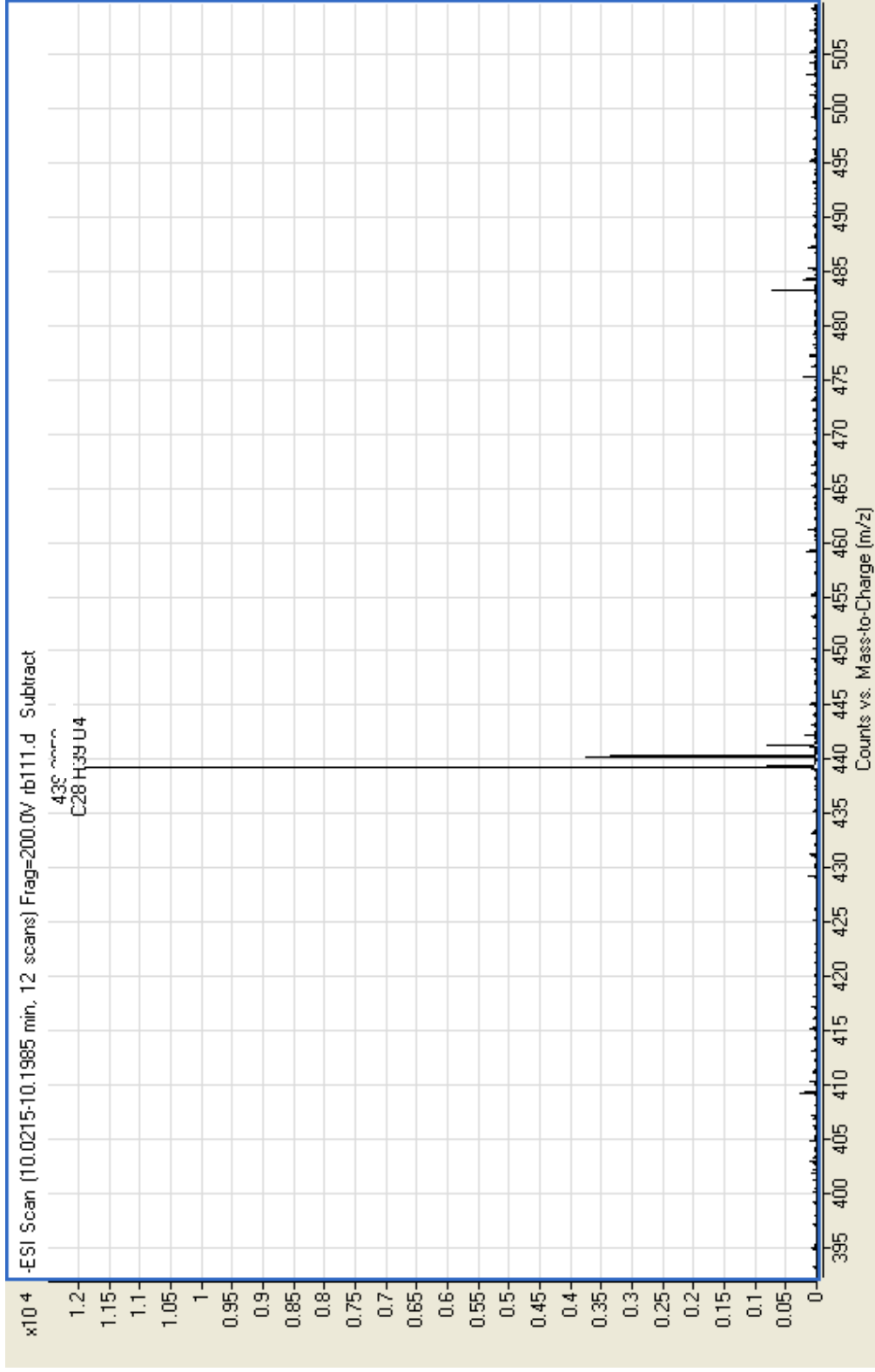


Figure S33. High resolution negative ESI-MS of peak G (9.81 min) (compound **10**) from HPLC-MS.

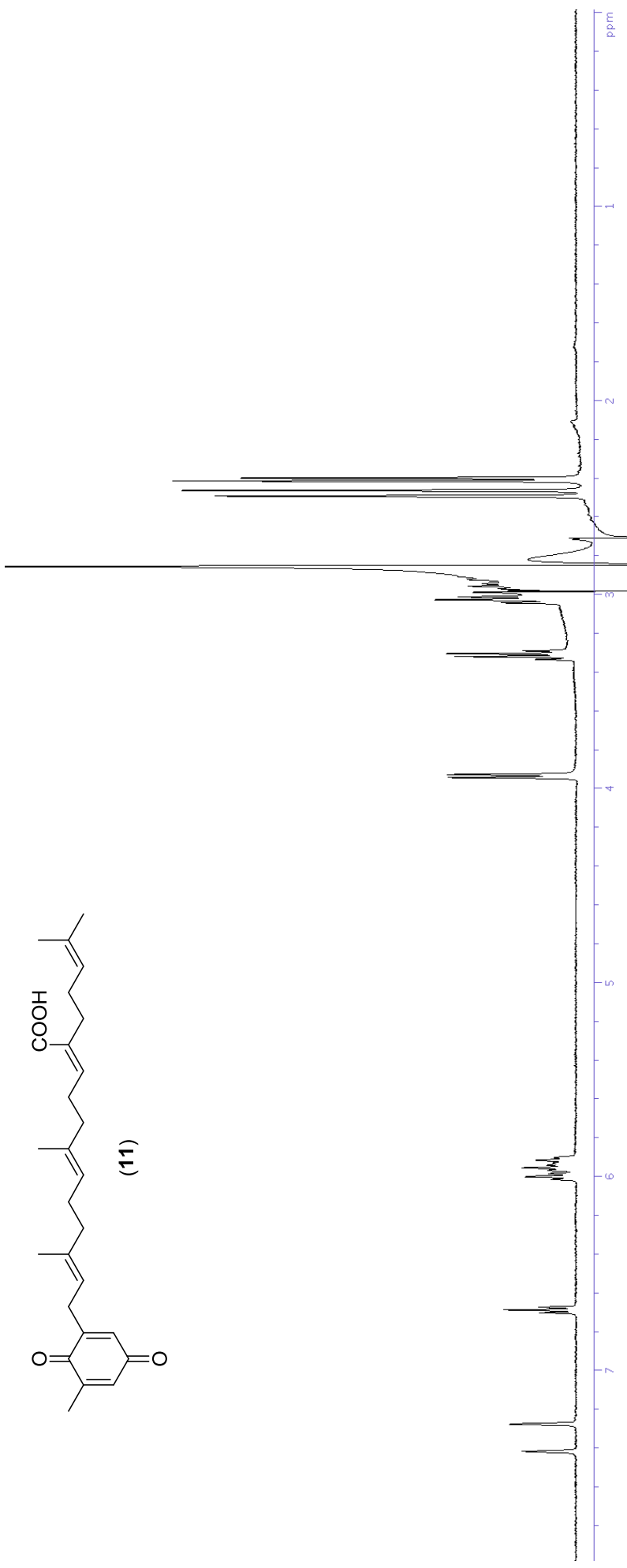


Figure S34. Stop-flow WETID Proton NMR spectrum of peak I (14.70 min) (compound **11**).

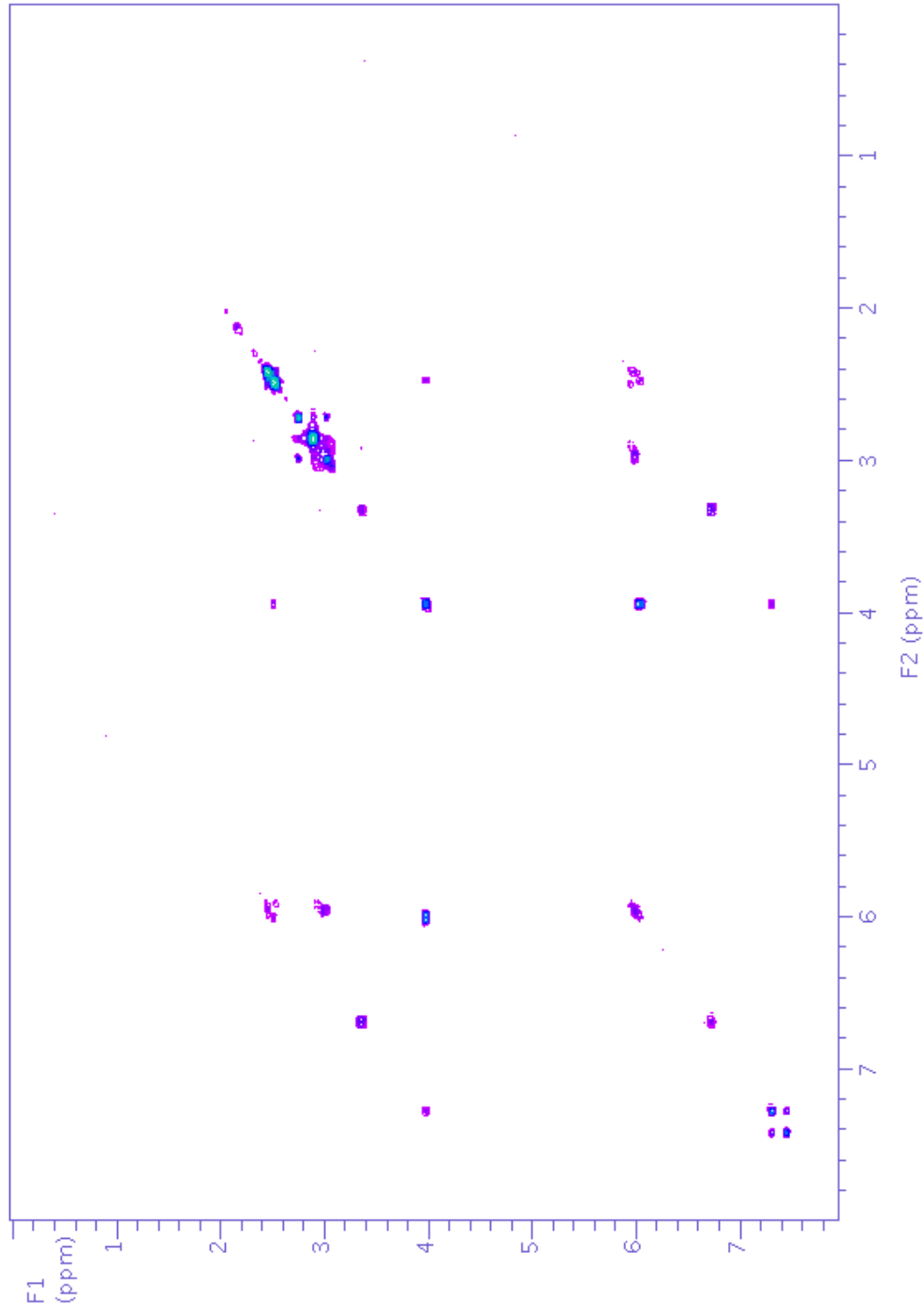


Figure S35. gCOSY NMR spectrum (from stop-flow HPLC-NMR) of peak I (14.70 min) (compound **11**).

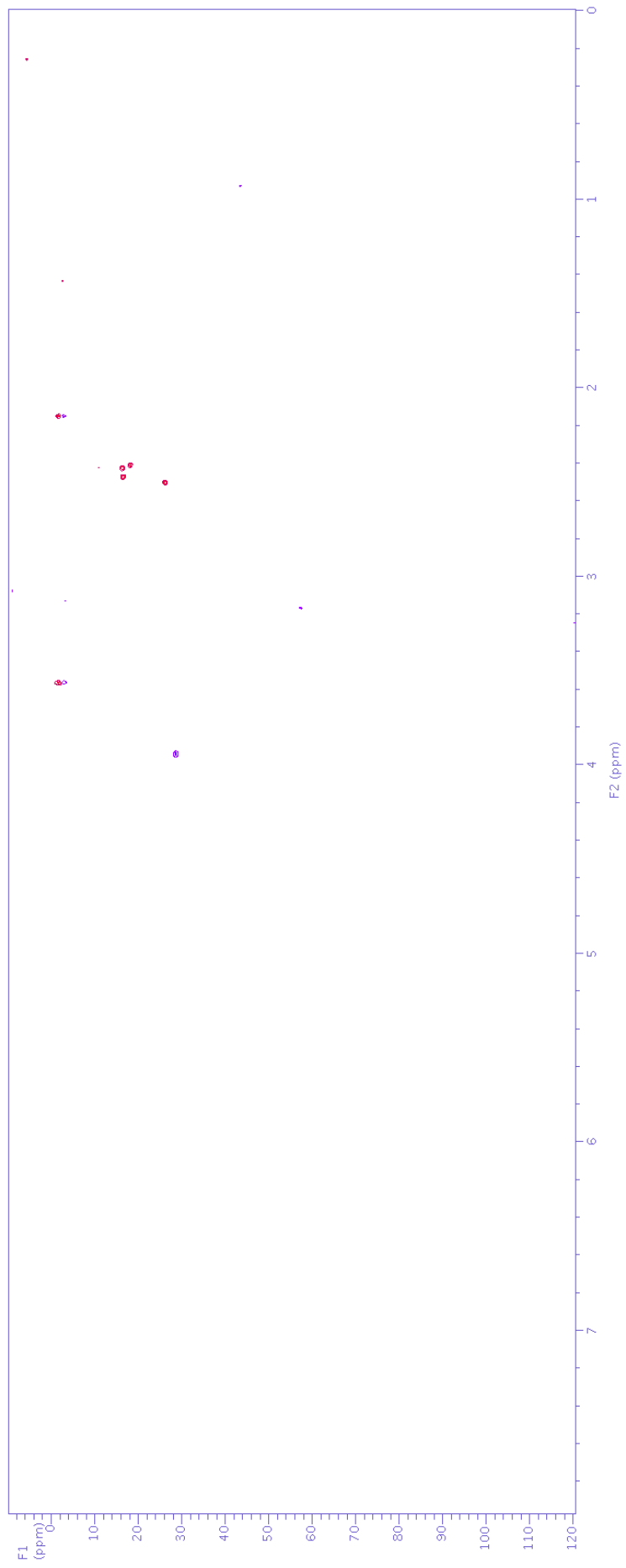


Figure S36. gHSQCAD NMR spectrum (from stop-flow HPLC-NMR) of peak I (14.70 min) (compound **11**).

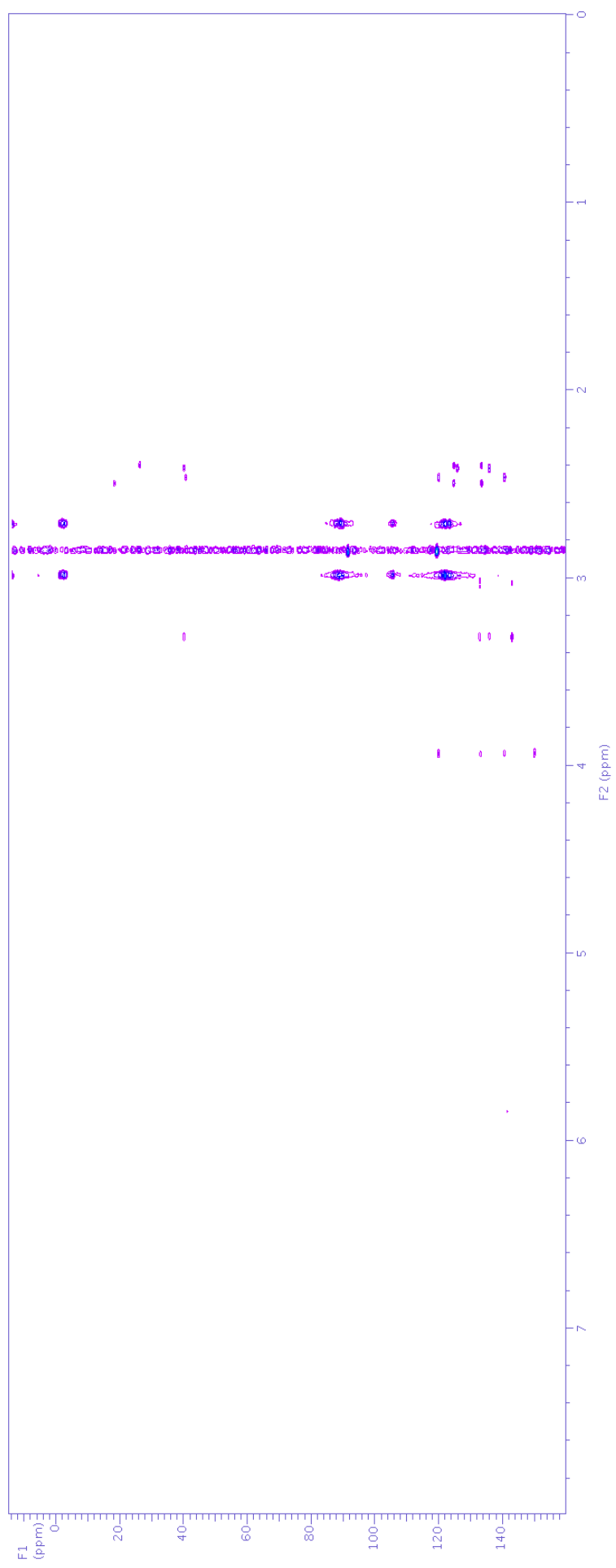


Figure S37. gHMBCAD NMR spectrum (from stop-flow HPLC-NMR) of peak I (14.70 min) (compound **11**).

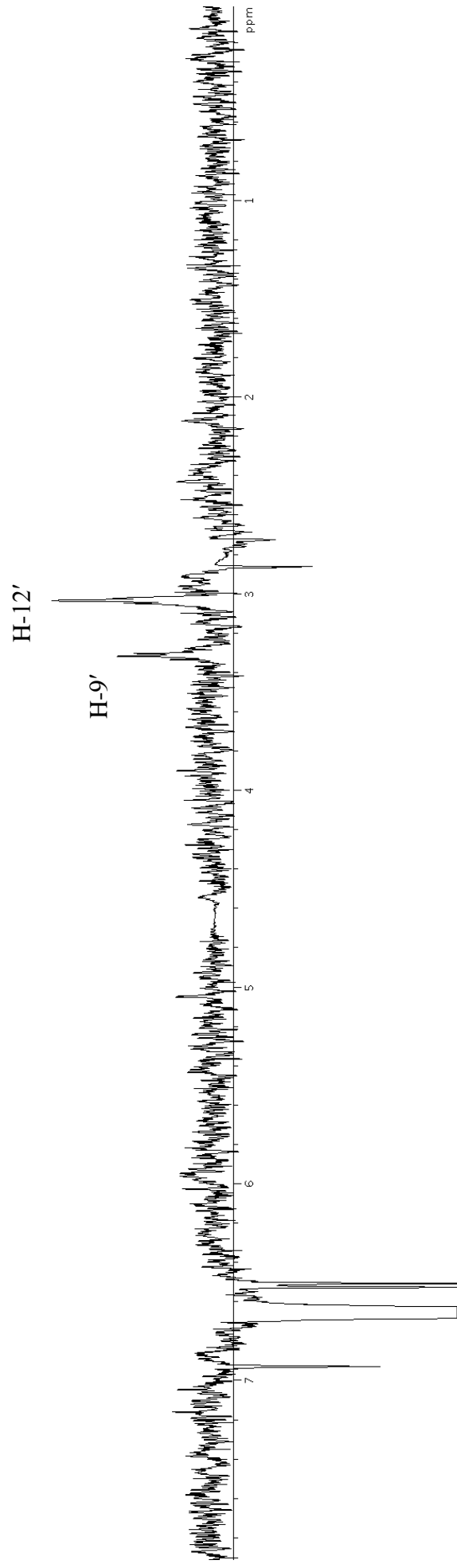
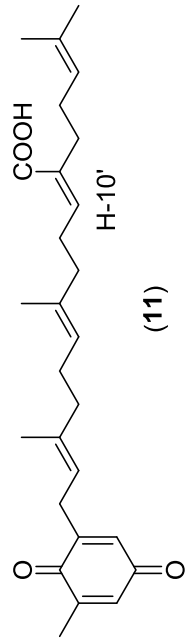


Figure S38. Single irradiation nOe NMR spectrum (from stop-flow HPLC-NMR) of peak **I** (compound **11**) showing the irradiation of $\delta_{\text{H}} 6.69$ (**H-10'**).

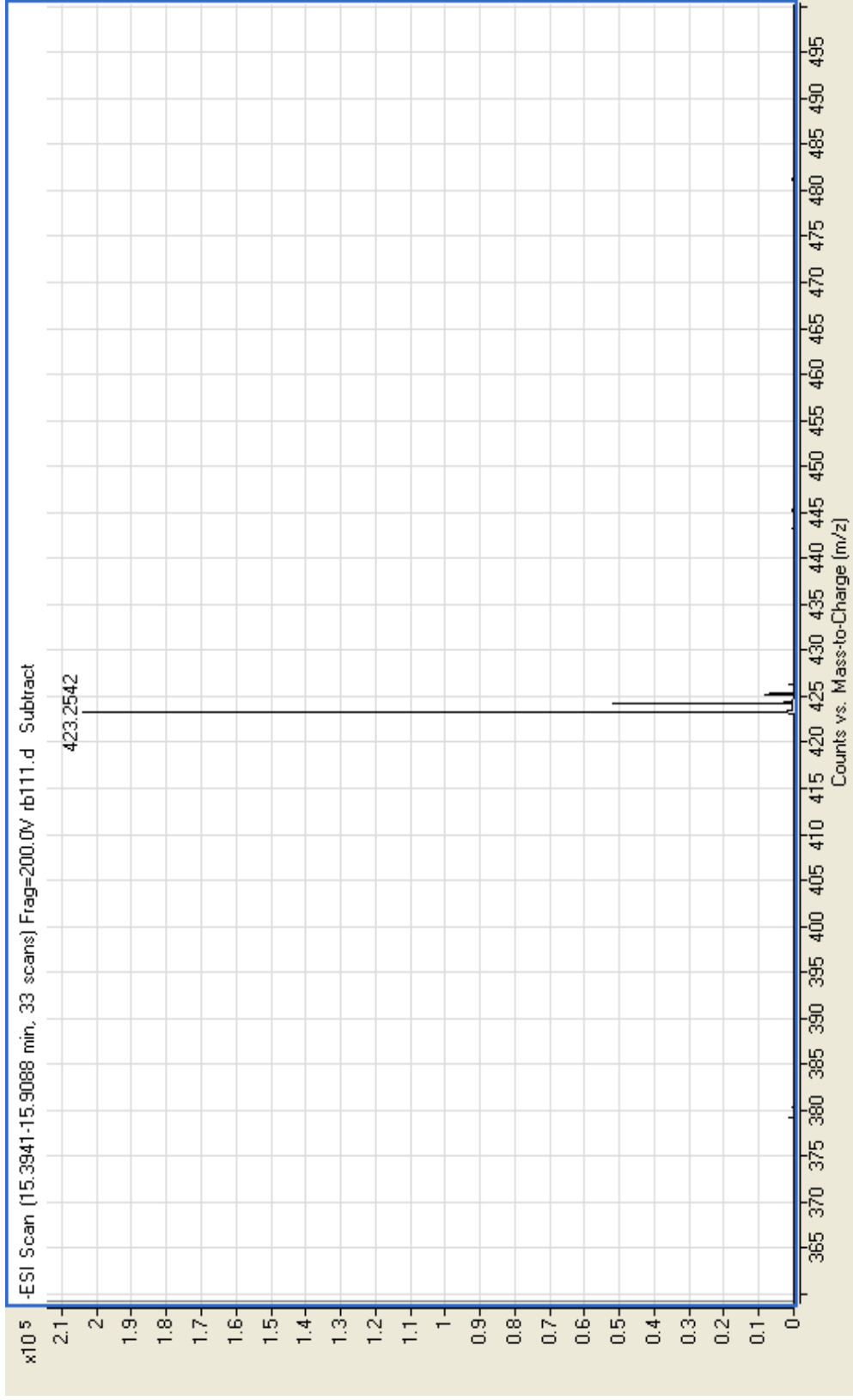


Figure S39. High resolution negative ESI-MS of peak I (14.70 min) (compound **11**) from HPLC-MS.

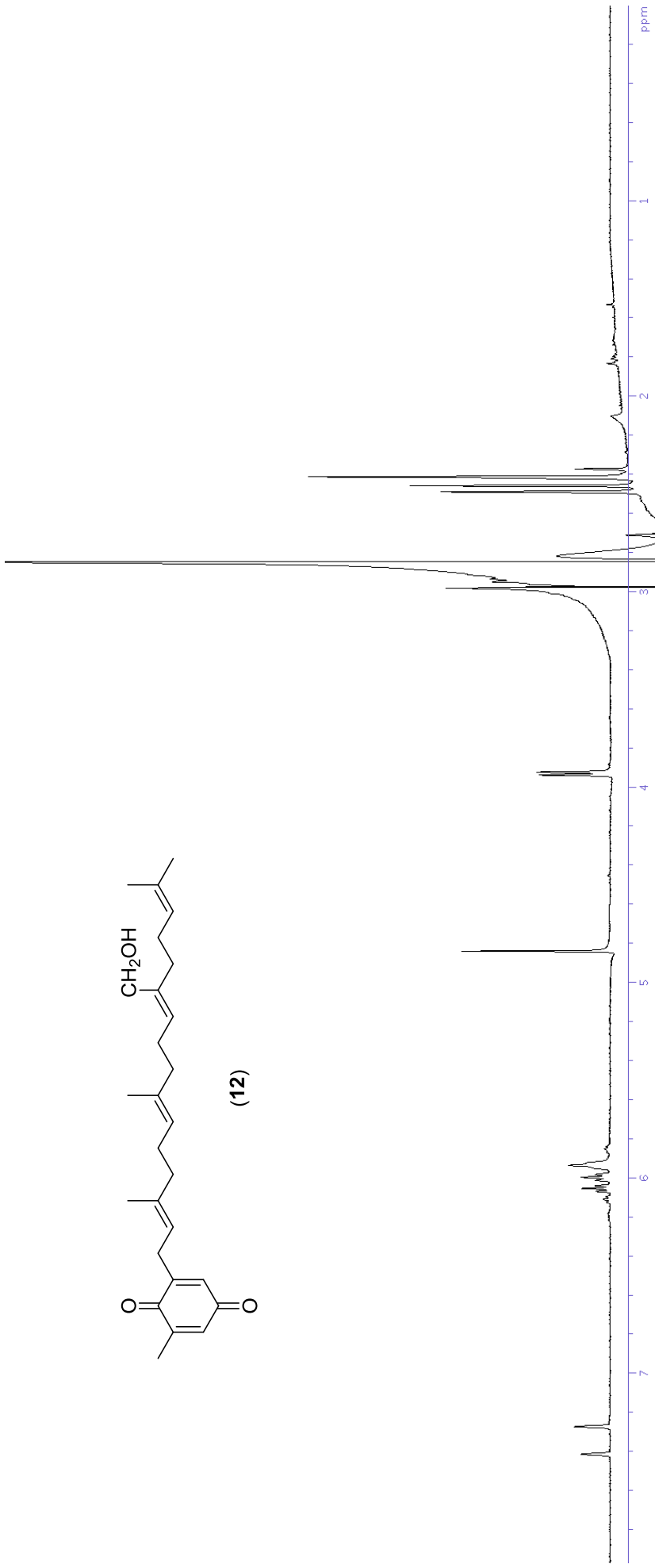
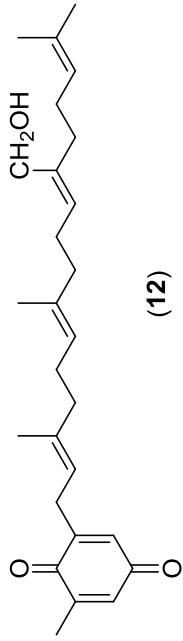


Figure S40. Stop-flow WETID Proton NMR spectrum of peak J (18.36 min) (compound **12**).

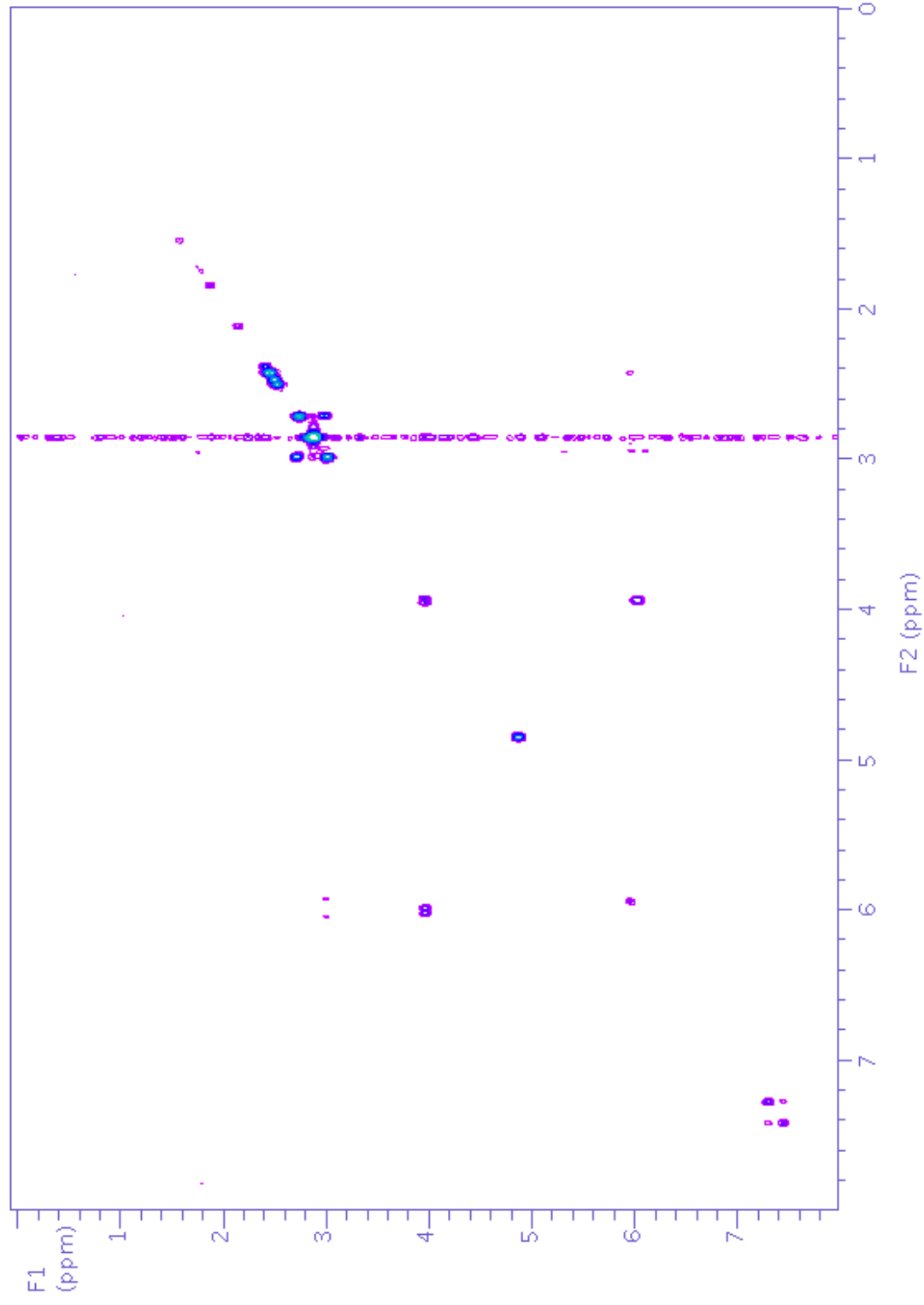


Figure S41. gCOSY NMR spectrum (from stop-flow HPLC-NMR) of peak J (18.36 min) (compound **12**).

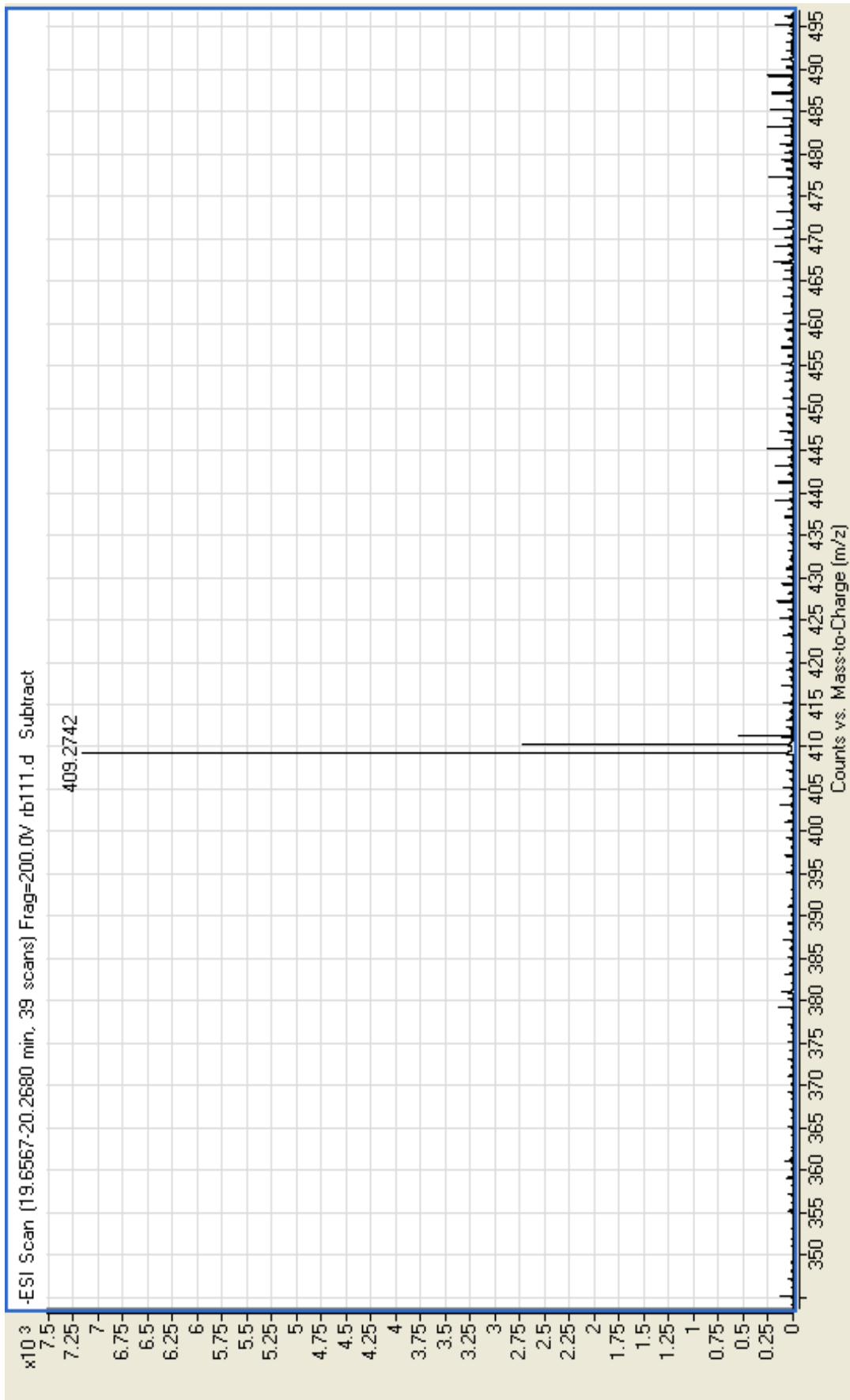


Figure S42. High resolution negative ESI-MS of peak J (18.36 min) (compound 12) from HPLC-MS.

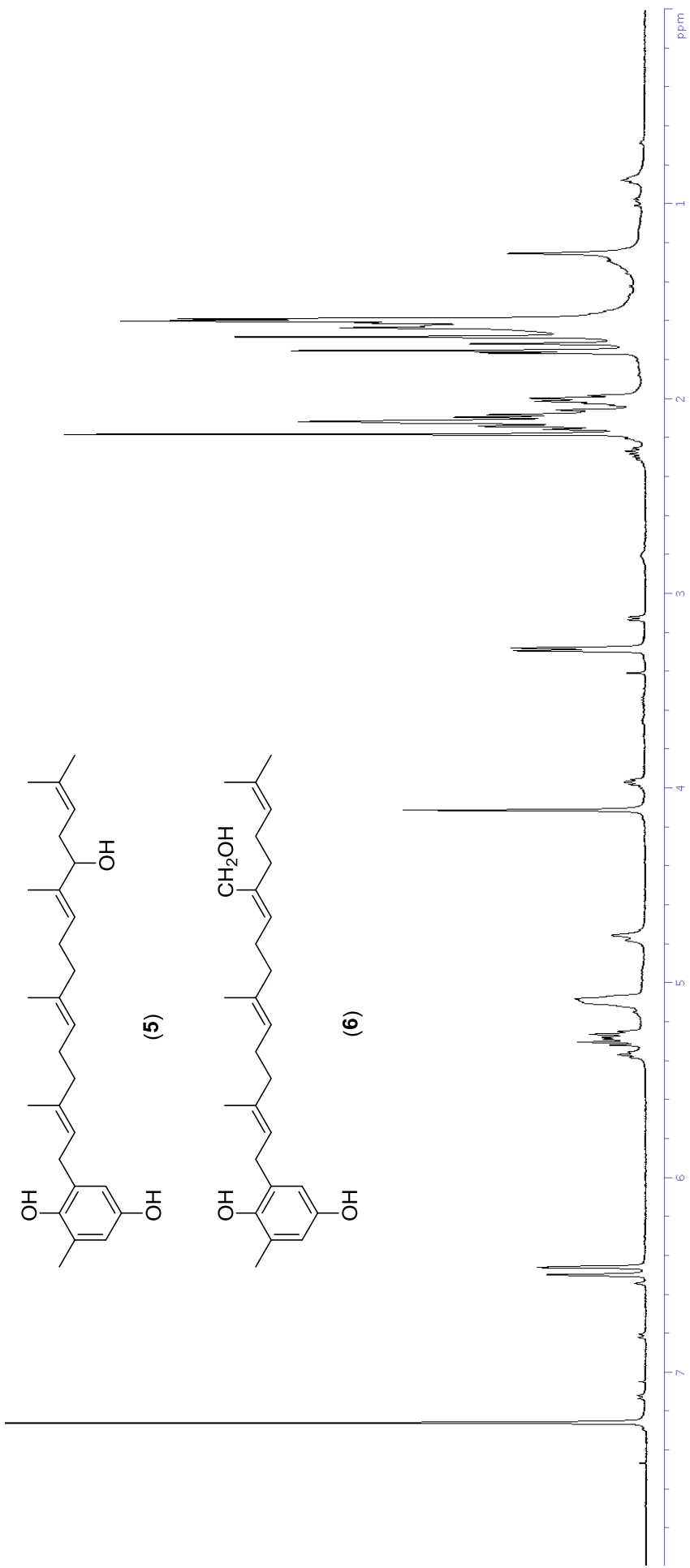


Figure S43. ¹H NMR spectrum (500 MHz, CDCl₃) of paradoxhydroquinone (5) and 2-[11-(hydroxymethyl)-3,7,15-trimethyl-2,6,10,14-hexadecatetraen-1-yl]-6-methyl-1,4-benzenediol (6) mixture.

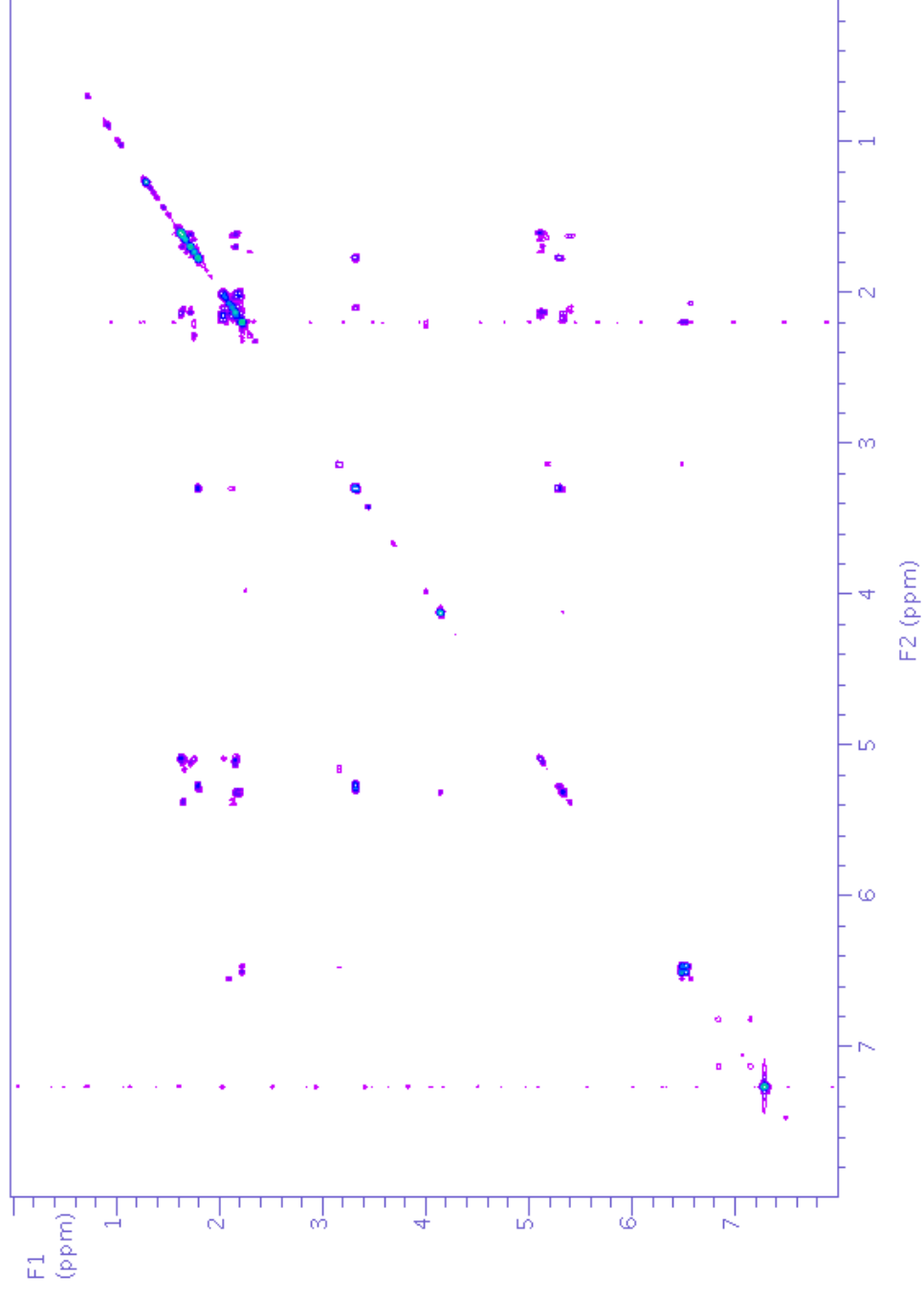


Figure S44. gCOSY NMR spectrum (500 MHz, CDCl₃) of paradoxhydroquinone (**5**) and 2-[11-(hydroxymethyl)-3,7,15-trimethyl-2,6,10,14-hexadecatetraen-1-yl]-6-methyl-1,4-benzenediol (**6**) mixture.

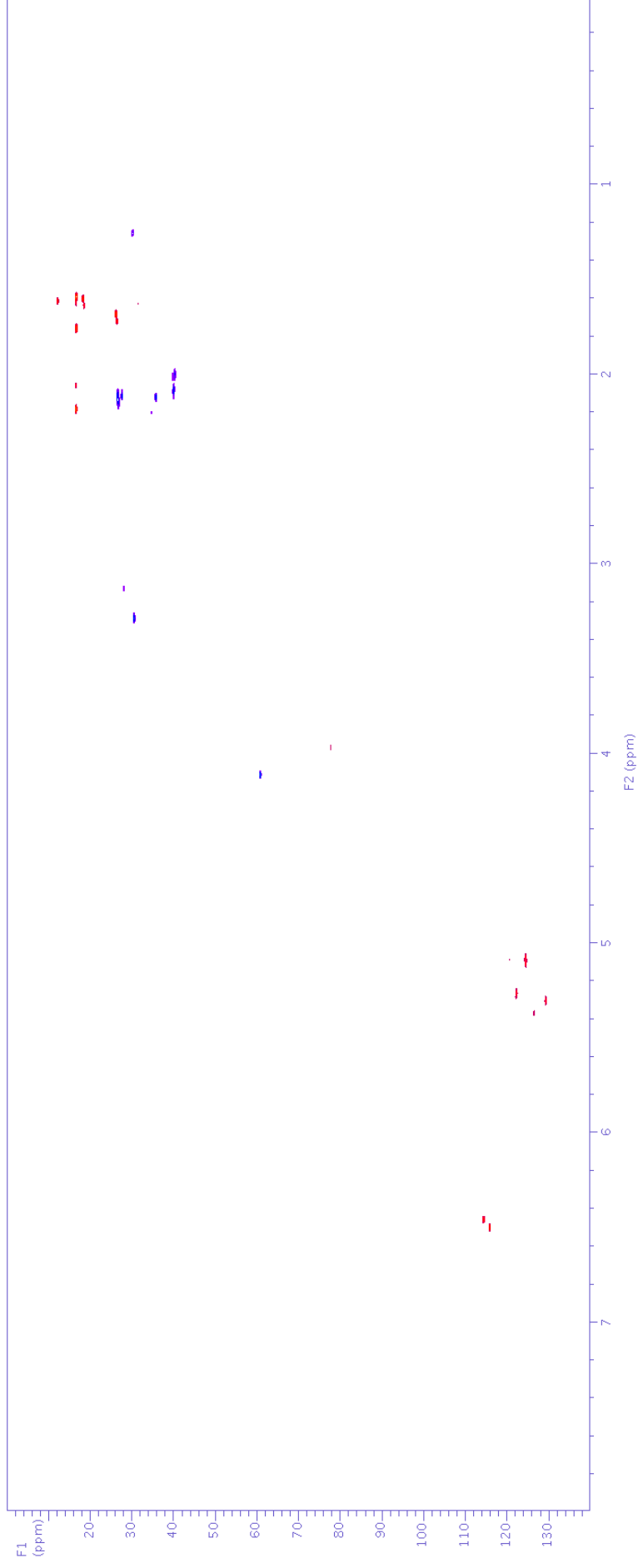


Figure S45. gHSQCAD NMR spectrum (500 MHz, CDCl₃) of parodoxhydroquinone (**5**) and 2-[11-(hydroxymethyl)-3,7,15-trimethyl-2,6,10,14-hexadecatetraen-1-yl]-6-methyl-1,4-benzenediol (**6**) mixture.

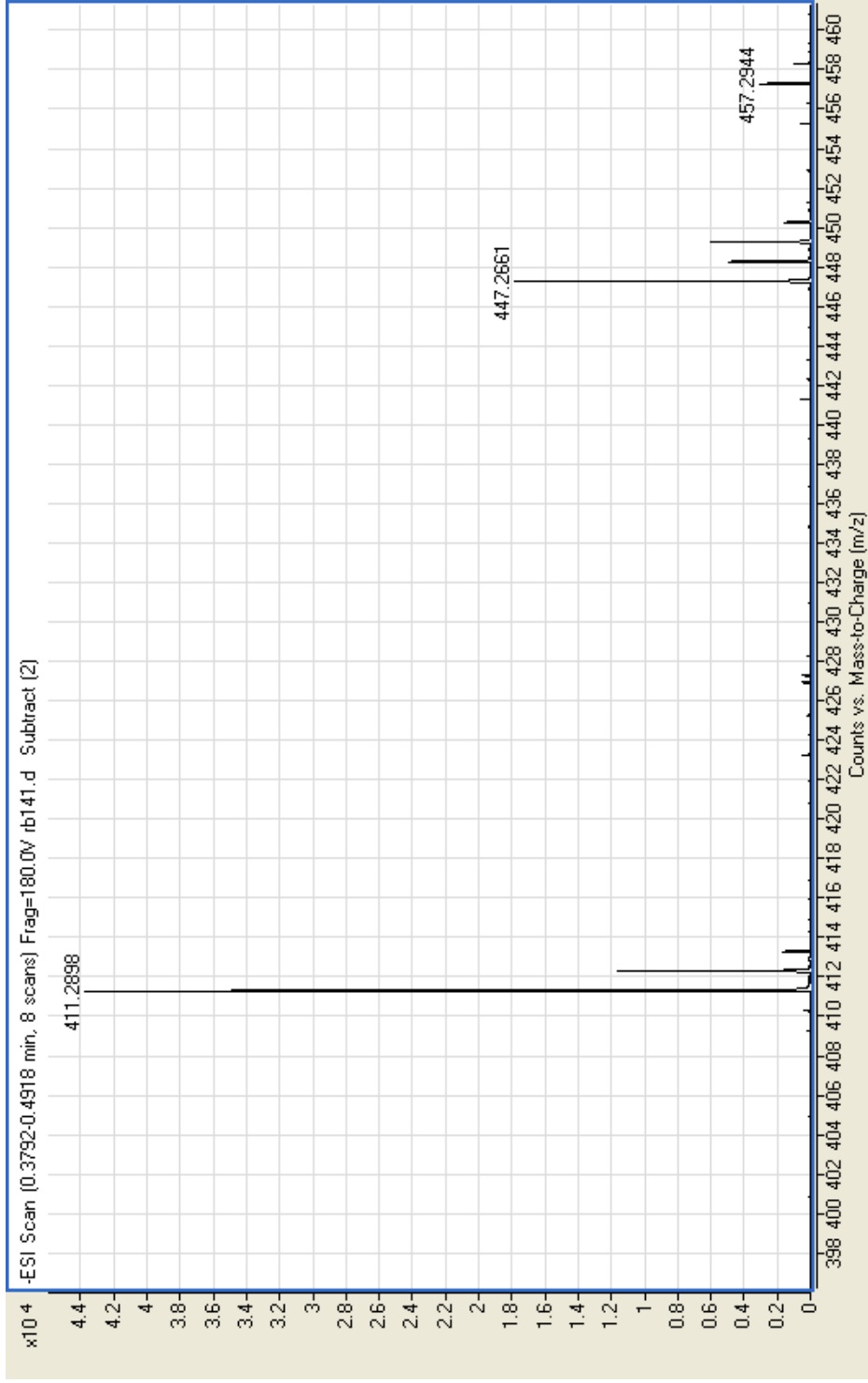


Figure S47. High resolution negative ESI-MS of parodoxhydroquinone (**5**) and 2-[11-(hydroxymethyl)-3,7,15-trimethyl]-2,6,10,14-hexadecatetraen-1-yl]-6-methyl-1,4-benzenediol (**6**) mixture.

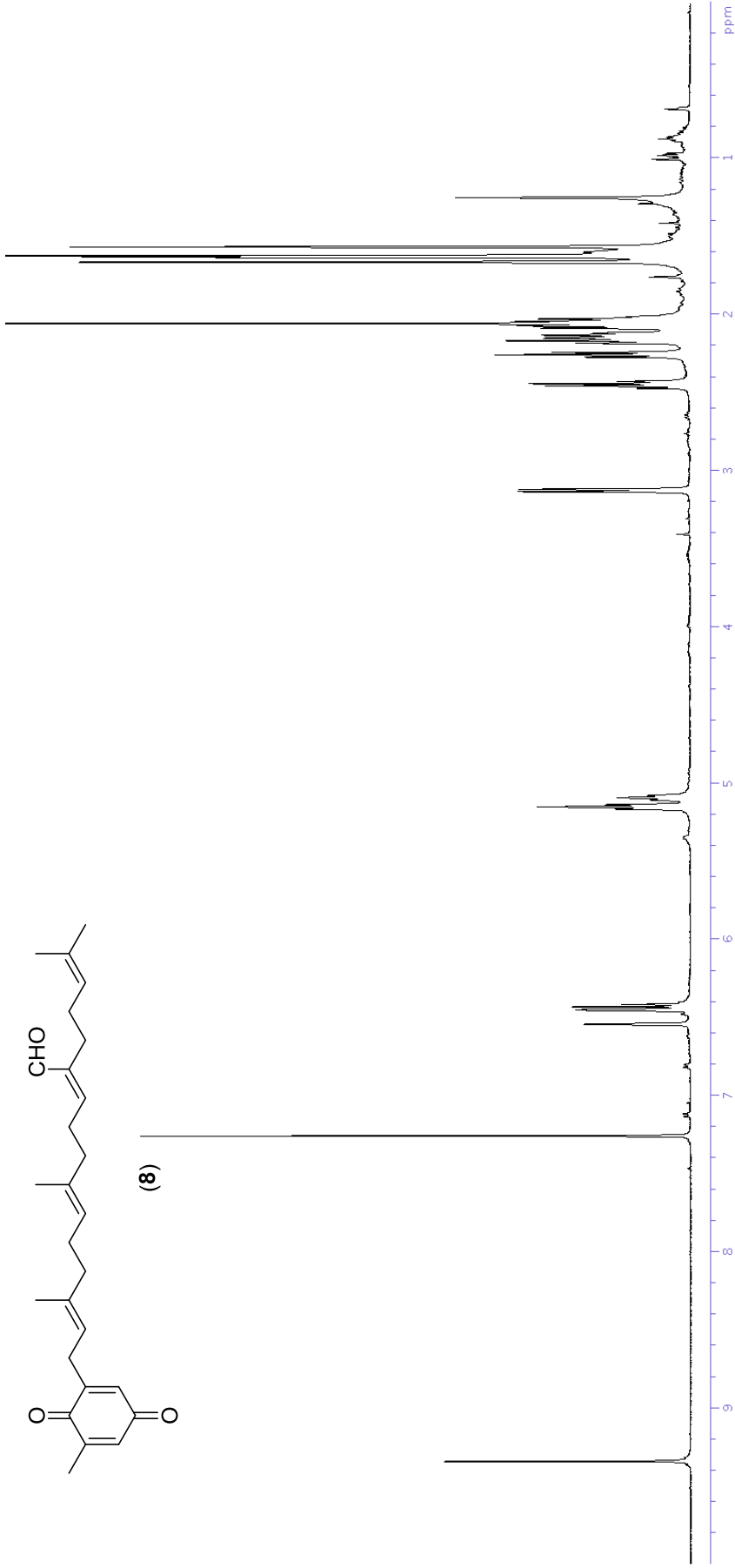


Figure S48. ¹H NMR spectrum (500 MHz, CDCl₃) of sargaquinal (8).

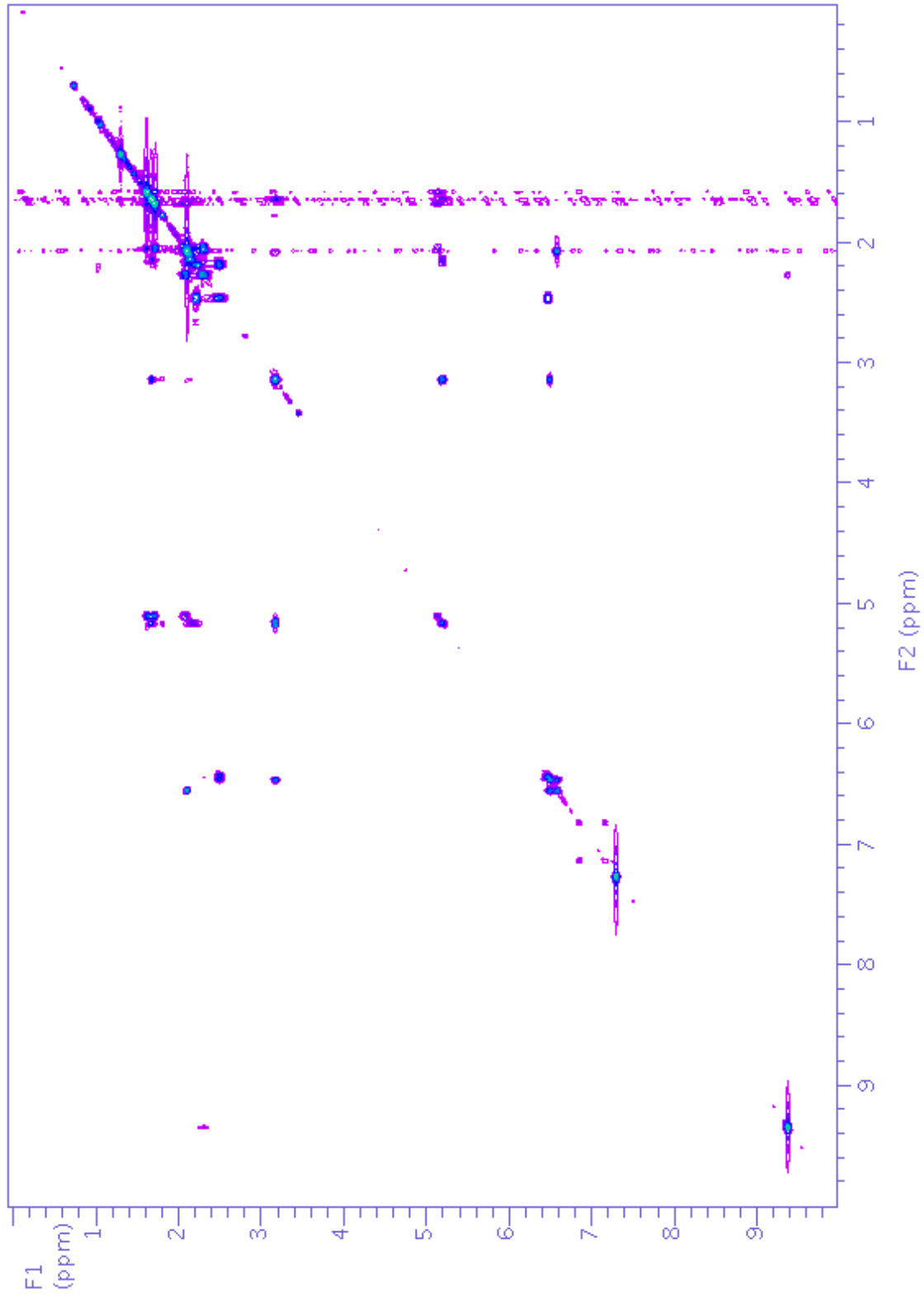


Figure S49. gCOSY NMR spectrum (500 MHz, CDCl₃) of sargaquinal (**8**).

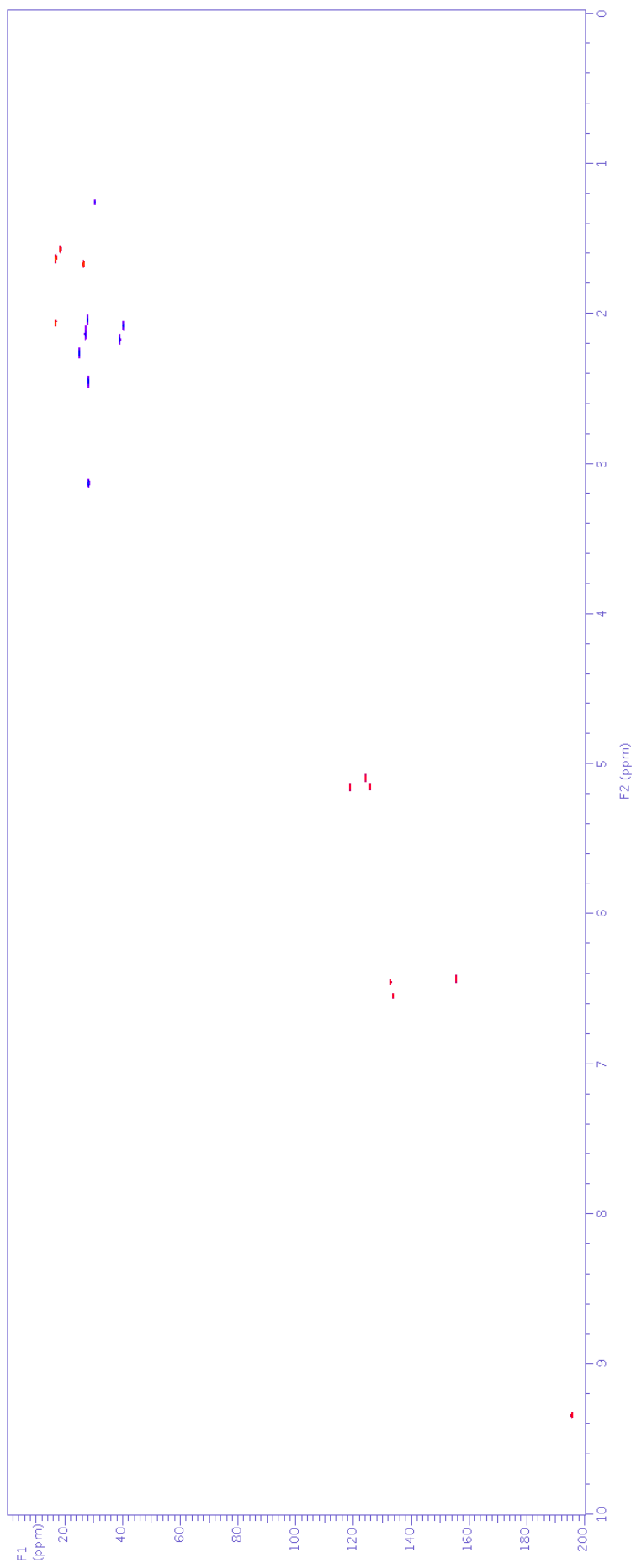


Figure S50. gHSQCAD NMR spectrum (500 MHz, CDCl₃) of sargaquinal (8).

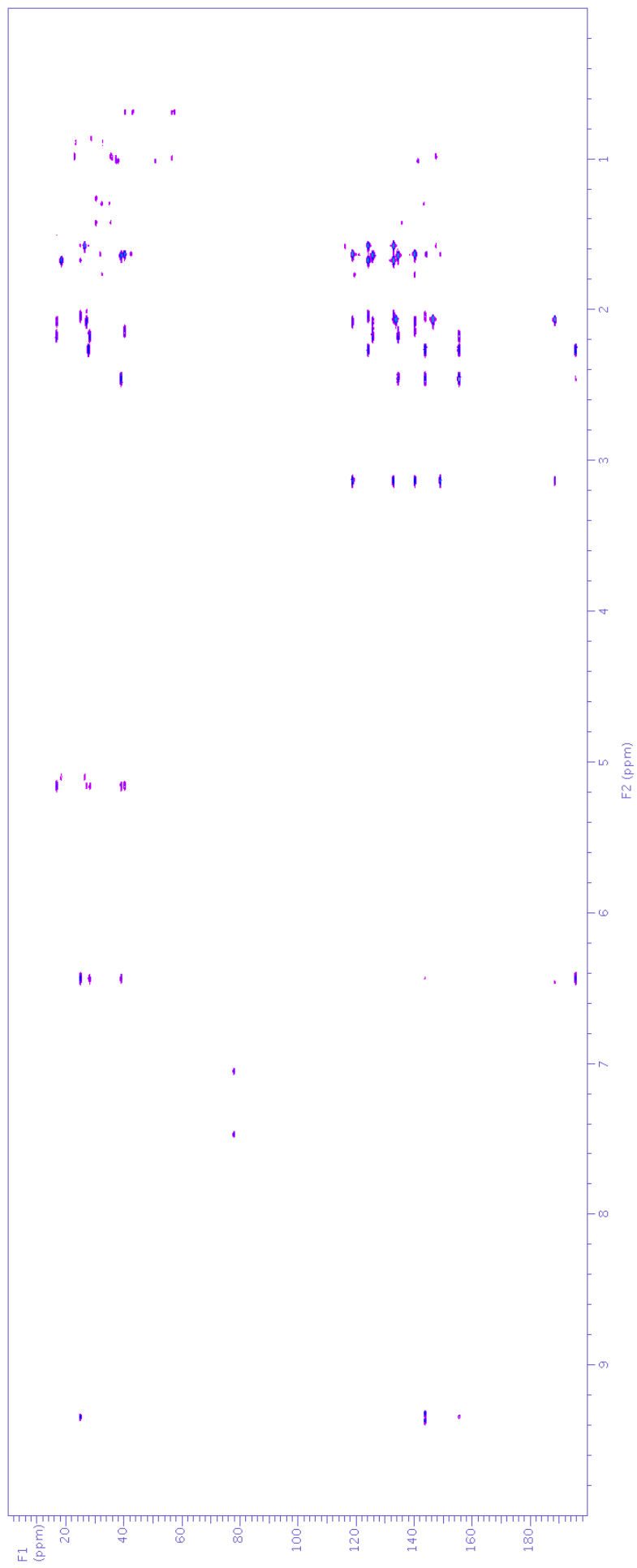


Figure S51. gHMBCAD NMR spectrum (500 MHz, CDCl₃) of sargaquinal (**8**).

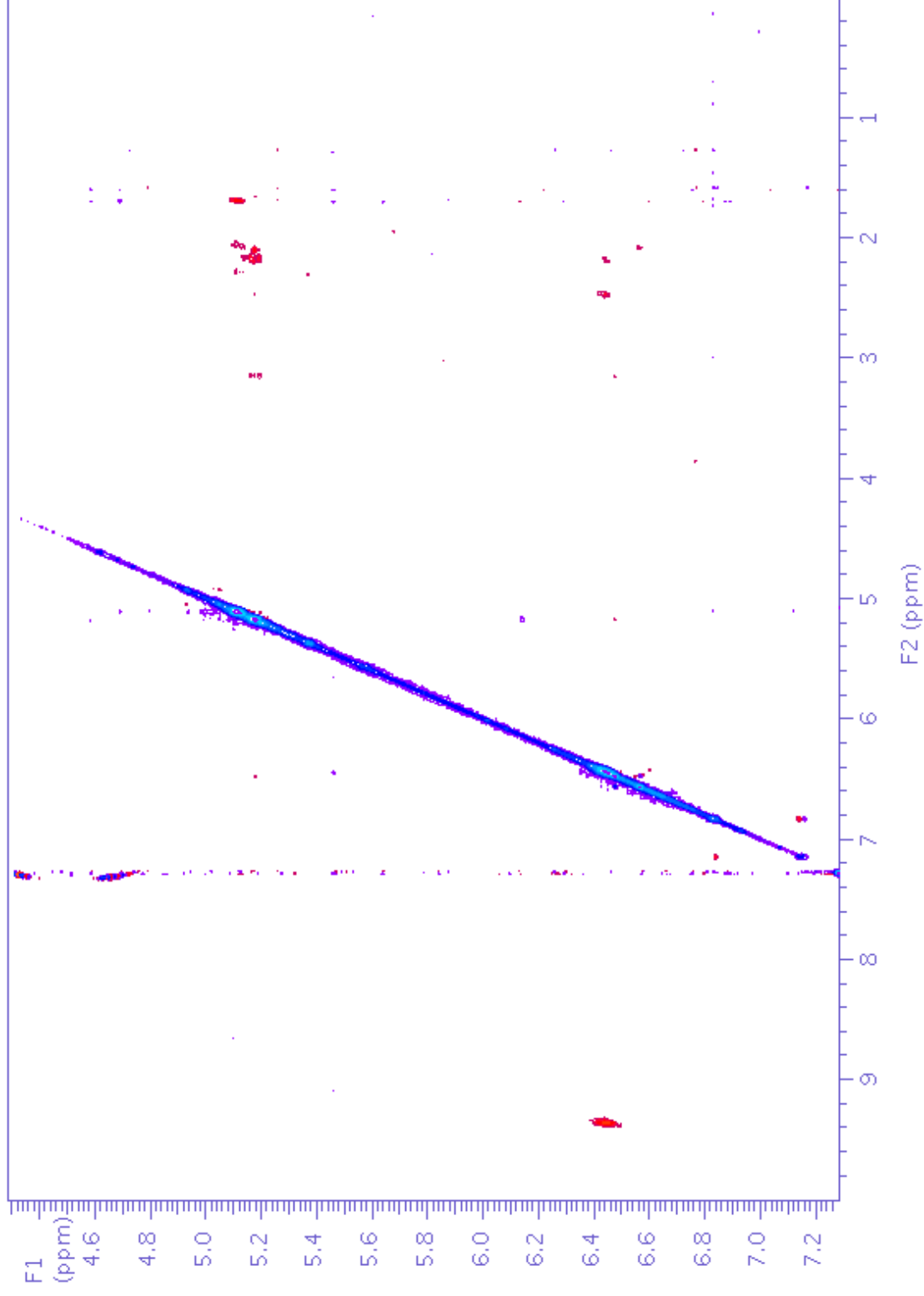


Figure S52. Band selective NOESY NMR spectrum (500 MHz, CDCl_3) of sargaquinal (**8**) showing the irradiation between δ_{H} 4.15-6.40.

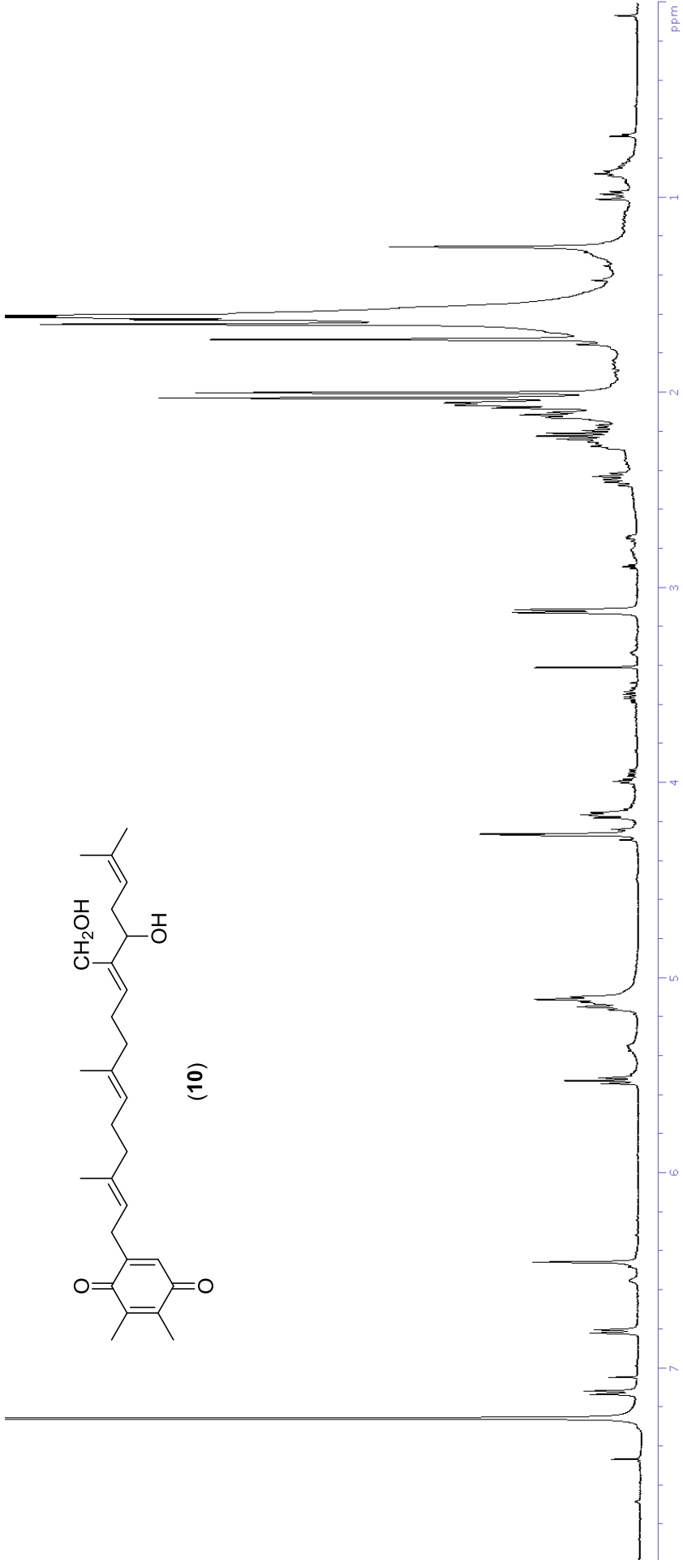


Figure S53. ^1H NMR spectrum (500 MHz, CDCl_3) of paradoxoquinone (**10**).

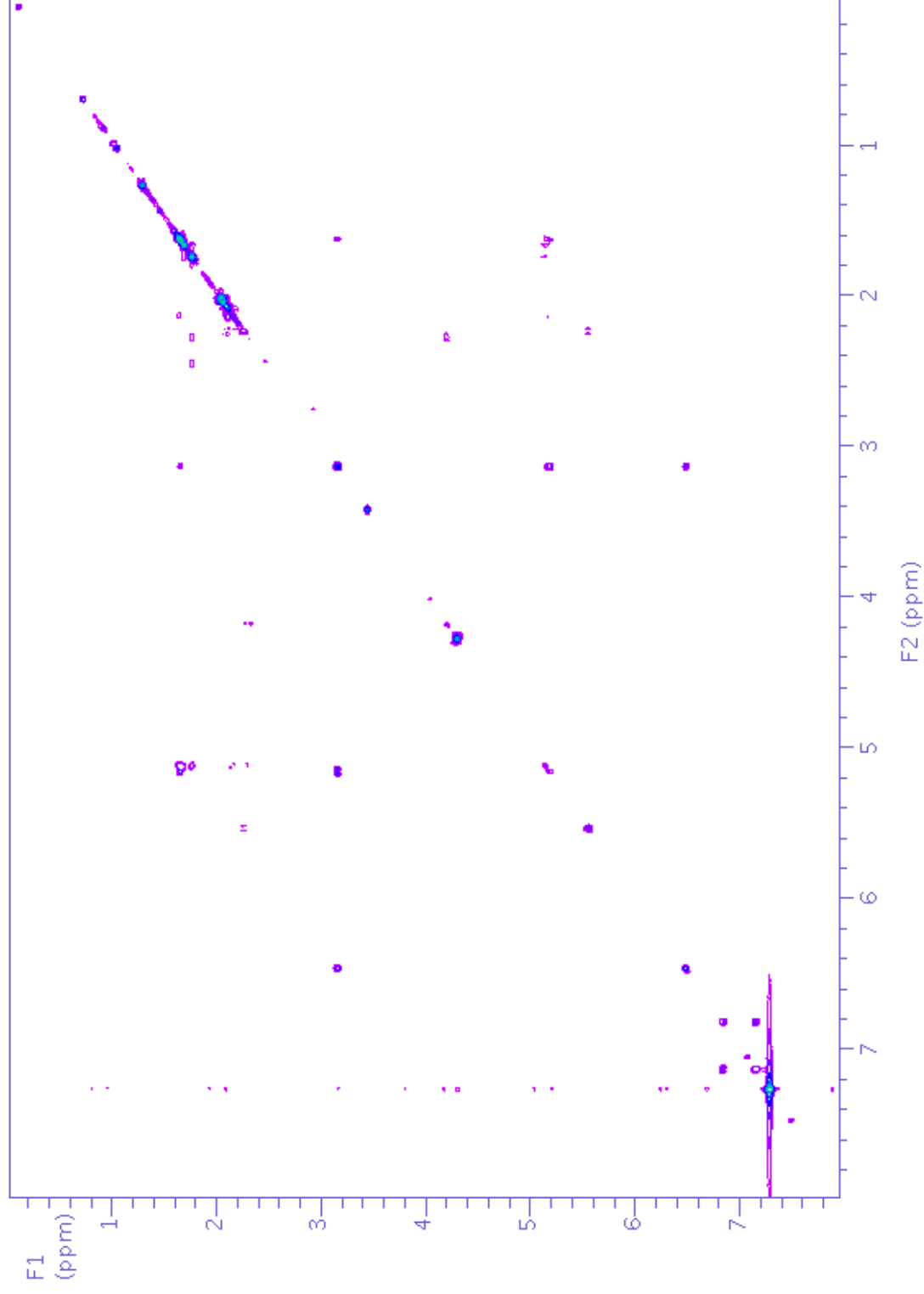


Figure S54. gCOSY NMR spectrum (500 MHz, CDCl₃) of parodoxquinone (**10**).

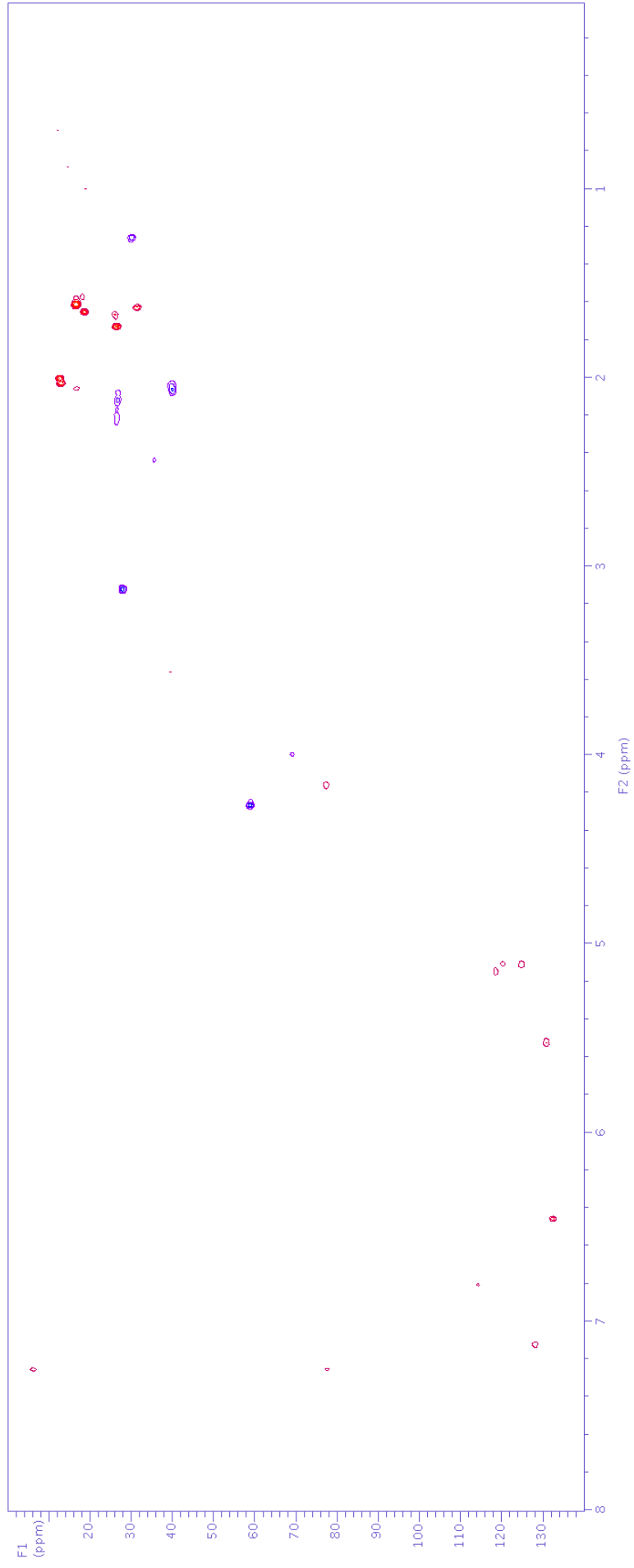


Figure S55. gHSQCAD NMR spectrum (500 MHz, CDCl₃) of parodoxquinone (**10**).

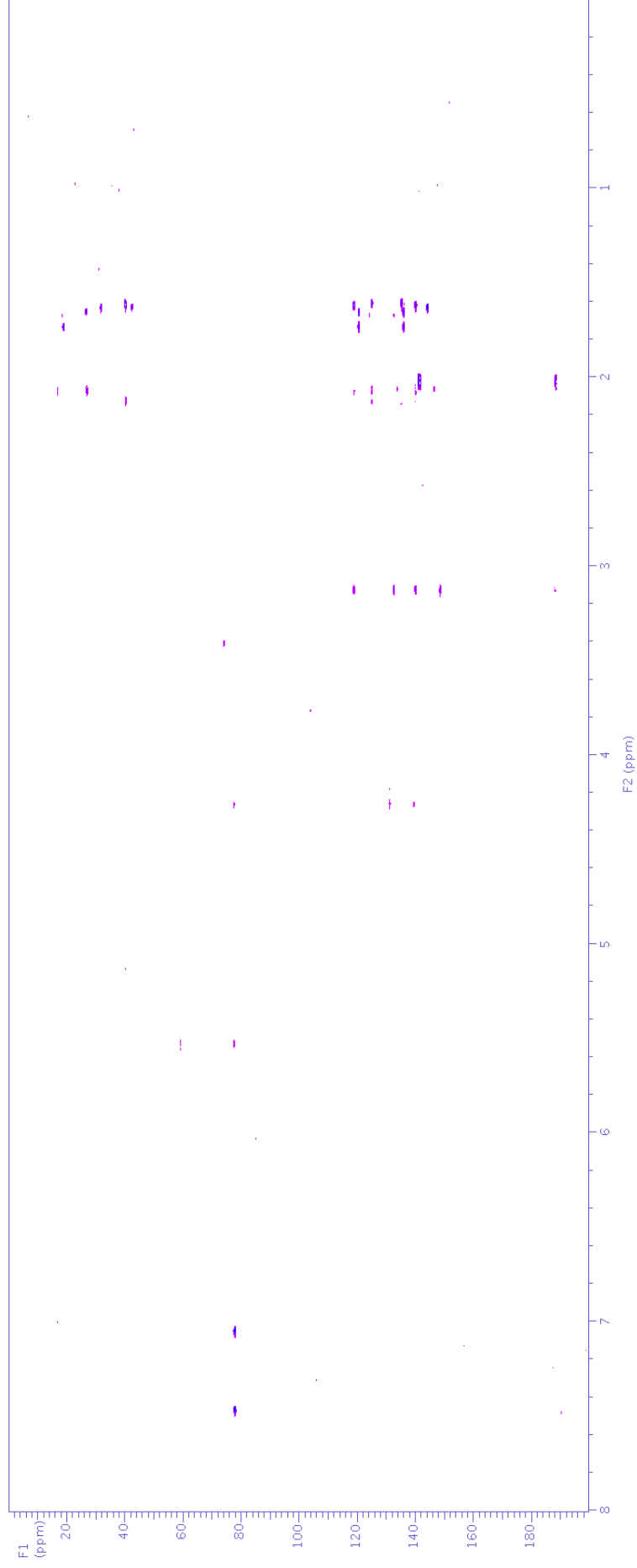


Figure S56. gHMBCAD NMR spectrum (500 MHz, CDCl_3) of parodoxquinone (**10**).

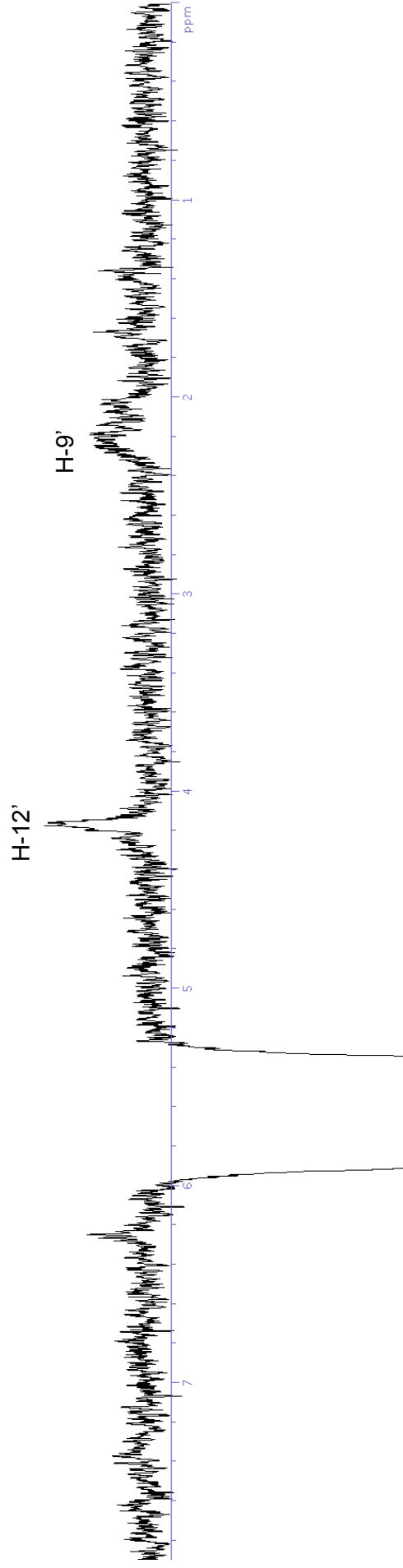
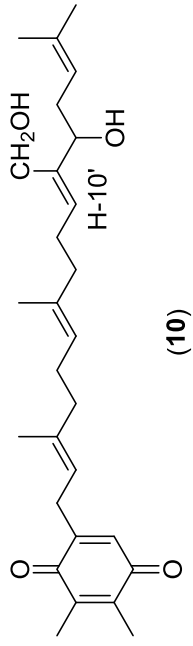


Figure S57. Single irradiation nOe NMR spectrum (500 MHz, CDCl_3) of parodoxquinone (**10**) showing the irradiation of δ_{H} 5.53 (H-10').

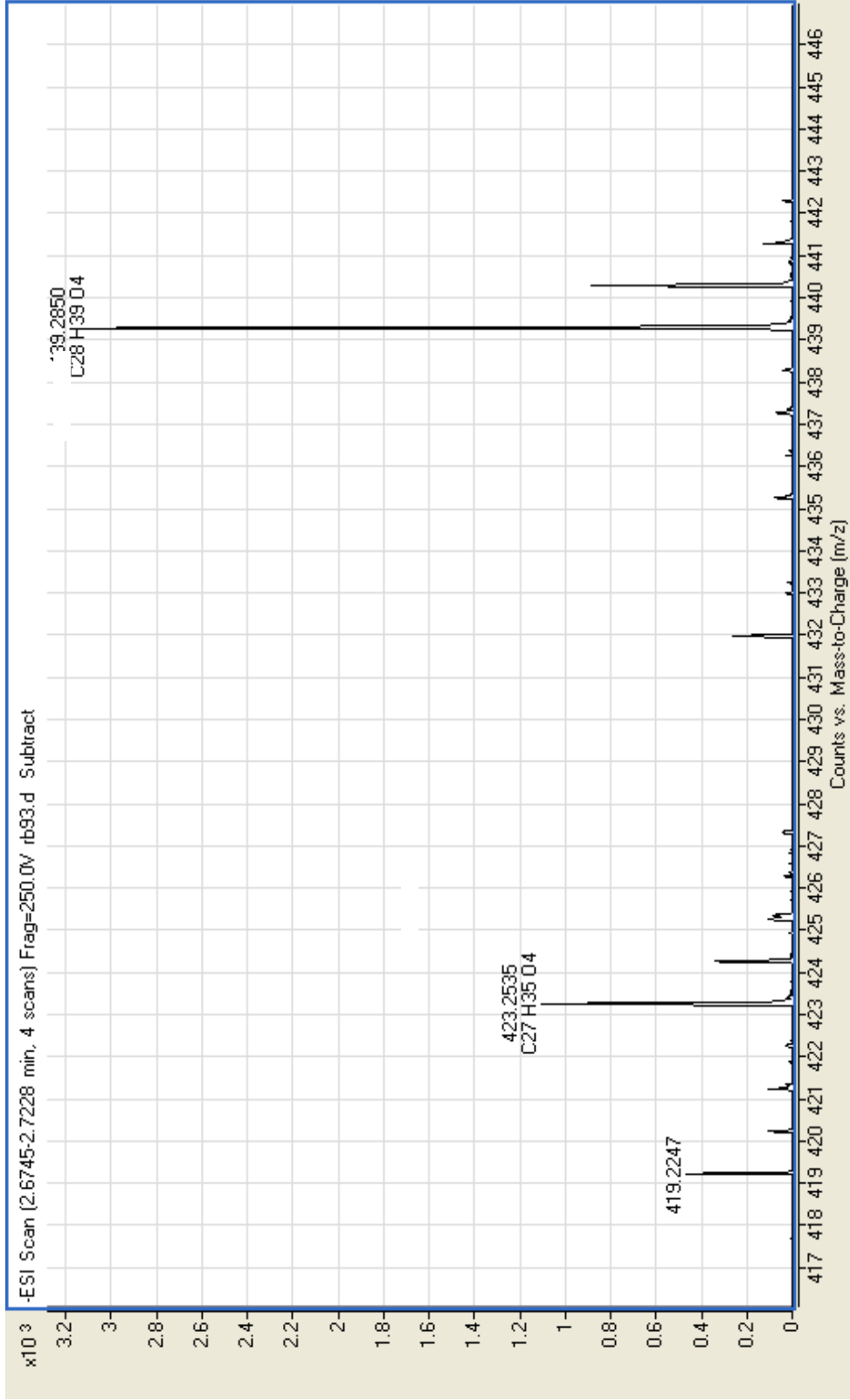


Figure S58. High resolution negative ESI-MS of paradoxquinone (**10**).

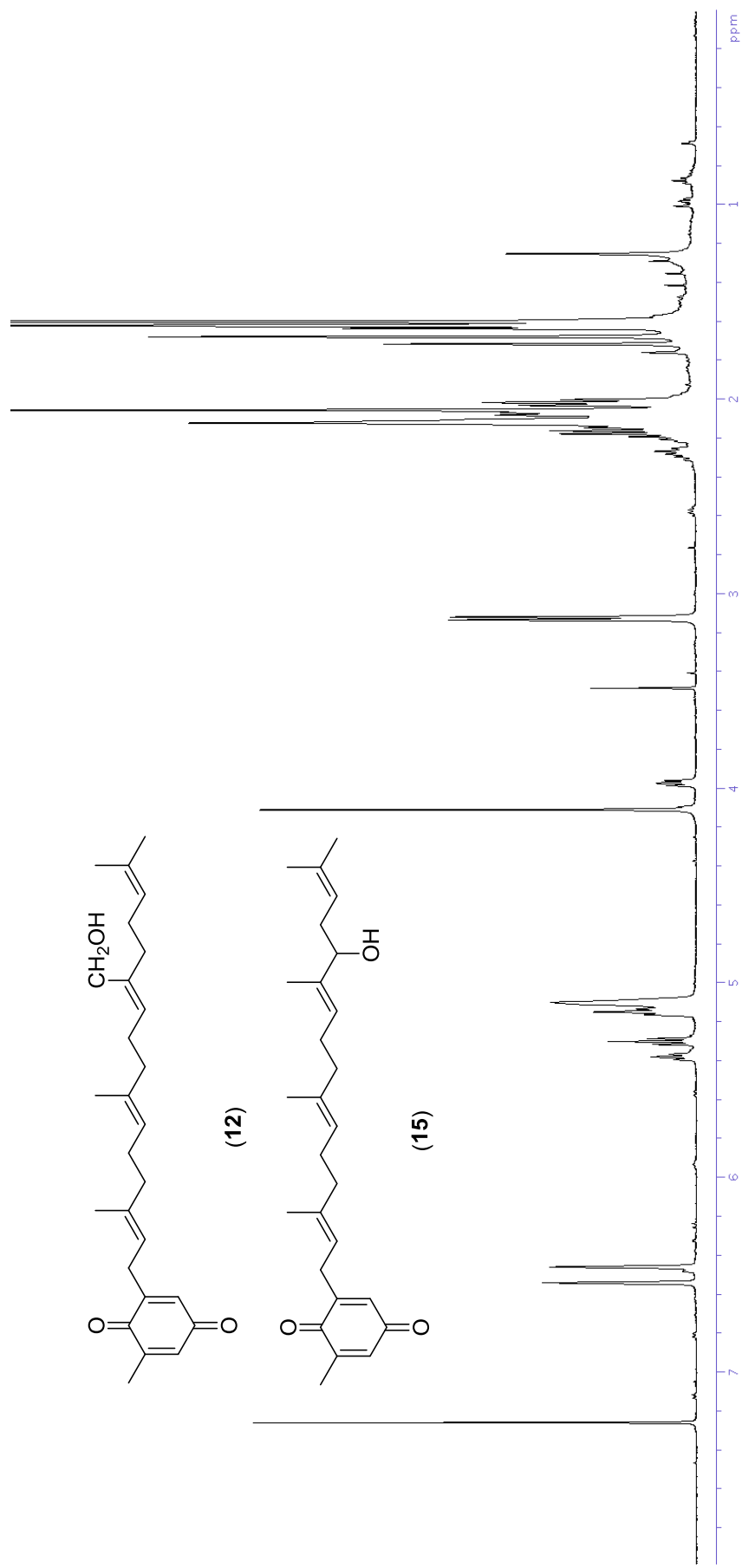


Figure S59. ¹H NMR spectrum (500 MHz, CDCl₃) of (2-[11-(hydroxymethyl)-3,7,15-trimethyl]-2,6,10,14-hexadecatetraen-1-yl]-6-methyl-1,4-benzoquinone (12) and paradoxquinone (15) mixture.

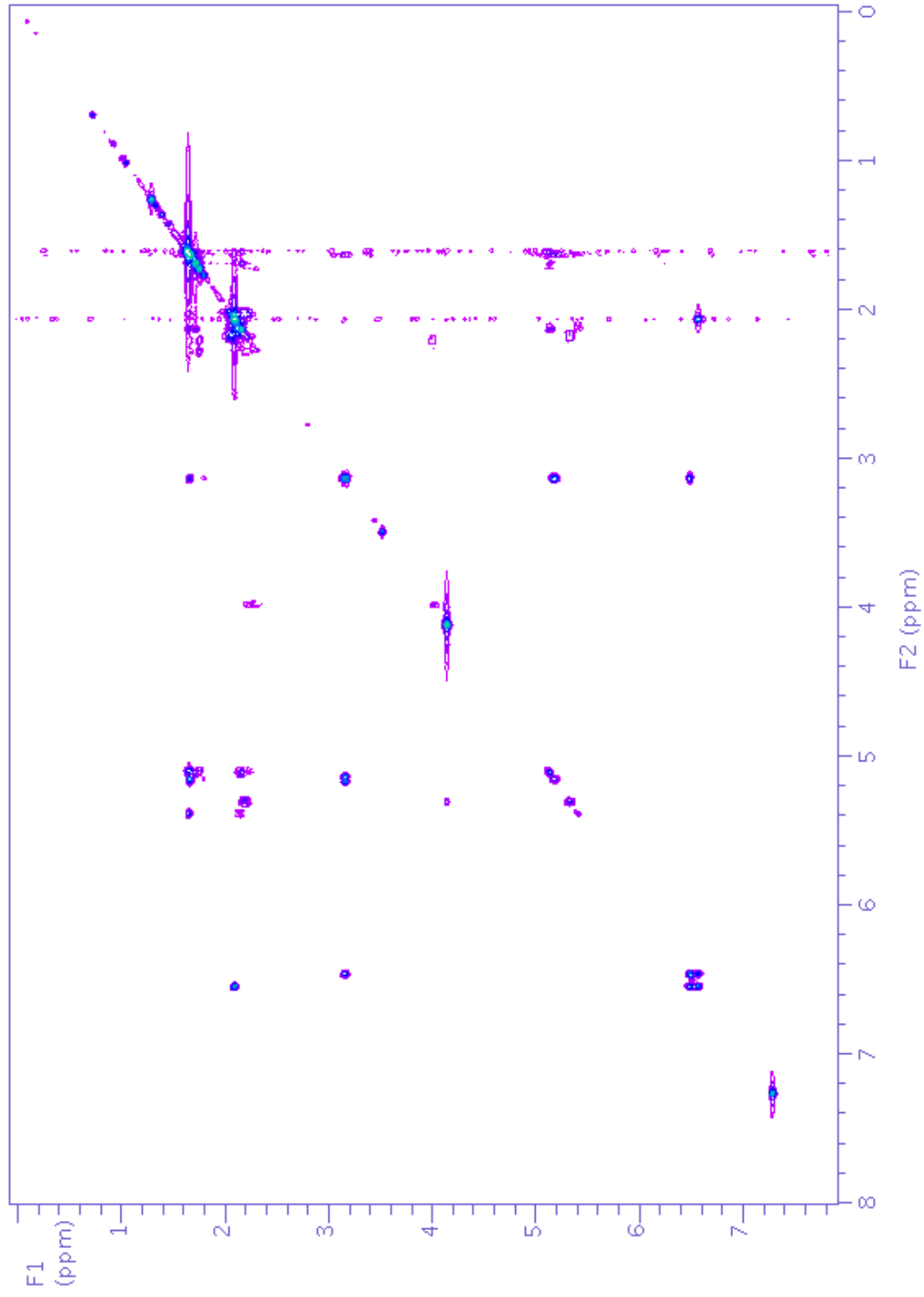


Figure S60. gCOSY NMR spectrum (500 MHz, CDCl₃) of (2-[11-(hydroxymethyl)-3,7,15-trimethyl-2,6,10,14-hexadecatetraen-1-yl]-6-methyl-1,4-benzoquinone (**12**) and paradoxquinone (**15**) mixture.

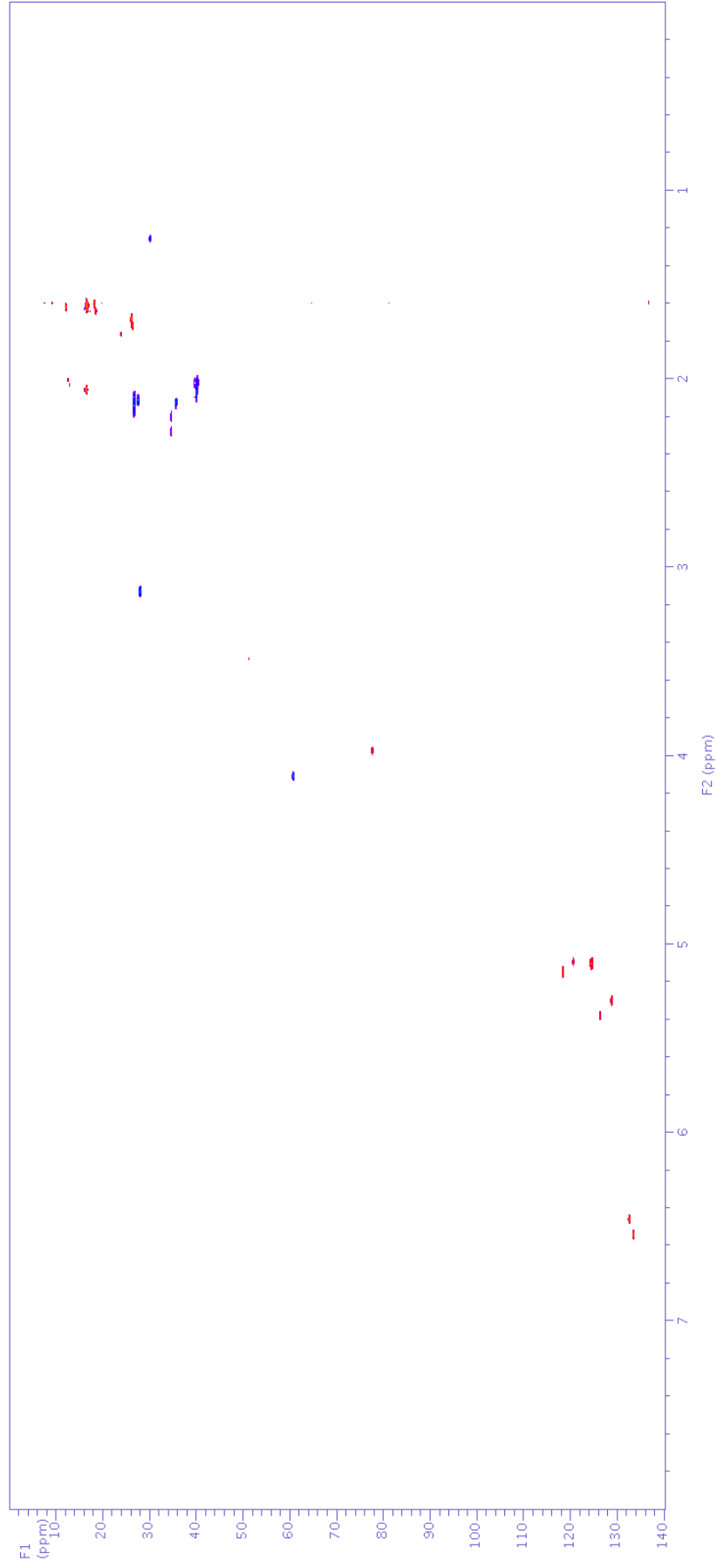


Figure S61. gHSQCAD NMR spectrum (500 MHz, CDCl₃) of (2-[11-(hydroxymethyl)-3,7,15-trimethyl-2,6,10,14-hexadecatetraen-1-yl]-6-methyl-1,4-benzoquinone (**12**) and paradoxquinone (**15**) mixture.

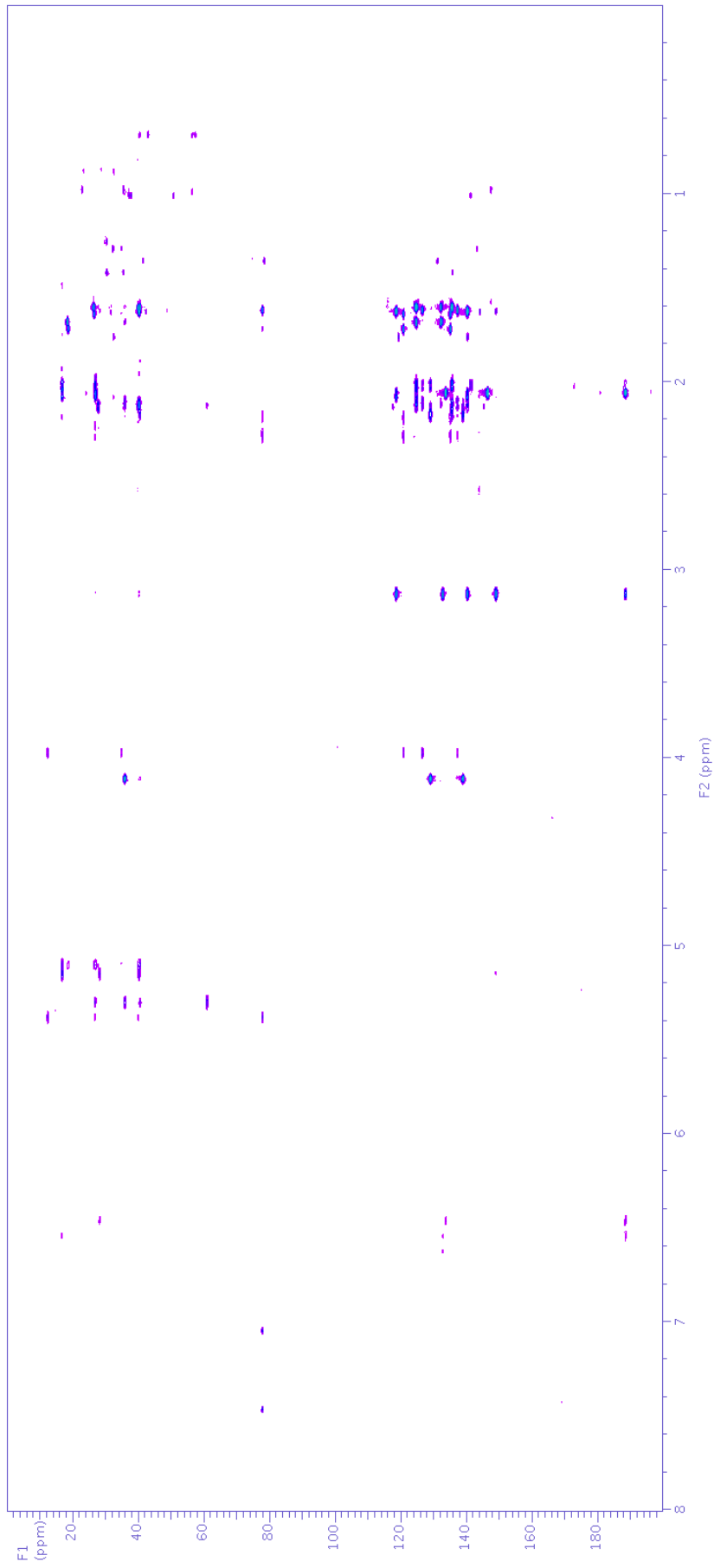


Figure S62. gHMBCAD NMR spectrum (500 MHz, CDCl₃) of (2-[11-(hydroxymethyl)-3,7,15-trimethyl]-2,6,10,14-hexadecatetraen-1-yl]-6-methyl-1,4-benzoquinone (**12**) and paradoxquinone (**15**) mixture.

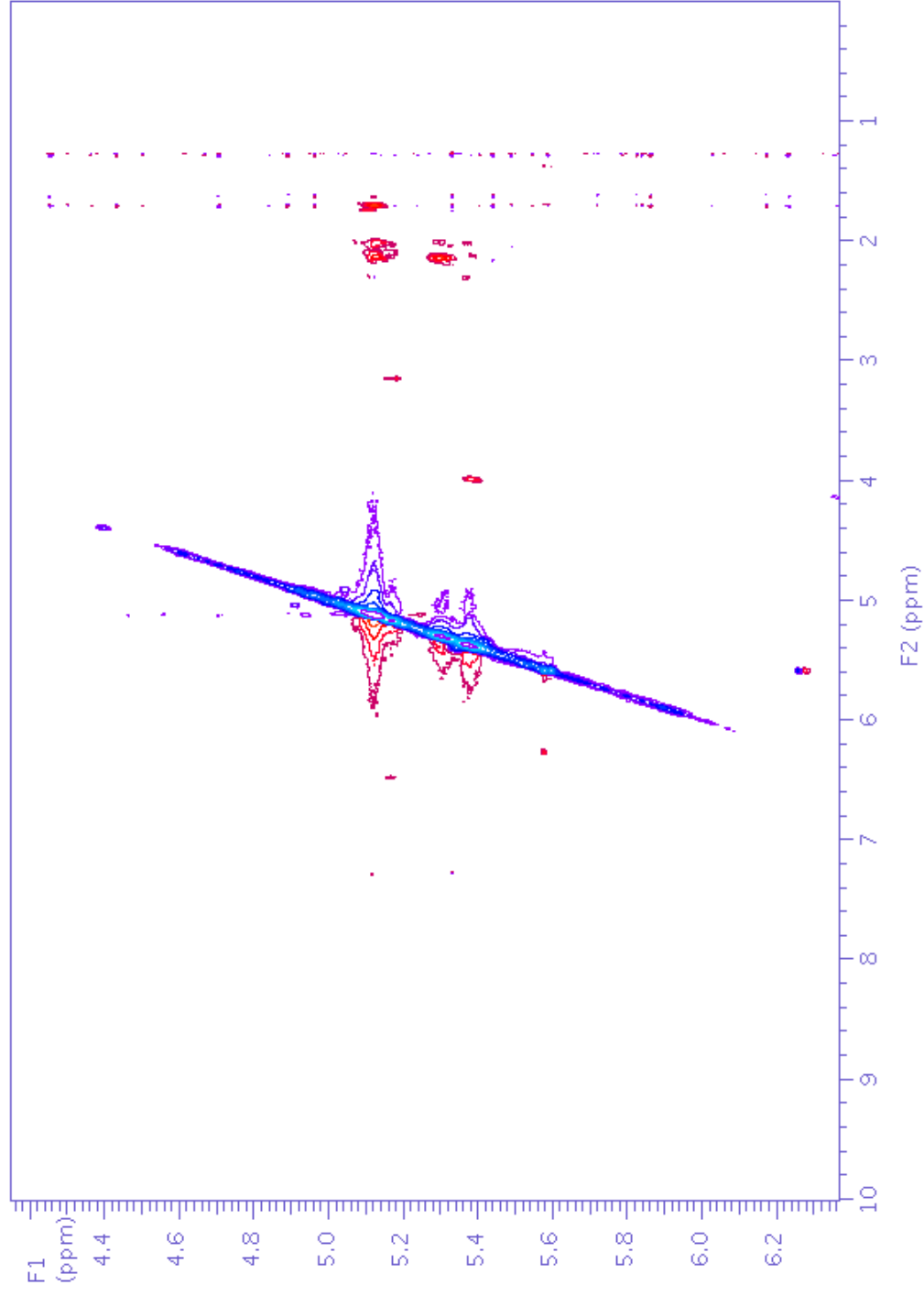


Figure S63. Band selective NOESY NMR spectrum (500 MHz, CDCl₃) of (2-[11-(hydroxymethyl)-3,7,15-trimethyl-2,6,10,14-hexadecatetraen-1-yl]-6-methyl-1,4-benzoquinone (**12**) and paradoxquinone (**15**) mixture showing the irradiation between δ_{H} 4.30–7.30.

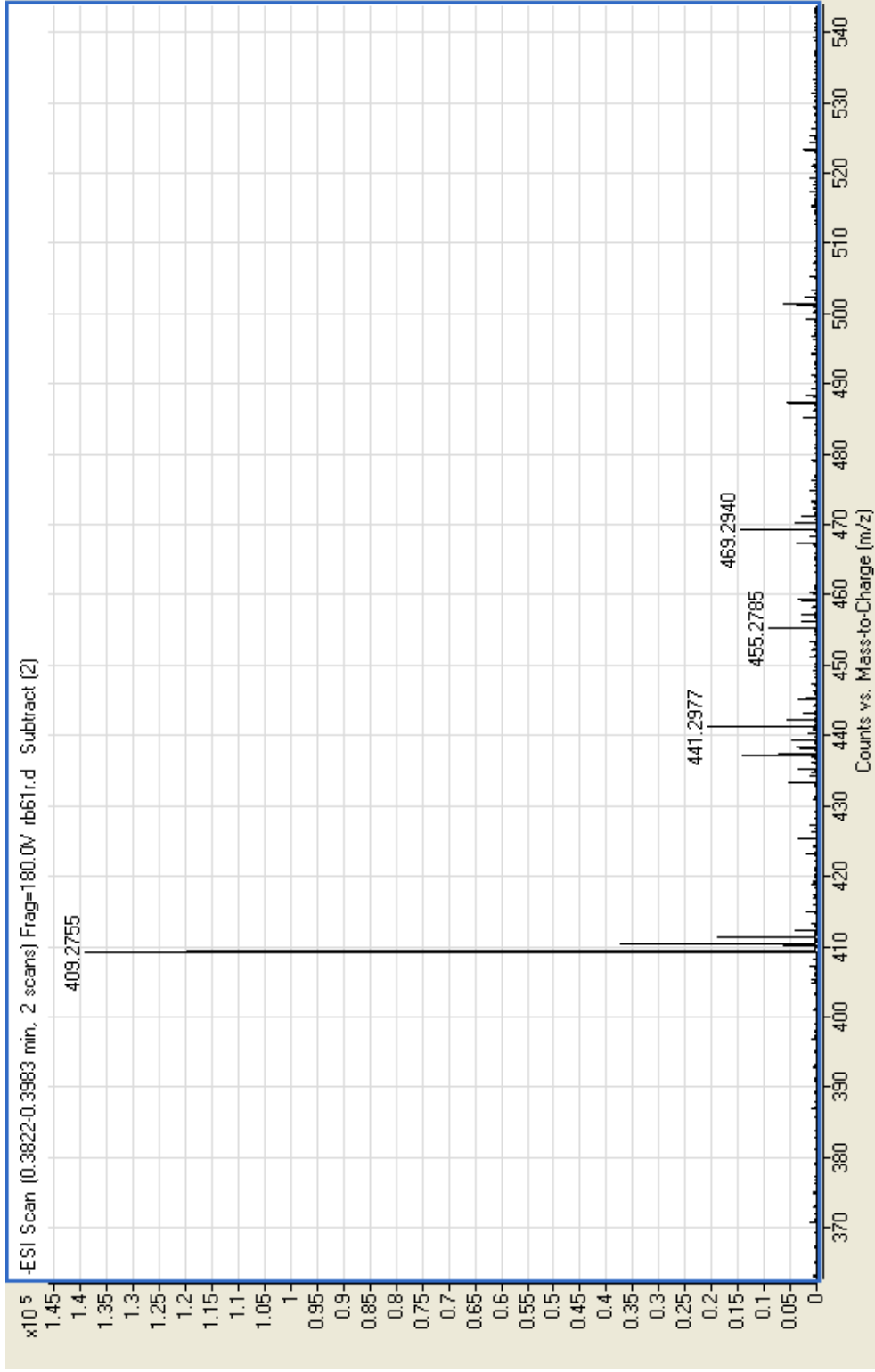
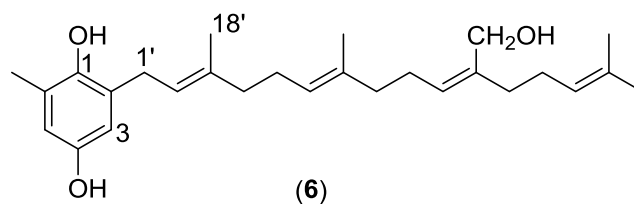


Figure S64. High resolution negative ESI-MS of (2-[11-(hydroxymethyl)-3,7,15-trimethyl-2,6,10,14-hexadecatetraen-1-yl]-6-methyl-1,4-benzoquinone (**12**) and paradoxquinone (**15**) mixture.

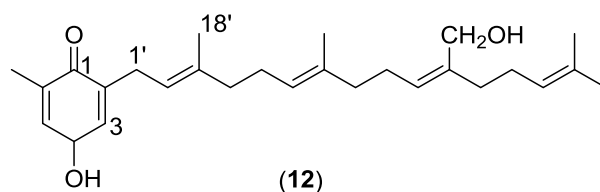
Table S1. NMR data (500 MHz, CDCl₃) of 2-[11-(hydroxymethyl)-3,7,15-trimethyl-2,6,10,14-hexadecatetraen-1-yl]-6-methyl-1,4-benzenediol (**6**).



Position	δ_C^a , mult	δ_H (J in Hz)	gCOSY	gHMBC
1	146.4, s			
2	127.6, s			
3	114.0, d	6.46, d (2.5)	5, 1'	1, 4, 5, 1'
4	149.0, s			
5	115.5, d	6.50, d (2.5)	3, 7	1, 3, 4, 7
6	125.5, s			
7	16.1, q	2.18, s	5	1, 5, 6
1'	30.0, t	3.28, d (7.0)	3, 2', 4' ^w , 18' ^w	1, 2, 3, 2', 3'
2'	122.0, d	5.26, t (7.0)	1', 4', 18'	1', 4', 18'
3'	138.1, s			
4'	39.5, t	2.08, m	1' ^w	5', 18'
5'	26.1, t	2.13, m		4', 7'
6'	124.4, d	5.09, m		4', 5', 19'
7'	135.1, s			
8'	39.8, t	2.00, m	9'	7', 9', 10', 19'
9'	26.1, t	2.13, m	8'	7', 10'
10'	128.9, d	5.30, t (7.5)	9', 20'	8', 9', 12', 20'
11'	138.2, s			
12'	35.2, t	2.12, m		11', 13', 14'
13'	27.1, t	2.11, m		11', 12', 14', 15'
14'	124.4, d	5.09, m	13', 16', 17'	
15'	131.8, s			
16'	17.7, q	1.60, s	13'	14', 15', 17'
17'	25.7, q	1.68, s	13', 14'	14', 15', 16'
18'	16.2, q	1.75, s	1', 2'	2', 3', 4'
19'	16.1, q	1.59, s	5', 6'	7', 8'
20'	60.4, t	4.11, s	10'	10', 11', 12'
1-OH		ND ^b		
4-OH		ND ^b		
20'-OH		ND ^b		

^a Carbon assignments made on the basis of gHSQCAD and gHMBCAD experiments. ^b indicates signal not detected. ^w Indicates weak or long range correlation.

Table S2. NMR data (500 MHz, CDCl₃) of 2-[11-(hydroxymethyl)-3,7,15-trimethyl-2,6,10,14-hexadecatetraen-1-yl]-6-methyl-1,4-benzoquinone (**12**).



Position	δ_C^a , mult	δ_H (J in Hz)	gCOSY	gHMBCAD	bsNOESY
1	188.0, s				
2	148.5, s				
3	132.3, d	6.46, bs	5, 1'	1, 4, 5	
4	188.0, s				
5	133.2, d	6.54, bs	3, 7	1, 3, 4	
6	145.9, s				
7	16.0, q	2.05, s	5	1, 5, 6	
1'	27.5, t	3.13, d (7.5)	3, 2', 18'	1, 2, 3, 2', 3'	
2'	118.1, d	5.15, t (7.5)	1', 18'	1', 4', 18'	5, 1', 4'
3'	139.8, s				
4'	39.6, t	2.07, m		2', 3', 5', 18'	
5'	26.2, t	2.11, m	6', 18' ^w , 19' ^w	3', 4', 6'	
6'	124.2, d	5.10, m	5'	4', 5', 19'	5', 8'
7'	135.1, s				
8'	39.8, t	2.01, m		6', 10'	
9'	26.2, t	2.16, m	10'	8', 10', 11'	
10'	128.5, d	5.30, t (7.0)	9', 20'	8', 9', 12', 20'	12'
11'	138.4, s				
12'	35.2, t	2.12, m		11', 13', 14', 15'	
13'	27.1, t	2.12, m	14', 17' ^w	11', 12', 14', 15'	
14'	124.2, d	5.10, m	13', 16'		17'
15'	131.7, s				
16'	17.7, q	1.60, s		14', 15'	
17'	25.7, q	1.68, s	13' ^w	14', 15', 16'	
18'	16.1, q	1.61, s		2', 3'	
19'	16.1, q	1.61, s			
20'	60.3, t	4.11, s		10', 11', 12'	
20'-OH		ND ^b			

^a Carbon assignments made on the basis of gHSQCAD and gHMBCAD experiments. ^b indicates signal not detected. ^c bs stands for band selective (Selective NOESY experiment). ^w Indicates weak or long range correlation.

APPENDIX F

Supplementary Information for the dereplication and structural identification studies of marine algae of the genus Cystophora

This appendix contains further information relevant to the dereplication (HPLC-NMR & HPLC-MS) and structural identification studies conducted of marine algae of the *Cystophora* genus as described in Chapter 10.

HPLC-NMR and HPLC-MS investigation of antimicrobial constituents in *Cystophora monilifera* and *Cystophora subfarcinata*

Robert Brkljača[†] and Sylvia Urban^{†*}

[†]School of Applied Sciences (Discipline of Chemistry), Health Innovations Research Institute (HIRi) RMIT University, GPO Box 2476V Melbourne, Victoria 3001, Australia).

Supporting Information Available

- S1.** Extracted UV profile (70% CH₃CN/D₂O) of **1** from HPLC-NMR.
- S2.** Stop-flow WET1D Proton NMR spectrum (70% CH₃CN/D₂O) of **1**.
- S3.** gCOSY NMR spectrum (70% CH₃CN/D₂O) (from stop-flow HPLC-NMR) of **1**.
- S4.** gHSQCAD NMR spectrum (70% CH₃CN/D₂O) (from stop-flow HPLC-NMR) of **1**.
- S5.** gHMBC NMR spectrum (70% CH₃CN/D₂O) (from stop-flow HPLC-NMR) of **1**.
- S6.** High resolution negative ESI-MS of **1** from HPLC-MS.
- S7.** Extracted UV profile (70% CH₃CN/D₂O) of **2** from HPLC-NMR.
- S8.** Stop-flow WET1D Proton NMR spectrum (70% CH₃CN/D₂O) of **2**.
- S9.** gCOSY NMR spectrum (70% CH₃CN/D₂O) (from stop-flow HPLC-NMR) of **2**.
- S10.** High resolution negative ESI-MS of **2** from HPLC-MS.
- S11.** Extracted UV profile (70% CH₃CN/D₂O) of **3** from HPLC-NMR.
- S12.** Stop-flow WET1D Proton NMR spectrum (70% CH₃CN/D₂O) of **3**.
- S13.** gCOSY NMR spectrum (70% CH₃CN/D₂O) (from stop-flow HPLC-NMR) of **3**.
- S14.** High resolution negative ESI-MS of **3** from HPLC-MS.

- S15.** Extracted UV profile (75% CH₃CN/D₂O) of **4** from HPLC-NMR.
- S16.** Stop-flow WET1D Proton NMR spectrum (75% CH₃CN/D₂O) of **4**.
- S17.** gCOSY NMR spectrum (75% CH₃CN/D₂O) (from stop-flow HPLC-NMR) of **4**.
- S18.** HSQCAD NMR spectrum (75% CH₃CN/D₂O) (from stop-flow HPLC-NMR) of **4**.
- S19.** gHMBCAD NMR spectrum (75% CH₃CN/D₂O) (from stop-flow HPLC-NMR) of **4**.
- S20.** High resolution negative ESI-MS of **4** from HPLC-MS.
- S21.** Extracted UV profile (70% CH₃CN/D₂O) of **5** from HPLC-NMR.
- S22.** Stop-flow WET1D Proton NMR spectrum (70% CH₃CN/D₂O) of **5**.
- S23.** gCOSY NMR spectrum (70% CH₃CN/D₂O) (from stop-flow HPLC-NMR) of **5**.
- S24.** High resolution negative ESI-MS of **5** from HPLC-MS.
- S25.** Extracted UV profile (75% CH₃CN/D₂O) of **6** from HPLC-NMR.
- S26.** Stop-flow WET1D Proton NMR spectrum (75% CH₃CN/D₂O) of **6**.
- S27.** gCOSY NMR spectrum (75% CH₃CN/D₂O) (from stop-flow HPLC-NMR) of **6**.
- S28.** High resolution negative ESI-MS of **6** from HPLC-MS.
- S29.** Extracted UV profile (75% CH₃CN/D₂O) of **7** from HPLC-NMR.
- S30.** Stop-flow WET1D Proton NMR spectrum (75% CH₃CN/D₂O) of **7**.
- S31.** gCOSY NMR spectrum (75% CH₃CN/D₂O) (from stop-flow HPLC-NMR) of **7**.
- S32.** Extracted UV profile (75% CH₃CN/D₂O) of **8** from HPLC-NMR.
- S33.** Stop-flow WET1D Proton NMR spectrum (75% CH₃CN/D₂O) of moniliferanone A (**8**).
- S34.** gCOSY NMR spectrum (75% CH₃CN/D₂O) (from stop-flow HPLC-NMR) of moniliferanone A (**8**).
- S35.** 1D TOCSY NMR spectrum (75% CH₃CN/D₂O) (from stop-flow HPLC-NMR) of moniliferanone A (**8**).
- S36.** HSQCAD NMR spectrum (75% CH₃CN/D₂O) (from stop-flow HPLC-NMR) of moniliferanone A (**8**).

- S37.** Expanded stop-flow WET1D Proton NMR spectrum (70% CH₃CN/D₂O) of moniliferanone A (**8**) and moniliferanone C (**11**) showing relative intensities from *C. monilifera*.
- S38.** Expanded stop-flow WET1D Proton NMR spectrum (70% CH₃CN/D₂O) of moniliferanone A (**8**) and moniliferanone C (**11**) showing relative intensities from *C. subfarcinata*.
- S39.** High resolution negative ESI-MS of moniliferanone A (**8**) from HPLC-MS.
- S40.** Extracted UV profile (75% CH₃CN/D₂O) of **9** from HPLC-NMR.
- S41.** Stop-flow WET1D Proton NMR spectrum (75% CH₃CN/D₂O) of moniliferanone B (**9**).
- S42.** gCOSY NMR spectrum (75% CH₃CN/D₂O) (from stop-flow HPLC-NMR) of moniliferanone B (**9**).
- S43.** High resolution negative ESI-MS of moniliferanone B (**9**) from HPLC-MS.
- S44.** ¹H NMR spectrum (500 MHz, CDCl₃) of moniliferanone A (**8**) and C (**11**) mixture.
- S45.** ¹³C NMR spectrum (125 MHz, CDCl₃) of moniliferanone A (**8**) and C (**11**) mixture.
- S46.** gCOSY NMR spectrum (500 MHz, CDCl₃) of moniliferanone A (**8**) and C (**11**) mixture.
- S47.** gHSQCAD NMR spectrum (500 MHz, CDCl₃) of moniliferanone A (**8**) and C (**11**) mixture.
- S48.** gHMBC NMR spectrum (500 MHz, CDCl₃) of moniliferanone A (**8**) and C (**11**) mixture.
- S49.** Expanded ¹H NMR spectrum (500 MHz, CDCl₃) of moniliferanone A (**8**) and moniliferanone C (**11**) showing relative intensities from *C. monilifera*.
- S50.** Expanded ¹H NMR spectrum (500 MHz, CDCl₃) of moniliferanone A (**8**) and moniliferanone C (**11**) showing relative intensities from *C. subfarcinata*.
- S51.** High resolution negative ESI-MS of moniliferanone A (**8**) and C (**11**) mixture.
- S52.** ¹H NMR spectrum (500 MHz, CDCl₃) of moniliferanone B (**9**).
- S53.** gCOSY NMR spectrum (500 MHz, CDCl₃) of moniliferanone B (**9**).
- S54.** gHSQCAD NMR spectrum (500 MHz, CDCl₃) of moniliferanone B (**9**).
- S55.** gHMBC NMR spectrum (500 MHz, CDCl₃) of moniliferanone B (**9**).
- S56.** High resolution negative ESI-MS of moniliferanone B (**9**).
- S57.** ¹H NMR spectrum (500 MHz, CDCl₃) of moniliferanone D (**12**).
- S58.** gCOSY NMR spectrum (500 MHz, CDCl₃) of moniliferanone D (**12**).

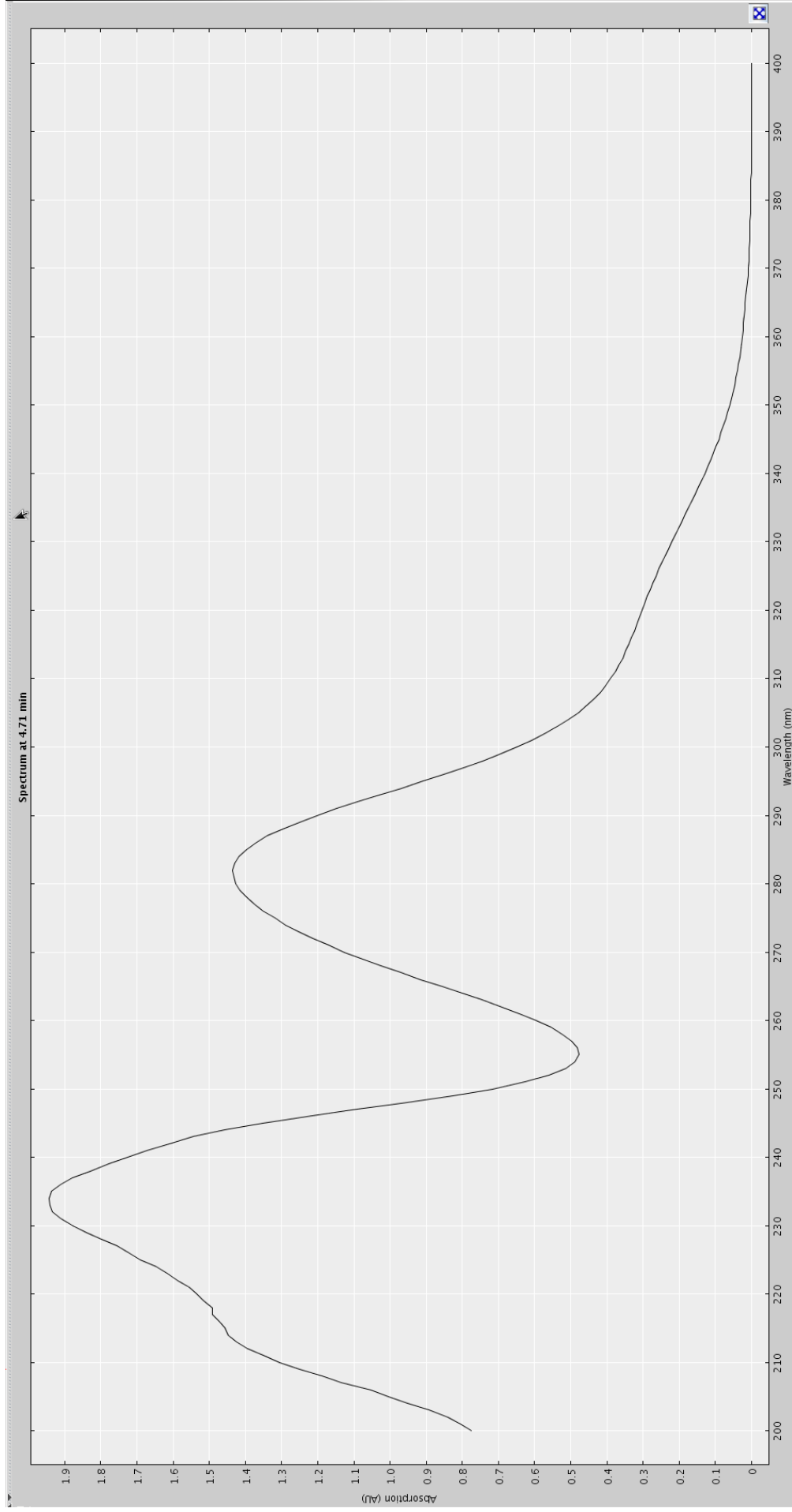
S59. gHSQCAD NMR spectrum (500 MHz, CDCl₃) of moniliferanone D (**12**).

S60. gHMBC NMR spectrum (500 MHz, CDCl₃) of moniliferanone D (**12**).

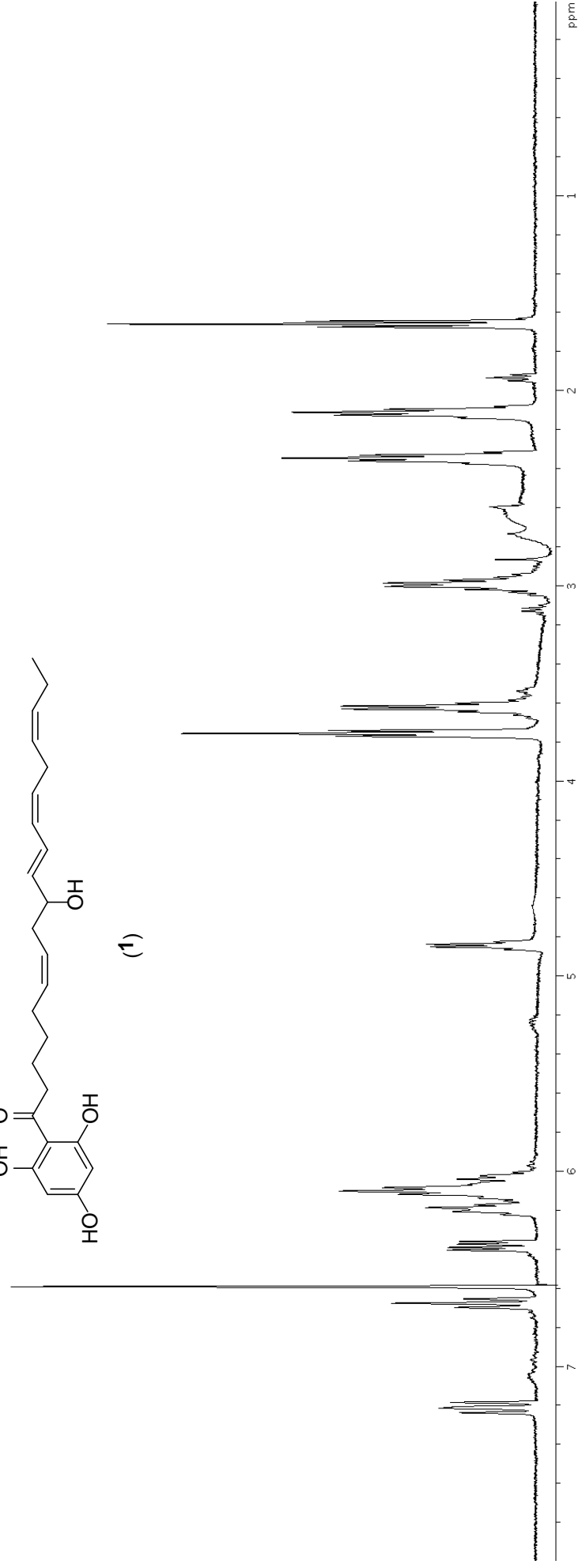
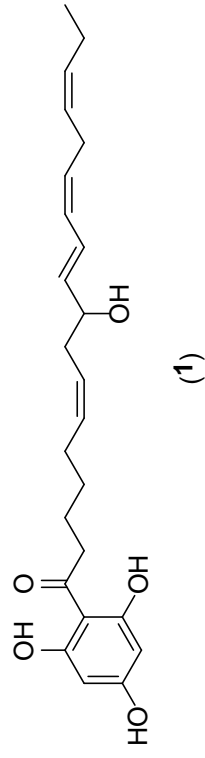
S61. High resolution negative ESI-MS of moniliferanone D (**12**).

*Corresponding author. Tel: +61 3 9925 3376; Fax: +61 3 9925 3747

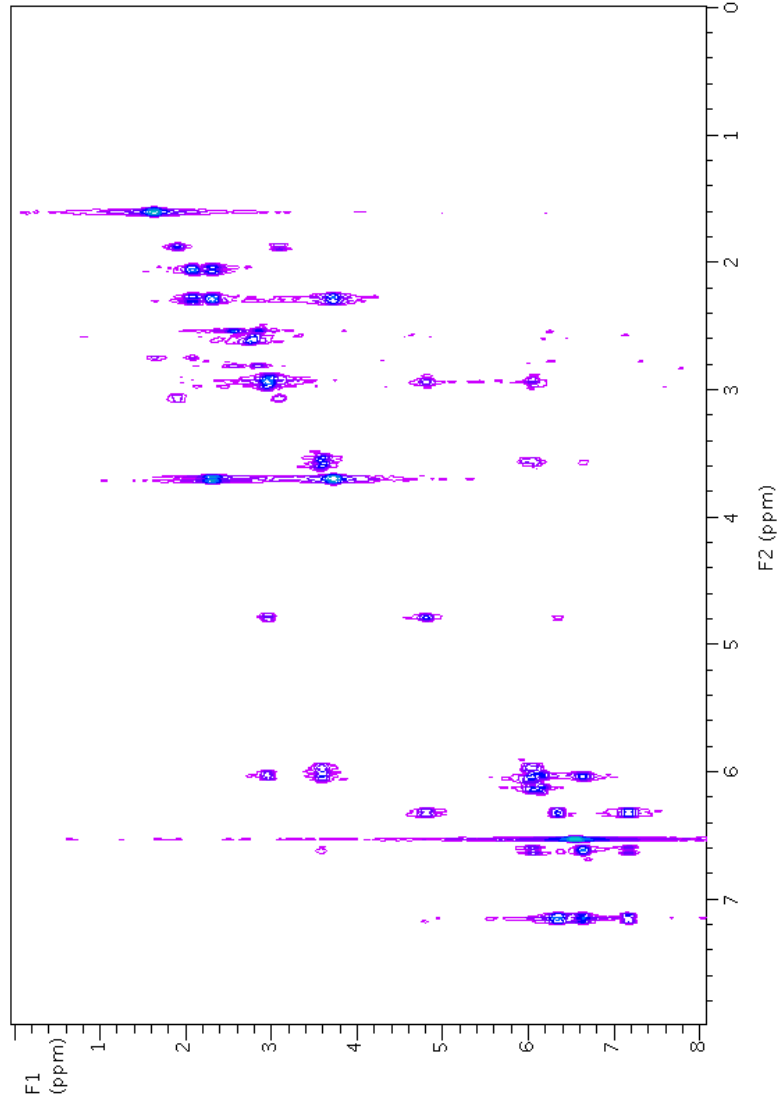
E-mail address: sylvia.urban@rmit.edu.au (S. Urban).



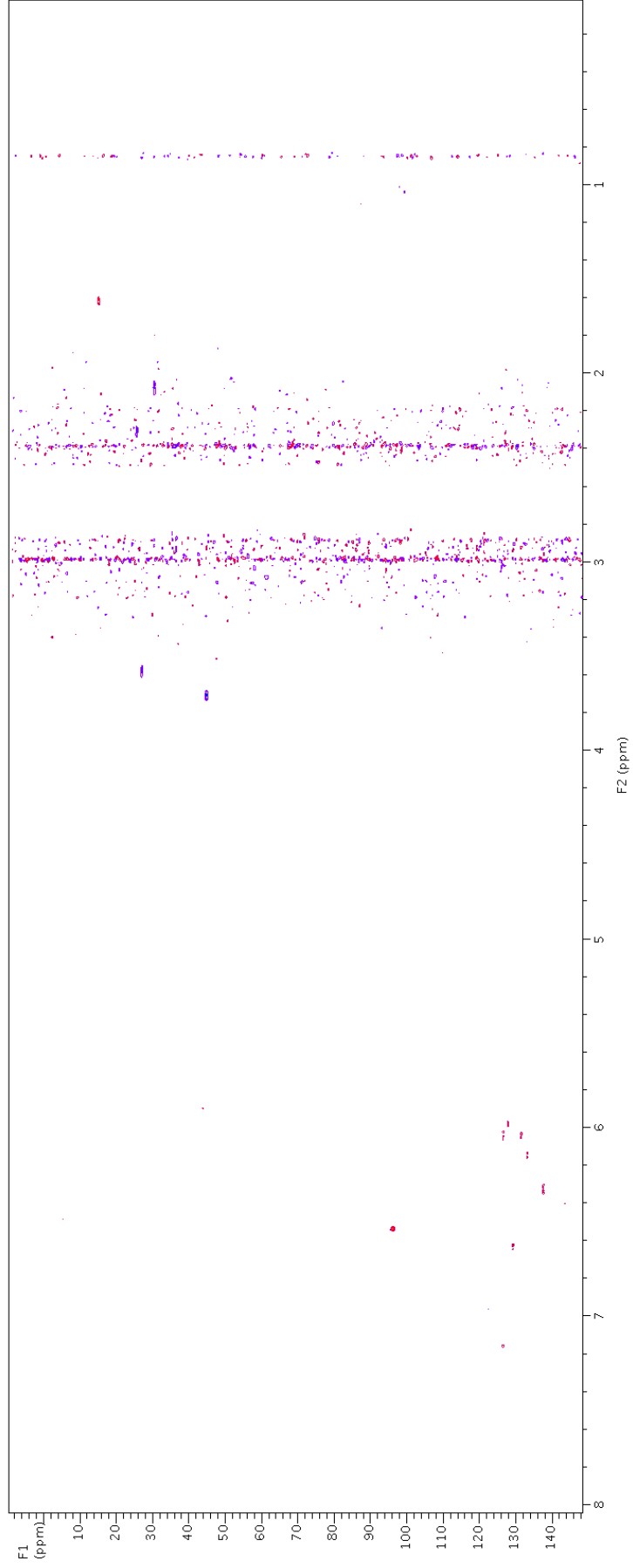
S1. Extracted UV profile (70% CH₃CN/D₂O) of **1** from HPLC-NMR.



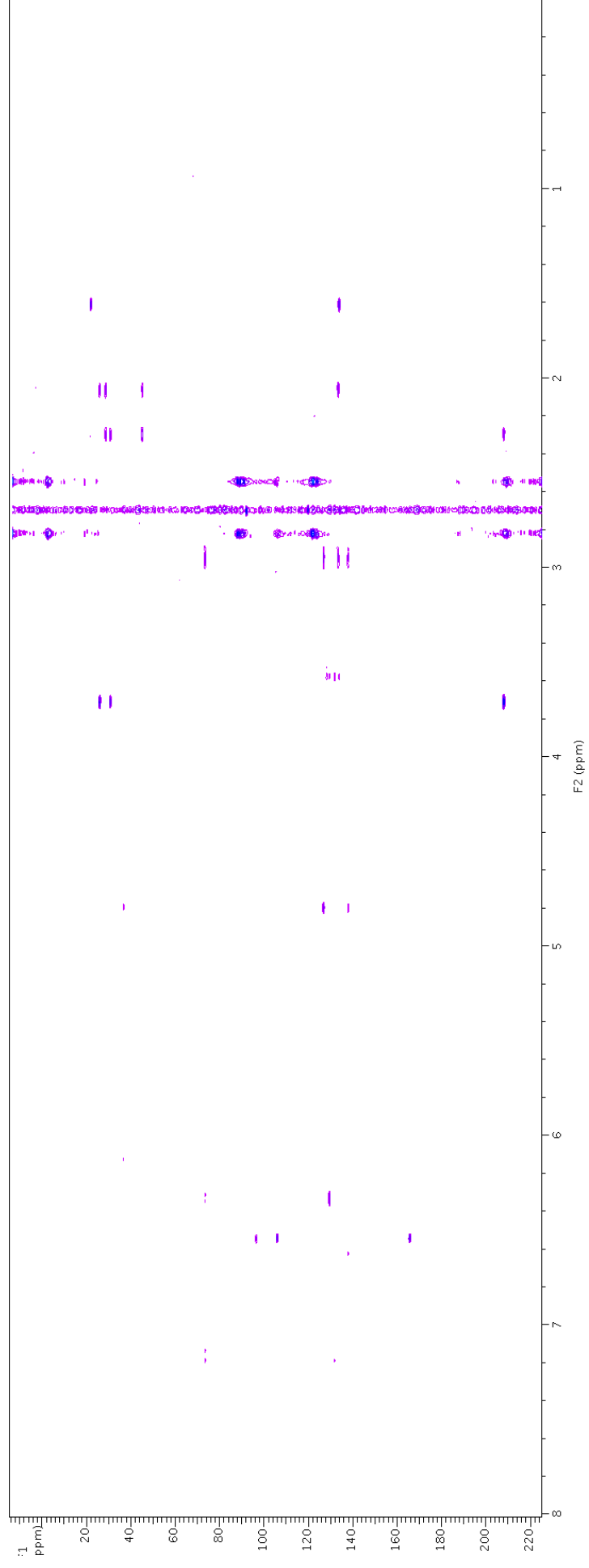
S2. Stop-flow WET1D Proton NMR spectrum (70% CH₃CN/D₂O) of **1**.



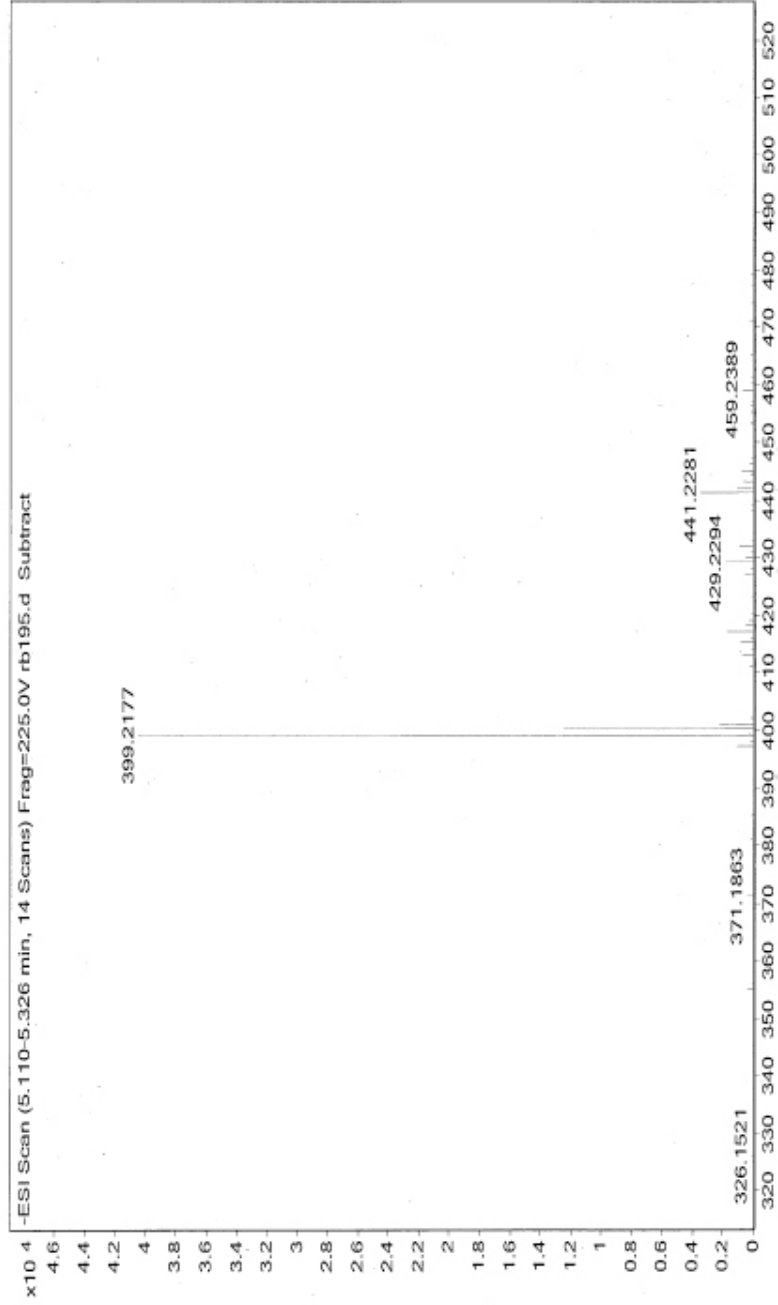
S3. gCOSY NMR spectrum (70% CH₃CN/D₂O) (from stop-flow HPLC-NMR) of **1**.



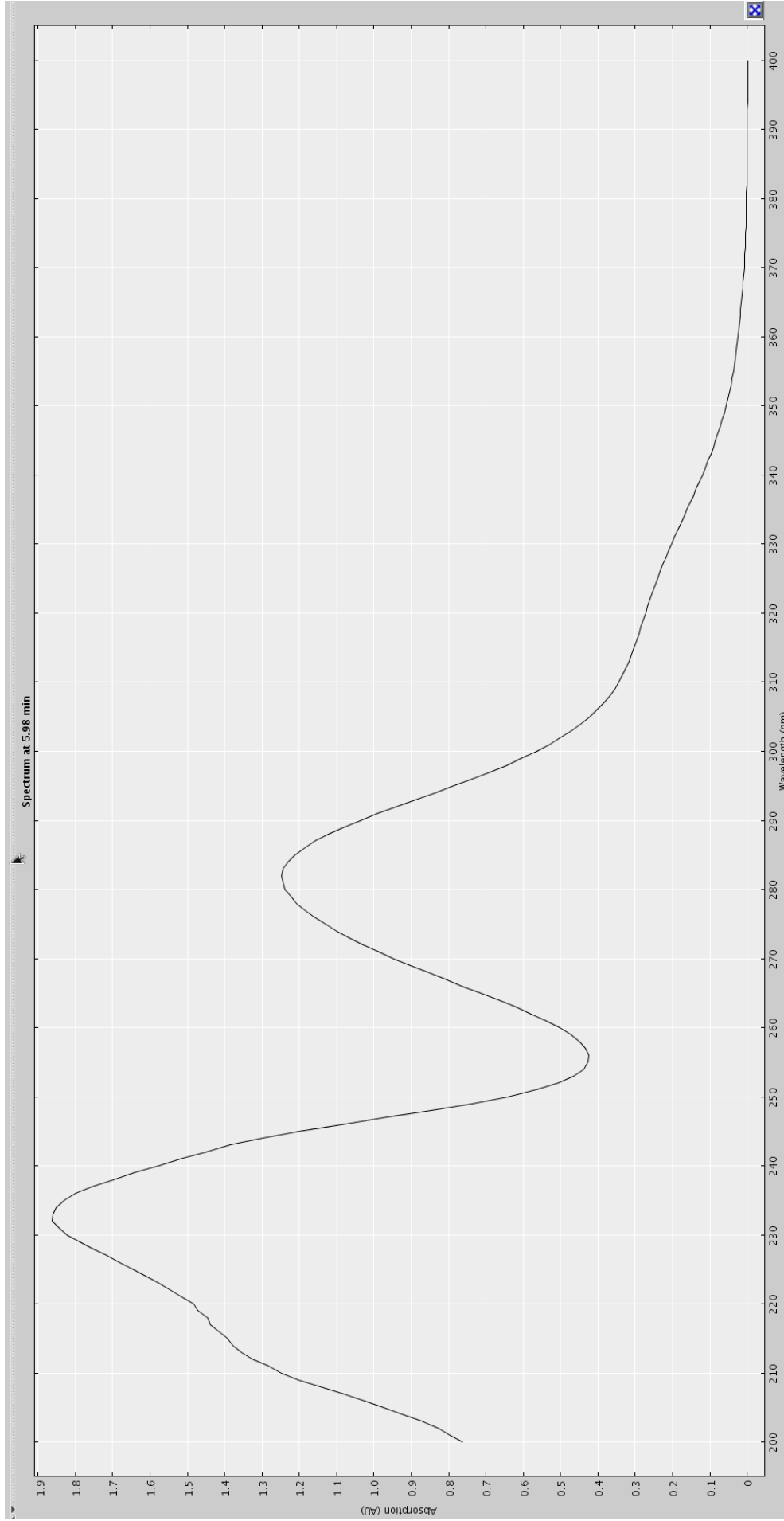
S4. gHSQCAD NMR spectrum (70% $\text{CH}_3\text{CN}/\text{D}_2\text{O}$) (from stop-flow HPLC-NMR) of **1**.



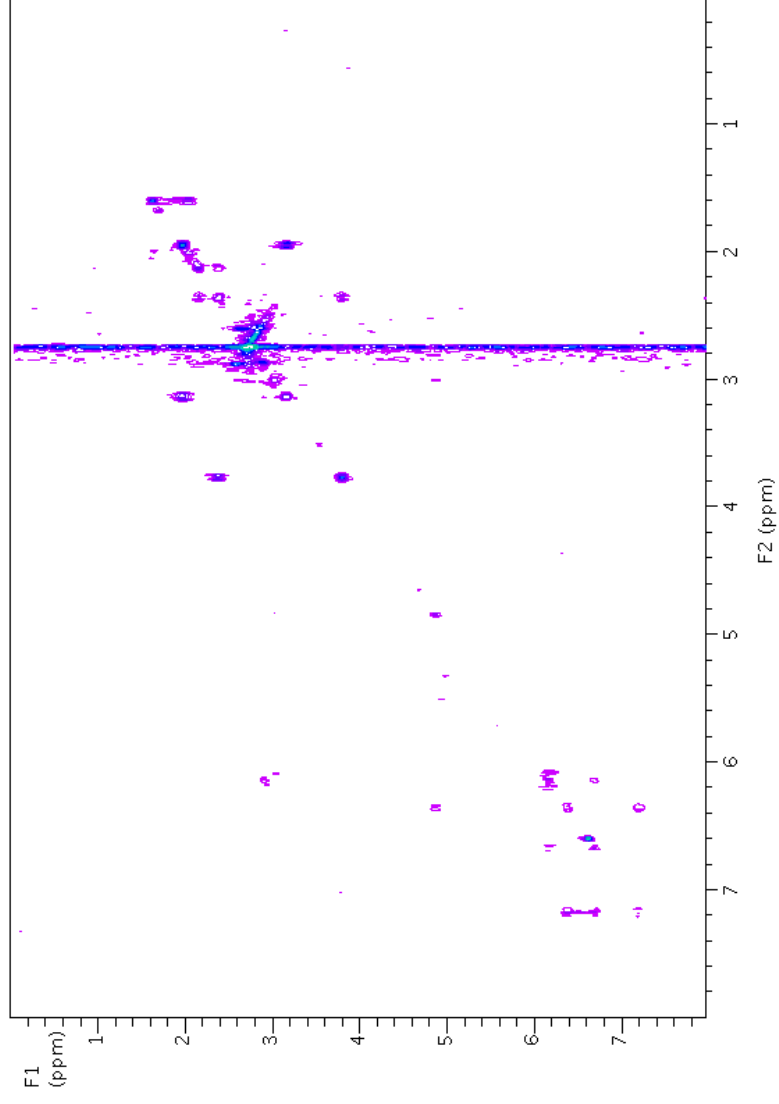
S5. gHMBC NMR spectrum (70% $\text{CH}_3\text{CN}/\text{D}_2\text{O}$) (from stop-flow HPLC-NMR) of **1**.



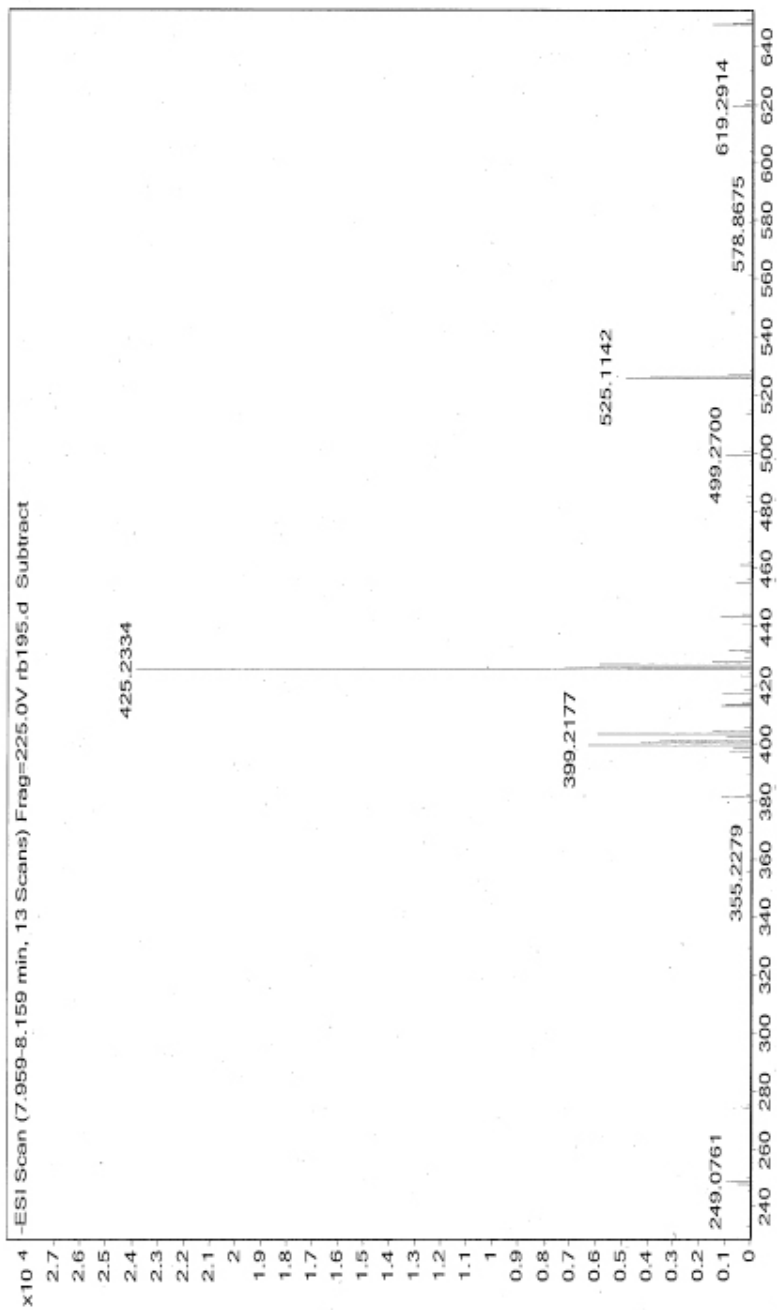
S6. High resolution negative ESI-MS of **1**.from HPLC-MS.



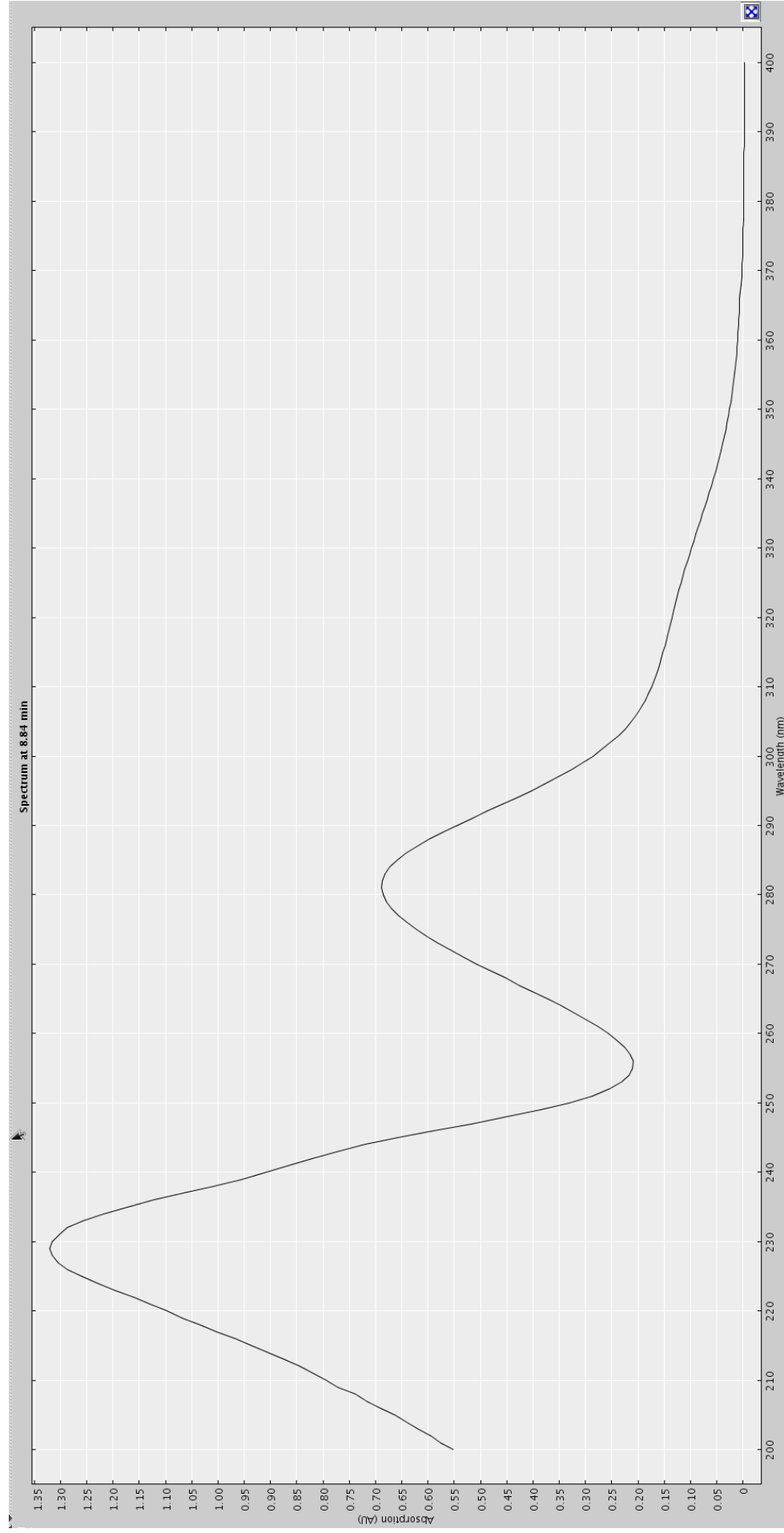
S7. Extracted UV profile (70% CH₃CN/D₂O) of **2** from HPLC-NMR.



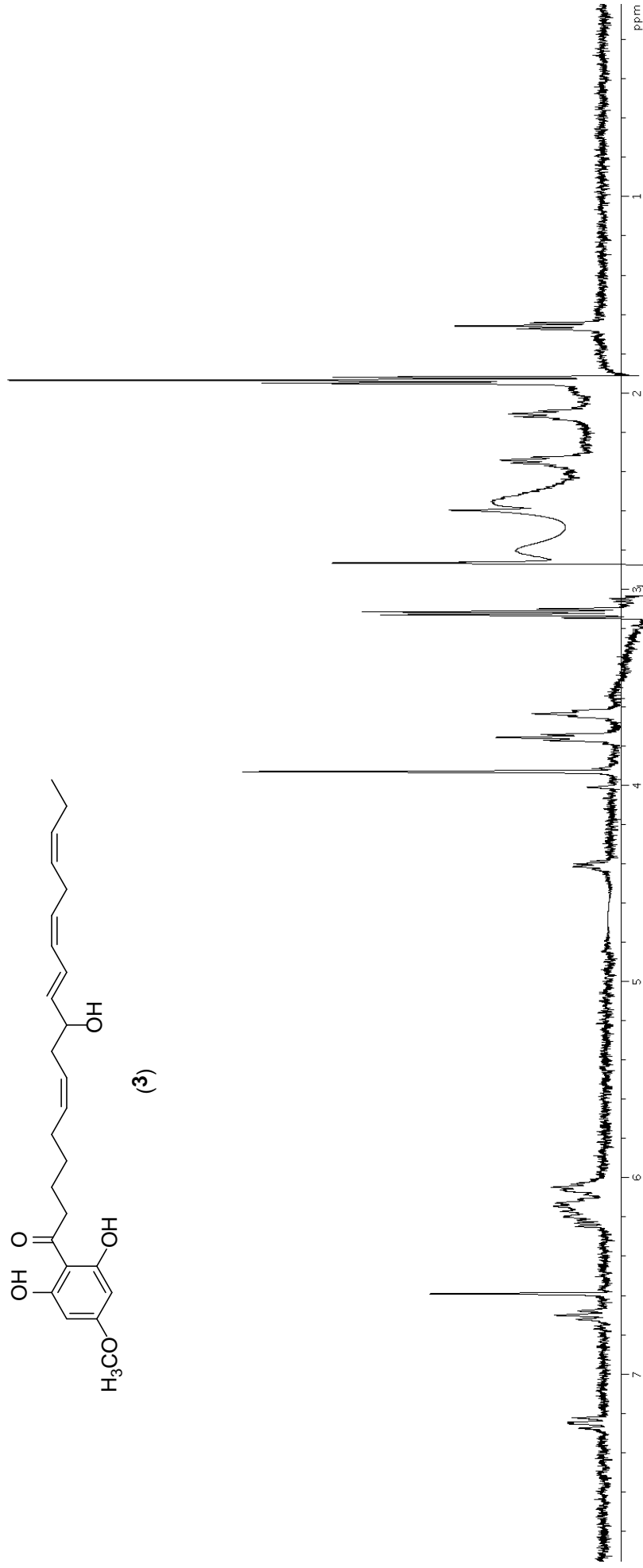
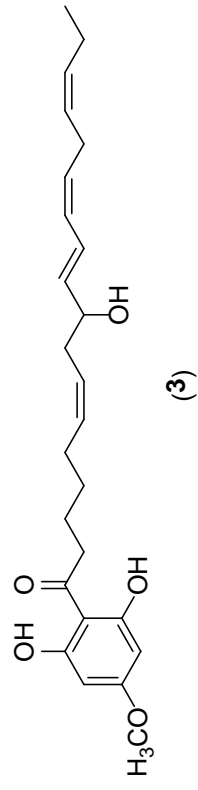
S9. gCOSY NMR spectrum (70% CH₃CN/D₂O) (from stop-flow HPLC-NMR) of **2**.



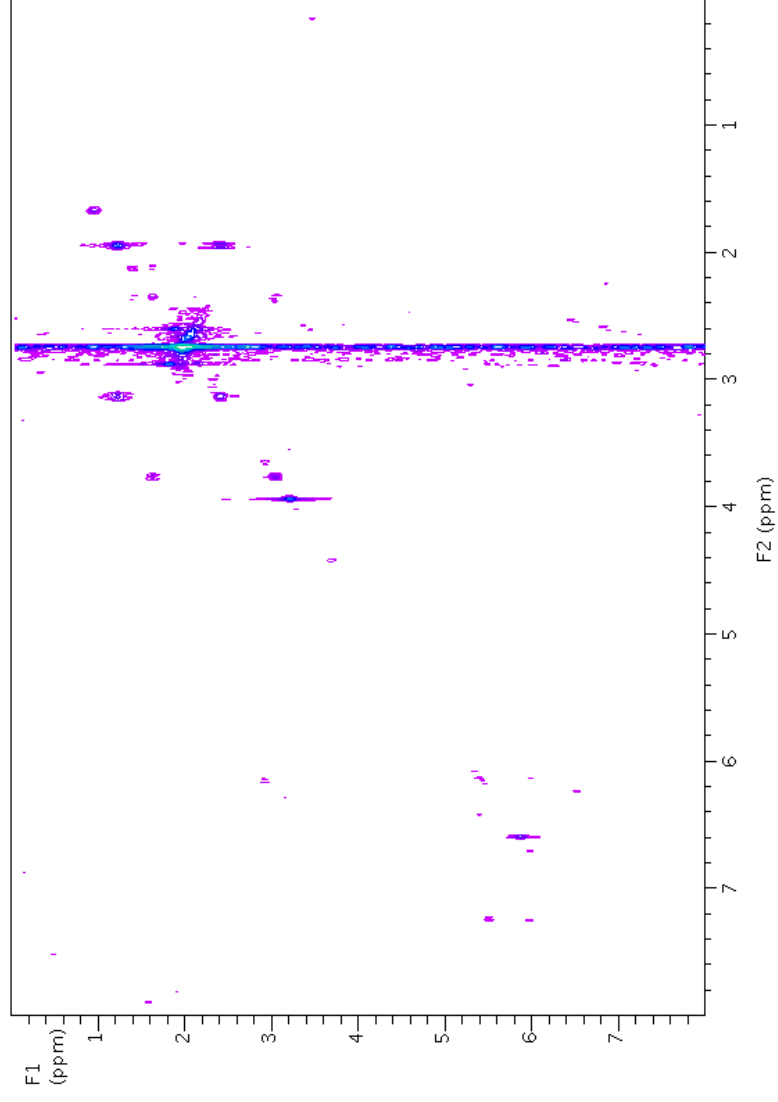
S10. High resolution negative ESI-MS of **2** from HPLC-MS.



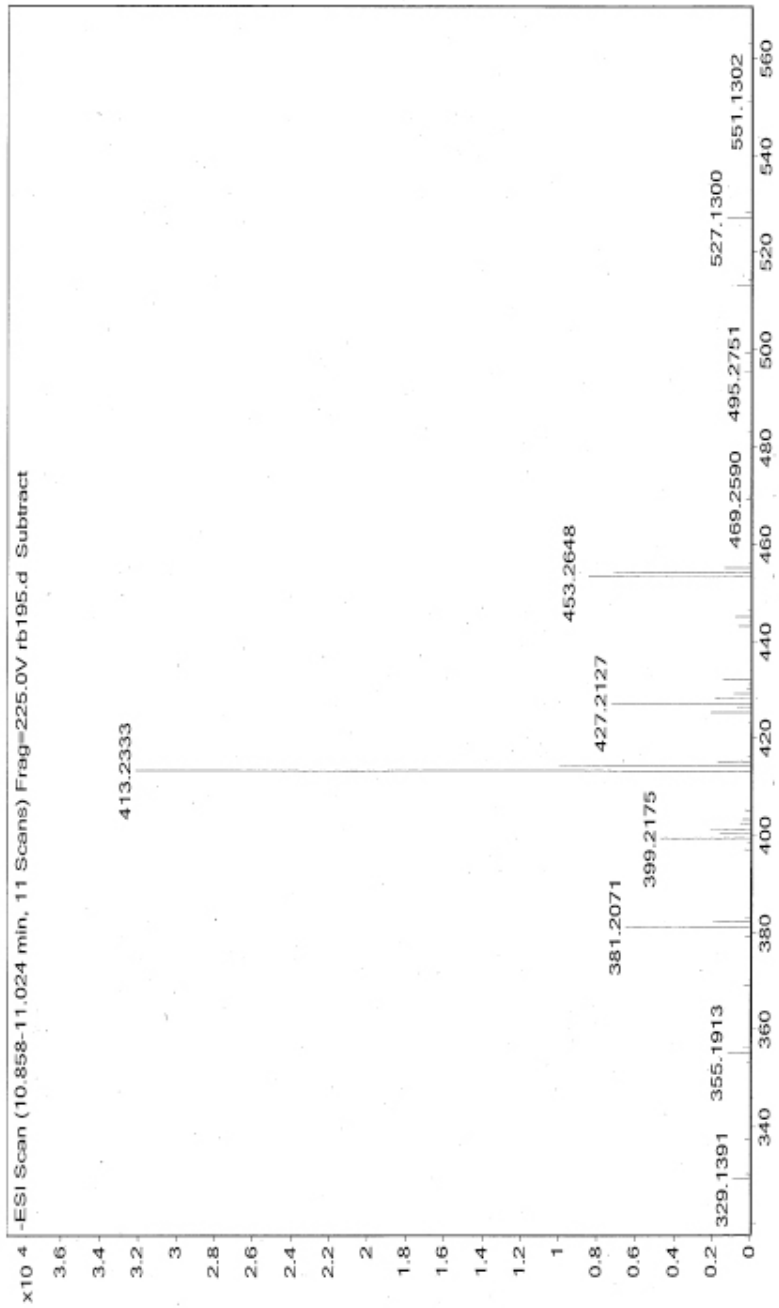
S11. Extracted UV profile (70% CH₃CN/D₂O) of **3** from HPLC-NMR.



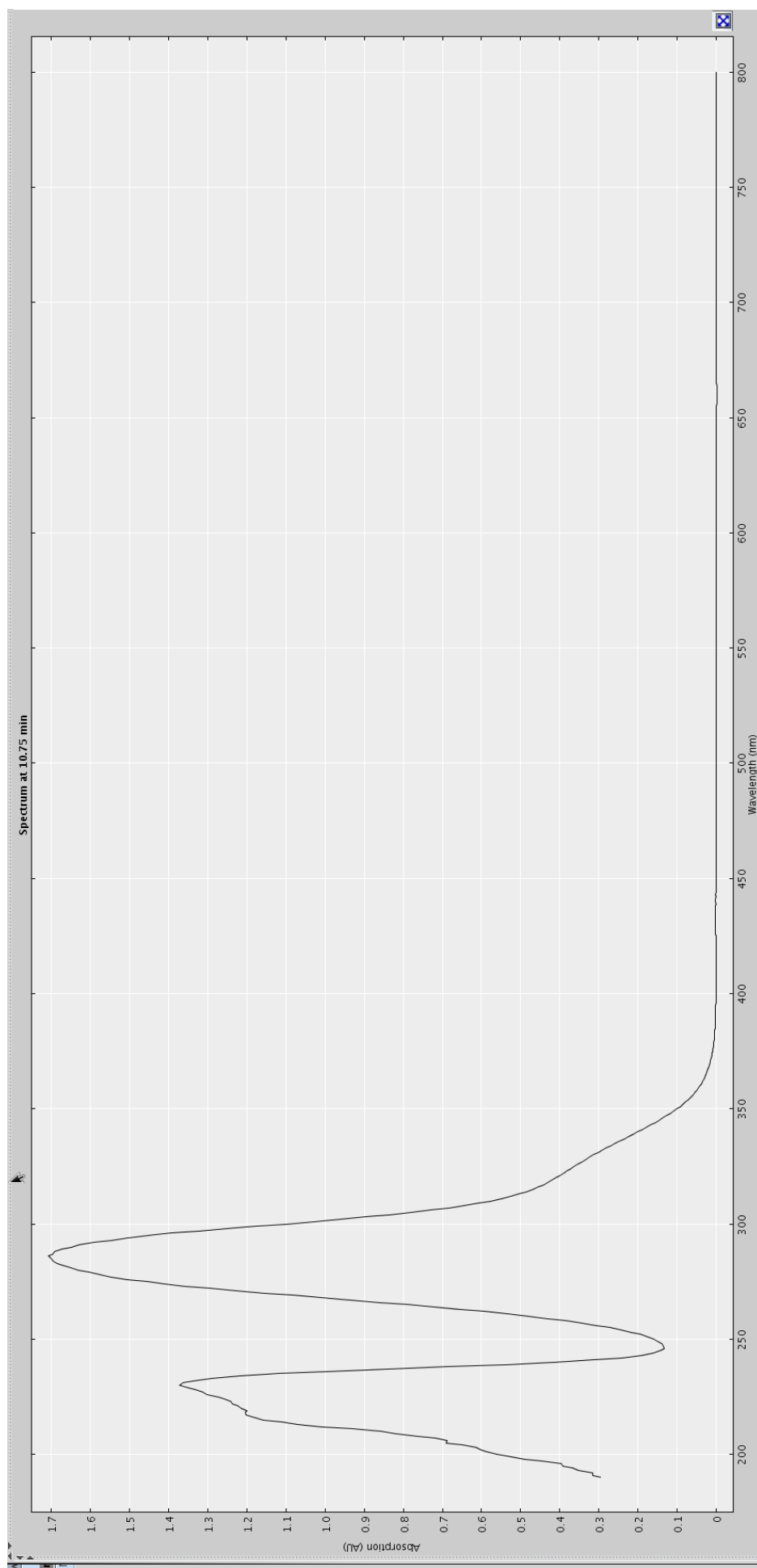
S12. Stop-flow WETID Proton NMR spectrum (70% CH₃CN/D₂O) of 3.



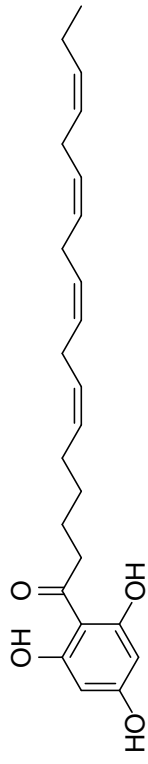
S13. gCOSY NMR spectrum (70% CH₃CN/D₂O) (from stop-flow HPLC-NMR) of **3**.



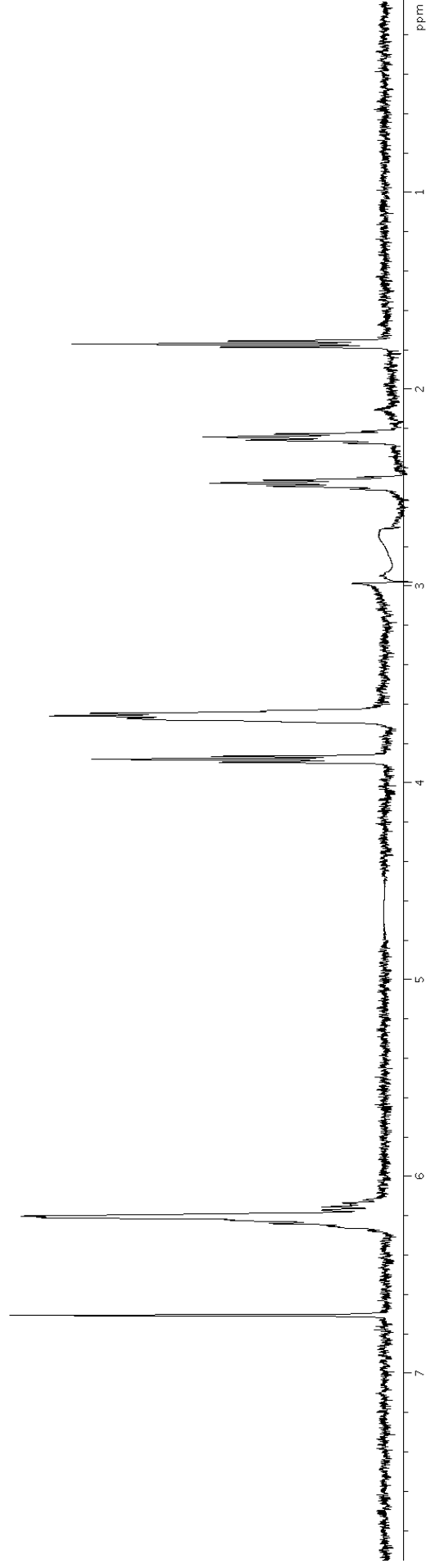
S14. High resolution negative ESI-MS of **3** from HPLC-MS.



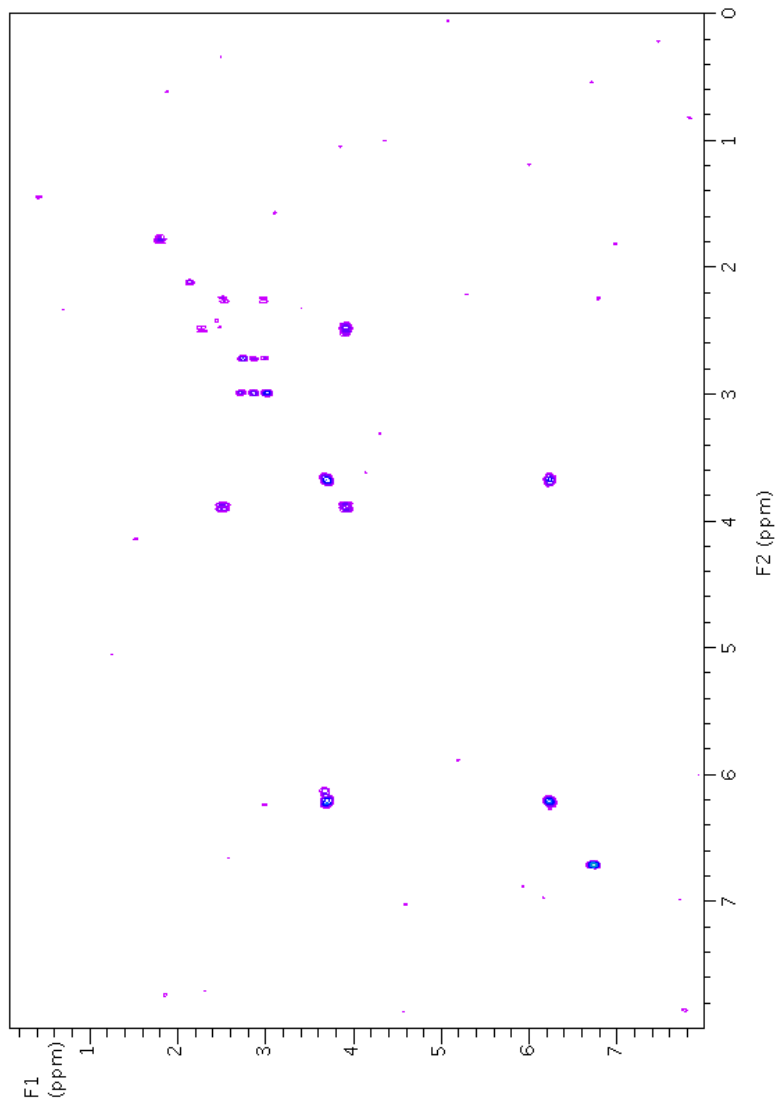
S15. Extracted UV profile (75% CH₃CN/D₂O) of **4** from HPLC-NMR.



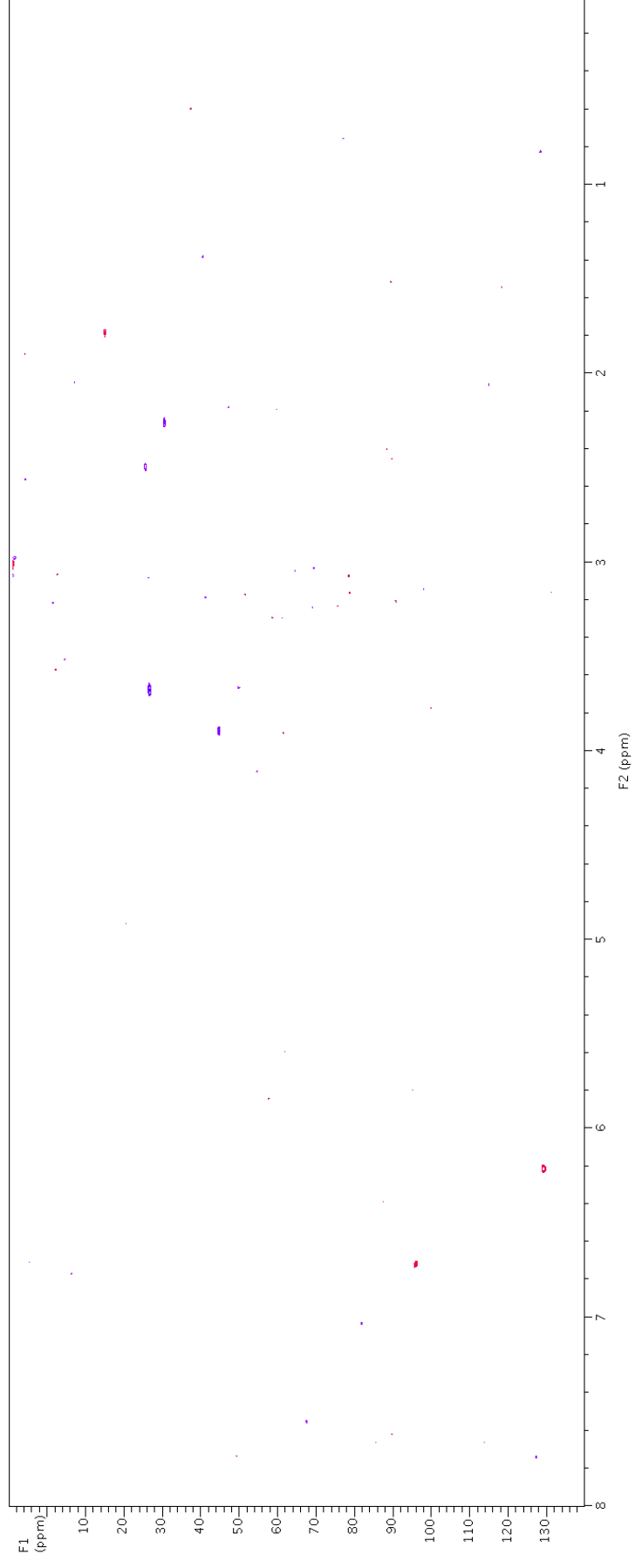
(4)



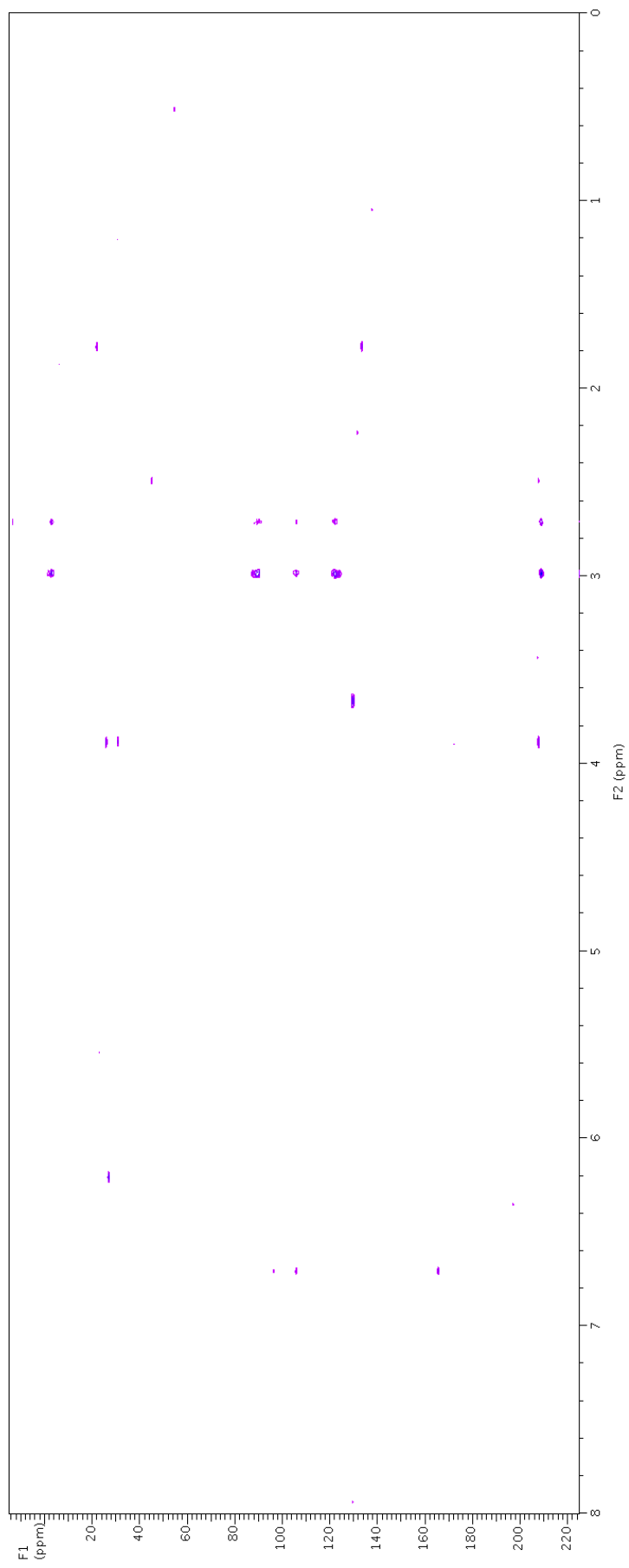
S16. Stop-flow WETID Proton NMR spectrum (75% CH₃CN/D₂O) of **4**.



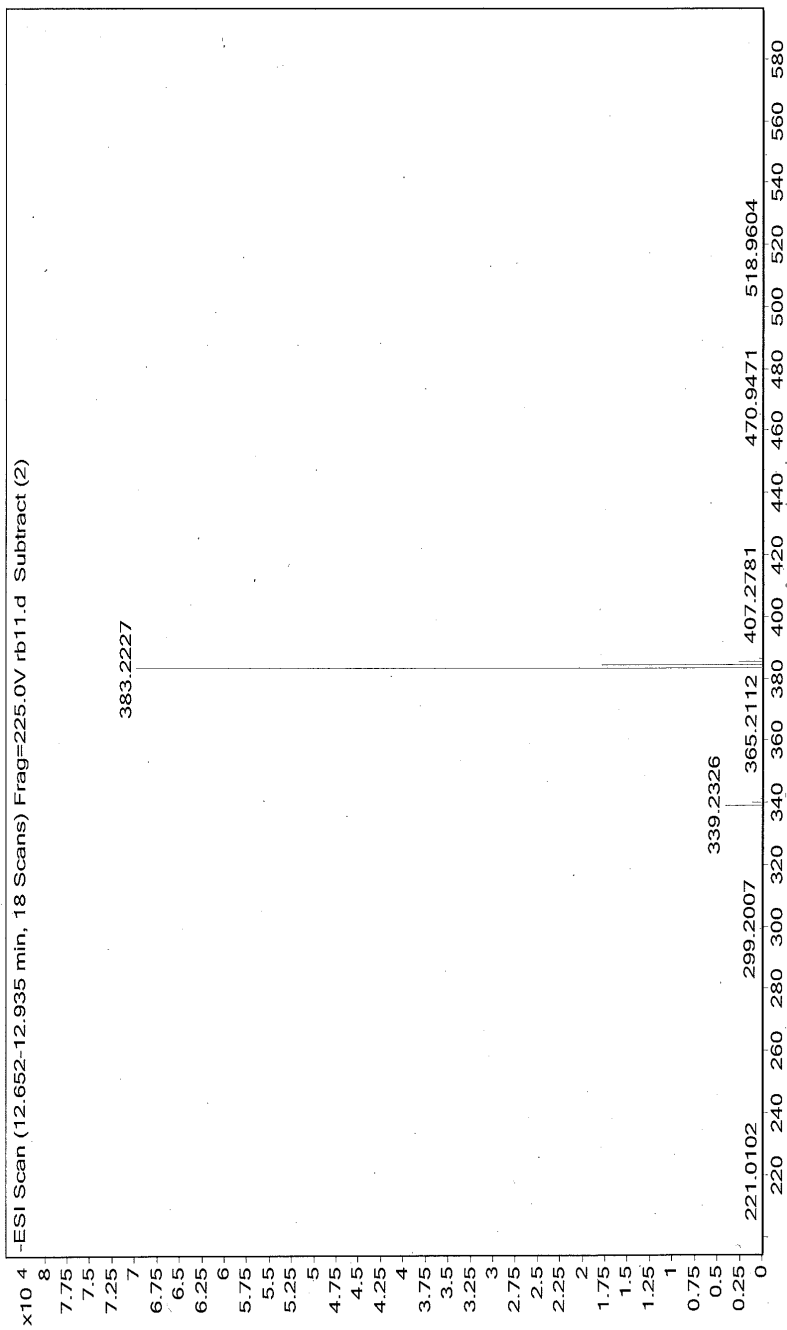
S17. gCOSY NMR spectrum (75% CH₃CN/D₂O) (from stop-flow HPLC-NMR) of **4**.



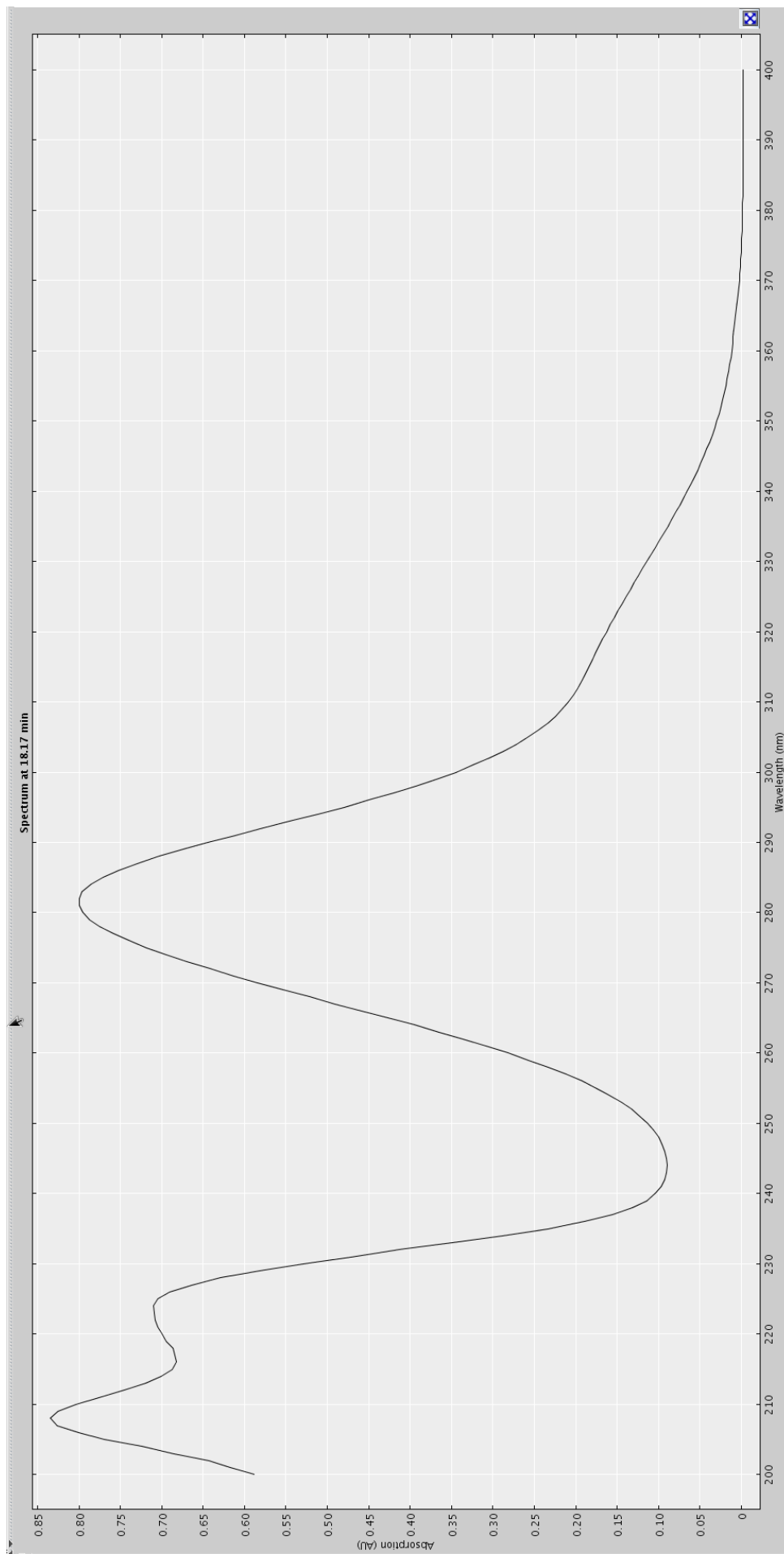
S18. HSQCAD NMR spectrum (75% CH₃CN/D₂O) (from stop-flow HPLC-NMR) of **4**.



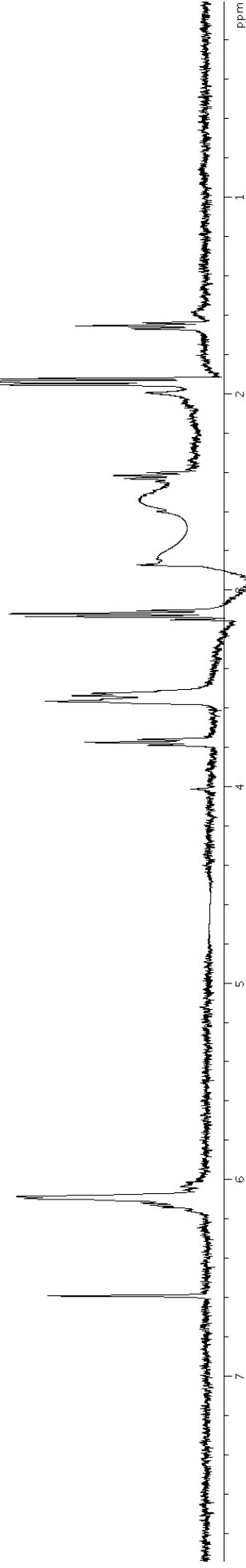
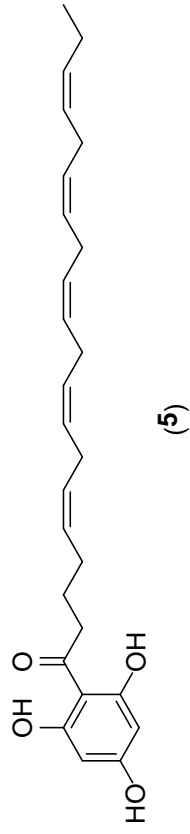
S19. gHMBCAD NMR spectrum (75% CH₃CN/D₂O) (from stop-flow HPLC-NMR) of **4**.



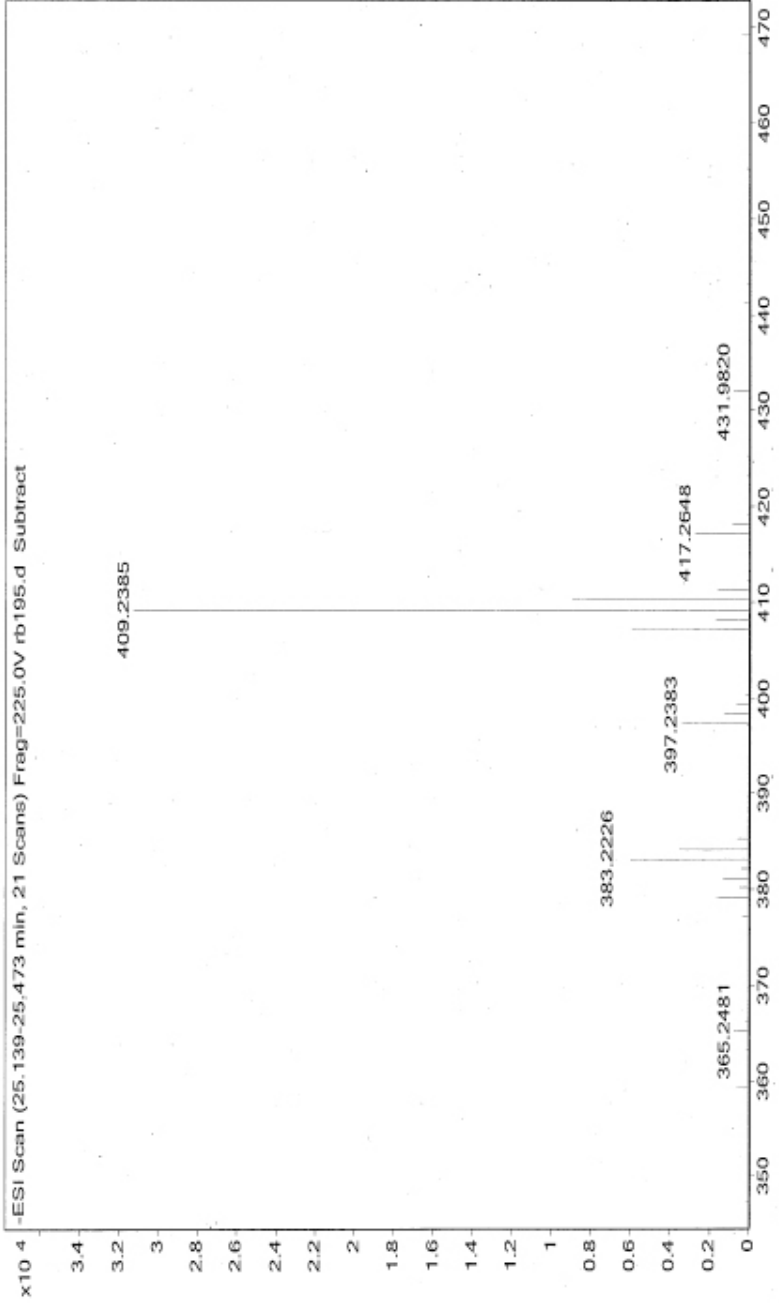
S20. High resolution negative ESI-MS of **4** from HPLC-MS.



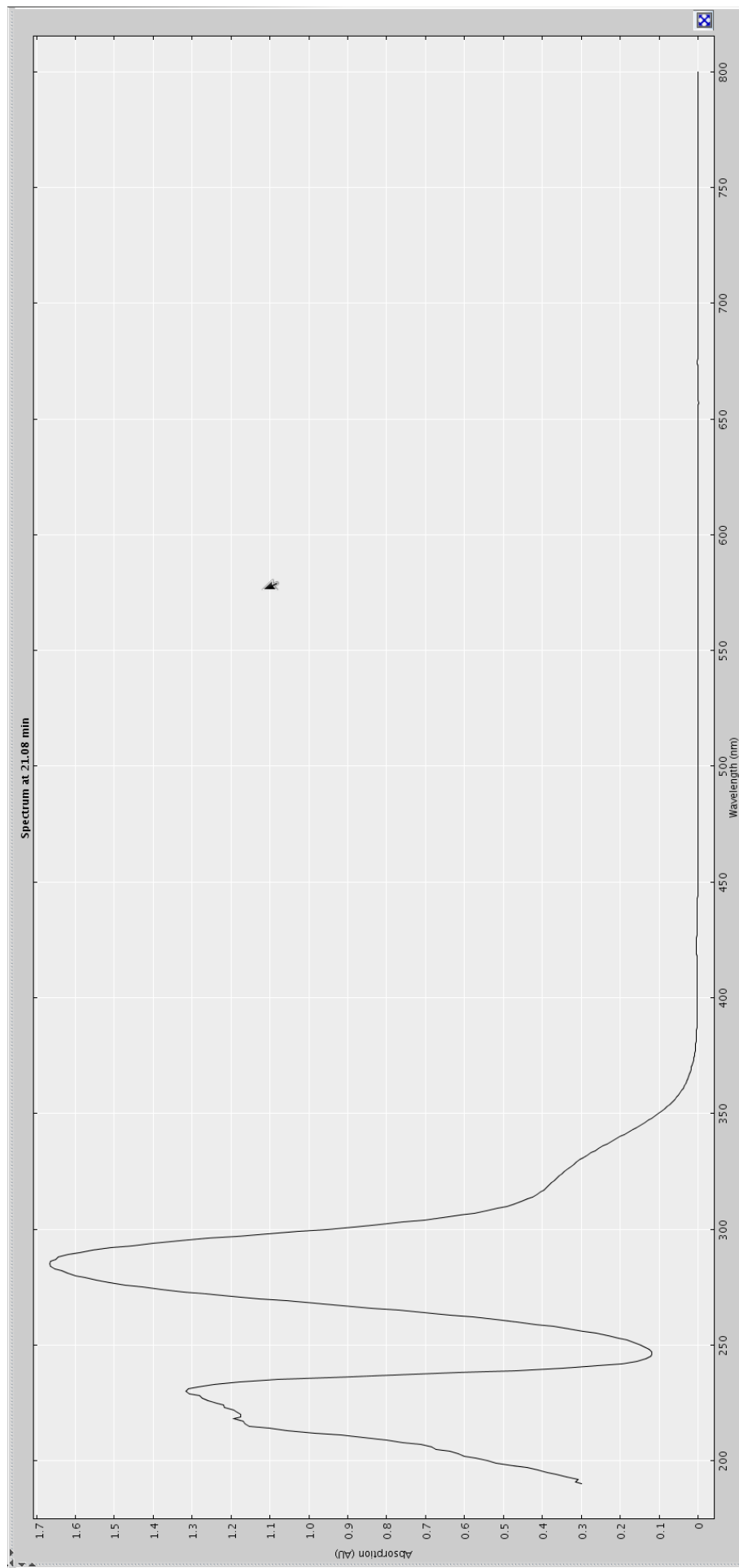
S21. Extracted UV profile (70% CH₃CN/D₂O) of **5** from HPLC-NMR.



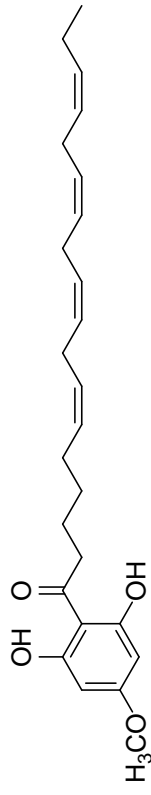
S22. Stop-flow WETID Proton NMR spectrum (70% CH₃CN/D₂O) of 5.



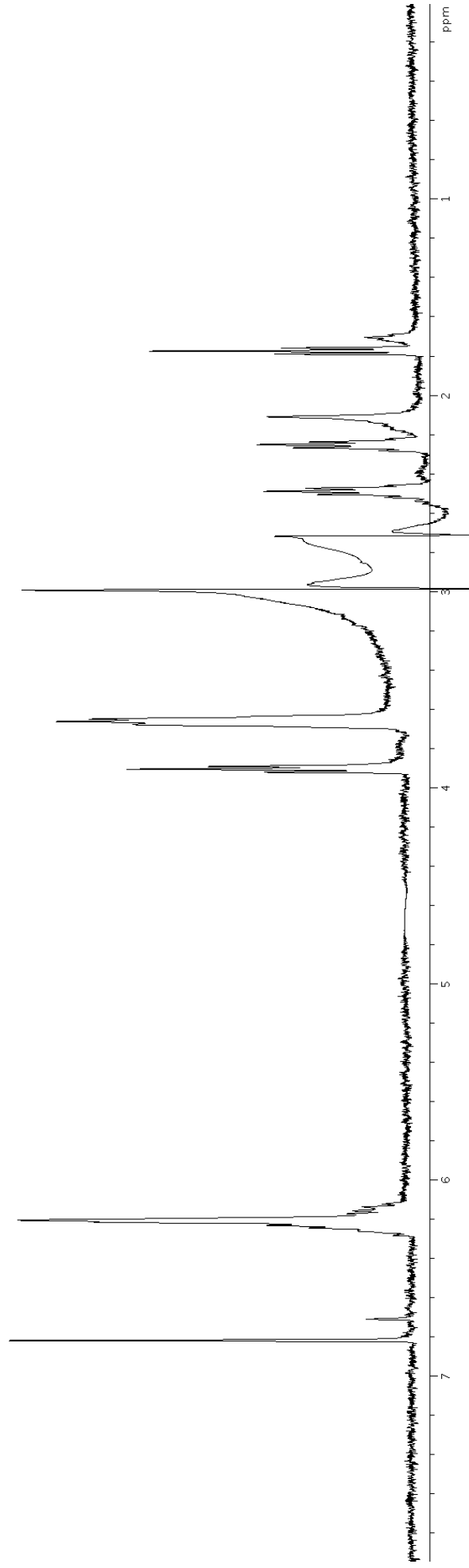
S24. High resolution negative ESI-MS of **5** from HPLC-MS.



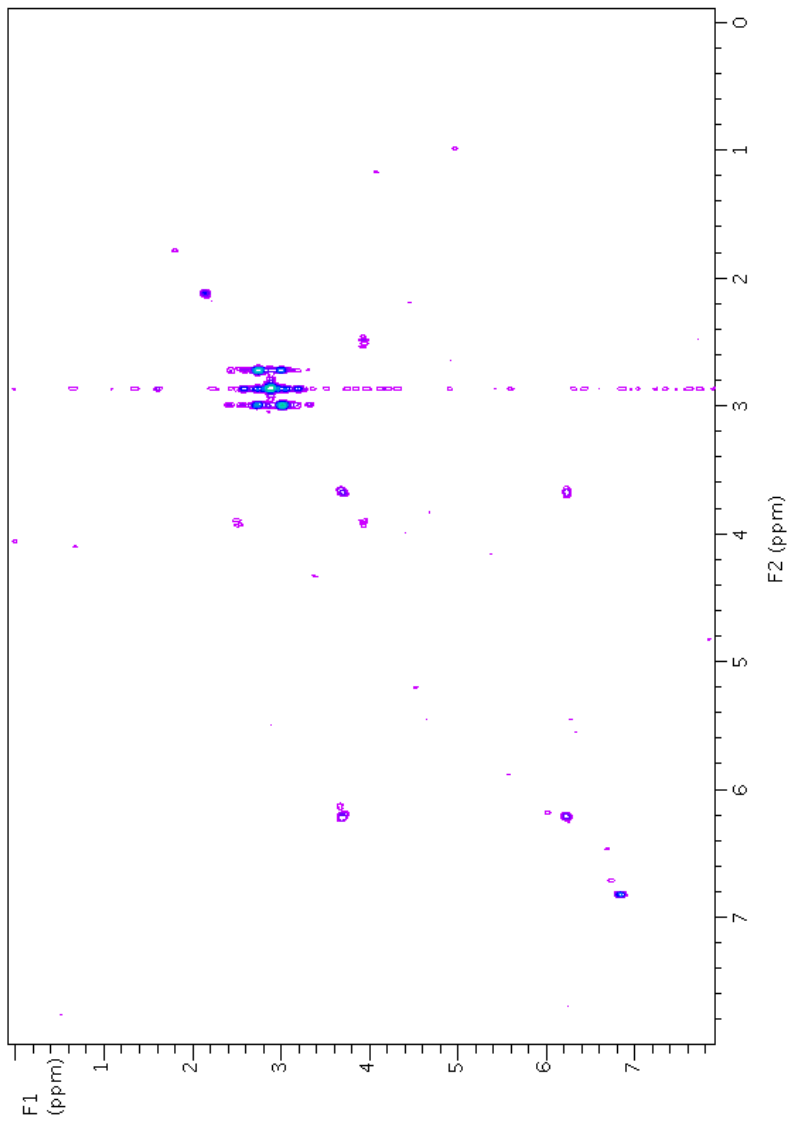
S25. Extracted UV profile (75% CH₃CN/D₂O) of **6** from HPLC-NMR.



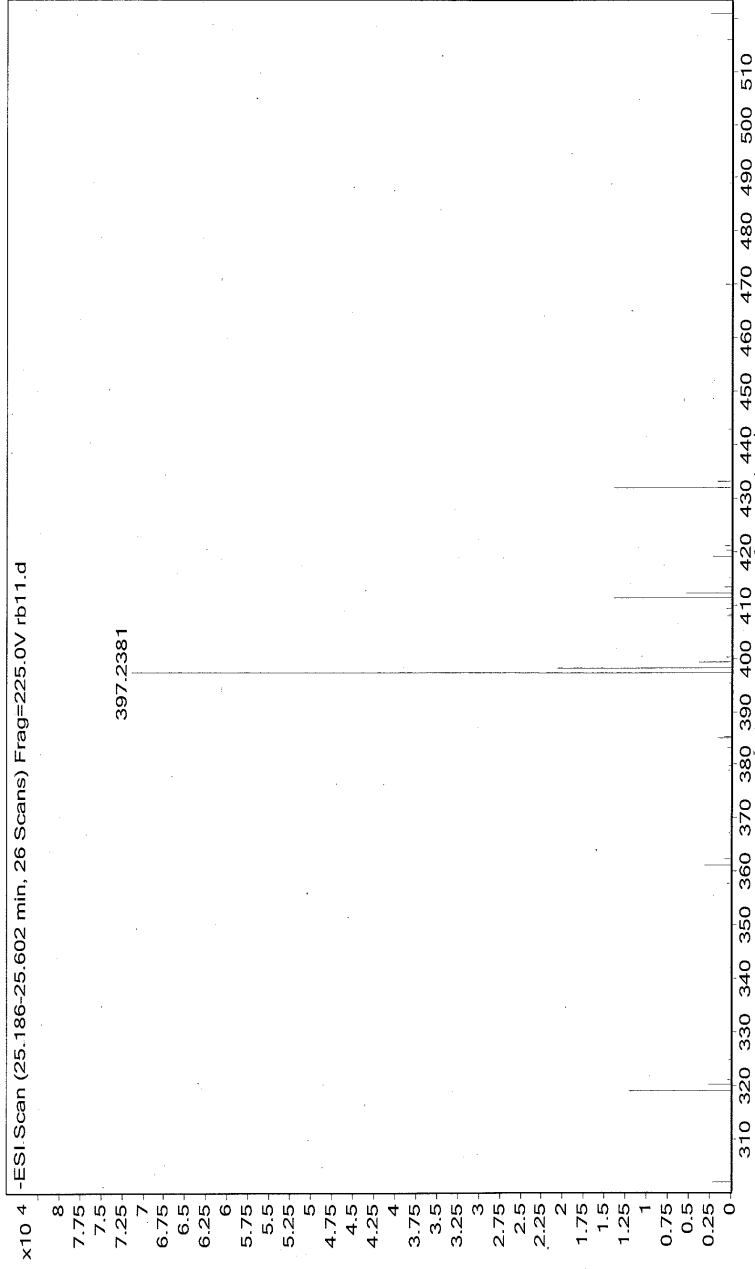
6



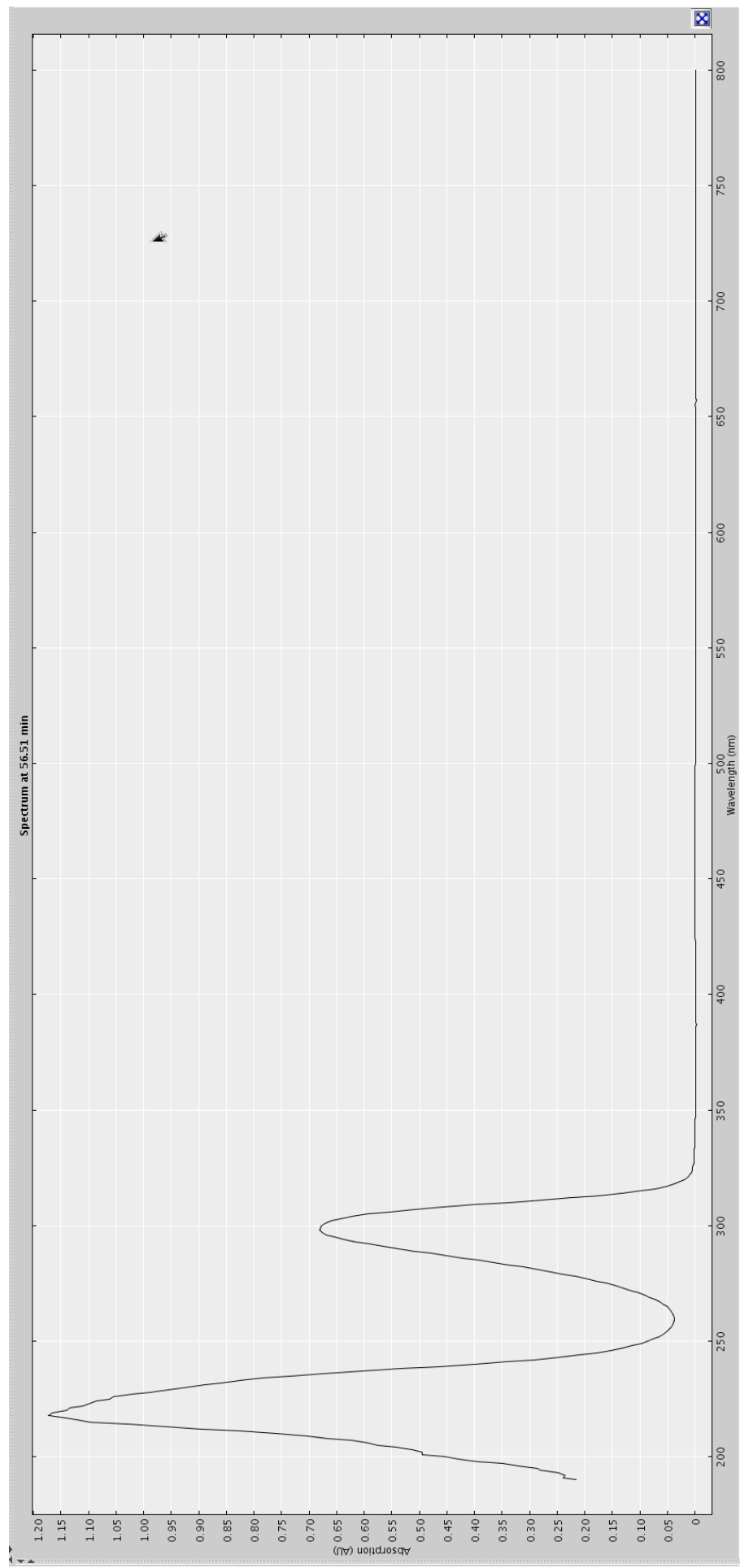
S26. Stop-flow WETID Proton NMR spectrum (75% CH₃CN/D₂O) of **6**.



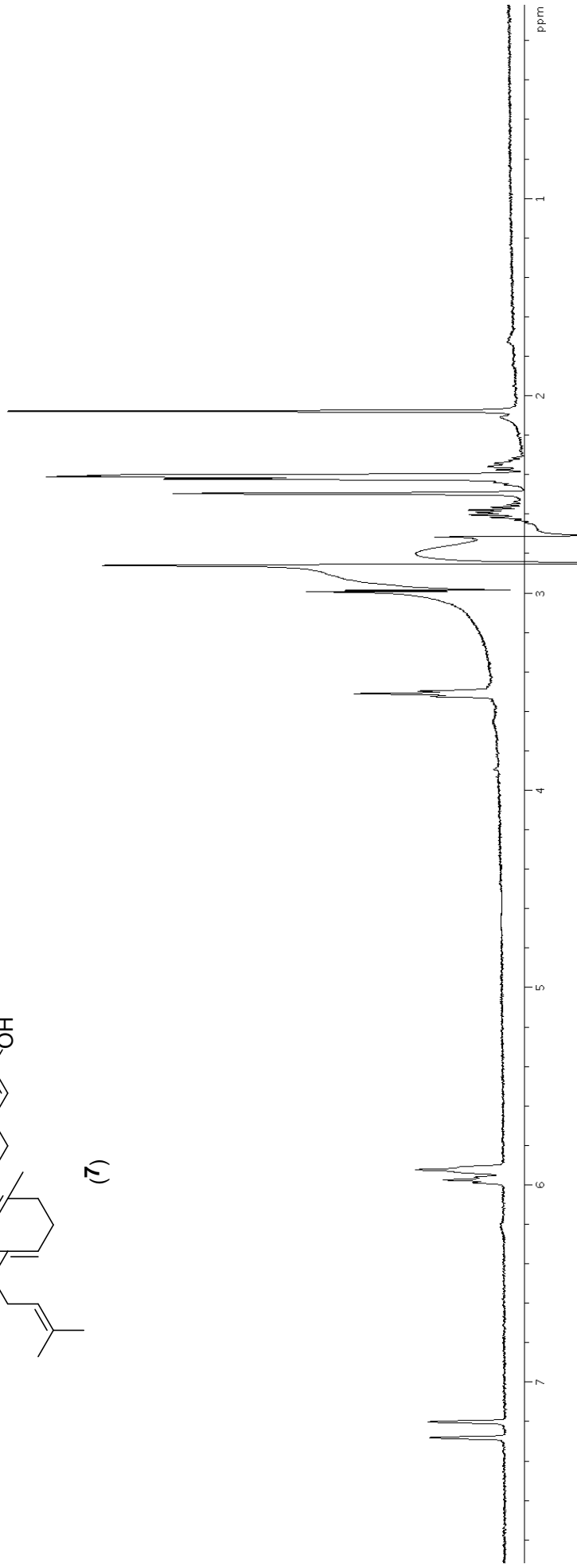
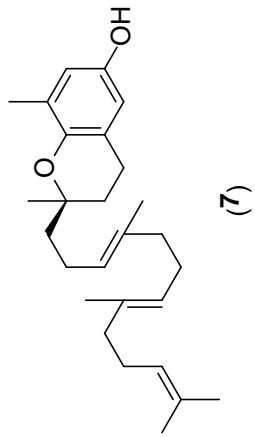
S27. gCOSY NMR spectrum (75% CH₃CN/D₂O) (from stop-flow HPLC-NMR) of **6**.



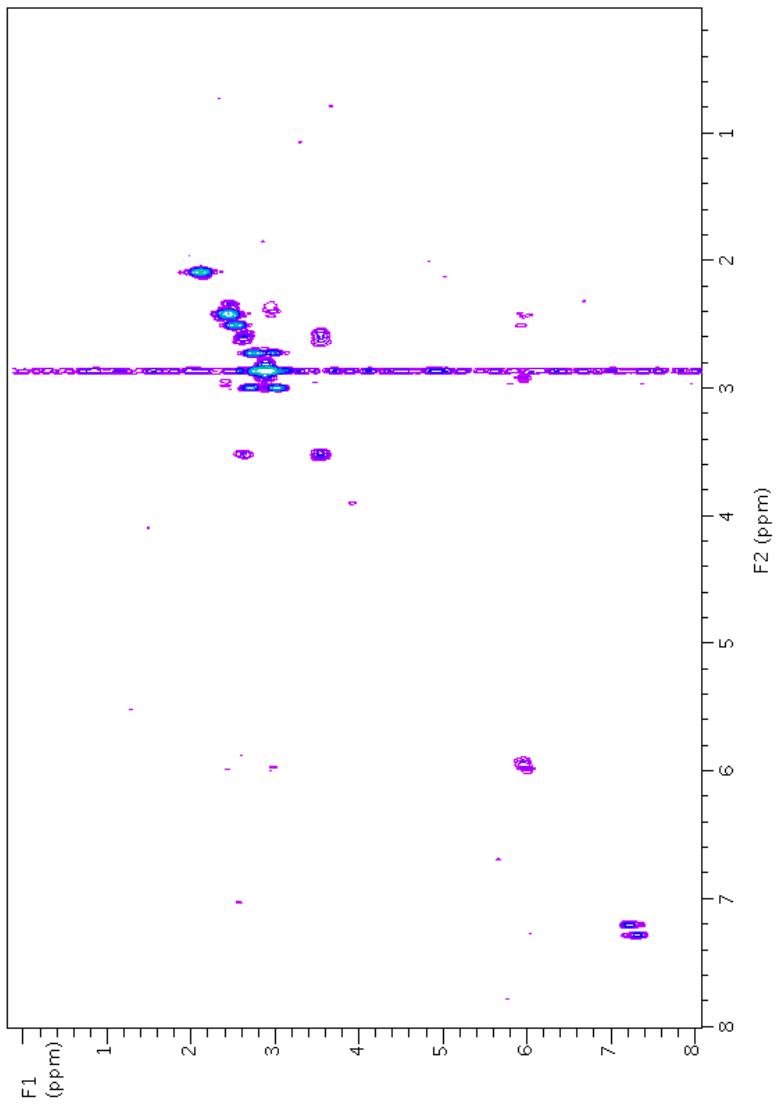
S28. High resolution negative ESI-MS of **6** from HPLC-MS.



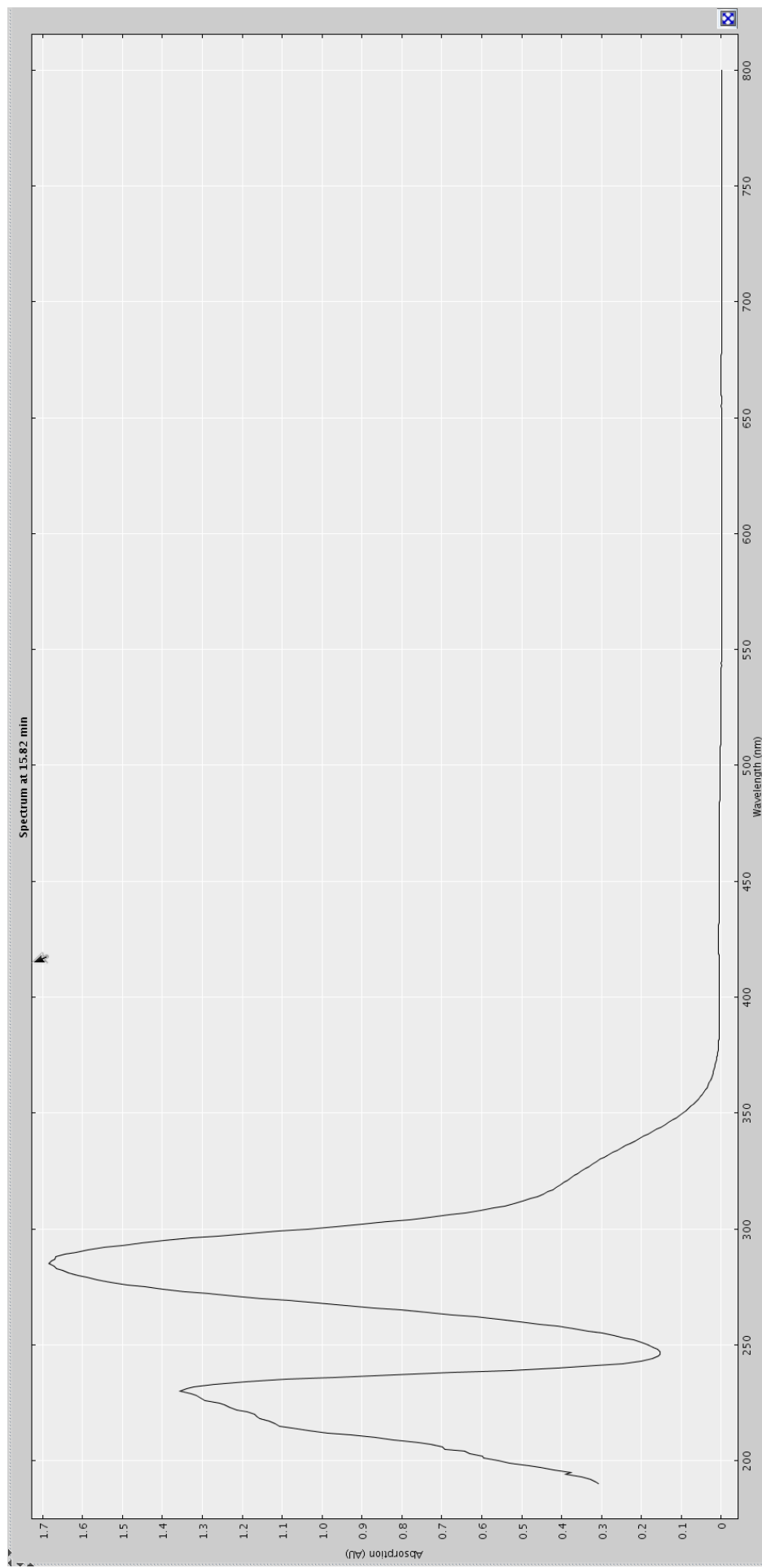
S29. Extracted UV profile (75% CH₃CN/D₂O) of **7** from HPLC-NMR.



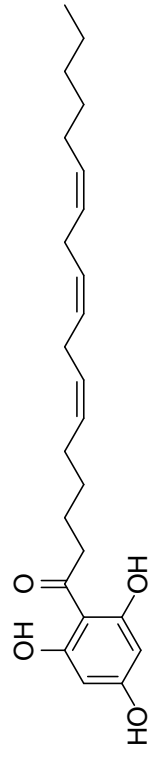
S30. Stop-flow WETID Proton NMR spectrum (75% CH₃CN/D₂O) of 7.



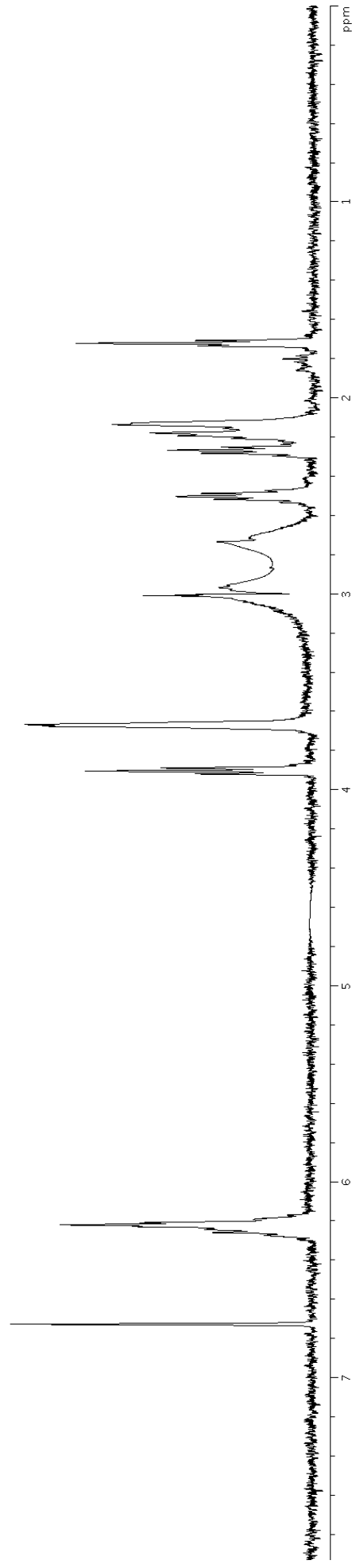
S31. gCOSY NMR spectrum (75% CH₃CN/D₂O) (from stop-flow HPLC-NMR) of **7**.



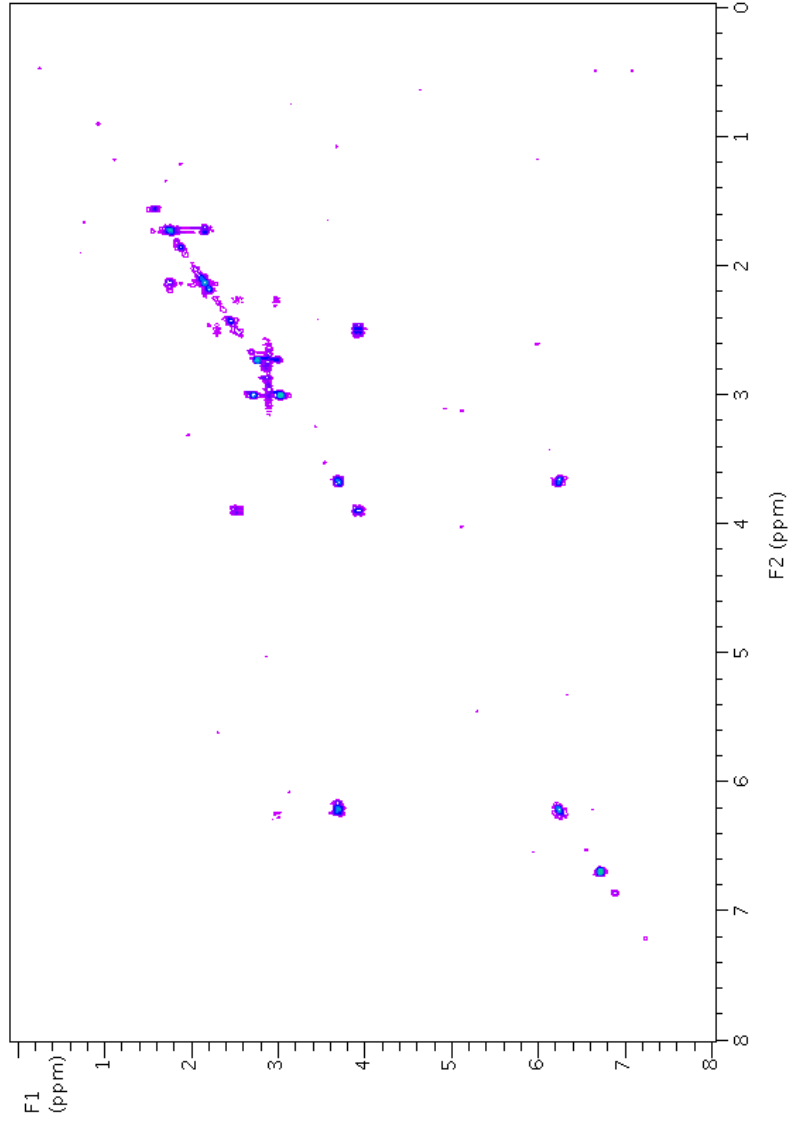
S32. Extracted UV profile (75% CH₃CN/D₂O) of **8** from HPLC-NMR.



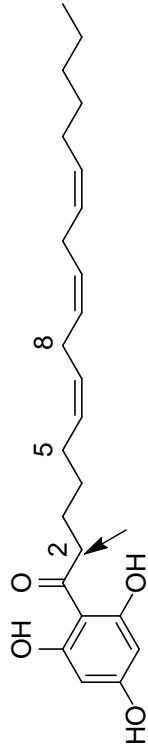
(8) - moniliferanone A



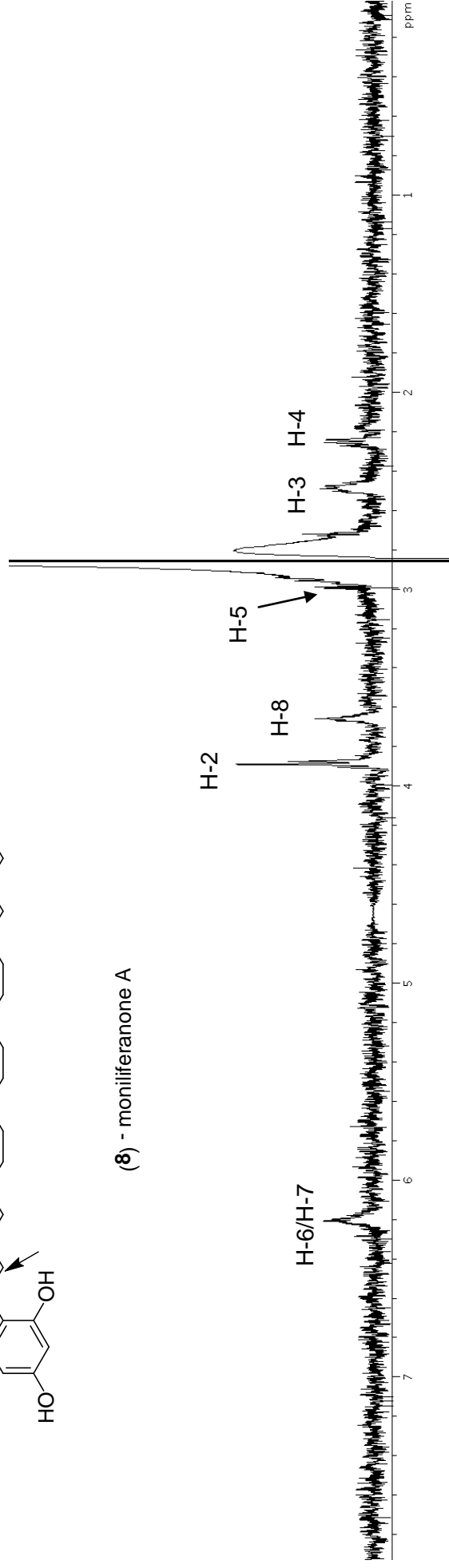
S33. Stop-flow WET1D Proton NMR spectrum (75% CH₃CN/D₂O) of moniliferanone A **(8)**.



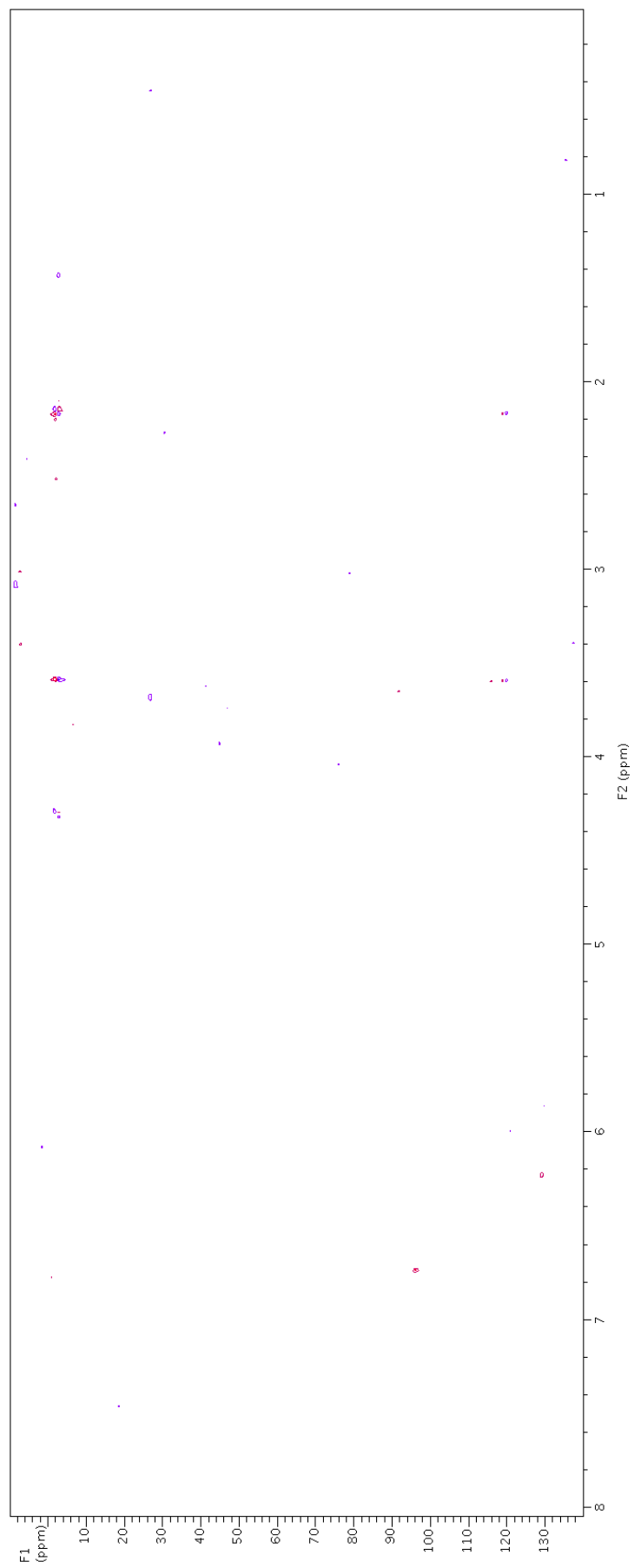
S34. gCOSY NMR spectrum (75% CH₃CN/D₂O) (from stop-flow HPLC-NMR) of moniferanone A (**8**).



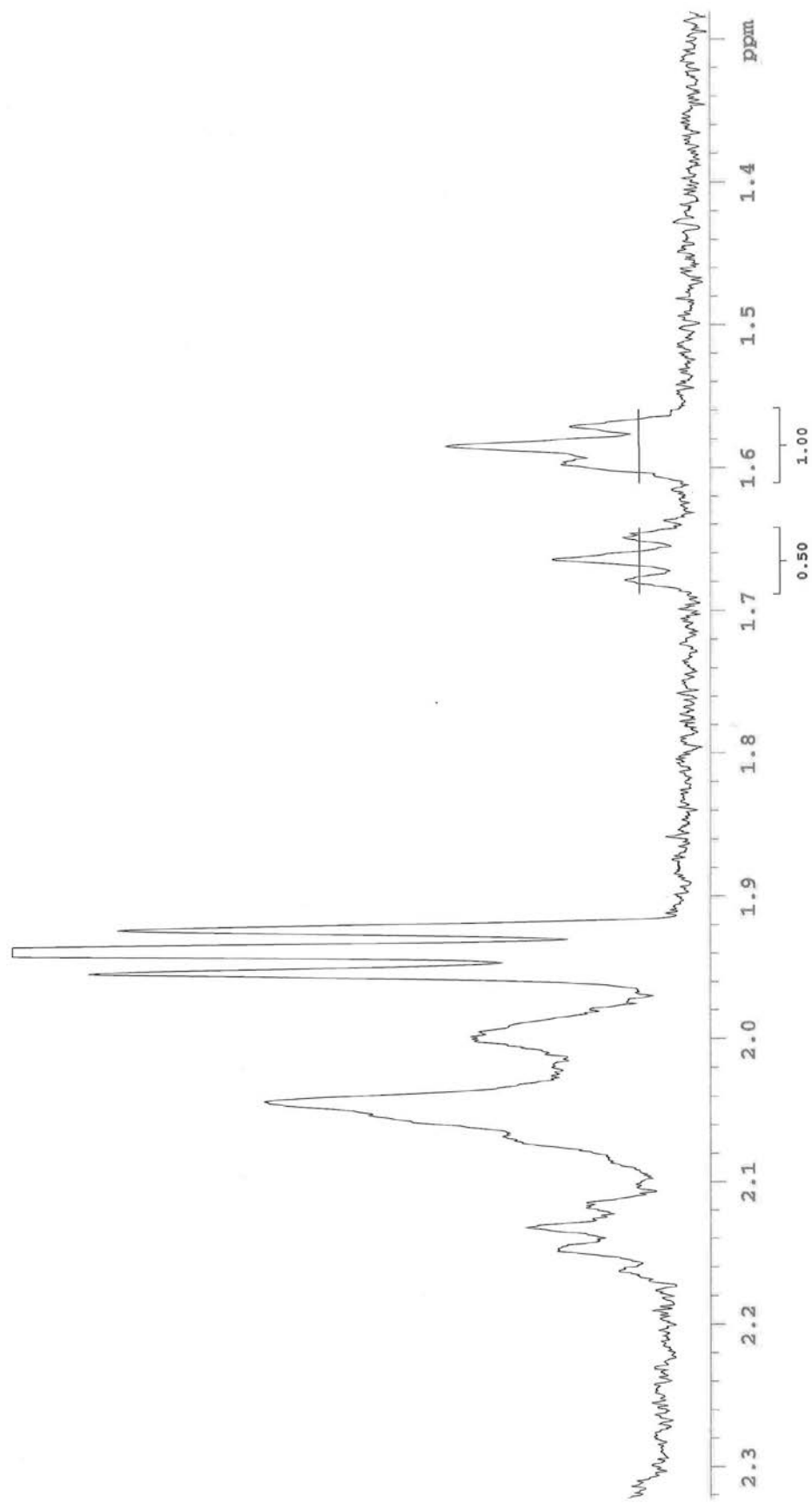
(8) - moniliferanone A



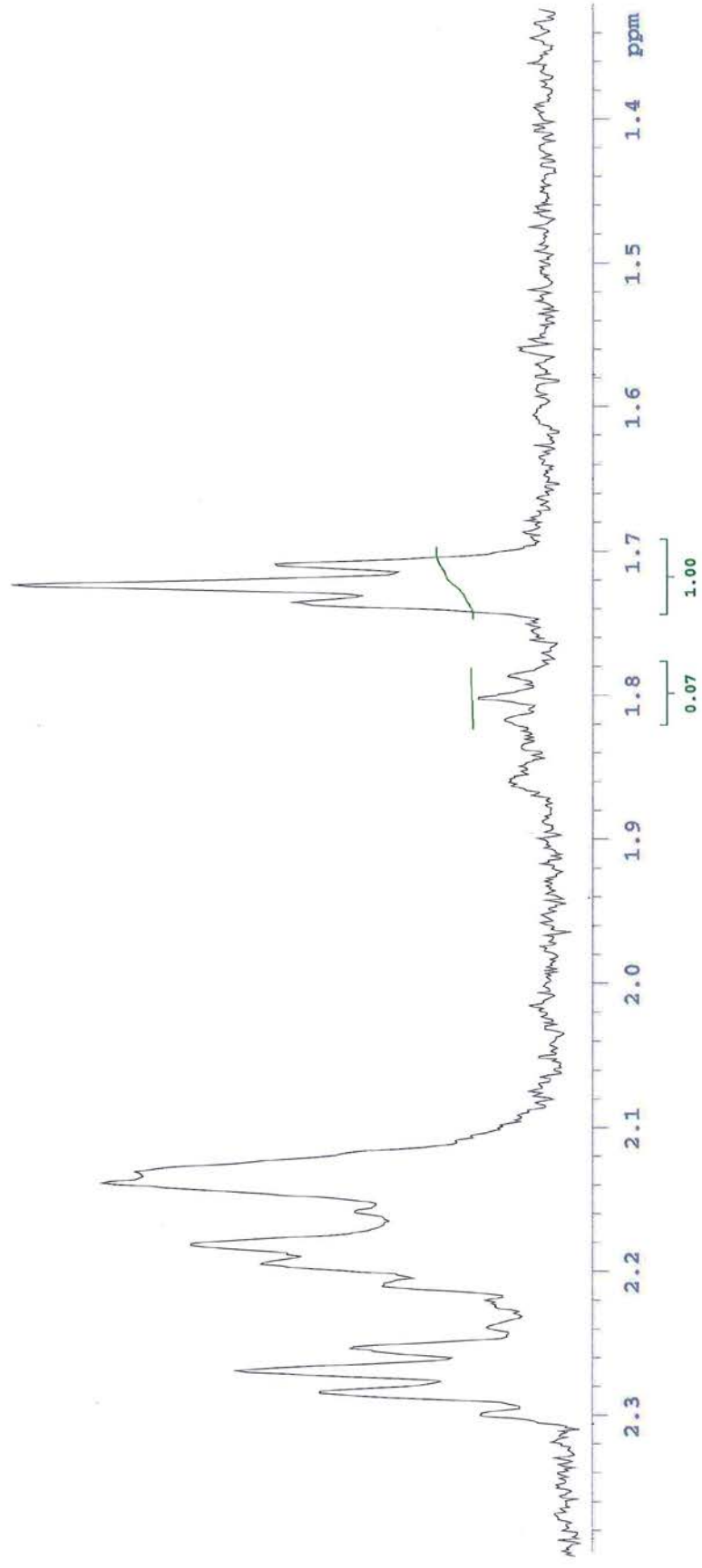
S35. 1D TOCSY NMR spectrum (75% CH₃CN/D₂O) (from stop-flow HPLC-NMR) of moniliferanone A (8).



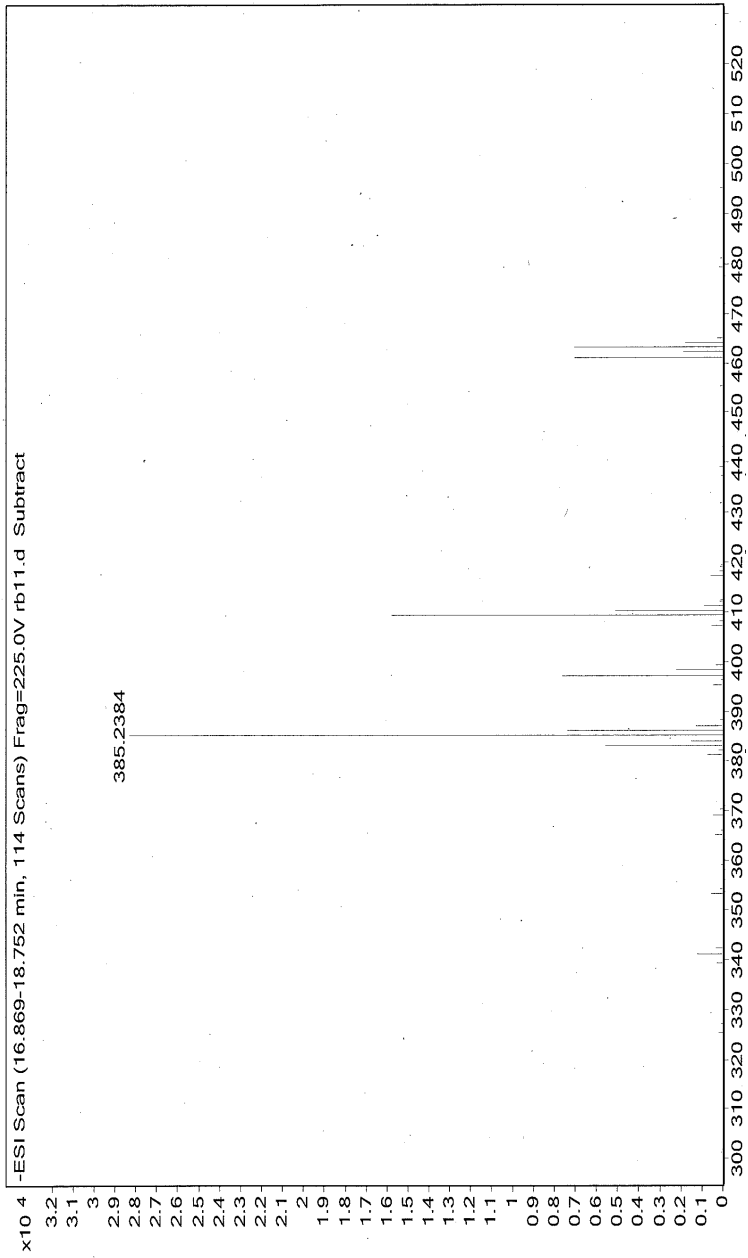
S36. HSQCAD NMR spectrum (75% CH₃CN/D₂O) (from stop-flow HPLC-NMR) of moniliferanone A (**8**).



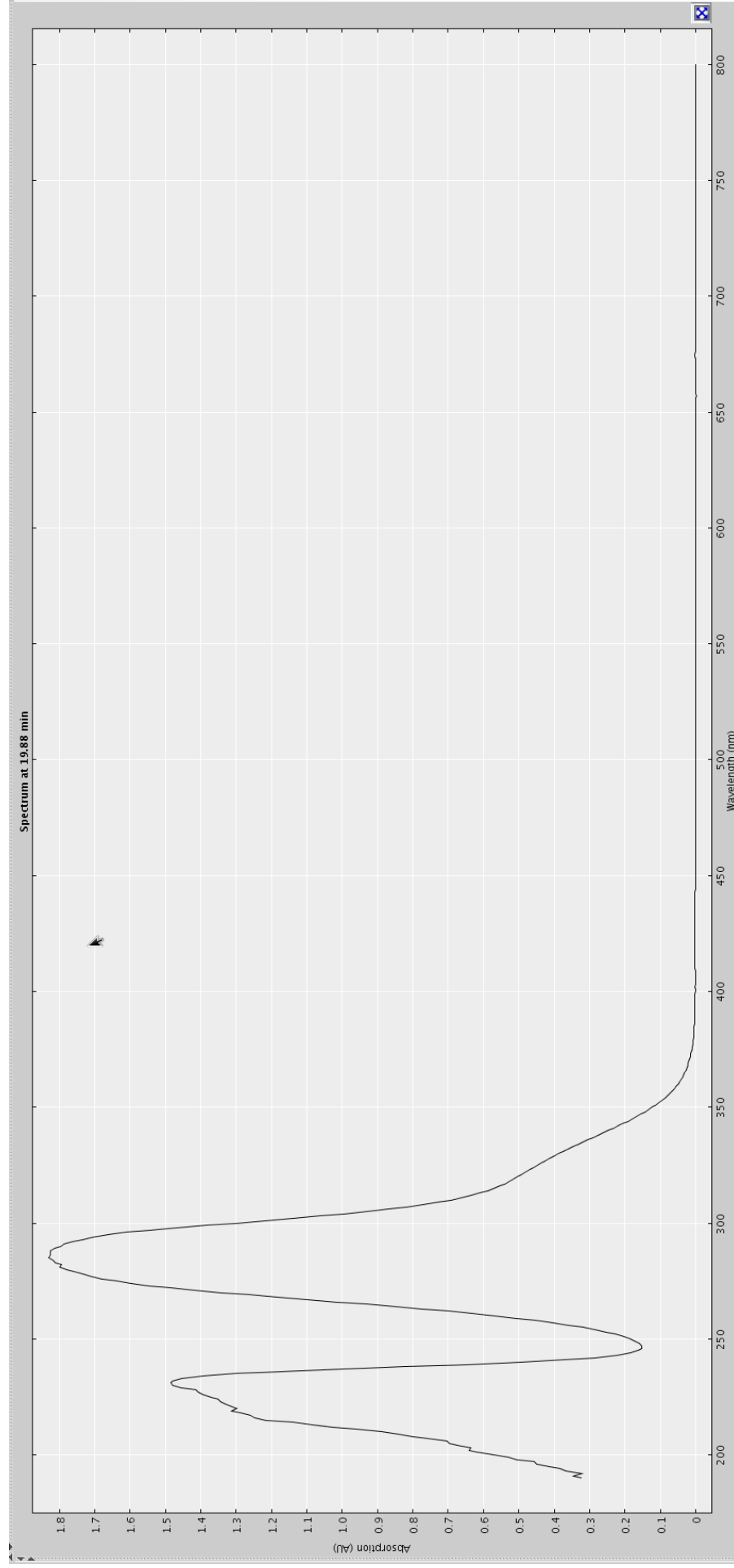
S37. Expanded stop-flow WET 1D Proton NMR spectrum (70% CH₃CN/D₂O) of moniliferanone A (**8**) and moniliferanone C (**11**) showing relative intensities from *C. monilifera*.



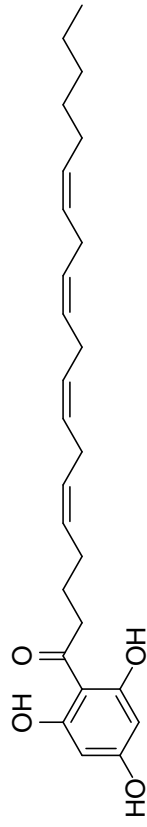
S38. Expanded stop-flow WET1D Proton NMR spectrum (70% CH₃CN/D₂O) of moniliferanone A (**8**) and moniliferanone C (**11**) showing relative intensities from *C. subfarcinata*.



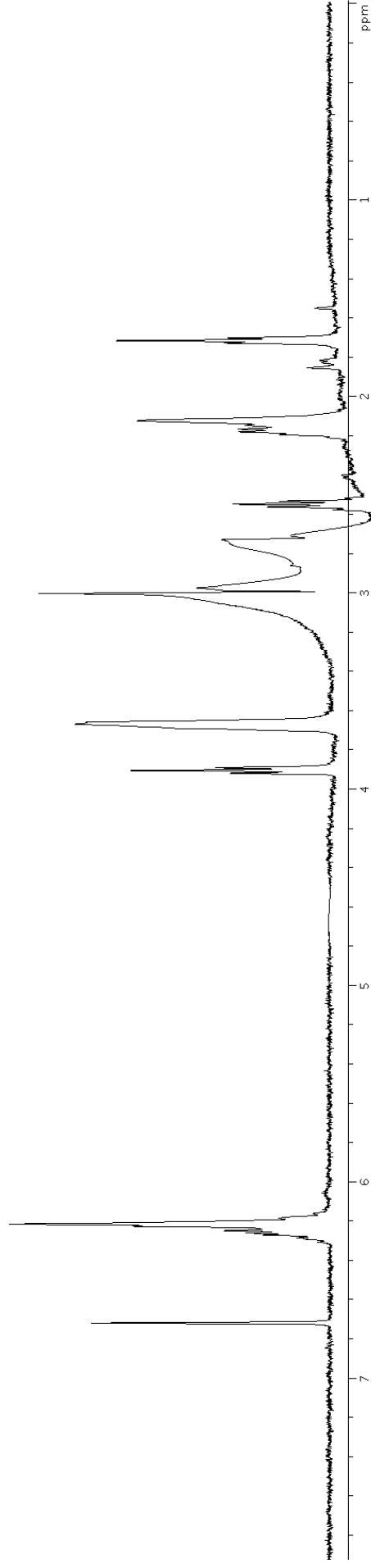
S39. High resolution negative ESI-MS of moniliferanone A (**8**) from HPLC-MS.



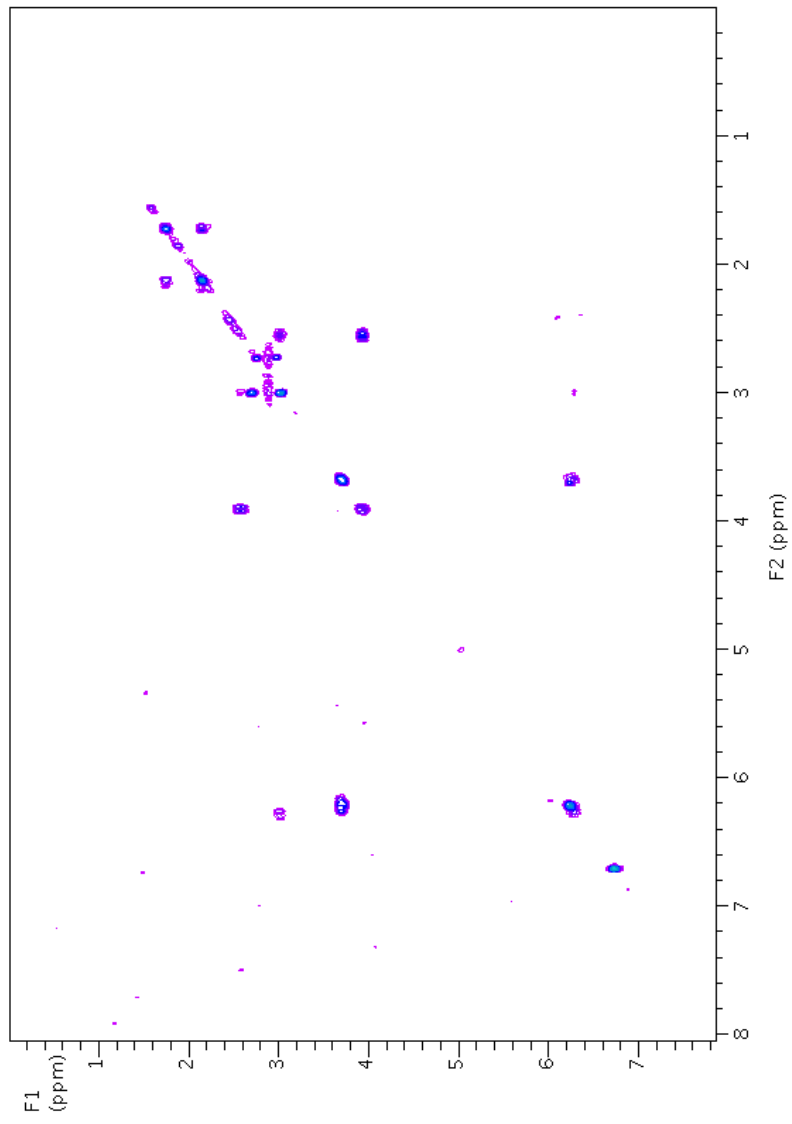
S40. Extracted UV profile (75% CH₃CN/D₂O) of **9** from HPLC-NMR.



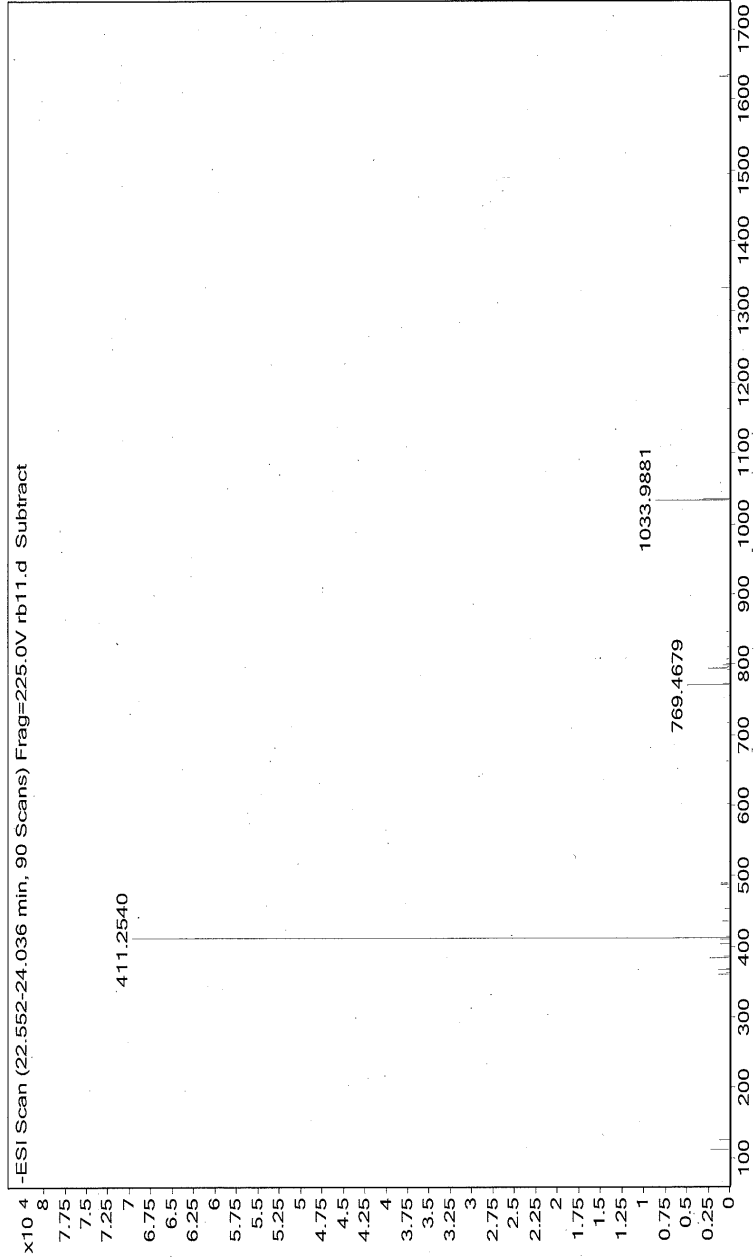
(9) - moniliferanone B



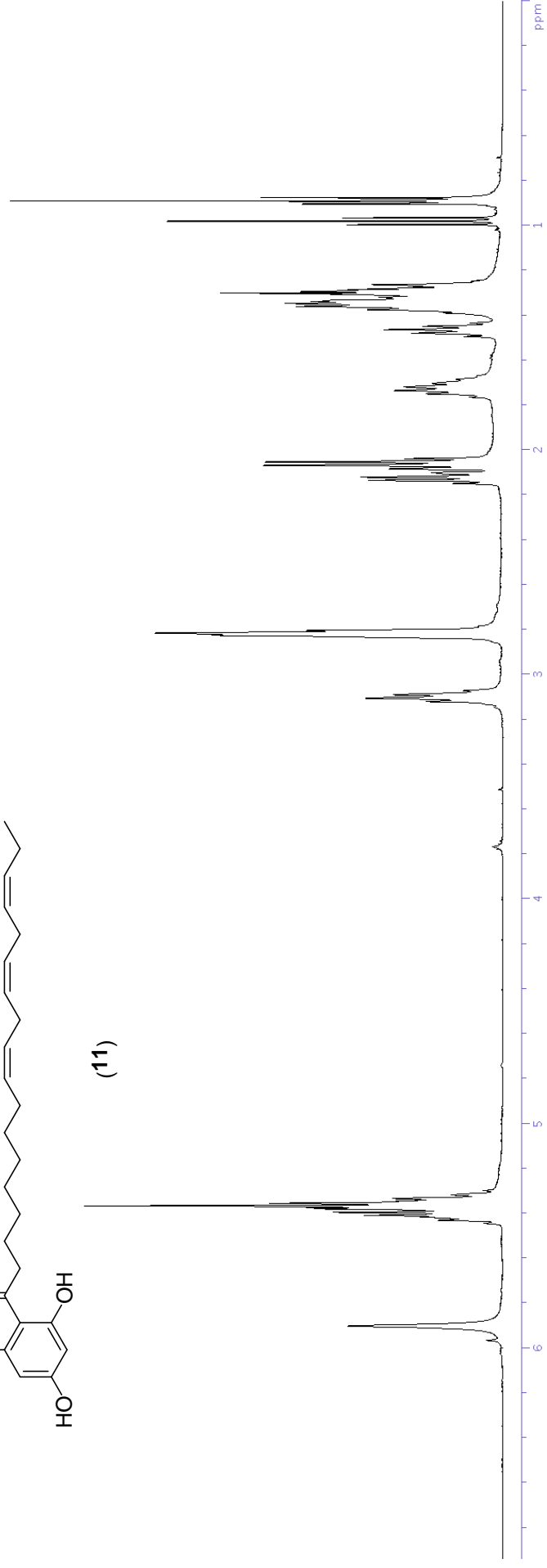
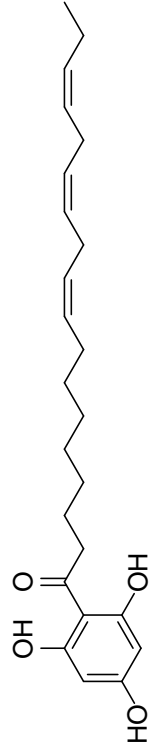
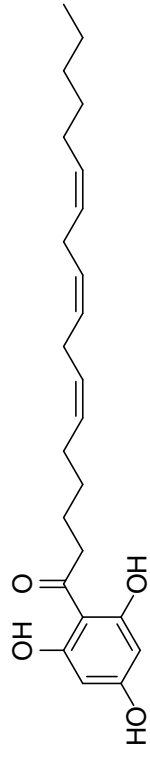
S41. Stop-flow WET1D Proton NMR spectrum (75% CH₃CN/D₂O) of moniliferanone B (**9**).



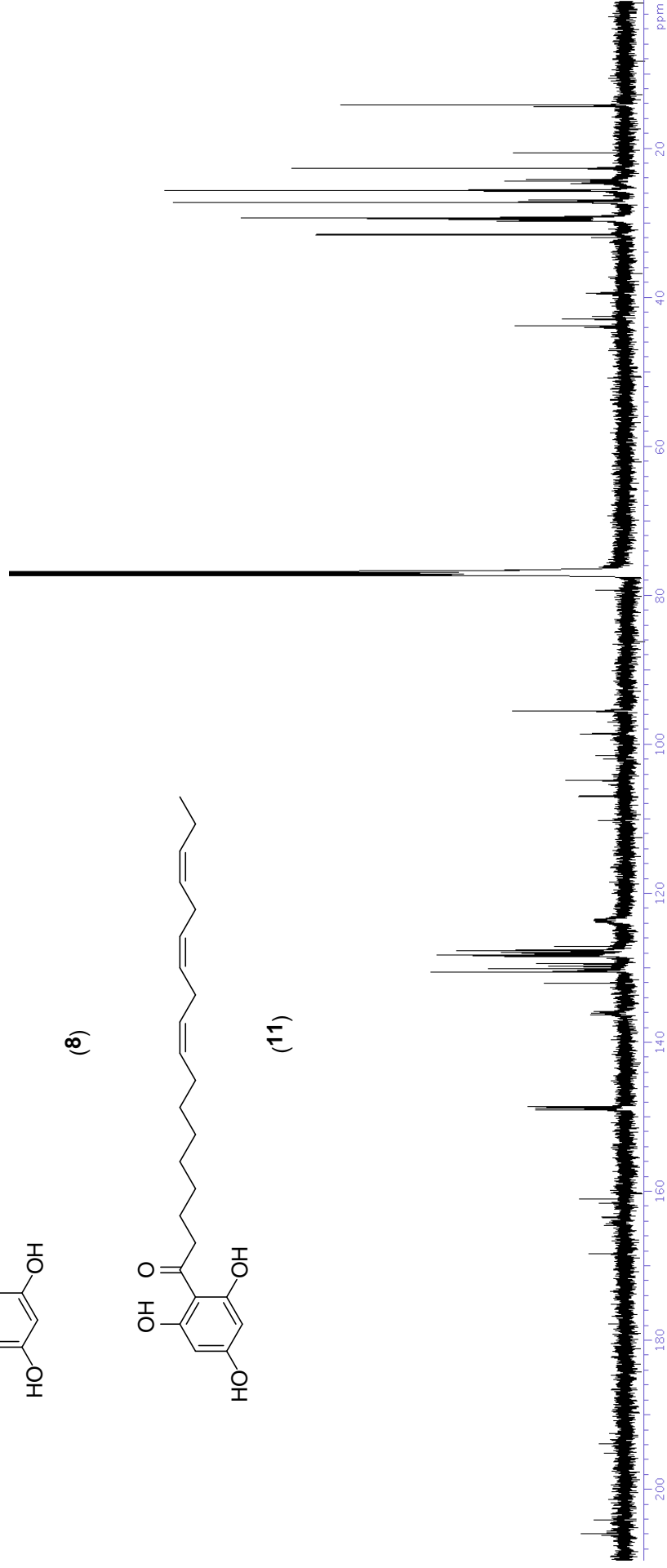
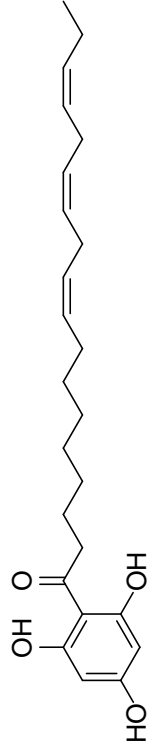
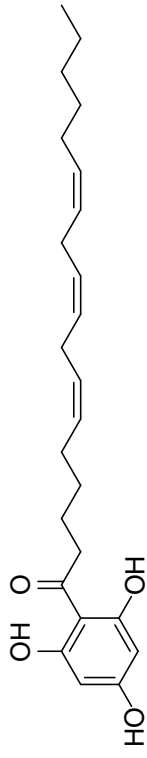
S42. gCOSY NMR spectrum (75% CH₃CN/D₂O) (from stop-flow HPLC-NMR) of moniferanone B (**9**).



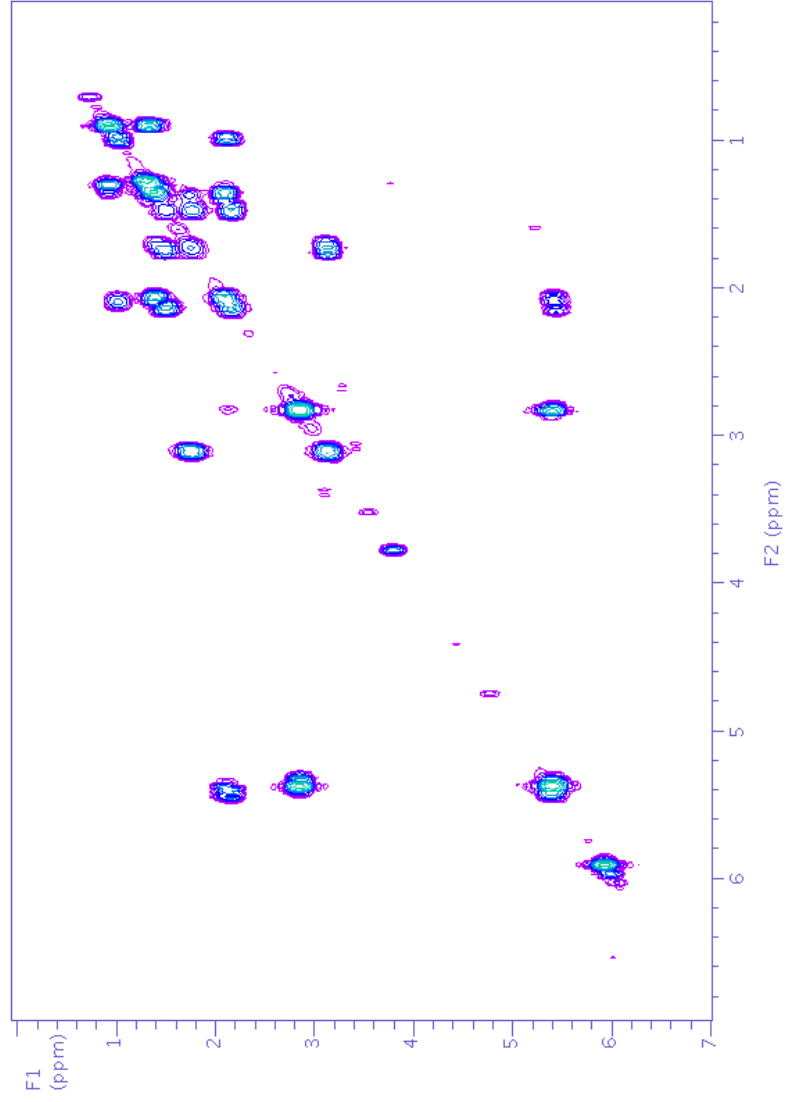
S43. High resolution negative ESI-MS of moniliferanone B (9) from HPLC-MS.



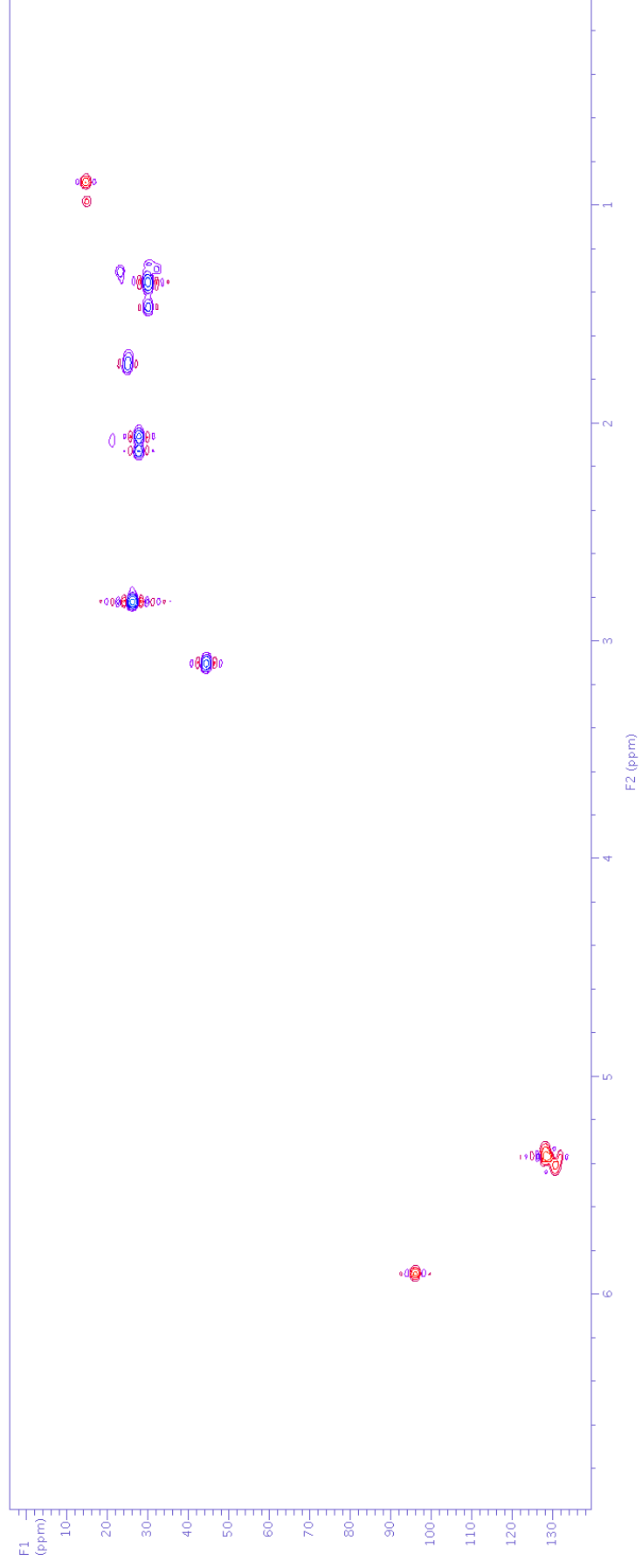
S44. ¹H NMR spectrum (500 MHz, CDCl₃) of moniferanone A (8) and C (11) mixture.



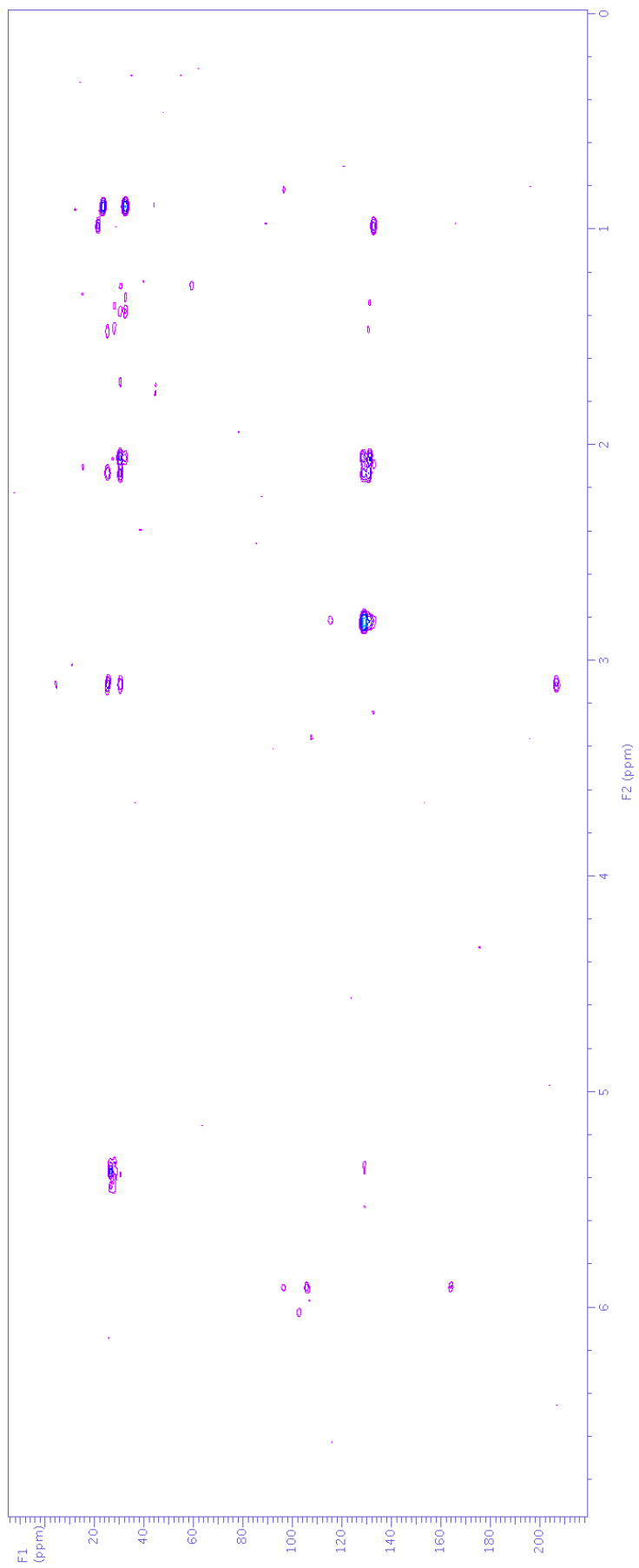
S45. ^{13}C NMR spectrum (125 MHz, CDCl_3) of moniliferanone A (8) and C (11) mixture.



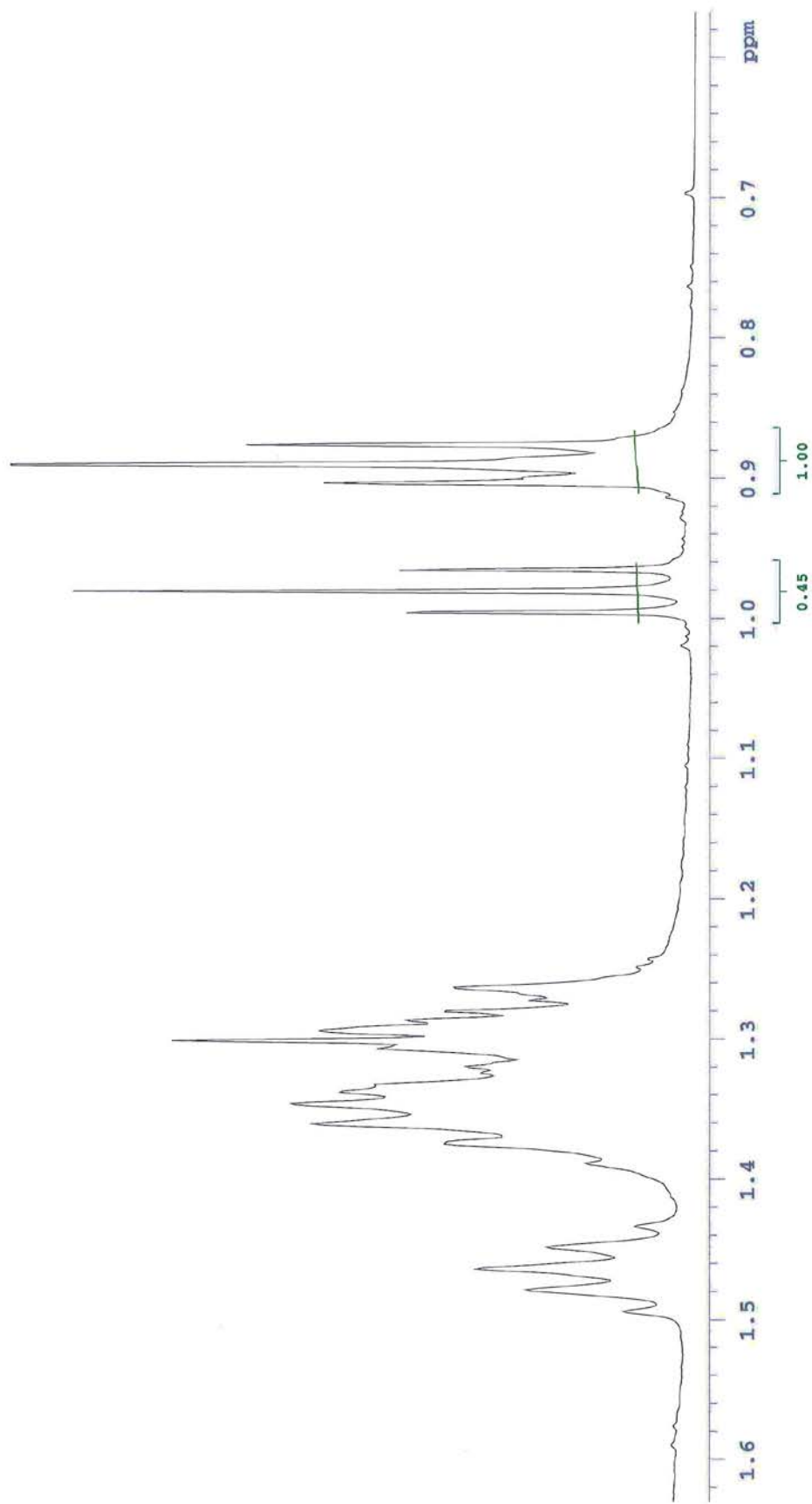
S46. gCOSY NMR spectrum (500 MHz, CDCl₃) of moniliferanone A (**8**) and C (**11**) mixture.



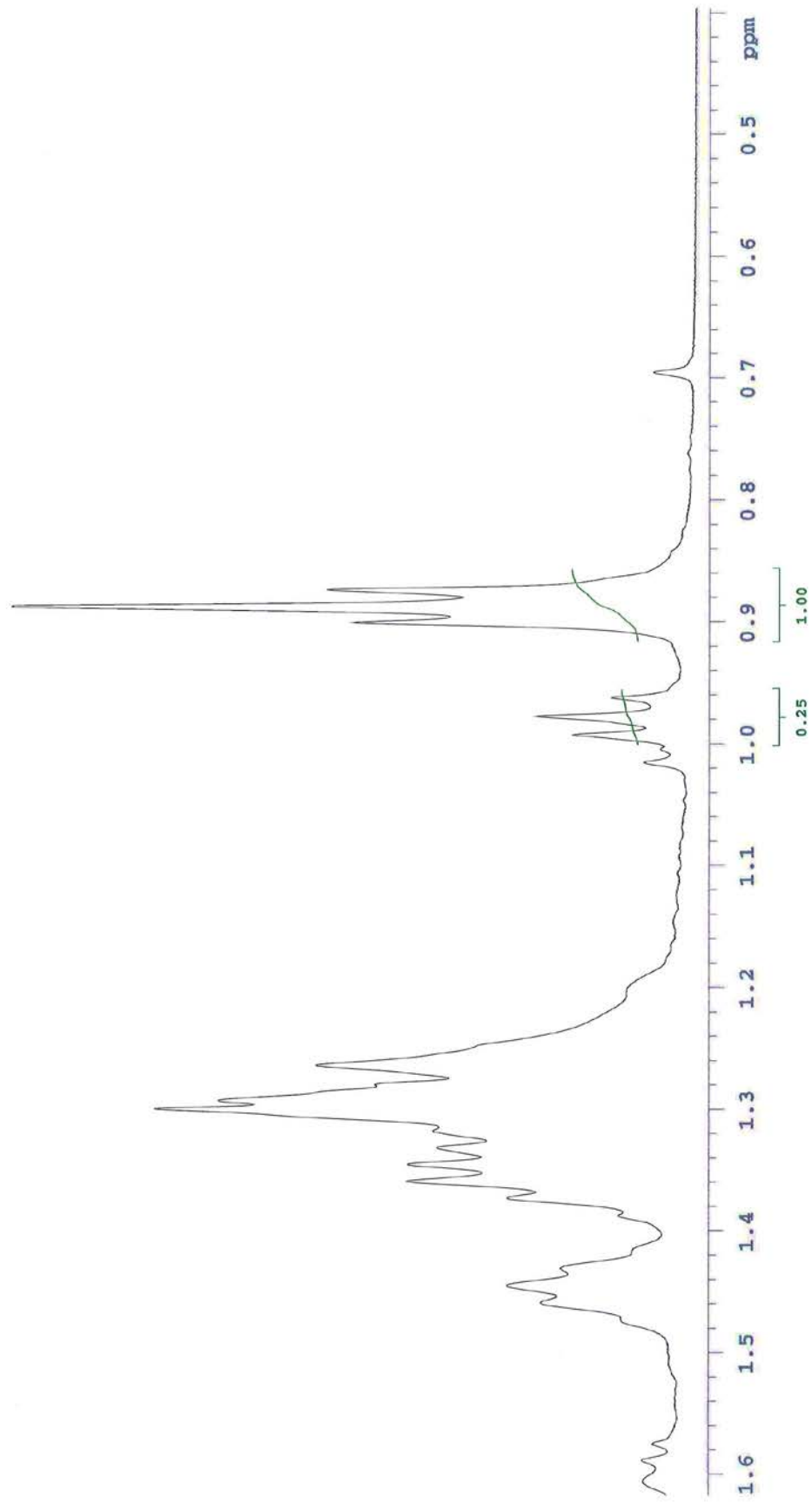
S47. gHSQCAD NMR spectrum (500 MHz, CDCl₃) of moniliferanone A (**8**) and C (**11**) mixture.



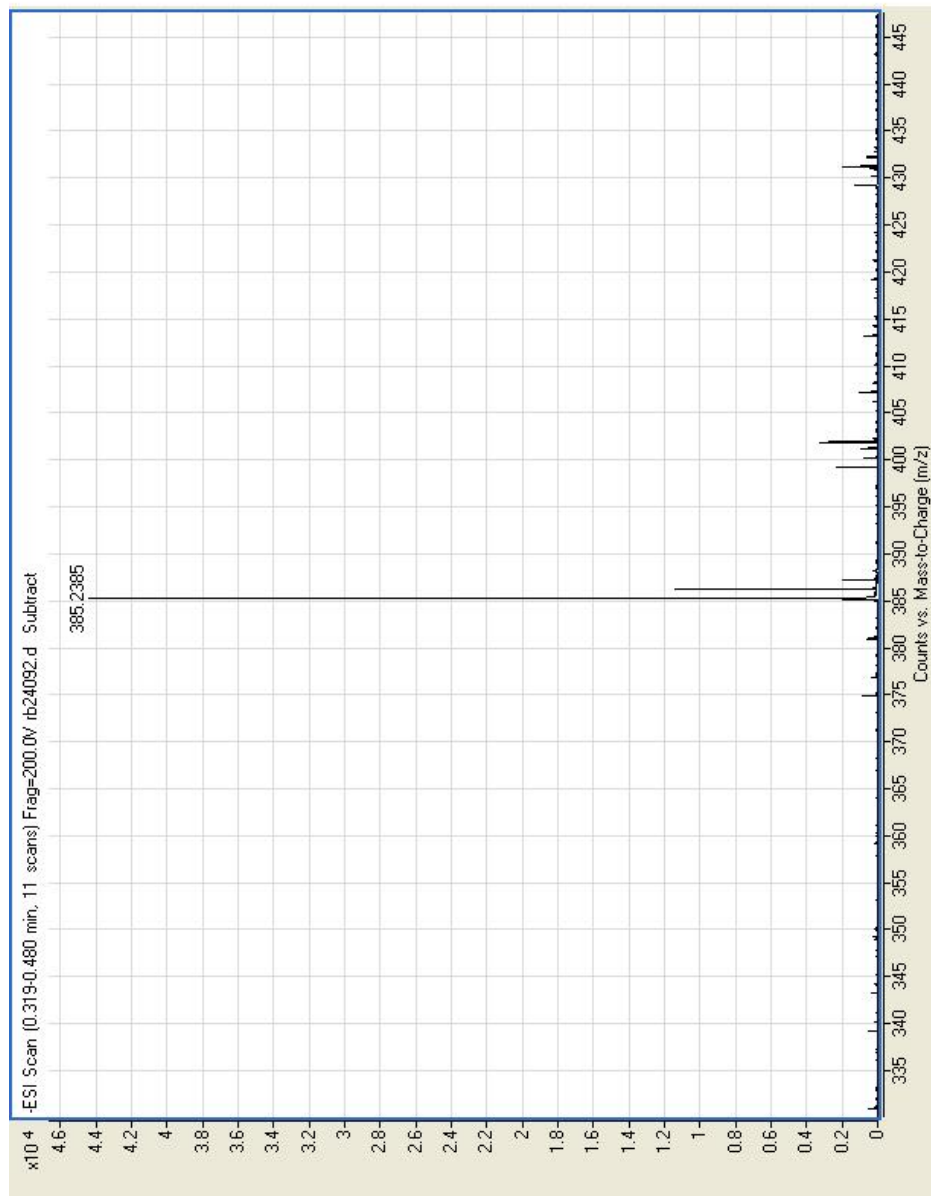
S48. gHMBC NMR spectrum (500 MHz, CDCl₃) of moniliferanone A (**8**) and C (**11**) mixture.



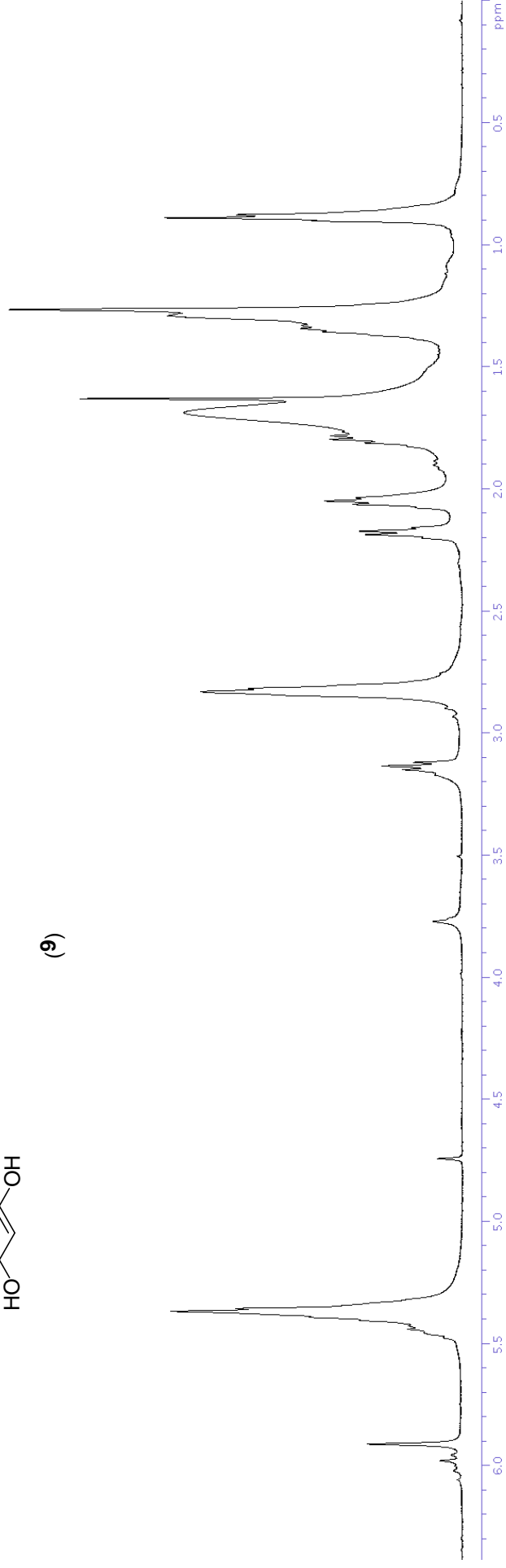
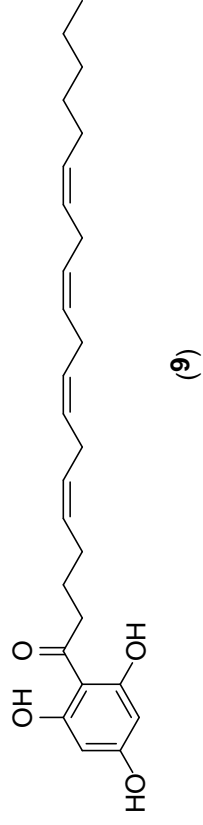
S49. Expanded ¹H NMR spectrum (500 MHz, CDCl₃) of moniliferanone A (**8**) and moniliferanone C (**11**) showing relative intensities from *C. monilifera*.



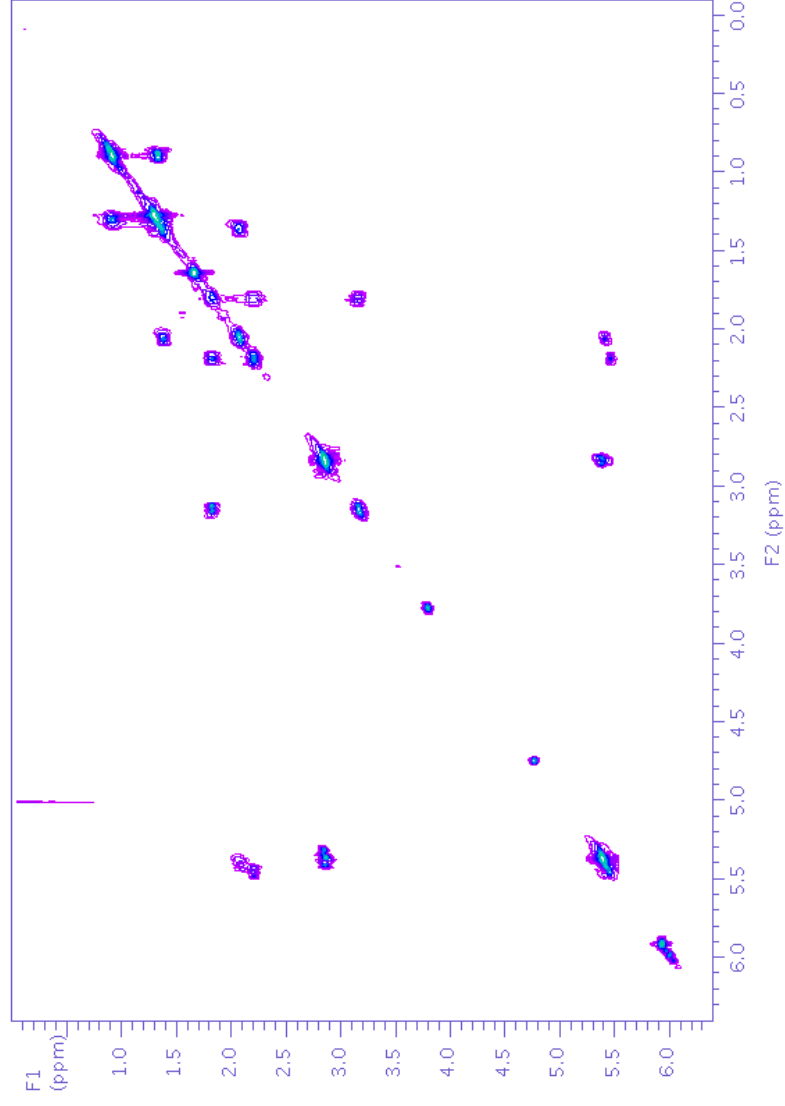
S50. Expanded ^1H NMR spectrum (500 MHz, CDCl_3) of moniliferanone A (**8**) and moniliferanone C (**11**) showing relative intensities from *C. subfarcinata*.



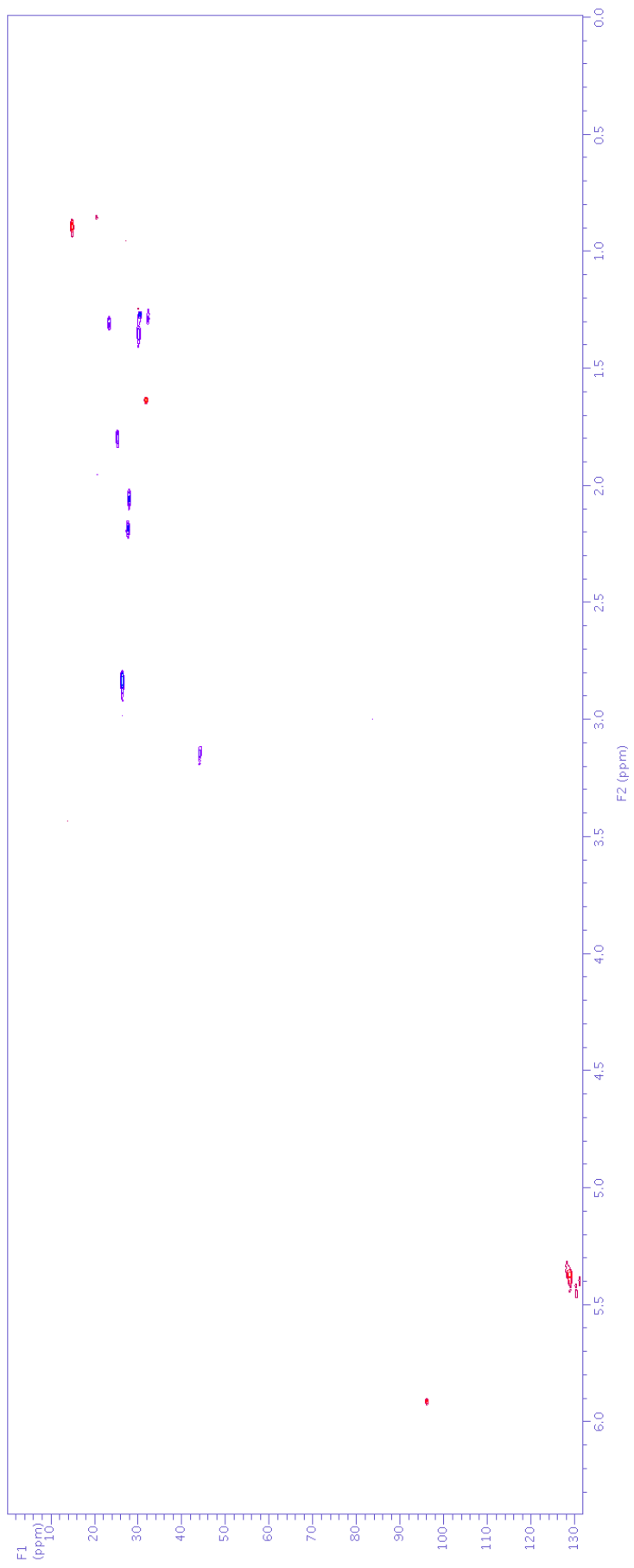
S51. High resolution negative ESI-MS of moniliferanone A (**8**) and C (**11**) mixture.



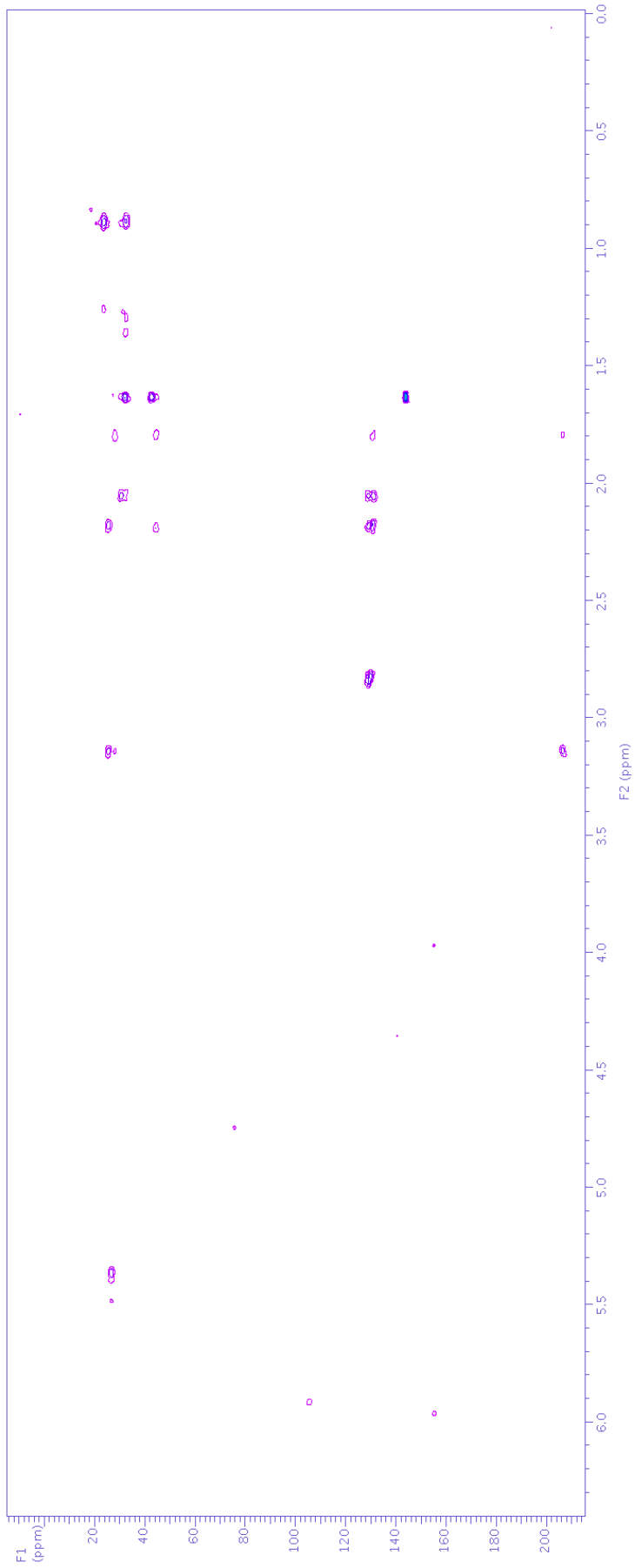
S52. ¹H NMR spectrum (500 MHz, CDCl₃) of moniliferanone B (**9**).



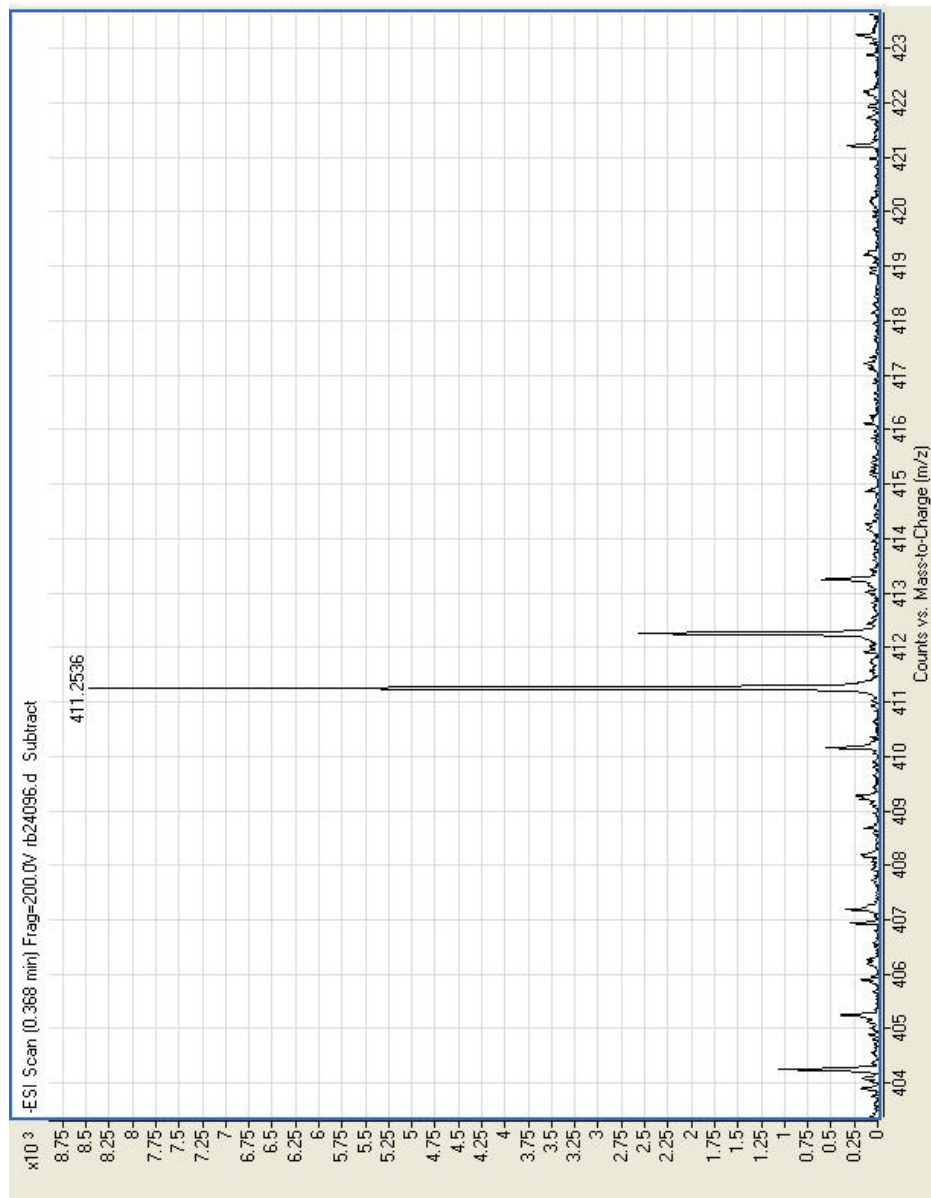
S53. gCOSY NMR spectrum (500 MHz, CDCl_3) of moniliferanone B (**9**).



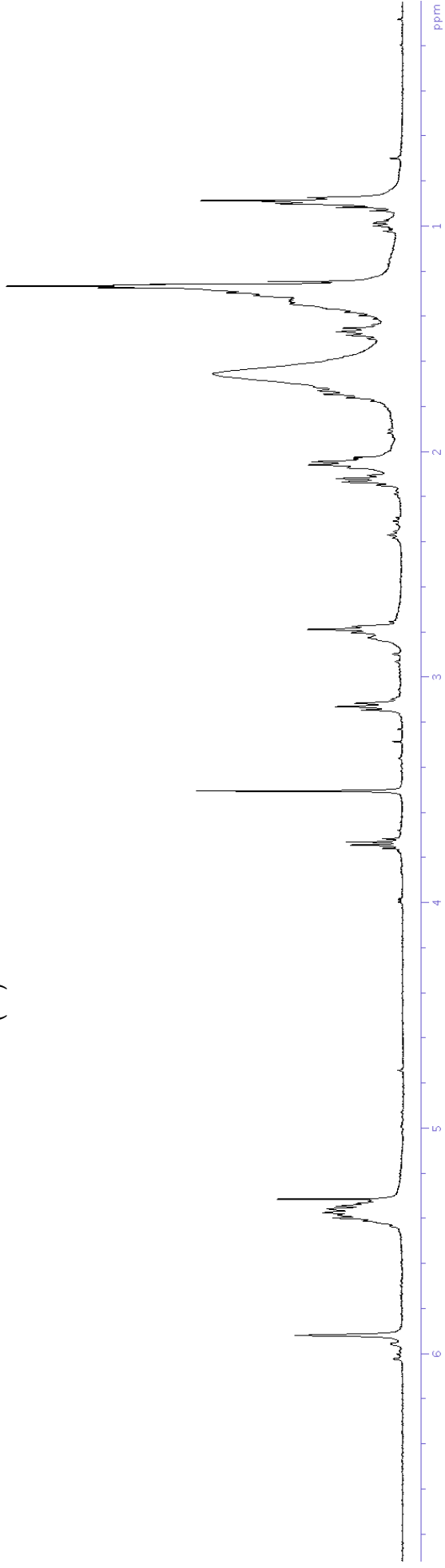
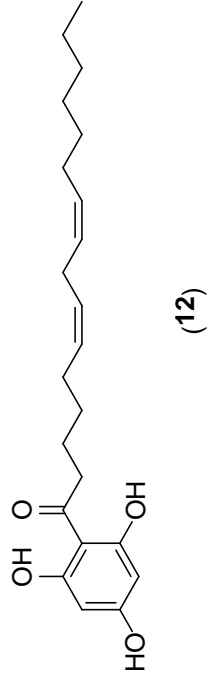
S54. gHSQCAD NMR spectrum (500 MHz, CDCl₃) of moniliferanone B (**9**).



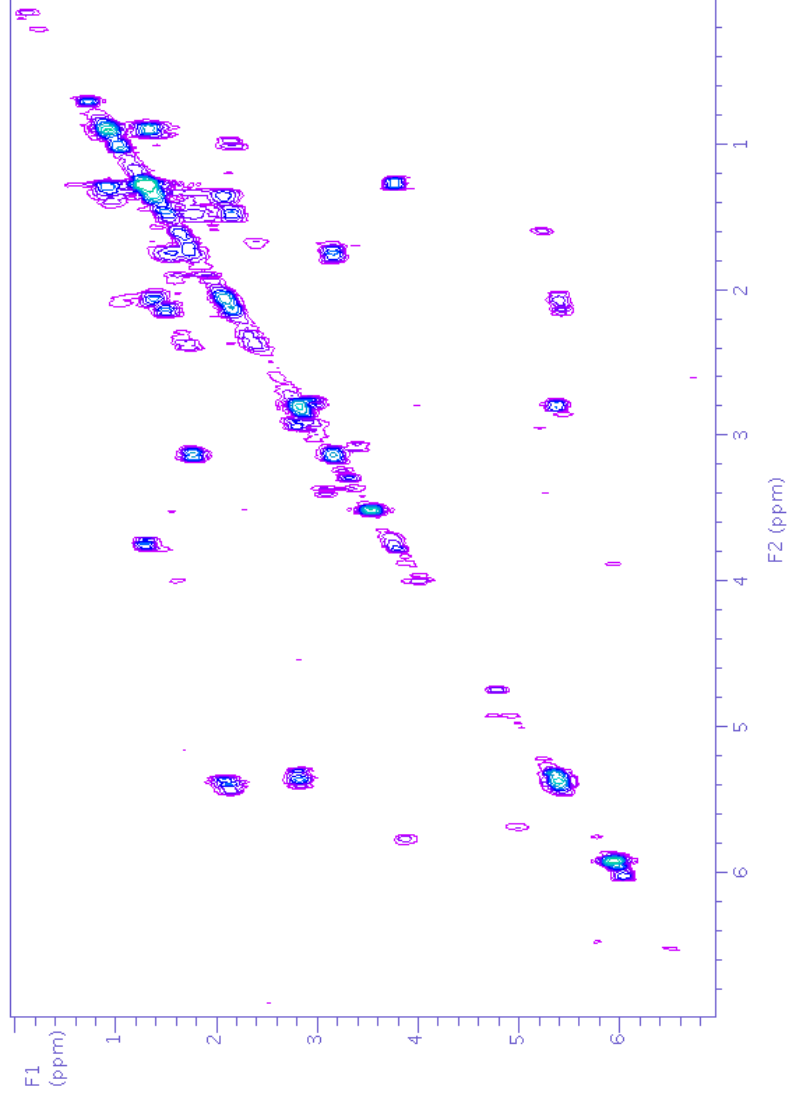
S55. gHMBC NMR spectrum (500 MHz, CDCl₃) of moniliferanone B (**9**).



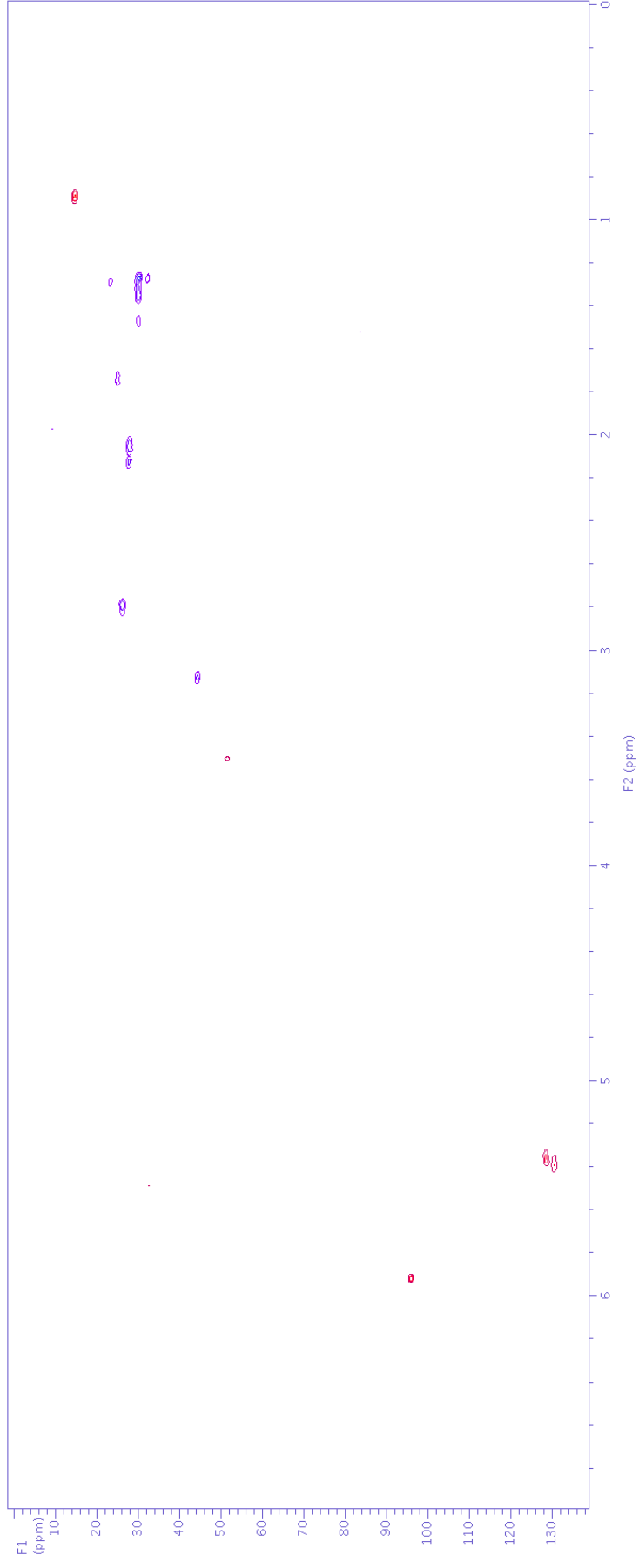
S56. High resolution negative ESI-MS of moniliferanone B (**9**).



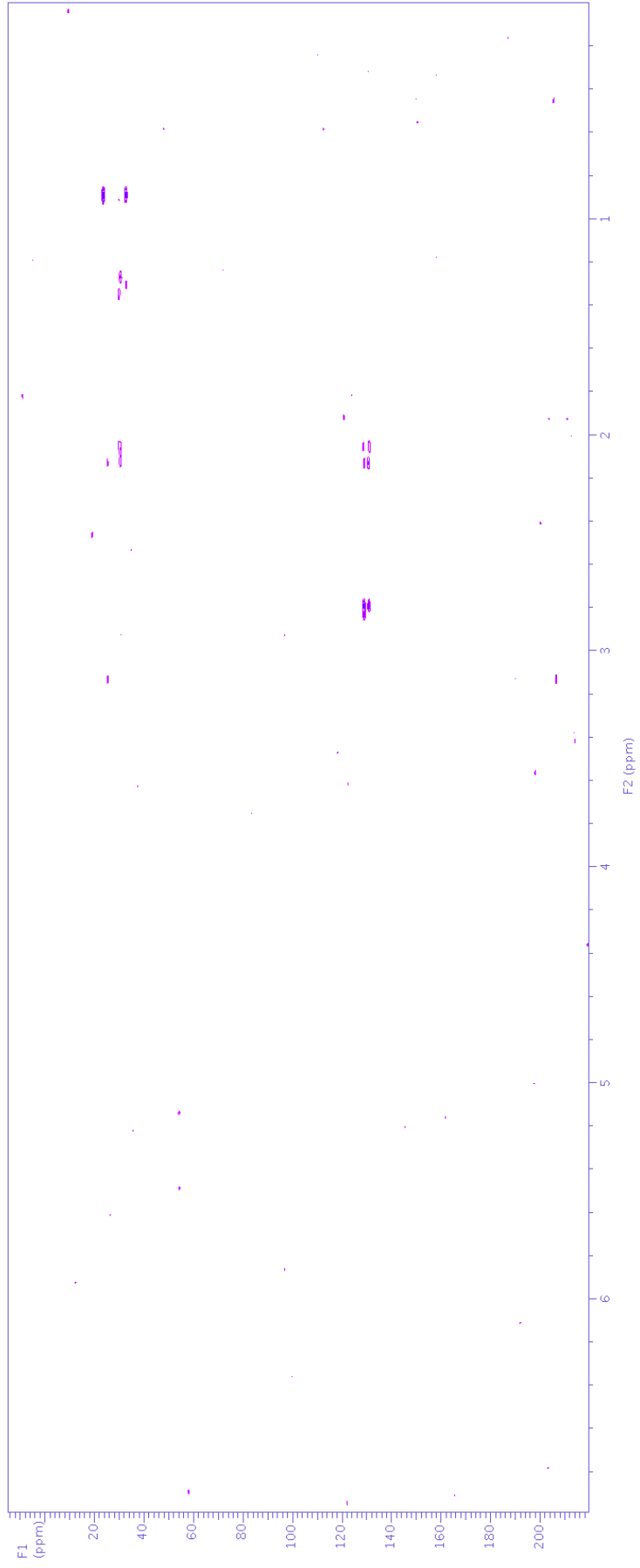
S57. ¹H NMR spectrum (500 MHz, CDCl₃) of moniliferanone D (**12**).



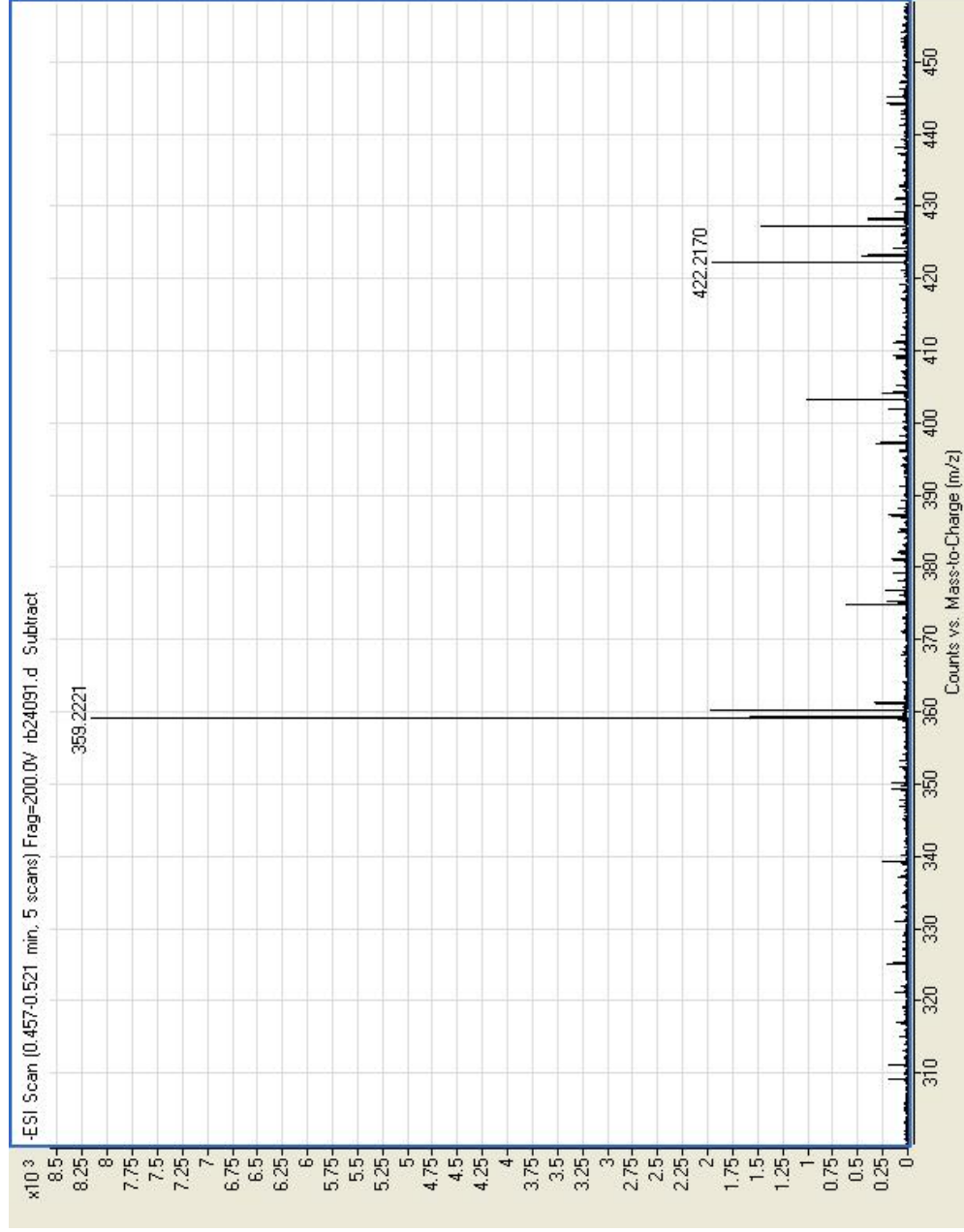
S58. gCOSY NMR spectrum (500 MHz, CDCl_3) of moniliferanone D (**12**).



S59. gHSQCAD NMR spectrum (500 MHz, CDCl₃) of moniliferanone D (**12**).



S60. gHMBC NMR spectrum (500 MHz, CDCl_3) of moniliferanone D (**12**).



S61. High resolution negative ESI-MS of moniliferanone D (**12**).